Intended for
Vistra Energy, dba
Dynegy Midwest Generation, LLC
13498 E 800th St
Hennepin, Illinois 61327

Date
March 7, 2025

Project No.
1940110241-006

CORRECTIVE ACTION PLAN

DYNEGY MIDWEST GENERATION, LLC, HENNEPIN POWER STATIONS, WEST ASH POND SYSTEM, IEPA ID NO. W1550100002-01 AND W1550100002-03

RAMBOLL Bright ideas. Sustainable change.

CORRECTIVE ACTION PLAN
DYNEGY MIDWEST GENERATION, LLC, HENNEPIN POWER STATIONS, WEST ASH POND SYSTEM, IEPA ID NO. W1550100002-01 AND W1550100002-03

Project name	**Hennepin West Ash Pond System**
Project no.	**1940110241-006**
Recipient	**Dynegy Midwest Generation**
Document type	**Corrective Action Plan**
Revision	**DRAFT**
Date	**March 7, 2025**
Prepared by	**Elizabeth (Richter) Rotstein, PE**
Checked by	**Lucas Carr, PE**
Approved by	**Brian Hennings, PG**
Description	**Corrective Action Plan for 35 I.A.C. § 845**

Lucas Carr, PE
Qualified Professional Engineer

Brian Hennings, PG
Project Officer, Hydrogeology

CONTENTS

TABLES (WITHIN TEXT)

TABLES

APPENDICES

ACRONYMS AND ABBREVIATIONS

%	percent
35 I.A.C.	Title 35 of the Illinois Administrative Code
40 C.F.R.	Title 40 of the Code of Federal Regulations
bgs	below ground surface
BMP	Best Management Practice
CAAA	Corrective Action Alternatives Analysis
CAAA-SIR	Corrective Action Alternatives Analysis Supporting Information Report
CAP	Corrective Action Plan
CBR	closure-by-removal
CCR	coal combustion residuals
CCS	continuous containment system
CIP	closure-in-place
cm/sec	centimeters per second
CMA	Corrective Measures Assessment
COC	constituent of concern
COI	constituent of interest
CP	Construction Permit
CWS	community water supply
DCW	Deep Cutoff Wall
DMG	Dynegy Midwest General, LLC
EAP	East Ash Pond
ft	feet
GMP	Groundwater Monitoring Plan
Gradient	Gradient Corporation
GWP	groundwater polishing
GWPS	groundwater protection standard(s)
HEN	Hennepin Power Station
HPP	Hennepin Power Plant
ID	identification
IEPA	Illinois Environmental Protection Agency
ISGS	Illinois State Geological Survey
ISS	*In-Situ* Stabilization/Solidification
ISWS	Illinois State Water Survey
LLDPE	linear low-density polyethylene
mg/L	milligram per liter
NAVD88	North American Vertical Datum of 1988
NID	National Inventory of Dams
No.	number
OP	Operating Permit
OWAP	Old West Ash Pond
OWPP	Old West Polishing Pond
PRB	permeable reactive barrier
PWS	public water system
Ramboll	Ramboll Americas Engineering Solutions, Inc.

SI	surface impoundment
UA	uppermost aquifer
USEPA	United States Environmental Protection Agency
WAPS	West Ash Pond System
WHPA	wellhead protection area

1. INTRODUCTION

1.1 Plant and Site Information

Dynegy Midwest Generation, LLC (DMG) is the owner of the inactive coal-fired Hennepin Power Plant (HPP), also referred to as the Hennepin Power Station (HEN), in Hennepin, Putnam County, Illinois. DMG intends to complete groundwater corrective action of the coal combustion residuals (CCR) surface impoundment (SI) West Ash Pond System (WAPS), which is identified by Illinois Environmental Protection Agency (IEPA) identification (ID) numbers (No.) W1550100002-01 and W1550100002-03, CCR Unit ID No. 804, and a National Inventory of Dams (NID) No. IL50698. The WAPS is comprised of the Old West Ash Pond (OWAP) and the Old West Polishing Pond (OWPP). The WAPS was constructed as a single unit with a single perimeter dike and subsequently internally divided into the OWAP and OWPP as part of operational practices. Source control (*e.g.*, closure) was completed in 2020; this included leaving CCR in place within the OWAP, removing all CCR from the OWPP, placing it within the OWAP, and installing a geomembrane final cover system over the consolidated OWAP [1, 2]. This document and all past engineering and hydrogeological studies consider the WAPS as a single CCR unit. This Corrective Action Plan (CAP) has been prepared for the WAPS at HPP under the requirements of Title 35 of the Illinois Administrative Code (35 I.A.C.) § 845, Standards for the Disposal of Coal Combustion Residuals in Surface Impoundments [3] and the requirements of Title 40 of the Code of Federal Regulations (40 C.F.R.) § 257, herein referred to as the Federal CCR Rule [4].

1.2 Organization of the Corrective Action Plan

This CAP is organized in the following manner:

- **Section 1** includes an introduction to the WAPS, lists the status of other 35 I.A.C. § 845 permit applications submitted to IEPA, identifies the selected remedy, and provides a narrative of remedy construction;
- **Section 2** includes an overview of the Corrective Action process, including the results of the Corrective Measures Assessment (CMA) and Corrective Action Alternatives Analysis (CAAA);
- **Section 3** provides the CAP requirements, the selected remedy, an evaluation of effectiveness and an implementation schedule, as required by 35 I.A.C. § 845.670; and
- **Section 4** includes reference documents used in the development of this CAP.

This CAP was prepared as an appendix to a Corrective Action Construction Permit (CP) application, to support obtaining a permit for Corrective Action Construction at the WAPS, as required by 35 I.A.C. § 845.220(a) and (c).

1.3 Permit Status

An Operating Permit (OP) application, as required by 35 I.A.C. § 845.230, was submitted on October 25, 2021 [5]. The permit application is currently under review by IEPA.

1.4 Closure and Source Control Status

DMG completed significant source control efforts in 2020 as part of final closure of the WAPS [1, 2]. The final closure was performed in accordance with the Closure and Post-Closure Care Plan [6] that was developed in accordance with 40 C.F.R. § 257, submitted to IEPA for review, and subsequently approved by IEPA [8]. IEPA found "*…the closure and post-closure care plan…to be an adequate corrective action*" [7]. The final closure was addressed in accordance with the IEPA Water Pollution Control Permit 202-EA-65026-1.

The WAPS closure included a hybrid consolidate-and-cap approach comprised of closure-by-removal (CBR) of the OWPP and closure-in-place (CIP) of the OWAP. This involved excavating CCR and approximately one foot of soil below the CCR from the OWPP and placing it into the OWAP, and installing a geomembrane final cover system over the consolidated OWAP in accordance with 40 C.F.R. § 257.102 [1, 2]. These source control activities serve as the primary groundwater corrective measure for the WAPS.

Since final closure in 2020, groundwater quality has improved evidenced by a decrease in boron concentrations [8] within the groundwater monitoring network. Specifically, many wells where boron concentrations were above the GWPS of 2 milligram per liter (mg/L) before closure, *e.g.*, wells 22, 21/21R, and 51, have, since closure, attained GWPS, or concentration levels have steadily decreased.

The remedy presented within this Corrective Action Plan is intended to be supplementary to the primary remedy, which is the completed source control.

1.5 Selected Corrective Action Remedy

A source control with continuous containment system (CCS), which combines source control that has been implemented at WAPS [1, 2] with a proposed deep cutoff wall (DCW) anchored (*i.e.,* extended) into competent bedrock, has been identified as the most appropriate remedy for the WAPS, based on the CAAA provided in **Appendix A**. The CCS will provide a continuous, passive, and essentially maintenance-free containment of the CCR within the WAPS, thereby controlling the source of releases of constituents listed in 35 I.A.C. § 845.60.

Potential remedies evaluated in the CAAA included Source Control with Groundwater Polishing (GWP) and Source Control with DCW. The CAAA, which was prepared by Gradient Corporation (Gradient), was based on a CAAA Supporting Information Report (CAAA-SIR) that was prepared by Ramboll Americas Engineering Solutions, Inc. (Ramboll) and is attached to the CAAA. The CAAA-SIR includes the results of groundwater modeling and feasibility-level design information for each remedy.

A Groundwater Polishing Evaluation Report [9] is also attached to the CAAA. This report presents results from geochemical modeling of exceedance[1] parameters addressed at WAPS by the CAP. Geochemical modeling is intended to contextualize the estimated time to reach the groundwater protection standard (GWPS) by evaluating the potential for chemical attenuation of exceedance parameters; and, for evaluating the potential for previously attenuated constituents of concern (COCs) to be remobilized under return-to-background conditions.

---

[1] Throughout this document, "exceedance" or "exceedances" is intended to refer only to potential exceedances of proposed applicable background statistics or GWPSs as described in the proposed groundwater monitoring program, which was submitted to the IEPA on October 25, 2021 as part of DMG's operating permit application for the HPP WAPS. That operating permit application, including the proposed groundwater monitoring program, remains under review by the IEPA and, therefore, DMG has not identified any actual exceedances.

1.5.1 Narrative Description of Selected Corrective Action Remedy

Corrective action will consist of supplementing the completed source control [1, 2] through the installation of a vertically- and laterally-continuous, permanent, and low-permeability DCW that will extend from the perimeter dikes of the WAPS into low-permeability competent bedrock beneath the WAPS. This will result in the CCR within the WAPS being physically isolated from the environment on all sides by a permanent, passive system of continuous low-permeability barriers, including the final cover system on the surface, the DCW laterally, and competent shale bedrock below the base.

Once installed, the CCS will be a permanent corrective action feature. Performance of the CCS as groundwater corrective action will be monitored in accordance with the Corrective Action Groundwater Monitoring Plan (GMP) attached to the CP Application.

Estimated times to reach the GWPS will be periodically reviewed and updated based on observed corrective action performance via an adaptive site management strategy. These periodic, updated estimates will be communicated to IEPA and the public within annual corrective action monitoring reports, in accordance with the corrective action GMP.

Corrective action will be considered complete when a demonstration that GWPS compliance beyond the waste boundary has been achieved for at least three years and a corrective action completion report and certification have been submitted to IEPA in accordance with 35 I.A.C. § 845.680(e).

1.5.1.1 Narrative Discussion of Remedy Design and Function

The CCS, which includes the DCW, final cover system, and competent bedrock base, includes the following features:

- The DCW portion of the remedy will be a continuous feature that will encircle the perimeter of the OWAP, with a total length of approximately 5,200 feet.
    - Since CCR from the OWPP was excavated and placed in the OWAP during WAPS closure [1, 2], this will encircle the remaining CCR contained within the WAPS.
- The DCW will be anchored (*i.e.,* extended) at least one foot into competent, low-permeability shale bedrock beneath the WAPS, which has a typical depth of approximately 90 feet below ground surface (bgs).
    - In 2024, packer testing was conducted at three boreholes (B-100, B-101, and B-102) adjacent to the WAPS. The results are summarized in a technical memorandum that will be included within an appendix to the CAAA (**Appendix A**) at a later date.
    - The competent shale bedrock was determined to have a hydraulic conductivity ranging from 1.1×10^{-5} centimeters per second (cm/sec) to 3.2×10^{-6} cm/sec, with a geometric mean hydraulic conductivity of 3.4×10^{-6} cm/sec.
    - As the field measured hydraulic conductivity from wells at the WAPS as approximately 1.2×10^{-2} cm/sec for the gravel deposits of the Henry Formation [10], the geometric mean of the hydraulic conductivity of the shale bedrock is on the order 3,500 times (*i.e.,* nearly 4 orders of magnitude) lower than that of the overlying aquifer materials. Additionally, the observed hydraulic conductivity of the competent shale bedrock either remained consistent or decreased with depth. This demonstrates

  - that the shale bedrock has an appropriately low hydraulic conductivity to function as a lower barrier layer for the CCS.
  - A summary of the 2024 packer testing results at boreholes B-100 through B-102 are presented in **Table 1**.
- The DCW will be constructed using a mixture of either soil and bentonite or cement and bentonite, and would have a typical thickness of approximately 3 to 4 feet.
  - The target hydraulic conductivity for the DCW will be 1×10^{-7} cm/sec. This is approximately 120,000 times (*i.e.*, 5 orders of magnitude) lower than that of the surrounding aquifer materials (1.2×10^{-2} cm/sec for the gravel deposits of the Henry Formation [10]). This will result in the wall having an appropriately lower hydraulic conductivity to function as a lateral barrier for the CCS.
- After installation of the DCW, the existing final cover system, which utilizes a low-permeability, 40-mil linear low-density polyethylene (LLDPE) geomembrane barrier layer, will be extended over the top of the final cover system.
- After CCS construction is complete, CCR within the WAPS will be continuously contained by low-permeability materials and isolated from the surrounding environment on all sides, including:
  - Surface containment will be provided by the existing and extended final cover system, which utilizes a low-permeability 40-mil LLDPE geomembrane, on the top of the CCR.
  - Lateral containment will be provided by the DCW on all sides of the CCR.
  - Lower containment will be provided by the low-permeability competent shale bedrock beneath the CCR.

Permit-level engineering drawings depicting the proposed DCW and other features, including areas of the WAPS where the final cover will be disturbed, repaired, and extended as part of DCW construction, are provided in **Appendix B**.

1.5.2 Narrative Description of Proposed Remedy Operations

No corrective action O&M is expected to be required following installation of the DCW with integration into the competent bedrock portions of the CCS, as they are passive, below-grade structures. However, O&M of the final cover system portion of the CCS remedy would continue in accordance with current post-closure care O&M practices [6].

1.5.3 Narrative Description of Proposed Groundwater Monitoring

Corrective action groundwater monitoring will be conducted in accordance with the Corrective Action GMP during remedy operation to evaluate the effectiveness of the corrective action remedy and whether groundwater concentrations are achieving the GWPS as predicted by the groundwater model. Groundwater data collected as part of the monitoring program will be analyzed to determine if the remedy is on track to meet GWPS and to inform adaptive management decisions if performance metrics are not achieved. Information associated with each of these activities is described below.

- Regular groundwater monitoring will be conducted utilizing a corrective action groundwater monitoring network designed in accordance with 35 I.A.C. § 845.680(a)(1).
- Laboratory parameters include major ions for evaluating groundwater chemistry and COCs (*i.e.*, reported exceedances in accordance with the Operating GMP) the Corrective Action is intended to address. Sampling to evaluate corrective action effectiveness will begin the quarter after the corrective action remedy is implemented and commissioned. Samples will be collected on a quarterly basis initially and potentially reduced to a semiannual basis once five years of monitoring have occurred, in accordance with 35 I.A.C. § 845.650(b)(4). Monitoring results will be submitted to IEPA for each monitoring event, in addition to an Annual Groundwater Monitoring and Corrective Action Report, in accordance with 35 I.A.C. § 845.610(e).
- Routine maintenance of the monitoring well network will include inspecting the wells, making repairs to the wells (as needed) and rehabilitating and/or replacing wells to improve performance (as needed).
- Adaptive site management strategies will be employed as an integral part of ongoing corrective action at the WAPS. The adaptive site management approach will allow timely incorporation of new site information to ensure the achievement of the GWPS. The effectiveness of the remedy at each phase is evaluated using performance metrics designed to assess the goals of that phase. Performance metrics answer questions designed to evaluate multiple aspects of remedy effectiveness with the ultimate goal of holistically guiding management decisions [11]. The goals and performance metrics of each phase of remedy evaluation are presented in Section 3 of the corrective action GMP included in the CP application.
- Documentation of remedy progress metrics will be provided in the Annual Groundwater Monitoring and Corrective Action Report beginning after the second year of data collection: a minimum of eight data points is required to complete meaningful statistical analysis required for evaluation of the remedy progress metrics, which will be available after two years of quarterly sampling. Per USEPA guidance [11], a thorough review of corrective action progress and remedy effectiveness will be conducted every five years. A Five-Year Annual Groundwater Monitoring and Corrective Action Report will evaluate the comprehensive data set and, if triggered by the results of the remedy progress evaluation metrics, evaluate whether adaptive management actions are needed. The five-year time frame allows adaptive management decisions to be based on a robust data sufficient to complete meaningful statistical analysis while remaining responsive to changing site conditions [11].
- Corrective Action Confirmation Monitoring and Completion
  - Per 35 I.A.C. § 845.680(c), corrective action is considered complete when compliance with the GWPS has been demonstrated at all points within the plume of contamination that lies beyond the waste boundary for a period of three consecutive years. At that time, an attainment evaluation will be implemented in accordance 35 I.A.C. § 845.680(c).
    - It should be noted that post-closure care groundwater monitoring required for a 30-year period or until GWPS is achieved whichever is longer by 35 I.A.C. § 845.780(c) will continue to occur after corrective action groundwater monitoring is expected to be completed.

- After completion of the corrective action confirmation monitoring period, a Corrective Action Completion Report and Certification will be prepared and submitted to IEPA, in accordance with 35 I.A.C. § 845.680(e).

2. CORRECTIVE ACTION OVERVIEW

This CAP is based on the tiered assessment and analysis of alternative remedial technologies and remedies that were completed via the CMA and CAAA (**Appendix A**). The objective of these assessments was to determine the optimal alternative for the WAPS that, when coupled with the source control that has been previously implemented [1, 2], would remediate groundwater and provide compliance with the GWPS specified under 35 I.A.C. § 845.600.

2.1 Corrective Measures Assessment

The CMA [12] was performed for the WAPS and submitted to the IEPA on May 8, 2024, after the exceedances of the GWPSs were identified. The CMA considered a total of five corrective measures for the WAPS, including:

- Source Control with GWP
- Source Control with *In-Situ* Stabilization/Solidification (ISS)
- Source Control with Groundwater Extraction (groundwater pumping wells or collection trenches)
- Source Control with Cutoff Wall
- Source Control with *In-Situ* Chemical Treatment (permeable reactive barrier [PRB])

Based on the CMA, three corrective measures, including source control with GWP, source control with cutoff wall, and source control with ISS[2], were identified as potentially viable corrective measures for the WAPS. The source control with cutoff wall remedy considered by the CMA was expanded into source control with CCS, which extends the cutoff wall to the competent bedrock and integrates it into the previously implemented final cover.

Of these corrective measures, source control with GWP and source control with CCS were selected for further evaluation, design advancement, and comparative assessment within the CAAA for the WAPS.

2.1.1 Corrective Action Alternatives Analysis Supporting Information Report

The CAAA for the WAPS was prepared by Gradient based on a CAAA-SIR prepared by Ramboll. The CAAA-SIR, which is included as Attachment B of the CAAA provided in **Appendix A**, included additional evaluation, design advancement, and comparative assessment of the source control with GWP and source control with CCS corrective measures identified as potentially viable for the WAPS. The evaluation included the completion of feasibility-level design activities for each alternative and incorporated the following tasks:

- Performing predictive groundwater modeling to evaluate the scope (*i.e.,* location and extents) of each alternative and the corresponding estimated time to achieve GWPS;
- Developing feasibility-level design drawings showing the extent in plan and elevation view of each engineered remedy;

---

[2] The source control with ISS remedy was evaluated further at a preliminary level and determined to be infeasible, as discussed in the CAAA provided in **Appendix A**.

- Estimating the time required to design, construct, and implement each remedy, in addition to ongoing operational and maintenance requirements;
- Identifying future tasks required to implement each alternative, including permitting, investigation, and design efforts; and
- Estimating relevant material quantities, labor hours, delivery miles, equipment miles, and daily commuting miles associated with constructing each remedy.

2.1.2 Corrective Action Alternatives Analysis

The CAAA (**Appendix A**) included a detailed analysis of each of the corrective action alternatives presented in the CAAA-SIR, including an evaluation of:

- Long and short-term effectiveness and protectiveness;
- Ease or difficulty of implementation;
- Degree to which community concerns are addressed; and
- Relative amount of contamination removed from the environment.

The CAAA identified source control with CCS as the most appropriate corrective action for the WAPS and this remedy was selected for further design development as part of this CAP.

It should be noted that the permit-level engineering assessments, groundwater modeling, and other information contained within this CAP were developed to a higher level of design and detail than for the source control with CCS within the CAAA; therefore, information on items such as permitting, remedy scope, estimated time to reach GWPS, implementation schedule, etc. may differ between this CAP and the included CAAA-SIR and CAAA. Information for the source control with CCS contained within the CAP should be considered to supersede information contained within the CAAA and CAAA-SIR.

3. CORRECTIVE ACTION PLAN

The 35 I.A.C. § 845 requirements for the CAP and corresponding demonstrations that the proposed corrective measures meet these requirements are discussed individually in this section. Many of the CAP requirements are discussed within the CMA and CAAA documents that have been prepared to support the CAP. Therefore, the demonstrations will also refer to those documents.

3.1 General Requirements

35 I.A.C. § 845.670(c): The corrective action plan must meet the following requirements:

(1) Be based on the results of the corrective measures assessment conducted under 35 I.A.C. § 845.660;

(2) Identify a selected remedy that at a minimum, meets the standards listed in subsection (d);

(3) Contain the corrective action alternatives analysis specified in subsection (e); and

(4) Contain proposed schedules for implementation, including an analysis of the factors in subsection (f).

This CAP is based on the results of the CMA and CAAA, which are included within **Appendix A**. The proposed schedule for implementing source control with CCS is provided in **Table 2**.

3.2 Remedy Selection

35 I.A.C. § 845.670(d): The selected remedy in the corrective action plan must:

(1) Be protective of human health and the environment;

Current conditions at the WAPS pose no risk to human health or environment (Appendix A). Concentrations of CCR-derived constituents are anticipated to continue to decline with the final cover that is in place, even without implementation of the DCW component of CCS. Once the DCW is installed, CCR within the WAPS would be contained within a continuous system of low-permeability materials and isolated from the surrounding environment on all sides.

(2) Attain the groundwater protection standards specified in 35 I.A.C. § 845.600;

Groundwater modeling used to support the design of the DCW (Appendix B of the CAAA-SIR) indicates the selected remedy of source control with CCS will attain the GWPS in approximately 33 years after complete implementation.

(3) Control the sources of releases to reduce or eliminate, to the maximum extent feasible, further releases of constituents listed in 35 I.A.C. § 845.600 into the environment;

The CCS will result in CCR within the WAPS being contained by a continuous system of low-permeability material on all sides of the WAPS. This includes the final cover system as surface containment, the DCW as lateral containment, and low-permeability competent bedrock as base containment beneath the CCR. This CCS would reduce, to the maximum extent feasible, further releases of constituents listed in 35 I.A.C. § 845.600 from the WAPS into the environment.

(4) *Remove from the environment as much of the contaminated material that was released from the CCR surface impoundment as is feasible, taking into account factors such as avoiding inappropriate disturbance of sensitive ecosystems; and*

No known releases of CCR due to structural integrity issue have occurred at the WAPS.

(5) Comply with standards for management of wastes as specified in 35 I.A.C. § 845.680(d).

Any CCR and associated waste encountered during construction of the selected corrective action (source control with CCS) will be managed in accordance with all 35 I.A.C. § 845.680(d) requirements.

3.3 Schedule for Implementation

The CCS is an effective engineered control as it provides hydraulic isolation at the limits of the WAPS and has been demonstrated as a reliable remedy by the USEPA [13]. The CCS will provide permanent hydraulic isolation of CCR within the WAPS from the surrounding environment. The CCS will remain in-place and functional even after GWPS have been met.

The CCS remedy was evaluated to determine if the DCW component of CCS can be successfully implemented to achieve GWPS compliance in a timely manner. Timeframes to attain GWPS in the corrective action monitoring network wells are estimated in **Table A**:

Table A. Estimated Timeframes to Attain GWPS in Groundwater Monitoring Wells

	2 years‡	5 years‡	10 years‡	20 years‡	33 years‡
Percentage of Wells predicted to attain GWPS†	67%	67%	67%	89%	100%

†: 9 wells were used to estimate time to reach GWPS in the 2025 Groundwater Modeling Technical Memorandum.

‡: Years counted starting from 2028, presumed completion of implementation of DCW portion of CCS.

35 I.A.C. § 845.670(f): The owner or operator must specify, as part of the corrective action plan, a schedule for implementing, of and completing, remedial activities. The schedule must require the completion of remedial activities within a reasonable time, taking into consideration the factors in this subsection (f). The owner or operator of the CCR surface impoundment must consider the following factors in determining the schedule of remedial activities:

The schedule for implementation and completion of the DCW component of the CCS remedy at the WAPS is included in **Table 2**. Implementation of the remedy will occur within 90 days of approval of the CAP, in accordance with 35 I.A.C. § 845.680(a)(1).

The schedule will result in completion of remedial activities within a reasonable timeframe considering the factors specified by 35 I.A.C. §§ 845.670(f)(1) through (5), as summarized below.

35 I.A.C. § 845.670(f)(1): Extent and nature of contamination, as determined by the characterization required under 35 I.A.C. § 845.650(d);

The Nature and Extent Report [14], which was submitted to the IEPA on April 18, 2024 and is included as an attachment to the CAAA provided as **Appendix A**, details exceedances of GWPS. Groundwater modeling and geochemical analysis was performed by Ramboll as part of the CAAA-SIR to design the remedy and the modeling considered the nature and extent of contamination.

35 I.A.C. § 845.670(f)(2): Reasonable probabilities of remedial technologies achieving compliance with the GWPS established by 35 I.A.C. § 845.600 and other objectives of the remedy;

Several remedies were evaluated in the CAAA (**Appendix A**) and results of groundwater modeling indicated that the selected remedy (source control with CCS) is expected to achieve compliance with 35 I.A.C. § 845.600. Groundwater modeling was performed to evaluate future groundwater quality in the vicinity of the WAPS. The results of the modeling indicate that groundwater will attain the GWPS for all constituents identified as having potential exceedances in the primary migration pathway (the uppermost aquifer [UA] groundwater unit) within approximately 33 years. As documented in the Groundwater Polishing Evaluation Report attached to the CAAA (**Appendix A**), attenuation of COCs, boron, lithium, sulfate, and TDS through sorption and chemical mechanisms will complement results of the groundwater transport modeling, in that time to reach GWPS may be shorter than the simulated timeframes. Remobilization of arsenic, which exceeds GWPS at two wells (51 and 21R), may increase the time to reach GWPS from the simulated results.

35 I.A.C. § 845.670(f)(3): Availability of treatment or disposal capacity for CCR managed during implementation of the remedy;

Excavated soils (*e.g.,* spoils) are expected to primarily be non-CCR material and will be placed into off-road dump trucks and disposed of in either the East Ash Pond (EAP) as contouring fill to support EAP closure in accordance with the submitted closure plan [15]. The EAP is expected to have sufficient disposal capacity for CCR wastes generated during remedy construction. After construction, the DCW component of CCS is not anticipated to result in the management of any appreciable volume of CCR.

35 I.A.C. § 845.670(f)(4): Potential risks to human health and the environment from exposure to contamination before completion of the remedy;

A Human Health and Ecological Risk Assessment was completed and included as an attachment to the CAAA (**Appendix A**). The overall conclusion is that groundwater from the WAPS impoundments and potential constituents of interest (COI) concentrations in groundwater contributions to surface water and sediment in the Illinois River pose no unacceptable risks to human health or the environment. However, the CAAA indicated that short-term negative impacts on surface water and sediment quality immediately adjacent to the site due to erosion and runoff from construction activities could occur, but will be mitigated using stormwater Best Management Practices (BMP) in accordance with applicable land disturbance permit requirements.

This conclusion is based on modeled and detected maximum concentrations of all COIs in surface water and sediment in the Illinois River, which were below conservative risk-based screening benchmarks. This conclusion was reached using methodology consistent with applicable United States Environmental Protection Agency (USEPA) risk assessment principles. The assessment relied on conservative assumptions meant to overestimate possible exposures and risks and provide an additional level of certainty in the conclusions.

35 I.A.C. § 845.670(f)(5): Resource value of the aquifer, including:

The resource value of the aquifer is discussed in the HCR, which is included as Appendix B to the closure CP application [10]. The HCR addresses paragraphs (A) through (F) from 35 I.A.C. § 845.670(f)(5), as summarized below.

35 I.A.C. § 845.670(f)(5)(A): Current and future uses, including potential residential, agricultural, commercial industrial and ecological uses;

Current uses and users of the groundwater are discussed in the HCR Section 3.5 and Appendix F. A water well inventory was completed in 2009 utilizing federal and state databases to assess nearby pumping wells, drinking water receptors, and other uses of water in the vicinity of the Hennepin Power Station property boundary inclusive of WAPS. Based on records obtained from IEPA, Illinois State Geological Survey (ISGS), and Illinois State Water Survey (ISWS), there are 2 wells located within 2,500-meters of WAPS. The two wells were reportedly constructed in 1844 and 1922 according to State of Illinois records have been verified and were most likely abandoned decades ago [10]. There are no public water supply (PWS), community water supply (CWS) or non-CWS wells or wellhead protection areas (WHPAs) within 2,500 feet of WAPS. There are four wells owned by DMG within the HPP property boundary all of which are non-potable and non-contact industrial wells.

35 I.A.C. § 845.670(f)(5)(B): Proximity and withdrawal rate of users;

See preceding discussion on 35 I.A.C. § 845.670(f)(5)(B) for a discussion on the proximity and withdrawal rates of users.

35 I.A.C. § 845.670(f)(5)(C): Groundwater quantity and quality;

Per 35 I.A.C. § 620.210, groundwater within the UA at the WAPS meets the definition of Class I – Potable Resource Groundwater. The Human Health and Ecological Risk Assessment (Appendix A in CAAA) concluded that groundwater from the WAPS impoundment and potential groundwater contributions to surface water pose no unacceptable risks to human health or the environment.

35 I.A.C. § 845.670(f)(5)(D): The potential impact to the subsurface ecosystem, wildlife, other natural resources, crops, vegetation, and physical structures caused by exposure to CCR constituents;

Potential surface receptors are discussed in the HCR for HPP East Ash Pond Sections 3.5 [16]. A survey to identify surface water features, nature preserves, and historic sites was conducted for a 1,000-meter radius around the WAPS. Section 3.5.1 of the Human Health and Ecological Risk Assessment included as Appendix A of the CAAA Report stated there are no current unacceptable risks to ecological receptors at the WAPS.

35 I.A.C. § 845.670(f)(5)(E): The hydrogeologic characteristic of the facility and surrounding land; and

The hydrogeological assessment identified that the stratigraphy within and immediately surrounding the WAPS consists of fill, unlithified river alluvium, and Pleistocene-age glacial outwash deposits overlying Pennsylvanian-age shale bedrock. Where undisturbed or partially excavated, the native surficial soil at the site is poorly drained, moderately permeable silty clay loam formed as alluvium in floodplains.

There are two hydrostratigraphic units:

- **Uppermost Aquifer (UA)**: Includes the unlithified natural geologic materials of the Cahokia Alluvium and Henry Formation extending from the upper saturated zone to the bedrock. The UA contains variable amounts of cobbles and boulders within a sand and gravel matrix. Both the prevalence and size of the cobbles and boulders increase with depth.
- **Bedrock Confining Unit**: Comprised of shales with thin limestone, sandstone, and coal beds. This bedrock confining unit is encountered at elevations ranging from 374.3 to 410.2 feet.[3]

35 I.A.C. § 845.670(f)(5)(F): The availability of alternative water supplies.

As discussed in subsection A, there are no extraction wells within 2,500 meters of the site. Therefore, an alternate water supply is not necessary.

3.3.1 Other Relevant Factors

35 I.A.C. § 845.670(f)(6): Other relevant factors.

No additional factors were identified for consideration.

3.4 Necessity of Interim Measures

Source control using the consolidate-and-cap approach has been completed [1, 2] and shown to be effective at remediating groundwater. Completion of DCW portion of CCS is projected to be complete within five to seven years after approval of the CAP. Source control followed by GWP alone was predicted by the groundwater supporting the closure plan would result in the decrease in CCR constituent concentrations in groundwater, and a contraction of the groundwater contaminant plume [6]. The prediction of the groundwater model is further supported by decrease in boron concentrations at a number of wells within the monitoring network upon closure. Therefore, no interim measure is required. Further, all subsections of this requirement are discussed as follows.

35 I.A.C. § 845.680(a)(3)(A): Time required to develop and implement a final remedy.

The final cover portion of the CCS remedy (source control) was implemented at the site in 2020 utilizing a consolidation and cap final closure approach [1, 2]. As presented in the Groundwater Modeling Technical Memorandum, source control alone is predicted to achieve the GWPS in approximately 30 years. The DCW portion of CCS remedy is supplemental to the current source control. Implementation of the DCW portion of the CCS is anticipated to take up to seven years following approval of the corrective action plan. Therefore, no interim measures are required as the primary corrective action has already been implemented.

35 I.A.C. § 845.680(a)(3)(B): Actual or potential exposure of nearby populations or environmental receptors to any of the constituents listed in 35 I.A.C. § 845.600.

---

[3] All elevation in this report are in the North American Vertical Datum of 1988 (NAVD88), unless otherwise noted.

There are no current unacceptable risks to human or ecological receptors at the site (**Appendix A**). It was concluded UA was not a source of drinking water [10].

35 I.A.C. § 845.680(a)(3)(C): Actual or potential contamination of sensitive ecosystems or current or potential drinking water supplies.

The nature and extent of exceedances have been evaluated in the Nature and Extent Report [15]. Although there are exceedances of GWPS, there are no impacts to current or potential drinking water supplies. As stated above, there are no current unacceptable risks to human or ecological receptors at the site.

35 I.A.C. § 845.680(a)(3)(D): Further degradation of the groundwater that may occur if remedial action is not initiated expeditiously.

The final cover portion of the CCS remedy (source control) was implemented at the site in 2020 utilizing a consolidation and cap final closure approach [1, 2], and corresponding decreases in boron concentrations have already been observed. No additional interim measures are needed to prevent further degradation of the groundwater more expeditiously than implementation of the selected remedy.

35 I.A.C. § 845.680(a)(3)(E): Weather conditions that may cause any of the constituents listed in 35 I.A.C. § 845.600 to migrate or be released.

As stated above, the final cover portion of the CCS was implemented in 2020 and provides surface containment that isolates CCR within the WAPS from typical site weather conditions.

35 I.A.C. § 845.680(a)(3)(F): Potential for exposure to any of the constituents listed in 35 I.A.C. § 845.600 as a result of accident or failure of a container or handling system.

As the WAPS is closed-in-place within a consolidated footprint, therefore no container or handling systems are currently in use, nor will they be in use in the future.

35 I.A.C. § 845.680(a)(3)(G): *Other situations that may pose threats to human health and the environment.*

No situations have been identified where WAPS CCR leachate poses threats to human health and environment.

4. REFERENCES

[1] Dynegy Midwest Generation, LLC, "Hennepin Power Station; Old West Ash Pond, Ash Pond No. 2, Notification of Completion of Closure," Luminant, December 17, 2020.

[2] Dynegy Midwest Generation, LLC, "Hennepin Power Station; Old West Polishing Pond, Notification of Completion of Closure," Luminant, December 17, 2020.

[3] "35 Ill. Admn. Code Part 845, Standards for the Disposal of Coal Combustion Residuals in Surface Impoundments," Illinois Environmental Protection Agency, Springfield, IL, 2021.

[4] Code of Federal Regulations, "Title 40, Chapter I, Subchapter I, Part 257, Subpart D, Standards for the Disposal of Coal Combustion Residuals in Landfills and Surface Impoundments," April 17, 2015.

[5] Burns & McDonnell, "Initial Operating Permit, Hennepin West Ash Pond System," October 25, 2021.

[6] Geosyntec Consultants, "Closure and Post-Closure Care Plan Old West Ash Pond Old West Polishing Pond at Hennepin Power Station," 2017.

[7] Illinois Environmental Protection Agency, "Correspondence with Luminant (formerly Dynegy Midwest Generation, LLC) regarding the Closure and Post-Closure Care Plan for Hennepin Old West Ash Pond System," July 19, 2018.

[8] Natural Resource Technology, "Groundwater Model Report - Hennepin West Ash Pond System," 2017.

[9] Geosyntec Consultants, Inc, "Groundwater Polishing Evaluation Report, Hennepin Power Plant, West Ash Pond System," 2025.

[10] Natural Resource Technology, Inc., "Hydrogeologic Site Characterization Report, Hennepin West Ash Pond System, Hennepin, Illinois," December 20, 2017.

[11] United States Environmental Protection Agency, "Groundwater Remedy Completion Strategy: Moving Forward with the End in Mind," Office of Solid Waste and Emergency Response, 2014.

[12] Ramboll, "Corrective Measures Assessment, Hennepin Power Plant, West Ash Pond," 2024.

[13] United States Environmental Protection Agency (USEPA), "Community Guide to Vertical Engineered Barriers. https://semspub.epa.gov/work/HQ/401627.pdf," 2021.

[14] Ramboll Americas Engineering Solutions, "Nature and Extent Report, Hennepin Power Plant, West Ash Pond System," 2024, May 8.

[15] Geosyntec Consultant, "CCR Surface Impoundment Final Closure Plan, Hennepin Power Plant, East Ash Pond," 2022.

[16] Ramboll Americas Engineering Solutions, Inc., "Hydrogeologic Site Characterization Report, East Ash Pond, Hennepin Power Plant, Hennepin, Illinois," October 25, 2021.

TABLES

Table 1. Summary of 2024 Bedrock Hydraulic Conductivity Testing

Bedrock Elevation Summary						Bedrock Packer Test Investigation		
Boring		Weathered Bedrock		Competent Bedrock		Packer Test Elevation Intervals		Hydraulic Conductivity
Number	Surface El. (ft)	Depth (ft-bgs)	Top El. (ft)	Depth (ft-bgs)	Top El. (ft)	Depth (ft-bgs)	El. (ft)	K_H (cm/s)
B-100	449.7	70.0	379.7	85.4	364.3	86.0 – 90.8	363.7 – 358.9	2.4×10^{-6}
						90.0 – 94.8	359.7 – 354.9	2.4×10^{-6}
						95.0 – 99.8	354.7 – 349.9	2.3×10^{-6}
B-101	459.3	85.0	374.3	95.0	364.3	95.0 – 98.3	364.3 – 361.0	2.3×10^{-6}
						98.0 – 101.3	361.3 – 358.0	2.2×10^{-6}
						100.0 – 103.3	359.3 – 356.0	2.2×10^{-6}
B-102	455.0	70.0	385.0	90.0	365.0	92.0 – 96.8	363.0 - 358.2	1.1×10^{-5}
						96.0 – 100.8	359.0 - 354.2	1.1×10^{-5}
						100.0 – 104.8	355.0 - 350.2	3.2×10^{-6}
Summary		Mean	379.7	Mean	364.5	Summary	Geomean	3.4×10^{-6}
		Min.	374.3	Min.	364.3		Min.	2.2×10^{-6}
		Max.	385.0	Max.	365.0		Max.	1.1×10^{-5}

Notes
El.: Elevation
ft: feet
Bgs: below ground surface
Surface El.: Reported in North American Vertical Datum of 1988 (NAVD88)
Geomean: Geometric mean
Min.: Minimum
Max.: Maximum
Detailed information on the hydraulic conductivity testing will be provided in an attachment to the Nature and Extent Report Addendum.

Table 2. Proposed Milestone Schedule for Implementing Corrective Action Remedy (Source Control with Continuous Containment System)

Implementation Phase	Implementation Task	Timeframe (Preliminary Estimates)
1: Pre-Construction Activities	Agency Coordination, Approvals, and Permitting	18 to 24 months
	Final Design and Bid Process	24 to 36 months
	Timeframe to Complete Corrective Pre-Construction Activities	42 to 60 months after CAP Approval
2: Corrective Action Construction	Corrective Action Construction	18 to 24 months
	Timeframe to Complete Corrective Action Construction	18 to 24 months
3: Corrective Action Monitoring and Closeout	Corrective Action Monitoring (Time to Meet GWPS)	396 months (33 years)
	Corrective Action Groundwater Confirmation Monitoring	36 months
	Corrective Action Completion	6 months
	Timeframe to Complete Corrective Action O&M and Closeout	438 months
Total Timeline to Complete Corrective Action (after approval of Corrective Action Plan)		498 to 522 months (42 to 44 years)

[1] All timeframes are preliminary and may change as the project develops. Timeframes may also be affected by regulatory review and/or permit approval processes, for both 35 I.A.C. § 845 and non-35 I.A.C. § 845 permits.

APPENDIX A

CORRECTIVE ACTION ALTERNATIVES ANALYSIS (845.670(E)), INCLUDING CORRECTIVE MEASURES ASSESSMENT (845.660)

Corrective Action Alternatives Analysis for the West Ash Pond System at the Hennepin Power Station, Hennepin, Illinois

March 7, 2025

GRADIENT

www.gradientcorp.com
One Beacon Street, 17th Floor
Boston, MA 02108
617-395-5000

Table of Contents

Page

List of Tables

List of Figures

Abbreviations

BCU	Bedrock Confining Unit
BMP	Best Management Practice
CAAA	Corrective Action Alternatives Analysis
CCR	Coal Combustion Residual
CCS	Continuous Containment System
CIP	Closure-in-Place
cm/s	Centimeters per Second
CMA	Corrective Measures Assessment
CO	Carbon Monoxide
CO_2	Carbon Dioxide
DMG	Dynegy Midwest Generation, LLC
HPP	Hennepin Power Plant
GHG	Greenhouse Gas
GMP	Groundwater Monitoring Plan
GWP	Groundwater Polishing
GWPS	Groundwater Protection Standard
IAC	Illinois Administrative Code
ID	Identification
IDNR	Illinois Department of Natural Resources
IEPA	Illinois Environmental Protection Agency
ISS	*In-Situ* Stabilization
LLDPE	Linear Low-Density Polyethylene
MW	Megawatt
N_2O	Nitrous Oxide
NID	National Inventory of Dams
NO_x	Nitrogen Oxide
NPDES	National Pollutant Discharge Elimination System
O&M	Operations and Maintenance
OWAP	Old West Ash Pond
OWPP	Old West Polishing Pond
PCB	Polychlorinated Biphenyl
PM	Particulate Matter
QA	Quality Assurance
QC	Quality Control
Source Control-CCS	Source Control with a Continuous Containment System
Source Control-GWP	Source-Control with Groundwater Polishing
Source Control-ISS	Source-Control with *In-Situ* Stabilization
TDS	Total Dissolved Solids
UA	Uppermost Aquifer
US DOT	United States Department of Transportation
US EPA	United States Environmental Protection Agency
VOC	Volatile Organic Compound
WAPS	Western Ash Pond System

Summary of Findings

Title 35, Part 845 of the Illinois Administrative Code (IAC) (IEPA, 2021) requires that a Corrective Action Alternatives Analysis (CAAA) be performed as part of the remedy selection, prior to undertaking any corrective actions at certain coal combustion residual (CCR)-containing impoundments, where exceedances of groundwater protection standards (GWPSs) have been identified. This report presents a CAAA for the West Ash Pond System (WAPS) at the Hennepin Power Plant (HPP) pursuant to the requirements under IAC Section 845.670. The goal of performing a CAAA is to holistically evaluate the potentially viable corrective actions identified in the Corrective Measures Assessment (CMA) (Appendix C; Ramboll, 2024a) in order to remediate groundwater and achieve compliance with the groundwater protection standards (GWPSs) specified under IAC Section 845.600 (IEPA, 2021). These analyses assess potentially viable corrective action alternatives based on a wide range of factors, including the efficiency, reliability, and ease of implementation of a corrective action; its potential positive and negative short- and long-term impacts on human health and the environment; and its ability to address concerns raised by the community (IEPA, 2021).

It is important to note that many CCR sites are complex groundwater environments where remedial actions will inherently take many years to complete. While no formal definition of a complex groundwater environment exists, most would agree that there are a number of common characteristics at complex groundwater sites, including the following (National Research Council, 2013):

- Highly heterogeneous subsurface environments;
- Large source zones;
- Multiple, recalcitrant constituents; and
- Long timeframes over which releases occurred.

Each of these characteristics are common at CCR sites. Surface impoundments are often tens to hundreds of acres in size and many have operated for decades, leading to large source zones and prolonged releases. Furthermore, CCR impoundments are often located in alluvial geologic settings where sands are interbedded with silts and clays. This results in a heterogeneous environment where constituent mass may persist for many years in low-permeability deposits. Finally, the constituents that are most common at CCR sites include metals and inorganics that do not naturally biodegrade. The combination of these factors results in a complex groundwater environment where remediation, even under the best of circumstances, may take many years to achieve GWPSs. It is for these reasons that the United States Environmental Protection Agency (US EPA) refused to specify what is a reasonable *vs.* an unreasonable timeframe for groundwater corrective actions at CCR sites, stating that it "was truly unable to establish an outer limit on the necessary timeframes – including even a presumptive outer bound" (US EPA, 2015a).

In this CAAA, all corrective actions that have been evaluated consist of source control and residual plume management. Source control is generally considered to be one of the more effective remedial action approaches. Source control involves removing the hydraulic head from an impoundment (*i.e.*, unwatering and dewatering) and preventing further downward migration of constituents. US EPA has found that "releases from surface impoundments [to groundwater] drop dramatically after closure" (US EPA, 2014, pp. 5-18 to 5-19). US EPA has also stated that source control is the most effective means of ensuring the timely attainment of remediation objectives (US EPA, 2015b). As a result, the implementation of source control often has a substantial and immediate effect on groundwater quality improvements.

The specific source control method that is the central component of all the corrective action alternatives evaluated in this CAAA is closure-in-place (CIP) using a consolidate-and-cap approach for the WAPS, which was approved of by IEPA in 2018 and completed in 2020 (Buscher, 2018; Tickner, 2020a,b). The WAPS consists of two sub-units, specifically, the Old West Ash Pond (OWAP) and the Old West Polishing Pond (OWPP). The source control included dewatering of coal combustion residuals (CCRs), excavation and consolidation of material from the OWPP into the OWAP, followed by the installation of an impermeable cap on the OWAP. Closure activities specifically included removal of impounded water and excavation of CCR and one foot of soil below the CCR from the OWPP, construction of a sheet pile wall and compacted clay buttress to separate the OWAP from the OWPP, and installation of a final cover system over the OWAP consisting of a geosynthetic layer, a protective soil layer to limit infiltration of precipitation into the impoundment, and establishment of a vegetative cover. These activities were designed to control, minimize or eliminate, post closure infiltration of liquids into the impounded CCR. As demonstrated by groundwater modeling in support of the Closure and Post-Closure Care Plan and this CAAA (Geosyntec Consultants, Inc., 2017; Appendix B; Ramboll, 2025a), the hydraulic pressure beneath the final cover system would drop to "near-zero levels" within 7 years after closure and cause constituent concentrations in groundwater to decrease and the groundwater plume to contract (Geosyntec Consultants, Inc., 2017). Due to the reduction in the hydraulic flux out of the WAPS, the mass flux out of the WAPS would also be controlled and minimized.

Two potential corrective actions are evaluated in this CAAA: Source Control with Groundwater Polishing (Source Control-GWP) and Source Control with a Continuous Containment System (Source Control-CCS). Both alternatives consist of source control and residual plume management; residual plume management for the two remedial approaches are groundwater polishing and a continuous containment system. Both alternatives were identified as viable approaches in the CMA (Appendix C; Ramboll, 2024a). It should be noted that Source Control-GWP, Source Control with a Cutoff Wall, and Source Control-ISS (Source Control with *In-Situ* Stabilization [ISS]) were identified in the CMA as viable remedial approaches (Appendix C; Ramboll, 2024a). However, during subsequent evaluations, the remedial approaches were modified. Remedy modifications include the following:

- Source Control-ISS was determined infeasible and excluded for further evaluation due to significant potential risks, including the need to temporarily remove half of the previously installed WAPS final cover. Removal of the final cover system would result in significant stormwater infiltration and potentially lead to reducing the effectiveness of the completed source control. In addition, ISS would involve managing tens of thousands of cubic yards of CCR and CCR-impacted cuttings on the WAPS surface, increasing the risk of releasing CCR-contaminated stormwater and sediments during construction, which could negatively impact nearby sensitive areas.
- Source Control-Cutoff Wall was expanded into the Source Control-CCS alternative, which is evaluated in this report. The continuous containment system (CCS) integrates the cutoff wall with the existing final cover to provide full lateral and surface isolation of CCR from the surrounding environment. The wall would be keyed into competent shale bedrock to provide additional base subsurface containment below the WAPS.

Under the Source Control-GWP alternative, active groundwater monitoring would supplement source control to verify and document the attenuation by natural physical and geochemical mechanisms of constituent concentrations in groundwater. Site-specific evaluations demonstrated that groundwater polishing is appropriate at the WAPS because Site conditions are favorable for natural attenuation of inorganic contaminants *via* adsorption and precipitation. However, it should be noted that some arsenic[1] re-mobilization may occur as groundwater returns to background conditions (Appendix E; Geosyntec Consultants, Inc., 2025). Under the Source Control-CCS alternative, the final cover system would be temporarily removed in the areas where the cutoff wall would be installed. An approximately 90 ft deep cutoff wall consisting of low-permeability material (either a mixture of soil and bentonite or cement and bentonite) would be constructed, extending from the top of the WAPS perimeter dikes completely through the Uppermost Aquifer (UA) and penetrate into the underlying competent shale bedrock. The final cover system would be extended across the top of the cutoff wall after installation. The final cover, the cutoff wall, and the competent shale bedrock would enclose the OWAP, which is the portion of the WAPS that was closed by CIP, resulting in CCR being contained within a continuous containment system, and would isolate CCR from the surrounding environment on all sides (Appendix B; Ramboll, 2025a).

Table S.1 evaluates the two potentially viable corrective actions evaluated in this CAAA (Source Control-GWP and Source Control-CCS) with regard to each of the factors specified under IAC Section 845.670(d) and IAC Section 845.670(e) (IEPA, 2021). Based on this evaluation and the details provided in Section 2 of this report, the most appropriate corrective action for this Site is Source Control-CCS. Although the expected impacts on workers, nearby communities, and the environment under the Source Control-GWP alternative are lower than the Source Control-CCS alternative, the Source Control-CCS alternative would provide full containment of the CCR within WAPS and be more effective at controlling sources of releases than Source Control-GWP. Controlling the source of releases using CCS is particularly important at this Site because of the high groundwater transmissivity associated with the sands and gravels in the UA. Thus, Source Control-CCS is the most appropriate corrective action alternative for the WAPS.

---

[1] It should be noted that not all arsenic in groundwater is associated with the WAPS. Some of the arsenic is likely naturally occurring and/or associated with other sources.

Table S.1 Comparison of Proposed Corrective Action Alternatives with Respect to Factors Specified in IAC Section 845.670(d) and IAC Section 845.670(e)

Evaluation Factor (Report Section; Part 845 Section)	Source Control-GWP	Source Control-CCS
Magnitude of Reduction of Existing Risks/Be Protective of Human Health and the Environment (Section 2.2.1; IAC Section 845.670(e)(1)(A)/ IAC Section 845.670(d)(1))	Because current conditions do not present a risk to human health or the environment at the WAPS, there will be no unacceptable risk to human health or the environment for future conditions since the unit was closed and source control was implemented. Concentrations of CCR-related constituents will decline over time and, consequently, potential exposures to CCR-related constituents in the environment will also decline. The magnitude of the reduction of existing risks is the same for all of the potential corrective action alternatives, and both corrective action alternatives are equally protective of human health and the environment.	Because current conditions do not present a risk to human health or the environment at the WAPS, there will be no unacceptable risk to human health or the environment for future conditions since the unit was closed and source control was implemented. Concentrations of CCR-related constituents will decline over time and, consequently, potential exposures to CCR-related constituents in the environment will also decline. The magnitude of the reduction of existing risks is the same for all of the potential corrective action alternatives, and both corrective action alternatives are equally protective of human health and the environment.
Effectiveness of the Remedy in Controlling the Source (Section 2.2.2; IAC Section 845.670(e)(2))		
Extent to Which Containment Practices Will Reduce Further Releases/Control the Sources of Releases to Reduce or Eliminate, to the Maximum Extent Feasible (IAC Section 845.670(e)(2)(A)/ IAC Section 845.670(d)(3))	Both alternatives include source control (which is the primary remedial measure) and residual plume management. Source control (*i.e.*, CIP using a consolidate-and-cap approach) was implemented in 2020. Modeling results in support of the Closure Plan indicated that source control would result in a significant reduction in groundwater concentrations and, overtime, reduce the extent of groundwater impacts to within the footprint of the impoundment (Geosyntec Consultants, Inc., 2017). Under residual plume management for this alternative, physical and geochemical attenuation mechanisms would mitigate impacts to downgradient groundwater quality and control the residual plume. However, it should be noted that some arsenic re-mobilization may occur as groundwater returns to background conditions, which may cause an impact to the time	Both alternatives include source control (which is the primary remedial measure) and residual plume management. Source control (*i.e.*, CIP using a consolidate-and-cap approach) was implemented in 2020. Modeling results in support of the Closure Plan indicated that source control would result in a significant reduction in groundwater concentrations and, overtime, reduce the extent of groundwater impacts to within the footprint of the impoundment (Geosyntec Consultants, Inc., 2017). Under residual plume management for this alternative, a cutoff wall would be constructed and incorporated into the existing final WAPS cover system. This would create a continuous low-permeability barrier that fully contains the CCR within the WAPS. This system ensures isolation from the surrounding environment through lateral containment by the deep cutoff wall,

Evaluation Factor (Report Section; Part 845 Section)	Source Control-GWP	Source Control-CCS
	required to achieve GWPS (Appendix E; Geosyntec Consultants, Inc., 2025). If necessary, remedy optimizations would be implemented under the adaptive site management program.	surface containment by the existing geomembrane cover, and a natural barrier provided by the competent shale bedrock below. Thus, this subsurface barrier will isolate the CCR from the surrounding environment and will control the sources of releases to the environment. If necessary, remedy optimizations would be implemented under the adaptive site management program. Source Control-CCS would be more effective at controlling releases than Source Control-GWP. CCS would isolate CCR from the surrounding environment on all sides and in particular would prevent releases of CCR-related constituents associated with the high groundwater transmissivity of the sand and gravel deposits in the UA.
Extent to Which Treatment Technologies May Be Used (IAC Section 845.670(e)(2)(B))	Source Control-GWP would rely on physical and geochemical attenuation processes. If necessary, remedy optimizations would be implemented under the adaptive site management program.	The Source Control-CCS alternative would utilize an engineered physical barrier to contain the CCR within WAPS. Contact stormwater may be generated during the construction phase, which would be pumped to the on-Site treatment pond before discharging *via* an NPDES permitted outfall. No additional treatment technologies would be required once the cutoff wall has been constructed. If necessary, remedy optimizations would be implemented under the adaptive site management program.
Likelihood of Future Releases of CCR (Section 2.2.3; IAC Section 845.670(e)(1)(B))	Both corrective action alternatives include source control using CIP with a consolidate-and-cap approach; the CIP source control was completed in in 2020 in compliance with 40 CFR Part 257, Subpart D. This included a geosynthetic layer, a protective soil layer to limit infiltration, and a vegetative cover. This cover system provides increased protection against berm and surface erosion, precipitation infiltration, and other adverse effects that could potentially trigger a release of CCR. Thus, there is minimal risk of	Both corrective action alternatives include source control using CIP with a consolidate-and-cap approach; the CIP source control was completed in in 2020 in compliance with 40 CFR Part 257, Subpart D. This included a geosynthetic layer, a protective soil layer to limit infiltration, and a vegetative cover. This cover system provides increased protection against berm and surface erosion, precipitation infiltration, and other adverse effects that could potentially trigger a release of CCR. Any CCR-contact stormwater

Evaluation Factor (Report Section; Part 845 Section)	Source Control-GWP	Source Control-CCS
	accidental CCR releases occurring post-closure under either of the alternatives.	generated during the construction phase would be managed through a contact stormwater management system. Thus, there would be minimal risk of accidental CCR releases occurring post-closure under either of the alternatives.
Type and Degree of Long-Term Management, Including Monitoring, Operation, and Maintenance (Section 2.2.4; IAC Section 845.670(e)(1)(C))	Minimal long-term O&M efforts would be required under Source Control-GWP because it would not require the installation, operation, or maintenance of any engineered systems or structures other than maintenance of the monitoring wells. Corrective action groundwater monitoring would continue until GWPSs have been achieved. Post-closure care groundwater monitoring would continue for a minimum of 30 years as required by IAC Section 845.780(c). Additionally, corrective action groundwater monitoring would continue for 3 years after GWPS have been achieved. Based on the adaptive site management approach, remedy optimizations might be implemented to ensure achievement of the GWPSs.	Residual plume management for the Source Control-CCS alternative would require construction of a deep cutoff wall that would occur in three phases. Once the cutoff wall has been installed, no O&M efforts would be required, because it is a passive and below-grade structure. However, post-construction quality assurance (QA) programs may be required to validate the quality of the constructed cutoff wall. Corrective action groundwater sampling would continue until GWPSs have been achieved. Post-closure care groundwater monitoring will continue for a minimum of 30 years as required by IAC Section. 845.780(c). Additionally, corrective action groundwater monitoring would continue for 3 years after GWPS have been achieved. Based on the adaptive site management approach, remedy optimizations may be implemented to ensure achievement of the GWPSs.
Short-Term Risks to the Community or the Environment During Implementation of Remedy (Section 2.2.5; IAC Section 845.670(e)(1)(D))		
Safety Impacts	Source control (*i.e.*, CIP using a consolidate-and-cap approach) was implemented in 2020. Thus, there is no further risk of accidents and injuries occurring during the implementation of the source control remedy. Overall, no worker accidents or injuries would be expected under the Source Control-GWP alternative because no installation, operation, and	Source control (*i.e.*, CIP using a consolidate-and-cap approach) was implemented in 2020. Thus, there is no further risk of accidents and injuries occurring during the implementation of the source control remedy. Overall, considering worker accidents occurring during residual plume management both on- and off-Site, 0.65 worker injuries and 0.013 worker

Evaluation Factor (Report Section; Part 845 Section)	**Source Control-GWP**	**Source Control-CCS**
	maintenance of engineered systems or structures would be required. Similarly, no off-Site impacts on nearby residents would be expected under the Source Control-GWP alternative.	fatalities would be expected under the Source Control-Cutoff Wall alternative. In total, an estimated 0.21 injuries and 2.5×10^{-3} fatalities would be expected to occur among community members due to off-Site activities under the Source Control-CCS alternative.
Cross-Media Impacts to Air	Source control (*i.e.*, CIP using a consolidate-and-cap approach) was implemented in 2020. No further air impacts associated with the implementation of the source control remedy are expected. Cross-media impacts to air associated with residual plume management can result from the emission of air pollutants and greenhouse gases (GHGs) from construction vehicles and equipment. These emissions are proportional to the use of construction vehicles and equipment that are required for residual plume management. Residual plume management for the Source Control-GWP alternative would be expected to have minimal air impacts, because it would not require the construction of any engineered systems or structures.	Source control (*i.e.*, CIP using a consolidate-and-cap approach) was implemented in 2020. No further air impacts associated with the implementation of the source control remedy are expected. Cross-media impacts to air associated with residual plume management can result from the emission of air pollutants and GHGs from construction vehicles and equipment. These emissions are proportional to the use of construction vehicles and equipment that are required for residual plume management. Residual plume management for the Source Control-CCS alternative would have greater air impacts than the Source Control-GWP alternative due to the increased construction activity required for this alternative.
Cross-Media Impacts to Surface Water and Sediments	Source control was implemented in 2020 for both corrective action alternatives, and constituent mass flux from groundwater into surface water will decline over time (Geosyntec Consultants, Inc., 2017). The source control approach minimizes the amount of water retained within the impoundment, which reduces the hydraulic flux through the CCR. Due to the reduction in the hydraulic flux out of the WAPS, the mass flux out of the WAPS will also be controlled or minimized. As demonstrated by the groundwater modeling in support of the Closure Plan, source control would result in a significant reduction in groundwater concentrations and, overtime, reduce the extent of groundwater impacts to within the	Source control was implemented in 2020 for both corrective action alternatives, and constituent mass flux from groundwater into surface water will decline over time (Geosyntec Consultants, Inc., 2017). The source control approach minimizes the amount of water retained within the impoundment, which reduces the hydraulic flux through the CCR. Due to the reduction in the hydraulic flux out of the WAPS, the mass flux out of the WAPS will also be controlled or minimized. As demonstrated by the groundwater modeling in support of the Closure Plan, source control would result in a significant reduction in groundwater concentrations and, overtime, reduce the extent of groundwater impacts to within the

Evaluation Factor (Report Section; Part 845 Section)	**Source Control-GWP**	**Source Control-CCS**
	footprint of the impoundment (Geosyntec Consultants, Inc., 2017). Under residual plume management for the Source Control-GWP alternative, minimal surface water and sediment impacts would be expected, because it would not require the construction of any engineered systems or structures.	footprint of the impoundment (Geosyntec Consultants, Inc., 2017). Under residual plume management for the Source Control-CCS alternative, surface water and sediment impacts would be higher than the Source Control-GWP alternative due to the construction of the cutoff wall. Any associated impacts would be addressed through best management practices (BMPs) in accordance with Site land disturbance permits.
Control of Exposure to Any Residual Contamination During Implementation of the Remedy	Source control (*i.e.*, CIP using a consolidate-and-cap approach) was implemented in 2020. Thus, there are no further risks of CCR exposure associated with source control implementation. Risks to workers arising from potential contact with residual contamination during construction activities associated with residual plume management would be minimal under the Source Control-GWP alternative, which would not involve exposure to soil or groundwater waste streams.	Source control (*i.e.*, CIP using a consolidate-and-cap approach) was implemented in 2020. Thus, there are no further risks of CCR exposure associated with source control implementation. Risks to workers arising from potential contact with residual contamination during construction activities associated with residual plume management would be higher for the Source Control-CCS alternative than for the Source Control-GWP alternative because the Source Control-CCS alternative would involve removal of a portion of the previously installed final cover system and excavation and subsequent disposal of Site spoils. Any potential CCR-exposures during the Source Control-CCS alternative would be managed through the use of rigorous safety protocols and personal protective equipment.
Other Identified Impacts	Source control (*i.e.*, CIP using a consolidate-and-cap approach) was implemented in 2020. Thus, there are no further impacts associated with the implementation of source control. The energy demands of construction equipment and vehicles associated with residual plume management would be lower under the Source Control-GWP alternative, because this alternative	Source control (*i.e.*, CIP using a consolidate-and-cap approach) was implemented in 2020. Thus, there are no further impacts associated with the implementation of source control. The energy demands of construction equipment and vehicles associated with residual plume management would be greater under the Source Control-CCS compared to the Source Control-GWP alternative, because the Source Control-

Evaluation Factor (Report Section; Part 845 Section)	Source Control-GWP	Source Control-CCS
	would not require any significant construction activity. Similarly, traffic and noise impacts associated with residual plume management are expected to be minimal because no installation, operation, and maintenance of engineered systems or structures would be required. There would be no impacts to natural resources and habitat under the Source Control-GWP alternative because no additional construction activities would be required.	CCS alternative would involve the construction of the barrier wall. Similarly, traffic and noise impacts associated with residual plume management are expected to be higher under the Source Control-CCS alternative than the Source Control-GWP alternative due to the construction activities that would be required to construct the cutoff wall. Under the Source Control-CCS alternative, some negative impacts on scenic and recreational value may occur along the Illinois River and within the Donnelley/DePue State Fish and Wildlife Areas complex, which borders the Site to the north and west. Given the proximity between these areas and the expected construction, it is likely that these areas would experience some adverse impacts such as visual disturbance, obstruction of view, and noise during the construction period. However, these impacts are expected to diminish once the construction is completed in 18 to 24 months. In addition, the construction of the cutoff wall under the Source Control-CCS alternative is expected to use a significant amount of cement or bentonite, which would be introduced into the UA and BCU. Adding substantial quantities of these materials into the subsurface environment may cause alteration in groundwater pH levels and affect geochemical conditions in the UA.
Time Until Groundwater Protection Standards Are Achieved/Attain the Groundwater Protection Standards Specified in Section 845.600 (Section 2.2.6; IAC Section 845.670(e)(1)(E); IAC Section 845.670(d)(2))	Groundwater modeling was performed in support of the Closure Plan (Geosyntec Consultants, Inc., 2017). The modeling predicted that source control would result in the reduction of leachate production, which facilitates the contraction of the contaminant plume in groundwater (Geosyntec Consultants, Inc., 2017).	Groundwater modeling was performed in support of the Closure Plan (Geosyntec Consultants, Inc., 2017). The modeling predicted that source control would result in the reduction of leachate production, which facilitates the contraction of the contaminant plume in groundwater (Geosyntec Consultants, Inc., 2017).

Evaluation Factor (Report Section; Part 845 Section)	Source Control-GWP	Source Control-CCS
	Additional modeling was conducted for each of the corrective action alternatives to evaluate future groundwater quality in the vicinity of the WAPS as a result of residual plume management (Appendix B; Ramboll, 2025b). The results of the modeling indicate that groundwater would attain the GWPSs for all of the constituents identified as having potential groundwater exceedances in the monitoring network within 29 years after approval of the Corrective Action Plan when the Source Control-GWP alternative is presumed to be initiated (Appendix B; Ramboll, 2025a).	Additional modeling was conducted for each of the corrective action alternatives to evaluate future groundwater quality in the vicinity of the WAPS as a result of residual plume management (Appendix B; Ramboll, 2025b). The results of the modeling indicate that groundwater would attain the GWPSs for all of the constituents identified as having potential groundwater exceedances in the monitoring network within 38 to 40 years (5 to 7 years of pre-construction and construction activities and 33 years after installation) after approval of the Corrective Action Plan when the Source Control-CCS alternative is presumed to be initiated (Appendix B; Ramboll, 2025a).
Potential for Exposure of Humans and Environmental Receptors to Remaining Wastes, Considering the Potential Threat to Human Health and the Environment Associated with Excavation, Transportation, Re-disposal, Containment, or Changes in Groundwater Flow (Section 2.2.7; IAC Section 845.670(e)(1)(F))	Source control (*i.e.*, CIP using a consolidate-and-cap approach) was implemented in 2020. Therefore, both corrective action alternatives are equally and fully protective with regard to exposure to residual CCR. As a result of the source control, there would be no risk of CCR releases post-closure. The Source Control-GWP alternative would not involve exposure to the soil or groundwater waste streams and thus, there is no potential for exposure of humans and environmental receptors to wastes.	Source control (*i.e.*, CIP using a consolidate-and-cap approach) was implemented in 2020. Therefore, both corrective action alternatives are equally and fully protective with regard to exposure to residual CCR. As a result of the source control, there would be no risk of CCR releases post-closure. For construction workers, risks arising from potential contact with residual contamination during construction, operation, and maintenance activities associated with residual plume management would be higher for the Source Control-CCS than for the Source Control-GWP alternative, because the Source Control-CCS alternative would involve the excavation and subsequent management of Site soils. In addition, Source Control-CCS would involve temporarily removing a portion of the final cover previously installed, which could potentially allow stormwater to be in contact with CCR material during construction. CCR-contact stormwater would be generated and managed through a CCR-contact stormwater management system during the times when the final cover would be removed.

Evaluation Factor (Report Section; Part 845 Section)	**Source Control-GWP**	**Source Control-CCS**
		Any potential CCR exposures occurring under Source Control-CCS during the installation of the cutoff wall would be managed through the use of rigorous safety protocols, personal protective equipment, and appropriate disposal practices. Hydrogeological changes would be expected under the Source Control-CCS alternative, such as altering flow patterns in the UA, redirecting groundwater flow around the cutoff wall, and causing changes to normal hydraulic gradients. However, changes to groundwater flow would not be expected to have an effect on the potential for the exposure of humans and environmental receptors to any wastes.
Long-Term Reliability of the Engineering and Institutional Controls (Section 2.2.8; IAC Section 845.670(e)(1)(G))	Source control (*i.e.*, CIP using a consolidate-and-cap approach) was implemented in 2020. Thus, long-term reliability of source control would be same for both corrective action alternatives. Residual plume management under the Source Control-GWP alternative would be reliable because it would rely on physical and geochemical attenuation processes and active monitoring. If necessary, remedy optimizations would be implemented under the adaptive site management program.	Source control (*i.e.*, CIP using a consolidate-and-cap approach) was implemented in 2020. Thus, long-term reliability of source control would be same for both corrective action alternatives. Cutoff walls are a proven remedy and have been implemented at many sites. Thus, residual plume management under the Source Control-CCS alternative would be reliable, provided it is constructed in accordance with standard design specifications. The remedy consists of a passive, below-grade structure, which would not require any O&M activities once it is installed. The construction of the cutoff wall would require temporarily removing a portion of the previously installed WAPS final cover. This procedure may allow additional stormwater to infiltrate the CCR, potentially leading to a temporary reversal of some positive effects that have occurred since the completion of the final cover system in 2020. A CCR-contact stormwater management

Evaluation Factor (Report Section; Part 845 Section)	**Source Control-GWP**	**Source Control-CCS**
		system would be required to manage and discharge the contact stormwater *via* an NPDES permitted outfall. Quality control (QC) and quality assurance (QA) programs will be required during and after the construction to ensure the effectiveness of the cutoff wall. If necessary, remedy optimizations would be implemented under the adaptive site management program.
Potential Need for Replacement of the Remedy (Section 2.2.9; IAC Section 845.670(e)(1)(H))	Replacement of the residual plume management remedy under the Source Control-GWP alternative would likely be unnecessary, because it would not require the installation, operation, and maintenance of engineered systems or structures. Adaptive site management strategies would be used to implement remedy optimizations, if necessary, to ensure that remedial goals are achieved.	Replacement of the residual plume management remedy under the Source Control-CCS alternative would likely be unnecessary, because the cutoff wall is a robust, engineered, and maintenance-free subsurface structure. The final cover system portion of this alternative would need ongoing maintenance per the IEPA approved Post-Closure Care Plan, but it is a passive and engineered structure that is unlikely to need replacement. Adaptive site management strategies would be used to implement remedy optimizations, if necessary, to ensure that remedial goals are achieved.
Degree of Difficulty Associated with Constructing the Remedy (Section 2.3.1; IAC Section 845.670 (e)(3)(A))	Source control (*i.e.*, CIP using a consolidate-and-cap approach) was implemented in 2020. Thus, there would be no further construction difficulties associated with the implementation of source control. Residual plume management under the Source Control-GWP alternative would rely on physical and geochemical attenuation processes and therefore would not pose any significant construction challenges.	Source control (*i.e.*, CIP using a consolidate-and-cap approach) was implemented in 2020. Thus, there would be no further construction difficulties associated with the implementation of Source Control. Residual plume management under the Source Control-CCS alternative would rely on a continuous containment system to enclose the CCR within the WAPS, and physical and geochemical attenuation processes to address downgradient groundwater quality impacts. Some challenges may be encountered during the construction of the cutoff wall, including the following: 1. Specialized equipment, including large cranes, clamshells, slurry cutters, batch plants, and grading

Evaluation Factor (Report Section; Part 845 Section)	Source Control-GWP	Source Control-CCS
		equipment may be needed to construct the cutoff wall. 2. Construction challenges, such as encountering highly permeable layers leading to slurry loss, facing obstructions that necessitate specialized techniques and/or equipment for progression, or experiencing sidewall instability, may arise. These challenges could be managed during cutoff wall construction. 3. Additional engineering assessments and monitoring programs would be necessary to monitor the embankment for indications of distress, such as deformation or cracking, throughout the cutoff wall construction process, because the cutoff wall would be installed through an existing impoundment embankment. 4. The construction of the cutoff wall would require temporarily removing a portion of the previously installed WAPS final cover in areas where conflict with the cutoff wall. This procedure may allow additional stormwater to infiltrate the CCR, potentially leading to a temporary reversal of some positive effects that have occurred since the completion of the final cover system in 2020. A CCR-contact stormwater management system would be required to manage and discharge the contact stormwater *via* an NPDES permitted outfall. 5. Ongoing QC is essential during construction, as part of QA activities, to prevent defective features. Additionally, post-construction QA programs, such as coring and testing, may be necessary to validate the quality of the constructed barrier.

Evaluation Factor (Report Section; Part 845 Section)	Source Control-GWP	Source Control-CCS
		6. Ongoing monitoring and QA/QC testing for slurry mixing, placement, or soil-bentonite mixing are critical to ensure the performance of the cutoff wall.
Expected Operational Reliability of the Remedy (Section 2.3.2; IAC Section 845.670 (e)(3)(B))	Source control (*i.e.*, CIP using a consolidate-and-cap approach) was implemented in 2020. The operational reliability of the source control would be the same for both corrective action alternatives. Residual plume management under the Source Control-GWP alternative would have high operational reliability because this alternative would rely on natural processes and active monitoring. However, it should be noted that some arsenic re-mobilization may occur as groundwater returns to background conditions, which may cause an impact to the time to achieve GWPS (Appendix E; Geosyntec Consultants, Inc., 2025). Adaptive site management strategies would be used to implement remedy optimizations, if necessary.	Source control (*i.e.*, CIP using a consolidate-and-cap approach) was implemented in 2020. The operational reliability of the source control would be the same for both corrective action alternatives. Residual plume management under the Source Control-CCS alternative would have high operational reliability because it is an established technology, as long as the cutoff wall is constructed in accordance with standard design specifications. This CCS would provide full isolation of all CCR from the surrounding environment as a result of the cutoff wall extending into bedrock and from the existing cover. However, this alternative would require the temporary removal of a portion of the completed cover over the WAPS, which could potentially cause additional stormwater to percolate into the CCR and result in a temporary reversal of certain positive effects that have occurred since the completion of source control in 2020. These temporary impacts would diminish once the final cover system is repaired. Adaptive site management strategies would be used to implement remedy optimizations, if necessary.
Need to Coordinate with and Obtain Necessary Approvals and Permits from Other Agencies (Section 2.3.3; IAC Section 845.670 (e)(3)(C))	Specific permits and approvals associated with source control were the same for both corrective action alternatives and were discussed in the Closure Plan (Geosyntec Consultants, Inc., 2017). Residual plume management under the Source Control-GWP alternative would	Specific permits and approvals associated with source control were the same for both corrective action alternatives and were discussed in the Closure Plan (Geosyntec Consultants, Inc., 2017). The Source Control-CCS alternative would require approvals and permits,

Evaluation Factor (Report Section; Part 845 Section)	**Source Control-GWP**	**Source Control-CCS**
	not need additional permits from other agencies, other than the approval of the Corrective Action Plan.	including construction stormwater controls and BMPs, a joint water pollution control construction and operating permit. An IDNR Dam Safety modification permit would be required for modifications of the WAPS embankment. A modification to the existing NPDES permit would be necessary to discharge the CCR-contact stormwater generated during the construction phase.
Availability of Necessary Equipment and Specialists (Section 2.3.4; IAC Section 845.670 (e)(3)(D))	Source control (*i.e.*, CIP using a consolidate-and-cap approach) was implemented in 2020. Thus, there are no further equipment and specialist needs associated with the implementation of the source control remedy. Residual plume management under the Source Control-GWP alternative would require standard environmental monitoring equipment and groundwater professionals. Specialists such as geologists, hydrogeologists, statisticians (*i.e.*, statistical analysis), and geochemists would be available to collect and evaluate the data.	Source control (*i.e.*, CIP using a consolidate-and-cap approach) was implemented in 2020. Thus, there are no further equipment and specialist needs associated with the implementation of the source control remedy. Residual plume management under the Source Control-CCS alternative would require standard environmental monitoring equipment similar to those under the Source Control-GWP alternative. In addition, building the cutoff wall requires the expertise of a specialized contractor with a background in constructing similar types of walls in comparable geologic environments. Specialized equipment, including large cranes, clamshell buckets, slurry cutters, batch plants, or other equipment would be required to construct the cutoff wall. Specialists, such as design engineers, construction managers, and contractor staff, involved in the design and construction of cutoff walls would be essential during both phases. Monitoring the WAPS embankments during cutoff wall construction would require expertise in geotechnical instrumentation, including the use of inclinometers, survey prisms, vibrating wire piezometers, and visual inspection for signs of distress. Equipment and experts with geosynthetics design and installation, specifically with seaming new geosynthetics to an existing final cover

Evaluation Factor (Report Section; Part 845 Section)	Source Control-GWP	Source Control-CCS
		system, would be required for the final cover system restoration. There may be backlogs associated with the equipment and specialists discussed above, due to the high existing demand for specialty ground improvement contractors and design specialists who are engaged with similar projects in sectors like electric utilities, dams/levees, solid waste management, and other areas.
Available Capacity and Location of Needed Treatment, Storage, and Disposal Services/Comply with Standards for Management of Wastes as Specified in Section 845.680(d) (Section 2.3.5; IAC Section 845.670 (e)(3)(D)/ IAC section 845.670(d)(5))	No treatment, storage, or disposal services would be required for residual plume management under Source Control-GWP alternative, as GWP would not generate any significant volume of waste or wastewater.	Residual plume management for the Source Control-CCS alternative would generate waste during the cutoff wall construction phase; waste would include geosynthetics and other debris from removing the final cover system, cutoff wall spoils, and contact stormwater. 1. Geosynthetics and other debris would be disposed of in an off-Site landfill that has sufficient volume. 2. CCR-containing cutoff wall spoils would be temporarily staged on-Site and then disposed off-Site or beneficially used on-Site as compacted contouring fill. 3. Non CCR-impacted spoils would be disposed of at an appropriate on-Site location. 4. CCR-contact stormwater generated during construction would be pumped to the on-Site treatment pond and then discharged *via* an NPDES permitted outfall. No wastes would be expected to be generated during operation of the cutoff wall; consequently, no additional treatment, storage, or disposal services would be necessary for this remedy.
The Degree to Which Community Concerns Are Addressed by the Remedy (Section 2.4; IAC Section 845.670(e)(4))	Some communities have expressed concerns over groundwater quality at CCR surface impoundments. The combination of source control (*i.e.*, CIP using a consolidate-and-cap approach)	Some communities have expressed concerns over groundwater quality at CCR surface impoundments. The combination of source control (*i.e.*, CIP using a consolidate-and-cap approach)

Evaluation Factor (Report Section; Part 845 Section)	Source Control-GWP	Source Control-CCS
	and residual plume management would cause groundwater concentrations to decline over time under all of the corrective action alternatives, as suggested by the groundwater modeling (Geosyntec Consultants, Inc., 2017; Appendix B Ramboll, 2025b), thus addressing these concerns. A public meeting will be held on April 8, 2025, pursuant to requirements under IAC Section 845.710(e). Questions raised by attendees will be answered at the meeting; subsequently, a written summary of all questions and responses will be made available to interested parties.	and residual plume management would cause groundwater concentrations to decline over time under all of the corrective action alternatives, as suggested by the groundwater modeling (Geosyntec Consultants, Inc., 2017; Appendix B; Ramboll, 2025b), thus addressing these concerns. A public meeting will be held on April 8, 2025, pursuant to requirements under IAC Section 845.710(e). Questions raised by attendees will be answered at the meeting; subsequently, a written summary of all questions and responses will be made available to interested parties.
Remove from the Environment as Much of the Contaminated Material That Was Released from the CCR Surface Impoundment as Is Feasible, Taking into Account Factors Such as Avoiding Inappropriate Disturbance of Sensitive Ecosystems (Section 2.5; IAC Section 845.670(d)(4))	There have been no known releases of CCR at the WAPS. Both potential corrective action alternatives include source control and residual plume management efforts. The source control included the a consolidate-and-cap approach to control, minimize or eliminate, post-closure infiltration of liquids into the impounded CCR. Therefore, this approach is preventing the release of contaminated material from the WAPS to the extent that is feasible. Additionally, residual plume management under the Source Control-GWP alternative would address impacted groundwater by relying on natural physical and geochemical attenuation processes to reduce the residual concentrations of CCR-related constituents in groundwater. Site-specific evaluations have shown that groundwater polishing would reduce the groundwater concentrations and mobility of inorganic contaminants (including boron and sulfate), through physical and geochemical attenuation mechanisms, especially after the implementation of source control (Appendix E; Geosyntec Consultants, Inc., 2025). However, it should be	There have been no known releases of CCR at the WAPS. Both potential corrective action alternatives include source control and residual plume management efforts. The source control included the a consolidate-and-cap approach to control, minimize or eliminate, post-closure infiltration of liquids into the impounded CCR. Therefore, this approach is preventing the release of contaminated material from the WAPS to the extent that is feasible. Additionally, residual plume management under the Source Control-CCS alternative would employ a cutoff wall which would be incorporated into the final WAPS cover system to create a continuous low-permeability barrier that fully contains the CCR within the WAPS. This system ensures isolation from the surrounding environment through lateral containment by the deep cutoff wall, surface containment by the existing geomembrane cover, and a natural barrier provided by the competent shale bedrock below. The temporary removal of the final cover system implemented during closure in 2020 would also occur during construction, which would generate

Evaluation Factor (Report Section; Part 845 Section)	Source Control-GWP	Source Control-CCS
	noted some arsenic re-mobilization may occur as groundwater returns to background conditions at the WAPS, which may cause an impact to the time required to achieve GWPS (Appendix E; Geosyntec Consultants, Inc., 2025). No ecosystems would be disturbed because no construction activities are expected under the Source Control-GWP alternative.	CCR-contact stormwater that would be managed appropriately. The construction activities may cause some negative impacts on natural resources and habitat located atop the WAPS final cover system and near the Site. However, the total duration of the construction is expected to be 18 to 24 months, so any construction-related impacts to ecosystems would be limited to the short term. Source Control-CCS would be more effective at controlling releases than Source Control-GWP. CCS would isolate CCR from the surrounding environment on all sides and in particular would prevent releases of CCR-related constituents associated with the high groundwater transmissivity of the sand and gravel deposits in the UA.

Notes:

BCU = Bedrock Confining Unit; CCR = Coal Combustion Residual; CCS = Continuous Containment System; CIP = Closure-in-Place; GWP = Groundwater Polishing; GWPS = Groundwater Protection Standard; IAC = Illinois Administrative Code; IDNR = Illinois Department of Natural Resources; NPDES = National Pollutant Discharge Elimination System; O&M = Operations and Maintenance; Source Control-CCS = Source Control with a Continuous Containment System; Source Control-GWP = Source Control with Groundwater Polishing; UA = Uppermost Aquifer; WAPS = Western Ash Pond System.

1 Introduction

1.1 Site Description and History

1.1.1 Site Location and History

Dynegy Midwest Generation, LLC's (DMG) Hennepin Power Plant is an electric power generating facility with coal-fired units located approximately 4 miles northeast of the Village of Hennepin, Illinois, along the Illinois River. The facility began operating in the early 1950s and was retired in 2019 (Ramboll, 2021). The plant had two coal-fired units constructed in 1953 and 1959 with a capacity of 70 megawatt (MW) and 210 MW, respectively (Ramboll, 2021).

1.1.2 CCR Impoundment

The Hennepin Power Plant produced and stored coal combustion residuals (CCRs) as a part of its historical operations. The West Ash Pond System (WAPS; which includes Illinois Environmental Protection Agency [IEPA] identification [ID] number [No.] W1550100002-01 and No. W1550100002-03, Vistra CCR Unit ID 804, and a National Inventory of Dams [NID] No. IL50698; Appendix B) is the subject of this report.

The WAPS was operated from 1952 through 1996. The impoundment is composed of two inactive sub-units, the Old West Ash Pond (OWAP) and the Old West Polishing Pond (OWPP) (Figure 1.1). Both sub-units were originally constructed as a single unit with a single perimeter dike and subsequently divided as part of operational procedures. The OWAP was approximately 27.7 acres in size and accepted mainly bottom ash, slag, as well as mixed coal ash. The 4.7-acre OWPP was used as a secondary pond and is located at the western end of the impoundment. Effluent from the impoundment was discharged to surface water until 1989 when the Ponds No. 1 and No. 3 were consolidated as OWAP and divided into primary and secondary cells within the OWAP. This report refers to the three sub-units as a single CCR unit, *i.e.*, WAPS (OBG, Part of Ramboll, 2019).

A Closure and Post-Closure Plan for the WAPS was developed in accordance with Title 40 Part 257 and was approved by IEPA in 2018. Source control using a consolidate-and-cap approach was completed in 2020 (Appendix C; Ramboll, 2024a), which is discussed in Section 2.1.

Figure 1.1 Site Location Map. Adapted from Ramboll (2025c).

1.1.3 Surface Water Hydrology

The WAPS is located within the DePue Lake-Ohio River Watershed (12-digit Hydrologic Unit Code: 071300010804), which is located in the greater Lower Illinois-Senachwine Lake (8-digit Hydrologic Unit Code: 07130001) (USGS, 2024). The Illinois River is located less than 200 ft north of the WAPS and flows from east to west (Geosyntec Consultants, Inc., 2017). As described below (Section 1.1.4, Hydrogeology), the Illinois River acts as a regional sink for surface water and groundwater in the vicinity of the Site.

The Illinois River is the largest surface water body in the area. The IEPA classifies the river as a General Use Water: it is designated for aquatic life and use in primary contact recreation; however, it is not designated for use in food processing or as a public water supply. The segment of the Illinois River adjacent to the Site (Section D-16) is listed on the 2022 Illinois Section 303(d) List as being impaired for fish consumption, due to mercury and polychlorinated biphenyls (PCBs). DePue Lake, which is located north of the Site along the north bank of the Illinois River, is listed as impaired for aquatic life due to cadmium, endrin, silver and zinc; it is also listed as impaired for fish consumption due to mercury and polychlorinated biphenyls (IEPA, 2022, 2019).

The former National Pollutant Discharge Elimination System (NPDES) permit (IL001554) outfall 005, which was a discharge culvert at the OWPP, was removed during closure of the WAPS in 2020 (IEPA, 2011; Geosyntec Consultants, Inc., 2017). During closure, free water pumped from the WAPS was eventually discharged through Outfall 003, which is located approximately one mile east of the WAPS, under the same permit (Geosyntec Consultants, Inc., 2017).

1.1.4 Hydrogeology

The geology underlying the Site in the vicinity of the WAPS consists of three distinct hydrostratigraphic units (Appendix C; Ramboll, 2024a; Geosyntec Consultants, Inc., 2017):

- **Uppermost Aquifer (UA):** The UA composed of mixed alluvial deposits (classified as Cahokia alluvium consisting of clay, silt, and sand), which overlie coarser grained outwash sand and gravel deposits (classified as Henry Formation). This unit is highly permeable and is the uppermost aquifer and primary groundwater transport pathway in the vicinity of the West Ash Pond System.
- **Bedrock Confining Unit (BCU):** The BCU is defined by Pennsylvanian age shale with minor layers of limestone, sandstone, and coal. This low permeability unit defines the lower boundary of the Uppermost Aquifer Unit at WAPS.

The groundwater movement in the unconsolidated materials is consistent with surface topography and flows north and west near the Site towards the Illinois River, which serves as a large regional hydraulic boundary. Precipitation infiltration recharges groundwater. Groundwater typically flows horizontally within the three hydrostratigraphic units at the Site, with converging upward flow near and beneath the river. Prior to the closure during the impoundment operations, substantial local recharge to groundwater from sluicing of ash created radial flow conditions near the impoundment. Groundwater flow direction is primarily northwest towards the river during post-closure conditions (Appendix C; Ramboll, 2024a; Appendix D; Ramboll, 2024b).

During groundwater's interaction with surface water, CCR-related constituents may partition between sediments and the surface water column. It should be noted that many CCR-related constituents can also arise from other industrial sources and occur naturally in sediments and surface water. As a result, their presence in the sediments and/or surface water of the Illinois River does not necessarily signify contributions from the WAPS.

1.1.5 Site Vicinity

The WAPS is surrounded by the Illinois River to the north, industrial properties to the east (Tri-Con Materials) and south (Tri-Con Materials and Washington Mills), agricultural land to the southwest, and the Hennepin Power Station to the west. Tri-Con Materials produces various fill and washed sand, gravel, rock and boulder products (Ramboll, 2018-2020). Washington Mills produces abrasive grains and specialty electro-fused minerals (Ramboll, 2018-2020).

Notable natural areas and recreational areas in the vicinity of the WAPS include the Illinois River and the Donnelley/DePue State Fish and Wildlife Areas complex, which is located opposite the WAPS along the northern bank of the Illinois River. The Illinois River is popular for canoeing and other forms of water recreation (IDNR, 2021). The nearby DePue Lake and Lyons Lake are popular areas for recreational boating and fishing (Illinois River Road National Scenic Byway, 2021; HookandBullet.com, 2021).

1.2 Part 845 Regulatory Review and Requirements

Title 35, Part 845 of the Illinois Administrative Code (IAC) (IEPA, 2021) requires that a Corrective Action Alternatives Analysis (CAAA) be performed as part of the remedy selection, prior to undertaking any corrective actions at certain CCR-containing impoundments where exceedances of GWPSs have been identified. Because exceedances[2] of GWPSs in groundwater associated with the WAPS have been identified for arsenic, boron, lithium, sulfate, and total dissolved solids (TDS) (Appendix D; Ramboll, 2024b), this report presents a CAAA for the WAPS pursuant to the requirements under IAC Section 845.670. The goal of a CAAA is to holistically evaluate a range of factors for the various corrective actions being considered at an impoundment, including the efficiency, reliability, and ease of implementation of the corrective action; its potential positive and negative short- and long-term impacts on human health and the environment; and its ability to address concerns raised by the community (IEPA, 2021). A CAAA is a decision-making tool that is designed to aid in the selection of a corrective action alternative.

---

[2] Throughout this document, "exceedance" or "exceedances" is intended to refer only to potential exceedances of proposed applicable background statistics or Groundwater Protection Standards (GWPS) as described in the proposed groundwater monitoring program, which was submitted to IEPA on October 25, 2021 as part of Dynegy Midwest Generation's operating permit application for the WAPS (Burns & McDonnell, 2021). The operating permit application, including the proposed groundwater monitoring program, remains under review by IEPA and therefore Dynegy Midwest Generation has not identified any actual exceedances.

2 Corrective Action Alternatives Analysis

This section presents the CAAA pursuant to requirements under IAC Section 845.670 (IEPA, 2021). The goal of a CAAA is to fully evaluate proposed viable corrective measures that were identified in the CMA. The CAAA evaluates potential corrective actions with respect to a wide range of factors, including the performance, reliability, and ease of implementation of the corrective action; its potential impacts on human health and the environment; and its ability to address concerns raised by the community (IEPA, 2021).

Per IAC Section 845.670(d) (IEPA, 2021), any corrective actions selected under a Corrective Action Plan must:

1. Be protective of human health and the environment;
2. Attain the groundwater protection standards specified in Section 845.600;
3. Control the sources of releases to reduce or eliminate, to the maximum extent feasible, further releases of constituents listed in Section 845.600 into the environment;
4. Remove from the environment as much of the contaminated material that was released from the CCR surface impoundment as is feasible, considering factors such as avoiding inappropriate disturbance of sensitive ecosystems; and
5. Comply with standards for management of wastes as specified in Section 845.680(d).

At the WAPS, a CAAA is required because groundwater monitoring associated with the WAPS identified exceedances of the GWPSs. Groundwater monitoring was conducted in accordance with the proposed groundwater monitoring plan (GMP) between 2015 and 2023 (Appendix D; Ramboll, 2024b). The groundwater samples collected from groundwater compliance monitoring wells were used to evaluate compliance with the groundwater quality standards listed in IAC Section 845.600(a). As of the date of this report, arsenic, boron, lithium, sulfate, and total dissolved solids (TDS) were identified as constituents/parameters with exceedances of their corresponding GWPSs (Appendix D; Ramboll, 2024b).

Two potential corrective actions are evaluated in this CAAA: Source Control with Groundwater Polishing (Source Control-GWP), and Source Control with a Continuous Containment System (Source Control-CCS). Both alternatives were identified as viable approaches in the CMA (Appendix C; Ramboll, 2024a). Each of these corrective action alternatives is described below in Section 2.1.

It should be noted that Source Control-GWP, Source Control with a Cutoff Wall, and Source Control with *In-Situ* Stabilization (ISS) were identified in the CMA as viable remedial approaches (Appendix C; Ramboll, 2024a). However, during subsequent evaluations, the remedial approaches were modified. Remedy modifications include the following:

- Source control-ISS was determined infeasible and excluded for further evaluation due to significant potential risks, including the need to temporarily remove half of the previously installed WAPS final cover. Removal of the final cover system would result in significant stormwater infiltration and potentially lead to reducing the effectiveness of the completed source control. In addition, ISS would involve managing tens of thousands of cubic yards of CCR and CCR-impacted cuttings on the WAPS surface, increasing the risk of releasing CCR-contaminated stormwater and sediments during construction, which could negatively impact nearby sensitive areas.

- Source Control-Cutoff Wall was expanded into the Source Control-CCS alternative, which is evaluated in this report. The continuous containment system (CCS) integrates the cutoff wall with the existing final cover to provide full lateral and surface isolation of CCR from the surrounding environment. The wall would be keyed into competent shale bedrock to provide base subsurface containment below the WAPS.

2.1 Corrective Action Alternative Descriptions

For both corrective actions evaluated in this CAAA, source control is the primary remedy. US EPA has stated that source control is the most effective means of ensuring the timely attainment of remediation objectives (US EPA, 2015b). The source control for the WAPS consisted of closure-in-place (CIP) using a consolidate-and-cap approach (Geosyntec Consultants, Inc., 2017). Specific elements of this approach competed in 2020 included:

- Removal of free water (unwatering) within the OWAP and OWPP *via* a pumping system and discharge through existing NPDES Outfall 003.
- Installation of a sheet pile wall and a compacted clay buttress at the splitter dike between the OWAP and OWPP for dike support and seepage control during excavation of the OWPP. The sheet pile and buttress remain in place after closure to physically separate CCR that were capped in the OWAP from the excavated area in the OWPP.
- Excavation of CCR and dike soils from the OWPP and placement of the excavated CCR in the OWAP as structural fill. The excavated area in OWPP resulted in a 6-acre depression, which was seeded to foster native vegetation growth and currently functions as an ephemeral pond for wildlife habitat.
- Placement of a geosynthetic cover system over the OWAP, which consisted of a 40-mil linear low-density polyethylene (LLDPE) geomembrane liner, 1.5 ft of soil cover and 0.5 ft vegetative layer.
- Removal of existing NPDES Outfall 005 and the associated discharge culvert at the OWPP.
- Establishing and maintaining native vegetative growth on the OWAP final cover, to minimize erosion.
- Establishing a gravel roadway along the south and west of the OWPP to allow for vehicular access to the adjacent Donnelly Wildlife Management Area.
- Installation of a stormwater management system.

These above source control activities included excavation of CCR from the OWPP and consolidation into OWAP, and the installation of a low-permeability final cover system. These activities were designed to control, minimize or eliminate, post closure infiltration of liquids into the impounded CCR. Closure activities specifically included removal of impounded water and excavation of CCR and one foot of soil below the CCR from OWPP to consolidate into OWAP, and installation of a final cover system consisting of a geosynthetic layer, a protective soil layer and establishment of a vegetative cover. These measures (installation of a geosynthetic cap and consolidation of CCR) control to the maximum extent feasible the migration of CCR constituents to groundwater, thus facilitating the achievement of the GWPSs in accordance with IAC Section 845.600. As demonstrated by the groundwater modeling in support of the Closure Plan, source control would result in a drop of hydraulic pressure beneath the final cover system, a significant reduction in groundwater concentrations, and over time would result in a reduction in the extent of groundwater impacts to within the footprint of the impoundment (Geosyntec Consultants, Inc., 2017). Due to the reduction in the hydraulic flux out of the WAPS, the mass flux out of the WAPS would also be controlled and minimized.

In addition to source control, the corrective actions evaluated in this CAAA include residual plume management. Two potential corrective actions, identified as viable in the CMA and after further assessment, are evaluated in this CAAA for the WAPS (Appendix B; Ramboll, 2025a):

- **Alternative 1:** Source Control with Groundwater Polishing (Source Control-GWP);
- **Alternative 2:** Source Control with a Continuous Containment System (Source Control-CCS).

For both corrective action alternatives, adaptive site management strategies would be integrated into residual plume management. This approach ensures the timely incorporation of new Site information throughout the corrective action process in order to optimize the remediation and expedite achievement of the GWPSs. As part of the adaptive site management approach, system performance and residual plume conditions would be monitored throughout the implementation of the selected corrective action. If groundwater concentrations do not respond as expected to the corrective action, the adaptive site management approach would enable prompt adjustments, optimizations, or replacement of the remedy to ensure overall effectiveness.

2.1.1 Alternative 1: Source Control-GWP

The first corrective action alternative is Source Control-GWP. This remedy includes source control (*i.e.*, CIP using a consolidate-and-cap approach) combined with residual plume management based on physical and geochemical processes that would reduce groundwater concentrations downgradient of the WAPS. Groundwater polishing mechanisms were evaluated using geochemical speciation and reaction models. The primary objective of the geochemical model was to support the evaluation of groundwater polishing as a potential remedy for the Site. The model focused on evaluating the dominant geochemical reactions that may occur at time scales relevant to groundwater flow, including adsorption and mineral dissolution/precipitation reactions (*i.e.*, iron and aluminum hydroxides, carbonates, and some sulfates) (Appendix E; Geosyntec Consultants, Inc., 2025). Model inputs included geochemically reactive solid mineral phases, downgradient groundwater composition, and background groundwater composition derived from Site-specific data. Speciation models analyzed the distribution of chemical constituents between solid and aqueous phases, while reaction models assessed how these distributions may shift in response to changing Site conditions (US EPA, 2015).

Components of residual plume management for the Source Control-GWP alternative include:

- Groundwater concentrations would be reduced in the downgradient plume as a result of physical and geochemical attenuation processes. Site-specific evaluations have shown that groundwater polishing would reduce the groundwater concentrations and mobility of inorganic contaminants (including boron, lithium, and sulfate), through natural physical and geochemical attenuation mechanisms, especially after the implementation of source control (Appendix E; Geosyntec Consultants, Inc., 2025). Specifically, chemical attenuation of contaminants is feasible *via* sorption to aquifer solids, particularly iron and aluminum oxides under current conditions. Attenuation *via* sorption onto mineral surfaces should remain stable for boron and sulfate under post-closure conditions. However, it should be noted some arsenic[3] re-mobilization may occur as groundwater returns to background conditions at the WAPS, which may cause an impact to the time to achieve GWPS (Appendix E; Geosyntec Consultants, Inc., 2025).

- Corrective action groundwater monitoring using a corrective action groundwater monitoring network designed in accordance with IAC Section 845.680(c), which would be installed within the plume that lies beyond the waste facility boundary.
- Adaptive site management strategies for this alternative would include geochemical modeling. Groundwater monitoring results would be evaluated and compared to the model-predicted concentrations. In situations in which observed groundwater concentrations deviate significantly from modeled conditions, alternative methods or techniques to achieve the GWPSs would be evaluated, and if viable, incorporated as per IAC Section 845.680(b).
- Corrective action confirmation groundwater sampling would be performed for 3 years after GWPSs have been achieved.
- Following the completion of the corrective action confirmation monitoring period, a report and certification for Corrective Action Completion would be prepared and submitted to IEPA as per IAC Section 845.680(e).

The overall corrective action implementation duration for this alternative is approximately 33 years (390 months) after approval of the corrective action plan (Appendix B; Ramboll, 2025a), including:

- Approximately 29 years (348 months) of corrective action monitoring (*i.e.*, time to meet GWPSs),
- At least 3 years (36 months) of corrective action confirmation monitoring,[4] and
- Approximately 6 months associated with post-closure reporting (Appendix B; Ramboll, 2025a).

2.1.2 Alternative 2: Source Control-CCS

The second corrective action alternative is Source Control-CCS. This remedy includes source control and uses a continuous containment system (*i.e.*, a deep groundwater cutoff wall tied into the existing the final cover system) as the residual plume management approach. The cutoff wall would extend from the top of the WAPS perimeter dikes completely through the UA and penetrate into the underlying competent shale bedrock. The total length of the cutoff wall is expected to be approximately 5,200 ft, enclosing the CIP portions of the WAPS. The wall would be constructed from ground surface to a depth of 90 ft below ground surface (bgs)[5] (Appendix B; Ramboll, 2025a). The cutoff wall would be constructed using either a mixture of soil and bentonite or cement and bentonite, with a thickness ranging from 2 to 3 ft, and would have a hydraulic conductivity of approximately 1.0×10^{-7} centimeters per second (cm/s). The existing final cover system would be extended and integrated with the cutoff wall, creating a continuous low-permeability physical barrier. This would fully contain the CCR within the WAPS, isolating it from the surrounding environment on all sides through:

- A deep cutoff wall ensuring lateral containment on all sides of the CCR;

---

[3] It should be noted that not all arsenic in groundwater is associated with the WAPS. Some of the arsenic is likely naturally occurring and/or associated with other sources.

[4] It should be noted that post-closure care groundwater monitoring would continue for a minimum of 30 years as required by IAC Section. 845.780(c).

[5] This depth corresponds to an approximate elevation of 375 ft. All elevations in this report are in the North American Vertical Datum of 1988 (NAVD88), unless otherwise noted.

- The existing low-permeability geomembrane final cover system providing surface containment over the CCR;
- Competent shale bedrock acting as a low-permeability barrier beneath the CCR.

The continuous containment system is a long-term, low-maintenance physical barrier between the WAPS and the surrounding environment. As indicated by groundwater modeling, the continuous containment system is unlikely to cause liquid buildup within the contained CCR mass, and thus supplemental groundwater extraction or active gradient control within the WAPS would be unnecessary. As a result, the system would control the source of releases of constituents to the environment.

Implementation of the Source Control-CCS is expected to include various tasks distributed across three major phases: pre-construction activities (Phase 1), corrective action construction (Phase 2), and corrective action operations and maintenance (O&M), groundwater monitoring, and closeout (Phase 3). The activities associated with the Source Control-CCS alternative are summarized below.

- **Phase 1:** Pre-construction activities including obtaining permits from agencies and completing Site investigations and engineering designs.
- **Phase 2:** Construction of the cutoff wall. Details pertaining to the construction activities are outlined below:
    - Mobilization of equipment and materials to the Site, and preparation for Site construction;
    - The final cover system previously installed would be temporarily removed in the areas where conflicts with the cutoff wall alignment; existing Site infrastructure (*i.e.*, access roads, piezometers, monitoring wells, stormwater structures, pressure relief vents) may also be removed.
    - Construction of a 60 ft wide working pad and temporary access road to allow construction equipment access and traffic;
    - Low-permeability backfill for the cutoff wall would be generated using an on-Site batch plant. A geotechnical monitoring system would be implemented during construction to monitor the WAPS perimeter dikes. The cutoff wall would be constructed using appropriate equipment, such as crane-mounted conventional constructional equipment. Other innovative methods would be utilized if determined to be appropriate during later phase.
    - Once the construction is completed, CCR-impacted spoils and/or work pad materials would be either disposed off-Site or beneficial used within the Hennepin East Ash Pond as compacted fill beneath the final cover system. Non-CCR impacted spoils would be disposed of at an appropriate on-Site location.
    - Appropriate stormwater management system would be constructed to discharge to an NPDES permitted outfall for any contact stormwater.
    - Site restoration would occur, which include replacement of Site infrastructure that are damaged or removed during construction, as well as the repair of the final cover system.
- **Phase 3:** Corrective action operations, maintenance (O&M), and closeout. Details pertaining to each of these activities are outlined below.
    - Corrective Action O&M: Because the deep cutoff wall is a passive, below-grade structure, no O&M would be needed following its installation. Maintenance of the final WAPS cover system (as part of the CCS) would proceed in accordance with current post-closure care O&M practices.

- Adaptive site management strategies would be employed to track remediation progress and incorporate new Site information to assure the achievement of the GWPSs.
- Corrective action monitoring would be performed using a corrective action groundwater monitoring network designed in accordance with IAC Section 845.680(c), which would be installed within the plume contamination that lies beyond the waste boundary.
- Corrective action confirmation monitoring would be performed for 3 years after GWPSs have been achieved.
- Following the completion of the corrective action confirmation monitoring period, a report and certification for Corrective Action Completion would be prepared and submitted to IEPA as per IAC Section 845.680(e).

The overall corrective action implementation duration is approximately 42 to 44 years (498 to 522 months) after approval of the corrective action plan (Appendix B), including:

- Approximately 4 to 5 years (42 to 60 months) of pre-construction activities (Phase 1),
- Approximately 18 to 24 months of corrective action construction (Phase 2), and
- Approximately 37 years (438 months) of O&M and closeout (Phase 3);
    - It includes 33 years (396 months) of corrective action monitoring (*i.e.*, time to meet GWPSs), at least 3 years (36 months) of corrective action confirmation monitoring,[6] and 6 months associated with post-closure reporting.

---

[6] It should be noted that post-closure care groundwater monitoring would continue for a minimum of 30 years as required by IAC Section 845.780(c).

Key parameters for the Source Control-Cutoff Wall corrective action alternative are shown in Table 2.1, below.

Table 2.1 Key Parameters for the Source Control-CCS Corrective Action Alternative[a]

Parameter[b]	Value[c]
Labor Hours	
Total On-Site Labor	29,400 hours
Total Off-Site Labor	0 hours
40% Contingency	11,800 hours
Total Labor Hours:	41,100 hours
Vehicle and Equipment Travel Miles	
Vehicles On-Site	95,600 miles
On-Site Haul Trucks (Unloaded + Loaded)	3,350 miles
Labor Mobilization	446,000 miles
Equipment Mobilization (Unloaded + Loaded)	54,100 miles
Off-Site Haul Trucks (Unloaded + Loaded)	121,000 miles
Material Deliveries (Unloaded + Loaded)	210,000 miles
Total On-Site Vehicle and Equipment Travel Miles:	99,000 miles
Total Off-Site Vehicle and Equipment Travel Miles:	831,000 miles
Total Vehicle and Equipment Travel Miles:	930,000 miles

Notes:
Source Control-CCS = Source Control with Continuous Containment System.
(a) Although source control (*i.e.*, closure-in-place [CIP]) is a primary component of the corrective action, the source control was previously completed in 2020 and the associated labor time, equipment usage, and mileage are not discussed in this analysis.
(b) Site activities are only expected to occur during the corrective action construction phase for this alternative.
(c) Values reported in this table were rounded to reflect 3 significant figures.
Source: Appendix B.

2.2 Long- and Short-Term Effectiveness and Protectiveness of Corrective Action Alternative (IAC Section 845.670(e)(1))

2.2.1 Magnitude of Reduction of Existing Risks/Be Protective of Human Health and the Environment (IAC Section 845.670(e)(1)(A)/IAC Section 845.670(d)(1))

There are no current unacceptable risks to human or ecological receptors at this Site associated with the WAPS (Appendix A; Gradient, 2025). Because current conditions do not present a risk to human health or the environment at the WAPS, there will be no unacceptable risk to human health or the environment for future conditions since the unit was already closed and source control was implemented. Concentrations of CCR-related constituents will decline over time and, consequently, potential exposures to CCR-related constituents in the environment will also decline. As a result of this, the magnitude of the reduction of existing risks is the same for the two potential corrective action alternatives (IAC Section 845.670(e)(1)(A)), and both corrective action alternatives are equally protective of human health and the environment (IAC Section 84.670(d)(1)).

2.2.2 Effectiveness of the Remedy in Controlling the Source (IAC Section 845.670(e)(2)/IAC Section 845.670(d)(3))

Extent to Which Containment Practices Will Reduce Further Releases/Control the Sources of Releases to Reduce or Eliminate, to the Maximum Extent Feasible (IAC Section 845.670(e)(2)(A)/IAC Section 845.670(d)(3))

Source control was implemented for both corrective action alternatives in 2020. Source control (*i.e.*, CIP using a dewatering-and-cap approach) which included dewatering and excavation of CCR from the OWPP and consolidation into the OWAP portion of the WAPS and the installation of a low-permeability final cover system. These source control activities would limit the infiltration of precipitation into the CCR, result in a significant reduction in groundwater concentrations, and, overtime, reduce the extent of groundwater impacts to within the footprint of the impoundment based on groundwater modeling conducted in support of the Closure Plan (Geosyntec Consultants, Inc., 2017). Therefore, both corrective action alternatives would be equally and fully protective with regard to source control. The effectiveness of residual plume management for each of the corrective action alternatives with respect to source control is summarized below.

- Under the Source Control-GWP alternative, the attenuation of dissolved constituent concentrations remaining after source control would be achieved through natural physical and geochemical processes. Site-specific evaluations have shown that groundwater polishing would reduce the groundwater concentrations and mobility of inorganic contaminants (including boron and sulfate), through natural physical and geochemical attenuation mechanisms, especially after the implementation of source control (Appendix E; Geosyntec Consultants, Inc., 2025). Specifically, chemical attenuation of contaminants is feasible to some extent *via* sorption to aquifer solids, particularly iron and aluminum oxides under current conditions. Attenuation *via* sorption onto mineral surfaces should remain stable for boron and sulfate under post-closure conditions. However, it should be noted some arsenic[7] re-mobilization may occur as groundwater returns to background conditions at WAPS, which may cause an impact to the time required to achieve GWPS (Appendix E; Geosyntec Consultants, Inc., 2025). In cases in which observed groundwater concentrations deviate significantly from modeled conditions, alternative methods or techniques to remove residual contamination to achieve the GWPSs would be evaluated under the adaptive site management program, and if viable, incorporated as per IAC Section 845.680(b);
- Under the Source Control-CCS alternative, residual plume management would be achieved by the installation of the continuous containment system. Cutoff walls are a frequently used corrective measures that have been determined to be an effective approach in preventing dissolved-phase groundwater plume migration. The final WAPS cover system would be extended and integrated with the cutoff wall, creating a continuous low-permeability barrier that fully contains the CCR within the WAPS. This system ensures isolation from the surrounding environment through lateral containment by the deep cutoff wall, surface containment by the existing geomembrane cover, and a natural barrier provided by the competent shale bedrock below. Thus, this continuous barrier will isolate the CCR from the surrounding environment thus reducing and eliminating further releases. If necessary, remedy optimizations would be implemented under the adaptive site management program.

---

[7] It should be noted that not all arsenic in groundwater is associated with the WAPS. Some of the arsenic is likely naturally occurring and/or associated with other sources.

Although both corrective action alternatives include source control and residual plume management, Source Control-CCS would be more effective at controlling sources of releases than Source Control-GWP. Source Control-CCS would isolate CCR from the surrounding environment on all sides and in particular would prevent releases of CCR-related constituents associated with the high groundwater transmissivity of the sand and gravel deposits of the UA.

Extent to Which Treatment Technologies May Be Used (IAC Section 845.670(e)(2)(B))

Because Source Control-GWP would rely on natural attenuation processes, no additional treatment technologies would be required under this alternative. Under the Source Control-CCS alternative, contact stormwater may be generated during the construction phase, which would be pumped to the on-Site treatment pond before discharging *via* an NPDES permitted outfall. No additional treatment technologies would be required for the Source Control-CCS alternative during the operation of the CCS, because the cutoff wall is an engineered physical barrier that does not require maintenance.

2.2.3 Likelihood of Future Releases of CCR (IAC Section 845.670(e)(1)(B))

Both corrective action alternatives include source control using CIP with a consolidate-and-cap approach. A geosynthetic cover system was installed over the WAPS in 2020 in compliance with 40 CFR Part 257, Subpart D, which included a geosynthetic layer, a protective soil layer to limit infiltration, and a vegetative cover. This cover system provides increased protection against berm and surface erosion, precipitation infiltration, and other adverse effects that could potentially trigger a release of CCR. During the construction phases of the Source Control-CCS alternative, a portion of the previously installed cover system would be temporarily removed near where the cutoff wall. Any CCR-contact stormwater generated during this time would be pumped to the on-Site treatment pond before discharged *via* an NPDES permitted outfall.

There would be minimal risk of accidental CCR releases occurring post-closure under either of the corrective action alternatives.

2.2.4 Type and Degree of Long-Term Management, Including Monitoring, Operation, and Maintenance (IAC Section 845.670(e)(1)(C))

The type and degree of long-term residual groundwater plume management associated with each corrective action alternative is summarized below.

- Residual plume management for the Source Control-GWP alternative would not require the installation, operation, or maintenance of any engineered systems or structures, other than maintenance of the monitoring well network. The only long-term management activity required under this alternative would be corrective action groundwater monitoring and routine maintenance of the monitoring wells, which would continue for at least 3 years after GWPSs have been achieved for all wells, in accordance with IAC Section 845.680(c)(2). Post-closure care groundwater monitoring would continue for a minimum of 30 years as required by IAC Section 845.780(c). Based on the adaptive site management approach, remedy optimization (additional methods or techniques) may be implemented to ensure the achievement of the GWPSs.
- Residual plume management for the Source Control-CCS alternative would require construction of a deep cutoff wall. Multiple tasks would be completed over three phases: pre-construction activities (Phase 1), corrective action construction (Phase 2), and corrective action operations, maintenance, and closeout (Phase 3). CCR-impacted spoils and/or work pad materials generated

during construction would be either disposed off-Site or beneficial used within the East Ash Pond as compacted fill beneath the final cover system. Non-CCR impacted spoils would be disposed of at an appropriate on-Site location (Appendix B; Ramboll, 2025a). After the installation of the cutoff wall, no O&M efforts will be required, because it is a passive, below-grade structure. However, quality assurance (QA) and quality control (QC) programs would be required as part of construction to validate the integrity of the constructed cutoff wall. Corrective action groundwater sampling and routine maintenance of the monitoring well network would continue for at least 3 years after GWPSs have been achieved for all wells, in accordance with IAC Section 845.680(c)(2). Post-closure care groundwater monitoring would continue for a minimum of 30 years as required by IAC Section 845.780(c). Based on the adaptive site management approach, remedy optimization (additional methods or techniques) may be implemented to ensure the achievement of the GWPSs.

2.2.5 Short-Term Risks to the Community or the Environment During Implementation of Remedy (IAC Section 845.670(e)(1)(D))

2.2.5.1 Safety Impacts

Best practices would be employed during construction in order to ensure worker safety and comply with all relevant regulations, permit requirements, and safety plans. However, it is impossible to completely eliminate risks to workers during construction and/or other corrective action activities. For example, injuries and fatalities can occur due to truck accidents or equipment malfunctions. Truck accidents that occur off-Site can also result in injuries or fatalities to community members. Because the source control was implemented in 2020, there is no further risk of accidents and injuries occurring during the implementation of the source control remedy. The safety impacts associated with residual plume management (*i.e.*, construction and/or O&M) for each corrective action alternative are described below.

- The Source Control-GWP alternative would not require the construction of any engineered systems or structures, and therefore no safety impacts are expected.
- The Source Control-CCS would include the construction of a deep cutoff wall to contain CCR within the WAPS. Because the cutoff wall is a passive, subsurface structure, no O&M would be needed following installation. Therefore, potential safety concerns are only associated with the construction of the cutoff wall.

Worker Risks

On-Site accidents include injuries and deaths arising from the use of heavy equipment and/or earthmoving operations during Site activities. Off-Site accidents include injuries and deaths due to vehicle accidents during labor and equipment mobilization/demobilization, as well as materials/supplies hauling and deliveries.

As discussed in Section 2.1.1, there are no construction activities or operational requirements associated with residual plume management for the Source Control-GWP alternative. Thus, no worker injuries or fatalities are expected under the Source Control-GWP alternative. Ramboll estimates that residual plume management for the Source Control-CCS corrective action alternative would require 29,400 on-Site labor hours (Appendix B; Ramboll, 2025a). The US Bureau of Labor Statistics (US DOL, 2020a,b) provides an estimate of the hourly fatality and injury rates for construction workers. Based on the accident rates reported by the US Bureau of Labor Statistics and the on-Site labor hours reported in Appendix B, we estimate that approximately 0.30 worker injuries and 2.7×10^{-3} worker fatalities would occur on-Site under the Source Control-CCS corrective action alternative (Table 2.2).

Table 2.2 Expected Number of On-Site Worker Accidents Under Each Corrective Action Alternative[a,b]

Corrective Action Alternative	Injuries	Fatalities
Source Control-GWP	0	0
Source Control-CCS	0.30	2.7×10^{-3}

Notes:
Source Control-CCS = Source Control with Continuous Containment System; Source Control-GWP = Source Control with Groundwater Polishing.
(a) Although source control (*i.e.*, closure-in-place [CIP]) is a primary component of the corrective action, the worker accidents associated with source control were previously estimated in the Closure and Closure Care Plan and are not repeated in this analysis.
(b) Worker accidents associated with groundwater sampling and monitoring are not included in this analysis for any of the alternatives.
Source: Appendix B; Ramboll, 2025a.

The Source Control-CCS alternative would result in off-Site hauling, labor and equipment mobilization/demobilization, and material deliveries (Table 2.1). For residual plume management under the Source Control-CCS alternative, a total of approximately 831,000 off-Site vehicle and equipment travel miles would be required. In contrast, for residual plume management under the Source Control-GWP corrective action alternative, no off-Site vehicle and equipment travel miles would be required (Appendix B; Ramboll, 2025a). The United States Department of Transportation (US DOT) provides estimates of the expected number of fatalities and injuries "per vehicle mile driven" for drivers and passengers of large trucks and passenger vehicles (US DOT, 2023). Table 2.3 shows the expected number of off-Site accidents under each corrective action alternative due to all categories of off-Site vehicle usage. For these calculations, it was assumed that labor mobilization/demobilization would rely upon passenger vehicles (cars or light trucks, including pickups, vans, and sport utility vehicles) and that hauling, equipment mobilization/demobilization, and material deliveries would rely upon large trucks. Based on US DOT's accident statistics and the mileage estimates in Appendix B, an estimated 0.35 worker injuries and 0.013 worker fatalities would be expected to occur due to off-Site activities under the Source Control-CCS alternative while there are no off-Site accidents expected under the Source Control-GWP alternative.

Table 2.3 Expected Number of Off-Site Worker Accidents Related to Off-Site Car and Truck Use Under Each Corrective Action Alternative[a]

Off-Site Vehicle Use Category	Source Control-GWP		Source Control-CCS	
	Injuries	Fatalities	Injuries	Fatalities
Hauling	0	0	0.025	1.9×10^{-3}
Labor Mobilization/Demobilization	0	0	0.27	4.2×10^{-3}
Equipment Mobilization/Demobilization	0	0	0.011	8.5×10^{-4}
Material Deliveries	0	0	0.044	3.3×10^{-3}
Total:	0	0	0.35	0.013

Notes:
Source Control-CCS = Source Control with Continuous Containment System; Source Control-GWP = Source Control with Groundwater Polishing.
(a) Although source control (*i.e.*, closure-in-place [CIP]) is a primary component of the corrective action, the source control was previously completed in 2020, and the worker accidents associated with source control are not discussed in this analysis.

Overall, considering accidents occurring both on- and off-Site, no worker injuries and worker fatalities would be expected to occur for residual plume management under the Source Control-GWP alternative;

and 0.65 worker injuries and 0.013 worker fatalities would be expected to occur for residual plume management under the Source Control-CCS alternative. Thus, overall risks to workers would be higher under the Source Control-CCS alternative and lower under Source Control-GWP alternative.

Community Risks

Vehicle accidents that occur off-Site can result in injuries or fatalities among community members as well as workers. Based on the accident statistics reported by US DOT (2023) and the off-Site travel mileages reported in Appendix B (and summarized in Table 2.1), off-Site vehicle accidents could result in an estimated 0.21 injuries and 2.5×10^{-3} fatalities among community members (*e.g.*, people involved in haul truck accidents that are neither haul truck drivers nor passengers, including pedestrians, drivers of other vehicles, *etc.*) for residual plume management under the Source Control-CCS alternative (Table 2.4). No off-Site mileage is expected under the Source Control-GWP alternative, and thus no off-Site risks are expected under the Source Control-GWP alternative. Therefore, off-Site impacts on nearby residents, including injuries or fatalities, would be higher under the Source Control-CCS alternative.

Table 2.4 Expected Number of Community Accidents Under Each Corrective Action Alternative[a]

Off-Site Vehicle Use Category	Source Control-GWP		Source Control-CCS	
	Injuries	Fatalities	Injuries	Fatalities
Hauling	0	0	0.032	2.3×10^{-4}
Labor Mobilization/Demobilization	0	0	0.11	1.7×10^{-3}
Equipment Mobilization/Demobilization	0	0	0.014	1.1×10^{-4}
Material Deliveries	0	0	0.055	4.1×10^{-4}
Total:	0	0	0.21	2.5×10^{-3}

Notes:
Source Control-CCS= Source Control with Continuous Containment System; Source Control-GWP = Source Control with Groundwater Polishing.
(a) Although source control (*i.e.*, closure-in-place [CIP]) is a primary component of the corrective action, the source control was previously completed in 2020, and the worker accidents associated with source control are not discussed in this analysis.

2.2.5.2 Cross-Media Impacts to Air

Air pollution can occur both on-Site (*e.g.*, construction activities) and off-Site (*e.g.*, along transportation routes), potentially impacting workers as well as community members. Diesel emissions are a major source of air pollutants and greenhouse gas (GHG) emissions at construction sites. Diesel exhaust contains air pollutants, including nitrogen oxides (NO_x), particulate matter (PM), carbon monoxide (CO), and volatile organic compounds (VOCs) (Hesterberg *et al.*, 2009; Mauderly and Garshick, 2009). Construction equipment also emits GHGs, including carbon dioxide (CO_2) and possibly nitrous oxide (N_2O). The potential impact of each corrective action alternative on GHG emissions is proportional to the use of construction vehicles and equipment that are required for residual plume management.

Source control (*i.e.*, CIP using a consolidate-and-cap approach) was implemented for both potential corrective action alternatives, and there are no further air impacts associated with source control. On-Site emissions would be higher for residual plume management under the Source Control-CCS alternative, due to the greater amount of on-Site vehicle travel miles required under this corrective action alternative (99,000 total on-Site travel miles under the Source Control-CCS alternative while no on-Site travel miles under the Source Control-GWP; Section 2.1.1 and Tables 2.1). Off-Site emissions would similarly be higher for residual plume management under the Source Control-CCS alternative due to the greater amount of off-Site vehicle and equipment travel miles required under this alternative (831,000 total off-Site travel miles under the Source Control-CCS alternative while no off-Site travel miles under the Source Control-GWP alternative). In summary, air impacts would be higher for the Source Control-CCS alternative than the Source Control-GWP alternative.

2.2.5.3 Cross-Media Impacts to Surface Water and Sediments

Under both corrective action alternatives, the source control was implemented in 2020 (*i.e.*, CIP using a consolidate-and-cap approach), and constituent mass flux from groundwater into surface water will decline over time (Geosyntec Consultants, Inc., 2017). The source control approach removes the amount of water retained within the impoundment, which further reduces the hydraulic flux through the CCR. Due to the reduction in the hydraulic flux out of the WAPS, the mass flux out of the WAPS would also be controlled and minimized. As demonstrated by the groundwater modeling in support of the Closure Plan, Source Control would result in a significant reduction in groundwater concentrations and, overtime, reduce the extent of groundwater impacts to within the footprint of the impoundment (Geosyntec Consultants, Inc., 2017).

Under the Source Control-GWP alternative, minimal surface water and sediment impacts would be expected to be associated with residual plume management because it would not require the construction of any engineered systems or structures (other than utilizing existing monitoring wells).

Under the Source Control-CCS alternative, surface water and sediment impacts would be higher than the Source Control-GWP alternative due to the construction of the cutoff wall. Due to erosion and runoff, construction can have short-term negative impacts on surface water and sediment quality immediately adjacent to a site. Any associated impacts would be addressed through best management practices (BMPs) in accordance with Site land disturbance permits.

2.2.5.4 Control of Exposure to Any Residual Contamination During Implementation of the Remedy

Source control (*i.e.*, CIP using a consolidate-and-cap approach) was implemented in 2020. Thus, there are no further risks of CCR exposure associated with source control implementation. However, impacted soils and groundwater can be a source of CCR-related constituent exposure for workers. Risks to workers arising from potential contact with residual contamination during construction activities associated with residual plume management would be higher for the Source Control-CCS alternative than for the Source Control-GWP alternative, because the Source Control-CCS alternative would involve removal of a portion of the previously installed final cover system and excavation and subsequent disposal of Site spoils. In contrast, the Source Control-GWP alternative would not involve exposure to either of these soil or groundwater waste streams. Any potential CCR-exposures during the Source Control-CCS alternative would be managed through the use of rigorous safety protocols and personal protective equipment.

2.2.5.5 Other Identified Impacts

Source control (*i.e.*, CIP using a consolidate-and-cap approach) was implemented in 2020. Thus, there are no further risks associated with source control implementation.

In addition to safety impacts, cross-media impacts, and the potential for workers to be exposed to residual contamination, construction activities and remedial operations can have significant energy demands and can cause nuisance impacts such as traffic and noise. Energy consumption at a construction site is synonymous with fossil fuel consumption, because the energy to power construction vehicles and equipment comes from the burning of fossil fuels. Fossil fuel demands considered here include the burning of diesel fuel during construction equipment and vehicle travel miles. Because GHG emission impacts and energy consumption impacts both arise from the same sources at construction sites, the trends discussed in Section 2.2.5.2 with respect to GHG emissions also apply to the evaluation of energy demands. Specifically, the energy demands of construction equipment and vehicles associated with residual plume management would be greater under the Source Control-CCS alternative, while the energy demands under the Source Control-GWP alternative associated with residual plume management are expected to be lower because this alternative would not require any significant construction activity. There is no operational energy expected under either of the alternatives, because the Source Control-GWP alternative would rely on physical and geochemical processes, while the Source Control-CCS alternative would rely on the constructed barrier wall.

Similarly, traffic and noise impacts associated with residual plume management are expected to be higher under the Source Control-CCS alternative than the Source Control-GWP alternative, due to the construction activities that would be required to construct the barrier wall. Traffic may increase temporarily around the Site under these alternatives due to the daily arrival and departure of the workforce, equipment mobilization/demobilization, and material deliveries. However, these impacts would be expected to largely occur at the beginning or end of each workday (for the arrival/departure of the work force), at the beginning or end of the construction period (for equipment mobilization/demobilization), and at specific times throughout the construction period (for material deliveries). Traffic and noise impacts associated with residual plume management from the Source Control-GWP are expected to be minimal due to the limited amount of construction and operation of the groundwater monitoring wells required.

Construction activities can negatively impact natural resources and habitat near the Site, as well as scenic, historical, and recreational value. Based on a review of the Illinois Department of Natural Resources (IDNR) Historic Preservation Division database and the Illinois State Archaeological Survey database, there are no historic sites located within 1,000 meters of the WAPS (Ramboll, 2021). There would be no impacts under the Source Control-GWP alternative because no additional construction activities would occur. However, negative impacts resulted from construction activities on scenic and recreational value may occur along the Illinois River and within the Donnelley/DePue State Fish and Wildlife Areas complex, under the Source Control-CCS alternative. The Donnelley/DePue State Fish and Wildlife Areas border the Hennepin Site to the north and west and includes DePue Lake, Spring Lake, and Coleman Lake. Under the Source Control-CCS, large cranes, batch plants, and other equipment could be utilized during construction phases. The Illinois River is popular for canoeing and other forms of water recreation (IDNR, 2021). Given the proximity between these areas and the expected construction, it is likely that these areas would experience some adverse impacts such as visual disturbance, obstruction of view, and noise during the construction period. However, these impacts are expected to diminish once the construction is completed in 18 to 24 months for the Source Control-CCS alternative.

In addition, the construction of the cutoff wall under the Source Control-CCS alternative is expected to use a significant amount of cement or bentonite, which would be introduced into the UA and the BCU. The process would use bentonite-based drilling mud with various additives, similar to the methods employed in well drilling but on a notably larger scale. Adding substantial quantities of these materials into the subsurface environment may cause alteration in groundwater pH levels and affect geochemical conditions in the UA.

2.2.6 Time Until Groundwater Protection Standards Are Achieved/Attain the Groundwater Protection Standards Specified in Section 845.600 (IAC Section 845.670(e)(1)(E)/IAC Section 845.680(d)(2))

This section of the report evaluates the time required to achieve GWPSs, pursuant to requirements under IAC Section 845.670(e)(1)(E) (IEPA, 2021) and under IAC Section 845.680(d)(2).

The groundwater movement in the unconsolidated materials is consistent with surface topography and flows north and west near the Site towards the Illinois River, which serves as a large regional hydraulic boundary. Precipitation infiltration recharges groundwater. Under normal post-closure conditions, groundwater flows northward toward the river at the WAPS (Appendix B; Ramboll, 2025b).

The source control activities were completed in 2020. Groundwater modeling was performed in support of the Closure Plan (Geosyntec Consultants, Inc., 2017). The modeling predicted that source control would result in the reduction of leachate production, which facilitates the contraction of the contaminant plume in groundwater (Geosyntec Consultants, Inc., 2017). Additional modeling was conducted for each of the corrective action alternatives to evaluate future groundwater quality in the vicinity of the WAPS as a result of residual plume management (Appendix B; Ramboll, 2025b). The results of the modeling and subsequent evaluation (Appendix E; Geosyntec Consultants, Inc., 2025) indicate that groundwater would attain the GWPSs for all of the constituents[8] identified as having potential groundwater exceedances in the groundwater monitoring network within 29 years under the Source Control-GWP alternative and 38 to 40 years under the Source Control-CCS alternative (5 to 7 years of pre-construction and construction activities followed by 33 years post-construction).[9] Both alternatives are assumed to start after approval of the Corrective Action Plan (Appendix B; Ramboll, 2025a). Table 2.5 summarizes and compares timeline and overall implementation schedule for both alternatives (also discussed in Sections 2.1.1 and 2.1.2).

---

[8] Boron was selected as a surrogate for the contaminant fate and transport simulations to evaluate the effectiveness of each of the corrective action alternative. Boron was detected in the greatest number of WAPS groundwater wells exceeding its GWPS, a statistically significant correlation has been identified between observations of boron in groundwater and observations of lithium and sulfate in groundwater and boron is expected to take the longest time to achieve GWPS. Modeling all constituents that exceed GWPS or have been detected at lower concentrations relative to their GWPSs is unnecessary, as these constituents will likely achieve their GWPSs more quickly (Appendix B; Ramboll, 2025).

[9] As suggested by the site-specific evaluations, some arsenic re-mobilization may occur as groundwater returns to background conditions at the Site, which may cause an impact and result uncertainty to the time to achieve GWPS (Section 2.1.1; Appendix E; Geosyntec Consultants, Inc., 2025).

Table 2.5 Estimated Timeline and Implementation Schedule for Source Control-GWP *vs.* Source Control-CCS

Implementation Phase[a]	Implementation Task	Timeframe	
		Source Control-GWP	Source Control-CCS
1: Pre-Construction Activities[a]	Agency Coordination, Approvals, and Permitting	NA	18 to 24 months
	Final Design and Bid Process		24 to 36 months
	Timeframe to Complete Corrective		42 to 60 months after CAP Approval (3.5 to 5 years)
	Pre-Construction Activities		
2: Corrective Action Construction	Corrective Action Construction	NA	18 to 24 months
	Timeframe to Complete Corrective Action Construction		18 to 24 months
3: Corrective Action O&M and Closeout	Corrective Action Monitoring (Time to Meet GWPS)	348 months (29 years)	396 months (33 years)
	Corrective Action Confirmation Monitoring	36 months	36 months
	Corrective Action Completion Reporting	6 months	6 months
Total Timeline to Complete Corrective Action (After CAP Approval)		390 months (33 years)	438 months (36.5 years)

Notes:
CAP = Corrective Action Plan; NA = Non-applicable; Source Control-CCS = Source Control with Continuous Containment System; Source Control-GWP = Source Control with Groundwater Polishing.
(a) Both corrective action alternatives are assumed to start after the approval of the corrective action plan.
Source: Appendix B; Ramboll, 2025d.

2.2.7 Potential for Exposure of Humans and Environmental Receptors to Remaining Wastes, Considering the Potential Threat to Human Health and the Environment Associated with Excavation, Transportation, Re-disposal, Containment, or Changes in Groundwater Flow (IAC Section 845.670(e)(1)(F))

Section 2.2.1 describes the magnitude of reduction of existing risks under each corrective action alternative. Section 2.2.2 describes the effectiveness of the remedy in controlling the source, including the extent to which containment practices would reduce further releases. Section 2.2.3 describes the likelihood of future releases of CCR occurring under each corrective action alternative, and Section 2.2.5 describes the short-term risks to workers, the community, and the environment during implementation of the remedy, including safety impacts and control of exposure to any residual contamination. In summary, source control measures (*i.e.*, CIP using a consolidate-and-cap approach) was implemented in 2020. Thus, both corrective action alternatives would essentially eliminate the potential for a sudden CCR release to occur post-closure (*e.g.*, a dike failure event) due to the absence of both free liquids and impounded water within the unit, and are equally and fully protective with regard to exposure to residual CCR.

For construction workers, risks arising from potential contact with residual contamination during construction, operation, and maintenance activities associated with residual plume management would be higher for the Source Control-CCS alternative than for the Source Control-GWP alternative, because the Source Control-CCS alternative would involve the excavation and subsequent management of Site spoils. In addition, Source Control-CCS would involve temporarily removing a portion of the final cover previously installed, which could potentially allow stormwater to be in contact with CCR material during construction. CCR-contact stormwater would be generated and managed through CCR-contact stormwater management system under this alternative while a portion of the final cover would be removed. Any potential CCR exposures occurring under Source Control-CCS during the installation of the cutoff would be managed through the use of rigorous safety protocols, personal protective equipment, and appropriate disposal practice. The Source Control-GWP alternative would not involve exposure to either of these soil or groundwater waste streams and thus, there is no potential for exposure of humans and environmental receptors to wastes.

Hydrogeological changes would be expected under the Source Control-CCS alternative, such as altering flow patterns in the UA, redirecting groundwater flow around the cutoff wall, and causing changes to normal hydraulic gradients. However, changes to groundwater flow would not be expected to have an effect on the potential for the exposure of humans and environmental receptors to any wastes.

2.2.8 Long-Term Reliability of the Engineering and Institutional Controls (IAC Section 845.670(e)(1)(G))

Source control (*i.e.*, CIP using a consolidate-and-cap approach) was implemented in 2020. Thus, the long-term reliability of source control would be the same for both corrective action alternatives (Geosyntec Consultants, Inc., 2017). The long-term reliability of the engineering and institutional controls associated with residual plume management of each corrective action alternative are summarized below.

- Residual plume management under the Source Control-GWP alternative would be reliable because it would rely on physical and geochemical processes, rather than the installation, operation, and maintenance of engineered systems or structures. Under this alternative, engineering failure would not occur and no O&M activities would be required to ensure the success of the alternative (other than those required for groundwater monitoring). Active groundwater monitoring would be in place to track the remediation progress. Should the predicted decrease in groundwater concentrations not occur, the adaptive site management approach would enable prompt adjustments or enhancements to the corrective action in accordance with IAC Section 845.680(b). This strategy would allow continuous improvement of the WAPS groundwater remediation in response to new Site information and/or the performance of the corrective action alternative.
- Cutoff walls are proven remedies that have been implemented at many sites. Thus, residual plume management under the Source Control-CCS alternative would be reliable provided it is constructed in accordance with standard design and specifications. The remedy consists of a passive, below-grade physical barrier, which would not require any O&M activities once it is installed. The final cover system would require ongoing maintenance per existing Post-Closure Care Plan but is a durable, engineered structure. Some challenges are expected during construction, necessitating specialized equipment deployment. Since the cutoff wall would be installed through an existing impoundment embankment, additional engineering assessments and monitoring programs would be necessary to the embankment for indications of distress, such as deformation or cracking, throughout the cutoff wall construction process. Appropriate measures would be taken to stabilize the embankment if instability is detected. The construction of the cutoff wall would require temporarily removing a portion of the previously installed WAPS final cover. This procedure may allow additional stormwater to infiltrate the CCR, potentially leading to a temporary reversal of some positive effects that have occurred since the completion of the final cover system in 2020. A CCR-contact stormwater management system would be required to manage and discharge the contact stormwater *via* an NPDES permitted outfall. The effectiveness of the cutoff wall relies on precise construction techniques, demanding ongoing QC. Other challenges include the management of the temporary removal of the already finished final cover system, which would require a contact stormwater management system during this time. However, post-construction QA programs may be required to validate the quality of the constructed cutoff wall. Ongoing

monitoring of the system may be required to ensure reliable operation. Active groundwater monitoring would be in place, similar to the monitoring required under the Source Control-GWP alternative.

- For both corrective action alternatives, remedy optimizations would be implemented if necessary under the adaptive site management.

2.2.9 Potential Need for Replacement of the Remedy (IAC Section 845.670(e)(1)(H))

The potential need for the eventual replacement of the residual plume management remedy under each corrective action alternative is summarized as follows:

- Residual plume management under Source Control-GWP would rely on physical and geochemical processes to achieve reductions in groundwater concentrations to below GWPSs. Because no installation, operation, and maintenance of engineered systems or structures would be required, it would be unlikely that the residual plume management remedy under the Source Control-GWP alternative would need to be replaced. Adaptive site management strategies would be used to implement remedy optimizations or replacement, as necessary based on data that are collected, to ensure that remedial goals are achieved.
- Residual plume management under Source Control-CCS would rely on a cutoff wall as a physical barrier to contain the CCR mass within the WAPS and achieve reductions in groundwater concentrations to below GWPSs. The deep cutoff wall is a robust, engineered, and maintenance-free subsurface structure. The final cover system portion of this alternative would need ongoing maintenance per the IEPA approved Post-Closure Care Plan, but it is a passive and engineered structure that is unlikely to need replacement. Therefore, it is unlikely that the residual plume management remedy under the Source Control-CCS alternative would need to be replaced. Adaptive site management strategies would be used to implement remedy optimizations or replacement, as necessary based on data that are collected, to ensure that remedial goals are achieved.

2.3 The Ease or Difficulty of Implementing a Remedy (IAC Section 845.670 (e)(3))

2.3.1 Degree of Difficulty Associated with Constructing the Remedy (IAC Section 845.670(e)(3)(A))

Source control (*i.e.*, CIP using a consolidate-and-cap approach) was implemented in 2020. Thus, there would be no further construction difficulties associated with source control. The expected degree of difficulty associated with residual plume management for each of the corrective action alternatives is summarized below.

- Residual plume management under the Source Control-GWP alternative would rely on physical and geochemical attenuation processes and therefore would not pose any significant construction challenges. Therefore, there would be minimal difficulty in constructing the Source Control-GWP remedy.
- Residual plume management under the Source Control-CCS alternative would rely on a continuous containment system to enclose the CCR within the WAPS, and physical and geochemical

attenuation processes to address downgradient groundwater quality impacts. However, it may have the following challenges during construction of the cutoff wall (Appendix B; Ramboll, 2025a):

- Implementing the remedy entails the mobilization of specialized equipment to the Site, including large cranes, clamshells, and slurry cutters, *etc*. Supporting equipment such as batch plants, excavation, and grading equipment may also be used.
- Although cutoff walls are commonly constructed to similar depths in comparable geologic environments, challenges during the cutoff wall's construction may still arise. These challenges may involve encountering highly permeable layers (leading to slurry loss), obstructions that necessitate specialized techniques and/or equipment for progression, or sidewall instability. These challenges could be particularly significant at the WAPS due to the presence of boulders and cobbles in the subsurface soils. While these challenges could be managed during cutoff wall construction, they may lead to potential schedule delays.
- The cutoff wall would be installed through an existing impoundment embankment, which is a dam regulated by IDNR. Therefore, additional engineering assessments and monitoring programs would be necessary to monitor the embankment for indications of distress, such as deformation or cracking, throughout the cutoff wall construction process. Appropriate measures would be taken to stabilize the embankment if instability is detected.
- The construction of the cutoff wall would require temporarily removing a portion of the previously installed WAPS final cover in areas where conflict with the cutoff wall. This procedure may allow additional stormwater to infiltrate the CCR, potentially leading to a temporary reversal of some positive effects that have occurred since the completion of the final cover system in 2020. A CCR-contact stormwater management system would be required to manage and discharge the contact stormwater *via* an NPDES permitted outfall.
- The effectiveness of the cutoff wall relies on the construction techniques employed to prevent gaps, voids, or other discontinuities in the structure. Ongoing QC is essential during construction as part of QA activities to prevent such defective features. Additionally, QA programs, such as coring and testing, may be necessary to validate the quality of the constructed barrier.
- The performance of the wall is contingent on its actual hydraulic conductivity. This necessitates ongoing monitoring and QA/QC testing for slurry mixing, placement, or soil-bentonite mixing. The goal is to ensure adherence to the designed mix and involves routine testing of samples from the wall material.

2.3.2 Expected Operational Reliability of the Remedy (IAC Section 845.670(e)(3)(B))

Source control (*i.e.*, CIP using a consolidate-and-cap approach) was implemented in 2020. Thus, the operational reliability of the remedy would be the same for both corrective action alternatives. Both corrective action alternatives would likely be highly reliable with respect to operational controls associated with residual plume management; specific details for each corrective action alternative are discussed below.

- Residual plume management under the Source Control-GWP alternative would have high operational reliability because it would rely on physical and geochemical processes and active monitoring, rather than the installation, operation, and maintenance of engineered systems or structures (other than monitoring wells). Under the Source Control-GWP alternative, engineering failure would not occur, and no O&M activities would be required to ensure the success of the alternative. However, it should be noted that some arsenic re-mobilization may occur as groundwater returns to background conditions at WAPS, which may cause an impact to the time to achieve GWPS (Appendix E; Geosyntec Consultants, Inc., 2025).

- Residual plume management under the Source Control-CCS alternative would also have high operational reliability, because it is an established remedial technology, as long as it is constructed in accordance with standard design specifications for barrier walls, and the final cover system is maintained according to the existing Post-Closure Care Plan. This continuous containment system would provide full lateral (*i.e.*, through the deep cutoff wall), surface (*i.e.*, through the existing cover) isolation of CCR from the surrounding environment. The wall would be keyed into competent shale bedrock to provide additional subsurface containment below the WAPS. However, the remedy would require the temporary removal of a portion of the completed cover over the WAPS and potentially cause additional stormwater to percolate into the CCR and result in a temporary reversal of certain positive effects that have occurred since the completion of source control in 2020. These temporary impacts would diminish once the final cover system is repaired, and the continuous containment system would be present.
- Adaptive site management strategies would be used to implement remedy optimizations, if necessary under both corrective action alternatives.

2.3.3 Need to Coordinate with and Obtain Necessary Approvals and Permits from Other Agencies (IAC Section 845.670(e)(3)(C))

Both corrective action alternatives would require regulatory approvals. Specific permits and approvals associated with source control were the same for both corrective action alternatives and were discussed in the Closure Plan (Geosyntec Consultants, Inc., 2017). The specific approvals and permits associated with residual plume management for both corrective action alternatives are discussed below.

- The Source Control-GWP alternative would not need additional permits from other agencies, other than the approval of the eventual Corrective Action Plan.
- The Source Control-CCS alternative would require approvals and permits, including construction stormwater controls and BMPs, a joint water pollution control construction and operating permit. An IDNR Dam Safety modification permit would also be required for modifications of the WAPS embankment. A modification to the existing NPDES permit would be necessary to discharge the CCR-contact stormwater generated during the construction phase. These permits and plans typically take 18 to 24 months to obtain.

2.3.4 Availability of Necessary Equipment and Specialists (IAC Sections 845.670(e)(3)(D) and 845.660(c)(1), "Ease of Implementation")

Source control (*i.e.*, CIP using a consolidate-and-cap approach) was implemented in 2020. Thus, there are no further equipment and specialist needs associated with the implementation of the source control remedy. Specialized equipment and personnel are essential for field data collection and groundwater sampling for residual plume management under both potential corrective action alternatives. Additionally, the assessment of groundwater concentrations for Site constituents would necessitate laboratory equipment and specialists for both alternatives. The availability of equipment and specialists for each corrective action alternative is summarized below.

- Residual plume management under the Source Control-GWP alternative would require groundwater professionals, such as geologists, hydrogeologists, statisticians, and geochemists to conduct statistical analyses, ensuring that natural geochemical processes functions as anticipated in this alternative. The equipment and specialists needed for Site groundwater monitoring and analysis are currently engaged in these tasks as part of the routine groundwater monitoring program outlined in accordance with IAC Section 845.220(c)(4).

- Residual plume management under the Source Control-CCS alternative would require specialists for the construction phase of the cutoff wall.
    - Building the cutoff wall requires the expertise of a specialized contractor with a background in constructing similar types of walls in comparable geologic environments, like those found in the Illinois, Mississippi, and Ohio River Valleys. The contractor would probably need specialized equipment, including large cranes, clamshell buckets, slurry cutters, batch plants, or other equipment.
    - Specialists involved in the design and construction of cutoff walls would be essential during both phases. This team of specialists should include design engineers, construction managers, and contractor staff with expertise in cutoff wall construction and equipment operation.
    - Monitoring the WAPS embankments during cutoff wall construction would require expertise in geotechnical instrumentation, including the use of inclinometers, survey prisms, vibrating wire piezometers, and visual inspection for signs of distress. Specialized drilling and installation contractor would be needed to construct the geotechnical instrumentation system.
    - The types of equipment and specialists should have been employed for projects similar to designing and building cutoff walls. However, there may be backlogs associated with the equipment and specialists, due to the high existing demand for specialty ground improvement contractors and design specialists who are engaged with similar projects in sectors like electric utilities, dams/levees, and other areas.
    - Equipment and experts with geosynthetics design and installation, specifically with seaming new geosynthetics to an existing final cover system, would be required for the final cover system restoration. However, the experts and equipment's availability could be limited due to the high existing backlog due to ongoing projects in the solid waste management, electric utility, and other areas.
    - This alternative would also require the use of equipment and the expertise of specialists for tasks such as field data collection, groundwater sampling, groundwater sample analysis, and periodic corrective action groundwater monitoring and reporting. Similar to those in the Source Control-GWP alternative, these activities are already being conducted as part of routine groundwater monitoring in accordance with IAC Section 845.220(c)(4).

2.3.5 Available Capacity and Location of Needed Treatment, Storage, and Disposal Services/Comply with Standards for Management of Wastes as Specified in Section 845.680(d) (IAC Section 845.670(e)(3)(D)/IAC Section 845.670(d)(5))

The available capacity and location of needed treatment, storage, and disposal services associated with residual plume management under each corrective action alternative is summarized below. All the practices employed in the three alternatives would comply with standards for the management of wastes as specified in IAC Section 845.670(e)(3)(D) and IAC Section 845.680(d)(5).

- Residual plume management for the Source Control-GWP remedy would not require any treatment, storage, or disposal services, because groundwater polishing (GWP) is not anticipated to produce a substantial amount of waste or wastewater, aside from minor purge water volumes generated during routine groundwater sampling activities for residual plume management. This could be managed by a standard waste management contractor.

- Residual plume management for the Source Control-CCS alternative would generate waste during the cutoff wall construction phase, which would include geosynthetics and other debris from removing the final cover system, cutoff wall spoils and contact stormwater.
  - Geosynthetics and other debris would be disposed of in an off-Site landfill that has sufficient volume to receive the relatively small amount of waste materials.
  - CCR-impacted cutoff wall spoils would be temporarily staged on-Site and then disposed either off-Site or beneficially used on-Site as compacted contouring fill beneath the East Ash Pond final cover system. The later disposal would require coordination with the East Ash Pond closure activities.
  - Non CCR-impacted spoils would be disposed of at an appropriate on-Site location.
  - CCR-contact stormwater generated during construction would be pumped to the on-Site treatment pond and then discharged *via* an NPDES permitted outfall.
  - No wastes would be expected to be generated after the cutoff wall is installed, and consequently, no additional treatment, storage, or disposal services would be necessary for this remedy.

2.4 The Degree to Which Community Concerns Are Addressed by the Remedy (IAC Section 845.670(e)(4))

Several nonprofits raised concerns regarding the potential impacts of the WAPS on groundwater and surface water quality (Earthjustice *et al*., 2018; Sierra Club and CIHCA, 2014). The combination of source control (*i.e.*, CIP using a consolidate-and-cap approach) and residual plume management would cause groundwater concentrations to decline over time under all of the corrective action alternatives, as suggested by the groundwater modeling (Geosyntec Consultants, Inc., 2017; Appendix B; Ramboll, 2025b), thus addressing these concerns.

A public meeting will be held on April 8, 2025, pursuant to requirements under IAC Section 845.710(e). Questions raised by attendees will be answered at the meeting; subsequently, a written summary of all questions and responses will be made available to interested parties.

2.5 Remove from the Environment as Much of the Contaminated Material that Was Released from the CCR Surface Impoundment as Is Feasible, Taking into Account Factors such as Avoiding Inappropriate Disturbance of Sensitive Ecosystems (IAC Section 845.670(d)(4))

There have been no known releases of CCR at the WAPS (Ramboll, 2025e). Both potential corrective action alternatives include source control and would have residual plume management efforts. The source control included the consolidation of CCR excavated from the OWPP into the OWAP portion of the WAPS and the installation of a low-permeability final cover system designed to limit the infiltration of precipitation into the impounded CCR. Groundwater modeling was performed in support of the Closure Plan (Geosyntec Consultants, Inc., 2017) predicted that source control would result in the reduction of leachate production, a decrease in CCR leachate constituent concentrations, and a contraction of the groundwater contaminant plume (Geosyntec Consultants, Inc., 2017). Due to the reduction in the hydraulic flux out of the WAPS, the mass flux out of the WAPS would also be controlled. Therefore, source control is preventing further releases of CCR constituents into the environment.

Moreover, residual plume management under each corrective action alternative will further result in the removal of contaminated material from the environment and/or the improvement of downgradient groundwater quality. Groundwater modeling has predicted that GWPSs would be achieved in all monitoring wells within 29 years, and 38 to 40 years (33 years as suggested by groundwater modeling and 5 to7 years of pre-construction under the Source Control-GWP and Source Control-CCS alternatives, respectively, assuming both alternatives start after approval of the corrective action plan) (Appendix B; Ramboll, 2025a). Specific considerations for residual plume management for each alternative are provided below.

- Residual plume management under the Source Control-GWP alternative would address impacted groundwater by relying on physical and geochemical attenuation processes to reduce the residual concentrations of CCR. Site-specific evaluations have shown that groundwater polishing would reduce the groundwater concentrations and mobility of inorganic contaminants (including boron and sulfate), through physical and geochemical attenuation mechanisms, especially after the implementation of source control (Appendix E; Geosyntec Consultants, Inc., 2025). However, it should be noted some arsenic re-mobilization may occur as groundwater returns to background conditions at WAPS, which may cause an impact to the time required to achieve GWPS (Appendix E; Geosyntec Consultants, Inc., 2025). In cases in which observed groundwater concentrations deviate significantly from modeled conditions, alternative methods or techniques to remove residual contamination to achieve the GWPSs would be evaluated under the adaptive site management, and if viable, incorporated as per IAC Section 845.680(b). No ecosystems would be disturbed because no construction activities are expected under the Source Control-GWP alternative.
- Residual plume management under the Source Control-CCS alternative would employ the cutoff wall which would be incorporated into the final WAPS cover system to create a continuous low-permeability barrier that fully contains the CCR within the WAPS. This system ensures isolation from the surrounding environment through lateral containment by the deep cutoff wall, surface containment by the existing geomembrane cover, and a natural barrier provided by the competent shale bedrock below. The temporary removal of a portion of the final cover system implemented during closure in 2020 would occur during construction, which would generate CCR-contact stormwater that would be managed appropriately. These construction activities may cause some negative impacts on natural resources and habitat located atop the WAPS final cover system and near the Site. However, the total duration of the construction is expected to be 18 to 24 months, so any construction-related impacts to ecosystems would be limited to the short term and would diminish once construction is completed.
- Although both corrective action alternatives include source control and residual plume management, Source Control-CCS would be more effective at controlling sources of releases than Source Control-GWP for the WAPS.

2.6 Summary

This CAAA evaluates both corrective action alternatives identified as potentially viable in the CMA with regard to each of the factors specified in IAC Section 845.670(d) and 845.670(e) (IEPA, 2021). Based on this evaluation, the most appropriate corrective action for this Site is Source Control-CCS.

Although the expected impacts on workers, nearby communities, and the environment under the Source Control-GWP alternative are lower than the Source Control-CCS alternative, the Source Control-CCS alternative would provide full containment of the CCR within WAPS and be more effective at controlling sources of releases than Source Control-GWP. Controlling the source of releases using CCS is particularly important at this Site because of the high groundwater transmissivity associated with the sands and gravels in the UA. Thus, Source Control-CCS is the most appropriate corrective action alternative for the WAPS.

References

Buscher, WE. [Illinois Environmental Protection Agency (IEPA)]. 2018. "Letter to P. Morris (Luminant) [re: Approval of Closure and Post-Closure Care Plan for the Hennepin Power Station Old West Ash Pond and Old West Polishing Pond]." 1p., June 19.

Earthjustice; Prairie Rivers Network; Environmental Integrity Project (EIP); Sierra Club. 2018. "Cap and Run: Toxic Coal Ash Left Behind by Big Polluters Threatens Illinois Water." 45p.

Geosyntec Consultants, Inc. 2017. "Closure and Post-Closure Care Plan: Old West Ash Pond, Old West Polishing Pond at Dynegy Midwest Generation, LLC Hennepin Power Station, 13498 East 800th Street, Hennepin, Illinois, 63127." Report to Dynegy Midwest Generation, LLC, Collinsville, IL. 1289p., December 20.

Geosyntec Consultants, Inc. 2025. "Groundwater Polishing Evaluation Report, Hennepin Power Plant - West Ash Pond System (IEPA ID No. 804) (Draft)." Report to Dynegy Midwest Generation, LLC, Collinsville, IL. February.

Gradient. 2025. "Human Health and Ecological Risk Assessment, West Ash Pond System, Hennepin Power Plant, Hennepin, Illinois (Draft)." 45p.

Hesterberg, TW; Valberg, PA; Long, CM; Bunn, WB III; Lapin, C. 2009. "Laboratory studies of diesel exhaust health effects: Implications for near-roadway exposures." *EM Mag.* (August):12-16. Accessed at http://pubs.awma.org/gsearch/em/2009/8/hesterberg.pdf.

HookandBullet.com. 2021. "Lyons Lake fishing near DePue, Illinois." Accessed at https://www.hookandbullet.com/fishing-lyons-lake-depue-il/.

Illinois Dept. of Natural Resources (IDNR). 2021. "Illinois River." Division of Fisheries. Accessed at https://www.ifishillinois.org/profiles/Illinois.php.

Illinois Environmental Protection Agency (IEPA). 2011. "Final NPDES Permit, Dynegy Midwest Generation, Inc. Hennepin Power Station." Submitted to Dynegy Midwest Generation, Inc., O'Fallon, IL. NPDES Permit No. IL0001554, 19p., May 24.

Illinois Environmental Protection Agency (IEPA). 2019. "Appendix A-1. Illinois' 2018 303(d) List and Prioritization." In "Illinois Integrated Water Quality Report and Section 303(d) List, 2018 (Final as submitted to US EPA Region V on February 22, 2021)." 40p., May 20. Accessed at https://www2.illinois.gov/epa/topics/water-quality/watershed-management/tmdls/Documents/Appendix%20A-1_303d_by_priority_FINAL_5-20-19.pdf.

Illinois Environmental Protection Agency (IEPA). 2021. "Standards for the disposal of coal combustion residuals in surface impoundments." Accessed at https://www.ilga.gov/commission/jcar/admincode/035/03500845sections.html.

Illinois Environmental Protection Agency (IEPA). 2022. "Appendix A-1. Specific Assessment Information for Streams, 2020/2022." In "Illinois Integrated Water Quality Report and Section 303(d) List, 2020/2022." Bureau of Water. 103p., May 26. Accessed at https://www2.illinois.gov/epa/topics/water-quality/watershed-management/tmdls/Documents/A1_Streams_FINAL_5-26-22.pdf.

Illinois River Road National Scenic Byway. 2021. "DePue Lake." Accessed at https://www.illinoisriverroad.org/places/united-states/illinois/depue/nature-outdoor-recreation/depue-lake/.

Lydersen, K. 2017. "Citizens fill void in oversight of potentially hazardous Illinois coal ash impoundments." *Energy News Network* January 20. Accessed at https://energynews.us/2017/01/20/citizens-fill-void-in-oversight-of-potentially-hazardous-illinois-coal-ash-impoundments/.

Mauderly, JL; Garshick, E. 2009. "Diesel exhaust." In *Environmental Toxicants: Human Exposures and Their Health Effects (Third Edition)*. (Ed.: Lippmann, M), John Wiley & Sons, Inc., Hoboken, NJ. p551-631.

National Research Council. 2013. "Alternatives for Managing the Nation's Complex Contaminated Groundwater Sites." Division of Earth and Life Sciences, Water Science and Technology Board, Committee on Future Options for Management in the Nation's Subsurface Remediation Effort. National Academies Press, Washington, DC, 422p. Accessed at http://www.nap.edu/catalog.php?record_id=14668.

OBG, Part of Ramboll. 2019. "Corrective Measures Assessment, Old West Ash Pond (Pond No. 1 and Pond No. 3) and Polishing Pond, Hennepin Power Station, 13498 East 800th Street, Hennepin, Illinois." Report to Dynegy Midwest Generation, LLC. 31p., September 5.

Ramboll. 2018-2020. "Final Closure and Post-Closure Plans for Hennepin East Ash Ponds No. 2 & No. 4." Report to Dynegy Midwest Generation, LLC. 1903p.

Ramboll. 2021. "Hydrogeologic Site Characterization Report, East Ash Pond, Hennepin Power Plant, Hennepin, Illinois (Final)." Report to Dynegy Midwest Generation, LLC. 342p., October 25.

Ramboll. 2024a. "35 I.A.C. § 845 Corrective Measures Assessment, Hennepin Power Plant, West Ash Pond System, IEPA ID: W1550100002-01 and W1550100002-03 (Final)." Report to Dynegy Midwest Generation, LLC. 34p., May 8.

Ramboll. 2024b. "Nature and Extent Report, Hennepin Power Plant, West Ash Pond System, IEPA ID No. W1550100002-01 and W1550100002-03 (Final)." Report to Dynegy Midwest Generation, LLC (Hennepin, IL). 232p., May 8.

Ramboll. 2025a. "Corrective Action Alternatives Analysis Supporting Information Report: Hennepin Power Station, West Ash Pond System, IEPA ID No. W1550100002-01 and W1550100002-03 (Final Draft)." Report to Dynegy Midwest Generation, LLC (Hennepin, IL)., March 7.

Ramboll. 2025b. "Groundwater Modeling Technical Memorandum, West Ash Pond System, Hennepin Power Plant, Hennepin, Illinois, IEPA ID No. W1550100002-01 and W1550100002-03 (Draft)." Report to Dynegy Midwest Generation, LLC. March 7.

Ramboll. 2025c. "Corrective Action Groundwater Monitoring Plan: Hennepin Power Plant, West Ash Pond System, IEPA ID No. W1550100002-01 and W1550100002-03 (Draft)." Report to Dynegy Midwest Generation, LLC, Hennepin, IL. March 7.

Ramboll. 2025d. "Corrective Measures Alternatives Analysis Supporting Information Report, Newton Power Plant, Primary Ash Pond, IEPA No. W0798070001-1 (Final Draft)." Report to Illinois Power Generating Co., Newton, IL. February 2.

Ramboll. 2025e. "Corrective Action Plan: Dynegy Midwest Generation, LLC, Hennepin Power Stations, West Ash Pond System, IEPA ID No. W1550100002-01 and W1550100002-03 (Draft)." Report to Vistra Energy, dba Dynegy Midwest Generation, LLC, Hennepin, IL., March 7.

Sierra Club. 2021. "Sierra Club statement on Joppa closure and settlement agreement with Vistra Energy." April 7. Accessed at https://www.sierraclub.org/press-releases/2021/09/sierra-club-statement-joppa-closure-and-settlement-agreement-vistra-energy.

Sierra Club; Central Illinois Healthy Community Alliance (CIHCA). 2014. "Dynegy's Toxic Assets: Legacy Coal Pollution in the Heartland." 17p.

Tickner, D. [Dynegy Midwest Generation, LLC]. 2020a. "Letter to D. LeCrone (IEPA) [re: Notification of completion of closure: Hennepin Power Station; Old West Ash Pond, Ash Pond No. 2]." 3p. December 17.

Tickner, D. [Dynegy Midwest Generation, LLC]. 2020b. "Letter to D. LeCrone (IEPA) [re: Notification of completion of closure: Hennepin Power Station; Old West Polishing Pond]." 2p., December 17.

US Dept. of Labor (US DOL). 2020a. "Fatal occupational injuries, total hours worked, and rates of fatal occupational injuries by selected worker characteristics, occupations, and industries, civilian workers, 2019." Bureau of Labor Statistics, December. Accessed at https://www.bls.gov/iif/oshwc/cfoi/cfoi_rates_2019hb.xlsx.

US Dept. of Labor (US DOL). 2020b. "Table R100. Incidence rates for nonfatal occupational injuries and illnesses involving days away from work per 10,000 full-time workers by occupation and selected events or exposures leading to injury or illness, private industry, 2019." Bureau of Labor Statistics, October. Accessed at https://www.bls.gov/iif/oshwc/osh/case/cd_r100_2019.xlsx.

US Dept. of Transportation (US DOT). 2023. "Large Truck and Bus Crash Facts 2021." Federal Motor Carrier Safety Administration, Analysis Division, FMCSA-RRA-23-002, 118p., November.

US EPA. 2014. "Human and Ecological Risk Assessment of Coal Combustion Residuals (Final)." Office of Solid Waste and Emergency Response (OSWER), Office of Resource Conservation and Recovery. Submitted to US EPA Docket. EPA-HQ-OLEM-2020-0107-0885, 1237p., December.

US EPA. 2015a. "Hazardous and solid waste management system; Disposal of coal combustion residuals from electric utilities (Final rule)." *Fed. Reg.* 80(74):21302-21501. 40 CFR 257, 40 CFR 261, April 17.

US EPA. 2015b. "Use of Monitored Natural Attenuation for Inorganic Contaminants in Groundwater at Superfund Sites." Office of Solid Waste and Emergency Response (OSWER), OSWER Directive 9283.1-36, 83p., August.

US Geological Survey (USGS). 2024. "USGS National Watershed Boundary Dataset (WBD)." April. Accessed on April 2, 2024 at https://hydro.nationalmap.gov/arcgis/rest/services/wbd/MapServer.

Appendix A

2024 Human Health and Ecological Risk Assessment

Human Health and Ecological Risk Assessment
West Ash Pond System
Hennepin Power Plant
Hennepin, Illinois

March 7, 2025

GRADIENT

www.gradientcorp.com
One Beacon Street, 17th Floor
Boston, MA 02108
617-395-5000

Table of Contents

Page

List of Tables

List of Figures

Abbreviations

ADI	Acceptable Daily Intake
BCF	Bioconcentration Factor
BCU	Bedrock Confining Unit
CAAA	Corrective Action Alternative Analysis
CCR	Coal Combustion Residual
CEM	Conceptual Exposure Model
CIP	Closure-In-Place
COI	Constituent of Interest
COPC	Constituent of Potential Concern
CSF	Cancer Slope Factor
CSM	Conceptual Site Model
CWS	Community Water Supply Well
DMG	Dynegy Midwest Generation
ESV	Ecological Screening Value
GWPS	Groundwater Protection Standards
GWQS	Groundwater Quality Standards
HPP	Hennepin Power Plant
HTC	Human Threshold Criteria
IAC	Illinois Administrative Code
ID	Identification
IEPA	Illinois Environmental Protection Agency
ISGS	Illinois State Geological Survey
MCL	Maximum Contaminant Level
NRWQC	National Recommended Water Quality Criteria
ORNL RAIS	Oak Ridge National Laboratory's Risk Assessment Information System
OWAP	Old West Ash Pond
OWPP	Old West Polishing Pond
PWS	Public Water System
RfD	Reference Dose
RME	Reasonable Maximum Exposure
RSL	Regional Screening Level
SDWIS	Safe Drinking Water Information System
SWQS	Surface Water Quality Standards
TDS	Total Dissolved Solids
TEC	Threshold Effect Concentration
UAU	Uppermost Aquifer Unit
US DOE	United States Department of Energy
US EPA	United States Environmental Protection Agency
USGS	US Geological Survey
WAPS	West Ash Pond System

1 Introduction

Dynegy Midwest Generation (DMG) Company's Hennepin Power Plant (HPP, or "the Site") is an electric power-generating facility with coal-fired units located in Hennepin, Illinois. The facility began operations in the early 1950s and was retired in 2019 (Ramboll, 2021). The HPP produced and stored coal combustion residuals (CCRs) as a part of its historical operations in several CCR ash ponds. Ponds located east of the power plant include East Ash Pond No. 2, East Ash Pond No. 4, East Ash Pond, Leachate Pond, and Polishing Pond. The West Ash Pond System (WAPS) consists of the Old West Ash Pond (OWAP, which includes Pond No. 1 and Pond No. 3) and Old West Polishing Pond (OWPP) (Vistra identification [ID] number [No.] 804, Illinois Environmental Protection Agency [IEPA] ID No. W1550100002-01 and W1550100002-03), and is the subject of this report.

This report presents the results of an evaluation that characterizes potential risk to human and ecological receptors that may be exposed to CCR constituents in environmental media potentially impacted by the WAPS. This risk evaluation was performed to support the Corrective Action Alternative Analysis (CAAA) for the WAPS in accordance with requirements in Title 35 Part 845.670 of the Illinois Administrative Code (IAC) (IEPA, 2021). Human and ecological risks were evaluated for Site-specific constituents of interest (COIs). The conceptual site model (CSM) assumed that Site-related COIs in groundwater may migrate to the Illinois River and affect surface water and sediment in the vicinity of the Site.

Consistent with United States Environmental Protection Agency (US EPA) guidance (US EPA, 1989), this report uses a tiered approach to evaluate potential risks, including the following steps:

1. Identify complete exposure pathways and develop a conceptual exposure model (CEM).
2. Identify Site-related COIs: Constituents detected in groundwater were considered COIs if their maximum detected concentration over the period from 2015 to 2021 exceeded a groundwater protection standard (GWPS), identified in Part 845.600 (IEPA, 2021), or a relevant surface water quality standard (IEPA, 2019a; US EPA Region IV, 2018).
3. Perform screening-level risk analysis: Compare maximum measured or modeled COI concentrations in surface water and sediment to conservative, health-protective benchmarks to determine constituents of potential concern (COPCs).
4. Perform refined risk analysis: If COPCs are identified, perform a refined analysis to evaluate potential risks associated with the COPCs.
5. Formulate risk conclusions and discuss any associated uncertainties.

This assessment relies on a conservative (*i.e.*, health-protective) approach and is consistent with the risk approaches outlined in US EPA guidance. Specifically, we considered evaluation criteria detailed in IEPA guidance documents (*e.g.*, IEPA, 2013, 2019a), incorporating principles and assumptions consistent with the Federal CCR Rule (US EPA, 2015a) and US EPA's "Human and Ecological Risk Assessment of Coal Combustion Residuals" (US EPA, 2014).

US EPA has established acceptable risk metrics. Risks above these US EPA-defined metrics are termed potentially "unacceptable risks." Based on the evaluation presented in this report, no unacceptable risks to human and ecological receptors resulting from CCR exposures associated with the WAPS were identified. Specific risk assessment results include the following:

- No completed exposure pathways were identified for any groundwater receptors; consequently, no risks were identified relating to the use of groundwater.
- No unacceptable risks were identified for recreators swimming or boating in the Illinois River adjacent to the Site.
- No unacceptable risks were identified for recreators exposed to sediment in the Illinois River adjacent to the Site.
- No unacceptable risks were identified for anglers consuming locally caught fish.
- No unacceptable risks were identified for ecological receptors exposed to surface water or sediment.
- No bioaccumulative ecological risks were identified.

It should be noted that this evaluation incorporates a number of conservative assumptions that tend to overestimate exposure and risk. Moreover, it should be noted that because current conditions do not present a risk to human health or the environment, there will also be no unacceptable risk to human health or the environment for future conditions because the WAPS was already closed in 2020. For all future closure scenarios, potential releases of CCR-related constituents will decline over time and consequently potential exposures to CCR-related constituents in the environment will also decline.

2 Site Overview

2.1 Site Description

The HPP is located four miles northeast of the Village of Hennepin in north central Illinois in Putnam County. The HPP property is bordered on the north by the Illinois River, on the south and east by industrial properties, and on the west by agricultural land. The Illinois River flows past the facility from east to west.

The CCR ash ponds located to the west of the power plant include the OWAP and the OWPP, collectively known as the WAPS (OBG, 2019) (Figure 2.1). The WAPS was closed in 2020 using closure-in-place (CIP) with a consolidate-and-cap approach, which included "removal of CCR and dike soils in the OWPP and consolidation of these materials into the OWAP" (OBG, 2019), and "capping [the OWAP] with a geosynthetic and soil final cover system" (Ramboll, 2024a). The WAPS is the subject of this report.

2.2 Geology/Hydrogeology

The geology underlying the Site in the vicinity of the WAPS consists of unlithified deposits of the Cahokia Alluvium and the Henry Formation, underlain by a thick shale bedrock (NRT, 2017; OBG, 2019). The Cahokia Alluvium consists of fine-grained silt, clay, and sand, whereas the underlying Henry Formation is composed of highly permeable sand and gravel (NRT, 2017; OBG, 2019). The Cahokia Alluvium deposits are absent in the eastern portion of the WAPS; in this area, the WAPS lies directly over Henry Formation (OBG, 2019). The thickness of the Cahokia Alluvium in the western part of the WAPS ranges from 10 to 40 ft (NRT, 2017). The Henry formation ranges from 5 to 35 ft thick (NRT, 2017).

Three distinct hydrostratigraphic units have been identified in the area near the WAPS (NRT, 2017; OBG, 2019):

- **Fill Unit:** The Fill Unit directly underlies the WAPS. It is comprised primarily of fly ash, with small amounts of bottom ash and slag mixed with sand, silt, and clay. During closure of the OWPP in 2020, CCRs in the ash pond and one foot of soils below the ash pond were removed.
- **Uppermost Aquifer Unit (UAU):** The UAU is comprised of mixed alluvial deposits (classified as Cahokia alluvium consisting of clay, silt, and sand) and coarser grained outwash sand and gravel deposits (classified as Henry Formation).
- **Bedrock Confining Unit (BCU):** The BCU consists of Pennsylvanian age shale bedrock with minor layers of limestone, sandstone, and coal. This low permeability unit defines the lower boundary of the Uppermost Aquifer Unit at the WAPS.

The Illinois River, located less than 0.1 mile north of the WAPS, is the major surface water body in the area. Groundwater in the UAU predominantly flows to the north/northwest, consistent with the surface topography, into the Illinois River (OBG, 2019). Prior to the closure during the impoundment operations, substantial local recharge to groundwater from sluicing of ash created radial flow conditions near the Site (Ramboll, 2024a). A groundwater flow reversal (*i.e.*, groundwater flows in a south to southwest direction toward the wetlands) may occur during high river stages or flooding events when the Illinois River stage elevation is higher than surrounding groundwater elevations. The normal horizontal hydraulic gradient near the WAPS is approximately 0.005 ft/ft (NRT, 2017; OBG, 2019). Under normal post-closure conditions, groundwater flows northward toward the river from the WAPS (Ramboll, 2024a). The low permeability bedrock aquitard acts as a barrier to downward migration of groundwater from the UAU (NRT, 2017).

2.3 Conceptual Site Model

A CSM describes sources of contamination, the hydrogeological units, and the physical processes that control the transport of water and solutes. In this case, the CSM describes how groundwater underlying the WAPS migrates and interacts with surface water and sediment in the adjacent Illinois River. The CSM was developed using available hydrogeological data (NRT, 2017; OBG, 2019; USGS, 2021a; Tetra Tech, 2012), including information on groundwater flow and surface water characteristics.

The highly permeable Henry Formation of the UAU, consisting of sands and gravels, is the primary conduit for groundwater flowing into the Illinois River (Ramboll, 2021). The downward groundwater migration from the UAU to underlying units is significantly limited due to the presence of thick, low-permeability shale bedrock, which acts as a confining layer (NRT, 2017). Other than flow into the Illinois River, no other potential groundwater transport pathways have been identified for the UAU (NRT, 2017). Because the Illinois River is a large regional hydraulic boundary (*i.e.*, serves as a sink for groundwater discharges in the area), all shallow groundwater underlying the WAPS is expected to flow into the river.

Near the WAPS, groundwater flowing into the Illinoi River mixes with surface water. During mixing, dissolved constituents in groundwater may partition between sediments and surface water.

Figure 2.1 Site Location Map. Source: Ramboll (2025).

2.4 Groundwater Monitoring

Thirteen wells screened in the UAU have been used to monitor the groundwater quality near and downgradient of the WAPS (Table 2.1). The analyses presented in this report relied on all available data from the 13 wells collected between 2018 and 2023. Groundwater samples were analyzed for a suite of metals, both total and dissolved, specified in Illinois CCR Rule Part 845.600 (IEPA, 2021).[1] A summary of the groundwater data used in this risk evaluation is presented in Table 2.2. The WAPS-related well locations are shown in Figure 2.2. The use of groundwater data in this risk evaluation does not imply that detected constituents are associated with the WAPS or that they have been identified as potential groundwater exceedances.

---

[1] Samples were analyzed for a longer list of inorganic constituents and general water quality parameters (chloride, fluoride, sulfate, and total dissolved solids), but these constituents were not evaluated in the risk evaluation.

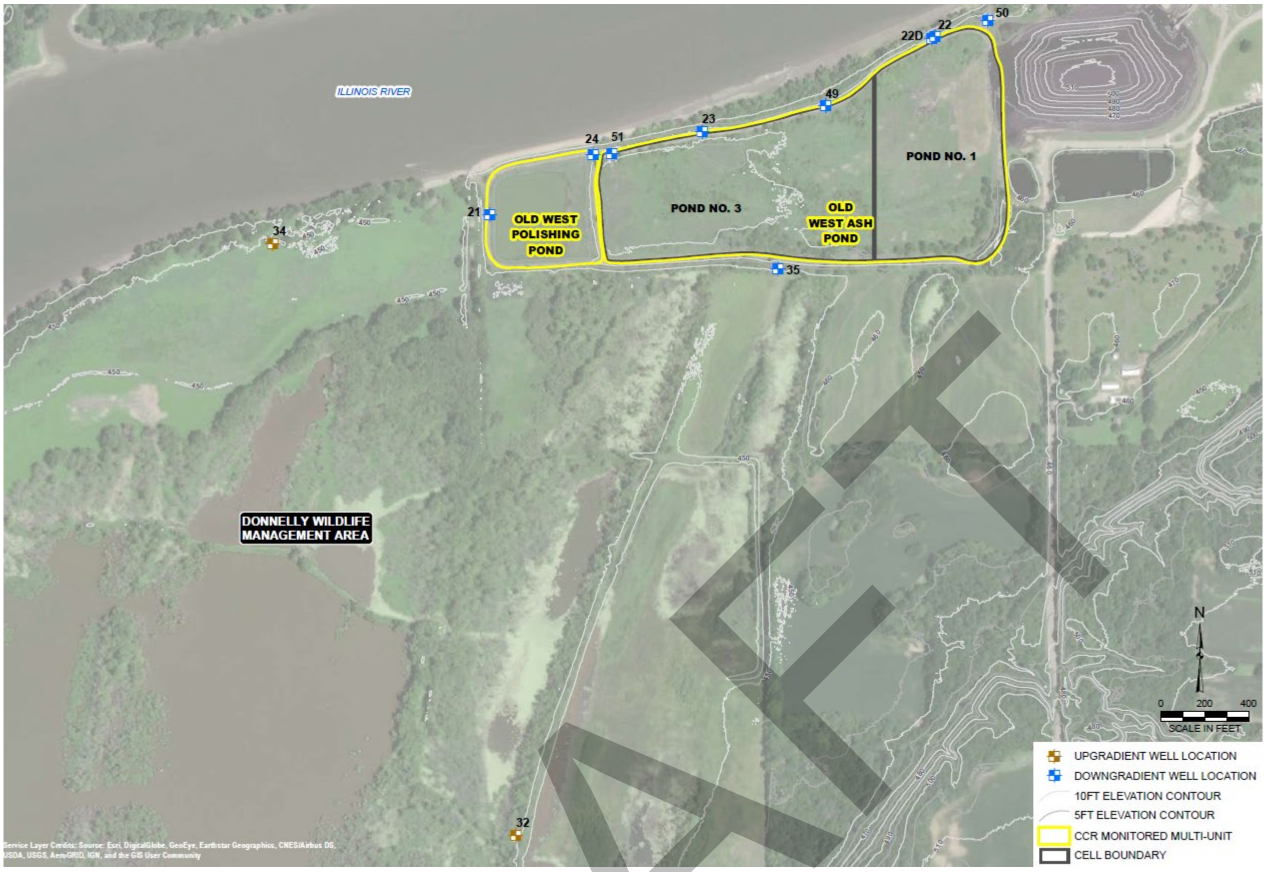

Figure 2.2 West Ash Pond Monitoring Well Locations. Source**:** OBG (2019). Well 51 was added from Ramboll (2023).

Table 2.1 Groundwater Monitoring Wells Related to Hennepin West Ash Pond[a]

Well ID	Date Constructed	Screen Top Depth (ft BGS)	Screen Bottom Depth (ft BGS)	Well Depth from Ground Surface (ft BGS)	Hydrogeologic Unit
21 (W-1)	Dec-1982	49.0	59.0	59.6	UAU
21R	Feb-2020	37.6	47.6	47.9	UAU
22 (W-2)	Dec-1982	24.4	34.4	34.6	UAU
22D	Aug-2019	49.7	59.7	59.7	UAU
23 (W-3)	Dec-1982	34.0	44.0	45.2	UAU
24 (W-4)	Dec-1982	56.4	66.4	64.5	UAU
27	Sep-1995	30.0	35.0	36.3	UAU
32	Aug-1996	7.0	17.0	17.3	UAU
34	Aug-1996	30.0	35.0	35.0	UAU
35	Sep-1999	8.0	18.0	17.6	UAU
49	Jul-2015	35.0	45.0	45.0	UAU
50	Aug-2019	19.6	29.6	29.6	UAU
51	Feb-2020	56	66	66.3	UAU

Notes:

BGS = Below Ground Surface; UAU = Uppermost Aquifer Unit.

(a) Table lists the wells with data from 2018-2023 that were used in this risk assessment.

Source: NRT (2017); Geosyntec (2020); Ramboll (2019).

Table 2.2 Groundwater Data Summary (2018-2023)

Parameter	Samples with Constituent Detected	Samples Analyzed	Minimum Detect	Maximum Detect	Maximum Detection Limit
Total Metals (mg/L)					
Antimony	7	231	0.00060	0.0012	0.0013
Arsenic	118	243	0.00028	0.038	0.0087
Barium	231	231	0.013	0.40	0.001
Beryllium	1	229	0.00030	0.00030	0.001
Boron	243	243	0.075	18	0.037
Cadmium	75	231	0.00020	0.0096	0.001
Chromium	39	231	0.00070	0.0078	0.0028
Cobalt	165	231	0.00020	0.0099	0.001
Iron	36	37	0.037	11	0.047
Lead	60	231	0.00020	0.0066	0.004
Lithium	241	243	0.0028	0.076	0.005
Manganese	37	37	0.012	1.3	0.0025
Mercury	1	220	0.00059	0.00059	0.0002
Molybdenum	219	243	0.00070	0.21	0.0037
Selenium	26	231	0.00070	0.032	0.001
Thallium	1	231	0.0036	0.0036	0.002
Dissolved Metals (mg/L)					
Antimony	0	3	ND	ND	0.001
Arsenic	8	15	0.0010	0.016	0.001
Barium	3	3	0.035	0.11	7E-07
Beryllium	0	3	ND	ND	0.001
Boron	129	129	0.069	17	0.015
Cadmium	1	3	0.0057	0.0057	0.001
Chromium	0	3	ND	ND	0.0015
Cobalt	1	3	0.0027	0.0027	0.001
Iron	28	44	0.028	6.8	0.047
Lead	0	3	ND	ND	0.001
Lithium	4	4	0.0047	0.058	0.0005
Manganese	44	44	0.0044	1.3	0.0025
Molybdenum	16	16	0.0058	0.14	0.0006
Selenium	1	3	0.021	0.021	0.001
Thallium	0	3	ND	ND	0.002
Other (mg/L or SU)					
Chloride	250	250	23	115	25
Fluoride	220	228	0.090	0.24	1
pH (field)	243	243	6.2	7.8	NA
Sulfate	250	250	37	1,190	307
Total Dissolved Solids	250	250	338	1,940	40
Radionuclides (pCi/L)					
Radium 226 + Radium 228	103	158	ND	3.1	1.8

Source: Ramboll (2024b).

Note: NA = Not Applicable; ND = Not Detected.

2.5 Surface Water Monitoring

Surface water samples were collected at 15 locations in September 2020 and one location in February 2021 in the Illinois River adjacent to the HPP. The 2020 samples were collected along five transects, with three samples per transect collected from the two edges and the center of the river (Figure 2.3). Sample set IR-01 was collected approximately one mile upstream of the HPP. Sample sets IR-02, IR-03, and IR-04 and IR-05 were located upstream of the WAPS, and set IR-05 was located downstream of the WAPS. Sample SG02 (February 2021) was located adjacent to the plant (Figure 2.3). It should be noted that many constituents occur naturally in the environment and/or could be associated with industrial activities unrelated to the WAPS. The use of surface water data in this risk assessment does not imply that any constituents are associated with the WAPS. A summary of the surface water data used in this risk evaluation is presented in Table 2.3.

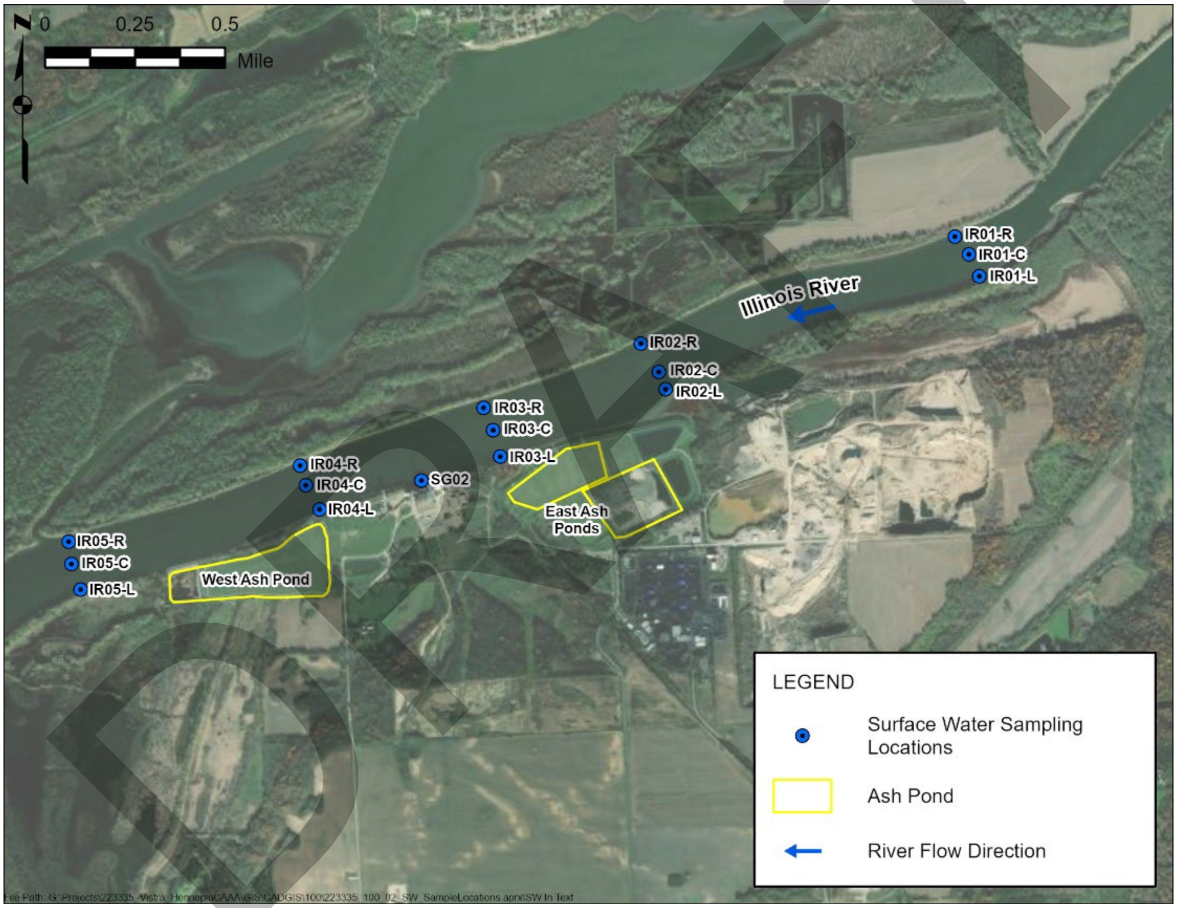

Figure 2.3 Surface Water Sampling Locations. Source: Modified from Geosyntec (2021).

Table 2.3 Surface Water Data Summary

Parameter	Samples with Constituent Detected	Samples Analyzed	Minimum Detect (mg/L)	Maximum Detect (mg/L)	Maximum Detection Limit (mg/L)
Total Metals					
Antimony	0	1	ND	ND	0.001
Arsenic	1	1	0.0012	0.0012	4E-07
Barium	1	1	0.052	0.052	7E-07
Beryllium	0	1	ND	ND	0.001
Boron	1	1	0.22	0.22	--
Cadmium	0	1	ND	ND	0.001
Calcium	1	1	88	88	--
Chromium	0	1	ND	ND	0.0015
Cobalt	0	1	ND	ND	0.001
Iron	1	1	0.24	0.24	1E-05
Lead	0	1	ND	ND	0.001
Lithium	1	1	0.0080	0.0080	--
Magnesium	1	1	35	35	--
Manganese	1	1	0.060	0.060	--
Molybdenum	1	1	0.0061	0.0061	6E-07
Potassium	1	1	6.6	6.6	8E-05
Selenium	0	1	ND	ND	0.001
Sodium	1	1	227	227	--
Thallium	0	1	ND	ND	0.002
Dissolved Metals					
Aluminum	1	15	0.64	0.64	0.025
Antimony	0	16	ND	ND	0.001
Arsenic	16	16	0.0011	0.0034	4E-07
Barium	16	16	0.035	0.049	7E-07
Beryllium	0	16	ND	ND	0.001
Boron	16	16	0.13	0.21	9E-06
Cadmium	0	16	ND	ND	0.001
Calcium	16	16	46	85	--
Chromium	1	16	0.015	0.015	0.015
Cobalt	0	16	ND	ND	0.001
Copper	15	15	0.0016	0.0035	–
Iron	1	16	1.1	1.1	0.025
Lead	1	16	0.0020	0.0020	0.001
Lithium	16	16	0.0071	0.0083	2E-06
Magnesium	16	16	24	30	2E-05
Manganese	3	16	0.010	0.083	0.002
Molybdenum	16	16	0.0048	0.0063	6E-07
Nickel	15	15	0.0026	0.0045	–
Potassium	1	1	6.3	6.3	8E-05
Selenium	0	16	ND	ND	0.001
Silver	0	15	ND	ND	0.001
Sodium	16	16	61	222	--
Strontium	15	15	0.23	0.26	–

Parameter	Samples with Constituent Detected	Samples Analyzed	Minimum Detect (mg/L)	Maximum Detect (mg/L)	Maximum Detection Limit (mg/L)
Thallium	0	16	ND	ND	0.002
Vanadium	0	15	ND	ND	0.005
Zinc	0	15	ND	ND	0.015
Other					
Chloride	16	16	97	282	5
pH	16	16	8.6	8.6	--
Sulfate	16	16	73	94	25
Total Dissolved Solids	11	11	368	878	16

Notes:
– = Not Available; ND = Not Detected.
Data collected 9/2/20 and 2/25/21.

3 Risk Evaluation

3.1 Risk Evaluation Process

A risk evaluation was conducted to determine whether constituents present in groundwater underlying and downgradient of the WAPS have the potential to pose adverse health effects to human and ecological receptors. The risk evaluation is consistent with the principles of risk assessment established by US EPA and has considered evaluation criteria detailed in Illinois guidance documents (*e.g.*, IEPA, 2013, 2019a).

The general risk evaluation approach is summarized in Figure 3.1 and discussed below.

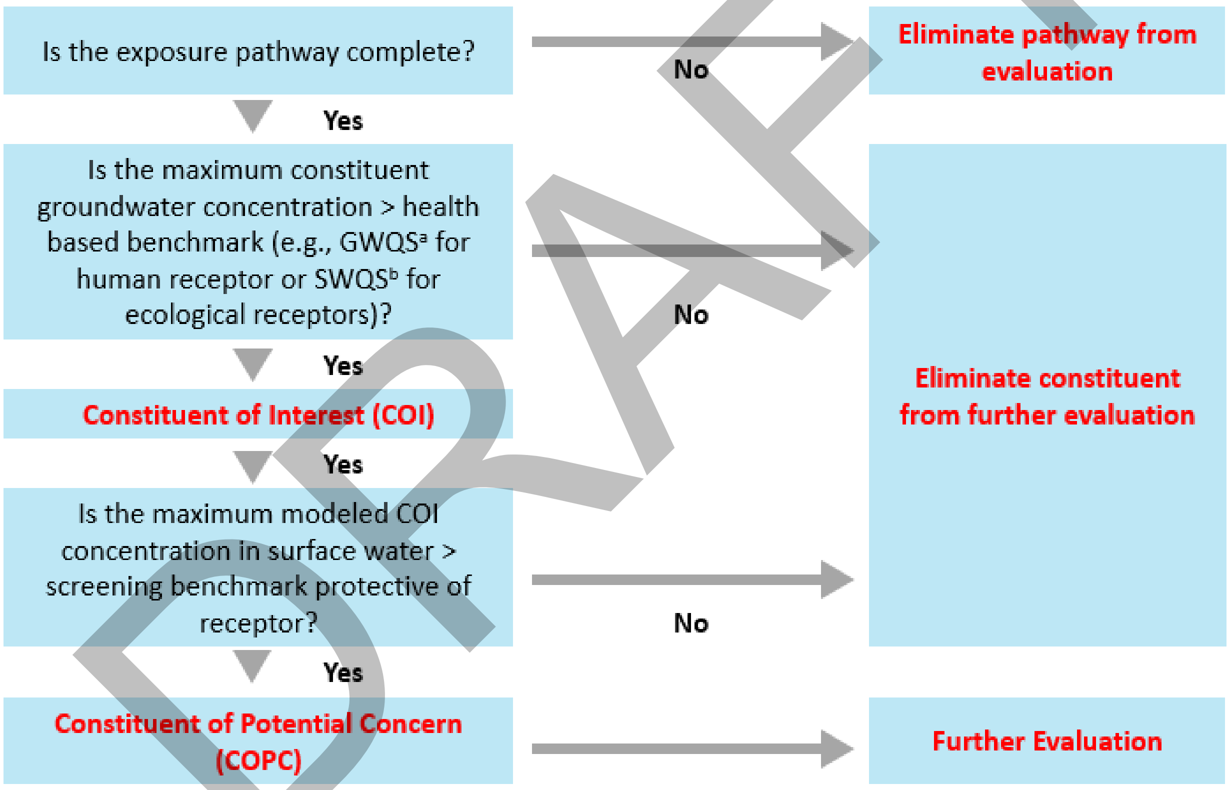

Figure 3.1 Overview of Risk Evaluation Methodology. Notes: IEPA = Illinois Environmental Protection Agency; GWQS = IEPA Groundwater Quality Standards; SWQS = IEPA Surface Water Quality Standards; US EPA = United States Environmental Protection Agency.
(a) The IEPA Part 845 groundwater protection standards were used to identify COIs.
(b) IEPA SWQS protective of chronic exposures to aquatic organisms were used to identify ecological COIs. In the absence of an SWQS, US EPA Region IV ecological screening values were used.

The first step in the risk evaluation was to develop the CEMs and identify complete exposure pathways. All potential receptors and exposure pathways based on groundwater use and surface water use in the vicinity of the Site were considered. Exposure pathways that are incomplete were excluded from the evaluation.

Groundwater data were used to identify COIs. COIs were identified as constituents with maximum concentrations in groundwater in excess of groundwater quality standards (GWQS)[2] for human receptors and surface water quality standards (SWQS) for ecological receptors. Based on the CSM (Section 2.2), groundwater underlying the WAPS flows from south to north toward the Illinois River. Therefore, any potential WAPS-related constituents in groundwater would flow toward and into surface water.

Surface water samples have been collected from the Illinois River adjacent to the Site; however, sediment samples have not been collected from the river. Gradient modeled the potential migration of COIs from groundwater to surface water and sediment to evaluate potential risks to receptors (see Section 3.3.3). Gradient modeled the COI concentrations in surface water and sediment based on the groundwater data from the WAPS-related groundwater monitoring wells. The measured and modeled COI concentrations in surface water and the modeled sediment concentrations were compared to conservative, generic risk-based screening benchmarks for human health and ecological receptors. These generic screening benchmarks rely on default assumptions with limited consideration of site-specific characteristics. Human health benchmarks are receptor-specific values calculated for each pathway and environmental medium that are designed to be protective of human health. Ecological benchmarks are medium-specific values designed to be protective of all potential ecological receptors exposed to surface water. Ecological and human health screening benchmarks are inherently conservative because they are intended to screen out chemicals that are of no concern with a high level of confidence. Therefore, a measured or modeled COI concentration exceeding a screening benchmark does not indicate an unacceptable risk, but only that further risk evaluation is warranted. COIs with maximum concentrations exceeding a conservative screening benchmark are identified as COPCs requiring further evaluation.

As described in more detail below, this evaluation relied on the screening assessment to demonstrate that constituents present in groundwater underlying the WAPS do not pose an unacceptable human health or ecological risk. That is, after the screening step, no COPCs were identified and further assessment was not warranted.

3.2 Human and Ecological Conceptual Exposure Models

A CEM provides an overview of the receptors and exposure pathways requiring risk evaluation. The CEM describes the source of the contamination, the mechanism that may lead to a release of contamination, the environmental media to which a receptor may be exposed, the route of exposure (exposure pathway), and the types of receptors that may be exposed to these environmental media.

3.2.1 Human Conceptual Exposure Model

The human CEM for the Site depicts the relationships between the off-Site environmental media potentially impacted by constituents in groundwater and human receptors that could be exposed to these media. Figure 3.2 presents a human CEM for the Site. It considers a human receptor who could be exposed to COIs hypothetically released from the WAPS into groundwater, surface water, sediment, and fish. The following human receptors and exposure pathways were evaluated for inclusion in the Site-specific CEM.

---

[2] As discussed further in Section 3.3.2, GWQS are protective of human health and not necessarily of ecological receptors. While ecological receptors are not exposed to groundwater, groundwater can potentially enter into the adjacent surface water and impact ecological receptors. Therefore, two sets of COIs were identified: one for humans and another for ecological receptors.

- Residents – exposure to groundwater/surface water as drinking water;
- Residents – exposure to groundwater/surface water used for irrigation;
- Recreators in the river near the Site:
  - Boaters – exposure to surface water and sediment while boating;
  - Swimmers – exposure to surface water and sediment while swimming;
  - Anglers – exposure to surface water and sediment and consumption of locally caught fish.

All of these exposure pathways were considered complete except for residential exposure to groundwater or surface water used for drinking water or irrigation. Section 3.2.1.1 explains why the residential drinking water and irrigation pathways are incomplete, and Section 3.2.1.2 provides additional description of the recreational exposures.

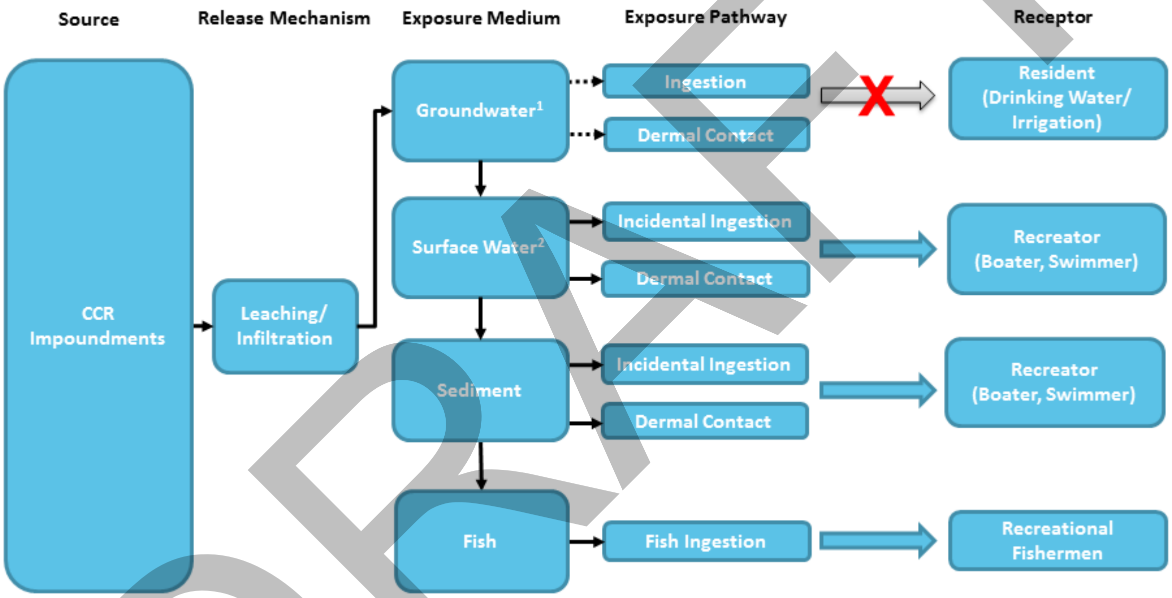

Figure 3.2 Human Conceptual Exposure Model. Notes: CCR = Coal Combustion Residual. Dashed line/Red X indicates incomplete or insignificant exposure pathway.
(1) Groundwater in the vicinity of the Site is not used as a drinking water or irrigation source.
(2) Surface water is not used as a drinking water source.

3.2.1.1 Groundwater or Surface Water as a Drinking Water/Irrigation Source

Groundwater as a source of drinking water and/or irrigation water is not a complete exposure pathway for CCR-related constituents originating from the WAPS. Specifically, shallow groundwater from the UAU in the vicinity of the WAPS is not used as a source of drinking water, and no public groundwater systems are downgradient of the site. Further, the downward migration of groundwater from the UAU is restricted due to the presence of a thick shale bedrock (NRT, 2017). A summary of the evidence supporting the conclusion that there are no residential uses of the shallow groundwater and Illinois River surface water as a source of drinking water is presented below:

- **No potential groundwater receptors are in the vicinity of the WAPS**. The public water systems (PWS) in the Putnam and Bureau Counties in the vicinity of the Hennepin WAPS rely on groundwater as a source of potable water. A review of existing drinking water intakes within the US EPA Safe Drinking Water Information System (SDWIS) (US EPA, 2024), IEPA Illinois Drinking Water Watch (IEPA, 2024a), and IEPA Map Server (IEPA, 2024b) databases yielded no PWS wells within 1,000 meters of the Site, as described below.
    - A total of 10 wells were identified within a 1,000-meter radius of the WAPS during a comprehensive search of the Illinois State Geological Survey (ISGS) Illinois Water and Related Wells (ILWATER) Map (ISGS, 2024b) (Figure 3.3). Under normal groundwater flow conditions, 2 out of the 10 wells are located downgradient from the WAPS (Well IDs 121552089500, and 121552089600), and the remaining 8 wells are located upgradient and/or side-gradient (Well IDs 121550009400, 121550009500, 121550012800, 121552043500, 121552059800, 121552059900, 121552070200, and 121552091200).
    - All 10 wells located within a 1,000-meter radius of the WAPS are listed as being owned by either "Power Plant", Illinois Power Company, Hennepin Power Station, or Dynegy Midwest-Hennepin Power (ISGS, 2024b). The wells include three monitoring wells; one irrigation well,[3] one industrial well, four wells with non-specific use, and one non-community public water well (ISGS, 2024b). The non-community public water well (121552043500) was installed in 1993 and is 120 feet deep; it is screened in sand and gravel from 90 to 115 feet bgs. However, this well is side-gradient to the WAPS (Figure 3.3).
    - A 2009 water well survey conducted in the area by Kelron/Natural Resource Technology concluded that CCR-impacted groundwater at the HPP is not likely to impact any existing potable or non-potable off-Site water wells that are located within 2,500 ft of the property boundary (Ramboll, 2018-2020; NRT, 2017).
    - In a letter to IEPA (Morris, 2021), DMG noted that 16 private wells were identified near the Site, with 1 well located potentially downgradient of the Site. However, DMG noted that this well is unlikely to be in use, based on the installation date (1884) and its remote floodplain location. DMG noted that three non-community water supply wells (CWS) were identified but that they are unlikely to be at risk because they are either inactive and/or not-located hydraulically downgradient of the WAPS.
- **There is no off-Site migration of WAPS-related constituents to nearby wells because all shallow groundwater flows into the Illinois River**. The Illinois River is the regional discharge point for groundwater in the UAU. Groundwater in the UAU flows to north/northwest into the Illinois River under normal conditions (OBG, 2019). Because the Illinois River is a large regional hydraulic boundary (*i.e.*, serves as a sink for groundwater discharges in the area), any potential constituents present in groundwater underlying the WAPS are not likely to migrate under or beyond the river.
- **The Illinois River adjacent to the Site is not used as a public water supply.** IEPA classified the Illinois River as a "General Use Water." IEPA fully supports the use of the Illinois River for aquatic life and primary contact recreation, but it is not designated for public and food processing water supplies. The segment of the Illinois River adjacent to the Site (Section D-16) is listed on the 2018 Illinois Section 303(d) List as being impaired for fish consumption, due to mercury and polychlorinated biphenyls (IEPA, 2016, IEPA, 2018 , IEPA, 2019b). Therefore, surface water adjacent to the Site is not used as a source of drinking water, and this exposure pathway was not evaluated further.

---

[3] The irrigation well is "used exclusively for irrigation of the coal pile." (NRT, 2017).

- **The WAPS has a limited hydraulic connection to underlying bedrock groundwater resources**. The bedrock aquitard is composed of a 300-400 ft thick shale unit of the Carbondale Formation (NRT, 2017). This thick, continuous shale bedrock forms a hydraulic barrier between the WAPS and deeper groundwater resources. Very low hydraulic conductivities of the shale bedrock and the lack of a downward gradient restrict any downward migration of shallow groundwater originating from the WAPS to the underlying aquifers (NRT, 2017).

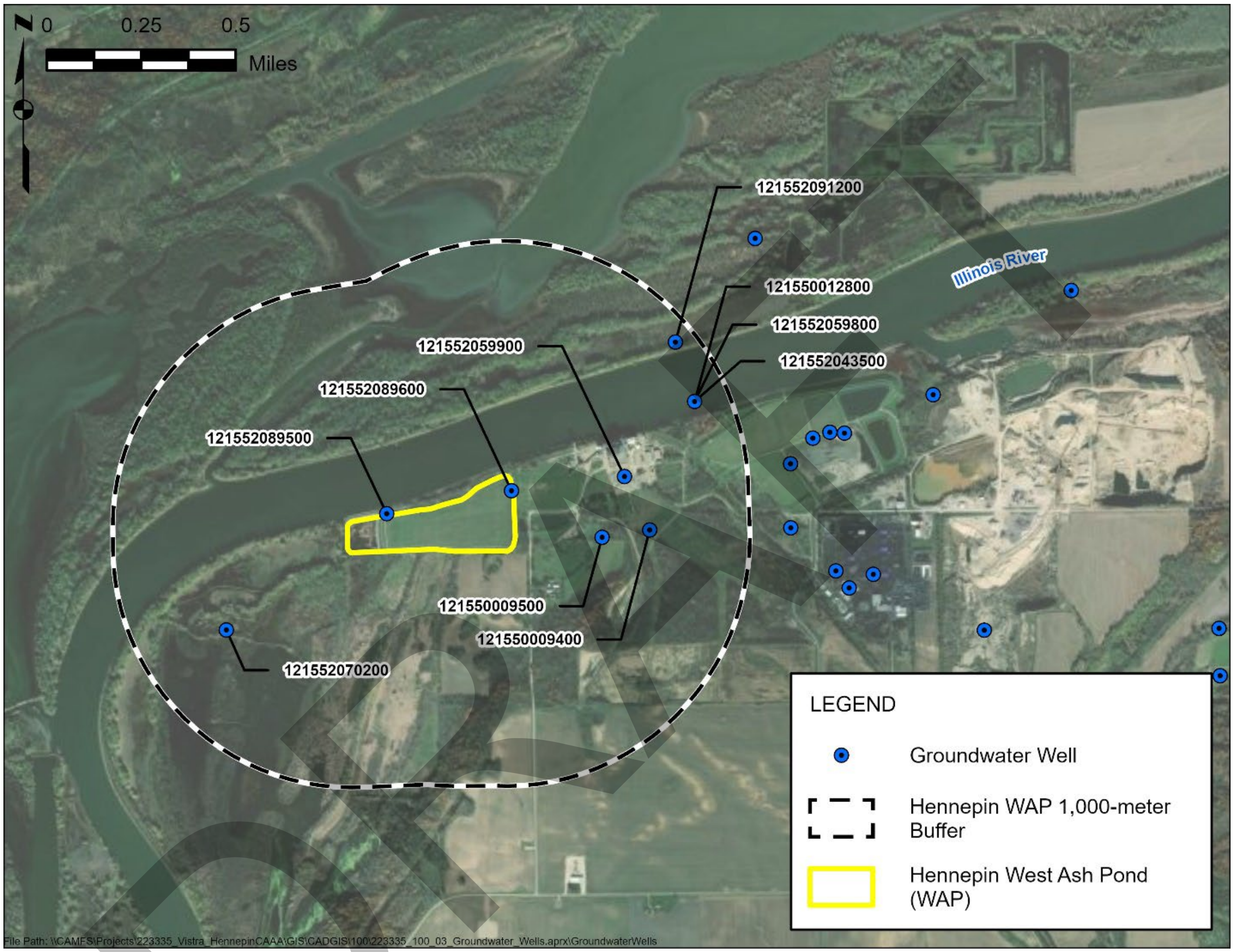

Figure 3.3 Water Wells Within 1,000 Meters of the West Ash Pond. Sources: Google LLC, 2024; ISGS, 2024b.

3.2.1.2 Recreational Exposures

The Illinois River flows east to west past the Site. Recreational exposure to surface water and sediment may occur during activities such as swimming or boating in the river. Exposure estimates for swimmers provide a health-protective means to evaluate exposure during other recreational activities. Recreational anglers may also consume locally caught fish from the Illinois River.

3.2.2 Ecological Conceptual Exposure Model

The ecological CEM for the Site depicts the relationships between off-Site environmental media (surface water and sediment) potentially impacted by COIs in groundwater and ecological receptors that may be exposed to these media. The ecological risk evaluation considered both direct toxicity as well as secondary toxicity *via* bioaccumulation. Figure 3.4 presents the ecological CEM for the Site. The following ecological receptor groups and exposure pathways were considered:

- **Ecological Receptors Exposed to Surface Water:**
  - Aquatic plants, amphibians, reptiles, and fish.
- **Ecological Receptors Exposed to Sediment:**
  - Benthic invertebrates (*e.g.*, insects, crayfish, mussels).
- **Ecological Receptors Exposed to Bioaccumulative COIs:**
  - Higher trophic-level wildlife (avian and mammalian) *via* direct exposures (surface water and sediment exposure) and secondary exposures through the consumption of prey (*e.g.*, plants, invertebrates, small mammals, fish).

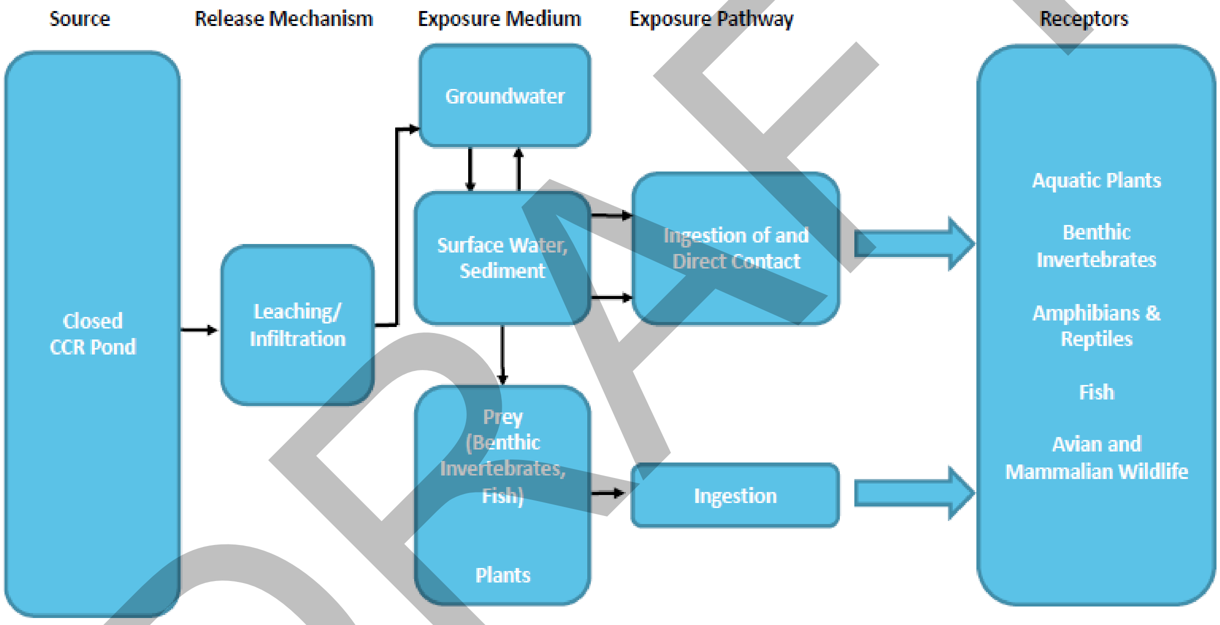

Figure 3.4 Ecological Conceptual Exposure Model. Notes: CCR = Coal Combustion Residual.

3.3 Identification of Constituents of Interest

Risks were evaluated for COIs. A constituent was considered a COI if the maximum detected constituent concentration in groundwater exceeded a health-based benchmark. According to US EPA risk assessment guidance (US EPA, 1989), this screening step is designed to reduce the number of constituents carried through the risk evaluation that are anticipated to have a minimal contribution to the overall risk. Identified COIs are the constituents that are most likely to pose a risk concern in the surface water adjacent to the Site.

3.3.1 Human Health Constituents of Interest

For the human health risk evaluation, COIs were conservatively identified as constituents with maximum concentrations in groundwater above the GWPSs listed in the Illinois CCR Rule Part 845.600 (IEPA, 2021). The use of groundwater data in this risk evaluation does not imply that detected constituents are associated with the WAPS or that they have been identified as potential groundwater exceedances. Using this approach, the COIs identified for the human health risk evaluation *via* a surface water pathway include arsenic, boron, cadmium, cobalt, iron, lithium, manganese, molybdenum, and thallium (Table 3.1).

The water quality parameters that exceeded the GWPS included sulfate and total dissolved solids (TDS); however, these constituents were not included in the risk evaluation because the GWPS are likely based on aesthetic quality. US EPA set secondary maximum contaminant levels (MCLs) for sulfate and TDS based on aesthetic quality. The sulfate (250 mg/L) MCL is based on salty taste. The secondary MCL for TDS (500 mg/L) is based on hardness, colored water, staining, and salty taste (US EPA, 2021). Given that these parameters are not likely to pose a human health risk concern in the event of exposure, they were not identified as COIs.

Table 3.1 Human Health Constituents of Interest

Analyte[a]	Maximum Groundwater Concentration[b]	GWPS[c]	Human Health COI[d]
Total Metals (mg/L)			
Antimony	0.0012	0.006	No
Arsenic	0.038	0.01	Yes
Barium	0.398	2	No
Beryllium	0.0003	0.004	No
Boron	18.1	2	Yes
Cadmium	0.0096	0.005	Yes
Chromium	0.0078	0.1	No
Cobalt	0.0099	0.006	Yes
Iron	11	5	Yes
Lead	0.0066	0.0075	No
Lithium	0.0764	0.04	Yes
Manganese	1.3	0.15	Yes
Mercury	0.00059	0.002	No
Molybdenum	0.206	0.1	Yes
Selenium	0.0322	0.05	No
Thallium	0.0036	0.002	Yes
Dissolved Metals (mg/L)			
Antimony	ND	0.006	No
Arsenic	0.0156	0.01	Yes
Barium	0.106	2	No
Beryllium	ND	0.004	No
Boron	16.5	2	Yes
Cadmium	0.0057	0.005	Yes
Chromium	ND	0.1	No
Cobalt	0.0027	0.006	No
Iron	6.8	5	Yes
Lead	ND	0.0075	No
Lithium	0.0583	0.04	Yes
Manganese	1.3	0.15	Yes
Molybdenum	0.14	0.1	Yes
Selenium	0.0212	0.05	No
Thallium	ND	0.002	No

Analyte[a]	Maximum Groundwater Concentration[b]	GWPS[c]	Human Health COI[d]
Other (mg/L)			
Chloride	115	200	No
Fluoride	0.24	4	No
pH (field) (SU)	7.8	9	No
Sulfate	1,190	400	No[e]
Total Dissolved Solids	1,940	1,200	No[e]
Radionuclides (pCi/L)			
Radium 226 + Radium 228	3.09	5	No

Notes:
COI = Constituent of Interest; GWPS = Groundwater Protection Standard; ND = Not Detected; SU = Standard Units
Shaded cell indicates a compound identified as a COI.
(a) The constituents are those listed in the IL Part 845.600 GWPS (IEPA, 2021).
(b) The maximum detected groundwater concentration was used to identify COIs.
(c) The IL Part 845.600 GWPS (IEPA, 2021) were used to identify COIs.
(d) COIs are constituents for which the maximum concentration exceeds the groundwater standard.
(e) Sulfate and TDS exceed the GWPS but are not considered to be COIs because the GWPS are likely based on aesthetic quality (see text above).

3.3.2 Ecological Constituents of Interest

The Illinois GWPS, as defined in IEPA's guidance, were developed to protect human health but not necessarily ecological receptors. While ecological receptors are not exposed to groundwater, groundwater can potentially migrate into the adjacent surface water and impact ecological receptors. Therefore, to identify ecological COIs, the maximum concentrations of analytes detected in groundwater were compared to ecological surface water benchmarks protective of aquatic life.

The surface water screening benchmarks for freshwater organisms were obtained from the following hierarchy of sources:

- IEPA (2019a) SWQS. IEPA SWQS are health-protective benchmarks for aquatic life exposed to surface water on a long-term basis (*i.e.*, chronic exposure). The SWQS for several metals are hardness dependent (cadmium, chromium, copper, fluoride, lead, manganese, nickel, and zinc). Screening benchmarks for these constituents were calculated assuming US EPA's (2019a) default hardness of 100 mg/L.[4]
- US EPA Region IV (2018) surface water Ecological Screening Values (ESVs) for hazardous waste sites.

For radium, benchmarks from the United States Department of Energy's (US DOE) guidance document, "A Graded Approach for Evaluating Radiation Doses to Aquatic and Terrestrial Biota" (US DOE, 2019), were used. US DOE presents benchmarks for radium-226 and radium-228 separately (4 and 3 pCi/L, respectively). Given that radium concentrations are expressed as total radium (radium-226+228, *i.e.*, the

---

[4] While hardness data are not available for the Illinois River adjacent to the Site, a US Geological Survey station (05556200) located at Hennepin, Illinois, approximately five miles downstream from the Site, measured hardness concentrations ranging from 200 to 370 mg/L, with a mean hardness of 288 mg/L, from 106 samples collected between 1980 and 1997 (USGS, 2021b). These are older data and may not reflect current conditions; therefore, US EPA's default hardness of 100 mg/L was used. However, use of a higher hardness value (288 mg/L) would result in less stringent screening values, and thus, use of the US EPA default hardness is conservative.

sum of radium-226 and radium-228), Gradient used the lower of the two benchmarks (3 pCi/L for radium-228) to evaluate total radium concentrations.

Consistent with the human health risk evaluation, Gradient used the maximum detected concentrations from groundwater samples collected from the WAPS-associated wells without considering spatial or temporal representativeness for ecological receptor exposures. The use of the maximum constituent concentrations in this evaluation is designed to conservatively identify COIs that warrant further investigation. Boron, cadmium, and iron were identified as COIs for ecological receptors (Table 3.2).

It should be noted that although cadmium and cobalt were screened in as ecological COIs based on the maximum groundwater concentration, neither constituent was detected in surface water (out of 17 samples) (Table 2.3). In addition, no constituent was detected in surface water at a concentration exceeding its ecological benchmark (Table 3.3). The maximum detection limit (0.001 mg/L) for cadmium and cobalt was just slightly above the ecological benchmark for cadmium, but below the ecological benchmark for cobalt (Table 3.3). A total of 158 groundwater samples were analyzed for radium-226+228; of these, only two samples had radium slightly above the ecological benchmark of 3 pCi/L (3.09 and 3.06 pCi/L). Based on a Rosner test for outliers (run in ProUCL 5.1), both samples were considered outliers at the 1% significance level. Thus, radium-226+228 was not considered an ecological COI.

Table 3.2 Ecological Constituents of Interest

Analyte[a]	Maximum Groundwater Concentration[b]	Ecological Benchmark	Basis	ECO COI[c]
Total Metals (mg/L)				
Antimony	0.0012	0.19	EPA R4 ESV	No
Arsenic	0.038	0.19	IEPA SWQC	No
Barium	0.398	5.0	IEPA SWQC	No
Beryllium	0.0003	0.064	EPA R4 ESV	No
Boron	18.1	7.6	IEPA SWQC	Yes
Cadmium	0.0096	0.0011	IEPA SWQC	Yes
Chromium	0.0078	0.21	IEPA SWQC	No
Cobalt	0.0099	0.019	EPA R4 ESV	No
Iron	11	1.0	EPA R4 ESV	Yes
Lead	0.0066	0.020	IEPA SWQC	No
Lithium	0.0764	0.44	EPA R4 ESV	No
Manganese	1.3	1.8	IEPA SWQC	No
Mercury	0.00059	0.0011	IEPA SWQC	No
Molybdenum	0.206	7.2	EPA R4 ESV	No
Selenium	0.0322	1.0	IEPA SWQC	No
Thallium	0.0036	0.0060	EPA R4 ESV	No
Dissolved Metals (mg/L)				
Antimony	ND	0.19	EPA R4 ESV	No
Arsenic	0.0156	0.19	IEPA SWQC	No
Barium	0.106	5.0	IEPA SWQC	No
Beryllium	ND	0.064	EPA R4 ESV	No
Boron	16.5	7.6	IEPA SWQC	Yes
Cadmium	0.0057	0.00093	IEPA SWQC	Yes
Chromium	ND	0.18	IEPA SWQC	No
Cobalt	0.0027	0.019	EPA R4 ESV	No

Analyte[a]	Maximum Groundwater Concentration[b]	Ecological Benchmark	Basis	ECO COI[c]
Iron	6.8	1.0	EPA R4 ESV	Yes
Lead	ND	0.016	IEPA SWQC	No
Lithium	0.0583	0.44	EPA R4 ESV	No
Manganese	1.3	1.8	IEPA SWQC	No
Molybdenum	0.14	0.80	EPA R4 ESV	No
Selenium	0.0212	1.0	IEPA SWQC	No
Thallium	ND	0.0060	EPA R4 ESV	No
Other (mg/L)				
Chloride	115	500	IEPA SWQC	No
Fluoride	0.24	4.0	IEPA SWQC	No
pH (field) (SU)	7.8	NA	NA	No
Sulfate	1,190	NA	NA	No
Total Dissolved Solids	1,940	NA	NA	No
Radionuclides (pCi/L)				
Radium 226 + Radium 228	3.09	3	US DOE	No[d]

Notes:

COI = Constituent of Interest; DOE = Department of Energy; EPA R4 ESV = US Environmental Protection Agency Region IV Ecological Screening Value; GWPS = Groundwater Protection Standards; IEPA SWQS = Illinois Environmental Protection Agency Surface Water Quality Standard; NA = Not Available; SU = Standard Unit.

A gray-shaded cell indicates a compound identified as a COI.

(a) The constituents are those listed in the IL Part 845.600 GWPS (IEPA, 2021) that were detected in at least one groundwater sample from the wells related to the Hennepin WAPS.

(b) Ecological benchmarks are from the hierarchy of sources discussed in Section 3.3.2: IEPA SWQS (IEPA, 2019a); US EPA Region IV, "Ecological Risk Assessment Supplemental Guidance" (US EPA Region IV, 2018); US DOE's guidance document, "A Graded Approach for Evaluating Radiation Doses to Aquatic and Terrestrial Biota" (US DOE, 2019).

(c) Analytes with maximum detected groundwater concentrations exceeding a benchmark protective of surface water exposure are considered ecological COIs.

(d) Of the 158 groundwater samples analyzed for radium-226+228, the two samples that were slightly above the ecological benchmark were considered outliers at the 1% significance level; therefore, radium-226+228 was not considered an ecological COI.

Table 3.3 Measured Surface Water Data Summary

Constituent	Maximum Detect (mg/L)	Maximum Detection Limit (mg/L)	Ecological Benchmark (mg/L)
Total Metals			
Antimony	ND	0.001	0.19
Arsenic	0.0012	4E-07	0.19
Barium	0.052	7E-07	5.0
Beryllium	ND	0.001	0.064
Boron	0.22	0.001	7.6
Cadmium	ND	0.001	0.0011
Chromium	ND	0.0015	0.21
Cobalt	ND	0.001	0.019
Iron	0.24	1E-05	1.0
Lead	ND	0.001	0.020
Lithium	0.0080	0.001	0.44
Manganese	0.060	0.001	1.8
Molybdenum	0.0061	6E-07	7.2
Selenium	ND	0.001	1.0
Thallium	ND	0.002	0.0060
Dissolved Metals			
Aluminum	0.64	0.025	–
Antimony	ND	0.001	0.19
Arsenic	0.0034	4E-07	0.19
Barium	0.049	7E-07	5.0
Beryllium	ND	0.001	0.064
Boron	0.21	9E-06	7.6
Cadmium	ND	0.001	0.00093
Chromium	0.015	0.015	0.18
Cobalt	ND	0.001	0.019
Iron	1.11	0.025	1.0
Lead	0.0020	0.001	0.016
Lithium	0.0083	2E-06	0.44
Manganese	0.083	0.002	1.8
Molybdenum	0.0063	6E-07	0.80
Selenium	ND	0.001	1.0
Thallium	ND	0.002	0.0060
Other			
Chloride	282	5	500
pH	8.6	NA	–
Sulfate	94	25	–
Total Dissolved Solids	878	16	–

Notes:
– = Not Available; NA = Not Applicable; ND = Not Detected.
Surface water data collected 9/2/20 and 2/25/21.

3.3.3 Surface Water and Sediment Modeling

Surface water sampling has been conducted in the Illinois River adjacent to the Site. To estimate the potential contribution to surface water (and sediment) from groundwater specifically associated with the WAPS, Gradient modeled concentrations in the Illinois River surface water and sediment from groundwater discharge to the Illinois River for the detected COIs. This is because the constituents detected in groundwater above a health-based benchmark are most likely to pose a risk concern in the adjacent surface water. Gradient modeled human health and ecological COI concentrations in the surface water and sediment using a mass balance calculation based on the surface water and groundwater mixing. The model assumes a well-mixed groundwater-surface water location.

The maximum detected concentrations in groundwater (regardless of well location) from 2018 to 2023 were conservatively used to model COI concentrations in surface water and sediment. For COIs that were measured as both total and dissolved fractions, we used the maximum of the total and dissolved COI concentrations for the modeling. In this case, the maximum concentration was from the total fraction for all COIs. Use of the total metal concentration for these COIs may overestimate surface water concentrations because dissolved concentrations, which are lower than total concentrations, represent the mobile fractions of constituents that could likely flow into and mix with surface water.

The modeling approach does not account for geochemical transformations that may occur during groundwater mixing with surface water. Gradient assumed that predicted surface water concentrations were influenced only by the physical mixing of groundwater as it enters the surface water and were not further influenced by the geochemical reactions in the water and sediment, such as precipitation. In addition, the model only predicts surface water and sediment concentrations as a result of the potential migration of COI concentrations in WAPS-related groundwater and does not account for background concentrations in surface water or sediment.

For this evaluation we adapted a simplified and conservative form of US EPA's indirect exposure assessment methodology (US EPA, 1998) that was used in US EPA's coal combustion waste risk assessment (US EPA, 2014). The original model is a mass balance calculation based on surface water and groundwater mixing and the concept that the dissolved and sorbed concentrations can be related through an equilibrium partitioning coefficient (K_d). The model assumes a well-mixed groundwater-surface water location, with partitioning among total suspended solids, dissolved water column, sediment porewater, and solid sediments.

Sorption to soil and sediment is highly dependent on the surrounding geochemical conditions. To be conservative, we ignored the natural attenuation capacity of soil and sediment and estimated the surface water concentration based only on the physical mixing of groundwater and surface water (*i.e.*, dilution) at the point of discharge of groundwater to the surface water.

The aquifer and surface water properties used to estimate the volume of groundwater flowing into the Illinois River and surface water concentrations are presented in Table 3.4. The COI concentrations in sediment were modeled using the COI-specific sediment-to-water partition coefficients and the sediment properties presented in Table 3.5. In the absence of Site-specific information for the Illinois River, we used default assumptions (*e.g.*, depth of the upper benthic layer and bed sediment porosity) to model sediment concentrations. The modeled surface water and sediment concentrations are presented in Table 3.6. These modeled concentrations reflect conservative contributions from groundwater flowing into the Illinois River. A description of the modeling and the detailed results are presented in Appendix A.

Table 3.4 Groundwater and Surface Water Properties Used in Modeling

Parameter	Unit	Values	Notes/Source
Groundwater			
COI Concentration	mg/L	Constituent-specific	Maximum detected concentration in groundwater
Cross Sectional Area for the UAU	m^2	11,613	Average thickness of the UAU (*i.e.*, 50 ft, or 15.2 m) multiplied by the length of WAPS adjacent to the Illinois River (2500 ft, or 762 m) (NRT, 2017)
Hydraulic Gradient	m/m	0.005	Horizontal hydraulic gradient from WAPS to off-site areas during normal river stage (NRT, 2017)
Hydraulic Conductivity of the UAU	cm/s	0.017	Geometric mean horizontal hydraulic conductivity measured for wells finished in gravel only (NRT, 2017)
Surface Water			
Surface Water Flow Rate	L/yr	4.56 x 10^{12}	Representative low flow (10th percentile) discharge rate for the Illinois River (5,100 cfs), as derived from USGS station at Henry (USGS 05558300) (USGS, 2021a)
Total Suspended Solids (TSS)	mg/L	40	Median TSS measured in Illinois River at Hennepin (Tetra Tech, 2012)
Depth of the Water Column	m	4	Maximum "water depth at the 75% exceedance discharge condition" is 4-5 m (USGS, 2024)
Suspended Sediment to Water Partition Coefficient	mg/L	Constituent-specific	Values based on US EPA (2014)

Notes:

cfs = Cubic Feet per Second; COI = Constituent of Interest; US EPA = United States Environmental Protection Agency.

Table 3.5 Sediment Properties Used in Modeling

Parameter	Unit	Value	Notes/Source
Sediment			
Depth of Upper Benthic Layer	m	0.03	Default (US EPA, 2014)
Depth of Water Body	m	4.03	Depth of water column (4 m) plus depth of upper benthic layer (0.03 m) (US EPA, 2014)
Bed Sediment Particle Concentration	g/cm^3	1	Default (US EPA, 2014)
Bed Sediment Porosity	-	0.6	Default (US EPA, 2014)
TSS Mass per Unit Area	kg/m^2	0.16	Depth of water column × TSS × conversion factors (10^6 kg/mg and 1,000 L/m^3)
Sediment Mass per Unit Area	kg/m^2	30	Depth of upper benthic layer × bed sediment particulate concentration × conversion factors (0.001 kg/g, 10^6 cm^3/m^3)
Sediment to Water Partition Coefficients	mg/L	Constituent specific	Values based on US EPA (2014)

Notes:

TSS = Total Suspended Solids; US EPA = United States Environmental Protection Agency.

Table 3.6 Surface Water and Sediment Modeling Results

COI	Maximum Measured Groundwater Concentration (mg/L)	Mass Discharge Rate (mg/year)	Modeled Surface Water Concentration (mg/L)	Modeled Sediment Concentration (mg/kg)
Arsenic	3.8E-02	1.2E+07	2.6E-06	5.0E-04
Boron	1.8E+01	5.6E+09	1.2E-03	6.0E-03
Cadmium	9.6E-03	3.0E+06	6.6E-07	3.2E-04
Cobalt	9.9E-03	3.1E+06	6.8E-07	2.4E-04
Iron	1.1E+01	3.4E+09	7.6E-04	1.9E-02
Lithium	7.6E-02	2.4E+07	5.3E-06	NA[a]
Manganese	1.3E+00	4.0E+08	9.0E-05	1.2E+00
Molybdenum	2.1E-01	6.4E+07	1.4E-05	2.2E-03
Thallium	3.6E-03	1.1E+06	2.5E-07	3.3E-06

Notes:

COI = Constituent of Interest; NA = Not Applicable.

(a) Lithium sorbed to sediment was not calculated because lithium lacks a K_d value.

3.4 Human Health Risk Evaluation

The section below presents the results of the human health risk evaluation for recreators (swimmers and anglers) along the Illinois River adjacent to the Site. Risks were assessed using the maximum measured and modeled COIs in surface water.

3.4.1 Recreators Exposed to Surface Water

Screening Exposures: Recreators could be exposed to surface water *via* incidental ingestion and dermal contact while swimming. In addition, anglers could consume fish caught in the Illinois River. The maximum measured or modeled COI concentrations in surface water were used as conservative upper-end estimates of the COI concentrations to which a recreator might be exposed directly (incidental ingestion of COIs in surface water while swimming) and indirectly (consumption of locally caught fish exposed to COIs in surface water).

Screening Benchmarks: Illinois surface water criteria (IEPA, 2019a), known as human threshold criteria (HTC), are based on incidental exposure through contact or ingestion of small volumes of water while swimming or during other recreational activities, as well as the consumption of fish. The HTC values were calculated from the following equation (IEPA, 2019a):

$$\mathrm{HTC} = \frac{\mathrm{ADI}}{\mathrm{W} + (\mathrm{F} \times \mathrm{BCF})}$$

where:

HTC = Human health protection criterion in milligrams per liter (mg/L)
ADI = Acceptable daily intake (mg/day)
W = Water consumption rate (L/day)
F = Fish consumption rate (kg/day)
BCF = Bioconcentration factor (L/kg)

Illinois defines the acceptable daily intake (ADI) as the "maximum amount of a substance which, if ingested daily for a lifetime, results in no adverse effects to humans" (IEPA, 2019a). US EPA defines its chronic reference dose (RfD) as an "estimate (with uncertainty spanning perhaps an order of magnitude) of a daily oral exposure for a chronic duration (up to a lifetime) to the human population (including sensitive subgroups) that is likely to be without an appreciable risk of deleterious effects during a lifetime" (US EPA, 2011a). Illinois lists methods to derive an ADI from the primary literature (IEPA, 2019a). In accordance with Illinois guidance, we derived an ADI by multiplying the MCL by the default water ingestion rate of 2 L/day (IEPA, 2019a). In the absence of an MCL, we used the RfD used by US EPA to derive its Regional Screening Levels (RSLs) (US EPA, 2023) as a conservative estimate of the ADI. The RfDs are given in mg/kg-day, while the ADIs are given in mg/day; thus, we multiplied the RfD by a standard body weight of 70 kg to obtain the ADI in mg/day. The calculation of the HTC values is shown in Appendix Table B.1.

We used bioconcentration factors (BCFs) from a hierarchy of sources. The primary BCFs were those that US EPA used to calculate the national recommended water quality criteria (NRWQC) for human health (US EPA, 2002, 2016). Other sources included BCFs used in the US EPA coal combustion ash risk assessment (US EPA, 2014) and BCFs reported by Oak Ridge National Laboratory's Risk Assessment Information System (ORNL RAIS).[5] Lithium did not have a BCF value available from any authoritative source. Therefore, the water quality criterion for lithium was calculated assuming a BCF of 1. This is a conservative assumption as lithium does not readily bioaccumulate in the aquatic environment (ECHA, 2020a,b; ATSDR, 2010).

Illinois recommends a fish consumption rate of 0.020 kg/day (20 g/day) for an adult weighing 70 kg (IEPA, 2019a). Illinois recommends a water consumption rate of 0.01 L/day for "incidental exposure through contact or ingestion of small volumes of water while swimming or during other recreational activities" (IEPA, 2019a). Appendix Table B.1 presents the calculated HTC for fish and water, and for fish consumption only.

Screening Risk Evaluation: The maximum modeled and measured COI concentrations in surface water were compared to the calculated Illinois HTC values (Table 3.7). All surface water concentrations were below their respective benchmarks. The HTC values are protective of recreational exposure *via* water and/or fish ingestion and do not account for dermal exposures to COIs in surface water while swimming. However, given that the modeled COI surface water concentrations are orders of magnitude below HTC protective of water and/or fish ingestion, dermal exposures to COIs are not expected to be a risk concern. Moreover, the dermal uptake of metals is considered to be minimal and only a small proportion of ingestion exposures. Thus, none of the COIs evaluated would be expected to pose an unacceptable risk to recreators exposed to surface water while swimming and anglers consuming fish caught in the Illinois River.

---

[5] Although recommended by US EPA (2015c), US EPA EpiSuite 4.1 (US EPA, 2019b) was not used as a source of BCFs because inorganic compounds are outside the estimation domain of the program.

Table 3.7 Risk Evaluation for Recreators Exposed to Surface Water

COI	Maximum Surface Water Concentration (modeled) (mg/L)	Maximum Surface Water Concentration (measured) (mg/L)	HTC for Water and Fish (mg/L)	HTC for Water Only (mg/L)	HTC for Fish Only (mg/L)	COPC based on modeled	COPC based on measured
Arsenic	2.6E-06	1.2E-03	2.2E-02	2.0E+00	2.3E-02	No	No
Boron	1.2E-03	2.2E-01	4.7E+02	1.4E+03	7.0E+02	No	No
Cadmium	6.6E-07	ND	1.8E-03	1.0E+00	1.9E-03	No	No
Cobalt	6.8E-07	ND	3.5E-03	2.1E+00	3.5E-03	No	No
Iron	7.6E-04	2.4E-01	1.3E+02	4.9E+03	1.3E+02	No	No
Lithium	5.3E-06	8.0E-03	4.7E+00	1.4E+01	7.0E+00	No	No
Manganese	9.0E-05	6.0E-02	9.3E+01	1.7E+02	2.1E+02	No	No
Molybdenum	1.4E-05	6.1E-03	3.9E+00	3.5E+01	4.4E+00	No	No
Thallium	2.5E-07	ND	1.7E-03	4.0E-01	1.7E-03	No	No

Notes:

COI = Constituent of Interest; COPC = Constituent of Potential Concern; HTC = Human Threshold Criteria; ND = Not Detected; SW = Surface Water; WAPS = West Ash Pond System.

(a) Measured surface water concentrations may be different from modeled concentrations because measured data include the effects of background and other industrial sources. Modeled concentrations only represent the potential effect on surface water quality resulting from the measured groundwater concentrations.

3.4.2 Recreators Exposed to Sediment

Recreational exposure to sediment may occur during boating and swimming activity along the Illinois River; exposure to sediment may occur through incidental ingestion and dermal contact.

Screening Exposures: COIs in impacted groundwater flowing into the river can sorb to sediments. In the absence of sediment data, sediment concentrations were modeled using maximum detected groundwater concentrations.

Screening Benchmarks: There are no established recreator RSLs that are protective of recreational exposures to sediment (US EPA, 2019c). Therefore, benchmarks that are protective of recreational exposures to sediment *via* incidental ingestion and dermal contact were calculated using US EPA's RSL guidance (US EPA, 2019c). These benchmarks were calculated using the recommended assumptions (*i.e.*, oral bioavailability, body weights, averaging time) and toxicity reference values (*i.e.*, RfD and cancer slope factor [CSF]), with the following changes: Recreators were assumed to be exposed to sediment while recreating 60 days a year (or 2 weekend days per week for 30 weeks a year, from April to October). The exposure duration was assumed for a child 6 years of age and an adult 20 years of age, per US EPA guidance (Stalcup, 2014). The daily recommended residential soil ingestion rates of 200 mg/day for a child and 100 mg/day for an adult are based on an all-day exposure to residential soils (Stalcup, 2014; US EPA, 2011b). Since recreational exposures to sediment are assumed to occur for less than 3 hours per day, one-third of the daily residential soil ingestion (67 mg/day for a child and 33 mg/day for an adult) was used as a conservative assumption.

For dermal exposures, recreators were assumed to be exposed to sediment on their lower legs and feet (1,026 cm^2 for the child and 3,026 cm^2 for the adult, based on the age-weighted surface areas reported in US EPA, 2011b). While other body parts may be exposed to sediment, the contact time will likely be very short, as the sediment would wash off in the surface water. We used US EPA's recommended adherence factor of 0.2 mg/cm^2 based on child exposure to wet soil (US EPA, 2004; Stalcup, 2014), which was used in the US EPA RSL User's Guide for a child recreator exposed to soil or sediment (US EPA, 2019c). The sediment screening benchmarks for cadmium and cobalt were calculated based on a target hazard quotient of 1. Appendix Table B.2 presents the calculation of RSLs protective of recreational exposures to sediment.

Screening Risk Evaluation: The modeled sediment concentrations were well below the recreational sediment RSLs (Table 3.8). Therefore, exposure to sediment is not expected to pose an unacceptable risk to recreators while swimming or boating.

Table 3.8 Risk Evaluation for Recreators Exposed to Sediment

COI	Modeled Sediment Concentration (mg/kg)	Recreator RSL (mg/kg)	COPC
Arsenic	5.0E-04	6.8E+01	No
Boron	6.0E-03	2.7E+05	No
Cadmium	3.2E-04	1.2E+02	No
Cobalt	2.4E-04	4.1E+02	No
Iron	1.9E-02	9.6E+05	No
Lithium	NA[a]	2.7E+03	No
Manganese	1.2E+00	3.3E+04	No
Molybdenum	2.2E-03	6.8E+03	No
Thallium	3.3E-06	1.4E+01	No

Notes:
COI = Constituent of Interest; COPC = Constituent of Potential Concern; NA = Not Available; RSL = Regional Screening Level.
(a) Lithium could not be modeled in sediment because it lacks a K_d value.

3.5 Ecological Risk Evaluation

Based on the ecological CEM (Figure 3.4), ecological receptors could be exposed to surface water and dietary items (*i.e.*, prey and plants) potentially impacted by identified COIs (cadmium and cobalt).

3.5.1 Ecological Receptors Exposed to Surface Water

Screening Exposures: The ecological evaluation considered aquatic communities in the Illinois River potentially impacted by identified ecological COIs. Measured and modeled surface water concentrations were compared to risk-based ecological screening benchmarks.

Screening Benchmarks: Surface water screening benchmarks protective of aquatic life were obtained from the following hierarchy of sources:

- IEPA SWQS (IEPA, 2019a), regulatory standards that are intended to protect aquatic life exposed to surface water on a long-term basis (*i.e.*, chronic exposure). For cadmium, the surface water benchmark is hardness dependent and calculated using a default hardness of 100 mg/L[6];
- NRWQC – Aquatic Life Criteria Table (US EPA, 2019a); and
- US EPA Region IV (2018) surface water ESVs for hazardous waste sites.

---

[6] While USGS hardness data are available, US EPA's (2019a) default hardness of 100 mg/L was conservatively used. Conservatisms associated with using a default hardness value are discussed in Section 3.4.

Risk Evaluation: The maximum modeled COI concentrations in surface water were compared to the benchmarks protective of aquatic life (Table 3.9). The measured and modeled surface water concentrations were below their respective benchmarks. Thus, none of the COIs evaluated are expected to pose an unacceptable risk to aquatic life in the Illinois River.

Table 3.9 Risk Evaluation of Ecological Receptors Exposed to Surface Water

COI	Maximum Surface Water Concentration, Modeled (mg/L)	Maximum Detected SW Conc (mg/L)	Ecological Freshwater Benchmark (mg/L)	Basis	COPC Based on Modeled Values	COPC Based on Measured Values
Boron	1.2E-03	2.2E-01	7.6E+00	IEPA (2019a)	No	No
Cadmium	6.6E-07	ND	1.1E-03	IEPA (2019a)	No	No
Iron	7.6E-04	2.4E-01	1.0E+00	US EPA Region IV (2018)	No	No

Notes:

COI = Constituent of Interest; COPC = Constituent of Potential Concern; IEPA = Illinois Environmental Protection Agency; N = No; ND = Not Detected; SW = Surface Water; US EPA R4 = United States Environmental Protection Agency Region IV.

(a) Modeled COI concentrations reflect the potential maximum COI surface water concentrations from groundwater mixing with surface water.

(b) A default hardness value of 100 mg/L was used to calculate this hardness-dependent benchmark.

3.5.2 Ecological Receptors Exposed to Sediment

Screening Exposures: COIs in impacted groundwater discharging into the Illinois River can sorb to sediments *via* chemical partitioning. In the absence of sediment data, sediment concentrations were modeled using maximum detected groundwater concentrations. Therefore, the modeled COI sediment concentrations reflect the potential maximum Site-related sediment concentration from groundwater discharge.

Screening Benchmarks: Sediment screening benchmarks were obtained from US EPA Region IV (2018). The majority of the sediment ESVs are based on threshold effect concentrations (TECs) from MacDonald *et al.* (2000), which provide consensus values that identify concentrations below which harmful effects on sediment-dwelling organisms are unlikely to be observed. The benchmarks used in this evaluation are listed in Table 3.10.

Screening Risk Results: The maximum modeled COI sediment concentrations were below their respective sediment screening benchmarks (Table 3.10). The modeled sediment concentrations attributed to potential contributions from Site groundwater for all COIs were less than 1% of the sediment screening benchmark. Therefore, the modeled sediment concentrations attributed to potential contributions from Site groundwater are not expected to significantly contribute to ecological exposures in the Illinois River adjacent to the Site.

Table 3.10 Risk Evaluation of Ecological Receptors Exposed to Sediment

COI	Modeled Sediment Concentration (mg/kg)	ESV[a] (mg/kg)	COPC	% of Benchmark
Boron	5.97E-03	38[c]	No	0.02%
Cadmium	3.16E-04	0.99	No	0.03%
Iron	1.90E-02	20,000	No	0.0001%

Notes:

COI = Constituent of Interest; COPC = Constituent of Potential Concern; ESV = Ecological Screening Value; NOEC = No Observed Effect Concentration; US EPA = United States Environmental Protection Agency.

(a) ESV from US EPA Region IV (2018).

(c) Boron NOEC of 38 mg/kg was used as a conservative benchmark for boron in the absence of an ESV (ECHA, 2019 219-6670).

3.5.3 Ecological Receptors Exposed to Bioaccumulative Constituents of Interest

Screening Exposures: COIs with bioaccumulative properties can impact higher-trophic-level wildlife exposed to these COIs *via* direct exposures (surface water and sediment exposure) and secondary exposures through the consumption of dietary items (*e.g.*, plants, invertebrates, small mammals, and fish).

Screening Benchmark: US EPA Region IV (2018) guidance and IEPA's SWQS (IEPA, 2019a) guidance were used to identify analytes with potential bioaccumulative effects.

Risk Evaluation: The ecological COIs (boron, cadmium and iron)[7] were not identified as having potential bioaccumulative effects. Therefore, these COIs are not considered to pose an ecological risk *via* bioaccumulation.

3.6 Uncertainties and Conservatisms

A number of uncertainties and their potential impact on the risk evaluation are discussed below. Wherever possible, conservative assumptions were used in an effort to minimize uncertainties and overestimate rather than underestimate risks.

Exposure Estimates:

- The risk evaluation included the IL Part 845.600 constituents detected in groundwater samples collected from wells downgradient of the WAPS. However, it is possible that not all of the detected constituents are related specifically to the WAPS, since there are several sources in this area.
- The human health and ecological risk characterizations were based on the maximum modeled COI concentrations, rather than on averages. Thus, the variability in exposure concentrations was not considered. Given that receptors are mobile and concentrations change over time, assuming continuous exposure to the maximum concentration overestimates human and ecological exposures. For example, US EPA guidance states that risks should be estimated using average exposure concentrations as represented by the 95% upper confidence limit on the mean (US EPA, 1992). Given that exposure estimates based on the maximum concentrations did not exceed risk benchmarks, we have greater confidence that there is no risk concern.

---

[7] US EPA Region IV (2018) identifies only mercury (including methyl mercury) and selenium as having potential bioaccumulative effects. IEPA (2019a) identifies mercury as the only metal with bioaccumulative properties. Mercury and selenium were detected in groundwater but were not considered ecological COIs.

- Only analytes detected in groundwater were used to identify COIs and model COI concentrations in surface water and sediment. For the constituents that were not detected in WAPS groundwater, the detection limits were below the IL Part 845 GWPS and thus do not require further evaluation.
- COI concentrations in surface water were modeled using the maximum detected total or dissolved COI concentrations. In this case, maximum detected concentrations for cadmium, cobalt, and lithium are based on total concentrations. Modeling surface water concentrations using total metal concentrations for these COIs may overestimate surface water concentrations because dissolved concentrations, which are lower than total concentrations, represent the mobile fractions of constituents that could likely flow into and mix with surface water.
- The COIs identified in this evaluation also occur naturally in the environment. Contributions to exposure from natural or other non-WAPS-related sources were not considered in the evaluation of modeled concentrations; only exposure contributions potentially attributable to Site groundwater mixing with surface water were evaluated. While not quantified, exposures from potential WAPS-related groundwater contributions are likely to represent only a small fraction of the overall human and ecological exposure to COIs that also have natural or non-WAPS-related sources.
- Screening benchmarks for human health were developed using exposure inputs based on US EPA's recommended values for reasonable maximum exposure (RME) assessments (Stalcup, 2014). RME is defined as "the highest exposure that is reasonably expected to occur at a site but that is still within the range of possible exposures" (US EPA, 2004). US EPA states the "intent of the RME is to estimate a conservative exposure case (*i.e.*, well above the average case) that is still within the range of possible exposures" (US EPA, 1989). US EPA also notes that this high-end exposure "is the highest dose estimated to be experienced by some individuals, commonly stated as approximately equal to the 90th percentile exposure category for individuals" (US EPA, 2015b). Thus, most individuals will have lower exposures than those presented in this risk assessment.
- Although the maximum radium-226+228 concentration in groundwater exceeded the ecological screening benchmark, radium-226+228 was not considered an ecological COI because the two highest results, detected slightly above the benchmark, were considered outliers at the 1% significance level. While risks to ecological receptors exposed to radium-226+228 in surface water, sediment, and diet were not evaluated, the risks are expected to be *de minimis*.[8]

Toxicity Benchmarks:

- Screening-level ecological benchmarks were compiled from IEPA and US EPA guidance and designed to be protective of the majority of Site conditions, leaving the option for Site-specific refinement. In some cases, these benchmarks may not be representative of the Site-specific conditions or receptors found at the Site, or may not accurately reflect concentration-response relationships encountered at the Site. For example, the ecological benchmark for cadmium is hardness dependent. While a US Geological Survey [USGS] station had available hardness data, we relied on US EPA's default hardness of 100 mg/L due to the limitations of the USGS data. USGS data from Hennepin, Illinois (five miles downstream of the Site) reported hardness ranging from 200 to 370 mg/L, with a mean hardness of 288 mg/L, based on samples collected in 1980-

---

[8] Radium was not analyzed in surface water. However, the surface water and sediment modeling for other ecological COIs demonstrate that the modeled concentrations are orders of magnitude lower than the measured COI concentration in surface water and sediment. Given that the maximum groundwater concentration slightly exceeds the surface water benchmark, the modeled surface water and sediment concentrations will be below their respective benchmarks. Furthermore, radium is not described in US EPA Region IV guidance, but it is identified as bioaccumulative by other entities (*e.g.*, ATSDR, 1990). However, the benchmark used to identify ecological COIs already considers bioaccumulative exposures. Given that the modeled concentrations are anticipated to be below benchmarks, which account for bioaccumulative exposures, radium-226+228 is not expected to pose a risk concern to ecological receptors based on its bioaccumulative properties.

1997 (USGS, 2021b). Increasing the hardness from 100 to 288 mg/L would increase the cadmium SWQS because benchmarks become less stringent with higher levels of hardness. Regardless of the hardness, the maximum modeled cadmium concentration is orders of magnitude below the SWQS.

- In addition, for the ecological evaluation, we conservatively assumed all constituents to be 100% bioavailable. Modeled COI concentrations in surface water are considered total COI concentrations. US EPA recommends using dissolved metals as a measure of exposure to ecological receptors because it represents the bioavailable fraction of metal in water (US EPA, 1993). Therefore, the modeled surface water COI concentrations may be an overestimation of exposure concentrations to ecological receptors.
- In general, it is important to appreciate that the human health toxicity factors used in this risk evaluation are developed to account for uncertainties, such that safe exposure levels used as benchmarks are often many times lower (even orders of magnitude lower) than the levels that cause effects that have been observed in human or animal studies. For example, toxicity factors incorporate a 10-fold safety factor to protect sensitive subpopulations. This means that a risk exceedance does not necessarily equate to actual harm.

4 Summary and Conclusions

A screening-level risk evaluation was performed for Site-related constituents in groundwater at the Hennepin Power Plant in Hennepin, Illinois. The CSM developed for the Site indicates that groundwater beneath the WAPS flows into the Illinois River adjacent to the Site and may potentially impact surface water and sediment.

CEMs were developed for human and ecological receptors. The complete exposure pathways for humans include recreators in the Illinois River who are exposed to surface water and sediment (boaters and swimmers) and anglers who consume locally caught fish. Based on the local hydrogeology, residential exposure to groundwater used for drinking water or irrigation is not a complete pathway and was not evaluated. The complete exposure pathways for ecological receptors include aquatic life (including aquatic and marsh plants, amphibians, reptiles, and fish) exposed to surface water; benthic invertebrates exposed to sediment; and avian and mammalian wildlife exposed to bioaccumulative COIs in surface water, sediment, and dietary items.

Surface water data collected in 2020 and 2021, and groundwater data collected from 2018 to 2023, were used to estimate exposures. The maximum detected concentrations in surface water were used for human and ecological receptors exposed to surface water. For analytes detected in groundwater, surface water concentrations were also modeled using the maximum detected groundwater concentration. In the absence of sediment data, modeled sediment concentrations based on the maximum detected groundwater concentrations were used as the exposure estimate for human and ecological receptors. Surface water and sediment exposure estimates were screened against benchmarks protective of human health and ecological receptors for this risk evaluation.

For recreators (boaters and swimmers) exposed to surface water, all COIs were below the conservative risk-based screening benchmarks. Therefore, none of the COIs evaluated in surface water are expected to pose an unacceptable risk to recreators swimming or boating in the Illinois River adjacent to the Site.

For recreators exposed to sediment *via* incidental ingestion and dermal contact, the modeled sediment concentrations for all COIs were below the health protective sediment benchmarks. Therefore, the modeled concentrations in sediment are not expected to pose an unacceptable risk to recreators exposed to sediment in the Illinois River adjacent to the Site.

For anglers consuming locally caught fish, the maximum measured and modeled concentrations of all COIs in surface water were below conservative benchmarks protective of fish consumption. Therefore, none of the COIs evaluated are expected to pose an unacceptable risk to recreators consuming fish caught in the Illinois River.

Ecological receptors exposed to surface water include aquatic and marsh plants, amphibians, reptiles, and fish. The risk evaluation showed that none of the modeled or measured COIs in surface water exceeded protective screening benchmarks. Ecological receptors exposed to sediment include benthic invertebrates. The modeled sediment COIs did not exceed the conservative screening benchmarks; therefore, none of the COIs evaluated in sediment are expected to pose an unacceptable risk to ecological receptors. Ecological receptors were also evaluated for exposure to bioaccumulative COIs. This evaluation considered higher-trophic-level wildlife with direct exposure to surface water and sediment and secondary exposure through the consumption of dietary items (*e.g.*, plants, invertebrates, small mammals, fish). The ecological COIs were not identified as having potential bioaccumulative effects. Therefore, these COIs are not considered to pose an ecological risk *via* bioaccumulation. Overall, this evaluation demonstrated that none of the COIs evaluated are expected to pose an unacceptable risk to ecological receptors.

It should be noted that this evaluation incorporates a number of conservative assumptions that tend to overestimate exposure and risk. The risk evaluation was based on the maximum detected COI concentration; however, US EPA guidance states that risks should be based on a representative average concentration such as the 95% upper confidence limit on the mean; thus, using the maximum concentration tends to overestimate exposure. Although the COIs identified in this evaluation also occur naturally in the environment, the contributions to exposure from natural background sources and nearby industry were not considered; thus, CCR-related exposures were likely overestimated. Exposure estimates assumed 100% metal bioavailability, which likely results in overestimates of exposure and risks. Exposure estimates were based on inputs to evaluate the RME; thus, most individuals will have lower exposures than those estimated in this risk assessment.

Finally, it should be noted that because current conditions do not present a risk to human health or the environment, there will also be no unacceptable risk to human health or the environment for future conditions when the WAPS is closed. For all future closure scenarios, potential releases of CCR-related constituents will decline over time and, consequently, potential exposures to CCR-related constituents in the environment will also decline.

References

Agency for Toxic Substances and Disease Registry (ATSDR). 1990. "Toxicological Profile for Radium." December.

Agency for Toxic Substances and Disease Registry (ATSDR). 2010. "Toxicological Profile for Boron." November. Accessed at http://www.atsdr.cdc.gov/ToxProfiles/tp26.pdf.

European Chemicals Agency (ECHA). 2020a. "REACH dossier for boron (CAS No. 7440-42-8)." Accessed at https://echa.europa.eu/registration-dossier/-/registered-dossier/14776.

European Chemicals Agency (ECHA). 2020b. "REACH dossier for lithium (CAS No. 7439-93-2)." Accessed at https://echa.europa.eu/registration-dossier/-/registered-dossier/14178.

Geosyntec Consultants. 2020. "MW 51 and 21R boring logs, Hennepin Power Station." 5p. February 4.

Geosyntec Consultants. 2021. "Surface Water Sampling Locations, Hennepin Power Plant, Hennepin, Illinois." 1p., July.

Google LLC. 2023. "Google Earth Pro." Accessed at https://www.google.com/earth/versions/#earth-pro.

Illinois Environmental Protection Agency (IEPA). 2013. "Title 35: Environmental Protection, Subtitle F: Public Water Supplies, Chapter I: Pollution Control Board, Part 620: Ground Water Quality." 60p. Accessed at https://www.ilga.gov/commission/jcar/admincode/035/035006200D04200R.html.

Illinois Environmental Protection Agency (IEPA). 2016. "Appendix A-5. 303(d) Listed Waters Maps." In "Illinois Integrated Water Quality Report and Section 303(d) List - Volume I: Surface Water - 2016 (Final as submitted to US EPA Region V on July 11, 2016)". 34p. Accessed at https://www2.illinois.gov/epa/Documents/iepa/water-quality/watershed-management/tmdls/2016/303-d-list/appendix-a5.pdf

Illinois Environmental Protection Agency (IEPA). 2018. "Illinois Integrated Water Quality Report and Section 303(d) List, 2018 (Draft)." 145p, November 1.

Illinois Environmental Protection Agency (IEPA). 2019a. "Title 35: Environmental Protection, Subtitle C: Water Pollution, Chapter I: Pollution Control Board, Part 302: Water Quality Standards." 194p. Accessed at https://www.epa.gov/sites/production/files/2019-11/documents/ilwqs-title35-part302.pdf.

Illinois Environmental Protection Agency (IEPA). 2019b. "Appendix A-1. Illinois' 2018 303(d) List and Prioritization." In "Illinois Integrated Water Quality Report and Section 303(d) List, 2018 (Final as submitted to US EPA Region V on February 22, 2021)." 40p., May 20. Accessed at https://www2.illinois.gov/epa/topics/water-quality/watershed-management/tmdls/Documents/Appendix%20A-1_303d_by_priority_FINAL_5-20-19.pdf

Illinois Environmental Protection Agency (IEPA). 2021. "Standards for the disposal of coal combustion residuals in surface impoundments." Accessed at https://www.ilga.gov/commission/jcar/admincode/035/03500845sections.html.

Illinois Environmental Protection Agency (IEPA). 2024a. "Public Water Supply Systems Search (SDWIS Version 3.02)." Accessed at http://water.epa.state.il.us/dww/index.jsp.

Illinois State Geological Survey (ISGS). 2024b. "Illinois Water Well (ILWATER) Interactive Map." Accessed at https://prairie-research.maps.arcgis.com/apps/webappviewer/index.html?id=e06b64ae0c814ef3a4e43a191cb57f87.

MacDonald, DD; Ingersoll, CG; Berger, TA. 2000. "Development and evaluation of consensus-based sediment quality guidelines for freshwater ecosystems." *Arch. Environ. Contam. Toxicol.* 39:20-31. doi: 10.1007/s002440010075.

Morris, P. [Dynegy Midwest Generation, LLC]. 2021. Letter to D. LeCrone (IEPA) re: CCR surface impoundment category designation and justification for Dynegy Midwest Generation, LLC. May 19.

Natural Resource Technology (NRT). 2017. "Hydrogeologic Site Characterization Report, Hennepin West Ash Pond System, Hennepin, Illinois (Final)." Report to Dynegy Midwest Generation, LLC, Collinsville, IL. 917p., December 20.

OBG. 2019. "Corrective Measures Assessment, Old West Ash Pond (Pond No. 1 and Pond No. 3) and Polishing Pond, Hennepin Power Station, 13498 East 800th Street, Hennepin, Illinois." Part of Ramboll. Report to Dynegy Midwest Generation, LLC. 31p., September 5.

Prothro, MG. [US EPA, Office of Water]. 1993. Memorandum to US EPA Directors and Regions re: Office of Water policy and technical guidance on interpretation and implementation of aquatic life metals criteria. EPA-822-F93-009. 49p., October 1.

Ramboll. 2018-2020. "Final Closure and Post-Closure Plans for Hennepin East Ash Ponds No. 2 & No. 4." Report to Dynegy Midwest Generation, LLC. 1903p.

Ramboll. 2019. "MW 50 and 22D boring logs, Hennepin Power Station - Hennepin West Delineation." 6p. August 7.

Ramboll. 2021. "Hydrogeologic Site Characterization Report, East Ash Pond, Hennepin Power Plant, Hennepin, Illinois (Final)." Report to Dynegy Midwest Generation, LLC. 342p., October 25.

Ramboll. 2024a. "Corrective Action Alternatives Analysis Supporting Information Report: Dynegy Midwest Generation, LLC, Hennepin Power Station, West Ash Pond System, IEPA ID NO. W1550100002-01 and W1550100002-03 (Draft)." Report to Dynegy Midwest Generation, LLC, Hennepin, IL. 106p., February 23.

Ramboll. 2024b. "Groundwater and surface water data for West Ash Pond System, Hennepin Power Plant, 1994-2023."

Ramboll. 2025. "Corrective Action Groundwater Monitoring Plan: Hennepin Power Plant, West Ash Pond System, IEPA ID No. W1550100002-01 and W1550100002-03 (Draft)." Report to Dynegy Midwest Generation, LLC, Hennepin, IL. February 7.

Stalcup, D. [US EPA, Office of Solid Waste and Emergency Response (OSWER)]. 2014. Memorandum to Superfund National Policy Managers, Regions 1-10 re: Human Health Evaluation Manual, Supplemental Guidance: Update of standard default exposure factors. OSWER Directive 9200.1-120. 7p., February 6. Accessed at https://www.epa.gov/sites/production/files/2015-11/documents/oswer_directive_9200.1-120_exposurefactors_corrected2.pdf.

Tetra Tech, Inc. 2012. "Final TMDL Report: Middle Illinois River Total Maximum Daily Load and Load Reduction Strategies." Report to US EPA Region V; Illinois Environmental Protection Agency. 325p., August 9.

US Dept. of Energy (US DOE). 2019. "A Graded Approach for Evaluating Radiation Doses to Aquatic and Terrestrial Biota." DOE-STD-1153-2019. 169p. Accessed at https://www.standards.doe.gov/standards-documents/1100/1153-astd-2019/@@images/file.

US EPA Region IV. 2018. "Region 4 Ecological Risk Assessment Supplemental Guidance (March 2018 Update)." Superfund Division, Scientific Support Section. 98p., March. Accessed at https://www.epa.gov/sites/production/files/2018-03/documents/era_regional_supplemental_guidance_report-march-2018_update.pdf

US EPA. 1989. "Risk Assessment Guidance for Superfund (RAGS). Volume I: Human Health Evaluation Manual (Part A) (Interim final)." Office of Emergency and Remedial Response. NTIS PB90-155581, EPA-540/1-89-002. 287p., December.

US EPA. 1992. "Risk Assessment Guidance for Superfund: Supplemental Guidance to RAGS: Calculating the Concentration Term." Office of Emergency and Remedial Response (Washington, DC). OSWER Directive 9285.7-08I, NTIS PB92-963373. 8p., May.

US EPA. 1998. "Methodology for assessing health risks associated with multiple pathways of exposure to combustor emissions." National Center for Environmental Assessment (NCEA), Cincinnati, OH. EPA 600/R-98/137. December. Accessed at http://www.epa.gov/nceawww1/combust.htm.

US EPA. 2002. "National Recommended Water Quality Criteria: 2002. Human Health Criteria Calculation Matrix." Office of Water. EPA-822-R-02-012. 23p., November.

US EPA. 2004. "Risk Assessment Guidance for Superfund (RAGS). Volume I: Human Health Evaluation Manual (Part E, Supplemental Guidance for Dermal Risk Assessment) (Final)." Office of Superfund Remediation and Technology Innovation, Washington, DC. EPA/540/R/99/005, OSWER 9285.7-02EP, PB99-963312. 156p., July. Accessed at http://www.epa.gov/oswer/riskassessment/ragse/pdf/part_e_final_revision_10-03-07.pdf.

US EPA. 2011a. "IRIS Glossary." 17p., August 31. Accessed at https://ofmpub.epa.gov/sor_internet/registry/termreg/searchandretrieve/glossariesandkeywordlists/search.do?details=&glossaryName=IRIS%20Glossary#formTop.

US EPA. 2011b. "Exposure Factors Handbook: 2011 Edition." Office of Research and Development. US EPA, National Center for Environmental Assessment (NCEA). EPA/600/R-090/052F. 1436p., September. Accessed at https://www.epa.gov/expobox/about-exposure-factors-handbook.

US EPA. 2014. "Human and Ecological Risk Assessment of Coal Combustion Residuals (Final)." Office of Solid Waste and Emergency Response (OSWER), Office of Resource Conservation and Recovery. Submitted to US EPA Docket. EPA-HQ-OLEM-2020-0107-0885. 1237p., December. Accessed at http://www.regulations.gov/#!documentDetail;D=EPA-HQ-RCRA-2009-0640-11993.

US EPA. 2015a. "Hazardous and solid waste management system; Disposal of coal combustion residuals from electric utilities (Final rule)." *Fed. Reg.* 80(74):21302-21501. 40 CFR 257, 40 CFR 261, April 17.

US EPA. 2015b. "Conducting a Human Health Risk Assessment." October 14. Accessed at http://www2.epa.gov/risk/conducting-human-health-risk-assessment#tab-4.

US EPA. 2015c. "Human Health Ambient Water Quality Criteria: 2015 Update." Office of Water EPA. 820-F-15-001. 3p., June.

US EPA. 2016. "National Recommended Water Quality Criteria - Aquatic Life Criteria Table." April 18. Accessed at https://www.epa.gov/wqc/national-recommended-water-quality-criteria-aquatic-life-criteria-table.

US EPA. 2019a. "National Recommended Water Quality Criteria - Aquatic Life Criteria Table." October 10. Accessed at https://www.epa.gov/wqc/national-recommended-water-quality-criteria-aquatic-life-criteria-table.

US EPA. 2019b. "EPI Suite™ - Estimation Program Interface." March 12. Accessed at https://www.epa.gov/tsca-screening-tools/epi-suitetm-estimation-program-interface.

US EPA. 2019c. "Regional Screening Levels (RSLs) - User's Guide." 105p., May. Accessed at https://www.epa.gov/risk/regional-screening-levels-rsls-users-guide

US EPA. 2021. "Secondary drinking water standards: Guidance for nuisance chemicals." January 7. Accessed at https://www.epa.gov/sdwa/secondary-drinking-water-standards-guidance-nuisance-chemicals.

US EPA. 2023. "Regional Screening Level (RSL) Summary Table (TR=1E-06, THQ=1.0)." November. Accessed at https://semspub.epa.gov/src/document/HQ/404331.

US Geological Survey (USGS). 2016. "Upper Mississippi River System - Systemic Spatial Data Viewer." Accessed at https://umesc.usgs.gov/management/dss/umrs_land_cover_viewer.html.

US Geological Survey (USGS). 2021a. "Discharge data for Illinois River at Henry, IL (1981-2021) [USGS 05558300]."

US Geological Survey (USGS). 2021b. "Streamgage data for Illinois River at Hennepin, IL [USGS 05556200] [Summary of all available data]." In "National Water Information System Web Interface." Accessed at https://waterdata.usgs.gov/il/nwis/inventory/?site_no=05556200&.

Appendix A

Surface Water and Sediment Modeling

Gradient modeled concentrations in river surface water and sediment based on available groundwater data. First, we estimated the flow rate of constituents of interest (COIs) flowing to the Illinois River *via* groundwater. Then, we adapted United States Environmental Protection Agency's (US EPA's) indirect exposure assessment methodology (US EPA, 1998) in order to model surface water and sediment water concentrations in the Illinois River.

Model Overview

The groundwater flow into the river is represented by a one-dimensional steady-state model. In this model, the groundwater plume migrates horizontally in the uppermost aquifer, from south to north, in the direction of the Illinois River. The groundwater flow entering the river is the flow going through a cross-sectional area that has a length equal to the length of the river adjacent to the West Ash Pond System (WAPS) with potential coal combustion residual (CCR)-related impacts and a height equal to the saturated thickness of the uppermost aquifer (Table 3.4). It was assumed that all the groundwater flowing through the uppermost aquifer flows into the Illinois River. The length of the river adjacent to the WAPS was estimated using Google Earth Pro.

The groundwater flow into the river mixes with the surface water in the Illinois River. The COIs entering the river *via* groundwater can dissolve into the water column, sorb to suspended sediments, or sorb to benthic sediments. Using US EPA's indirect exposure assessment methodology (US EPA, 1998), the model evaluates the surface water and sediment concentrations at a location downstream of the groundwater discharge, assuming a well-mixed water column.

Groundwater Discharge Rate

We used conservative assumptions to evaluate the groundwater discharge rate of the COIs. We conservatively assumed that the groundwater concentrations were uniformly equal to the maximum detected concentration for each individual COI. We ignored adsorption by subsurface soil and assumed that all the groundwater flowing through the uppermost aquifer flows into the river.

For each groundwater unit, the groundwater flow rate into the river was derived using Darcy's Law:

$$Q = KiA$$

where:

Q = Groundwater flow rate (m^3/s)
K = Hydraulic conductivity (m/s)
i = Hydraulic gradient (m/m)
A = Cross-sectional area (m^2)

For each COI, the mass discharge rate into the river was then calculated by:

$$m_c = C_c \times Q \times CF$$

where:

m_c = Mass discharge rate of the COI (mg/year)
C_c = Maximum groundwater concentration of the COI (mg/L)
CF = Conversion factors needed for unit conversion: 1,000 L/m^3; 31,557,600 s/year

The values of the aquifer parameters used for these calculations are provided in Table A.1. The calculated mass discharge rates were then used as inputs for the surface water and sediment partitioning model.

Surface Water and Sediment Concentration

Groundwater flowing into the river gets diluted in the surface water flow. Constituents transported by groundwater into the surface water migrate into the water column and the bed sediments. The surface water model we used to estimate the surface water and sediment concentrations is a steady-state model described in US EPA's indirect exposure assessment methodology (US EPA, 1998) and also used in US EPA's "Human and Ecological Risk Assessment of Coal Combustion Residuals" (US EPA, 2014). This model describes the partitioning of constituents between surface water, suspended sediments, and benthic sediments based on equilibrium partition coefficients. It estimates the concentrations of constituents in surface water, suspended sediments, and benthic sediments at steady-state equilibrium at a theoretical location downstream of the discharge point after complete mixing of the water column. In our analysis, we used the partitioning coefficients given in Table J-1 of the US EPA CCR Risk Assessment for all COIs (US EPA, 2014). These coefficients are presented in Table A.2.

To be conservative, we assumed that the constituents were not affected by dissipation or degradation once they entered the water body. The total water body concentration of the COI was calculated as (US EPA, 1998):

$$C_{wtot} = \frac{m_c}{V_f \times f_{water}}$$

where:

C_{wtot} = Total water body concentration of the constituent (mg/L)
V_f = Water body annual flow (L/year)
f_{water} = Fraction of COI in the water column (unitless)
m_c = Mass discharge rate of the COI (mg/year)

For the Illinois River annual flow rate, we conservatively used the low flow (10th percentile) discharge rate of about 5,100 cubic feet per second (cfs) based on the daily mean discharge rates measured at Henry (USGS station #05558300)[9] between 1981 and 2021 (USGS, 2021).

The fraction of COIs in the water column was calculated for each COI using the sediment/water and suspended solids/water partition coefficients (US EPA, 2014). The fraction of COIs in the water column is defined as (US EPA, 2014):

$$f_{water} = \frac{(1 + [K_{dsw} \times TSS \times 0.000001]) \times \frac{d_w}{d_z}}{\left([1 + (K_{dsw} \times TSS \times 0.000001)] \times \frac{d_w}{d_z}\right) + ([bsp + K_{dbs} \times bsc] \times \frac{d_b}{d_z})}$$

where:

K_{dsw} = Suspended sediment-water partition coefficient (mL/g)
K_{dbs} = Sediment-water partition coefficient (mL/g)

---

[9] The USGS station at Henry, located approximately 18 miles downstream of the Hennepin plant, is the closest USGS gauging station with surface water flow data.

TSS = Total suspended solids in the surface water body (mg/L), set equal to the median river concentration of 40 mg/L (TetraTech, 2012)
0.000001 = Units conversion factor
d_w = Depth of the water column (m)
d_b = Depth of the upper benthic layer (m), set equal to 0.03 m (US EPA, 2014)
$d_z = d_w + d_b$ = Depth of the water body (m)
bsp = Bed sediment porosity (unitless), set equal to 0.6 (US EPA, 2014)
bsc = Bed sediment particle concentration (g/cm^3), set equal to 1.0 g/cm^3 (US EPA, 2014)

The fraction of COIs dissolved in the water column (f_d) is calculated as (US EPA 2014):

$$f_d = \frac{1}{1 + K_{dsw} \times TSS \times 0.000001}$$

The values of the fraction of COIs in the water column and other calculated parameters are presented in Table A.3. Other water body parameters are presented in Table A.4.

The total water column concentration (C_{wcTot}) of the COIs, comprising both the dissolved and suspended sediment phases, is then calculated as (US EPA, 2014):

$$C_{wcTot} = C_{wtot} \times f_{water} \times \frac{d_z}{d_w}$$

Finally, the dissolved water column concentration (C_{dw}) for the COIs is calculated as (US EPA, 2014):

$$C_{dw} = f_d \times C_{wcTot}$$

The dissolved water column concentration was then used to calculate the concentration of COIs sorbed to suspended solids in the water column (US EPA, 1998):

$$C_{sw} = C_{dw} \times K_{dsw}$$

where:

C_{sw} = Concentration sorbed to suspended solids (mg/kg)
C_{dw} = Concentration dissolved in the water column (mg/L)
K_{dsw} = Suspended solids/water partition coefficient (mL/g)

In the same way, using the total water body concentration and the fraction of COIs in the benthic sediments, the model derives the total concentration in benthic sediments (US EPA, 2014):

$$C_{bstot} = f_{benth} \times C_{wtot} \times \frac{d_z}{d_b}$$

where:

C_{bstot} = Total concentration in bed sediment (mg/L or g/m^3)

C_{wtot} = Total water body concentration of the constituent (mg/L)
f_{benth} = Fraction of contaminant in benthic sediments (unitless)
d_b = Depth of the upper benthic layer (m)
$d_z = d_w + d_b$ = Depth of the water body (m)

This value can be used to calculate dry weight sediment concentration as follows:

$$C_{sed-dw} = \frac{C_{bstot}}{bsc}$$

where:

C_{sed-dw} = Dry weight sediment concentration (mg/kg)
C_{bstot} = Total sediment concentration (mg/L)
bsc = Bed sediment bulk density (used the default value of 1 g/cm^3 from US EPA, 2014)

The total sediment concentration is composed of the concentration dissolved in the bed sediment pore water (equal to the concentration dissolved in the water column) and the concentration sorbed to benthic sediments (US EPA, 1998).

The concentration sorbed to benthic sediments was calculated from (US EPA, 1998):

$$C_{sb} = C_{dbs} \times K_{dbs}$$

where:

C_{sb} = Concentration sorbed to bottom sediments (mg/kg)
C_{dbs} = Concentration dissolved in the sediment pore water (mg/L)
K_{dbs} = Sediments/water partition coefficient (mL/kg)

For each COI, the modeled total water column concentration, the modeled dry weight sediment concentration, and the modeled concentration sorbed to sediment are presented in Table A.5.

Table A.1 Parameters Used to Estimate Groundwater Discharge to Surface Water

GW Unit	Parameter	Full Name	Value	Unit
Uppermost Aquifer	A	Cross-Sectional Area	11,613	m^2
Uppermost Aquifer	i	Hydraulic Gradient	0.005	m/m
Uppermost Aquifer	K	Hydraulic Conductivity	0.017	cm/s

Notes:
GW = Groundwater, UA = Uppermost Aquifer.
Average thickness of the UA (*i.e.*, 50 ft or 15.2 m) multiplied by the length of the WAP-intersecting Illinois River (2,500 ft, or 762 m).
Source: NRT (2017).

Table A.2 Partition Coefficients

Constituent	Sediment-Water, Mean, K_{dbs}		Suspended Sediment-Water, Mean, K_{dsw}	
	Value ($\log_{10}$) (mL/g)	Value (mL/g)	Value ($\log_{10}$) (mL/g)	Value (mL/g)
Arsenic (III)	2.4	2.51E+02	3.9	7.94E+03
Boron	0.8	6.31E+00	3.9	7.94E+03
Cadmium	3.3	2.00E+03	4.9	7.94E+04
Cobalt	3.1	1.26E+03	4.8	6.31E+04
Iron	1.4	2.51E+01	1.4	2.51E+01
Lithium	Not Available	Not Available	Not Available	Not Available
Manganese	4.4	2.80E+04	4.4	2.80E+04
Molybdenum	2.5	3.16E+02	4.4	2.51E+04
Thallium	1.3	2.00E+01	4.1	1.26E+04

Notes:

Lithium was not modeled because it lacks a K_d value in US EPA (2014).

Source: US EPA (2014).

Table A.3 Calculated Parameters

Constituent	Fraction of Constituent in the Water Column f_{water}	Fraction of Constituent in the Benthic Sediments $f_{benthic}$	Fraction of Constituent Dissolved in the Water Column $f_{dissolved}$
Arsenic (III)	0.4110	0.5890	0.7589
Boron	0.9622	0.0378	0.7589
Cadmium	0.2182	0.7818	0.2394
Cobalt	0.2717	0.7283	0.2838
Iron	0.8384	0.1616	0.9990
Lithium	0.9955	0.0045	1.0
Manganese	0.00999	0.9900	0.4717
Molybdenum	0.4576	0.5424	0.4988
Thallium	0.9070	0.0930	0.6651

Table A.4 Surface Water Parameters

Parameter	Full Name	Value	Unit
TSS	Total Suspended Solids	40	mg/L
V_{fx}	Surface Water Flow Rate	4.56E+12	L/yr
db	Depth of Upper Benthic Layer (default: 0.03)	0.03	m
dw	Depth of Water Column	4	m
dz	Depth of Water Body	4.03	m
bsc	Bed Sediment Particle Concentration (default)	1	g/cm^3
bsp	Bed Sediment Porosity (default: 0.6)	0.6	-
M_{TSS}	TSS Mass per Unit Area	0.16	kg/m^2
M_S	Sediment Mass per Unit Area	30	kg/m^2

Notes:

Source of input values: Flow rate value from USGS (2021), total suspended solids value from Tetra Tech (2012), and depth of water column value from USGS (2016). Remaining values from US EPA (2014).

Table A.5 Input Groundwater Concentrations and Output Surface Water and Sediment Concentrations

Constituent	Groundwater Concentration (mg/L)	Mass Discharge Rate to Surface Water (mg/year)	Total Water Column Concentration (mg/L)	Concentration Sorbed to Bottom Sediments (mg/kg)
Arsenic (III)	3.8E-02	1.2E+07	2.6E-06	5.0E-04
Boron	1.8E+01	5.6E+09	1.2E-03	6.0E-03
Cadmium	9.6E-03	3.0E+06	6.6E-07	3.2E-04
Cobalt	9.9E-03	3.1E+06	6.8E-07	2.4E-04
Iron	1.1E+01	3.4E+09	7.6E-04	1.9E-02
Lithium	7.6E-02	2.4E+07	5.3E-06	NA[a]
Manganese	1.3E+00	4.0E+08	9.0E-05	1.2E+00
Molybdenum	2.1E-01	6.4E+07	1.4E-05	2.2E-03
Thallium	3.6E-03	1.1E+06	2.5E-07	3.3E-06

Note:
(a) Lithium was not modeled in sediment due to a lack of K_d value in US EPA (2014).

References

Natural Resource Technology (NRT). 2017. "Hydrogeologic Site Characterization Report, Hennepin West Ash Pond System, Hennepin, Illinois (Final)." Report to Dynegy Midwest Generation, LLC, Collinsville, IL. 917p., December 20.

Tetra Tech, Inc. 2012. "Final TMDL Report: Middle Illinois River Total Maximum Daily Load and Load Reduction Strategies." Report to US EPA Region V; Illinois Environmental Protection Agency. 325p., August 9.

US EPA. 1998. "Methodology for assessing health risks associated with multiple pathways of exposure to combustor emissions." National Center for Environmental Assessment (NCEA), Cincinnati, OH. EPA 600/R-98/137. December. Accessed at http://www.epa.gov/nceawww1/combust.htm.

US EPA. 2014. "Human and Ecological Risk Assessment of Coal Combustion Residuals (Final)." Office of Solid Waste and Emergency Response (OSWER), Office of Resource Conservation and Recovery. Submitted to US EPA Docket. EPA-HQ-OLEM-2020-0107-0885. 1237p., December. Accessed at http://www.regulations.gov/#!documentDetail;D=EPA-HQ-RCRA-2009-0640-11993.

US Geological Survey (USGS). 2016. "Upper Mississippi River System - Systemic Spatial Data Viewer." Accessed at https://umesc.usgs.gov/management/dss/umrs_land_cover_viewer.html.

US Geological Survey (USGS). 2021. "Discharge data for Illinois River at Henry, IL (1981-2021) [USGS 05558300]."

Appendix B

Screening Benchmarks

Table B.1 Calculated Water Quality Standards Protective of Incidental Ingestion and Fish Consumption

Analytes	Bioconcentration Factor (BCF)		Average Daily Intake (ADI)			Human Threshold Criteria (HTC)		
	BCF[a] (L/kg-tissue)	Basis	MCL (mg/L)	RfD (mg/kg-d)	ADI[b] (mg/day)	Water & Fish (mg/L)	Water Only (mg/L)	Fish Only (mg/L)
Arsenic	44	NRWQC, 2002	0.010	0.00030	0.020	0.022	2.0	0.023
Boron	1	(d)	NC	0.20	14	467	1400	700
Cadmium	270	US EPA, 2014	0.0050	0.00050	0.010	0.0018	1.0	0.0019
Cobalt	300	ORNL RAIS	NC	0.00030	0.021	0.0035	2.1	0.0035
Iron	19	US EPA, 2014	NC	0.70	49	126	4900	129
Lithium	1	(d)	NC	0.002	0.14	4.7	14	7.0
Manganese	0.4	US EPA, 2014	NC	0.024	1.7	93	168	210
Molybdenum	4	US EPA, 2014	NC	0.00500	0.3500	3.9	35	4.4
Thallium	116	NRWQC, 2002	0.0020	0.000010	0.0040	0.0017	0.40	0.0017

Notes:

ADI = Average Daily Intake; BCF = Bioconcentration Factor; F = Fish Consumption Rate; HTC = Human Threshold Criteria; IEPA = Illinois Environmental Protection Agency; MCL = Maximum Contaminant Level; NA = BCF Not Available and Therefore, WQC for Fish Only Not Calculated; NC = No Criterion Available; NRWQC = National Recommended Water Quality Criteria; ORNL RAIS = Oak Ridge National Laboratory Risk Assessment Information System; RfD = Reference Dose; W = Water Consumption Rate; WQC = Water Quality Criteria; SWQC = Surface Water Quality Criteria; US EPA = United States Environmental Protection Agency.

(a) BCFs from the following hierarchy of sources:

NRWQC (US EPA, 2016). National Recommended Water Quality Criteria.
NRWQC (US EPA, 2002). National Recommended Water Quality Criteria: 2002. Human Health Criteria Calculation Matrix.
US EPA (2014). Human and Ecological Risk Assessment of Coal Combustion Residuals.
ORNL RAIS (ORNL, 2023). Risk Assessment Information System (RAIS) Chemical Toxicity Values.

(b) ADI based on the MCL is calculated as the MCL (mg/L) multiplied by a water ingestion rate of 2 L/day. In the absence of an MCL, the ADI was calculated as the RfD (mg/kg-d) multiplied by the body weight (70 kg).

(c) SWQC based on US EPA's action level.

(d) BCF of 1 was used as a conservative assumption, due to lack of published BCF.

Equations from IEPA (2019a):

Consumption of Water and Fish

$$\text{HTC} = \frac{\text{ADI}}{\text{W} + (\text{F} \times \text{BCF})}$$

Incidental Consumption of Water only

$$\text{HTC} = \frac{\text{ADI}}{\text{W}}$$

Consumption of Fish only

$$\text{HTC} = \frac{\text{ADI}}{\text{F} \times \text{BCF}}$$

Where

Average Daily Intake (ADI) = Chem. Specific mg/day
Fish Consumption Rate (F) = 0.02 kg/day
Bioconcentration Factor (BCF) = Chem. Specific L/kg-tissue
Water Consumption Rate (W) = 0.01 L/day

Table B.2 Recreator Exposure to Sediment

COI	Relative Bioavailability B (unitless)	Dermal Absorption Fraction ABS (unitless)	Cancer				Cancer SL (mg/kg)	Non-Cancer								Recreator RSL Sediment (mg/kg)	Basis
			TRV		Child + Adult			TRV		Child		Adult		Child	Adult		
			CSF $(mg/kg\text{-}d)^{-1}$	Derm. CSF $(mg/kg\text{-}d)^{-1}$	Incidental Ingestion SL_{ing} (mg/kg)	Dermal Contact SL_{derm} (mg/kg)		RfD (mg/kg-d)	Derm. RfD (mg/kg-d)	Incidental Ingestion SL_{ing} (mg/kg)	Dermal Contact SL_{derm} (mg/kg)	Incidental Ingestion SL_{ing} (mg/kg)	Dermal Contact SL_{derm} (mg/kg)	Non-Cancer SL (mg/kg)			
Arsenic	1	0.03	1.5E+00	1.5E+00	8.1E+01	4.1E+02	6.8E+01	3.0E-04	3.0E-04	4.1E+02	4.4E+03	4.4E+03	8.0E+03	3.8E+02	2.8E+03	6.8E+01	c
Boron	1	NA	NC	NC	NC	NC	NC	2.0E-01	2.0E-01	2.7E+05	NA	2.9E+06	NA	2.7E+05	2.9E+06	2.7E+05	nc
Cadmium	1	0.001	NC	NC	NC	NC	NC	1.0E-04	2.5E-06	1.4E+02	1.1E+03	1.5E+03	2.0E+03	1.2E+02	8.5E+02	1.2E+02	nc
Cobalt	1	NA	NC	NC	NC	NC	NC	3.0E-04	3.0E-04	4.1E+02	NA	4.4E+03	NA	4.1E+02	4.4E+03	4.1E+02	nc
Iron	1	NA	NC	NC	NC	NC	NC	7.0E-01	7.0E-01	9.6E+05	NA	1.0E+07	NA	9.6E+05	1.0E+07	9.6E+05	nc
Lithium	1	NA	NC	NC	NC	NC	NC	2.0E-03	2.0E-03	2.7E+03	NA	2.9E+04	NA	2.7E+03	2.9E+04	2.7E+03	nc
Manganese	1	NA	NC	NC	NC	NC	NC	2.4E-02	9.6E-04	3.3E+04	NA	3.5E+05	NA	3.3E+04	3.5E+05	3.3E+04	nc
Molybdenum	1	NA	NC	NC	NC	NC	NC	5.0E-03	5.0E-03	6.8E+03	NA	7.3E+04	NA	6.8E+03	7.3E+04	6.8E+03	nc
Thallium	1	NA	NC	NC	NC	NC	NC	1.0E-05	1.0E-05	1.4E+01	NA	1.5E+02	NA	1.4E+01	1.5E+02	1.4E+01	nc

Notes:

AL = EPA Action Level; COI = Constituent of Interest; CSF = Cancer Slope Factor; derm = Dermal Contact; ing = Ingestion; NC = No Criterion Available; RfD = Reference Dose; SL = Screening Level; TRV = Toxicity Reference Value.

Health Benchmark defined as the lower of the screening levels for cancer and non-cancer. The basis of the Health Benchmark is presented as c = based on cancer endpoint, or nc = based on non-cancer endpoint.

$$\text{Screening Benchmark} = \frac{1}{\frac{1}{SL_{ing}} + \frac{1}{SL_{derm}}}$$

$$\text{Non-cancer } SL_{ing} = \frac{THQ * RfD}{Intake} \qquad \text{Cancer } SL_{ing} = \frac{TR}{Intake * CSF}$$

$$\text{Non-cancer } SL_{derm} = \frac{THQ * RfD}{Intake * ABS} \qquad \text{Cancer } SL_{derm} = \frac{TR}{Intake * ABS * CSF}$$

Target Cancer Risk (TR) = 1E-05

Target Hazard Quotient (THQ) = 1

Sediment – Ingestion (Chemical)

		Non-Cancer		Cancer		
Intake Factor (IF) = $\frac{IR \times EF \times ED \times CF}{BW \times AT}$ =		7.3E-07 Child	6.8E-08 Adult	6.3E-08 Child	2.0E-08 Adult	Basis
IR	Ingestion Rate (mg/day)	67	33	67	33	One-third of US EPA residential soil ingestion rate (Prof. Judgment)
EF	Sediment Exposure Frequency (days/year)	60	60	60	60	2 days/week between April and Oct when air temp. > 70°F (Prof. Judgment)
ED	Exposure Duration (years)	6	20	6	20	Default value for Resident (US EPA, 2023)
CF	Conversion Factor (kg/mg)	0.000001	0.000001	0.000001	0.000001	
BW	Body Weight (kg)	15	80	15	80	Default value for Resident (US EPA, 2023)
AT	Averaging Time (d)	2,190	7,300	25,550	25,550	Default value for Resident (US EPA, 2023)

Sediment – Dermal Contact (Chemical)

		Non-Cancer		Cancer		
Intake Factor (IF) = $\frac{SA \times AF \times EF \times ED \times CF}{BW \times AT}$ =		2.2E-06 Child	1.2E-06 Adult	1.9E-07 Child	3.6E-07 Adult	Basis
SA	Surface Area Exposed to Sediment (cm²/day)	1,026	3,026	1,026	3,026	Age weighted SA for lower legs and feet (US EPA, 2011b)
AF	Sediment Skin Adherence Factor (mg/cm²)	0.2	0.2	0.2	0.2	Age weighted AF for children exposed to sediment (US EPA, 2011b)
EF	Sediment Exposure Frequency (days/year)	60	60	60	60	2 days/week between April and Oct when air temp. > 70°F (Prof. Judgment)
ED	Exposure Duration (years)	6	20	6	20	Default value for Resident (US EPA, 2023)
CF	Conversion Factor (kg/mg)	0.000001	0.000001	0.000001	0.000001	
BW	Body Weight (kg)	15	80	15	80	Default value for Resident (US EPA, 2023)
AT	Averaging Time (d)	2,190	7,300	25,550	25,550	Default value for Resident (US EPA, 2023)

Appendix B

Corrective Action Alternatives Analysis – Supporting Information Report

Intended for
Dynegy Midwest Generation, LLC
13498 E 800th St
Hennepin, Illinois 61327

Date
March 7, 2025

Project No.
1940103584-005

CORRECTIVE ACTION ALTERNATIVES ANALYSIS SUPPORTING INFORMATION REPORT

HENNEPIN POWER STATION, WEST ASH POND SYSTEM, IEPA ID NO. W1550100002-01 AND W1550100002-03

RAMBOLL Bright ideas. Sustainable change.

CORRECTIVE ACTION ALTERNATIVES ANALYSIS SUPPORTING INFORMATION REPORT HENNEPIN POWER STATION, WEST ASH POND SYSTEM, IEPA ID NO. W1550100002-01 AND W1550100002-03

Project name	**Hennepin West Ash Pond System**
Project no.	**1940103584-005**
Recipient	**Dynegy Midwest Generation, LLC**
Document type	**Supporting Information Report**
Revision	**DRAFT**
Date	**March 7, 2025**
Prepared by	**Elizabeth (Richter) Rotstein, PE**
Checked by	**Lucas Carr, PE**
Approved by	**Brian G. Hennings, PG**
Description	**Corrective Action Alternatives Analysis Supporting Information Report**

Ramboll
234 W. Florida Street
Fifth Floor
Milwaukee, WI 53204
USA

T 414-837-3607
F 414-837-3608
https://ramboll.com

Lucas Carr, PE
Qualified Professional Engineer

Brian G. Hennings, PG
Project Officer, Hydrogeology

CONTENTS

TABLES

APPENDICES

ACRONYMS AND ABBREVIATIONS

35 I.A.C.	Title 35 of the Illinois Administrative Code
40 C.F.R.	Title 40 of the Code of Federal Regulations
2020 closure	WAPS source control by consolidate-and-cap approach completed in 2020
bgs	below ground surface
BMP	best management practices
CAAA	Corrective Action Alternatives Analysis
CAAA-SIR	Corrective Action Alternatives Analysis Supporting Information Report
CAP	Corrective Action Plan
CCR	coal combustion residuals
CCR Rule	40 C.F.R. § 257 Subpart D
CIP	closure-in-place
cm/s	centimeters per second
CMA	Corrective Measures Assessment
COC	constituent of concern
CSM	conceptual site model
DMG	Dynegy Midwest Generation, LLC
gpm	gallons per minute
Gradient	Gradient Corporation
GWPS	groundwater protection standard(s)
HEN	Hennepin Power Station
HPP	Hennepin Power Plant
ID	identification
IDNR	Illinois Department of Natural Resources
IEPA	Illinois Environmental Protection Agency
ISS	in-situ solidification/stabilization
Kd	soil adsorption coefficient
mL/g	milliliters per gram
NAVD88	North American Vertical Datum of 1988
No.	number
NPDES	National Pollutant Discharge Elimination System
O&M	operation & maintenance
OWAP	Old West Ash Pond
OWPP	Old West Polishing Pond
PRB	Permeable Reactive Barrier
Ramboll	Ramboll Americas Engineering Solutions, Inc.
RS Means	RS Means Heavy Construction Cost Data
SI	surface impoundment
TDS	total dissolved solids
UA	uppermost aquifer
USEPA	United States Environmental Protection Agency
WAPS	West Ash Pond System

1. INTRODUCTION AND BACKGROUND

1.1 Plant and Site Information

Dynegy Midwest Generation, LLC (DMG) is the owner of the inactive coal-fired Hennepin Power Plant (HPP), also referred to as the Hennepin Power Station (HEN), in Hennepin, Putnam County, Illinois. DMG intends to complete groundwater corrective action at the coal combustion residuals (CCR) surface impoundment (SI) West Ash Pond System (WAPS), which is identified by Illinois Environmental Protection Agency (IEPA) identification (ID) numbers (No.) W1550100002-01 and W1550100002-03, CCR Unit ID 804, and National Inventory of Dams Number IL50698. The WAPS is comprised of the Old West Ash Pond (OWAP) and the Old West Polishing Pond (OWPP). WAPS was constructed as a single unit with a single perimeter dike and subsequently internally divided into the OWAP and OWPP as part of operational practices. Source control (*e.g.*, closure) was completed in 2020; this included leaving CCR in place within the OWAP, removing all CCR from the OWPP, placing it within the OWAP, and installing a geomembrane final cover system over the consolidated OWAP [1, 2]. This document and all past engineering and hydrogeological studies consider the WAPS as a single CCR unit. Groundwater corrective action for the HEN WAPS will be performed under the requirements of Title 35 of the Illinois Administrative Code (35 I.A.C.) § 845, Standards for the Disposal of Coal Combustion Residuals in Surface Impoundments [3] and the requirements of Title 40 of the Code of Federal Regulations (40 C.F.R.) § 257, herein referred to as the Federal CCR Rule [4].

1.2 CAAA-SIR Background and Scope

35 I.A.C. § 845 requires a Corrective Action Alternatives Analysis (CAAA) to be completed as part of remedy selection, pursuant to the requirements of 35 I.A.C. § 845.670(e). The CAAA for the HEN WAPS will be prepared by Gradient Corporation (Gradient). Ramboll Americas Engineering Solutions, Inc. (Ramboll) has prepared this Corrective Action Alternatives Analysis Supporting Information Report (CAAA-SIR) to provide information requested by Gradient to support the CAAA for the HEN WAPS.

This CAAA-SIR is a feasibility-level assessment utilized to evaluate multiple groundwater corrective action alternatives. The remedy that is selected within the CAAA, to which this CAAA-SIR is attached, is then further developed into a permit-level remedy within the Corrective Action Plan (CAP), to which the CAAA is attached. Therefore, there may be minor differences in information presented for the selected remedy between this CAAA-SIR and the CAP. Information that may be different includes, but is not limited to, groundwater quality data, groundwater modeling inputs and results, implementation schedules, time to reach GWPSs, physical dimensions and scope of the remedy, and engineering design parameters. These differences are due to the further remedy refinement that is inherent with advancing the selected alternative into the permit-level remedy that is included within the CAP.

1.2.1 Identified Corrective Action Alternatives

Corrective action remedies selected for evaluation within this CAAA-SIR include:

- Alternative 1: Source control with groundwater polishing (GWP); and
- Alternative 2: Source control with continuous containment system.

Multiple remedies were evaluated in the Corrective Measures Assessment (CMA), prepared by Ramboll and attached to the CAAA prepared by Gradient, including source control with GWP, source control with cutoff wall, source control with *in-situ* stabilization (ISS), source control with permeable reactive barrier (PRB), source control with in-situ chemical treatment, and source control with groundwater extraction.

Out of these remedies, source control with GWP, source control with cutoff wall, and source control with ISS were identified for further assessment, while the remaining remedies were determined to be infeasible. As part of further assessment performed during this CAAA-SIR modeling and development, the following adjustments were made to the remedies identified by the CMA:

- Following groundwater modeling, the source control with ISS remedy was determined to be infeasible and omitted for inclusion in this CAAA-SIR, for the reasons described below:
    - ISS would require the temporary removal of approximately 15 acres of the 30-acre completed WAPS final cover system. Removal of the final cover system could allow for significant stormwater infiltration into CCR within the WAPS, potentially leading to temporary reductions in the effectiveness of the completed source control.
    - ISS would require handling of tens of thousands of cubic yards of CCR and CCR-impacted ISS cuttings on the surface of the WAPS. These activities could lead to an elevated risk of releasing CCR-impacted stormwater and sediments during construction activities, which could result in negative impacts to adjacent environmentally sensitive areas.
- The source control with cutoff wall remedy was expanded into the source control with continuous containment system remedy. The remedy includes a deep cutoff wall that is integrated with the existing cover system to provide lateral and surface isolation of the CCR from the surrounding environment and keyed into the competent shale bedrock which will provide isolation below the WAPS. Additional information on the expanded remedy is provided in Section 3.

1.2.2 Scope of CAAA-SIR

Ramboll completed the following tasks and documented the tasks within this CAAA-SIR, for each of the corrective action alternative remedies listed in **Section 1.2.1**:

- Feasibility-level design drawings (**Appendix A**) were developed to show the approximate extents and typical details of the Alternative 2 remedy (source control with continuous containment system). Drawings were not prepared for the Alternative 1 remedy as it does not involve construction at the site.
- Narratives describing the implementation of each remedy were developed, including the pre-design, design, construction, and closeout phases.
- Feasibility-level schedules providing the estimated time to implement the remedy were developed, including design, permitting, and construction.
- Information required to evaluate specific portions of 35 I.A.C. § 845.670(e) requirements were prepared, as requested by Gradient, including 35 I.A.C. § 845.670(e)(1)(H) and 35 I.A.C. § 845.670(e)(3).

- Estimates of implementation-based equipment mileage, vehicle delivery mileage, labor hour, and labor commuting mileage, were developed for each remedy alternative where physical construction activities are expected to occur.

All remedies presented in this CAAA-SIR are in conjunction with source control for the WAPS, which was completed in 2020 ("2020 closure") in accordance with the closure plan and supporting groundwater modeling that was submitted to and approved by IEPA in 2018 [6, 7, 1, 2]. Source control was the primary corrective action completed for the WAPS and utilized a consolidate-and-cap approach. The consolidate-and-cap approach included excavating all CCR from the OWPP portion of the WAPS, constructing a sheet pile wall and compacted clay buttress to separate the closure-by-removal and closure-in-place (CIP) portions of the WAPS, placing the CCR excavated from the OWPP in the OWAP portion of the WAPS, and then capping the CIP area with a geosynthetic and soil final cover system ("completed WAPS final closure"). The design of the source control was supported by groundwater modeling included in the IEPA-approved 2017 closure plan (**Appendix B2**).

1.2.3 Criterion for Estimating Time to Achieve GWPS

Times to achieve GWPS for each of the remedial alternative remedies were estimated for the wells within the existing WAPS compliance monitoring system, using updated groundwater modeling that incorporated the 2020 closure, as provided in **Appendix B1**. This approach was utilized to provide a consistent comparison of the estimated time to reach GWPS for each remedy, as required by 35 I.A.C. § 845.670(e)(f).

Closure for the WAPS serves as the primary corrective action for the unit and was completed in 2020, as discussed in **Section 1.2.2**. Supplemental remedial alternatives for the WAPS will need to be integrated with the completed closure. This affects the time to reach GWPS for each remedy, as the timeframe for each remedial alternative to become functional varies based on the required level of remedy permitting, design, and construction, or lack thereof. To provide a simplified comparative framework for the remedial alternatives, the groundwater modeling provided in **Appendix B1** assumed that Corrective Action Plans would be approved in 2026 and that construction for the source control with continuous containment system remedy would be completed in 2028.

1.3 Report Contents

The following information is included within this report:

- **Section 1** includes the introduction and background;
- **Section 2** includes information for the Alternative 1 remedy: source control with GWP;
- **Section 3** includes information for the Alternative 2 remedy: source control with continuous containment system;
- **Section 4** includes a brief summary of times to reach GWPS for Alternatives 1 through 3;
- **Section 5** includes information used to develop estimates of material quantities, labor hours, and mileage; and
- **Section 6** includes reference documents used in the development of this CAAA-SIR.

2. ALTERNATIVE 1 REMEDY: SOURCE CONTROL WITH GROUNDWATER POLISHING

The Alternative 1 remedy, source control with GWP, includes the already completed consolidate-and-cap approach for source control, after which GWP would be implemented via a formalized process. GWP is a remedial alternative that relies on natural geochemical processes and may be appropriate as recognized by the United States Environmental Protection Agency (USEPA) in a final policy directive for groundwater remediation [8]. GWP has been naturally occurring at the WAPS since source control was completed in 2020. For the purposes of this CAAA-SIR, the Alternative 1 remedy would involve formalizing the ongoing natural GWP processes as the corrective action remedy for the WAPS.

2.1 Supporting Groundwater Modeling and Time to Reach GWPS

The COCs exceeding[1] the GWPS at compliance groundwater monitoring wells as of the 2024 Annual Report [5] include arsenic, boron, lithium, sulfate, and TDS. Boron was selected for modeling the source control presented in the Final Closure Plan and was identified as a surrogate for other exceedances of the GWPS (**Appendix B2**). For modeling purposes, it was assumed that boron would not significantly sorb or chemically react with aquifer solids (soil adsorption coefficient [Kd] was set to 0 milliliters per gram [mL/g]) which is a conservative estimate for predicting contaminant transport times in the model. Boron transport is likely to be affected by both chemical and physical attenuation mechanisms (*i.e.,* adsorption and/or precipitation reactions as well as dilution and dispersion). Physical attenuation (dilution and dispersion) of contaminants in groundwater is simulated in the groundwater computer models. Chemical attenuation mechanisms and their effect on modeled times for exceedances to reach the GWPS are discussed in the Groundwater Polishing Evaluation Report [9] which is attached to the CAAA and discussed herein.

Groundwater modeling was performed to support the closure plan for the WAPS in 2017 (**Appendix B2**). This groundwater modeling identified that removing CCR from the OWPP portions of the WAPS was necessary to reduce times to reach GWPS. This was incorporated into the closure plan, and closure in accordance with the IEPA-approved closure plan was implemented in 2020 [1, 2]. More than three years of post-closure groundwater monitoring has subsequently been collected. The calibration associated with the 2017 groundwater model was updated to include that data as part of this CAAA-SIR, as discussed in the Groundwater Modeling Technical Memorandum included in **Appendix B1** [10]. The updated groundwater model estimated, for an assumed start of remedial action in 2026, that GWPS would be met for all wells in the monitoring system in 2055. This is 29 years after the assumed start of corrective action for all wells and 6 years on average (mean) for wells in the current monitoring system.

2.2 Remedy Implementation

Implementation of the source control portion of this remedy was completed in 2020 [1, 2]. Although a formal GWP remedy has not yet been initiated and approved by IEPA, GWP processes

---

[1] Throughout this document, "exceedance" or "exceedances" is intended to refer only to potential exceedances of proposed applicable background statistics or GWPSs as described in the proposed groundwater monitoring program, which was submitted to the IEPA on October 25, 2021 as part of DMG's operating permit application for the HPP WAPS. That operating permit application, including the proposed groundwater monitoring program, remains under review by the IEPA and, therefore, DMG has not identified any actual exceedances.

have been ongoing since the closure was completed. Implementation of GWP would include formalizing the GWP remedy. This would include performing corrective action groundwater monitoring, enacting an adaptive management strategy, and, after GWPS have been met, performing corrective action closure and completion activities. Information associated with each of these activities is described below.

- Corrective Action Groundwater Monitoring
  - Regular corrective action groundwater monitoring would be conducted utilizing a corrective action groundwater monitoring system designed in accordance with 35 I.A.C. § 845.680(c), which specifies that wells must be installed in the plume of contamination that lies beyond the waste boundary.
    - Samples would be collected for major ions for evaluating groundwater chemistry and COCs. Samples would be collected on a quarterly basis initially and potentially reduced to a semiannual basis once five years of monitoring have occurred, in accordance with 35 I.A.C. § 845.650(b)(4).
    - Monitoring results would be submitted to IEPA for each monitoring event, in addition to an annual groundwater monitoring and corrective action report, in accordance with 35 I.A.C. § 845.610(e).
    - Routine maintenance of the monitoring well system would occur during the monitoring period. This would include inspecting the wells, making repairs to the wells (as and if needed), and rehabilitating and/or replacing wells to improve performance (as and if needed).
- Adaptive Management during Monitoring
  - Groundwater monitoring results would be evaluated and documented in the monitoring reports submitted to IEPA, in accordance with 35 I.A.C. § 845.610(e).
  - If remedy progress does not correspond with expectations, additional methods or techniques to achieve compliance with GWPS would be evaluated and, if feasible, implemented in accordance with 35 I.A.C. § 845.680(b).
- Corrective Action Confirmation Monitoring and Completion
  - After GWPS have been met for all corrective action monitoring wells, corrective action confirmation groundwater monitoring would be implemented. This would include monitoring each well for three additional years to confirm that GWPS have been achieved, in accordance 35 I.A.C. § 845.680(c).
    - It should be noted that this could occur prior to or after completion of the 30-year post-closure care groundwater monitoring requirement associated with 35 I.A.C. § 845.780(c).
  - After completion of the corrective action confirmation monitoring period, a Corrective Action Completion Report and Certification would be prepared and submitted to IEPA, in accordance with 35 I.A.C. § 845.680(e).

2.2.1 Remedy Implementation Schedule

A feasibility-level implementation schedule for the Alternative 1 source control with GWP remedy is provided in **Table A** below.

Table A. Feasibility-Level Implementation Schedule – Alternative 1 Source Control with GWP

Implementation Phase	Implementation Task	Timeframe (Preliminary Estimates)
Corrective Action Monitoring and Closeout	Corrective Action Monitoring (Time to Meet GWPS)	348 months (29 years)
	Corrective Action Groundwater Confirmation Monitoring	36 months
	Corrective Action Completion	6 months
	Timeframe to Complete Corrective Action Implementation	390 months
Total Timeline to Complete Corrective Action (after approval of Corrective Action Plan)		390 months (33 years)

2.2.2 Management of Extracted Groundwater

No groundwater extraction would occur under this remedy.

2.2.3 35 I.A.C. § 845.670(e)(1)(H) and 35 I.A.C. § 845.670(e)(3) Information

As requested by Gradient, the following information required by 35 I.A.C. § 845.670(e)(1)(H) and 35 I.A.C. § 845.670(e)(3) has been developed for the remedy. The information was developed based on preliminary-level information contained within the CMA for the HEN WAPS and then refined based on additional feasibility-level design activities performed as part of the development of this CAAA-SIR.

- Potential Need for Replacement of the Remedy – 35 I.A.C. § 845.670(e)(1)(H)
  - No replacement of the remedy would be required for source control with GWP, as a physical remedy would not be constructed.
- Degree of Difficulty Associated with Constructing the Remedy – 35 I.A.C. § 845.670(e)(3)(A)
  - No construction would be required with the source control with GWP remedy; therefore, there is no difficulty in constructing the remedy.
- Expected Operational Reliability of the Remedy - 35 I.A.C. § 845.670(e)(3)(B)
  - A report detailing the GWP process [9] has been developed and evaluates the reliability and the potential for reversibility of the chemical attenuation mechanisms. This report is attached to the Gradient CAAA.
- Need to Coordinate with and Obtain Necessary Approvals and Permits from Other Agencies - 35 I.A.C. § 845.670(e)(3)(C)
  - No permits are needed outside of approval of the eventual CAP.

- Availability of Necessary Equipment and Specialists - 35 I.A.C. § 845.670(e)(3)(D)
  - Equipment and specialists for field data collection and groundwater sampling are required for the GWP alternative. Laboratory equipment and specialists would also be required to assess groundwater concentrations of site constituents. Groundwater professionals (*i.e.*, geologists, hydrogeologists, statisticians, geochemists) would be required to perform statistical analysis and other assessments to confirm that GWP is functioning as intended and prepare corrective action-related groundwater monitoring and progress reports.
  - The equipment and specialists required for site groundwater monitoring and analysis are currently performing this work as part of the routine groundwater monitoring program in accordance with 35 I.A.C. § 845.220(c)(4). Therefore, no new equipment or specialists are required for groundwater monitoring for this alternative.
- Available Capacity and Location of Needed Treatment, Storage, and Disposal Services – 35 I.A.C. § 845.670(e)(3)(E)
  - No treatment, storage, or disposal services would be required with the source control with GWP remedy, as GWP would not generate any appreciable volume of waste or wastewater.

3. ALTERNATIVE 2 REMEDY: SOURCE CONTROL WITH CONTINUOUS CONTAINMENT SYSTEM

The Alternative 2 remedy, source control with continuous containment system, includes the completed source control supplemented by the construction of a cutoff wall that would extend from the top of the WAPS perimeter dikes (approximate elevation of 462-465 feet[2]) completely through the highly pervious uppermost aquifer (UA) and penetrate (*i.e.*, anchor) into shale bedrock at an approximate elevation of 375 feet (*i.e.*, a deep cutoff wall). The deep cutoff wall would encircle the perimeter of the CIP portions of the WAPS, with a total length of approximately 5,200 feet and a typical depth of 90 feet below ground surface (bgs). The existing final cover system would be extended over the top of and tied into the deep cutoff wall. This would result in CCR within the WAPS being contained within a continuous system of low-permeability materials and isolated from the surrounding environment on all sides, which includes the highly pervious UA, through:

- The deep cutoff wall, providing lateral containment on all sides of the CCR,
- The existing low-permeability geomembrane final cover system, providing surface containment on the top of the CCR,
- Low-permeability competent shale bedrock, providing base containment below the CCR.

This continuous containment system would provide a physical barrier between the CCR and the surrounding environment. Modeling indicates the continuous containment system is unlikely to result in the buildup of liquids within the contained CCR mass, and therefore supplemental groundwater extraction and/or active gradient control within the WAPS to remove accumulated liquids is not expected to be necessary. Therefore, the continuous containment system would control the source of releases of constituents.

The deep cutoff wall portion of the system would be constructed using either a mixture of soil and bentonite or cement and bentonite and would have a typical thickness of 2 to 3 feet. The cutoff wall would have a typical hydraulic conductivity value of approximately 1×10^{-7} centimeters per second (cm/s) or lower.

A feasibility-level design drawing of the Alternative 2 source control with continuous containment system remedy is provided as **Figure 2** in **Appendix A.**

3.1 Remedy Scoping and Groundwater Modeling Results

The location of the deep cutoff wall portion of the continuous containment system remedy was selected by reviewing physical constraints around the WAPS and designating locations on the DMG property where the wall could feasibly be constructed. The objective of selecting the wall location was to limit impacts to existing site infrastructure and sensitive areas such as wetlands, regulatory floodplains, or areas with documented decurrent false aster plants[3] while also limiting adverse impacts or conflicts with the 2020 WAPS final closure. This assessment resulted in the selection of a wall alignment along and outside of the existing site access road around the crest

---

[2] All elevations in this report are in the North American Vertical Datum of 1988 (NAVD88), unless otherwise noted.

[3] The decurrent false aster (*Boltonia decurrents*), a threatened species in Illinois, has been identified along the southern boundary of the OWAP [12, 13, 14]

of the WAPS perimeter dikes, which is not within regulatory floodplains or known wetlands, avoids known decurrent false asters, and provides generally level alignment for the wall. The location also allows the cutoff wall to act as a lateral barrier between the CCR contained within the OWAP and the surrounding environment and reduces, but does not eliminate, conflicts with the 2020 WAP closure. The location of the wall would allow the final cover to be extended over the top of the wall as surface containment, while also allowing the wall to completely encircle CCR within the WAPS.

Other locations were considered and determined to be infeasible for construction of the deep cutoff wall portion of the continuous containment system remedy. One location was outside the OWAP perimeter dikes, such as at the toe of the OWAP dikes or within adjacent portions of the OWAP that were closed by removal of CCR (*i.e.,* the OWPP). This is because these areas are within the 100-year floodplain of the Illinois River and are often flooded by seasonal high-water events, located near or beyond DMG property boundaries, in areas that are considered regulatory wetlands, or home to rare and endangered species (*e.g.*, decurrent false aster known to be present along the southern boundary of OWAP [11]). Therefore, both permitting and constructing the cutoff wall portion of the remedy in these areas was determined to be impracticable due to a high likelihood for flood-related impacts during wall construction, multiple floodplain and wetland-related permits required for the construction, the potential need to purchase or obtain access easements from adjacent landowners, the potential for a release of impacted stormwater and/or sediments to the wetlands or river during construction, and the potential adverse impacts to rare and/or endangered species previously discussed. Adjacent wetlands, floodplains, and rare plant locations are shown on the drawings provided in **Appendix A**.

Groundwater modeling estimated that, for an assumed start of remedial action in 2028, GWPS would be met for all wells in the monitoring network in 2061. This is 33 years after the start of corrective action that was assumed in the groundwater model. The attached Groundwater Modeling Technical Memorandum, which provides additional information on the updated groundwater modeling used to support the feasibility-level design of this remedy, is provided in **Appendix B1**.

3.2 Remedy Implementation

Implementation of the Alternative 2 source control with continuous containment system remedy is expected to include multiple tasks spread out over three phases, including pre-construction activities (Phase 1), corrective action construction (Phase 2), and corrective action operations, maintenance, and closeout (Phase 3). Information for each phase is described in this section.

3.2.1 Phase 1: Pre-Construction Activities

Pre-construction activities would include further pre-design investigation, obtaining permits from other agencies, completing the final design of the remedy, and selecting a remedy implementation contractor via a bidding process. Information associated with each of these activities is described below.

- Completing pre-design investigation, final design, and bid activities, including:
  - Completion of final pre-design subsurface investigations, laboratory soil testing, engineering calculations, bench-scale testing of proposed wall construction materials, design drawings, specifications, and a construction quality assurance plan.

  - Bidding and selection of a cutoff wall construction contractor.
- Obtaining permits from other agencies including:
  - A general stormwater permit for construction site activities through IEPA, including construction of stormwater controls and other best management practices (BMPs) such as silt fences.
  - An Illinois Department of Natural Resources (IDNR) Office of Water Resources, Dam Safety modification permit would be likely be required for modification of the WAPS embankment.
  - A National Pollutant Discharge Elimination System (NPDES) permit modification to allow CCR-contact stormwater generated during construction to be collected and transmitted to the existing on-site treatment pond for discharge to the Illinois River via Outfall 003.

3.2.2 Phase 2: Corrective Action Construction

Corrective action construction would be initiated after pre-construction activities are complete. It would include mobilizing construction equipment to the site, preparing the site for construction activities, construction of the cutoff wall (which would include removal and replacement of existing subgrade soils with low-permeability wall materials), and performing post-construction and site restoration activities including integrating the deep cutoff wall with the completed final closure to provide the continuous containment system.

Information associated with each of these activities is described below.

- The contractor would mobilize equipment and materials to the site, install stormwater BMPs around the construction area, construct a staging and laydown area, and construct a level working pad and/or temporary construction access roads along the cutoff wall alignment.
- The cutoff wall alignment would likely conflict with the completed geosynthetic and soil final cover system for the WAPS. To allow for cutoff wall construction, the final cover system would be temporarily removed in these areas.
  - This would include stripping topsoil and cover soil from the geomembrane, stockpiling the materials in the former Hennepin Coal Yard for future final cover restoration, removing the geosynthetics, and disposing of them in an off-site landfill.
  - Any conflicting site infrastructure (i.e., access roads, piezometers, monitoring wells, stormwater channels, stormwater letdown structures, pressure relief vents) would also be removed as part of the activities.
- A level, approximately 60-feet wide working pad and temporary construction access road would be constructed along the cutoff wall alignment to allow construction equipment (*i.e.*, cranes, haul trucks, light vehicles) access and traffic.
  - Due to the expected high ground pressures of the construction equipment, there is a high potential for damage to final cover system geosynthetics beneath access roads and working pads, even in areas outside of the cutoff wall alignment itself. For this reason, the final cover system soils and geosynthetics would also be removed beneath the footprint of the working pad and access road, in the same manner as final cover system removal completed directly beneath the cutoff wall alignment.

- A temporary contact water stormwater management system would be constructed to collect CCR-impacted stormwater generated during construction. This is expected to include temporary drainage sumps, pumps, and piping required to collect contact stormwater and pump it to the existing on-site treatment pond for discharge via NPDES Outfall 003.
- A temporary on-site batch plant and/or material handling system would be established for the purpose of generating low permeability backfill for the cutoff wall. This would include either mixing bentonite with the subgrade soils or producing a cement-bentonite slurry to place into the wall.
- A geotechnical monitoring system would be installed to monitor the WAPS perimeter dikes for movement when the dike is loaded with heavy construction equipment with the potential to destabilize the slurry construction. The monitoring system may consist of survey monuments, survey prisms, inclinometers, piezometers, and/or other appropriate monitoring devices.
- The wall would likely be constructed utilizing either crane-mounted conventional construction equipment (*i.e.,* clamshell, slurry cutter, and/or hydromill); however, other innovative methods could be utilized if determined to be appropriate based on site-specific subsurface conditions and constructability considerations.
- Installation of the cutoff wall would occur concurrently with the removal of some of the subsurface soils (soil-bentonite walls) or all of the subsurface soils (cement-bentonite wall).
- The wall would likely require installation in discontinuous panels (*i.e.,* primary panels) with secondary panels installed for connection after the primary panels have sufficiently cured/hardened, in order to support the stability of the sides of the wall during construction and reduce the destabilizing effects of slurry within the perimeter embankments.
- Excavated soils (*e.g.,* spoils) would be placed into off-road dump trucks and hauled to the former Hennepin Coal Yard for temporary stockpiling.
- After the cutoff wall construction is complete, CCR-impacted cutoff wall spoils and/or work pad materials would be managed either off-site or beneficially used within the Hennepin East Ash Pond as compacted contouring fill beneath the final cover system.
  - Cutoff wall spoils that are not CCR-impacted would be disposed of on-site at the HPP.
- The final cover system would then be restored. This would include placing new geosynthetics and tying them into the existing, un-damaged geosynthetics, extending the final cover system across the deep cutoff wall to provide the continuous containment system, and replacing the cover soil and topsoil with the previously removed and stockpiled final cover system soils.
- The temporary contact water management system would be decommissioned as part of final cover system replacement.
- Piezometers, monitoring wells, pressure relief vents, stormwater channels, stormwater letdown structures, and access roads damaged or removed during construction would also be replaced, and the final cover system would be revegetated via seeding.
- Temporary BMPs would also be installed during the site restoration period, if required in accordance with site land disturbance permits. The BMPs would be removed once vegetation is established.

3.2.3 Phase 3: Corrective Action Operations, Maintenance, and Closeout

Corrective action operations, maintenance, and closure would be initiated after corrective action construction is completed. Phase 3 would include performing corrective action groundwater monitoring, and, after GWPS have been met, performing corrective action closeout and completion activities. Information associated with each of these activities is described below.

- Corrective Action O&M
  - No corrective action O&M is required for the deep cutoff wall or shale bedrock portions of the continuous containment system remedy, as these features are passive, below-grade structure without maintenance or operational needs.
  - Maintenance of the WAPS final cover system portion of the continuous containment system remedy would continue in accordance with current post-closure care O&M practices.
- Corrective Action Groundwater Monitoring
  - Regular corrective action groundwater monitoring would be conducted utilizing a corrective action groundwater monitoring system designed in accordance with 35 I.A.C. § 845.680(c), which specifies that wells must be installed within the plume of contamination that lies beyond the waste boundary.
    - Samples would be collected for COCs required by 35 I.A.C. § 845.600(a)(1). Samples would be collected on a quarterly basis initially and potentially reduced to a semiannual basis once five years of monitoring have occurred, in accordance with 35 I.A.C. § 845.650(b)(4).
    - Monitoring results would be submitted to IEPA after each monitoring event, in addition to an annual groundwater monitoring and corrective action report, in accordance with 35 I.A.C. § 845.640(e). The annual corrective action report would include an evaluation of the actual performance of the remedy relative to the remedy's expected performance.
    - Routine maintenance of the monitoring well system would be conducted during the monitoring period. This would include inspection of the wells, making repairs to the wells (as and if needed), and rehabilitation and/or replacing the wells to improve performance (as and if needed).
  - If the remedy does not achieve its expected performance, additional methods or techniques to achieve compliance with GWPS would be evaluated and, if feasible, implemented in accordance with 35 I.A.C. § 845.680(b).
- Adaptive Management during Monitoring
  - Groundwater monitoring results would be evaluated and documented in the monitoring reports submitted to IEPA, in accordance with 35 I.A.C. § 845.610(e).
  - Remedy progress evaluation as part of adaptive site management may include additional investigation to inform updates to the conceptual site model (CSM), groundwater, and geochemical models.
  - If remedy progress does not correspond with expectations, additional methods or techniques to achieve compliance with GWPS would be evaluated and, if feasible, implemented in accordance with 35 I.A.C. § 845.680(b).

- Corrective Action Completion
  - After GWPS have been met for all compliance wells for a period of three years, corrective action would be considered complete, per 35 I.A.C. § 845.680(c).
    - It should be noted that this could occur prior to or after completion of the 30-year post-closure care groundwater monitoring requirement associated with 35 I.A.C. § 845.780(c).
  - After completion of the corrective action confirmation monitoring period, a Corrective Action Completion Report and Certification would then be submitted to IEPA, in accordance with 35 I.A.C. § 845.680(e).

3.2.4 Remedy Implementation Schedule

A feasibility-level implementation schedule for the Alternative 2 source control with continuous containment system remedy is provided in **Table B** below.

Table B. Feasibility-Level Implementation Schedule – Alternative 2 Source Control with Continuous Containment System

Implementation Phase	Implementation Task	Timeframe (Preliminary Estimates)
1: Pre-Construction Activities	Agency Coordination, Approvals, and Permitting	18 to 24 months
	Final Design and Bid Process	24 to 36 months
	Timeframe to Complete Corrective Pre-Construction Activities	42 to 60 months after CAP Approval
2: Corrective Action Construction	Corrective Action Construction	18 to 24 months
	Timeframe to Complete Corrective Action Construction	18 to 24 months
3: Corrective Action Monitoring and Closeout	Corrective Action Monitoring (Time to Meet GWPS)	396 months (33 years)
	Corrective Action Groundwater Confirmation Monitoring	36 months
	Corrective Action Completion	6 months
	Timeframe to Complete Corrective Action O&M and Closeout	438 months
	Total Timeline to Complete Corrective Action (after approval of Corrective Action Plan)	498 to 522 months (42 to 44 years)

3.2.5 Management of Extracted Groundwater

No groundwater extraction would occur under this remedy.

3.2.6 35 I.A.C. § 845.670(e)(1)(H) and 35 I.A.C. § 845.670(e)(3) Information

As requested by Gradient, the following information required by 35 I.A.C. § 845.670(e)(1)(H) and 35 I.A.C. § 845.670(e)(3) has been developed for the remedy. The information was developed based on preliminary-level information contained within the CMA for the HEN WAPS and then refined based on additional feasibility-level design activities performed as part of the development of this CAAA-SIR.

- Potential Need for Replacement of the Remedy – 35 I.A.C. § 845.670(e)(1)(H)
  - The deep cutoff wall and underlying shale bedrock remedy would be unlikely to require replacement, as the cutoff wall would be a robust, engineered, and maintenance-free subsurface structure.
  - The final cover system portion of the remedy will require continual maintenance in accordance with existing post-closure care plans, but is an engineered and passive structure that is unlikely to require replacement.
- Degree of Difficulty Associated with Constructing the Remedy – 35 I.A.C. § 845.670(e)(3)(A)
  - The remedy would require mobilizing specialty equipment to the site (*i.e.,* large cranes, clamshells, or slurry cutters) to construct the deep cutoff wall in addition to other supporting equipment (*i.e.,* batch plants, excavation, and grading equipment).
  - While cutoff walls are routinely constructed to similar depths in similar geologic environments, they often encounter difficulties during construction. The difficulties could include encountering especially pervious layers and resulting slurry loss or encountering obstructions that require specialized techniques and/or equipment to advance past, or instability or caving in the sidewalls prior to hardening of the slurry backfill. These difficulties can be problematic at the WAPS due to the known presence of boulders and cobbles within the subsurface soils. While these challenges can be addressed during cutoff wall construction, they may result in schedule delays.
  - The cutoff wall would be installed through an existing CCR surface impoundment embankment that is also a dam regulated by IDNR. This would require placing heavy construction equipment (*i.e.*, cranes) at the crest of the embankment as well as placing a slurry fluid within the embankment that may cause temporary destabilization of the embankments until curing occurs. While these challenges are common to constructing cutoff walls in embankments, additional engineering assessments and monitoring systems/programs would be required to monitor the embankment for signs of distress (*i.e.*, deformation, cracking) during cutoff wall construction and take appropriate means to stabilize the embankment if signs of potential instability are noted.
    - Furthermore, the act of placing the crane at the top of the embankment and placing slurry within the embankment may result in temporary destabilization of the embankment relative to current conditions. This would be addressed by performing detailed engineering assessments to evaluate the stability of the WAPS embankments during cutoff wall construction.
  - CCR-contact stormwater management is an obligatory part of construction that is necessary in order to comply with site-specific land disturbance permits and reduce the potential for the release of contact stormwater into the adjacent wetlands or Illinois River. This would require the installation and operation of a contact stormwater management system to pump contact stormwater approximately 1.3 miles to the existing on-site treatment pond for discharge via NPDES Outfall 003. Additional management of outfall water quality may also be required during construction.
  - The performance of the cutoff wall portion of the remedy would be dependent on the construction techniques of the wall, in order to avoid gaps, voids, or other discontinuous features or defects in the wall. Continuous quality control monitoring would be required

  during construction as part of construction quality control and quality assurance activities in order to avoid these features. The wall may also require post-construction quality assurance activities (*i.e.,* coring and testing) to verify the quality of the constructed barrier.

  - The performance of the deep cutoff wall portion of the remedy would also be dependent on the actual hydraulic conductivity of the wall. This would require continual monitoring, quality control testing, and quality assurance testing of slurry mixing and placement or soil-bentonite mixing to verify that the as-designed mix is utilized.

- Expected Operational Reliability of the Remedy - 35 I.A.C. § 845.670(e)(3)(B)
  - The continuous containment system wall is expected to have high operational reliability if the deep cutoff wall is constructed in accordance with standard design specifications for barrier walls and the final cover system is maintained in accordance with the existing post-closure care plan. This is because the remedy provides continuous surface, lateral, and lower containment of the CCR using both engineered and natural inert, low-permeability groundwater flow barriers (*i.e.*, the existing cover, the deep cutoff wall, and competent shale bedrock).
  - Temporarily removing portions of the completed WAPS final cover is required to allow for installation of the cutoff wall portion of the remedy. The final cover system will be restored around one year later. This process may allow additional stormwater to percolate into the CCR while the final cover system is removed and potentially cause a temporary reversal of some of the positive effects of the completed final cover system (*e.g.*, source control).
    - However, these effects would be expected to diminish after the final cover system is repaired, as the continuous containment system will then be present.
- Need to Coordinate with and Obtain Necessary Approvals and Permits from Other Agencies - 35 I.A.C. § 845.670(e)(3)(C)
  - Agency permits would need to be obtained from IEPA for construction stormwater controls and BMPs, in addition to a joint water pollution control construction and operating permit and IDNR Dam Safety modification permit to allow for modifications of the WAPS embankment.
  - A modification to the site's NPDES permit would also be required to allow for the discharge of CCR-contact stormwater generated during construction. These permits typically take 18 to 24 months to obtain.
- Availability of Necessary Equipment and Specialists - 35 I.A.C. § 845.670(e)(3)(D)
  - Construction of the deep cutoff wall portion of the remedy would require a specialized contractor experienced with construction of similar types of walls in similar geologic environments (*i.e.,* the Illinois, Mississippi, and/or Ohio River Valleys), particularly in environments with a prevalence of boulders and cobbles in the subsurface. The contractor would likely need specialized equipment, such as large cranes, clamshell buckets, slurry cutters, hydromills, batch plants, or other types of specialized equipment.
  - Specialists in cutoff wall design and construction would also need to be utilized during the design and construction phase of the cutoff wall. The specialists would include design

  engineers, construction managers, and contractor staff experienced with cutoff wall construction and equipment operation.

  - Monitoring of the WAPS embankments during cutoff wall construction would require specialists in geotechnical instrumentation (*i.e.,* inclinometers, survey prisms, vibrating wire piezometers) and visual observation of embankments for signs of distress. Additionally, a specialized drilling and instrumentation installation contractor would be needed to construct the geotechnical instrumentation system. Surveyors or other specialists may also be needed to collect routine readings from the system.
  - These types of equipment and specialists have been utilized in the past for other similar types of deep cutoff wall design and construction projects. However, there may be shortages associated with the equipment and specialists, due to high existing backlog for specialty ground improvement contractors and design specialists who are supporting similar types of projects in the electric utility, dam/levee, and other market sectors.
  - Specialists, with the necessary equipment, experienced with geosynthetics design and installation, specifically with seaming new geosynthetics to an existing final cover system, would be required for the final cover system restoration portion of the remedy. These types of equipment and specialists are available; however, they may have a high existing backlog due to ongoing projects in the solid waste management, electric utility, and other market sectors.
  - Equipment and specialists for field data collection, groundwater sampling, analysis, and periodic corrective action groundwater monitoring and reporting would be required for the remedy. As described in **Section 2.2.3,** the equipment and specialists required to support these activities are currently performing routine groundwater monitoring in accordance with 35 I.A.C. § 845.220(c)(4). Therefore, no new equipment or specialists are required for groundwater monitoring in this alternative.
    - The equipment and specialists required for site groundwater monitoring and analysis are currently performing this work in accordance with 35 I.A.C. § 845.220(c)(4). Therefore, no new equipment or specialists are required for groundwater monitoring for this alternative.

- Available Capacity and Location of Needed Treatment, Storage, and Disposal Services - 35 I.A.C. § 845.670(e)(3)(E)
  - Wastes generated during cutoff wall construction would be limited to geosynthetics and other debris from removing the final cover system, cutoff wall spoils, and contact stormwater.
    - Geosynthetics and other debris would be disposed at an off-site landfill. Multiple off-site landfills are located within the region, and all are expected to have sufficient volume to receive the relatively low quantities of geosynthetics and other debris.
    - Cutoff wall spoils containing CCR-impacted material would be temporarily staged on-site during construction and ultimately be managed either off-site or beneficially utilized as compacted contouring fill on-site beneath the Hennepin East Ash Pond final cover system during restoration. This would require coordination with the East Ash Pond closure.

  - Cutoff wall spoils that do not contain CCR-impacted material would be disposed of at an appropriate on-site location at the HPP.
  - Contact stormwater would be pumped to the existing on-site treatment pond for discharge via NPDES Outfall 003. The treatment pond and outfall previously received much higher flow volumes during operation and are therefore expected to have sufficient capacity for contact stormwater management.
- No wastes would be generated during operation of the continuous containment system; therefore, no additional treatment, storage or disposal services would be required with the source control with cutoff wall remedy.

4. MATERIAL QUANTITY, LABOR, AND MILEAGE ESTIMATES

Estimates of material quantities, total labor hours, and mileage were prepared for Alternative 2 source control with continuous containment system remedy, to support Gradient in preparing a CAAA. Estimates were not prepared for Alternative 1 source control with GWP as the alternative does not require remedial construction or operations and maintenance of a physical remedy.

These estimates were prepared utilizing the following approach:

- Major implementation (*e.g.*, construction) components and line items were identified in accordance with the remedy implementation narratives contained within this CAAA-SIR.
- Construction quantities were estimated based on quantity estimates for volumes, areas, and units, as obtained from the feasibility-level engineering drawings and schedules included within this CAAA-SIR.
- RS Means Heavy Construction Cost Data (RS Means) [12] was utilized to estimate the crew size, equipment description, and daily output associated with each line item.
- For line-items where RS Means data was not available, the crew size, equipment description, and daily output were estimated based on Ramboll's experience, information from contractors, and/or information from material suppliers.
- For the Alternative 2 source control with continuous containment system remedy, daily construction and oversight were estimated assuming an average one-way commute of 35 miles for each individual working on-site. The number of working days and hours per week were estimated from the construction schedule developed for each remedy.
- Estimates of material delivery miles were prepared based on Ramboll's experience.

The detailed material quantity, labor, and mileage estimates are provided in **Appendix C** for each alternative.

5. REFERENCES

[1] Dynegy Midwest Generation, LLC, "Hennepin Power Station; Old West Ash Pond, Ash Pond No. 2, Notification of Completion of Closure," Luminant, December 17, 2020.

[2] Dynegy Midwest Generation, LLC, "Hennepin Power Station; Old West Polishing Pond, Notification of Completion of Closure," Luminant, December 17, 2020.

[3] "35 Ill. Admn. Code Part 845, Standards for the Disposal of Coal Combustion Residuals in Surface Impoundments," Illinois Environmental Protectoin Agency, Springfield, IL, 2021.

[4] Code of Federal Regulations, "Title 40, Chapter I, Subchapter I, Part 257, Subpart D, Standards for the Disposal of Coal Combustion Residuals in Landfills and Surface Impoundments," April 17, 2015.

[5] Ramboll Americas Engineering Solutions, Inc., "2024 35 I.A.C. § 845 Annual Groundwater Monitoring and Corrective Action Report. West Ash Pond System, Hennepin Power Plant, Hennepin, Illinois.," 2025. January 31.

[6] Geosyntec Consultants, "Closure and Post-Closure Care Plan Old West Ash Pond Old West Polishing Pond at Hennepin Power Station," 2017.

[7] Natural Resource Technology, "Groundwater Model Report - Hennepin West Ash Pond System," 2017.

[8] United States Environmental Protection Agency, "Use of Monitored Natural Attenuation at Superfund, RCRA Corrective Action, and Underground Storage Tank Sites," OSWER Directive Number 9200.4-17P, April 21, 1999.

[9] Geosyntec Consultants, "Groundwater Polishing Evaluation Report, West Ash Pond System, Hennepin Power Plant, Hennepin, Illinois," 2025.

[10] Ramboll Americas Engineering Solutions, Inc., Groundwater Modeling Technical Memorandum, 2025.

[11] SCI Engineering, Inc., "Decurrent False Aster Survey, Hennepin Power Station - Old West Ash Pond," September 27, 2019.

[12] Gordian, RS Means Data version 8.7: Gordian, 2023.

[13] U.S. Fish and Wildlife Service, "National Wetlands Inventory, Surface Waters and Wetlands," [Online]. Available: https://fwsprimary.wim.usgs.gov/wetlands/apps/wetlands-mapper/.

[14] Federal Emergency Management Agency, "National Flood Hazard Layer," U.S. Department of Homeland Security, 26 August 2021. [Online]. Available: https://www.fema.gov/flood-maps/national-flood-hazard-layer.

[15] Geosyntec Consultants, "Construction Certification Report Closure of the Old West Ash Pond and Old West Polishing Pond," 2021.

[16] Ramboll Americas Engineering Solutions, Inc., "River Flood Evaluation Report, Hennepin East Ash Pond No. 2 and No. 4, Closure Plan Addendum 3," 2020.

APPENDIX A
FEASIBILITY-LEVEL DESIGN DRAWINGS FOR ALTERNATIVE 2 REMEDY

c:\DC\ACCDocs\ramboll gruppen as\rus-1940103584-005 vistra energy hen\project files\4 delivery\40 WIP\401 civil\Drawings\03_CAAA-SIR\F-1_HEN-OWAP_CAAA-SIR.dwg

PROJECT: ----

DATED: 2/21/2024

DESIGNER: LEMMONBN

NOTE:

1. SITE GRADING REPRESENTED PER FINAL CLOSURE DRAWINGS OF OLD WEST ASH POND AND OLD WEST POLISHING POND, COMPLETED BY CEC, OCTOBER 2020.
2. WETLANDS REPRESENTED AS PER ILLINOIS NATIONAL WETLANDS INVENTORY.
3. BOLTONIA PLANTS AND AREAS BASED ON SCI'S DECURRENT FALSE ASTER SURVEY, SEPTEMBER 27, 2019.
4. 100-YEAR FLOODPLAIN REPRESENTED AS PER FEDERAL EMERGENCY MANAGEMENT AGENCY,"FLOOD INSURANCE RATE MAP, JASPER COUNTY, ILLINOIS (UNINCORPORATED AREAS)," NATIONAL FLOOD INSURANCE PROGRAM, JANUARY 17, 1985. BASE FLOOD LEVEL EL. 461.9 FT.

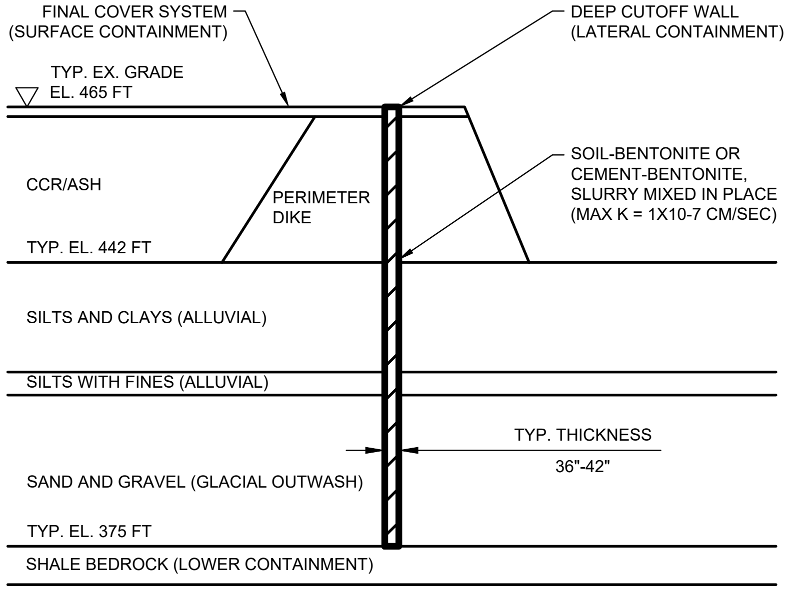

CONTINUOUS CONTAINMENT SYSTEM DETAIL

NOT TO SCALE

🟩	WETLANDS BOUNDARY (SEE NOTE 2)	●	BOLTONIA PLANTS (SEE NOTE 3)
⬚	BODY OF WATER	▨	BOLTONIA AREAS (SEE NOTE 3)
		— - —	100-YR FLOODPLAIN (SEE NOTE 4)
		—	PROPOSED CUTOFF WALL LOCATION

0 250 Feet

SOURCE CONTROL WITH CONTINUOUS CONTAINMENT SYSTEM

FEASABILITY-LEVEL DESIGN

Hennepin Power Plant
Hennepin Power Plant 13498 E 800th St Hennepin, IL 61327

FIGURE 1

RAMBOLL AMERICAS
ENGINEERING SOLUTIONS, INC.
A RAMBOLL COMPANY

RAMBOLL

APPENDIX B
GROUNDWATER MODELING DOCUMENTS

APPENDIX B1
GROUNDWATER MODELING TECHNICAL MEMORANDUM

Intended for
Dynegy Midwest Generation, LLC

Date
March 7, 2025

Project No.
1940103584-005

GROUNDWATER MODELING TECHNICAL MEMORANDUM

WEST ASH POND SYSTEM
HENNEPIN POWER PLANT
HENNEPIN, ILLINOIS
IEPA ID NO. W1550100002-01 AND W1550100002-03

RAMBOLL Bright ideas. Sustainable change.

GROUNDWATER MODELING TECHNICAL MEMORANDUM
WEST ASH POND SYSTEM
HENNEPIN POWER PLANT

Project Name	**Hennepin Power Plant West Ash Pond System**
Project No.	**1940101010-005**
Recipient	**Dynegy Midwest Generation, LLC**
Document Type	**Groundwater Corrective Action Alternatives Modeling Report**
Revision	**DRAFT**
Date	**March 7, 2025**
Prepared by	**Katie Moran**
Checked by	**Lucas Carr**
Approved by	**Brian G. Hennings, PG**

Katie Moran
Senior Scientist

Brian G. Hennings, PG
Project Officer, Hydrogeology

CONTENTS

TABLES (IN TEXT)

TABLES (ATTACHED)

FIGURES (IN TEXT)

FIGURES (ATTACHED)

APPENDICES

Appendix A MODFLOW and MT3DMS Modeling Files (Electronic Only)

ACRONYMS AND ABBREVIATIONS

35 I.A.C.	Title 35 of the Illinois Administrative Code
40 C.F.R.	Title 40 of the Code of Federal Regulations
ASD	Alternative Source Demonstration
CAAA	Corrective Action Alternatives Analysis
CAP	Corrective Action Plan
CBR	closure-by-removal
CCR	coal combustion residuals
CCR Rule	40 C.F.R. § 257 Subpart D
cm/s	centimeters per second
COC	constituent of concern
DMG	Dynegy Midwest Generation, LLC
ft/day	feet per day
ft^2/day	square feet per day
ft/ft	foot per foot
GMR	Groundwater Modeling Report
GPR	Groundwater Polishing Evaluation Report
GWP	groundwater polishing
GWPS	groundwater protection standard(s)
HCR	Hydrogeologic Site Characterization Report
HELP	Hydrologic Evaluation of Landfill Performance
HFB	horizontal flow barrier
HPP	Hennepin Power Plant
ID	identification
IEPA	Illinois Environmental Protection Agency
in/yr	inch per year
ISS	in-situ solidification/stabilization
Kd	soil adsorption coefficient
mg/L	milligrams per liter
mL/g	milliliters per gram
MW	megawatt
NAD83	North American Datum of 1983
NAVD88	North American Vertical Datum of 1988
NGVD29	National Geodetic Vertical datum of 1929
No.	number
NRT	Natural Resources Technology, Inc.
OWAP	Old West Ash Pond
OWPP	Old West Polishing Pond
Ramboll	Ramboll Americas Engineering Solutions, Inc.
TDS	total dissolved solids
UA	uppermost aquifer
USEPA	United States Environmental Protection Agency
WAPS	West Ash Pond System

EXECUTIVE SUMMARY

Ramboll Americas Engineering Solutions, Inc. (Ramboll) has prepared this Groundwater Modeling Technical Memorandum on behalf of the Hennepin Power Plant (HPP), operated by Dynegy Midwest Generation, LLC (DMG), in accordance with requirements of Title 35 of the Illinois Administrative Code (35 I.A.C.) § 845, Standards for the Disposal of Coal Combustion Residuals in Surface Impoundments. This document presents the groundwater flow and transport models for the West Ash Pond System (WAPS) and the results of predictive groundwater modeling simulations for proposed corrective action. The coal combustion residuals (CCR) unit is the WAPS, composed of the Old West Polishing Pond (OWPP) and the Old West Ash Pond (OWAP), both closed in 2020 (Vistra identification [ID] number [No.] 804). The WAPS was operated from the 1960s until 1996. The Illinois Environmental Protection Agency (IEPA)-approved closure of the WAPS consisted of excavation of ash material from the OWPP, consolidation of ash from the OWPP into the OWAP, and capping of the OWAP with a geomembrane and soil cover. The closure plan for the WAPS was described in Closure and Post-Closure Care Plan (Geosyntec, 2017) and approved by the IEPA in a letter dated June 19, 2018.

A detailed summary of site conditions was provided in the Hydrogeologic Site Characterization Report (HCR; Natural Resources Technology, Inc. (NRT), 2017a). The principal stratigraphic layers encountered at the WAPS and adjacent areas (from top to bottom) are CCRs consisting primarily of fly ash with lesser amounts of bottom ash and slag, alluvial fine-grained silts and clays classified as Cahokia Alluvium, alluvial fine to medium sands, and sand and gravel with boulders deposited by glacial meltwaters, which are classified as Henry formation. Bedrock is encountered at an approximate elevation of 375 feet[1] and consists of interbedded layers of shales and thin limestone, sandstone, and coal beds.

The overall groundwater flow regime consists of surface recharge to groundwater, with flow directions towards the Illinois River. Flow patterns within the site hydrostratigraphic units are typically horizontal, with components of converging vertical (upward) flow near and below the river. Under typical post-closure conditions, groundwater flow directions at the OWAP are north, towards the river. During the former operation of the impoundments, high local recharge to groundwater from sluicing of ash created radial flow conditions near the impoundment; while groundwater flow was still predominantly towards the river, some of the groundwater beneath the impoundment flowed outwards towards the south and west of the OWAP.

Boron transport in groundwater was evaluated with the groundwater model because it is a primary indicator of coal ash leachate, exceeds the Class I standard, is mobile in groundwater, and is more representative of coal ash leachate than sulfate at this site, which may originate from other anthropogenic or natural sources. Boron enters groundwater via vertical recharge through coal ash, and horizontal groundwater flow through coal ash where it lies below the water table. Solutes are transported in groundwater towards the Illinois River which is the primary receiving body of water adjacent to the WAPS. The conceptual transport model assumes that boron concentration in leachate does not vary as a function of time, although the volume and flux rate of leachate decreases over time as a function of pond dewatering and capping. It is assumed in this model there is no removal of mass from the groundwater system via adsorption or decay.

---

[1] All elevations and total heads in this report and the subsequent attachments are referenced to North American Vertical Datum of 1988 (NAVD88), unless otherwise noted.

For modeling purposes, it was assumed that boron would not significantly sorb or chemically react with aquifer solids (soil adsorption coefficient [Kd] was set to 0 milliliters per gram [mL/g]) which is a conservative estimate for predicting contaminant transport times in the model.

This Correction Action Plan (CAP) model update is a revision to the model developed for the WAPS in 2014 and updated in 2017 (NRT, 2017b). Generally, the model boundaries, parameters, and calibration (heads, flow directions, and boron distributions) were retained from the 2017 model; however, some small adjustments were made to parameter and boundary conditions to preserve model calibration (flow and transport) following updates to the model resolution and base-of-ash elevations within the OWAP. The objectives of the model update were to refine model specifications to include data collected since 2017 (*i.e.,* the closure conditions of the OWAP) while maintaining the previous quality of calibration, and to generate results consistent with the 2017 model predictions.

Model prediction scenarios were simulated to evaluate potential groundwater corrective action alternatives for boron in groundwater. Prediction models were evaluated from projected remedy completion of 2028 to 200 years in the future (2228). The objective of predictive modeling of the corrective action scenarios listed below is to simulate boron concentrations in groundwater for different corrective actions to evaluate if implementation of these actions will reduce the amount of time to meet the groundwater protection standard (GWPS) of 2 mg/L for boron at the nine compliance monitoring wells; and, within groundwater at the site.

The following corrective action alternatives were simulated:

- Alternative 1, Source Control with Groundwater Polishing (GWP)
- Alternative 2, Source Control with Cutoff Wall
    - 2a, Continuous Containment System with Deep Cutoff Wall
    - 2b, Partial-Depth Cutoff Wall
    - 2c, Shallow Cutoff Wall
- Alternative 3, Source Control with In-situ Solidification/Stabilization (ISS)

Simulation of the corrective action alternatives indicated that concentrations of boron at the nine site compliance wells have decreased as a result of the closure in 2020 and will continue to decrease. Each of the five alternatives results in reduction of boron at the compliance wells within approximately 30 years following corrective action. Small differences in cleanup time were identified for each of the different alternatives. Comparison of predicted concentrations at the compliance wells indicates that the time to reach GWPS is similar across each of the evaluated remedies, with Alternatives 1, 2b, 2c, and 3 reaching GWPS in 2055 (27 years after implementation), and Alternative 2a reaching GWPS by 2061 (33 years after implementation).

1. INTRODUCTION

1.1 Overview

NRT, an OBG Company, documented site-specific MODFLOW and MT3DMS groundwater flow and transport models in a Groundwater Modeling Report (GMR) submitted to IEPA in 2017 (Appendix D of the Closure and Post-Closure Care Plan; Geosyntec, 2017). The groundwater modeling activities documented in the 2017 GMR were performed to support closure of the WAPS at the Hennepin Power Station, Hennepin, Illinois. This document presents the MODFLOW and MT3DMS groundwater flow and transport models developed in 2023 (CAP model update) to meet the Corrective Action requirements of 35 I.A.C. § 845.220(c)(2) and 845.670. These models contain minor refinements to reflect current conditions at the now-closed WAPS and enable improved simulation of future conditions.

Closure of the WAPS consisted of excavation of ash material from the OWPP, consolidation of ash from the OWPP into the OWAP, and capping of the OWAP with a geomembrane and soil cover. The closure plan for the WAPS was described in Closure and Post-Closure Care Plan (Geosyntec, 2017) and approved by the IEPA in a letter dated June 19, 2018. The WAPS closure was completed in 2020 (Dynegy, 2020a; Dynegy, 2020b).

Site hydrogeology and groundwater quality are summarized below , and described in detail in a separate Hydrogeologic Characterization Report (NRT, 2017a) and the Nature and Extent Report (Ramboll, 2024b) The Hydrogeologic Investigation Report was completed to summarize data collected to comply with the requirements of Title 40 of the Code of Federal Regulations (40 C.F.R.) § 257, herein referred to as the Federal CCR Rule, as well as comprehensive data collection and evaluations from prior hydrogeologic investigation reports completed at the site. In addition, Hydrologic Evaluation of Landfill Performance (HELP) modeling was conducted to enable estimation of the time required for hydrostatic equilibrium of groundwater to be achieved beneath the final cover system of the WAPS. The HELP modeling also provided percolation rates for existing conditions and predicted cap scenario that were used as inputs in the groundwater flow and transport model. A description of the HELP model inputs and modeling results are found in the Hydrostatic Modeling Report (NRT, 2017c). Groundwater transport modeling was performed to assess the effects of impoundment closure on groundwater quality. Model development and calibration is documented in **Section 2**. The model prediction results are presented in **Sections 4** and conclusions are summarized in **Section 5**.

1.2 Background

1.2.1 Site History

The Hennepin Power Station has two coal-fired generating units with a total capacity of 280 megawatts (MW). The units were constructed in 1953 and 1959, respectively. DMG operated the WAPS at the Hennepin Power Station from 1952 until late 1996 when the WAPS was removed from service.

The impoundment originally consisted of three ponds: Pond 1 (9.3 acres), at the eastern end of the impoundment, primarily contained bottom ash and slag. Pond 3 (16.4 acres), in the central portion of the impoundment, contained mixed coal ash. A polishing pond (4.7 acres) was located at the western end of the impoundment. The berms, which are 15 feet above grade, were constructed from locally occurring sandy soils. During operation, service water was used to sluice fly ash, bottom ash, and low-volume wastes to the impoundment.

Closure of the WAPS consisted of excavation of ash material from the OWPP *(*closure-by-removal [CBR]), consolidation of ash from the OWPP into the OWAP, and capping of the OWAP with a geomembrane and soil cover. The WAPS closure was completed in 2020 (Dynegy, 2020a; Dynegy, 2020b).

Site Hydrogeology

In addition to the CCR fill material, the four principal stratigraphic layers (from top to bottom) encountered at the WAPS and adjacent areas are:

- Alluvial fine-grained silts and clays;
- Alluvial fine to medium sands;
- Sand and gravel with boulders, deposited by glacial meltwaters and classified as Henry Formation;
- Bedrock, consisting of interbedded layers of shales and thin limestone, sandstone, and coal beds.

The river-laid deposits are classified as Cahokia Alluvium. The Henry Formation sands and gravels make up the upper and lower terraces, contain frequent boulders, and fill the valley beneath the alluvium. An additional stratigraphic layer, loamy and sandy diamicton (*i.e.*, till) of the Wedron or Glasford Formation, was encountered at one location (Boring 32) approximately 2,560 feet (½ mile) south of the western end of the impoundment; however, this layer is not significant to the hydrogeology at the impoundment.

The uppermost bedrock near the Hennepin Power Station, including the WAPS, is the Pennsylvanian Carbondale Formation, which consists of shale with thin limestone, sandstone, and coal beds. Depth to bedrock in this area varies based upon data available from the Illinois Geological Survey (Chenoweth, et al., 1994) A bedrock investigation conducted in 2025 encountered shale bedrock at a depth of approximately 85 feet beneath the WAPS (Ramboll, 2025).

The WAPS lies over both glacial deposits (Henry Formation) and alluvium (Cahokia Alluvium). Pond 1 lies on top of lower terrace glacial sand and gravel deposits. The eastern portion of Pond 3 overlies alluvial sand, while the western portion of Pond 3 and the Polishing Pond overlay silty clay alluvial channel fill deposits. The Cahokia Alluvium and Henry Formation materials together comprise the uppermost aquifer at the WAPS, which extends from the water table to the top of the bedrock. More details are presented in the HCR (NRT, 2017a).

Groundwater elevation data is available beginning in 1993. The Illinois River is the local and regional receiving body of water for groundwater, and river stage is controlled by dams located upstream and downstream. River stage is usually lowest during the months of August through October. The river basin experiences annual spring flooding during the months of March, April, May, and sometimes June, while lesser flooding occasionally occurs during autumn. River stage during high precipitation and/or flood events seasonally rises above adjacent groundwater elevations and in low lying areas of the floodplain, particularly within the Donnelley WMA at wells 32, 33, and 34. Stage of the Illinois River typically measures 441-442 feet elevation during baseflow conditions (low stage); the 10-year flood level is 457 feet, and annual floods typically reach elevations of 450 feet or above.

Review of groundwater elevation data for the site, including transducer data collected in 2023, indicates that groundwater levels across the system vary system-wide, with variations in head tied to river stage and/or seasonal recharge. Horizontal hydraulic gradients from the WAPS to off-site areas ranges from 0.001 foot per foot (ft/ft) during Illinois River flood stage to about 0.005 ft/ft during normal river stage, yielding a groundwater velocity ranging from 0.1 to 1.1 ft/day (NRT, 2017a).

1.2.2 Groundwater Quality

35 I.A.C. § 845 groundwater monitoring began in 2023. Exceedances[2] to the GWPS were identified for boron, cadmium, lithium, sulfate, total dissolved solids, and arsenic. An Alternate Source Demonstration (ASD) was approved for cadmium. The remainder of the constituents with groundwater exceedances were discussed in the Groundwater Monitoring Data and Detected Exceedances, Quarter 4, 2023 (Ramboll, 2024a) and the Nature and Extent Report (Ramboll, 2024b).

1.3 Conceptual Model

The WAPS overlays alluvium and outwash deposits in the Illinois River valley. The principal stratigraphic layers encountered at the WAPS and adjacent areas (from top to bottom) are CCRs and fill consisting primarily of fly ash with lesser amounts of bottom ash and slag, alluvial fine grained silts and clays classified as Cahokia Alluvium, alluvial fine to medium sands, and sand and gravel with boulders deposited by glacial meltwaters which are classified as Henry formation.

The overall groundwater flow regime within the unlithified materials is consistent with topographically-controlled flow patterns, where infiltration of surface precipitation recharges groundwater and flows north and west near the Site towards the Illinois River. Flow patterns within the site hydrostratigraphic units are typically horizontal, with components converging vertical (upward) flow near and underneath the river. Under typical post-closure conditions, groundwater flow directions at the WAPS are north, towards the river. During the operation of the impoundments, high local recharge to groundwater from sluicing of ash created radial flow conditions near the impoundment; while groundwater flow was still predominantly towards the river, some of the groundwater beneath the impoundment flowed towards the adjacent wetlands located south and west of the WAPS (NRT, 2017a; Ramboll, 2024b).

The CCR materials are the primary source of constituent loading to the CCR porewater (*i.e.*, CCR source water). Over an extended period (*e.g.*, months to years), the CCR source water (*i.e.*, water contained within the interstitial pore spaces of the CCR that can be sampled by low-flow groundwater sampling methods) reaches equilibrium with the CCR materials. The porewater is therefore representative of the mobile phase constituents capable of migrating into the underlying materials and potentially downgradient in groundwater. The WAPS CCR source water is therefore the primary indicator of constituents available to the groundwater and is considered

---

[2] Throughout this document, “exceedance” or “exceedances” is intended to refer only to potential exceedances of proposed applicable background statistics or GWPSs as described in the proposed groundwater monitoring program, which was submitted to the IEPA on October 25, 2021 as part of DMG’s operating permit application for the HPP WAPS. That operating permit application, including the proposed groundwater monitoring program, remains under review by the IEPA and, therefore, DMG has not identified any actual exceedances.

the primary source term for environmental investigation and fate and transport modeling (Ramboll, 2024b).

Boron was simulated and considered a surrogate for other 35 I.A.C. § 845.600 constituents because (1) it is commonly present at elevated concentrations in coal ash leachate; (2) it is mobile and typically not very reactive but conservative (*i.e.*, low rates of sorption or degradation) in groundwater; and (3) it is less likely than other constituents to be present at elevated concentrations in background groundwater from natural or other anthropogenic sources. The surrogate selected for groundwater flow and transport modeling is conservative (*i.e.*, aqueous concentrations are predominantly affected by physical processes such as dilution and dispersion rather than by chemical attenuation mechanisms) and therefore represent the maximum plume extent. The use of a conservative parameter to represent plume extent and clean-up times is consistent with United States Environmental Protection Agency (USEPA) modeling examples intended for evaluating relative remedy effectiveness (USEPA, 1994) as well as an independent subject matter expert review validating the modeling approach for evaluating closure alternatives (Gradient, 2024).

Conservative parameters are most acutely affected by closure: once the source is controlled via closure, concentrations of surrogate parameters in the groundwater will respond in timeframes consistent with groundwater flow. Source control will control, minimize, or eliminate, to the maximum extent feasible, infiltration of liquids through the CCR (per 35 I.A.C. § 845.750(a)(1)), mitigating the flux of not only the surrogate parameters but all other parameters potentially leaching from the unit. The time to reach the GWPS determined by modeling surrogate parameters correlates to the effectiveness of the proposed closure as source control. Therefore, the existing model is appropriate for assessing the effect of closure on the flux of all CCR SI porewater constituents.

The conceptual model for transport assumes two boron sources: boron that leaches to recharge water during percolation through ash above the water table; and boron that leaches to water that may infiltrate from the sides or base of the CCR unit below the water table. Therefore, mass is added to groundwater via vertical recharge through coal ash, and horizontal exfiltration of water from coal ash where it lies below the water table. Mass is transported along with groundwater toward the Illinois River, which is the primary receiving body of water adjacent to the WAPS. The conceptual transport model assumes that boron concentration in leachate does not vary as a function of time, although the volume of leachate decreases over time as a function of capping.

For modeling purposes, it was assumed that boron would not significantly sorb or chemically react with aquifer solids (Kd was set to 0 mL/g) which is a conservative estimate for predicting contaminant transport times in the model. Boron transport is likely to be affected by both chemical and physical attenuation mechanisms (*i.e.,* adsorption and/or precipitation reactions as well as dilution and dispersion). Physical attenuation (dilution and dispersion) of contaminants in groundwater is simulated in the groundwater computer models. Chemical attenuation mechanisms and their effect on modeled times for exceedances to reach the GWPS are discussed in the Groundwater Polishing Evaluation Report [GPR, Geosyntec, 2025] and summarized in **Section 3.2**.

1.3.1 Correlation of Boron with Sulfate, Lithium, and Arsenic

Boron is considered a surrogate for other parameters that exceed the GWPS that do not have approved alternative source demonstrations (arsenic, lithium, and sulfate) because it occurs above the GWPS in the greatest number of wells and it is the constituent at the site that will likely require the longest time to achieve the GWPS. In addition, comparisons of observed sulfate and lithium to boron concentrations (**Figures A and B** below) indicate a statistically significant correlation between these parameters in downgradient uppermost aquifer (UA) wells with exceedances. The correlation coefficient (R^2) and p values (indicator of statistical significance) are also provided on **Figures A and B**. Higher R^2 values (*i.e.,* closer to 1) indicate stronger correlation between parameters. A correlation is considered statistically significant when the p value is lower than 0.05. The p values are less than the target of 0.05, indicating correlations are statistically significant. The statistically significant correlations between sulfate and boron and lithium and boron indicate boron is an appropriate surrogate for sulfate and lithium in the groundwater model, and concentrations of these parameters are expected to change consistent with model predicted boron concentrations.

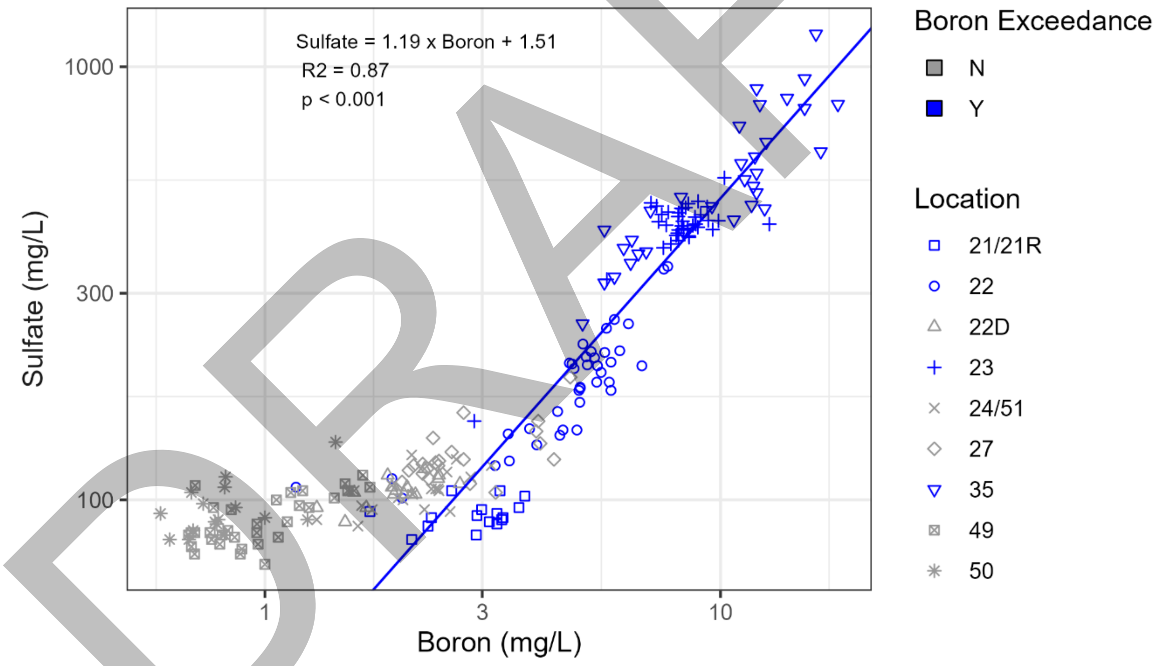

Figure A Correlation of Observed Sulfate and Boron Concentrations in Downgradient Wells (Linear regression for wells with exceedances only)

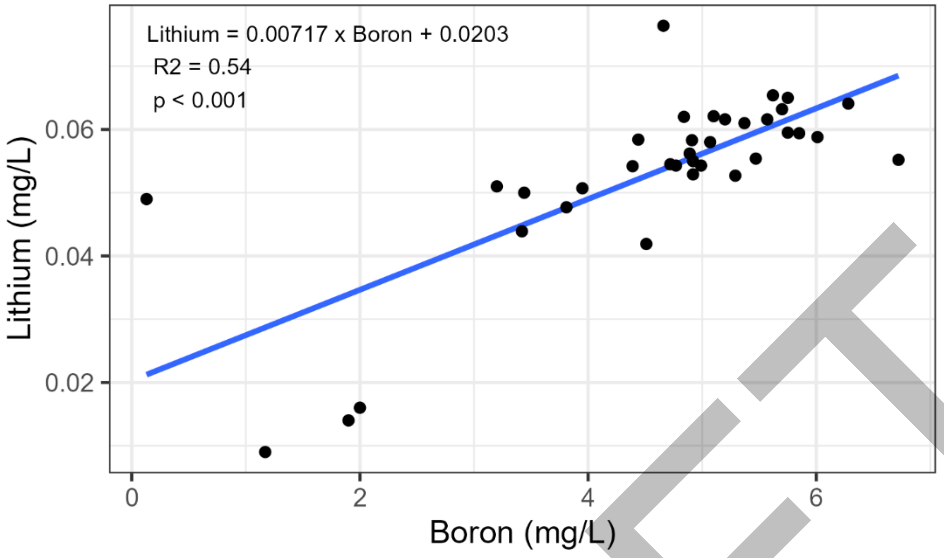

Figure B Correlation of Observed Lithium and Boron Concentrations in Well 22

Boron and arsenic concentrations in downgradient wells with an arsenic (21R and 51) and/or boron exceedance were also evaluated for correlation (**Figure C**). The arsenic data set contains a large number of non-detect values and as a result no statistically significant correlation was found. Arsenic is a reactive CCR constituent, and concentrations within the aquifer will be influenced by geochemical conditions and changes following closure. Localized effects on arsenic geochemistry and expected behavior following closure at these two well locations are further discussed in the Groundwater Polishing Evaluation Report (Geosyntec, 2025) and **Section 3.2**.

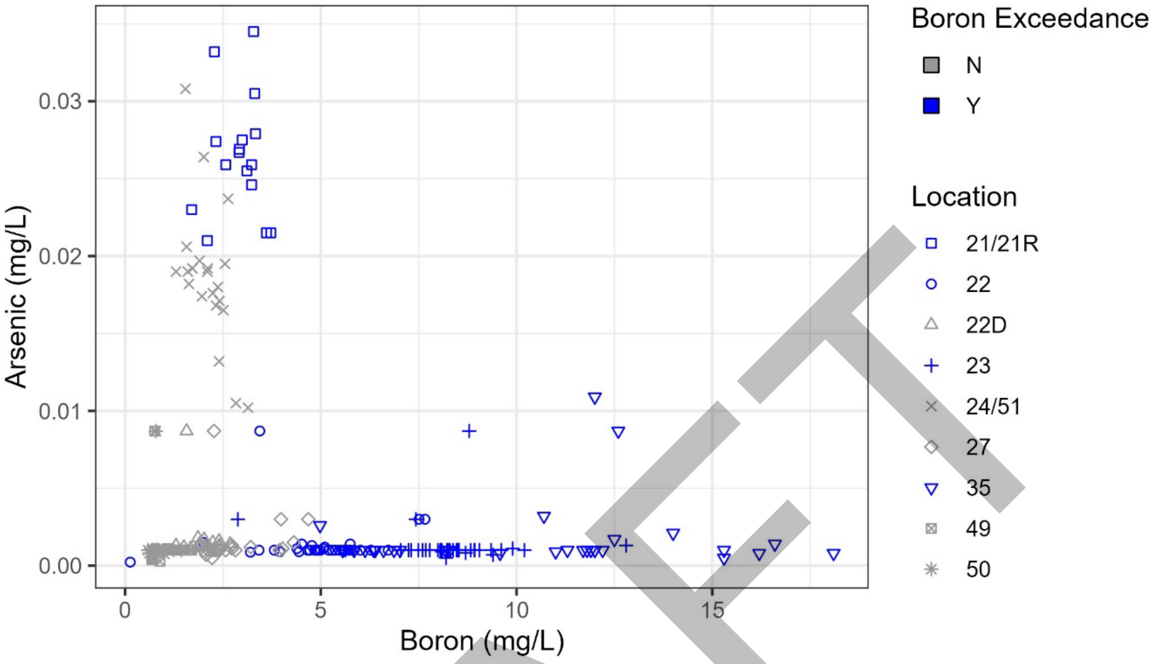

Figure C Correlation of Arsenic and Boron Concentrations in Downgradient Wells

2. GROUNDWATER MODEL DEVELOPMENT AND CALIBRATION

The CAP model update described herein consists of an update to the model developed for the WAPS in 2014 and 2017 (NRT, 2017b). Generally, the model boundaries, parameters, and calibration (heads, flow directions, and boron distributions) were retained from the 2017 model; however, some small adjustments were made to parameter and boundary conditions to preserve model calibration (flow and transport) following updates described in **Section 2.1**. The objectives of the model update were to incorporate information collected since 2017 (including the 2020 closure of the OWAP) while maintaining the previous quality of calibration. Since the model update is predicated on the need to simulate additional corrective action for boron concentrations in groundwater at the site, it was important to retain to the extent practicable the previous model components and calibrations, to ensure that predicted results would be comparable to the 2017 model predictions for WAPS closure.

Specifications and results of the MODFLOW/MT3DMS modeling are presented below. Electronic copies of the model files are provided with this report (**Appendix A**).

2.1 Model Background

Model updates / revisions completed for the CAP model update consist of the following:

- Model Discretization
  - The model extents (domain) and origin were adjusted to correctly align with Illinois state plane coordinates (North American Datum of 1983 [NAD83]).
  - Model resolution was increased, with the horizontal grid spacing decreased from 100 to 25 feet at the WAPS.
  - The bottom of model layer 1 was revised to better match the base of ash elevations within the footprint of the OWAP with the increased resolution of the model. A bottom elevation of 444 feet was assigned to the former OWPP, and model layer 1 bottom elevations were set to 440 feet outside of the WAPS.
  - The bottom of model layer 6 was revised from 390 to 375 feet to better match the estimated bedrock elevation at the WAPS.
- Model Approach and Codes
  - The model time frames were adjusted to simulate current conditions in 2023 and future conditions. The transient calibration model was extended from 2017 to 2023; the previous stress period (2) was extended from 2017 to 2020, and a new stress period (3) was used to simulate closure of the WAPS which was performed in 2020. Stress period 3 was extended to the current time for the calibration model, and until 2028 for the prediction models.
  - The simulation of conditions for unit closure are documented later in **Section 2.4.4**. Simulation specifications for unit closure were consistent with the predictive modeling for capping of the OWAP performed in 2017.
  - New model simulations were performed using MODFLOW 2005, instead of MODFLOW-2000, which was used for the 2017 model simulations. Different versions of MODFLOW are

similar but offer slightly different functionalities that can be useful for various simulated conditions. MT3DMS was retained as the transport model code.

- Boundaries and Parameters
  - Assigned hydraulic conductivity for the glacial outwash material in model layer 6 was decreased to 100 ft/day to retain a consistent transmissivity value after increasing the thickness of the layer.
  - Minor modifications were made to the representation of the Illinois River. The river stage of 441.7 feet National Geodetic Vertical Datum (NGVD29) was retained[3], with the bottom elevation changed to 435 feet to better match river depths. Consequently, the river cells were moved from layer 1 to layer 2 to better match the layer elevations. The river cell conductance values were adjusted in areas away from the WAPS to preserve the calibration and heads from the previous version of the model with the adjustments to the model extent and grid.
  - The conductance values for the river cells used to represent the duck ponds and wetland areas southeast of the impoundments were adjusted to preserve calibration and flow directions with changes to grid cell size.
  - Minor adjustments were made to the alignment of hydraulic conductivity zones to preserve model calibration and flow directions following other minor changes to boundaries and the model grid.
  - Minor adjustments were made to assigned model recharge to preserve model calibration.
  - The no-flow cells in model layer 1 used to represent the areas of the OWAP which were unsaturated under typical conditions were removed to allow model cells to convert from wet to dry during model simulations as warranted by simulated groundwater elevations.
  - Specific yield was decreased from 0.3 to 0.2 to be consistent with porosity (0.2) for each of the transient flow models.
- Transport Model
  - Assignment of a Kd of 1 mL/g for the silt/clay materials was removed to maintain a Kd of 0 mL/g for the entire model domain (no retardation). This is consistent with MT3DMS modeling performed to simulate boron transport at other Luminant/DMG CCR impoundments regulated by 35 I.A.C. § 845.

2.2 Model Approach

Three modeling codes were used to model groundwater flow and contaminant transport: (1) percolation through the cap system was modeled using the HELP model. All details regarding closure configurations and HELP model establishment are presented in a separate Hydrostatic Equilibrium Report (NRT, 2017c); (2) groundwater flow was modeled in three dimensions using MODFLOW 2005; and (3) contaminant transport was modeled in three dimensions using MT3DMS.

---

[3] All river stages are referenced to NGVD29, which is the USACE gauge datum. The NGVD29 and NAVD88 datums have a difference of around 0.2’ in Putnam County, IL. Due to the difference being relatively minor in the context of the model size and accuracy, the river stage elevations were not corrected from the NGVD29 gauge datum to NAVD88.

A three-dimensional groundwater flow and transport model was developed to represent the conceptual flow system described above and then calibrated to match the groundwater monitoring results since 1994. A number of simulations were created to represent different periods of time (below and in **Table A**):

- A steady-state flow model was calibrated to approximate head distributions observed while the impoundment was in service, based on median heads observed from 1994 through 1996 (steady-state flow model)
- The accompanying transport model was calibrated to approximate concentrations observed while the impoundment was in service, based on observations from 1994 through 1996. A 30-year period of impoundment operation was simulated to represent the years 1966 to 1996.
- A transient flow model was created from the steady-state flow model and calibrated to match the decreasing heads measured after the impoundment was removed from service. The model period was December 1996 through December 2016 (transient calibration model stress periods 1 and 2). For this CAP model update, stress period 2 was extended from December 2016 to July 2020.
- The transport model was calibrated to approximate boron concentration trends observed since the impoundment was removed from service. The model period was December 1996 through July 2020 (transient model stress periods 1 and 2).
- New for the CAP model update: A new stress period 3 was added to the transient flow and transport models to simulate closure of the WAPS in 2020. Simulation specifications for the completed closure of the WAPS were consistent with the predictive model for the capping scenario performed in 2017.
- New for the CAP model update: Predictive modeling was performed to evaluate the effects of additional corrective action alternatives on boron concentrations. Flow conditions and concentrations were simulated for a number of scenarios (**Section 3**) from the current time to 2228.

Table A. Model Simulation Stress Periods

Model Stage	Time Period	Model Description
Steady State Flow Model / Transport Model	1966 - 1996	30-year simulation of flow directions and boron transport under operating conditions
	Steady-State Flow Calibration	
	Transient Transport Calibration	
Transient Flow Model and Transport Model	Stress Period 1 (1997 - May 1998)	SP1 – natural dewatering of OWAP after closure
	Stress Period 2 (May 1998 – July 2020)	SP2 – dormant period
	Stress Period 3 (August 2020 - December 2023)	SP3 – post-closure period
Predictive Corrective Action Alternative Simulations (Flow and Transport)	Stress Period 3, extended to 2028	Predictive scenario simulations
	Predictive Scenarios (2028 - 2228)	

2.3 Model Codes

MODFLOW uses a finite difference approximation to solve a three-dimensional head distribution in a transient, multi-layer, heterogeneous, anisotropic, variable-gradient, variable-thickness, confined or unconfined flow system—given user-supplied inputs of hydraulic conductivity, aquifer/layer thickness, recharge, wells and boundary conditions. The program also calculates water balance at wells, rivers and drains.

MODFLOW was developed by the United States Geological Survey (McDonald and Harbaugh, 1988) and has been updated several times since. Major assumptions of the code are: (1) groundwater flow is governed by Darcy's law; (2) the formation behaves as a continuous porous medium; (3) flow is not affected by chemical, temperature, or density gradients; and (4) hydraulic properties are constant within a grid cell. Other assumptions concerning the finite difference equation can be found in McDonald and Harbaugh (1988). MODFLOW 2005 (Harbaugh et al., 2017) was used for this model revision using Groundwater Vistas 8 software for model pre- and post-processing tasks (Rumbaugh, 2020).

MT3DMS (Zheng and Wang, 1998) is an update of MT3D and calculates concentration distribution for a single dissolved solute as a function of time and space. Concentration is distributed over a three-dimensional, non-uniform, transient flow field. Solute mass may be input at discrete points (wells, drains, river nodes, constant head cells), or distributed evenly or unevenly over the land surface (recharge).

MT3DMS accounts for advection, dispersion, diffusion, first-order decay and sorption. Sorption can be calculated using linear, Freundlich, or Langmuir isotherms. First-order decay terms may be differentiated for the adsorbed and dissolved phases.

Major assumptions are: (1) changes in the concentration field do not affect the flow field; (2) changes in the concentration of one solute do not affect the concentration of another solute; (3) chemical and hydraulic properties are constant within a grid cell; and (4) sorption is instantaneous and fully reversible, while decay is not reversible.

2.4 Model Setup

2.4.1 Grid and Boundary Conditions

The discretization of the model consists of six layers, 119 rows, and 178 columns. Variable horizontal grid spacing was used with grid spacing of up to 200 feet at the edges of the model and 25 feet in the area of interest (**Figure 2-1**). Model layers are simulated with uniform top and bottom elevation, with the exception of model layer 1. Variable bottom elevations for model layer 1 were used within the former OWAP to represent the base of ash material (approximately 438-450 feet, 444 feet in the former OWPP, and 440 feet for the remainder of model layer 1).

Flow and transport model domain boundaries were the same for all scenarios. The upgradient (east and south) edge of the model is a no-flow boundary. The downgradient (north) and lateral (west) boundaries are either MODFLOW river (mixed) boundaries (layer 2) or no-flow (layers 1 and 3 to 6). The upper boundary is a time-dependent specified flux (Neumann) boundary, with specified flux rates equal to the recharge rate (from precipitation) or the rate of percolation from the impoundment. The base of the model is a no-flow boundary, at the base of layer 6 (bedrock surface). Additional information on these boundaries is discussed in the subsequent section of this report.

The model included two types of transport boundaries (constant concentration and recharge), both in layer 1. Ash materials within the impoundments were explicitly simulated using both constant concentration cells and recharge. Representation of ash with both boundaries is conservative, in that source concentrations are assigned to active model cells by the constant concentration cells and assigned to inactive or dry cells by recharge concentrations to represent precipitation infiltrating vertically through the ash to the underlying groundwater table. The distribution of these boundaries was adjusted within the ash ponds for the different transport model stress periods to match actual conditions.

2.4.2 Flow Model Input Values

Flow model input values are described below and summarized in **Table 2-1** (Steady-State Flow Model / Transport Model Input Values) and **Table 2-2** (Transient Model Input Values). Sensitivity analysis of input values was performed and documented in the 2017 model update but is not included in this report. Input values were generally retained from the 2017 model, with revisions noted above and in **Table 2-1** and **Table 2-2**.

Layer Bottom
Layer bottoms were set for each of the six layers (**Table B)**. The bottom of model layer 1 was revised from the 2017 model by increasing the grid discretization to better match the base of ash elevations within the footprint of the OWAP. The bottom elevation of model layer 6 was changed from 390 feet to 375 feet to better match the estimated bedrock elevation at the WAPS.

Table B. Model Layer Bottom Elevations

Model Layer	2017 Model	Model Revision
1	440+	437+
2	430	430
3	420	420
4	410	410
5	400	400
6	390	375

Note: Elevations are in feet referenced to NAVD88.

Hydraulic Conductivity
Hydraulic conductivity values were initially derived from field-measured and laboratory tested values and adjusted during calibration. Calibrated values were within observed ranges for the formations present at the site. Vertical anisotropy ratios were set at 2.0 for the sand and gravel and 10 for the silty clay and alluvium. The Kx/Kz ratios represent expected stratification within the formations. **Figures 2-2** through **2-7** present hydraulic conductivity zones and boundary conditions for model layers 1 through 6 for the steady-state and transient calibration models, with a summary of hydraulic conductivity zones in **Table 2-1**. Modifications were made to the boundary conditions and the hydraulic conductivity distribution in model layer 1 at the WAPS to represent closure conditions in stress period 3 (**Figure 2-8**).

Storage
No field data was available defining these terms, so representative values for similar materials were obtained from Smith and Wheatcraft (1993). Sensitivity analysis was not performed on this

parameter. The storage coefficient used in the model was 0.01 and the specific yield was 0.2 (revised from 2017 model). A value of 0.2 was assigned for model porosity for all layers.

Recharge
Recharge rates for the impoundment while in service and during dewatering were assigned during model calibration. Recharge rates for the model domain were adopted from the previous 2017 model and were adjusted during calibration. **Figures 2-9** through **2-12** present the recharge distributions for the steady-state flow model, transient model stress period 1 (1996 to 1997), transient stress period 2 (1998 to 2020), and OWAP closure conditions (stress period 3). A summary of model recharge is provided on **Tables 2-1** and **2-2**.

River Parameters
River boundary cells were used to represent the Illinois River, the waterfowl ponds south and west of the impoundments, and a small creek leading from the waterfowl ponds **(Figures 2-2** and **2-3)**. **Table 2-1** presents stage, river bottom, and conductance for these features used for each of the model simulations. The characteristics of the river boundaries in the model were retained from the 2017 model with a few adjustments to conductance to account for revisions to the model grid and to preserve the previous calibration (head and flow directions). The river was specified in model layer 2 to better match river geometry (depth and stage).

An Illinois River stage of 441.7 feet was retained from the 2017 model, which represents a relatively low stage for typical baseflow conditions. Since groundwater elevations near the OWAP are controlled primarily by river stage, this selection is consistent with simulation of baseflow *(i.e.*, low) groundwater elevations, which is reflected in selected calibration targets for the steady-state flow model.

2.4.3 Transport Model Input Values

Transport model input values are listed in **Tables 2-1** and **2-2** and described below. Sensitivity analysis of transport model inputs was conducted as part of the model development and is documented in the 2017 GMR. Transport calibration was performed during the 2017 model development; minor adjustments to transport parameters were performed to retain calibration of the model with respect to other modifications to grid size and refinements to the base of ash elevations (layer 1 bottom elevations).

Initial Concentration
Initial concentrations for the 1966 to 1996 model were set to zero to represent the background concentration for boron. The final concentrations from the steady-state flow / transient transport calibration model (1966 to 1996) were used as the initial concentrations for the subsequent transient transport model representing the years 1996 and later.

Source Concentration
Boron source concentrations were set during model calibration at values between 7 and 19 milligrams per liter (mg/L), the range observed in monitoring wells near the impoundment. These values were assigned during model calibration conducted in 2017 and retained for the CAP model update.

Ash materials within the impoundments were explicitly simulated using both constant concentration cells and recharge. Representation of ash with both boundaries is conservative, in that source concentrations are assigned active cells by the constant concentration cells and assigned to inactive or dry cells by recharge concentrations to represent precipitation infiltrating through the ash to the underlying groundwater table. Equivalent concentrations were assigned at each location through recharge (**Tables 2-1** and **2-2**) and using constant concentration cells.

Dispersivity
Dispersivity was set during model calibration, with sensitivity testing performed as part of the 2017 model revision. Transverse and vertical dispersion were estimated according to ratios developed by Gelhar et al. (1985). Calibrated concentrations at some wells distant from the impoundment (wells 26, 30, 31, and 36) were highly sensitive to the longitudinal dispersivity value and to the vertical dispersivity multiplier.

Retardation
Retardation was calculated by the model based on the Kd, which was set during calibration during previous models. The 2017 model assigned a Kd value of 1.0 mL/g to the silty units (channel-fill deposits and alluvium), and a Kd of zero for the sand and gravel units. The simulated Kd was set to zero for the entire model domain (including for the silty units) in the CAP model update to be more consistent with other Luminant/DMG CCR models, and due to low sensitivity of 2017 model results to the Kd for the silty units.

Diffusion
Diffusion was set to 0 square feet per day for the entire model domain.

2.4.4 Simulation of OWAP Closure (Stress Period 3)

Closure of the OWAP was completed in July 2020 in a manner consistent with the specifications simulated in the 2017 predictive modeling, specifically in that the OWPP was removed, and Pond 1 and Pond 3 (the OWAP) were fully capped by a geomembrane cover, comprised of (from top to bottom) a 6-inch vegetative layer, 18-inch protective soil layer, a 0.2-inch geocomposite drainage layer, and a 40-mil geomembrane layer. These conditions were simulated as stress period 3 according to the following model changes:

- All observed ash was excavated from the OWPP and consolidated within the footprint of the OWAP. This was simulated in the flow and transport model by setting the hydraulic conductivity and recharge to the values assigned to the channel fill silts (K of 1.4 ft/day, recharge of 2.2 inch per year (in/yr) and concentration of 0 mg/L), and by removing the constant-concentration cells from the OWPP.
- A structural steel sheet pile wall was installed between the OWAP and the former OWPP. This was represented in the model using the horizontal flow boundary package in MODFLOW. Horizontal flow barriers (HFBs) were assigned to the locations corresponding to the sheet pile installation with an assigned hydraulic conductivity of 1×10^{-6} cm/s (simulated conductance of 2.36×10^{-4} square feet per day [ft^2/day]). This component of the OWAP closure was not simulated in the 2017 model.
- Recharge values in the OWAP were modified to reflect capping of the OWAP with soil and a geomembrane final cover system, consistent with the simulation of this scenario in the 2017 model. Areal recharge was reduced to 0.0024 in/yr across the OWAP, and concentration recharge values of 7 to 19 mg/L were retained to represent concentrations in the limited vertical infiltration through the ash material under the cap (**Table 2-2**).

2.5 Flow and Transport Model Assumptions and Limitations

Simplifying assumptions are necessary when numerically representing the natural environment in a groundwater flow and transport model. Outside of assumptions inherent to the codes used to develop the model, several simplifying assumptions were made, including:

- Recharge instantaneously migrates to groundwater (*e.g.,* rapid vertical infiltration through the unsaturated zone).
- Fluctuations in river stage are short in duration and do not materially affect long-term groundwater flow.
- Source concentrations remain constant over time.
- Boron minimally adsorbs and does not decay, and mixing and dispersion are the primary attenuation mechanisms.
- Cap construction has an instantaneous effect on recharge and percolation because they are constructed over a brief period relative to the length of the model simulation.

The model is limited by the data used for calibration, which adequately define the local groundwater flow system and the source and extent of the plume. These data, collected from 1994 through 2023, are from points near the WAPS. Model predictions of transport distant from the impoundment will not be as reliable as predictions of transport near the impoundment, and the reliability of model predictions decreases with increasing time because changes to the system may occur that the model does not account for.

2.6 Steady-State Flow Model and Transport Model Calibration

Calibration of a groundwater flow or transport model refers to the iterative process of adjusting model parameters and boundary conditions to obtain a reasonable match between observed conditions and simulation results. The primary criterion for evaluating the calibration of a groundwater flow model is the difference between observed and simulated water levels at a set of calibration targets. Calibration targets are a set of field measurements, typically groundwater elevations. For the calibration of a steady-state (time-invariant) model, the goal in selecting calibration targets is to define a set of water level measurements that represent the average elevation of the water table or potentiometric surface at locations throughout the site. The calibration of a groundwater flow model should rely on spatially discrete measurements of groundwater elevation to avoid the potential for interpretive bias that may result from attempting to match a contoured potentiometric surface (Kalikow, 1978; Anderson and Woessner, 1992).

A model residual is defined as the calculated difference between the observed and simulated hydraulic head at a specific location (observed–simulated). Residual statistics are used to quantify and evaluate the relative fit of a model simulation to measured water level targets. The mean of model residuals is a representation of overall model bias; a value near zero is desired. The steady-state flow model and accompanying transport model were developed to represent conditions from 1966 to 1996, during operation of the impoundments. The steady-state flow and transport model targets used in the 2017 modeling were retained for this model revision, with the objective of a similar level of calibration (equivalent match to calibration targets) for the revised flow and transport models. Flow and transport model calibration targets and statistics are presented on **Table 2-3**. Both sets of targets were originally developed from data collected from 1994 to 1996; transport target simulated values were retrieved from the end of the model simulation (1996). Calibration plots showing observed vs simulated residuals are presented in **Figure 2-13**.

Simulated groundwater model heads (model layer 1) and boron concentrations (maximum concentration from across the model layers) from 1996 are presented in **Figure 2-14**. The mean residual for this calibration is -0.5 (**Table 2-3**). The residual standard deviation indicates the magnitude and spread of the residuals. A residual standard deviation of less than 10 percent of the total range of water level targets is desirable. The residual standard deviation for this calibration is 1.29, which is approximately 10 percent of the observation range (12.7). The residual statistics and simulated hydraulic head distributions indicate a satisfactory model match to observed groundwater flow conditions, and model calibration for the CAP model update is generally consistent with the 2017 model calibration.

2.7 Transient Flow and Transport Model Calibration

The transient flow and transport models, which represented conditions from 1996 to 2023, were qualitatively calibrated by graphically comparing observed and simulated heads and boron concentrations from 1996 to 2023 to provide a qualitative assessment of calibration. Plots comparing simulated and observed heads and boron concentrations at the nine compliance wells are presented in **Figures 2-15** and **2-16**, respectively. The transient model calibration is consistent with the simulation results from the 2017 calibration; consistency with the previous model results was a primary objective of the CAP model update. Several observations regarding the transient model flow and transport model calibrations are further discussed below.

Flow Calibration
As shown in **Figure 2-15**, observed groundwater elevations at site wells fluctuate over time, between approximately 3 and 8 feet, depending on the well location. Generally, simulated heads are consistent with the lower elevation measurements, as is reasonable considering the intended simulation of baseflow conditions (*i.e.,* conditions of low river stage and groundwater elevations). Additionally, wells 22D, 50, 51 were installed after the 2017 model update, therefore these wells were not used as calibration targets during the 2017 model update.

Transport Calibration
Comparison of model simulated boron concentrations in **Figure 2-16** to the calibration obtained by the 2017 modeling (NRT, 2017b) indicates that the CAP model update is generally consistent with the calibration of the 2017 model). However, a number of the compliance wells used for evaluation of this revision were not installed or available for calibration in 2017. The simulated boron concentrations at wells 22D, 49, 50, and 51 are overpredicted. However, since an objective of this model revision was to retain similar predicted conditions and boron concentrations compared to the 2017 modeling, model parameters were not adjusted to improve the calibration at these locations. The overprediction of boron concentrations at these wells is not considered significant for this evaluation since observed concentrations at these four wells are either below the GWPS of 2 mg/L at the current time, or near the GWPS and trending downward. Model calibration to observed concentrations at well 35 is satisfactory from 1997-2019, but do not represent well the concentrations observed at this location from 2020 onward.

3. PREDICTIVE MODELING

Prediction models were evaluated from projected remedy completion of 2028 to 200 years in the future (2228). The objective of predictive modeling of the corrective action scenarios described below is to simulate boron concentrations in groundwater for different corrective actions to evaluate if implementation of these actions will reduce the amount of time to meet the GWPS of 2 mg/L for boron in groundwater. Simulated concentrations of boron were evaluated spatially using maps of maximum boron concentration within each layer at various points in time, and through time-series plots of boron concentrations for the compliance monitoring wells.

Figure 3-1 presents simulated boron concentrations in 2024 and 2028 as initial conditions for evaluation (maximum concentration of boron at each location across all model layers).

3.1 Model Prediction Scenarios

The physical components of each scenario, their representation within the model, and simulation results are presented below. 2028 was used as ”time zero” for completion of the construction of the corrective actions for the model prediction scenarios; discussion of cleanup times in years assumes 2028 as the starting point.

3.1.1 Alternative 1 - Source Control with Groundwater Polishing (GWP)

This scenario is consistent with the closure conditions (capping of the OWAP and Closure-by-removal of the OWPP) initially simulated in the 2017 model report and used to represent current conditions in the revised model as stress period 3. The completed closure and capping of the OWAP and OWPP provides source control for this scenario.

Simulation of GWP was performed by extending stress period 3 from 2028 to 2228. Boron concentrations at the compliance monitoring wells are shown in **Figure 3-2** and **Figure 3-3** presents a map of maximum boron concentrations at 30 years (2058) and 100 years (2128), respectively. Although model simulations were completed for a time frame of 200 years (2228), results were not presented beyond 2128, since concentrations decrease to GWPS at the compliance wells well within this 100-year time frame.

3.1.2 Alternative 2 – Source Control with Cutoff Walls

Alternative 2 consists of installation of a slurry wall cutoff wall surrounding the former OWAP, placed within the OWAP berm from ground surface to various depths with the deep cutoff wall combined with existing site features forming a continuous containment system. Cutoff walls were simulated using the HFB package in MODFLOW, with a thickness of 3 feet and a hydraulic conductivity of 1 x 10^{-7} cm/s. These scenarios assume no changes to the cover system installed during OWAP closure (*i.e.,* any disturbance to the existing cap on the OWAP will be remedied following cutoff wall installation).

- **Alternative 2a – Deep Cutoff Wall (continuous containment system)**. This simulation assumed the cutoff wall was keyed into the relatively impermeable bedrock beneath the overlying unlithified materials, with HFBs simulated in model layers 1 through 6.
- **Alternative 2b – Partial Cutoff Wall**. This simulation assumed the cutoff wall was placed to a base elevation of 400 feet, in order to promote constructability by avoiding cobbles and boulders within deeper layers. HFBs were simulated in model layers 1 through 5.

- **Alternative 2c – Shallow Cutoff Wall**. This simulation assumed the cutoff wall was placed to a base elevation of 420 feet, in order to further improve constructability of the wall. HFBs were simulated in model layers 1 through 3.

Simulation of the cutoff walls assumed remedy completion (begin simulation) in 2028. Boron concentrations at compliance monitoring wells for each of the three cutoff wall alternatives are shown in **Figure 3-4**. Maps of maximum boron concentrations for each of the three cutoff wall alternatives are shown in **Figure 3-5** (30 years, 2058) and **Figure 3-6** (100 years, 2128).

Simulated hydraulics were evaluated for each of the three Alternative 2 scenarios to identify any potential mounding of groundwater inside of the cutoff wall (**Figures 3-5** and **3-6**). Simulation results before and after remedy implementation for the deep cutoff wall (2a) indicated that heads inside the cutoff wall vary from 443.16 to 444.6 feet prior to implementation, and are uniform at 444.19 feet 200 years after implementation. Due to the average of less than 1 foot of head increase within the pond footprint 200 years after implementation of the deep cutoff wall, mitigation of mounding through use of pumping wells or other action was not required to reduce mounding or time to meet GWPS. Minimal change to pre-implementation heads on the interior of the cutoff wall for scenarios 2b and 2c were simulated.

3.1.3 Alternative 3 – Source Control - In-Situ Solidification/Stabilization (ISS)

The third simulated alternative consists of ISS across a portion of the OWAP. The target area for ISS was assigned based upon the estimated extent of CCR present at portions of the WAPS with the lower base elevations. The ISS target area consisted of portions of the OWAP below an elevation of 445.7 feet; portions of the former ash pond where the base of ash elevation was higher than this value were not included in the ISS footprint. **Figure 3-7** depicts the target area for ISS and the estimated thickness of ash where ISS would be conducted at each location.

Simulation of ISS was performed by assigning a hydraulic conductivity of 1×10^{-7} cm/s to the ISS target area. The constant-concentration boundary cells within the footprint were removed to represent immobilization or treatment of dissolved phase mass in the solidified material; however, the recharge concentrations were retained for the OWAP to represent assignment of boron concentration to vertical infiltration through the overlying ash material. The final cover of the OWAP is assumed to be replaced or repaired consistent with the 2017 design specifications (Geosyntec, 2017) following ISS, therefore the simulated rate of vertical surface infiltration through the final cover did not change relative to current conditions for this alternative.

Boron concentrations at the compliance monitoring wells are shown in **Figure 3-8**, and **Figure 3-9** presents a map of maximum boron concentrations at 30 years (2058) and 100 years (2128).

3.2 Assessment of Geochemical Processes

This groundwater transport model estimates the time for boron to reach the GWPS under different potential corrective actions, incorporating the physical components of groundwater polishing. As described above, it was assumed that boron would not significantly sorb or chemically react with aquifer solids (Kd was set to 0 mL/g, which is a conservative estimate for estimating contaminant transport times).

The GPR was prepared as an attachment to the Corrective Actions Alternative Analysis (CAAA). The geochemical modeling effort presented in the GPR supports the assessment of groundwater polishing as a component of the proposed corrective action by evaluating the potential for chemical attenuation of constituents of concern (COCs) (and for previously attenuated COCs to be mobilized to groundwater as groundwater quality returns to background conditions) as a means of contextualizing the times estimated in the flow and transport model. The GPR also provides a foundation for understanding groundwater chemistry to inform adaptive site management as a key component of the Corrective Action Groundwater Monitoring Program.

As concluded in the GPR:

> *"The results of the groundwater polishing evaluation indicate that chemical attenuation of modeled COCs (arsenic, boron and sulfate) is feasible under current conditions through sorption to iron and aluminum oxide minerals. Though some degree of desorption is predicted with background water interaction, aqueous boron and sulfate (and therefore TDS) concentrations should decrease below the GWPS at all wells in the compliance monitoring network following source control. Remobilization of boron and sulfate is unlikely to affect the estimated time to reach the GWPS based on modeling results. Aqueous arsenic concentrations are predicted to increase at wells with current exceedances following remobilization of arsenic in post-source control conditions. Remobilization may impact the time to reach the GWPS for arsenic. Lithium was not evaluated in the geochemical modeling because lithium concentrations continue to decline following unit closure."*

The results of the GPR geochemical modeling indicate attenuation of COCs boron, lithium, sulfate, and TDS through sorption and chemical mechanisms will complement results of the groundwater transport modeling, in that time to reach GWPS may be shorter than the simulated timeframes. Remobilization of arsenic, which exceeds GWPS at two wells (51 and 21R), may increase the time to reach GWPS from the simulated results.

3.3 Prediction Scenario Results Discussion

Simulation of corrective action alternatives for the OWAP through the next 200 years indicates that concentrations of boron in groundwater will decrease over time regardless of the remedy selected. A summary of predicted boron concentrations and time to meet the GWPS at the compliance monitoring wells is provided in **Table 3-1** and summarized below in **Table C** for Alternative 2a. As shown, concentrations are expected to fall below 2 mg/L by 2061 for all corrective action alternatives, with the majority of wells (6 of 9) reaching GWPS by 2030 (two years after remedy implementation) regardless of the selected corrective action alternative.

Table C. Estimated Timeframes to Attain GWPS in Groundwater Monitoring Wells†

	Alternative	2 years‡	5 years‡	10 years‡	20 years‡	33 years‡
Percentage of Wells predicted to attain GWPS†	1	67%	89%	89%	89%	100%
Percentage of Wells predicted to attain GWPS†	2a	67%	67%	67%	89%	100%
Percentage of Wells predicted to attain GWPS†	2b	89%	89%	89%	89%	100%
Percentage of Wells predicted to attain GWPS†	2c	67%	89%	89%	89%	100%
Percentage of Wells predicted to attain GWPS†	3	67%	89%	89%	89%	100%

†: Estimated timeframes per the 9 compliance wells
‡: Years counted starting from 2028

3.3.1 Comparison of Corrective Action Alternatives

Comparison of predicted concentrations at the compliance wells indicates that the time to reach GWPS is similar across each of the evaluated remedies, with Alternatives 1, 2b, 2c, and 3 reaching GWPS in 2055 (27 years after 2028), and Alternative 2a reaching GWPS by 2061 (33 years after 2028). Comparison of the engineered corrective action alternatives to GWP shows that Alternatives 2b, 2c, and 3 produce similar cleanup times to Alternative 1, with only slight decreases in time to reach GWPS in 1, 2, or 3 wells (less than 5 years improvement). Alternative 2a results in increased time to reach GWPS in wells 23 and 49 due to reduced advection of groundwater immediately downgradient of the deep cutoff wall (*i.e.,* stagnation of groundwater near wells 23 and 49).

Well 21R is the last to meet GWPS in four of five alternatives; this result is due to the simulated location of this well within the silt and clays, which results in lower groundwater velocities and a consequently longer time for flushing of concentrations after closure of the OWAP in 2020 than for the higher-permeability materials. The cleanup time at well 21R (27 years) is also reduced compared to the cleanup time at this well from the 2017 simulation of OWAP closure; this is due to the assignment of a Kd of 0 mL/g to the silts and clays in this model revision (no retardation of boron).

4. CONCLUSIONS

Existing site-specific three-dimensional groundwater flow (MODFLOW) and transport models (MT3DMS) were revised and employed to evaluate the effectiveness of groundwater corrective action alternatives in reduction of time to reach GWPS in groundwater at the Hennepin WAPS following the closure of the OWAP and OWPP, which were completed in 2020. Boron was selected for simulation of groundwater quality changes resulting from the WAPS. It was assumed that boron would not significantly sorb or chemically react with aquifer solids (Kd was set to 0 mL/g) which is a conservative estimate for predicting contaminant transport times in the model.

Five corrective action alternatives were simulated, consisting of GWP (Alternative 1), three configurations of a cutoff wall surrounding the OWAP (Alternatives 2a, 2b, and 2c), and ISS (Alternative 3). Comparison of predicted concentrations at the compliance wells indicates that the time to reach GWPS is similar for each of the evaluated remedies, with Alternatives 1, 2b, 2c, and 3 reaching GWPS in 2055, and Alternative 2a reaching GWPS by 2061. Comparison of the "engineered" corrective action alternatives to GWP indicates that Alternatives 2b, 2c, and 3 produce similar cleanup times to Alternative 1, with only slight decreases in time to reach GWPS. Alternative 2a, the continuous containment system, results in a longer time to reach the GWPS due to the creation of a stagnant flow zone (area of reduced advection) downgradient of the cutoff wall.

5. REFERENCES

Anderson, Mary P., and Woessner, William W., 1992. Applied groundwater modeling: simulation of flow and advective transport, Academic Press, Inc., San Diego, CA.

Chenoweth, Cheri; Herzog, BL; JB Sievering; KL Warner; Stiff, Barbara J., 1994. Buried Bedrock Surface (Illinois). Illinois Geospatial Data Clearinghouse; B1G Academic Alliance Geospatial Information Network.

Code of Federal Regulations, Title 40, Chapter I, Subchapter I, Part 257, Subpart D, Standards for the Disposal of Coal Combustion Residuals in Landfills and Surface Impoundments, effective April 17, 2015.

Dynegy, 2020a. Hennepin Power Station; Old West Ash Pond, Ash Pond No. 2 Notification of Completion of Closure. Dynegy Midwest Generation, LLC; Collinsville, IL, December 17, 2020.

Dynegy, 2020b. Hennepin Power Station; Old West Polishing Pond Notification of Completion of Closure. Dynegy Midwest Generation, LLC; Collinsville, IL, December 17, 2020.

Gelhar et al., 1985. A review of field-scale physical solute transport processes in saturated and unsaturated porous media. Electric Power Research Institute, Rep. EA-4190

Geosyntec Consultants (Geosyntec), 2017. Closure and Post-Closure Care Plan, Old West Ash Pond, Old West Polishing Pond at Dynegy Midwest Generation, LLC Hennepin Power Station, Chicago, Illinois, December 2017.

Geosyntec Consultants (Geosyntec), 2025. Groundwater Polishing Evaluation Report. Hennepin Power Plant, West Ash Pond System, Hennepin, Illinois.

Gradient Corporation (Gradient), 2004. Closure Alternatives Analysis Groundwater Modeling Review at the Coffeen Power Plant, Edwards Power Plant, Newton Power Plant, and Hennepin Power Plant. Expert Report of Andrew Bittner, P.E, prepared for ArentFox Schiff LLP, Chicago, IL. January 24, 2024.

Harbaugh, A.W., Langevin, C.D., Hughes, J.D., Niswonger, R.N., and Konikow, L. F., 2017. MODFLOW-2005 version 1.12.00, the U.S. Geological Survey modular groundwater model: U.S. Geological Survey Software Release, 03 February 2017.

Illinois Administrative Code, Title 35, Subtitle G, Chapter I, Subchapter J, Part 845: Standards for The Disposal of Coal Combustion Residuals In Surface Impoundments, effective April 21, 2021.

Konikow, L., 1978. Calibration of Groundwater Models, in Proceedings of the Specialty Conferences on Verification of Mathematical and Physical Models in Hydraulic Engineering. College Park, Maryland, August 9-11, 1978.

McDonald, M.G., and A.W. Harbaugh, 1988. A Modular Three-Dimensional Finite-Difference Ground-Water Flow Model: Techniques of Water-Resources Investigations, Techniques of Water-Resources of the United States Geological Survey, Book 6, Chapter A1.

Natural Resource Technology, Inc. (NRT), 2017a. Hydrogeologic Site Characterization Report; Hennepin Power Station Putnam County, West Ash Impoundment, Illinois. September, 2017.

Natural Resource Technology, Inc. (NRT), 2017b. Groundwater Modeling Report; Hennepin Power Station Putnam County, West Ash Impoundment, Illinois. September, 2017.

Natural Resource Technology, Inc. (NRT), 2017c. Hydrostatic Modeling Report; Hennepin Power Station Putnam County, West Ash Impoundment, Illinois. September, 2017.

Ramboll, 2024a. Groundwater Monitoring Data and Detected Exceedances Quarter 4, 2023, West Ash Pond System, Hennepin Power Plant, Hennepin, Illinois.

Ramboll, 2024b. Nature and Extent Report, Hennepin Power Station, West Ash Pond System. Hennepin, Illinois, May 2024.

Ramboll, 2025. Technical Memorandum: Summary of Bedrock Investigation Results. Hennepin Power Station, West Ash Pond System. Hennepin, Illinois, March 2025.

Rumbaugh, J. O. D. B., 2020. Groundwater Vistas 9 Advanced. Reinholds, PA: Environmental Simulations, Inc.

Smith, L. and S.J. Wheatcraft, 1993. Chapter 6: Groundwater Flow, in: Maidment, D.R. (ed) Handbook of Hydrology. McGraw-Hill, New York, NY.

United States Environmental Protection Agency (USEPA). 1994. Ground-Water Modeling Compendium. Second Edition. Office of Solid Waste and Emergency Response. 500-B-94-004. July.

Zheng, Z., and P.P. Wang, 1998. MT3DMS, a Modular Three-Dimensional Multispecies Transport Model, Model documentation and user’s guide prepared by the University of Alabama Hydrogeology Group for the US Army Corps of Engineers.

TABLES

Table 2-1
Model Input Values: Steady-State Flow Model / Transport Model
Groundwater Modeling Technical Memorandum
West Ash Pond System, Hennepin Power Plant

Horizontal Hydraulic Conductivity	**ft/d**	**cm/s**		**Revision Notes**
Sand & River Sand (Zone 1)	30.0	1.1E-02		
Outwash Gravel, Layers 1-5 (Zone 2)	200.0	7.1E-02		
Alluvium (Zone 3)	1.5	5.3E-04		
Channel Fill Silts (Zone 4)	1.4	4.9E-04		
Ash (Zone 10)	0.05	1.8E-05		
Outwash Gravel, Layer 6 (Zone 12)	100.0	3.5E-02		New for Rev1

Vertical Hydraulic Conductivity	**ft/d**	**Kh/Kv**		**Revision Notes**
Sand & River Sand (Zone 1)	15.0	2.0		
Outwash Gravel (Zone 2)	100.0	2.0		
Alluvium (Zone 3)	0.15	10.0		
Channel Fill Silts (Zone 4)	0.14	10.0		
Ash (Zone 10)	0.05	1.0		
Outwash Gravel, Layer 6 (Zone 12)	50	2.0		New for Rev1

Recharge[2]	ft/d	in/yr	**Boron Concentration (mg/L**	**Revision Notes**
Sand & River Sand (Zone 1)	1.0E-03	4.4		Decreased by 10%
Outwash Gravel (Zone 2)	1.0E-03	4.4		Decreased by 10%
Channel Fill Silts (Zone 4)	5.0E-04	2.2		
Ash-Pond 1 (Zone 9)	3.83E-03	16.8	9.0	
Ash-Pond 3 East (Zone 8)	4.0E-02	175.2	9.0	Increased by 10%
Ash-Pond 3 Center (Zone 10)	2.7E-02	118.3	9.0	Increased by 5%
Ash-Pond 3 West (Zone 6)	2.7E-02	118.3	19.0	
Ash-Pond 3 Northwest (Zone 5)	2.7E-02	118.3	7.0	
Ash-Secondary Pond (Zone 7)	2.0E-02	87.6	7.0	

River Parameters	**Illinois Riv.**	**Duck Ponds**	**Duck Pond (Creek)**	**Revision Notes**
Stage (ft)	441.7	445.5	444.8	Retained
Bottom (ft)	435	440	440	Modified (Illinois River)
Conductance (ft2/d)	200-1000	62.5-10,000	2.5E+05	Modified (see report)

Dispersivity	**dispersivity (ft^2/d)**			**Revision Notes**
Longitudinal (all layers)	50			Retained
Transverse (all layers)	6.25			Retained
Vertical (all layers)	0.313			Retained

Storage/Porosity	**S_S (1/ft)**	**Sy**	**porosity**	**Revision Notes**
Entire Domain	0.01	0.20	0.20	Retained

Notes:

1 The steady-state flow model and transient transport calibration represent conditions from 1966-1996 (30 years) during ash pond operation

2 See figures for delineation of model zones

Table 2-2
Model Input Values: Transient Flow Model / Transport Model
Groundwater Modeling Technical Memorandum
West Ash Pond System, Hennepin Power Plant

	Calibration		
Stress Periods[1]	**Days, # of time steps**	**Dates**	
Stress Period 1	**500, 6**	**1/1997-5/1998**	
Stress Period 2	**8096, 20**	**5/1998-7/2020**	
Stress Period 3	**2710, 10**	**8/2020-1/2028**	
Recharge[2] (Stress Period 1)	**ft/d**	**in/yr**	**Boron Concentration (mg/L)**
Ash-Pond 1 (Zone 9)	3.83E-03	16.8	9.0
Ash-Pond 3 East (Zone 8)	2.E-02	87.6	9.0
Ash-Pond 3 Center (Zone 10)	2.E-02	87.6	9.0
Ash-Pond 3 Center (Zone 6)	2.E-02	87.6	9.0
Ash-Pond 3 West (Zone 12)	2.E-02	87.6	19.0
Ash-Pond 3 West (Zone 13)	2.E-02	87.6	19.0
Ash-Pond 3 Northwest (Zone 5)	2.E-02	87.6	7.0
Ash-Pond 3 Northwest (Zone 11)	2.E-02	87.6	9.0
Ash-Old West Polishing Pond (Zone 7)	2.E-02	87.6	7.0
Recharge[2] (Stress Period 2)	**ft/d**	**in/yr**	**Boron Concentration (mg/L)**
Ash-Pond 1 (Zone 9)	3.83E-03	16.8	9.0
Ash-Pond 3 East (Zone 8)	2.96E-03	13.0	9.0
Ash-Pond 3 Center (Zone 10)	2.96E-03	13.0	9.0
Ash-Pond 3 Center (Zone 6)	2.E-02	87.6	9.0
Ash-Pond 3 West (Zone 12)	2.E-02	87.6	19.0
Ash-Pond 3 West (Zone 13)	2.96E-03	13.0	19.0
Ash-Pond 3 Northwest (Zone 5)	2.96E-03	13.0	7.0
Ash-Pond 3 Northwest (Zone 11)	2.E-02	87.6	9.0
Ash-Old West Polishing Pond (Zone 7)	2.96E-03	13.0	7.0
Recharge[2] (Stress Period 3)	**ft/d**	**in/yr**	**Boron Concentration (mg/L)**
Ash-Pond 3 East (Zone 8)	5.55E-07	0.0	9.0
Ash-Pond 3 Center (Zone 10)	5.55E-07	0.0	9.0
Ash-Pond 3 West (Zone 12)	5.55E-07	0.0	19.0
Ash-Pond 3 Northwest (Zone 11)	5.55E-07	0.0	7.0

Notes:

1 Transient flow and transport models described above represent years 1996-2023 (2028)

2 See figures for delineation of model zones; recharge values outside ash pond are same as Table 2-1.

Table 2-3
Calibration Targets and Statistics: Steady-State Flow Model / Transport Model
Groundwater Modeling Technical Memorandum
West Ash Pond System, Hennepin Power Plant

Flow Model Calibration Targets

Well ID	Model Layer	Observed Head (feet)	Simulated Head (feet)	Residual (observed - simulated, feet)	Simulated Head, 1997 model (feet)
21	5	446.89	446.38	0.51	446.00
23	3	446.56	445.92	0.64	445.36
24	5	446.85	446.07	0.78	445.54
26	1	446.82	446.94	-0.12	446.10
27	4	446.02	446.06	-0.04	445.95
30	4	446.15	446.49	-0.34	446.10
31	1	446.09	446.49	-0.40	446.10
32	1	446.10	446.39	-0.29	446.17
33	5	444.46	444.43	0.03	444.37
34	4	441.56	442.40	-0.84	441.69
L1	1	454.25	455.96	-1.71	455.22
L4	1	448.10	452.32	-4.22	451.59

Notes:

Flow Model targets were developed using data collected from 1994-1996.

Flow model targets were retained from the previous (2017) model.

Flow Model Calibration Statistics		
Residual Mean	-0.50	ft
Absolute Residual Mean	0.83	ft
Residual Std. Deviation	1.29	ft
Sum of Squares	23.1	ft^2
RMS Error	1.4	
Number of Observations	12	
Range in Observations	12.7	

Transport Model Calibration Targets

Well ID	Model layer	Observed boron concentration (mg/L)	Simulated boron concentration (mg/L)	Residual (Observed - Simulated, mg/L)	Simulated boron concentration, 1997 model (mg/L)
21	5	4.9	7.0	-2.0	5.8
22	1	8.1	7.7	0.4	8.9
23	3	6.9	9.2	-2.3	8.7
24	5	7.7	8.6	-1.0	8.7
26	1	1.1	0.2	0.9	0.4
27	4	6.0	5.4	0.6	7.5
30	4	2.3	2.0	0.3	1.5
31	1	0.2	0.4	-0.2	0.7
32	1	0.1	0.0	0.1	0.0
33	5	0.1	0.0	0.1	0.0
34	4	0.1	0.0	0.1	0.0
L1	1	14.4	18.5	-4.1	18.9
L4	1	26.1	7.3	18.8	4.8

Notes:

Transport model targets were developed using data collected from 1994-1996. Calibration targets were retained from the previous (2017) model.

Table 3-1

Estimated Time to Achieve GWPS at Compliance Wells
Groundwater Modeling Technical Memorandum
West Ash Pond System, Hennepin Power Plant

	Simulated Boron Concentrations (mg/L)		Years to Reach GWPS (2 mg/L) from 2028				
Compliance Wells	7/30/2020 (Completed Closure)	1/1/2028 (Completed Remedy)	1 - GWP + Source Control	2A –Bedrock Wall	2B – Partial Wall	2C – Shallow Wall	3 – ISS
21R- L5	6.4	5.7	**27**	20	27	27	27
22- L1	7.8	3.5	**2**	2	1	2	2
22D- L5	5.2	*1.4*					
23- L3	8.4	3.2	**4**	16	1	4	4
27- L4	2.1	*1.2*					
35- L1	5.5	2.4	**2**	0	1	1	2
49- L3	7.1	3.4	**5**	33	0	3	4
50-L2	4.4	*0.6*					
51- L6	9.8	*1.1*					
		Year for GWPS	2055 (21R)	2061 (49)	2055 (21R)	2055 (21R)	2055 (21R)

Notes

The GWPS for Boron is 2 mg/L.

Years to reach GWPS are in BOLD for Alternative 1. Blue shading denotes faster cleanup, gold denotes slower cleanup compared to Alternative 1.

Current concentrations are at or below GWPS of 2 mg/L at wells 22D, 49, 50, and 51; concentrations are overpredicted at these wells for 2023.

FIGURES

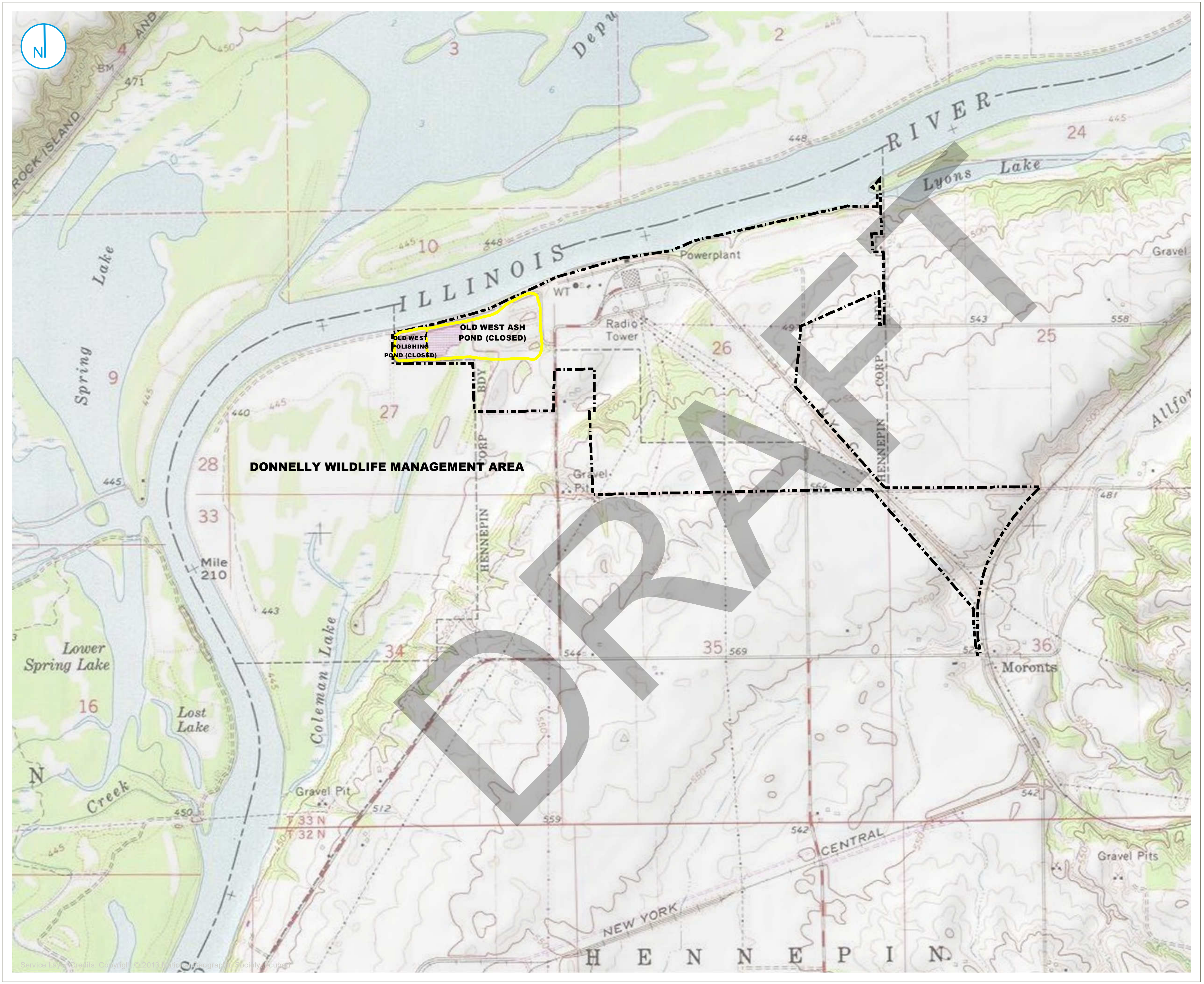

🟨 REGULATED UNIT (SUBJECT UNIT)

▭ PROPERTY BOUNDARY

0 750 1,500 Feet

SITE LOCATION MAP

GROUNDWATER MODELING
TECHNICAL MEMORANDUM
WEST ASH POND SYSTEM
HENNEPIN POWER PLANT
HENNEPIN, ILLINOIS

FIGURE 1-1

RAMBOLL AMERICAS
ENGINEERING SOLUTIONS, INC.

Y:\Mapping\Projects\22\2285\MXD\Model_Figures\Hennepin\OWAP_804\Figure 1-1. Site Location Map.mxd

PROJECT: 169000XXXX | DATED: 1/10/2024 | DESIGNER: GALARNMC

Service Layer Credits: Source: Esri, Maxar, Earthstar Geographics, and the GIS User Community

SITE FEATURES AND MONITORING WELLS

GROUNDWATER MODELING TECHNICAL MEMORANDUM
WEST ASH POND SYSTEM
HENNEPIN POWER PLANT
HENNEPIN, ILLINOIS

FIGURE 1-2

RAMBOLL AMERICAS
ENGINEERING SOLUTIONS, INC.

Y:\Mapping\Projects\22\2285\MXD\Model_Figures\Hennepin\OWAP_804\Figure 1-2. Site Features and Monitoring Wells.mxd

PROJECT: 169000XXXX | DATED: 1/10/2024 | DESIGNER: GALARNMC

FIGURE 2-1

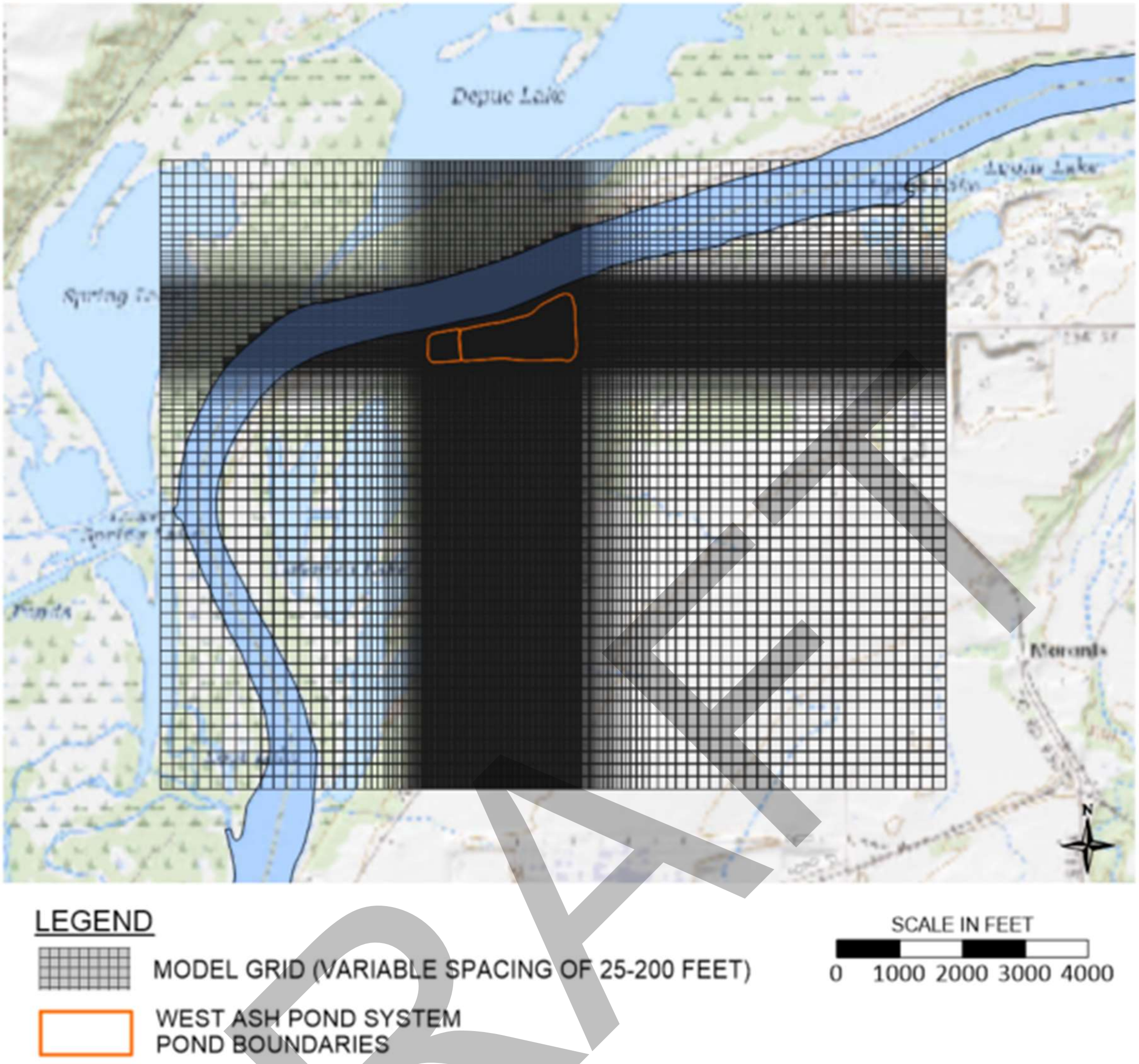

MODEL GRID

GROUNDWATER MODELING TECHNICAL MEMORANDUM
WEST ASH POND SYSTEM
HENNEPIN POWER PLANT
HENNEPIN, ILLINOIS

RAMBOLL

FIGURE 2-2

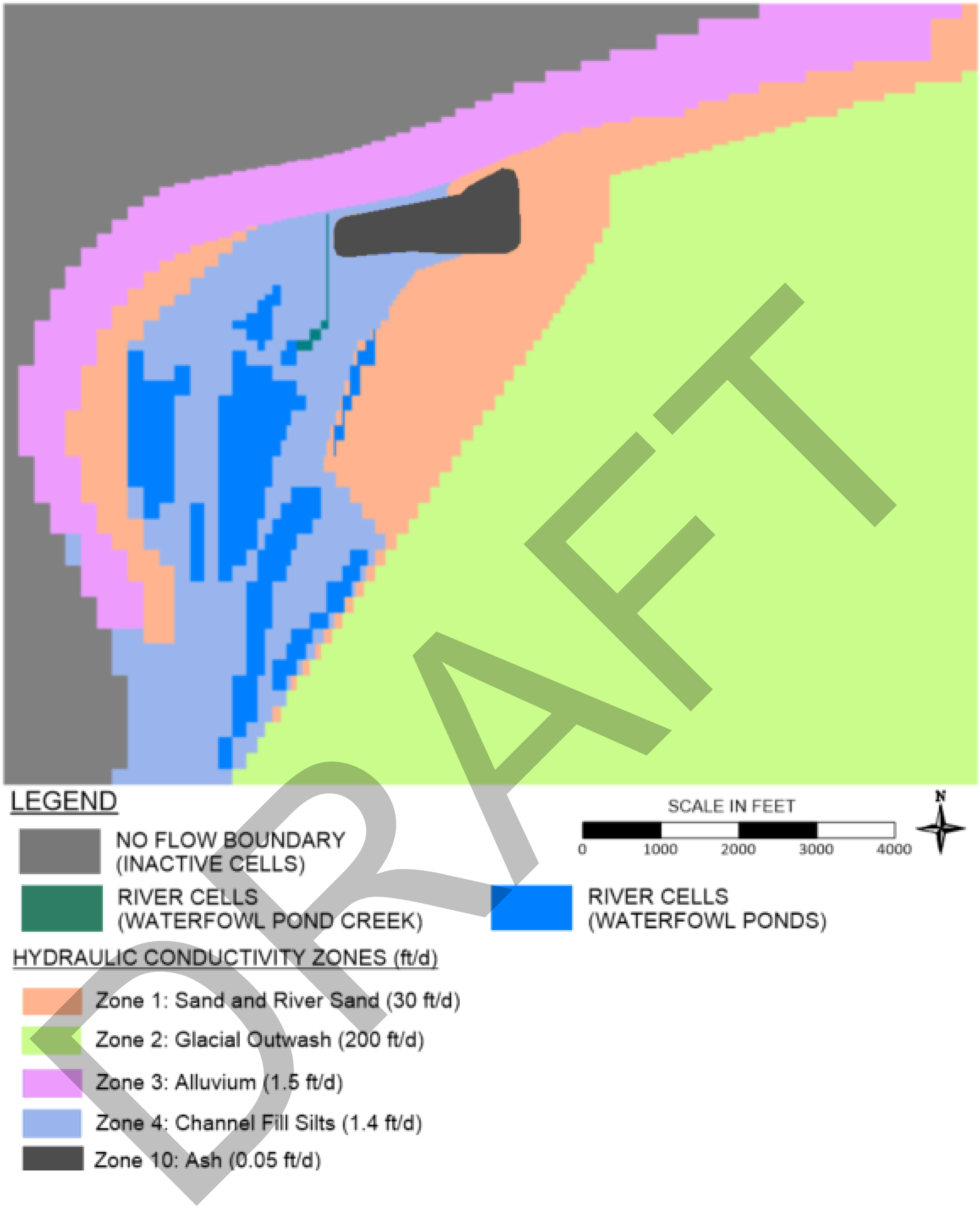

Notes

Constant-concentration cells representing the ash in model layer 1 are presented in Figures 2-9 through 2-12.

BOUNDARY CONDITIONS AND HYDRAULIC CONDUCTIVITY (K) ZONES
MODEL LAYER 1

GROUNDWATER MODELING TECHNICAL MEMORANDUM
WEST ASH POND SYSTEM
HENNEPIN POWER PLANT
HENNEPIN, ILLINOIS

FIGURE 2-3

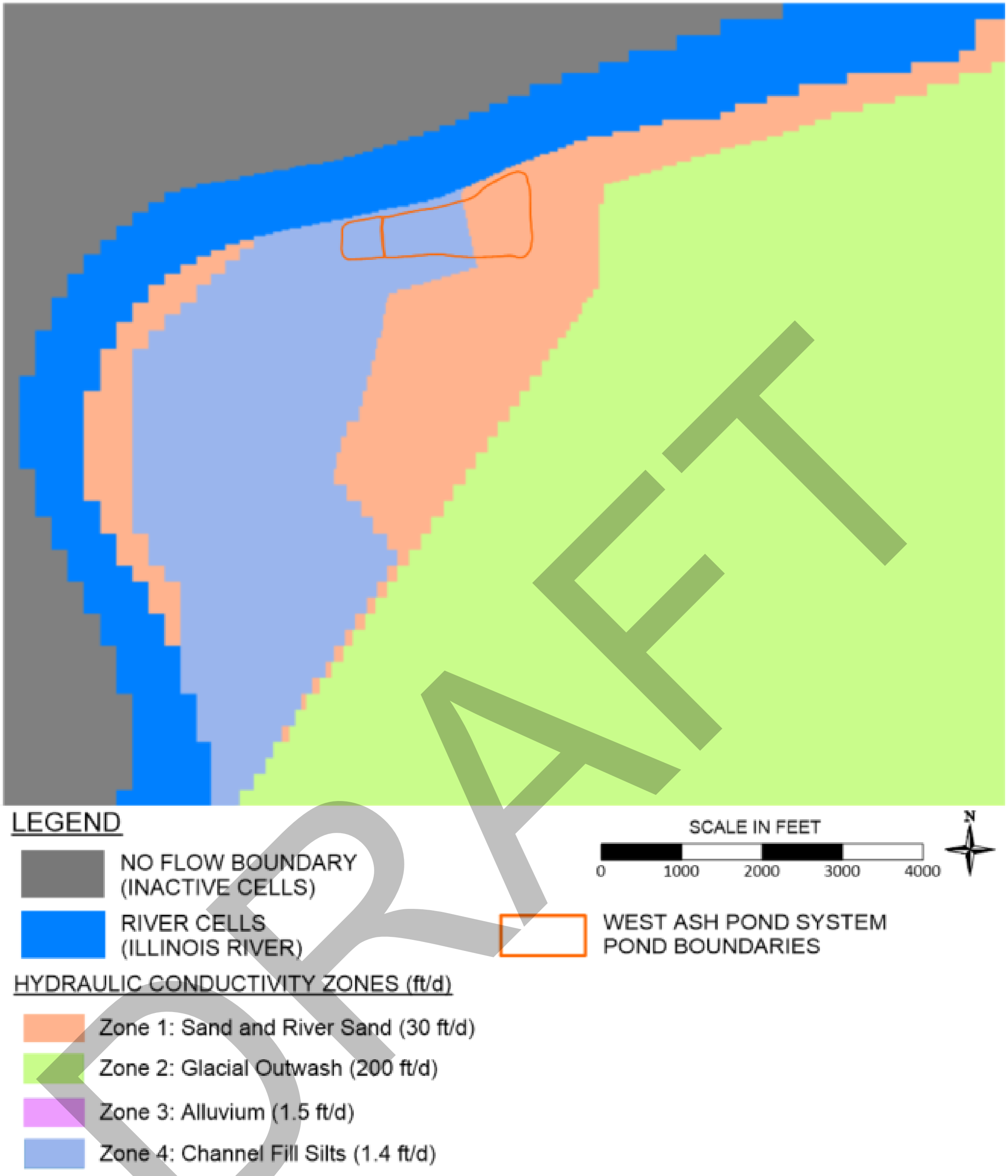

Notes

The river boundary cells representing the Illinois River are coincident with K zone 3 (Alluvium).

BOUNDARY CONDITIONS AND HYDRAULIC CONDUCTIVITY (K) ZONES
MODEL LAYER 2

GROUNDWATER MODELING TECHNICAL
MEMORANDUM
WEST ASH POND SYSTEM
HENNEPIN POWER PLANT
HENNEPIN, ILLINOIS

FIGURE 2-4

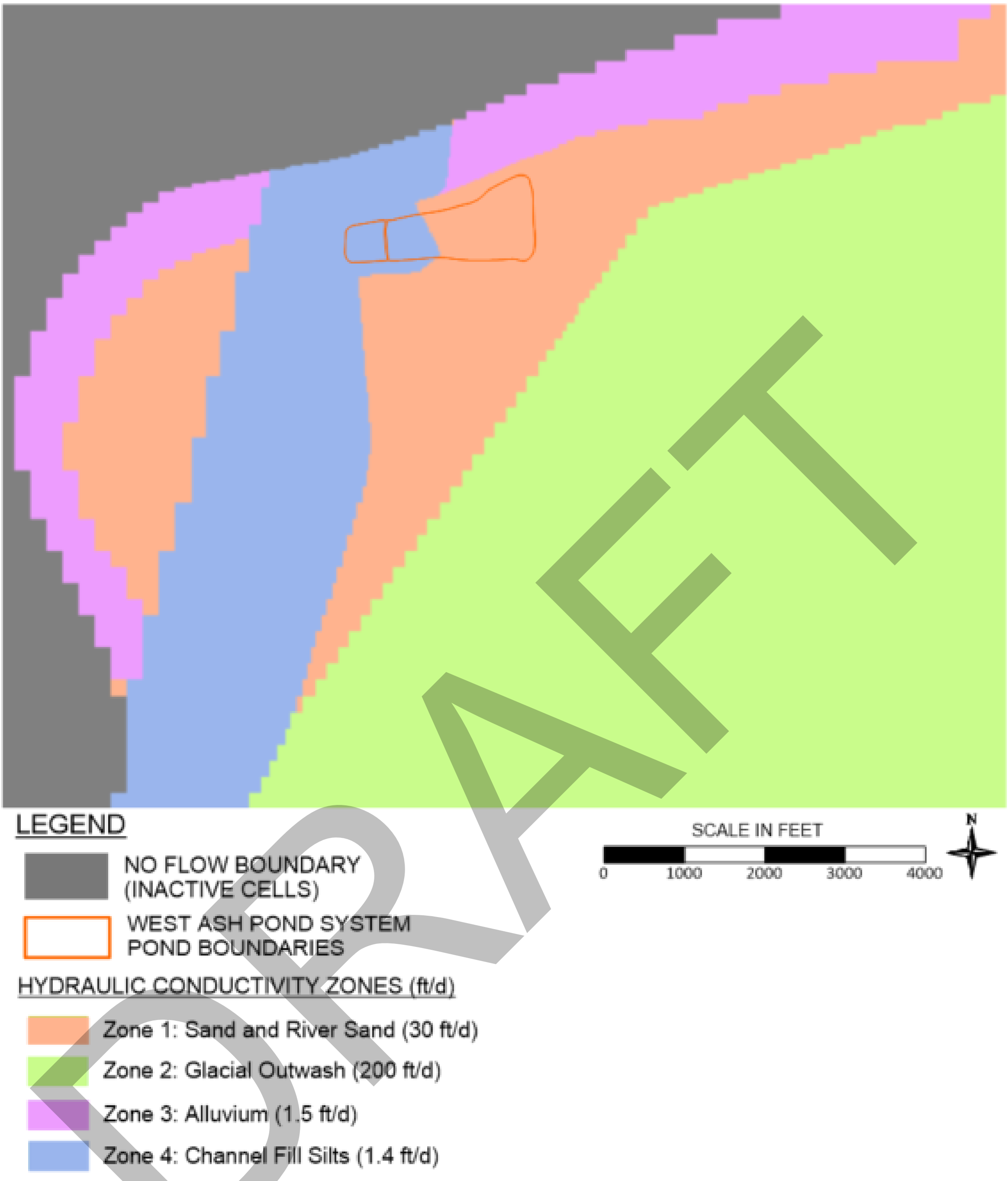

BOUNDARY CONDITIONS AND HYDRAULIC CONDUCTIVITY (K) ZONES
MODEL LAYER 3

GROUNDWATER MODELING TECHNICAL MEMORANDUM
WEST ASH POND SYSTEM
HENNEPIN POWER PLANT
HENNEPIN, ILLINOIS

FIGURE 2-5

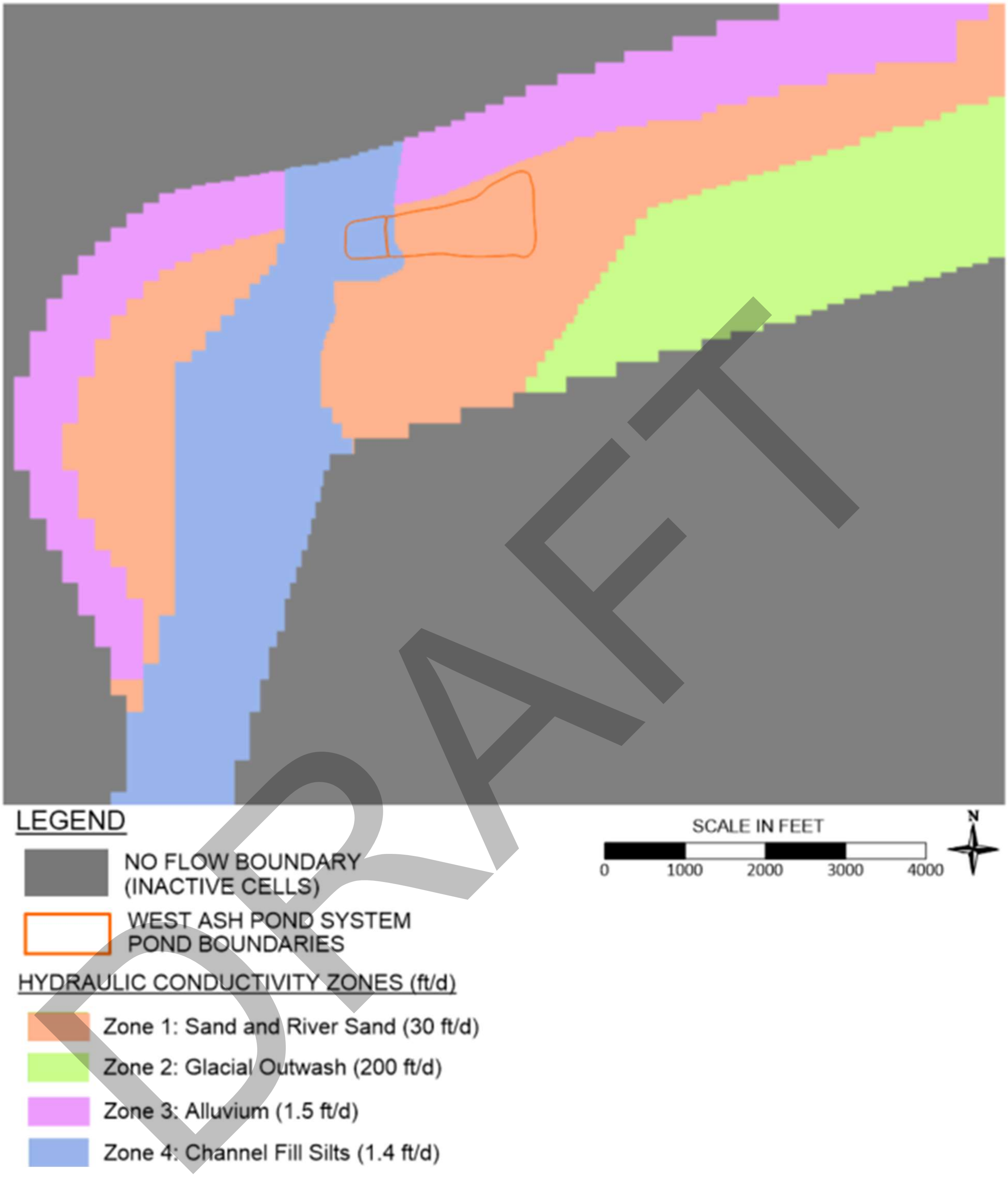

BOUNDARY CONDITIONS AND HYDRAULIC CONDUCTIVITY (K) ZONES
MODEL LAYER 4

GROUNDWATER MODELING TECHNICAL
MEMORANDUM
WEST ASH POND SYSTEM
HENNEPIN POWER PLANT
HENNEPIN, ILLINOIS

FIGURE 2-6

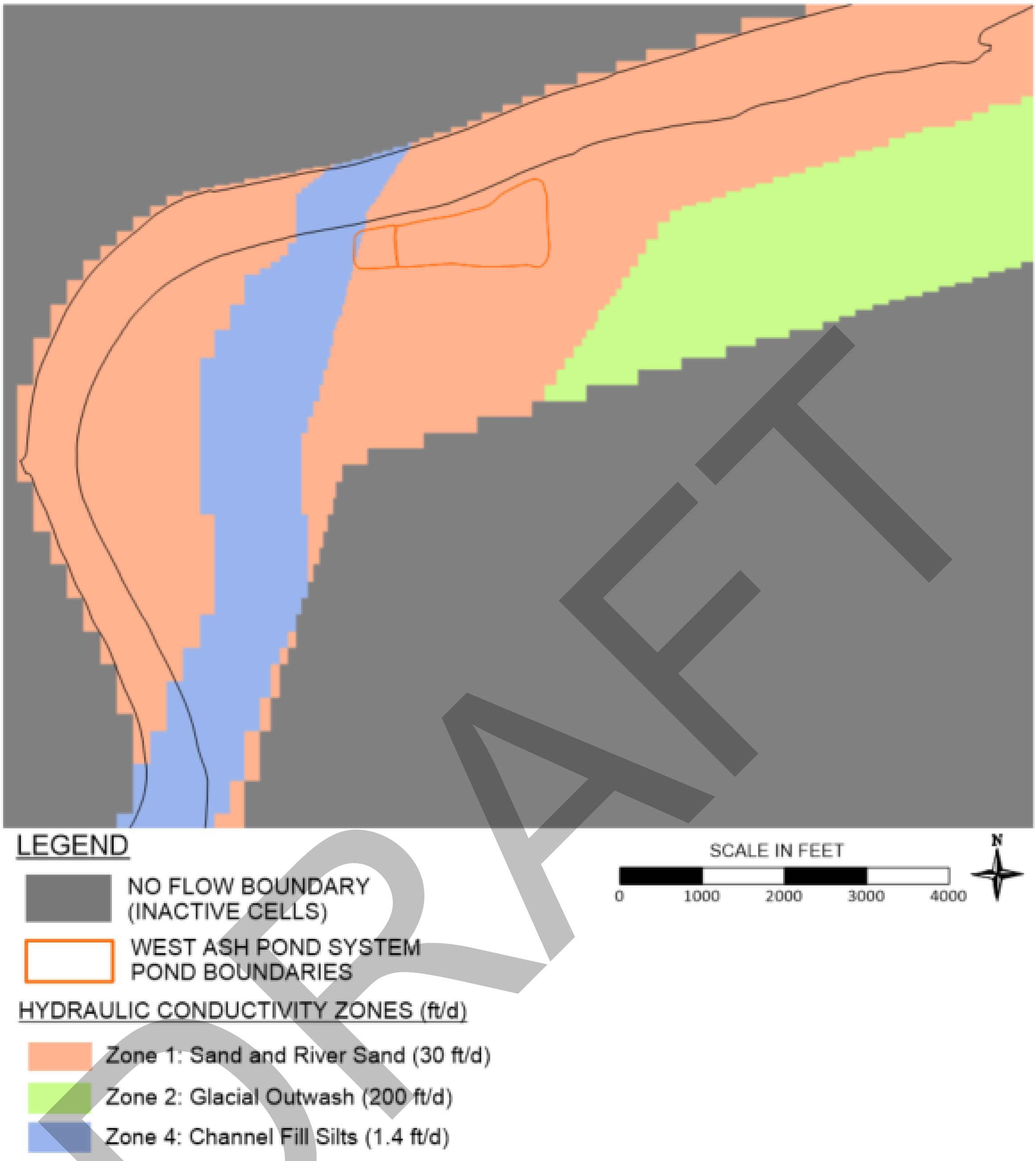

BOUNDARY CONDITIONS AND HYDRAULIC CONDUCTIVITY (K) ZONES
MODEL LAYER 5

GROUNDWATER MODELING TECHNICAL MEMORANDUM

WEST ASH POND SYSTEM
HENNEPIN POWER PLANT
HENNEPIN, ILLINOIS

RAMBOLL

FIGURE 2-7

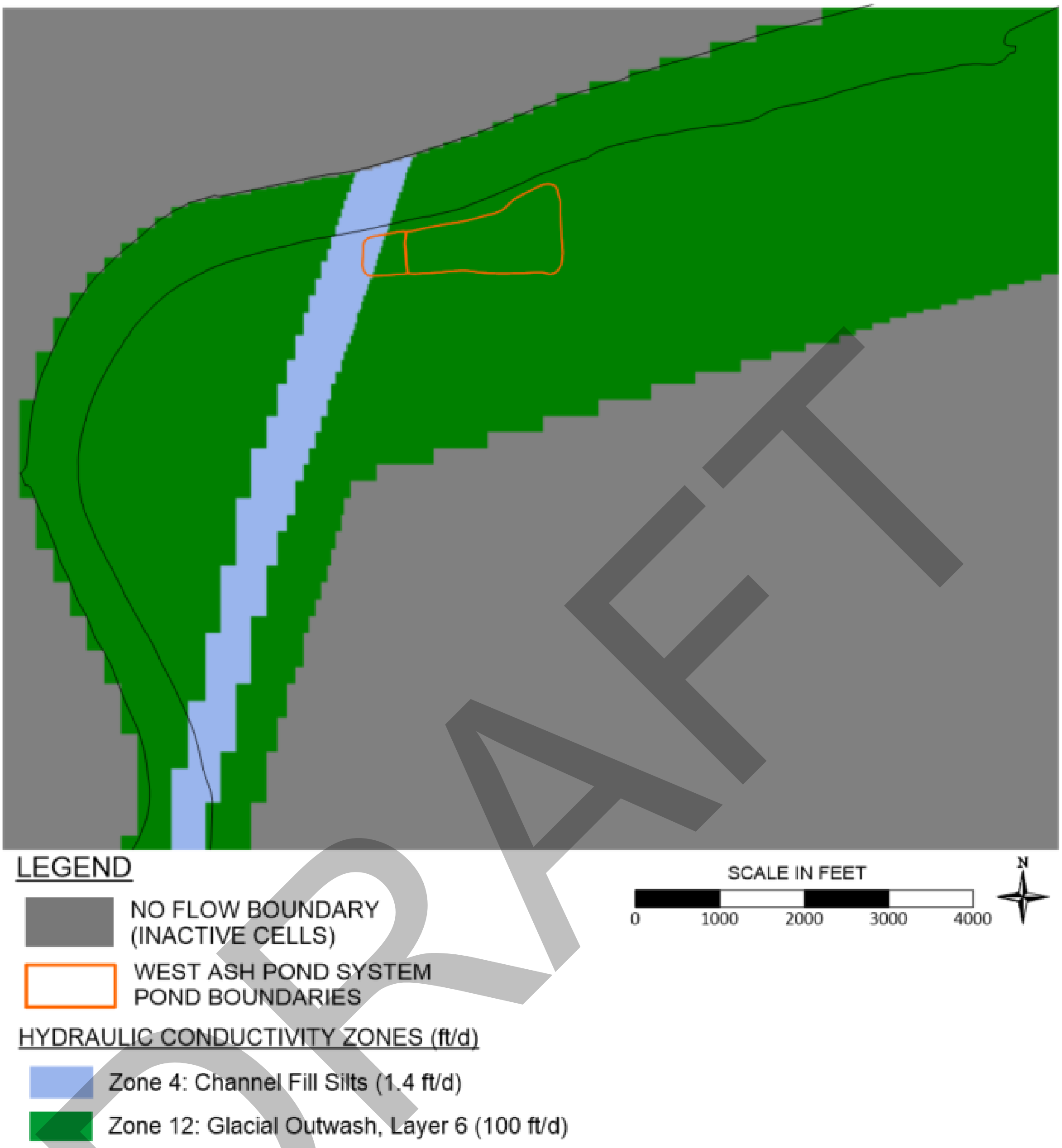

BOUNDARY CONDITIONS AND HYDRAULIC CONDUCTIVITY (K) ZONES
MODEL LAYER 6

GROUNDWATER MODELING TECHNICAL MEMORANDUM
WEST ASH POND SYSTEM
HENNEPIN POWER PLANT
HENNEPIN, ILLINOIS

RAMBOLL

FIGURE 2-8

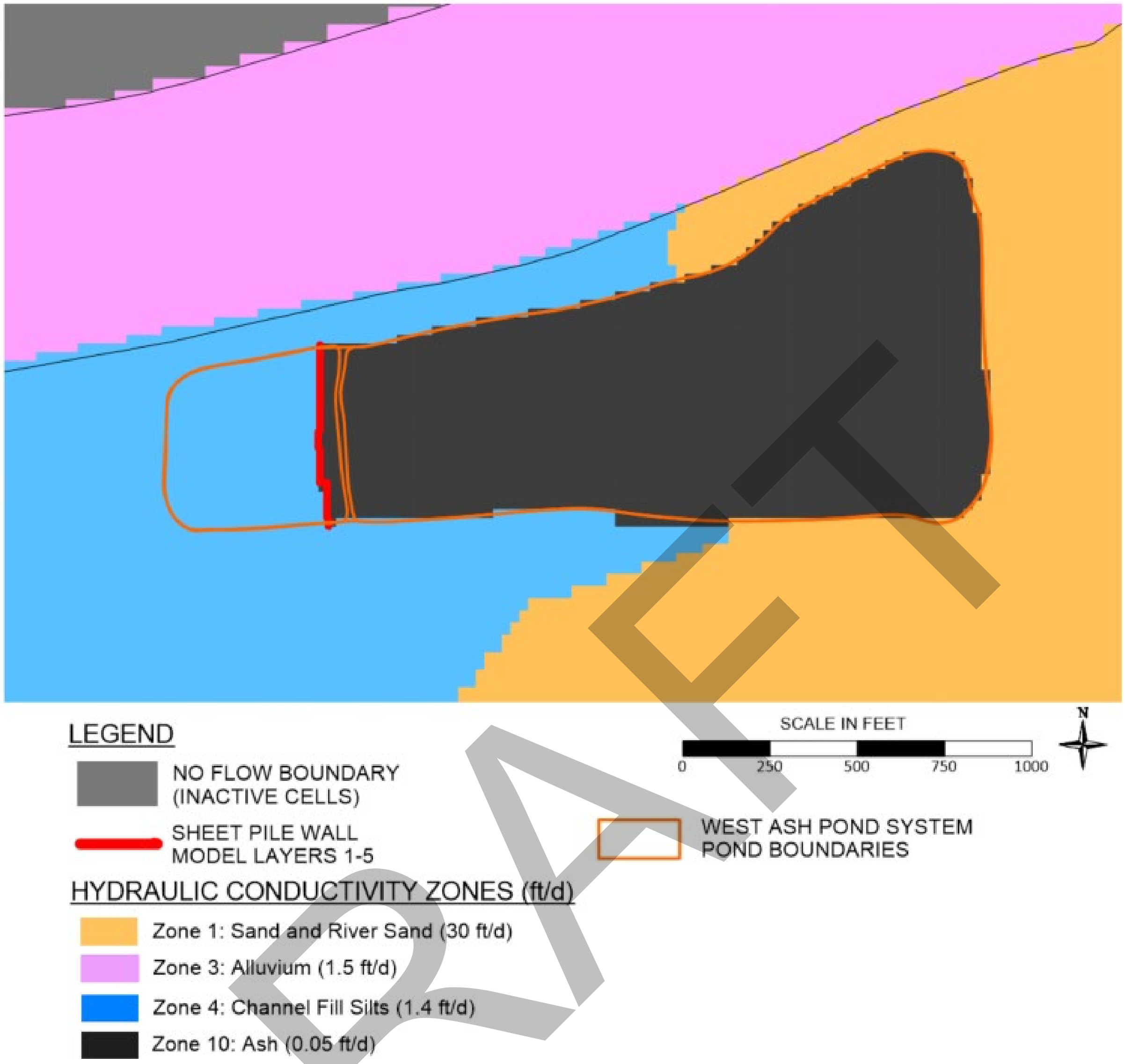

BOUNDARY CONDITIONS AND HYDRAULIC CONDUCTIVITY (K) ZONES
MODEL LAYER 1, STRESS PERIOD 3

GROUNDWATER MODELING TECHNICAL MEMORANDUM
WEST ASH POND SYSTEM
HENNEPIN POWER PLANT
HENNEPIN, ILLINOIS

FIGURE 2-9

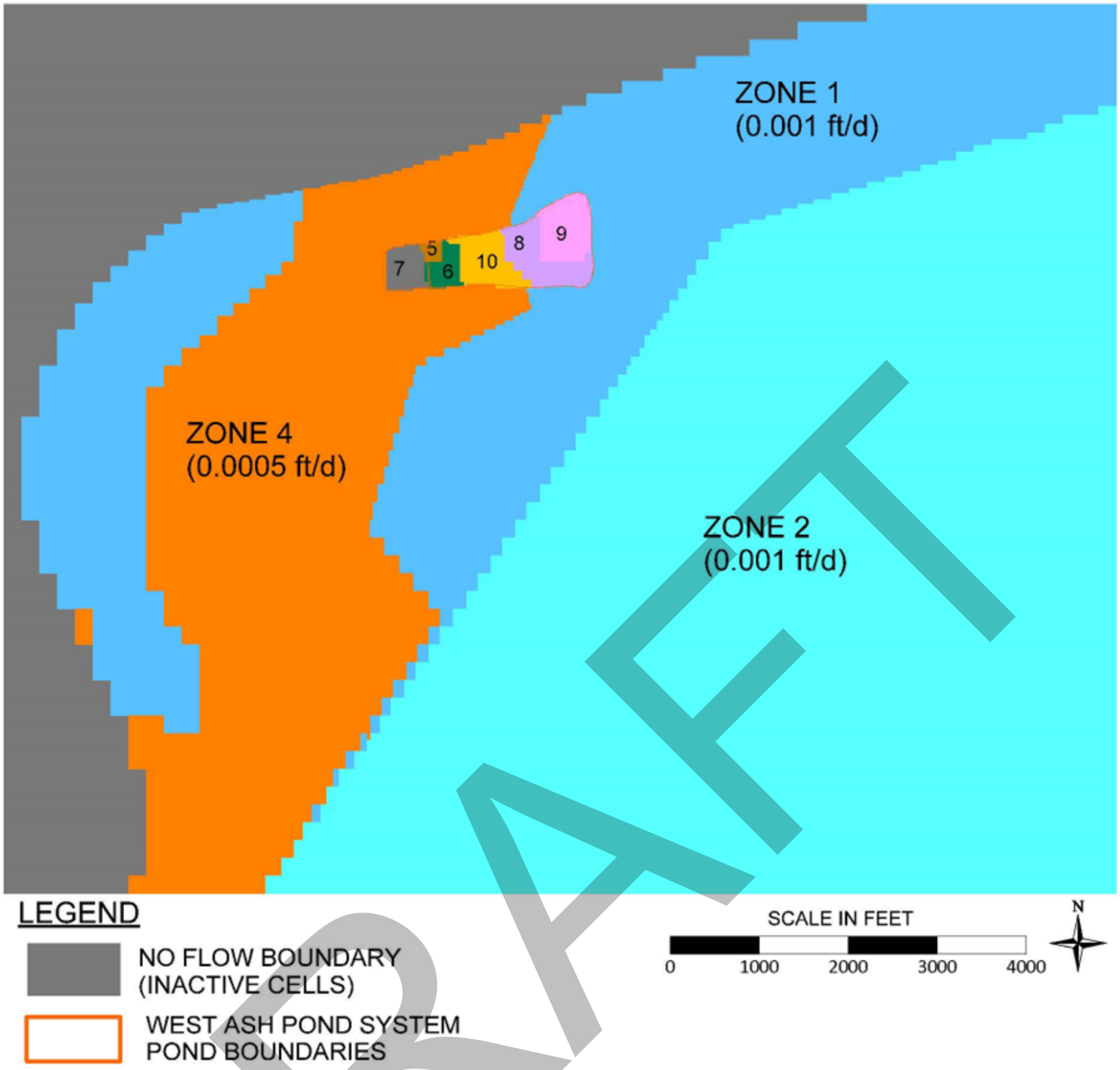

RECHARGE ZONES (ft/d) WITH BORON [mg/L] marked on map

Model Recharge	ft/d	in/yr	Boron Concentration (mg/L)
Sand & River Sand (Zone 1)	1.0E-03	4.4	
Outwash Gravel (Zone 2)	1.0E-03	4.4	
Channel Fill Silts (Zone 4)	5.0E-04	2.2	
Ash-Pond 1 (Zone 9)	3.8E-03	16.8	9.0
Ash-Pond 3 East (Zone 8)	4.0E-02	175.2	9.0
Ash-Pond 3 Center (Zone 10)	2.7E-02	118.3	9.0
Ash-Pond 3 West (Zone 6)	2.7E-02	118.3	19.0
Ash-Pond 3 Northwest (Zone 5)	2.7E-02	118.3	7.0
Ash-Secondary Pond (Zone 7)	2.0E-02	87.6	7.0

Note: Constant-concentration boundaries specified in model layer 1 are consistent with boron recharge values.

MODEL RECHARGE, STEADY-STATE FLOW MODEL / TRANSPORT MODEL

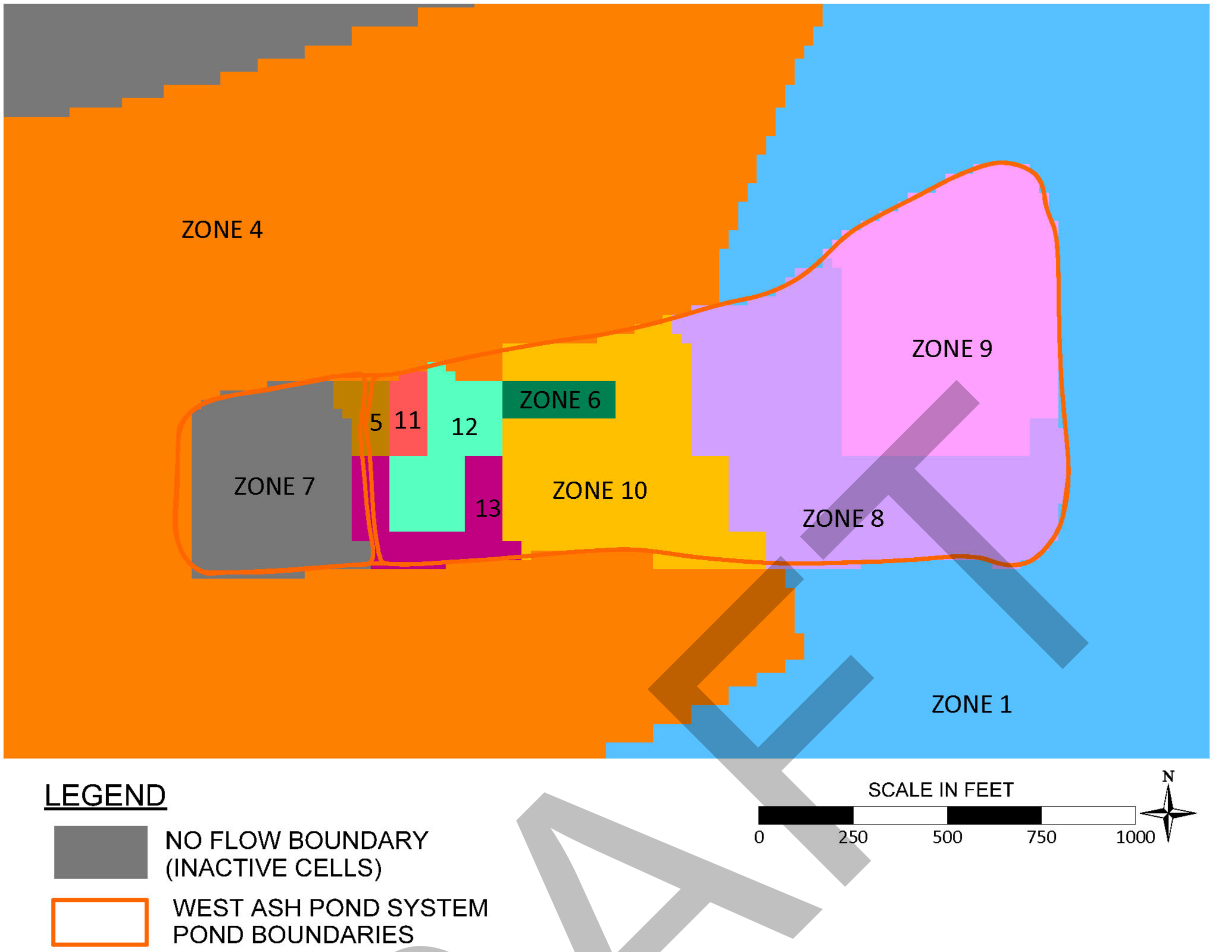

RECHARGE ZONES (ft/d) WITH BORON [mg/L] marked on map

Model Recharge	ft/d	in/yr	**Boron Concentration (mg/L)**
Sand & River Sand (Zone 1)	1.0E-03	4.4	
Outwash Gravel (Zone 2)	1.0E-03	4.4	
Channel Fill Silts (Zone 4)	5.0E-04	2.2	
Ash-Pond 1 (Zone 9)	3.8E-03	16.8	9.0
Ash-Pond 3 East (Zone 8)	2.0E-02	87.6	9.0
Ash-Pond 3 Center (Zone 10)	2.0E-02	87.6	9.0
Ash-Pond 3 Center (Zone 6)	2.0E-02	87.6	9.0
Ash-Pond 3 West (Zone 12)	2.0E-02	87.6	19.0
Ash-Pond 3 West (Zone 13)	2.0E-02	87.6	19.0
Ash-Pond 3 Northwest (Zone 5)	2.0E-02	87.6	7.0
Ash-Pond 3 Northwest (Zone 11)	2.0E-02	87.6	9.0
Ash-Old West Polishing Pond (Zone 7)	2.0E-02	87.6	7.0

Note: Constant-concentration boundaries specified in model layer 1 are consistent with boron recharge values.

MODEL RECHARGE, TRANSIENT MODEL STRESS PERIOD 1

FIGURE 2-11

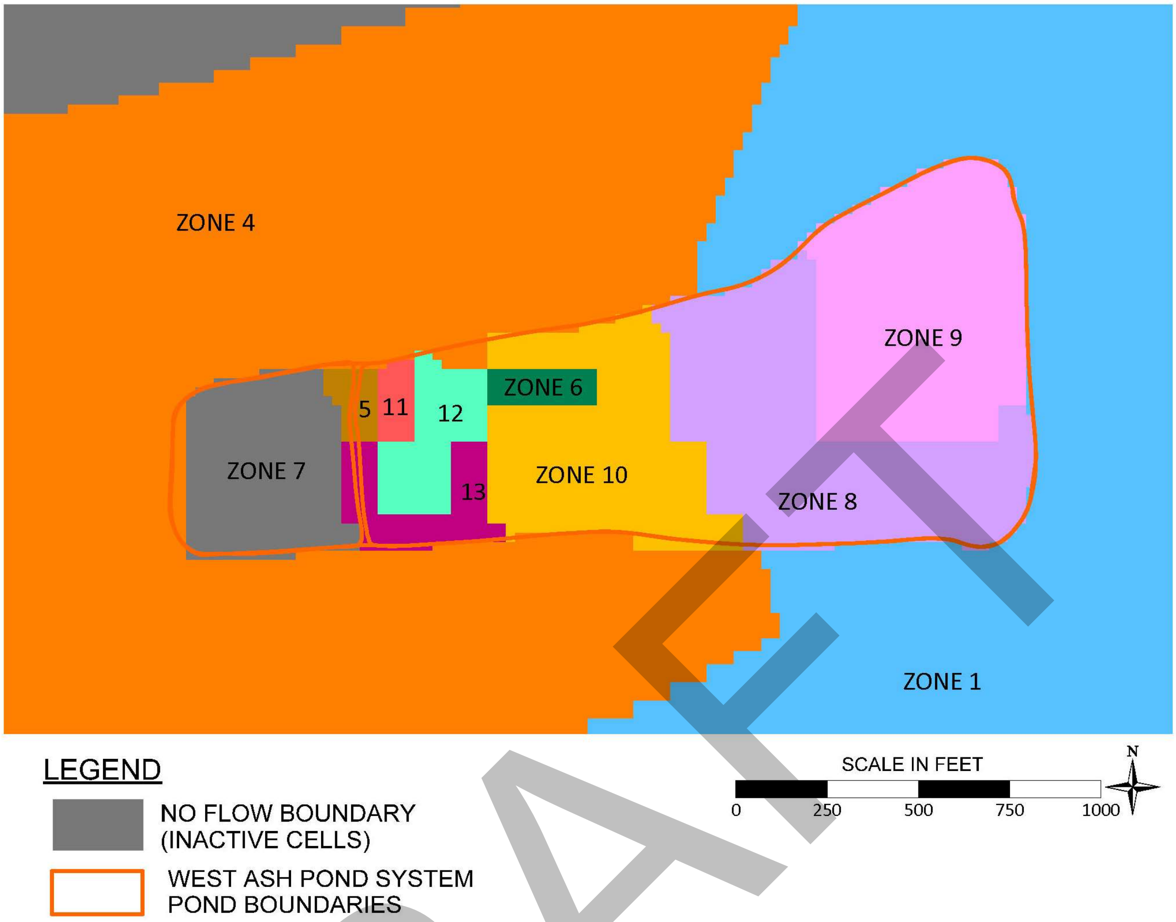

RECHARGE ZONES (ft/d) WITH BORON [mg/L] marked on map

Model Recharge	ft/d	in/yr	**Boron Concentration (mg/L)**
Sand & River Sand (Zone 1)	1.0E-03	4.4	
Outwash Gravel (Zone 2)	1.0E-03	4.4	
Channel Fill Silts (Zone 4)	5.0E-04	2.2	
Ash-Pond 1 (Zone 9)	3.8E-03	16.8	9.0
Ash-Pond 3 East (Zone 8)	3.0E-03	13.0	9.0
Ash-Pond 3 Center (Zone 10)	3.0E-03	13.0	9.0
Ash-Pond 3 Center (Zone 6)	2.0E-02	87.6	9.0
Ash-Pond 3 West (Zone 12)	2.0E-02	87.6	19.0
Ash-Pond 3 West (Zone 13)	3.0E-03	13.0	19.0
Ash-Pond 3 Northwest (Zone 5)	3.0E-03	13.0	7.0
Ash-Pond 3 Northwest (Zone 11)	2.0E-02	87.6	9.0
Ash-Old West Polishing Pond (Zone 7)	3.0E-03	13.0	7.0

Note: Constant-concentration boundaries specified in model layer 1 are consistent with boron recharge values.

MODEL RECHARGE, TRANSIENT MODEL STRESS PERIOD 2

GROUNDWATER MODELING TECHNICAL MEMORANDUM
WEST ASH POND SYSTEM
HENNEPIN POWER PLANT
HENNEPIN, ILLINOIS

RAMBOLL

FIGURE 2-12

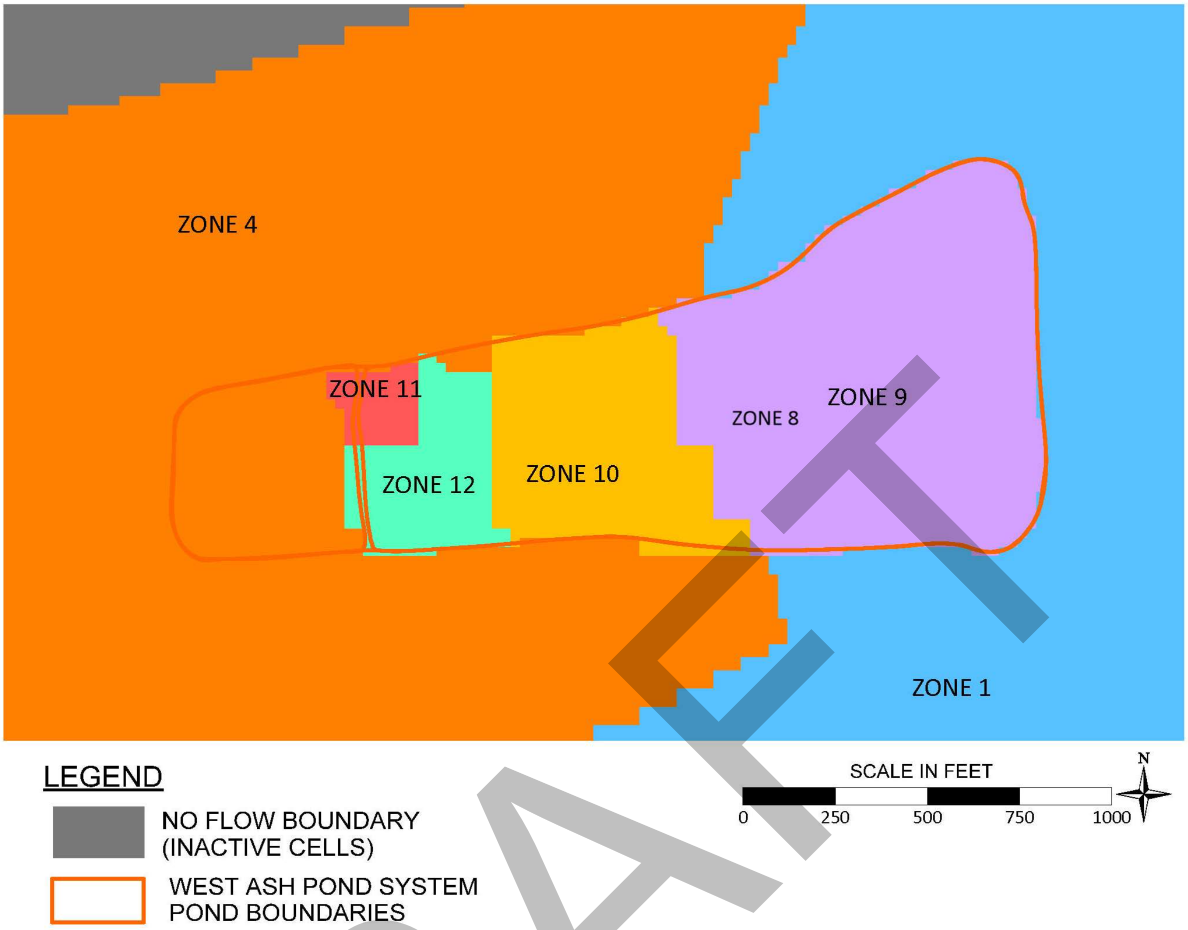

RECHARGE ZONES (ft/d) WITH BORON [mg/L] marked on map

Model Recharge	ft/d	in/yr	**Boron Concentration (mg/L)**
Sand & River Sand (Zone 1)	1.0E-03	4.4	
Outwash Gravel (Zone 2)	1.0E-03	4.4	
Channel Fill Silts (Zone 4)	5.0E-04	2.2	
Ash-Pond 3 East (Zone 8)	5.6E-07	0.0	9.0
Ash-Pond 3 Center (Zone 10)	5.6E-07	0.0	9.0
Ash-Pond 3 West (Zone 12)	5.6E-07	0.0	19.0
Ash-Pond 3 Northwest (Zone 11)	5.6E-07	0.0	7.0

Note: Constant-concentration boundaries specified in model layer 1 are consistent with boron recharge values.

MODEL RECHARGE, TRANSIENT MODEL STRESS PERIOD 3
GROUNDWATER MODELING TECHNICAL MEMORANDUM
WEST ASH POND SYSTEM
HENNEPIN POWER PLANT
HENNEPIN, ILLINOIS

RAMBOLL

Figure 2-13

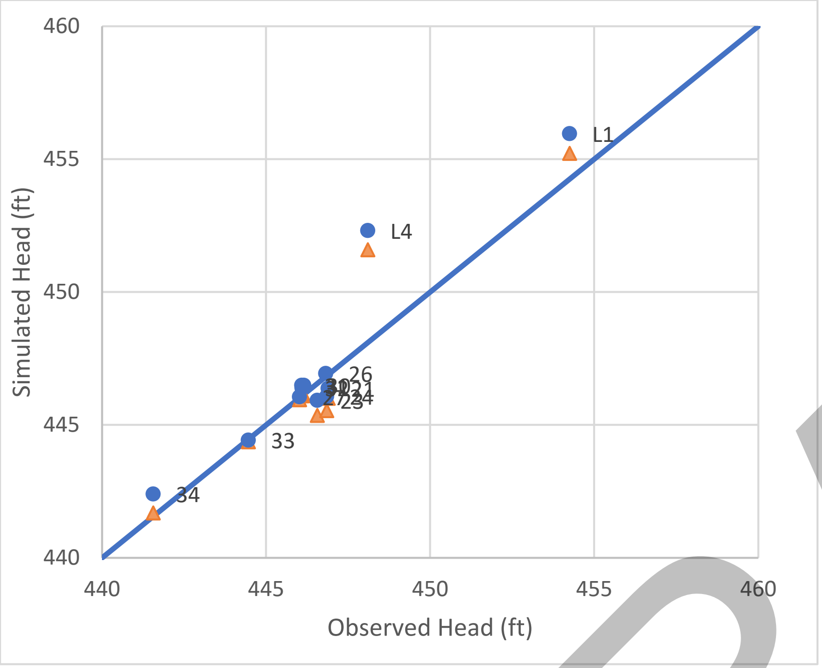

Flow Model Observed vs Simulated Heads

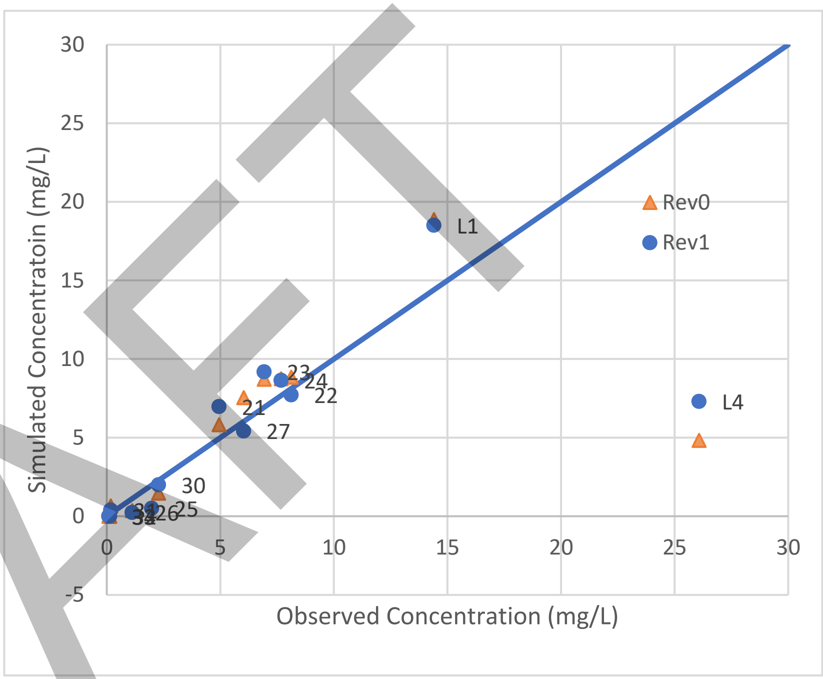

Transport Model Observed vs Simulated Boron Concentrations

Notes:

1. The steady-state flow model and paired transport model were calibrated using data collected from 1994-1996, summarized as 1996.

2. Calibration targets (heads and boron concentrations) were preserved from the 2017 model update (Rev0) for this model revision (Rev1)
3. Plots show the 1:1 line for reference (equivalent observed and simulated)

CALIBRATION PLOTS: STEADY-STATE FLOW MODEL / TRANSPORT MODEL
GROUNDWATER MODELING TECHNICAL MEMORANDUM

WEST ASH POND SYSTEM
HENNEPIN POWER PLANT
HENNEPIN, ILLINOIS

RAMBOLL

FIGURE 2-14

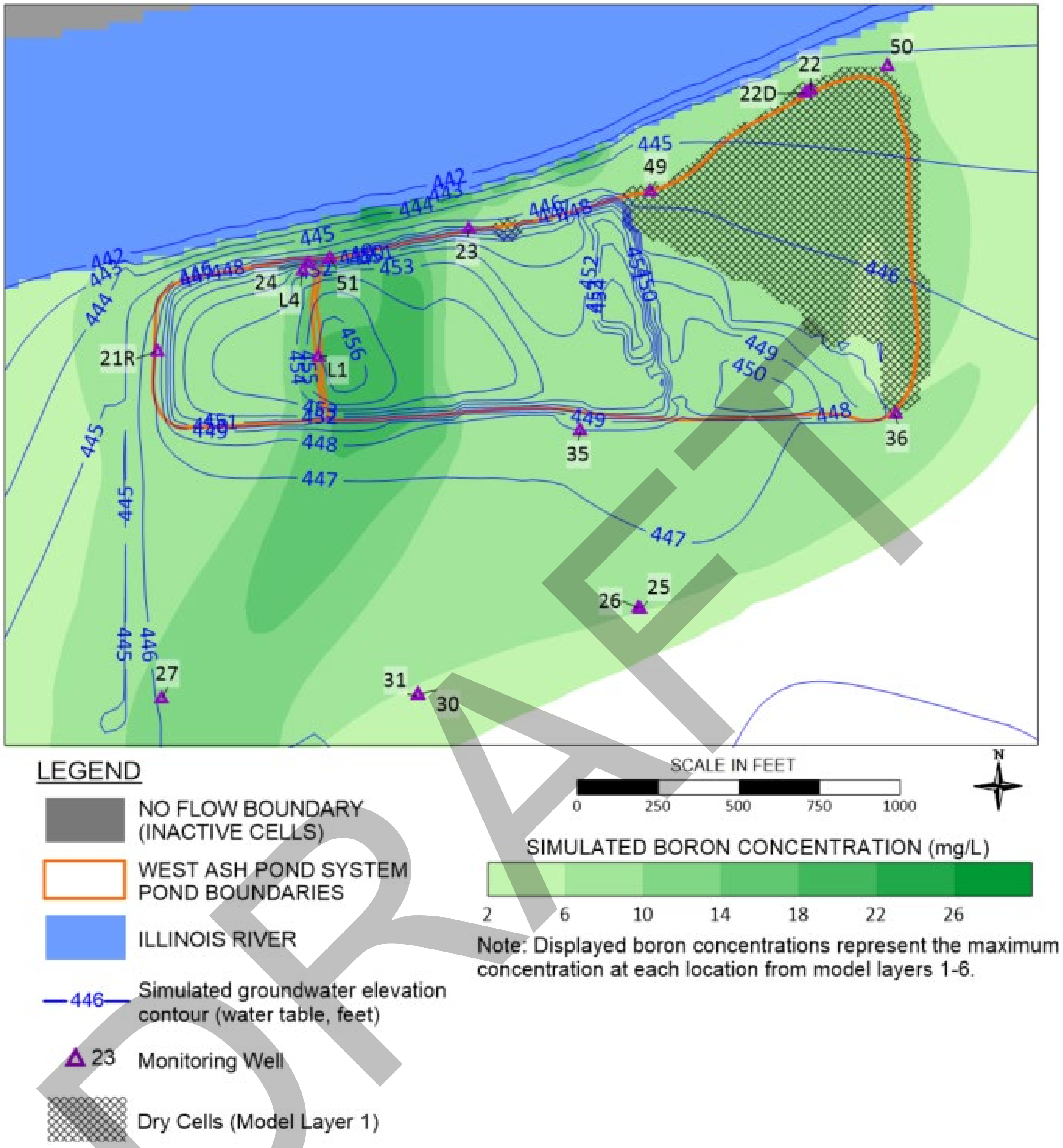

Note: Displayed boron concentrations represent the maximum concentration at each location from model layers 1-6.

SIMULATED GROUNDWATER ELEVATIONS AND BORON CONCENTRATIONS, STEADY-STATE FLOW MODEL / TRANSPORT MODEL (1996)
GROUNDWATER MODELING TECHNICAL MEMORANDUM
WEST ASH POND SYSTEM
HENNEPIN POWER PLANT
HENNEPIN, ILLINOIS

RAMBOLL

Figure 2-15

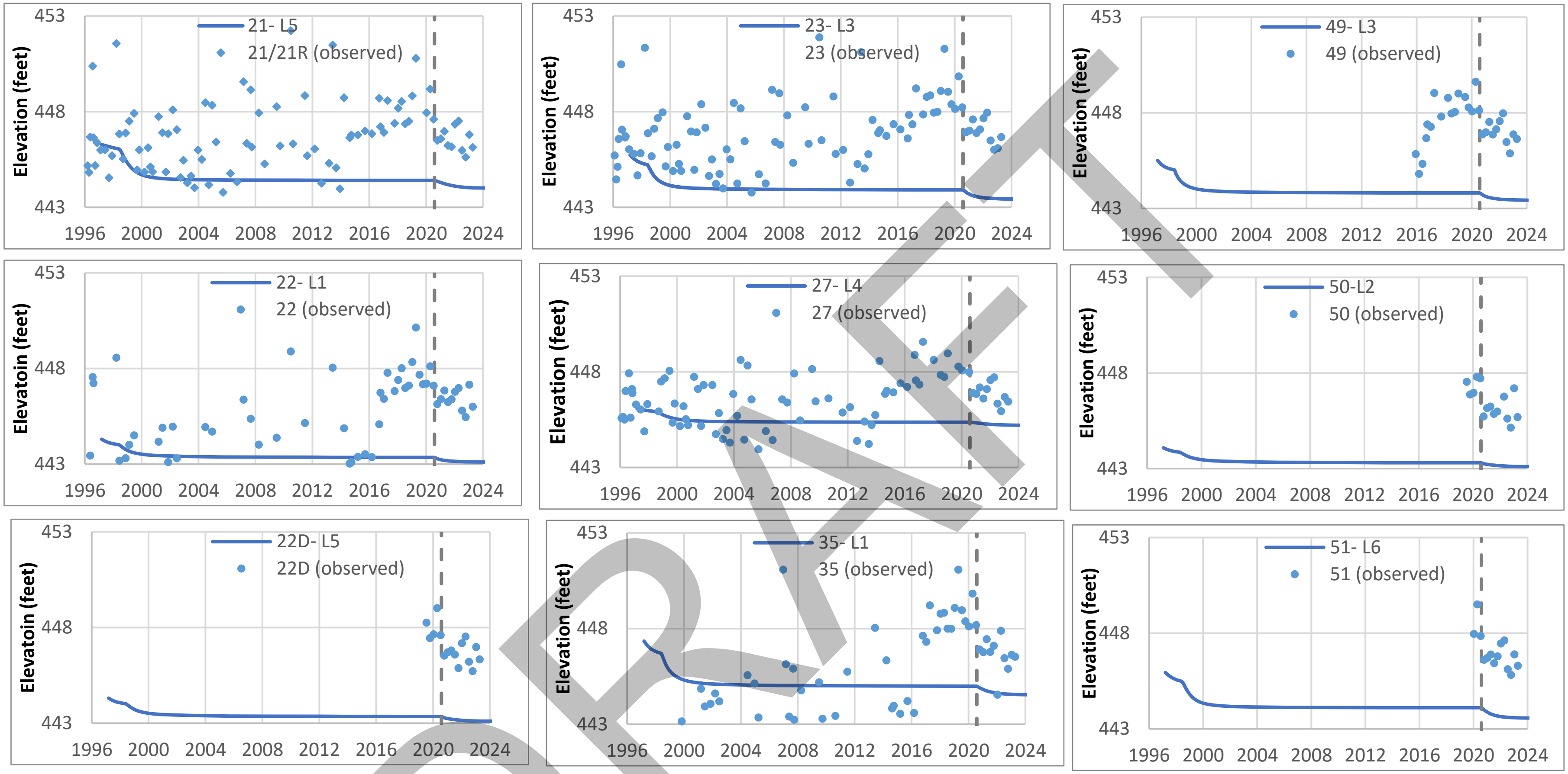

TRANSIENT FLOW MODEL CALIBRATION: OBSERVED VS SIMULATED HEADS (1997-2023)

GROUNDWATER MODELING TECHNICAL MEMORANDUM
WEST ASH POND SYSTEM
HENNEPIN POWER PLANT
HENNEPIN, ILLINOIS

RAMBOLL

Figure 2-16

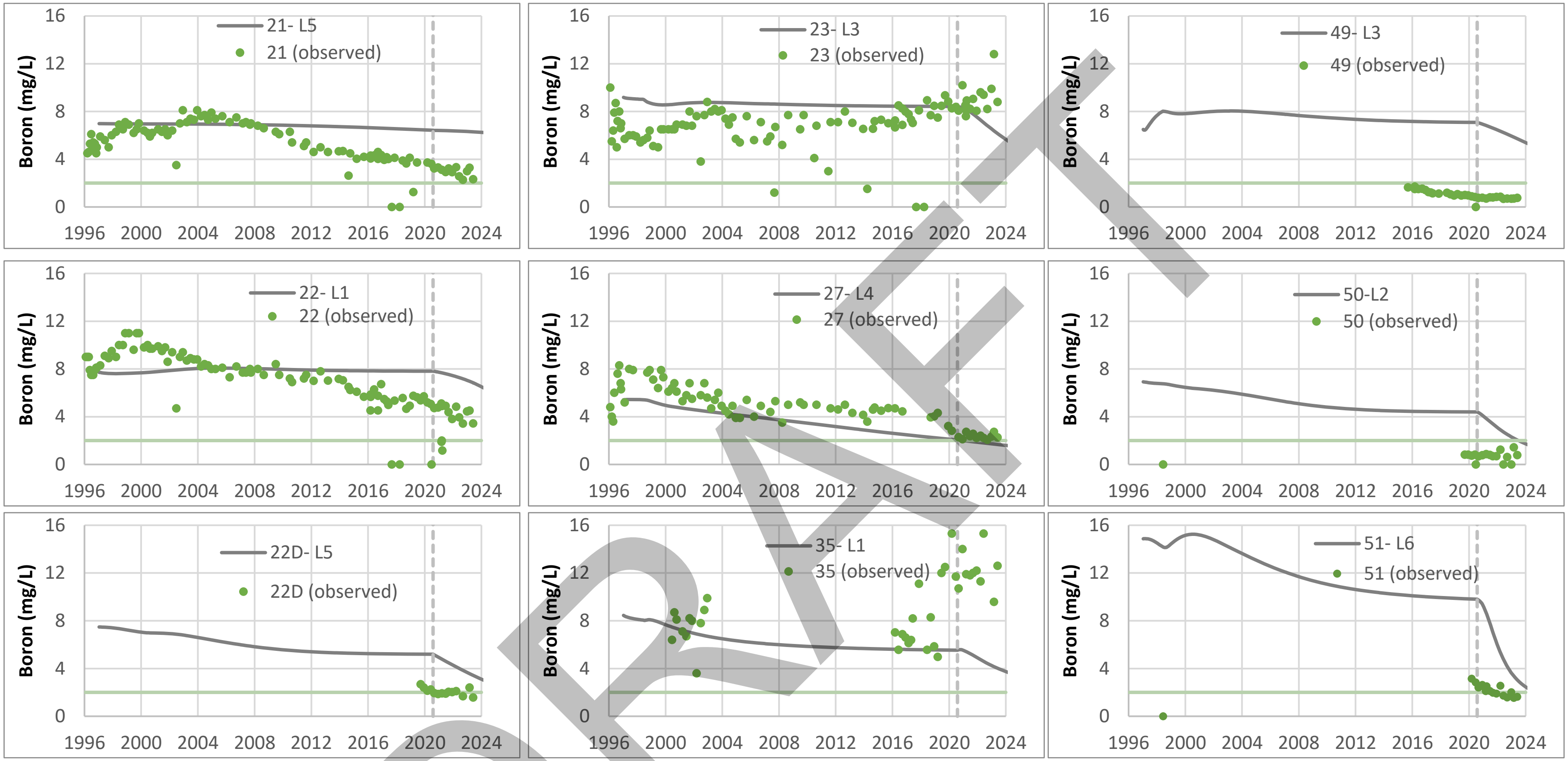

TRANSIENT TRANSPORT MODEL CALIBRATION: OBSERVED VS SIMULATED BORON CONCENTRATIONS (1997-2023)

GROUNDWATER MODELING TECHNICAL MEMORANDUM
WEST ASH POND SYSTEM
HENNEPIN POWER PLANT
HENNEPIN, ILLINOIS

FIGURE 3-1

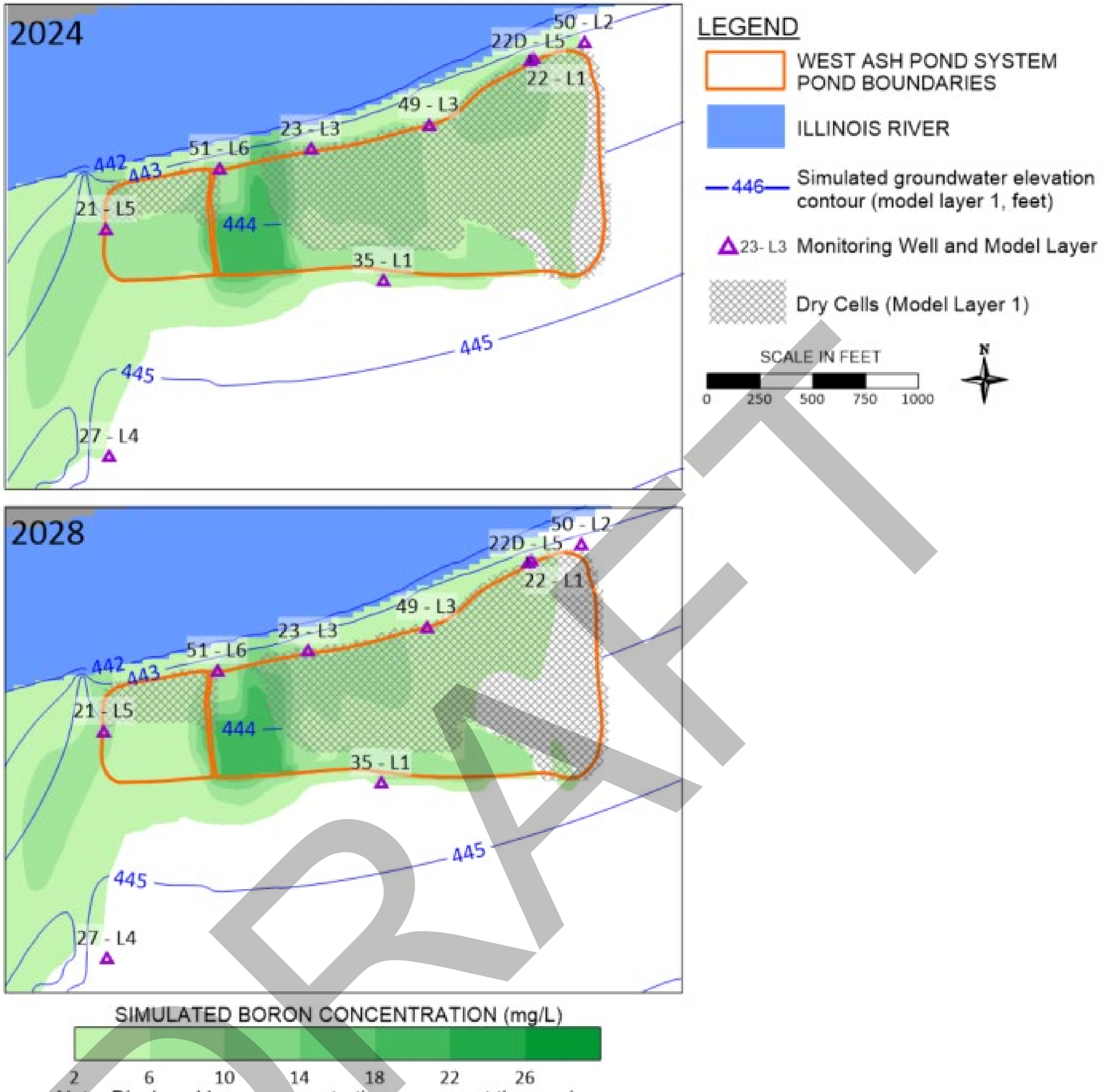

Note: Displayed boron concentrations represent the maximum concentration at each location from model layers 1-6.

SIMULATED GROUNDWATER ELEVATIONS AND BORON CONCENTRATIONS, 2024 and 2028

GROUNDWATER MODELING TECHNICAL MEMORANDUM
WEST ASH POND SYSTEM
HENNEPIN POWER PLANT
HENNEPIN, ILLINOIS

FIGURE 3-2

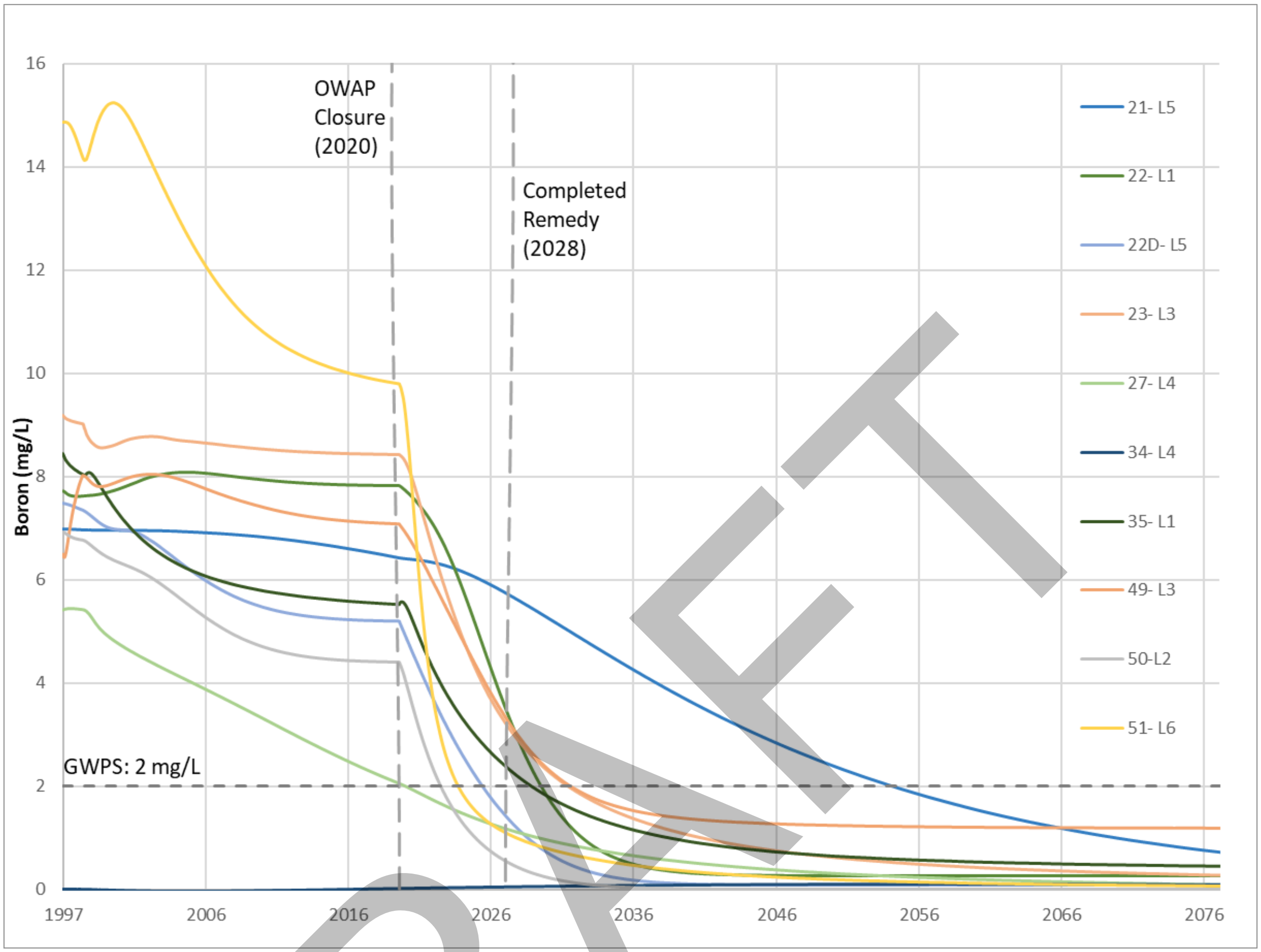

Concentrations of Boron at Site Monitoring Wells, Groundwater Polishing (GWP)

Notes

Concentrations were simulated through 2228, however the chart is truncated at 2078 (50 years following remedy completion) due to decrease of concentrations below GWPS by that time.

SIMULATED BORON CONCENTRATIONS AT COMPLIANCE MONITORING WELLS:
ALTERNATIVE 1 (GWP)

GROUNDWATER MODELING TECHNICAL MEMORANDUM
WEST ASH POND SYSTEM
HENNEPIN POWER STATION
HENNEPIN, ILLINOIS

RAMBOLL

FIGURE 3-3

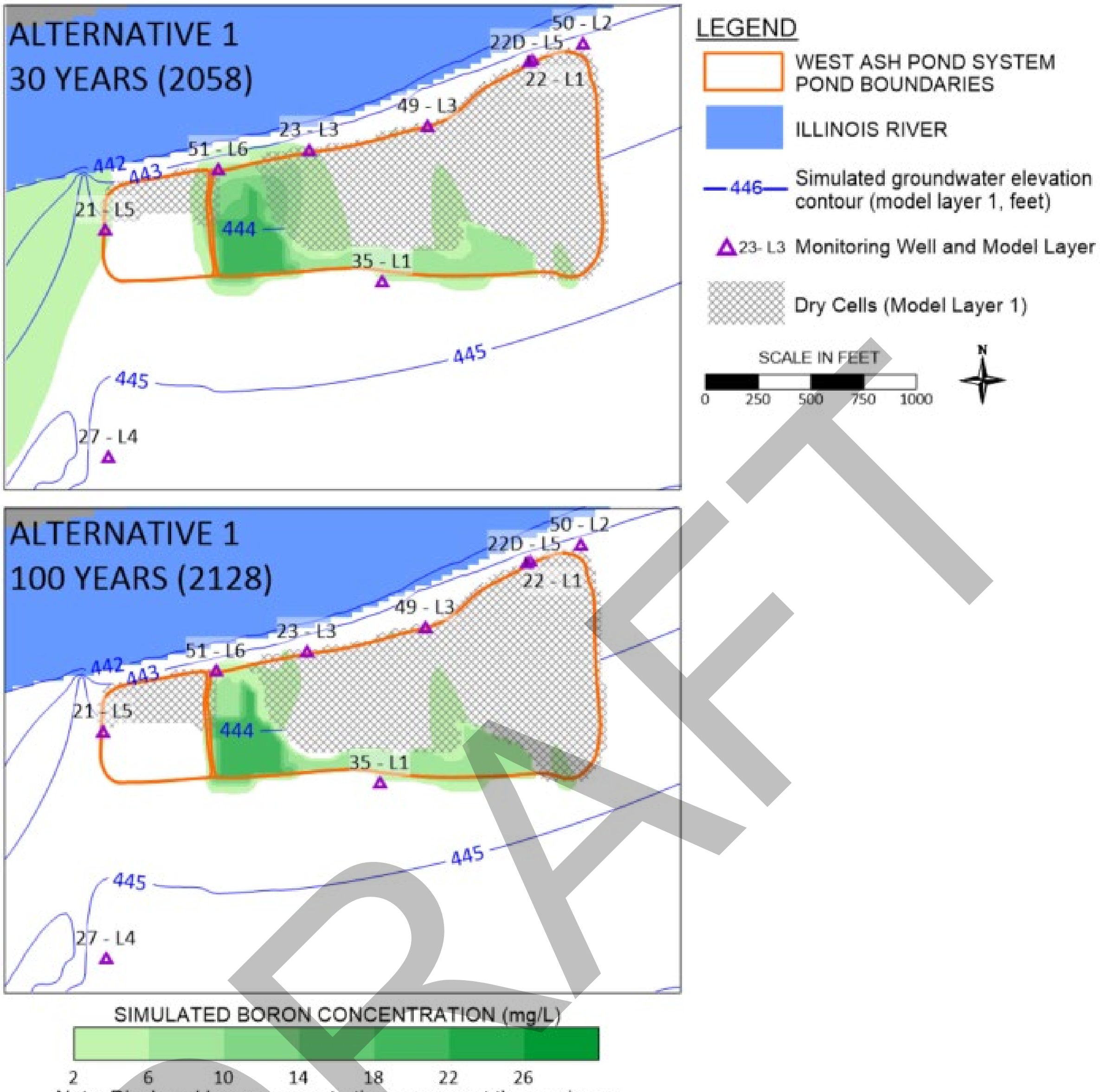

Note: Displayed boron concentrations represent the maximum concentration at each location from model layers 1-6.

SIMULATED BORON CONCENTRATIONS, 30 AND 100 YEARS, ALTERNATIVE 1 (GWP)

GROUNDWATER MODELING TECHNICAL MEMORANDUM
WEST ASH POND SYSTEM
HENNEPIN POWER PLANT
HENNEPIN, ILLINOIS

RAMBOLL

FIGURE 3-4

Concentrations of Boron at Site Monitoring Wells, Alternative 2a (Full-Depth Cutoff Wall)

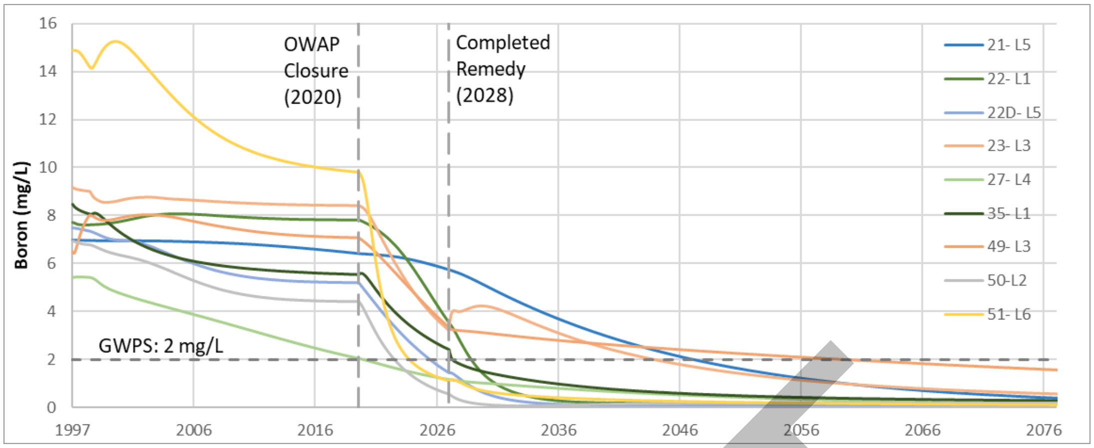

Concentrations of Boron at Site Monitoring Wells, Alternative 2b (Partial-Depth Cutoff Wall)

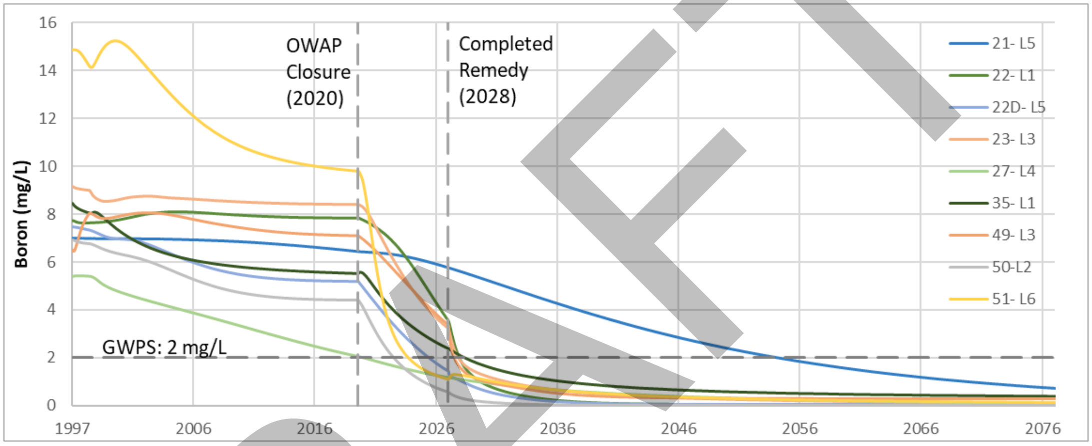

Concentrations of Boron at Site Monitoring Wells, Alternative 2a (Shallow Cutoff Wall)

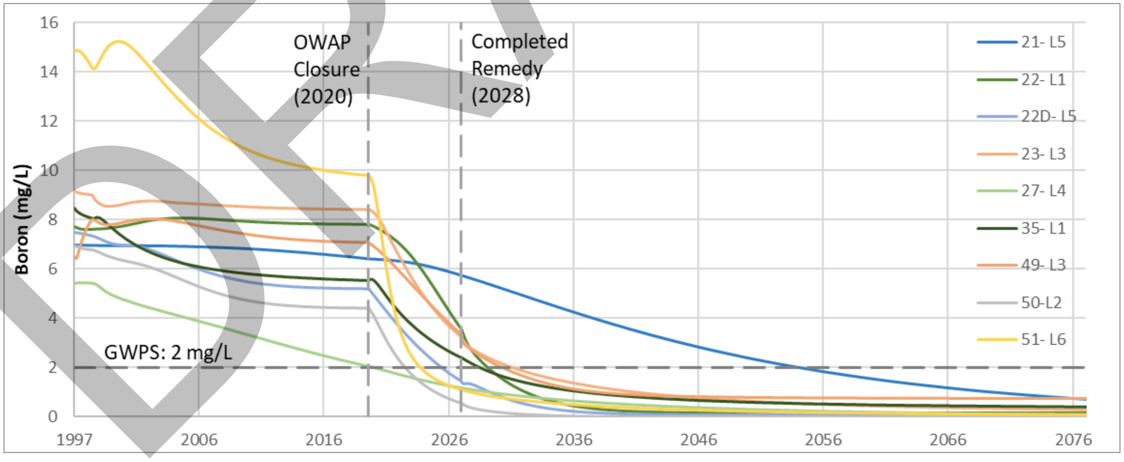

Notes

Concentrations were simulated through 2228, however the chart is truncated at 2078 (50 years following remedy completion) due to decrease of concentrations below GWPS by that time.

SIMULATED BORON CONCENTRATIONS AT COMPLIANCE MONITORING WELLS:
ALTERNATIVES 2a, 2b, 2c (CUTOFF WALLS)

GROUNDWATER MODELING TECHNICAL MEMORANDUM
WEST ASH POND SYSTEM
HENNEPIN POWER PLANT
HENNEPIN, ILLINOIS

FIGURE 3-5

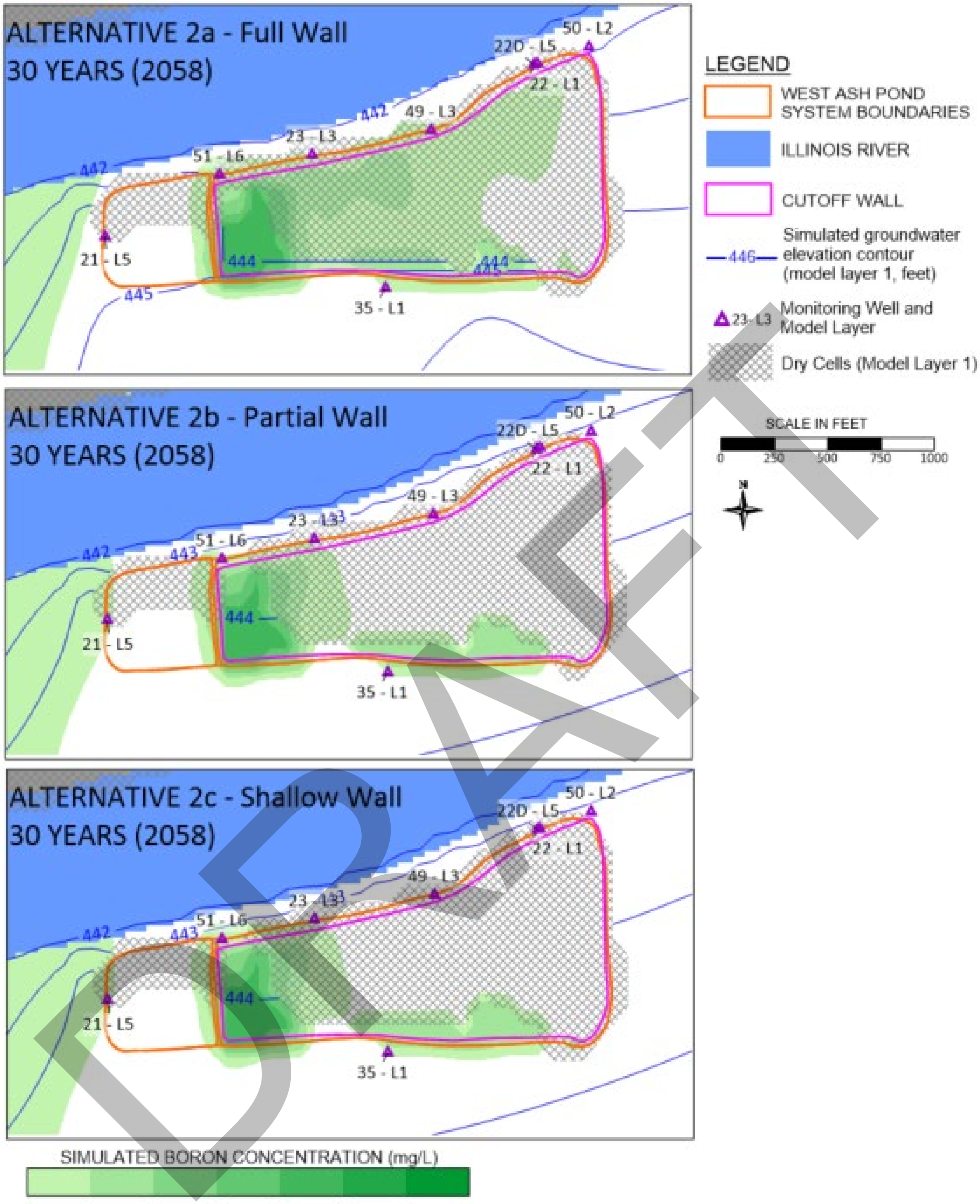

Note: Displayed boron concentrations represent the maximum concentration at each location from model layers 1-6.

SIMULATED BORON CONCENTRATIONS, 30 YEARS: ALTERNATIVES 2a, 2b, 2c
(CUTOFF WALLS)

GROUNDWATER MODELING TECHNICAL MEMORANDUM
WEST ASH POND SYSTEM
HENNEPIN POWER PLANT
HENNEPIN, ILLINOIS

FIGURE 3-6

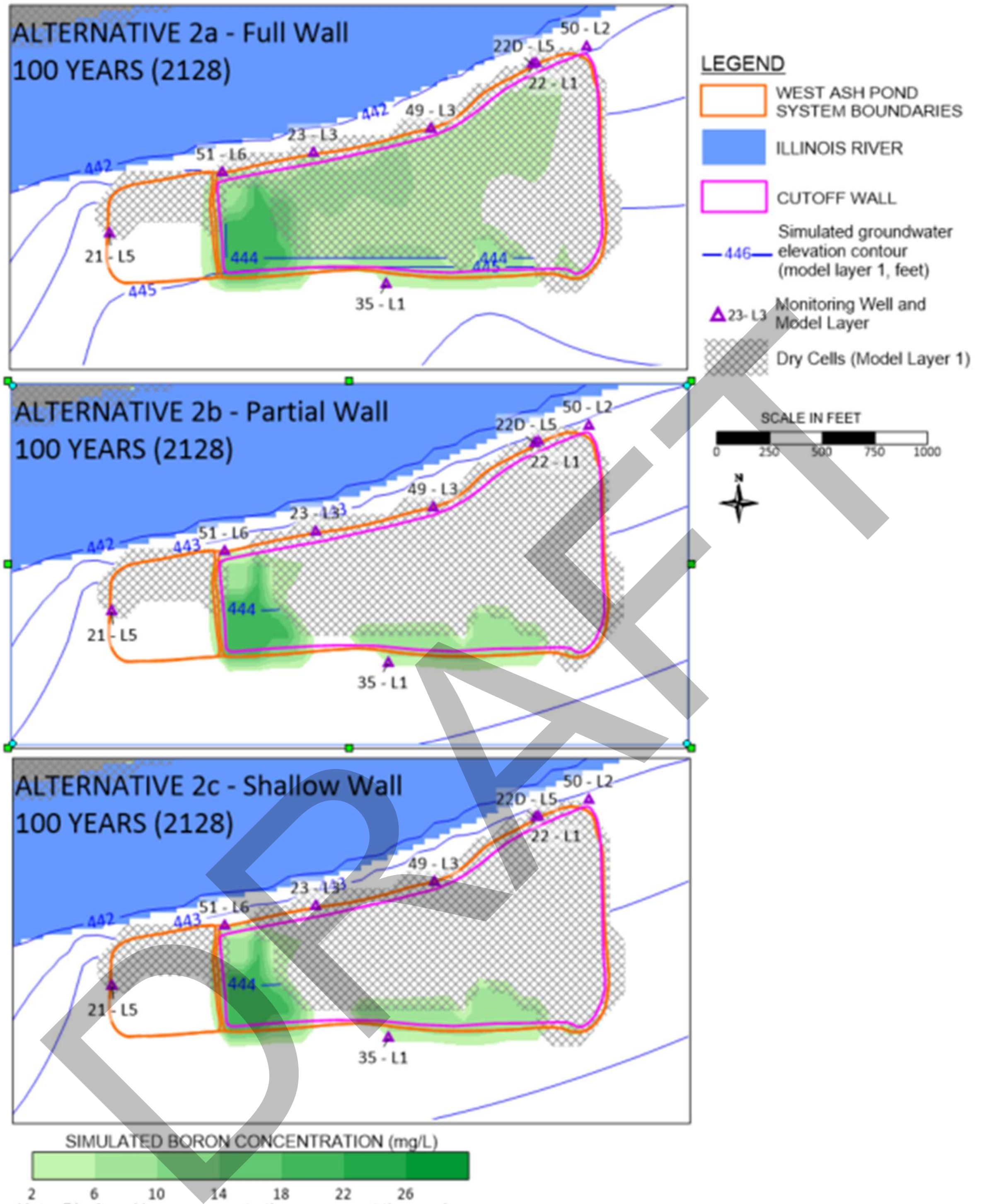

Note: Displayed boron concentrations represent the maximum concentration at each location from model layers 1-6.

SIMULATED BORON CONCENTRATIONS, 100 YEARS: ALTERNATIVES 2a, 2b, 2c (CUTOFF WALLS)

GROUNDWATER MODELING TECHNICAL MEMORANDUM
WEST ASH POND SYSTEM
HENNEPIN POWER PLANT
HENNEPIN, ILLINOIS

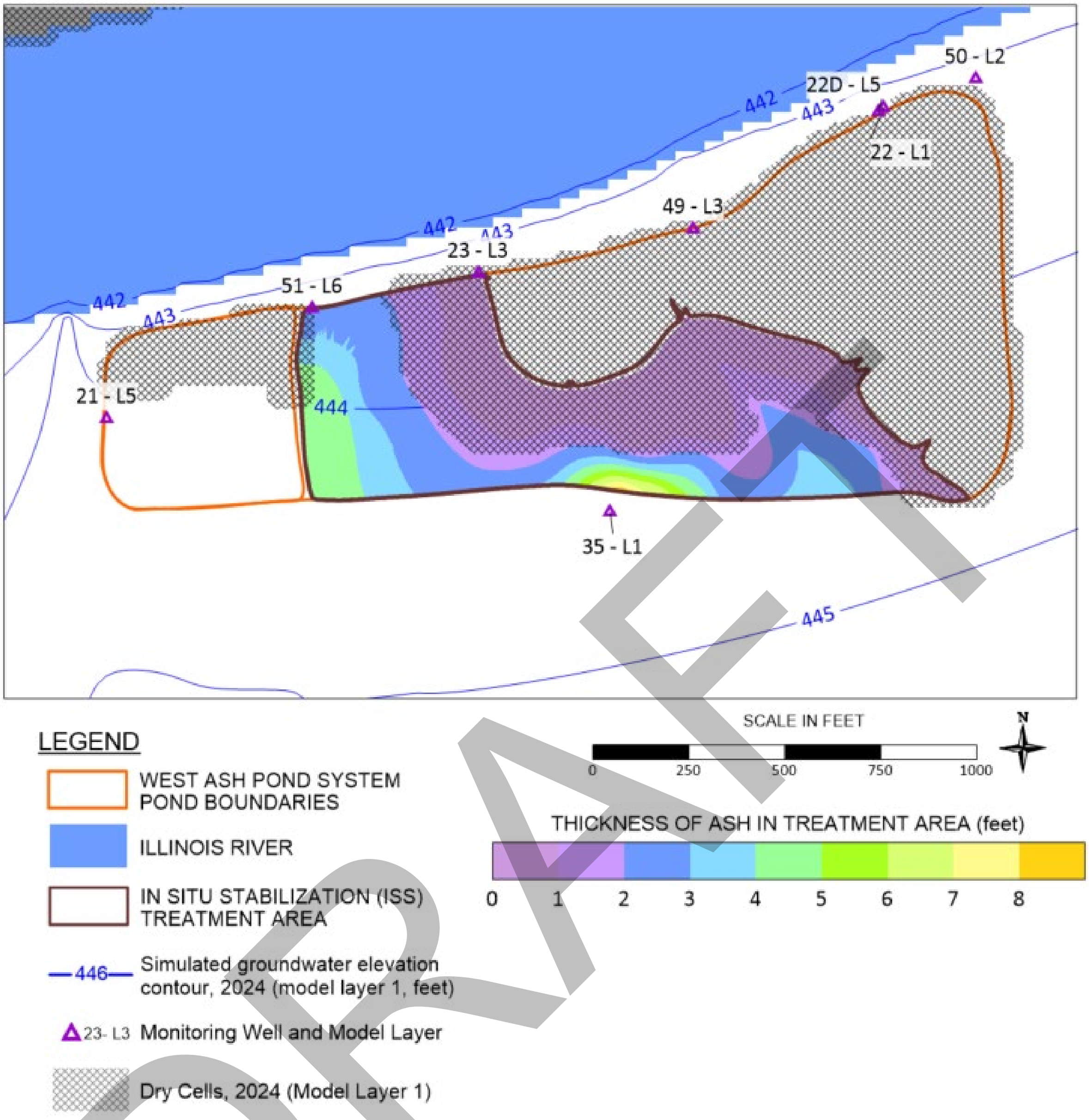

ISS TREATMENT AREA
GROUNDWATER MODELING TECHNICAL MEMORANDUM
WEST ASH POND SYSTEM
HENNEPIN POWER PLANT
HENNEPIN, ILLINOIS

Concentrations of Boron at Site Monitoring Wells, In-Situ Stabilization (ISS)

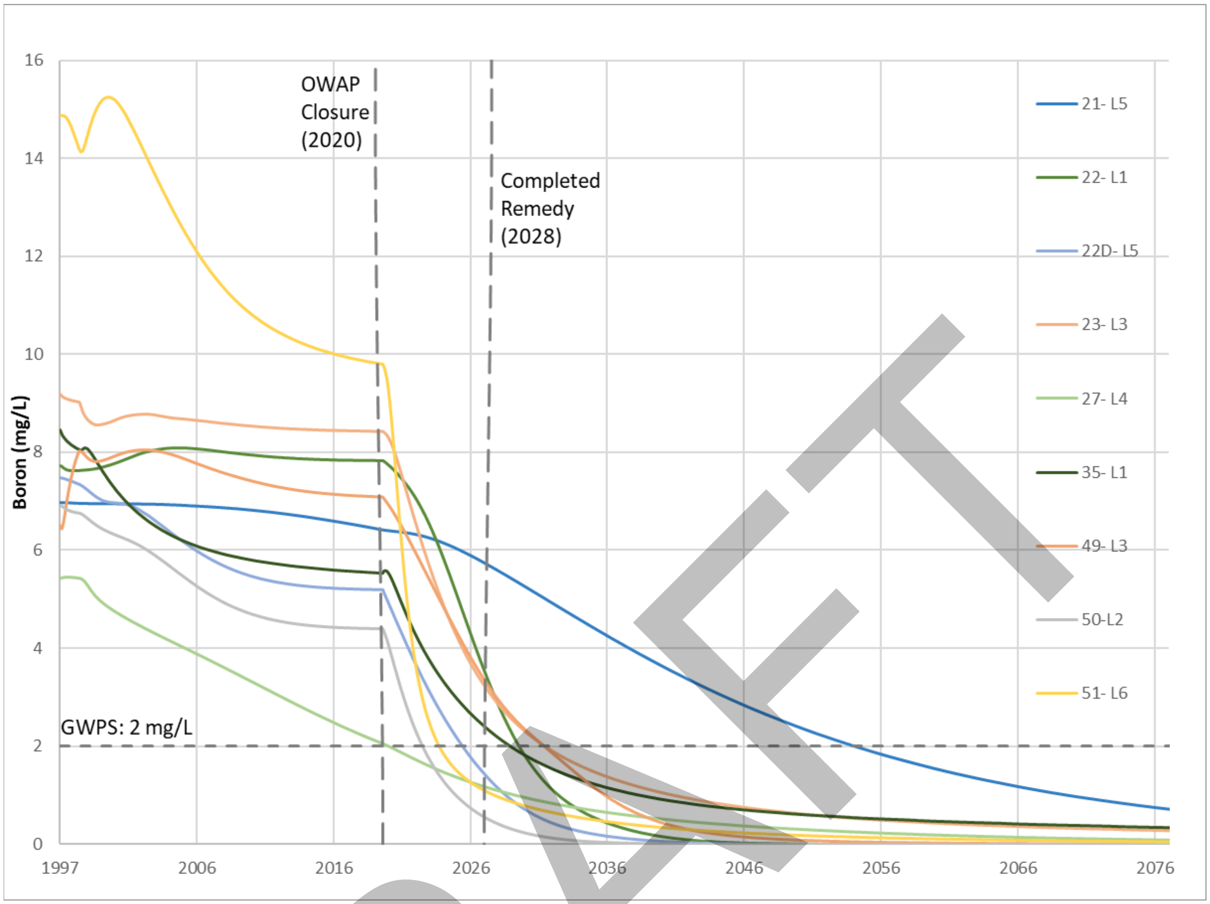

Notes

Concentrations were simulated through 2228, however the chart is truncated at 2078 (50 years following remedy completion) due to decrease of concentrations below GWPS by that time.

SIMULATED BORON CONCENTRATIONS AT COMPLIANCE MONITORING WELLS: ALTERNATIVE 3 (ISS)

GROUNDWATER MODELING TECHNICAL MEMORANDUM
WEST ASH POND SYSTEM
HENNEPIN POWER PLANT
HENNEPIN, ILLINOIS

FIGURE 3-9

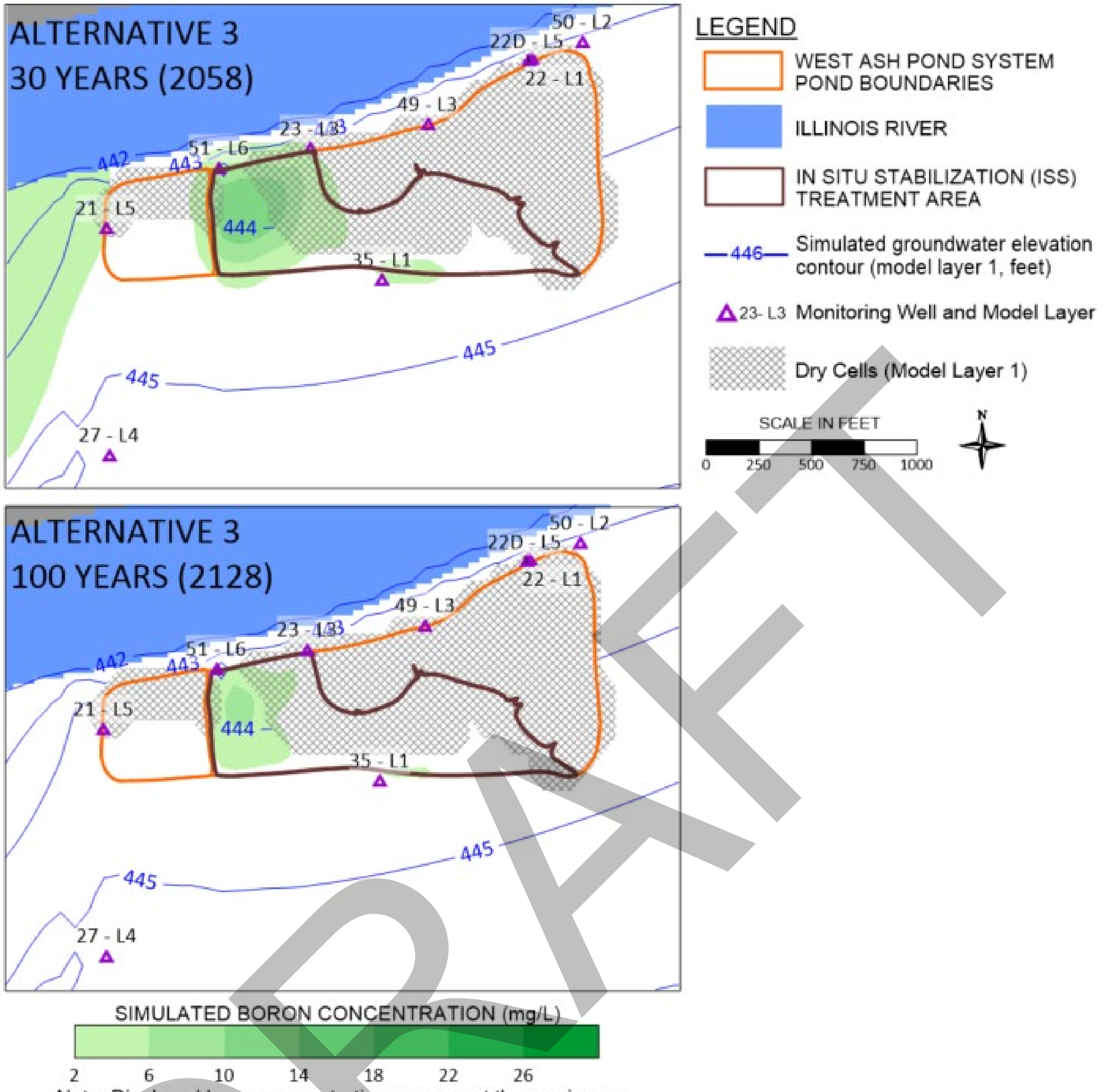

Note: Displayed boron concentrations represent the maximum concentration at each location from model layers 1-6.

SIMULATED BORON CONCENTRATIONS, 30 AND 100 YEARS: ALTERNATIVE 3 (ISS)

GROUNDWATER MODELING TECHNICAL MEMORANDUM
WEST ASH POND SYSTEM
HENNEPIN POWER PLANT
HENNEPIN, ILLINOIS

RAMBOLL

APPENDIX A
MODFLOW AND MT3DMS MODELING FILES

(ELECTRONIC ONLY)

APPENDIX B2
GROUNDWATER MODEL REPORT

OBG

Groundwater Model Report

Hennepin West Ash Pond System

Hennepin, Illinois

Dynegy Midwest Generation, LLC

FINAL

December 20, 2017

Natural Resource Technology

AN OBG COMPANY

HENNEPIN WEST ASH POND SYSTEM | GROUNDWATER MODEL REPORT

DECEMBER 20, 2017 | FINAL | PROJECT #2413

Groundwater Model Report

Hennepin West Ash Pond System
Hennepin, Illinois

Prepared for:

Dynegy Midwest Generation, LLC
1500 Eastport Plaza Drive
Collinsville, IL 62234

STUART J. CRAVENS, PG
Principal Hydrogeologist

MENG WANG, PHD, PE
Data Innovation Engineer

TABLE OF CONTENTS

LIST OF TABLES

LIST OF FIGURES

LIST OF APPENDICES

ACRONYMS AND ABBREVIATIONS

CCR	coal combustion residual
CEC	Civil & Environmental Consultants, Inc.
WAPC	West Ash Pond Complex
DMG	Dynegy Midwest Generation, LLC
in/yr	inches per year
ft	feet
HELP	Hydrologic Evaluation of Landfill Performance
IAC	Illinois Administrative Code
IDNR	Illinois Department of Natural Resources
K_d	distribution coefficient
mg/L	milligrams per liter
mL/g	milliliters per gram
MW	megawatt
NRT	Natural Resource Technology, an OBG Company
WMA	Wildlife Management Area
yr	year

1 INTRODUCTION

1.1 OVERVIEW

This Groundwater Model Report has been prepared by Natural Resource Technology (NRT), an OBG company, on behalf of Dynegy Midwest Generation, LLC (DMG) to document the impact of proposed capping system for closure of the West Ash Pond Complex (WAPC) at the Hennepin Power Station, Hennepin, Illinois (Figure 1-1). The WAPS is located in the northeast quarter of Section 27, Township 33 North, Range 2 West, Putnam County, Illinois. The impoundment is situated less than 200 feet south of the Illinois River, and comprised of the Old West Ash Pond which includes Pond No. 1, Pond No. 3, and the Old West Polishing (Secondary) Pond. It is bordered to the southeast by agricultural fields, to the southwest and west by low lying floodplain within the Donnelley Wildlife Management Area (Donnelley WMA) administered by the Illinois Department of Natural Resources (IDNR) and to the east by the coal pile and power generating facility.

Site hydrogeology, and groundwater quality are summarized in Section 1, and described in detail in a separate *Hydrogeologic Investigation Report* (NRT, 2017b). The Hydrogeologic Investigation Report was completed to summarize data collected to comply with Federal Coal Combustion Residual (CCR) Rule (40 CFR Part 257) as well as comprehensive data collection and evaluations from prior hydrogeologic investigation reports completed at the Site. A Groundwater Monitoring Plan (NRT, 2017c) and a Groundwater Management Zone Application (NRT, 2017d) are also being prepared to support the closure of the WAPS. In addition, Hydrologic Evaluation of Landfill Performance (HELP) modeling has also been conducted to enable estimation of the time required for hydrostatic equilibrium of groundwater to be achieved beneath the WAPS. The HELP modeling also provided percolation rates for existing conditions and predicted cap scenario that were used as inputs in the groundwater flow and transport model. A description of the HELP model inputs and modeling results are found in the Hydrostatic Modeling Report (NRT, 2017a).

Groundwater transport modeling was established to assess the effects of the proposed capping system on surrounding groundwater quality, and is documented in Section 2. The model calibration and prediction results are presented in Sections 3 and 4, respectively. The report is summarized in Section 5.

1.2 BACKGROUND

1.2.1 Site History

The Hennepin Power Station has two coal-fired generating units with a total capacity of 280 megawatts (MW). The units were constructed in 1953 and 1959, respectively. DMG operated the WAPS at the Hennepin Power Station from 1952 until late 1996 when the WAPS was removed from service. All coal ash disposed to the WAPS is derived from Illinois coal.

The impoundment consists of the Old West Ash Pond (Figure 1-1) including Pond No. 1 (9.3 acres), at the eastern end of the impoundment, which primarily contains bottom ash and slag and Pond No. 3 (16.4 acres), in the central portion of the impoundment, which contains mixed coal ash. The Old West Polishing Pond (4.7 acres) is located at the western end of the impoundment. The berms, which are 15 feet above grade, were constructed from locally occurring sandy soils. Top of ash elevation in all three ponds is lower than the surrounding berms, providing full containment. There are no controls to collect storm water, so all runoff collects in the lowest portion of each pond, where it evaporates or infiltrates through the ash.

During operation, service water was used to sluice fly ash, bottom ash, and low-volume wastes to the impoundment. There was initially a surface water discharge from this impoundment; however, that discharge stopped after the impoundment was reworked in 1989. At the time the impoundment was removed from service in late 1996, there was no surface water discharge and all sluice water exfiltrated via evapotranspiration, seepage through the berms, or leakage through the base of the ponds. The ash is currently dry over most of the surface through most of the year with the exception of: (1) the Old West Polishing Pond, which always contains water; and, (2) within the Old West Ash Pond on the western end of Pond No. 3, where runoff water collects and is ponded most of the year.

1.2.2 Site Hydrogeology

Four principal stratigraphic layers (from top to bottom) encountered at the WAPS and adjacent areas are:

- Fill - coal combustion residuals (CCRs) consisting primarily of fly ash with lesser amounts of bottom ash and slag. This layer also includes the constructed fill berms around the ash ponds, which contain variable admixtures of CCRs and re-worked native silt, clay and sand.
- Alluvial fine grained silts and clays, classified as Cahokia Alluvium.
- Alluvial fine to medium sands.
- Sand and gravel with boulders, deposited by glacial meltwaters and classified as Henry Formation.

The river-laid deposits are classified as Cahokia Alluvium. The Henry Formation sands and gravels make up the upper and lower terraces, and fill the valley beneath the alluvium. A fifth stratigraphic layer (Layer 5) – loamy and sandy diamicton (i.e., till) of the Wedron or Glasford Formation – was encountered at one location (Boring 32) approximately 2,560 feet (½ mile) south of the western end of the impoundment; however, this layer is not significant to the hydrogeology at the impoundment.

The stratigraphy of unlithified materials underlying the Henry Formation is uncertain, but it is assumed based on nearby borings at the power plant, East Ash Pond System, and vicinity that the Henry Formation most likely sits directly on top of bedrock near the WAPS. However, based on the identification of till approximately ½ mile south of the impoundment, it is possible that till of the Wedron or Glasford Formation or an older sand formation, the Sankoty Sand, lies between the Henry Formation and bedrock.

The uppermost bedrock near the Hennepin Power Station, including the West Ash Pond Complex, is the Pennsylvanian Carbondale Formation, which consists of shale with thin limestone, sandstone, and coal beds. Three deeper borings around the perimeter of the East Ash Pond System indicate the presence of shale bedrock between elevations 400 and 410. Water well logs at the power plant indicate shale bedrock at an elevation of roughly 350.

The WAPS lies over both glacial deposits (Henry Formation) and alluvium (Cahokia Alluvium). The Old West Ash Pond, specifically Pond No. 1 lies on top of lower terrace glacial sand and gravel deposits, the eastern portion of Pond No. 3 overlies alluvial sand, while the western portion of Pond No. 3 and the Old West Polishing Pond overlay silty clay alluvial channel fill deposits. More details are presented in the *Hydrogeologic Investigation Report* (NRT, 2017b).

Monitoring wells installed at the West Ash Pond System are shown on Figure 1-2. Groundwater elevation data is available beginning in 1993. The Illinois River is the local and regional groundwater discharge area under normal river stage. River stage is usually lowest during the months of August through October. The river basin experiences annual spring flooding during the months of March, April, May, and sometimes June, while lesser flooding occasionally occurs during autumn. River stage during high precipitation and/or flood events seasonally rises above adjacent groundwater elevations and in low lying areas of the floodplain, particularly within the Donnelley WMA at wells 32, 33, and 34. Horizontal hydraulic gradients from the West Ash Pond Complex to off-site areas ranges from 0.001 foot per foot (ft/ft) during Illinois River flood stage to about 0.005 ft/ft during normal river stage, yielding a groundwater velocity ranging from 0.1 ft/day to 1.1 ft/day.

1.2.3 Groundwater Quality

Groundwater monitoring was performed for selected analytes in 1983, but consistent data collection began in 1996. The monitoring program in 2016 included the full list of inorganic and organic parameters listed in IAC 35 Part 620 Section 410 except for radium 224/226. The most recent data and analysis were submitted in the 2016 Closure Work Plan Annual Report (NRT, 2016).

Parameters that have historically (1996 to 2016) exceeded Class I groundwater standards include boron, iron, manganese and sulfate. Additional parameters that exceeded Class I Standards during the expanded monitoring performed for the hydrogeologic investigation from June 2013 through March 2014 were arsenic, selenium, nitrate and lead but none of them were attributed to the WAPS.

1.3 CONCEPTUAL MODEL

The WAPS overlays alluvium, and outwash deposits in the Illinois River valley. The principal stratigraphic layers encountered at the WAPS and adjacent areas (from top to bottom) are coal combustion residuals (CCRs) consisting primarily of fly ash with lesser amounts of bottom ash and slag, alluvial fine grained silts and clays classified as Cahokia Alluvium, alluvial fine to medium sands as well as sand and gravel with boulders, deposited by glacial meltwaters which are classified as Henry formation. The primary directions of groundwater flow are north and west, with discharge to the Illinois River – a regional groundwater sink. There are two sources of water: natural recharge within the model domain; and, recharge (percolation) through the impoundment.

Boron was modeled because it is a primary indicator of coal ash leachate, exceeds the Class I standard, is mobile in groundwater, and is more representative of coal ash leachate than sulfate, which may originate from other anthropogenic or natural sources. The monitoring network of boron observations is shown in Figure 1-2. The conceptual model for transport assumes two boron sources: boron that leaches to recharge water during percolation through ash above the water table; and boron that leaches to groundwater as it flows through ash below the water table. Therefore, mass is added to groundwater via vertical recharge through coal ash, and horizontal groundwater flow through coal ash where it lies below the water table. Mass is discharged at the model representation of the Illinois River. The conceptual transport model assumes that boron concentration in leachate does not vary as a function of time, although the volume of leachate decreases over time as a function of pond dewatering and capping. There is no removal of mass from the groundwater system via adsorption or decay.

2 MODEL ESTABLISHMENT

2.1 MODEL BACKGROUND

The 2017 model is an update to, and was derived from, a model developed for the WAPS in 2014 (NRT, 2014). Updates made to this 2017 model include the following:

- The transient calibration period was extended through December 2016 to incorporate all available monitoring data.
- The WAPS ash thickness was re-assessed during a geological investigation conducted by Civil & Environmental Consultants, Inc. (CEC) in March, 2017. Accordingly, the bottom elevations of model Layer 1 at the WAPS location were adjusted to reflect the new data.
- The bottom elevations of model Layer 1 were also adjusted to meet model convergence criteria. One additional layer was inserted beneath Layer 1 to maintain the geological layering in the model.
- The hydraulic conductivities of coal ash, silt and sand were revised to improve calibration results. The updated values of coal ash and silt are close to laboratory conductivity measurements performed by AECOM in December, 2015.
- The river stage was revised to improve calibration results.
- Newly installed monitoring well MW-49 (built in 2016) was added to the monitoring network.
- The recalibrated model was then used to simulate the closure scenario, which was modeled over a period of 200 years, beginning in Year 2017.

2.2 MODEL APPROACH

Three modeling codes were used to model groundwater flow and contaminant transport: 1) percolation through the cap system was modeled using the Hydrologic Evaluation of Landfill Performance (HELP) model. All details regarding closure configurations and HELP model establishment are presented in a separate Hydrostatic Equilibrium Report (NRT, 2017a); 2) groundwater flow was modeled in three dimensions using MODFLOW; and, 3) contaminant transport was modeled in three dimensions using MT3DMS.

A three-dimensional groundwater flow and transport model was established to represent the conceptual flow system described above and then calibrated to match the groundwater monitoring results since 1994. The model was calibrated in four stages:

1. Stage 1: A steady-state flow model was calibrated to approximate head distributions observed while the impoundment was in service, based on median heads observed from 1994 through 1996.
2. Stage 2: The steady state transport model was calibrated to approximate concentrations observed while the impoundment was in service, based on observations from 1994 through 1996.
3. Stage 3: The steady state flow model was converted to a transient flow model and calibrated to match the decreasing heads measured after the impoundment was removed from service. The model period was December 1996 through December 2016 (Transient model stress periods 1 and 2).
4. Stage 4: The transport model was calibrated to approximate boron concentration trends observed since the impoundment was removed from service, using heads from the transient flow calibration model. The model period was December 1996 through December 2016 (Transient model stress periods 1 and 2).

Each subsequent calibration stage required changes to and recalibration of previous stages. The results provide a representative simulation of groundwater flow and transport conditions near the WAPS. The calibrated model was then used as a starting point to predict changes in boron concentrations over a transport period of 200 years under a baseline scenario and a closure configuration:

- Baseline: assumes no action is undertaken.
- Closure Configuration: Old West Polishing Pond is removed. Old West Ash Pond (Pond No. 1 and Pond No. 3) are fully capped by a geomembrane cover, comprised of (from top to bottom) 6-inch vegetative layer, 18-inch protective soil layer, a 0.2-inch geocomposite drainage layer and a 40-mil geomembrane layer.

Two transient stress periods (periods 3 and 4) were added at the end of the transient calibration model to simulate groundwater flow and transport after the capping system was completed (prediction modeling stress periods). The HELP model results (NRT, 2017a) indicated it would take seven years for percolation rates through the cover and CCR material to stabilize (reach equilibrium) after completion of the capping system. Therefore, transient stress period 3 was used for Years 2017 to 2024 to simulate dewatering of the material below the cap and stress period 4 was used to simulate the stabilized percolation rate for the remaining period of 193 years.

2.3 MODEL DESCRIPTION

MODFLOW uses a finite difference approximation to solve a three-dimensional head distribution in a transient, multi-layer, heterogeneous, anisotropic, variable-gradient, variable-thickness, confined or unconfined flow system. User-supplied inputs are hydraulic conductivity, aquifer/layer thickness, recharge, wells and boundary conditions. The program also calculates water balance at wells, rivers and drains.

MODFLOW was developed by the United States Geological Survey (McDonald and Harbaugh, 1988) and has been updated several times since. Major assumptions of the code are: 1) groundwater flow is governed by Darcy's law; 2) the formation behaves as a continuous porous medium; 3) flow is not affected by chemical, temperature, or density gradients; and 4) hydraulic properties are constant within a grid cell. Other assumptions concerning the finite difference equation can be found in McDonald and Harbaugh (1988).

MT3DMS (Zheng and Wang, 1998) is an update of MT3D. It calculates concentration distribution for a single dissolved solute as a function of time and space. Concentration is distributed over a three-dimensional, non-uniform, transient flow field. Solute mass may be input at discrete points (wells, drains, river nodes, constant head cells), or distributed evenly or unevenly over the land surface (recharge).

MT3DMS accounts for advection, dispersion, diffusion, first-order decay and sorption. Sorption can be calculated using linear, Freundlich, or Langmuir isotherms. First-order decay terms may be differentiated for the adsorbed and dissolved phases.

The program uses the standard finite difference method, the particle-tracking-based Eulerian-Lagrangian methods and the higher-order finite-volume TVD method for the solution schemes. The finite difference solution can be prone to numerical dispersion for low-dispersivity transport scenarios, and the particle-tracking method has problems in conserving mass-balance. The TVD solution is not subject to numerical dispersion and conserves mass well, but is computationally intensive. For this modeling, the TVD solution was used.

Major assumptions are: 1) changes in the concentration field do not affect the flow field; 2) changes in the concentration of one solute do not affect the concentration of another solute; 3) chemical and hydraulic properties are constant within a grid cell; and 4) sorption is instantaneous and fully reversible, while decay is not reversible.

2.4 MODEL SETUP

2.4.1 Grid and Boundary Conditions

A six layer, 63 by 79 node grid, was established with variable grid spacing ranging from 100 feet to 200 feet (Figure 2-1). The largest node spacing was upgradient at the lateral model boundary, and the finest node spacing was near the impoundment.

Flow and transport boundaries were the same for all scenarios. The upgradient (east and south) edge of the model was a no-flow boundary (Figure 2-1). The downgradient (north) and lateral (west) boundaries were either MODFLOW river (Mixed) boundaries (layer 1) or no flow (layers 2-5). Pond No. 1 (Layer 1) was set as no flow condition to ensure the ash remained unsaturated during model simulations. The upper boundary was a time-dependent specified flux (Neumann) boundary, with specified flux rates equal to the recharge rate or the rate of percolation from the impoundment.

The model included two types of transport boundaries (constant concentration and recharge), both in layer 1 (Figure 2-2). Saturated ash areas were represented by constant concentration boundaries. All water passing through these boundaries was assigned a specified concentration representative of ash leachate concentration. The base elevation of nodes representing saturated ash was set to represent depth of ash borings observed in the field. In addition, recharge water in areas overlain by ash was assigned a specified concentration, and the concentration in the underlying node was a result of mixing the recharge flux with the flux passing laterally through the node (unless that node was a saturated ash area, in which case all water passing through was assigned the maximum observed leachate concentration by the constant concentration boundary cell).

2.4.2 Flow Model Input Values and Sensitivity

Flow model input values and results of sensitivity analyses are listed in Table 2-1 and described below.

Layer Top/Bottom

The top of layer 1 was the water table, therefore the elevation of model layer 1 was set at 460 feet, a value higher than the maximum water table elevation (in the impoundment). The top of layers 2 through 6 were set to the base of the overlying layer. The saturated thickness of layer 1 depended on modeled water table elevation. The base of layer 1 at the WAPS was set as the bottom of coal ash elevations and the bottom elevation of the surrounding cells were adjusted to meet the model convergence criteria (Figure 2-3). The base of layer 2 was set at 430 feet and each underlying layer (Layer 3 to Layer 6) was 10 feet thick.

Hydraulic Conductivity

Hydraulic conductivity values (Figure 2-4) were initially derived from field-measured and laboratory tested values and adjusted during calibration. Calibrated values were within observed ranges for the formations present at the site. Vertical anisotropy ratios were set at 2.0 for the sand and gravel and 10 for the silty clay and alluvium. The Kx/Kz ratios represent expected stratification within the formations.

The model had moderate to high sensitivity to the horizontal hydraulic conductivity used over most of the domain. Sensitivity to vertical hydraulic conductivity varied, with the low permeability zones being most sensitive.

Storage

No field data was available defining these terms, so representative values for similar materials were obtained from Smith and Wheatcraft (1993). Sensitivity analysis was not performed on this parameter. The storage coefficient used in the model was 0.01 and the specific yield was 0.30.

Recharge

Recharge rates for the impoundment while in-service and during dewatering were determined during model calibration. Recharge rates for the model domain were adopted from the previous 2014 model and were adjusted during calibration. Recharge zones during the transient calibration period are illustrated in Figure 2-5. Recharge rates after cap completion were set based on the HELP simulations and shown in Figure 2-6. Transient stress period 3 was used for Years 2017 to 2024 to simulate dewatering of the material below the cap. Transient stress period 4 was used to simulate the stabilized percolation rate for the remaining period of 193 years.

Calibrated heads were highly sensitive to changes in recharge rates in zones 5, 6, and 7 of Ash Pond 3 and the outwash gravel (Zone 2). The flow model displayed low to moderate sensitivity to the other recharge zones in the model.

River Parameters

The Illinois River was represented by head-dependent flux nodes that required inputs for river stage, width, bed thickness and bed hydraulic conductivity. The latter three parameters are used to calculate a conductance term for the boundary node. This conductance term was determined by adjusting hydraulic conductivity during model calibration. For simplicity, it was assumed that river stage does not fluctuate and that river gradient is negligible along the reach modeled. In addition, the waterfowl ponds and a small creek that feeds the waterfowl ponds were simulated using MODFLOW river nodes (Figure 2-1).

Sensitivity analysis showed that the model was highly sensitive to river stage, and insensitive to conductance values.

2.4.3 Transport Model Input Values and Sensitivity

Transport model input values are listed in Table 2-2 and described below. The results of sensitivity analyses are also presented in Table 2-2.

Initial Concentration

Initial concentration for the steady state calibration model was set at zero, implying a background concentration of zero, which is reasonable for boron. The final concentrations from the steady state calibration model were used as the initial concentration for the transient calibration model. The prediction model was built by adding two transient stress periods to the transient calibration model as discussed above. The transient calibration model is stress periods 1 and 2, the dewatering phase of the prediction model is stress period 3, and the hydrostatic equilibrium phase of the prediction model is stress period 4.

Source Concentration

Boron source concentrations (from saturated ash) were set during model calibration at values between 7 and 19 mg/L, the range observed in monitoring wells near the impoundment. The setting of source concentration is consistent with the 2014 model. As mentioned in Section 2.4.1, Pond No. 1 (Layer 1) was set as no flow condition instead of a constant concentration boundary to simulate unsaturated ash observed at Pond No. 1. Source concentration originating from Pond No. 1 (leachate percolating through the unsaturated ash) was simulated by applying concentration to the recharge zone above the no flow cells, which was then applied to the highest active layer (Layer 2). Using a combination of no flow cells and recharge inputs for simulating Pond No. 1 ensures the only source concentration entering the model from Pond No. 1 is in the form of leachate through the base of the unsaturated ash.

Since clean closure will be applied to the Old West Polishing pond, the source concentration at the Old West Polishing pond was set as zero during stress periods 3 and 4 (Figure 2-7).

Boron source concentrations from recharge were also determined during model calibration (Table 2-2) and remained the same during the prediction stress periods 3 and 4. The recharge rates were reduced as discussed above.

Effective Porosity

Effective porosity values were based on ranges provided by Mercer and Waddell (1993). Predicted concentrations at some wells distant from the impoundment (wells 26, 30, 31) had moderate sensitivity to this parameter (Table 2-2).

Dispersivity

Dispersivity was set during model calibration. Transverse and vertical dispersion were estimated according to ratios developed by Gelhar et al. (1985). Calibrated concentrations at some wells distant from the impoundment (wells 26, 30, 31, 36) were highly sensitive to the longitudinal dispersivity value and to the vertical dispersivity multiplier, while calibrated concentrations were not sensitive to the transverse dispersivity multiplier.

Retardation

Retardation was calculated by the model based on the distribution coefficient (K_d), which was set during calibration. Concentration match was best when K_d was set at zero for the sand and gravel units, and at 1.0 mL/g in the silty units (channel-fill deposit and alluvium) (Figure 2-8). The K_d value of 1.0 mL/g resulted in a retardation factor of 9.0 in the silt units. Calibrated concentrations at wells distant from the impoundment (wells 26, 27, 30, 31, 36) were highly sensitive to the K_d value modeled for the sand units, while the model exhibited low sensitivity to the range of K_d values tested for the silt units.

Diffusion

Diffusion was also set to 0 for the entire model domain.

3 MODEL RESULTS

3.1 Flow and Transport Model Assumptions and Limitations

Simplifying assumptions are necessary when numerically representing the natural environment in a groundwater flow and transport model. Outside of assumptions inherent to the codes used to develop the model, several simplifying assumptions were made, including:

- Leachate instantaneously migrates to groundwater (e.g., rapid migration through the unsaturated zone).
- Fluctuations in river stage are short in duration and do not affect groundwater flow and transport.
- Recharge rate outside the impoundment is constant over time.
- Source concentrations remain constant over time.
- Boron minimally adsorbs and does not decay, and mixing and dispersion are the primary attenuation mechanisms.
- Cap construction has an instantaneous effect on recharge and percolation because it is constructed over a brief period relative to the length of the model simulation.

The model is limited by the data used for calibration, which adequately define the local groundwater flow system and the source and extent of the plume. These data, collected from 1994 through 2016, are from points near the WAPC. Model predictions of transport distant from the impoundment will not be as reliable as predictions of transport near the impoundment, and the reliability of model predictions decreases with increasing time because changes to the system may occur that the model does not account for.

3.2 Calibration Flow and Transport Model Results

Results of the MODFLOW/MT3DMS modeling are presented below. A CD containing the model files is attached to this report (Appendix A).

Figure 3-1 compares modeled versus observed steady-state heads for the period while the impoundment was in service. Figure 3-2 compares modeled versus observed heads for the period 1994 through 2016 at Wells 21, 22, 23, 24, 25/26, 27, 30, 31, 32, 33, 34, 35, 36, L1, L4 and 49. Modeled heads at all monitoring wells fall within the range of observed values. The modeled and observed heads demonstrate a linear trend that falls just above the ideal 1 to 1 line, which indicates the calibrated groundwater elevations are slightly higher than observed but adequately represent the calibration data across the range of observed values. The graph of observed values and calibration residuals indicates most of the residuals are negative, which also suggests the steady state model results are biased a little high. However, the data have a good degree of scatter, indicating the model is not biased across the range of elevations observed. The relative standard deviation, given as a percentage of standard deviation to data mean, was determined to be 7.1%, which is within the acceptable target of less than 10%. This statistical result is strong evidence of the steady state model's ability to simulate flow within the range of groundwater elevations observed. Modeled heads in the transient model follow observed trends observed from 1997 through 2016, and successfully capture the hydraulic head drops after the impoundments were removed from service (Figure 3-2). The consistency between observable data and modeling results indicate that this model provides a reasonable simulation of the effects of the WAPS on groundwater flow.

The simulated boron concentration trends are compared to observed data in Figure 3-3. The simulated boron concentrations reasonably match the observed concentrations. For example, the transport model exhibits a successful simulation of the short-term concentration increase at Well 24 between 1998 and 2000, and captures the decreasing concentration trends at wells 22, 24, 25/26, 27, 30 and 31 after removing the impoundment from service (well locations are shown on Figure 1-2). It also predicts no decrease in concentration relative to initial conditions at wells 21 and 23. The model made conservative simulations of boron concentration at Well 24 after Year 2009 and at Well 49, which was installed in 2015 and has limited data. The agreement between modeled and predicted concentrations demonstrates the capability of the transport model for the prediction of contaminant transport in groundwater at the site.

3.3 Model Prediction

As stated in the previous sections, the prediction model was extended 200 years following the cap completion (2017 to 2217) to evaluate boron concentrations in groundwater under a baseline (no action) scenario and the closure configuration. The predicted hydraulic heads under the two conditions are compared in Figure 3-4. The predicted boron concentrations under the two conditions are compared in Figure 3-5.

3.3.1 Baseline

Under the baseline scenario, it was assumed that no action was taken to cover or remove existing ash. As shown in Figures 3-4 and 3-5, both hydraulic head and boron concentrations are predicted to remain stable except at Well 27, in which the boron concentration would decrease even when no action was applied. As shown in Figure 1-2, Well 27 is located further downgradient from the pond. The continuous decrease of boron concentration at this location under the baseline scenario is its response to the pond removal from service.

Figure 3-6 depicts the predicted boron plume where it exceeds the Illinois Class I groundwater protection standard (2 mg/L) 50 years after cap completion. The boron plume is predicted to extend north beneath the Illinois River. As illustrated in Figure 3-5, the boron concentrations at wells become asymptotic; no further reduction is expected with time and most wells with boron concentrations that exceed the standard will remain above the standard after 200 years.

3.3.2 Capping Scenario

Under the capping scenario, it was assumed that the Old West Polishing Pond would be excavated and the remaining WAPS (Old West Ash Pond, including Pond No. 1 and Pond No. 3) would be capped in place with a geosynthetic cover that was expected to yield a percolation rate as low as 0.002 inch/yr (NRT, 2017a).

Comparing the baseline to the capping option, significant reduction in boron concentrations is predicted in monitoring wells (Figure 3-5). All wells would reach the standard in 50 years except wells 21 and 23, the concentrations of which will eventually decrease to meet the criterion within the 200-year simulation. Slight drops in hydraulic heads are observed after the cap is in place, which is due to the infiltration decrease.

As shown in Figure 3-6 (50-year plume), the footprint of the plume under the capping scenario is significantly reduced and the highest boron concentrations are focused within the pond footprint. Groundwater impacts beneath the eastern portion of the pond are attenuated by 50 years. The remaining impacts are focused around the capped and saturated ash along with the lower permeability silty/clay material beneath the western portion of the pond. This lower permeability material results in slower release/attenuation of the impacts as compared to other portions of the site which are underlain by higher permeability sands. Figure 3-7 shows the plume configuration in Layer 4, where boron is slowly attenuated. The north-south shape of the western portion of the boron plume is consistent with the north-south hydraulic conductivity distribution shown in layers 4 through 6 on Figure 2-4.

After 200 years (year 2217), as shown in Figure 3-8, the footprint of exceedances (boron concentrations greater than 2 mg/L) will be limited to the property except for a few isolated areas where the western extent of the plume lingers in association with the silty material. The modeling results show that the proposed closure configuration effectively consolidates groundwater impacts to the footprint of the capped impoundment.

4 SUMMARY

A 3-dimensional groundwater flow and transport model was established to evaluate the effectiveness of the proposed closure plan on the WAPS at the Hennepin Power Station. The proposed closure configuration includes clean closure of the Old West Polishing Pond and capping the remaining impoundments in place with a geosynthetic cover, which consists of a 6-inch surface soil layer, a 18-inch soil layer, a geocomposite drainage layer and a geosynthetic layer. The model was developed based on a previous 2014 model with incorporation of new field and laboratory measurements and was recalibrated to fit additional monitoring data. In summary, the results of the modeling are:

- The consistency between modeling results and the observable data collected from 1994 through 2016 exhibits a successful calibration of the updated model, demonstrating the model's capability for the prediction of hydraulic flow and contaminant transport in groundwater at the site.
- When no action is taken, groundwater impacts will not be contained within the property and groundwater protection standards will not be met for boron. Boron concentrations become asymptotic after approximately 50 years (Year 2067) and no further reduction is expected with time.
- Under the proposed closure scenario, significant reduction in groundwater impacts are expected. Boron concentrations in most wells will meet the groundwater protection standards in 50 years upon cap completion (Year 2067) and all wells will meet the standards within 200 years (Year 2217).
- At 50 years after cap completion, the remaining impacts outside the footprint of the capped impoundment appear to be attributed to lower permeability silty/clay material beneath the western portion of the pond. After 200 years (year 2217), groundwater impacts are nearly removed and only isolated areas of impacts remain (also associated with the silty/clay materials). The proposed closure configuration effectively consolidates groundwater impacts to the footprint of the capped impoundment.

REFERENCES

Anderson, Mary P., and Woessner, William W., 1992, Applied groundwater modeling: simulation of flow and advective transport, Academic Press, Inc., San Diego, CA.

Fetter, C. W., 1988, Applied Hydrogeology, Merrill Publishing Company, Columbus Ohio.

McDonald, M.G., and A.W. Harbaugh, 1988, A Modular Three-Dimensional Finite-Difference Ground-Water Flow Model: Techniques of Water-Resources Investigations, Techniques of Water-Resources of the United States Geological Survey, Book 6, Chapter A1.

Mercer, J.W., and R.K. Waddell, 1993, Contaminant Transport in Groundwater, in Handbook of Hydrology, D.R. Maidment (ed.), McGraw-Hill Inc., pp. 16.1-16.41, New York, NY.

Natural Resource Technology, Inc. (NRT), 2002. Model Recalibration and Prediction of Closure Options for the West Ash Impoundment; Hennepin Power Station Putnam County, Illinois. October, 2002.

Natural Resource Technology, Inc. (NRT), 2014. Closure Alternatives Evaluation; Hennepin Power Station Putnam County, West Ash Impoundment, Illinois. July, 2014.

Natural Resource Technology, Inc. (NRT), 2016. 2016 Closure Work Plan Annual Report; Hennepin Power Station Putnam County, West Ash Impoundment, Illinois. 2016.

Natural Resource Technology, Inc. (NRT), 2017a. Hydrostatic Modeling Report; Hennepin Power Station Putnam County, West Ash Pond System, Illinois. September, 2017.

Natural Resource Technology, Inc. (NRT), 2017b. Hydrogeologic Site Characterization Report; Hennepin Power Station Putnam County, West Ash Pond System, Illinois. September, 2017.

Natural Resource Technology, Inc. (NRT), 2017c. Groundwater Monitoring Plan; Hennepin Power Station Putnam County, West Ash Pond System, Illinois. September, 2017.

Natural Resource Technology, Inc. (NRT), 2017d. Groundwater Management Zone Application; Hennepin Power Station Putnam County, West Ash Pond System, Illinois. September, 2017.

Zheng, Z., and P.P. Wang, 1998, MT3DMS, a Modular Three-Dimensional Multispecies Transport Model, Model documentation and user's guide prepared by the University of Alabama Hydrogeology Group for the US Army Corps of Engineers.

Tables

Table 2-1a. Flow Model Input Values (steady-state calibration)
Groundwater Model Report
West Ash Pond System, Hennepin Power Station

Horizontal Hydraulic Conductivity	**ft/d**	**cm/s**	**Sensitivity[1]**
Sand & River Sand (Zone 1)	30.0	1.1E-02	high
Outwash Gravel (Zone 2)	200.0	7.1E-02	high
Alluvium (Zone 3)	1.5	5.3E-04	moderate
Channel Fill Silts (Zone 4)	1.4	4.9E-04	moderately high
Ash (Zone 10)	0.05	1.8E-05	moderate

Vertical Hydraulic Conductivity	**ft/d**	**Kh/Kv**	**Sensitivity[1]**
Sand & River Sand (Zone 1)	15.0	2.0	moderate
Outwash Gravel (Zone 2)	100.0	2.0	negligible
Alluvium (Zone 3)	0.15	10.0	high
Channel Fill Silts (Zone 4)	0.14	10.0	high
Ash (Zone 10)	0.05	1.0	high

Recharge[2]	**ft/d**	**in/yr**	**Sensitivity[1]**
Sand & River Sand (Zone 1)	1.1E-03	4.8	moderately high
Outwash Gravel (Zone 2)	1.1E-03	4.8	high
Channel Fill Silts (Zone 4)	5.0E-04	2.2	low
Ash-Pond No. 1 (Zone 9)	3.83E-03	16.8	low
Ash-Pond No. 3 East (Zone 8)	4.0E-02	175.2	moderately high
Ash-Pond No. 3 Center (Zone 10)	2.7E-02	118.3	moderately high
Ash-Pond No. 3 West (Zone 6)	2.7E-02	118.3	high
Ash-Pond No. 3 Northwest (Zone 5)	2.7E-02	118.3	high
Ash-Old West Polishing Pond (Zone 7)	2.0E-02	87.6	high

River Parameters	**Illinois Riv.**	**Duck Ponds/Creek**	**Sensitivity[1]**
Stage (ft)	441.7	445.5	high
Bed Thickness (ft)	1	1	not tested
Hydraulic Conductivity (ft/d)	10	1/5	not tested
Conductance (ft^2/d, normalized per ft^2 area)	10	1/5	negligible
River Width (ft)	100-200	100-200/10	not tested
River Cell Length (ft)	100-200	100-200/100	not tested

Notes:

1 - Sensitivity Explanation, based on maximum change in Sum of Squared Residuals (SSR)
- Negligible - SSR changed by less than 1%
- Low - SSR change between 1% and 10%
- Moderate - SSR change between 10% and 50%
- Moderately High - SSR change between 50% and 100%
- High - SSR change greater than 100%

2 - See Table 2-1b for transient recharge values.

3 - See figures for delineation of model zones

Table 2-1b. Flow Model Input Values (transient calibration)
Groundwater Model Report
West Ash Pond System, Hennepin Power Station

	Calibration	
Stress Periods[1]	**Days, #TS**	**Dates**
Stress Period 1	**500, 6**	**1/1997-5/1998**
Stress Period 2	**6804, 20**	**5/1998-12/2016**
Recharge[2] (Calibration SP1)	**ft/d**	**in/yr**
Ash-Pond No. 1 (Zone 9)	3.83E-03	16.8
Ash-Pond No. 3 East (Zone 8)	2.E-02	87.6
Ash-Pond No. 3 Center (Zone 10)	2.E-02	87.6
Ash-Pond No. 3 Center (Zone 6)	2.E-02	87.6
Ash-Pond No. 3 West (Zone 12)	2.E-02	87.6
Ash-Pond No. 3 West (Zone 13)	2.E-02	87.6
Ash-Pond No. 3 Northwest (Zone 5)	2.E-02	87.6
Ash-Pond No. 3 Northwest (Zone 11)	2.E-02	87.6
Ash-Old West Polishing Pond (Zone 7)	2.E-02	87.6
Recharge[2] (Calibration SP2)	**ft/d**	**in/yr**
Ash-Pond No. 1 (Zone 9)	3.83E-03	16.8
Ash-Pond No. 3 East (Zone 8)	2.96E-03	13.0
Ash-Pond No. 3 Center (Zone 10)	2.96E-03	13.0
Ash-Pond No. 3 Center (Zone 6)	2.E-02	87.6
Ash-Pond No. 3 West (Zone 12)	2.E-02	87.6
Ash-Pond No. 3 West (Zone 13)	2.96E-03	13.0
Ash-Pond No. 3 Northwest (Zone 5)	2.96E-03	13.0
Ash-Pond No. 3 Northwest (Zone 11)	2.E-02	87.6
Ash-Old West Polishing Pond (Zone 7)	2.96E-03	13.0
Storage/Porosity	**S_S/S_Y**	**Porosity**
Entire Domain	0.01/0.30	0.20

Notes:

1 - First column is model days and number of time steps, second column is approximate dates in mm/yyyy format.

2 - See figures for delineation of model zones; recharge values outside ash pond are same as Table 2-1a.

Table 2-1c. Flow Model Input Values (prediction)
Groundwater Model Report
West Ash Pond System, Hennepin Power Station

	Prediction	
Stress Periods[1]	**Days, #TS**	**Dates**
Stress Period 3	**2555, 10**	**1/2017-1/2024**
Stress Period 4	**70497, 50**	**1/2024-1/2217**
Recharge[2] **(Closure Scenario SP3)**	**ft/d**	**in/yr**
Ash-Pond No. 1 (Zone 14)	2.E-03	9.1
Ash-Pond No. 3 East (Zone 14)	2.E-03	9.1
Ash-Pond No. 3 Center (Zone 15)	2.E-03	9.1
Ash-Pond No. 3 West (Zone 17)	2.E-03	9.1
Ash-Pond No. 3 Northwest (Zone 16)	2.E-03	9.1
Ash-Old West Polishing Pond (Zone 4)	5.0E-04	2.2
Recharge[2] **(Closure Scenario SP4)**	**ft/d**	**in/yr**
Ash-Pond No. 1 (Zone 14)	5.53E-07	0.002
Ash-Pond No. 3 East (Zone 14)	5.53E-07	0.002
Ash-Pond No. 3 Center (Zone 15)	5.53E-07	0.002
Ash-Pond No. 3 West (Zone 17)	5.53E-07	0.002
Ash-Pond No. 3 Northwest (Zone 16)	5.53E-07	0.002
Ash-Old West Polishing Pond (Zone 4)	5.00E-04	2.2

Notes:

1 - First column is model days and number of time steps, second column is approximate dates in mm/yyyy format.

2 - See figures for delineation of model zones; recharge values outside ash pond are same as Table 2-1b (SP2).

3 - Cap percolation rate is applied to the impoundment.

Table 2-2. Transport Model Input Values
Groundwater Model Report
West Ash Pond System, Hennepin Power Station

Initial Concentration (mg/L)	**Base Case**	**Alternatives**	**Sensitivity[1]**
Entire Domain	0.0	not tested	-
Source Concentration	**Base Case**	**Alternatives**	**Sensitivity[1]**
(Constant Concentration Zone/Recharge Zone)			
Pond No. 3 East (Zone 2 / Zone 14)	9	not tested	high[2]
Pond No. 3 Center (Zone 6 / Zone 15)	9	not tested	moderately high[2]
Pond No. 3 West (Zone 4 / Zone 17)	19	not tested	high[2]
Pond No. 3 Northwest (Zone 5 / Zone 16)	7	not tested	high[2]
Polishing Pond (Zone 3 / Zone 4)	7	not tested	high[2]
Pond No. 1 (no flow / Zones 9 & 14)	9	not tested	high[2]
Effective Porosity	**Base Case**	**Alternatives**	**Sensitivity[1]**
Entire Domain	0.20	0.15, 0.25	moderate
Dispersivity (ft)	**Base Case**	**Alternatives**	**Sensitivity[1]**
Entire Domain	50	25, 75	high
Transverse (all layers)	Dl / 8	Dl / 10	negligible
Vertical (all layers)	Dl / 160	Dl / 100	high
Retardation	**Base Case**	**Alternatives**	**Sensitivity[1]**
Bulk Density (g/cm^3)	1.6	not tested	-
Distribution Coefficient - Gravel, Ash, River Sands (mL/g)	0.0	0.5	high
Distribution Coefficient - Channel Fill (mL/g)	1.0	0.5, 1.5	moderate

Notes:

1 - Sensitivity Explanation

- Negligible - little effect on concentrations
- Low - concentrations at two or more wells changed by 2 to 10 percent
- Moderate - concentrations at two or more wells changed by 10 to 20 percent
- High - concentration at two or more wells changed by more than 20 percent

2 - Determined to be highly sensitive during transport model calibration

Figures

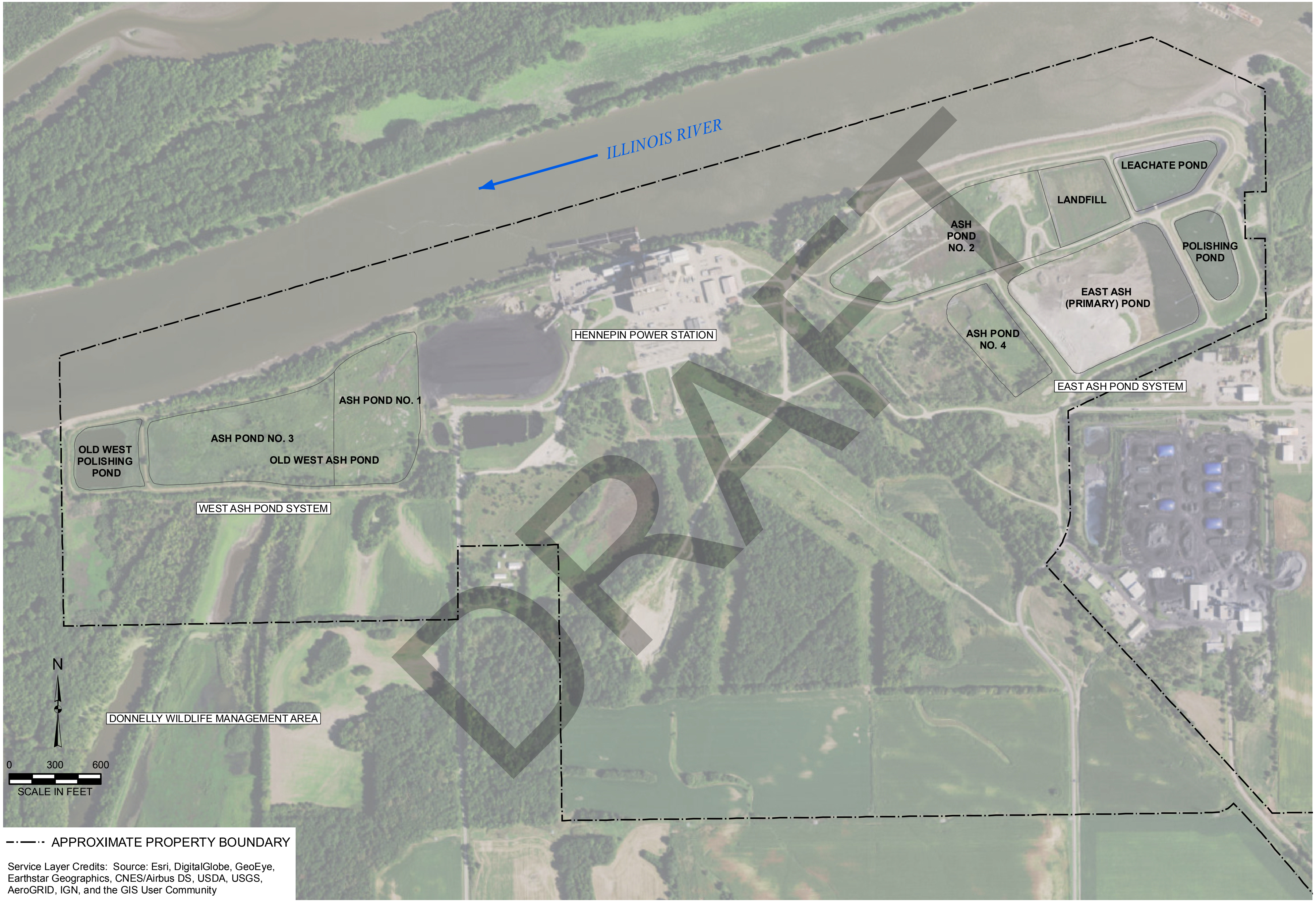

-·- APPROXIMATE PROPERTY BOUNDARY

Service Layer Credits: Source: Esri, DigitalGlobe, GeoEye, Earthstar Geographics, CNES/Airbus DS, USDA, USGS, AeroGRID, IGN, and the GIS User Community

DRAWN BY/DATE:
SDS 8/29/17
REVIEWED BY/DATE:
RJK 8/30/17
APPROVED BY/DATE:
SJC 8/31/17

SITE MAP

GROUNDWATER MODEL REPORT
WEST ASH POND SYSTEM
DYNEGY MIDWEST GENERATION, LLC
HENNEPIN POWER STATION, HENNEPIN, ILLINOIS

PROJECT NO: 2413

FIGURE NO: 1-1

Natural Resource Technology
AN OBG COMPANY

Y:\Mapping\Projects\24\2413\MXD\GW_Model_Report\Figure 1-1_Site Map.mxd Author: stolzsd; Date/Time: 12/15/2017, 3:37:35 PM

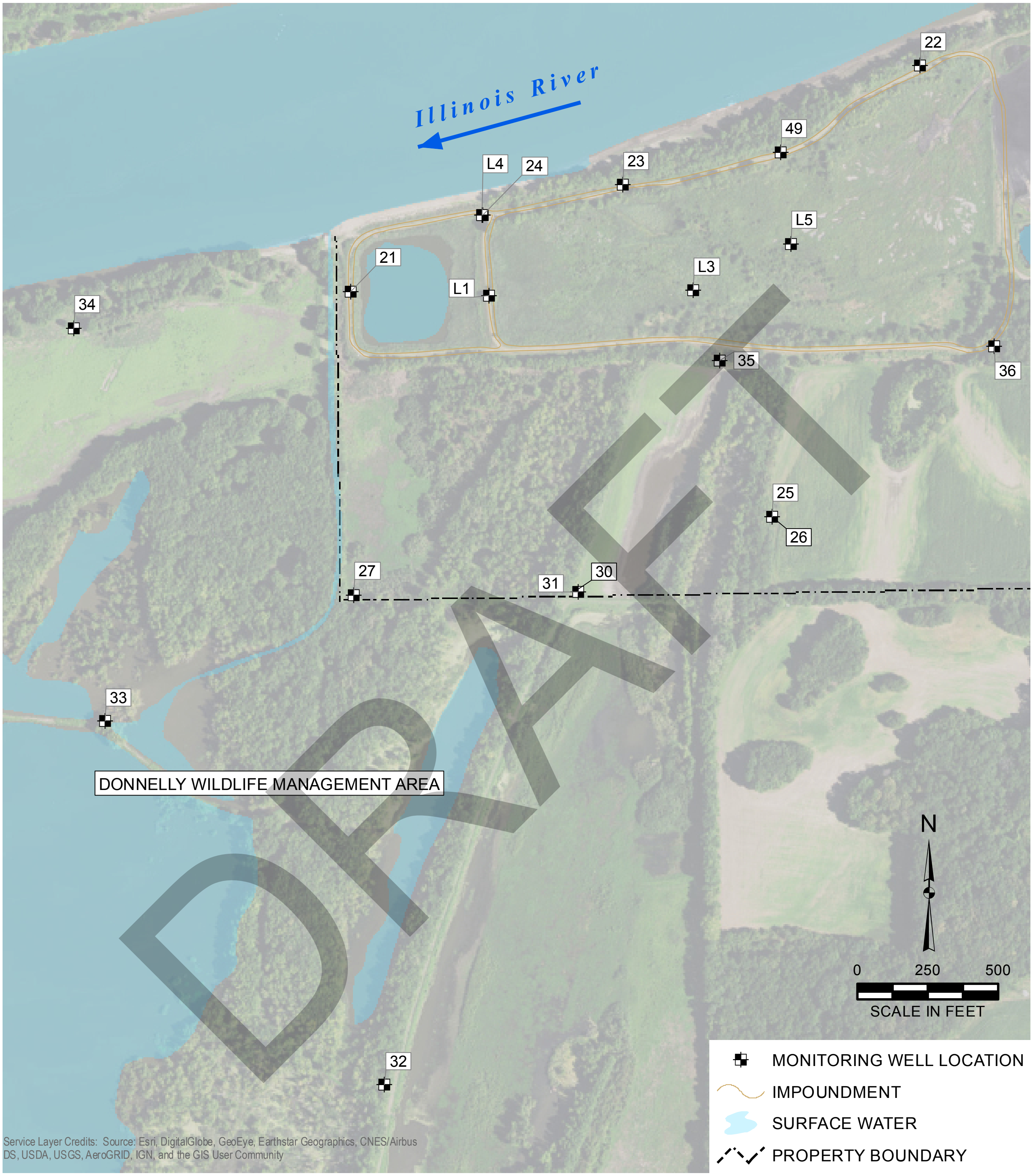

Service Layer Credits: Source: Esri, DigitalGlobe, GeoEye, Earthstar Geographics, CNES/Airbus DS, USDA, USGS, AeroGRID, IGN, and the GIS User Community

DRAWN BY/DATE:
SDS 8/29/17
REVIEWED BY/DATE:
RJK 8/30/17
APPROVED BY/DATE:
SJC 8/31/17

MONITORING WELL LOCATION MAP

GROUNDWATER MODEL REPORT
WEST ASH POND SYSTEM
DYNEGY MIDWEST GENERATION, LLC
HENNEPIN POWER STATION, HENNEPIN, ILLINOIS

PROJECT NO: 2413

FIGURE NO: 1-2

Natural Resource Technology
AN OBG COMPANY

Y:\Mapping\Projects\24\2413\MXD\GW_Model_Report\Figure 1-2_Monitoring Well Location Map.mxd Author: stolzsd; Date/Time: 12/15/2017, 3:40:08 PM

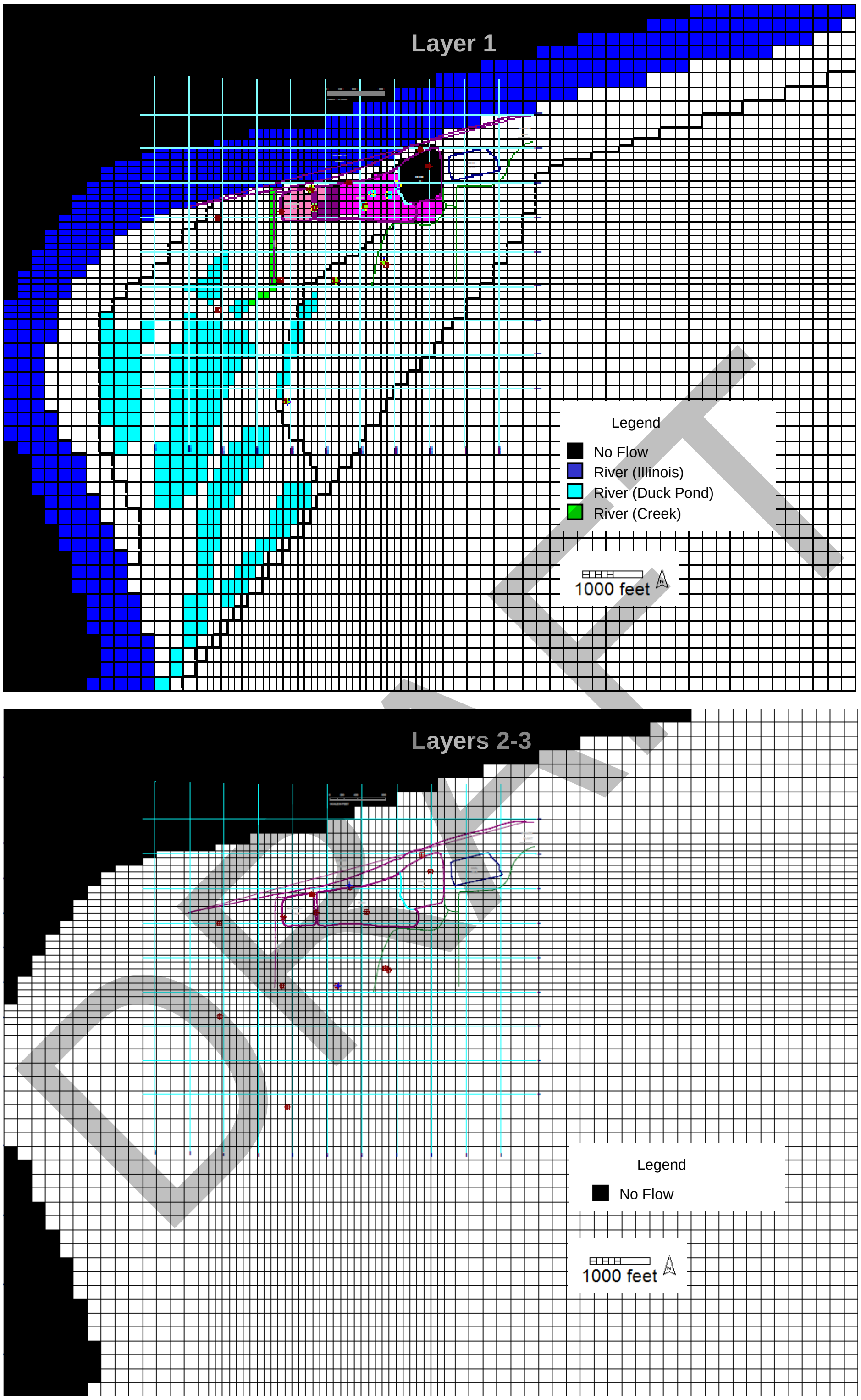

PREPARED BY/DATE:
M_W /08072017
REVIEWED BY/DATE:
BGH /08252017

MODFLOW Grid and Boundary Conditions for Layers 1 (top) and 2-3 (bottom)

GROUNDWATER MODEL REPORT
HENNEPIN POWER STATION, WEST ASH POND SYSTEM
DYNEGY MIDWEST GENERATION, LLC

PROJECT NO: 2413

FIGURE NO: 2-1

Natural Resource Technology
AN OBG COMPANY

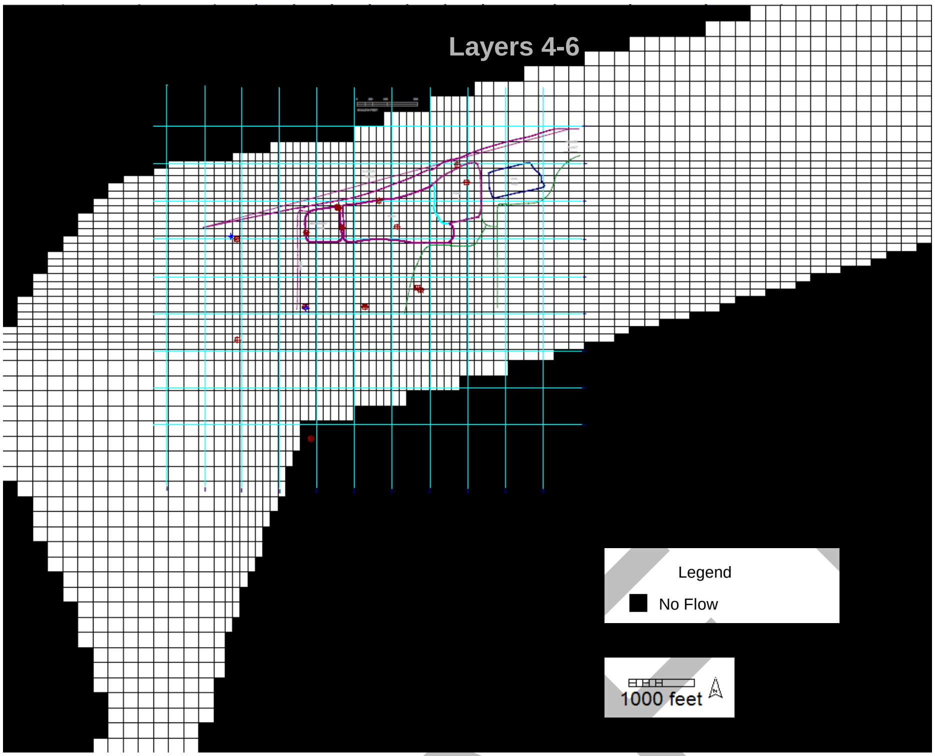

PREPARED BY/DATE:
M_W /08072017
REVIEWED BY/DATE:
BGH /08252017

MODFLOW Grid and Boundary Conditions for Layers 4-6

GROUNDWATER MODEL REPORT
HENNEPIN POWER STATION, WEST ASH POND SYSTEM
DYNEGY MIDWEST GENERATION, LLC

PROJECT NO: 2413

FIGURE NO: 2-1

Natural Resource Technology
AN OBG COMPANY

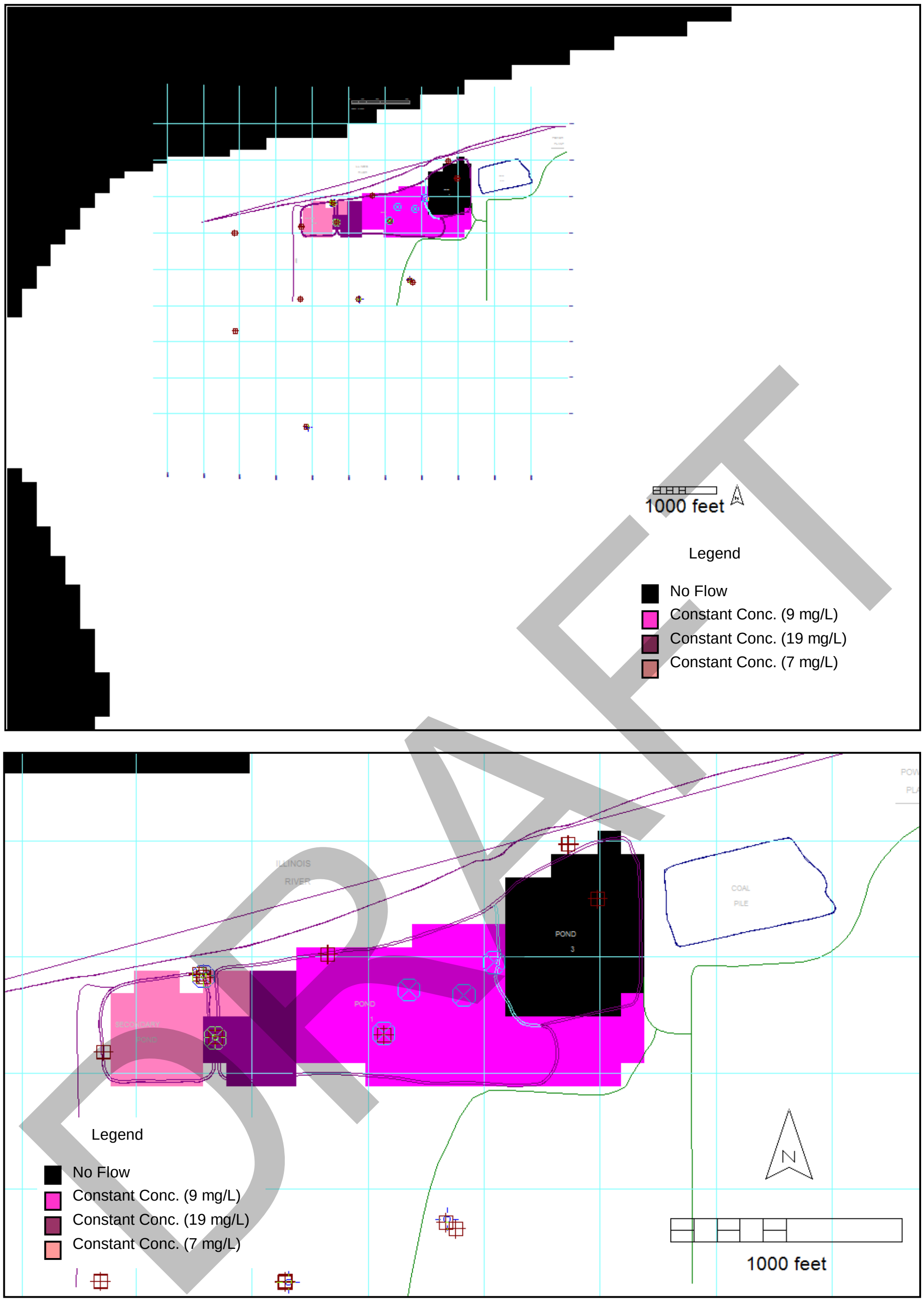

Note: Layers 2 through 6 only contain no-flow boundaries identical to the MODFLOW grid.

PREPARED BY/DATE:
M_W /08072017
REVIEWED BY/DATE:
BGH /08252017

MT3DMS Grid and Boundary Conditions for Layer 1

GROUNDWATER MODEL REPORT
HENNEPIN POWER STATION, WEST ASH POND SYSTEM
DYNEGY MIDWEST GENERATION, LLC

PROJECT NO: 2413

FIGURE NO: 2-2

Natural Resource Technology
AN OBG COMPANY

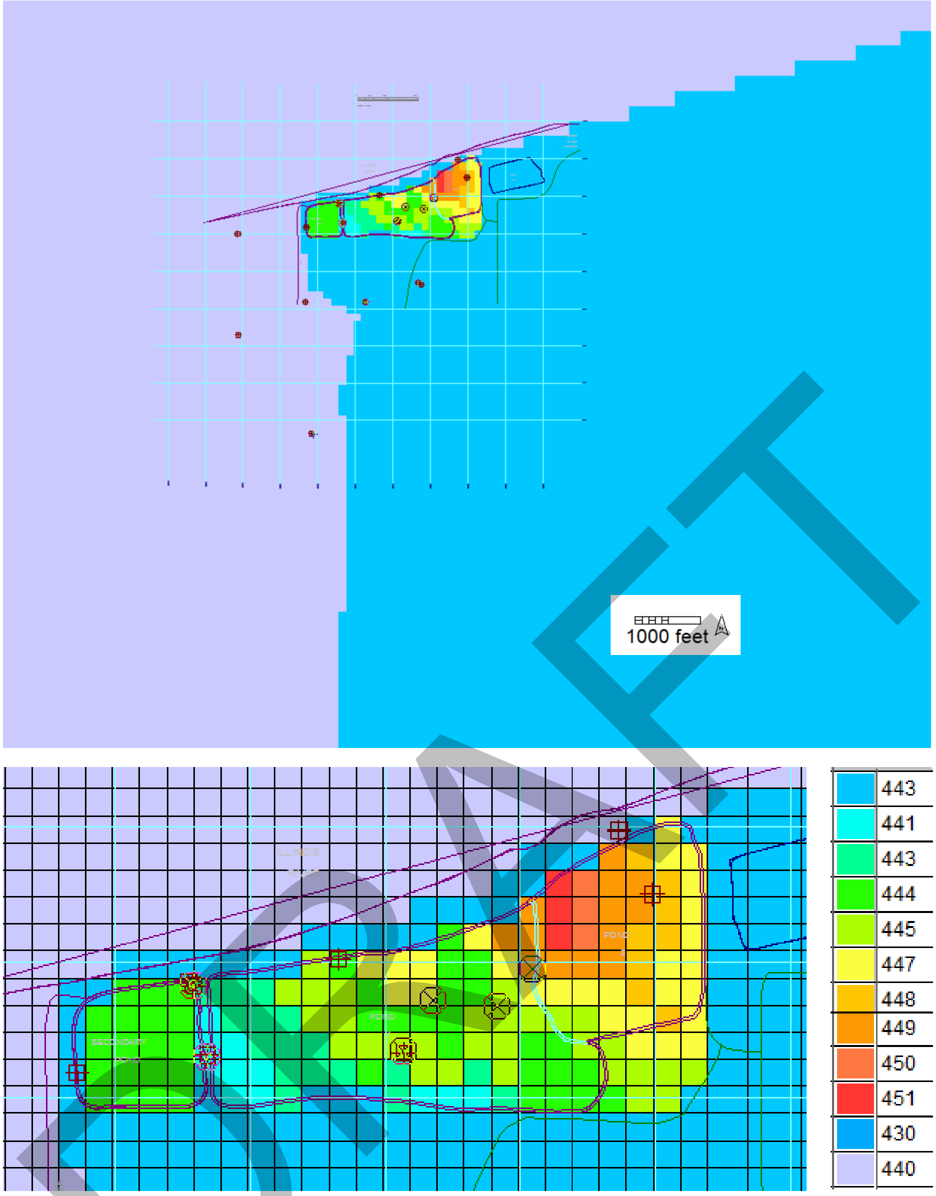

Note:

Top is entire model, bottom is zoomed around impoundment.

Layers 2-5 have uniform bottom elevations; 420, 410, 400, 390 feet, respectively.

PREPARED BY/DATE:
M_W /08072017
REVIEWED BY/DATE:
BGH /08252017

Bottom Elevation (feet) Array for Layer 1

GROUNDWATER MODEL REPORT
HENNEPIN POWER STATION, WEST ASH POND SYSTEM
DYNEGY MIDWEST GENERATION, LLC

PROJECT NO: 2413

FIGURE NO: 2-3

Natural Resource Technology
AN OBG COMPANY

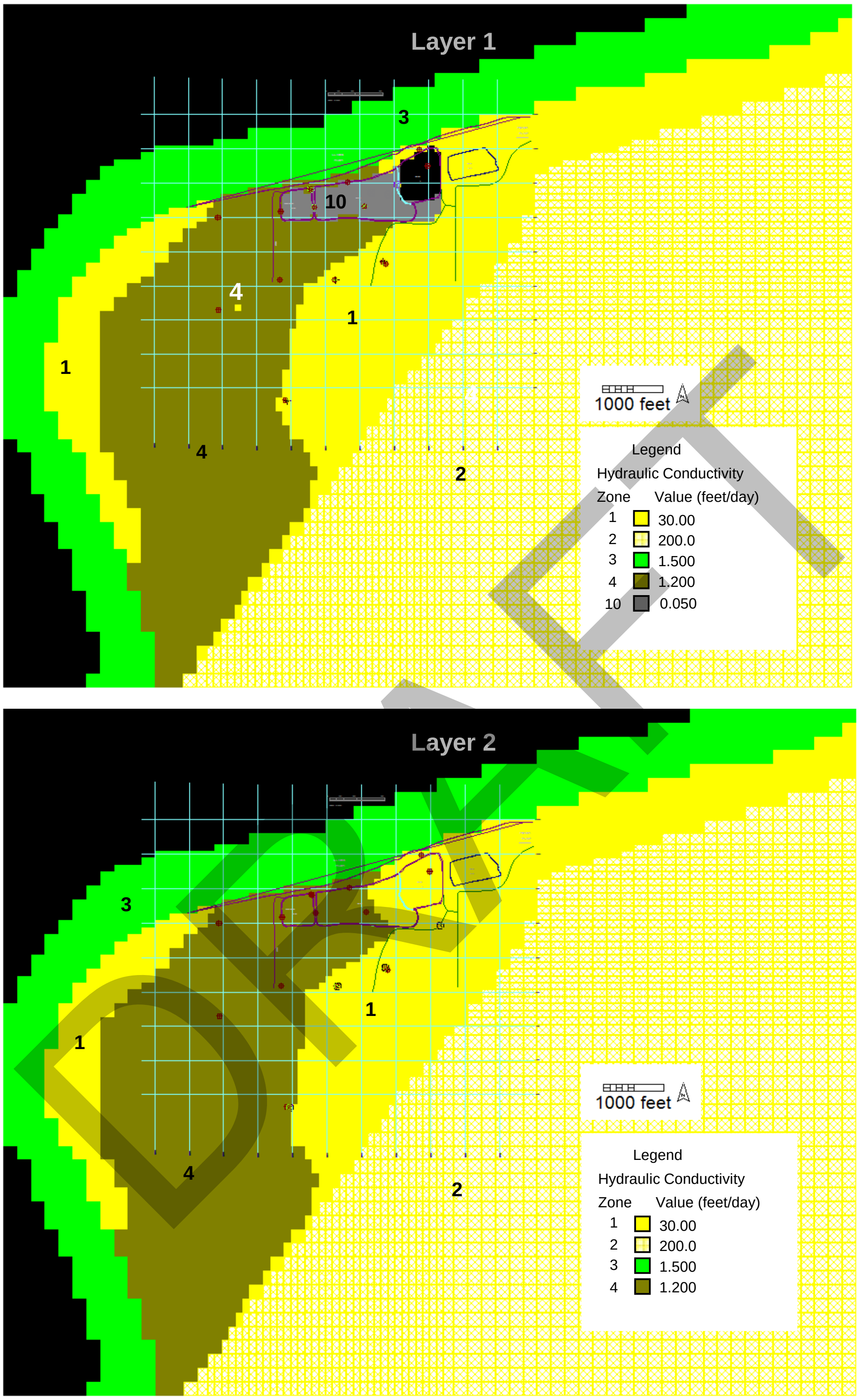

PREPARED BY/DATE:
M_W /08072017
REVIEWED BY/DATE:
BGH /08252017

Hydraulic Conductivity (ft/d) Array - Layers 1 (top) and 2 (bottom)

GROUNDWATER MODEL REPORT
HENNEPIN POWER STATION, WEST ASH POND SYSTEM
DYNEGY MIDWEST GENERATION, LLC

PROJECT NO: 2413

FIGURE NO: 2-4

Natural Resource Technology
AN OBG COMPANY

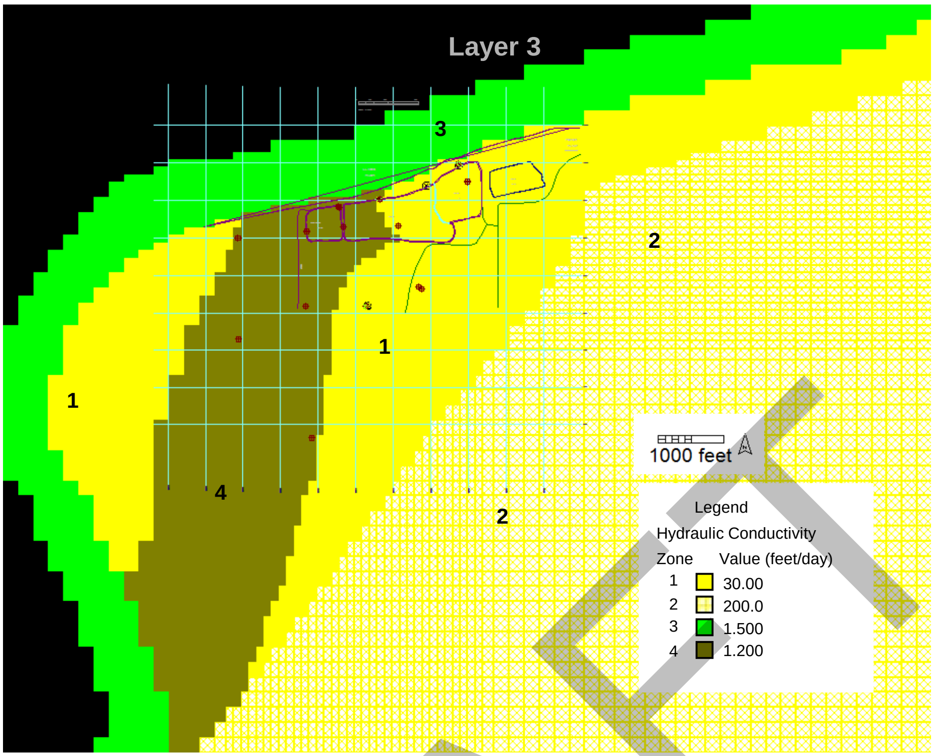

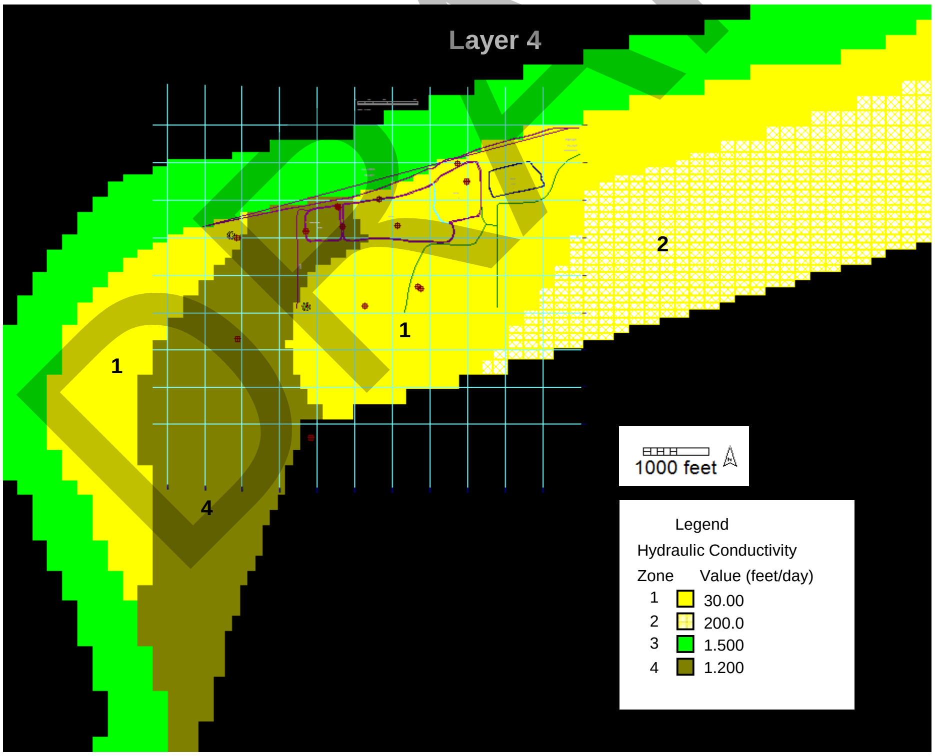

PREPARED BY/DATE:
M_W /08072017
REVIEWED BY/DATE:
BGH /08252017

Hydraulic Conductivity (ft/d) Array - Layers 3 (top) and 4 (bottom)

GROUNDWATER MODEL REPORT
HENNEPIN POWER STATION, WEST ASH POND SYSTEM
DYNEGY MIDWEST GENERATION, LLC

PROJECT NO: 2413

FIGURE NO: 2-4

Natural Resource Technology
AN OBG COMPANY

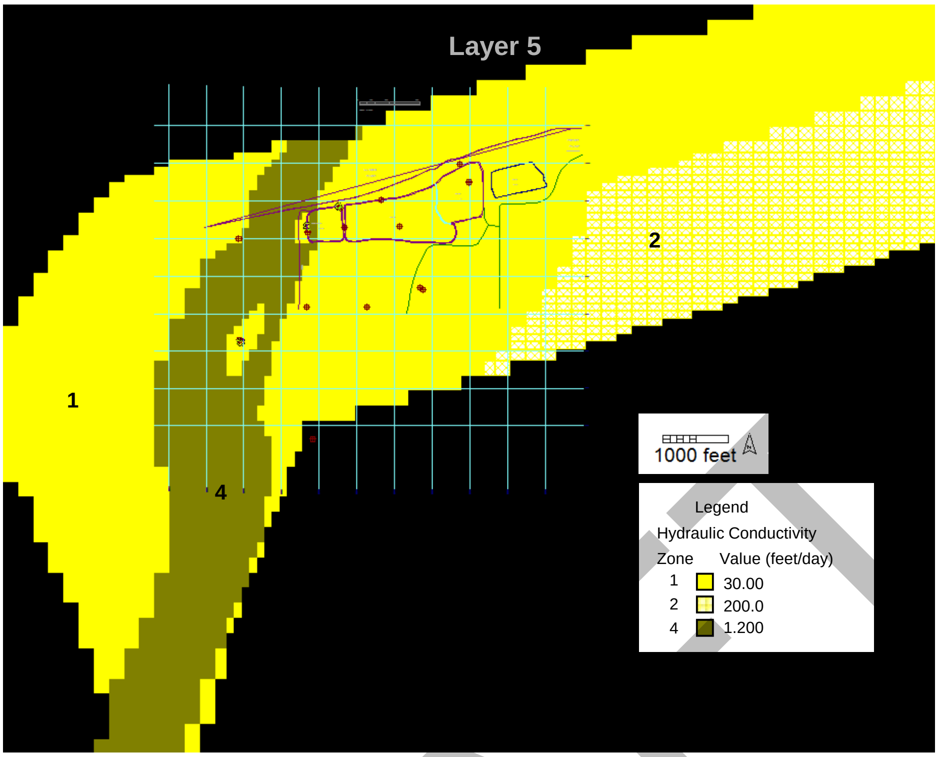

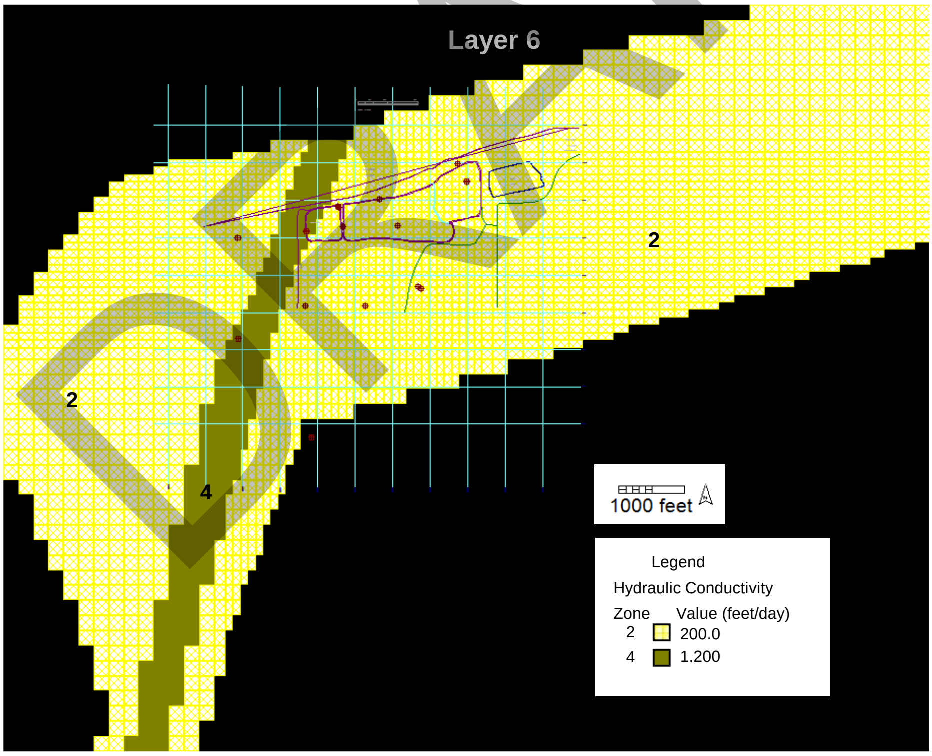

PREPARED BY/DATE:
M_W /08072017
REVIEWED BY/DATE:
BGH /08252017

Hydraulic Conductivity (ft/d) Array - Layers (top) 5 and 6 (bottom)

GROUNDWATER MODEL REPORT
HENNEPIN POWER STATION, WEST ASH POND SYSTEM
DYNEGY MIDWEST GENERATION, LLC

PROJECT NO: 2413

FIGURE NO: 2-4

Natural Resource Technology
AN OBG COMPANY

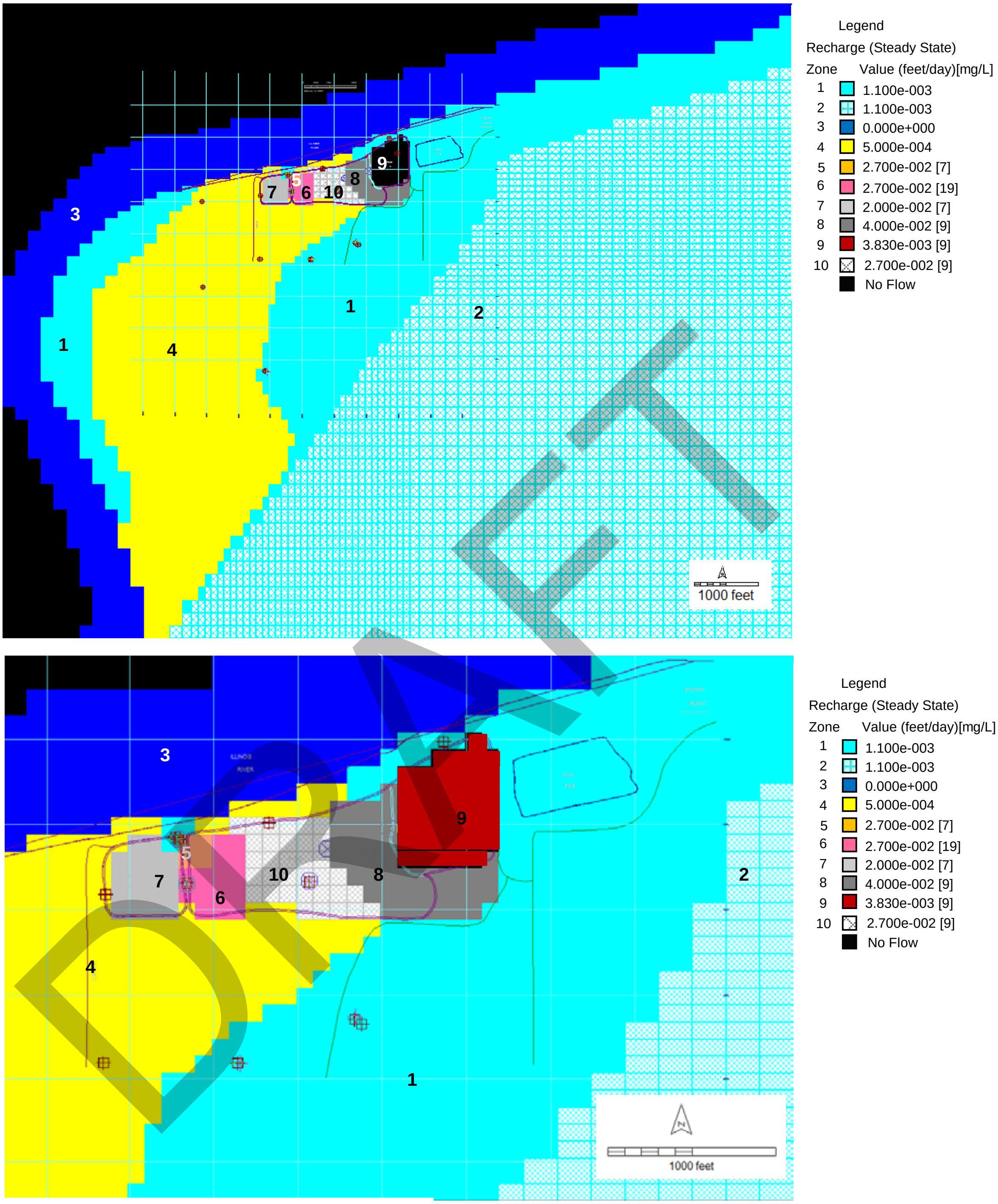

Note: Top is entire model, bottom is zoomed around impoundment. Values listed in legend are for the steady state model.

PREPARED BY/DATE:
M_W /08072017
REVIEWED BY/DATE:
BGH /08252017

Recharge (ft/d) Array (Steady State Model)

GROUNDWATER MODEL REPORT
HENNEPIN POWER STATION, WEST ASH POND SYSTEM
DYNEGY MIDWEST GENERATION, LLC

PROJECT NO: 2413

FIGURE NO: 2-5

Natural Resource Technology
AN OBG COMPANY

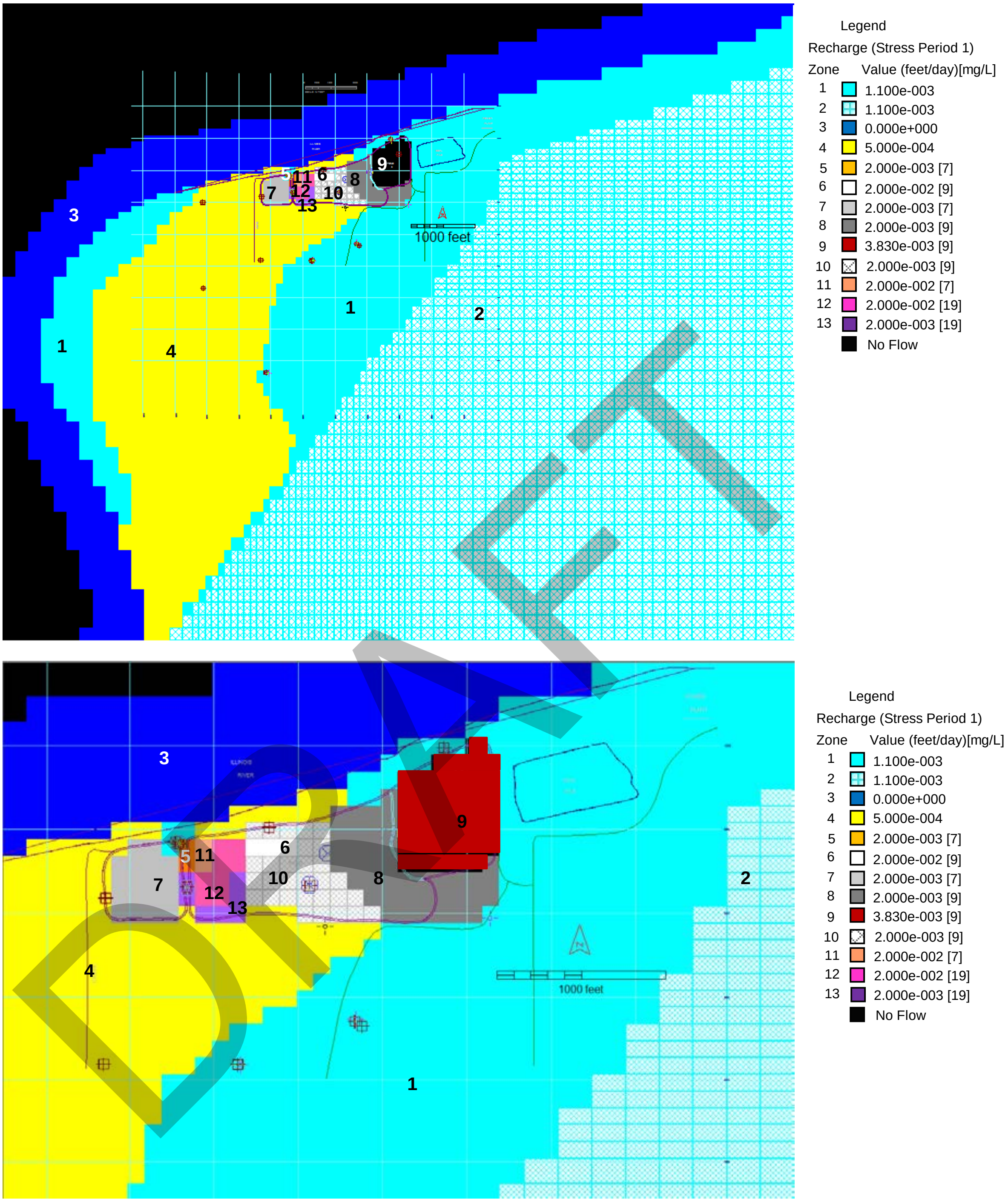

Note: Top is entire model, bottom is zoomed around impoundment. Values listed in legend are for the transient calibration scenario.

PREPARED BY/DATE:
M_W /08072017
REVIEWED BY/DATE:
BGH /08252017

Recharge (ft/d) Array (Transient Model, Stress Period 1)

GROUNDWATER MODEL REPORT
HENNEPIN POWER STATION, WEST ASH POND SYSTEM
DYNEGY MIDWEST GENERATION, LLC

PROJECT NO: 2413

FIGURE NO: 2-5

Natural Resource Technology
AN OBG COMPANY

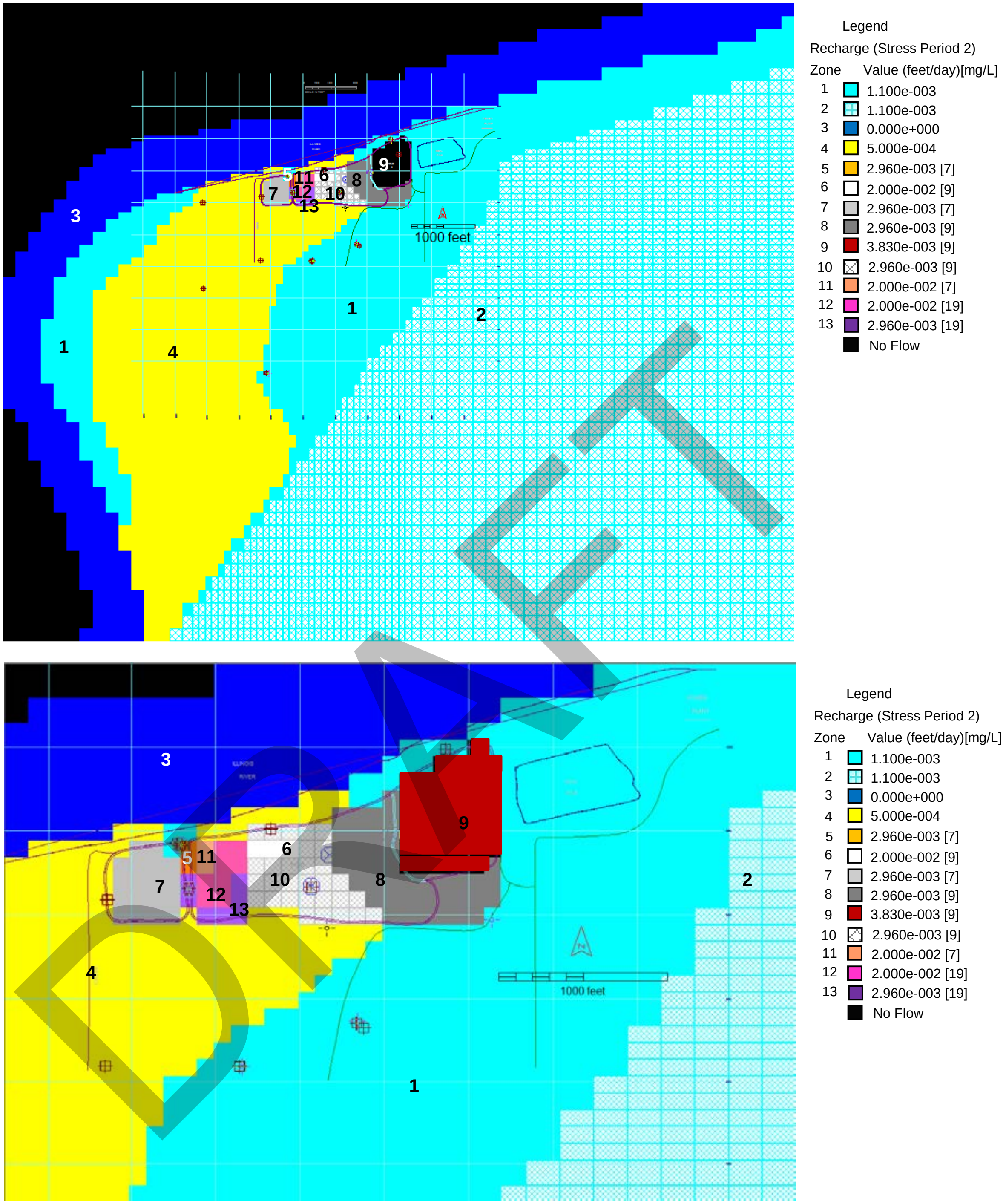

Note: Top is entire model, bottom is zoomed around impoundment. Values listed in legend are for the transient calibration scenario.

PREPARED BY/DATE:
M_W /08072017
REVIEWED BY/DATE:
BGH /08252017

Recharge (ft/d) Array (Transient Model, Stress Period 2)

GROUNDWATER MODEL REPORT
HENNEPIN POWER STATION, WEST ASH POND SYSTEM
DYNEGY MIDWEST GENERATION, LLC

PROJECT NO: 2413

FIGURE NO: 2-5

Natural Resource Technology
AN OBG COMPANY

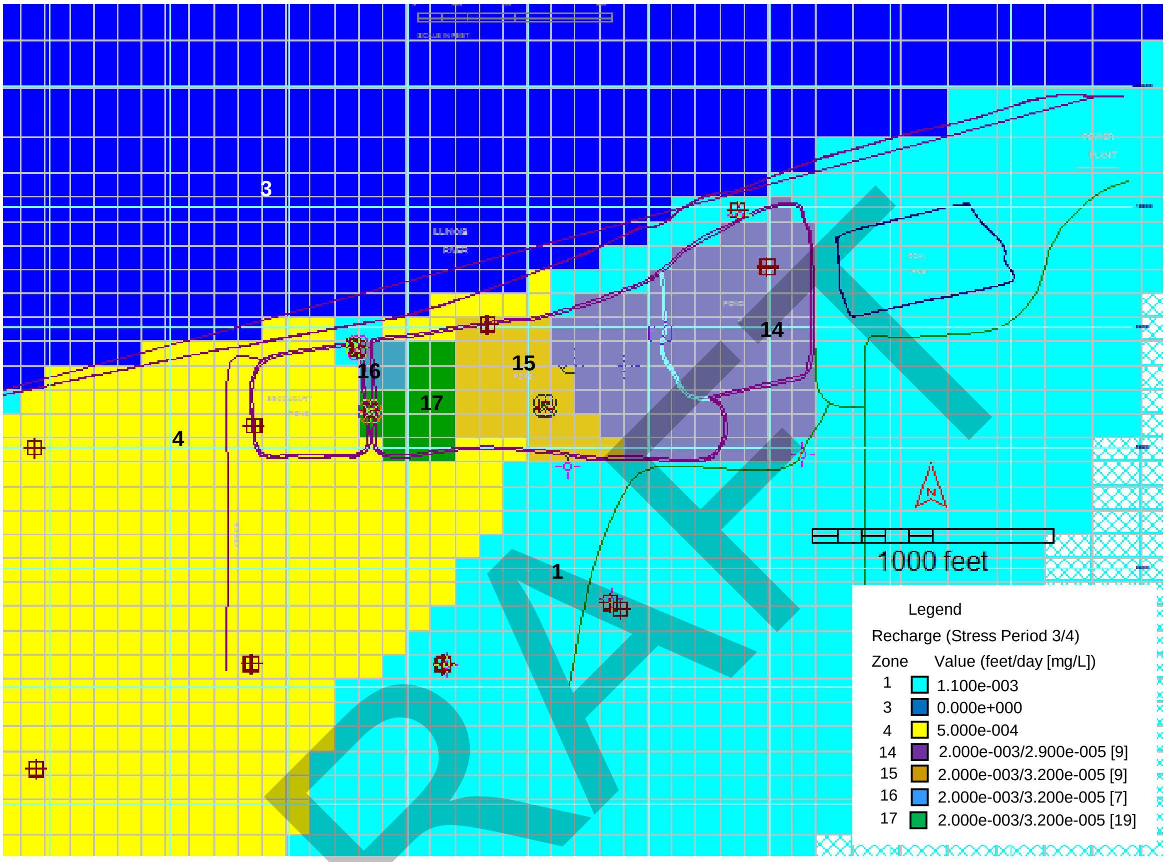

PREPARED BY/DATE:
M_W /08072017
REVIEWED BY/DATE:
BGH /08252017

Recharge (ft/d) Array
(Prediction Model, Stress Periods 3 & 4)

GROUNDWATER MODEL REPORT
HENNEPIN POWER STATION, WEST ASH POND SYSTEM
DYNEGY MIDWEST GENERATION, LLC

PROJECT NO: 2413

FIGURE NO: 2-6

Natural Resource Technology
AN OBG COMPANY

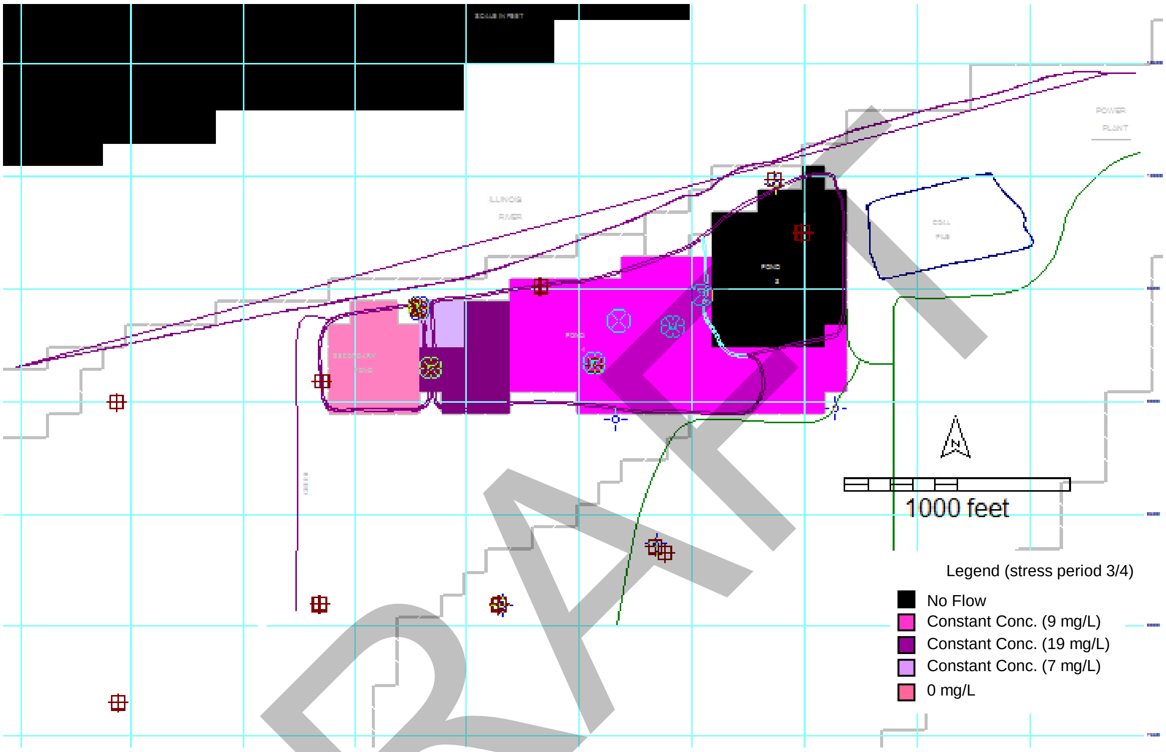

PREPARED BY/DATE:
M_W /08072017
REVIEWED BY/DATE:
BGH /08252017

Constant Concentration Boundary Conditions (Prediction Model, Stress Periods 3 & 4)

GROUNDWATER MODEL REPORT
HENNEPIN POWER STATION, WEST ASH POND SYSTEM
DYNEGY MIDWEST GENERATION, LLC

PROJECT NO: 2413

FIGURE NO: 2-7

Natural Resource Technology
AN OBG COMPANY

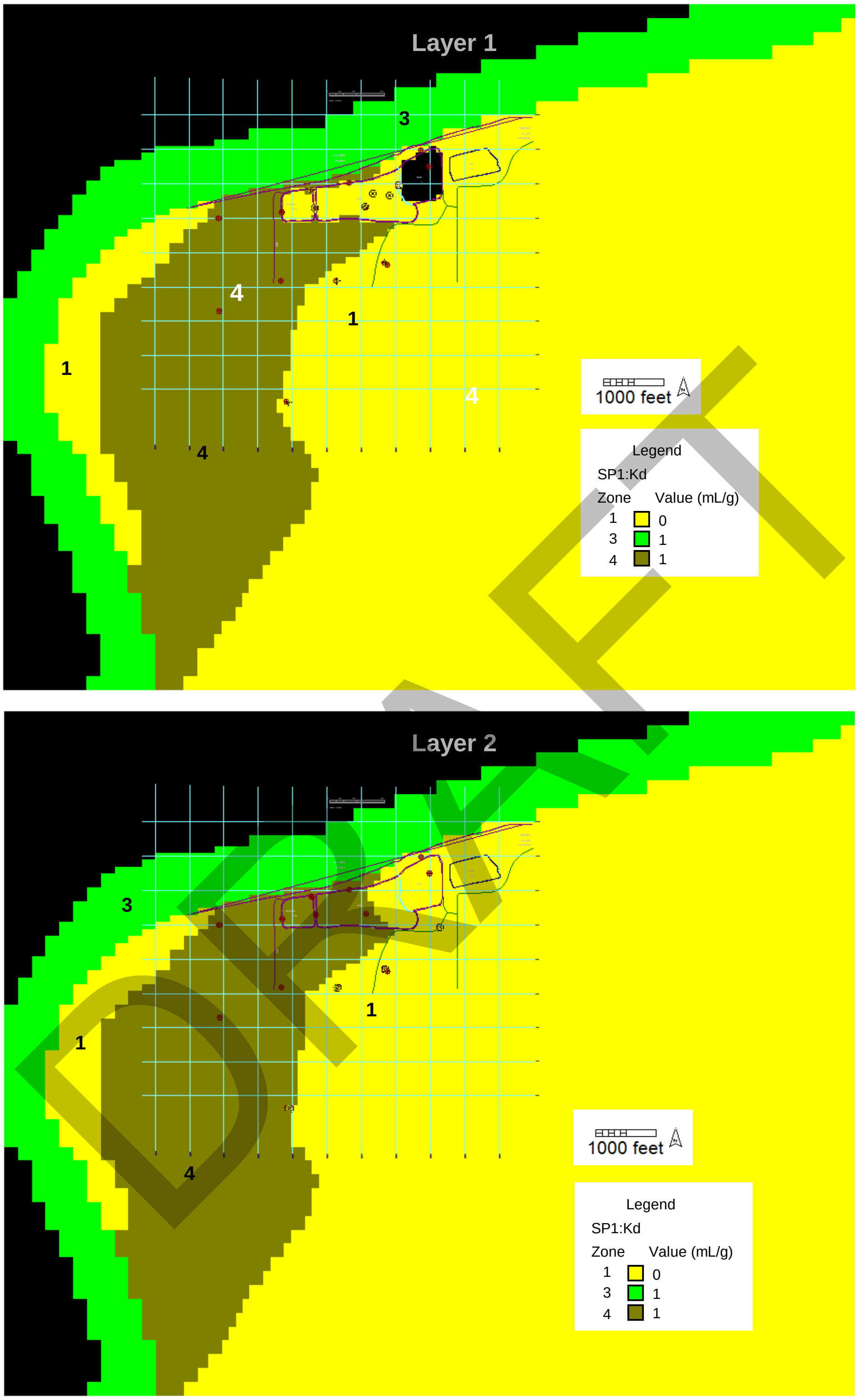

PREPARED BY/DATE:
M_W /08072017
REVIEWED BY/DATE:
BGH /08252017

Distribution Coefficient (mL/g) Array - Layers 1 (top) and 2 (bottom)

GROUNDWATER MODEL REPORT
HENNEPIN POWER STATION, WEST ASH POND SYSTEM
DYNEGY MIDWEST GENERATION, LLC

PROJECT NO: 2413

FIGURE NO: 2-8

Natural Resource Technology
AN OBG COMPANY

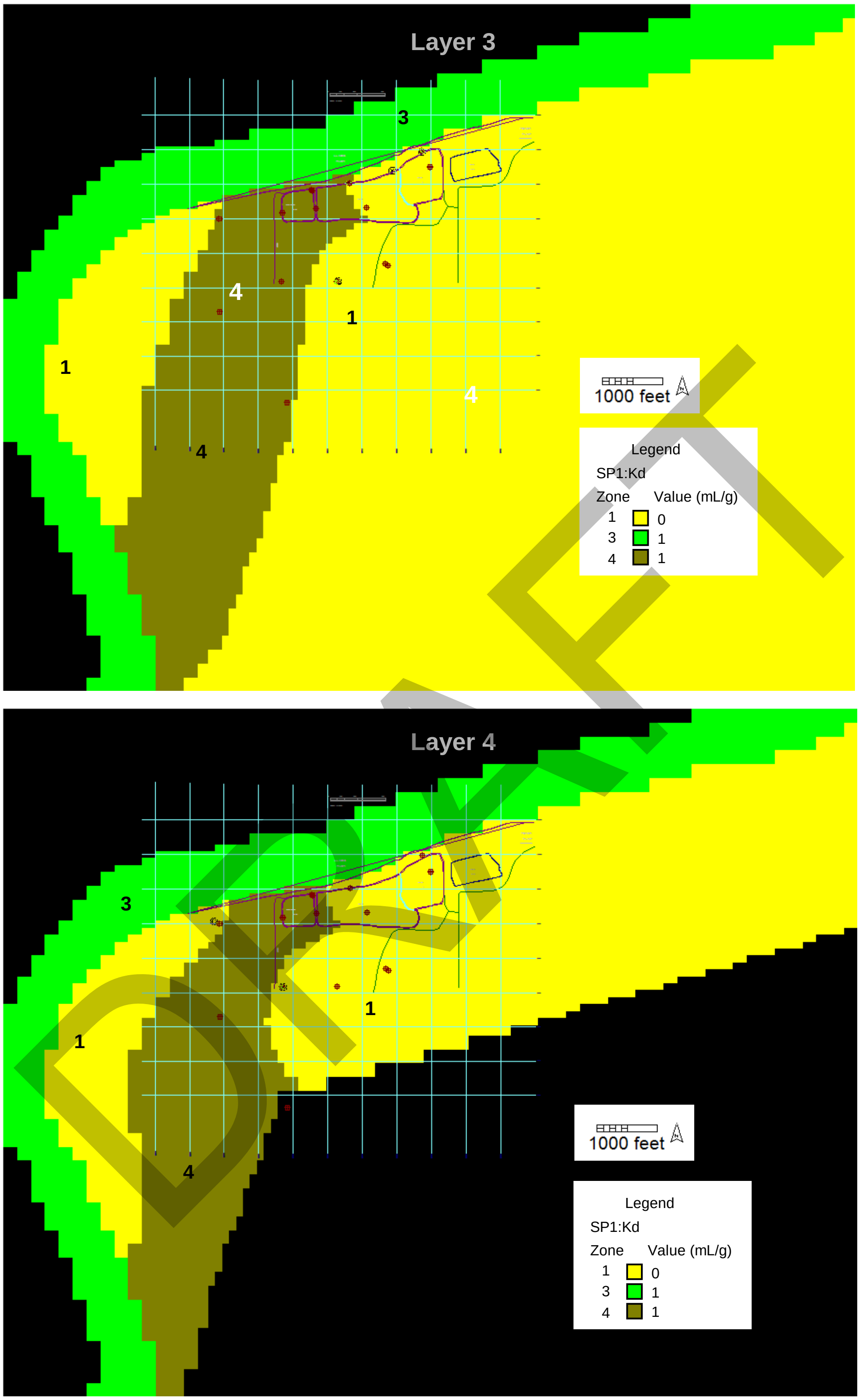

PREPARED BY/DATE:
M_W /08072017
REVIEWED BY/DATE:
BGH /08252017

Distribution Coefficient (mL/g) Array - Layers 3 (top) and 4 (bottom)

GROUNDWATER MODEL REPORT
HENNEPIN POWER STATION, WEST ASH POND SYSTEM
DYNEGY MIDWEST GENERATION, LLC

PROJECT NO: 2413

FIGURE NO: 2-8

Natural Resource Technology
AN OBG COMPANY

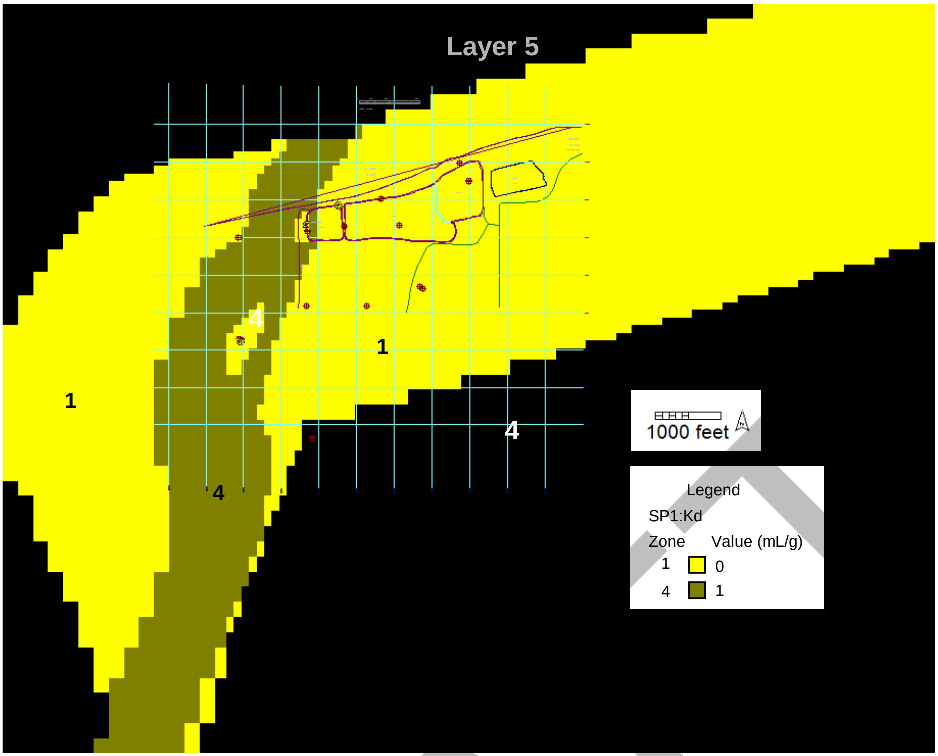

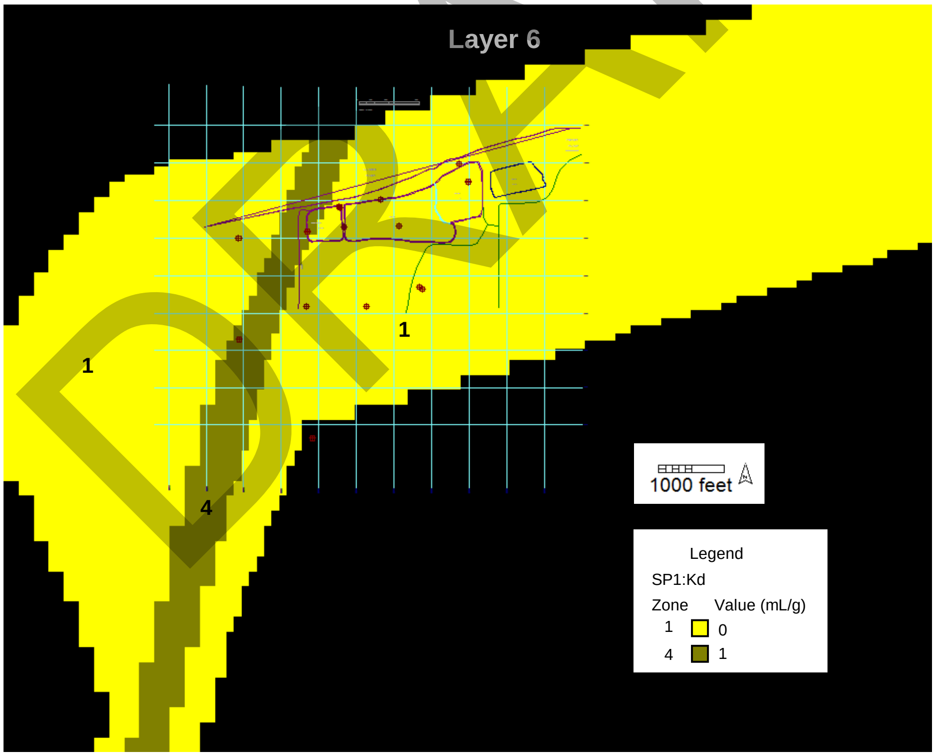

PREPARED BY/DATE:
M_W /08072017
REVIEWED BY/DATE:
BGH /08252017

Distribution Coefficient (mL/g) Array - Layers 5 (top) and 6 (bottom)

GROUNDWATER MODEL REPORT
HENNEPIN POWER STATION, WEST ASH POND SYSTEM
DYNEGY MIDWEST GENERATION, LLC

PROJECT NO: 2413

FIGURE NO: 2-8

Natural Resource Technology
AN OBG COMPANY

Observed vs. Computed Target Values

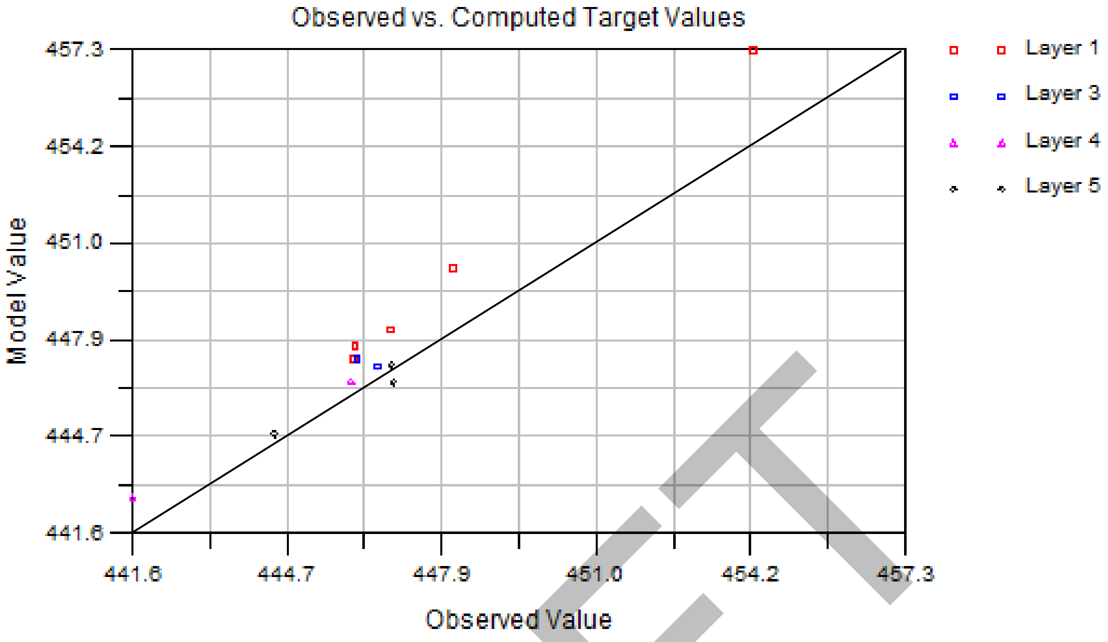

Observed vs. Residuals

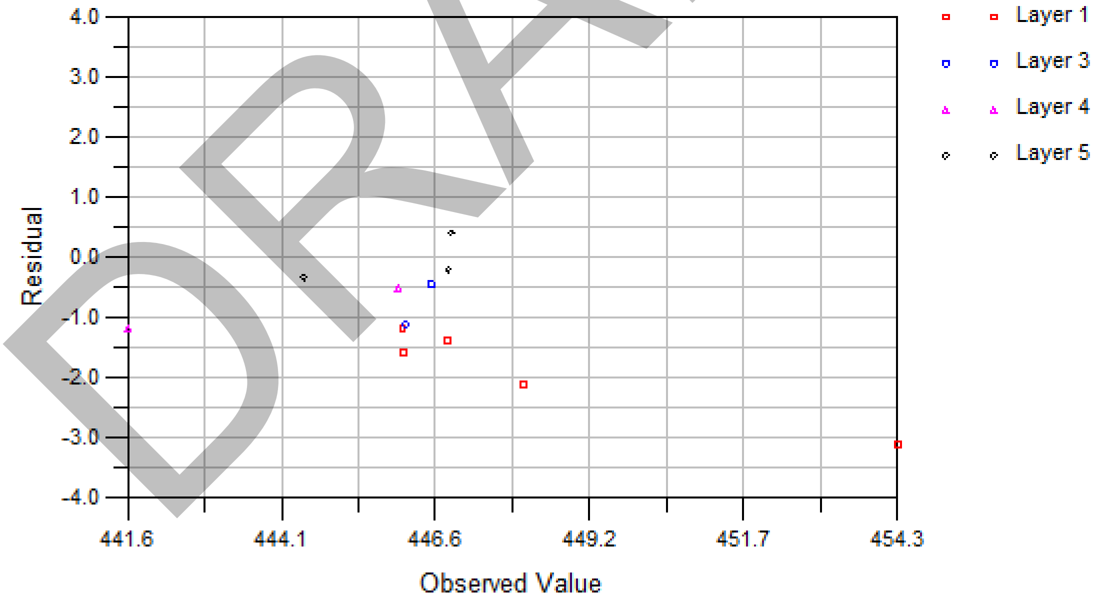

Note: Top plot displays observed heads versus simulated heads, and bottom plots displays observed heads versus residuals.

PREPARED BY/DATE:
M_W /08072017
REVIEWED BY/DATE:
BGH /08252017

Steady-State MODFLOW Model Calibration Results

GROUNDWATER MODEL REPORT
HENNEPIN POWER STATION, WEST ASH POND SYSTEM
DYNEGY MIDWEST GENERATION, LLC

PROJECT NO: 2413

FIGURE NO: 3-1

Natural Resource Technology
AN OBG COMPANY

PREPARED BY/DATE:
M_W /08072017
REVIEWED BY/DATE:
BGH /08252017

Comparison of Calibration Heads to Observations from 1994 through 2016

GROUNDWATER MODEL REPORT
HENNEPIN POWER STATION, WEST ASH POND SYSTEM
DYNEGY MIDWEST GENERATION, LLC

PROJECT NO: 2413

FIGURE NO: 3-2

Natural Resource Technology
AN OBG COMPANY

PREPARED BY/DATE:
M_W /08072017
REVIEWED BY/DATE:
BGH /08252017

Comparison of Calibration Heads to Observations from 1994 through 2016

GROUNDWATER MODEL REPORT
HENNEPIN POWER STATION, WEST ASH POND SYSTEM
DYNEGY MIDWEST GENERATION, LLC

PROJECT NO: 2413

FIGURE NO: 3-2

Natural Resource Technology
AN OBG COMPANY

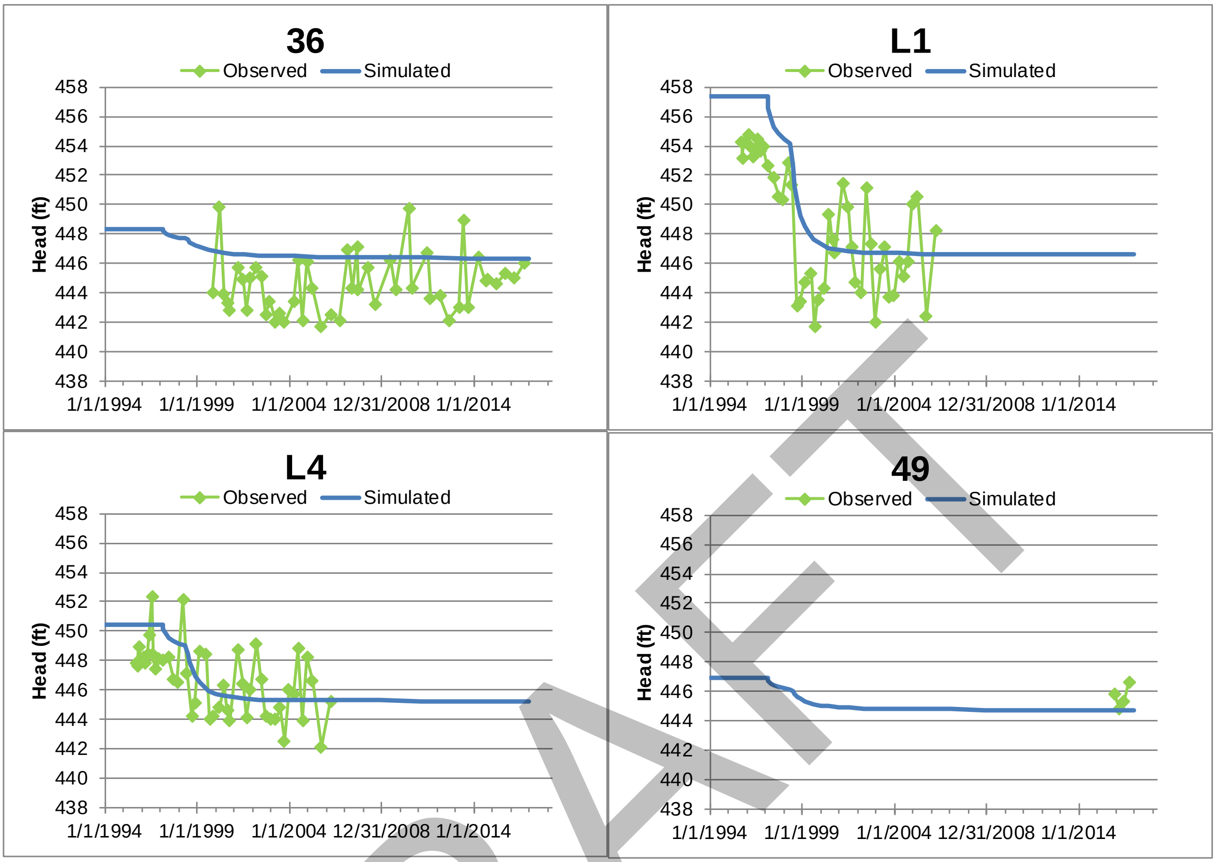

Figure 2-11(Cont'd). Comparison of Calibration Heads to Observations from 1994 through 2013.

PREPARED BY/DATE:
M_W /08072017
REVIEWED BY/DATE:
BGH /08252017

Comparison of Calibration Heads to Observations from 1994 through 2016

GROUNDWATER MODEL REPORT
HENNEPIN POWER STATION, WEST ASH POND SYSTEM
DYNEGY MIDWEST GENERATION, LLC

PROJECT NO: 2413

FIGURE NO: 3-2

Natural Resource Technology
AN OBG COMPANY

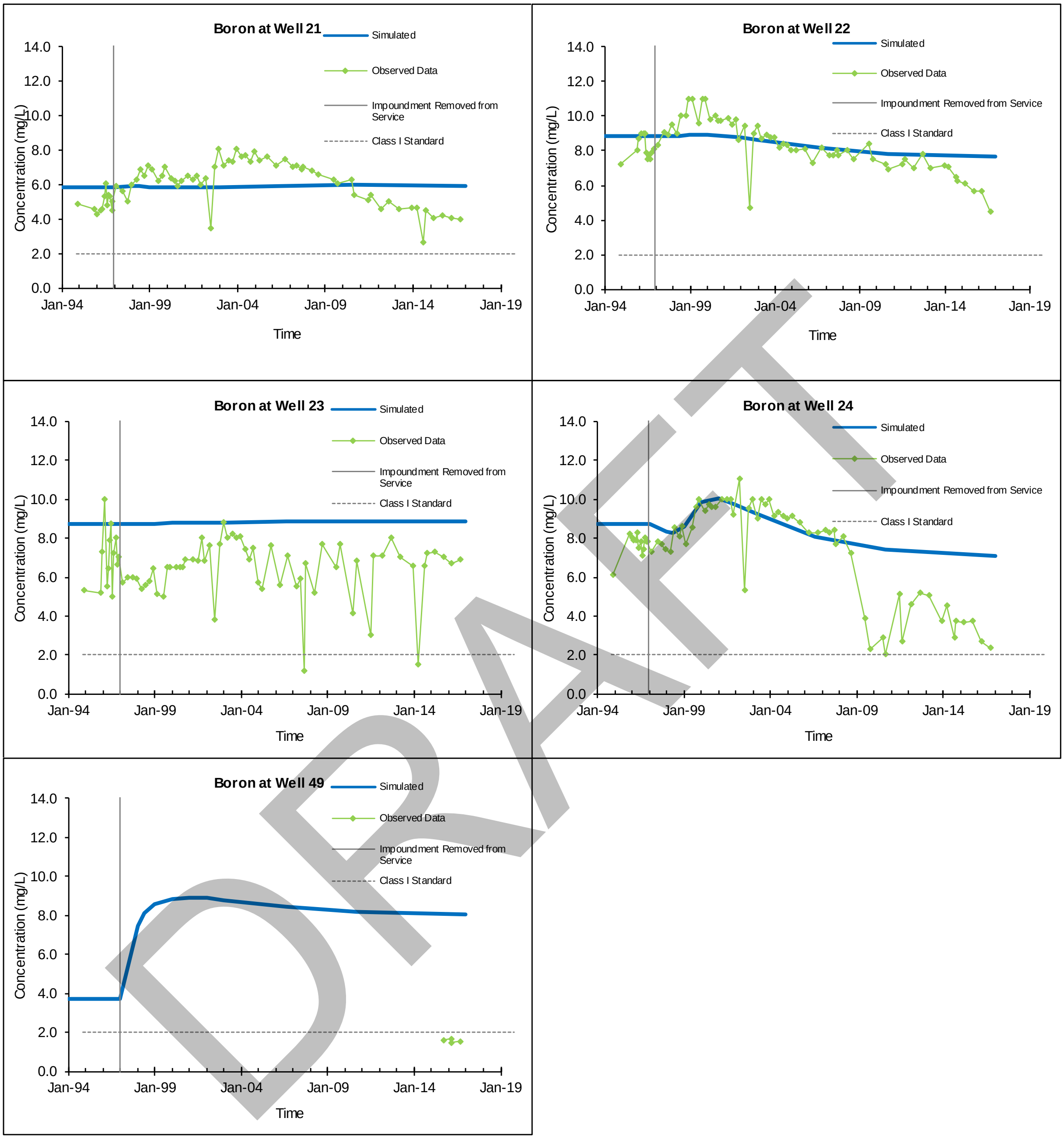

PREPARED BY/DATE:
M_W /08072017
REVIEWED BY/DATE:
BGH /08252017

Comparison of Calibration Boron Concentrations to Observations from 1994 through 2016

GROUNDWATER MODEL REPORT
HENNEPIN POWER STATION, WEST ASH POND SYSTEM
DYNEGY MIDWEST GENERATION, LLC

PROJECT NO: 2413

FIGURE NO: 3-3

Natural Resource Technology
AN OBG COMPANY

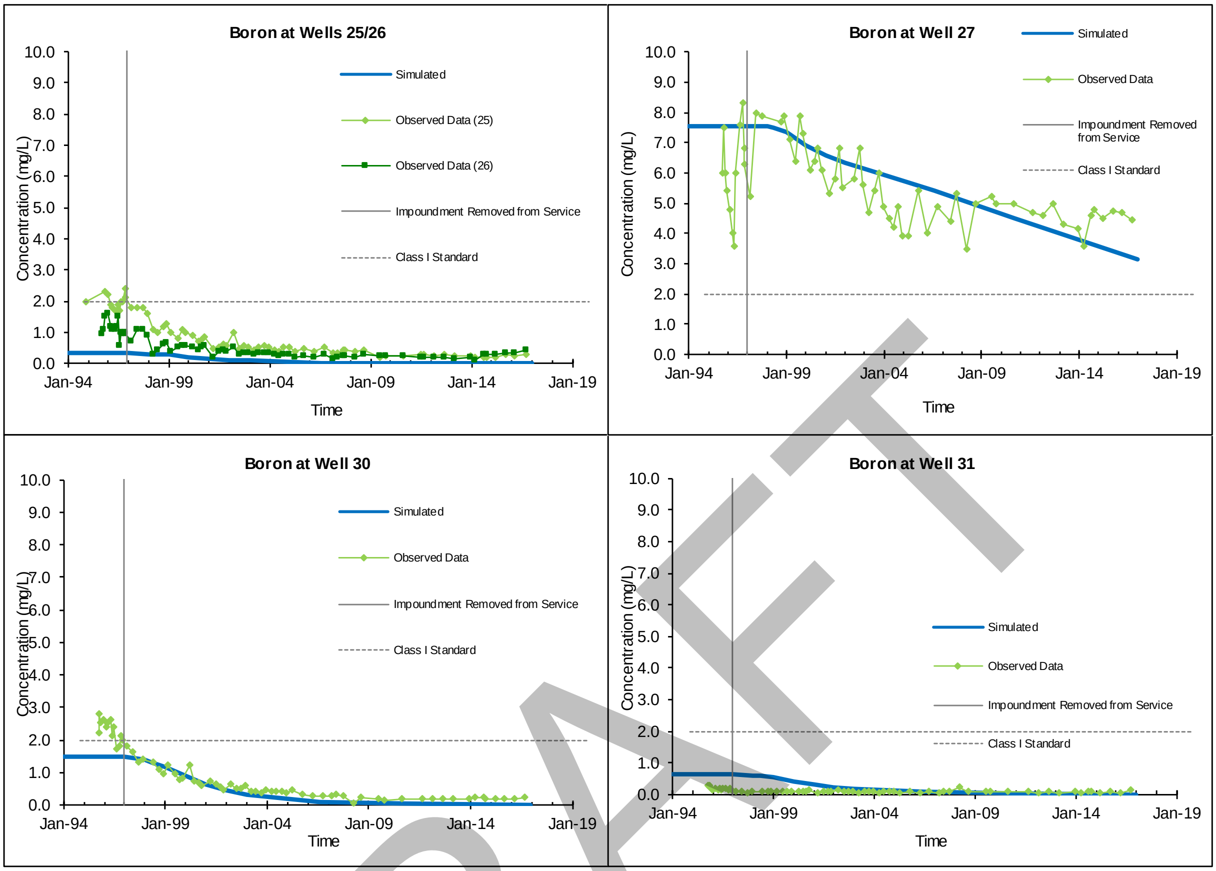

PREPARED BY/DATE:
M_W /08072017
REVIEWED BY/DATE:
BGH /08252017

Comparison of Calibration Boron Concentrations to Observations from 1994 through 2016

GROUNDWATER MODEL REPORT
HENNEPIN POWER STATION, WEST ASH POND SYSTEM
DYNEGY MIDWEST GENERATION, LLC

PROJECT NO: 2413

FIGURE NO: 3-3

Natural Resource Technology
AN OBG COMPANY

PREPARED BY/DATE:
M_W /08072017
REVIEWED BY/DATE:
BGH /08252017

Comparison of Predicted Heads between Baseline and Capping Scenarios

GROUNDWATER MODEL REPORT
HENNEPIN POWER STATION, WEST ASH POND SYSTEM
DYNEGY MIDWEST GENERATION, LLC

PROJECT NO: 2413

FIGURE NO: 3-4

Natural Resource Technology
AN OBG COMPANY

PREPARED BY/DATE:
M_W /08072017
REVIEWED BY/DATE:
BGH /08252017

Comparison of Predicted Heads between Baseline and Capping Scenarios

GROUNDWATER MODEL REPORT
HENNEPIN POWER STATION, WEST ASH POND SYSTEM
DYNEGY MIDWEST GENERATION, LLC

PROJECT NO: 2413

FIGURE NO: 3-4

Natural Resource Technology
AN OBG COMPANY

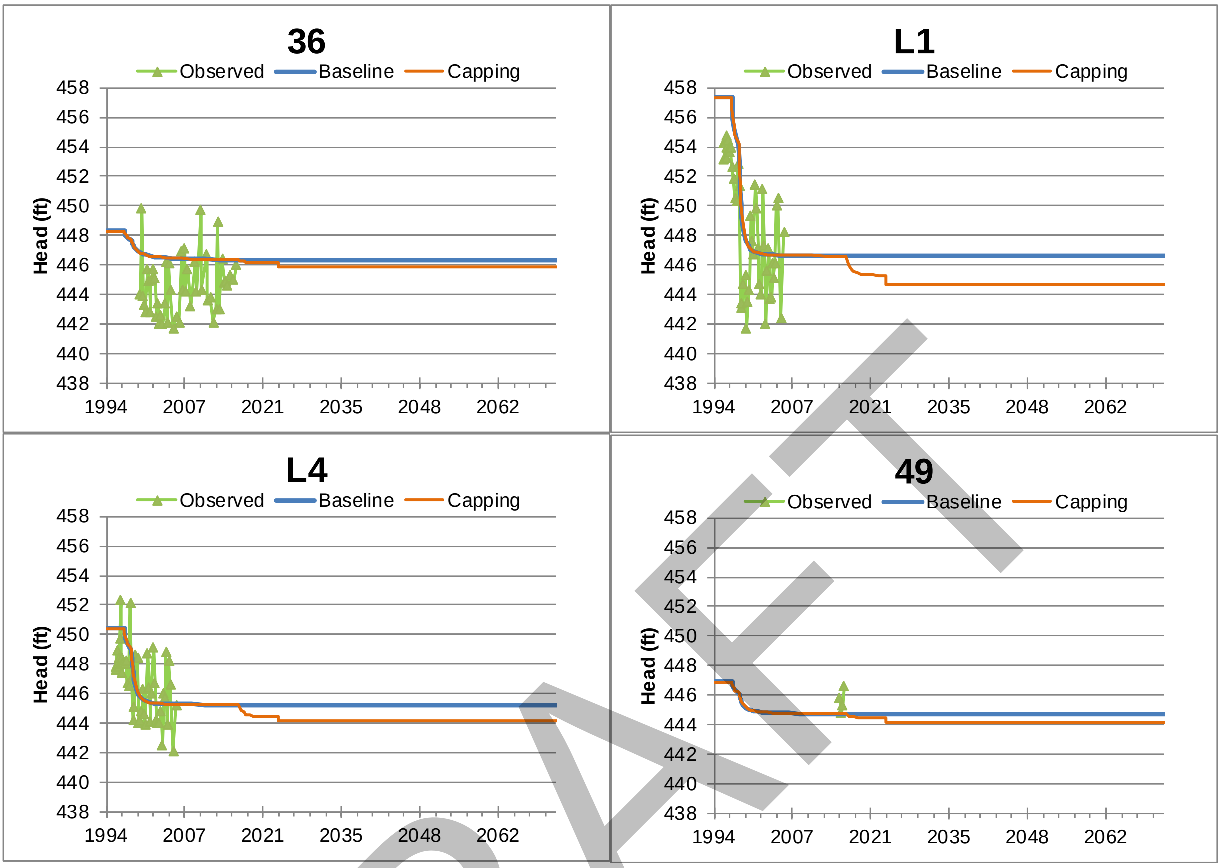

PREPARED BY/DATE:
M_W /08072017
REVIEWED BY/DATE:
BGH /08252017

Comparison of Predicted Heads between Baseline and Capping Scenarios

GROUNDWATER MODEL REPORT
HENNEPIN POWER STATION, WEST ASH POND SYSTEM
DYNEGY MIDWEST GENERATION, LLC

PROJECT NO: 2413

FIGURE NO: 3-4

Natural Resource Technology
AN OBG COMPANY

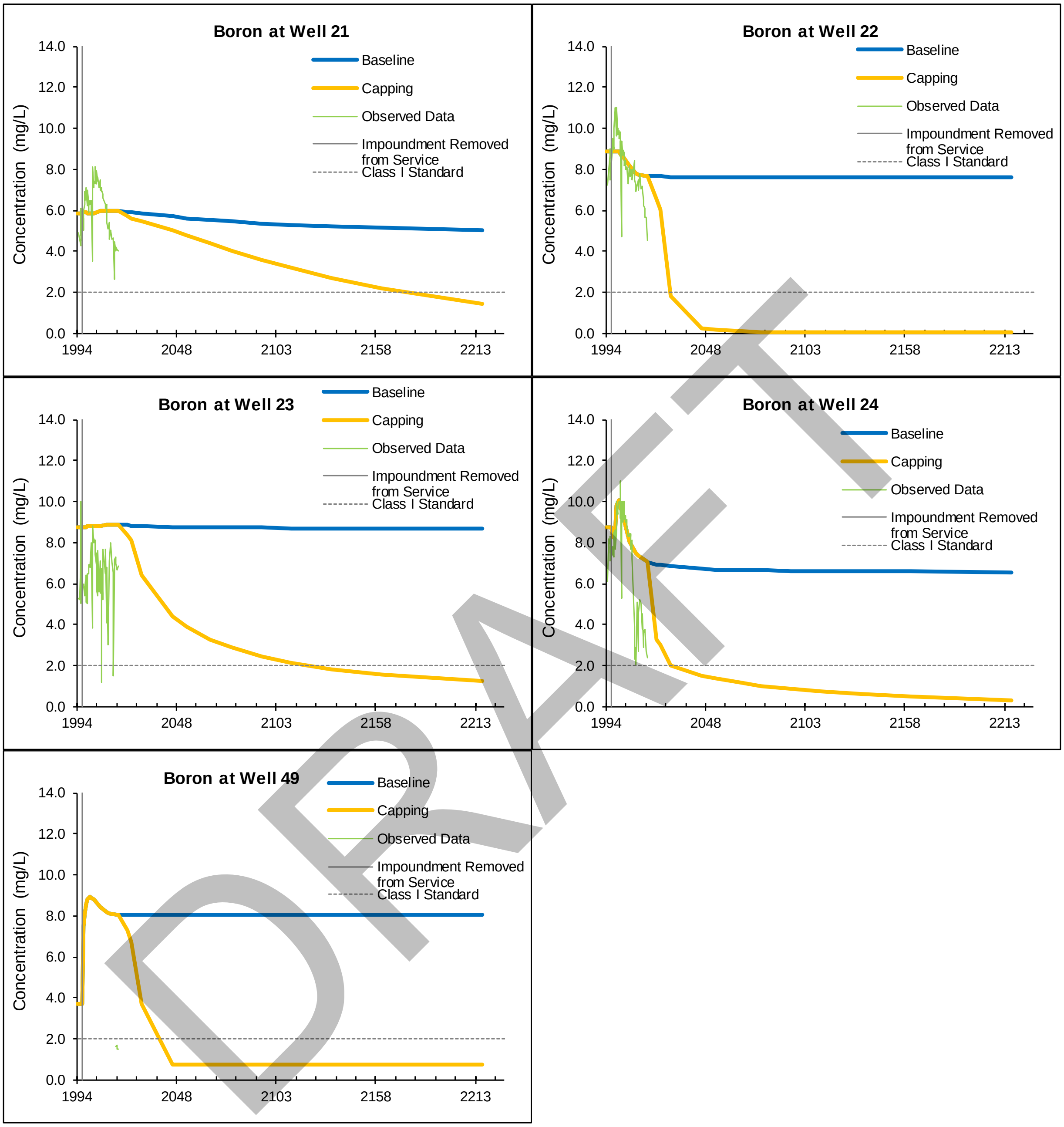

PREPARED BY/DATE:
M_W /08072017
REVIEWED BY/DATE:
BGH /08252017

Comparison of Predicted Boron Concentrations between Baseline and Capping Scenarios

GROUNDWATER MODEL REPORT
HENNEPIN POWER STATION, WEST ASH POND SYSTEM
DYNEGY MIDWEST GENERATION, LLC

PROJECT NO: 2413

FIGURE NO: 3-5

Natural Resource Technology
AN OBG COMPANY

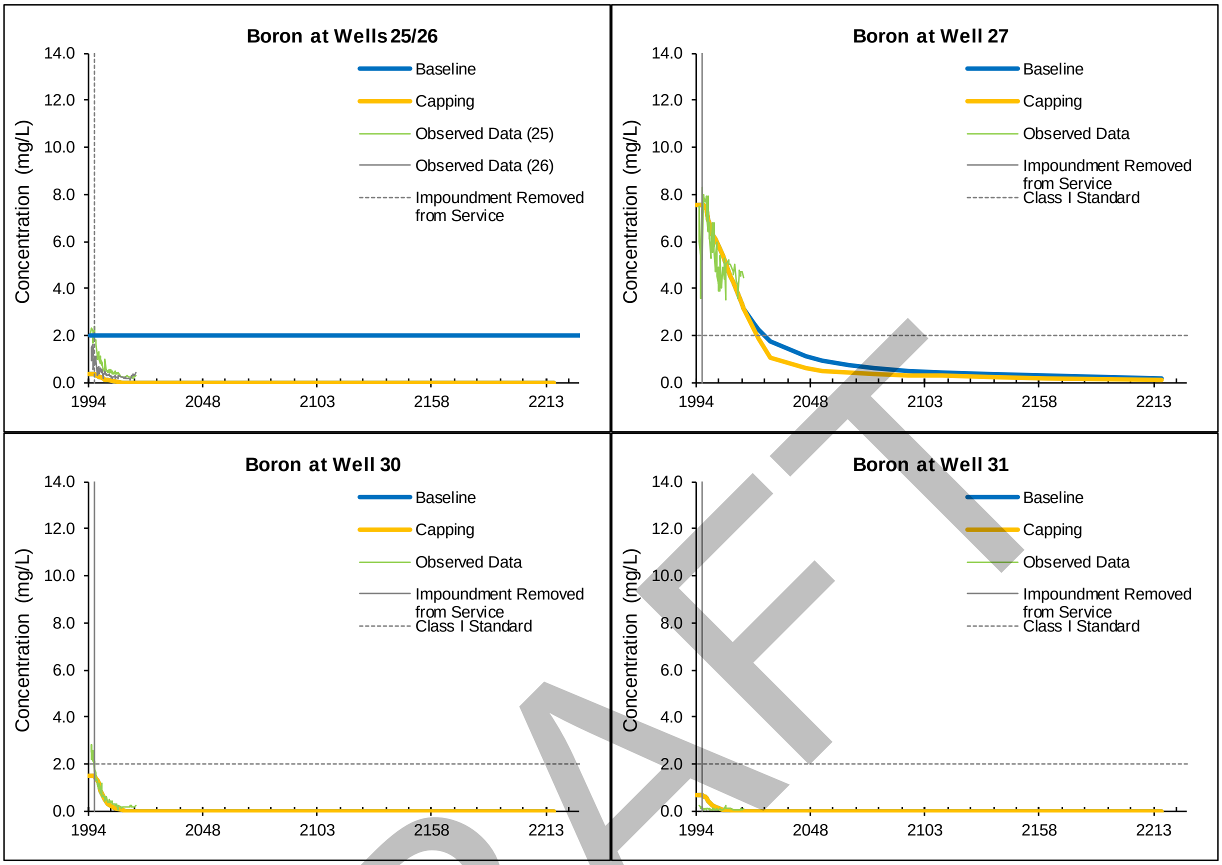

PREPARED BY/DATE:
M_W /08072017
REVIEWED BY/DATE:
BGH /08252017

Comparison of Predicted Boron Concentrations between Baseline and Capping Scenarios

GROUNDWATER MODEL REPORT
HENNEPIN POWER STATION, WEST ASH POND SYSTEM
DYNEGY MIDWEST GENERATION, LLC

PROJECT NO: 2413

FIGURE NO: 3-5

Natural Resource Technology
AN OBG COMPANY

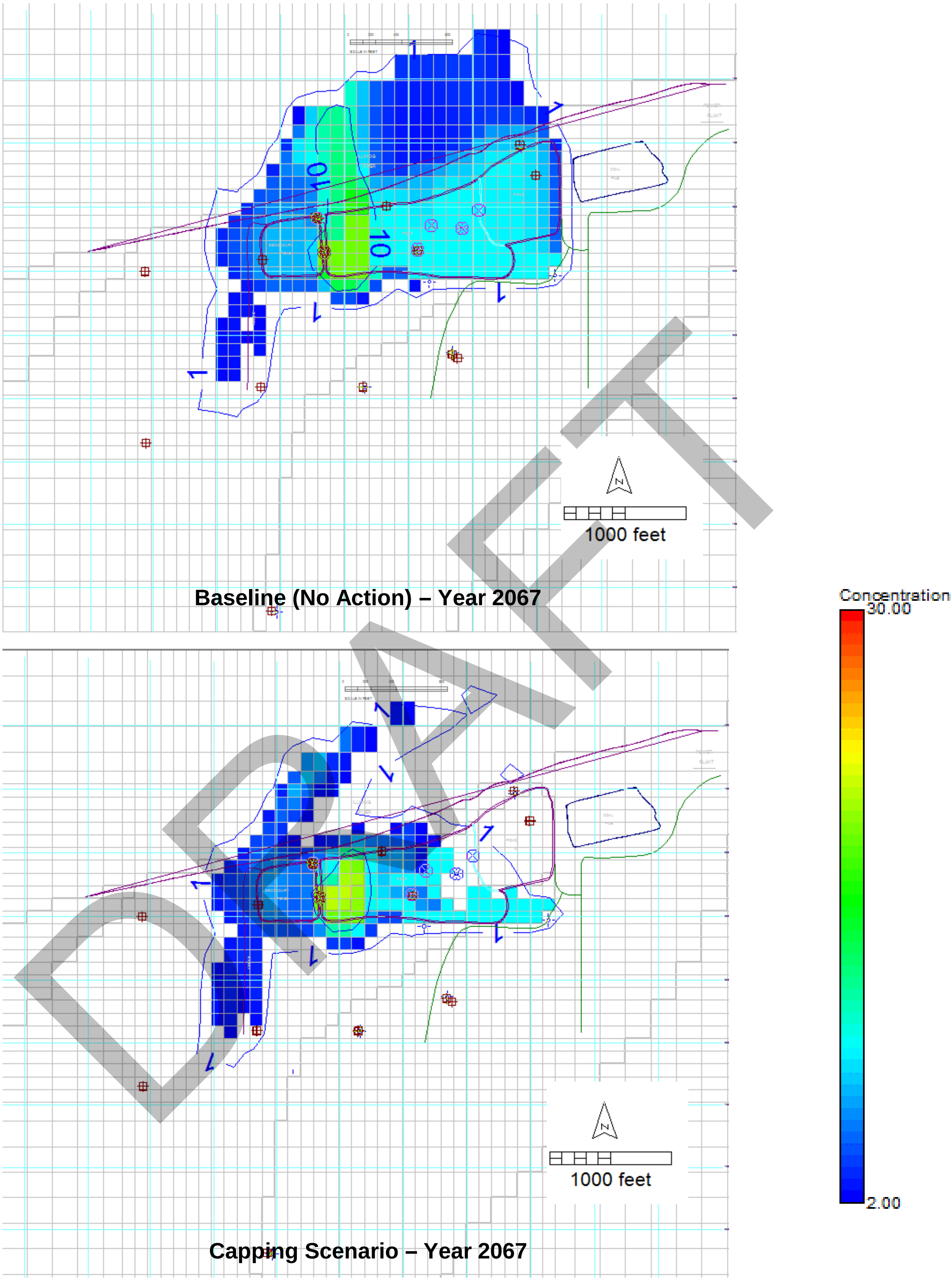

PREPARED BY/DATE:
M_W /08072017
REVIEWED BY/DATE:
BGH /08252017

Footprint of Boron Plume over 2 mg/L in Year 2067

GROUNDWATER MODEL REPORT
HENNEPIN POWER STATION, WEST ASH POND SYSTEM
DYNEGY MIDWEST GENERATION, LLC

PROJECT NO: 2413

FIGURE NO: 3-6

Natural Resource Technology
AN OBG COMPANY

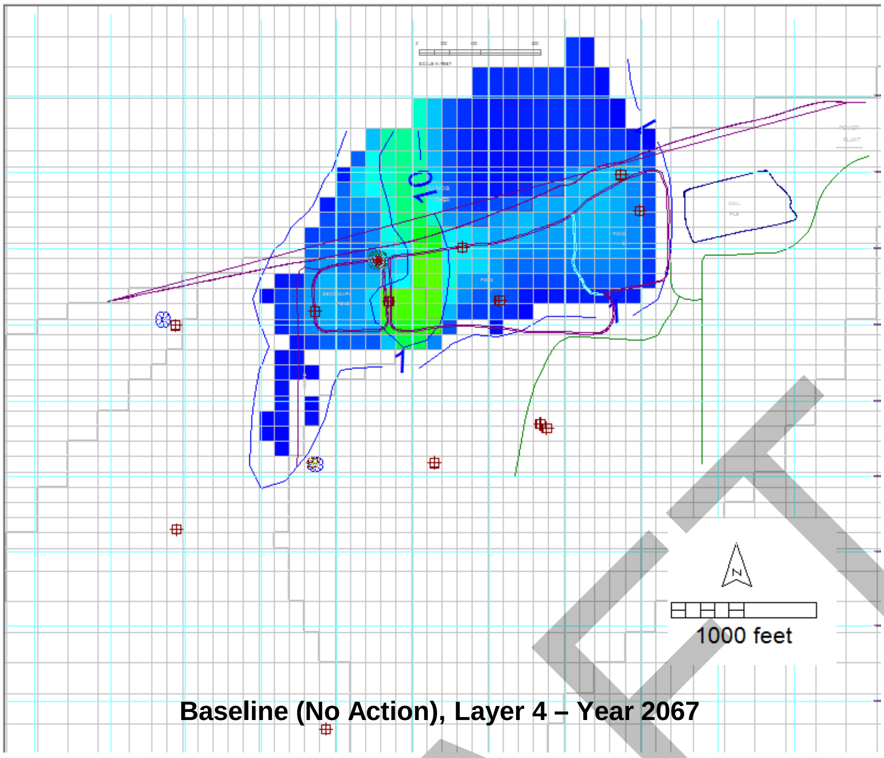

Baseline (No Action), Layer 4 – Year 2067

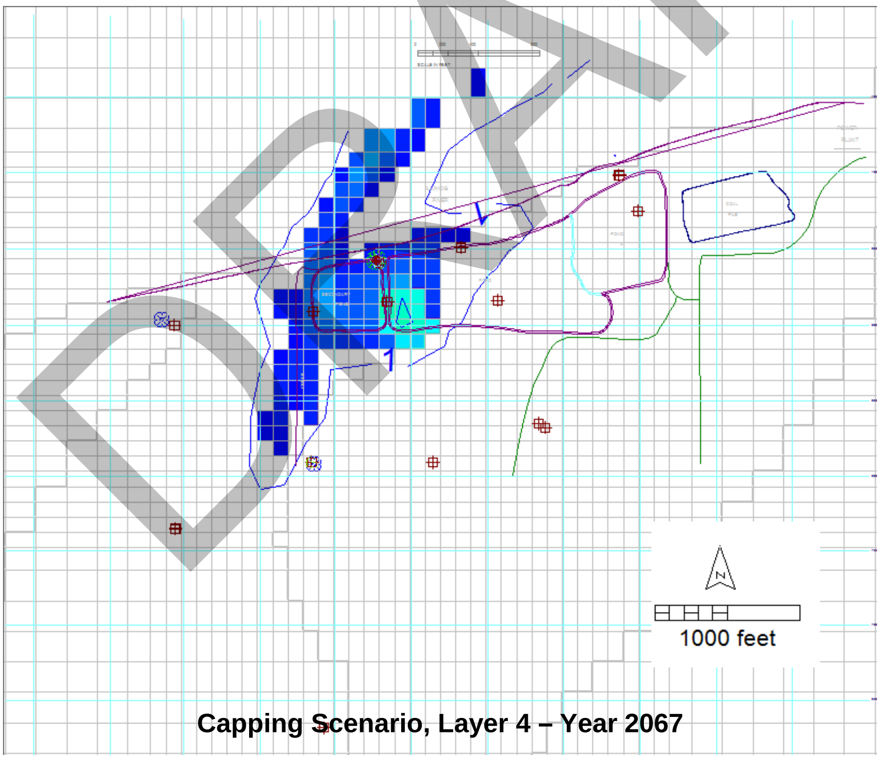

Capping Scenario, Layer 4 – Year 2067

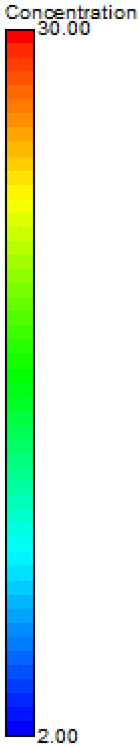

PREPARED BY/DATE:
M_W /08072017
REVIEWED BY/DATE:
BGH /08252017

Footprint of Boron Plume over 2 mg/L in Year 2067 (Layer 4)

GROUNDWATER MODEL REPORT
HENNEPIN POWER STATION, WEST ASH POND SYSTEM
DYNEGY MIDWEST GENERATION, LLC

PROJECT NO: 2413

FIGURE NO: 3-7

Natural Resource Technology
AN OBG COMPANY

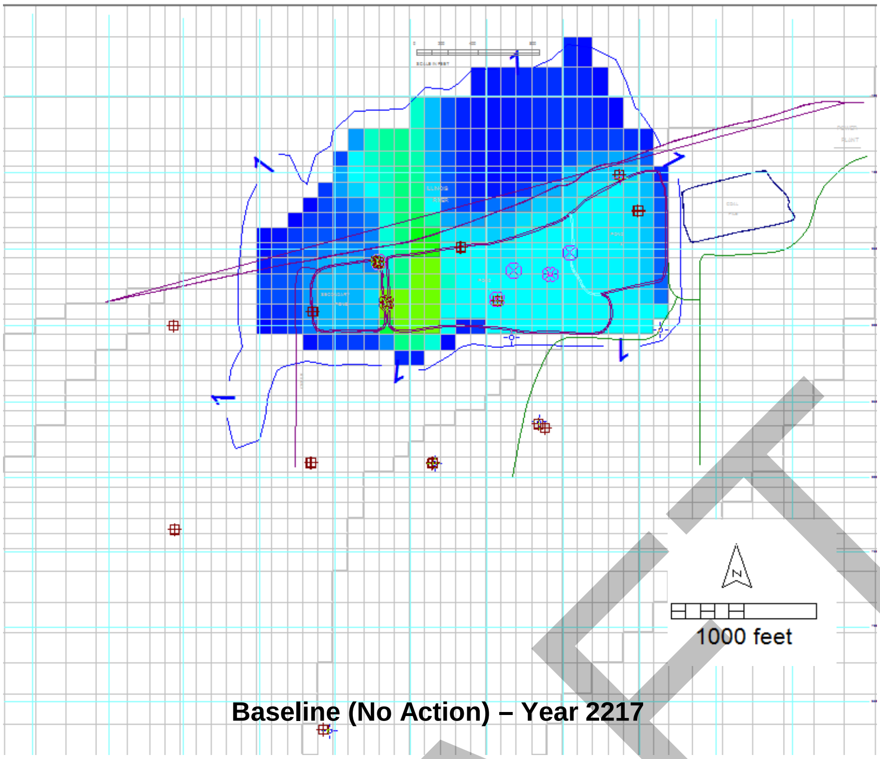

Baseline (No Action) – Year 2217

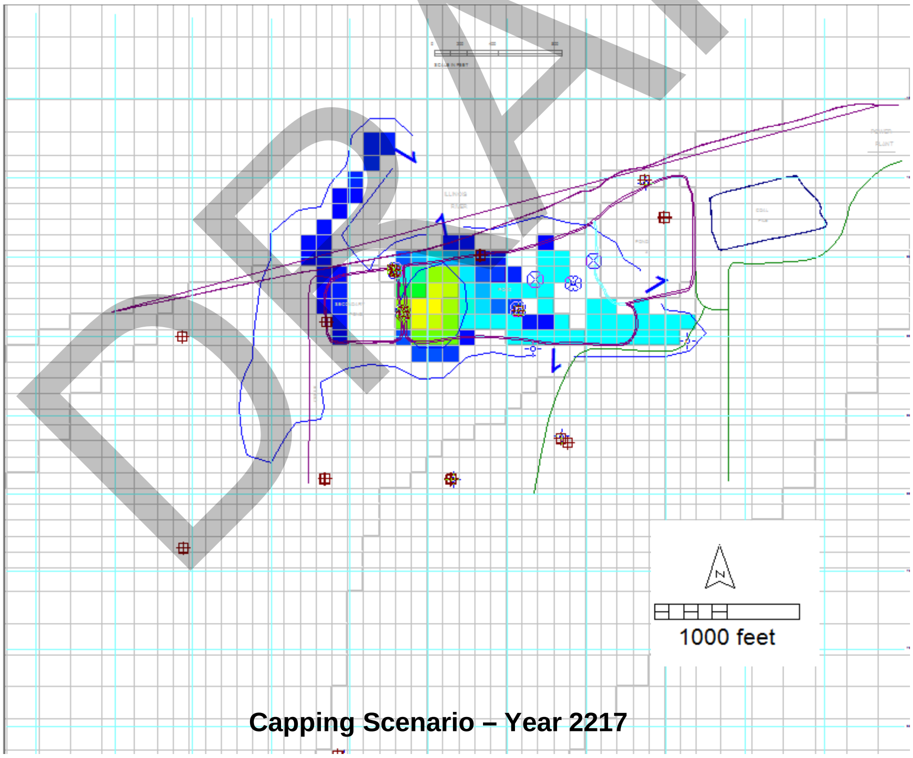

Capping Scenario – Year 2217

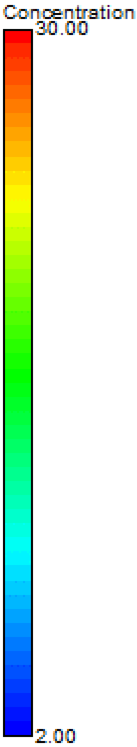

PREPARED BY/DATE:
M_W /08072017
REVIEWED BY/DATE:
BGH /08252017

Footprint of Boron Plume over 2 mg/L in Year 2217

GROUNDWATER MODEL REPORT
HENNEPIN POWER STATION, WEST ASH POND SYSTEM
DYNEGY MIDWEST GENERATION, LLC

PROJECT NO: 2413

FIGURE NO: 3-8

Natural Resource Technology
AN OBG COMPANY

Appendix A

MODFLOW and MT3DMS Modeling Files

(on CD)

OBG

THERE’S A WAY

Natural Resource Technology
AN OBG COMPANY

APPENDIX C

MATERIAL QUANTITY, LABOR, AND MILEAGE ESTIMATES FOR ALTERNATIVE 2 REMEDY

DYNEGY MIDWEST GENERATION, LLC - HENNEPIN POWER PLANT
CORRECTIVE ACTION ALTERNATIVES ANALYSIS SUPPORTING INFORMATION REPORT (CAAA-SIR)
ALTERNATIVE 2 - SOURCE CONTROL WITH CONTINUOUS CONTAINMENT SYSTEM[1]

ITEM NO.	ENGINEERING, PRE-CONSTRUCTION, AND CONSTRUCTION SUPPORT TASKS	Units	Quantity	Crew	Daily Output	Labor Hours	Equipment Hours	Notes
1	Engineering Support and CQA During Construction	LS	1	Eng	12	6,240	2,080	Assumed labor and equipment hours based on Ramboll project experience.
	ENGINEERING, PRE-CONSTRUCTION, AND CONSTRUCTION SUPPORT ESTIMATED SUBTOTAL					**6,240**	**2,080**	
ITEM NO.	**SITE PREPARATION**	**Units**	**Quantity**	**Crew**	**Daily Output**	**Labor Hours**	**Equipment Hours**	**Notes**
2	Staging/Laydown Area Preparation	-	-	-	-	1,295	390	Assumes the general work area associated with the cutoff wall will need to be graded and built-up in order to make way for construction equipment needed for the install.
	Subsurface Stabilization Nonwoven Geotextile	SY	19,400	2 Clab	2500	124	0	313219161550: Geosynthetic soil stabilization, geotextile fabric, non-woven, 120 lb tensile strength includes scarifying and compaction. This assumes stabilization of access roads, staging area, and material handling system.
	Construct Staging/Laydown Areas	SY	15,000	B14	615	1,171	390	015523500100: Temporary, roads, gravel fill, 8" gravel depth, excluding surfacing. Assumes 3-acre staging/laydown area.
3	Construction Soil Erosion & Sediment Controls	-	-	-	-	774	258	Assumes soil erosion and sediment controls will be implemented only during the cutoff wall construction.
	Silt Fence	LF	20,800	B62	650	768	256	312514161000: Synthetic erosion control, silt fence, install and remove, 3' high. Assumes silt fence is installed down both sides of the cutoff wall alignment (5,200 ft total per side) and the silt fence is replaced once during cutoff wall construction. (20,800 ft total)
	Straw Wattles	LF	250	A2	1000	6	2	312514160705: Sediment Log, Filter Sock, 9". Assume straw wattles are needed along perimeter of cutoff wall and staging/laydown area at an occurrence of 1 every 50 feet. Replaced straw wattles once.
4	Construction Facilities	MO - in use	-	-	-	24	-	Assumes office trailer, storage boxes, and portable toilets are required during the construction phase of the alternative.
	Office Trailer	MO - in use	24	B66	-	8	-	015213200350: Office trailer, furnished, no hookups, 32' x 8'. Assume quantity of one (1). Duration is assumed to be 24 months for construction with winter contingency.
	Storage Trailers	MO - in use	24	B66	-	8	-	015213201350: Storage boxes, 40' x 8'. Assume quantity of three (3). Duration is assumed to be 24 months for construction with winter contingency.
	Portable Toilet	MO - in use	24	B66	-	8	-	015433406410: Toilet, portable chemical. Assume quantity of four (4). Duration is assumed to be 24 months for construction with winter contingency.
5	Temporary Contact Stormwater Management System					2,731	710	System to transfer CCR-contact stormwater to the existing onsite settling ponds for treatment prior to discharge
	Install Sump	EA	6	SI	4	24	12	Crew and Daily Output based on experience. Assumed one sump every 5 acres.
	Install 8" HDPE Conveyance Pipe	LF	11,200	B22A	320	1,400	280	331413350300: Water supply distribution piping, piping HDPE, butt fusion joints, 40' lengths, 8" diameter, SDR 21. Includes labor, materials, and machine for installation and welding of HDPE pipe for conveying extracted water from sumps to EAP.
	Install Transfer Pump and Controller	EA	1	B6	1	52	0	Installation of transfer pump and pump controller to convey water from sumps to discharge outfall based on Ramboll project experience. Assumes inclusion of housing structure. Assume 2 days for installation.
	Install Equilibrium Tank	EA	2	B6	1	180	60	Installation of equalization tank at each trench and associated site preparation and instrumentation. Assumes 2 days for installation.
	Pipe Abandonment	LF	11,200	B6	250	1,075	358	024113380090: Selective demolition of 8" pipe.
6	Cutoff Wall Alignment Preparation Work Pad	-	-	-	-	2,263	754	Construct a temporary gravel work pad along entire cutoff wall alignment.
	Install Crushed Gravel Road (18" Thick) - Right of Way	SY	29,000	B14	615	2,263	754	015523500100: Temporary, roads, gravel fill, 8" gravel depth, excluding surfacing. Spanning 5,200-feet long and 50-feet wide.
	SITE PREPARATION ESTIMATED SUBTOTAL					**7,088**	**2,113**	
ITEM NO.	**CUTOFF WALL CONSTRUCTION**	**Units**	**Quantity**	**Crew**	**Daily Output**	**Labor Hours**	**Equipment Hours**	**Notes**
7	Temporary Final Cover Removal		-	-	-	482	140	Remove the final cover including cover soil and geosynthetics along the cutoff wall alignment to minimize damage to the final cover system over WAPS.
	Cover Removal	CY	2,300	B10X	575	48	32	312316465570: Excavating, bulk, dozer, open site, bank measure, common earth, 460 HP dozer, 300' haul Assumed 2 feet of thickness over 7 acres, is removed and stockpiled at coal yard.
	Geosynthetic Layers Removal	SF	305,000	B63B	22500	434	108	310519531200: Pond and reservoir liners, membrane lining systems HDPE, 100,000 S.F. or more, 60 mil thick, per S.F. Assumed removal of 7 acres. Also assumed removed geomembranes will be disposed of beneath the repaired final cover system to minimize off-site hauling/disposal.
8	Installation of Cutoff Wall	SF	504,400	-	-	10,761	2,690	Spoils to be temporarily placed in Hennepin Coal Yard and ultimately be placed in WAPS beneath the final cover system. Assumes 5,200-foot wall alignment, 3-foot wall width, and 97-foot wall depth. Assumes 5 feet thick layer that consists of boulders that require the use of hydromill. 312316420550: Excavating, bulk bank measure, 1 C.Y. capacity = 35 C.Y./hour, clamshell, excluding truck loading. This line item was included to quantify labor and equipment hours.
	Contruction Through Layer with Ash, Sand, Silt, and Clay - Heavy Equipment	SF	478,400	B12H	1500	5,103	2,551	Excavation of 92 feet of materials that do not require a hydromill.
	Contruction Through Layer with Ash, Sand, Silt, and Clay - Labor	SF	478,400	2 Clab	1500	5,103	0	Additional laborers to assist excavation
	Contruction Through Layer with Ash, Sand, Silt, and Clay - Heavy Equipment	SF	26,000	B12H	1500	277	139	Excavation of 5-foot layer with boulders that require the use of a hydromill. Assumed a total of 5 feet of the entire cutoff wall may require advancement through boulders or other obstructions.
	Contruction Through Layer with Ash, Sand, Silt, and Clay - Labor	SF	26,000	2 Clab	1500	277	0	Additional laborers to assist excavation
9	Spoils Management	CY - Loose	57,000	-	-	2,846	2,255	Quantity based on surface to surface calculation. Spoils assumed to be temporarily staged in Hennepin Coal Yard Area and then moved to EAP for use as contouring fill.
	Loading	CY - as excavated	114,000	B14B	5000	274	182	312316435320: Excavating, large volume projects; excavation with truck loading; excavator, 6 C.Y. bucket, 100% fill factor (assume 10% fluff factor from ground to excavated).
	Double Hauling and Placement at Coal Yard area	CY - as excavated	114,000	B34G	850	1,073	1,073	312323206170: Hauling; no loading equipment, including hauling, waiting, loading/dumping; 34 C.Y. off-road, 15 min wait/ld./uld., 15 MPH, cycle 1 mile. Daily output extrapolated down to 10 min wait.
	Spreading/Drying Moisture Conditioning	CY - as excavated	57,000	B10B	1000	684	456	312323170020: Spread dumped material, no compaction, by dozer. Daily output edited to match excavation based on experience. Quantity assumes 50% of volume requires moisture conditioning.
	Spreading Lifts	CY - as excavated	57,000	B10B	1000	684	456	312323170020: Spread dumped material, no compaction, by dozer. Daily output edited to match excavation based on experience.

	Compaction of Material	CY - in place	57,000	B10G	5200	132	88	312323235680: Compaction; Riding, sheepsfoot or wobbly wheel roller, 12" lifts, 2 passes. Assuming material to be compacted will be fine and not coarse.
10	Geotechnical Monitoring	LS	-			1,176	-	Geotechnical monitoring of embankment stability during wall construction
	Installation Fee	LS	1	GM	-	600	-	Assumes installation of inclinometers, survey prisms, and settlement monitoring devices along the WAPS dikes. Assumes a 4-person crew installs the monitoring system over a period of 3 weeks. Based on Ramboll experience
	Monthly O&M Fee	MO	24	Eng	-	576	-	Assumes crew to make two-day visits for monthly calibration, etc for duration of construction.
11	Contact Water Storm Water Management					236	11	Contact storm water will be collected from the sumps and pumped to the Leachate Pond or Secondary Settling Pond near EAP.
	Field Maintenance (O&M)	Event	104	OM	-	208	0	Assumes weekly maintenance visits on pumps and conduits during construction. Each visit assumes 2 staff for 2 days to check, clean, and service all mechanical parts. Assumes 24 months of contruction.
	Generator Charges	Ea	1	R3	1	28	11	263213160300. Gasoline, 3 phase 4 wire, 277/480 V, 11.5 kW generator
	CUTOFF WALL CONSTRUCTION					**15,501**	**5,097**	
ITEM NO.	**SITE RESTORATION**	**Units**	**Quantity**	**Crew**	**Daily Output**	**Labor Hours**	**Equipment Hours**	**Notes**
12	Replacement of Cover Soils/Vegetation	-	-	-	-	118	99	Assumes restoration of chain link fence along property boundary and restoration of grade surface following cutoff wall installation
	Loading and Spreading Stockpiled Cover Material	CY	2,300	B10B	1000	28	18	312323170011: Fill, dumped material, spread, by dozer, excludes compaction Assumed 2 feet of thickness over 7 acres, returned from stockpile staged at coal yard
	Grading	Ea	1	B62	2	16	5	312213200130: Rough grading sites, 1,100-3,000 S.F., skid steer & labor
	Lime	MSF	455	B66	700	5	5	329113234250: Soil preparation, structural soil mixing, spread soil conditioners, ground limestone, 1#/S.Y., tractor spreader. Assume soils possibly being void of nutrients.
	Fertilizer	MSF	455	B66	700	5	5	329113234150: Soil preparation, structural soil mixing, spread soil conditioners, fertilizer, 0.2#/S.Y., tractor spreader. Assume soils possibly being void of nutrients.
	Grassland Mix	MSF	350	B66	52	54	54	329219142300: Seeding athletic fields, seeding fescue, tall, 5.5 lb. per M.S.F., tractor spreader. Quantity all disturbed areas minus wetland area, pollinator area, and 15-acre pond in consolidated area.
	Mulch	MSF	350	B65	530	11	11	329113160350: Mulching, Hay, 1" deep, power mulcher, large.
13	Replacement of Liner Materials	-	-	-	-	441	0	Assumes replacing damaged liners along the cutoff wall alignment
	Geotextile	SF	310,000	2 Clab	22500	220	0	313219161550: Geotextile soil stabilization; non-woven 120 lb. tensile strength (Assume heavier geotextile based on experience)
	Geomembrane	SF	310,000	2 Clab	22500	220	0	310519531200: Pond and reservoir liners, membrane lining systems HDPE, 100,000 S.F. or more, 60 mil thick, per S.F.
	SITE RESTORATION ESTIMATED SUBTOTAL					**559**	**99**	
						Total Labor Hours	**Total Equipment Hours**	
	ENGINEERING AND CONSTRUCTION SUBTOTAL					**29,387**	**9,389**	
	CORRECTIVE ACTION OPERATION AND MAINTENANCE SUBTOTAL					**-**	**-**	
	ALTERNATIVE 2 SUBTOTAL					**29,400**	**9,400**	

NOTES:

1. Alternative 2: Source Control with continous containment system is estimated to take approximately 33 years to achieve groundwater protection standards (GWPS-35 I.A.C Section 845.600) at a majority of perimeter wells associated with the West Ash Pond System (WAPS). The monitoring period has been capped at 30 years total, plus 3 additional years of compliance monitoring.
2. RS Means refers to the 2023 online edition of RS Means Heavy Construction.
3. See crew tab (Alt 2 - Crew) for assumptions regarding crew size, total labor hours and required construction equipment, as needed, for each task.
4. See mileage tab (Alt 2 - Mileage) for assumptions regarding total mileage for tasks outlined in this alternative.

ACRONYMS:

AC = Acre
CY = Cubic Yard
  Bank: Material in natural compacted state
  Loose: Material swelled when removed from compacted state
EAP = East Ash Pond
EA = Each
WAPS = West Ash Pond System
GWPS = groundwater protection standards
LF = Linear Foot
LS = Lump Sum
MSF = square feet divided by 1000
MO = Month

RAMBOLL

CREW CODES
DYNEGY MIDWEST GENERATION, LLC - HENNEPIN POWER PLANT
CORRECTIVE ACTION ALTERNATIVES ANALYSIS SUPPORTING INFORMATION REPORT (CAAA-SIR)
ALTERNATIVE 2 - SOURCE CONTROL WITH CONTINUOUS CONTAINMENT SYSTEM

Item No.	Crew Code	Labor	Daily Labor Hours	Equipment	Daily Equipment Hours	Crew Size	Onsite Labor Hours	Onsite Heavy Equipment Hours
Construction								
2, 8, 13	2 Clab	Laborer x2	16	None	0	2	5,945	0
3	A2	Laborer x2 Truck Driver x1	24	Flatbed Truck, Gas, 1.5 ton	8	3	6	2
5	B6	Laborer x 2 Operator (light) x 1	24	Backhoe Loader, 48 H.P.	8	3	1,307	418
9, 12	B10B	Operator x1 Laborer x0.5	12	Dozer, 200 H.P.	8	1.5	1,396	930
9	B10G	Operator (med) x1 Laborer x0.5	12	Sheepsfoot Roller, 240 H.P.	8	1.5	132	88
7	B10X	Operator (med) x1 Laborer x0.5	12	Dozer, 105 H.P.	8	1.5	48	32
8	B12H	Laborer x1 Operator x1	16	1 Crawler Crane, 25 Ton 1 Clamshell Bucket, 1 C.Y.	8	2	5,380	2,690
2, 6	B14	Labor Foreman x 1 Operator (light) x1 Laborer x 4	48	Hyd. Excavator, 4.5 C.Y.. Backhoe Loader, 48 H.P.	16	6	3,434	1,145
9	B14B	Operator x1 Laborer x0.5	12	Hyd. Excavator, 6 C.Y.	8	1.5	274	182
5	B22A	Labor Foreman x1 Skilled Worker x1 2 Laborers 1 Equipment Operator, crane	40	1 S.P. Crane 4x4	8	5	1,400	280
9	B34G	Truck Driver x1	8	Dump Truck, Off Hwy., 50 ton	8	1	1,073	1,073
3, 12	B62	Laborer x2 Operator x 1	24	Loader, Skid Steer, 30 H.P.	8	3	784	261
7	B63B	Labor Foreman x1 Laborer x2 Operator x1	32	Loader, Skid Steer, 78 H.P.	8	4	434	108
12	B65	Laborer x1 Truck Driver (light) x1	16	Power Mulcher (large) x1 Flatbed Truck, Gas, 1.5 Ton x1	16	2	11	11
4, 12	B66	Operator (light) x1	8	Flatbed Truck, Gas, 1.5 Ton x1	8	1	88	64
11	R3	1 Electrician Foreman 1 Electrician 0.5 Operator (crane)	20	0.5 S.P. Crane, 4x4, 5 Ton	8	2.5	28	11
10	GM	Engineering Staff x4	40	Service Vehicle X 2	0	4	600	0
1, 10	Eng	Engineering Staff x1.2	10	Side by Side x1	4	1.2	6,816	2,080
5	SI	Laborer x1 Operator x1	16	Hyd. Excavator, 4.5 C.Y.	8	2	24	12
11	OM	Laborer x1	10	None	0	1	208	0
				Construction Subtotals			29,387	9,389
Note: Blue shaded crew codes were created by Ramboll based on experience (not pulled from RS Means).					**Totals**		**29,400**	**9,400**

CONSTRUCTION MILEAGE AND LABOR ESTIMATES
DYNEGY MIDWEST GENERATION, LLC - HENNEPIN POWER PLANT
CORRECTIVE ACTION ALTERNATIVES ANALYSIS SUPPORTING INFORMATION REPORT (CAAA-SIR)
ALTERNATIVE 2 - SOURCE CONTROL WITH CONTINUOUS CONTAINMENT SYSTEM

Construction Mileage and Labor Estimates

Item	Quantity	Assumptions
Labor Total Hours	29,387	Per projected Construction total in cost estimate (does not include contingency)
Duration of Onsite Construction Days	520	Total Days
Average Daily Crew Size	12.3	10 hour days (5 days per week) Assumes 11 workers for site preparation for duration of 2 months, 13 workers for construction for duration of 17 months, 6 workers for site restoration for 2 months
Daily Labor Mobilization Miles	445,900	Inlcudes light and medium commercial vehicles Average of 70 miles round trip per day
Vehicles Miles Onsite	95,550	1 mile per day round trip from gate to parking 5 miles per day for groundwater sampling and well maintenance staff 9 miles per day local trips (Vil. of Hennepin) No contingency Included
Equipment Mobilization Miles - Unloaded	27,040	Average of 260 miles round trip for equipment hauling Average 1 load of equipment per working week
Equipment Mobilization Miles - Loaded	27,040	Average of 260 miles round trip for equipment hauling Average 1 load of equipment per working week
Onsite Haul Truck Miles - Unloaded	1,676	34 CY Off Road Dump Truck 2 mile round trip per load
Onsite Haul Truck Miles - Loaded	1,676	34 CY Off Road Dump Truck 2 mile round trip per load
Offsite Haul Truck Miles - Unloaded	60,417	Assumes 16 CY loads of gravel are delivered to the site from a regional supplier located within 100 miles of the site
Offsite Haul Truck Miles - Loaded	60,417	Assumes truck is returning to the regional supplier located within 100 miles of the site
Material Delivery Miles - Unloaded	105,000	Misc. construction materials (cement, bails, etc) Assumes 200 mile round trip on a daily basis 1 delivery of geomembrane (1,000 miles)
Material Delivery Miles - Loaded	105,000	Misc. construction materials (cement, bails, etc) Assumes 200 mile round trip on a daily basis 1 delivery of geomembrane (1,000 miles)

O&M Mileage and Labor Estimates - Alternative 2: Source Control with Continuous Containment System

Item	Quantity	Assumptions
Labor Total Hours	0	No O&M for Alt 2
Duration of Onsite OMM Days	0	-
Average Daily Crew Size	0	-
Daily Labor Mobilization Miles	0	-
Vehicles Miles Onsite	0	-
Equipment Mobilization Miles - Unloaded	0	-
Equipment Mobilization Miles - Loaded	0	
Onsite Haul Truck Miles - Unloaded	0	-
Onsite Haul Truck Miles - Loaded	0	-
Offsite Haul Truck Miles - Unloaded	0	-
Offsite Haul Truck Miles - Loaded	0	-
Material Delivery Miles - Unloaded	0	-
Material Delivery Miles - Loaded	0	-

Legend:
CAGM = Corrective Action Groundwater Monitoring
O&M = Operation & Maintenance

Appendix C

Corrective Measures Assessment

Intended for
Dynegy Midwest Generation, LLC

Date
May 8, 2024

Project No.
1940103584-005

35 I.A.C. § 845 CORRECTIVE MEASURES ASSESSMENT

HENNEPIN POWER PLANT, WEST ASH POND SYSTEM, IEPA ID: W1550100002-01 AND W1550100002-03

RAMBOLL Bright ideas. Sustainable change.

35 I.A.C. § 845 CORRECTIVE MEASURES ASSESSMENT HENNEPIN POWER PLANT, WEST ASH POND SYSTEM, IEPA ID: W1550100002-01 AND W1550100002-03

Project name	**Hennepin Power Plant West Ash Pond System**
Project no.	**1940103584-005**
Recipient	**Dynegy Midwest Generation, LLC**
Document type	**35 I.A.C. § 845 Corrective Measures Assessment**
Revision	**FINAL**
Date	**May 8, 2024**
Prepared by	**Frances Ackerman, RG, PE**
Checked by	**Lucas P. Carr, PE**
Approved by	**Brian G. Hennings, PG**

Frances Ackerman, RG, PE
Senior Managing Engineer

Brian Hennings, PG
Project Officer, Hydrogeology

CONTENTS

TABLES

FIGURES

ATTACHMENTS

ACRONYMS AND ABBREVIATIONS

35 I.A.C.	Title 35 of the Illinois Administrative Code
40 C.F.R.	Title 40 of the Code of Federal Regulations
ASD	Alternative Source Demonstration
CAAA	corrective action alternatives analysis
CAP	Corrective Action Plan
CBR	closure-by-removal
CCR	coal combustion residuals
CIP	closure-in-place
Closure Plan	Closure and Post-Closure Care Plan
CMA	Corrective Measures Assessment
CSM	conceptual site model
DMG	Dynegy Midwest Generation, LLC
E001	monitoring event 1
E002	monitoring event 2
E003	monitoring event 3
EPRI	Electric Power Research Institute
Geosyntec	Geosyntec Consultants, Inc.
GMP	groundwater monitoring plan
GWPS	groundwater protection standard(s)
HCR	Hydrogeologic Site Characterization Report
HPP	Hennepin Power Plant
ID	identification
IDNR	Illinois Department of Natural Resources
IEPA	Illinois Environmental Protection Agency
ISS	In-situ stabilization
ITRC	National Research Council, Interstate Technology & Regulatory Council
IX	ion exchange
NAVD88	North American Vertical Datum of 1988
NID	National Inventory of Dams
No.	number
NPDES	National Pollutant Discharge Elimination System
NRT/OBG	Natural Resource Technology, an OBG Company
OWAP	Old West Ash Pond
OWPP	Old West Polishing Pond
PRB	permeable reactive barrier
psi	pounds per square inch
Ramboll	Ramboll Americas Engineering Solutions, Inc.
SI	surface impoundment
Site	Hennepin Power Plant
TDS	total dissolved solids
UA	uppermost aquifer
USEPA	United States Environmental Protection Agency
WAPS	West Ash Pond System
ZVI	zero-valent iron

1. INTRODUCTION

1.1 Overview

Ramboll Americas Engineering Solutions, Inc. (Ramboll) has developed this assessment of groundwater corrective measures on behalf of the Hennepin Power Plant (HPP), owned and operated by Dynegy Midwest Generation, LLC (DMG), to assist in the compliance with the requirements of Title 35 of the Illinois Administrative Code (35 I.A.C.) § 845: Standards for the Disposal of Coal Combustion Residuals in Surface Impoundments. This assessment applies specifically to the coal combustion residuals (CCR) surface impoundments (SI) referred to as the West Ash Pond System (WAPS), also referred to as the Old West Ash Pond (OWAP [Illinois Environmental Protection Agency [IEPA] identification [ID] number (No.) W1550100002-01]) and Old West Polishing Pond (OWPP, [IEPA ID No. W1550100002-03]), and CCR Unit ID No. 804, and National Inventory of Dams (NID) No. IL50698. This report addresses content requirements specific to 35 I.A.C. § 845.660 (Assessment of Corrective Measures) for exceedances of arsenic, boron, sulfate, lithium, and total dissolved solids (TDS) at the WAPS.

1.2 Source Control and Residual Plume Management

DMG completed significant source control and residual plume management efforts in 2020 as part of final closure of the WAPS. The final closure was performed in accordance with the Closure and Post-Closure Care Plan (Closure Plan; Geosyntec Consultants, Inc. [Geosyntec], 2017) that was developed in accordance with Title 40 of the Code of Federal Regulations (40 C.F.R.) § 257 and submitted to IEPA for review. IEPA approved the Closure Plan and found *"…the closure and post-closure care plan…to be an adequate corrective action"* (IEPA, 2018). The final closure was addressed in accordance with the IEPA Water Pollution Control permit 2020-EA-65026-1.

The WAPS closure construction included a hybrid consolidate-and-cap approach comprised of closure-by-removal (CBR) of the OWPP and closure-in-place (CIP) of the OWAP. This was accomplished by removing impounded water from within the OWAP and OWPP, excavating CCR and approximately one foot of soil below the CCR, from the OWPP and placing it into the OWAP, and constructing an alternate soil and geosynthetic cover system over the OWAP, in accordance with 40 C.F.R. § 257.102. These source control activities will serve as the primary groundwater corrective measure at the WAPS. The potentially feasible corrective measures presented herein are intended to be supplementary to the primary source control and are intended to serve as management measures to address any residual plumes that remain after completion of source control.

Attachment A includes summary figures (from the final closure plan) showing the final IEPA approved source control and primary corrective action.

1.3 Adaptive Site Management

Adaptive site management strategies will be employed as an integral part of ongoing corrective action at the WAPS. The adaptive site management approach will allow timely incorporation of new site information over the post-closure life cycle of the WAPS to ensure the achievement of the groundwater protection standards (GWPS). The adaptive site management approach is proposed to expedite progress toward meeting the GWPS while acknowledging uncertainties, such as the persistence of current groundwater flow directions and flux quantities and potential related changes in geochemical conditions. A structured decision-making process and explicitly planned iterations between the implemented corrective measures and monitoring results will ensure that remediation is occurring. System performance and the condition of the residual plume will be monitored as the corrective measure(s) selected through the I.A.C. § 845.710 Corrective Action Plan (CAP) process are implemented to supplement the source control measures described above. If the groundwater concentrations do not decrease consistent with the modeling prediction, the adaptive site management approach will facilitate timely modifications or enhancements to the corrective measure(s), as needed in accordance with 35 I.A.C. §845.680(b). This approach will be employed to provide continuous improvement to the WAPS groundwater remediation in response to new site information and/or the performance of the selected corrective measure(s).

The planned adaptive site management strategies are generally consistent with National Research Council, Interstate Technology & Regulatory Council (ITRC) and United States Environmental Protection Agency (USEPA) methodologies developed to address sites with long remediation times and high levels of uncertainty regarding the remedial actions necessary to achieve final and protective remediation goals (USEPA, 2022). The elements of the proposed adaptive site management strategy at the WAPS will be responsive to the changing conditions associated with pond closure and performance of the selected corrective measure(s) and will include the following:

1. Implementing the groundwater corrective measure(s) selected as part of the CAP for the current conditions at the WAPS. The selected corrective measures may include a combination of the technologies presented in this Corrective Measures Assessment (CMA).
2. Establishing both the absolute remedial objective and functional (interim) goals to monitor progress toward the remedial objective. Achieving the GWPS for 35 I.A.C. § 845.600 constituents at the downgradient waste boundary is the remedial objective for the WAPS. Specific functional goals will be developed as part of the CAP process. The functional goals will be measurable thresholds for future action and may include short-term or technology-specific objectives and triggers. Functional goals may vary for different locations, CCR constituents or other site-specific considerations (ITRC, 2017) and will serve as benchmarks for comparison to ongoing groundwater monitoring at the WAPS.
3. Ongoing groundwater monitoring at the WAPS will continue throughout at least the post-closure care period. Post-closure monitoring will continue for a period of at least 30 years, in accordance I.A.C. § 845.780(c), or until GWPS have been met for at least 3 years, whichever is longer. A comprehensive groundwater monitoring plan (GMP) will be developed as part of the CAP process in accordance with 35 I.A.C. § 845.670 and 35 I.A.C. § 845.220(c)(4). The GMP will include the functional goals and proposed action levels.
4. Groundwater monitoring information will be used to guide decisions regarding whether progress toward the remedial goal is advancing as expected and/or whether additional actions may be needed to achieve the remedial objective, in conjunction with IEPA, as required by 35 I.A.C. § 845.680(b).

2. SITE INFORMATION

The HPP is located in the northwest quarter of Section 26, Township 33 North, Range 2 West, Putnam County, Illinois and approximately 3 miles north-northeast of the Village of Hennepin. The WAPS is located west of the power plant and situated in an area that is a mixture of agricultural and undeveloped land use (**Figure 2-1**). The WAPS is a closed CCR SI consisting of two closed, unlined CCR sub-units including the OWAP (IEPA Unit ID W1550100002-01) and the OWPP (IEPA Unit ID W1550100002-03). The two sub-units formerly comprised the WAPS and were surrounded by a continuous earthen embankment. Prior to closure, the sub-units were divided utilizing an internal splitter dike to support plant operations, where CCR was deposited within the OWAP and the OWPP was utilized as a polishing pond prior to discharging process water to the Illinois River via a National Pollutant Discharge Elimination System (NPDES) outfall. As part of closure, the OWPP, all CCR within the OWPP, and the OWPP perimeter dikes were removed and placed within the WAPS. The pre-closure surface area of the WAPS was approximately 35 acres. The current surface area of the OWAP final cover area is approximately 29 acres (**Figure 2-2**). The Illinois River is connected to the post-closure OWPP by a culvert, allowing for the water level in the OWPP to be similar to the Illinois River. The OWPP functions as post-closure wildlife habitat.

The Closure Plan was submitted to IEPA in 2017 (Geosyntec, 2017). The Closure Plan was approved by IEPA in a letter dated June 19, 2018. The approved Closure Plan summarized the planned closure of the WAPS, which included dewatering the CCR, mechanical excavation of material from the OWPP for use as structural fill in the WAPS, grading within the WAPS, constructing an alternative cover system consisting of geomembrane and vegetated cover soils in direct contract with the graded CCR, and establishment of a vegetative cover. Closure construction was completed by November 17, 2020 (DMG, 2020a; DMG 2020b).

2.1 Conceptual Site Model

Significant site investigation has been completed at the HPP to characterize the geology, hydrogeology, and groundwater quality. Based on extensive investigation and monitoring, the WAPS has been well characterized and detailed in the Hydrogeologic Site Characterization Report (HCR; Natural Resource Technology, an OBG Company [NRT/OBG], 2017c). The conceptual site model (CSM) is presented below.

There are three dominant geomorphic features in the immediate vicinity of the HPP: an upper river terrace at an elevation of about 500 to 550 feet[1], a lower river terrace at an elevation of about 450 to 460 feet, and the current river valley filled with alluvium to an elevation of about 445 feet. The HPP and the eastern portion of the WAPS are on the lower terrace. The western portion of the WAPS overlies alluvium.

The hydrogeological assessment identified that the stratigraphy within and immediately surrounding the WAPS consists of fill, unlithified river alluvium, and Pleistocene-age glacial outwash deposits overlying Pennsylvanian-age shale bedrock. Where undisturbed or partially excavated, the native surficial soil at the site is poorly drained, moderately permeable silty clay loam formed as alluvium in floodplains.

---

[1] All elevations in this report are refenced to North American Vertical Datum of 1988 (NAVD88) unless otherwise noted.

The Site is characterized by two hydrostratigraphic units:

- **Uppermost Aquifer (UA)**: Includes the unlithified natural geologic materials of the Cahokia Alluvium and Henry Formation extending from the upper saturated zone to the bedrock. The UA contains variable amounts of cobbles and boulders within a sand and gravel matrix. Both the prevalence and size of the cobbles and boulders increase with depth.
- **Bedrock Confining Unit**: Comprised of shales with thin limestone, sandstone, and coal beds. This bedrock confining unit is encountered at elevations ranging from 399.2 to 410.2 feet.

The direction of groundwater flow and hydraulic gradient within the UA varies with the elevation of the Illinois River. During normal river stage the direction of groundwater flow is most often toward the river, but comparison of groundwater and river elevation data indicate reversals in this flow direction during times of high river elevations. The relative duration of these events is short, which leads to the determination of a predominant groundwater flow direction toward the river. Groundwater elevations and contours for the May 2023 monitoring event (Event 1 [E001]) are presented in **Figure 2-3**.

2.2 Groundwater Quality

Groundwater monitoring in accordance with the GMP and sampling methodologies provided in the operating permit application for the WAPS began in the second quarter of 2023. The 35 I.A.C § 845 groundwater monitoring system is displayed on **Figure 2-4** and consists of 11 wells screened in the UA (two background and nine compliance) and one temporary water level only surface water staff gauge. The groundwater samples collected from the 11 wells are used to monitor and evaluate groundwater quality and demonstrate compliance with the groundwater quality standards listed in 35 I.A.C. § 845.600(a). The proposed monitoring wells yield groundwater samples that represent the quality of downgradient groundwater at the CCR boundary (as required by 35 I.A.C. § 845.630(a)(2)).

The E001 sampling event was completed on June 1, 2023. In accordance with 35 I.A.C. § 845.610(b)(3)(C), statistically derived values were compared with the GWPSs summarized in 35 I.A.C. § 845.600 to determine exceedances of the GWPS (Ramboll, 2023a). The statistical determination identified the following GWPS exceedances at compliance groundwater monitoring wells:

- Arsenic at wells 21R and 51
- Boron at wells 21R, 22, 23, and 35
- Cadmium at well 22
- Sulfate at wells 23 and 35
- Lithium at well 22

Subsequent compliance sampling events for Quarter 3 and Quarter 4 2023 (Event 2 [E002] and Event 3 [E003]) were completed in August and November 2023 and groundwater samples were evaluated for exceedances of the GWPS as described in 35 I.A.C. § 845.600 (Ramboll, 2024a; Ramboll, 2024b). The following additional exceedances were identified during the E002 and E003 monitoring events:

- Lithium at well 22
- TDS as well 35

Pursuant to 35 I.A.C. § 845.650(e), an alternative source demonstration (ASD) was prepared and submitted to IEPA that presented evidence demonstrating that sources other than the WAPS were the cause of the cadmium GWPS exceedance listed above (Ramboll, 2023b). The IEPA concurred with the ASD; therefore, arsenic, boron, sulfate, lithium, and TDS exceedances are addressed in this CMA, in accordance with 35 I.A.C. § 845.660.

3. CORRECTIVE MEASURES ASSESSMENT METHODOLOGY

This section describes the CMA methodology initiated in response to the identification of exceedances of the GWPS for 35 I.A.C. § 845.600 constituents at the downgradient waste boundary of the WAPS during the E001 groundwater monitoring event (Ramboll, 2023a). The CMA was initiated on December 10, within 90 days after the detection of exceedance(s) of GWPS. Under 35 I.A.C. § 845, owners and operators of existing CCR SIs must initiate the assessment of corrective measures in accordance with 35 I.A.C. § 845.660 if one or more constituents are detected, and confirmed by an immediate resample, to be in exceedance of a GWPS in 35 I.A.C. § 845.600, and the owner or operator has not demonstrated that: a source other than the CCR SI caused the exceedance, or; that the exceedance of the GWPS resulted from error in sampling, analysis, statistical evaluation, natural variation in groundwater quality or a change in the potentiometric surface and groundwater flow direction (an ASD).

The CMA is the first step in developing a long-term CAP to address the GWPS exceedances at CCR SIs. The process provides a systematic, rational method for evaluating potential corrective measures by first identifying potentially applicable technologies and evaluating them using qualitative information to eliminate from consideration infeasible or otherwise unacceptable remedial technologies (*i.e.,* the 35 I.A.C. § 845.660 CMA). The remaining technologies will be evaluated individually, or assembled into combined alternatives, and further evaluated under the 35 I.A.C. § 845.670 CAP process. The final outcome of the process will be to select an appropriate and protective corrective action(s) for the WAPS.

This CMA identified applicable corrective measure technologies and evaluated them for viability, given the site-specific conditions and considerations at the WAPS, by addressing the following 35 I.A.C § 845.660 evaluation criteria:

- Performance, reliability, ease of implementation and potential impacts of appropriate potential remedies, including safety impacts, cross-media impacts, and control of exposure to any residual contamination;
- Time required to begin and complete the CAP; and
- Institutional requirements, such as State or local permit requirements or other environmental or public health requirements that may substantially affect implementation of the CAP.

The evaluation included qualitative and/or semi-quantitative screening of the potential corrective measures (technologies) relative to their general performance, reliability, and ease of implementation characteristics and their potential impacts, timeframes, and institutional requirements to assess the viability of each technology to address the GWPS exceedances at the WAPS. This approach provided a reasoned set of corrective measures that could be used, either individually or in combination, to supplement the source control measures described in **Section 1.2** and achieve GWPSs in the most effective and protective manner. This set of corrective measures will be further evaluated in the Corrective Action Alternatives Analysis (CAAA).

4. DESCRIPTION OF POTENTIAL CORRECTIVE TECHNOLOGIES

The potential groundwater corrective measures summarized below are applicable to the WAPS and were included in the CMA development and analysis. Site-specific considerations regarding the WAPS provided in **Section 2** were used to evaluate potential groundwater corrective measures. Each of the corrective measures evaluated may be capable of satisfying the requirements and objectives, listed in **Section 3**, to varying degrees of effectiveness. The corrective measure review process was intended to yield a set of applicable corrective measures that could be used to supplement the completed source control activities described in **Section 1.2** (CBR of the OWPP and CIP with a geosynthetic cap at the OWAP). The completed source control has significantly reduced infiltration rates relative to pre-closure conditions. Ongoing monitoring will be an integral part of all corrective measures to verify and document the remedial process. The corrective measures ultimately advanced to the CAAA and selected in the CAP will be used to enhance the effectiveness of the source control and may be used independently or may be combined into specific remedial alternatives to leverage the advantages of multiple corrective measures to attain GWPSs.

Source control measures were completed in 2020 for the WAPS, as described in **Section 1.2**; all of the evaluated corrective technologies are proposed to be supplemental and complementary to source control activities. The following potential corrective measures, commonly used to mitigate groundwater impacts, were considered as a part of the CMA process:

- Source Control with Groundwater Polishing;
- Source Control with In-Situ Stabilization (ISS);
- Source Control with Groundwater Extraction (groundwater pumping wells or collection trenches);
- Source Control with a Cutoff Wall; and
- Source Control with In-Situ Chemical Treatment (permeable reactive barrier [PRB]).

4.1 Source Control with Groundwater Polishing

Both federal and state regulators have long recognized that natural geochemical processes can be an acceptable component of a remedial action when it can achieve remedial action objectives in a reasonable timeframe. In 1999, USEPA published a final policy directive for groundwater remediation and described the process as follows:

- *"The reliance on natural attenuation processes (within the context of a carefully controlled and monitored site cleanup approach) to achieve site-specific remediation objectives within a time frame that is reasonable compared to that offered by other more active methods. The 'natural attenuation processes' that are at work in such a remediation approach include a variety of physical, chemical, or biological processes that, under favorable conditions, act without human intervention to reduce the mass, toxicity, mobility, volume, or concentration of contaminants in soil or groundwater. These in-situ processes include biodegradation; dispersion; dilution; sorption; volatilization; radioactive decay; and chemical or biological stabilization, transformation, or destruction of contaminants."* (USEPA, 1999).

The USEPA has stated that source control is the most effective means of ensuring the timely attainment of remediation objectives (USEPA, 1999). Natural geochemical processes may be appropriate as a "finishing step" after effective source control implementation (*i.e.*, groundwater polishing), to reduce the residual mass remaining in the groundwater after closure, if there are no risks to receptors and/or the contaminant plume is not expanding. Thus, groundwater polishing would be used in conjunction with the significant planned source control effort at the site, which will consist of a hybrid consolidate-and-cap approach with a final cover system described in **Section 1.2**.

In 2015, USEPA addressed remediation of inorganic compounds in groundwater and noted that the use of natural geochemical processes to address inorganic contaminants: (1) is not intended to constitute a treatment process for inorganic contaminants; (2) when appropriately implemented, can help to restore an aquifer to beneficial uses by immobilizing contaminants onto aquifer solids and providing the primary means for attenuation of contaminants in groundwater; and (3) is not intended to be a "do nothing" response (USEPA, 2015). Rather, documenting the applicability of natural geochemical processes for groundwater remediation should be thoroughly and adequately supported with site-specific characterization data and analysis (USEPA, 1999; USEPA, 2007; USEPA, 2015):

Both physical and chemical processes can contribute to the reduction of the small amount of residual mass remaining after closure of the WAPS, and the toxicity, mobility, volume, or concentration of contaminants in groundwater. Physical processes applicable to CCR include dilution, dispersion, and flushing. Chemical processes applicable to CCR include precipitation and coprecipitation (*e.g.,* incorporation into sulfide minerals) and sorption (*e.g.,* to iron, manganese, aluminum; to other metal oxides or oxyhydroxides; or to sulfide minerals or organic matter), and ion exchange (IX).

All inorganic compounds are subject to physical processes and under typical environmental conditions, physical mechanisms most often exert the dominant control on the CCR constituents of interest. Chemical mechanisms are also likely to be active, though not often dominant, such as adsorption, IX, and organic complexation. In combination with source control, these natural controls can provide an effective means to polish residual loading and achieve the GWPS in a reasonable timeframe. Additional data collection and analysis may be required to support the USEPA's evaluation framework (USEPA, 2015) and obtain regulatory approval.

4.2 Source Control with In-Situ Stabilization

ISS is a technology to treat impacted material using large diameter augers or other equipment to mix a slurry of pozzolanic additives, or reagents, into soils to solidify them in-situ. As the augers are advanced into the subsurface, the slurried reagent is blended with the soil, resulting in a subsurface mixture of soil and reagent. ISS results in a solidified mass with similar unit weights but with greater strength, lower permeability, and reduced contaminant mobility. ISS results in a column of mixed material which cures to a desired unconfined compressive strength of approximately 50 to 200 pounds per square inch (psi) after 28 days. Mixed columns typically cure relatively quickly, generally able to support construction equipment within 24 to 48 hours. Typically mixing sequencing will call for allowing mixed columns to cure for 24 to 48 hours before mixing a directly adjacent column. To treat all soil within a targeted area, adjacent columns are overlapped.

Typical ISS construction uses using large diameter rotary augers or hydraulic excavators to solidify/stabilize soil in place by mixing a cementitious grout with impacted soil. ISS implementation creates a stable and relatively impermeable, continuous, monolith having an unconfined compressive strength of greater than 50 psi. Full-scale ISS construction will result in volumetric expansion of the treated soil. The expansion, often referred to as "swell," is a result of blending reagent mixtures with the soil.

Typical ISS column diameters range from 3 to 12 feet. Various diameter columns may be used depending on the subsurface soil conditions, site constraints or layout, or project schedule. ISS columns will overlap forming a continuous solidified monolith. Columns will be spaced and overlapped to ensure all soils within the targeted area are thoroughly mixed. Each ISS column will include continuous application of reagent from the ISS platform surface (*i.e.,* base of excavation) to the design depth. There may be some limited areas where a shallower mixing profile is designed and mixing using a backhoe/excavator, commonly referred to as bucket mixing, may prove to be more efficient than vertical rotary mixing system. Bucket mixing operations consist of using the excavator to mix the soils to the design depth. Grout is pumped into the excavation from the grout plant via hoses. The soil is mixed with the grout from the base to the top of the treatment cell until the material appears adequately homogenized.

ISS is not widely used as a corrective measure for CCR applications but has been successfully implemented at power stations for other (*i.e.,* structural) applications. A combination of factors, including geologic heterogeneities and potential subsurface obstructions in the ash could limit the effectiveness of implementation.

4.3 Source Control with Groundwater Extraction

Groundwater extraction is one of the most widely used groundwater corrective technologies and has a long history of performance. This corrective measure includes installation of one or more groundwater pumping wells or trenches to control and extract impacted groundwater. Groundwater extraction captures and contains impacted groundwater and can limit plume expansion and/or off-site migration. Construction of a groundwater extraction system typically includes, but is not limited to, the following primary components:

- Designing and constructing a groundwater extraction system consisting of one or more extraction wells and operating at a rate to allow capture of CCR impacted groundwater within the UA.
- Management of extracted groundwater, which may include modification to the existing NPDES permit.
- Ongoing inspection and maintenance of the groundwater extraction system.

Remediation of inorganics by groundwater extraction can be effective, but systems do not always perform as expected. A combination of factors, including geologic heterogeneities, difficulty in flushing low-permeability zones, and rates of contaminant desorption from aquifer solids can limit effectiveness. Groundwater extraction systems require ongoing operation and maintenance to address issues such as iron bacteria and well fouling and to ensure optimal performance. The extracted groundwater must be managed, either by ex-situ treatment or disposal.

Groundwater extraction may reduce the timeframe to achieve GWPS and contain the groundwater constituents that exceed the GWPS. Extraction could be accomplished using a groundwater pumping well system or an extraction trench.

4.4 Source Control with a Cutoff Wall

Since the late 1970s and early 1980s, vertical cutoff walls have been used to control and/or isolate impacted groundwater. Low-permeability cutoff walls can be used to prevent horizontal off-site migration of potentially impacted groundwater. Cutoff walls act as barriers to transport of impacted groundwater and can isolate soils that have been impacted by CCR to prevent contact with unimpacted groundwater. Cutoff walls are often used in conjunction with an interior pumping system to establish an inward gradient within the cutoff wall. The gradient imparted by the pumping system maintains an inward flow through the wall, keeping it from acting as a groundwater dam and controlling potential end-around or breakout flow of contaminated groundwater. Constructing the cutoff wall such that it intersects a low-permeability material at its base, referred to as “keying”, greatly increases its effectiveness.

A commonly used cutoff wall construction technology is the slurry trench method, which consists of excavating a trench and backfilling it with a soil-bentonite mixture, often created with the excavated soils, or, for deeper walls, a cement-bentonite mixture that is produced at an onsite batch plant. The trench is temporarily supported with bentonite slurry pumped into the trench during excavation (D’Appolonia & Ryan, 1979). Cutoff wall excavation uses conventional hydraulic excavators, hydraulic excavators equipped with specialized booms to extend their reach (*i.e.,* long-stick excavators), clamshells, or more specialized equipment such as hydromills or secant-pile drill rigs, depending upon trench depth, material excavated, and type of material that the wall is keyed into.

Cutoff walls are a widely accepted technology for containing impacted groundwater. Combining groundwater polishing with a limited cutoff wall and groundwater extraction in specific areas may provide advantages over independent use of these potential corrective technologies. Cutoff walls can be used in combination with groundwater extraction or as part of a PRB system (as the “funnel” in a funnel-and-gate system; **Section 4.5**).

4.5 Source Control with In-Situ Chemical Treatment

The use of in-situ treatment, either by injection or PRBs is a widely used technology for treating impacted groundwater. However, in-situ treatment techniques for arsenic, boron, lithium, and sulfate are not well established; therefore, performance is unknown.

Chemical treatment could consist of injection of reactive materials into the subsurface to treat contaminants at specific, targeted locations. Alternately, treatment via PRB, where reactive materials are placed in the subsurface at locations designed to direct the contaminant plume along a flow path through the reactive media. In either system, the contaminants are transformed or otherwise rendered into environmentally acceptable forms to attain remediation concentration goals downgradient of the barrier (Electric Power Research Institute [EPRI], 2006).

As groundwater passes through the PRB under natural gradients, dissolved constituents in the groundwater react with the media and are transformed or immobilized. A variety of media have been used or proposed for use in PRBs. Zero-valent iron (ZVI) has been shown to effectively immobilize some CCR constituents, including arsenic, chromium, cobalt, molybdenum, selenium, and sulfate. Use of a combination media consisting of ZVI and a boron-selective IX resin to treat boron has been documented in a pilot-scale test (EPRI, 2006).

System configurations include continuous PRBs, in which the reactive media extends across the entire path of the contaminant plume; and funnel-and-gate systems, where low-permeability barriers are installed to control groundwater flow through a permeable gate containing the reactive media. Continuous PRBs intersect the entire contaminant plume and do not materially impact the groundwater flow system. Design may or may not include keying the PRB into a low-permeability unit at depth. Funnel-and-gate systems utilize a system of barriers to groundwater flow (funnels) to direct the contaminant plume through the reactive gate. The barriers, typically some form of cutoff wall, are keyed into a low-permeability unit at depth to prevent short circuiting of the plume. Funnel-and-gate design must consider the residence time to allow chemical reactions to occur. Directing the contaminant plume through the reactive gate can significantly increase the flow velocity, thus reducing residence time.

Design of in-situ treatment systems requires rigorous site investigation to characterize the site hydrogeology and to delineate the contaminant plume. A thorough understanding of the geochemical and redox characteristics of the plume is critical to assess the feasibility of the process and select appropriate reactive media. Laboratory studies, including batch studies and column studies using samples of site groundwater, are needed to determine the effectiveness of the selected reactive media at the site (EPRI, 2006). The main considerations in selecting reactive media are as follows (Gavaskar et al., 1998 as cited by EPRI, 2006):

- Reactivity - The media should be of adequate reactivity to immobilize a contaminant within the residence time of the design.
- Hydraulic performance - The media should provide adequate flow through the PRB, meaning a greater particle size than the surrounding aquifer materials. Alternatively, gravel beds have been emplaced in front of barriers to direct flow through the barrier.
- Stability - The media should remain reactive for an amount of time that makes its use economically advantageous over other technologies.
- Environmentally compatible by-products - Any by-products of media reaction should be environmentally acceptable. For example, iron released by zero-valent iron corrosion should not occur at levels exceeding regulatory acceptance levels. Availability and price: The media should be easy to obtain in large quantities at a price that does not negate the economic feasibility of using a PRB.
- Availability and price: The media should be easy to obtain in large quantities at a price that does not negate the economic feasibility of using a PRB.

5. ASSESSMENT OF CORRECTIVE MEASURE TECHNOLOGIES

This CMA was initiated to address exceedances of the 35 I.A.C. § 845.600 GWPS at the downgradient waste boundary of the WAPS identified during the E001 groundwater monitoring event (**Section 2.2**).

5.1 Requirements

The potential groundwater corrective technologies described in the previous section were evaluated relative to the requirements presented in **Section 3** and reiterated below:

- Performance, reliability, ease of implementation and potential impacts of appropriate potential remedies, including safety impacts, cross-media impacts, and control of exposure to any residual contamination;
- Time required to begin and complete the CAP; and
- Institutional requirements, such as State or local permit requirement or other environmental or public health requirements that may substantially affect implementation of the CAP.

Table 5-1 presents the qualitative CMA evaluations of the of each groundwater technology against these requirements, as well as their ability to address GWPS exceedances. The following sections provide a summary of these evaluations and a discussion of the potential groundwater corrective measure technologies that may be viable, either independently or in combination, to address GWPS exceedances. This section also provides a summary of corrective measure technologies that have been retained and advanced for evaluation as part of the CAAA process for selecting the final remedy for the WAPS per 35 I.A.C. § 845.670.

5.2 Groundwater Corrective Technology Assessment

Source control, consisting of a hybrid consolidate-and-cap approach comprised of CBR of the OWPP and CIP of the OWAP, will be the primary groundwater corrective measure for the WAPS. Closure was completed in 2020 and each of the potential groundwater corrective measure technologies would supplement the positive impact of prior closure activities. The following sections evaluate groundwater corrective measure technologies that, when combined with site closure, may be viable to address GWPS exceedances. Technologies that are not viable for addressing the GWPS at the WAPS will be eliminated from further evaluation and viable technologies will be advanced for further evaluation as part of the CAAA process per 35 I.A.C. § 845.600.

5.2.1 Source Control with Groundwater Polishing

Source control construction (**Section 1.2**) has reduced the mass loading to the groundwater system to the extent that aquifer polishing process could act upon CCR constituents in the UA. Hydrostatic modeling and groundwater flow and fate and transport modeling indicated that source control construction would reduce the hydraulic head to near-zero level (equilibrium condition) within seven years after completion of cap construction and decrease transport of CCR constituents off-site. Ongoing groundwater modeling, which is expected to be completed in 2025, indicates that GWPS will be met approximately 30 years after the remedy implementation for the wells currently included in the compliance well network.

Groundwater polishing by natural geochemical processes is a widely accepted component of groundwater remediation and is routinely approved by the IEPA when paired with source control. The performance of groundwater polishing as a groundwater corrective measure varies based on site-specific conditions and additional data collection may be needed to support the design and regulatory approval. The sandy nature of the UA suggests good performance by physical processes in addressing the arsenic, boron, sulfate, lithium, and TDS in the UA.

Naturally occurring geochemical processes are ongoing at the WAPS and will continue to affect groundwater constituent concentrations. Ongoing monitoring of groundwater conditions is needed to better understand the mechanisms and efficacy of the groundwater polishing process and to confirm the effectiveness over time. Thus, additional groundwater sample collection and analyses would be required to characterize potential mechanisms, as discussed above, and to provide long term monitoring of the remedial progress. Enhancements to the groundwater monitoring system may be required to ensure that the aquifer polishing is occurring as predicted, consistent with the adaptive site management approach. The reliability of aquifer polishing as a groundwater corrective measure is high because operation and maintenance requirements are limited. However, the reliability can also vary based on site-specific hydrogeologic and geochemical conditions.

Following characterization and approval of the CAP, monitoring of the groundwater polishing processes and comparison to functional goals established to monitor progress toward the remedial objective could begin as quickly as within a few months of CAP approval.

No potential safety impacts or exposure to human health or environmental receptors are expected to result from the groundwater polishing processes. Timeframes to achieve GWPS are dependent on site-specific conditions, which require detailed technical analysis (ongoing at this time). Selecting groundwater polishing as a corrective measure for the WAPS will require approval of the CAP permits by the IEPA.

Monitoring the groundwater polishing to track progress toward achievement of the GWPS after the 2020 completion of source control construction at the WAPS would require long-term maintenance and monitoring of the groundwater monitoring system to confirm source control and verify the effectiveness in reducing groundwater concentrations to levels below the GWPS. Monitoring activities could be initiated immediately after approval of the CAP permit.

Groundwater polishing processes will continue to occur naturally at the FAPS. It may be a viable corrective measure for the arsenic, boron, sulfate, lithium, and TDS exceedances at the WAPS. Therefore, these processes are being advanced to the CAAA for further evaluation.

5.2.2 Source Control with In-Situ Stabilization

Source control will reduce the mass loading to the groundwater system and ISS was considered as a method of supplementing the completed source control. ISS is typically infeasible for large site and/or deep CCR; however, it was considered at the WAPS due to the limited size of the impoundment and limited depth to CCR. Implementing additional groundwater corrective measures may reduce the time required to attain the GWPS in the UA. Targeting zones of the CCR in the WAPS using ISS to solidify/stabilize CCR that is present at and below the groundwater level observed in surrounding monitoring wells at normal conditions could reduce or prevent the continued migration of CCR-related constituents away from the WAPS. When combined with groundwater polishing, ISS may reduce the time required to attain GWPS.

ISS is not a common corrective measure for CCR impacted groundwater, but it is a widely accepted corrective measure used to control and/or isolate impacted groundwater and it is routinely approved by regulatory agencies. ISS have a long history of reliable performance as a groundwater remediation technique.

ISS construction may be challenging due to the presence of potential obstructions in the CCR (*i.e.,* debris in the ash) which could impede advancement of the large diameter augers used to construct the ISS monolith. ISS construction in the already closed WAPS would be complicated and would likely require removal and reconstruction of the final cover system, which could cause a temporary reversal of some of the completed source control activities.

Construction could be completed within 2 to 3 years. Time of implementation is approximately 4 to 5 years, including characterization, design, permitting and construction. ISS would be used to supplement the completed source control and may require additional corrective measures, such as groundwater polishing, to attain GWPS.

Completing ISS in the WAPS would require IEPA approval of the CAP permit and, depending on the location, an IDNR dam safety modification permit may be required.

Supplementing source control using ISS could be used to reduce or prevent the continued migration of CCR-related constituents away from the WAPS. When combined with groundwater polishing, ISS may reduce the time required to attain GWPS. Therefore, ISS is being advanced to the CAAA for further evaluation.

5.2.3 Source Control with Groundwater Extraction

The completed source control is reducing the mass loading to the groundwater system and implementing additional groundwater corrective measures may reduce the time required to attain the GWPS in the UA.

Groundwater extraction is a widely accepted corrective measure with a long track record of performance and reliability. It is routinely approved by the IEPA. For a corrective measure using groundwater extraction to effectively control off-site flow and/or to remove potentially contaminated groundwater, horizontal and vertical capture zone(s) must be created. The performance of a groundwater extraction system would be expected to be effective in the high permeability UA. However, the proximity and influence of the Illinois River to the impacted area of the UA would potentially result in large volumes of extracted groundwater and river water. Cutoff walls (**Section 4.4**) could be used in conjunction with a pumping system to control potential groundwater movement from the river.

Implementation of a groundwater extraction system presents design challenges due to the proximity to the Illinois River. An extraction system in the UA would have to consider the potential for extracting unimpacted river water. Construction of an extraction system may be challenging due to the presence of cobbles and potentially large boulders in the UA. Specialty drilling methods may be required to construct the extraction system. Extracted groundwater (and potentially river water) would need to be managed, which may include modification to the existing NPDES permit and treatment prior to discharge, if necessary. Specialized treatment equipment may be required, and ongoing operations and maintenance activities would be necessary.

There could be some impacts associated with constructing and operating a groundwater extraction system, including some limited exposure to extracted groundwater. Additional data collection and analyses would be required to design an extraction system. Construction could be completed within 1 year following completion of a final design. Time of implementation is approximately 3 to 4 years after approval of the CAP permit, including characterization, design, permitting, and construction. Timeframes to achieve GWPS are dependent on site-specific conditions. An extraction system may reduce the time to attain GWPS in the UA relative to the post-closure timeframe predicted by the groundwater modeling. However, the relatively long expected GWPS attainment times may result in operations and maintenance of a groundwater extraction system for decades of years or more.

Implementing a groundwater extraction system at the WAPS would require IEPA approval of the CAP permit, and discharge of extracted groundwater may require a modification to the NPDES permit, as well as possibly permitting and construction of a new outfall. Depending upon the location of the extraction system an Illinois Department of Natural Resources (IDNR) dam safety modification permit may also be required to construct an extraction system.

Groundwater extraction could be viable corrective measure for the arsenic, boron, sulfate, lithium, and TDS exceedances at the WAPS. Implementation of groundwater extraction would require combining an extraction system with a cutoff wall to prevent very high inflow volumes from the Illinois River. Therefore, groundwater extraction is not being advanced to the CAAA for further evaluation.

5.2.4 Source Control with Groundwater Cutoff Wall

The completed source control is reducing the mass loading to the groundwater system and implementing additional groundwater corrective measures may reduce the time required to attain the GWPS in the UA. A low permeability cutoff wall could provide long-term, maintenance-free physical barrier to significantly reduce or prevent horizontal migration of CCR-impacted groundwater away from the WAPS. A cutoff wall could be used in combination with a groundwater extraction system in the UA to reduce the potentially high volumes of extracted groundwater that would be captured by and extraction system between the WAPS and the Illinois River. A cutoff wall could reduce the water management and treatment requirements for an extraction system.

Groundwater cutoff walls are a widely accepted corrective measure used to control and/or isolate impacted groundwater and are routinely approved by the IEPA. Cutoff walls have a long history of reliable performance as hydraulic barriers, provided they are properly designed and constructed. However, if not coupled with a groundwater extraction system, a cutoff wall will provide directional groundwater control only and may result in redistribution of contaminants and potentially GWPS exceedances at new locations.

Cutoff walls are designed to act as hydraulic barriers; as a result, cutoff walls inherently alter the existing groundwater flow system. Changes to the existing groundwater flow system may need to be controlled to maximize the effectiveness of the remedy by, for example, combining a cutoff wall with groundwater extraction to control build-up of hydraulic head upgradient and around the cutoff walls. Construction of a cutoff wall extending into the UA would be challenging, if it is possible, and would require specialized and highly experienced contractors with non-standard construction equipment due to the presence of subsurface cobbles and boulders.

Constructing a cutoff wall may also be challenging due to the physical site constraints (limited construction area due to the proximity of the Illinois River), particularly if used in combination with an extraction system. In that case, both the extraction system and the cutoff wall would need to be located between the WAPS and the river, which would increase the construction complexity and could result in structural impacts to the embankment dikes, depending on the location of the wall.

Additional data collection and analyses would be required to design a cutoff wall. Construction could be completed within 2 to 3 years. Time of implementation is approximately 5 to 8 years, including characterization, design, permitting, and construction. To attain GWPS, cutoff walls require a separate groundwater corrective measure to operate in concert with the cutoff wall(s). Cutoff walls are commonly coupled with aquifer polishing and/or groundwater extraction as groundwater corrective measures. The time to attain GWPS is dependent on the selected groundwater corrective measure or measures that are coupled with the cutoff walls.

Constructing a cutoff wall at the WAPS would require IEPA approval of the CAP permit and, depending on the location, an IDNR dam safety modification permit may be required.

A cutoff wall alone would not be a viable corrective measure for the arsenic, boron, sulfate, lithium, and TDS exceedances at the WAPS. Cutoff walls are commonly coupled with groundwater polishing and/or groundwater extraction as groundwater corrective measures. However, a cutoff wall could provide long-term, maintenance-free physical barrier to significantly reduce or prevent horizontal migration of CCR-impacted groundwater away from the WAPS. Therefore, the cutoff wall is being advanced to the CAAA for further evaluation.

5.2.5 Source Control with In-Situ Chemical Treatment

Source control will reduce the mass loading to the groundwater system and implementing additional groundwater corrective measures may reduce the time required to attain the GWPS in the UA. Use of in-situ treatment, either through targeted injection of reactive media or in PRB systems, to transform contaminants into environmentally acceptable forms to attain the GWPS was considered.

In-situ treatment using IX to address arsenic, boron, lithium, sulfate, and TDS exceedances in groundwater is not an established or widely accepted groundwater corrective measure; therefore, its performance and reliability are unknown. Regulatory acceptance of this innovative approach to achieving the GWPS is uncertain.

In-situ treatment in the granular UA is expected to be relatively straightforward using targeted reactive media delivery via injection, however use of a PRB would present design and construction challenges similar to the challenges with constructing a cutoff wall discussed above due to the presence of cobbles and boulders. Depending upon the location of the PRB system, construction may affect the WAPS embankment and/or final cover system and periodic change-outs of IX resin media may be required.

Additional data collection and analyses would be required to design an in-situ treatment system and bench scale and/or pilot scale testing may be required to demonstrate performance and reliability. Time of implementation is approximately 4 to 6 years after approval of the CAP permit, including characterization, design, permitting, and construction. Timeframes to achieve GWPS are dependent on demonstrations of performance and reliability and on ultimate regulatory acceptance. It is not known whether in-situ treatment would reduce the time to attain GWPS in the UA relative to the post-closure timeframe predicted by the groundwater modeling.

Due to the uncertain performance, reliability and potential for regulatory acceptance, in-situ chemical treatment is not a viable corrective measure for the arsenic, boron, sulfate, lithium, and TDS exceedances at the WAPS and is not being advanced to the CAAA for further evaluation.

5.3 Technologies Advanced to CAAA

Based on the evaluations presented above, the following potential corrective technologies are being advanced to the CAAA for more detailed evaluations, individually or in combination, and cost estimation:

- Source control with groundwater polishing;
- Source control and with ISS; and
- Source control with a groundwater cutoff wall.

6. REFERENCES

D'Appolonia, D.J., and Ryan, C.R., 1979, *Soil-Bentonite Slurry Trench Cut-Off Walls*, Geotechnical Exhibition and Technical Conference, Chicago, Illinois.

Electric Power Research Institute (EPRI), 2006. *Groundwater Remediation of Inorganic Constituents at Coal Combustion Project Management Sites, Technical Report #1012584*, October 2006.

Dynegy Midwest Generation (DMG), 2020a. *Hennepin Power Station; Old West Polishing Pond Notification of Completion of Closure.* December 17, 2020.

Dynegy Midwest Generation (DMG), 2020b. *Hennepin Power Station; Old West Ash Pond, Ash Pond No. 2 Notification of Completion of Closure.* December 17, 2020.

Gavaskar, A.R., N Gupta, B.M. Sass, R.J. Janosy and D. O'Sullivan, 1998. *Permeable Reactive Barriers for Groundwater Remediation: Design, Construction and Monitoring*. Battelle Press.

Geosyntec Consultants, Inc. (Geosyntec), 2017. *Closure and Post Closure Care Plan, Old West Ash Pond, Old West Polishing Pond at Dynegy Midwest Generation, LLC, Hennepin Power Station*. December 20, 2017.

Illinois Environmental Protection Agency, 2018. *Correspondence with Luminant (formerly Dynegy Midwest Generation, LLC regarding the Closure and Post-Closure Care Plan for Hennepin Old West Ash Pond System*, July 19, 2018.

National Research Council, Interstate Technology & Regulatory Council (ITRC), 2017. *Remediation Management of Complex Sites*. RMCS-1. Washington, D.C.: Interstate Technology & Regulatory Council, Remediation Management of Complex Sites Team. http//rmcs-1.itrcweg.org.

Natural Resource Technology, an OBG Company (NRT/OBG), 2017c. *Hydrogeologic Site Characterization Report, Hennepin West Ash Pond System, Hennepin, Illinois*. December 20, 2017.

Ramboll Americas Engineering Solutions, Inc. (Ramboll), 2023a. 35 I.A.C. § 845.610(B)(3)(D) *Groundwater Monitoring Data and Detected Exceedances, 2023 Quarter 2, West Ash Pond System, Hennepin Power Plant, Hennepin, Illinois*. September 11, 2023.

Ramboll Americas Engineering Solutions, Inc. (Ramboll), 2023b. 35 I.A.C. § 845.650(E): *Alternative Source Demonstration, West Ash Pond System, Hennepin Power Plant, Hennepin, Illinois*. November 10, 2023.

Ramboll Americas Engineering Solutions, Inc. (Ramboll), 2024a. 35 I.A.C. § 845.610(B)(3)(D) *Groundwater Monitoring Data and Detected Exceedances – Quarter 3, 2023. West Ash Pond System, Hennepin Power Plant, Baldwin, Illinois*. January 15, 2024.

Ramboll Americas Engineering Solutions, Inc. (Ramboll), 2024b. *35 I.A.C. § 845.610(B)(3)(D) Groundwater Monitoring Data and Detected Exceedances – Quarter 4, 2023. West Ash Pond System, Hennepin Power Plant, Baldwin, Illinois*. March 4, 2024.

United States Environmental Protection Agency (USEPA), 1999. *Use of Monitored Natural Attenuation at Superfund, RCRA Corrective Action, and Underground Storage Tank Sites.*

Directive No. 9200.U-17P. Washington, D.C.: EPA, Office of Solid Waste and Emergency Response.

United States Environmental Protection Agency (USEPA), 2007*. Monitored Natural Attenuation of Inorganic Contaminants in Ground Water, Volume 1 – Technical Basis for Assessment. EPA/600/R-07/139*. National Risk Management Research Laboratory, Office of Research and Development, U.S. Environmental Protection Agency, Cincinnati, Ohio. October 2007.

United States Environmental Protection Agency (USEPA), 2015. *Use of Monitored Natural Attenuation for Inorganic Contaminants in Groundwater at Superfund Sites. Directive No. 9283.1-36*. U.S. Environmental Protection Agency, Office of Solid Waste and Emergency Response. August 2015.

United States Environmental Protection Agency (USEPA), 2022. *Adaptive Site Management – A Framework for Implementing Adaptive Management at Contaminated Sediment Superfund Sites. Directive No. 9200.1-166*. U.S. Environmental Protection Agency. June 2022.

Tables

TABLE 5-1.
Corrective Measures Assessment Matrix
WEST ASH POND SYSTEM
HENNEPIN POWER PLANT
HENNEPIN, ILLINOIS
5/8/2024

Remedy	**Evaluation Factors**						
	Performance	**Reliability**	**Ease of Implementation**	**Potential Impacts of Remedy (safety impacts, cross-media impacts, control of exposure to any residual contamination)**	**Time Required to Begin and Implement Remedy[1]**	**Time to Attain Groundwater Protection Standards**	**Institutional Requirements (state/local permit requirements, environmental/public health requirements that affect implementation of remedy)**
Source Control with Groundwater Polishing	Performs best paired with source control which was completed in 2020.	Ongoing analysis will evaluate if the attenuation mechanism has low reversibility, if the aquifer has sufficient capacity, and if the hydrogeology is favorable for arsenic, boron, sulfate and/or lithium physical processes. Arsenic in the uppermost aquifer conditions may be more amenable to physical processes.	Evaluation is underway and is expected to be completed in 2024. Long-term monitoring would be required. Implementing would not require extensive specialized equipment or contractors	None identified.	Approximately 90 days after CAP permit approval.	Dependent on site-specific conditions. Ongoing analysis will evaluate attenuation rate and capacity.	IEPA approval of the CAP permit is required. No institutional requirements are anticipated. The approved the Closure Plan for source control included a Groundwater Management Zone application for locations and identified parameters.
Source Control with In-Situ Stabilization	Supplement source control using in-situ stabilization within targeted zones of the CCR, combined with groundwater polishing for impacts beyond the CCR.	Not widely used as a corrective measure for CCR applications but has been successfully implemented at power stations for other (*i.e.,* structural) applications.	Presence of potential obstructions (*i.e.,* debris) in the ash could inhibit implementation.	Would require temporarily disturbing and reconstructing the existing final cover system; this may temporarily reverse some of the completed source control effects.	Design, permitting and construction is expected to take 4 to 5 years after CAP approval.	Would likely reduce the time to less than the post closure timeframe predicted by the groundwater model for source control and groundwater polishing only.	IEPA approval of the CAP permit is required. A IDNR dam safety modification permit might also be required, depending on the location of the ISS installation.
Source Control with Groundwater Extraction	A widely accepted, routinely approved technology. Performance is generally good in granular aquifers, however the highly permeable nature of the Uppermost Aquifer would likely require high flow rates. May be uncertainty in expected performance due to the proximity to the river and potential for flood events.	Reliable if properly designed, constructed and maintained. Likely not reliable without cutoff wall due to the high permeability of the Uppermost Aquifer and proximity to the river.	Specialized drilling techniques (*i.e.,* sonic) may necessary for groundwater extraction system construction due to the presence of cobbles/boulders. Extracted groundwater flow rates could be very high and would require management, possibly including treatment, which may also require specialized equipment/contractors.	Alters groundwater flow system. Potential for some limited exposure to extracted groundwater. Groundwater extraction may induce settlement, which could cause structural impacts to the embankments, final cover system and/or adjacent structures. High flow rates may increase the difficulty in water management/treatment requirements.	Design, permitting and construction is expected to take 3 to 4 years after CAP permit approval.	Dependent on site-specific conditions. Less than the post-closure timeframe predicted by the groundwater model for source control and groundwater polishing.	IEPA approval of the CAP permit is required. IEPA approval is anticipated to be required for discharge of extracted groundwater via a NPDES discharge permit. An IDNR dam safety modification permit might also be required, depending on location of wells and settlement potential.
Source Control with Groundwater Cutoff Wall	Widely accepted, routinely approved, good performance if properly designed and constructed. May need to be combined with another groundwater corrective measure, such as groundwater polishing or extraction, to achieve GWPS.	Reliable for groundwater directional control if properly designed and constructed.	Widely used, established technology. Due to the depth to the uppermost aquifer and presence of cobbles/boulders, construction would likely require specialized, highly experienced contractors with non-standard construction equipment. Space limitations may be challenging for installing the wall and relocating compliance well system.	Alters groundwater flow system but does not provide any treatment. Can result in unintended consequences resulting from redirecting contaminants to areas where they are not currently present. May cause structural impacts to the embankment dikes, depending on the location of the wall. May require disturbing and reconstructing portions of the existing final cover system and other aspects of the completed closure, depending on the location of the wall; this may temporarily reverse some of the completed source control effects.	Design, permitting and construction is expected to take 5 to 8 years after CAP permit approval. Uncertainty in implementation time due to need for specialty contractors and expected difficult installation conditions.	Needs to be combined with other groundwater corrective measure(s). Time required to attain GWPS dependent on combined measures.	IEPA approval of the CAP permit is required. An IDNR dam safety permit may also be required depending on the location of the cutoff wall.
Source Control with In-Situ Chemical Treatment	In-Situ treatment not well established for boron, sulfate or lithium, therefore performance is unknown. In-situ treatment of arsenic is feasible. Performance would be poor because it would be limited to a single constituent.	Unknown reliability for arsenic, boron, sulfate, and/or lithium.	The granular nature of uppermost aquifer would likely be amenable to in-situ chemical delivery.	May require disturbing and reconstructing portions of the existing final cover system and other aspects of the completed closure, depending on the type and delivery method for the treatment. This may temporarily reverse some of the completed source control effects.	May require bench scale and/or pilot scale testing as part of design. Design, permitting and construction is expected to take 4 to 6 years after CAP approval.	There is uncertainty regarding whether a in-situ treatment would reduce arsenic, boron, sulfate, or lithium concentrations to achieve the GWPS. Dependent on conditions specific to the reactive media used and the site. Treatment technology is not well understood.	IEPA approval of the CAP permit is required. IEPA approval of this innovative and relatively unproved solution may be challenging. A IDNR dam safety permit may also be required if a PRB is used, depending on the location.

Notes:
[1] Time required to begin and implement remedy includes design, permitting, and construction.
CAP - Corrective Action Plan
CCR - coal combustion residuals
GWPS - Groundwater Protection Standards
IDNR - Illinois Department of Natural Resources
IEPA - Illinois Environmental Protection Agency
ISS - In-Situ Stabilization
NPDES - National Pollutant Discharge Elimination System
PRB - Permeable Reactive Barrier

Figures

Y:\Mapping\Projects\22\2285\MXD\845_Operating_Permit\Hennepin\GMP_804\Figure 1-1_Site Location Map.mxd

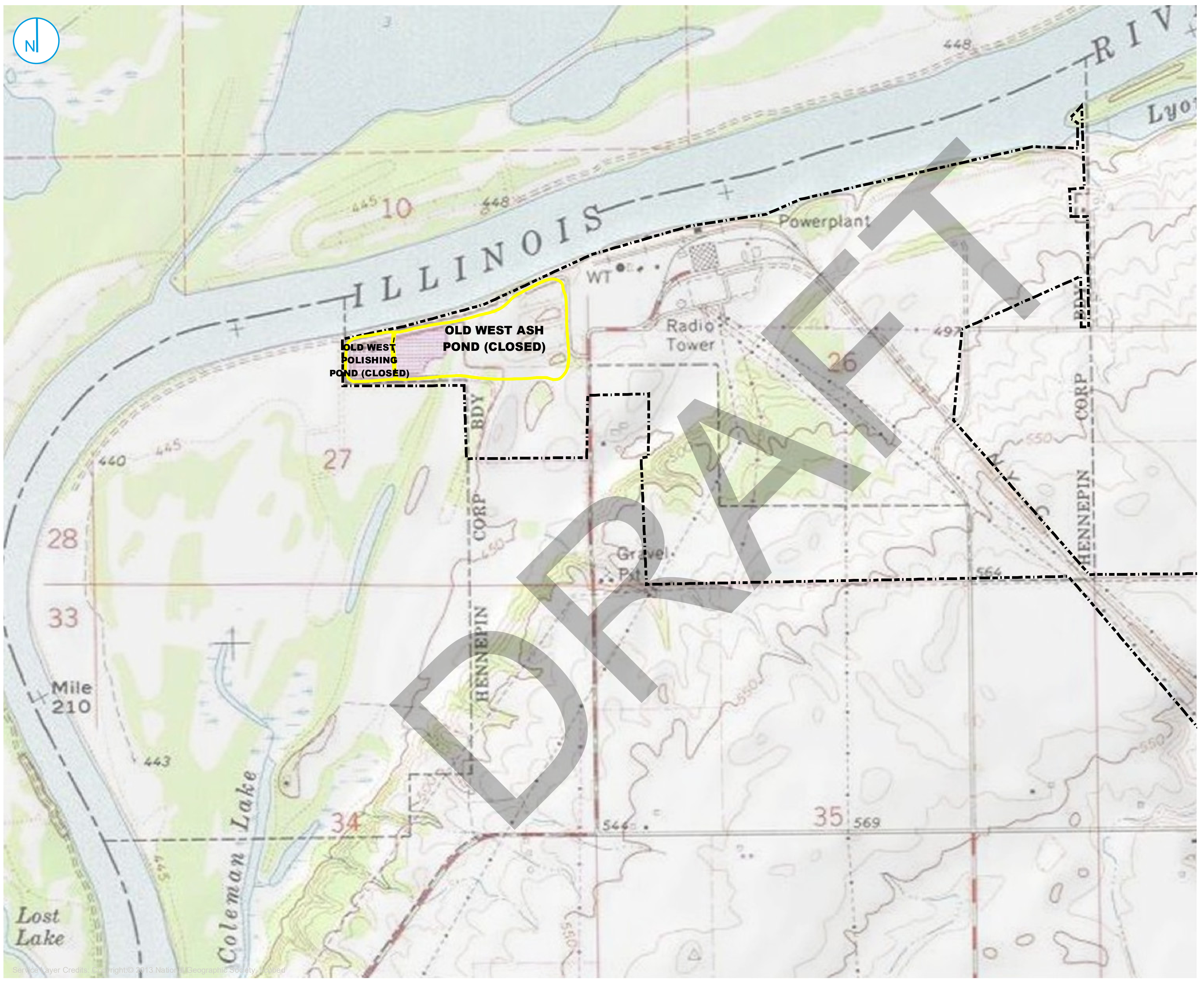

🟨 REGULATED UNIT (SUBJECT UNIT)

▭ PROPERTY BOUNDARY

0 500 1,000 Feet

SITE LOCATION MAP

35 I.A.C. § 845 CORRECTIVE MEASURES ASSESSMENT
WEST ASH POND SYSTEM
HENNEPIN POWER PLANT
HENNEPIN, ILLINOIS

FIGURE 2-1

RAMBOLL AMERICAS
ENGINEERING SOLUTIONS, INC.

RAMBOLL

PROJECT: 169000XXXX | DATED: 9/29/2021 | DESIGNER: STOLZSD

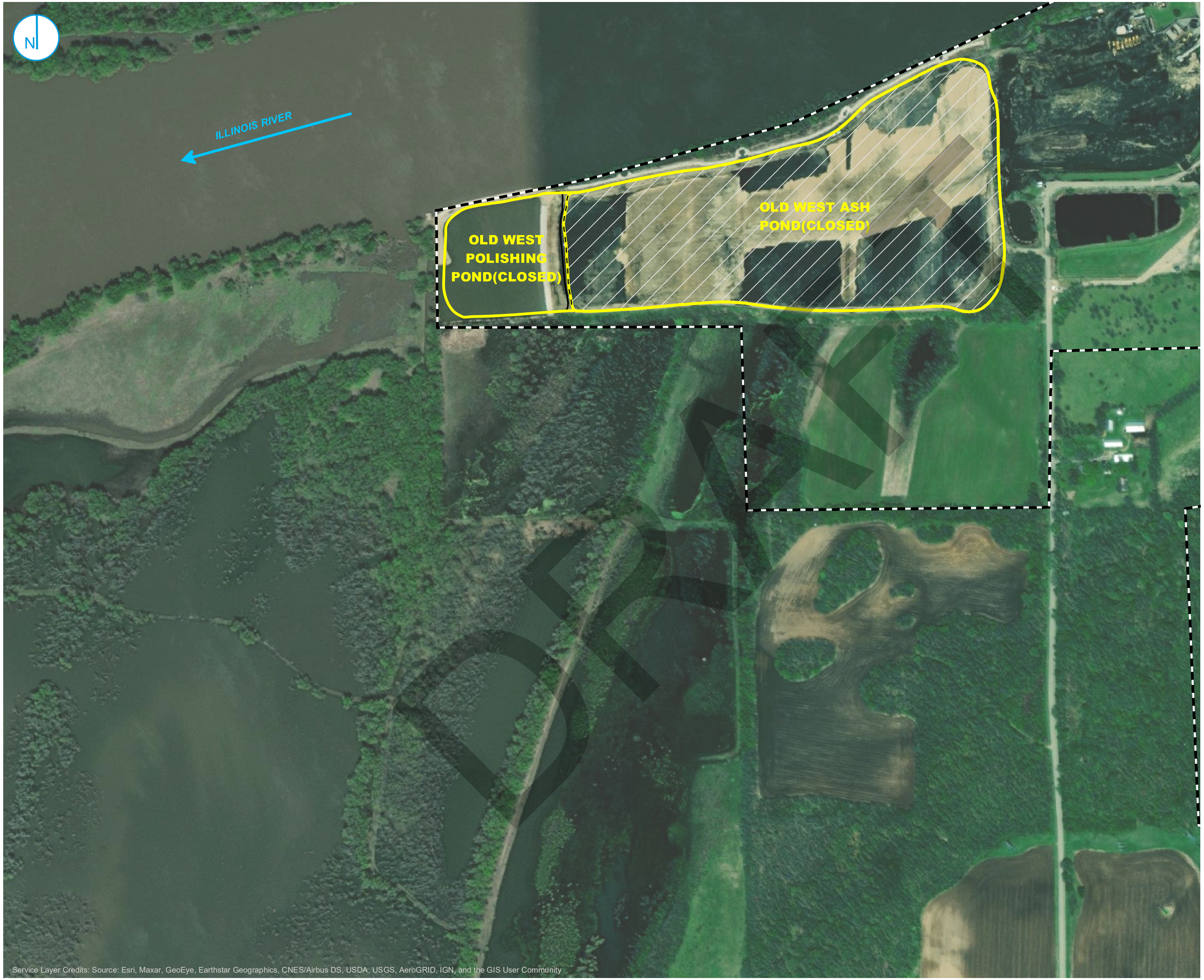

Service Layer Credits: Source: Esri, Maxar, GeoEye, Earthstar Geographics, CNES/Airbus DS, USDA, USGS, AeroGRID, IGN, and the GIS User Community

🟨 REGULATED UNIT (SUBJECT UNIT)
▨ LIMITS OF FINAL COVER
⬚ PROPERTY BOUNDARY

0 200 400 Feet

SITE MAP

35 I.A.C. § 845 CORRECTIVE MEASURES ASSESSMENT
WEST ASH POND SYSTEM
HENNEPIN POWER PLANT
HENNEPIN, ILLINOIS

FIGURE 2-2

RAMBOLL AMERICAS
ENGINEERING SOLUTIONS, INC.

Y:\Mapping\Projects\22\2285\MXD\845_Operating_Permit\Hennepin\GMP_804\Figure 1-2_Site Map.mxd

PROJECT: 169000XXXX | DATED: 9/29/2021 | DESIGNER: STOLZSD

⊞	COMPLIANCE MONITORING WELL
⊞	BACKGROUND MONITORING WELL
⊞	MONITORING WELL
—	GROUNDWATER ELEVATION CONTOUR (1 FT CONTOUR INTERVAL, NAVD88)
- -	INFERRED GROUNDWATER ELEVATION CONTOUR
→	GROUNDWATER FLOW DIRECTION
▭	REGULATED UNIT (SUBJECT UNIT)
▨	LIMITS OF FINAL COVER
⬚	PROPERTY BOUNDARY

NOTES:
1.ELEVATIONS IN PARENTHESES WERE NOT USED FOR CONTOURING.
2. ELEVATION CONTOURS SHOWN IN FEET, NORTH AMERICAN VERTICAL DATUM OF 1988 (NAVD88)
*ILLINOIS RIVER ELEVATION OBTAINED FROM STAFF GAGE SG02, LOCATED AT THE HENNEPIN POWER PLANT

0 200 400
Feet

UPPERMOST AQUIFER POTENTIOMETRIC SURFACE MAP
MAY 30, 2023

35 I.A.C. § 845 CORRECTIVE MEASURES ASSESSMENT
WEST ASH POND SYSTEM
HENNEPIN POWER PLANT
HENNEPIN, ILLINOIS

FIGURE 2-3

RAMBOLL AMERICAS
ENGINEERING SOLUTIONS, INC.

Service Layer Credits: Source: Esri, Maxar, GeoEye, Earthstar Geographics, CNES/Airbus DS, USDA, USGS, AeroGRID, IGN, and the GIS User Community

- ✚ COMPLIANCE MONITORING WELL
- ✚ BACKGROUND MONITORING WELL
- ✚ MONITORING WELL
- ▭ REGULATED UNIT (SUBJECT UNIT)
- ▨ LIMITS OF FINAL COVER
- ▭ SITE FEATURE
- ⬚ PROPERTY BOUNDARY

0 200 400
Feet

MONITORING WELL LOCATION MAP

35 I.A.C. § 845 CORRECTIVE MEASURES ASSESSMENT
WEST ASH POND SYSTEM
HENNEPIN POWER PLANT
HENNEPIN, ILLINOIS

FIGURE 2-4

RAMBOLL AMERICAS
ENGINEERING SOLUTIONS, INC.

Y:\Mapping\Projects\22\2285\MXD\2021_AnnualGWM_CAR\Hennepin\OWAP_804\Figure 1 HEN OWAP MW Location Map.mxd

PROJECT: 169000XXXX | DATED: 1/5/2022 | DESIGNER: galarmc

Attachments

Attachment A – Selected Closure Plan Drawings

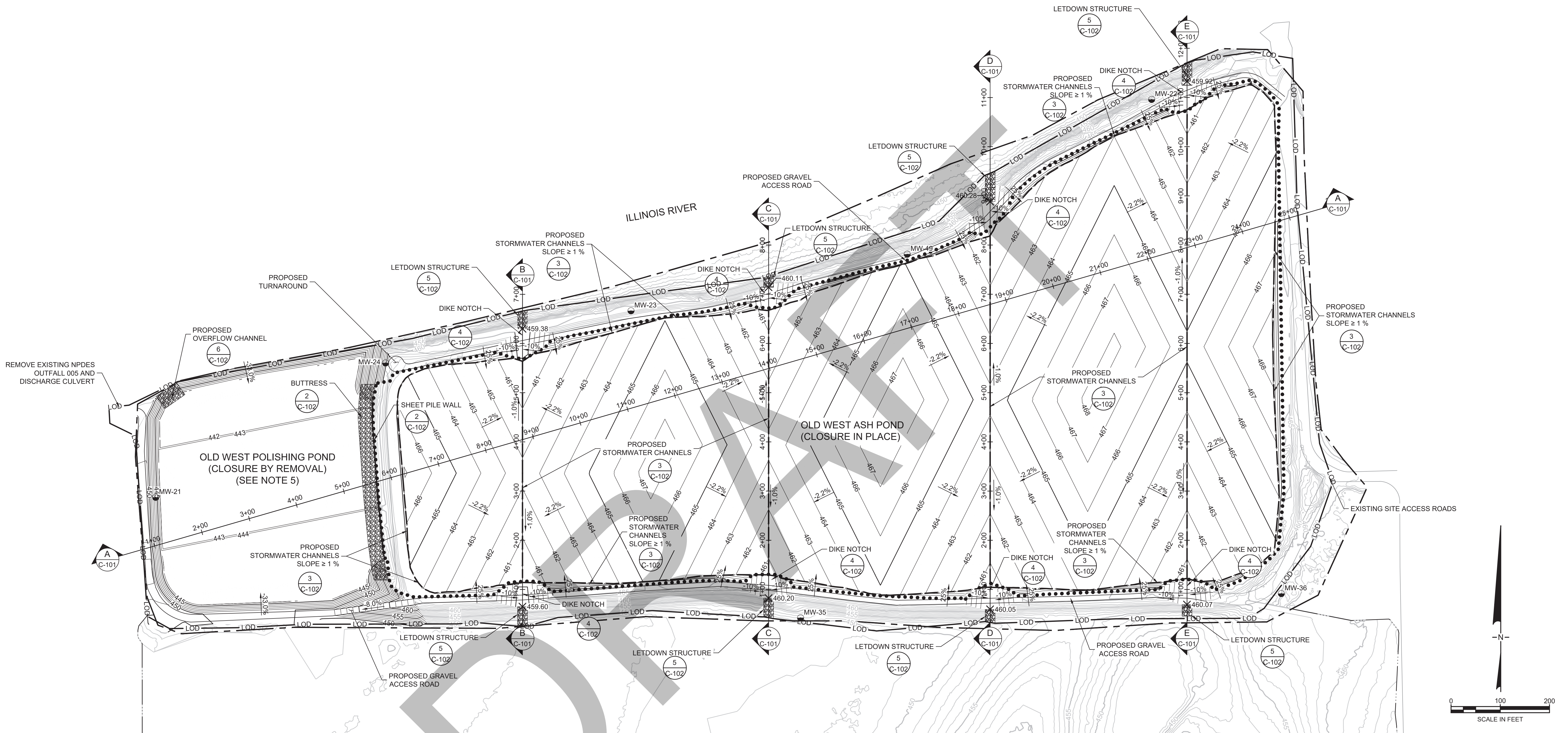

EARTHWORK VOLUMES TO REACH DESIGN SUBGRADES

CUT (PRE-COMPACTION)		FILL (POST COMPACTION)	
OLD WEST POLISHING POND	61,000 CY	OLD WEST POLISHING POND	0 CY
OLD WEST ASH POND	36,000 CY	OLD WEST ASH POND	80,000 CY
TOTAL	97,000 CY	TOTAL	80,000 CY

NOTES:

1. CUT MATERIAL IS ASSUMED TO REDUCE IN VOLUME BY 18% DUE TO COMPACTION. THEREFORE, THE TOTAL VOLUME OF CUT MATERIAL AVAILABLE FOR COMPACTED FILL IS 80,000 CY, RESULTING IN BALANCED CUT AND FILL QUANTITIES.
2. CUT AND FILL QUANTITIES ARE ONLY THOSE REQUIRED TO REACH DESIGN SUBGRADES. OTHER EARTHWORK QUANTITIES, SUCH COVER SOIL, BUTTRESS FILL, AND LETDOWN STRUCTURES ARE NOT INCLUDED IN THESE QUANTITIES.

NOTES:

1. WEST ASH BASIN TOPOGRAPHIC SURVEY PROVIDED BY DYNEGY, TITLED "HENNEPIN 2015 AERIAL TOPOGRAPHY EXISTING SITE CONDITIONS", SURVEYED BY WEAVER CONSULTANTS GROUP, DATED DECEMBER 1, 2015.
2. TOPOGRAPHIC SURVEY SOUTH OF THE OLD WEST ASH POND AND OLD WEST POLISHING POND WAS PROVIDED BY INGENAE, TITLED "2017 TOPOGRAPHY", DATED JUNE 15, 2017.
3. COORDINATES AND DIRECTIONS SHOWN ON THIS DRAWING ARE BASED ON ILLINOIS STATE PLANE COORDINATE SYSTEM (NAD83) (US FEET). ELEVATIONS ARE BASED ON NORTH AMERICAN VERTICAL DATUM OF 1988 (NAVD88) (US FEET).
4. GRADING SHOWN ON THIS PLAN IS THE TOP OF FINAL COVER, WHICH IS TWO FEET ABOVE TOP OF SUBGRADE.
5. THE OLD WEST POLISHING POND WILL BE CLOSED BY REMOVAL OF CCR. AFTER CLOSURE, THE FORMER OLD WEST POLISHING POND WILL BE VEGETATED AND FUNCTION AS SHALLOW POND. THE ONLY INFLOW INTO THE FORMER OLD WEST POLISHING POND WILL BE PRECIPITATION THAT FALLS DIRECTLY INTO THE POND AND WATER FROM THE ADJACENT ILLINOIS RIVER THAT WILL FLOW INTO THE POND DURING HIGH-WATER EVENTS.
6. ALL DENSE, WOODY VEGETATION (I.E. TREES, SHRUBS) INSIDE THE LIMITS OF DISTURBANCE WILL BE REMOVED AS PART OF CLOSURE CONSTRUCTION. THE DISTURBED AREAS WILL BE RE-VEGETATED WITH GRASSES AS PART OF CLOSURE CONSTRUCTION.

BASE MAP LEGEND

460	EXISTING GROUND SURFACE ELEVATION (MAJOR) (5-FT INTERVAL)
	EXISTING GROUND SURFACE ELEVATION (MINOR) (1-FT INTERVAL)
— —	WEAVER SURVEY LIMITS
— · · · —	INGENAE SURVEY LIMITS
— LOD —	LIMITS OF DISTURBANCE
MW-23	EXISTING MONITORING WELL

PROPOSED CONDITION LEGEND

465	TOP OF FINAL COVER ELEVATION ELEVATION (MAJOR) (5-FT INTERVAL)
465	TOP OF FINAL COVER ELEVATION (MINOR) (1-FT INTERVAL)
—●●●●●—	APPROXIMATE LIMITS OF FINAL COVER AND ANCHOR TRENCH
→ → →	PROPOSED STORMWATER CHANNELS

CLOSURE PLAN SUBMITTAL
NOT FOR CONSTRUCTION

REV	DATE	DESCRIPTION	DRN	APP

Geosyntec consultants
134 NORTH LASALLE STREET, SUITE 300
CHICAGO, IL 60602 USA
TELEPHONE: 312 658 0500

DYNERGY MIDWEST GENERATION, LLC
1500 EASTPORT PLAZE DRIVE
COLLINSVILLE, IL 62234 USA

TITLE:
OVERALL GRADING PLAN

PROJECT:
SWPPP DRAWINGS FOR CLOSURE OF THE
OLD WEST ASH POND AND OLD WEST POLISHING POND

SITE:
HENNEPIN POWER STATION
HENNEPIN, ILLINOIS

THIS DRAWING MAY NOT BE ISSUED FOR PROJECT TENDER OR CONSTRUCTION, UNLESS SEALED.

SIGNATURE

DATE

DESIGN BY: LPC		DATE:	DECEMBER 2017
DRAWN BY: CT/MK		PROJECT NO.:	CHE8356
CHECKED BY: SH		FILE:	CHE8356-003
REVIEWED BY: PA		DRAWING NO.:	C-100
APPROVED BY: JPC			

H:\D\DYNEGY\HENNEPIN\CLOSURE PROJECT - CHE8356\DRAWINGS\CHE8356-003

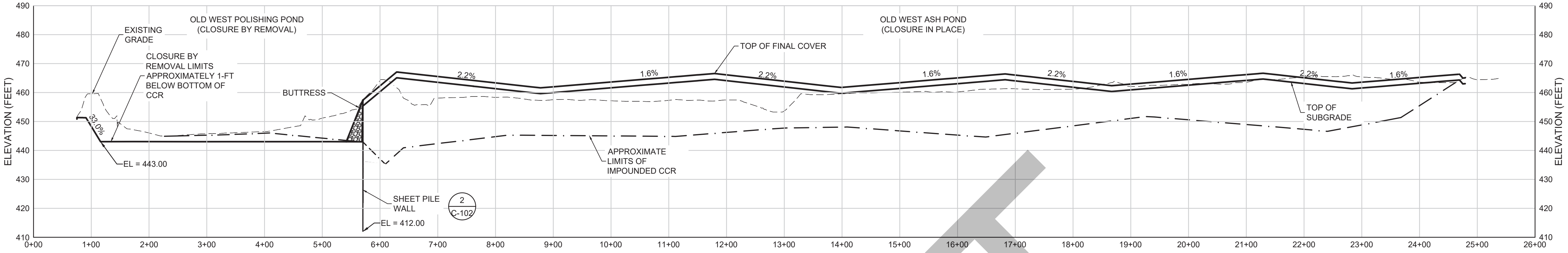

A
C-100

SECTION

PROPOSED DESIGH GRADING SECTION A-A

HORIZONTAL SCALE: 1" = 100'
VERTICAL SCALE: 1" = 20'

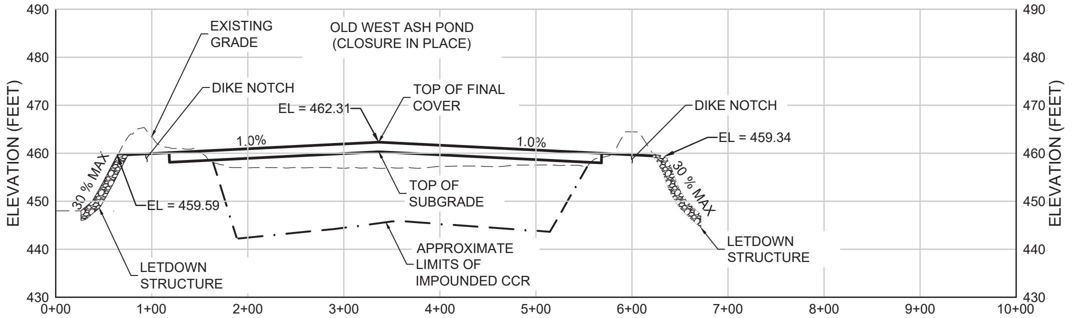

B
C-100

SECTION

CHANNEL SECTION B-B

HORIZONTAL SCALE: 1" = 100'
VERTICAL SCALE: 1" = 20'

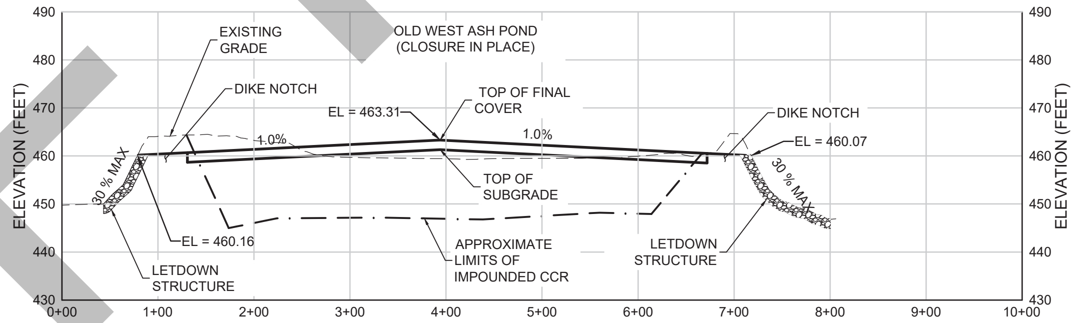

C
C-100

SECTION

CHANNEL SECTION C-C

HORIZONTAL SCALE: 1" = 100'
VERTICAL SCALE: 1" = 20'

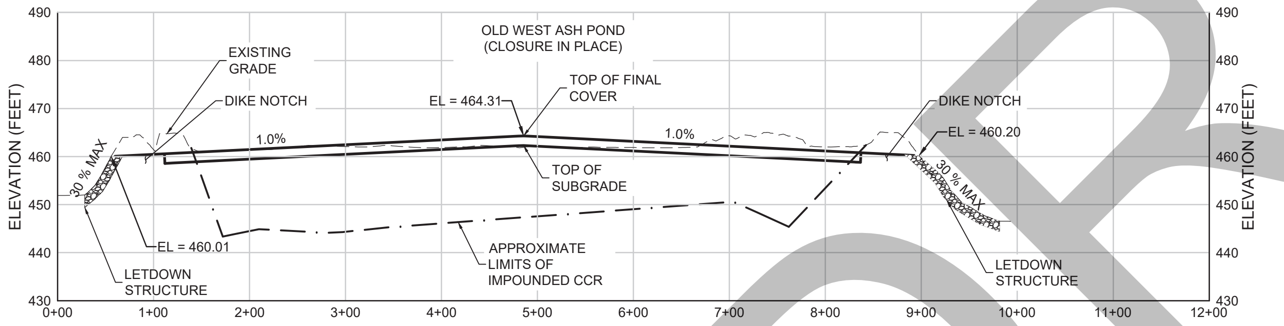

D
C-100

SECTION

CHANNEL SECTION D-D

HORIZONTAL SCALE: 1" = 100'
VERTICAL SCALE: 1" = 20'

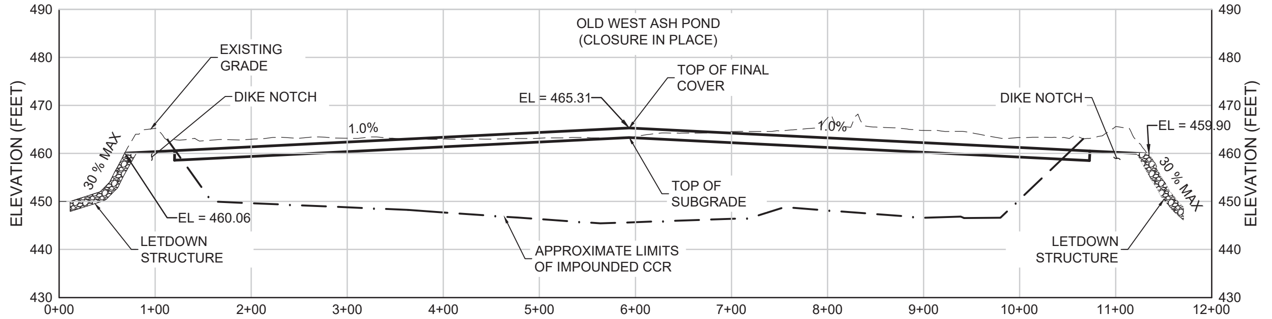

E
C-100

SECTION

CHANNEL SECTION E-E

HORIZONTAL SCALE: 1" = 100'
VERTICAL SCALE: 1" = 20'

NOTE:

1. APPROXIMATE LIMITS OF IMPOUNDED CCR DEVELOPED USING AVAILABLE BORING DATA FROM THE 2016 AECOM, 2016 CEC, AND 2017 CEC GEOTECHNICAL EXPLORATIONS. CCR LIMITS BETWEEN BORINGS WERE INTERPOLATED USING AUTOCAD CIVIL3D SOFTWARE AND IMPOUNDMENT DESIGN AND CONSTRUCTION INFORMATION FROM THE CCR RULE HISTORY OF CONSTRUCTION REPORT FOR THE HENNEPIN POWER STATION (AECOM, 2016).

CLOSURE PLAN SUBMITTAL
NOT FOR CONSTRUCTION

REV	DATE	DESCRIPTION	DRN	APP

Geosyntec consultants
134 NORTH LASALLE STREET, SUITE 300
CHICAGO, IL 60602 USA
TELEPHONE: 312 658 0500

DYNERGY MIDWEST GENERATION, LLC
1500 EASTPORT PLAZE DRIVE
COLLINSVILLE, IL 62234 USA

TITLE: SECTIONS

PROJECT: SWPPP DRAWINGS FOR CLOSURE OF THE
OLD WEST ASH POND AND OLD WEST POLISHING POND

SITE: HENNEPIN POWER STATION
HENNEPIN, ILLINOIS

THIS DRAWING MAY NOT BE ISSUED FOR PROJECT TENDER OR CONSTRUCTION, UNLESS SEALED.

SIGNATURE

DATE

DESIGN BY:	LPC	DATE:	DECEMBER 2017
DRAWN BY:	CT/MK	PROJECT NO.:	CHE8356
CHECKED BY:	SH	FILE:	CHE8356-004
REVIEWED BY:	PA	DRAWING NO.:	
APPROVED BY:	JPC		C-101

H:\DYNEGY\HENNEPIN\CLOSURE PROJECT - CHE8356\DRAWINGS\CHE8356-004

Appendix D

Nature and Extent Report

Intended for
Dynegy Midwest Generation , LLC
13498 E 800th St.
Hennepin, Illinois, 61327

Date
May 8, 2024

Project No.
1940103584-005

NATURE AND EXTENT REPORT

HENNEPIN POWER PLANT, WEST ASH POND SYSTEM, IEPA ID NO. W1550100002-01 AND W1550100002-03

RAMBOLL Bright ideas. Sustainable change.

NATURE AND EXTENT REPORT
HENNEPIN POWER PLANT, WEST ASH POND SYSTEM, IEPA ID NO. W1550100002-01 AND W1550100002-03

Project name	**Hennepin Power Plant West Ash Pond System**
Project no.	**1940103584-005**
Recipient	**Dynegy Midwest Generation, LLC**
Document type	**Nature and Extent Report**
Revision	**FINAL**
Date	**May 8, 2024**
Prepared by	**Nathaniel Keller, Bryan Donaldson**
Checked by	**Melanie Conklin**
Approved by	**Brian G. Hennings, PG**

Ramboll
234 W. Florida Street
Fifth Floor
Milwaukee, WI 53204
USA

T 414-837-3607
F 414-837-3608
https://ramboll.com

Alison OConnor

Alison O'Connor, PhD
Geochemist

Nathaniel R Keller

Nathaniel R. Keller
Senior Technical Manager, Hydrogeology

Brian G. Hennings, PG
Project Officer, Hydrogeology

CONTENTS

TABLES (ATTACHED)

FIGURES (ATTACHED)

APPENDICES

ACRONYMS AND ABBREVIATIONS

35 I.A.C.	Title 35 of the Illinois Administrative Code
ASD	Alternative Source Demonstration
CCR	coal combustion residuals
Closure Plan	Closure and Post-Closure Care Plan
CMA	Corrective Measures Assessment
cm/s	centimeters per second
COC	chemicals of concern
CSM	conceptual site model
DMG	Dynegy Midwest Generation, LLC
E001	Event 1
E002	Event 2
E003	Event 3
GCSM	geochemical conceptual site model
GWPS	groundwater protection standard
HELP	Hydrologic Evaluation of Landfill Performance
HPP	Hennepin Power Plant
HCR	Hydrogeologic Site Characterization Report
ID	Identification
IEPA	Illinois Environmental Protection Agency
LCL	lower confidence limit
mg/L	milligrams per liter
NAVD88	North American Vertical Datum 1988
No.	Number
OWAP	Old West Ash Pond (Pond No. 1 and Pond No. 3)
OWPP	Old West Polishing Pond
SI	surface impoundment
TDS	total dissolved solids
UA	uppermost aquifer
WAPS	West Ash Pond System

EXECUTIVE SUMMARY

Groundwater samples collected at the Hennepin Power Plant (HPP) West Ash Pond System (WAPS) during May and June 2023 for the Quarter 2, 2023 compliance sampling event (Event 1 [E001]) were evaluated for exceedances of the groundwater protection standards (GWPS) described in Title 35 of the Illinois Administrative Code (35 I.A.C.) § 845.600. Exceedances were identified in the following wells in the uppermost aquifer (UA):

- Arsenic at 21R and 51
- Boron at 21R, 22, 23, and 35
- Cadmium at 22
- Sulfate at 23 and 35

In accordance with 35 I.A.C. § 845.650(e), an Alternative Source Demonstration (ASD) was completed for the cadmium exceedance at well 22 and received concurrence in a letter from the Illinois Environmental Protection Agency (IEPA) dated December 11, 2023 [1, 2]. A Corrective Measures Assessment (CMA) was initiated on December 10, 2023 and submitted on May 8, 2024 in accordance with 35 I.A.C. § 845.660 for the remaining E001 exceedances [3].

The subsequent compliance sampling events for the Quarter 3 and Quarter 4, 2023 sampling events (Event 2 [E002] and Event 3 [E003]) were completed in August and November 2023 and groundwater samples were evaluated for exceedances of the GWPS as described in 35 I.A.C. § 845.600. Additional exceedances were identified in the following wells in the UA during the E002 and E003 events:

- Lithium at 22
- Total Dissolved Solids (TDS) at 35

The E002 and E003 exceedances of lithium at well 22 and TDS at well 35 were evaluated with respect to the groundwater model, potentially feasible corrective measures, and remedy extents and were determined not to substantially affect the findings and conclusions of the previously initiated CMA evaluation and therefore have been incorporated into the CMA and this report.

As required by 35 I.A.C. § 845.650(d)(1) this report characterizes the nature and extent of arsenic, boron, lithium, sulfate, and TDS and relevant site conditions to determine how they may affect the corrective measures ultimately selected for the WAPS and documents the additional measures taken in accordance with 35 I.A.C. § 845.650(d).

All of the aforementioned chemicals of concern (COCs) were detected above the GWPS within the UA. The lateral and downgradient extent of these COCs in the UA is adequately defined by sampling of existing monitoring wells and surface water samples. The vertical migration of these COCs above the GWPS in the UA is limited by low hydraulic conductivity of the Bedrock Confining Unit (Carbondale Formation) underlying the UA [4]. The concentrations of arsenic, boron, lithium, sulfate and TDS within the UA are attenuated physically through dilution and dispersion; and may be geochemically attenuated by surface complexation reactions with metal oxyhydroxides and clays. Concentrations of exceedance parameters in the Illinois River were evaluated and they do not exceed their respective GWPS.

1. INTRODUCTION

35 I.A.C. § 845.650(d)(1) requires the owner or operator of a coal combustion residuals (CCR) surface impoundment (SI) to characterize the nature and extent of a release and relevant site conditions that may affect the remedy ultimately selected for a CCR SI if any constituent regulated under 35 I.A.C. § 845 is found to exceed the GWPS. This report documents the nature and extent of constituents detected above the GWPS that are attributable to the HPP WAPS.

The groundwater data and analysis in this report includes results from historical sampling (initiated in 2015) through E003, which was completed on November 15, 2023. Results of the events E001, E002, and E003 were submitted and placed in the facility's operating record within 60 days of receiving final laboratory analytical data [5, 6, 7] as required by 35 I.A.C. § 845.800(d)(15). The statistical determination presented in these reports identified the following exceedances of the GWPS at compliance groundwater wells in the UA:

- Arsenic at 21R and 51
- Boron at 21R (E001 only), 22, 23, and 35
- Cadmium at 22
- Lithium at 22
- Sulfate at 23 and 35
- TDS at 35

An ASD, as allowed by 35 I.A.C. § 845.650(e), was completed for the cadmium exceedance at UA monitoring well 22 [2]. The IEPA concurred with the ASD in a letter dated December 11, 2023 [1]. Therefore, the nature and extent of cadmium is not discussed in this document. This Nature and Extent Report discusses in detail the extent of arsenic, boron, lithium, sulfate, and TDS exceedances as well as a geochemical conceptual site model (GCSM) describing the nature of these exceedances.

2. UNIT BACKGROUND

2.1 Site Location and Description

The HPP is an approximately 504-acre property consisting of 19 parcels positioned adjacent to the Illinois River, including a retired coal-fired power plant, CCR landfill and SIs, and farmland, located approximately 3 miles north-northeast of the Village of Hennepin, Illinois, in Putnam County. The HPP construction history includes construction of Unit 1 in 1953 and Unit 2 in 1969, with capacities of 70 megawatts (MW) and 210 MW, respectively. The plant initially burned high-sulfur Illinois coal and switched to sub-bituminous Powder River Basin coal in 1999 [8]. The HPP ceased operations in 2019 when the power plant was retired.

The WAPS is one of three CCR units at the HPP regulated under 35 I.A.C. § 845. The other two CCR units regulated under 35 I.A.C. § 845 (Ash Pond Number [No.] 2 and No. 4 multi-unit [AP2/AP4] and the East Ash Pond) are located adjacent to each other and the Landfill, east of the HPP. The WAPS is located west of the HPP. Areas surrounding the WAPS include agricultural land, with scattered groupings or rows of trees to the southeast, and low-lying floodplains of the Donnelley Wildlife Management Area to the southwest and west. The WAPS and surrounding properties are shown on **Figure 2-1**.

2.2 Description of CCR Unit

Dynegy Midwest Generation, LLC (DMG) operated the WAPS from 1952 through 1996. It consists of two closed units, the Old West Ash Pond (OWAP; IEPA Unit Identification [ID] W1550100002-01) and the Old West Polishing Pond (OWPP; IEPA Unit ID W1550100002-03) (**Figure 2-2**). The OWAP consists of the 9.3-acre Pond No. 1 at the eastern end of the impoundment and the 16.4-acre Pond No. 3 within the central portion of the impoundment. The 4.7-acre OWPP is situated at the western end of the impoundment. All ponds were previously bermed to approximately 15 feet above grade primarily using locally occurring soils. The OWPP berms were excavated and removed to obtain access to CCR material used within and below them during closure construction of this unit in 2020.

During operation, water was used to sluice fly ash, bottom ash, and low-volume wastes to the WAPS. At the time it was removed from service in late 1996, there was no surface water discharge. Coal ash sluiced to the WAPS was a by-product of the combustion of high-sulfur Illinois coal. CCR fill, consisting primarily of fly ash, bottom ash, and boiler slag is present from approximately 460 feet[1] to a minimum elevation of approximately 440 feet along the west side of the OWAP (**Figure 2-3**). The unit is encompassed by fill deposits of predominantly sand, clay, and silt materials from on-site excavations that were used to construct berms and roads surrounding the various impoundments across the Site.

Water that may come into contact with CCR within the footprint of the WAPS becomes CCR source water. CCR source water samples, collected from the porewater monitoring wells (**Figure 2-4**) screened within the CCR materials at the WAPS were used to provide information for ASDs

---

[1] All elevations in this report are referenced to North American Vertical Datum of 1988 (NAVD88) unless otherwise noted.

and groundwater transport modeling[2]. As a result of declining water levels within the unit post-closure, the remaining porewater monitoring wells have become dry, thus preventing further sample collection.

The Closure and Post-Closure Care Plan, Old West Ash Pond, Old West Polishing Pond at DMG, Hennepin Power Station (Closure Plan) was submitted to IEPA in 2017 [9] and approved by IEPA in a letter dated June 19, 2018. The approved Closure Plan summarized the planned closure of the WAPS, which included dewatering the CCR, if needed, mechanical excavation of material from the OWPP for use as structural fill in the WAPS, grading within the WAPS, constructing an alternate cover system consisting of geomembrane and vegetated cover soils in direct contact with the graded CCR, and establishment of a vegetative cover. Closure construction was completed on November 17, 2020 [10].

2.3 Geology and Hydrogeology

Significant site investigation has been completed at the HPP to characterize the geology, hydrogeology, and groundwater quality. Based on extensive investigation and monitoring, the WAPS has been well characterized and detailed in the October 25, 2021 operating permit application and the Hydrogeologic Site Characterization Report (HCR) submitted as part of the Closure Plan [4, 11, 9]. Those materials, in addition to data collected from the nearby East Ash Pond System, where representative of Site conditions, are incorporated herein.

2.3.1 Hydrostratigraphic Units

In addition to CCR, materials at the site have been categorized into two hydrostratigraphic units at the WAPS based on stratigraphic relationships, geologic composition, and common hydrogeologic properties. Cross-sections developed for the HCR are included in **Appendix A**. The units, listed from surface downward, are summarized as follows:

- **Uppermost Aquifer (UA)**: Includes the Cahokia Alluvium which consists of fine-grained river deposits comprised of silts and clays (upper UA), fine-medium sands (middle UA), and highly permeable glacial outwash sands and gravels of the Henry Formation (lower UA). The UA contains variable amounts of cobbles and boulders within a sand and gravel matrix. Both the prevalence and size of the cobbles and boulders increase with depth.

- **Bedrock Confining Unit**: Comprised of interbedded layers of shales with thin limestone, sandstone, and coal beds. Representative hydraulic conductivity for shale ranges from 5×10^{-6} to 5×10^{-10} centimeters per second (cm/s) and this unit defines the lower boundary of the UA. Borings along the perimeter of the nearby East Ash Pond System confirm the presence of shale bedrock between elevations ranging from 399.2 to 410.2 feet [12].

2.3.2 Uppermost Aquifer

The unlithified geologic deposits of the UA surrounding the WAPS are derived from recent river deposition, glacial outwash, and glacial tills. The WAPS overlies both glacial outwash deposits (Henry Formation) and alluvium (Cahokia Alluvium). OWAP Pond No. 1 rests on top of lower terrace glacial deposits, and the eastern portion of Pond No. 3 overlies alluvial sand. Whereas the

---

[2] Per Federal Register 80 (21302), which promulgated the final C.F.R. 40 § 257 rule, porewater concentrations should be used to characterize potential leaching from impoundments. As discussed further in USEPA's risk assessment of CCR surface impoundments (USEPA 2014), porewater is "collected from the interstitial water between waste particles in surface impoundments as it occurs in the field," and concentrations within the porewater are "the most representative data available for impoundments because these data are field-measured concentrations of leachate." Therefore, CCR source water collected from porewater wells screened near the base of ash within the unit represents the CCR source term.

western portion of Pond No. 3 and the OPP overlies silty clay alluvial channel fill deposits (**Figure 2-3**). The total thickness of the UA varies in thickness ranging from 50 to 200 feet. Groundwater monitoring for the UA is focused on the sand and gravel zone because it is continuous, exhibits high groundwater velocities, and is most likely to indicate potential migration of impacts from the WAPS. The top of the sand and gravel portion of the UA is shown on **Figure 2-5**. The sand and gravel is present at the surface at an approximate elevation of 450 feet (no overlying clay/silt) near wells 25, 26, and within 5 feet of the surface at wells 30, 31, 35, and 36. CCR is also near the top of the sand and gravel in eastern areas of the WAPS. From the topographic highs, the top of the sand and gravel slopes downward toward the river to approximately 410 feet near well 21/21R and 51. The direction of groundwater flow and hydraulic gradient is contingent on the elevation of the Illinois River which is directly adjacent to the WAPS.

2.3.3 Regional Bedrock Geology

The bedrock geology near the Hennepin Power Station is primarily comprised of the Pennsylvanian Carbondale Formation, which is characterized by shale with thin limestone, sandstone, and coal beds. The bedrock surface elevation ranges from 400 to 450 feet, with shale bedrock confirmed between elevations of 400 and 410 feet in the vicinity of the WAPS. The thickness of Pennsylvanian rocks varies from 150 to 525 feet across Putnam County and is estimated to be around 300 to 400 feet near the site. Beneath the Pennsylvanian rocks lie Mississippian and Devonian-age interbedded layers of limestone and shale over Silurian-age dolomite, with aquifer depths ranging from less than 1,000 feet to over 1,800 feet. [4].

2.3.4 Water Table Elevation and Groundwater Flow Direction

Measured water table elevations in the UA during the quarterly sampling events in 2023 ranged from approximately 440 feet in the northwest portion of the site (well 34) to approximately 449 feet south of the WAPs in well 26 (**Table 2-1**; **Figure 2-6** to **Figure 2-9**). Increased groundwater elevations measured near the river in wells 22, 34, and 50 during periods of flooding (**Figure 2-5**) indicate there is a potential connection between the river and the sand and gravel of the UA in this area. Groundwater elevations following closure have been relatively stable, generally varying less than approximately 2 feet.

The primary groundwater flow direction within the UA is generally northwest from areas where the sand and gravel in the UA is closest to the surface (wells 25, 26, 30, 31, 35, and 36) toward the river and locations where the UA potentially interacts with the base of the river (*i.e.,* wells 22, 34, and 50).

2.3.4.1 Impact of Surface Water Bodies on Groundwater Flow

Under normal river stage conditions, the Illinois River serves as the primary local and regional receiving body of water for groundwater in the area, with its lowest stage typically occurring between August and October [4]. Historically during this period, a groundwater divide becomes apparent beneath the WAPS, directing flow north towards the river and southwestward, eventually migrating west of the WAPS. Surface water elevations in the Donnelley Wildlife Management Area (DWMA) are expected to be similar to elevations measured in wells 32, 33, and 34. Groundwater flow patterns are depicted in potentiometric surface maps for quarters 1 through 4 of 2023 (**Figures 2-6 through 2-9**), which align with historical observations.

During annual spring flooding from March to June, and sporadic flood events, river stages exceed adjacent groundwater levels, resulting in temporary aquifer recharge and a reversal of groundwater flow direction. Horizontal gradients across the site flatten during these events. A representative potentiometric surface map for February 28 and March 1, 2023 (**Figure 2-6**), illustrates groundwater flow conditions during flood stage, with an approximate river elevation of 449.50 feet. These reversals are temporary and limited in duration and extent. Horizontal hydraulic gradients from the WAPS to off-site areas vary from 0.001 during Illinois River flood stage to about 0.005 during normal river stage.

2.3.5 Hydraulic Conductivities

2.3.5.1 Field Hydraulic Conductivities

Hydraulic conductivity was calculated based on field tests at seven wells in proximity to the WAPS. Hydraulic conductivity ranged from 1.2 x 10^{-2} cm/s in the Henry Formation (deep UA) to 1.3 x 10^{-4} cm/s in the Cahokia Alluvium silt (shallowest UA). The geometric mean hydraulic conductivity for the sand and gravel portion of the UA is 6 x 10^{-3} cm/s. The geometric mean for wells finished in the glacial outwash gravels of the Henry Formation is 1.7 x 10^{-2} cm/s [4].

A pump test was also performed in the Henry Formation using a “fire well” which resulted in a reported hydraulic conductivity of 1.3 x 10^{-1} cm/s. The well is located in proximity to the southwest corner of the HPP, east of the WAPS [4].

2.3.5.2 Laboratory Hydraulic Conductivities

Hydraulic conductivity laboratory tests were performed for two samples collected in boring HEN-B010 (fly ash with sand and gravel) near the south berm of Old West Pond 3 and HEN-B017 (gray lean clay with sand) near the west berm of the OWPP. Hydraulic conductivities were calculated to be 1.2 x 10^{-5} cm/s and 6.8 x 10^{-7} cm/s, respectively [4].

2.3.5.3 Groundwater Velocity and Vertical Gradients

Hydraulic gradients were calculated from water-level elevations at wells 21 to 34 and wells 27 to 33 in June and September 2013 [4] as representative gradients for the predominant direction of lateral flow at the WAPS. Hydraulic gradients ranged from 0.005 (21 to 34) to 0.001 (27 to 37) during both periods of measurement [4].

Groundwater velocities were calculated using geometric means of the field calculated hydraulic conductivities of 1.7 x 10^{-2} cm/s (glacial outwash gravels) and 6.0 x 10^{-3} cm/s (sand and gravel), an effective porosity of 0.22 and the hydraulic gradients listed above. Groundwater velocities calculated in proximity to the WAPS, between wells 21 to 34 and wells 27 to 33, range from 0.03 meters per day (m/day) to 0.34 m/day [4].

Vertical gradients evaluated in wells 22 and 22D in 2023 indicate groundwater generally has an upward gradient in this area, which is consistent with the Illinois River being the receiving water body for regional groundwater. Downward gradients observed in February and November are potentially a result of delayed response to changes in river stage in the deeper well, and a measurement anomaly, respectively (**Figure 2-10**).

2.4 Groundwater Monitoring

The monitoring system for the WAPS is shown on **Figure 2-11** and consists of two background monitoring wells (32 and 34) and nine compliance monitoring wells (21R, 22, 22D, 23, 27, 35, 49, 50, and 51). These monitoring wells are screened within the UA along the perimeter of the WAPS to monitor potential impacts from the SI [13]. During remedial construction performed in February 2020, wells 21 and 24 were abandoned and replaced with wells 21R and 51, respectively. Discussion of historical groundwater data from wells 21 and 24 is presented in **Section 3** of this report and will refer to their respective replacement wells.

2.5 Hydrogeologic Conceptual Site Model

The overall groundwater flow regime within the unlithified materials is consistent with topographically-controlled flow patterns, where infiltration of precipitation recharges groundwater and flows north and west near the site towards the Illinois River. Flow patterns within the site hydrostratigraphic units are typically horizontal, with components of converging vertical (upward) flow near and underneath the river. Under typical post-closure conditions, groundwater flow directions at the OWAP are north, towards the river. During the operation of the impoundments, high local recharge to groundwater from sluicing of CCR created radial flow conditions near the impoundment; while groundwater flow was still predominantly towards the river, some of the groundwater beneath the impoundment flowed towards the adjacent wetlands located south and west of the OWAP.

After sluicing was halted, recharge continued to infiltrate the CCR in the WAPS. The recharge in the footprint of the OWAP migrated within the CCR into the OWPP (through ash within the former western separator berm), and downward into the UA at a reduced rate (since sluice water was no longer present). During closure the OWPP was dewatered, a temporary sheet pile wall was constructed along its eastern side to facilitate the excavation of ash in the OWPP, and a solid clay berm along the west side of the OWAP was constructed. The unit was then closed with a geomembrane cover system to significantly reduce and control infiltration into the CCR material. The sheet pile was left in place at the completion of the construction.

Currently, little to no precipitation enters the remaining CCR in the WAPS due to the geomembrane cover system; however, during high river stage the heads within the UA may become elevated and potentially intersect the base of the CCR. The extent and magnitude of these events is based on the stage of the Illinois River and the duration of the elevated levels.

Conceptually, source water from the WAPS, if present, migrates downward into the materials of the UA, either sand or silt/clay, and mixes with groundwater. Groundwater continues to migrate vertically in the low permeability materials until it encounters the sand and gravel portions of the UA. In the sand and gravel, groundwater migrates horizontally to the north towards the Illinois River, and depending on elevations, may also have a component to the southwest/west which eventually intersects the Illinois River.

Based on the conceptual model discussed above, the compliance wells at the WAPS have been grouped into the following categories based on their location within the flow system (**Figure 2-5**):

- Unconfined UA wells: Monitoring wells located in areas where the sand and gravel unit is near the land surface (wells 22, 22D, 32, 35, 36, 49, and 50). These wells are located on the eastern half of the unit or southeast of the WAPS. The bottom of the screened intervals are at an elevation greater than 420 feet (except 22D) and the sand and gravel is overlain by less than 8 feet of fine-grained material.

- Transitional UA wells: Monitoring wells within sand and gravel that is overlain by 15 to 25 feet of fine-grained material (wells 23, 27, and 34). The base of the screens are at an elevation between 410 and 420 feet and the wells are located in a “U” shape around the former OWPP.
- Confined UA wells: Wells within sand and gravel at depth below 30 to 40 feet of fine-grained material (wells 21R and 51). These wells are located on the west and northeast side of the OWPP, and the base of the wells are at an elevation below 405 feet.

3. OCCURRENCE AND DISTRIBUTION OF GROUNDWATER EXCEEDANCES (EXTENT)

As described in Section 1, exceedances from sampling events E001, E002, and E003 include the following parameters and wells within the UA:

- Arsenic at 21R and 51
- Boron at 21R, 22, 23, and 35
- Sulfate at 23 and 35
- Lithium at 22
- TDS at 35

The extents of exceedances discussed below were defined using existing monitoring wells, including wells present onsite (**Table 3-1**) that may not be included in the 35 I.A.C. § 845 monitoring program.

3.1 Additional Investigation to Further Evaluate Nature and Extent

Solid phase data were collected and evaluated to assess potential geological sources of exceedance parameters and to inform the GCSM (discussed further in **Section 4**). Solid phase data were not collected from the CCR source material prior to completion of closure of the unit in 2020. A total of three borings were advanced adjacent to locations with potential exceedances (wells 22 and 51), and background well (34). Four solids samples were collected and analyzed for the following:

- EPA 6010B for 7-step sequential extraction (iron, aluminum, arsenic, manganese, lithium, and boron);
- EPA 6010B for Total Metals (35 I.A.C. § 845.600 parameters [minus radium] plus aluminum, bismuth, copper, iron, magnesium, manganese, nickel, potassium, silver, strontium, tin, titanium, uranium, vanadium, yttrium, and zinc) via Bulk Characterization;
- Bulk Mineralogy by Reitveld x-ray diffraction analysis;
- Sulfate and Sulfide Analysis via anion chromatography;
- Total Organic Carbon Analysis; and,
- Loss on Ignition Analysis.

In addition, fifteen surface water samples were collected to characterize the water quality in the Illinois River upgradient and adjacent to the WAPS (**Figure 3-1**). Surface water samples were analyzed for dissolved (*i.e.*, filtered) fractions of arsenic, lithium, and boron, and total (*i.e.*, unfiltered) sulfate. Data from this investigation is presented in **Table 3-2** and has been incorporated into this report where applicable.

3.2 Extents in the Uppermost Aquifer

Exceedances are identified quarterly following comparison of lower confidence limits (LCLs) to the GWPSs described in 35 I.A.C. § 845.600. The LCLs vary as the dataset is updated to include additional quarterly events (**Table 3-3**). The discussion below includes ranges of concentrations measured in wells with exceedances, because there is no single value for LCLs. The statistical results from the three compliance monitoring events are presented in **Table 3-3** and all data evaluated has been summarized in **Table 3-4**.

3.2.1 Arsenic

Arsenic concentrations in monitoring wells 21R and 51 resulted in exceedances of the GWPS (0.010 milligrams per liter [mg/L], **Figure 3-2**). The concentrations and extent of arsenic exceedances at the WAPS are summarized as follows:

- 21R and 51 – Exceedances were reported in all three compliance sampling events. Data collected between 2015 and 2023 reported arsenic concentrations ranging from 0.0024 to 0.0345 mg/L in well 21/21R and from 0.0102 to 0.038 mg/L in well 24/51 (**Table 3-4**). The lateral extent of elevated arsenic concentrations are defined by adjacent monitoring wells 34 (non-detect to 0.0005 mg/L) located west of 21R, and 23 (non-detect to 0.0005 mg/L), located east of 51 (**Figure 2-11**, **Table 3-4**). The downgradient extent is defined by the Illinois River, where arsenic concentrations measured in 2020 at sample locations IR04-C/L/R and IR05-C/L/R were all less than 0.0031 mg/L (**Table 3-2).** Surface water samples of the Illinois River upgradient, midgradient, and downgradient of the HPP were indistinguishable for arsenic concentrations, indicating that there is no measurable impact to the Illinois River from groundwater relative to the WAP or HPP. Downward vertical migration of arsenic concentrations above the GWPS is limited by regional upward gradients to the Illinois river, as observed in wells 22/22D.

3.2.2 Boron

Boron concentrations in monitoring wells 21R (E001 only), 22, 23, and 35 resulted in exceedances of the GWPS (2 mg/L, **Figure 3-2**). The concentrations and extent of boron exceedances at the WAPS are summarized as follows:

- 21R (E001 only) – The concentrations of boron in 21/21R ranged from 1.25 to 4.60 mg/L (**Table 3-4**) and LCLs have declined between events E001 and E003. The lateral extent of elevated boron concentrations are defined by adjacent monitoring wells 34 (0.075 to 0.206 mg/L) located west of 21R, and 24/51 (1.3 to 3.84 mg/L), located east of 21R (**Figure 2-11**, **Table 3-4**).
- 22 – Concentrations of boron in monitoring well 22 range from 0.13 to 6.72 mg/L (**Table 3-4**) and LCLs have declined between events E001 and E003. Concentrations above the GWPS are defined laterally by well 49 (0.68 to 1.70 mg/L) located west of 22, and by well 50 (0.59 to 1.43 mg/L) located east of well 22 (**Table 3-4**). Vertical extent of boron concentrations above the GWPS is defined by nested well 22D (1.63 to 2.68 mg/L).
- 23 – Concentrations of boron range in well 23 from 5.63 to 12.8 mg/L (**Table 3-4**) and LCLs are variable during events E001 through E003. The extent of boron concentrations above the GWPS is defined laterally by well 51 (1.30 to 3.14 mg/L) to the west and well 49 (0.68 to 1.70 mg/L) to the east.
- 35 – Concentrations of boron in well 35 range from 4.98 to 18.1 mg/L (**Table 3-4**) and LCLs have declined during events E001 through E003. The extent of elevated boron concentrations is defined in the downgradient direction of flow (towards both 23 and 27) by concentrations measured in well 27 (2.00 to 4.31 mg/L) and the Illinois River (discussed below).

The extent of boron concentrations above the GWPS downgradient from all locations is defined by the results of surface water sampling from the Illinois River completed in 2020 (**Figure 3-1**). Concentrations of boron measured at sample locations IR04-C/L/R and IR05-C/L/R were all less than 0.14 mg/L. Surface water samples of the Illinois River upgradient, midgradient, and downgradient of the HPP were indistinguishable for boron concentrations, indicating that there is no measurable impact to the Illinois River from groundwater relative to the WAP or HPP. Downward migration of boron concentrations within the UA is limited by the presence of regional upward gradients to the Illinois River, as observed in wells 22/22D.

3.2.3 Lithium

Lithium concentrations in monitoring well 22 resulted in the only exceedance of the GWPS (0.04 mg/L, **Figure 3-2**). The concentrations of lithium within well 22 range from 0.0090 to 0.0764 mg/L (**Table 3-4**) and LCLs have increased during events E001 through E003 as concentrations stabilize. The extent of lithium concentrations above the GWPS is defined laterally by well 50 (0.0071 to 0.0300 mg/L) to the east and well 49 (0.0202 to 0.0297 mg/L) to the west. Surface water samples collected from the Illinois River in 2020 (**Figure 3-1**) at sample locations IR04-C/L/R and IR05-C/L/R had lithium concentrations below 0.008 mg/L. Surface water samples of the Illinois River upgradient, midgradient, and downgradient of the HPP were indistinguishable for lithium concentrations, indicating that there is no measurable impact to the Illinois River from groundwater relative to WAP or HPP. The vertical extent of lithium is defined by concentrations measured in well 22D which are below the GWPS, ranging from 0.0123 to 0.0190 mg/L (**Table 3-4**).

3.2.4 Sulfate

Sulfate concentrations in monitoring wells 23 and 35 resulted in exceedances of the GWPS (400 mg/L, **Figure 3-2**). The concentrations and extent of sulfate exceedances at the WAPS are summarized as follows:

- 23 – Concentrations of sulfate range from 323 to 554 mg/L and LCLs exhibit no trend during events E001 through E003. The extent of sulfate concentrations above the GWPS, like boron, is defined by well 24/51 (87.0 to 162 mg/L) to the west and well 49 (71.0 to 114 mg/L) to the east (**Table 3-4**).
- 35 – Concentrations of sulfate in well 35 range from 255 to 1,190 mg/L and LCLs have increased during events E001 through E003. The extent of elevated sulfate concentrations is defined in the downgradient direction of flow (towards both 23 and 27) by well 27 (104 to 228 mg/L) and the Illinois River.

Surface water samples collected from the Illinois River in 2020 (**Figure 3-1**) at sample locations IR04-C/L/R and IR05-C/L/R had sulfate concentrations ranging from 73 to 75 mg/L. Surface water samples of the Illinois River upgradient, midgradient, and downgradient of the HPP were indistinguishable for sulfate concentrations, indicating that there is no measurable impact to the Illinois River from groundwater relative to WAP or HPP. The vertical migration of sulfate is limited by the regional upward gradients near the Illinois River, as observed onsite in wells 22 and 22D.

3.2.5 Total Dissolved Solids

TDS results indicate the mass of dissolved material in groundwater and is a representation of multiple constituents present in the groundwater. Typically, major ions (such as sulfate) represent the primary contributors to TDS. TDS detected in monitoring well 35 resulted in an exceedance of the GWPS (1200 mg/L, **Figure 3-2**). This TDS exceedance is coincident with the sulfate exceedance observed at well 35. The concentrations and extent of TDS exceedances at the WAPS are defined downgradient of well 35 by wells 23, 27, 49, and 51 (**Table 3-4**).

The vertical migration of TDS is limited by the regional upward gradients near the Illinois River, as observed onsite in wells 22 and 22D.

4. GEOCHEMICAL CONCEPTUAL SITE MODEL (NATURE)

A GCSM was developed to describe the conditions of the groundwater in the vicinity of the HPP WAPS and is summarized here (full analysis presented in **Appendix B**). The GCSM describes the geochemical processes that contribute to the mobilization, distribution, and attenuation of chemicals in the environment. Only parameters that have exceeded the GWPS in WAPS groundwater, to be addressed in the corrective action plan, are included in the GCSM. As discussed in previous sections the exceedances observed at the WAPS include arsenic, boron, lithium, sulfate, and TDS.

The CCR materials are the primary source of constituent loading to the CCR porewater (*i.e.*, CCR source water). Over an extended period (*e.g.*, months to years), the CCR source water (*i.e.*, water contained within the interstitial pore spaces of the CCR that can be sampled by low-flow groundwater sampling methods) reaches equilibrium with the CCR materials. The porewater is therefore representative of the mobile phase constituents capable of migrating into the underlying materials and potentially downgradient in groundwater. The WAPS CCR source water is therefore the primary indicator of constituents *available* to the groundwater and is considered as the primary source term for environmental investigation and fate and transport modeling.

Arsenic, boron, lithium, and sulfate are naturally present in coal deposits and are concentrated in CCR. TDS is a measure of inorganic and organic substances in solution and, as such, TDS trends are generally consistent with those of major ions in the WAPS groundwater system. Arsenic, boron, and lithium were identified in UA solids adjacent to downgradient and background wells, which suggests that aquifer solids could provide a secondary natural geogenic source of arsenic, boron, and lithium to the groundwater. Redox conditions vary across the site, with more oxidizing conditions on the east side of the WAPS and more reducing conditions on the west. Reducing conditions may be enhancing arsenic mobility and thus aqueous arsenic concentrations at select wells on the west of the WAPS. The principal source of arsenic, boron, lithium, sulfate, and TDS exceedances to groundwater of the UA is currently expected to be the WAPS CCR porewater.

Arsenic, boron, lithium, and sulfate in the groundwater system may be attenuated via surface complexation reactions with metal (*i.e.*, aluminum, iron, and manganese) oxyhydroxides. Iron oxides were detected in aquifer solids and are generally predicted to be stable at monitoring wells across the monitoring system. Clay minerals were also identified in aquifer solids and may provide an additional attenuation mechanism for arsenic, boron, lithium, and sulfate in groundwater. At the limited locations across the monitoring system where reducing conditions are present, microbial sulfate reduction may also contribute to decreased sulfate concentrations in the groundwater. Attenuation of the constituents contributing to TDS, such as sulfate, will reduce TDS concentrations as well.

5. COMBINED GEOCHEMICAL AND HYDROGEOLOGIC CONCEPTUAL SITE MODELS

5.1 Arsenic Conceptual Site Model

The conceptual site model (CSM) describing current conditions at the WAPS combining the hydrogeologic and geochemical CSMs for arsenic is as follows. Water that may come into contact with CCR in the WAPS becomes porewater within the unlined CCR unit. During operations, sluicing of CCR with elevated heads in the unit resulted in radial flow, likely causing porewater, potentially impacted with arsenic, to migrate downward into the UA. In the UA, porewater mixes with groundwater and the resulting geochemical conditions influence the mobility of arsenic and concentrations observed in compliance wells. In the unconfined/oxidizing portions of the UA, arsenic concentrations do not exceed the GWPS, while in the deeper confined portions of the UA, reducing concentrations result in elevated arsenic concentrations that exceed the GWPS. In addition to physical attenuation mechanisms of dilution and dispersion, elevated arsenic concentrations may be attenuated via surface complexation reactions with metal (*i.e.,* aluminum, iron, and manganese) oxyhydroxides or reactions with clay minerals.

5.2 Boron Conceptual Site Model

The CSM describing current conditions at the WAPS combining the hydrogeologic and geochemical CSMs for boron is as follows. Water that may come into contact with CCR in the WAPS becomes porewater within the unlined CCR unit. During operations, sluicing of CCR with elevated heads in the unit resulted in radial flow, likely causing porewater, impacted with boron, to migrate downward and outward into the UA. In the UA, porewater mixes with groundwater and migrates toward the Illinois River. After sluicing operations ceased in 1996 boron concentrations began to decline in all wells (except 23 and 35) and continued on that trajectory following closure of the unit in 2020. The reduction in infiltration has generally resulted in lower boron concentrations and small shifts in groundwater flow directions (*i.e.,* boron concentrations in well 27 have declined and no longer exceed the GWPS). At well 35 (and 23, which is downgradient of 35), localized flow conditions following closure appear to be influencing boron concentrations at this location while head within the WAPS approaches equilibrium. The Hydrologic Evaluation of Landfill Performance (HELP) model completed for closure indicated that hydrostatic equilibrium would be achieved in approximately 7 years following closure (or approximately 2027) [14]. In addition to physical attenuation mechanisms of dilution and dispersion, elevated boron concentrations may be attenuated via surface complexation reactions with metal (*i.e.,* aluminum, iron, and manganese) oxyhydroxides or reactions with clay minerals.

5.3 Lithium Conceptual Site Model

Similar to arsenic and boron CSMs, water that may come into contact with CCR in the WAPS becomes porewater within the unlined CCR unit. During operations, sluicing of CCR with elevated heads in the unit resulted in radial flow, likely causing porewater, potentially impacted with lithium, to migrate downward into the UA. In the UA, porewater mixes with groundwater and the resulting geochemical conditions influence the concentrations observed in compliance wells. Lithium concentrations are above the GWPS only in well 22 at the WAPS. The well is located north of the CCR unit and is the only compliance location directly downgradient of the CCR unit without a clay/silt layer above the well screen. In addition to physical attenuation mechanisms of dilution and dispersion, elevated lithium concentrations may be attenuated via surface complexation reactions with metal (*i.e.,* aluminum, iron, and manganese) oxyhydroxides or reactions with clay minerals. The lack of clay at this location may have resulted in migration of lithium to this location and observations following closure indicate concentrations are declining.

5.4 Sulfate and TDS Conceptual Site Model

Consistent with the other CSMs, water that may come into contact with CCR in the WAPS becomes porewater within the unlined CCR unit. During operations, sluicing of CCR with elevated heads in the unit resulted in radial flow, likely causing porewater, impacted with sulfate, to migrate downward and outward into the UA. In the UA, porewater mixes with groundwater and migrates toward the Illinois River with concentrations attenuating due to physical mechanisms (dilution and dispersion), and potentially through surface complexation reactions with metal (*i.e.*, aluminum, iron, and manganese) oxyhydroxides or reactions with clay minerals. Under sufficient reducing conditions, microbial sulfate reduction may also contribute to decreased sulfate concentrations in the groundwater. After sluicing operations ceased in 1996 sulfate concentrations began to decline in all wells (except 23 and 35) and continued on that trajectory following closure of the unit in 2020. The reduction in infiltration has generally resulted in lower sulfate concentrations and small shifts in groundwater flow directions. At well 35 (and 23, which is downgradient of 35), localized flow conditions following closure appear to be influencing sulfate concentrations at this location while head within the WAPS approaches equilibrium. The HELP model completed for closure indicated that hydrostatic equilibrium would be achieved in approximately 7 years following closure (or approximately 2027) [14] . Lack of elevated sulfate (while boron persists) at UA well 21R provides evidence that sulfate reduction may be occurring.

6. CONCLUSIONS AND FUTURE ACTIVITIES

In accordance with 35 I.A.C. § 845.650(d)(1), the nature and extent of GWPS exceedances of arsenic, boron, lithium, sulfate, and TDS have been described in sufficient detail to support a complete and accurate assessment of the corrective measures necessary to effectively clean up all releases from the WAPS. As discussed in Sections 3.3.1 and 3.3.2, the horizontal delineation of all constituents has been defined by a combination of results at existing wells and surface water results that indicate concentrations are below the GWPS.

Following closure, groundwater monitoring results are generally consistent with the conclusions in the Closure Plan [9] and site conditions are improving as follows:

- Water levels within the CCR are declining. Porewater monitoring wells have gone dry, indicating the level in the unit has declined.
- Trends for boron and sulfate (**Appendix B** [GCSM]), which are conservative indicators of CCR impacts, indicate concentrations are declining in all wells except wells 23 and 35. Concentrations at these two locations are potentially related to localized flow conditions that originated as a result of closure, but are expected to dissipate as the unit reaches equilibrium (predicted to occur in 2027).

These observations are consistent with the conceptual site models and constituent extents provided in **Section 5.**

Boron was selected for modeling source control presented in the Final Closure Plan, as described in the Groundwater Model Report (GMR) [14]. Boron is considered a surrogate parameter for arsenic, lithium, sulfate and TDS because it is the constituent at the site that will likely require the longest time to achieve the GWPS. Further modeling selected constituents is a common industry approach for evaluation of environmental systems and is sufficient to achieve the modeling objectives in support of the closure alternatives analysis [15]. Ongoing groundwater modeling, which includes recent data following closure and is expected to be completed in 2025, indicates that the GWPS will be met approximately 30 years after the initiation of groundwater polishing (which starts when the Corrective Action Plan permit is issued). Additional geochemical modeling will be completed to evaluate how surface complexation reactions with metal oxyhydroxides and clay minerals or changes in redox conditions may affect arsenic, boron, lithium, and sulfate mobility or in the case and therefore the time to reach the GWPS for these parameters.

7. REFERENCES

[1] Illinois Environmental Protection Agency (IEPA), *Letter from Michael Summers (IEPA) to Phil Morris (Dynegy Midwest Generation, LLC), Re: Hennepin Power Plant West Ash Pond System; W1550100002-01 & 03, Alternative Source Demonstration (ASD) Submittal.,* December 11, 2023.

[2] Ramboll Americas Engineering Solutions, Inc. , "35 I.A.C. § 845.650(E): Alternative Source Demonstration, West Ash Pond System, Hennepin Power Plant, Hennepin, IL, IEPA ID: W1550100002-01 and W1550100002-03," November 10, 2023.

[3] Ramboll Americas Enginering Solutions, Inc., "35 I.A.C. § 845 Corrective Measures Assesment, Hennepin Power Plant, West Ash Pond System," Hennepin, Illinois, May 8, 2024.

[4] Natural Resource Technology, an OBG Company, Hydrogeologic Site Characterization Report, West Ash Pond System, Hennepin Power Station, Hennepin, Illinois, December 20, 2017.

[5] Ramboll Americas Engineering Solutions, Inc., "35 I.A.C. § 845.610(B)(3)(D) Groundwater Monitoring Data and Detected Exceedances, 2023 Quarter 2, West Ash Pond System, Hennepin Power Plant, Hennepin, Illinois," September 11, 2023.

[6] Ramboll Americas Engineering Solutions, Inc., "35 I.A.C. § 845.610(B)(3)(D) Groundwater Monitoring Data and Detected Exceedances, 2023 Quarter 3, West Ash Pond System, Hennepin Power Plant, Hennepin, Illinois," January 15, 2024.

[7] Ramboll Americas Engineering Solutions, Inc., "35 I.A.C. § 845.610(B)(3)(D) Groundwater Monitoring Data and Detected Exceedances, 2023 Quarter 4, West Ash Pond System, Hennepin Power Plant, Hennepin, Illinois," March 4, 2024.

[8] Science and Technology Management, Inc. , "Investigation of Site Closure Options at Illinois Power Company's Hennepin East Ash Impoundment. Report No. STMI/135/96-02," Brookfield, Wisconsin, June 1996.

[9] Geosyntec Consultants Inc., "Closure and Post Closure Care Plan, Old West Ash Pond, Old West Polishing Pond at Dynegy Midwest Generation, LLC, Hennepin Power Station," 2017.

[10] Dynegy Midwest Generation, LLC, "Hennepin Power Station; Old West Polishing Pond Notification of Completion of Closure.," December 17, 2020.

[11] Burns & McDonnell, "Initial Operating Permit, Hennepin West Ash Pond System," October 25, 2021.

[12] Ramboll Americas Engineering Solutions, Inc. , "Hydrogeologic Site Characterization Report, East Ash Pond, Hennepin Power Plant, Hennepin, Illinois," October 25, 2021.

[13] Ramboll Americas Engineering Solutions, Inc. , "Addendum to the Groundwater Monitoring Plan, Hennepin Power Plant, West Ash Pond System, Hennepin, Illinois, Dynegy Midwest Generation, LLC.," October 25, 2021.

[14] Natural Resource Technology, an OBG Company, "Groundwater Model Report, Hennepin West Ash System, Hennepin, Illinois," December 20, 2017.

[15] P. Andrew Bittner and Gradient, *Closure Alternatives Analysis Groundwater Modeling Review at the Coffeen Power Plant, Edwards Power Plant, Newton Power Plant, and Hennepin Power Plant,* January 24, 2024.

TABLES

Table 2-1. Groundwater Elevation Data
Nature and Extent Report
Hennepin Power Plant
West Ash Pond System
Hennepin, Illinois

Well ID	Well Type	Monitored Unit	Date	Depth to Groundwater (feet BMP)	Groundwater Elevation (feet NAVD88)
21R	Compliance	UA	4/30/2023	5.16	446.88
21R	Compliance	UA	5/30/2023	5.92	446.13
21R	Compliance	UA	6/21/2023	6.36	445.68
21R	Compliance	UA	7/21/2023	6.11	445.93
21R	Compliance	UA	8/21/2023	6.36	445.68
21R	Compliance	UA	9/30/2023	6.52	445.53
21R	Compliance	UA	10/31/2023	5.67	446.38
21R	Compliance	UA	11/13/2023	5.77	446.28
21R	Compliance	UA	12/21/2023	6.18	445.87
22	Compliance	UA	4/30/2023	17.85	446.59
22	Compliance	UA	5/30/2023	18.45	446.00
22	Compliance	UA	6/21/2023	18.73	445.71
22	Compliance	UA	7/21/2023	18.52	445.92
22	Compliance	UA	8/21/2023	18.68	445.76
22	Compliance	UA	9/30/2023	19.54	444.91
22	Compliance	UA	10/31/2023	18.87	445.58
22	Compliance	UA	11/13/2023	18.43	446.02
22	Compliance	UA	12/21/2023	18.84	445.61
22D	Compliance	UA	4/30/2023	18.43	446.99
22D	Compliance	UA	5/30/2023	19.10	446.33
22D	Compliance	UA	6/21/2023	19.42	446.00
22D	Compliance	UA	7/21/2023	19.19	446.23
22D	Compliance	UA	8/21/2023	19.40	446.02
22D	Compliance	UA	10/31/2023	18.90	446.53
22D	Compliance	UA	11/13/2023	22.10	443.33
22D	Compliance	UA	12/21/2023	19.54	445.89
23	Compliance	UA	4/30/2023	15.90	447.48
23	Compliance	UA	5/30/2023	16.72	446.67
23	Compliance	UA	6/21/2023	17.08	446.30
23	Compliance	UA	7/21/2023	16.83	446.55
23	Compliance	UA	8/21/2023	17.08	446.30
23	Compliance	UA	9/30/2023	17.38	446.01
23	Compliance	UA	10/31/2023	16.45	446.94
23	Compliance	UA	11/13/2023	17.64	445.75
23	Compliance	UA	12/21/2023	17.18	446.21

Table 2-1. Groundwater Elevation Data

Nature and Extent Report
Hennepin Power Plant
West Ash Pond System
Hennepin, Illinois

Well ID	Well Type	Monitored Unit	Date	Depth to Groundwater (feet BMP)	Groundwater Elevation (feet NAVD88)
27	Compliance	UA	4/30/2023	3.33	447.24
27	Compliance	UA	5/30/2023	4.14	446.44
27	Compliance	UA	6/21/2023	4.53	446.04
27	Compliance	UA	7/21/2023	4.31	446.27
27	Compliance	UA	8/21/2023	4.56	446.02
27	Compliance	UA	10/31/2023	3.72	446.86
27	Compliance	UA	11/13/2023	3.91	446.67
27	Compliance	UA	12/21/2023	4.38	446.20
32	Background	UA	4/30/2023	4.36	447.02
32	Background	UA	5/30/2023	5.22	446.16
32	Background	UA	6/21/2023	5.63	445.75
32	Background	UA	7/21/2023	5.42	445.96
32	Background	UA	8/21/2023	5.60	445.78
32	Background	UA	9/30/2023	5.74	445.64
32	Background	UA	10/31/2023	4.62	446.76
32	Background	UA	11/13/2023	4.79	446.59
32	Background	UA	12/21/2023	5.20	446.18
34	Background	UA	4/30/2023	7.69	441.86
34	Background	UA	5/30/2023	8.66	440.90
34	Background	UA	6/21/2023	9.16	440.39
34	Background	UA	8/25/2023	NA	440.58
34	Background	UA	10/31/2023	7.74	441.82
34	Background	UA	11/13/2023	8.37	441.19
34	Background	UA	12/21/2023	7.76	441.80
35	Compliance	UA	4/30/2023	7.69	447.13
35	Compliance	UA	5/30/2023	8.30	446.53
35	Compliance	UA	6/21/2023	8.84	445.98
35	Compliance	UA	7/21/2023	8.58	446.24
35	Compliance	UA	8/21/2023	8.87	445.96
35	Compliance	UA	9/30/2023	9.05	445.78
35	Compliance	UA	10/31/2023	7.97	446.86
35	Compliance	UA	11/13/2023	8.15	446.68
35	Compliance	UA	12/21/2023	8.70	446.13

Table 2-1. Groundwater Elevation Data

Nature and Extent Report
Hennepin Power Plant
West Ash Pond System
Hennepin, Illinois

Well ID	Well Type	Monitored Unit	Date	Depth to Groundwater (feet BMP)	Groundwater Elevation (feet NAVD88)
49	Compliance	UA	5/30/2023	21.54	446.63
49	Compliance	UA	8/25/2023	19.65	448.52
49	Compliance	UA	9/30/2023	22.16	446.01
49	Compliance	UA	10/31/2023	21.33	446.84
49	Compliance	UA	11/13/2023	21.49	446.68
49	Compliance	UA	12/21/2023	22.02	446.15
50	Compliance	UA	5/30/2023	18.25	445.69
50	Compliance	UA	10/31/2023	18.06	445.88
50	Compliance	UA	11/13/2023	18.24	445.70
50	Compliance	UA	12/21/2023	18.61	445.33
51	Compliance	UA	4/30/2023	17.74	447.05
51	Compliance	UA	5/30/2023	18.50	446.30
51	Compliance	UA	6/21/2023	18.94	445.85
51	Compliance	UA	7/21/2023	18.69	446.10
51	Compliance	UA	8/21/2023	18.92	445.87
51	Compliance	UA	9/30/2023	19.17	445.63
51	Compliance	UA	10/31/2023	18.22	446.58
51	Compliance	UA	11/13/2023	18.59	446.21
51	Compliance	UA	12/21/2023	18.84	445.96
SG02	Water Level	SW	4/30/2023	NA	448.50
SG02	Water Level	SW	5/30/2023	NA	440.50
SG02	Water Level	SW	6/21/2023	NA	440.50
SG02	Water Level	SW	7/21/2023	NA	441.75
SG02	Water Level	SW	8/21/2023	NA	440.75
SG02	Water Level	SW	9/30/2023	NA	440.75
SG02	Water Level	SW	10/31/2023	NA	441.50
SG02	Water Level	SW	11/13/2023	NA	441.00
SG02	Water Level	SW	12/21/2023	NA	441.75

Notes:

BMP = below measuring point
NAVD88 = North American Vertical Datum 1988
UA = uppermost aquifer
SW = Illinois River surface water

Table 3-1. Monitoring Well Construction Details

Nature and Extent Report
Hennepin Power Plant
West Ash Pond System
Hennepin, Illinois

Location	HSU	Date Constructed	Top of PVC Elevation (ft)	Measuring Point Elevation (ft)	Measuring Point Description	Ground Elevation (ft)	Screen Top Depth (ft bgs)	Screen Bottom Depth (ft bgs)	Screen Top Elevation (ft)	Screen Bottom Elevation (ft)	Well Depth (ft bgs)	Bottom of Boring Elevation (ft)	Screen Length (ft)	Screen Diameter (inches)	Latitude (Decimal Degrees)	Longitude (Decimal Degrees)
21	UA	12/9/1982	459.3	459.3	Top of PVC	459.8	49	59	410.8	400.8	59.6	400.1	10	2	41.299866	-89.328905
21R	UA	2/6/2020	452.1	452.2	Top of PVC	449.4	37.6	47.6	411.8	401.8	50	399.4	10	2	41.299866	-89.328914
22	UA	12/9/1982	464.4	464.6	Top of PVC	461.5	24.4	34.4	437.1	427.1	34.6	426.9	10	2	41.302032	-89.321512
22D	UA	8/7/2019	465.4	465.6	Top of PVC	461.8	49.7	59.7	412.2	402.2	59.67	401.8	10	2	41.302017	-89.321572
23	UA	12/10/1982	463.4	463.6	Top of PVC	460.9	34	44	426.9	416.9	45.2	415.7	10	2	41.300881	-89.325376
24	UA	12/13/1982	462.1	462.1	Top of PVC	461.1	56.4	66.4	404.7	394.7	64.5	396.6	10	2	41.300602	-89.327186
27	UA	9/11/1995	450.6	450.8	Top of PVC	448.2	30	35	418.2	413.2	36.3	412.0	5	2	41.296911	-89.328898
32	UA	8/21/1996	451.4	451.6	Top of PVC	448.8	7	17	441.8	431.8	17.3	431.4	10	2	41.292128	-89.328563
34	UA	8/22/1996	449.6	449.7	Top of PVC	448.2	30	35	418.2	413.2	35	413.2	5	2	41.299538	-89.33249
35	UA	9/8/1999	454.8	454.9	Top of PVC	451.5	8	18	443.5	433.5	17.6	433.9	10	2	41.29916	-89.324145
49	UA	7/6/2015	468.2	468.3	Top of PVC	465.8	35	45	430.8	420.8	45	420.8	10	2	41.301182	-89.32333
50	UA	8/7/2019	463.9	464.1	Top of PVC	460.6	19.6	29.6	441.0	431.0	29.6	430.6	10	2	41.302243	-89.320647
51	UA	2/4/2020	464.8	464.9	Top of PVC	461.5	56	66	405.5	395.5	66.3	394.5	10	2	41.300639	-89.326953
L4	CCR	8/21/1995	460.9	460.9	Top of PVC	461.3	13.0	23.0	448.3	438.3	28.0	29.0	10	2	41.30061	-89.327193
LPZ17	CCR	3/14/2017	463.9	463.9	Top of PVC	460.9	10.1	21.1	450.8	439.8	21.1	21.1	10	2	41.299504	-89.321795

Notes:

All elevation data are presented relative to the North American Vertical Datum 1988 (NAVD88), GEOID 12A
bgs = below ground surface
ft = foot or feet
HSU = Hydrostratigraphic Unit
UA = Uppermost Aquifer
CCR = Coal Combustion Residuals
PVC = polyvinyl chloride

Table 3-2. Illinois River Surface Water Data

Nature and Extent Report
Hennepin Power Plant
West Ash Pond System
Hennepin, Illinois

Sample Location	Sample Date	Fraction	Analyte	Unit	Result
IR01-C	9/2/2020	D	Arsenic	mg/L	0.0028
IR01-L	9/2/2020	D	Arsenic	mg/L	0.0027
IR01-R	9/2/2020	D	Arsenic	mg/L	0.0028
IR02-C	9/2/2020	D	Arsenic	mg/L	0.0028
IR02-L	9/2/2020	D	Arsenic	mg/L	0.0028
IR02-R	9/2/2020	D	Arsenic	mg/L	0.0027
IR03-C	9/2/2020	D	Arsenic	mg/L	0.0027
IR03-L	9/2/2020	D	Arsenic	mg/L	0.0027
IR03-R	9/2/2020	D	Arsenic	mg/L	0.0028
IR04-C	9/2/2020	D	Arsenic	mg/L	0.0027
IR04-L	9/2/2020	D	Arsenic	mg/L	0.0029
IR04-R	9/2/2020	D	Arsenic	mg/L	0.0027
IR05-C	9/2/2020	D	Arsenic	mg/L	0.003075
IR05-L	9/2/2020	D	Arsenic	mg/L	0.0027
IR05-R	9/2/2020	D	Arsenic	mg/L	0.0026
IR01-C	9/2/2020	D	Boron	mg/L	0.126
IR01-L	9/2/2020	D	Boron	mg/L	0.139
IR01-R	9/2/2020	D	Boron	mg/L	0.137
IR02-C	9/2/2020	D	Boron	mg/L	0.135
IR02-L	9/2/2020	D	Boron	mg/L	0.13
IR02-R	9/2/2020	D	Boron	mg/L	0.132
IR03-C	9/2/2020	D	Boron	mg/L	0.136
IR03-L	9/2/2020	D	Boron	mg/L	0.147
IR03-R	9/2/2020	D	Boron	mg/L	0.131
IR04-C	9/2/2020	D	Boron	mg/L	0.127
IR04-L	9/2/2020	D	Boron	mg/L	0.128
IR04-R	9/2/2020	D	Boron	mg/L	0.134
IR05-C	9/2/2020	D	Boron	mg/L	0.13225
IR05-L	9/2/2020	D	Boron	mg/L	0.134
IR05-R	9/2/2020	D	Boron	mg/L	0.125
IR01-C	9/2/2020	D	Lithium	mg/L	0.0075
IR01-L	9/2/2020	D	Lithium	mg/L	0.0072
IR01-R	9/2/2020	D	Lithium	mg/L	0.0078
IR02-C	9/2/2020	D	Lithium	mg/L	0.0071
IR02-L	9/2/2020	D	Lithium	mg/L	0.0073
IR02-R	9/2/2020	D	Lithium	mg/L	0.0075
IR03-C	9/2/2020	D	Lithium	mg/L	0.0072
IR03-L	9/2/2020	D	Lithium	mg/L	0.0072
IR03-R	9/2/2020	D	Lithium	mg/L	0.0075
IR04-C	9/2/2020	D	Lithium	mg/L	0.0072
IR04-L	9/2/2020	D	Lithium	mg/L	0.0071

Table 3-2. Illinois River Surface Water Data

Nature and Extent Report
Hennepin Power Plant
West Ash Pond System
Hennepin, Illinois

Sample Location	Sample Date	Fraction	Analyte	Unit	Result
IR04-R	9/2/2020	D	Lithium	mg/L	0.0071
IR05-C	9/2/2020	D	Lithium	mg/L	0.00775
IR05-L	9/2/2020	D	Lithium	mg/L	0.0076
IR05-R	9/2/2020	D	Lithium	mg/L	0.0071
IR01-C	9/2/2020	T	Sulfate	mg/L	76
IR01-L	9/2/2020	T	Sulfate	mg/L	77
IR01-R	9/2/2020	T	Sulfate	mg/L	79
IR02-C	9/2/2020	T	Sulfate	mg/L	74
IR02-L	9/2/2020	T	Sulfate	mg/L	75
IR02-R	9/2/2020	T	Sulfate	mg/L	77
IR03-C	9/2/2020	T	Sulfate	mg/L	77
IR03-L	9/2/2020	T	Sulfate	mg/L	75
IR03-R	9/2/2020	T	Sulfate	mg/L	77
IR04-C	9/2/2020	T	Sulfate	mg/L	73
IR04-L	9/2/2020	T	Sulfate	mg/L	73
IR04-R	9/2/2020	T	Sulfate	mg/L	75
IR05-C	9/2/2020	T	Sulfate	mg/L	75
IR05-L	9/2/2020	T	Sulfate	mg/L	75
IR05-R	9/2/2020	T	Sulfate	mg/L	74

Notes:

Results presented represent the mean of field duplicates where collected.
D = dissolved
T = total
mg/L = milligrams per liter

Table 3-3. Exceedance Parameter Statistical Results

Nature and Extent Report
Hennepin Power Plant
West Ash Pond System
Hennepin, Illinois

Location	Parameter	Unit	Groundwater Protection Standard	2023 Q2 LCL	2023 Q3 LCL	2023 Q4 LCL
21/21R	Arsenic, total	mg/L	0.010	0.0198	0.0194	0.0189
24/51	Arsenic, total	mg/L	0.010	0.0204	0.0204	0.0203
21/21R	Boron, total	mg/L	2	2.22	1.96	1.95
22	Boron, total	mg/L	2	3.33	3.15	3.04
23	Boron, total	mg/L	2	8.74	8.30	8.34
35	Boron, total	mg/L	2	12.4	12.3	12.1
22	Lithium, total	mg/L	0.04	0.0395	0.0405	0.0436
23	Sulfate, total	mg/L	400	422	423	423
35	Sulfate, total	mg/L	400	618	649	659
35	Total Dissolved Solids	mg/L	1,200	1,200	1,250	1,280

Notes:

LCL = Lower Confidence Level
mg/L = milligrams per liter

Table 3-4. Summary of Groundwater Data

Nature and Extent Report
Hennepin Power Plant
West Ash Pond System
Hennepin, Illinois

HSU	Location	Well Type	Parameter	Unit	Sample Count	Non-Detect Results	Percent Non-Detect Results	First Sample	Last Sample	Minimum	Median	Mean	Maximum
UA	21	MWO	Sulfate, total	mg/L	18	0	0	3/18/2015	6/19/2019	51.0	140	130	169
UA	21	MWO	Total Dissolved Solids	mg/L	18	0	0	3/18/2015	6/19/2019	338	560	550	644
UA	21	MWO	Arsenic, total	mg/L	13	0	0	12/10/2015	6/19/2019	0.00240	0.0091	0.0083	0.0128
UA	21	MWO	Boron, total	mg/L	14	0	0	12/10/2015	6/19/2019	1.25	4.1	3.9	4.60
UA	21	MWO	Lithium, total	mg/L	13	0	0	12/10/2015	6/19/2019	0.00640	0.014	0.014	0.0208
UA	21R	C	Arsenic, total	mg/L	16	0	0	3/11/2020	11/14/2023	0.0210	0.026	0.026	0.0345
UA	21R	C	Boron, total	mg/L	16	0	0	3/11/2020	11/14/2023	1.70	3.0	2.9	3.72
UA	21R	C	Lithium, total	mg/L	16	0	0	3/11/2020	11/14/2023	0.0167	0.021	0.022	0.0280
UA	21R	C	Sulfate, total	mg/L	16	0	0	3/11/2020	11/14/2023	81.0	92	93	105
UA	21R	C	Total Dissolved Solids	mg/L	16	0	0	3/11/2020	11/14/2023	540	680	670	918
UA	22	C	Sulfate, total	mg/L	41	0	0	3/18/2015	11/15/2023	101	200	180	261
UA	22	C	Arsenic, total	mg/L	36	23	64	12/10/2015	11/15/2023	<0.00023	0.0010	0.0012	<0.0087
UA	22	C	Boron, total	mg/L	37	0	0	12/10/2015	11/15/2023	0.130	4.9	4.6	6.72
UA	22	C	Lithium, total	mg/L	36	0	0	12/10/2015	11/15/2023	0.00900	0.055	0.053	0.0764
UA	22	C	Total Dissolved Solids	mg/L	41	0	0	3/18/2015	11/15/2023	586	680	680	800
UA	22D	C	Arsenic, total	mg/L	16	1	6	9/17/2019	11/15/2023	0.00110	0.0013	0.0018	<0.0087
UA	22D	C	Boron, total	mg/L	16	0	0	9/17/2019	11/15/2023	1.30	2.0	2.0	2.68
UA	22D	C	Lithium, total	mg/L	16	0	0	9/17/2019	11/15/2023	0.0123	0.016	0.016	0.0190
UA	22D	C	Sulfate, total	mg/L	16	0	0	9/17/2019	11/15/2023	89.0	100	110	118
UA	22D	C	Total Dissolved Solids	mg/L	16	0	0	9/17/2019	11/15/2023	550	630	630	690
UA	23	C	Sulfate, total	mg/L	41	0	0	3/18/2015	11/15/2023	323	430	440	554
UA	23	C	Total Dissolved Solids	mg/L	41	0	0	3/18/2015	11/15/2023	820	890	910	1,020
UA	23	C	Arsenic, total	mg/L	36	30	83	12/10/2015	11/15/2023	0.000500	0.0010	0.0012	<0.0087
UA	23	C	Boron, total	mg/L	37	0	0	12/10/2015	11/15/2023	5.63	8.3	8.5	12.8
UA	23	C	Lithium, total	mg/L	36	2	6	12/10/2015	11/15/2023	<0.0019	0.0051	0.0050	0.00670
UA	24	MWO	Sulfate, total	mg/L	18	0	0	3/18/2015	6/9/2019	95.0	140	130	162
UA	24	MWO	Total Dissolved Solids	mg/L	18	0	0	3/18/2015	6/9/2019	458	650	640	822
UA	24	MWO	Arsenic, total	mg/L	13	0	0	12/10/2015	6/19/2019	0.0254	0.032	0.031	0.0380
UA	24	MWO	Boron, total	mg/L	14	0	0	12/10/2015	6/19/2019	2.11	2.5	2.7	3.84
UA	24	MWO	Lithium, total	mg/L	13	0	0	12/10/2015	6/19/2019	0.0193	0.022	0.023	0.0270

Table 3-4. Summary of Groundwater Data
Nature and Extent Report
Hennepin Power Plant
West Ash Pond System
Hennepin, Illinois

HSU	Location	Well Type	Parameter	Unit	Sample Count	Non-Detect Results	Percent Non-Detect Results	First Sample	Last Sample	Minimum	Median	Mean	Maximum
UA	27	C	Sulfate, total	mg/L	26	0	0	3/18/2015	11/14/2023	104	120	140	228
UA	27	C	Total Dissolved Solids	mg/L	26	0	0	3/18/2015	11/14/2023	442	660	670	808
UA	27	C	Arsenic, total	mg/L	19	9	47	9/12/2018	11/14/2023	0.000500	0.0010	0.0014	<0.0087
UA	27	C	Boron, total	mg/L	19	0	0	9/12/2018	11/14/2023	2.00	2.4	2.7	4.31
UA	27	C	Lithium, total	mg/L	19	0	0	9/12/2018	11/14/2023	0.0174	0.023	0.023	0.0266
UA	32	B	Sulfate, total	mg/L	35	0	0	3/18/2015	11/14/2023	37.0	60	58	82.0
UA	32	B	Total Dissolved Solids	mg/L	35	0	0	3/18/2015	11/14/2023	450	490	510	600
UA	32	B	Arsenic, total	mg/L	30	26	87	12/10/2015	11/14/2023	0.000370	0.0010	0.0011	<0.0087
UA	32	B	Boron, total	mg/L	31	0	0	12/10/2015	11/14/2023	0.0681	0.11	0.12	0.199
UA	32	B	Lithium, total	mg/L	30	0	0	12/10/2015	11/14/2023	0.00220	0.0037	0.0036	0.00510
UA	34	B	Sulfate, total	mg/L	32	0	0	3/18/2015	11/14/2023	45.0	77	80	117
UA	34	B	Total Dissolved Solids	mg/L	32	0	0	3/18/2015	11/14/2023	640	740	750	846
UA	34	B	Arsenic, total	mg/L	29	24	83	12/9/2015	11/14/2023	0.000500	0.0010	0.0012	<0.0087
UA	34	B	Boron, total	mg/L	30	0	0	12/9/2015	11/14/2023	0.0750	0.14	0.14	0.206
UA	34	B	Lithium, total	mg/L	29	0	0	12/9/2015	11/14/2023	0.00320	0.013	0.013	0.0160
UA	35	C	Arsenic, total	mg/L	31	20	65	12/9/2015	11/15/2023	0.000500	0.0010	0.0017	0.0109
UA	35	C	Boron, total	mg/L	32	0	0	12/9/2015	11/15/2023	4.98	11	10	18.1
UA	35	C	Lithium, total	mg/L	31	0	0	12/9/2015	11/15/2023	0.0128	0.029	0.028	0.0374
UA	35	C	Sulfate, total	mg/L	32	0	0	12/9/2015	11/15/2023	255	510	570	1,190
UA	35	C	Total Dissolved Solids	mg/L	32	0	0	12/9/2015	11/15/2023	708	1100	1200	1,940
UA	49	C	Arsenic, total	mg/L	31	27	87	12/10/2015	11/15/2023	0.000280	0.0010	0.0011	<0.0087
UA	49	C	Boron, total	mg/L	32	0	0	12/10/2015	11/15/2023	0.680	0.92	1.0	1.70
UA	49	C	Lithium, total	mg/L	31	0	0	12/10/2015	11/15/2023	0.0202	0.025	0.025	0.0297
UA	49	C	Sulfate, total	mg/L	32	0	0	12/10/2015	11/15/2023	71.0	84	90	114
UA	49	C	Total Dissolved Solids	mg/L	32	0	0	12/10/2015	11/15/2023	566	640	640	710
UA	50	C	Arsenic, total	mg/L	16	13	81	9/17/2019	11/14/2023	0.000760	0.0010	0.0015	<0.0087
UA	50	C	Boron, total	mg/L	16	0	0	9/17/2019	11/14/2023	0.590	0.79	0.83	1.43
UA	50	C	Lithium, total	mg/L	16	0	0	9/17/2019	11/14/2023	0.00710	0.023	0.022	0.0300
UA	50	C	Sulfate, total	mg/L	16	0	0	9/17/2019	11/14/2023	81.0	90	95	136
UA	50	C	Total Dissolved Solids	mg/L	16	0	0	9/17/2019	11/14/2023	580	620	630	700

Table 3-4. Summary of Groundwater Data
Nature and Extent Report
Hennepin Power Plant
West Ash Pond System
Hennepin, Illinois

HSU	Location	Well Type	Parameter	Unit	Sample Count	Non-Detect Results	Percent Non-Detect Results	First Sample	Last Sample	Minimum	Median	Mean	Maximum
UA	51	C	Arsenic, total	mg/L	21	0	0	11/3/2020	11/15/2023	0.0102	0.019	0.019	0.0308
UA	51	C	Boron, total	mg/L	21	0	0	11/3/2020	11/15/2023	1.30	2.1	2.1	3.14
UA	51	C	Lithium, total	mg/L	21	0	0	11/3/2020	11/15/2023	0.0210	0.024	0.026	0.0714
UA	51	C	Sulfate, total	mg/L	21	0	0	11/3/2020	11/15/2023	87.0	100	100	127
UA	51	C	Total Dissolved Solids	mg/L	21	0	0	11/3/2020	11/15/2023	584	630	640	702
CCR	L4	Porewater	Boron, total	mg/L	3	0	0	12/7/2016	9/6/2017	21.2	32	30	37.4
CCR	L4	Porewater	Sulfate, total	mg/L	3	0	0	12/7/2016	9/6/2017	370	420	430	509
CCR	L4	Porewater	Arsenic, total	mg/L	2	0	0	4/25/2017	9/6/2017	0.0351	0.048	0.048	0.0610
CCR	L4	Porewater	Lithium, total	mg/L	2	0	0	4/25/2017	9/6/2017	0.0455	0.054	0.054	0.0627
CCR	L4	Porewater	Total Dissolved Solids	mg/L	2	0	0	4/25/2017	9/6/2017	900	940	940	972
CCR	LPZ17	Porewater	Arsenic, total	mg/L	2	0	0	4/25/2017	9/6/2017	0.0265	0.032	0.032	0.0381
CCR	LPZ17	Porewater	Boron, total	mg/L	2	0	0	4/25/2017	9/6/2017	26.9	28	28	28.6
CCR	LPZ17	Porewater	Lithium, total	mg/L	2	0	0	4/25/2017	9/6/2017	0.0903	0.094	0.094	0.0975
CCR	LPZ17	Porewater	Sulfate, total	mg/L	2	0	0	4/25/2017	9/6/2017	1,120	1200	1200	1,270
CCR	LPZ17	Porewater	Total Dissolved Solids	mg/L	2	0	0	4/25/2017	9/6/2017	1,910	2000	2000	2,090

Notes:
< = result less than the method detection limit
B = Background
C = Compliance
CCR = Coal Combustion Residuals
HSU = Hydrostratigraphic Unit
MWO - Water Level Only
mg/L = milligrams per liter
SU = Standard Unit
UA = Uppermost Aquifer

FIGURES

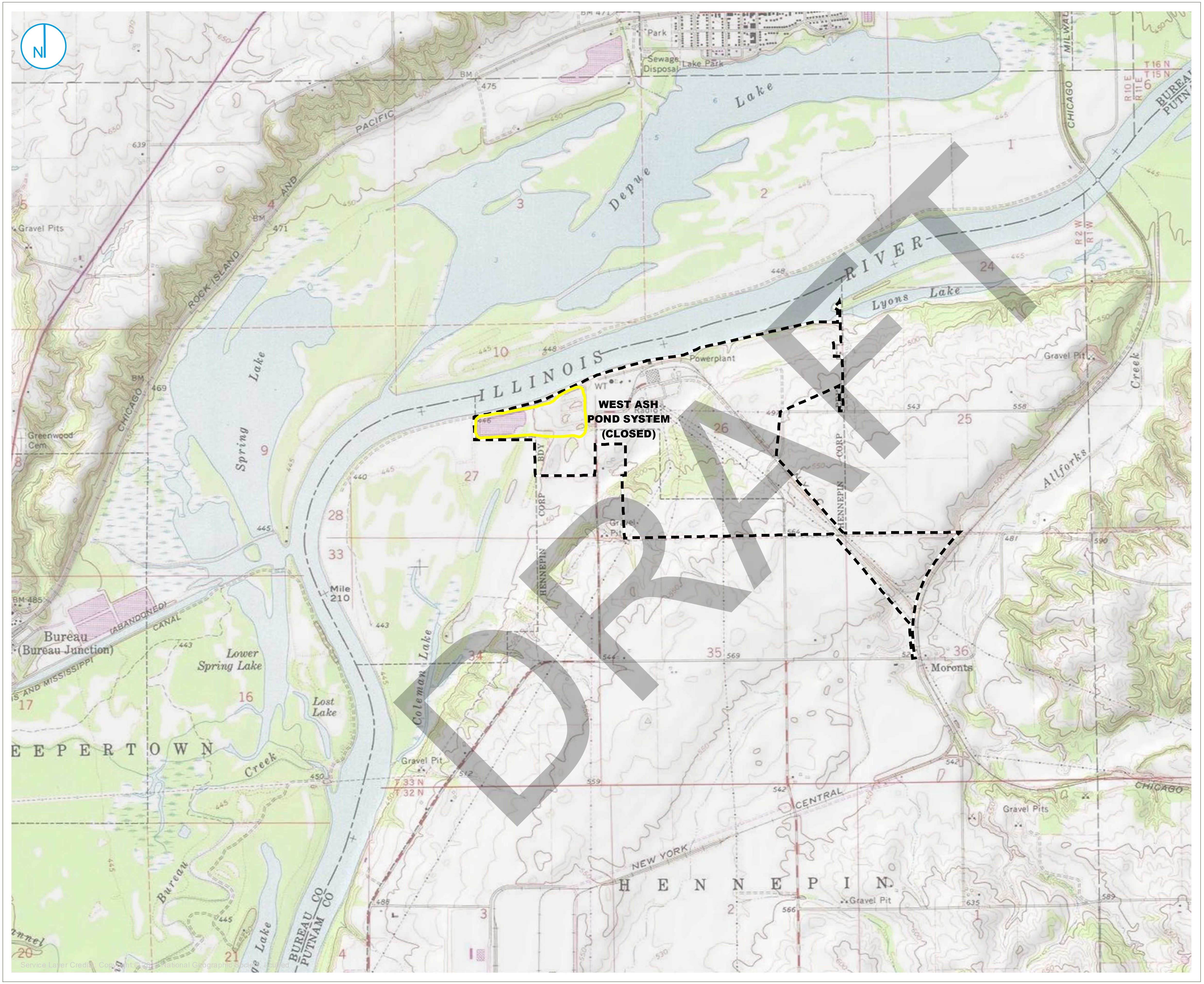

🟨 REGULATED UNIT (SUBJECT UNIT)
⬚ PROPERTY BOUNDARY

0 1,000 2,000
Feet

SITE LOCATION MAP

NATURE AND EXTENT REPORT
WEST ASH POND SYSTEM
HENNEPIN POWER PLANT
HENNEPIN, ILLINOIS

FIGURE 2-1

RAMBOLL AMERICAS
ENGINEERING SOLUTIONS, INC.

Y:\Mapping\Projects\22\22285\MXD\Nature_and_Extent\HEN\Nature_and_Extent_Report_HenWest\Figure 1-1_Site Location Map.mxd

PROJECT: 169000XXXX | DATED: 4/23/2024 | DESIGNER: galarnmc

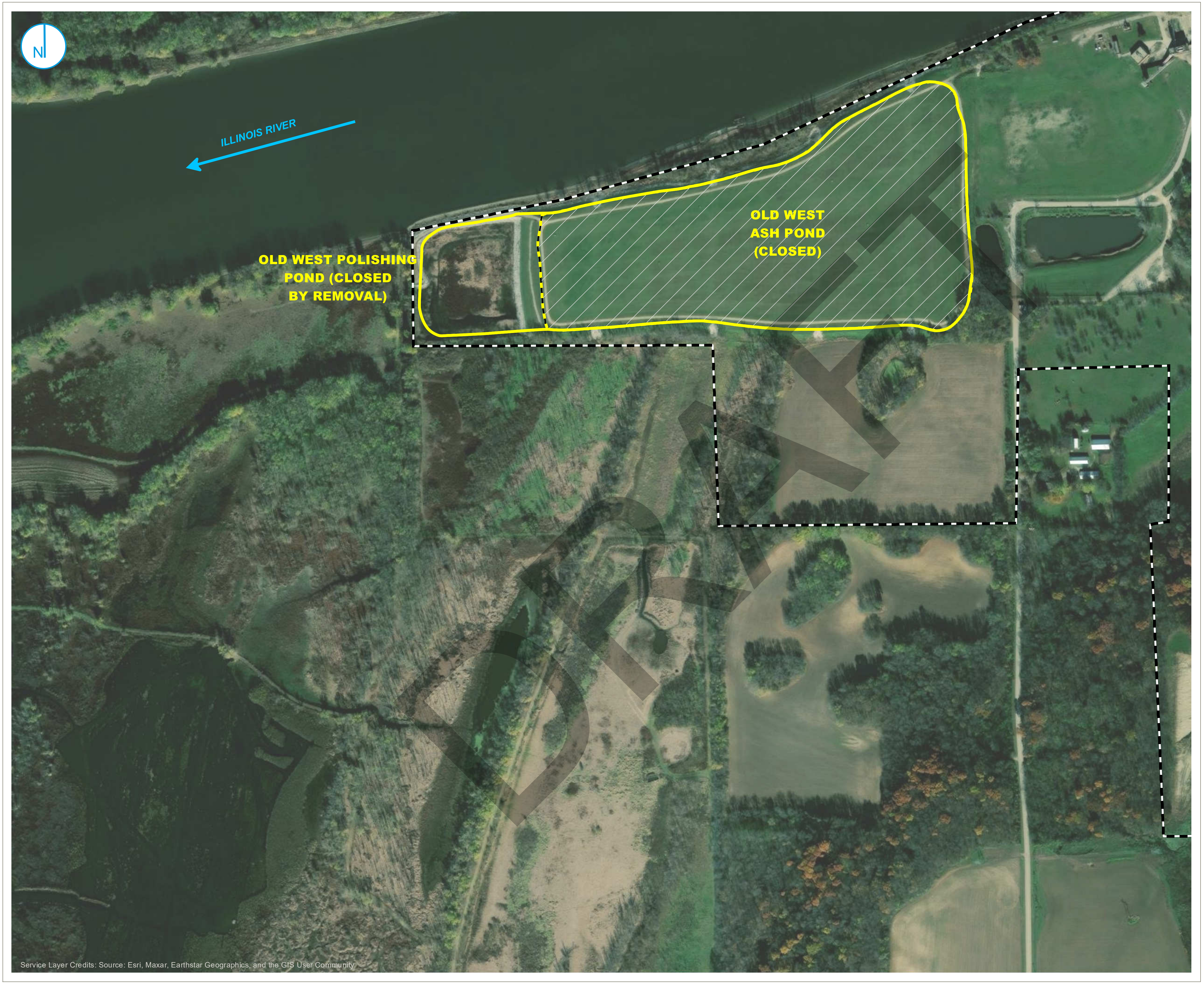

🟨 REGULATED UNIT (SUBJECT UNIT)
▨ LIMITS OF FINAL COVER
⬚ PROPERTY BOUNDARY

SITE MAP

NATURE AND EXTENT REPORT
WEST ASH POND SYSTEM
HENNEPIN POWER PLANT
HENNEPIN, ILLINOIS

FIGURE 2-2

RAMBOLL AMERICAS
ENGINEERING SOLUTIONS, INC.

RAMBOLL

Y:\Mapping\Projects\22\2285\MXD\Nature_and_Extent\HEN\Nature_and_Extent_Report_HenWest\Figure 2-2_Site Map.mxd

PROJECT: 169000XXXX | DATED: 4/24/2024 | DESIGNER: galarmmc

Y:\Mapping\Projects\22\2285\MXD\Nature_and_Extent\HEN\Nature_and_Extent_Report_HenWest\Figure 2-1_Bottom of Ash Map.mxd

● B006 0 ft BORING LOCATION WHERE ASH IS UNDERLAIN BY SAND AND/OR GRAVEL

● B007 2 ft BORING LOCATION AND KNOWN MINIMUM THICKNESS OF CLAY UNDERLYING ASH

INTERPOLATED BOTTOM OF ASH ELEVATION CONTOUR

REGULATED UNIT (SUBJECT UNIT)

LIMITS OF FINAL COVER

PROPERTY BOUNDARY

0 100 200 Feet

BASE OF CCR AND OBSERVED CLAY THICKNESS

NATURE AND EXTENT REPORT
WEST ASH POND SYSTEM
HENNEPIN POWER PLANT
HENNEPIN, ILLINOIS

FIGURE 2-3

RAMBOLL AMERICAS
ENGINEERING SOLUTIONS, INC.

PROJECT: 169000XXXX | DATED: 4/23/2024 | DESIGNER: galarmmc

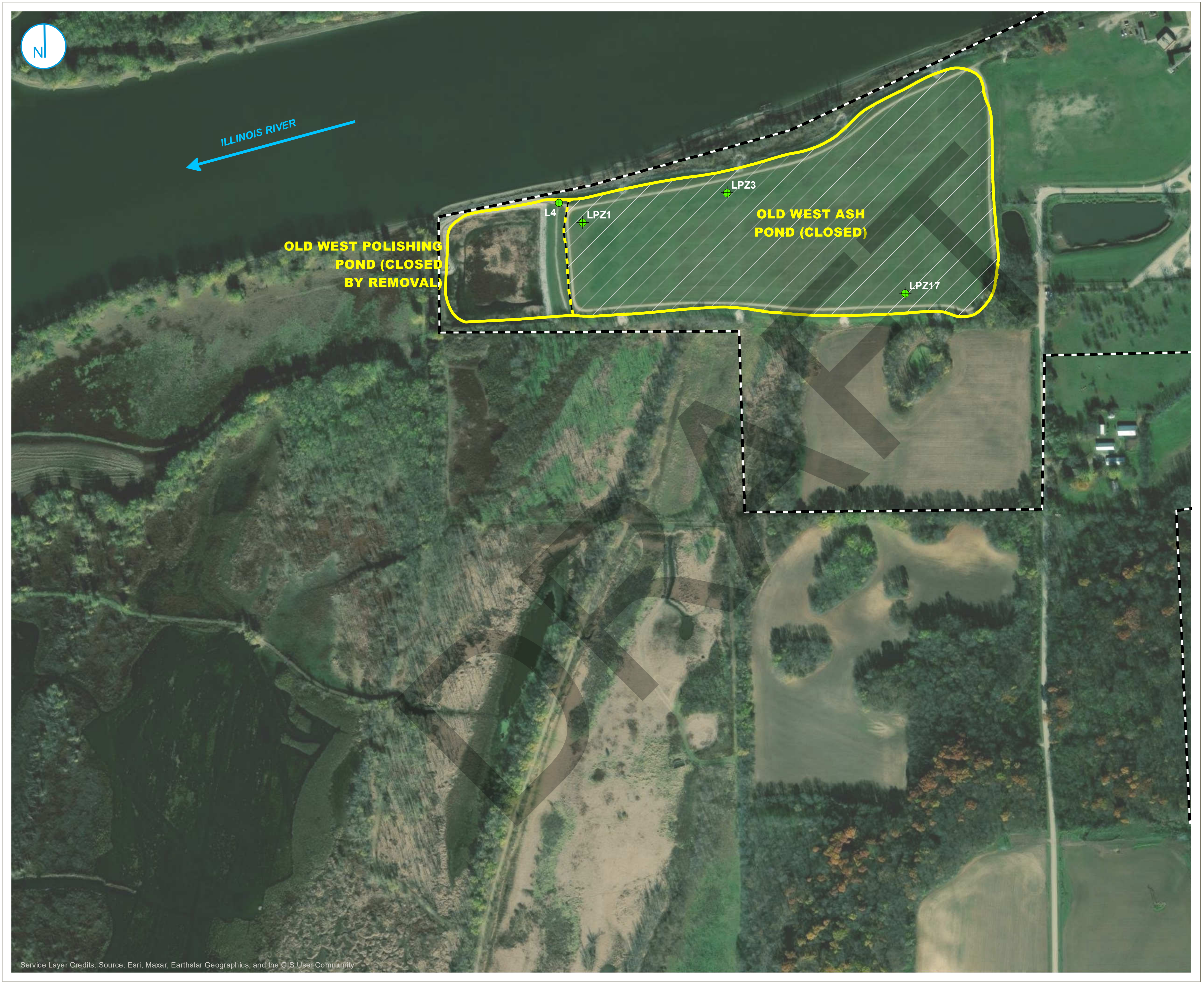

Service Layer Credits: Source: Esri, Maxar, Earthstar Geographics, and the GIS User Community

⊕ LEACHATE WELL
▭ REGULATED UNIT (SUBJECT UNIT)
▨ LIMITS OF FINAL COVER
⬚ PROPERTY BOUNDARY

0 200 400 Feet

POREWATER SAMPLE LOCATION MAP

NATURE AND EXTENT REPORT
WEST ASH POND SYSTEM
HENNEPIN POWER PLANT
HENNEPIN, ILLINOIS

FIGURE 2-4

RAMBOLL AMERICAS
ENGINEERING SOLUTIONS, INC.

Y:\Mapping\Projects\22\2285\MXD\Nature_and_Extent\HEN\Nature_and_Extent_Report_HenWest\Figure 2-4. Leachate Sample Location Map.mxd

PROJECT: 169000XXXX | DATED: 4/24/2024 | DESIGNER: galarnmc

Service Layer Credits: Source: Esri, Maxar, Earthstar Geographics, and the GIS User Community

⊞	MONITORING WELL
—	TOP OF SAND ELEVATION CONTOUR (5 FT CONTOUR INTERVAL, NAVD88)
- -	INFERRED TOP OF SAND ELEVATION CONTOUR
☐	REGULATED UNIT (SUBJECT UNIT)
▨	LIMITS OF FINAL COVER
⬚	PROPERTY BOUNDARY

TOP OF SAND AND GRAVEL IN UPPERMOST AQUIFER

NATURE AND EXTENT REPORT
WEST ASH POND SYSTEM
HENNEPIN POWER PLANT
HENNEPIN, ILLINOIS

FIGURE 2-5

RAMBOLL AMERICAS
ENGINEERING SOLUTIONS, INC.

Y:\Mapping\Projects\22\2285\MXD\Nature_and_Extent\HEN\Nature_and_Extent_Report_HenWest\Figure 2-5_Top of Aquifer Map.mxd

PROJECT: 169000XXXX | DATED: 5/6/2024 | DESIGNER: GALARNMC

Y:\Mapping\Projects\22\2285\MXD\GW_Contours\Round_2023\Hennepin\OWAP_804\HEN 804 OWAP Pot Surface 20230228.mxd

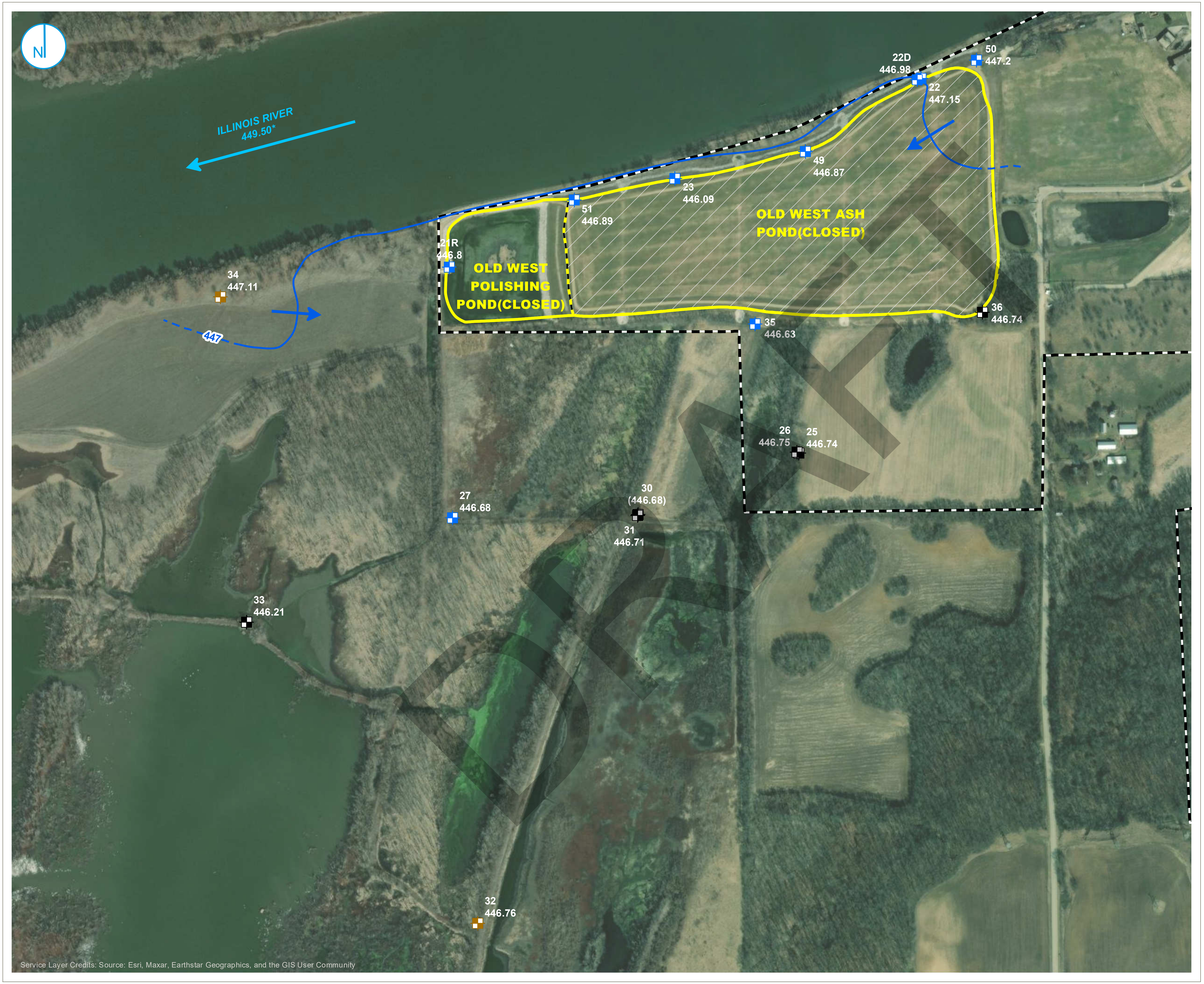

Service Layer Credits: Source: Esri, Maxar, Earthstar Geographics, and the GIS User Community

PROJECT: 169000XXXX | DATED: 9/15/2023 | DESIGNER: GALARNMC

- 🟦 COMPLIANCE MONITORING WELL
- 🟫 BACKGROUND MONITORING WELL
- ⬛ MONITORING WELL
- ― GROUNDWATER ELEVATION CONTOUR (1 FT CONTOUR INTERVAL, NAVD88)
- - - INFERRED GROUNDWATER ELEVATION CONTOUR
- → GROUNDWATER FLOW DIRECTION
- ▭ REGULATED UNIT (SUBJECT UNIT)
- ▨ LIMITS OF FINAL COVER
- ⬚ PROPERTY BOUNDARY

NOTES:
1.ELEVATIONS IN PARENTHESES WERE NOT USED FOR CONTOURING.
2. ELEVATION CONTOURS SHOWN IN FEET, NORTH AMERICAN VERTICAL DATUM OF 1988 (NAVD88)
*ILLINOIS RIVER ELEVATION OBTAINED FROM STAFF GAGE SG02, LOCATED AT THE HENNEPIN POWER PLANT

0 200 400 Feet

POTENTIOMETRIC SURFACE MAP FEBRUARY 28 AND MARCH 1, 2023

NATURE AND EXTENT REPORT
WEST ASH POND SYSTEM
HENNEPIN POWER PLANT
HENNEPIN, ILLINOIS

FIGURE 2-6

RAMBOLL AMERICAS
ENGINEERING SOLUTIONS, INC.

RAMBOLL

- COMPLIANCE MONITORING WELL
- BACKGROUND MONITORING WELL
- MONITORING WELL
- GROUNDWATER ELEVATION CONTOUR (1 FT CONTOUR INTERVAL, NAVD88)
- INFERRED GROUNDWATER ELEVATION CONTOUR
- GROUNDWATER FLOW DIRECTION
- REGULATED UNIT (SUBJECT UNIT)
- LIMITS OF FINAL COVER
- PROPERTY BOUNDARY

NOTES:

1.ELEVATIONS IN PARENTHESES WERE NOT USED FOR CONTOURING.

2. ELEVATION CONTOURS SHOWN IN FEET, NORTH AMERICAN VERTICAL DATUM OF 1988 (NAVD88)

*ILLINOIS RIVER ELEVATION OBTAINED FROM STAFF GAGE SG02, LOCATED AT THE HENNEPIN POWER PLANT

0 200 400
Feet

POTENTIOMETRIC SURFACE MAP
MAY 30, 2023 (E001)

NATURE AND EXTENT REPORT
WEST ASH POND SYSTEM
HENNEPIN POWER PLANT
HENNEPIN, ILLINOIS

FIGURE 2-7

RAMBOLL AMERICAS
ENGINEERING SOLUTIONS, INC.

RAMBOLL

Y:\Mapping\Projects\22\2285\MXD\GW_Contours\Round_2023\Hennepin\OWAP_804\HEN 804 OWAP Pot Surface 20230530.mxd

PROJECT: 169000XXXX | DATED: 7/6/2023 | DESIGNER: GALARNMC

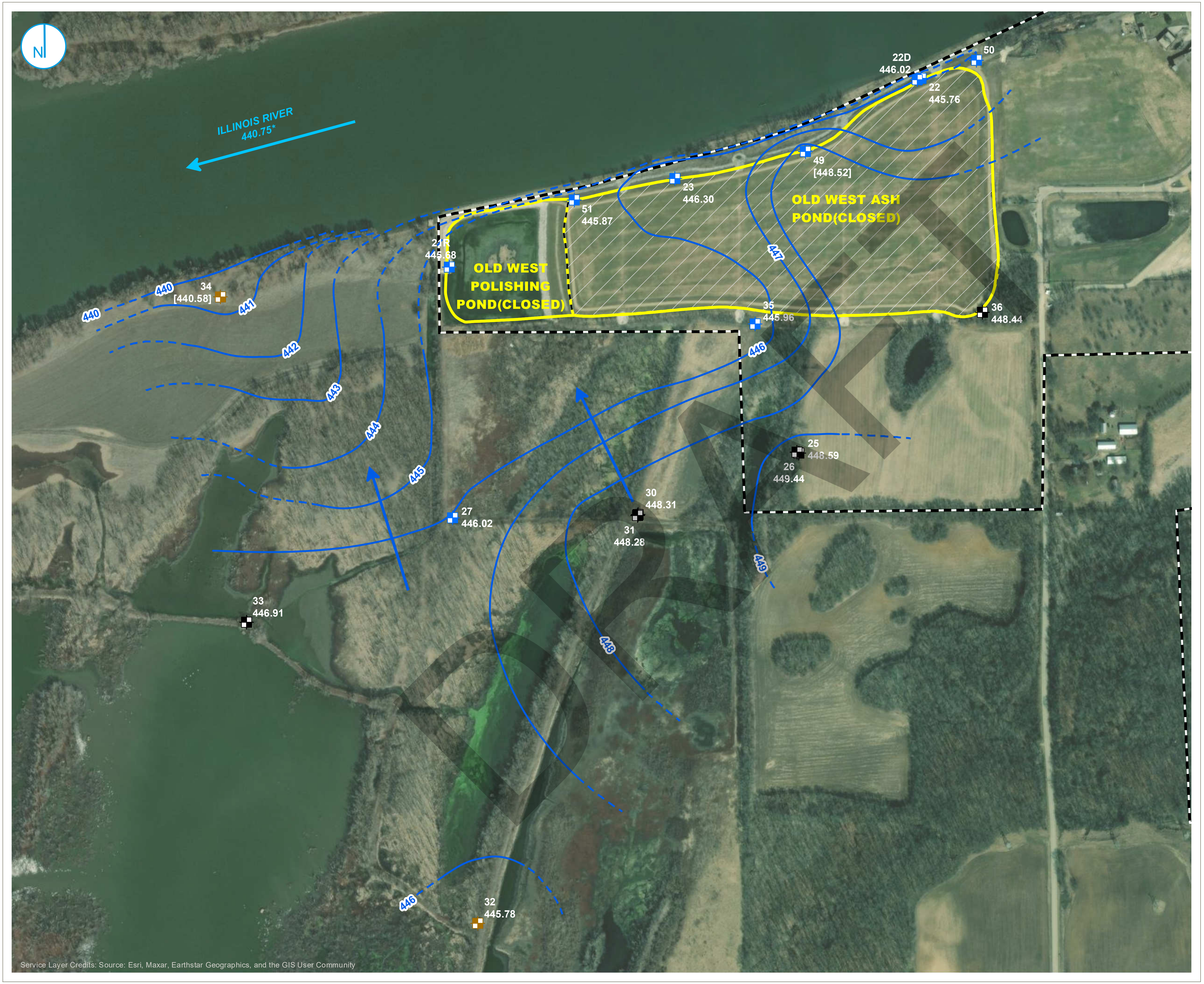

▦ COMPLIANCE MONITORING WELL

▦ BACKGROUND MONITORING WELL

▦ MONITORING WELL

— GROUNDWATER ELEVATION CONTOUR (1 FT CONTOUR INTERVAL, NAVD88)

- - INFERRED GROUNDWATER ELEVATION CONTOUR

→ GROUNDWATER FLOW DIRECTION

▭ REGULATED UNIT (SUBJECT UNIT)

▨ LIMITS OF FINAL COVER

⬚ PROPERTY BOUNDARY

NOTES:

1.ELEVATIONS IN PARENTHESES WERE NOT USED FOR CONTOURING.

2. ELEVATIONS IN BRACKETS WERE OBTAINED OUTSIDE OF THE 24 HOUR PERIOD FROM INITIATION OF DEPTH TO GROUNDWATER MEASUREMENTS BUT WITHIN THE SAME SAMPLING EVENT.

3. ELEVATION CONTOURS SHOWN IN FEET, NORTH AMERICAN VERTICAL DATUM OF 1988 (NAVD88)

*ILLINOIS RIVER ELEVATION OBTAINED FROM STAFF GAGE SG02, LOCATED AT THE HENNEPIN POWER PLANT

0 200 400
Feet

POTENTIOMETRIC SURFACE MAP
AUGUST 21 AND 22, 2023
(E002)

NATURE AND EXTENT REPORT
WEST ASH POND SYSTEM
HENNEPIN POWER PLANT
HENNEPIN, ILLINOIS

FIGURE 2-8

RAMBOLL AMERICAS
ENGINEERING SOLUTIONS, INC.

Y:\Mapping\Projects\22\2285\MXD\GW_Contours\Round_2023\Hennepin\OWAP_804\HEN 804 OWAP Pot Surface 20230821.mxd

PROJECT: 169000XXXX | DATED: 12/18/2023 | DESIGNER: GALARNMC

Y:\Mapping\Projects\22\2285\MXD\GW_Contours\Round_2023\Hennepin\OWAP_804\HEN 804 OWAP Pot Surface 20231113.mxd

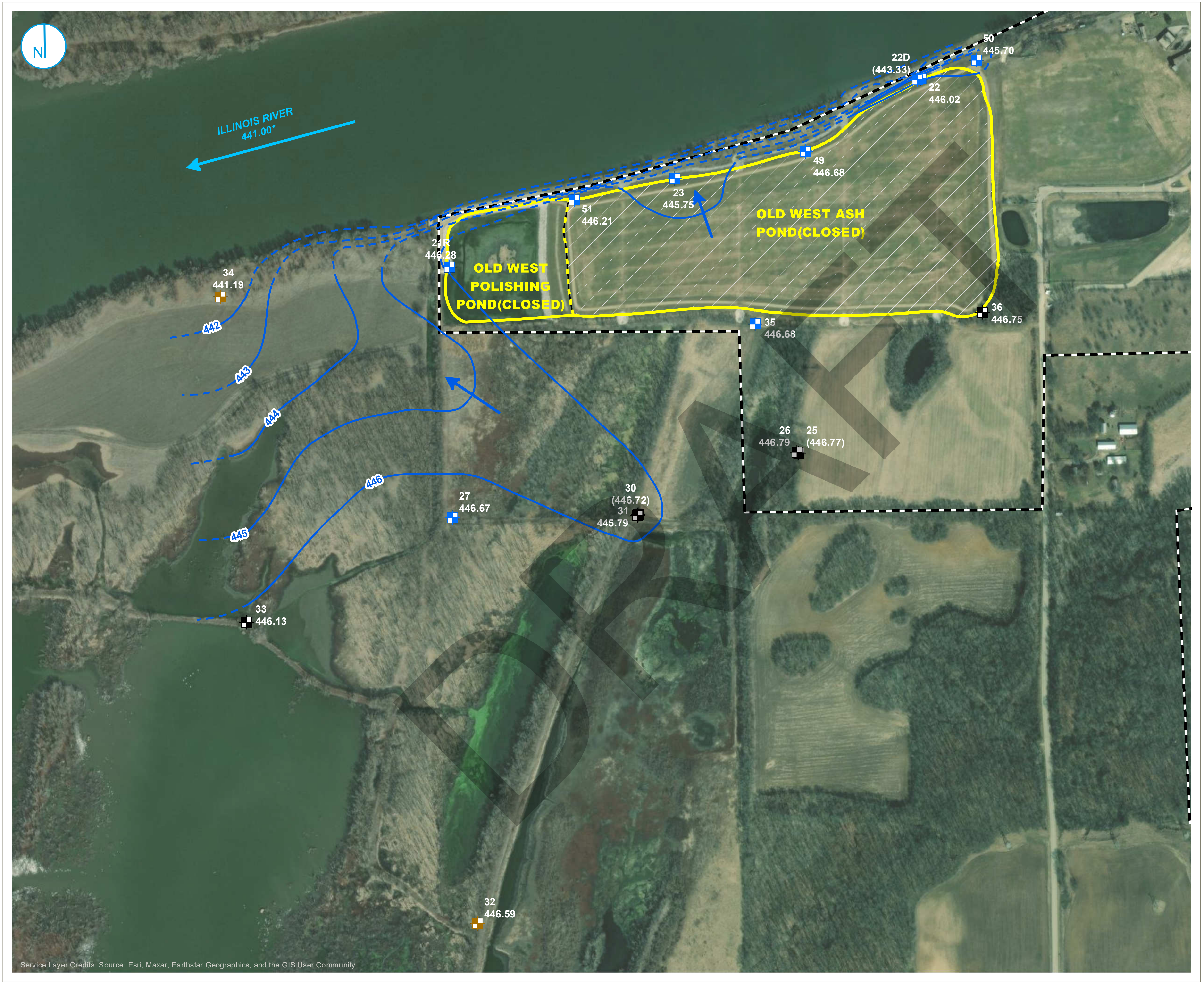

- ▣ COMPLIANCE MONITORING WELL
- ▣ BACKGROUND MONITORING WELL
- ▣ MONITORING WELL
- ― GROUNDWATER ELEVATION CONTOUR (1 FT CONTOUR INTERVAL, NAVD88)
- - - INFERRED GROUNDWATER ELEVATION CONTOUR
- → GROUNDWATER FLOW DIRECTION
- ☐ REGULATED UNIT (SUBJECT UNIT)
- ▨ LIMITS OF FINAL COVER
- ☐ PROPERTY BOUNDARY

NOTES:

1.ELEVATIONS IN PARENTHESES WERE NOT USED FOR CONTOURING.

2. ELEVATION CONTOURS SHOWN IN FEET, NORTH AMERICAN VERTICAL DATUM OF 1988 (NAVD88)

*ILLINOIS RIVER ELEVATION OBTAINED FROM STAFF GAGE SG02, LOCATED AT THE HENNEPIN POWER PLANT

0 200 400
Feet

POTENTIOMETRIC SURFACE MAP
NOVEMBER 13, 2023 (E003)

NATURE AND EXTENT REPORT
WEST ASH POND SYSTEM
HENNEPIN POWER PLANT
HENNEPIN, ILLINOIS

FIGURE 2-9

RAMBOLL AMERICAS
ENGINEERING SOLUTIONS, INC.

RAMBOLL

PROJECT: 169000XXXX | DATED: 12/18/2023 | DESIGNER: GALARNMC

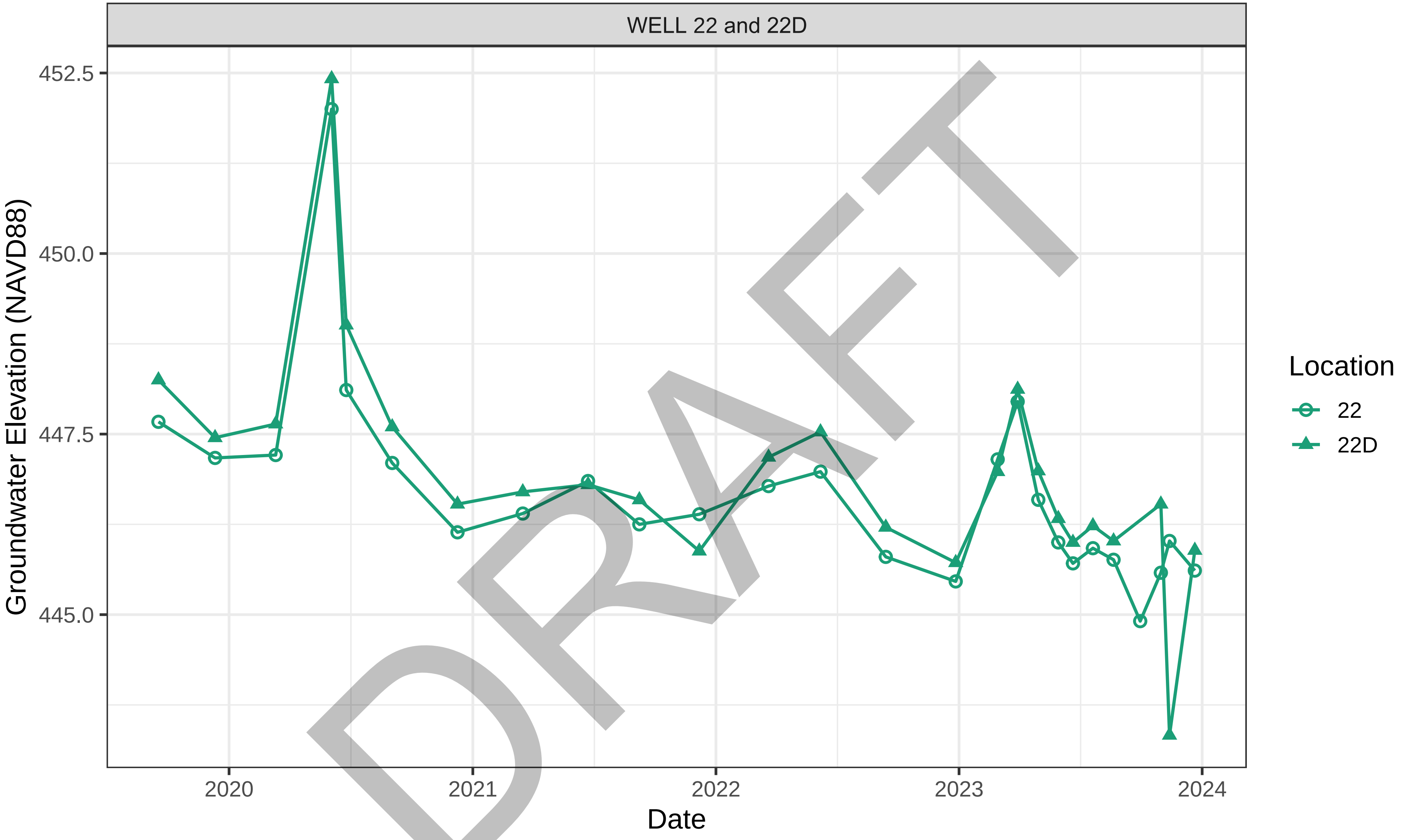

RAMBOLL

HYDROGRAPH - WELLS 22 and 22D

Nature and Extent Report
Hennepin West Ash Pond System
Hennepin, IL

Figure

2-10

Drafter: AOC Date: 2024−04−24 Contract Number: 1940103584

Y:\Mapping\Projects\22\2285\MXD\Nature_and_Extent\HEN\Nature_and_Extent_Report_HenWest\Figure 2-10. Monitoring Well Location Map.mxd

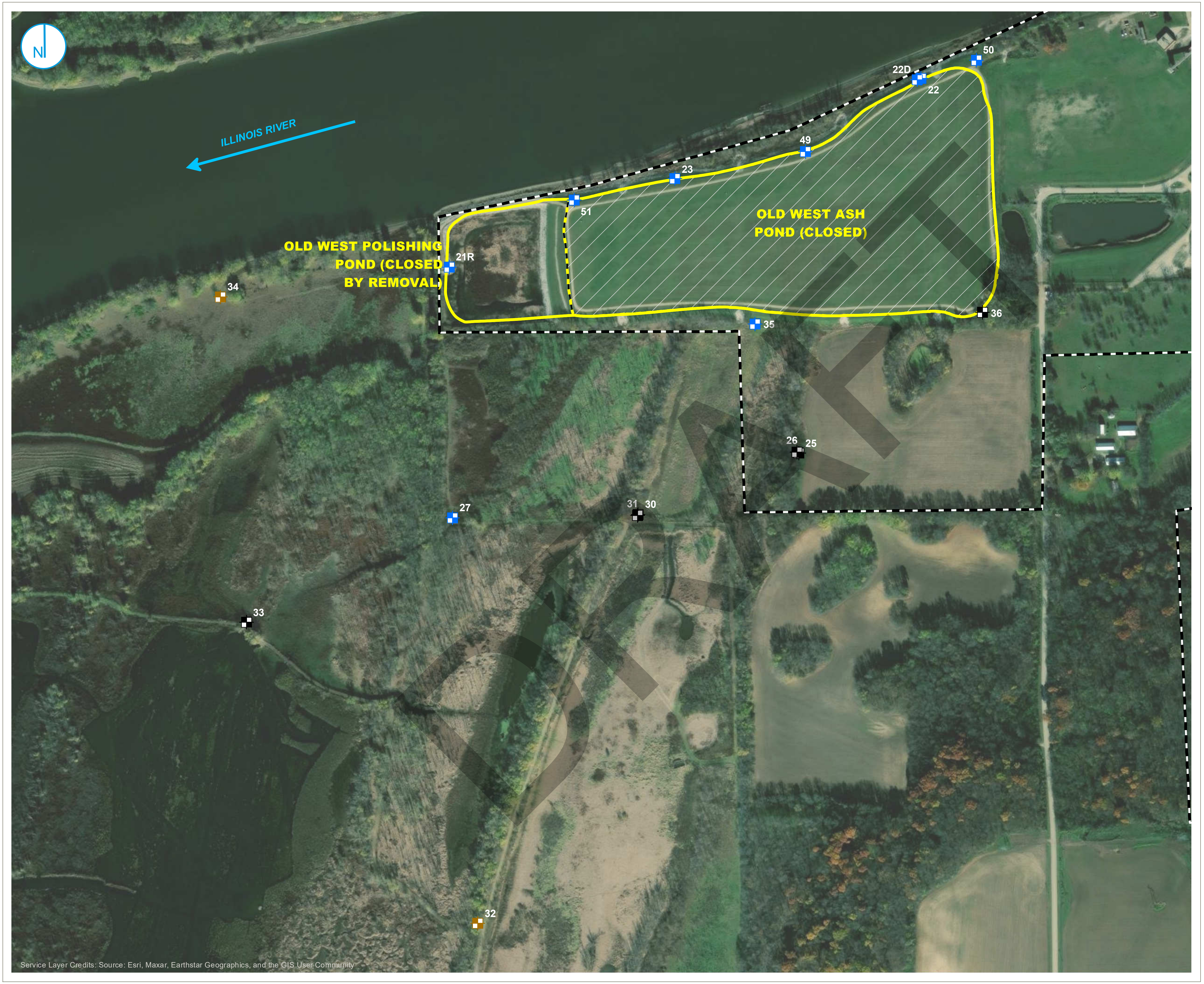

Service Layer Credits: Source: Esri, Maxar, Earthstar Geographics, and the GIS User Community

- ▣ COMPLIANCE MONITORING WELL
- ▣ BACKGROUND MONITORING WELL
- ▣ MONITORING WELL
- ▭ REGULATED UNIT (SUBJECT UNIT)
- ▨ LIMITS OF FINAL COVER
- ⬚ PROPERTY BOUNDARY

0 200 400 Feet

MONITORING WELL LOCATION MAP

NATURE AND EXTENT REPORT
WEST ASH POND SYSTEM
HENNEPIN POWER PLANT
HENNEPIN, ILLINOIS

FIGURE 2-11

RAMBOLL AMERICAS
ENGINEERING SOLUTIONS, INC.

RAMBOLL

PROJECT: 169000XXXX | DATED: 4/24/2024 | DESIGNER: galarnmc

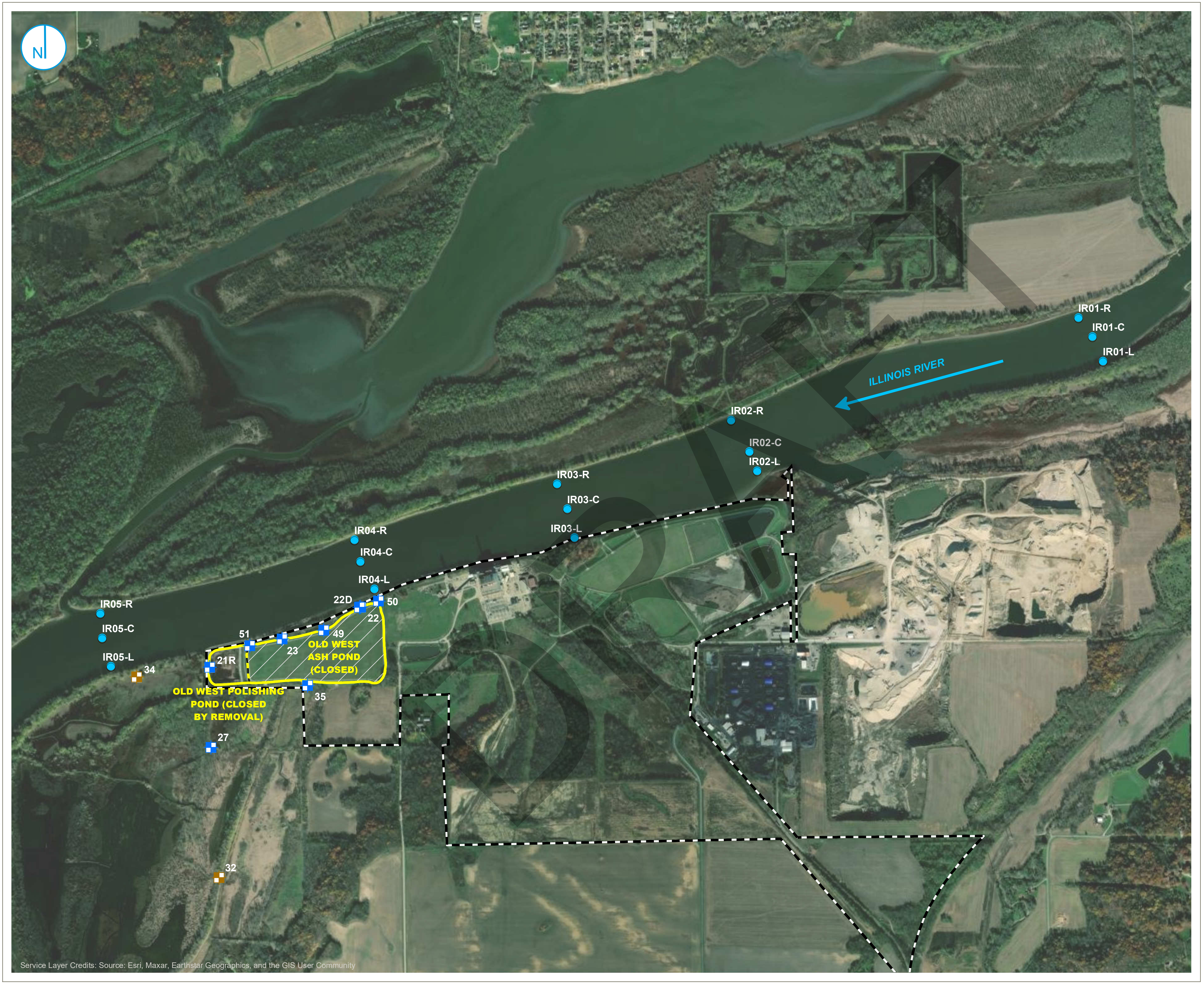

● SURFACE WATER SAMPLE

▣ COMPLIANCE MONITORING WELL

▣ BACKGROUND MONITORING WELL

▭ REGULATED UNIT (SUBJECT UNIT)

▨ LIMITS OF FINAL COVER

▭ PROPERTY BOUNDARY

0 625 1,250
Feet

ILLINOIS RIVER SURFACE WATER SAMPLING LOCATIONS

NATURE AND EXTENT REPORT
WEST ASH POND SYSTEM
HENNEPIN POWER PLANT
HENNEPIN, ILLINOIS

FIGURE 3-1

RAMBOLL AMERICAS
ENGINEERING SOLUTIONS, INC.

Y:\Mapping\Projects\22\2285\MXD\Nature_and_Extent\HEN\Nature_and_Extent_Report_HenWest\Figure 3-2. Illinois River Surface Water Sampling Locations.mxd

PROJECT: 169000XXXX | DATED: 5/6/2024 | DESIGNER: GALARNMC

Y:\Mapping\Projects\22\2285\MXD\Nature_and_Extent\HEN\Nature_and_Extent_Report_HenWest\Figure 3-1. HEN 804 GWPS UA.mxd

PROJECT: 169000XXXX | DATED: 4/24/2024 | DESIGNER: galarnmc

GWPS EXCEEDANCE MAP
UPPERMOST AQUIFER

NATURE AND EXTENT REPORT
WEST ASH POND SYSTEM
HENNEPIN POWER PLANT
HENNEPIN, ILLINOIS

FIGURE 3-2

RAMBOLL AMERICAS
ENGINEERING SOLUTIONS, INC.

APPENDICES

APPENDIX A
Geologic Cross-Sections (NRT, 2017)

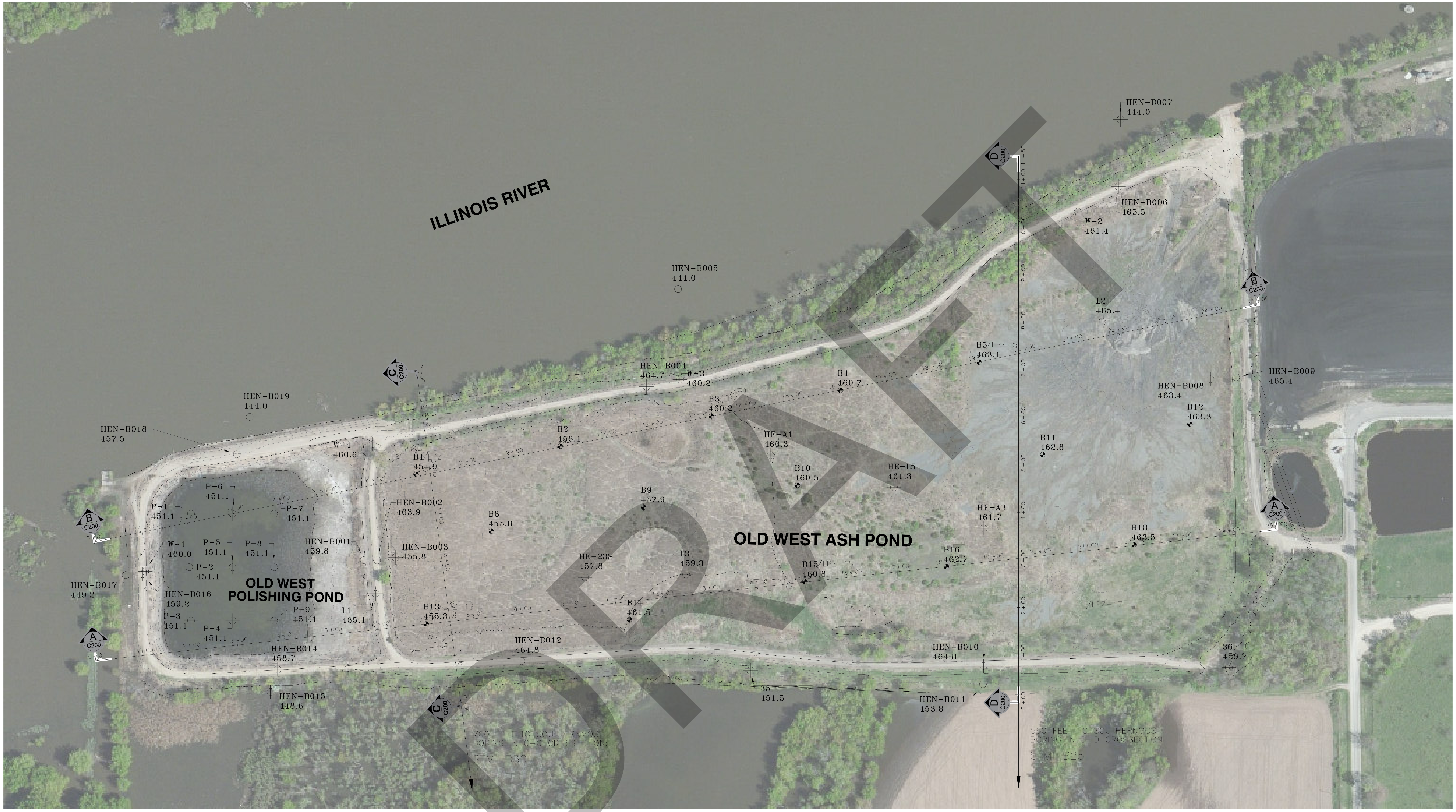

Aug 31, 2017 1:53pm PLOTTED BY: Oneilljm SAVED BY: Oneilljm
I:\Abbott-Nut.15090\STDS\GIS_NRT\Hennepin\OBG MOD - 164478-CV01-C100-Cross Sections.dwg Plan View
IMAGES: I:\Abbott-Nut.15090\STDS\GIS_NRT\Hennepin\CEC B-Series Borings.tif; .\Images\GoogleEarth Site.jpg;
XREFS:

REFERENCES

1. SOURCE DRAWING DERIVED FROM CEC, INC.; PROJECT NUMBER 164-478, DRAWING NUMBER C200, DATED 3/27/17.
2. TOPOGRAPHIC INFORMATION BASED ON AERIAL SURVEY COMPLETED BY SURDEX ON AUGUST 17, 2015 AND TOPOGRAPHIC/BATHYMETRIC SURVEY COMPLETED BY WEAVER CONSULTANTS GROUP ON SEPTEMBER 22, 2015.
3. IMAGE PROVIDED BY GOOGLE EARTH. DATE OF IMAGE: SEPTEMBER 20,2015.

LEGEND

━━ ‒ ‒ ━━	WEST ASH POND SYSTEM LIMITS
— — —450— — —	EXISTING 10 FT CONTOUR
- - - - -452- - - - -	EXISTING 2 FT CONTOUR
◐ B13	CEC BORING LOCATION
⊕ P-1	SOIL BORING BY OTHERS
Ⓐ Ⓐ	CROSS SECTION LOCATION

DRAWN BY:	AGC	DATE:	02/15/2017
CHECKED BY:	NRK	DATE:	02/21/2017
APPROVED BY:	SJC	DATE:	08/25/2017
DRAWING NO:	OBG MOD - 16448 CROSS SECTIONS		
REFERENCE:	.		

MONITORING WELL AND BORING LOCATIONS

HYDROGEOLOGIC CHARACTERIZATION REPORT
WEST ASH POND SYSTEM
DYNEGY MIDWEST GENERATION, LLC
HENNEPIN POWER STATION, HENNEPIN, ILLINOIS

Natural Resource Technology
AN OBG COMPANY

PROJECT NO.
2421

FIGURE NO.
7

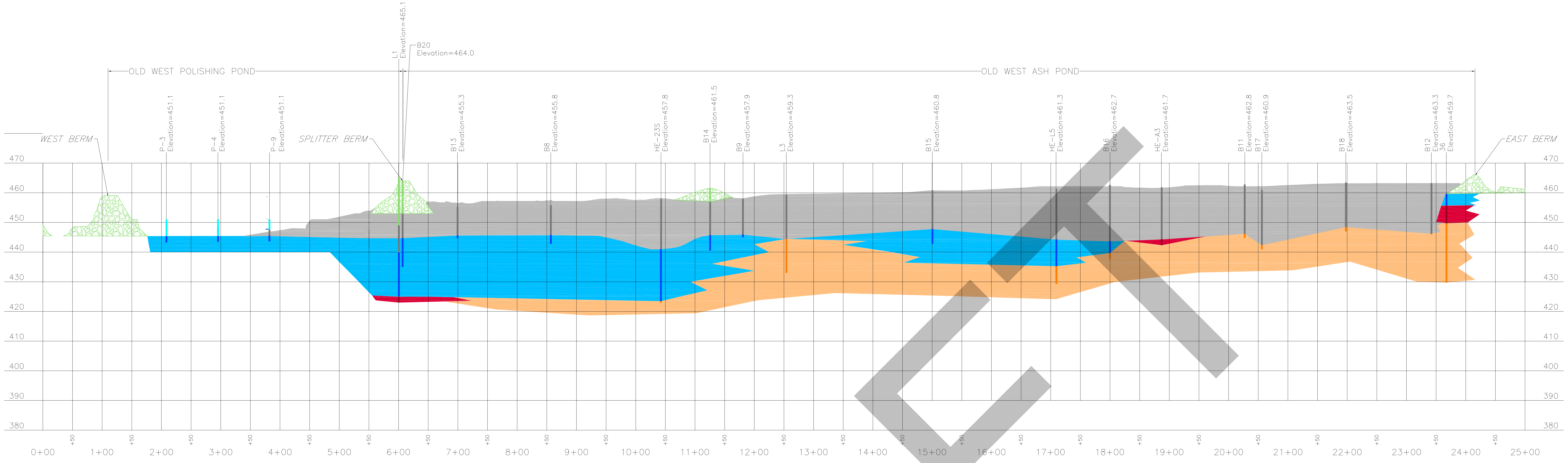

A PROFILE

SCALE H:1"=100'; V:1"=20'

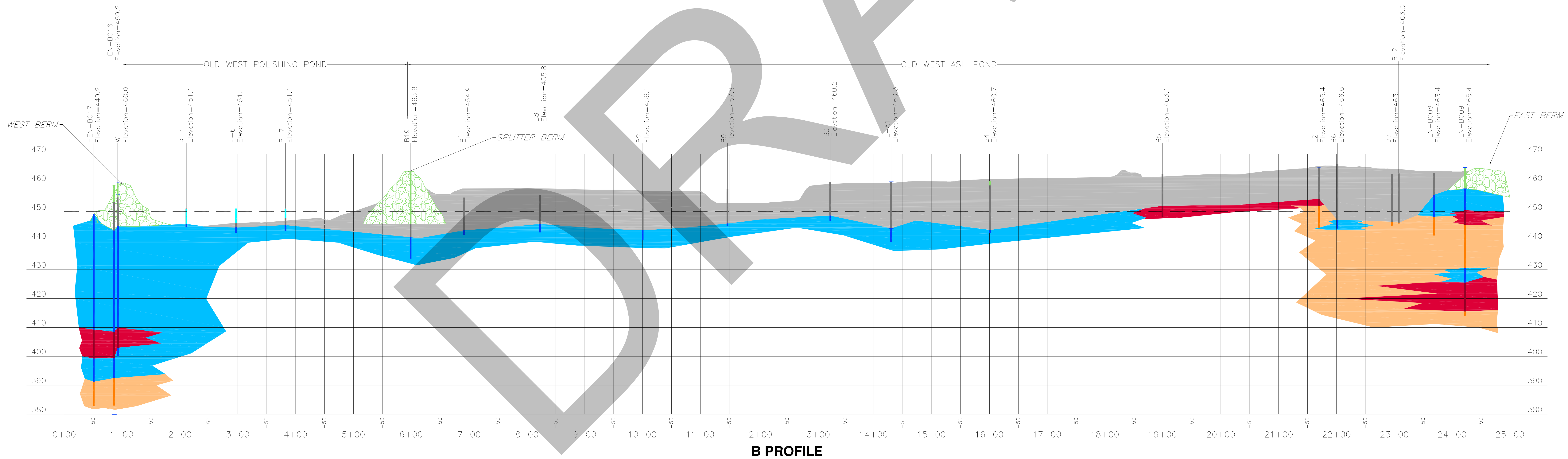

B PROFILE

SCALE H:1"=100'; V:1"=20'

Aug 29, 2017 1:07pm PLOTTED BY: Oneilljm SAVED BY: Oneilljm
I:\Abbott-Nut.15090\STDS\GIS_NRT\Hennepin\OBG MOD - 164478-CV01-C100-Cross Sections.dwg A-A' & B-B'
IMAGES: .\Images\GoogleEarth Site.jpg;
XREFS:

REFERENCES

1. SOURCE DRAWING DERIVED FROM CEC, INC.; PROJECT NUMBER 164-478, DRAWING NUMBER C200, DATED 3/27/17.
2. TOP OF EXISTING GRADE BASED ON DATA PROVIDED BY WEAVER CONSULTING GROUP SURVEY (2015) AS PRESENTED BY CEC INC.
3. GEOLOGIC INTERPRETATIONS ARE BASED ON BORING LOGS PERFORMED BY CEC INC., AECOM, SCIENCE AND TECHNOLOGY MANAGEMENT INC., JOHN MATHES & ASSOCIATES INC., AND NATURAL RESOURCE TECHNOLOGY INC.

LEGEND

🟩	MISCELLANEOUS BERM SOIL FILL
⬜	CCR/ASH
🟦	SILTS AND CLAYS (ALLUVIAL)
🟥	SANDS WITH FINES (ALLUVIAL)
🟧	SAND AND GRAVEL (GLACIAL OUTWASH)

GEOLOGIC CONDITIONS

1. THE TEST BORING INFORMATION PRESENTED HEREIN DEPICTS SUBSURFACE CONDITIONS AT THE TEST BORING LOCATIONS AND AT THE TIME OF DRILLING. SOIL CONDITIONS AT OTHER LOCATIONS MAY DIFFER.
2. GEOLOGIC CORRELATIONS BETWEEN TEST BORINGS ARE GENERALLY BASED ON STRAIGHT-LINE INTERPOLATION. ACTUAL CONDITIONS BETWEEN TEST BORINGS MAY DIFFER.

DRAWN BY: AGC DATE: 02/15/2017
CHECKED BY: NRK DATE: 02/21/2017
APPROVED BY: SJC DATE: 08/25/2017
DRAWING NO: OBG MOD - 16448 CROSS SECTIONS
REFERENCE: .

CROSS-SECTION A-A' AND B-B'

HYDROGEOLOGIC CHARACTERIZATION REPORT

WEST ASH POND SYSTEM
DYNEGY MIDWEST GENERATION, LLC
HENNEPIN POWER STATION, HENNEPIN, ILLINOIS

Natural Resource Technology
AN OBG COMPANY

PROJECT NO.
2421

FIGURE NO.
9

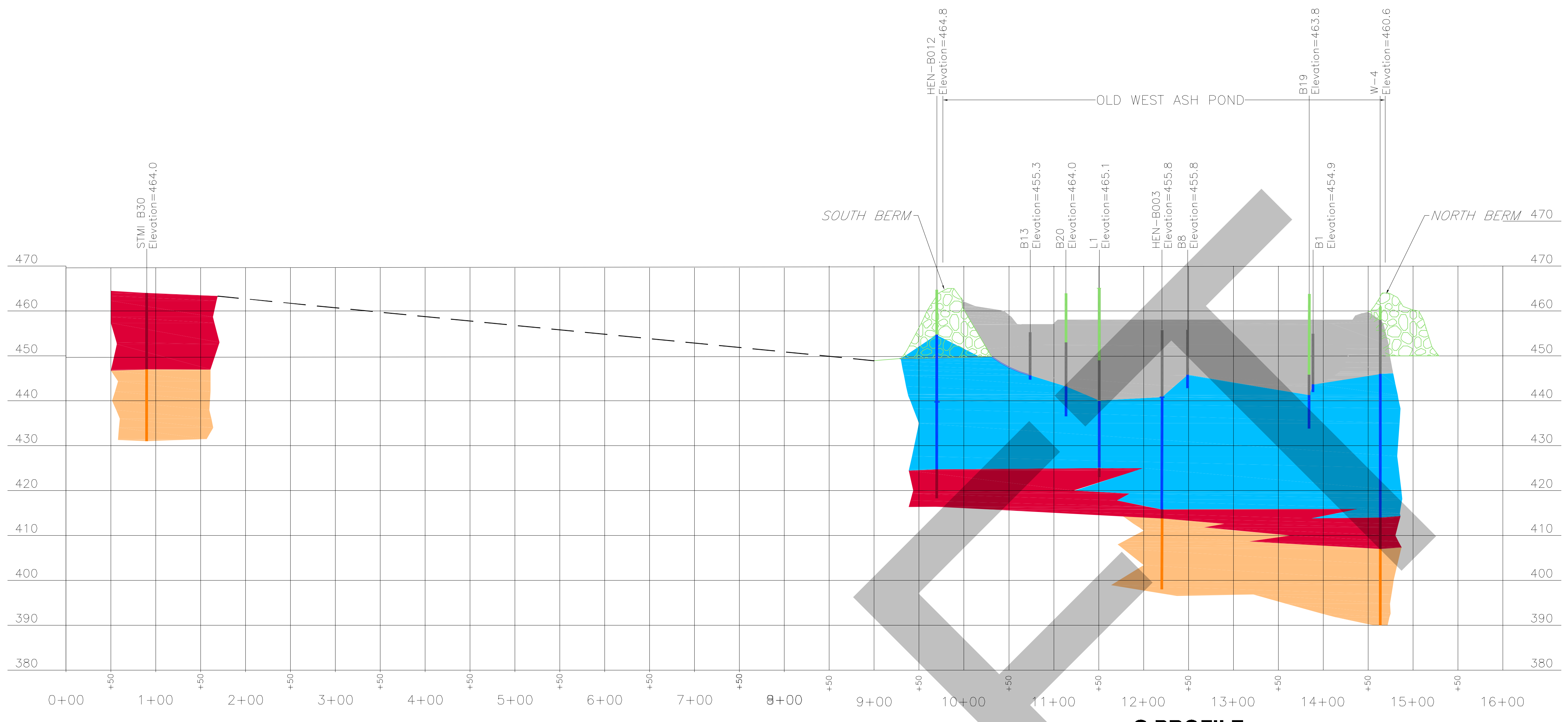

C PROFILE

SCALE H:1"=100'; V:1"=20'

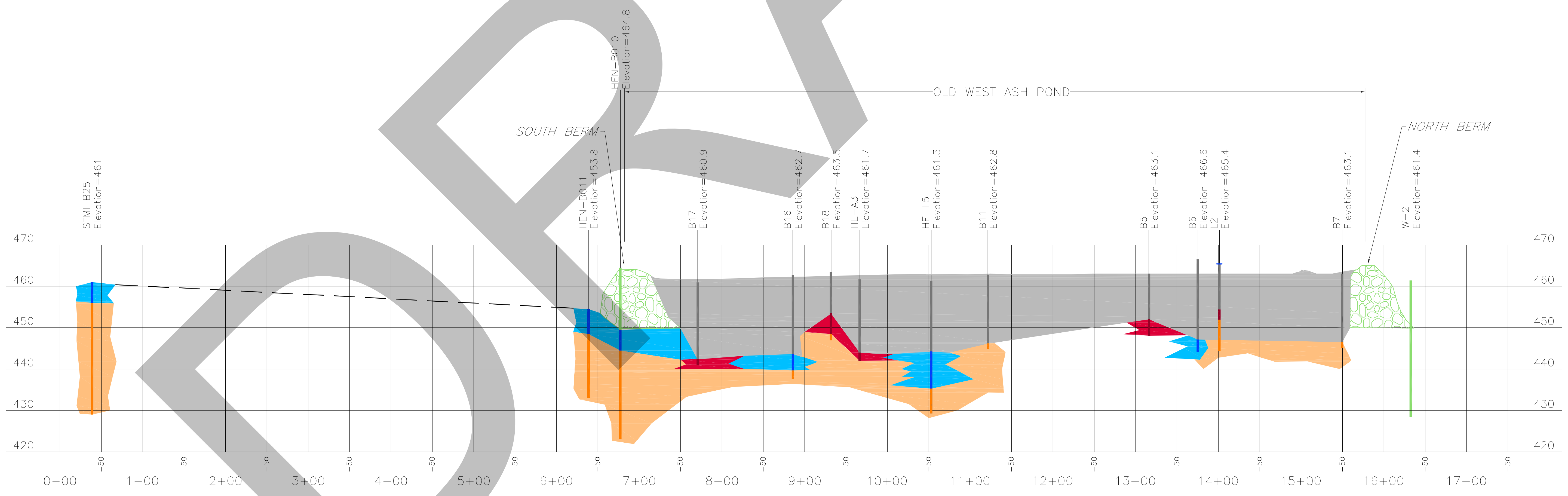

D PROFILE

SCALE H:1"=100'; V:1"=20'

Aug 29, 2017 1:06pm PLOTTED BY: Oneilljm SAVED BY: Oneilljm
I:\Abbott-Nut.15090\STDS\GIS_NRT\Hennepin\OBG MOD - 164478-CV01-C100-Cross Sections.dwg C-C' & D-D'
IMAGES: .\Images\GoogleEarth Site.jpg;
XREFS:

REFERENCES

1. SOURCE DRAWING DERIVED FROM CEC, INC.; PROJECT NUMBER 164-478, DRAWING NUMBER C200, DATED 3/27/17.
2. TOP OF EXISTING GRADE BASED ON DATA PROVIDED BY WEAVER CONSULTING GROUP SURVEY (2015) AS PRESENTED BY CEC INC.
3. GEOLOGIC INTERPRETATIONS ARE BASED ON BORING LOGS PERFORMED BY CEC INC., AECOM, SCIENCE AND TECHNOLOGY MANAGEMENT INC., JOHN MATHES & ASSOCIATES INC., AND NATURAL RESOURCE TECHNOLOGY INC.

LEGEND

▨	MISCELLANEOUS BERM SOIL FILL
⬜	CCR/ASH
🟦	SILTS AND CLAYS (ALLUVIAL)
🟥	SANDS WITH FINES (ALLUVIAL)
🟧	SAND AND GRAVEL (GLACIAL OUTWASH)
— — —	INTERPRETED NATURAL GROUND SURFACE OUTSIDE OF ASH POND

GEOLOGIC CONDITIONS

1. THE TEST BORING INFORMATION PRESENTED HEREIN DEPICTS SUBSURFACE CONDITIONS AT THE TEST BORING LOCATIONS AND AT THE TIME OF DRILLING. SOIL CONDITIONS AT OTHER LOCATIONS MAY DIFFER.
2. GEOLOGIC CORRELATIONS BETWEEN TEST BORINGS ARE GENERALLY BASED ON STRAIGHT-LINE INTERPOLATION. ACTUAL CONDITIONS BETWEEN TEST BORINGS MAY DIFFER.

DRAWN BY:	AGC	DATE:	02/15/2017
CHECKED BY:	NRK	DATE:	02/21/2017
APPROVED BY:	SJC	DATE:	08/25/2017
DRAWING NO:	OBG MOD - 16448 CROSS SECTIONS		
REFERENCE:	.		

CROSS-SECTION C-C' AND D-D'

HYDROGEOLOGIC CHARACTERIZATION REPORT

WEST ASH POND SYSTEM
DYNEGY MIDWEST GENERATION, LLC
HENNEPIN POWER STATION, HENNEPIN, ILLINOIS

Natural Resource Technology
AN OBG COMPANY

PROJECT NO.
2421

FIGURE NO.
10

APPENDIX B
Geochemical Conceptual Site Model (Geosyntec Consultants, Inc., 2024)

Geosyntec consultants

engineers | scientists | innovators

Geochemical Conceptual Site Model

Hennepin Power Plant – West Ash Pond System

(CCR Unit #804)

Prepared for

Dynegy Midwest Generation, LLC
1500 Eastport Plaza Drive
Collinsville, Illinois 62234

Prepared by

Geosyntec Consultants, Inc.
134 N. Lasalle Street, Suite 300
Chicago, Illinois 60602

Project Number: GLP8079

May 2024

TABLE OF CONTENTS

LIST OF FIGURES

LIST OF TABLES

LIST OF ATTACHMENTS

ACRONYMS AND ABBREVIATIONS

ASD	alternative source demonstration
CCR	coal combustion residuals
COCs	constituents of concern
ft bg	feet below ground surface
GCSM	geochemical conceptual site model
GWPS	groundwater protection standard
HPP	Hennepin Power Plant
HSU	hydrostratigraphic unit
I.A.C.	Illinois Administrative Code
IEPA	Illinois Environmental Protection Agency
LOI	loss on ignition
mg/L	milligrams per liter
µg/g	micrograms per gram
N&E	nature and extent
ORP	oxidation-reduction potential
OWAP	Old West Ash Pond
OWPP	Old West Polishing Pond
SEP	sequential extraction procedure
SU	standard units
TDS	total dissolved solids
TOC	total organic carbon
UA	uppermost aquifer
WAPS	West Ash Pond System
wt %	weight percent
XRD	X-Ray diffraction

1. EXECUTIVE SUMMARY

This report documents the development of a geochemical conceptual site model (GCSM) to describe conditions at the Hennepin Power Plant (HPP) West Ash Pond System (WAPS) coal combustion residuals (CCR) unit (Unit #804). A GCSM describes the geochemical processes that contribute to the mobilization, distribution, and attenuation of chemicals in the subsurface soil and groundwater environment. The GCSM was prepared in support of an evaluation of the nature and extent (N&E) of exceedances of constituents of concern (COCs) above the groundwater protection standards (GWPS) at the WAPS. Through the second, third, and fourth quarters of 2023, COC exceedances of arsenic, boron, lithium, sulfate, and total dissolved solids (TDS) were reported at WAPS compliance wells. The exceedances occur exclusively in the uppermost aquifer (UA), which consists of fill, unconsolidated alluvium, and Pleistocene-age glacial outwash and till deposits.

The CCR materials are the primary source of constituent loading to the CCR porewater (i.e., CCR source water). Over an extended period (e.g., months to years), the CCR source water (i.e., water contained within the interstitial pore spaces of the CCR that can be sampled by low-flow groundwater sampling methods) reaches equilibrium with the CCR materials. The porewater is therefore representative of the mobile phase constituents capable of migrating into the underlying materials and potentially downgradient in groundwater. The WAPS CCR source water is therefore the primary indicator of boron and sulfate *available* to the groundwater and is considered as the primary source term for environmental investigation and fate and transport modeling.

Arsenic, boron, lithium, and sulfate are naturally present in coal deposits and are concentrated in CCR. TDS is a measure of inorganic and organic substances in solution and, as such, TDS trends are generally consistent with those of major ions in the WAPS groundwater system. Arsenic, boron, and lithium were identified in UA solids adjacent to downgradient and background wells, which suggests that aquifer solids could provide a secondary natural geogenic source of arsenic, boron, and lithium to the groundwater. Redox conditions vary across the site, with more oxidizing conditions on the east side of the WAPS and more reducing conditions on the west. Reducing conditions may be enhancing arsenic mobility and thus aqueous arsenic concentrations at select wells on the west of the WAPS. The source of arsenic, boron, lithium, sulfate, and TDS to groundwater of the UA is currently expected to be the WAPS CCR porewater.

Arsenic, boron, lithium, and sulfate in the groundwater system may be attenuated via surface complexation reactions with metal (i.e., aluminum, iron, and manganese) oxyhydroxides. Iron oxides were detected in aquifer solids and are generally predicted to be stable at monitoring wells across the network. Clay minerals were also identified in aquifer solids and may provide an additional attenuation mechanism for arsenic, boron, lithium, and sulfate in groundwater. At the limited locations across the network where reducing conditions are present, microbial sulfate reduction may also contribute to decreased sulfate concentrations in the groundwater. Attenuation of the constituents contributing to TDS, such as sulfate, will reduce TDS concentrations as well.

2. INTRODUCTION

This report documents the development of a geochemical conceptual site model (GCSM) to describe conditions at the Hennepin Power Plant (HPP) West Ash Pond System (WAPS) coal combustion residuals (CCR) unit (Unit #804). A GCSM describes the geochemical processes that contribute to the mobilization, distribution, and attenuation of chemicals in the subsurface soil and groundwater environment. The GCSM was prepared in support of an evaluation of the nature and extent (N&E) of exceedances of constituents of concern (COCs) above the groundwater protection standards (GWPS) at the WAPS. This document has been prepared as an appendix to the HPP WAPS N&E Report prepared by Ramboll Americas Engineering Solutions, Inc. (Ramboll). Parameters with exceedances above the GWPS at the HPP WAPS compliance wells for the second, third, and fourth quarters of 2023 (Q2 2023, Q3 2023, and Q4 2023) sampling events completed under Illinois Administrative Code (I.A.C.) Title 35 Section 845.630 include arsenic, boron, lithium, sulfate, and total dissolved solids (TDS). Arsenic exceedances were observed at compliance wells 21R and 51. Boron exceedances were observed at compliance wells 21R, 22, 23, 35, and 27. Lithium was an exceedance at compliance well 22, and sulfate exceedances were observed at compliance wells 23 and 35. TDS exceeded the GWPS at compliance well 35. The exceedances identified at the WAPS occur exclusively in the uppermost aquifer (UA), the only monitored unit at the WAPS.

An exceedance of cadmium was observed at compliance monitoring well 22 during the Q2 2023 sampling event. However, an alternative source demonstration (ASD), as allowed by I.A.C. 845.650(e), was completed for the cadmium exceedance (Ramboll 2023). The cadmium ASD was accepted by the Illinois Environmental Protection Agency (IEPA) on December 7, 2023 (IEPA 2023); therefore, cadmium is not included as a COC in this GCSM.

3. SITE BACKGROUND

3.1 Site Overview

An overview of site characteristics and hydrogeology is presented in the HPP WAPS N&E Report. A site layout figure is provided in Attachment A.[1] The Hennepin WAPS consists of the Old West Ash Pond (OWAP) (Ponds No. 1 and No. 3) and the Old West Polishing Pond (OWPP). Pond No. 1 of the OWAP was constructed in 1951 and 1952, and Pond No 3. was constructed in 1968. Ponds No. 1 and No. 3 comprising the OWAP were merged in 1988 and 1989 when the embankment surrounding OWAP was raised. The OWPP was also constructed during this time (1988-1989). The WAPS operated between 1952 to 1996, and closure occurred between August 2019 and November 2020. The OWPP was closed by removal and consolidation of the CCR into OWAP, and subsequently, the OWAP was closed with a geomembrane and vegetated soil cover. A steel sheetpile wall was installed between the OWAP and the OWPP during closure as a temporary support-of-excavation feature to facilitate CCR consolidation and a compacted clay dike was constructed in front of the steel sheet pile wall to provide a permanent and continuous earthen containment system around the consolidated WAPS. The steel sheetpile was left in place following closure of the unit.

The Hennepin WAPS is located west of the HPP and adjacent to the Illinois River. The HPP property is bordered by farm fields to the east and south, low lying floodplains to the west, and the Illinois River to the north.

A Hydrogeologic Site Characterization Report (NRT 2017) and a Hydrogeologic Monitoring Plan (OBG 2017) previously described the hydrostratigraphic units (HSUs) present in the vicinity of the Hennepin WAPS. These reports indicate that the subsurface stratigraphy of the WAPS consists of fill, unconsolidated alluvium, and Pleistocene-age glacial outwash and till deposits, which comprise the UA. Sand and gravel deposits are thicker underneath the eastern portion of the WAPS, while the western portion is underlain by less permeable, silty and clay material (OBG, 2017). The UA may be up to 130 feet thick beneath the WAPS and is underlain by Pennsylvanian-age shale bedrock with interbedded limestone, sandstone, and coal seams.

3.2 Groundwater Monitoring Network

A groundwater monitoring network was proposed in accordance with I.A.C. Title 35 Section 845.630 to monitor groundwater quality which passes the waste boundary as part of the Operating Permit application to IEPA for the WAPS. The proposed groundwater monitoring network is

---

[1] This figure is also provided as Figure 2-2 of the HPP WAPS N&E Report.

described in the Addendum to the Groundwater Monitoring Plan (Ramboll 2021) and shown in Attachment B.[2] Well construction information is provided in Attachment C.[3]

Groundwater flow beneath the WAPS within the UA is predominantly to the north and northwest, towards the Illinois River, although the flow direction varies with the elevation of the river. During a high river stage, the groundwater flow direction may reverse, saturating the ash in the OWAP (NRT 2017; NRT 2018). There are localized flow conditions near the south boundary of the WAPS (near compliance well 35) as a result of the elevation of the top of the sand and gravel portion of the UA at this location, continuity of the silt and clay underlying the WAPS, and the presence of drainage features and wetlands south of the unit. A detailed discussion of the hydrogeology of the Site is presented in Section 2 of the HPP WAPS N&E Report.

---

[2] This figure is also provided as Figure 2-10 of the HPP WAPS N&E Report.
[3] This table is also provided as Table 3-1 of the HPP WAPS N&E Report.

4. GEOCHEMICAL SITE CONDITIONS

4.1 Constituent Transport and Fate

As described in Section 2 and the HPP WAPS N&E Report, arsenic, boron, lithium, sulfate, and TDS exceeded the GWPS at the HPP WAPS. These constituents are frequently present and detectable in CCR porewater and groundwater impacted by CCR.

Arsenic speciation in groundwater is dependent on both pH and oxidation/reduction reactions and is typically present as arsenic (III) or arsenic (V) in environmental systems. Arsenic (III) is the predominant species under relatively reducing conditions and, a pH values less than 9 standard units (SU), forms the neutral complex $As(OH)_3$. Arsenic (V) is the predominant species under relatively oxidizing conditions and typically exists as $HAsO_4^{2-}$ at pH values above 7 SU. Arsenic (V) is more likely to be attenuated than neutral arsenic (III) species due to its negative charge and electrostatic interactions with soil/aquifer solids. In general, arsenic has a high sorption affinity for metal (i.e., aluminum, iron, and manganese) oxyhydroxides and may also sorb to clay minerals (Rahman et al. 2019, Nguyen et al. 2021). Arsenic sorption is typically highest at lower pH values where favorable electrostatics enhance attenuation, and also under oxidizing conditions due to the greater propensity for attenuation of the negatively charged $HAsO_4^{2-}$ species relative to neutral $As(OH)_3$ species. Further, the presence of divalent cations (such as calcium [Ca^{2+}]) can promote arsenic (V) absorption (Nguyen et al. 2021).

Boron is primarily present in groundwater as boric acid (H_3BO_3) or borate ($B[OH]^{4-}$) (Bolan et al. 2023). The speciation of boron depends on pH: at pH below 9.2 standard units (SU), H_3BO_3 is the dominant species (NCBI 2024a). Boron is not subject to oxidation/reduction reactions (Lemarchand et al. 2015; Bolan et al. 2023). Boron primarily adsorbs to positively charged sites on solid metal oxide phases, including iron and aluminum oxides (Goldberg and Glaubig 1985; Bolan et al. 2023). Boron sorbs most extensively to amorphous metal oxides between pH 7 SU and 8 SU (Goldberg and Glaubig 1985). Boron can also sorb onto natural organic substances such as humic acids or coal under favorable conditions, most extensively between pH 8 and 10 SU (LeMarchand et al. 2015). Clay minerals have been correlated with boron sorption in soils (Goldberg 1997), with this sorption mechanism presenting an additional potential attenuation mechanism for boron under certain geochemical conditions.

Lithium in solution is typically conservative. Lithium is more hydrated than other similarly charged cations, which reduces its ability to bind to soil colloids (Robinson et al. 2018, Elbana and Osman 2023). Lithium in groundwater may adsorb to iron and manganese oxides and clay minerals, though retention is often weak, and sorption may decrease with increasing lithium concentrations and/or decreasing pH (Robinson et al. 2018, Elbana and Osman 2023; Steinhoefel et al., 2021). However, lithium sorbed to secondary clays may be incorporated deeper into the mineral matrix for more permanent immobilization (Li and Liu, 2020; Steinhoefel et al., 2021).

Sulfate is the primary form of oxidized sulfur (S(VI)) in the environment and is a divalent oxyanion at pH values greater than 2 SU (Stumm and Morgan 1996). Sulfate in groundwater may adsorb onto positively charged sites on solid metal oxide phases, most commonly iron and manganese oxides (Brown et al. 1999). The extent and strength of sulfate adsorption to metal oxide surfaces depends on pH, ionic strength, and oxide surface area available for sorption. Sulfate can also form insoluble complexes such as barite ($BaSO_4$) (NCBI 2024b). Sulfate in groundwater may be reduced to elemental sulfur (S[0]) or sulfide (S[-II]) under sufficiently reducing conditions, a process governed by local microbial communities (Stumm and Morgan 1996). Generally, reduced sulfur is less mobile in groundwater than sulfate. Reduced sulfur readily precipitates as metal sulfides and adsorbs to solid phases such as iron and manganese oxides (Stumm and Morgan 1996).

TDS is a measure of the mass of dissolved material in water, rather than a specific chemical constituent. Individual constituent contributions to TDS depend on both the concentration and molar mass of each contributor. Typically, major ions (i.e., calcium, sodium, magnesium, potassium, chloride, sulfate, and carbonate species) represent the primary contributors to TDS. As such, TDS is often positively correlated with electrical conductivity and ionic strength (Rusydi 2018, Ghalib et al. 2020). TDS concentrations can be reduced by the removal from aqueous phases of the individual constituents that contribute to TDS.

4.2 Site Solids Characterization

Solid phase data were not collected from the CCR source material prior to completion of unit closure with a geomembrane cover system in 2020.

Site solids were characterized to determine the type and abundance of minerals present in the UA, their geochemical properties, and their effect on the aqueous geochemistry of the groundwater system. Solids were characterized using a variety of analytical techniques, the results of which are presented in Tables 1 to 4. Aquifer solids were collected from three locations within the UA adjacent to existing wells in the WAPS monitoring network:

- SB-22, located downgradient of the WAPS to the northeast adjacent to well 22. Solids were collected from two intervals within the UA (26-27 feet below ground surface [ft bgs] and 29-30 ft bgs). Exceedances of boron and lithium above the GWPS were first observed at well 22 during the Q2 and Q3 2023 statistical evaluations, respectively.

- SB-34, adjacent to background well 34, which is unimpacted by the WAPS. Solids were collected from one interval within the UA (32-33 ft bgs).

- SB-51, located downgradient and northwest of the WAPS adjacent to well 51. Solids were collected from one interval within the UA (42-43 ft bgs). An exceedance of arsenic above the GWPS was first observed at well 51 during the Q2 2023 statistical evaluation.

The monitoring well locations are shown in Attachment B. Boring logs for these locations are provided in Attachment D.

4.2.1 Total Organic Carbon, Loss on Ignition, Sulfate, and Sulfide

Total organic carbon (TOC) represents only the carbon component of organic matter within a solid material, while loss on ignition (LOI) represents the combustible portions of a solid material and is often used as an approximation of organic matter in a sample. The TOC and LOI values for aquifer solids from SB-22, SB-34, and SB-51 are presented in Table 1. TOC values range from 0.34 to 4.6 percent weight [% wt] and LOI values vary from 11.6 to 21.5% wt, indicating that the aquifer solids contain a moderate amount of organic matter. Solids adjacent to well 51 generally contained a higher proportion of organic matter compared to wells to the east based on the LOI results.

Sulfate, as measured in solid leachate after HCl digestion, and sulfide, as measured by combustion-infrared absorption after digestion, were also quantified for the aquifer solids. Observed concentrations of sulfate were below detection (0.1%) in the samples (see Table 1). Total sulfide ranged from below the detection limit (0.04%) at SB-22 (26-27 ft bgs) to 0.18% at SB-51. The presence of sulfides may indicate that sulfate reduction is actively occurring, particularly at well 51 which has reducing conditions (as discussed in Subsection 4.3.2). The laboratory analytical results for TOC, LOI, sulfate, and sulfide are available in Attachment E.

4.2.2 Total Metals via Bulk Characterization

Total metals were analyzed to determine the major and trace metal content of the aquifer solids with results presented in Table 2. The laboratory analytical results are available in Attachment E. Arsenic, boron, and lithium were detected in solids adjacent to wells 22, 34 and 51. The solids from SB-22 had the highest arsenic concentrations while solids from SB-34 (background) and SB-51 had comparable arsenic concentrations (though of these two, only well 51 has an arsenic exceedance in groundwater). Lithium and boron concentrations were both highest in the solids from SB-51. Total iron concentrations were relatively low in aquifer solids sampled from the three wells, with values ranging from 9,400 to 14,000 micrograms per gram (µg/g). Similarly, total manganese concentrations were also relatively low, with values ranging from 220 to 350 µg/g. Both iron and manganese were highest in the aquifer solids from SB-51. Aluminum was also present in the solids from the three wells, with the highest value (8,200 µg/g) at SB-51. The presence of these metals (aluminum, iron, and manganese) in the aquifer solids may provide potential attenuation sites for COCs in the form of metal oxyhydroxides.

4.2.3 Sequential Extraction Procedure Analysis of Metals

A sample of composited material from each boring location was submitted to SGS Canada Inc. (Lakefield, ON, CA) for sequential extraction procedure (SEP). SEPs are chemical extractions used to dissolve metals from specific solid-associated phases. SEPs use progressively stronger reagents to solubilize metals from increasingly recalcitrant phases. Although these procedures do not quantitatively identify the specific metal phases in a soil/aquifer matrix, they do provide a means to evaluate the class of solids and relative stability in relation to oxidation/reduction (redox) potential and pH fluctuations (Tessier et al. 1979, Kuo et al. 1983, Sposito et al. 1984, Hickey and Kittrick 1984, Gruebel et al. 1988). Therefore, SEP data are useful to interpret the mechanism and potential reversibility of attenuation processes. The 6-step extraction procedure is briefly described, and the results of the SEP analysis are provided in Table 3 and Attachment F.

Manganese was primarily detected in fractions associated with carbonates, iron and manganese oxides, and residual metals, with lesser amounts bound to organic material. Between 8.8% and 25.5% of the iron extracted from the aquifer solids was associated with metal oxide phases, indicating that iron oxides are present at significant concentrations and may provide potential sorption sites for COCs. Arsenic in aquifer solids from SB-34 (background) and SB-51 were bound to the fraction associated with iron and manganese oxides at similar concentrations (0.8 and 0.9 µg/g [29.6% and 25%], respectively). This suggests that iron and manganese oxides in the solids have some capacity to serve as adsorption sites for arsenic and that arsenic may be naturally present in background. Lithium was only identified in association with the residual fraction, which could indicate incorporation into clay minerals. While boron was largely identified in association with the residual fraction, some portion (6.7 to 16.7%) was also identified in the fraction associated with metal oxides (Table 3). SEP data indicated that there was little association of arsenic, boron, and lithium to organics. Overall, these results suggest some attenuation via interaction with metal oxides may be feasible in the aquifer.

4.2.4 Mineralogical Analysis

X-Ray diffraction (XRD) with Rietveld refinement was conducted for identification of minerals in aquifer solid samples. XRD is an analytical technique that provides information about the identity of the crystalline material within a sample but does not provide information about non-crystalline or amorphous phases. XRD results are normalized to 100% of the total weight, meaning that material not characterized by XRD is ignored in the percent calculation. The four samples analyzed by XRD were determined to be primarily composed of quartz (SiO_2), ranging from 33.1 to 57.0 percent by weight (wt%) of the minerals present (Table 4; Attachment G). The second most abundant mineral was either dolomite (ranging from 11.4 to 14.4 wt% in SB-22) or calcite (11.1 wt% in well 34; 20.9 wt% in SB-51), both of which are carbonate minerals. These results are consistent with the field observations documented in the boring logs provided in Attachment D.

Magnetite, which is a mixed valence iron oxide, was identified in the aquifer solids from 0.2 to 0.5 wt%. Magnetite contains both ferrous (2+) and ferric (3+) forms of iron and is therefore considered to be one of the more stable iron oxide minerals in the environment (Cornell and Schwertmann 2003). Magnetite provides adsorption sites to attenuate constituents in solution. Magnetite concentrations do not correlate well with observations of total iron in the solids (i.e., samples with higher iron concentrations do not necessarily have higher abundances of iron oxides minerals as identified in the XRD results). This may be related to the presence of non-crystalline, amorphous iron oxides that are not detected by XRD (described above), which provide additional adsorption capacity in the aquifer.

The aquifer solids samples also had measurable proportions of kaolinite (0.6 to 3.4%) and chlorite, (1.9 to 6.8%; Table 4). Clay minerals, such as kaolinite and chlorite, provide potential attenuation sites for arsenic, boron, lithium, and/or sulfate due to the presence of surface hydroxyl groups (Goldberg 1997; Lins and Puls, 2002; Mohapatra et al. 2007; Sokolova and Alekseeva 2008; Li and Liu 2020). Chlorite is of particular importance for the attenuation of arsenic, as it is an iron-rich mineral which contains a hydroxide interlayer that provides adsorption sites (Lin and Puls, 2002). Kaolinite, a secondary clay mineral commonly formed during feldspar weathering, provides a particularly strong (i.e., irreversible) sorbing surface for lithium (Li and Liu 2020). Naturally occurring kaolinites tend to be enriched in lithium attenuated from groundwater (Anderson et al. 1989; Pogge von Strandmann et al. 2021; Steinhoefel et al., 2021).

4.3 Aqueous Geochemistry

UA groundwater from wells across the delineation network were analyzed for a range of geochemical parameters and data from October 2012 to November 2023 are presented in Figures 1 through 8. For clarity in interpretation, wells are arranged from east to west in the legends, with a warm (east) to cold (west) color scheme. Concentrations discussed in the following subsections are inclusive of the two most recent years of monitoring data (December 2021 to November 2023). The groundwater data used in the site evaluation are presented in Attachment H.

CCR porewater (i.e., CCR source water) from porewater wells (L4, LPZ-1, LPZ-3, and LPZ-17) distributed across the WAPS were collected April 2017 and analyzed for a range of geochemical parameters. The United States Environmental Protection Agency (USEPA) considers the use of porewater data as the most appropriate approach to estimate constituent fluxes to groundwater from CCR surface impoundments. As per USEPA, “this is because porewater better represents the leachate seeping from the bottom of the impoundment than impoundment water samples” (USEPA 2015). CCR porewater data are presented in Table 5 and discussed in the following subsections.

4.3.1 Exceedance Parameters

Arsenic concentrations in groundwater were consistently below the GWPS of 0.010 milligrams per liter (mg/L) in background wells and compliance wells, with two exceptions, 21R and 51. Arsenic concentrations in exceedance of the GWPS were identified[4] at compliance wells 21R (21R was installed to replace 21; 21 was decommissioned in 2019) and 51 (51 was installed to replace 24; 24 was decommissioned in 2019) (Figure 1). Wells 21R and 51 are located near the northwest corner of the WAPS. Arsenic at well 21R has been elevated post-closure, with concentrations ranging from 0.0210 to 0.0345 mg/L for the last two years of monitoring data (December 2021 to November 2023). Arsenic at well 51 has also been elevated post-closure, with concentrations ranging from 0.0182 to 0.0308 mg/L. The trends at well 51 are consistent with previous arsenic values measured in well 24 prior to decommissioning. Arsenic concentrations at wells 21R and 51 are also consistent with those of porewater wells, which had arsenic concentrations ranging from

---

[4] Using data pooled from both original and replacement wells collected from 2015 onward.

0.0123 to 0.0351 mg/L during the 2017 sampling event. Arsenic concentrations at other wells within the delineation network (including background wells) were low, with concentrations ranging from below detection to 0.0017 mg/L.[5]

Boron concentrations were generally stable or decreased through time across the site (Figure 2). In background wells 32 and 34, boron concentrations were consistently low (between 0.075 and 0.206 mg/L). Boron concentrations at wells 49, 50, and 51 are slightly elevated above background but below the GWPS of 2.0 mg/L during recent events. Exceedances above the GWPS were reported in compliance wells 21R, 22, 23, 35, and 27. Boron at wells 21R, 22, and 27 decreases over time, with values ranging from 0.13 to 4.84 mg/L. The exceedance at monitoring well 27 may be attributed to groundwater flow conditions prior to closure, wherein groundwater was mounded within the WAPS and flowed radially from the unit and migrated to the nearby wetland (Section 2 of the N&E Report). Concentrations at well 23 have an average value of 9.3 mg/L for the previous two years of data. Well 35 has exhibited an increase in boron since closure activities started in 2019, with a range of concentrations (9.58 to 18.1 mg/L) reported over the last two years. Localized post-closure flow conditions at well 35 are likely contributing to the increase in boron. However, once water levels in the WAPS reach equilibrium, concentrations of boron are expected to stabilize and decline in the future. Boron concentrations in porewater wells ranged from 21 to 28 mg/L in 2017. These concentrations suggest that the porewater may be contributing to the stable to increasing boron concentrations observed at wells 23 and 35.

Lithium concentrations remained stable or decreased over time in the wells across the delineation network (Figure 3). Concentrations at background wells 32 and 34 have been consistently low, ranging from 0.0029 to 0.0051 mg/L and 0.0032 to 0.0160 mg/L for wells 32 and 34, respectively. Lithium concentrations across the site have generally been below the GWPS of 0.040 mg/L but elevated relative to background wells, with two exceptions. Lithium exceeds the GWPS at well 22 but exhibits a decreasing trend over time, with concentrations ranging from 0.0419 to 0.0620 mg/L. There was a spike in lithium during the May 2023 sampling event at well 51, but this was not determined to represent an exceedance and all other data points for well 51 are below the lithium GWPS. Lithium concentrations at porewater wells were generally similar to or greater than that of well 22, with reported values ranging from 0.046 to 0.109 mg/L during the 2017 sampling event.

Sulfate concentrations across the site were stable or decreased over time, except in well 35 (Figure 4). In background wells 32 and 34, sulfate concentrations were consistently low (between 45 and 82 mg/L). Exceedances above the sulfate GWPS of 400 mg/L were reported at wells 23 and 35. Sulfate concentrations remained relatively stable in well 23, unlike the increasing boron concentration, ranging from 413 to 471 mg/L. In well 35, sulfate concentrations exhibited an increasing trend post-closure, similar to boron, with variable sulfate concentrations (476 to 1190

---

[5] The apparent spike in arsenic concentrations in most wells (except 21R and 51) during the May 2023 sampling event is a result of the higher detection limit (0.0087 mg/L) that was used during analysis on that date, rather than an increase in arsenic in the groundwater.

mg/L) over the last two years. Other compliance and monitoring wells had sulfate concentrations below the GWPS. Concentrations at these wells were similar to or slightly greater than that of background wells, ranging from 77 to 159 mg/L. Porewater wells exhibited a wide range of sulfate concentrations during the 2017 sampling event (370 to 1270 mg/L), which is generally consistent with the range of concentrations observed at wells 23 and 35.

TDS concentrations across the network were stable over time, with the exception of well 35 (Figure 5). In background wells 32 and 34, TDS concentrations ranged from 514 to 845 mg/L. TDS in well 35 exceeded the GWPS of 1,200 mg/L and has increased following closure activities in 2019. TDS trends in well 35 have a positive and linear correlation with sulfate trends ($R^2 = 0.97$, Figure 6), which indicates that sulfate may be a major contributor to elevated TDS at well 35. Other compliance and monitoring wells had TDS concentrations that were generally within the range of background measurements, though well 23 consistently had TDS concentrations above background but below the GWPS. TDS concentrations at the porewater wells ranged from 768 to 2090 mg/L, which is similar to the range observed at well 35 in the last two years (918 to 1940 mg/L).

4.3.2 Redox/pH Summary

The oxidation-reduction (redox) potential (ORP) and pH in aqueous systems are major controls on the speciation of redox-active chemicals. ORP and pH will affect arsenic and sulfate (COCs for WAPS groundwater) mobility in groundwater and determine the stability of iron and manganese oxyhydroxides.

In wells across the groundwater monitoring network, groundwater pH values have declined since placement of CCR and use of the WAPS ceased in the late 1990s (Figure 7). In recent years, pH values are circumneutral and fairly consistent across the site (ranging between 6.8 to 7.7 standard units [SU]), though compliance wells along the north side of the WAPS tend to have slightly higher pH values than background wells. This may reflect a consistent influence from the pond water, which had reported pH values ranging from 7.6 to 10 SU (Table 5).

Redox conditions vary across the site, with the east side of the WAPS generally exhibiting more oxidizing conditions and the west side exhibiting more reducing conditions (Figure 8). The oxidizing conditions are a result of these wells being located closer to a recharge zone where sand and/or gravel are near the land surface. The presence of a silty, organic-rich deposit on the west side of the WAPS may be creating the observed reducing conditions in that area (EPRI 2002). More reducing conditions exist at compliance wells 21R, 22D, 23, 27, and 51, background well 34, and leachate porewater wells. Reducing conditions at 21R and 51 are consistent with the elevated arsenic concentrations at these wells, which is likely attributed to the lower stability of iron and/or manganese oxyhydroxides and the desorption of arsenic associated with these phases and/or changes in arsenic speciation as discussed in Section 4.3.3.

4.3.3 Pourbaix Diagrams

Eh-pH, or Pourbaix, diagrams can be used to illustrate the predicted stability of specific phases at thermodynamic equilibrium under the conditions observed for a groundwater sample. Select crystalline mineral species were suppressed to be representative of groundwater conditions (e.g., mineral formation not anticipated to be kinetically favored), except when identified in XRD data from solids in the site (e.g., magnetite). Conditions observed at well 21R on 22 August 2023 were used to represent wells with arsenic exceedances, which tend to be more reducing (Table 6). Conditions observed at well 22 on 25 August 2023 were used to represent wells with more oxidizing conditions (Table 6).[6]

Using conditions observed at wells 22 and 21R in August 2023 (Table 6), magnetite is predicted to be stable in the aquifer (Figure 9a and Figure 9b) The predicted stability of magnetite is consistent with XRD analysis which detected magnetite in aquifer solids at abundances ranging between 0.2 and 0.5 wt% (Table 4). When magnetite is suppressed, amorphous iron oxyhydroxides (represented by ferrihydrite) are generally predicted to be stable in the aquifer at locations with oxidizing (Figure 9c) conditions. Iron oxides, whether crystalline or amorphous, may provide potential mineral surfaces for sorption of arsenic, boron, lithium, and/or sulfate within the aquifer. Ankerite, which is represented by siderite in Figures 10a – 10d, may be stable under reducing conditions (Figure 9d), which is consistent with XRD detection of ankerite in aquifer solids at abundances ranging from 1.3 to 6.0 wt%. In general, iron oxyhydroxide minerals appear to be less stable under the more reducing conditions observed in site groundwater and as such, select wells (21R, 23, 34, and 51) may experience dynamic equilibrium conditions in which dissolution and subsequent precipitation of these minerals are more likely occur.

Arsenic is predicted to primarily exist as the arsenic (V) species $HAsO_4^{2-}$ even under reducing aquifer conditions at well 21R (Figure 10), which is a more readily attenuated arsenic (V) species. Under oxidizing conditions, the presence of $HAsO_4^{2-}$ in combination with more stable ferrihydrite suggests the potential for arsenic attenuation via interaction of arsenic (V) species with iron oxides.

A review of Eh-pH conditions for manganese found that solid phase manganese minerals are not predicted to be stable under conditions that exist at the compliance and background wells (Figures 11a and 11b).

4.3.4 Total and Dissolved Iron and Manganese Concentrations

The distribution of iron and manganese between total and dissolved phases can provide insights on site redox conditions and constituent behavior. A comparison of the total and dissolved iron and manganese data for the Q2 and Q3 2023 sampling events is provided in Table 7. Total iron was detected at least once at all sample locations, with values ranging from 0.037 mg/L (well 22, Q2 2023) to 8.5 mg/L (well 21R, Q2 2023). Dissolved iron was detected at 6 of the 11 sample

---

[6] Field ORP measurements were converted to Eh by adding +200 millivolts to correct for the Ag/AgCl electrode.

locations, with values ranging from 0.14 mg/L (well 23, Q3 2023) to 6.8 mg/L (background well 34, Q3 2023). Reducing conditions exist at all six sampling locations that had detectable dissolved iron, indicating that reducing conditions are contributing to dissolved iron in the groundwater. Where dissolved iron was detected, the dissolved concentrations were typically a significant (>50%) portion of the total iron identified. These results align with the findings of the Pourbaix diagrams, which predicted lower ferrihydrite stability at wells with more reducing conditions (Figures 10c and 10d).

Total manganese was detected at all locations analyzed, with reported values ranging from 0.012 mg/L (well 22, Q3 2023) to 1.3 mg/L (background well 34, Q3 2023). Dissolved manganese was detected at 12 of the 13 locations, with values ranging from 0.0044 (well 49, Q3 2023) to 1.3 (background well 34, Q3 2023). Where dissolved manganese was detected, dissolved concentrations as a percent of total concentrations varied widely, from 0 to greater than 100%. This is consistent with the widespread mobilization of manganese to the aqueous phase predicted by the Pourbaix diagrams (Figures 11a and 11b) and the lack of observed crystalline manganese-bearing minerals (like rhodochrosite) across the site (Table 4).

4.3.5 Total and Dissolved Organic Carbon Concentrations

Concentrations of organic carbon in groundwater can provide insights into redox conditions and constituent mobility. A comparison of aqueous TOC and dissolved organic carbon (DOC) concentrations for the Q2 and Q3 2023 sampling events is provided in Table 8. TOC and DOC were detected at all sampling locations during this time period. TOC concentrations ranged from 0.83 mg/L (well 27, Q3 2023) to 8.9 mg/L (well 35, Q2 2023) and DOC ranged from 0.88 mg/L (background well 32, Q3 2023) to 26 mg/L (well 22D, Q3 2023). The silty, organic-rich deposit on the west side of the WAPS likely contributes to higher TOC and DOC concentrations, particularly at well 34 which had higher TOC and DOC concentrations than most wells for both the 2023 Q2 and Q3 sampling events. In most cases, DOC concentrations were greater than or equal to TOC, suggesting that much of the organic carbon in the aquifer is dissolved. The presence of organic carbon can contribute to reducing conditions, which impacts the speciation and mobility of arsenic, iron, and manganese and the reduction of sulfate. Further, DOC can influence arsenic mobility by competing for binding sites on iron oxides, passivating the surface of iron oxides to reduce their reactivity, or serving as a substrate for iron-reducing microbial species, all of which could increase arsenic mobility via reduced attenuation with iron mineral surfaces (Aftabtalab et al. 2022). Wells with arsenic exceedances (51 and 21R) had TOC and DOC concentrations ranging from 1.5 to 3.3 mg/L and 1.6 to 2.6 mg/L (TOC and DOC, respectively), which are similar to that of other wells in the network.

4.3.6 Major Ion Distribution and Groundwater Signatures

A piper diagram was constructed using data from the delineation network and leachate to visualize major ion distributions in UA groundwater. Piper diagrams are a common tool for assessing geochemical similarities or differences between aqueous samples. The major ion distribution is similar for most wells in the delineation network (Figure 12) and is characterized by relatively high contributions of calcium and bicarbonate ions. The relatively high contribution of carbonate species to groundwater composition is consistent with the abundance of carbonate-bearing minerals such as calcite and dolomite in the site solids (Table 4). Wells 23 and 35, which have boron and sulfate exceedances, exhibit a different ion distribution, with higher abundances of sulfate and lower abundances of bicarbonate relative to other wells in the network. The major groundwater composition in wells 23 and 35 is similar to that of the source water samples, which suggests that porewater may have contributed to boron and sulfate exceedances at these wells.

5. LABORATORY ATTENUATION TESTING

The aquifer solids described in Section 4.2 were submitted to SIREM laboratory to test attenuation behavior of arsenic using batch testing. Batch test studies combine soil and groundwater collected from the site to evaluate the sorption and desorption of chemical constituents. The methods and results of batch adsorption testing completed to evaluate attenuation of the arsenic with Site solids is described below. Batch desorption testing was not completed due to the redox sensitivity of arsenic, which contributed to poor recoveries in the batch attenuation testing.

5.1 Batch Attenuation Testing Methods

Aquifer solids from boring SB-34 and groundwater from well 51 were used for the batch attenuation tests. Test bottles (referred to as a microcosm) were constructed with five soil to water ratios (Table 9). The groundwater added to the microcosms was spiked with sodium arsenite to a target concentration of 0.1 mg/L arsenic, and the sample bottles were allowed to tumble for seven days. An initial sample of the stock solution was collected on Day 0 and a control sample (i.e., MW-51 groundwater with no aquifer solids) was collected on Day 7 following tumbling to evaluate any less to interactions with the bottleware or ambient conditions. Duplicates were constructed for each microcosm, including the control sample.

After seven days of contact time, an aliquot of the free liquid was collected and filtered through a 0.45-micron filter prior to analysis for dissolved arsenic. Analysis of the dissolved phase is important to adequately measure the partitioning of mass between the solid and liquid fractions of the experiment. The redox and pH were measured for each batch test at the beginning and end of the contact period and in the control samples.

5.2 Batch Attenuation Testing Results

While pH between the initial and final control samples remained consistent, ORP increased from -136 mV to -58 mV, suggesting a slight oxidation of the sample bottles during the experimental period. pH and redox results were generally consistent between the control and test samples, except for the 1:1 soil:water ratio microcosms which had a significantly lower ORP recorded (Table 9). The cause of the anomalously low ORP values for this soil:water ratio is not immediately apparent. The recovery of arsenic in the control samples was approximately 58% of the initial total, with the loss of aqueous arsenic likely associated with the observed change in redox conditions in the control.

While interpretation of the data is limited by the poor recovery in the control samples, the data obtained from the tests (Table 9) were used to construct 5-point isotherms for arsenic by averaging duplicate results for each soil:solution ratio. Mathematical fitting was used to calculate the attenuation distribution coefficients (K_d), assuming linear adsorption. The linear adsorption equation was used:

$$q_e = K_d \times C_e \qquad \text{Eq. 1}$$

where q_e is the mass of constituent adsorbed to the solid phase at equilibrium, C_e is the remaining aqueous constituent concentration at equilibrium, and K_d is the linear sorption coefficient (reported in liters per kilogram [L/kg]). The linear data output is provided as Figure 13.

The data were also fitted to a non-linear Langmuir isotherm:

$$q_e = \frac{q_m K_L C_e}{1 + K_L C_e} \qquad \text{Eq. 2}$$

where q_m is the inverse of the slope and K_L is the Langmuir distribution coefficient. The adsorption data were linearized according to:

$$\frac{C_e}{q_e} = \frac{1}{(K_L \times q_m)} + \frac{C_e}{q_m} \qquad \text{Eq. 3}$$

A common non-linear Freundlich equation was also used:

$$q_e = K_F (C_e)^{1/n} \qquad \text{Eq. 4}$$

where q_e is the mass of constituent adsorbed to the solid phase at equilibrium, C_e is the remaining aqueous constituent concentration at equilibrium, K_F is the Freundlich distribution coefficient, and *1/n* is a non-linearity constant. The adsorption data were plotted as log-transformed values to perform the non-linear isotherm fitting using the linearized Freundlich equation:

$$log(q_e) = \log(K_F) + (1/n)\log(C_e) \qquad \text{Eq. 5}$$

The calculated linear, Langmuir, and Freundlich distribution coefficients (K_d, K_L, and K_F, respectively) and 1/*n* values are shown in Table 10.

The linear K_d of 36.4 L/kg was selected for well 51 based on its goodness-of-fit ($R^2 = 0.69$) and compatibility with values reported in literature (which range from several orders of magnitude from 1 to 1×10^5; USEPA 2005). As noted above, the calculated K_d may be influenced by the loss of arsenic in the control solution; the batch attenuation results instead may serve as a proof of concept for the attenuation of arsenic in the system in lieu of a more quantitative measurement.

6. GEOCHEMICAL CONCEPTUAL SITE MODEL

6.1 Source and Mobilization Mechanisms

Arsenic, boron, sulfate, and lithium are naturally present in coal deposits and are concentrated within CCR. Sulfate may also be present in CCR as a byproduct of flue gas desulphurization. Arsenic, boron, and lithium were detected within UA aquifer solids from compliance and background wells, although groundwater concentrations of these constituents in background wells consistently do not exceed GWPSs. Arsenic, boron, sulfate, and lithium all exhibited elevated concentration in CCR porewater at the time of collection (2017). While naturally occurring sources of arsenic, boron, and lithium are present in the UA as supported by solid phase characterization of background material, the primary source of these constituents, as well as sulfate, in the UA is expected to be the WAPS CCR porewater. The elevated concentrations of sulfate are a major contributor to the exceedance of TDS identified at well 35.

6.2 Potential Attenuation Mechanisms

Arsenic is predicted to exist primarily as the arsenic (V) species $HAsO_4^{2-}$ which has a high affinity for metal (hydr)oxides. Neutral arsenic (III) species $As(OH)_3$ may also be present in the UA, particularly under reducing conditions. Boron is anticipated to largely be present as the neutral H_3BO_3 species, as groundwater pH values are below the pK_a for boric acid (9.2 SU). The presence of iron oxides in aquifer solids (Table 4) suggests that a portion of the arsenic, boron, lithium, and/or sulfate in the groundwater could be attenuated via surface (inner- and outer-sphere) complexation reactions. Aluminum and manganese oxyhydroxides, clay minerals, and calcite (Table 4) in the aquifer solids may also serve as sorption sites for arsenic, boron, lithium, and/or sulfate (Goldberg 1997, Sokolova and Alekseeva 2008, Robinson et al. 2018, Rahman et al. 2019, Nguyen et al. 2021, Elbana and Osman 2023). This suggests that attenuation of these constituents via sorption mechanisms is possible, though it will be dependent on speciation, redox conditions, and pH in the UA. In addition, bioremediation of sulfate (via microbial sulfate reduction) may naturally occur in the UA under reducing conditions. Attenuation of sulfate will likely contribute to a reduction of TDS in the groundwater.

7. REFERENCES

Aftabtalab, A, J Rinklebe, S M Shaheen, N K Niazi, E Moreno-Jiménez, J Schaller, K-H K. 2022. “Review on the Interactions of Arsenic, Iron (Oxy)(hydr)oxides, and Dissolved Organic Matter in Soils, Sediments, and Groundwater in a Ternary System.” Chemosphere 286(2), 131790.

Anderson, M. A., Bertsch, P. M., & Miller, W. P. 1989. “Exchange and Apparent Fixation of Lithium in Selected Soils and Clay Minerals”. Soil Science, 148(1), 46–52.

Bolan, S, H Wijesekara, D Amarasiri, T Zhang, P Ragályi, M Brdar-Jokanović, M Rékási, J Lin, L Padhye, H Zhao, L Wang, J Rinklebe, H Wang, K Siddique, M Kirkhamn, N Bolan. 2023. "Boron Contamination and its Risk Management in Terrestrial and Aquatic Environmental Settings”. Sci. Total Environ. 164744.

Brown, G E J, V Henrich, W Casey, D Clark, C Eggleston, A Felmy, D W Goodman, M Gratzel, G Maciel, M I McCarthy, K H Nealson, D Sverjensky, M Toney, J M Zachara. 1999. “Metal Oxide Surfaces and Their Interactions with Aqueous Solutions and Microbial Organisms”. Chem Rev. 99, 77-174.

Cornell, R M, and U Schwertmann. 2003. “The Iron Oxides: Structure, Properties, Reactions, Occurrences, and Uses." Wiley-VCH Verlag GmbH, Weinheim.

Elbana, T A, and M A Osman. 2023. “Lithium Sorption/Desorption in Some Alkaline Soils: Modeling of the Kinetics Behavior.” Water Air Soil Poll. 234, 33.

Electric Power Research Institute (EPRI). 2002. “Manganese Occurrence Near Three Coal Ash Impoundments in Illinois”. Report 1005257.

Ghalib, H B, M B Yaqoob, A M Al-Abadi. 2020. “Assessment of the Groundwater at Ali Al-Garbi Area, Iraq using Geochemical Modeling and Environmental Isotopes.” Desalination Water Treat. 176, 114-122.

Goldberg, S. 1997. “Reactions of Boron with Soils.” Plant and Soil 193, 35-48.

Goldberg, S. and Glaubig, R.A. 1985. “Boron Adsorption on Aluminum and Iron Oxide Minerals.” Soil Sci. Soc. Am. J. 49: 1374-1379.

Gruebel, K A, J A Davies, and J O Leckie. 1988. “The Feasibility of Using Sequential Extraction Techniques for Arsenic and Selenium in Soils and Sediments.” Soil Sci. Soc. Am. J. 52, 390-397.

Hickey, M G, and J A Kittrick. 1984. “Chemical Partitioning of Cadmium, Copper, Nickel, and Zinc in Soils and Sediments Containing High Levels of Heavy Metals.” J. Environ. Qual. 13, 372-376.

IEPA. 2023. "Hennepin Power Plan West Ash Pond System; W1550100002-01 & 03, Alternative Source Demonstration (ASD) Submittal." Letter from Michael Summers (Illinois Environmental Protection Agency) to Phil Morris (Dynegy Midwest Generation, LLC). December 7.

Kuo, S, P E Heilman, and A S Baker. 1983. "Distribution and Forms of Copper, Zinc, Cadmium, Iron, and Manganese in Soils Near a Copper Smelter." Soil Sci. 135, 101-109.

Lemarchand, D, A D Jacobson, D Cividini, and F Chabaux. 2015. "The Major Ion, 87Sr/86Sr, and d11B Geochemistry of Groundwater in the Wyodak-Anderson Coal Bed Aquifer (Powder River Basin, Wyoming, USA)". Comptes Rendus Geoscience 347, 348-357.

Li W. and Liu X.-M. 2020. "Experimental investigation of lithium isotope fractionation during kaolinite adsorption: Implications for chemical weathering." Geochim Cosmochim Acta**,** 284, 156–172.

Lin, Z., Puls, R. 2000. "Adsorption, desorption and oxidation of arsenic affected by clay minerals and aging process". Environmental Geology 39, 753-759.

Mohapatra, D, D Mishra, G R Chaudhury, R P Das. 2007. "Arsenic(V) Adsorption Mechanism Using Kaolinite, Montmorillonite, and Illite from Aqueous Medium." J. Environ. Sci. Health A. 42(4), 453-469.

National Center for Biotechnology Information (NCBI). 2024a. PubChem Compound Summary for CID 7628, Boric Acid. https://pubchem.ncbi.nlm.nih.gov/compound/Boric-Acid. Accessed Mar. 19, 2024.

National Center for Biotechnology Information (NCBI). 2024b. PubChem Compound Summary for CID 24414, Barium Sulfate. https://pubchem.ncbi.nlm.nih.gov/compound/Barium-Sulfate. Accessed Mar. 19, 2024.

Nguyen, K T, M B Ahmed, A Mojiri, Y Huang, J L Zhou, and D Li. 2021. "Advances in As Contamination and Adsorption in Soil for Effective Management." J. Environ. Manage. 295, 113274.

NRT. 2017 "Hydrogeologic Site Characterization Report – Hennepin West Ash Pond System." December.

NRT. 2018. "Groundwater Management Zone Application Revision 1 – Hennepin West Ash Pond System." May.

OBG. 2017. "Hydrogeologic Monitoring Plan – Hennepin West Ash Pond System." Hennepin Power Station, Hennepin, Illinois. October.

Pogge von Strandmann, P. A. E., Burton, K. W., Opfergelt, S., Genson, B., Guicharnaud, R. A., & Gislason, S. R. 2021. "The lithium isotope response to the variable weathering of soils in Iceland." Geochimica et Cosmochimica Acta, 313, 55–73

Rahman, M S, M W Clark, L H Yee, M J Comarmond, T E Payne, and E D Burton. 2019. "Effects of pH, Competing Ions and Aging on Arsenic(V) Sorption and Isotopic Exchange in Contaminated Soils." Appl. Geochem. 105, 114-124.

Ramboll Americas Engineering Solutions, Inc. (Ramboll). 2021. "Addendum to the Groundwater Monitoring Plan, West Ash Pond System, Hennepin Power Plant, Hennepin, Illinois." October

Ramboll Americas Engineering Solutions, Inc. (Ramboll). 2023. "35 I.A.C. § 845.640(E): Alternative Source Demonstration. West Ash Pond System, Hennepin Power Plant, Hennepin, Illinois." November.

Robinson, B H, R Yalamanchali, R Reiser, and N M Dickinson. 2018. "Lithium as an Emerging Environmental Contaminant: Mobility in the Soil-plant System." Chemosphere 197, 1-6.

Rusydi, A. 2018. "Correlation Between Conductivity and Total Dissolved Solids in Various Types of Water: A Review." IOP Conference Series: Earth and Environmental Science. 118, 012019.

Sokolova, T A, and A S Alekseeva. 2008. "Adsorption of Sulfate Ions by Soils (A Review)." Eurasian Soil Sci. 41(2), 140-148.

Sposito, G, C S LeVesque, J P LeClaire, and N Senesi. 1984. "Methodologies to Predict the Mobility and Availability of Hazardous Metals in Sludge-Amended Soils." California Water Resource Center. University of California, Davis, CA.

Steinhoefel G., Brantley S. L. and Fantle M. S. 2021. "Lithium isotopic fractionation during weathering and erosion of shale." Geochim Cosmochim Acta, 295, 155–177.

Stumm, W, J J Morgan. 1996. Aquatic Chemistry: Chemical Equilibria and Rates in Natural Waters, 3rd ed. Wiley-Interscience. New York, NY.

Tessier A, P G C Campbell, and M Bisson, 1979. "Sequential Extraction Procedures for the Speciation of Particulate Trace Metals." Anal. Chem. 51(7), 844-851.

USEPA. 2005. "Partition Coefficients for Metals in Surface Water, Soil, and Waste". EPA/600/R-05/074. United States Environmental Protection Agency. July.

USEPA. 2015. Federal Register, Vol. 80, No. 74, Rules and Regulations, April 17, 2015.

TABLES

Table 1 - Total Organic Carbon, Loss on Ignition, Sulfate, and Sulfide in Aquifer Solids
Geochemical Conceptual Site Model
Hennepin West Ash Pond System, Illinois

Field Boring Location	**SB-22**		**SB-34**	**SB-51**
Sample Depth (ft bgs)	**26-27**	**29-30**	**32-33**	**42-43**
Location	**Downgradient**		**Background**	**Downgradient**
Sample Collection Date	**4-Mar-21**	**4-Mar-21**	**4-Mar-21**	**4-Mar-21**
Field Boring Description	**Fine sand**	**Gravel with sand and trace clay**	**Fine-medium sand**	**Silty clay with trace sand**
TOC %	0.34	4.6	1.9	3.6
LOI %	11.6	15.3	13.3	21.5
Sulfate (%)	< 0.1	< 0.1	< 0.1	< 0.1
Sulfide (%)	< 0.04	0.06	0.09	0.18

Notes

Sample depth is shown in feet below ground surface (ft bgs)
TOC - total organic carbon
LOI - loss on ignition
Non-detects are shown as less than the reporting limit.

Table 2 - Bulk Characterization of Aquifer Solids
Geochemical Conceptual Site Model
Hennepin West Ash Pond System, Illinois

Field Boring Location	**SB-22**		**SB-34**	**SB-51**
Sample Depth (ft bgs)	**26-27**	**29-30**	**32-33**	**42-43**
Location	**Downgradient**		**Background**	**Downgradient**
Sample Collection Date	**4-Mar-21**	**4-Mar-21**	**4-Mar-21**	**4-Mar-21**
Field Boring Description	**Fine sand**	**Gravel with sand and trace clay**	**Fine-medium sand**	**Silty clay with trace sand**
Aluminum	2800	3700	5000	8200
Antimony	< 0.8	< 0.8	< 0.8	< 0.8
Arsenic	5.1	8.4	2.7	3.5
Barium	20	31	47	84
Beryllium	0.20	0.87	0.29	0.50
Bismuth	0.13	0.26	0.23	0.59
Boron	6	7	5	10
Cadmium	0.76	2.9	0.53	0.89
Calcium	56000	36000	52000	91000
Chromium	79	130	45	27
Cobalt	5.2	9.8	6.9	9.3
Copper	11	25	8	14
Iron	9400	12000	10000	14000
Lead	7.7	28	6.1	11
Lithium	4	6	6	12
Magnesium	21000	16000	13000	15000
Manganese	310	220	260	350
Molybdenum	3.1	5.0	0.9	2.0
Nickel	15	43	12	19
Potassium	910	1200	1200	1900
Phosphorous	350	330	380	430
Selenium	< 0.7	0.8	< 0.7	1.1
Silicon	5400	1600	7200	4500
Silver	< 0.05	0.08	< 0.05	0.06
Sodium	190	160	180	170
Thallium	0.13	0.26	0.16	0.25
Tin	< 0.5	0.5	1.1	0.6
Tungsten	0.07	0.10	0.06	0.05
Uranium	1.3	1.8	0.65	1.2
Vanadium	17	41	12	18
Yttrium	6.1	7.6	5.7	8.0
Zinc	46	91	40	67

Notes

Sample depth is shown in feet below ground surface (ft bgs)

All results are shown in µg/g (microgram per gram).

Total metals samples prepared via method SW 3050 and analyzed via USEPA method 6020A.

Non-detect results are shown as less than the reporting limit.

Table 3 - SEP Analysis of Aquifer Solids
Geochemical Conceptual Site Model
Hennepin West Ash pond System, Illinois

Field Boring Location			**SB-22**				**SB-34**		**SB-51**	
Sample Depth (ft bgs)			**26-27**		**29-30**		**32-33**		**42-43**	
Location			**Downgradient**				**Background**		**Downgradient**	
Sample Collection Date			**4-Mar-21**		**4-Mar-21**		**4-Mar-21**		**4-Mar-21**	
Field Boring Description			**Fine sand**		**Gravel with sand and trace clay**		**Fine-medium sand**		**Silty clay with trace sand**	
Fraction	**Reagent**	**Arsenic SEP**	µg/g	% of Total	µg/g	% of Total	µg/g	% of Total	µg/g	% of Total
1	Deionized Water	Water Soluble Metals	< 0.5	-	< 0.5	-	< 0.5	-	< 0.5	-
2	$MgCl_2$	Exchangeable Metals	< 0.5	-	< 0.5	-	< 0.5	-	< 0.5	-
3	Sodium acetate, acetic acid	Metals Bound to Carbonates	< 0.5	-	< 0.5	-	< 0.5	-	< 0.5	-
4	Hydroxylamine HCl and acetic acid	Metals Bound to Fe and Mn Oxides	< 0.5	-	< 0.5	-	0.8	29.6%	0.9	25.0%
5	HNO_3, H_2O_2, and ammonium acetate	Bound to Organic Material	< 0.5	-	< 0.5	-	< 0.5	-	< 0.5	-
6	HNO_3, HCl, and HF	Residual Metals	3.9	100%	6.6	100%	1.9	70.4%	2.7	75.0%
SEP Total			**3.9**	-	**6.6**	**-**	**2.7**	**-**	**3.6**	-
Fraction	**Reagent**	**Boron SEP**	µg/g	% of Total	µg/g	% of Total	µg/g	% of Total	µg/g	% of Total
1	Deionized Water	Water Soluble Metals	< 1	-	1	4.5%	< 1	-	1	3.3%
2	$MgCl_2$	Exchangeable Metals	< 1	-	< 1	-	< 1	-	< 1	-
3	Sodium acetate, acetic acid	Metals Bound to Carbonates	< 1	-	1	4.5%	< 1	-	< 1	-
4	Hydroxylamine HCl and acetic acid	Metals Bound to Fe and Mn Oxides	2	16.7%	2	9.1%	1	7.1%	2	6.7%
5	HNO_3, H_2O_2, and ammonium acetate	Bound to Organic Material	< 1	-	< 1	-	< 1	-	1	3.3%
6	HNO_3, HCl, and HF	Residual Metals	10	83.3%	18	81.8%	13	92.9%	26	86.7%
SEP Total			**12**	-	**22**	**-**	**14**	**-**	**30**	-
Fraction	**Reagent**	**Lithium SEP**	µg/g	% of Total	µg/g	% of Total	µg/g	% of Total	µg/g	% of Total
1	Deionized Water	Water Soluble Metals	< 2	-	< 2	-	< 2	-	< 2	-
2	$MgCl_2$	Exchangeable Metals	< 2	-	< 2	-	< 2	-	< 2	-
3	Sodium acetate, acetic acid	Metals Bound to Carbonates	< 2	-	< 2	-	< 2	-	< 2	-
4	Hydroxylamine HCl and acetic acid	Metals Bound to Fe and Mn Oxides	< 2	-	< 2	-	< 2	-	< 2	-
5	HNO_3, H_2O_2, and ammonium acetate	Bound to Organic Material	< 2	-	< 2	-	< 2	-	< 2	-
6	HNO_3, HCl, and HF	Residual Metals	5	100%	13	100%	11	100%	18	100%
SEP Total			**5**	-	**13**	**-**	**11**	**-**	**18**	-

Table 3 - SEP Analysis of Aquifer Solids
Geochemical Conceptual Site Model
Hennepin West Ash Pond System, Illinois

Field Boring Location			**SB-22**				**SB-34**		**SB-51**	
Sample Depth (ft bgs)			**26-27**		**29-30**		**32-33**		**42-43**	
Location			**Downgradient**				**Background**		**Downgradient**	
Sample Collection Date			**4-Mar-21**		**4-Mar-21**		**4-Mar-21**		**4-Mar-21**	
Field Boring Description			**Fine sand**		**Gravel with sand and trace clay**		**Fine-medium sand**		**Silty clay with trace sand**	
Fraction	**Reagent**	**Aluminum SEP**	µg/g	% of Total	µg/g	% of Total	µg/g	% of Total	µg/g	% of Total
1	Deionized Water	Water Soluble Metals	32	0.2%	310	1.7%	120	0.5%	140	0.6%
2	$MgCl_2$	Exchangeable Metals	<1	-	3	0.0%	3	0.0%	4	0.0%
3	Sodium acetate, acetic acid	Metals Bound to Carbonates	28	0.2%	6	0.0%	5	0.0%	2	0.0%
4	Hydroxylamine HCl and acetic acid	Metals Bound to Fe and Mn Oxides	270	1.9%	230	1.3%	270	1.2%	320	1.3%
5	HNO_3, H_2O_2, and ammonium acetate	Bound to Organic Material	150	1.0%	630	3.5%	77	0.3%	120	0.5%
6	HNO_3, HCl, and HF	Residual Metals	14,000	96.7%	17,000	93.5%	22,000	97.9%	24,000	97.6%
SEP Total			**14,480**	-	**18,179**	-	**22,475**	-	**24,586**	-
Fraction	**Reagent**	**Iron SEP**	µg/g	% of Total	µg/g	% of Total	µg/g	% of Total	µg/g	% of Total
1	Deionized Water	Water Soluble Metals	22	0.2%	310	2.5%	72	0.6%	68	0.4%
2	$MgCl_2$	Exchangeable Metals	< 1	-	2	0.0%	5	0.0%	6	0.0%
3	Sodium acetate, acetic acid	Metals Bound to Carbonates	41	0.4%	32	0.3%	8	0.1%	4	0.0%
4	Hydroxylamine HCl and acetic acid	Metals Bound to Fe and Mn Oxides	1,600	15.7%	1,100	8.8%	3,100	25.5%	2,500	14.9%
5	HNO_3, H_2O_2, and ammonium acetate	Bound to Organic Material	34	0.3%	1,100	8.8%	170	1.4%	180	1.1%
6	HNO_3, HCl, and HF	Residual Metals	8,500	83.4%	10,000	79.7%	8,800	72.4%	14,000	83.5%
SEP Total			**10,197**	-	**12,544**	-	**12,155**	-	**16,758**	-
Fraction	**Reagent**	**Manganese SEP**	µg/g	% of Total	µg/g	% of Total	µg/g	% of Total	µg/g	% of Total
1	Deionized Water	Water Soluble Metals	0.5	0.2%	4.0	1.8%	1.4	0.5%	1.3	0.4%
2	$MgCl_2$	Exchangeable Metals	1.5	0.5%	17	7.7%	6.5	2.4%	8.5	2.4%
3	Sodium acetate, acetic acid	Metals Bound to Carbonates	140	47.4%	69	31.4%	78	29.0%	74	20.8%
4	Hydroxylamine HCl and acetic acid	Metals Bound to Fe and Mn Oxides	90	30.5%	65	29.5%	110	40.9%	170	47.7%
5	HNO_3, H_2O_2, and ammonium acetate	Bound to Organic Material	3.5	1.2%	11	5.0%	5.1	1.9%	7.5	2.1%
6	HNO_3, HCl, and HF	Residual Metals	60	20.3%	54	24.5%	68	25.3%	95	26.7%
SEP Total			**296**	-	**220**	-	**269**	-	**356**	-

Notes
Sample depth is shown in feet below ground surface (ft bgs)
Non-detect values are shown as less than the detection limit
SEP - sequential extraction procedure
µg/g - microgram per gram

Table 4 - XRD Analysis of Aquifer Solids
Geochemical Conceptual Site Model
Hennepin West Ash Pond System, Illinois

Field Boring Location			**SB-22**		**SB-34**	**SB-51**
Sample Depth (ft bgs)			**26-27**	**29-30**	**32-33**	**42-43**
Location			**Downgradient**		**Background**	**Downgradient**
Sample Collection Date			**4-Mar-21**	**4-Mar-21**	**4-Mar-21**	**4-Mar-21**
Field Boring Description			**Fine sand**	**Gravel with sand and trace clay**	**Fine-medium sand**	**Silty clay with trace sand**
Mineral/Compound	**Formula**	**Mineral Type**	**(wt %)**	**(wt %)**	**(wt %)**	**(wt %)**
Quartz	SiO_2	Silicate	57.0	54.5	53.0	33.1
Calcite	$CaCO_3$	Carbonate	7.2	3.3	11.1	20.9
Albite	$NaAlSi_3O_8$	Feldspar	7.3	9.8	7.1	6.6
Muscovite	$KAl_2(AlSi_3O_{10})(OH)_2$	Mica	2.1	7.4	7.9	12.5
Dolomite	$CaMg(CO_3)_2$	Carbonate	14.4	11.4	2.6	5.0
Microcline	$KAlSi_3O_8$	Feldspar	5.2	5.2	5.1	9.8
Ankerite	$CaFe(CO_3)_2$	Carbonate	2.9	2.8	6.0	1.3
Actinolite	$Ca_2(Mg,Fe)_5Si_8O_{22}(OH)_2$	Amphibole	0.8	ND	ND	ND
Magnetite	Fe_3O_4	Oxide	0.5	0.4	0.4	0.2
Kaolinite	$Al_2Si_2O_5(OH)_4$	Clay	0.6	2.5	3.4	3.4
Chlorite	$(Fe,(Mg,Mn)_5,Al)(Si_3Al)O_{10}(OH)_8$	Clay	1.9	2.7	3.4	6.8
Pyrite	FeS_2	Sulfide	ND	ND	0.2	0.3

Notes

Sample depth is shown in feet below ground surface (ft bgs)
wt % - percentage by weight
ND - not detected in the sample

Table 5 - Porewater Geochemistry Results
Geochemical Conceptual Site Model
Hennepin West Ash Pond System, Illinois

Porewater Well Location		**L4**	**LPZ-1**	**LPZ-3**	**LPZ-17**
Sample Collection Date		**25-Apr-17**	**25-Apr-17**	**25-Apr-17**	**25-Apr-17**
Parameter	**Units**				
pH	SU	7.6	9.1	10	10
Turbidity	NTU	< 1.0	5.6	< 1.0	28
Oxidation Reduction Potential	mV	-149	-177	-87.0	-163
Carbonate Alkalinity	mg/L $CaCO_3$	0	84	52	80
Bicarbonate Alkalinity	mg/L $CaCO_3$	316	0	0	0
Total Dissolved Solids	mg/L	900	1600	768	2090
Sulfate	mg/L	370	926	375	1270
Fluoride	mg/L	0.28	< 0.10	< 0.10	< 0.10
Chloride	mg/L	10	39	7	< 5
Calcium	mg/L	190	370	214	578
Magnesium	mg/L	27	8.5	0.96	1.3
Potassium	mg/L	9.3	46	13	27
Sodium	mg/L	58	65	7.4	16
Arsenic	µg/L	35	31	12	27
Barium	µg/L	51	60	25	92
Boron	mg/L	21	28	22	27
Cadmium	µg/L	< 1.0	< 1.0	< 1.0	< 1.0
Chromium	µg/L	< 1.0	2.1	32	4
Lead	µg/L	< 1.0	1.2	8.9	7.7
Lithium	µg/L	46	109	52	98
Molybdenum	µg/L	78	3400	264	289
Selenium	µg/L	1.4	8.6	112	118

Notes

mg/L - milligram per liter
mV - millivolts
NTU - nephelometric turbidity units
SU - standard units
µg/L - microgram per liter

Table 6 - Eh-pH Diagram Inputs
Geochemical Conceptual Site Model
Hennepin West Ash Pond System, Illinois

Well ID		**21R**	**22**
Sample Collection Date		**22-Aug-23**	**25-Aug-23**
Input Parameter	**Units**		
pH	SU	7.51	7.67
Arsenic	mg/L	0.0230	0.0002
Bicarbonate Alkalinity	mg/L $CaCO_3$	370	240
Calcium	mg/L	120	23
Chloride	mg/L	95	89
Iron	mg/L	7.90	0.07
Magnesium	mg/L	39	7
Manganese	mg/L	0.14	0.012
Sodium	mg/L	45	12
Sulfate	mg/L	94	120
Temperature	℃	16.6	16.1

Notes

mg/L - milligram per liter
SU - standard units

Table 7 - Total and Dissolved Aqueous Iron and Manganese Results
Geochemical Conceptual Site Model
Hennepin West Ash Pond System, Illinois

Well ID	Well Classification	General Redox Condition	Date	Dissolved Iron (mg/L)	Total Iron (mg/L)	Dissolved Manganese (mg/L)	Total Manganese (mg/L)
50	Downgradient	Oxidizing	31-May-23	< 0.02	0.11	0.18	0.28
			25-Aug-23	< 0.047	0.27	0.27	0.052
22	Downgradient	Oxidizing	31-May-23	< 0.02	0.037	0.034	0.051
			25-Aug-23	< 0.047	0.070	0.036	0.012
22D	Downgradient	Reducing	31-May-23	1.9	2.4	0.065	0.070
			22-Aug-23	2.2	2.3	0.065	0.063
49	Downgradient	Oxidizing	31-May-23	< 0.02	0.91	0.0045	0.57
			25-Aug-23	< 0.047	0.22	0.0044	0.049
35	Downgradient	Oxidizing	31-May-23	< 0.02	0.054	0.57	0.76
			24-Aug-23	< 0.047	< 0.047	0.50	0.52
23	Downgradient	Reducing	31-May-23	0.15	0.21	1.2	1.2
			22-Aug-23	0.14	0.21	1.1	1.1
51	Downgradient	Reducing	31-May-23	6.5	7.8	0.17	0.20
			22-Aug-23	6.1	6.7	0.15	0.15
21R	Downgradient	Reducing	31-May-23	5.6	8.5	0.11	0.16
			22-Aug-23	5.4	7.9	0.11	0.14
27	Downgradient	Reducing	31-May-23	0.26	0.53	0.66	0.68
			24-Aug-23	0.21	0.24	0.66	0.67
32	Background	Oxidizing	31-May-23	< 0.02	0.30	0.050	0.10
			22-Aug-23	< 0.047	0.11	0.092	0.11
34	Background	Reducing	31-May-23	4.9	6.2	1.2	1.1
			25-Aug-23	6.8	6.7	1.3	1.3

Notes

Non-detect values are shown as less than the reporting limit
mg/L - milligrams per liter

Table 8 - Total and Dissolved Organic Carbon Results
Geochemical Conceptual Site Model
Hennepin West Ash Pond System, Illinois

Well ID	Well Classification	General Redox Condition	Date	Dissolved Organic Carbon (mg/L)	Total Organic Carbon (mg/L)
50	Downgradient	Oxidizing	31-May-23	1.8	1.2
			25-Aug-23	1.7	1.4
22	Downgradient	Oxidizing	31-May-23	3.1	3.1
			25-Aug-23	1.5	1.4
22D	Downgradient	Reducing	31-May-23	2.4	2.4
			22-Aug-23	26	0.97
49	Downgradient	Oxidizing	31-May-23	1.6	1.2
			25-Aug-23	1.1	5.1
35	Downgradient	Oxidizing	31-May-23	1.9	8.9
			24-Aug-23	1.4	1.2
23	Downgradient	Reducing	31-May-23	1.6	3.2
			22-Aug-23	6.0	1.0
51	Downgradient	Reducing	31-May-23	1.6	1.5
			22-Aug-23	2.2	2.5
21R	Downgradient	Reducing	31-May-23	2.4	3.3
			22-Aug-23	2.6	1.7
27	Downgradient	Reducing	31-May-23	1.4	1.4
			24-Aug-23	2.1	0.83
32	Background	Oxidizing	31-May-23	1.0	1.0
			22-Aug-23	0.88	0.94
34	Background	Reducing	31-May-23	4.6	4.6
			25-Aug-23	5.3	6.1

Notes

Non-detect values are shown as less than the reporting limit

mg/L - milligrams per liter

Table 9 - Batch Attenuation Results
Geochemical Coneptual Site Model
Hennepin West Ash Pond System, Illinois

Groundwater Sample ID	Geologic Material	Treatment	Date	Day	Replicate	Dissolved Arsenic	pH	ORP
						mg/L	SU	mV
MW-51	--	Water Only Control	17-Oct-22	0				
					MW-51-1	0.10	6.90	-149
					MW-51-2	0.093	6.82	-122
					Average Result	**0.10**	**6.9**	**-136**
			24-Oct-22	7	MW-51-1	0.057	6.85	-61
					MW-51-2	0.059	6.89	-55
					Average Result	**0.058**	**6.9**	**-58**
	SB-34 32-33'	2:1 Soil:Water Ratio	17-Oct-22	0				
			24-Oct-22	7	SB-34 32-33':MW-51 2:1-1	0.0040	6.81	-2
					SB-34 32-33':MW-51 2:1-2	0.0030	6.78	6
					Average Result	**0.0035**	**6.8**	**2**
		1:1 Soil:Water Ratio	17-Oct-22	0				
			24-Oct-22	7	SB-34 32-33':MW-51 1:1-1	0.0090	6.79	-278
					SB-34 32-33':MW-51 1:1-2	0.0090	6.77	-179
					Average Result	**0.0090**	**6.8**	**-229**
		1:5 Soil:Water Ratio	17-Oct-22	0				
			24-Oct-22	7	SB-34 32-33':MW-51 1:5-1	0.035	6.84	-9
					SB-34 32-33':MW-51 1:5-2	0.033	6.88	-15
					Average Result	**0.034**	**6.9**	**-12**
		1:10 Soil:Water Ratio	17-Oct-22	0				
			24-Oct-22	7	SB-34 32-33':MW-51 1:10-1	0.025	6.91	-81
					SB-34 32-33':MW-51 1:10-2	0.030	6.85	-11
					Average Result	**0.028**	**6.9**	**-46**
		1:20 Soil:Water Ratio	17-Oct-22	0				
			24-Oct-22	7	SB-34 32-33':MW-51 1:20-1	0.041	6.89	-23
					SB-34 32-33':MW-51 1:20-2	0.044	6.86	-12
					Average Result	**0.043**	**6.9**	**-18**

Notes:

mg/L - milligrams per liter
mV - millivoltes
SU - standard units

Table 10 - Arsenic Partition Coefficients
Geochemical Conceptual Site Model
Hennepin West Ash Pond System, Illinois

Groundwater Sample ID	Geologic Material Sample ID	Analyte	Isotherm	Variable	Value
MW-51	**SB-34 23-33'**	**Arsenic**	Linear	R^2	0.69
				K_d (L/kg)	**36.40**
			Langmuir	R^2	0.90
				q_m (mg/g)	0.004
				K_L (L/kg)	**2.43E+08**
			Freundlich	R^2	0.60
				1/n	0.15
				K_F (L/kg)	**109.5**

Notes

K_d - linear partition coefficient

K_L - Langmuir partition coefficient

K_F - Freundlich partition coefficient

q_m - inverse of the slope of the linearized Langmuir isotherm

n - non-linearity constant of the Freundlich isotherm

ft bgs - feet below ground surface

L/kg - liters per kilogram

mg/g - milligrams of arsenic per gram of soil

FIGURES

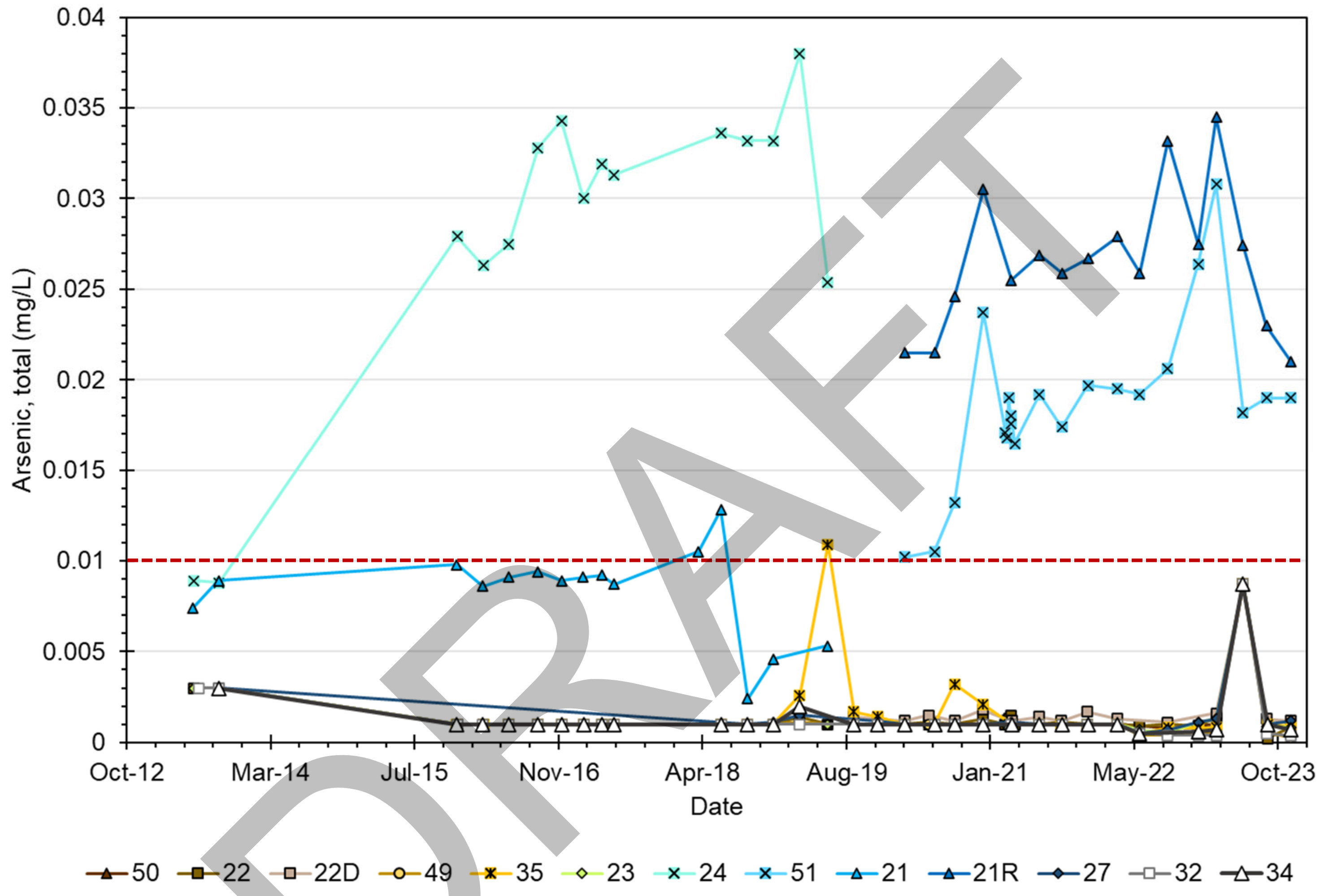

Notes:
1. Wells 21 and 24 were abandoned during closure activities and replaced with 21R and 51, respectively.
2. mg/L: milligrams per liter
3. Red dashed line denotes groundwater protection standard.

Arsenic Concentration Time Series

Hennepin West Ash Pond System

Geosyntec consultants

Figure 1

Chicago, Illinois

April 2024

Geosyntec\Vistra - Groundwater Compliance - Documents\General\GCSM\Hennepin

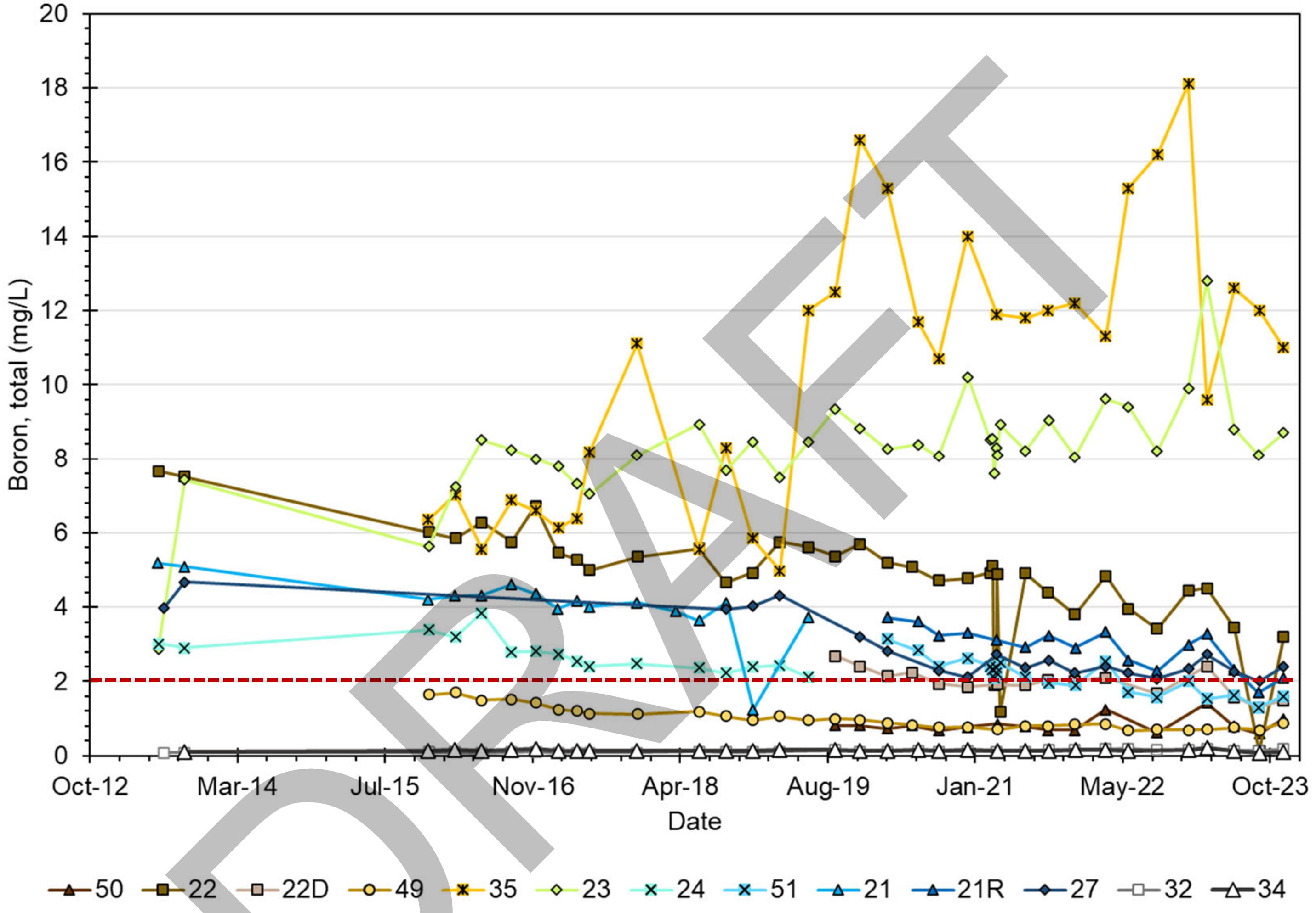

Notes:
1. Wells 21 and 24 were abandoned during closure activities and replaced with 21R and 51, respectively.
2. mg/L: milligrams per liter
3. Red dashed line denotes groundwater protection standard.

Boron Concentration Time Series

Hennepin West Ash Pond System

Geosyntec consultants

Figure 2

Chicago, Illinois

April 2024

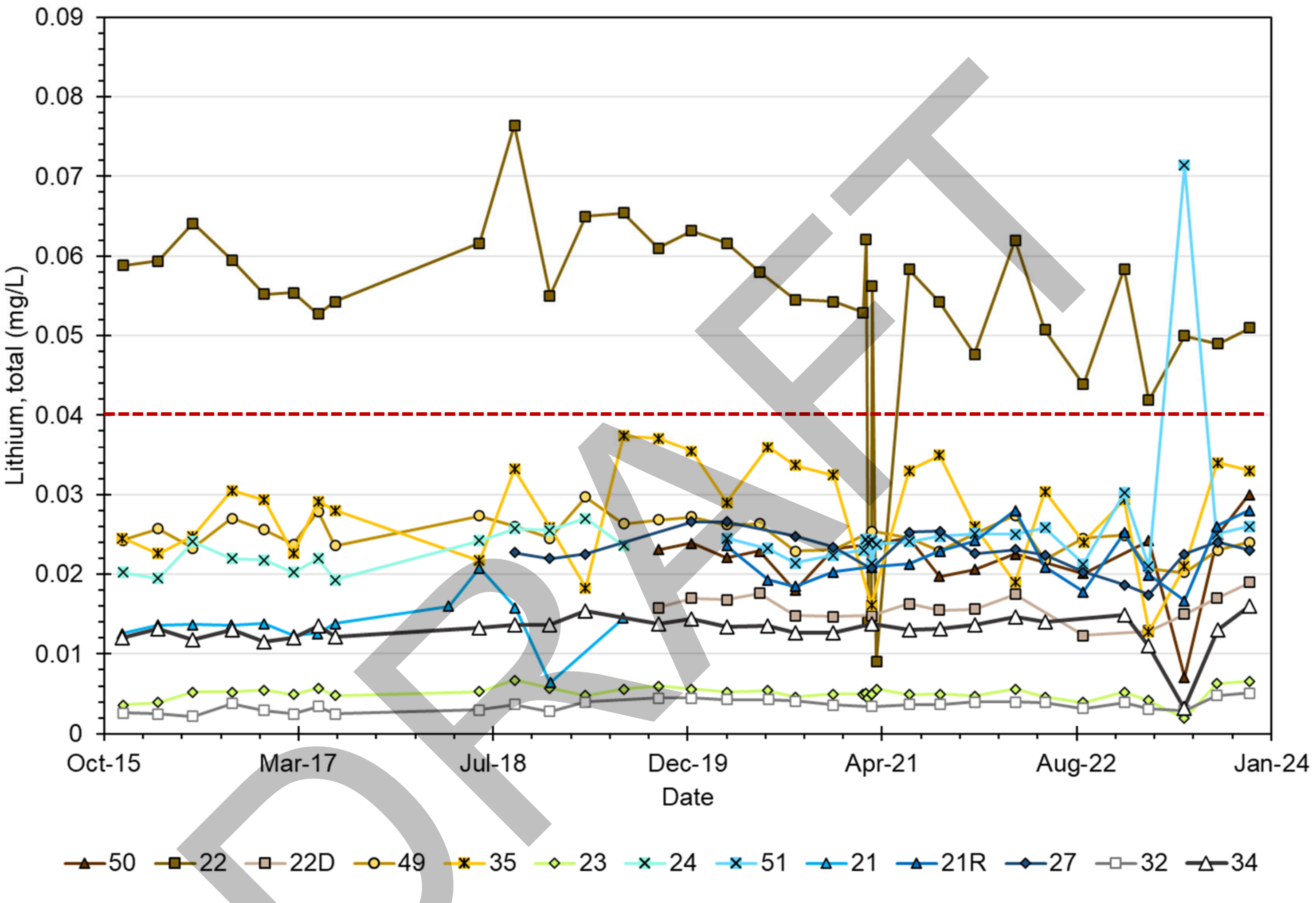

Notes:
1. Wells 21 and 24 were abandoned during closure activities and replaced with 21R and 51, respectively.
2. mg/L: milligrams per liter
3. Red dashed line denotes groundwater protection standard.

Lithium Concentration Time Series

Hennepin West Ash Pond System

Geosyntec consultants

Figure 3

Chicago, Illinois

April 2024

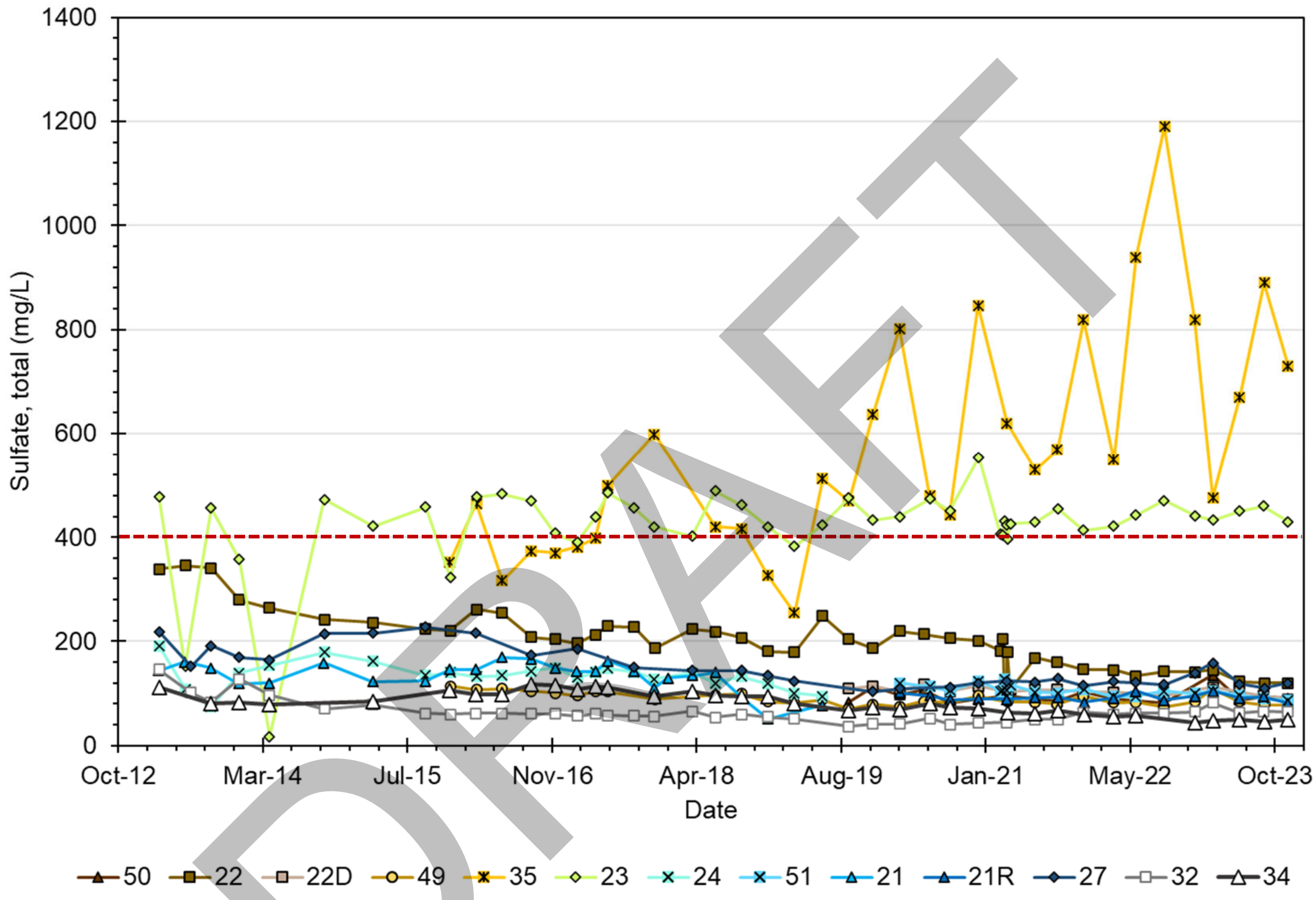

Notes:
1. Wells 21 and 24 were abandoned during closure activities and replaced with 21R and 51, respectively.
2. mg/L: milligrams per liter
3. Red dashed line denotes groundwater protection standard.

Sulfate Concentration Time Series

Hennepin West Ash Pond System

Geosyntec consultants

Figure 4

Chicago, Illinois

April 2024

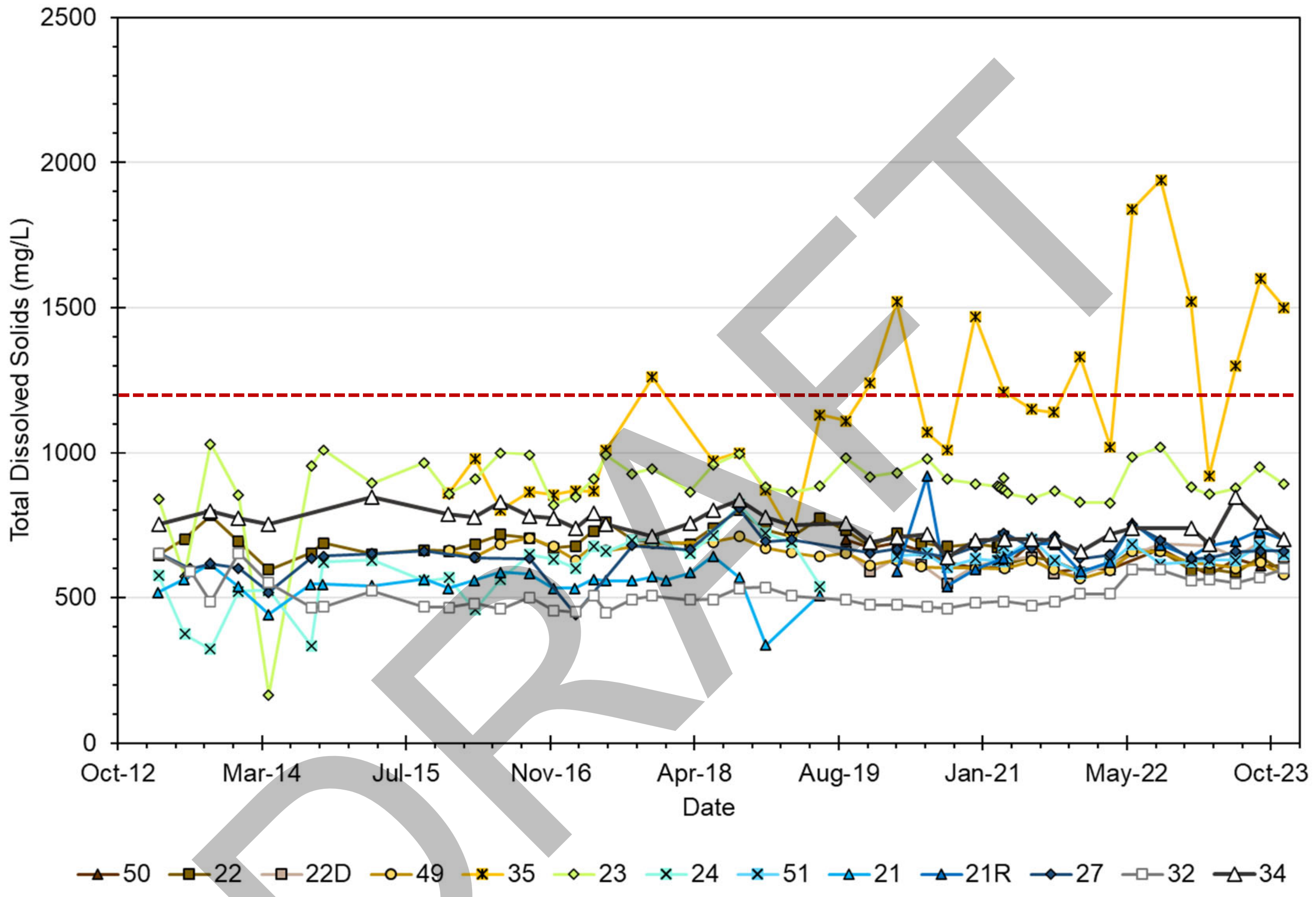

Notes:
1. Wells 21 and 24 were abandoned during closure activities and replaced with 21R and 51, respectively.
2. mg/L: milligrams per liter
3. Red dashed line denotes groundwater protection standard.

TDS Concentration Time Series

Hennepin West Ash Pond System

Geosyntec consultants

Figure
5

Chicago, Illinois

April 2024

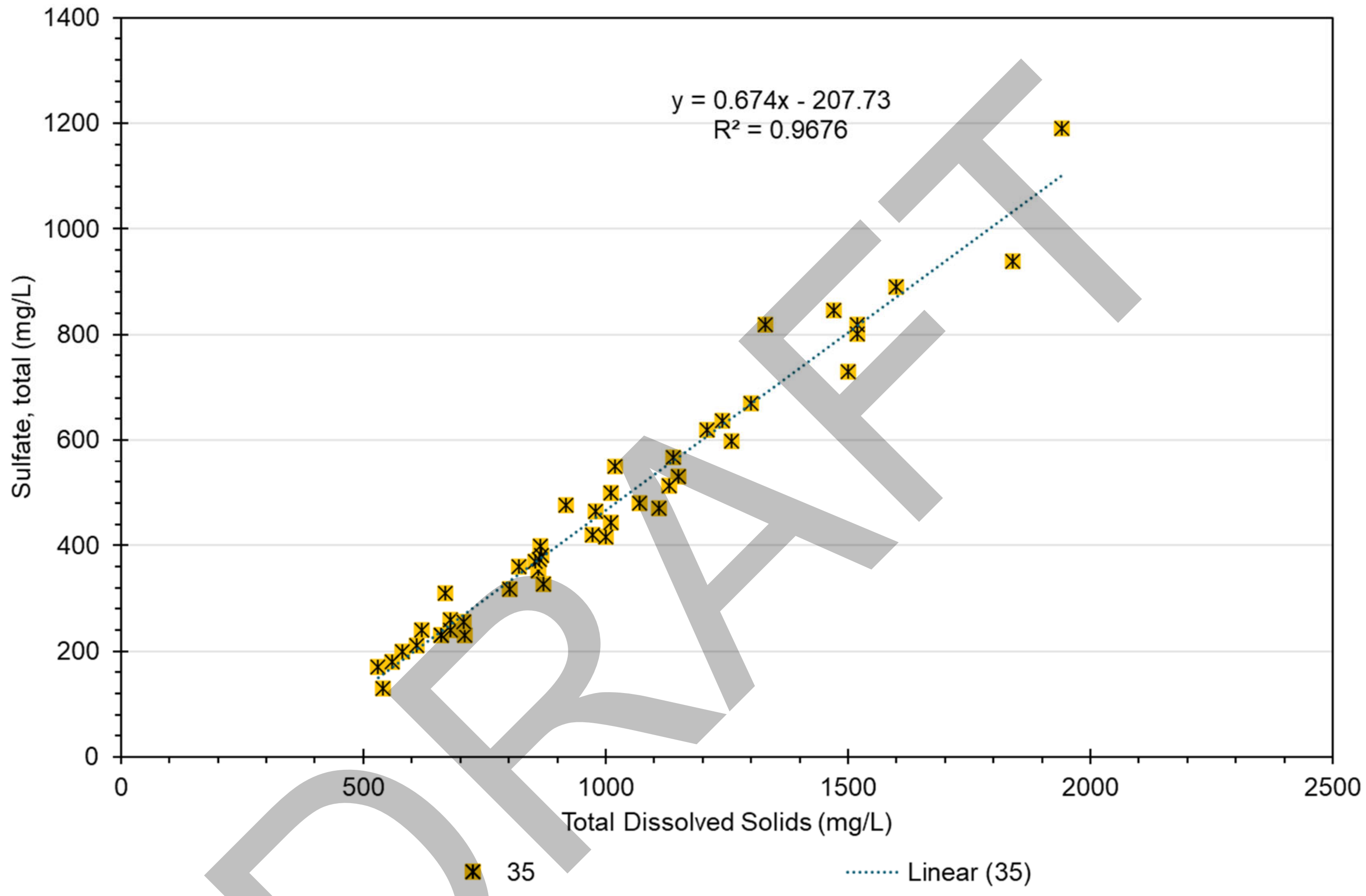

Notes:
1. mg/L: milligrams per liter

Sulfate and Total Dissolved Solids Correlation, Well 35
Hennepin West Ash Pond System

Geosyntec consultants

Figure 6

Chicago, Illinois | April 2024

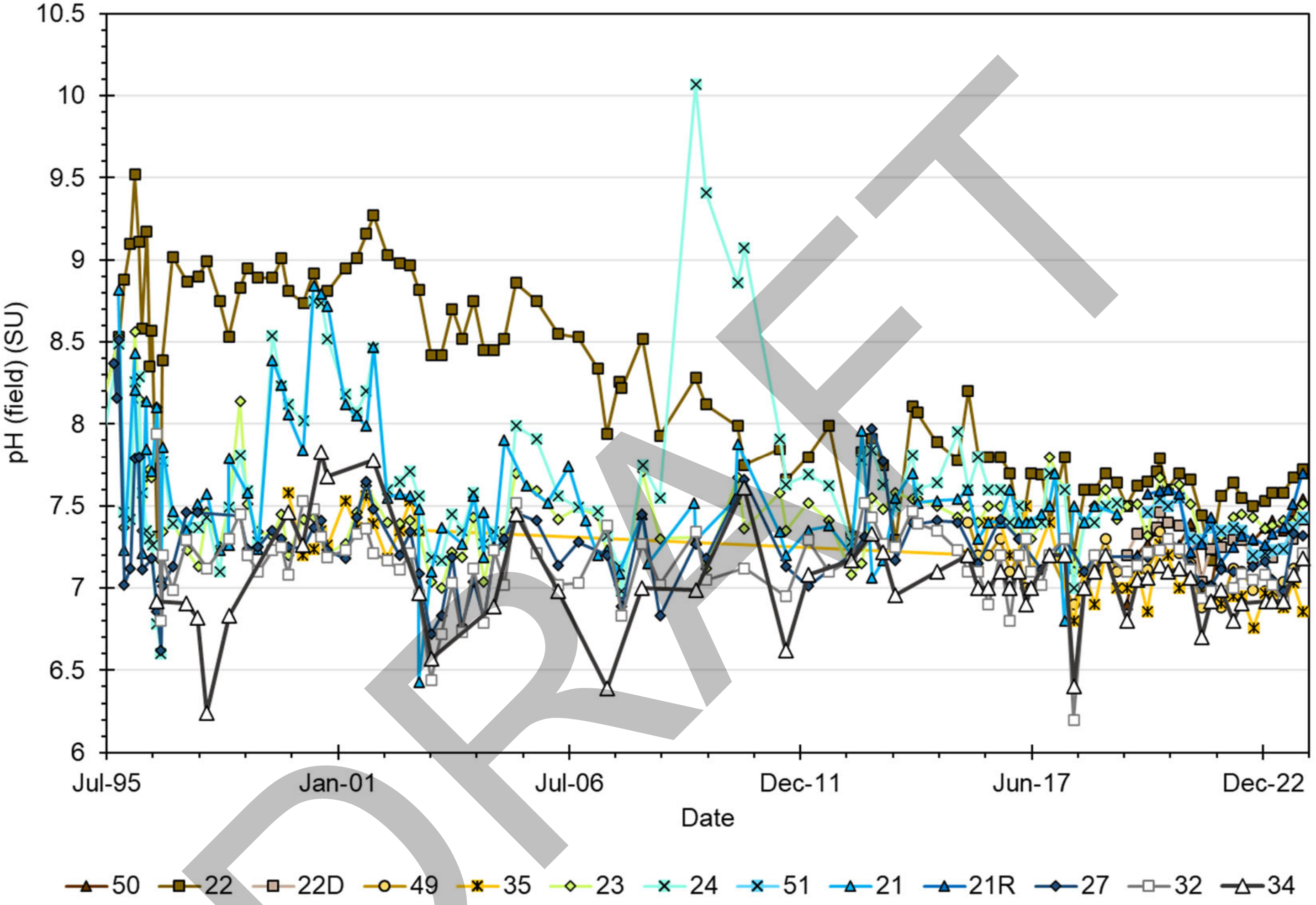

Notes:
1. Wells 21 and 24 were abandoned during closure activities and replaced with 21R and 51, respectively.
2. SU: standard units

pH Time Series

Hennepin West Ash Pond System

Geosyntec consultants

Figure 7

Chicago, Illinois

April 2024

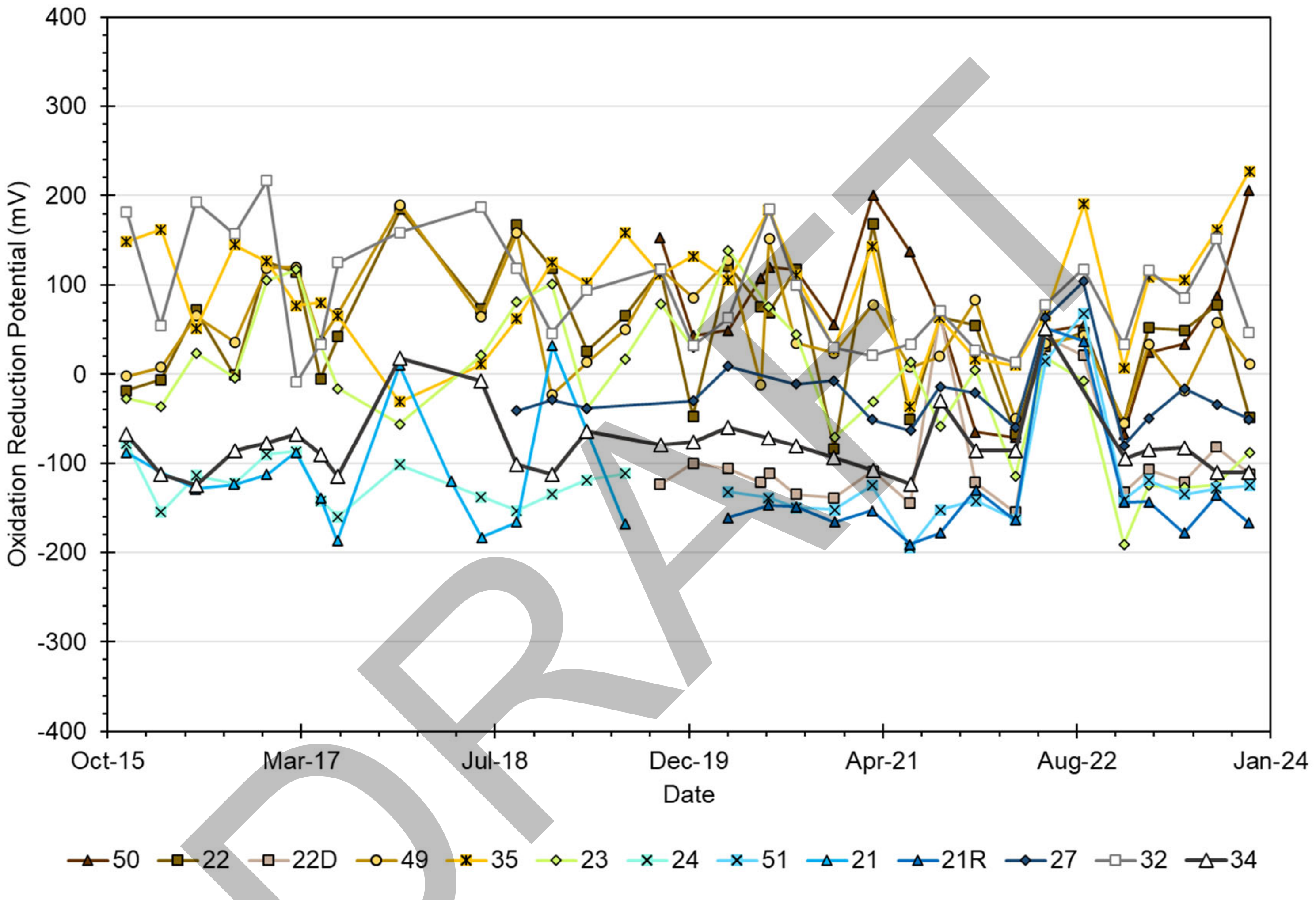

Notes:
1. Wells 21 and 24 were abandoned during closure activities and replaced with 21R and 51, respectively.
2. mV: millivolts

ORP Time Series

Hennepin West Ash Pond System

Geosyntec consultants

Figure 8

Chicago, Illinois

April 2024

Geosyntec\Vistra - Groundwater Compliance - Documents\General\GCSM\Hennepin

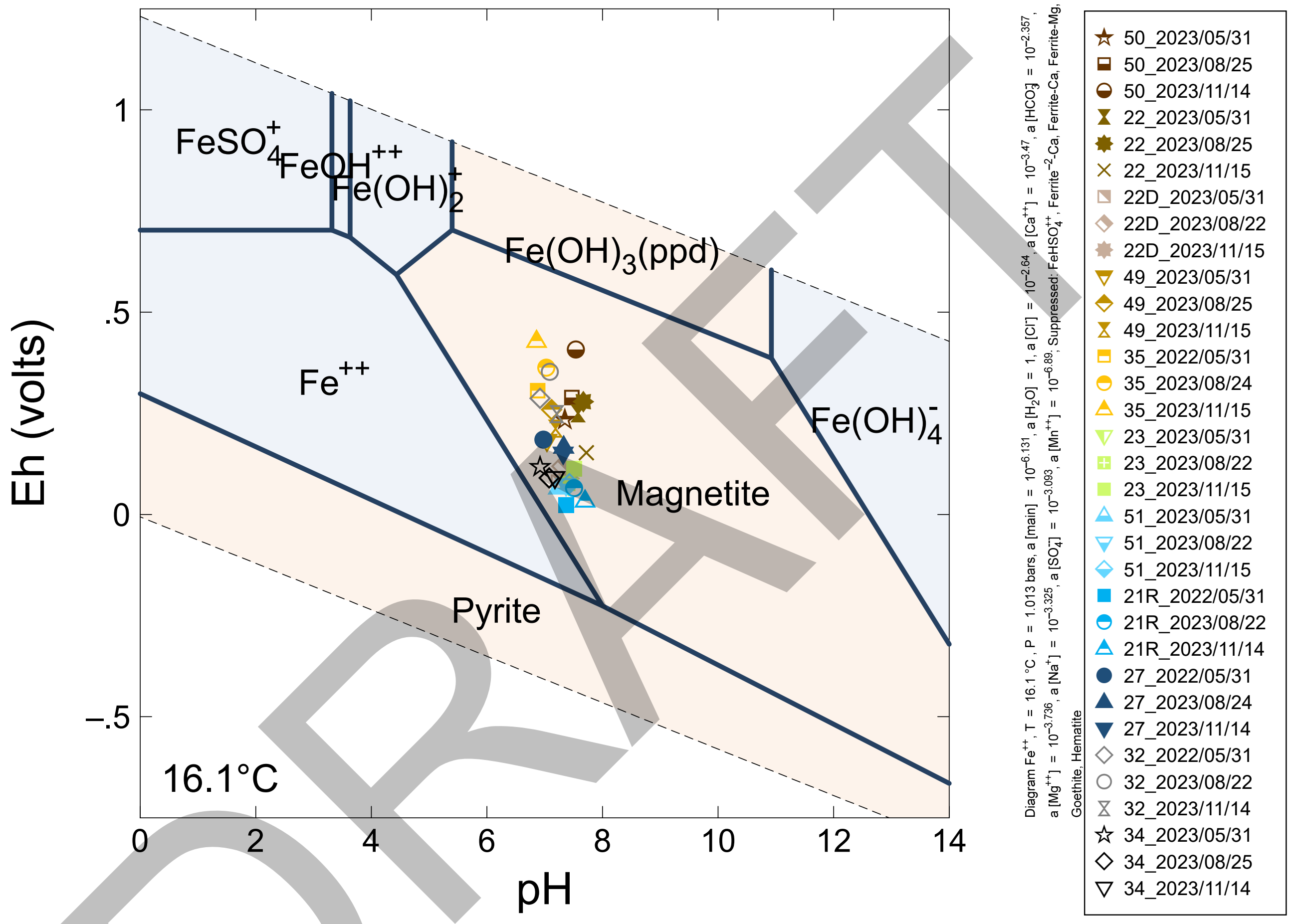

Notes:
1. Diagram generated using conditions at well 22 on August 25, 2023 to represent iron stability under more oxidizing conditions.
2. Crystalline phases ferrite-Ca, ferrite-Mg, goethite, and hematite are suppressed.

Geosyntec\Vistra - Groundwater Compliance - Documents\General\GCSM\Hennepin

Iron Pourbaix Diagram, Magnetite - 22

Hennepin West Ash Pond System

Geosyntec consultants

Figure
9a

Chicago, Illinois

April 2024

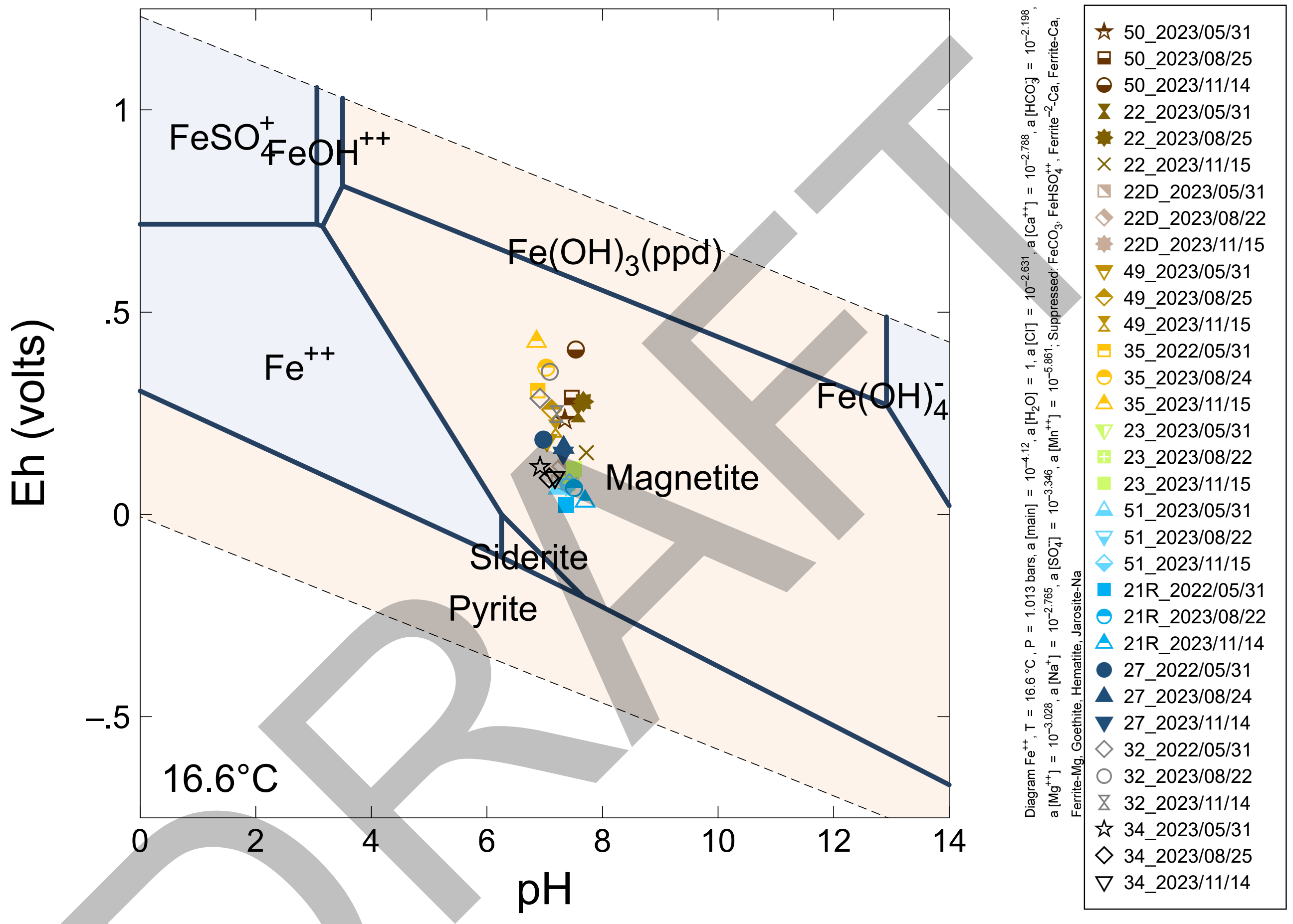

Notes:
1. Diagram generated using conditions at well 21R on August 22, 2023 to represent iron stability under more reducing conditions.
2. Crystalline phases ferrite-Ca, ferrite-Mg, goethite, hematite, and jarosite-Na are suppressed.

Iron Pourbaix Diagram, Magnetite – 21R

Hennepin West Ash Pond System

Geosyntec consultants

Figure 9b

Chicago, Illinois

April 2024

Geosyntec\Vistra - Groundwater Compliance - Documents\General\GCSM\Hennepin

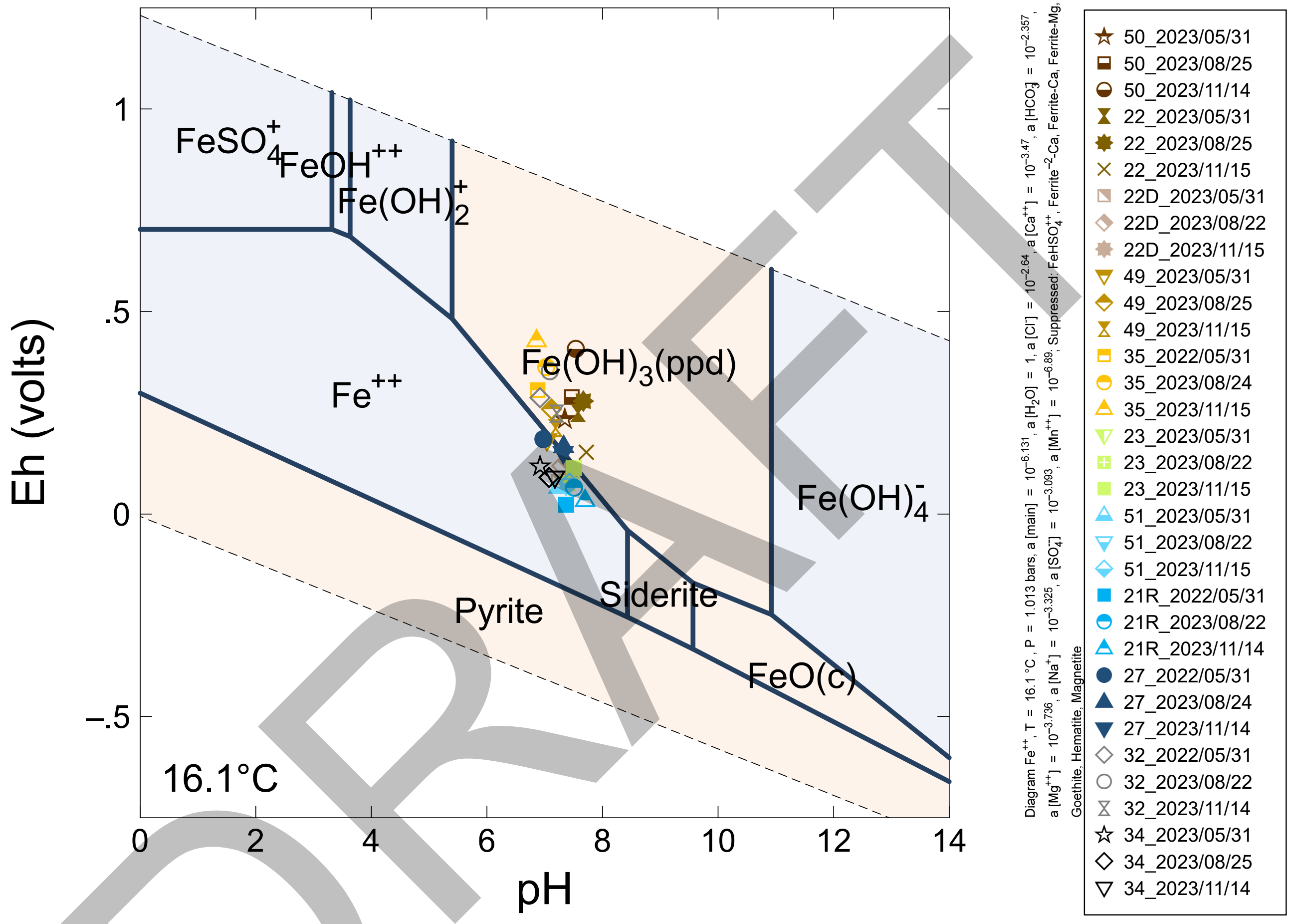

Notes:
1. Diagram generated using conditions at well 22 on August 25, 2023 to represent iron stability under more oxidizing conditions.
2. Crystalline iron phases ferrite-Ca, ferrite-Mg, goethite, hematite, and magnetite are suppressed.

Iron Pourbaix Diagram, Ferrihydrite - 22

Hennepin West Ash Pond System

Geosyntec consultants

Figure 9c

Chicago, Illinois

April 2024

Geosyntec\Vistra - Groundwater Compliance - Documents\General\GCSM\Hennepin

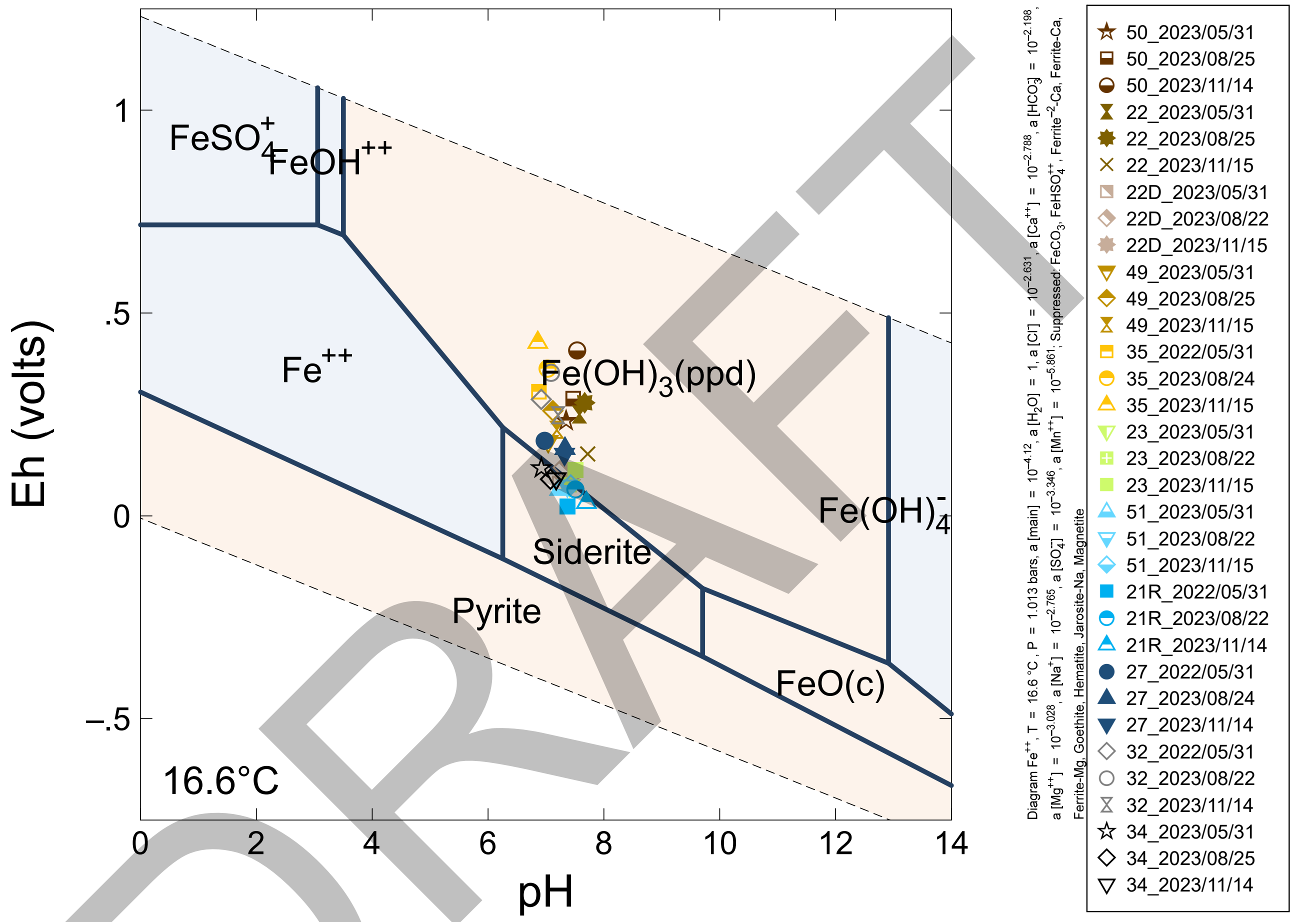

Notes:

1. Diagram generated using conditions at well 21R on August 22, 2023 to represent iron stability under more reducing conditions.
2. Crystalline phases ferrite-Ca, ferrite-Mg, goethite, hematite, magnetite, and jarosite-Na are suppressed.

Iron Pourbaix Diagram, Ferrihydrite – 21R

Hennepin West Ash Pond System

Geosyntec consultants

Figure 9d

Chicago, Illinois

April 2024

Geosyntec\Vistra - Groundwater Compliance - Documents\General\GCSM\Hennepin

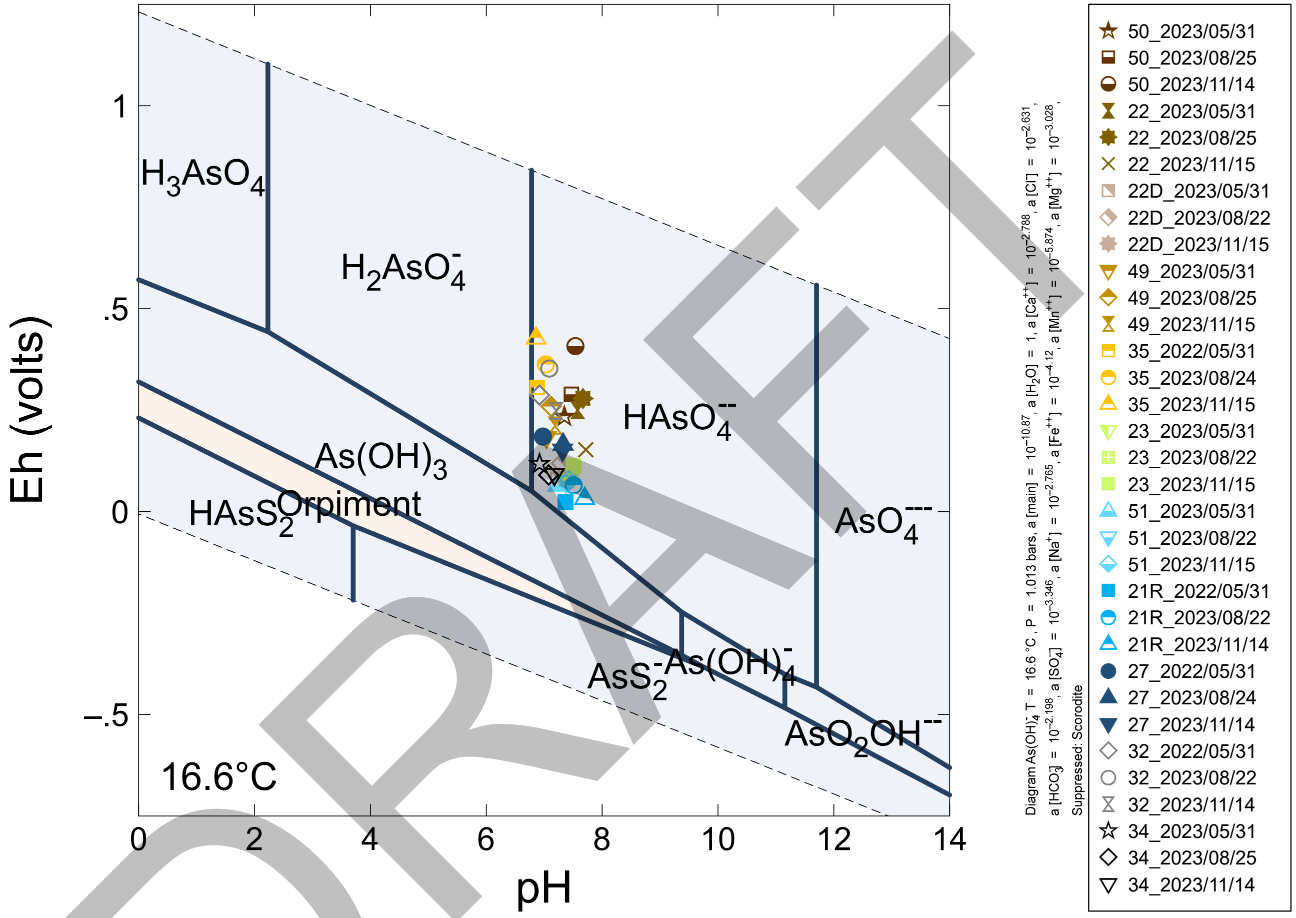

Notes:
1. Diagram generated using conditions at well 21R on August 22, 2023 to represent arsenic stability under more reducing conditions.
2. Crystalline phase scorodite is suppressed.

Arsenic Pourbaix Diagram - 21R

Hennepin West Ash Pond System

Geosyntec consultants

Figure 10

Chicago, Illinois

April 2024

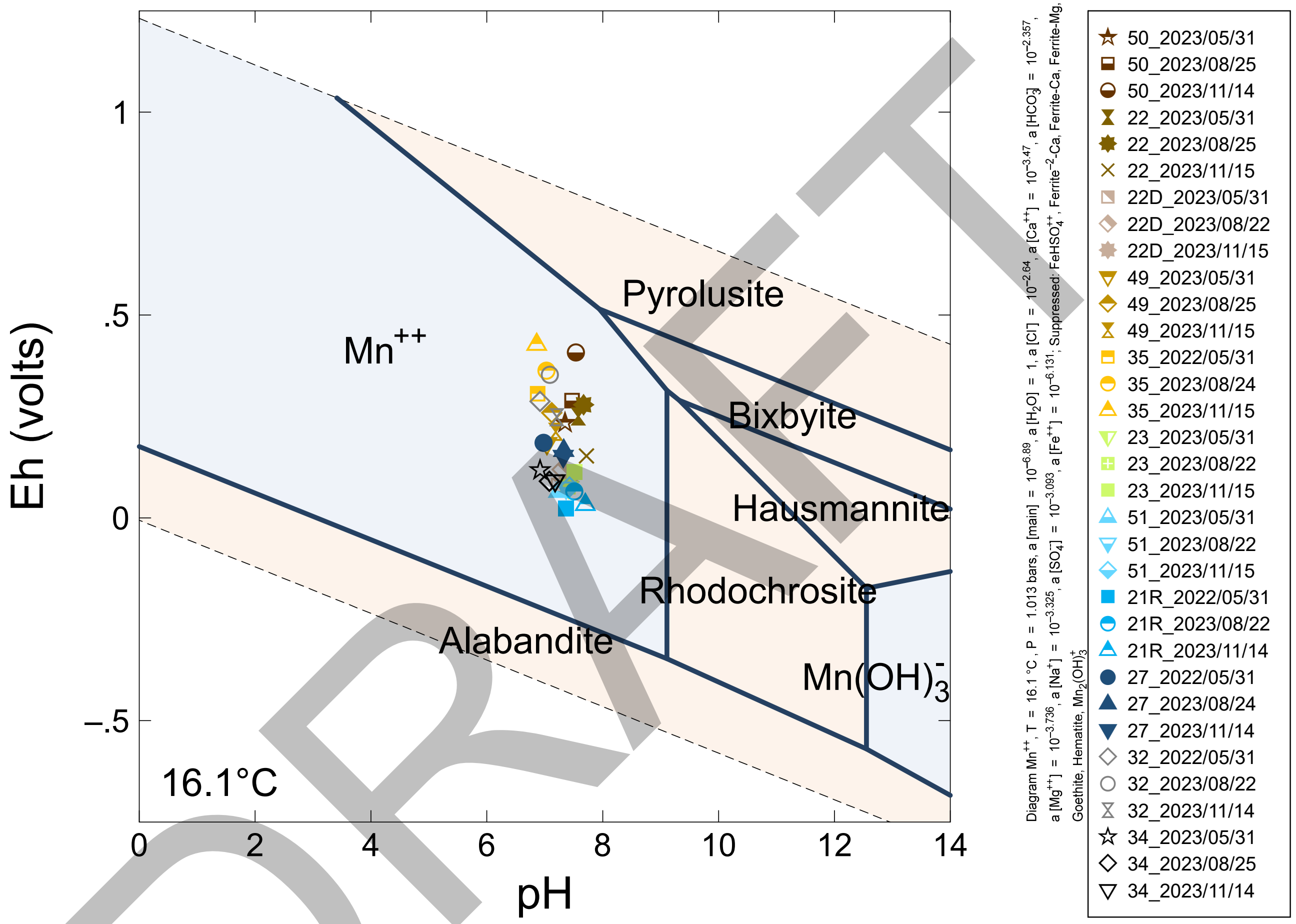

Notes:
1. Diagram generated using conditions at well 22 on August 25, 2023 to represent manganese stability under more oxidizing conditions.

Manganese Pourbaix Diagram - 22

Hennepin West Ash Pond System

Geosyntec consultants

Figure 11a

Chicago, Illinois

April 2024

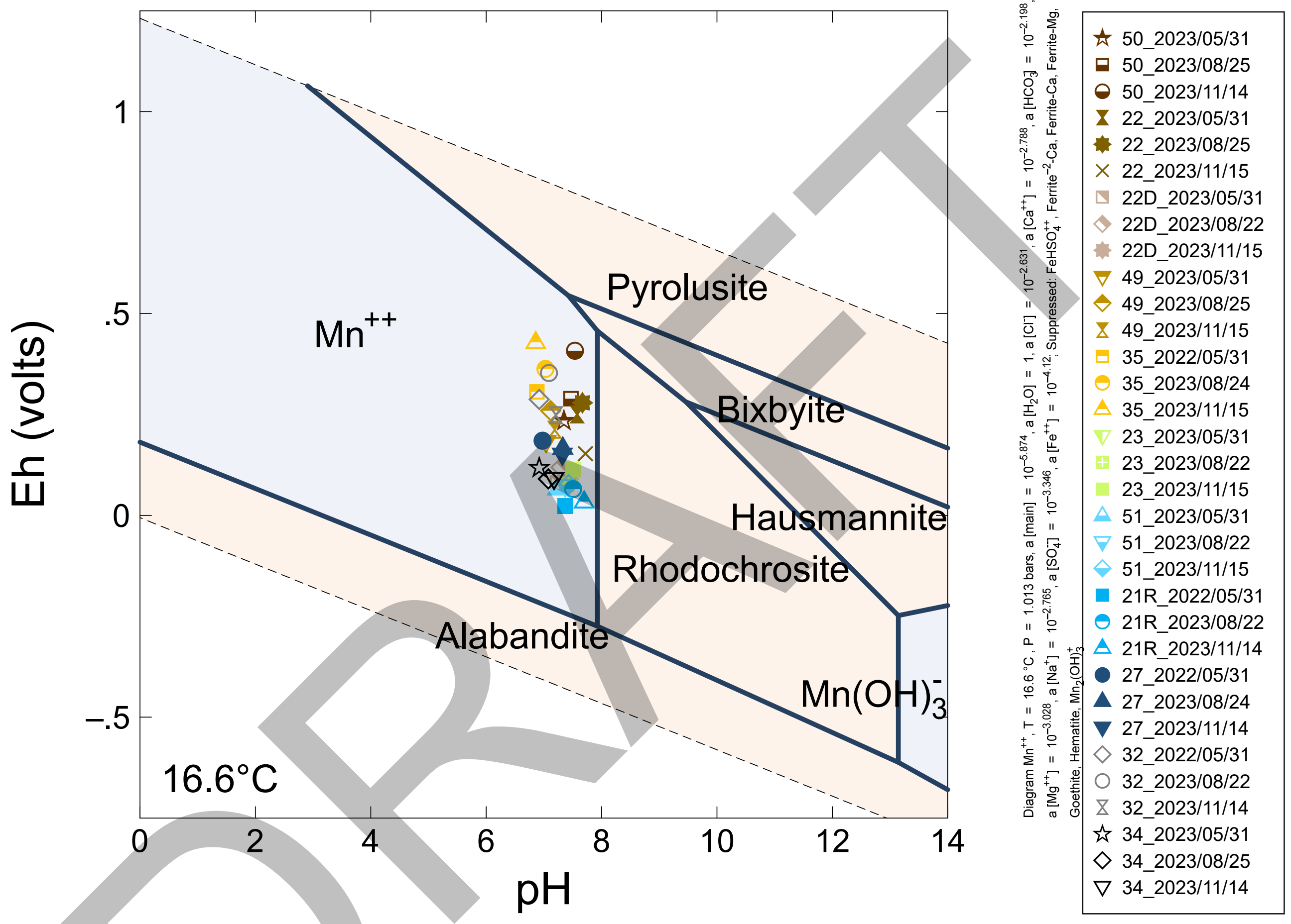

Notes:
1. Diagram generated using conditions at well 21R on August 22, 2023 to represent manganese stability under more reducing conditions.

Manganese Pourbaix Diagram – 21R

Hennepin West Ash Pond System

Geosyntec consultants

Chicago, Illinois | April 2024

Figure
11b

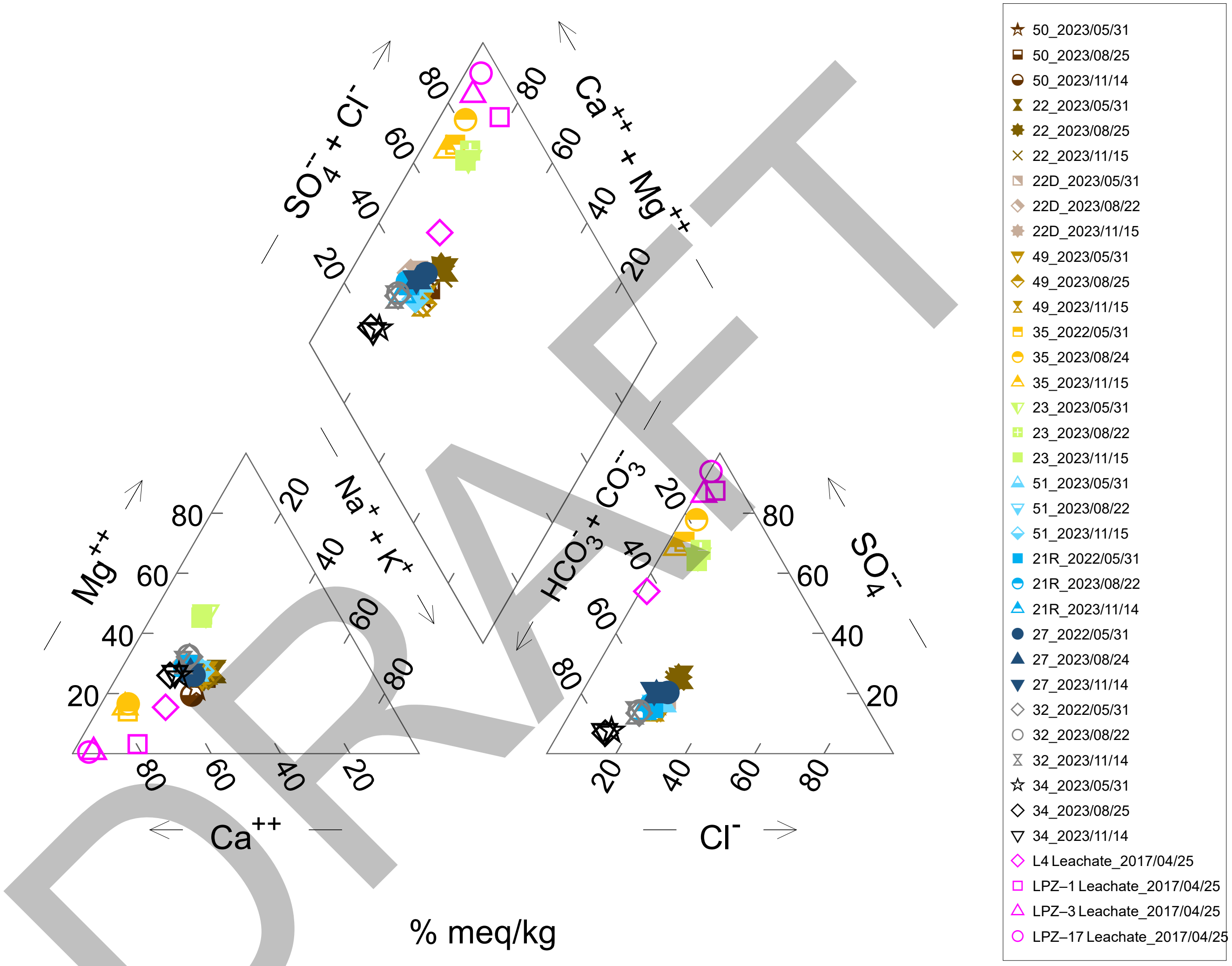

Notes:
1. meq/kg: milliequivalents per kilogram

Piper Diagram

Hennepin West Ash Pond System

Geosyntec consultants

Figure 12

Chicago, Illinois

April 2024

Geosyntec\Vistra - Groundwater Compliance - Documents\General\GCSM\Hennepin

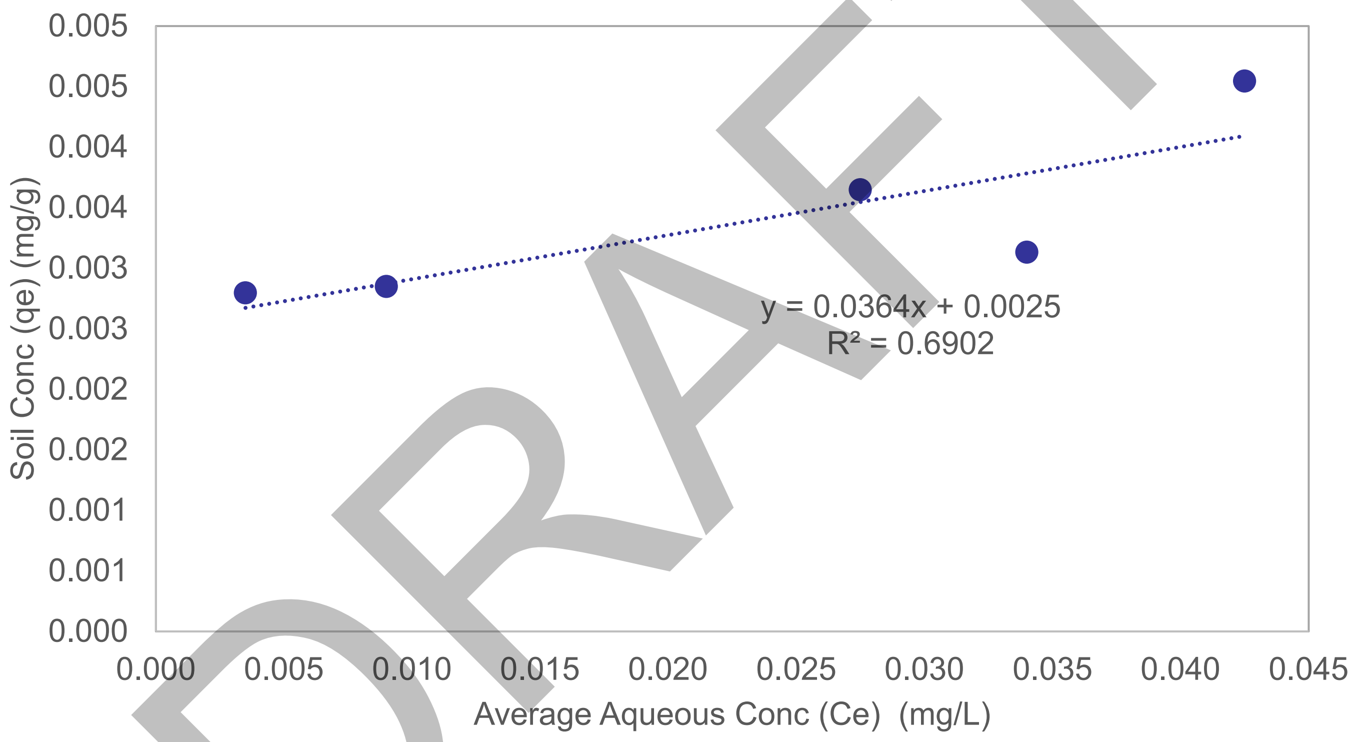

Notes:
1. mg/L: milligrams per liter
2. mg/g: milligrams of arsenic per gram of soil

Batch Adsorption Testing – Linear Isotherm

Hennepin West Ash Pond System

Geosyntec consultants

Chicago, Illinois

April 2024

Figure 13

ATTACHMENT A

Site Layout Figure

Y:\Mapping\Projects\22\2285\MXD\Nature_and_Extent\HEN\Nature_and_Extent_Report_HenWest\Figure 2-2_Site Map.mxd

PROJECT: 169000XXXX | DATED: 4/24/2024 | DESIGNER: galarmmc

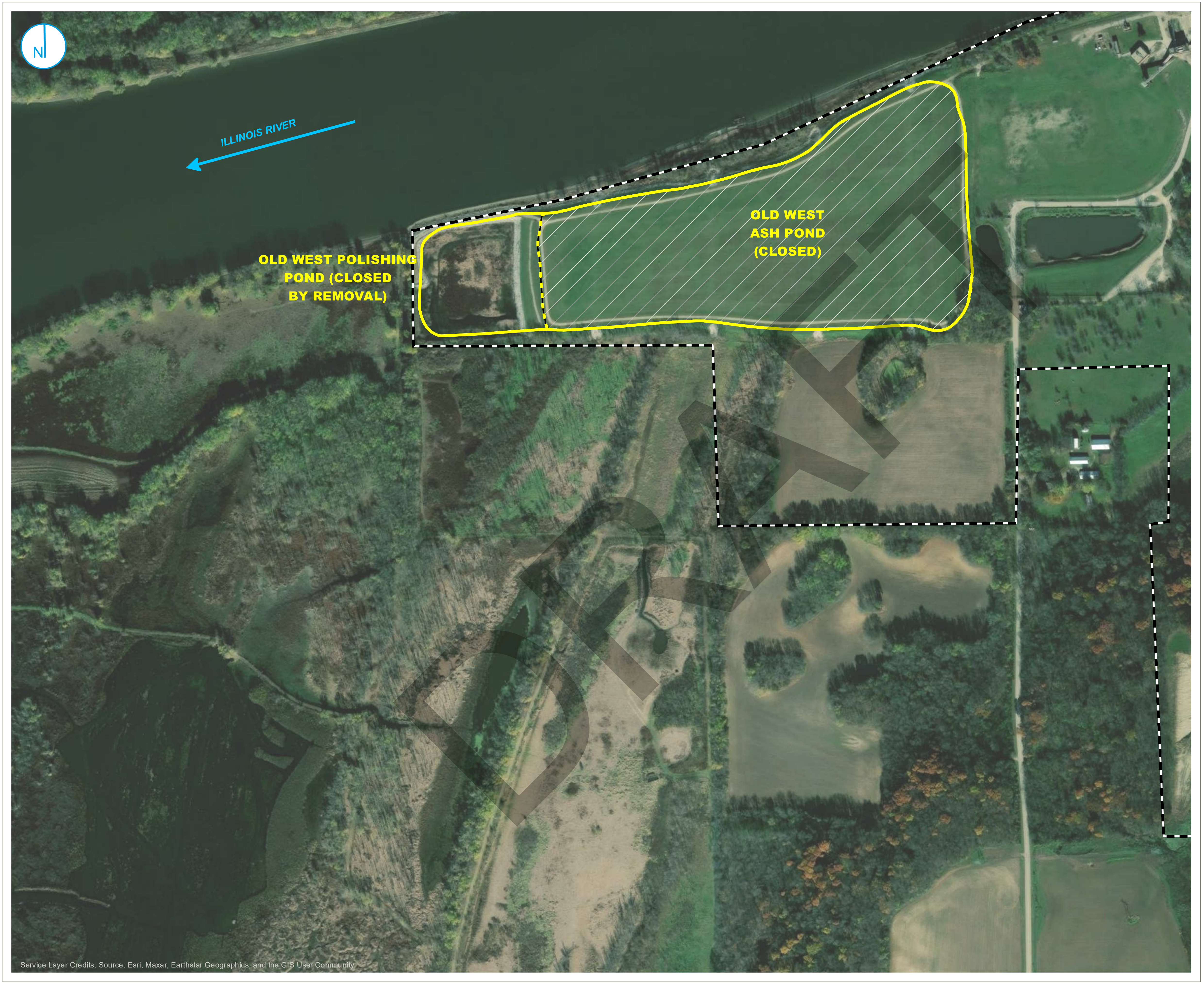

Service Layer Credits: Source: Esri, Maxar, Earthstar Geographics, and the GIS User Community

▭ REGULATED UNIT (SUBJECT UNIT)
▨ LIMITS OF FINAL COVER
⬚ PROPERTY BOUNDARY

0 200 400 Feet

SITE MAP

NATURE AND EXTENT REPORT
WEST ASH POND SYSTEM
HENNEPIN POWER PLANT
HENNEPIN, ILLINOIS

FIGURE 2-2

RAMBOLL AMERICAS
ENGINEERING SOLUTIONS, INC.

RAMBOLL

ATTACHMENT B

Proposed Part 845 Groundwater Monitoring Network

Service Layer Credits: Source: Esri, Maxar, GeoEye, Earthstar Geographics, CNES/Airbus DS, USDA, USGS, AeroGRID, IGN, and the GIS User Community

PROPOSED PART 845 GROUNDWATER MONITORING WELL NETWORK

ADDENDUM TO THE
GROUNDWATER MONITORING PLAN
WEST ASH POND SYSTEM
HENNEPIN POWER PLANT
HENNEPIN, ILLINOIS

FIGURE 2-1

RAMBOLL AMERICAS
ENGINEERING SOLUTIONS, INC.

Y:\Mapping\Projects\22\2285\MXD\845_Operating_Permit\Hennepin\GMP_804\Figure 2-1_Proposed Monitoring Well Network.mxd

PROJECT: 169000XXXX | DATED: 9/29/2021 | DESIGNER: STOLZSD

ATTACHMENT C

Monitoring Well Construction Information

TABLE 2-1. MONITORING WELL LOCATIONS AND CONSTRUCTION DETAILS
ADDENDUM TO THE GROUNDWATER MONITORING PLAN
HENNEPIN POWER PLANT
WEST ASH POND SYSTEM
HENNEPIN, ILLINOIS

Well Number	Type	HSU	Date Constructed	Top of PVC Elevation (ft)	Measuring Point Elevation (ft)	Measuring Point Description	Ground Elevation (ft)	Screen Top Depth (ft BGS)	Screen Bottom Depth (ft BGS)	Screen Top Elevation (ft)	Screen Bottom Elevation (ft)	Well Depth (ft BGS)	Bottom of Boring Elevation (ft)	Screen Length (ft)	Screen Diameter (inches)	Latitude (Decimal Degrees)	Longitude (Decimal Degrees)
21R	C	UA	02/06/2020	452.05	452.05	Top of PVC	449.37	37.60	47.60	411.77	401.77	50.00	399.40	10	2	41.299866	-89.328914
22	C	UA	12/09/1982	464.45	464.45	Top of PVC	461.46	24.40	34.40	437.06	427.06	34.60	426.90	10	2	41.302032	-89.321512
22D	C	UA	08/07/2019	465.43	465.43	Top of PVC	461.83	49.70	59.70	412.16	402.16	59.67	401.80	10	2	41.302017	-89.321572
23	C	UA	12/10/1982	463.39	463.39	Top of PVC	460.88	34.00	44.00	426.88	416.88	45.20	415.70	10	2	41.300881	-89.325376
27	C	UA	09/11/1995	450.58	450.58	Top of PVC	448.21	30.00	35.00	418.21	413.21	36.30	412.00	5	2	41.296911	-89.328898
32	B	UA	08/21/1996	451.38	451.38	Top of PVC	448.75	7.00	17.00	441.75	431.75	17.30	431.40	10	2	41.292128	-89.328563
34	B	UA	08/22/1996	449.56	449.56	Top of PVC	448.23	30.00	35.00	418.23	413.23	35.00	413.20	5	2	41.299538	-89.33249
35	C	UA	09/08/1999	454.83	454.83	Top of PVC	451.51	8.00	18.00	443.51	433.51	17.60	433.90	10	2	41.29916	-89.324145
49	C	UA	07/06/2015	468.17	468.17	Top of PVC	465.76	35.00	45.00	430.76	420.76	45.00	420.80	10	2	41.301182	-89.32333
50	C	UA	08/07/2019	463.94	463.94	Top of PVC	460.59	19.60	29.60	440.99	430.99	29.60	430.60	10	2	41.302243	-89.320647
51	C	UA	02/04/2020	464.80	464.80	Top of PVC	461.50	56.00	66.00	405.50	395.50	66.30	394.50	10	2	41.300639	-89.326953

Notes:
All elevation data are presented relative to the North American Vertical Datum 1988 (NAVD88), GEOID 12A
Type refers to the role of the well in the monitoring network: background (B), compliance (C), or water level measurements only (WLO)
WLO wells are temporary pending implementation of impoundment closure per an approved Construction Permit application
BGS = below ground surface
ft = foot or feet
HSU = Hydrostratigraphic Unit
PVC = polyvinyl chloride
UA = uppermost aquifer
generated 10/05/2021, 3:14:31 PM CDT

ATTACHMENT D

Boring Logs

PROJECT Hydrogeologic Study
Hennepin Power Plant
JOB NO. 82-1293

BORING W-2
SHEET 1 **OF** 1

22

DEPTH (ft)	SAMPLE NUMBER	SAMPLE INTERVAL AND TYPE	SAMPLE ADVANCED / RECOVERED (in)	SEE REMARK #	DESCRIPTION OF MATERIALS (Color Modifier MATERIAL. Classification) Soil Classification System Unified; Surface Elevation 461.4'	BLOWS (per 6 in)	DRY UNIT WEIGHT (pcf)
	1	AS			Brown Sandy CLAY, CL		
5	2	SS	18/9		Gray - Brown Silty CLAY Trace Sand, CL	3-5-5	
					Brown Fine SAND w/Silt Trace Gravel, SM		
10	3	SS	18/16			5-7-5	
15	4	SS	18/16			19-20-28	
					Gray-Brown GRAVEL w/ Sand Trace Clay, GP		
20	5	SS	18/18			17-27-38	
25	6	SS	18/13		-Coal @ 25.4'	23-18-12	
					Brown Fine SAND, SP		
30	7	SS	18/15			6-11-11	
					Brown GRAVEL w/Sand Trace Clay, GP-GC		
35	8	SS	18/6		TOB	0-4-6	

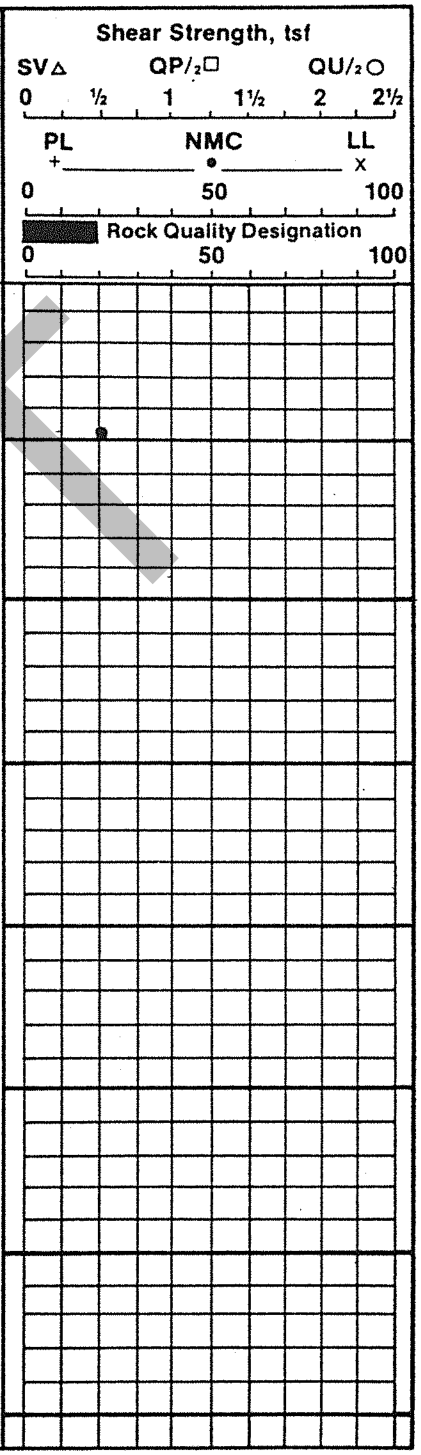

DRILLING METHOD Hollow Auger
DATE DRILLED 12/9/82
DRILLED BY Roberts
LOGGED BY Maxeiner
PIEZOMETER Yes

GROUNDWATER LEVELS

Encountered at 8.0 Feet
___ Hours after completion ___ Feet
6 Days after completion 8.0 Feet
___ after completion ___ Feet

NOTE: Refer to the attached GENERAL NOTES and NOTATION USED ON RECORDS OF SUBSURFACE EXPLORATION for abbreviations, explanations, and qualifications relative to this log.

mathes

John Mathes & Associates, Inc.

Monitoring Well No. 34

PROJECT Title: Hennepin West Ash Impoundment
DRILL RIG: Hollow Stem Auger
DRILLER: Boart Longyear

DATE: 8-22-96
HOLE DIA.: 7 in.
FINAL GW: 7.54 ft.

LOGGED BY: Mueller/Tu
SAMPLER: Split Spoon
HOLE ELEV.: 448.19 ft. MSL

DESCRIPTION

USCS CLASS

Silty clay, trace of plant debris, little fine-grained sand, very dark brown in color, medium to high plasticity (alluvium).

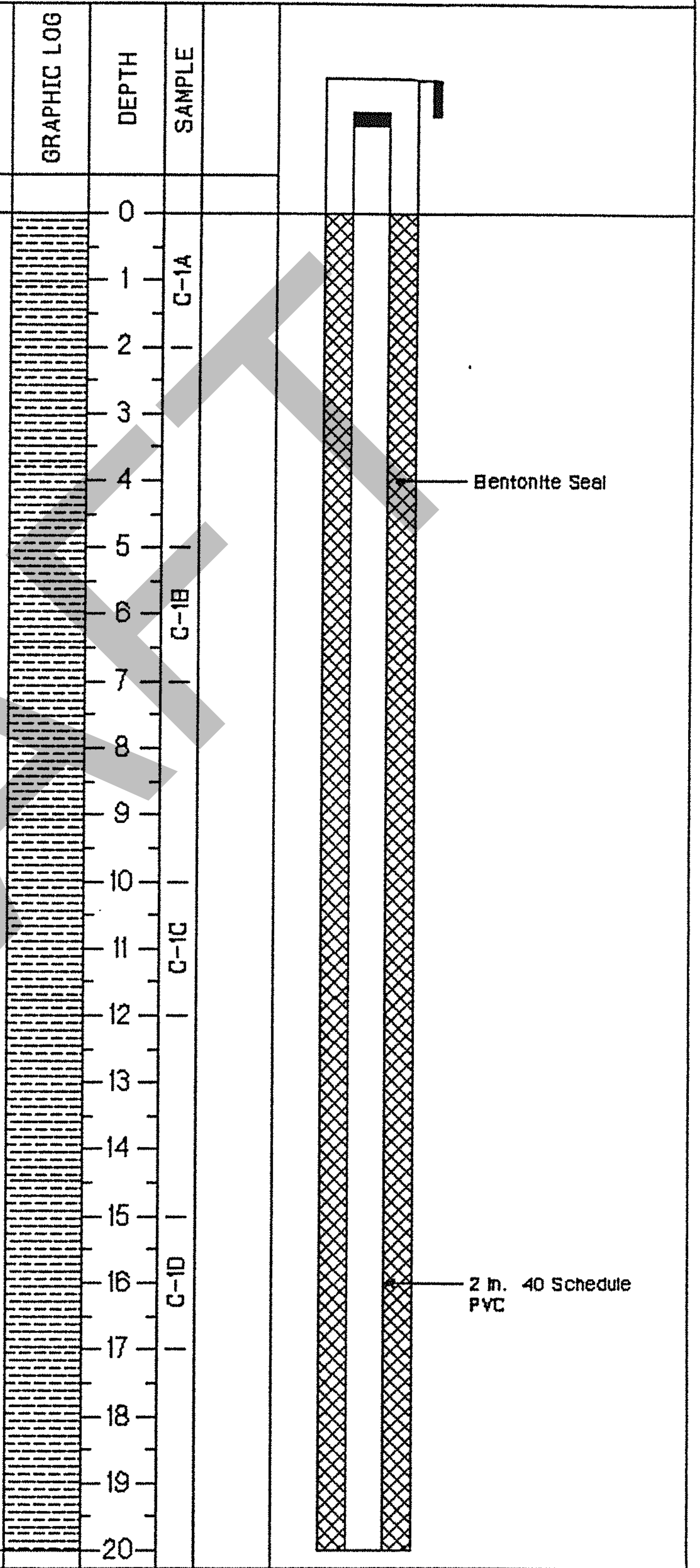

STMI

2511 N. 124th St. Suite 205
Brookfield, Wisconsin 53005-8208

Notes:

Project No.
135-1.31

Monitoring Well No. 34

PROJECT Title: Hennepin West Ash Impoundment
DATE: 8-22-96
LOGGED BY: Mueller/Tu
DRILL RIG: Hollow Stem Auger
HOLE DIA.: 7 in.
SAMPLER: Split Spoon
DRILLER: Boart Longyear
FINAL GW: 7.54 ft.
HOLE ELEV.: 448.19 ft. MSL

DESCRIPTION	USCS CLASS
Clayey silt, trace to little fine-grained sand and shell fragments, soft, olive-gray. Wet.	
Sand, fine-grained to medium-grained, well-sorted, quartz, trace of silt, loose. Yellowish brown color grades to olive gray below 31 ft.	

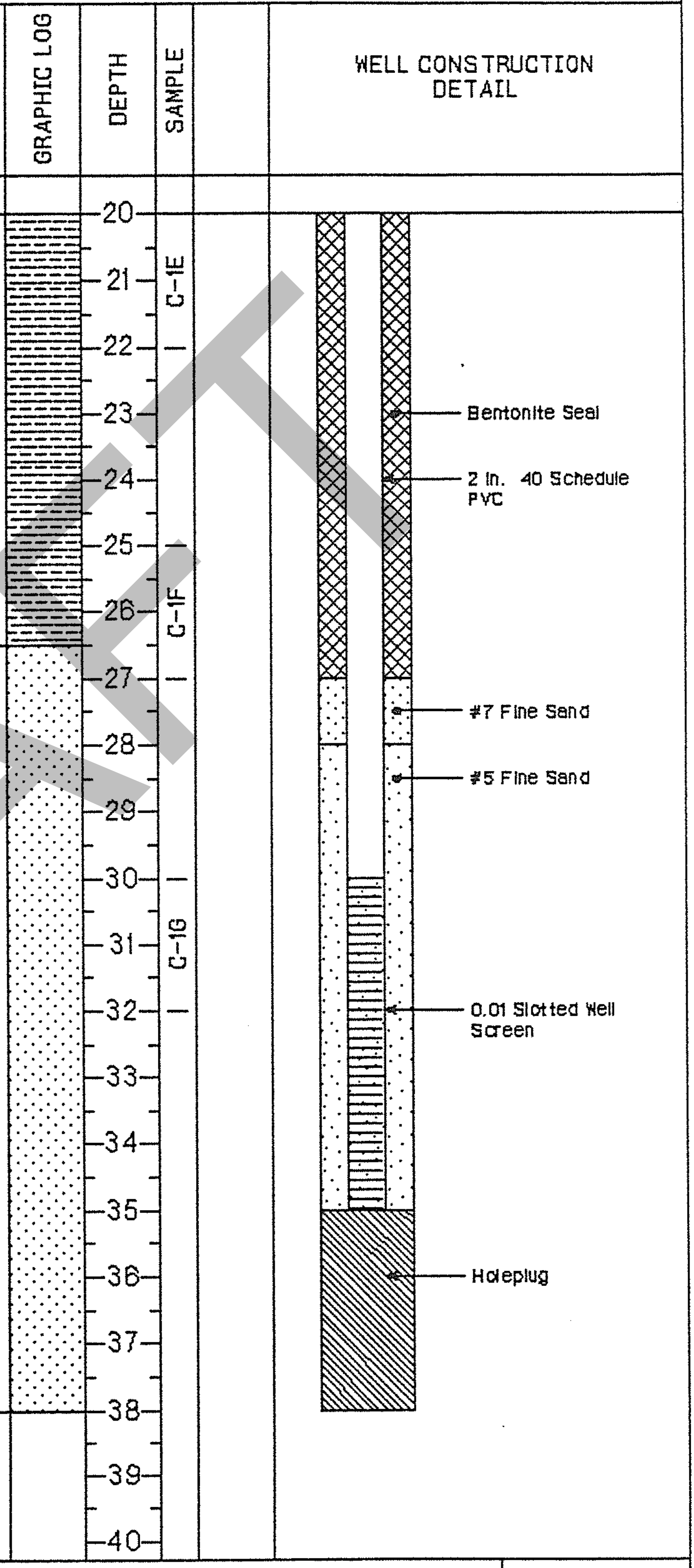

STMI

2511 N. 124th St. Suite 205
Brookfield, Wisconsin 53005-8208

Notes:

Project No.
135-1.31

Page 2 of 2

Geosyntec consultants

1 McBride and Sons Center Dr
Suite 202
Chesterfield, MO 63005

GS FORM:
WELL BORE 01/04

BOREHOLE LOG

BORING MW-51 **SHEET** 1 **OF** 3
START DRILL DATE February 4, 2020
FINISH DRILL DATE February 4, 2020
LOCATION PUTNAM COUNTY, HENNEPIN IL
PROJECT HENNEPIN POWER STATION
NUMBER CHE8400

ELEVATION DATA:
GROUND SURF. (Ft) 461.50
TOP OF CASING (Ft) 464.80
DATUM NAVD 1988

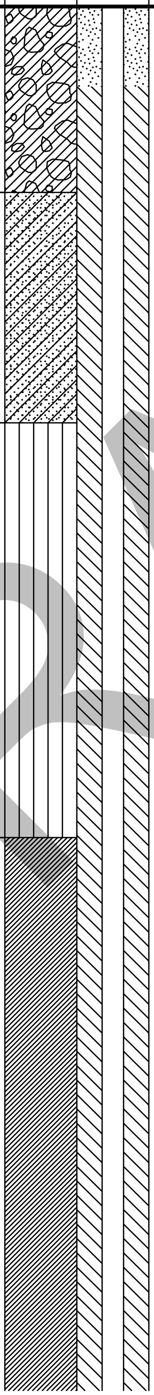

DEPTH (ft-bgs)	DESCRIPTION 1) Unit/Formation, Mem. 2) USCS Name 3) Color 4) Moisture 5) Percent Grain Size 6) Plasticity 7) Density/Consistency 8) Structure 9) Other (Mineralization, Discoloration, Odor, etc.)	GROUNDWATER OR STRUCTURE	ELEVATION (ft)	SAMPLE NO.	TYPE	BLOW COUNT	N-Value	RECOVERY (%)	COMMENTS 1) Rig Behavior 2) Air Monitoring
	Brown/red, clayey gravel, GC, fill material		460	01		2 4 4 3	8	17/24	
				02		5 3 11 12	14	18/24	
5	Brown/red, clayey sand with trace coarse sand, SC, low plasticity			03		5 6 9 5	15	16/24	
			455	04		6 3 4 5	7	2/24	
	Dark gray, fly ash, ML, non-plastic, non-cohesive			05		3 4 5 9	9	21/24	
10			450	06		3 3 3 4	6	24/24	
				07		2 1 1 2	2	24/24	
15	@14 ft changes to dark gray/black			08		4 4 32 40	36	24/24	
			445	09		3 3 3 4	6	24/24	
	Dark gray/black silty clay, CL, medium plasticity, damp			10		2 3 3 3	6	24/24	
20			440	11		2 1 3 2	4	18/24	
				12		0 1 2 2	3	24/24	
25	@ 24 ft red brown coarse gravel lens			13		0 2 3 4	5	24/24	
	@ 26 ft changes to dark gray		435	14		0 1 1 1	2	24/24	
	@ 28 ft changes to medium stiff			15		1 2 2 3	4	18/24	
30									

CONTRACTOR TSC
EQUIPMENT CME 75
DRILL MTHD HOLLOWSTEM AUGER
DIAMETER 6-inch
LOGGER C. CHRISTENSON **REVIEWER** L. CARR

NORTHING 1688814.68
EASTING 2527303.58
COORDINATE SYSTEM:
STATE PLANE ILLINOIS WEST

NOTES:

SEE KEY SHEET FOR SYMBOLS AND ABBREVIATIONS

Geosyntec consultants

1 McBride and Sons Center Dr
Suite 202
Chesterfield, MO 63005

GS FORM:
WELL BORE 01/04

BOREHOLE LOG

BORING	MW-51	**SHEET**	2 OF 3
START DRILL DATE	February 4, 2020	**ELEVATION DATA:**	
FINISH DRILL DATE	February 4, 2020	**GROUND SURF. (Ft)**	461.50
LOCATION	PUTNAM COUNTY, HENNEPIN IL	**TOP OF CASING (Ft)**	464.80
PROJECT	HENNEPIN POWER STATION	**DATUM**	NAVD 1988
NUMBER	CHE8400		

DESCRIPTION: 1) Unit/Formation, Mem. 2) USCS Name 3) Color 4) Moisture 5) Percent Grain Size 6) Plasticity 7) Density/Consistency 8) Structure 9) Other (Mineralization, Discoloration, Odor, etc.)

COMMENTS: 1) Rig Behavior 2) Air Monitoring

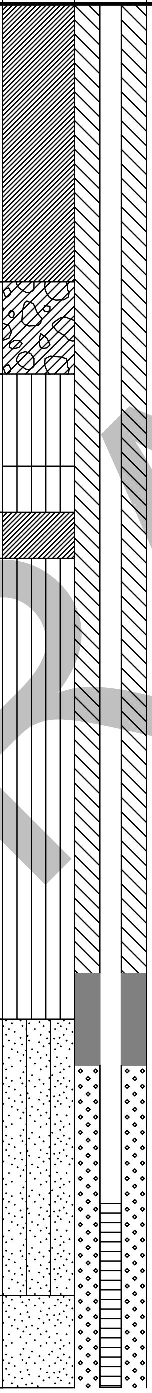

DEPTH (ft-bgs)	DESCRIPTION	GROUNDWATER OR STRUCTURE	ELEVATION (ft)	SAMPLE NO.	BLOW COUNT	N-Value	RECOVERY (%)	COMMENTS
	@ 31 ft medium gravel lens		430	16	3 4 5 5	8	6/24	
				17	0 1 2 2	3	19/24	
35				18	2 3 4 5	7	24/24	
	Dark gray clay and gravel mixture, wet, GC		425	19	2 2 3 5	5	6/24	
	Dark gray, silt with trace clay, ML, low plasticity, damp			20	0 0 2 2	2	24/24	
40	Dark gray silt with trace clay, ML, low plasticity, damp Dark gray silty clay, CL, medium plasticity, damp, medium stiff		420	21	2 1 1 2	2	24/24	
	Dark gray silt with trace clay, ML, low plasticity, damp, medium stiff			22	2 2 2 3	4	24/24	
45				23	1 1 2 3	3	24/24	
	@ 47 ft few diatomaceous/shells		415	24	0 0 2 2	2	24/24	
				25	0 1 2 2	3	10/24	
50			410	26	3 4 4 7	8	14/24	
	Dark gray, fine to medium sand, trace coarse sand, SM			27		0	24/24	
55				28	1 3 5 7	8	24/24	
	@ 56 ft changes to some coarse sand, SM-SP		405	29	7 6 7 6	13	24/24	
	Dark gray, medium sand with some fine and coarse sand, SP, wet			30	3 3 9 1	12	24/24	
60								

CONTRACTOR TSC
EQUIPMENT CME 75
DRILL MTHD HOLLOWSTEM AUGER
DIAMETER 6-inch
LOGGER C. CHRISTENSON **REVIEWER** L. CARR

NORTHING 1688814.68
EASTING 2527303.58
COORDINATE SYSTEM:
STATE PLANE ILLINOIS WEST

NOTES:

SEE KEY SHEET FOR SYMBOLS AND ABBREVIATIONS

Geosyntec consultants

1 McBride and Sons Center Dr
Suite 202
Chesterfield, MO 63005

GS FORM:
WELL BORE 01/04

BOREHOLE LOG

BORING MW-51 **SHEET** 3 **OF** 3
START DRILL DATE February 4, 2020
FINISH DRILL DATE February 4, 2020
LOCATION PUTNAM COUNTY, HENNEPIN IL
PROJECT HENNEPIN POWER STATION
NUMBER CHE8400

ELEVATION DATA:
GROUND SURF. (Ft) 461.50
TOP OF CASING (Ft) 464.80
DATUM NAVD 1988

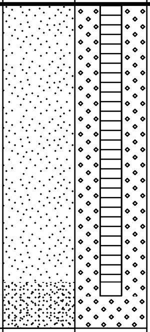

DEPTH (ft-bgs)	DESCRIPTION 1) Unit/Formation, Mem. 2) USCS Name 3) Color 4) Moisture 5) Percent Grain Size 6) Plasticity 7) Density/Consistency 8) Structure 9) Other (Mineralization, Discoloration, Odor, etc.)	GRAPHIC LOG	WELL LOG	GROUNDWATER OR STRUCTURE	ELEVATION (ft)	SAMPLE NO.	TYPE	BLOW COUNT	N-Value	RECOVERY (%)	COMMENTS 1) Rig Behavior 2) Air Monitoring
	Dark gray, medium sand with some fine and coarse sand, SP, wet				400	31		1 1 3 4	4	2/24	
	@ 62 ft, changes to few fine gravel, fine sand absent, SW					32		5 7 13 18	20	24/24	
65						33		5 8 14 17	22	24/24	
	Dark gray, medium-fine sand with some coarse sand, SW				395	34		3 10	13	12/12	
	@ 67 ft lens of medium gravel										
	End of boring at 67 ft.										
70					390						
75					385						
80					380						
85					375						
90											

CONTRACTOR TSC
EQUIPMENT CME 75
DRILL MTHD HOLLOWSTEM AUGER
DIAMETER 6-inch
LOGGER C. CHRISTENSON **REVIEWER** L. CARR

NORTHING 1688814.68
EASTING 2527303.58
COORDINATE SYSTEM:
STATE PLANE ILLINOIS WEST

NOTES:

SEE KEY SHEET FOR SYMBOLS AND ABBREVIATIONS

ATTACHMENT E

Site Solids Bulk Characterization and Total Metals Analytical Data

SGS Canada Inc.
P.O. Box 4300 - 185 Concession St.
Lakefield - Ontario - KOL 2HO
Phone: 705-652-2000 FAX: 705-652-6365

Project : Hennepin MNA

06-April-2021

SiREM Laboratory
Attn : Michael Healey

130 Stone Road W
Guelph, ON
N1G 3Z2, Canada

Phone: 519-822-2265
Fax:519-822-3151

Date Rec. : 05 March 2021
LR Report: **CA14198-MAR21**
Reference: P.O# 80003210A

Copy: #1

CERTIFICATE OF ANALYSIS

Final Report

Analysis	1: Analysis Start Date	2: Analysis Start Time	3: Analysis Completed Date	4: Analysis Completed Time	5: SB-34 32-33'	6: SB-51 42-43'	7: SB-22 26-27'	8: SB-22 29-30'
Sample Date & Time					04-Mar-21 12:15	04-Mar-21 12:30	04-Mar-21 12:40	04-Mar-21 13:00
Sulphide [%]	22-Mar-21	12:31	22-Mar-21	17:06	0.09	0.18	< 0.04	0.06
SO4 [%]	23-Mar-21	07:20	25-Mar-21	09:13	< 0.1	< 0.1	< 0.1	< 0.1
TOC [%]	22-Mar-21	02:08	22-Mar-21	17:06	1.92	3.55	0.339	4.55
TS LOI [mg/L]	11-Mar-21	19:34	16-Mar-21	09:39	64100	70500	15400	74800
Ag [µg/g]	05-Apr-21	14:43	06-Apr-21	11:29	< 0.05	0.06	< 0.05	0.08
Al [µg/g]	05-Apr-21	14:43	06-Apr-21	11:29	5000	8200	2800	3700
As [µg/g]	05-Apr-21	14:43	06-Apr-21	11:29	2.7	3.5	5.1	8.4
Ba [µg/g]	05-Apr-21	14:43	06-Apr-21	11:29	47	84	20	31
Be [µg/g]	05-Apr-21	14:43	06-Apr-21	11:29	0.29	0.50	0.20	0.87
B [µg/g]	05-Apr-21	14:43	06-Apr-21	11:29	5	10	6	7
Bi [µg/g]	05-Apr-21	14:43	06-Apr-21	11:29	0.23	0.59	0.13	0.26
Ca [µg/g]	05-Apr-21	14:43	06-Apr-21	11:29	52000	91000	56000	36000
Cd [µg/g]	05-Apr-21	14:43	06-Apr-21	11:29	0.53	0.89	0.76	2.9
Co [µg/g]	05-Apr-21	14:43	06-Apr-21	11:29	6.9	9.3	5.2	9.8
Cr [µg/g]	05-Apr-21	14:43	06-Apr-21	11:29	45	27	79	130
Cu [µg/g]	05-Apr-21	14:43	06-Apr-21	11:29	8	14	11	25
Fe [µg/g]	05-Apr-21	14:43	06-Apr-21	11:29	10000	14000	9400	12000
K [µg/g]	05-Apr-21	14:43	06-Apr-21	11:29	1200	1900	910	1200
Li [µg/g]	05-Apr-21	14:43	06-Apr-21	11:29	6	12	4	6
Mg [µg/g]	05-Apr-21	14:43	06-Apr-21	11:29	13000	15000	21000	16000
Mn [µg/g]	05-Apr-21	14:43	06-Apr-21	11:29	260	350	310	220
Mo [µg/g]	05-Apr-21	14:43	06-Apr-21	11:29	0.9	2.0	3.1	5.0
Na [µg/g]	05-Apr-21	14:43	06-Apr-21	11:29	180	170	190	160
Ni [µg/g]	05-Apr-21	14:43	06-Apr-21	11:29	12	19	15	43
Pb [µg/g]	05-Apr-21	14:43	06-Apr-21	11:29	6.1	11	7.7	28
P [µg/g]	05-Apr-21	14:43	06-Apr-21	11:29	380	430	350	330
Se [µg/g]	05-Apr-21	14:43	06-Apr-21	11:29	< 0.7	1.1	< 0.7	0.8
Si [µg/g]	05-Apr-21	14:43	06-Apr-21	11:29	7200	4500	5400	1600
Sb [µg/g]	05-Apr-21	14:43	06-Apr-21	11:29	< 0.8	< 0.8	< 0.8	< 0.8
Sn [µg/g]	05-Apr-21	14:43	06-Apr-21	11:29	1.1	0.6	< 0.5	0.5
Tl [µg/g]	05-Apr-21	14:43	06-Apr-21	11:29	0.16	0.25	0.13	0.26
U [µg/g]	05-Apr-21	14:43	06-Apr-21	11:29	0.65	1.2	1.3	1.8
V [µg/g]	05-Apr-21	14:43	06-Apr-21	11:29	12	18	17	41

Analysis	**1: Analysis Start Date**	**2: Analysis Start Time**	**3: Analysis Completed Date**	**4: Analysis Completed Time**	**5: SB-34 32-33'**	**6: SB-51 42-43'**	**7: SB-22 26-27'**	**8: SB-22 29-30'**
W [µg/g]	05-Apr-21	14:43	06-Apr-21	11:29	0.06	0.05	0.07	0.10
Y [µg/g]	05-Apr-21	14:43	06-Apr-21	11:29	5.7	8.0	6.1	7.6
Zn [µg/g]	05-Apr-21	14:43	06-Apr-21	11:29	40	67	46	91

Catharine Arnold

ASSOCIATION OF THE CHEMICAL PROFESSION OF ONTARIO
CHARTERED
CATHARINE ARNOLD
CHEMIST

Catharine Arnold, B.Sc., C.Chem
Project Specialist,
Environment, Health & Safety

ATTACHMENT F

Sequential Extraction Procedure Analytical Data

SGS Canada Inc.
P.O. Box 4300 - 185 Concession St.
Lakefield - Ontario - KOL 2HO
Phone: 705-652-2000 FAX: 705-652-6365

water soluble

Project : Hennepin MNA

30-March-2021

SiREM Laboratory
Attn : Michael Healey

130 Stone Road W
Guelph, ON
N1G 3Z2, Canada

Phone: 519-822-2265
Fax:519-822-3151

Date Rec. : 05 March 2021
LR Report: **CA14201-MAR21**
Reference: P.O# 800003210A

Copy: #1

CERTIFICATE OF ANALYSIS

Final Report

Analysis	**1: Analysis Start Date**	**2: Analysis Start Time**	**3: Analysis Completed Date**	**4: Analysis Completed Time**	**5: SB-34 32-33'**	**6: SB-51 42-43'**	**7: SB-22 26-27'**	**8: SB-22 29-30'**
Sample Date & Time					04-Mar-21 12:15	04-Mar-21 12:30	04-Mar-21 12:40	04-Mar-21 13:00
Ag [µg/g]	26-Mar-21	11:11	26-Mar-21	17:50	< 0.05	< 0.05	< 0.05	< 0.05
Al [µg/g]	26-Mar-21	11:11	26-Mar-21	17:50	120	140	32	310
As [µg/g]	26-Mar-21	11:11	26-Mar-21	17:50	< 0.5	< 0.5	< 0.5	< 0.5
Ba [µg/g]	26-Mar-21	11:11	26-Mar-21	17:50	0.8	0.9	0.2	1.5
Be [µg/g]	26-Mar-21	11:11	26-Mar-21	17:50	< 0.02	< 0.02	< 0.02	0.02
B [µg/g]	26-Mar-21	11:11	26-Mar-21	17:50	< 1	1	< 1	1
Bi [µg/g]	26-Mar-21	11:11	26-Mar-21	17:50	< 0.09	< 0.09	< 0.09	< 0.09
Ca [µg/g]	26-Mar-21	11:11	26-Mar-21	17:50	500	600	220	410
Cd [µg/g]	26-Mar-21	11:11	26-Mar-21	17:50	< 0.02	< 0.02	< 0.02	0.04
Co [µg/g]	26-Mar-21	11:11	26-Mar-21	17:50	0.03	0.04	0.02	0.23
Cr [µg/g]	26-Mar-21	11:11	26-Mar-21	17:50	< 0.5	< 0.5	< 0.5	1.6
Cu [µg/g]	26-Mar-21	11:11	26-Mar-21	17:50	< 0.1	< 0.1	< 0.1	0.5
Fe [µg/g]	26-Mar-21	11:11	26-Mar-21	17:50	72	68	22	310
K [µg/g]	26-Mar-21	11:11	26-Mar-21	17:50	110	140	99	220
Li [µg/g]	26-Mar-21	11:11	26-Mar-21	17:50	< 2	< 2	< 2	< 2

SGS Canada Inc.
P.O. Box 4300 - 185 Concession St.
Lakefield - Ontario - KOL 2HO
Phone: 705-652-2000 FAX: 705-652-6365

water soluble

Project : Hennepin MNA

LR Report : **CA14201-MAR21**

Analysis	**1: Analysis Start Date**	**2: Analysis Start Time**	**3: Analysis Completed Date**	**4: Analysis Completed Time**	**5: SB-34 32-33'**	**6: SB-51 42-43'**	**7: SB-22 26-27'**	**8: SB-22 29-30'**
Mg [µg/g]	26-Mar-21	11:11	26-Mar-21	17:50	89	120	100	140
Mn [µg/g]	26-Mar-21	11:11	26-Mar-21	17:50	1.4	1.3	0.5	4.0
Mo [µg/g]	26-Mar-21	11:11	26-Mar-21	17:50	0.1	0.6	0.1	0.3
Na [µg/g]	26-Mar-21	11:11	26-Mar-21	17:50	28	35	40	52
Ni [µg/g]	26-Mar-21	11:11	26-Mar-21	17:50	< 0.5	< 0.5	< 0.5	0.7
P [µg/g]	26-Mar-21	11:11	26-Mar-21	17:50	4	4	< 3	10
Pb [µg/g]	26-Mar-21	11:11	26-Mar-21	17:50	< 0.1	< 0.1	< 0.1	0.7
Si [µg/g]	26-Mar-21	11:11	26-Mar-21	17:50	300	290	120	740
Sb [µg/g]	26-Mar-21	11:11	26-Mar-21	17:50	< 0.8	< 0.8	< 0.8	< 0.8
Se [µg/g]	26-Mar-21	11:11	26-Mar-21	17:50	< 0.7	< 0.7	< 0.7	< 0.7
Sn [µg/g]	26-Mar-21	11:11	26-Mar-21	17:50	< 0.5	< 0.5	< 0.5	< 0.5
Tl [µg/g]	26-Mar-21	11:11	26-Mar-21	17:50	< 0.02	< 0.02	< 0.02	< 0.02
U [µg/g]	26-Mar-21	11:11	26-Mar-21	17:50	0.016	0.043	0.004	0.069
V [µg/g]	26-Mar-21	11:11	26-Mar-21	17:50	< 3	< 3	< 3	4
W [µg/g]	26-Mar-21	11:11	26-Mar-21	17:50	< 0.04	< 0.04	< 0.04	< 0.04
Y [µg/g]	26-Mar-21	11:11	26-Mar-21	17:50	0.045	0.042	0.029	0.15
Zn [µg/g]	26-Mar-21	11:11	26-Mar-21	17:50	< 0.7	< 0.7	< 0.7	2.5

`Fraction 1 - Water Soluble`

Catharine Arnold

Catharine Arnold, B.Sc., C.Chem
Project Specialist,
Environment, Health & Safety

SGS Canada Inc.
P.O. Box 4300 - 185 Concession St.
Lakefield - Ontario - KOL 2HO
Phone: 705-652-2000 FAX: 705-652-6365

Fraction 1 Exchangeable Metals

Project : Hennepin MNA

30-March-2021

SiREM Laboratory
Attn : Michael Healey

130 Stone Road W
Guelph, ON
N1G 3Z2, Canada

Phone: 519-822-2265
Fax:519-822-3151

Date Rec. : 05 March 2021
LR Report: **CA14202-MAR21**
Reference: P.O# 800003210A

Copy: #1

CERTIFICATE OF ANALYSIS

Final Report

Analysis	**1: Analysis Start Date**	**2: Analysis Start Time**	**3: Analysis Completed Date**	**4: Analysis Completed Time**	**5: SB-34 32-33'**	**6: SB-51 42-43'**	**7: SB-22 26-27'**	**8: SB-22 29-30'**
Sample Date & Time					04-Mar-21 12:15	04-Mar-21 12:30	04-Mar-21 12:40	04-Mar-21 13:00
Ag [µg/g]	26-Mar-21	11:11	26-Mar-21	17:51	< 0.05	< 0.05	< 0.05	< 0.05
Al [µg/g]	26-Mar-21	11:11	26-Mar-21	17:51	3	4	< 1	3
As [µg/g]	26-Mar-21	11:11	26-Mar-21	17:51	< 0.5	< 0.5	< 0.5	< 0.5
Ba [µg/g]	26-Mar-21	11:11	26-Mar-21	17:51	4.0	4.7	1.5	5.0
Be [µg/g]	26-Mar-21	11:11	26-Mar-21	17:51	< 0.02	< 0.02	< 0.02	< 0.02
B [µg/g]	26-Mar-21	11:11	26-Mar-21	17:51	< 1	< 1	< 1	< 1
Bi [µg/g]	26-Mar-21	11:11	26-Mar-21	17:51	< 0.09	< 0.09	< 0.09	< 0.09
Ca [µg/g]	26-Mar-21	11:11	26-Mar-21	17:51	2200	3200	1000	3500
Cd [µg/g]	26-Mar-21	11:11	26-Mar-21	17:51	< 0.02	< 0.02	< 0.02	0.24
Co [µg/g]	26-Mar-21	11:11	26-Mar-21	17:51	0.02	0.03	< 0.01	0.10
Cr [µg/g]	26-Mar-21	11:11	26-Mar-21	17:51	< 0.5	< 0.5	< 0.5	< 0.5
Cu [µg/g]	26-Mar-21	11:11	26-Mar-21	17:51	0.1	< 0.1	< 0.1	< 0.1
Fe [µg/g]	26-Mar-21	11:11	26-Mar-21	17:51	5	6	< 1	2
K [µg/g]	26-Mar-21	11:11	26-Mar-21	17:51	57	88	58	92
Li [µg/g]	26-Mar-21	11:11	26-Mar-21	17:51	< 2	< 2	< 2	< 2

OnLine LIMS

SGS Canada Inc.
P.O. Box 4300 - 185 Concession St.
Lakefield - Ontario - KOL 2HO
Phone: 705-652-2000 FAX: 705-652-6365

Fraction 1 Exchangeable Metals

Project : Hennepin MNA
LR Report : **CA14202-MAR21**

Analysis	1: Analysis Start Date	2: Analysis Start Time	3: Analysis Completed Date	4: Analysis Completed Time	5: SB-34 32-33'	6: SB-51 42-43'	7: SB-22 26-27'	8: SB-22 29-30'
Mn [µg/g]	26-Mar-21	11:11	26-Mar-21	17:51	6.5	8.5	1.5	17
Mo [µg/g]	26-Mar-21	11:11	26-Mar-21	17:51	< 0.1	0.1	< 0.1	< 0.1
Na [µg/g]	26-Mar-21	11:11	26-Mar-21	17:51	8	9	11	12
Ni [µg/g]	26-Mar-21	11:11	26-Mar-21	17:51	< 0.5	< 0.5	< 0.5	< 0.5
Pb [µg/g]	26-Mar-21	11:11	26-Mar-21	17:51	< 0.1	< 0.1	< 0.1	< 0.1
P [µg/g]	26-Mar-21	11:11	26-Mar-21	17:51	< 3	< 3	< 3	< 3
Sb [µg/g]	26-Mar-21	11:11	26-Mar-21	17:51	< 0.8	< 0.8	< 0.8	< 0.8
Se [µg/g]	26-Mar-21	11:11	26-Mar-21	17:51	< 0.7	< 0.7	< 0.7	< 0.7
Si [µg/g]	26-Mar-21	11:11	26-Mar-21	17:51	32	30	45	30
Sn [µg/g]	26-Mar-21	11:11	26-Mar-21	17:51	< 0.5	< 0.5	< 0.5	< 0.5
Tl [µg/g]	26-Mar-21	11:11	26-Mar-21	17:51	< 0.02	< 0.02	< 0.02	< 0.02
U [µg/g]	26-Mar-21	11:11	26-Mar-21	17:51	0.017	0.061	0.021	0.024
V [µg/g]	26-Mar-21	11:11	26-Mar-21	17:51	< 3	< 3	< 3	< 3
W [µg/g]	26-Mar-21	11:11	26-Mar-21	17:51	< 0.04	< 0.04	< 0.04	< 0.04
Y [µg/g]	26-Mar-21	11:11	26-Mar-21	17:51	0.006	0.006	0.004	0.008
Zn [µg/g]	26-Mar-21	11:11	26-Mar-21	17:51	< 0.7	< 0.7	< 0.7	< 0.7

`Exchangeable Metals`

Catharine Arnold

ASSOCIATION OF THE CHEMICAL PROFESSION OF ONTARIO
CHARTERED
CATHARINE ARNOLD
CHEMIST

Catharine Arnold, B.Sc., C.Chem
Project Specialist,
Environment, Health & Safety

SGS Canada Inc.
P.O. Box 4300 - 185 Concession St.
Lakefield - Ontario - KOL 2HO
Phone: 705-652-2000 FAX: 705-652-6365

Fraction 2 Metals Bound to Carbonates

Project : Hennepin MNA

30-March-2021

SiREM Laboratory
Attn : Michael Healey

130 Stone Road W
Guelph, ON
N1G 3Z2, Canada

Phone: 519-822-2265
Fax:519-822-3151

Date Rec. : 05 March 2021
LR Report: **CA14203-MAR21**
Reference: P.O# 800003210A

Copy: #1

CERTIFICATE OF ANALYSIS

Final Report

Analysis	1: Analysis Start Date	2: Analysis Start Time	3: Analysis Completed Date	4: Analysis Completed Time	5: SB-34 32-33'	6: SB-51 42-43'	7: SB-22 26-27'	8: SB-22 29-30'
Sample Date & Time					04-Mar-21 12:15	04-Mar-21 12:30	04-Mar-21 12:40	04-Mar-21 13:00
Ag [µg/g]	26-Mar-21	11:11	26-Mar-21	17:51	< 0.05	< 0.05	< 0.05	< 0.05
Al [µg/g]	26-Mar-21	11:11	26-Mar-21	17:51	5	2	28	6
As [µg/g]	26-Mar-21	11:11	26-Mar-21	17:51	< 0.5	< 0.5	< 0.5	< 0.5
Ba [µg/g]	26-Mar-21	11:11	26-Mar-21	17:51	20	22	6.0	7.5
Be [µg/g]	26-Mar-21	11:11	26-Mar-21	17:51	< 0.02	< 0.02	< 0.02	0.03
B [µg/g]	26-Mar-21	11:11	26-Mar-21	17:51	< 1	< 1	< 1	1
Bi [µg/g]	26-Mar-21	11:11	26-Mar-21	17:51	< 0.09	< 0.09	< 0.09	< 0.09
Ca [µg/g]	26-Mar-21	11:11	26-Mar-21	17:51	30000	30000	24000	13000
Cd [µg/g]	26-Mar-21	11:11	26-Mar-21	17:51	0.12	0.11	0.37	0.69
Co [µg/g]	26-Mar-21	11:11	26-Mar-21	17:51	0.39	0.39	1.1	1.1
Cr [µg/g]	26-Mar-21	11:11	26-Mar-21	17:51	< 0.5	< 0.5	2.6	9.6
Cu [µg/g]	26-Mar-21	11:11	26-Mar-21	17:51	< 0.1	< 0.1	0.2	< 0.1
Fe [µg/g]	26-Mar-21	11:11	26-Mar-21	17:51	8	4	41	32
K [µg/g]	26-Mar-21	11:11	26-Mar-21	17:51	41	49	45	67
Li [µg/g]	26-Mar-21	11:11	26-Mar-21	17:51	< 2	< 2	< 2	< 2

OnLine LIMS

0002446258

SGS Canada Inc.
P.O. Box 4300 - 185 Concession St.
Lakefield - Ontario - KOL 2HO
Phone: 705-652-2000 FAX: 705-652-6365

Fraction 2 Metals Bound to Carbonates

Project : Hennepin MNA
LR Report : **CA14203-MAR21**

Analysis	**1: Analysis Start Date**	**2: Analysis Start Time**	**3: Analysis Completed Date**	**4: Analysis Completed Time**	**5: SB-34 32-33'**	**6: SB-51 42-43'**	**7: SB-22 26-27'**	**8: SB-22 29-30'**
Mg [µg/g]	26-Mar-21	11:11	26-Mar-21	17:51	2800	4700	2200	7000
Mn [µg/g]	26-Mar-21	11:11	26-Mar-21	17:51	78	74	140	69
Mo [µg/g]	26-Mar-21	11:11	26-Mar-21	17:51	< 0.1	< 0.1	< 0.1	< 0.1
Ni [µg/g]	26-Mar-21	11:11	26-Mar-21	17:51	< 0.5	< 0.5	2.7	1.9
Pb [µg/g]	26-Mar-21	11:11	26-Mar-21	17:51	0.2	0.2	0.3	0.6
P [µg/g]	26-Mar-21	11:11	26-Mar-21	17:51	< 3	< 3	< 3	< 3
Sb [µg/g]	26-Mar-21	11:11	26-Mar-21	17:51	< 0.8	< 0.8	< 0.8	< 0.8
Se [µg/g]	26-Mar-21	11:11	26-Mar-21	17:51	< 0.7	< 0.7	< 0.7	< 0.7
Si [µg/g]	26-Mar-21	11:11	26-Mar-21	17:51	90	77	70	110
Sn [µg/g]	26-Mar-21	11:11	26-Mar-21	17:51	< 0.5	< 0.5	< 0.5	< 0.5
Tl [µg/g]	26-Mar-21	11:11	26-Mar-21	17:51	< 0.02	< 0.02	< 0.02	< 0.02
U [µg/g]	26-Mar-21	11:11	26-Mar-21	17:51	0.039	0.15	0.089	0.030
V [µg/g]	26-Mar-21	11:11	26-Mar-21	17:51	< 3	< 3	< 3	< 3
W [µg/g]	26-Mar-21	11:11	26-Mar-21	17:51	< 0.04	< 0.04	< 0.04	< 0.04
Y [µg/g]	26-Mar-21	11:11	26-Mar-21	17:51	0.57	0.26	1.0	0.23
Zn [µg/g]	26-Mar-21	11:11	26-Mar-21	17:51	1.4	1.4	1.6	1.7

Fraction 2 Metals Bound to Carbonates

Catharine Arnold

CHARTERED CATHARINE ARNOLD CHEMIST

Catharine Arnold, B.Sc., C.Chem
Project Specialist,
Environment, Health & Safety

SGS Canada Inc.
P.O. Box 4300 - 185 Concession St.
Lakefield - Ontario - KOL 2HO
Phone: 705-652-2000 FAX: 705-652-6365

Fraction 3 Metals Bound to Fe and Mn Oxides

Project : Hennepin MNA

30-March-2021

SiREM Laboratory
Attn : Michael Healey

130 Stone Road W
Guelph, ON
N1G 3Z2, Canada

Phone: 519-822-2265
Fax:519-822-3151

Date Rec. : 05 March 2021
LR Report: **CA14204-MAR21**
Reference: P.O# 800003210A

Copy: #1

CERTIFICATE OF ANALYSIS

Final Report

Analysis	**3: Analysis Completed Date**	**4: Analysis Completed Time**	**5: SB-34 32-33'**	**6: SB-51 42-43'**	**7: SB-22 26-27'**	**8: SB-22 29-30'**
Sample Date & Time			04-Mar-21 12:15	04-Mar-21 12:30	04-Mar-21 12:40	04-Mar-21 13:00
Ag [µg/g]	26-Mar-21	17:51	< 0.05	< 0.05	< 0.05	< 0.05
Al [µg/g]	26-Mar-21	17:51	270	320	270	230
As [µg/g]	26-Mar-21	17:51	0.8	0.9	< 0.5	< 0.5
Ba [µg/g]	26-Mar-21	17:51	8.6	29	3.4	5.9
Be [µg/g]	26-Mar-21	17:51	0.14	0.22	0.07	0.48
B [µg/g]	26-Mar-21	17:51	1	2	2	2
Bi [µg/g]	26-Mar-21	17:51	0.12	0.29	< 0.09	< 0.09
Ca [µg/g]	26-Mar-21	17:51	18000	49000	30000	18000
Cd [µg/g]	26-Mar-21	17:51	0.25	0.59	0.16	1.1
Co [µg/g]	26-Mar-21	17:51	1.4	2.2	0.70	2.6
Cr [µg/g]	26-Mar-21	17:51	14	5.3	30	28
Cu [µg/g]	26-Mar-21	17:51	0.1	< 0.1	1.6	0.3
Fe [µg/g]	26-Mar-21	17:51	3100	2500	1600	1100
K [µg/g]	26-Mar-21	17:51	54	73	61	82
Li [µg/g]	26-Mar-21	17:51	< 2	< 2	< 2	< 2

Analysis	**3: Analysis Completed Date**	**4: Analysis Completed Time**	**5: SB-34 32-33'**	**6: SB-51 42-43'**	**7: SB-22 26-27'**	**8: SB-22 29-30'**
Mg [µg/g]	26-Mar-21	17:51	9000	7000	17000	10000
Mn [µg/g]	26-Mar-21	17:51	110	170	90	65
Mo [µg/g]	26-Mar-21	17:51	0.1	0.2	0.5	0.2
Na [µg/g]	26-Mar-21	17:51	850	3700	540	2200
Ni [µg/g]	26-Mar-21	17:51	2.9	3.7	3.1	9.9
Pb [µg/g]	26-Mar-21	17:51	3.1	5.7	3.1	7.7
P [µg/g]	26-Mar-21	17:51	100	71	59	35
Sb [µg/g]	26-Mar-21	17:51	< 0.8	< 0.8	< 0.8	< 0.8
Se [µg/g]	26-Mar-21	17:51	< 0.7	< 0.7	< 0.7	< 0.7
Si [µg/g]	26-Mar-21	17:51	480	450	410	410
Sn [µg/g]	26-Mar-21	17:51	< 0.5	< 0.5	< 0.5	< 0.5
Tl [µg/g]	26-Mar-21	17:51	0.02	0.03	0.03	< 0.02
U [µg/g]	26-Mar-21	17:51	0.095	0.19	0.27	0.31
V [µg/g]	26-Mar-21	17:51	< 3	< 3	< 3	4
W [µg/g]	26-Mar-21	17:51	< 0.04	< 0.04	< 0.04	< 0.04
Y [µg/g]	26-Mar-21	17:51	1.8	2.6	1.8	1.4
Zn [µg/g]	26-Mar-21	17:51	14	24	7.4	26

Fraction 3 Metals Bound to Fe and Mn Oxides

Catharine Arnold

CATHARINE ARNOLD

Catharine Arnold, B.Sc., C.Chem
Project Specialist,
Environment, Health & Safety

SGS Canada Inc.
P.O. Box 4300 - 185 Concession St.
Lakefield - Ontario - KOL 2HO
Phone: 705-652-2000 FAX: 705-652-6365

Fraction 4 Bound to Organic Material

30-March-2021

SiREM Laboratory
Attn : Michael Healey

130 Stone Road W
Guelph, ON
N1G 3Z2, Canada

Phone: 519-822-2265
Fax:519-822-3151

Date Rec. : 08 March 2021
LR Report: **CA14205-MAR21**
Reference: P.O# 800003210A

Copy: #1

CERTIFICATE OF ANALYSIS

Final Report

Analysis	**3: Analysis Completed Date**	**4: Analysis Completed Time**	**5: SB-34 32-33'**	**6: SB-51 42-43'**	**7: SB-22 26-27'**	**8: SB-22 29-30'**
Sample Date & Time			04-Mar-21 12:15	04-Mar-21 12:30	04-Mar-21 12:40	04-Mar-21 13:00
Ag [µg/g]	26-Mar-21	17:51	< 0.05	< 0.05	< 0.05	< 0.05
Al [µg/g]	26-Mar-21	17:51	77	120	150	630
As [µg/g]	26-Mar-21	17:51	< 0.5	< 0.5	< 0.5	< 0.5
Ba [µg/g]	26-Mar-21	17:51	1.5	5.5	1.1	2.4
Be [µg/g]	26-Mar-21	17:51	< 0.02	< 0.02	< 0.02	0.18
B [µg/g]	26-Mar-21	17:51	< 1	1	< 1	< 1
Bi [µg/g]	26-Mar-21	17:51	< 0.09	< 0.09	< 0.09	< 0.09
Ca [µg/g]	26-Mar-21	17:51	1800	3700	600	1300
Cd [µg/g]	26-Mar-21	17:51	0.03	0.03	0.03	0.25
Co [µg/g]	26-Mar-21	17:51	1.0	0.87	0.12	1.1
Cr [µg/g]	26-Mar-21	17:51	3.8	2.5	3.3	20
Cu [µg/g]	26-Mar-21	17:51	2.0	3.4	1.0	11
Fe [µg/g]	26-Mar-21	17:51	170	180	34	1100
K [µg/g]	26-Mar-21	17:51	12	22	24	45
Li [µg/g]	26-Mar-21	17:51	< 2	< 2	< 2	< 2

Analysis	**3: Analysis Completed Date**	**4: Analysis Completed Time**	**5: SB-34 32-33'**	**6: SB-51 42-43'**	**7: SB-22 26-27'**	**8: SB-22 29-30'**
Mg [µg/g]	26-Mar-21	17:51	1800	3400	240	490
Mn [µg/g]	26-Mar-21	17:51	5.1	7.5	3.5	11
Mo [µg/g]	26-Mar-21	17:51	0.2	0.1	0.3	1.0
Na [µg/g]	26-Mar-21	17:51	10	65	15	36
Ni [µg/g]	26-Mar-21	17:51	1.1	1.8	0.7	15
Pb [µg/g]	26-Mar-21	17:51	0.2	0.2	0.2	1.9
P [µg/g]	26-Mar-21	17:51	70	51	23	24
Sb [µg/g]	26-Mar-21	17:51	< 0.8	< 0.8	< 0.8	< 0.8
Se [µg/g]	26-Mar-21	17:51	< 0.7	0.9	< 0.7	< 0.7
Si [µg/g]	26-Mar-21	17:51	130	160	220	480
Sn [µg/g]	26-Mar-21	17:51	< 0.5	< 0.5	< 0.5	< 0.5
Tl [µg/g]	26-Mar-21	17:51	0.03	0.04	< 0.02	0.02
U [µg/g]	26-Mar-21	17:51	0.097	0.086	0.12	0.48
V [µg/g]	26-Mar-21	17:51	< 3	< 3	< 3	8
W [µg/g]	26-Mar-21	17:51	< 0.04	< 0.04	< 0.04	< 0.04
Y [µg/g]	26-Mar-21	17:51	0.42	0.31	1.0	3.0
Zn [µg/g]	26-Mar-21	17:51	2.5	2.8	1.7	9.7

`Fraction 4 Bound to Organic Material`

Catharine Arnold

CATHARINE ARNOLD

Catharine Arnold, B.Sc., C.Chem
Project Specialist,
Environment, Health & Safety

OnLine LIMS

0002446266

SGS Canada Inc.
P.O. Box 4300 - 185 Concession St.
Lakefield - Ontario - KOL 2HO
Phone: 705-652-2000 FAX: 705-652-6365

Fraction 5 Residual metals

Project : Hennepin MNA

30-March-2021

SiREM Laboratory
Attn : Michael Healey

130 Stone Road W
Guelph, ON
N1G 3Z2, Canada

Phone: 519-822-2265
Fax:519-822-3151

Date Rec. : 05 March 2021
LR Report: **CA14206-MAR21**
Reference: P.O# 800003210A

Copy: #1

CERTIFICATE OF ANALYSIS

Final Report

Analysis	**3: Analysis Completed Date**	**4: Analysis Completed Time**	**5: SB-34 32-33'**	**6: SB-51 42-43'**	**7: SB-22 26-27'**	**8: SB-22 29-30'**
Sample Date & Time			04-Mar-21 12:15	04-Mar-21 12:30	04-Mar-21 12:40	04-Mar-21 13:00
Ag [µg/g]	26-Mar-21	17:52	0.06	0.09	0.07	0.09
Al [µg/g]	26-Mar-21	17:52	22000	24000	14000	17000
As [µg/g]	26-Mar-21	17:52	1.9	2.7	3.9	6.6
Ba [µg/g]	26-Mar-21	17:52	190	170	130	130
Be [µg/g]	26-Mar-21	17:52	0.46	0.74	0.29	0.47
B [µg/g]	26-Mar-21	17:52	13	26	10	18
Bi [µg/g]	26-Mar-21	17:52	< 0.09	0.21	< 0.09	0.16
Ca [µg/g]	26-Mar-21	17:52	3000	4400	1800	1700
Cd [µg/g]	26-Mar-21	17:52	0.05	0.07	0.10	0.23
Co [µg/g]	26-Mar-21	17:52	3.9	5.4	2.9	3.9
Cr [µg/g]	26-Mar-21	17:52	37	39	54	98
Cu [µg/g]	26-Mar-21	17:52	5.7	9.6	7.4	9.7
Fe [µg/g]	26-Mar-21	17:52	8800	14000	8500	10000
K [µg/g]	26-Mar-21	17:52	9500	10000	6500	7500
Li [µg/g]	26-Mar-21	17:52	11	18	5	13

Analysis	**3: Analysis Completed Date**	**4: Analysis Completed Time**	**5: SB-34 32-33'**	**6: SB-51 42-43'**	**7: SB-22 26-27'**	**8: SB-22 29-30'**
Mg [µg/g]	26-Mar-21	17:52	1900	2300	1100	1100
Mn [µg/g]	26-Mar-21	17:52	68	95	60	54
Mo [µg/g]	26-Mar-21	17:52	0.5	0.9	1.8	3.4
Na [µg/g]	26-Mar-21	17:52	4100	3200	3600	3900
Ni [µg/g]	26-Mar-21	17:52	8.2	14	7.4	11
Pb [µg/g]	26-Mar-21	17:52	5.2	6.5	5.3	17
P [µg/g]	26-Mar-21	17:52	130	210	160	200
Sb [µg/g]	26-Mar-21	17:52	< 0.8	< 0.8	< 0.8	1.0
Se [µg/g]	26-Mar-21	17:52	< 0.7	< 0.7	< 0.7	< 0.7
Si [µg/g]	26-Mar-21	17:52	8500	25000	34000	31000
Sn [µg/g]	26-Mar-21	17:52	2.9	3.6	2.9	4.3
Tl [µg/g]	26-Mar-21	17:52	0.23	0.34	0.15	0.29
U [µg/g]	26-Mar-21	17:52	0.84	1.4	1.0	1.3
V [µg/g]	26-Mar-21	17:52	28	49	25	78
W [µg/g]	26-Mar-21	17:52	0.24	0.40	0.15	0.23
Y [µg/g]	26-Mar-21	17:52	4.1	4.1	3.3	3.1
Zn [µg/g]	26-Mar-21	17:52	24	39	33	62

`Fraction 5 Residual metals`

Catharine Arnold

CHARTERED
CATHARINE ARNOLD
CHEMIST

Catharine Arnold, B.Sc., C.Chem
Project Specialist,
Environment, Health & Safety

ATTACHMENT G

X-Ray Diffraction Analytical Data

Quantitative X-Ray Diffraction by Rietveld Refinement

Report Prepared for:	*Environmental Services*
Project Number/ LIMS No.	*Custom XRD/MI4516-MAR21*
Sample Receipt:	*March 12, 2021*
Sample Analysis:	*March 25, 2021*
Reporting Date:	*April 8, 2021*

Instrument:	BRUKER AXS D8 Advance Diffractometer
Test Conditions:	Co radiation, 35 kV, 40 mA Regular Scanning: Step: 0.02°, Step time: 1s, 2θ range: 3-80°
Interpretations :	PDF2/PDF4 powder diffraction databases issued by the International Center for Diffraction Data (ICDD). DiffracPlus Eva and Topas software.
Detection Limit :	0.5-2%. Strongly dependent on crystallinity.

Contents:

1) Method Summary
2) Quantitative XRD Results
3) XRD Pattern(s)

Kim Gibbs

Kim Gibbs, H.B.Sc., P.Geo.
Senior Mineralogist

Huyun Zhou

Huyun Zhou, Ph.D., P.Geo.
Senior Mineralogist

ACCREDITATION: SGS Minerals Services Lakefield is accredited to the requirements of ISO/IEC 17025 for specific tests as listed on our scope of accreditation, including geochemical, mineralogical and trade mineral tests. To view a list of the accredited methods, please visit the following website and search SGS Canada - Minerals Services - Lakefield: http://palcan.scc.ca/SpecsSearch/GLSearchForm.do.

Method Summary

The Rietveld Method of Mineral Identification by XRD (ME-LR-MIN-MET-MN-D05) method used by SGS Minerals Services is accredited to the requirements of ISO/IEC 17025.

Mineral Identification and Interpretation:

Mineral identification and interpretation involves matching the diffraction pattern of an unknown material to patterns of single-phase reference materials. The reference patterns are compiled by the Joint Committee on Powder Diffraction Standards - International Center for Diffraction Data (JCPDS-ICDD) database and released on software as Powder Diffraction Files (PDF).

Interpretations do not reflect the presence of non-crystalline and/or amorphous compounds, except when internal standards have been added by request. Mineral proportions may be strongly influenced by crystallinity, crystal structure and preferred orientations. Mineral or compound identification and quantitative analysis results should be accompanied by supporting chemical assay data or other additional tests.

Quantitative Rietveld Analysis:

Quantitative Rietveld Analysis is performed by using Topas 4.2 (Bruker AXS), a graphics based profile analysis program built around a non-linear least squares fitting system, to determine the amount of different phases present in a multicomponent sample. Whole pattern analyses are predicated by the fact that the X-ray diffraction pattern is a total sum of both instrumental and specimen factors. Unlike other peak intensity-based methods, the Rietveld method uses a least squares approach to refine a theoretical line profile until it matches the obtained experimental patterns.

Rietveld refinement is completed with a set of minerals specifically identified for the sample. Zero values indicate that the mineral was included in the refinement calculations, but the calculated concentration was less than 0.05wt%. Minerals not identified by the analyst are not included in refinement calculations for specific samples and are indicated with a dash.

Summary of Rietveld Quantitative Analysis X-Ray Diffraction Results

Mineral/Compound	**SB-34 32-33'** **MAR4516-01** (wt %)	**SB-51 42-43'** **MAR4516-02** (wt %)	**SB-22 26-27'** **MAR4516-03** (wt %)	**SB-22 29-30'** **MAR4516-04** (wt %)
Quartz	53.0	33.1	57.0	54.5
Microcline	5.1	9.8	5.2	5.2
Chlorite	3.4	6.8	1.9	2.7
Kaolinite	3.4	3.4	0.6	2.5
Muscovite	7.9	12.5	2.1	7.4
Calcite	11.1	20.9	7.2	3.3
Dolomite	2.6	5.0	14.4	11.4
Ankerite	6.0	1.3	2.9	2.8
Pyrite	0.2	0.3	-	-
Magnetite	0.4	0.2	0.5	0.4
Albite	7.1	6.6	7.3	9.8
Actinolite	-	-	0.8	-
TOTAL	100	100	100	100

Zero values indicate that the mineral was included in the refinement, but the calculated concentration is below a measurable value.

Dashes indicate that the mineral was not identified by the analyst and not included in the refinement calculation for the sample.

The weight percent quantities indicated have been normalized to a sum of 100%. The quantity of amorphous material has not been determined.

Mineral/Compound	**Formula**
Quartz	SiO_2
Microcline	$KAlSi_3O_8$
Chlorite	$(Fe,(Mg,Mn)_5,Al)(Si_3Al)O_{10}(OH)_8$
Kaolinite	$Al_2Si_2O_5(OH)_4$
Muscovite	$KAl_2(AlSi_3O_{10})(OH)_2$
Calcite	$CaCO_3$
Dolomite	$CaMg(CO_3)_2$
Ankerite	$CaFe(CO_3)_2$
Pyrite	FeS_2
Magnetite	Fe_3O_4
Albite	$NaAlSi_3O_8$
Actinolite	$Ca_2(Mg,Fe)_5Si_8O_{22}(OH)_2$

SB-34 32-33'

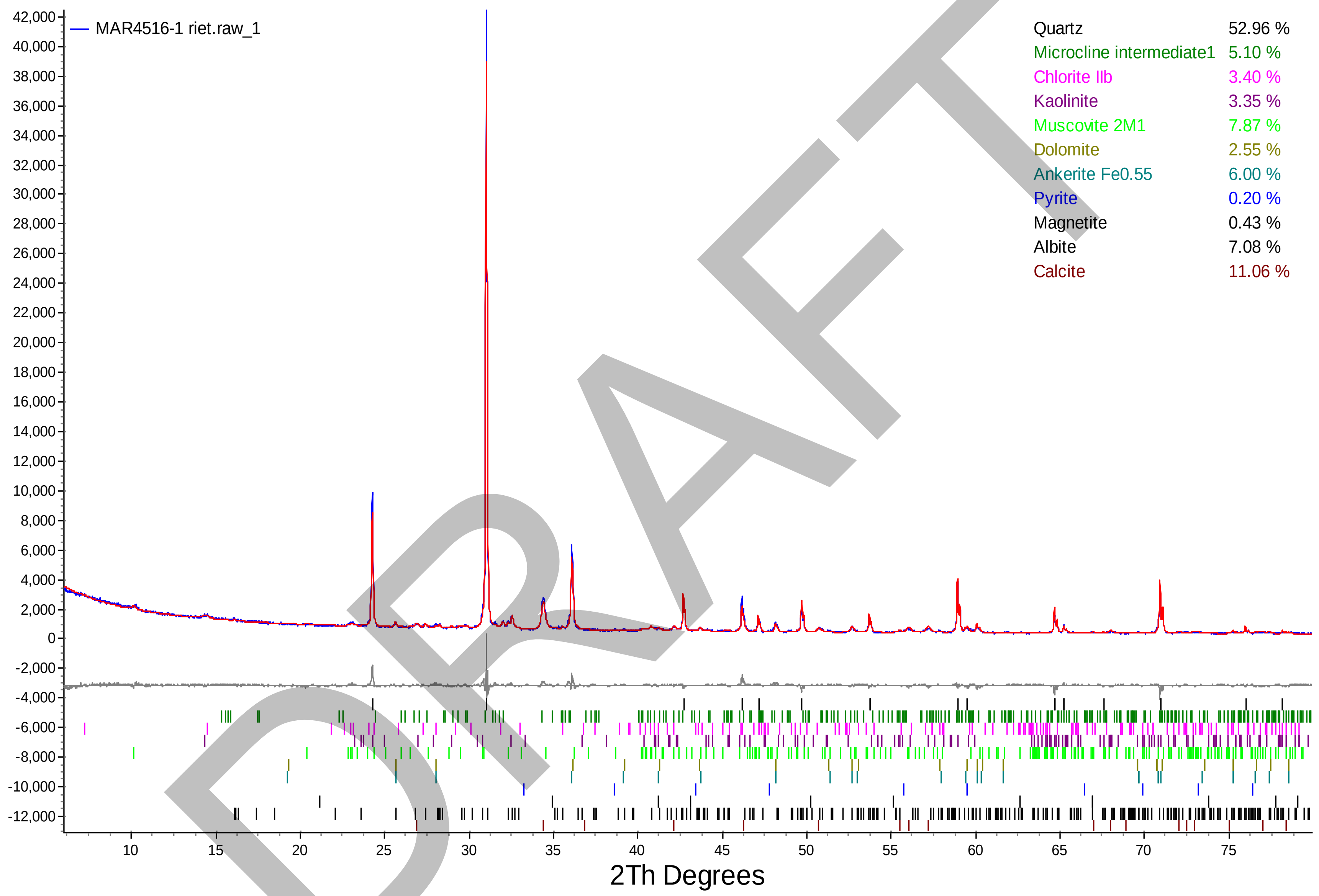
MAR4516-1 riet.raw_1
Quartz 52.96 %
Microcline intermediate1 5.10 %
Chlorite IIb 3.40 %
Kaolinite 3.35 %
Muscovite 2M1 7.87 %
Dolomite 2.55 %
Ankerite Fe0.55 6.00 %
Pyrite 0.20 %
Magnetite 0.43 %
Albite 7.08 %
Calcite 11.06 %
42,000
40,000
38,000
36,000
34,000
32,000
30,000
28,000
26,000
24,000
22,000
20,000
18,000
16,000
14,000
12,000
10,000
8,000
6,000
4,000
2,000
0
-2,000
-4,000
-6,000
-8,000
-10,000
-12,000
10
15
20
25
30
35
40
45
50
55
60
65
70
75
2Th Degrees

SB-51 42-43'

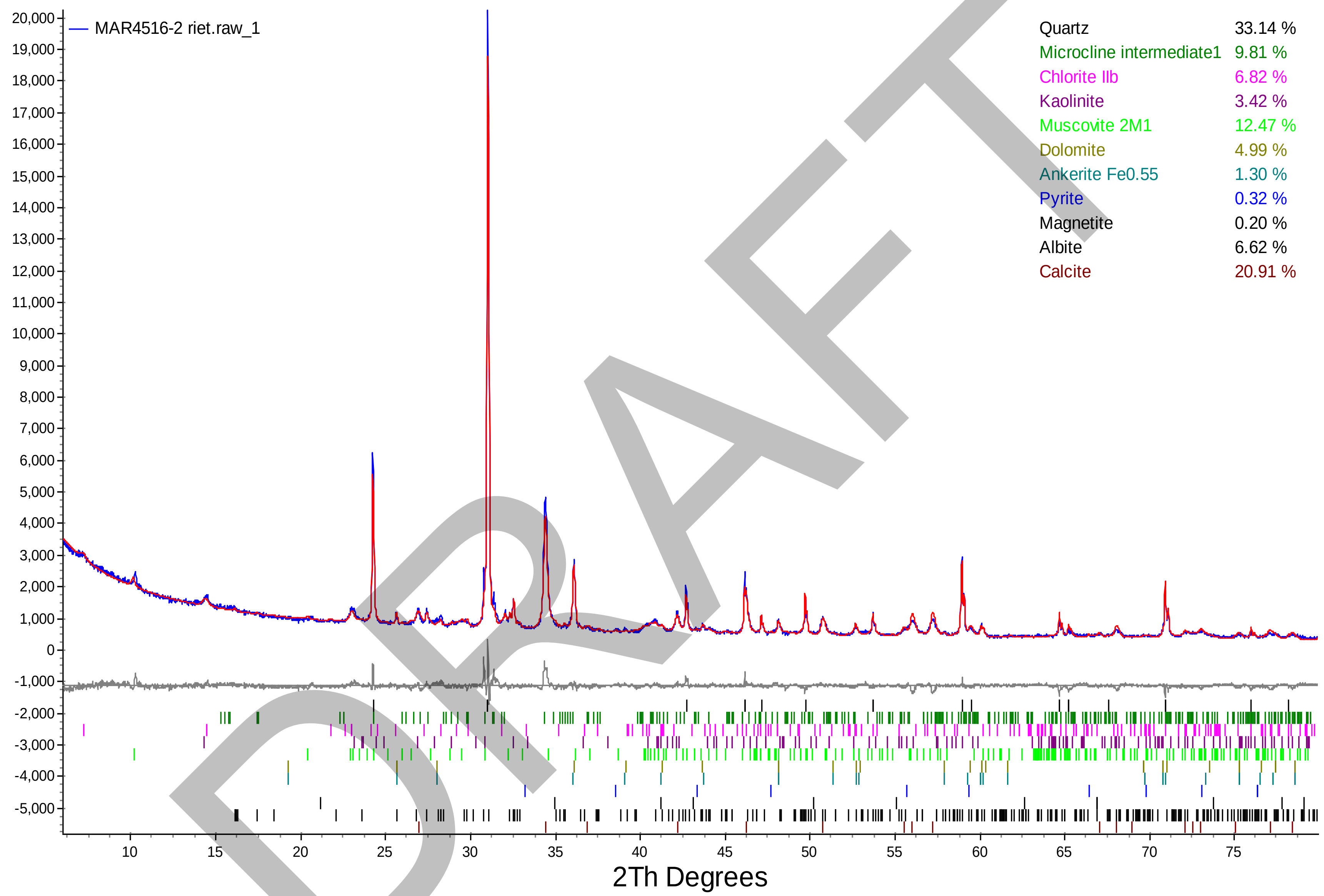

Quartz	33.14 %
Microcline intermediate1	9.81 %
Chlorite IIb	6.82 %
Kaolinite	3.42 %
Muscovite 2M1	12.47 %
Dolomite	4.99 %
Ankerite Fe0.55	1.30 %
Pyrite	0.32 %
Magnetite	0.20 %
Albite	6.62 %
Calcite	20.91 %

SB-22 26-27'

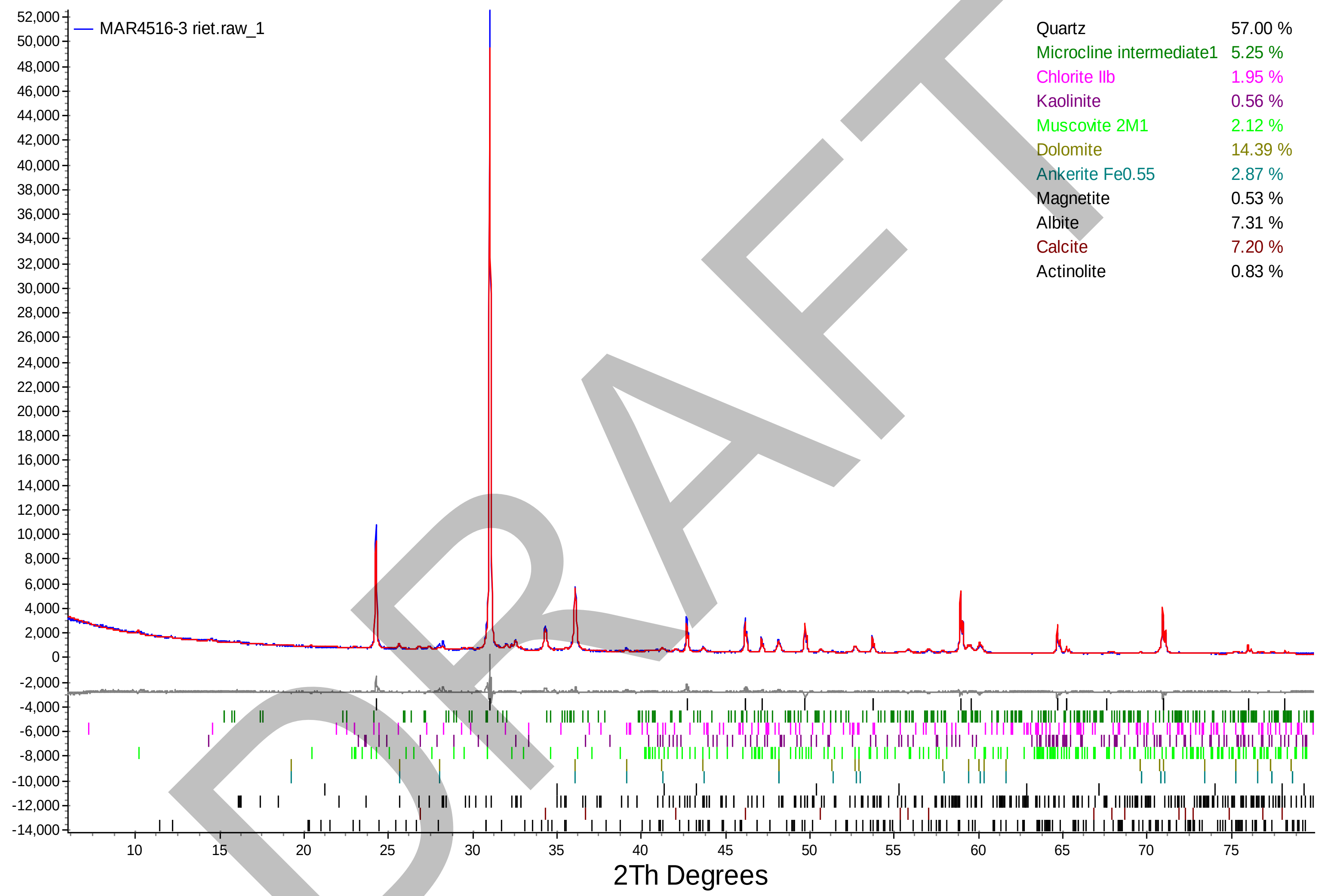

Quartz	57.00 %
Microcline intermediate1	5.25 %
Chlorite IIb	1.95 %
Kaolinite	0.56 %
Muscovite 2M1	2.12 %
Dolomite	14.39 %
Ankerite Fe0.55	2.87 %
Magnetite	0.53 %
Albite	7.31 %
Calcite	7.20 %
Actinolite	0.83 %

SB-22 29-30'

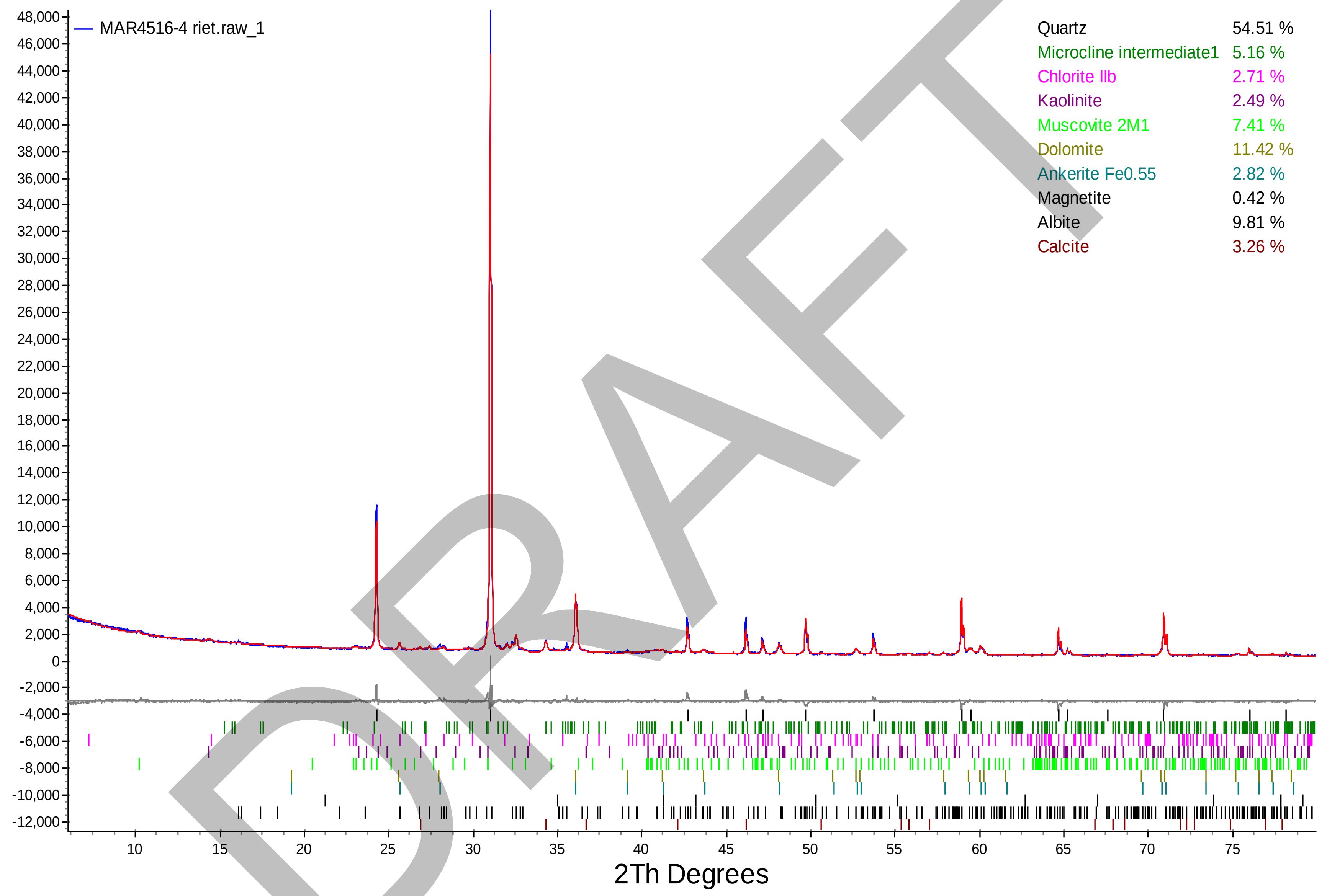
MAR4516-4 riet.raw_1
Quartz 54.51 %
Microcline intermediate1 5.16 %
Chlorite IIb 2.71 %
Kaolinite 2.49 %
Muscovite 2M1 7.41 %
Dolomite 11.42 %
Ankerite Fe0.55 2.82 %
Magnetite 0.42 %
Albite 9.81 %
Calcite 3.26 %
48,000
46,000
44,000
42,000
40,000
38,000
36,000
34,000
32,000
30,000
28,000
26,000
24,000
22,000
20,000
18,000
16,000
14,000
12,000
10,000
8,000
6,000
4,000
2,000
0
-2,000
-4,000
-6,000
-8,000
-10,000
-12,000
10
15
20
25
30
35
40
45
50
55
60
65
70
75
2Th Degrees

ATTACHMENT H

Groundwater Data Summary

Attachment H. Groundwater Data Summary
Geochemical Conceptual Site Model
Hennepin West Ash Pond System
Hennepin Power Plant
Hennepin, IL

HSU	Location	Well Type	Date	Parameter	Unit	Result
UA	32	B	2013/03/08	pH (field)	SU	7.2
UA	32	B	2013/06/26	pH (field)	SU	7.5
UA	32	B	2013/09/03	pH (field)	SU	7.4
UA	32	B	2013/12/10	pH (field)	SU	7.3
UA	32	B	2014/03/25	pH (field)	SU	7.2
UA	32	B	2014/08/19	pH (field)	SU	7.5
UA	32	B	2014/09/30	pH (field)	SU	7.4
UA	32	B	2015/03/18	pH (field)	SU	7.3
UA	32	B	2015/09/16	pH (field)	SU	7.2
UA	32	B	2015/12/10	pH (field)	SU	7.1
UA	32	B	2016/03/08	pH (field)	SU	7.1
UA	32	B	2016/06/07	pH (field)	SU	6.9
UA	32	B	2016/09/15	pH (field)	SU	7.2
UA	32	B	2016/12/07	pH (field)	SU	6.8
UA	32	B	2017/02/21	pH (field)	SU	7.2
UA	32	B	2017/04/25	pH (field)	SU	7.3
UA	32	B	2017/06/08	pH (field)	SU	7.1
UA	32	B	2017/09/06	pH (field)	SU	7.0
UA	32	B	2017/11/15	pH (field)	SU	7.2
UA	32	B	2018/03/26	pH (field)	SU	7.3
UA	32	B	2018/06/13	pH (field)	SU	6.2
UA	32	B	2018/09/12	pH (field)	SU	7.0
UA	32	B	2018/12/12	pH (field)	SU	7.2
UA	32	B	2019/03/13	pH (field)	SU	7.2
UA	32	B	2019/09/18	pH (field)	SU	7.1
UA	32	B	2019/12/11	pH (field)	SU	7.1
UA	32	B	2020/03/11	pH (field)	SU	7.2
UA	32	B	2020/06/25	pH (field)	SU	7.2
UA	32	B	2020/09/02	pH (field)	SU	7.3
UA	32	B	2020/12/09	pH (field)	SU	7.2
UA	32	B	2021/03/17	pH (field)	SU	7.1
UA	32	B	2021/06/24	pH (field)	SU	6.9
UA	32	B	2021/09/09	pH (field)	SU	7.0
UA	32	B	2021/12/08	pH (field)	SU	7.0
UA	32	B	2022/03/22	pH (field)	SU	7.0
UA	32	B	2022/06/07	pH (field)	SU	7.1
UA	32	B	2022/09/13	pH (field)	SU	7.0
UA	32	B	2022/12/27	pH (field)	SU	7.1
UA	32	B	2023/02/28	pH (field)	SU	7.0
UA	32	B	2023/05/31	pH (field)	SU	6.9
UA	32	B	2023/08/22	pH (field)	SU	7.1
UA	32	B	2023/11/14	pH (field)	SU	7.2
UA	32	B	2015/12/10	Oxidation Reduction Potential	mV	182
UA	32	B	2016/03/08	Oxidation Reduction Potential	mV	54.0
UA	32	B	2016/06/07	Oxidation Reduction Potential	mV	193
UA	32	B	2016/09/15	Oxidation Reduction Potential	mV	157
UA	32	B	2016/12/07	Oxidation Reduction Potential	mV	217
UA	32	B	2017/02/21	Oxidation Reduction Potential	mV	-9.00
UA	32	B	2017/04/25	Oxidation Reduction Potential	mV	34.0
UA	32	B	2017/06/08	Oxidation Reduction Potential	mV	125
UA	32	B	2017/11/15	Oxidation Reduction Potential	mV	159
UA	32	B	2018/06/13	Oxidation Reduction Potential	mV	187
UA	32	B	2018/09/12	Oxidation Reduction Potential	mV	119
UA	32	B	2018/12/12	Oxidation Reduction Potential	mV	46.0
UA	32	B	2019/03/13	Oxidation Reduction Potential	mV	94.0

UA	32	B	2019/09/18	Oxidation Reduction Potential	mV	118
UA	32	B	2019/12/11	Oxidation Reduction Potential	mV	32.0
UA	32	B	2020/03/11	Oxidation Reduction Potential	mV	63.0
UA	32	B	2020/06/25	Oxidation Reduction Potential	mV	185
UA	32	B	2020/09/02	Oxidation Reduction Potential	mV	100
UA	32	B	2020/12/09	Oxidation Reduction Potential	mV	30.0
UA	32	B	2021/03/17	Oxidation Reduction Potential	mV	21.0
UA	32	B	2021/06/24	Oxidation Reduction Potential	mV	34.0
UA	32	B	2021/09/09	Oxidation Reduction Potential	mV	71.0
UA	32	B	2021/12/08	Oxidation Reduction Potential	mV	27.0
UA	32	B	2022/03/22	Oxidation Reduction Potential	mV	13.0
UA	32	B	2022/06/07	Oxidation Reduction Potential	mV	78.0
UA	32	B	2022/09/13	Oxidation Reduction Potential	mV	118
UA	32	B	2022/12/27	Oxidation Reduction Potential	mV	33.0
UA	32	B	2023/02/28	Oxidation Reduction Potential	mV	116
UA	32	B	2023/05/31	Oxidation Reduction Potential	mV	86.0
UA	32	B	2023/08/22	Oxidation Reduction Potential	mV	152
UA	32	B	2023/11/14	Oxidation Reduction Potential	mV	46.9
UA	32	B	2015/12/10	Eh	V	0.38
UA	32	B	2016/03/08	Eh	V	0.25
UA	32	B	2016/06/07	Eh	V	0.39
UA	32	B	2016/09/15	Eh	V	0.35
UA	32	B	2016/12/07	Eh	V	0.41
UA	32	B	2017/02/21	Eh	V	0.19
UA	32	B	2017/04/25	Eh	V	0.23
UA	32	B	2017/06/08	Eh	V	0.32
UA	32	B	2017/11/15	Eh	V	0.36
UA	32	B	2018/06/13	Eh	V	0.38
UA	32	B	2018/09/12	Eh	V	0.32
UA	32	B	2018/12/12	Eh	V	0.24
UA	32	B	2019/03/13	Eh	V	0.29
UA	32	B	2019/09/18	Eh	V	0.31
UA	32	B	2019/12/11	Eh	V	0.23
UA	32	B	2020/03/11	Eh	V	0.26
UA	32	B	2020/06/25	Eh	V	0.38
UA	32	B	2020/09/02	Eh	V	0.30
UA	32	B	2020/12/09	Eh	V	0.23
UA	32	B	2021/03/17	Eh	V	0.22
UA	32	B	2021/06/24	Eh	V	0.23
UA	32	B	2021/09/09	Eh	V	0.27
UA	32	B	2021/12/08	Eh	V	0.22
UA	32	B	2022/03/22	Eh	V	0.21
UA	32	B	2022/06/07	Eh	V	0.28
UA	32	B	2022/09/13	Eh	V	0.31
UA	32	B	2022/12/27	Eh	V	0.23
UA	32	B	2023/02/28	Eh	V	0.31
UA	32	B	2023/05/31	Eh	V	0.28
UA	32	B	2023/08/22	Eh	V	0.35
UA	32	B	2023/11/14	Eh	V	0.24
UA	32	B	2019/09/18	Alkalinity, bicarbonate	mg/L CaCO3	294
UA	32	B	2020/03/11	Alkalinity, bicarbonate	mg/L CaCO3	324
UA	32	B	2021/03/17	Alkalinity, bicarbonate	mg/L CaCO3	324
UA	32	B	2021/09/09	Alkalinity, bicarbonate	mg/L CaCO3	335
UA	32	B	2022/03/22	Alkalinity, bicarbonate	mg/L CaCO3	317
UA	32	B	2022/09/13	Alkalinity, bicarbonate	mg/L CaCO3	326
UA	32	B	2023/02/28	Alkalinity, bicarbonate	mg/L CaCO3	341
UA	32	B	2023/05/31	Alkalinity, bicarbonate	mg/L CaCO3	329
UA	32	B	2023/08/22	Alkalinity, bicarbonate	mg/L CaCO3	320
UA	32	B	2023/11/14	Alkalinity, bicarbonate	mg/L CaCO3	340
UA	32	B	2013/06/26	Arsenic, total	mg/L	<0.0007
UA	32	B	2013/09/03	Arsenic, total	mg/L	<0.0007
UA	32	B	2015/12/10	Arsenic, total	mg/L	<0.0002

UA	32	B	2016/03/08	Arsenic, total	mg/L	<0.0002
UA	32	B	2016/06/07	Arsenic, total	mg/L	<0.0002
UA	32	B	2016/09/15	Arsenic, total	mg/L	<0.0002
UA	32	B	2016/12/07	Arsenic, total	mg/L	<0.0002
UA	32	B	2017/02/21	Arsenic, total	mg/L	<0.0002
UA	32	B	2017/04/25	Arsenic, total	mg/L	<0.0002
UA	32	B	2017/06/08	Arsenic, total	mg/L	<0.0002
UA	32	B	2018/06/13	Arsenic, total	mg/L	<0.0004
UA	32	B	2018/09/12	Arsenic, total	mg/L	<0.0004
UA	32	B	2018/12/12	Arsenic, total	mg/L	<0.0004
UA	32	B	2019/03/13	Arsenic, total	mg/L	0.00100
UA	32	B	2019/09/18	Arsenic, total	mg/L	<0.0004
UA	32	B	2019/12/11	Arsenic, total	mg/L	<0.0004
UA	32	B	2020/03/11	Arsenic, total	mg/L	<0.0004
UA	32	B	2020/06/25	Arsenic, total	mg/L	<0.0004
UA	32	B	2020/09/02	Arsenic, total	mg/L	<0.0004
UA	32	B	2020/12/09	Arsenic, total	mg/L	<0.0004
UA	32	B	2021/03/17	Arsenic, total	mg/L	<0.0004
UA	32	B	2021/06/24	Arsenic, total	mg/L	<0.0004
UA	32	B	2021/09/09	Arsenic, total	mg/L	<0.0004
UA	32	B	2021/12/08	Arsenic, total	mg/L	<0.0004
UA	32	B	2022/03/22	Arsenic, total	mg/L	<0.0004
UA	32	B	2022/06/07	Arsenic, total	mg/L	0.000500
UA	32	B	2022/09/13	Arsenic, total	mg/L	<0.0004
UA	32	B	2022/12/27	Arsenic, total	mg/L	<0.0004
UA	32	B	2023/02/28	Arsenic, total	mg/L	<0.0004
UA	32	B	2023/05/31	Arsenic, total	mg/L	<0.0087
UA	32	B	2023/08/22	Arsenic, total	mg/L	0.000490
UA	32	B	2023/11/14	Arsenic, total	mg/L	0.000370
UA	32	B	2013/06/26	Barium, total	mg/L	0.0421
UA	32	B	2013/09/03	Barium, total	mg/L	0.0438
UA	32	B	2015/12/10	Barium, total	mg/L	0.0332
UA	32	B	2016/03/08	Barium, total	mg/L	0.0340
UA	32	B	2016/06/07	Barium, total	mg/L	0.0290
UA	32	B	2016/09/15	Barium, total	mg/L	0.0347
UA	32	B	2016/12/07	Barium, total	mg/L	0.0387
UA	32	B	2017/02/21	Barium, total	mg/L	0.0317
UA	32	B	2017/04/25	Barium, total	mg/L	0.0329
UA	32	B	2017/06/08	Barium, total	mg/L	0.0340
UA	32	B	2018/06/13	Barium, total	mg/L	0.0338
UA	32	B	2018/09/12	Barium, total	mg/L	0.0403
UA	32	B	2018/12/12	Barium, total	mg/L	0.0407
UA	32	B	2019/03/13	Barium, total	mg/L	0.0420
UA	32	B	2019/09/18	Barium, total	mg/L	0.0412
UA	32	B	2019/12/11	Barium, total	mg/L	0.0458
UA	32	B	2020/03/11	Barium, total	mg/L	0.0419
UA	32	B	2020/06/25	Barium, total	mg/L	0.0426
UA	32	B	2020/09/02	Barium, total	mg/L	0.0449
UA	32	B	2020/12/09	Barium, total	mg/L	0.0577
UA	32	B	2021/03/17	Barium, total	mg/L	0.0399
UA	32	B	2021/06/24	Barium, total	mg/L	0.0392
UA	32	B	2021/09/09	Barium, total	mg/L	0.0428
UA	32	B	2021/12/08	Barium, total	mg/L	0.0429
UA	32	B	2022/03/22	Barium, total	mg/L	0.0407
UA	32	B	2022/06/07	Barium, total	mg/L	0.0575
UA	32	B	2022/09/13	Barium, total	mg/L	0.0380
UA	32	B	2022/12/27	Barium, total	mg/L	0.0406
UA	32	B	2023/02/28	Barium, total	mg/L	0.0590
UA	32	B	2023/05/31	Barium, total	mg/L	0.0410
UA	32	B	2023/08/22	Barium, total	mg/L	0.0390
UA	32	B	2023/11/14	Barium, total	mg/L	0.0430
UA	32	B	2013/06/26	Boron, total	mg/L	0.0833

UA	32	B	2013/09/03	Boron, total	mg/L	0.0859
UA	32	B	2015/12/10	Boron, total	mg/L	0.101
UA	32	B	2016/03/08	Boron, total	mg/L	0.101
UA	32	B	2016/06/07	Boron, total	mg/L	0.0749
UA	32	B	2016/09/15	Boron, total	mg/L	0.0980
UA	32	B	2016/12/07	Boron, total	mg/L	0.108
UA	32	B	2017/02/21	Boron, total	mg/L	0.0681
UA	32	B	2017/04/25	Boron, total	mg/L	0.0844
UA	32	B	2017/06/08	Boron, total	mg/L	0.0859
UA	32	B	2017/11/15	Boron, total	mg/L	0.0801
UA	32	B	2018/06/13	Boron, total	mg/L	0.113
UA	32	B	2018/09/12	Boron, total	mg/L	0.0974
UA	32	B	2018/12/12	Boron, total	mg/L	0.0926
UA	32	B	2019/03/13	Boron, total	mg/L	0.115
UA	32	B	2019/09/18	Boron, total	mg/L	0.150
UA	32	B	2019/12/11	Boron, total	mg/L	0.110
UA	32	B	2020/03/11	Boron, total	mg/L	0.110
UA	32	B	2020/06/25	Boron, total	mg/L	0.132
UA	32	B	2020/09/02	Boron, total	mg/L	0.117
UA	32	B	2020/12/09	Boron, total	mg/L	0.124
UA	32	B	2021/03/17	Boron, total	mg/L	0.107
UA	32	B	2021/06/24	Boron, total	mg/L	0.109
UA	32	B	2021/09/09	Boron, total	mg/L	0.162
UA	32	B	2021/12/08	Boron, total	mg/L	0.154
UA	32	B	2022/03/22	Boron, total	mg/L	0.183
UA	32	B	2022/06/07	Boron, total	mg/L	0.188
UA	32	B	2022/09/13	Boron, total	mg/L	0.152
UA	32	B	2022/12/27	Boron, total	mg/L	0.151
UA	32	B	2023/02/28	Boron, total	mg/L	0.199
UA	32	B	2023/05/31	Boron, total	mg/L	0.143
UA	32	B	2023/08/22	Boron, total	mg/L	0.140
UA	32	B	2023/11/14	Boron, total	mg/L	0.180
UA	32	B	2013/06/26	Cadmium, total	mg/L	<0.0003
UA	32	B	2013/09/03	Cadmium, total	mg/L	<0.0003
UA	32	B	2015/12/10	Cadmium, total	mg/L	<0.0002
UA	32	B	2016/03/08	Cadmium, total	mg/L	<0.0002
UA	32	B	2016/06/07	Cadmium, total	mg/L	<0.0002
UA	32	B	2016/09/15	Cadmium, total	mg/L	<0.0002
UA	32	B	2016/12/07	Cadmium, total	mg/L	<0.0002
UA	32	B	2017/02/21	Cadmium, total	mg/L	<0.0002
UA	32	B	2017/04/25	Cadmium, total	mg/L	<0.0002
UA	32	B	2017/06/08	Cadmium, total	mg/L	<0.0002
UA	32	B	2018/06/13	Cadmium, total	mg/L	<0.0002
UA	32	B	2018/09/12	Cadmium, total	mg/L	<0.0002
UA	32	B	2018/12/12	Cadmium, total	mg/L	<0.0002
UA	32	B	2019/03/13	Cadmium, total	mg/L	<0.0002
UA	32	B	2019/09/18	Cadmium, total	mg/L	<0.0002
UA	32	B	2019/12/11	Cadmium, total	mg/L	<0.0002
UA	32	B	2020/03/11	Cadmium, total	mg/L	<0.0002
UA	32	B	2020/06/25	Cadmium, total	mg/L	<0.0002
UA	32	B	2020/09/02	Cadmium, total	mg/L	<0.0002
UA	32	B	2020/12/09	Cadmium, total	mg/L	<0.0002
UA	32	B	2021/03/17	Cadmium, total	mg/L	<0.0002
UA	32	B	2021/06/24	Cadmium, total	mg/L	<0.0002
UA	32	B	2021/09/09	Cadmium, total	mg/L	<0.0002
UA	32	B	2021/12/08	Cadmium, total	mg/L	<0.0002
UA	32	B	2022/03/22	Cadmium, total	mg/L	<0.0002
UA	32	B	2022/06/07	Cadmium, total	mg/L	0.000200
UA	32	B	2022/09/13	Cadmium, total	mg/L	<0.0002
UA	32	B	2022/12/27	Cadmium, total	mg/L	<0.0002
UA	32	B	2023/02/28	Cadmium, total	mg/L	0.000200
UA	32	B	2023/05/31	Cadmium, total	mg/L	<0.0005

UA	32	B	2023/08/22	Cadmium, total	mg/L	0.000210
UA	32	B	2023/11/14	Cadmium, total	mg/L	<0.00017
UA	32	B	2015/12/10	Calcium, total	mg/L	93.2
UA	32	B	2016/03/08	Calcium, total	mg/L	99.1
UA	32	B	2016/06/07	Calcium, total	mg/L	94.3
UA	32	B	2016/09/15	Calcium, total	mg/L	96.0
UA	32	B	2016/12/07	Calcium, total	mg/L	95.0
UA	32	B	2017/02/21	Calcium, total	mg/L	102
UA	32	B	2017/04/25	Calcium, total	mg/L	84.9
UA	32	B	2017/06/08	Calcium, total	mg/L	92.1
UA	32	B	2017/11/15	Calcium, total	mg/L	107
UA	32	B	2018/06/13	Calcium, total	mg/L	96.8
UA	32	B	2018/09/12	Calcium, total	mg/L	107
UA	32	B	2018/12/12	Calcium, total	mg/L	115
UA	32	B	2019/03/13	Calcium, total	mg/L	104
UA	32	B	2019/09/18	Calcium, total	mg/L	95.9
UA	32	B	2019/12/11	Calcium, total	mg/L	98.6
UA	32	B	2020/03/11	Calcium, total	mg/L	98.0
UA	32	B	2020/06/25	Calcium, total	mg/L	89.5
UA	32	B	2020/09/02	Calcium, total	mg/L	96.3
UA	32	B	2020/12/09	Calcium, total	mg/L	141
UA	32	B	2021/03/17	Calcium, total	mg/L	101
UA	32	B	2021/06/24	Calcium, total	mg/L	106
UA	32	B	2021/09/09	Calcium, total	mg/L	115
UA	32	B	2021/12/08	Calcium, total	mg/L	101
UA	32	B	2022/03/22	Calcium, total	mg/L	110
UA	32	B	2022/06/07	Calcium, total	mg/L	115
UA	32	B	2022/09/13	Calcium, total	mg/L	113
UA	32	B	2022/12/27	Calcium, total	mg/L	112
UA	32	B	2023/02/28	Calcium, total	mg/L	122
UA	32	B	2023/05/31	Calcium, total	mg/L	102
UA	32	B	2023/08/22	Calcium, total	mg/L	100
UA	32	B	2023/11/14	Calcium, total	mg/L	110
UA	32	B	2013/03/08	Chloride, total	mg/L	119
UA	32	B	2013/06/26	Chloride, total	mg/L	69.0
UA	32	B	2013/09/03	Chloride, total	mg/L	54.0
UA	32	B	2013/12/10	Chloride, total	mg/L	109
UA	32	B	2014/03/25	Chloride, total	mg/L	107
UA	32	B	2014/09/30	Chloride, total	mg/L	41.0
UA	32	B	2015/03/18	Chloride, total	mg/L	53.0
UA	32	B	2015/09/16	Chloride, total	mg/L	38.0
UA	32	B	2015/12/10	Chloride, total	mg/L	42.0
UA	32	B	2016/03/08	Chloride, total	mg/L	51.0
UA	32	B	2016/06/07	Chloride, total	mg/L	47.0
UA	32	B	2016/09/15	Chloride, total	mg/L	47.0
UA	32	B	2016/12/07	Chloride, total	mg/L	48.0
UA	32	B	2017/02/21	Chloride, total	mg/L	44.0
UA	32	B	2017/04/25	Chloride, total	mg/L	51.0
UA	32	B	2017/06/08	Chloride, total	mg/L	47.0
UA	32	B	2017/09/06	Chloride, total	mg/L	48.0
UA	32	B	2017/11/15	Chloride, total	mg/L	57.0
UA	32	B	2018/03/26	Chloride, total	mg/L	59.0
UA	32	B	2018/06/13	Chloride, total	mg/L	64.0
UA	32	B	2018/09/12	Chloride, total	mg/L	73.0
UA	32	B	2018/12/12	Chloride, total	mg/L	61.0
UA	32	B	2019/03/13	Chloride, total	mg/L	61.0
UA	32	B	2019/09/18	Chloride, total	mg/L	56.0
UA	32	B	2019/12/11	Chloride, total	mg/L	61.0
UA	32	B	2020/03/11	Chloride, total	mg/L	57.0
UA	32	B	2020/06/25	Chloride, total	mg/L	52.0
UA	32	B	2020/09/02	Chloride, total	mg/L	52.0
UA	32	B	2020/12/09	Chloride, total	mg/L	56.0

UA	32	B	2021/03/17	Chloride, total	mg/L	54.0
UA	32	B	2021/06/24	Chloride, total	mg/L	57.0
UA	32	B	2021/09/09	Chloride, total	mg/L	57.0
UA	32	B	2021/12/08	Chloride, total	mg/L	68.0
UA	32	B	2022/03/22	Chloride, total	mg/L	68.0
UA	32	B	2022/06/07	Chloride, total	mg/L	73.0
UA	32	B	2022/09/13	Chloride, total	mg/L	74.0
UA	32	B	2022/12/27	Chloride, total	mg/L	80.0
UA	32	B	2023/02/28	Chloride, total	mg/L	83.0
UA	32	B	2023/05/31	Chloride, total	mg/L	70.0
UA	32	B	2023/08/22	Chloride, total	mg/L	68.0
UA	32	B	2023/11/14	Chloride, total	mg/L	67.0
UA	32	B	2013/03/08	Iron, dissolved	mg/L	0.100
UA	32	B	2013/12/10	Iron, dissolved	mg/L	0.294
UA	32	B	2014/03/25	Iron, dissolved	mg/L	<0.007
UA	32	B	2014/08/19	Iron, dissolved	mg/L	<0.007
UA	32	B	2014/09/30	Iron, dissolved	mg/L	<0.007
UA	32	B	2015/03/18	Iron, dissolved	mg/L	<0.007
UA	32	B	2015/09/16	Iron, dissolved	mg/L	<0.007
UA	32	B	2016/03/08	Iron, dissolved	mg/L	<0.007
UA	32	B	2016/09/15	Iron, dissolved	mg/L	<0.007
UA	32	B	2017/02/21	Iron, dissolved	mg/L	<0.007
UA	32	B	2017/09/06	Iron, dissolved	mg/L	<0.007
UA	32	B	2018/03/26	Iron, dissolved	mg/L	<0.007
UA	32	B	2023/05/31	Iron, dissolved	mg/L	<0.02
UA	32	B	2023/08/22	Iron, dissolved	mg/L	<0.047
UA	32	B	2015/12/10	Lithium, total	mg/L	0.00260
UA	32	B	2016/03/08	Lithium, total	mg/L	0.00250
UA	32	B	2016/06/07	Lithium, total	mg/L	0.00220
UA	32	B	2016/09/15	Lithium, total	mg/L	0.00380
UA	32	B	2016/12/07	Lithium, total	mg/L	0.00290
UA	32	B	2017/02/21	Lithium, total	mg/L	0.00250
UA	32	B	2017/04/25	Lithium, total	mg/L	0.00340
UA	32	B	2017/06/08	Lithium, total	mg/L	0.00250
UA	32	B	2018/06/13	Lithium, total	mg/L	0.00300
UA	32	B	2018/09/12	Lithium, total	mg/L	0.00370
UA	32	B	2018/12/12	Lithium, total	mg/L	0.00280
UA	32	B	2019/03/13	Lithium, total	mg/L	0.00400
UA	32	B	2019/09/18	Lithium, total	mg/L	0.00450
UA	32	B	2019/12/11	Lithium, total	mg/L	0.00450
UA	32	B	2020/03/11	Lithium, total	mg/L	0.00430
UA	32	B	2020/06/25	Lithium, total	mg/L	0.00430
UA	32	B	2020/09/02	Lithium, total	mg/L	0.00410
UA	32	B	2020/12/09	Lithium, total	mg/L	0.00360
UA	32	B	2021/03/17	Lithium, total	mg/L	0.00340
UA	32	B	2021/06/24	Lithium, total	mg/L	0.00370
UA	32	B	2021/09/09	Lithium, total	mg/L	0.00370
UA	32	B	2021/12/08	Lithium, total	mg/L	0.00400
UA	32	B	2022/03/22	Lithium, total	mg/L	0.00400
UA	32	B	2022/06/07	Lithium, total	mg/L	0.00390
UA	32	B	2022/09/13	Lithium, total	mg/L	0.00320
UA	32	B	2022/12/27	Lithium, total	mg/L	0.00390
UA	32	B	2023/02/28	Lithium, total	mg/L	0.00310
UA	32	B	2023/05/31	Lithium, total	mg/L	0.00290
UA	32	B	2023/08/22	Lithium, total	mg/L	0.00480
UA	32	B	2023/11/14	Lithium, total	mg/L	0.00510
UA	32	B	2019/09/18	Magnesium, total	mg/L	33.6
UA	32	B	2020/03/11	Magnesium, total	mg/L	36.1
UA	32	B	2020/06/25	Magnesium, total	mg/L	34.9
UA	32	B	2021/03/17	Magnesium, total	mg/L	36.8
UA	32	B	2021/09/09	Magnesium, total	mg/L	42.0
UA	32	B	2022/03/22	Magnesium, total	mg/L	39.0

UA	32	B	2022/09/13	Magnesium, total	mg/L	39.6
UA	32	B	2023/02/28	Magnesium, total	mg/L	42.4
UA	32	B	2023/05/31	Magnesium, total	mg/L	39.5
UA	32	B	2023/08/22	Magnesium, total	mg/L	39.0
UA	32	B	2023/11/14	Magnesium, total	mg/L	38.0
UA	32	B	2013/03/08	Manganese, dissolved	mg/L	1.19
UA	32	B	2013/12/10	Manganese, dissolved	mg/L	0.411
UA	32	B	2014/03/25	Manganese, dissolved	mg/L	0.266
UA	32	B	2014/08/19	Manganese, dissolved	mg/L	<0.0016
UA	32	B	2014/09/30	Manganese, dissolved	mg/L	<0.0005
UA	32	B	2015/03/18	Manganese, dissolved	mg/L	0.00540
UA	32	B	2015/09/16	Manganese, dissolved	mg/L	0.0504
UA	32	B	2016/03/08	Manganese, dissolved	mg/L	<0.0005
UA	32	B	2016/09/15	Manganese, dissolved	mg/L	0.00720
UA	32	B	2017/02/21	Manganese, dissolved	mg/L	0.00700
UA	32	B	2017/09/06	Manganese, dissolved	mg/L	0.00860
UA	32	B	2018/03/26	Manganese, dissolved	mg/L	0.00700
UA	32	B	2023/05/31	Manganese, dissolved	mg/L	0.0495
UA	32	B	2023/08/22	Manganese, dissolved	mg/L	0.0920
UA	32	B	2023/05/31	Phosphate, dissolved	mg/L	0.175
UA	32	B	2023/08/22	Phosphate, dissolved	mg/L	<0.073
UA	32	B	2019/09/18	Potassium, total	mg/L	2.30
UA	32	B	2020/03/11	Potassium, total	mg/L	2.27
UA	32	B	2020/06/25	Potassium, total	mg/L	2.34
UA	32	B	2021/03/17	Potassium, total	mg/L	2.06
UA	32	B	2021/09/09	Potassium, total	mg/L	2.37
UA	32	B	2022/03/22	Potassium, total	mg/L	2.08
UA	32	B	2022/09/13	Potassium, total	mg/L	2.24
UA	32	B	2023/02/28	Potassium, total	mg/L	1.95
UA	32	B	2023/05/31	Potassium, total	mg/L	2.22
UA	32	B	2023/08/22	Potassium, total	mg/L	2.10
UA	32	B	2023/11/14	Potassium, total	mg/L	2.10
UA	32	B	2023/05/31	Silicon, dissolved	mg/L	5.65
UA	32	B	2023/08/22	Silicon, dissolved	mg/L	6.90
UA	32	B	2019/09/18	Sodium, total	mg/L	29.9
UA	32	B	2020/03/11	Sodium, total	mg/L	33.0
UA	32	B	2020/06/25	Sodium, total	mg/L	32.4
UA	32	B	2021/03/17	Sodium, total	mg/L	34.5
UA	32	B	2021/09/09	Sodium, total	mg/L	33.4
UA	32	B	2022/03/22	Sodium, total	mg/L	38.0
UA	32	B	2022/09/13	Sodium, total	mg/L	38.6
UA	32	B	2023/02/28	Sodium, total	mg/L	39.7
UA	32	B	2023/05/31	Sodium, total	mg/L	40.1
UA	32	B	2023/08/22	Sodium, total	mg/L	38.0
UA	32	B	2023/11/14	Sodium, total	mg/L	39.0
UA	32	B	2013/03/08	Sulfate, total	mg/L	146
UA	32	B	2013/06/26	Sulfate, total	mg/L	102
UA	32	B	2013/09/03	Sulfate, total	mg/L	83.0
UA	32	B	2013/12/10	Sulfate, total	mg/L	128
UA	32	B	2014/03/25	Sulfate, total	mg/L	97.0
UA	32	B	2014/09/30	Sulfate, total	mg/L	71.0
UA	32	B	2015/03/18	Sulfate, total	mg/L	78.0
UA	32	B	2015/09/16	Sulfate, total	mg/L	62.0
UA	32	B	2015/12/10	Sulfate, total	mg/L	60.0
UA	32	B	2016/03/08	Sulfate, total	mg/L	62.0
UA	32	B	2016/06/07	Sulfate, total	mg/L	62.0
UA	32	B	2016/09/15	Sulfate, total	mg/L	61.0
UA	32	B	2016/12/07	Sulfate, total	mg/L	61.0
UA	32	B	2017/02/21	Sulfate, total	mg/L	57.0
UA	32	B	2017/04/25	Sulfate, total	mg/L	61.0
UA	32	B	2017/06/08	Sulfate, total	mg/L	58.0
UA	32	B	2017/09/06	Sulfate, total	mg/L	57.0

UA	32	B	2017/11/15	Sulfate, total	mg/L	56.0
UA	32	B	2018/03/26	Sulfate, total	mg/L	66.0
UA	32	B	2018/06/13	Sulfate, total	mg/L	54.0
UA	32	B	2018/09/12	Sulfate, total	mg/L	60.0
UA	32	B	2018/12/12	Sulfate, total	mg/L	55.0
UA	32	B	2019/03/13	Sulfate, total	mg/L	51.0
UA	32	B	2019/09/18	Sulfate, total	mg/L	37.0
UA	32	B	2019/12/11	Sulfate, total	mg/L	42.0
UA	32	B	2020/03/11	Sulfate, total	mg/L	42.0
UA	32	B	2020/06/25	Sulfate, total	mg/L	52.0
UA	32	B	2020/09/02	Sulfate, total	mg/L	41.0
UA	32	B	2020/12/09	Sulfate, total	mg/L	44.0
UA	32	B	2021/03/17	Sulfate, total	mg/L	45.0
UA	32	B	2021/06/24	Sulfate, total	mg/L	50.0
UA	32	B	2021/09/09	Sulfate, total	mg/L	50.0
UA	32	B	2021/12/08	Sulfate, total	mg/L	64.0
UA	32	B	2022/03/22	Sulfate, total	mg/L	60.0
UA	32	B	2022/06/07	Sulfate, total	mg/L	62.0
UA	32	B	2022/09/13	Sulfate, total	mg/L	62.0
UA	32	B	2022/12/27	Sulfate, total	mg/L	65.0
UA	32	B	2023/02/28	Sulfate, total	mg/L	82.0
UA	32	B	2023/05/31	Sulfate, total	mg/L	63.0
UA	32	B	2023/08/22	Sulfate, total	mg/L	66.0
UA	32	B	2023/11/14	Sulfate, total	mg/L	65.0
UA	32	B	2013/03/08	Temperature (Celsius)	degrees C	6.50
UA	32	B	2013/06/26	Temperature (Celsius)	degrees C	12.8
UA	32	B	2013/09/03	Temperature (Celsius)	degrees C	12.9
UA	32	B	2013/12/10	Temperature (Celsius)	degrees C	10.5
UA	32	B	2014/03/25	Temperature (Celsius)	degrees C	5.90
UA	32	B	2014/08/19	Temperature (Celsius)	degrees C	12.0
UA	32	B	2014/09/30	Temperature (Celsius)	degrees C	12.0
UA	32	B	2015/03/18	Temperature (Celsius)	degrees C	8.50
UA	32	B	2015/09/16	Temperature (Celsius)	degrees C	13.1
UA	32	B	2015/12/10	Temperature (Celsius)	degrees C	13.5
UA	32	B	2016/03/08	Temperature (Celsius)	degrees C	10.4
UA	32	B	2016/06/07	Temperature (Celsius)	degrees C	11.2
UA	32	B	2016/09/15	Temperature (Celsius)	degrees C	15.1
UA	32	B	2016/12/07	Temperature (Celsius)	degrees C	12.1
UA	32	B	2017/02/21	Temperature (Celsius)	degrees C	11.8
UA	32	B	2017/04/25	Temperature (Celsius)	degrees C	14.6
UA	32	B	2017/06/08	Temperature (Celsius)	degrees C	12
UA	32	B	2017/09/06	Temperature (Celsius)	degrees C	13.5
UA	32	B	2017/11/15	Temperature (Celsius)	degrees C	14.0
UA	32	B	2018/03/26	Temperature (Celsius)	degrees C	11.1
UA	32	B	2018/06/13	Temperature (Celsius)	degrees C	12.4
UA	32	B	2018/09/12	Temperature (Celsius)	degrees C	13.9
UA	32	B	2018/12/12	Temperature (Celsius)	degrees C	11.9
UA	32	B	2019/03/13	Temperature (Celsius)	degrees C	10.0
UA	32	B	2019/09/18	Temperature (Celsius)	degrees C	13.6
UA	32	B	2019/12/11	Temperature (Celsius)	degrees C	12.9
UA	32	B	2020/03/11	Temperature (Celsius)	degrees C	9.60
UA	32	B	2020/06/25	Temperature (Celsius)	degrees C	10.7
UA	32	B	2020/09/02	Temperature (Celsius)	degrees C	13.7
UA	32	B	2020/12/09	Temperature (Celsius)	degrees C	13.1
UA	32	B	2021/03/17	Temperature (Celsius)	degrees C	9.80
UA	32	B	2021/06/24	Temperature (Celsius)	degrees C	11.6
UA	32	B	2021/09/09	Temperature (Celsius)	degrees C	13.9
UA	32	B	2021/12/08	Temperature (Celsius)	degrees C	13.6
UA	32	B	2022/03/22	Temperature (Celsius)	degrees C	10.1
UA	32	B	2022/06/07	Temperature (Celsius)	degrees C	11.0
UA	32	B	2022/09/13	Temperature (Celsius)	degrees C	14.3
UA	32	B	2022/12/27	Temperature (Celsius)	degrees C	12.0

UA	32	B	2023/02/28	Temperature (Celsius)	degrees C	10.2
UA	32	B	2023/05/31	Temperature (Celsius)	degrees C	11.0
UA	32	B	2023/08/22	Temperature (Celsius)	degrees C	13.8
UA	32	B	2023/11/14	Temperature (Celsius)	degrees C	14.1
UA	32	B	2013/03/08	Total Dissolved Solids	mg/L	652
UA	32	B	2013/06/26	Total Dissolved Solids	mg/L	592
UA	32	B	2013/09/03	Total Dissolved Solids	mg/L	486
UA	32	B	2013/12/10	Total Dissolved Solids	mg/L	654
UA	32	B	2014/03/25	Total Dissolved Solids	mg/L	552
UA	32	B	2014/08/19	Total Dissolved Solids	mg/L	466
UA	32	B	2014/09/30	Total Dissolved Solids	mg/L	468
UA	32	B	2015/03/18	Total Dissolved Solids	mg/L	524
UA	32	B	2015/09/16	Total Dissolved Solids	mg/L	468
UA	32	B	2015/12/10	Total Dissolved Solids	mg/L	466
UA	32	B	2016/03/08	Total Dissolved Solids	mg/L	480
UA	32	B	2016/06/07	Total Dissolved Solids	mg/L	462
UA	32	B	2016/09/15	Total Dissolved Solids	mg/L	502
UA	32	B	2016/12/07	Total Dissolved Solids	mg/L	456
UA	32	B	2017/02/21	Total Dissolved Solids	mg/L	452
UA	32	B	2017/04/25	Total Dissolved Solids	mg/L	508
UA	32	B	2017/06/08	Total Dissolved Solids	mg/L	450
UA	32	B	2017/09/06	Total Dissolved Solids	mg/L	494
UA	32	B	2017/11/15	Total Dissolved Solids	mg/L	506
UA	32	B	2018/03/26	Total Dissolved Solids	mg/L	492
UA	32	B	2018/06/13	Total Dissolved Solids	mg/L	494
UA	32	B	2018/09/12	Total Dissolved Solids	mg/L	532
UA	32	B	2018/12/12	Total Dissolved Solids	mg/L	536
UA	32	B	2019/03/13	Total Dissolved Solids	mg/L	506
UA	32	B	2019/09/18	Total Dissolved Solids	mg/L	492
UA	32	B	2019/12/11	Total Dissolved Solids	mg/L	476
UA	32	B	2020/03/11	Total Dissolved Solids	mg/L	476
UA	32	B	2020/06/25	Total Dissolved Solids	mg/L	468
UA	32	B	2020/09/02	Total Dissolved Solids	mg/L	464
UA	32	B	2020/12/09	Total Dissolved Solids	mg/L	482
UA	32	B	2021/03/17	Total Dissolved Solids	mg/L	488
UA	32	B	2021/06/24	Total Dissolved Solids	mg/L	474
UA	32	B	2021/09/09	Total Dissolved Solids	mg/L	486
UA	32	B	2021/12/08	Total Dissolved Solids	mg/L	514
UA	32	B	2022/03/22	Total Dissolved Solids	mg/L	514
UA	32	B	2022/06/07	Total Dissolved Solids	mg/L	598
UA	32	B	2022/09/13	Total Dissolved Solids	mg/L	596
UA	32	B	2022/12/27	Total Dissolved Solids	mg/L	560
UA	32	B	2023/02/28	Total Dissolved Solids	mg/L	564
UA	32	B	2023/05/31	Total Dissolved Solids	mg/L	550
UA	32	B	2023/08/22	Total Dissolved Solids	mg/L	570
UA	32	B	2023/11/14	Total Dissolved Solids	mg/L	600
UA	34	B	2013/03/08	pH (field)	SU	7.2
UA	34	B	2013/09/04	pH (field)	SU	7.3
UA	34	B	2013/12/10	pH (field)	SU	7.2
UA	34	B	2014/03/25	pH (field)	SU	7.0
UA	34	B	2015/03/18	pH (field)	SU	7.1
UA	34	B	2015/12/09	pH (field)	SU	7.2
UA	34	B	2016/03/08	pH (field)	SU	7.0
UA	34	B	2016/06/07	pH (field)	SU	7.0
UA	34	B	2016/09/15	pH (field)	SU	7.1
UA	34	B	2016/12/07	pH (field)	SU	7.0
UA	34	B	2017/02/21	pH (field)	SU	7.1
UA	34	B	2017/04/25	pH (field)	SU	6.9
UA	34	B	2017/06/08	pH (field)	SU	7.0
UA	34	B	2017/11/15	pH (field)	SU	7.2
UA	34	B	2018/03/26	pH (field)	SU	7.2
UA	34	B	2018/06/13	pH (field)	SU	6.4

UA	34	B	2018/09/12	pH (field)	SU	7.0
UA	34	B	2018/12/12	pH (field)	SU	7.1
UA	34	B	2019/03/13	pH (field)	SU	7.2
UA	34	B	2019/09/18	pH (field)	SU	6.8
UA	34	B	2019/12/11	pH (field)	SU	7.0
UA	34	B	2020/03/11	pH (field)	SU	7.1
UA	34	B	2020/06/24	pH (field)	SU	7.1
UA	34	B	2020/09/02	pH (field)	SU	7.1
UA	34	B	2020/12/09	pH (field)	SU	7.1
UA	34	B	2021/03/19	pH (field)	SU	7.1
UA	34	B	2021/06/24	pH (field)	SU	6.7
UA	34	B	2021/09/09	pH (field)	SU	6.9
UA	34	B	2021/12/09	pH (field)	SU	7.0
UA	34	B	2022/03/22	pH (field)	SU	6.8
UA	34	B	2022/06/07	pH (field)	SU	6.9
UA	34	B	2022/12/29	pH (field)	SU	6.9
UA	34	B	2023/02/28	pH (field)	SU	6.9
UA	34	B	2023/05/31	pH (field)	SU	6.9
UA	34	B	2023/08/25	pH (field)	SU	7.1
UA	34	B	2023/11/14	pH (field)	SU	7.2
UA	34	B	2015/12/09	Oxidation Reduction Potential	mV	-67.0
UA	34	B	2016/03/08	Oxidation Reduction Potential	mV	-113
UA	34	B	2016/06/07	Oxidation Reduction Potential	mV	-125
UA	34	B	2016/09/15	Oxidation Reduction Potential	mV	-86.0
UA	34	B	2016/12/07	Oxidation Reduction Potential	mV	-77.0
UA	34	B	2017/02/21	Oxidation Reduction Potential	mV	-67.0
UA	34	B	2017/04/25	Oxidation Reduction Potential	mV	-90.0
UA	34	B	2017/06/08	Oxidation Reduction Potential	mV	-115
UA	34	B	2017/11/15	Oxidation Reduction Potential	mV	18.0
UA	34	B	2018/06/13	Oxidation Reduction Potential	mV	-8.00
UA	34	B	2018/09/12	Oxidation Reduction Potential	mV	-101
UA	34	B	2018/12/12	Oxidation Reduction Potential	mV	-113
UA	34	B	2019/03/13	Oxidation Reduction Potential	mV	-64.0
UA	34	B	2019/09/18	Oxidation Reduction Potential	mV	-79.0
UA	34	B	2019/12/11	Oxidation Reduction Potential	mV	-76.0
UA	34	B	2020/03/11	Oxidation Reduction Potential	mV	-60.0
UA	34	B	2020/06/24	Oxidation Reduction Potential	mV	-72.0
UA	34	B	2020/09/02	Oxidation Reduction Potential	mV	-80.0
UA	34	B	2020/12/09	Oxidation Reduction Potential	mV	-94.0
UA	34	B	2021/03/19	Oxidation Reduction Potential	mV	-108
UA	34	B	2021/06/24	Oxidation Reduction Potential	mV	-124
UA	34	B	2021/09/09	Oxidation Reduction Potential	mV	-30.0
UA	34	B	2021/12/09	Oxidation Reduction Potential	mV	-86.0
UA	34	B	2022/03/22	Oxidation Reduction Potential	mV	-86.0
UA	34	B	2022/06/07	Oxidation Reduction Potential	mV	51.0
UA	34	B	2022/12/29	Oxidation Reduction Potential	mV	-95.0
UA	34	B	2023/02/28	Oxidation Reduction Potential	mV	-84.5
UA	34	B	2023/05/31	Oxidation Reduction Potential	mV	-83.0
UA	34	B	2023/08/25	Oxidation Reduction Potential	mV	-111
UA	34	B	2023/11/14	Oxidation Reduction Potential	mV	-111
UA	34	B	2015/12/09	Eh	V	0.13
UA	34	B	2016/03/08	Eh	V	0.085
UA	34	B	2016/06/07	Eh	V	0.072
UA	34	B	2016/09/15	Eh	V	0.11
UA	34	B	2016/12/07	Eh	V	0.12
UA	34	B	2017/02/21	Eh	V	0.13
UA	34	B	2017/04/25	Eh	V	0.10
UA	34	B	2017/06/08	Eh	V	0.075
UA	34	B	2017/11/15	Eh	V	0.21
UA	34	B	2018/06/13	Eh	V	0.19
UA	34	B	2018/09/12	Eh	V	0.090
UA	34	B	2018/12/12	Eh	V	0.085

UA	34	B	2019/03/13	Eh	V	0.13
UA	34	B	2019/09/18	Eh	V	0.12
UA	34	B	2019/12/11	Eh	V	0.12
UA	34	B	2020/03/11	Eh	V	0.14
UA	34	B	2020/06/24	Eh	V	0.13
UA	34	B	2020/09/02	Eh	V	0.12
UA	34	B	2020/12/09	Eh	V	0.10
UA	34	B	2021/03/19	Eh	V	0.090
UA	34	B	2021/06/24	Eh	V	0.073
UA	34	B	2021/09/09	Eh	V	0.17
UA	34	B	2021/12/09	Eh	V	0.11
UA	34	B	2022/03/22	Eh	V	0.11
UA	34	B	2022/06/07	Eh	V	0.25
UA	34	B	2022/12/29	Eh	V	0.10
UA	34	B	2023/02/28	Eh	V	0.11
UA	34	B	2023/05/31	Eh	V	0.11
UA	34	B	2023/08/25	Eh	V	0.086
UA	34	B	2023/11/14	Eh	V	0.087
UA	34	B	2019/09/18	Alkalinity, bicarbonate	mg/L CaCO3	496
UA	34	B	2020/03/11	Alkalinity, bicarbonate	mg/L CaCO3	504
UA	34	B	2021/03/19	Alkalinity, bicarbonate	mg/L CaCO3	514
UA	34	B	2021/09/09	Alkalinity, bicarbonate	mg/L CaCO3	516
UA	34	B	2022/03/22	Alkalinity, bicarbonate	mg/L CaCO3	527
UA	34	B	2023/02/28	Alkalinity, bicarbonate	mg/L CaCO3	575
UA	34	B	2023/05/31	Alkalinity, bicarbonate	mg/L CaCO3	521
UA	34	B	2023/08/25	Alkalinity, bicarbonate	mg/L CaCO3	570
UA	34	B	2023/11/14	Alkalinity, bicarbonate	mg/L CaCO3	570
UA	34	B	2013/09/04	Arsenic, total	mg/L	<0.0007
UA	34	B	2015/12/09	Arsenic, total	mg/L	<0.0002
UA	34	B	2016/03/08	Arsenic, total	mg/L	<0.0002
UA	34	B	2016/06/07	Arsenic, total	mg/L	<0.0002
UA	34	B	2016/09/15	Arsenic, total	mg/L	<0.0002
UA	34	B	2016/12/07	Arsenic, total	mg/L	<0.0002
UA	34	B	2017/02/21	Arsenic, total	mg/L	<0.0002
UA	34	B	2017/04/25	Arsenic, total	mg/L	<0.0002
UA	34	B	2017/06/08	Arsenic, total	mg/L	<0.0002
UA	34	B	2018/06/13	Arsenic, total	mg/L	<0.0004
UA	34	B	2018/09/12	Arsenic, total	mg/L	<0.0004
UA	34	B	2018/12/12	Arsenic, total	mg/L	<0.0004
UA	34	B	2019/03/13	Arsenic, total	mg/L	0.00200
UA	34	B	2019/09/18	Arsenic, total	mg/L	<0.0004
UA	34	B	2019/12/11	Arsenic, total	mg/L	<0.0004
UA	34	B	2020/03/11	Arsenic, total	mg/L	<0.0004
UA	34	B	2020/06/24	Arsenic, total	mg/L	<0.0004
UA	34	B	2020/09/02	Arsenic, total	mg/L	<0.0004
UA	34	B	2020/12/09	Arsenic, total	mg/L	<0.0004
UA	34	B	2021/03/19	Arsenic, total	mg/L	<0.0004
UA	34	B	2021/06/24	Arsenic, total	mg/L	<0.0004
UA	34	B	2021/09/09	Arsenic, total	mg/L	<0.0004
UA	34	B	2021/12/09	Arsenic, total	mg/L	<0.0004
UA	34	B	2022/03/22	Arsenic, total	mg/L	<0.0004
UA	34	B	2022/06/07	Arsenic, total	mg/L	0.000500
UA	34	B	2022/12/29	Arsenic, total	mg/L	0.000600
UA	34	B	2023/02/28	Arsenic, total	mg/L	0.000700
UA	34	B	2023/05/31	Arsenic, total	mg/L	<0.0087
UA	34	B	2023/08/25	Arsenic, total	mg/L	<0.00023
UA	34	B	2023/11/14	Arsenic, total	mg/L	0.000690
UA	34	B	2013/09/04	Barium, total	mg/L	0.126
UA	34	B	2015/12/09	Barium, total	mg/L	0.123
UA	34	B	2016/03/08	Barium, total	mg/L	0.124
UA	34	B	2016/06/07	Barium, total	mg/L	0.0987
UA	34	B	2016/09/15	Barium, total	mg/L	0.107

UA	34	B	2016/12/07	Barium, total	mg/L	0.156
UA	34	B	2017/02/21	Barium, total	mg/L	0.116
UA	34	B	2017/04/25	Barium, total	mg/L	0.107
UA	34	B	2017/06/08	Barium, total	mg/L	0.126
UA	34	B	2018/06/13	Barium, total	mg/L	0.108
UA	34	B	2018/09/12	Barium, total	mg/L	0.120
UA	34	B	2018/12/12	Barium, total	mg/L	0.106
UA	34	B	2019/03/13	Barium, total	mg/L	0.120
UA	34	B	2019/09/18	Barium, total	mg/L	0.102
UA	34	B	2019/12/11	Barium, total	mg/L	0.103
UA	34	B	2020/03/11	Barium, total	mg/L	0.0970
UA	34	B	2020/06/24	Barium, total	mg/L	0.101
UA	34	B	2020/09/02	Barium, total	mg/L	0.105
UA	34	B	2020/12/09	Barium, total	mg/L	0.129
UA	34	B	2021/03/19	Barium, total	mg/L	0.114
UA	34	B	2021/06/24	Barium, total	mg/L	0.105
UA	34	B	2021/09/09	Barium, total	mg/L	0.0933
UA	34	B	2021/12/09	Barium, total	mg/L	0.0957
UA	34	B	2022/03/22	Barium, total	mg/L	0.102
UA	34	B	2022/06/07	Barium, total	mg/L	0.115
UA	34	B	2022/12/29	Barium, total	mg/L	0.129
UA	34	B	2023/02/28	Barium, total	mg/L	0.139
UA	34	B	2023/05/31	Barium, total	mg/L	0.0995
UA	34	B	2023/08/25	Barium, total	mg/L	0.110
UA	34	B	2023/11/14	Barium, total	mg/L	0.110
UA	34	B	2013/09/04	Boron, total	mg/L	0.104
UA	34	B	2015/12/09	Boron, total	mg/L	0.140
UA	34	B	2016/03/08	Boron, total	mg/L	0.146
UA	34	B	2016/06/07	Boron, total	mg/L	0.140
UA	34	B	2016/09/15	Boron, total	mg/L	0.162
UA	34	B	2016/12/07	Boron, total	mg/L	0.190
UA	34	B	2017/02/21	Boron, total	mg/L	0.133
UA	34	B	2017/04/25	Boron, total	mg/L	0.145
UA	34	B	2017/06/08	Boron, total	mg/L	0.130
UA	34	B	2017/11/15	Boron, total	mg/L	0.130
UA	34	B	2018/06/13	Boron, total	mg/L	0.143
UA	34	B	2018/09/12	Boron, total	mg/L	0.137
UA	34	B	2018/12/12	Boron, total	mg/L	0.132
UA	34	B	2019/03/13	Boron, total	mg/L	0.158
UA	34	B	2019/09/18	Boron, total	mg/L	0.153
UA	34	B	2019/12/11	Boron, total	mg/L	0.128
UA	34	B	2020/03/11	Boron, total	mg/L	0.127
UA	34	B	2020/06/24	Boron, total	mg/L	0.149
UA	34	B	2020/09/02	Boron, total	mg/L	0.136
UA	34	B	2020/12/09	Boron, total	mg/L	0.151
UA	34	B	2021/03/19	Boron, total	mg/L	0.142
UA	34	B	2021/06/24	Boron, total	mg/L	0.122
UA	34	B	2021/09/09	Boron, total	mg/L	0.145
UA	34	B	2021/12/09	Boron, total	mg/L	0.147
UA	34	B	2022/03/22	Boron, total	mg/L	0.158
UA	34	B	2022/06/07	Boron, total	mg/L	0.127
UA	34	B	2022/12/29	Boron, total	mg/L	0.153
UA	34	B	2023/02/28	Boron, total	mg/L	0.206
UA	34	B	2023/05/31	Boron, total	mg/L	0.125
UA	34	B	2023/08/25	Boron, total	mg/L	0.0750
UA	34	B	2023/11/14	Boron, total	mg/L	0.110
UA	34	B	2013/09/04	Cadmium, total	mg/L	<0.0003
UA	34	B	2015/12/09	Cadmium, total	mg/L	<0.0002
UA	34	B	2016/03/08	Cadmium, total	mg/L	<0.0002
UA	34	B	2016/06/07	Cadmium, total	mg/L	<0.0002
UA	34	B	2016/09/15	Cadmium, total	mg/L	<0.0002
UA	34	B	2016/12/07	Cadmium, total	mg/L	<0.0002

UA	34	B	2017/02/21	Cadmium, total	mg/L	<0.0002
UA	34	B	2017/04/25	Cadmium, total	mg/L	<0.0002
UA	34	B	2017/06/08	Cadmium, total	mg/L	<0.0002
UA	34	B	2018/06/13	Cadmium, total	mg/L	<0.0002
UA	34	B	2018/09/12	Cadmium, total	mg/L	<0.0002
UA	34	B	2018/12/12	Cadmium, total	mg/L	<0.0002
UA	34	B	2019/03/13	Cadmium, total	mg/L	<0.0002
UA	34	B	2019/09/18	Cadmium, total	mg/L	<0.0002
UA	34	B	2019/12/11	Cadmium, total	mg/L	<0.0002
UA	34	B	2020/03/11	Cadmium, total	mg/L	<0.0002
UA	34	B	2020/06/24	Cadmium, total	mg/L	<0.0002
UA	34	B	2020/09/02	Cadmium, total	mg/L	<0.0002
UA	34	B	2020/12/09	Cadmium, total	mg/L	<0.0002
UA	34	B	2021/03/19	Cadmium, total	mg/L	<0.0002
UA	34	B	2021/06/24	Cadmium, total	mg/L	<0.0002
UA	34	B	2021/09/09	Cadmium, total	mg/L	<0.0002
UA	34	B	2021/12/09	Cadmium, total	mg/L	<0.0002
UA	34	B	2022/03/22	Cadmium, total	mg/L	<0.0002
UA	34	B	2022/06/07	Cadmium, total	mg/L	<0.0002
UA	34	B	2022/12/29	Cadmium, total	mg/L	<0.0002
UA	34	B	2023/02/28	Cadmium, total	mg/L	<0.0002
UA	34	B	2023/05/31	Cadmium, total	mg/L	<0.0005
UA	34	B	2023/08/25	Cadmium, total	mg/L	<0.00017
UA	34	B	2023/11/14	Cadmium, total	mg/L	<0.00017
UA	34	B	2015/12/09	Calcium, total	mg/L	162
UA	34	B	2016/03/08	Calcium, total	mg/L	168
UA	34	B	2016/06/07	Calcium, total	mg/L	161
UA	34	B	2016/09/15	Calcium, total	mg/L	156
UA	34	B	2016/12/07	Calcium, total	mg/L	165
UA	34	B	2017/02/21	Calcium, total	mg/L	170
UA	34	B	2017/04/25	Calcium, total	mg/L	142
UA	34	B	2017/06/08	Calcium, total	mg/L	160
UA	34	B	2017/11/15	Calcium, total	mg/L	170
UA	34	B	2018/06/13	Calcium, total	mg/L	162
UA	34	B	2018/09/12	Calcium, total	mg/L	170
UA	34	B	2018/12/12	Calcium, total	mg/L	153
UA	34	B	2019/03/13	Calcium, total	mg/L	165
UA	34	B	2019/09/18	Calcium, total	mg/L	165
UA	34	B	2019/12/11	Calcium, total	mg/L	161
UA	34	B	2020/03/11	Calcium, total	mg/L	157
UA	34	B	2020/06/24	Calcium, total	mg/L	152
UA	34	B	2020/09/02	Calcium, total	mg/L	159
UA	34	B	2020/12/09	Calcium, total	mg/L	208
UA	34	B	2021/03/19	Calcium, total	mg/L	177
UA	34	B	2021/06/24	Calcium, total	mg/L	167
UA	34	B	2021/09/09	Calcium, total	mg/L	180
UA	34	B	2021/12/09	Calcium, total	mg/L	175
UA	34	B	2022/03/22	Calcium, total	mg/L	167
UA	34	B	2022/06/07	Calcium, total	mg/L	166
UA	34	B	2022/12/29	Calcium, total	mg/L	163
UA	34	B	2023/02/28	Calcium, total	mg/L	184
UA	34	B	2023/05/31	Calcium, total	mg/L	149
UA	34	B	2023/08/25	Calcium, total	mg/L	150
UA	34	B	2023/11/14	Calcium, total	mg/L	150
UA	34	B	2013/03/08	Chloride, total	mg/L	97.0
UA	34	B	2013/09/04	Chloride, total	mg/L	81.0
UA	34	B	2013/12/10	Chloride, total	mg/L	83.0
UA	34	B	2014/03/25	Chloride, total	mg/L	82.0
UA	34	B	2015/03/18	Chloride, total	mg/L	97.0
UA	34	B	2015/12/09	Chloride, total	mg/L	88.0
UA	34	B	2016/03/08	Chloride, total	mg/L	108
UA	34	B	2016/06/07	Chloride, total	mg/L	107

UA	34	B	2016/09/15	Chloride, total	mg/L	104
UA	34	B	2016/12/07	Chloride, total	mg/L	108
UA	34	B	2017/02/21	Chloride, total	mg/L	101
UA	34	B	2017/04/25	Chloride, total	mg/L	105
UA	34	B	2017/06/08	Chloride, total	mg/L	101
UA	34	B	2017/11/15	Chloride, total	mg/L	88.0
UA	34	B	2018/03/26	Chloride, total	mg/L	90.0
UA	34	B	2018/06/13	Chloride, total	mg/L	90.0
UA	34	B	2018/09/12	Chloride, total	mg/L	87.0
UA	34	B	2018/12/12	Chloride, total	mg/L	80.0
UA	34	B	2019/03/13	Chloride, total	mg/L	78.0
UA	34	B	2019/09/18	Chloride, total	mg/L	72.0
UA	34	B	2019/12/11	Chloride, total	mg/L	74.0
UA	34	B	2020/03/11	Chloride, total	mg/L	72.0
UA	34	B	2020/06/24	Chloride, total	mg/L	73.0
UA	34	B	2020/09/02	Chloride, total	mg/L	74.0
UA	34	B	2020/12/09	Chloride, total	mg/L	75.0
UA	34	B	2021/03/19	Chloride, total	mg/L	73.0
UA	34	B	2021/06/24	Chloride, total	mg/L	76.0
UA	34	B	2021/09/09	Chloride, total	mg/L	70.0
UA	34	B	2021/12/09	Chloride, total	mg/L	74.0
UA	34	B	2022/03/22	Chloride, total	mg/L	74.0
UA	34	B	2022/06/07	Chloride, total	mg/L	76.0
UA	34	B	2022/12/29	Chloride, total	mg/L	83.0
UA	34	B	2023/02/28	Chloride, total	mg/L	80.0
UA	34	B	2023/05/31	Chloride, total	mg/L	71.0
UA	34	B	2023/08/25	Chloride, total	mg/L	69.0
UA	34	B	2023/11/14	Chloride, total	mg/L	67.0
UA	34	B	2013/03/08	Iron, dissolved	mg/L	6.82
UA	34	B	2013/12/10	Iron, dissolved	mg/L	6.81
UA	34	B	2014/03/25	Iron, dissolved	mg/L	3.49
UA	34	B	2015/03/18	Iron, dissolved	mg/L	8.63
UA	34	B	2016/03/08	Iron, dissolved	mg/L	6.69
UA	34	B	2017/02/21	Iron, dissolved	mg/L	5.76
UA	34	B	2018/03/26	Iron, dissolved	mg/L	1.90
UA	34	B	2023/05/31	Iron, dissolved	mg/L	4.85
UA	34	B	2023/08/25	Iron, dissolved	mg/L	6.80
UA	34	B	2015/12/09	Lithium, total	mg/L	0.0120
UA	34	B	2016/03/08	Lithium, total	mg/L	0.0132
UA	34	B	2016/06/07	Lithium, total	mg/L	0.0118
UA	34	B	2016/09/15	Lithium, total	mg/L	0.0130
UA	34	B	2016/12/07	Lithium, total	mg/L	0.0115
UA	34	B	2017/02/21	Lithium, total	mg/L	0.0120
UA	34	B	2017/04/25	Lithium, total	mg/L	0.0135
UA	34	B	2017/06/08	Lithium, total	mg/L	0.0122
UA	34	B	2018/06/13	Lithium, total	mg/L	0.0133
UA	34	B	2018/09/12	Lithium, total	mg/L	0.0136
UA	34	B	2018/12/12	Lithium, total	mg/L	0.0136
UA	34	B	2019/03/13	Lithium, total	mg/L	0.0154
UA	34	B	2019/09/18	Lithium, total	mg/L	0.0138
UA	34	B	2019/12/11	Lithium, total	mg/L	0.0144
UA	34	B	2020/03/11	Lithium, total	mg/L	0.0134
UA	34	B	2020/06/24	Lithium, total	mg/L	0.0135
UA	34	B	2020/09/02	Lithium, total	mg/L	0.0127
UA	34	B	2020/12/09	Lithium, total	mg/L	0.0127
UA	34	B	2021/03/19	Lithium, total	mg/L	0.0138
UA	34	B	2021/06/24	Lithium, total	mg/L	0.0130
UA	34	B	2021/09/09	Lithium, total	mg/L	0.0132
UA	34	B	2021/12/09	Lithium, total	mg/L	0.0137
UA	34	B	2022/03/22	Lithium, total	mg/L	0.0146
UA	34	B	2022/06/07	Lithium, total	mg/L	0.0140
UA	34	B	2022/12/29	Lithium, total	mg/L	0.0149

UA	34	B	2023/02/28	Lithium, total	mg/L	0.0111
UA	34	B	2023/05/31	Lithium, total	mg/L	0.00320
UA	34	B	2023/08/25	Lithium, total	mg/L	0.0130
UA	34	B	2023/11/14	Lithium, total	mg/L	0.0160
UA	34	B	2019/09/18	Magnesium, total	mg/L	42.0
UA	34	B	2020/03/11	Magnesium, total	mg/L	41.7
UA	34	B	2020/06/24	Magnesium, total	mg/L	42.0
UA	34	B	2021/03/19	Magnesium, total	mg/L	43.2
UA	34	B	2021/09/09	Magnesium, total	mg/L	48.6
UA	34	B	2022/03/22	Magnesium, total	mg/L	43.0
UA	34	B	2023/02/28	Magnesium, total	mg/L	47.7
UA	34	B	2023/05/31	Magnesium, total	mg/L	41.8
UA	34	B	2023/08/25	Magnesium, total	mg/L	40.0
UA	34	B	2023/11/14	Magnesium, total	mg/L	42.0
UA	34	B	2013/03/08	Manganese, dissolved	mg/L	1.12
UA	34	B	2013/12/10	Manganese, dissolved	mg/L	1.24
UA	34	B	2014/03/25	Manganese, dissolved	mg/L	1.26
UA	34	B	2015/03/18	Manganese, dissolved	mg/L	1.24
UA	34	B	2016/03/08	Manganese, dissolved	mg/L	1.18
UA	34	B	2017/02/21	Manganese, dissolved	mg/L	1.17
UA	34	B	2018/03/26	Manganese, dissolved	mg/L	1.18
UA	34	B	2023/05/31	Manganese, dissolved	mg/L	1.12
UA	34	B	2023/08/25	Manganese, dissolved	mg/L	1.30
UA	34	B	2023/05/31	Phosphate, dissolved	mg/L	0.365
UA	34	B	2023/08/25	Phosphate, dissolved	mg/L	0.500
UA	34	B	2019/09/18	Potassium, total	mg/L	0.381
UA	34	B	2020/03/11	Potassium, total	mg/L	0.360
UA	34	B	2020/06/24	Potassium, total	mg/L	0.433
UA	34	B	2021/03/19	Potassium, total	mg/L	0.414
UA	34	B	2021/09/09	Potassium, total	mg/L	0.788
UA	34	B	2022/03/22	Potassium, total	mg/L	0.414
UA	34	B	2023/02/28	Potassium, total	mg/L	0.423
UA	34	B	2023/05/31	Potassium, total	mg/L	0.450
UA	34	B	2023/08/25	Potassium, total	mg/L	0.420
UA	34	B	2023/11/14	Potassium, total	mg/L	0.480
UA	34	B	2023/05/31	Silicon, dissolved	mg/L	11.4
UA	34	B	2023/08/25	Silicon, dissolved	mg/L	13.0
UA	34	B	2019/09/18	Sodium, total	mg/L	52.1
UA	34	B	2020/03/11	Sodium, total	mg/L	54.7
UA	34	B	2020/06/24	Sodium, total	mg/L	55.7
UA	34	B	2021/03/19	Sodium, total	mg/L	55.8
UA	34	B	2021/09/09	Sodium, total	mg/L	49.5
UA	34	B	2022/03/22	Sodium, total	mg/L	53.7
UA	34	B	2023/02/28	Sodium, total	mg/L	54.7
UA	34	B	2023/05/31	Sodium, total	mg/L	53.5
UA	34	B	2023/08/25	Sodium, total	mg/L	44.0
UA	34	B	2023/11/14	Sodium, total	mg/L	49.0
UA	34	B	2013/03/08	Sulfate, total	mg/L	111
UA	34	B	2013/09/04	Sulfate, total	mg/L	80.0
UA	34	B	2013/12/10	Sulfate, total	mg/L	83.0
UA	34	B	2014/03/25	Sulfate, total	mg/L	78.0
UA	34	B	2015/03/18	Sulfate, total	mg/L	85.0
UA	34	B	2015/12/09	Sulfate, total	mg/L	106
UA	34	B	2016/03/08	Sulfate, total	mg/L	99.0
UA	34	B	2016/06/07	Sulfate, total	mg/L	98.0
UA	34	B	2016/09/15	Sulfate, total	mg/L	117
UA	34	B	2016/12/07	Sulfate, total	mg/L	115
UA	34	B	2017/02/21	Sulfate, total	mg/L	107
UA	34	B	2017/04/25	Sulfate, total	mg/L	113
UA	34	B	2017/06/08	Sulfate, total	mg/L	112
UA	34	B	2017/11/15	Sulfate, total	mg/L	94.0
UA	34	B	2018/03/26	Sulfate, total	mg/L	104

UA	34	B	2018/06/13	Sulfate, total	mg/L	97.0
UA	34	B	2018/09/12	Sulfate, total	mg/L	94.0
UA	34	B	2018/12/12	Sulfate, total	mg/L	95.0
UA	34	B	2019/03/13	Sulfate, total	mg/L	81.0
UA	34	B	2019/09/18	Sulfate, total	mg/L	68.0
UA	34	B	2019/12/11	Sulfate, total	mg/L	74.0
UA	34	B	2020/03/11	Sulfate, total	mg/L	69.0
UA	34	B	2020/06/24	Sulfate, total	mg/L	80.0
UA	34	B	2020/09/02	Sulfate, total	mg/L	74.0
UA	34	B	2020/12/09	Sulfate, total	mg/L	72.0
UA	34	B	2021/03/19	Sulfate, total	mg/L	64.0
UA	34	B	2021/06/24	Sulfate, total	mg/L	61.0
UA	34	B	2021/09/09	Sulfate, total	mg/L	67.0
UA	34	B	2021/12/09	Sulfate, total	mg/L	60.0
UA	34	B	2022/03/22	Sulfate, total	mg/L	56.0
UA	34	B	2022/06/07	Sulfate, total	mg/L	57.0
UA	34	B	2022/12/29	Sulfate, total	mg/L	45.0
UA	34	B	2023/02/28	Sulfate, total	mg/L	48.0
UA	34	B	2023/05/31	Sulfate, total	mg/L	49.0
UA	34	B	2023/08/25	Sulfate, total	mg/L	46.0
UA	34	B	2023/11/14	Sulfate, total	mg/L	49.0
UA	34	B	2013/03/08	Temperature (Celsius)	degrees C	11.0
UA	34	B	2013/09/04	Temperature (Celsius)	degrees C	13.0
UA	34	B	2013/12/10	Temperature (Celsius)	degrees C	9.80
UA	34	B	2014/03/25	Temperature (Celsius)	degrees C	11.0
UA	34	B	2015/03/18	Temperature (Celsius)	degrees C	11.9
UA	34	B	2015/12/09	Temperature (Celsius)	degrees C	12.9
UA	34	B	2016/03/08	Temperature (Celsius)	degrees C	11.7
UA	34	B	2016/06/07	Temperature (Celsius)	degrees C	12.6
UA	34	B	2016/09/15	Temperature (Celsius)	degrees C	13.8
UA	34	B	2016/12/07	Temperature (Celsius)	degrees C	10.8
UA	34	B	2017/02/21	Temperature (Celsius)	degrees C	13.2
UA	34	B	2017/04/25	Temperature (Celsius)	degrees C	22.5
UA	34	B	2017/06/08	Temperature (Celsius)	degrees C	22.2
UA	34	B	2017/11/15	Temperature (Celsius)	degrees C	13
UA	34	B	2018/03/26	Temperature (Celsius)	degrees C	12.8
UA	34	B	2018/06/13	Temperature (Celsius)	degrees C	15.1
UA	34	B	2018/09/12	Temperature (Celsius)	degrees C	21.1
UA	34	B	2018/12/12	Temperature (Celsius)	degrees C	11.8
UA	34	B	2019/03/13	Temperature (Celsius)	degrees C	12.6
UA	34	B	2019/09/18	Temperature (Celsius)	degrees C	12.6
UA	34	B	2019/12/11	Temperature (Celsius)	degrees C	12.2
UA	34	B	2020/03/11	Temperature (Celsius)	degrees C	11.8
UA	34	B	2020/06/24	Temperature (Celsius)	degrees C	12.6
UA	34	B	2020/09/02	Temperature (Celsius)	degrees C	12.8
UA	34	B	2020/12/09	Temperature (Celsius)	degrees C	12.4
UA	34	B	2021/03/19	Temperature (Celsius)	degrees C	12.0
UA	34	B	2021/06/24	Temperature (Celsius)	degrees C	12.4
UA	34	B	2021/09/09	Temperature (Celsius)	degrees C	12.8
UA	34	B	2021/12/09	Temperature (Celsius)	degrees C	12.3
UA	34	B	2022/03/22	Temperature (Celsius)	degrees C	12.1
UA	34	B	2022/06/07	Temperature (Celsius)	degrees C	12.6
UA	34	B	2022/12/29	Temperature (Celsius)	degrees C	12.4
UA	34	B	2023/02/28	Temperature (Celsius)	degrees C	11.2
UA	34	B	2023/05/31	Temperature (Celsius)	degrees C	12.3
UA	34	B	2023/08/25	Temperature (Celsius)	degrees C	12.8
UA	34	B	2023/11/14	Temperature (Celsius)	degrees C	12.6
UA	34	B	2013/03/08	Total Dissolved Solids	mg/L	754
UA	34	B	2013/09/04	Total Dissolved Solids	mg/L	798
UA	34	B	2013/12/10	Total Dissolved Solids	mg/L	772
UA	34	B	2014/03/25	Total Dissolved Solids	mg/L	752
UA	34	B	2015/03/18	Total Dissolved Solids	mg/L	846

UA	34	B	2015/12/09	Total Dissolved Solids	mg/L	786
UA	34	B	2016/03/08	Total Dissolved Solids	mg/L	776
UA	34	B	2016/06/07	Total Dissolved Solids	mg/L	830
UA	34	B	2016/09/15	Total Dissolved Solids	mg/L	780
UA	34	B	2016/12/07	Total Dissolved Solids	mg/L	772
UA	34	B	2017/02/21	Total Dissolved Solids	mg/L	740
UA	34	B	2017/04/25	Total Dissolved Solids	mg/L	790
UA	34	B	2017/06/08	Total Dissolved Solids	mg/L	752
UA	34	B	2017/11/15	Total Dissolved Solids	mg/L	710
UA	34	B	2018/03/26	Total Dissolved Solids	mg/L	758
UA	34	B	2018/06/13	Total Dissolved Solids	mg/L	800
UA	34	B	2018/09/12	Total Dissolved Solids	mg/L	836
UA	34	B	2018/12/12	Total Dissolved Solids	mg/L	776
UA	34	B	2019/03/13	Total Dissolved Solids	mg/L	748
UA	34	B	2019/09/18	Total Dissolved Solids	mg/L	756
UA	34	B	2019/12/11	Total Dissolved Solids	mg/L	690
UA	34	B	2020/03/11	Total Dissolved Solids	mg/L	708
UA	34	B	2020/06/24	Total Dissolved Solids	mg/L	718
UA	34	B	2020/09/02	Total Dissolved Solids	mg/L	640
UA	34	B	2020/12/09	Total Dissolved Solids	mg/L	696
UA	34	B	2021/03/19	Total Dissolved Solids	mg/L	702
UA	34	B	2021/06/24	Total Dissolved Solids	mg/L	702
UA	34	B	2021/09/09	Total Dissolved Solids	mg/L	696
UA	34	B	2021/12/09	Total Dissolved Solids	mg/L	658
UA	34	B	2022/03/22	Total Dissolved Solids	mg/L	720
UA	34	B	2022/06/07	Total Dissolved Solids	mg/L	740
UA	34	B	2022/12/29	Total Dissolved Solids	mg/L	738
UA	34	B	2023/02/28	Total Dissolved Solids	mg/L	685
UA	34	B	2023/05/31	Total Dissolved Solids	mg/L	845
UA	34	B	2023/08/25	Total Dissolved Solids	mg/L	760
UA	34	B	2023/11/14	Total Dissolved Solids	mg/L	700
UA	21R	C	2020/03/11	pH (field)	SU	7.6
UA	21R	C	2020/06/24	pH (field)	SU	7.6
UA	21R	C	2020/09/02	pH (field)	SU	7.6
UA	21R	C	2020/12/10	pH (field)	SU	7.6
UA	21R	C	2021/03/17	pH (field)	SU	7.2
UA	21R	C	2021/06/23	pH (field)	SU	7.3
UA	21R	C	2021/09/09	pH (field)	SU	7.4
UA	21R	C	2021/12/09	pH (field)	SU	7.2
UA	21R	C	2022/03/22	pH (field)	SU	7.2
UA	21R	C	2022/06/07	pH (field)	SU	7.3
UA	21R	C	2022/09/13	pH (field)	SU	7.3
UA	21R	C	2022/12/27	pH (field)	SU	7.3
UA	21R	C	2023/02/28	pH (field)	SU	7.3
UA	21R	C	2023/05/31	pH (field)	SU	7.4
UA	21R	C	2023/08/22	pH (field)	SU	7.5
UA	21R	C	2023/11/14	pH (field)	SU	7.7
UA	21R	C	2020/03/11	Oxidation Reduction Potential	mV	-161
UA	21R	C	2020/06/24	Oxidation Reduction Potential	mV	-147
UA	21R	C	2020/09/02	Oxidation Reduction Potential	mV	-149
UA	21R	C	2020/12/10	Oxidation Reduction Potential	mV	-166
UA	21R	C	2021/03/17	Oxidation Reduction Potential	mV	-153
UA	21R	C	2021/06/23	Oxidation Reduction Potential	mV	-191
UA	21R	C	2021/09/09	Oxidation Reduction Potential	mV	-178
UA	21R	C	2021/12/09	Oxidation Reduction Potential	mV	-130
UA	21R	C	2022/03/22	Oxidation Reduction Potential	mV	-164
UA	21R	C	2022/06/07	Oxidation Reduction Potential	mV	52.0
UA	21R	C	2022/09/13	Oxidation Reduction Potential	mV	37.0
UA	21R	C	2022/12/27	Oxidation Reduction Potential	mV	-144
UA	21R	C	2023/02/28	Oxidation Reduction Potential	mV	-143
UA	21R	C	2023/05/31	Oxidation Reduction Potential	mV	-178
UA	21R	C	2023/08/22	Oxidation Reduction Potential	mV	-136

UA	21R	C	2023/11/14	Oxidation Reduction Potential	mV	-167
UA	21R	C	2020/03/11	Eh	V	0.037
UA	21R	C	2020/06/24	Eh	V	0.050
UA	21R	C	2020/09/02	Eh	V	0.047
UA	21R	C	2020/12/10	Eh	V	0.031
UA	21R	C	2021/03/17	Eh	V	0.045
UA	21R	C	2021/06/23	Eh	V	0.0056
UA	21R	C	2021/09/09	Eh	V	0.017
UA	21R	C	2021/12/09	Eh	V	0.067
UA	21R	C	2022/03/22	Eh	V	0.034
UA	21R	C	2022/06/07	Eh	V	0.25
UA	21R	C	2022/09/13	Eh	V	0.23
UA	21R	C	2022/12/27	Eh	V	0.054
UA	21R	C	2023/02/28	Eh	V	0.055
UA	21R	C	2023/05/31	Eh	V	0.019
UA	21R	C	2023/08/22	Eh	V	0.058
UA	21R	C	2023/11/14	Eh	V	0.029
UA	21R	C	2020/03/11	Alkalinity, bicarbonate	mg/L CaCO3	360
UA	21R	C	2021/03/17	Alkalinity, bicarbonate	mg/L CaCO3	367
UA	21R	C	2021/09/09	Alkalinity, bicarbonate	mg/L CaCO3	370
UA	21R	C	2022/03/22	Alkalinity, bicarbonate	mg/L CaCO3	372
UA	21R	C	2022/09/13	Alkalinity, bicarbonate	mg/L CaCO3	376
UA	21R	C	2023/02/28	Alkalinity, bicarbonate	mg/L CaCO3	378
UA	21R	C	2023/05/31	Alkalinity, bicarbonate	mg/L CaCO3	388
UA	21R	C	2023/08/22	Alkalinity, bicarbonate	mg/L CaCO3	370
UA	21R	C	2023/11/14	Alkalinity, bicarbonate	mg/L CaCO3	390
UA	21R	C	2020/03/11	Arsenic, total	mg/L	0.0215
UA	21R	C	2020/06/24	Arsenic, total	mg/L	0.0215
UA	21R	C	2020/09/02	Arsenic, total	mg/L	0.0246
UA	21R	C	2020/12/10	Arsenic, total	mg/L	0.0305
UA	21R	C	2021/03/17	Arsenic, total	mg/L	0.0255
UA	21R	C	2021/06/23	Arsenic, total	mg/L	0.0269
UA	21R	C	2021/09/09	Arsenic, total	mg/L	0.0259
UA	21R	C	2021/12/09	Arsenic, total	mg/L	0.0267
UA	21R	C	2022/03/22	Arsenic, total	mg/L	0.0279
UA	21R	C	2022/06/07	Arsenic, total	mg/L	0.0259
UA	21R	C	2022/09/13	Arsenic, total	mg/L	0.0332
UA	21R	C	2022/12/27	Arsenic, total	mg/L	0.0275
UA	21R	C	2023/02/28	Arsenic, total	mg/L	0.0345
UA	21R	C	2023/05/31	Arsenic, total	mg/L	0.0274
UA	21R	C	2023/08/22	Arsenic, total	mg/L	0.0230
UA	21R	C	2023/11/14	Arsenic, total	mg/L	0.0210
UA	21R	C	2020/03/11	Barium, total	mg/L	0.274
UA	21R	C	2020/06/24	Barium, total	mg/L	0.295
UA	21R	C	2020/09/02	Barium, total	mg/L	0.311
UA	21R	C	2020/12/10	Barium, total	mg/L	0.360
UA	21R	C	2021/03/17	Barium, total	mg/L	0.329
UA	21R	C	2021/06/23	Barium, total	mg/L	0.316
UA	21R	C	2021/09/09	Barium, total	mg/L	0.304
UA	21R	C	2021/12/09	Barium, total	mg/L	0.316
UA	21R	C	2022/03/22	Barium, total	mg/L	0.326
UA	21R	C	2022/06/07	Barium, total	mg/L	0.287
UA	21R	C	2022/09/13	Barium, total	mg/L	0.378
UA	21R	C	2022/12/27	Barium, total	mg/L	0.331
UA	21R	C	2023/02/28	Barium, total	mg/L	0.398
UA	21R	C	2023/05/31	Barium, total	mg/L	0.296
UA	21R	C	2023/08/22	Barium, total	mg/L	0.300
UA	21R	C	2023/11/14	Barium, total	mg/L	0.310
UA	21R	C	2020/03/11	Boron, total	mg/L	3.72
UA	21R	C	2020/06/24	Boron, total	mg/L	3.61
UA	21R	C	2020/09/02	Boron, total	mg/L	3.23
UA	21R	C	2020/12/10	Boron, total	mg/L	3.31

UA	21R	C	2021/03/17	Boron, total	mg/L	3.11
UA	21R	C	2021/06/23	Boron, total	mg/L	2.92
UA	21R	C	2021/09/09	Boron, total	mg/L	3.23
UA	21R	C	2021/12/09	Boron, total	mg/L	2.91
UA	21R	C	2022/03/22	Boron, total	mg/L	3.33
UA	21R	C	2022/06/07	Boron, total	mg/L	2.57
UA	21R	C	2022/09/13	Boron, total	mg/L	2.28
UA	21R	C	2022/12/27	Boron, total	mg/L	2.99
UA	21R	C	2023/02/28	Boron, total	mg/L	3.28
UA	21R	C	2023/05/31	Boron, total	mg/L	2.32
UA	21R	C	2023/08/22	Boron, total	mg/L	1.70
UA	21R	C	2023/11/14	Boron, total	mg/L	2.10
UA	21R	C	2020/03/11	Cadmium, total	mg/L	<0.0002
UA	21R	C	2020/06/24	Cadmium, total	mg/L	<0.0002
UA	21R	C	2020/09/02	Cadmium, total	mg/L	<0.0002
UA	21R	C	2020/12/10	Cadmium, total	mg/L	<0.0002
UA	21R	C	2021/03/17	Cadmium, total	mg/L	<0.0002
UA	21R	C	2021/06/23	Cadmium, total	mg/L	<0.0002
UA	21R	C	2021/09/09	Cadmium, total	mg/L	<0.0002
UA	21R	C	2021/12/09	Cadmium, total	mg/L	<0.0002
UA	21R	C	2022/03/22	Cadmium, total	mg/L	<0.0002
UA	21R	C	2022/06/07	Cadmium, total	mg/L	<0.0002
UA	21R	C	2022/09/13	Cadmium, total	mg/L	<0.0002
UA	21R	C	2022/12/27	Cadmium, total	mg/L	<0.0002
UA	21R	C	2023/02/28	Cadmium, total	mg/L	0.000200
UA	21R	C	2023/05/31	Cadmium, total	mg/L	<0.0005
UA	21R	C	2023/08/22	Cadmium, total	mg/L	<0.00017
UA	21R	C	2023/11/14	Cadmium, total	mg/L	0.000240
UA	21R	C	2020/03/11	Calcium, total	mg/L	137
UA	21R	C	2020/06/24	Calcium, total	mg/L	125
UA	21R	C	2020/09/02	Calcium, total	mg/L	123
UA	21R	C	2020/12/10	Calcium, total	mg/L	162
UA	21R	C	2021/03/17	Calcium, total	mg/L	139
UA	21R	C	2021/06/23	Calcium, total	mg/L	144
UA	21R	C	2021/09/09	Calcium, total	mg/L	145
UA	21R	C	2021/12/09	Calcium, total	mg/L	154
UA	21R	C	2022/03/22	Calcium, total	mg/L	146
UA	21R	C	2022/06/07	Calcium, total	mg/L	139
UA	21R	C	2022/09/13	Calcium, total	mg/L	135
UA	21R	C	2022/12/27	Calcium, total	mg/L	135
UA	21R	C	2023/02/28	Calcium, total	mg/L	147
UA	21R	C	2023/05/31	Calcium, total	mg/L	121
UA	21R	C	2023/08/22	Calcium, total	mg/L	120
UA	21R	C	2023/11/14	Calcium, total	mg/L	120
UA	21R	C	2020/03/11	Chloride, total	mg/L	70.0
UA	21R	C	2020/06/24	Chloride, total	mg/L	70.0
UA	21R	C	2020/09/02	Chloride, total	mg/L	75.0
UA	21R	C	2020/12/10	Chloride, total	mg/L	90.0
UA	21R	C	2021/03/17	Chloride, total	mg/L	88.0
UA	21R	C	2021/06/23	Chloride, total	mg/L	96.0
UA	21R	C	2021/09/09	Chloride, total	mg/L	97.0
UA	21R	C	2021/12/09	Chloride, total	mg/L	107
UA	21R	C	2022/03/22	Chloride, total	mg/L	99.0
UA	21R	C	2022/06/07	Chloride, total	mg/L	97.0
UA	21R	C	2022/09/13	Chloride, total	mg/L	104
UA	21R	C	2022/12/27	Chloride, total	mg/L	107
UA	21R	C	2023/02/28	Chloride, total	mg/L	108
UA	21R	C	2023/05/31	Chloride, total	mg/L	103
UA	21R	C	2023/08/22	Chloride, total	mg/L	95.0
UA	21R	C	2023/11/14	Chloride, total	mg/L	89.0
UA	21R	C	2023/08/22	Ferrous Iron, dissolved	mg/L	0.916
UA	21R	C	2023/05/31	Iron, dissolved	mg/L	5.64

UA	21R	C	2023/08/22	Iron, dissolved	mg/L	5.40
UA	21R	C	2020/03/11	Lithium, total	mg/L	0.0236
UA	21R	C	2020/06/24	Lithium, total	mg/L	0.0193
UA	21R	C	2020/09/02	Lithium, total	mg/L	0.0185
UA	21R	C	2020/12/10	Lithium, total	mg/L	0.0203
UA	21R	C	2021/03/17	Lithium, total	mg/L	0.0209
UA	21R	C	2021/06/23	Lithium, total	mg/L	0.0213
UA	21R	C	2021/09/09	Lithium, total	mg/L	0.0229
UA	21R	C	2021/12/09	Lithium, total	mg/L	0.0242
UA	21R	C	2022/03/22	Lithium, total	mg/L	0.0280
UA	21R	C	2022/06/07	Lithium, total	mg/L	0.0209
UA	21R	C	2022/09/13	Lithium, total	mg/L	0.0178
UA	21R	C	2022/12/27	Lithium, total	mg/L	0.0252
UA	21R	C	2023/02/28	Lithium, total	mg/L	0.0199
UA	21R	C	2023/05/31	Lithium, total	mg/L	0.0167
UA	21R	C	2023/08/22	Lithium, total	mg/L	0.0260
UA	21R	C	2023/11/14	Lithium, total	mg/L	0.0280
UA	21R	C	2020/03/11	Magnesium, total	mg/L	44.2
UA	21R	C	2020/06/24	Magnesium, total	mg/L	42.7
UA	21R	C	2021/03/17	Magnesium, total	mg/L	45.6
UA	21R	C	2021/09/09	Magnesium, total	mg/L	47.4
UA	21R	C	2022/03/22	Magnesium, total	mg/L	46.6
UA	21R	C	2022/09/13	Magnesium, total	mg/L	42.0
UA	21R	C	2023/02/28	Magnesium, total	mg/L	44.7
UA	21R	C	2023/05/31	Magnesium, total	mg/L	41.7
UA	21R	C	2023/08/22	Magnesium, total	mg/L	39.0
UA	21R	C	2023/11/14	Magnesium, total	mg/L	39.0
UA	21R	C	2023/05/31	Manganese, dissolved	mg/L	0.111
UA	21R	C	2023/08/22	Manganese, dissolved	mg/L	0.110
UA	21R	C	2023/05/31	Phosphate, dissolved	mg/L	0.666
UA	21R	C	2023/08/22	Phosphate, dissolved	mg/L	<0.073
UA	21R	C	2020/03/11	Potassium, total	mg/L	4.02
UA	21R	C	2020/06/24	Potassium, total	mg/L	2.78
UA	21R	C	2021/03/17	Potassium, total	mg/L	3.08
UA	21R	C	2021/09/09	Potassium, total	mg/L	3.16
UA	21R	C	2022/03/22	Potassium, total	mg/L	3.10
UA	21R	C	2022/09/13	Potassium, total	mg/L	2.81
UA	21R	C	2023/02/28	Potassium, total	mg/L	2.91
UA	21R	C	2023/05/31	Potassium, total	mg/L	3.01
UA	21R	C	2023/08/22	Potassium, total	mg/L	2.80
UA	21R	C	2023/11/14	Potassium, total	mg/L	3.00
UA	21R	C	2023/05/31	Silicon, dissolved	mg/L	8.17
UA	21R	C	2023/08/22	Silicon, dissolved	mg/L	10.0
UA	21R	C	2020/03/11	Sodium, total	mg/L	32.6
UA	21R	C	2020/06/24	Sodium, total	mg/L	32.8
UA	21R	C	2021/03/17	Sodium, total	mg/L	40.2
UA	21R	C	2021/09/09	Sodium, total	mg/L	37.8
UA	21R	C	2022/03/22	Sodium, total	mg/L	47.5
UA	21R	C	2022/09/13	Sodium, total	mg/L	45.1
UA	21R	C	2023/02/28	Sodium, total	mg/L	52.5
UA	21R	C	2023/05/31	Sodium, total	mg/L	49.4
UA	21R	C	2023/08/22	Sodium, total	mg/L	45.0
UA	21R	C	2023/11/14	Sodium, total	mg/L	47.0
UA	21R	C	2020/03/11	Sulfate, total	mg/L	102
UA	21R	C	2020/06/24	Sulfate, total	mg/L	96.0
UA	21R	C	2020/09/02	Sulfate, total	mg/L	88.0
UA	21R	C	2020/12/10	Sulfate, total	mg/L	90.0
UA	21R	C	2021/03/17	Sulfate, total	mg/L	89.0
UA	21R	C	2021/06/23	Sulfate, total	mg/L	92.0
UA	21R	C	2021/09/09	Sulfate, total	mg/L	93.0
UA	21R	C	2021/12/09	Sulfate, total	mg/L	83.0
UA	21R	C	2022/03/22	Sulfate, total	mg/L	91.0

UA	21R	C	2022/06/07	Sulfate, total	mg/L	105
UA	21R	C	2022/09/13	Sulfate, total	mg/L	87.0
UA	21R	C	2022/12/27	Sulfate, total	mg/L	95.0
UA	21R	C	2023/02/28	Sulfate, total	mg/L	105
UA	21R	C	2023/05/31	Sulfate, total	mg/L	91.0
UA	21R	C	2023/08/22	Sulfate, total	mg/L	94.0
UA	21R	C	2023/11/14	Sulfate, total	mg/L	81.0
UA	21R	C	2020/03/11	Temperature (Celsius)	degrees C	11.7
UA	21R	C	2020/06/24	Temperature (Celsius)	degrees C	13.3
UA	21R	C	2020/09/02	Temperature (Celsius)	degrees C	14.2
UA	21R	C	2020/12/10	Temperature (Celsius)	degrees C	12.3
UA	21R	C	2021/03/17	Temperature (Celsius)	degrees C	10.8
UA	21R	C	2021/06/23	Temperature (Celsius)	degrees C	13.5
UA	21R	C	2021/09/09	Temperature (Celsius)	degrees C	15.8
UA	21R	C	2021/12/09	Temperature (Celsius)	degrees C	12.4
UA	21R	C	2022/03/22	Temperature (Celsius)	degrees C	11.8
UA	21R	C	2022/06/07	Temperature (Celsius)	degrees C	13.5
UA	21R	C	2022/09/13	Temperature (Celsius)	degrees C	14.3
UA	21R	C	2022/12/27	Temperature (Celsius)	degrees C	12.1
UA	21R	C	2023/02/28	Temperature (Celsius)	degrees C	10.9
UA	21R	C	2023/05/31	Temperature (Celsius)	degrees C	13.2
UA	21R	C	2023/08/22	Temperature (Celsius)	degrees C	16.6
UA	21R	C	2023/11/14	Temperature (Celsius)	degrees C	13.4
UA	21R	C	2020/03/11	Total Dissolved Solids	mg/L	590
UA	21R	C	2020/06/24	Total Dissolved Solids	mg/L	918
UA	21R	C	2020/09/02	Total Dissolved Solids	mg/L	540
UA	21R	C	2020/12/10	Total Dissolved Solids	mg/L	598
UA	21R	C	2021/03/17	Total Dissolved Solids	mg/L	636
UA	21R	C	2021/06/23	Total Dissolved Solids	mg/L	686
UA	21R	C	2021/09/09	Total Dissolved Solids	mg/L	684
UA	21R	C	2021/12/09	Total Dissolved Solids	mg/L	590
UA	21R	C	2022/03/22	Total Dissolved Solids	mg/L	622
UA	21R	C	2022/06/07	Total Dissolved Solids	mg/L	758
UA	21R	C	2022/09/13	Total Dissolved Solids	mg/L	682
UA	21R	C	2022/12/27	Total Dissolved Solids	mg/L	642
UA	21R	C	2023/02/28	Total Dissolved Solids	mg/L	678
UA	21R	C	2023/05/31	Total Dissolved Solids	mg/L	695
UA	21R	C	2023/08/22	Total Dissolved Solids	mg/L	730
UA	21R	C	2023/11/14	Total Dissolved Solids	mg/L	700
UA	22	C	2013/03/08	pH (field)	SU	7.3
UA	22	C	2013/06/07	pH (field)	SU	7.8
UA	22	C	2013/09/03	pH (field)	SU	7.9
UA	22	C	2013/12/10	pH (field)	SU	7.8
UA	22	C	2014/03/25	pH (field)	SU	7.3
UA	22	C	2014/08/19	pH (field)	SU	8.1
UA	22	C	2014/09/30	pH (field)	SU	8.1
UA	22	C	2015/03/18	pH (field)	SU	7.9
UA	22	C	2015/09/16	pH (field)	SU	7.8
UA	22	C	2015/12/10	pH (field)	SU	8.2
UA	22	C	2016/03/09	pH (field)	SU	7.8
UA	22	C	2016/06/07	pH (field)	SU	7.8
UA	22	C	2016/09/15	pH (field)	SU	7.8
UA	22	C	2016/12/07	pH (field)	SU	7.7
UA	22	C	2017/02/21	pH (field)	SU	7.4
UA	22	C	2017/04/25	pH (field)	SU	7.5
UA	22	C	2017/06/08	pH (field)	SU	7.7
UA	22	C	2017/09/06	pH (field)	SU	7.7
UA	22	C	2017/11/16	pH (field)	SU	7.4
UA	22	C	2018/03/26	pH (field)	SU	7.8
UA	22	C	2018/06/13	pH (field)	SU	7.2
UA	22	C	2018/09/12	pH (field)	SU	7.6
UA	22	C	2018/12/12	pH (field)	SU	7.6

UA	22	C	2019/03/13	pH (field)	SU	7.7
UA	22	C	2019/06/19	pH (field)	SU	7.6
UA	22	C	2019/09/17	pH (field)	SU	7.5
UA	22	C	2019/12/11	pH (field)	SU	7.6
UA	22	C	2020/03/11	pH (field)	SU	7.7
UA	22	C	2020/06/03	pH (field)	SU	7.7
UA	22	C	2020/06/25	pH (field)	SU	7.8
UA	22	C	2020/09/02	pH (field)	SU	7.6
UA	22	C	2020/12/09	pH (field)	SU	7.7
UA	22	C	2021/03/19	pH (field)	SU	7.7
UA	22	C	2021/06/23	pH (field)	SU	7.4
UA	22	C	2021/09/08	pH (field)	SU	7.2
UA	22	C	2021/12/08	pH (field)	SU	7.6
UA	22	C	2022/03/22	pH (field)	SU	7.6
UA	22	C	2022/06/07	pH (field)	SU	7.6
UA	22	C	2022/09/13	pH (field)	SU	7.5
UA	22	C	2022/12/27	pH (field)	SU	7.5
UA	22	C	2023/02/28	pH (field)	SU	7.6
UA	22	C	2023/05/31	pH (field)	SU	7.6
UA	22	C	2023/08/25	pH (field)	SU	7.7
UA	22	C	2023/11/15	pH (field)	SU	7.7
UA	22	C	2015/12/10	Oxidation Reduction Potential	mV	-18.0
UA	22	C	2016/03/09	Oxidation Reduction Potential	mV	-6.00
UA	22	C	2016/06/07	Oxidation Reduction Potential	mV	72.0
UA	22	C	2016/09/15	Oxidation Reduction Potential	mV	-1.00
UA	22	C	2016/12/07	Oxidation Reduction Potential	mV	126
UA	22	C	2017/02/21	Oxidation Reduction Potential	mV	114
UA	22	C	2017/04/25	Oxidation Reduction Potential	mV	-5.00
UA	22	C	2017/06/08	Oxidation Reduction Potential	mV	42.0
UA	22	C	2017/11/16	Oxidation Reduction Potential	mV	185
UA	22	C	2018/06/13	Oxidation Reduction Potential	mV	73.0
UA	22	C	2018/09/12	Oxidation Reduction Potential	mV	167
UA	22	C	2018/12/12	Oxidation Reduction Potential	mV	119
UA	22	C	2019/03/13	Oxidation Reduction Potential	mV	26.0
UA	22	C	2019/06/19	Oxidation Reduction Potential	mV	65.0
UA	22	C	2019/09/17	Oxidation Reduction Potential	mV	117
UA	22	C	2019/12/11	Oxidation Reduction Potential	mV	-47.0
UA	22	C	2020/03/11	Oxidation Reduction Potential	mV	121
UA	22	C	2020/06/03	Oxidation Reduction Potential	mV	76.0
UA	22	C	2020/06/25	Oxidation Reduction Potential	mV	69.2
UA	22	C	2020/09/02	Oxidation Reduction Potential	mV	118
UA	22	C	2020/12/09	Oxidation Reduction Potential	mV	-84.0
UA	22	C	2021/03/19	Oxidation Reduction Potential	mV	168
UA	22	C	2021/06/23	Oxidation Reduction Potential	mV	-51.0
UA	22	C	2021/09/08	Oxidation Reduction Potential	mV	64.0
UA	22	C	2021/12/08	Oxidation Reduction Potential	mV	55.0
UA	22	C	2022/03/22	Oxidation Reduction Potential	mV	-67.0
UA	22	C	2022/06/07	Oxidation Reduction Potential	mV	31.0
UA	22	C	2022/09/13	Oxidation Reduction Potential	mV	47.0
UA	22	C	2022/12/27	Oxidation Reduction Potential	mV	-54.0
UA	22	C	2023/02/28	Oxidation Reduction Potential	mV	51.9
UA	22	C	2023/05/31	Oxidation Reduction Potential	mV	49.0
UA	22	C	2023/08/25	Oxidation Reduction Potential	mV	77.8
UA	22	C	2023/11/15	Oxidation Reduction Potential	mV	-48.4
UA	22	C	2015/12/10	Eh	V	0.18
UA	22	C	2016/03/09	Eh	V	0.19
UA	22	C	2016/06/07	Eh	V	0.27
UA	22	C	2016/09/15	Eh	V	0.20
UA	22	C	2016/12/07	Eh	V	0.32
UA	22	C	2017/02/21	Eh	V	0.31
UA	22	C	2017/04/25	Eh	V	0.19
UA	22	C	2017/06/08	Eh	V	0.24

UA	22	C	2017/11/16	Eh	V	0.38
UA	22	C	2018/06/13	Eh	V	0.27
UA	22	C	2018/09/12	Eh	V	0.36
UA	22	C	2018/12/12	Eh	V	0.32
UA	22	C	2019/03/13	Eh	V	0.22
UA	22	C	2019/06/19	Eh	V	0.26
UA	22	C	2019/09/17	Eh	V	0.31
UA	22	C	2019/12/11	Eh	V	0.15
UA	22	C	2020/03/11	Eh	V	0.32
UA	22	C	2020/06/03	Eh	V	0.27
UA	22	C	2020/06/25	Eh	V	0.26
UA	22	C	2020/09/02	Eh	V	0.31
UA	22	C	2020/12/09	Eh	V	0.11
UA	22	C	2021/03/19	Eh	V	0.36
UA	22	C	2021/06/23	Eh	V	0.14
UA	22	C	2021/09/08	Eh	V	0.26
UA	22	C	2021/12/08	Eh	V	0.25
UA	22	C	2022/03/22	Eh	V	0.13
UA	22	C	2022/06/07	Eh	V	0.23
UA	22	C	2022/09/13	Eh	V	0.24
UA	22	C	2022/12/27	Eh	V	0.14
UA	22	C	2023/02/28	Eh	V	0.25
UA	22	C	2023/05/31	Eh	V	0.24
UA	22	C	2023/08/25	Eh	V	0.27
UA	22	C	2023/11/15	Eh	V	0.15
UA	22	C	2019/09/17	Alkalinity, bicarbonate	mg/L CaCO3	242
UA	22	C	2020/03/11	Alkalinity, bicarbonate	mg/L CaCO3	230
UA	22	C	2021/02/24	Alkalinity, bicarbonate	mg/L CaCO3	230
UA	22	C	2021/03/04	Alkalinity, bicarbonate	mg/L CaCO3	210
UA	22	C	2021/03/09	Alkalinity, bicarbonate	mg/L CaCO3	327
UA	22	C	2021/03/17	Alkalinity, bicarbonate	mg/L CaCO3	332
UA	22	C	2021/03/19	Alkalinity, bicarbonate	mg/L CaCO3	216
UA	22	C	2021/03/30	Alkalinity, bicarbonate	mg/L CaCO3	346
UA	22	C	2021/09/08	Alkalinity, bicarbonate	mg/L CaCO3	249
UA	22	C	2022/03/22	Alkalinity, bicarbonate	mg/L CaCO3	236
UA	22	C	2022/09/13	Alkalinity, bicarbonate	mg/L CaCO3	248
UA	22	C	2023/02/28	Alkalinity, bicarbonate	mg/L CaCO3	237
UA	22	C	2023/05/31	Alkalinity, bicarbonate	mg/L CaCO3	243
UA	22	C	2023/08/25	Alkalinity, bicarbonate	mg/L CaCO3	240
UA	22	C	2023/11/15	Alkalinity, bicarbonate	mg/L CaCO3	260
UA	22	C	2013/06/07	Arsenic, total	mg/L	<0.0007
UA	22	C	2013/09/03	Arsenic, total	mg/L	<0.0007
UA	22	C	2015/12/10	Arsenic, total	mg/L	<0.0002
UA	22	C	2016/03/09	Arsenic, total	mg/L	<0.0002
UA	22	C	2016/06/07	Arsenic, total	mg/L	<0.0002
UA	22	C	2016/09/15	Arsenic, total	mg/L	<0.0002
UA	22	C	2016/12/07	Arsenic, total	mg/L	<0.0002
UA	22	C	2017/02/21	Arsenic, total	mg/L	<0.0002
UA	22	C	2017/04/25	Arsenic, total	mg/L	<0.0002
UA	22	C	2017/06/08	Arsenic, total	mg/L	<0.0002
UA	22	C	2018/06/13	Arsenic, total	mg/L	<0.0004
UA	22	C	2018/09/12	Arsenic, total	mg/L	<0.0004
UA	22	C	2018/12/12	Arsenic, total	mg/L	<0.0004
UA	22	C	2019/03/13	Arsenic, total	mg/L	0.00140
UA	22	C	2019/06/19	Arsenic, total	mg/L	<0.0004
UA	22	C	2019/09/17	Arsenic, total	mg/L	<0.0004
UA	22	C	2019/12/11	Arsenic, total	mg/L	<0.0004
UA	22	C	2020/03/11	Arsenic, total	mg/L	<0.0004
UA	22	C	2020/06/03	Arsenic, total	mg/L	0.00110
UA	22	C	2020/09/02	Arsenic, total	mg/L	<0.0004
UA	22	C	2020/12/09	Arsenic, total	mg/L	0.00130
UA	22	C	2021/02/24	Arsenic, total	mg/L	<0.0000004

UA	22	C	2021/03/04	Arsenic, total	mg/L	0.00120
UA	22	C	2021/03/09	Arsenic, total	mg/L	0.00130
UA	22	C	2021/03/17	Arsenic, total	mg/L	0.00150
UA	22	C	2021/03/19	Arsenic, total	mg/L	<0.0004
UA	22	C	2021/03/30	Arsenic, total	mg/L	<0.0004
UA	22	C	2021/06/23	Arsenic, total	mg/L	<0.0004
UA	22	C	2021/09/08	Arsenic, total	mg/L	0.00110
UA	22	C	2021/12/08	Arsenic, total	mg/L	0.00100
UA	22	C	2022/03/22	Arsenic, total	mg/L	<0.0004
UA	22	C	2022/06/07	Arsenic, total	mg/L	0.000900
UA	22	C	2022/09/13	Arsenic, total	mg/L	0.00100
UA	22	C	2022/12/27	Arsenic, total	mg/L	0.000900
UA	22	C	2023/02/28	Arsenic, total	mg/L	0.00140
UA	22	C	2023/05/31	Arsenic, total	mg/L	<0.0087
UA	22	C	2023/08/25	Arsenic, total	mg/L	<0.00023
UA	22	C	2023/11/15	Arsenic, total	mg/L	0.000870
UA	22	C	2013/06/07	Barium, total	mg/L	0.0615
UA	22	C	2013/09/03	Barium, total	mg/L	0.0657
UA	22	C	2015/12/10	Barium, total	mg/L	0.0604
UA	22	C	2016/03/09	Barium, total	mg/L	0.0634
UA	22	C	2016/06/07	Barium, total	mg/L	0.0657
UA	22	C	2016/09/15	Barium, total	mg/L	0.0620
UA	22	C	2016/12/07	Barium, total	mg/L	0.0760
UA	22	C	2017/02/21	Barium, total	mg/L	0.0628
UA	22	C	2017/04/25	Barium, total	mg/L	0.0605
UA	22	C	2017/06/08	Barium, total	mg/L	0.0673
UA	22	C	2018/06/13	Barium, total	mg/L	0.0688
UA	22	C	2018/09/12	Barium, total	mg/L	0.0816
UA	22	C	2018/12/12	Barium, total	mg/L	0.0902
UA	22	C	2019/03/13	Barium, total	mg/L	0.0669
UA	22	C	2019/06/19	Barium, total	mg/L	0.0744
UA	22	C	2019/09/17	Barium, total	mg/L	0.0687
UA	22	C	2019/12/11	Barium, total	mg/L	0.0736
UA	22	C	2020/03/11	Barium, total	mg/L	0.0731
UA	22	C	2020/06/03	Barium, total	mg/L	0.0731
UA	22	C	2020/09/02	Barium, total	mg/L	0.0722
UA	22	C	2020/12/09	Barium, total	mg/L	0.0931
UA	22	C	2021/02/24	Barium, total	mg/L	0.0655
UA	22	C	2021/03/19	Barium, total	mg/L	0.0669
UA	22	C	2021/06/23	Barium, total	mg/L	0.0699
UA	22	C	2021/09/08	Barium, total	mg/L	0.0622
UA	22	C	2021/12/08	Barium, total	mg/L	0.0635
UA	22	C	2022/03/22	Barium, total	mg/L	0.0616
UA	22	C	2022/06/07	Barium, total	mg/L	0.0678
UA	22	C	2022/09/13	Barium, total	mg/L	0.0652
UA	22	C	2022/12/27	Barium, total	mg/L	0.0676
UA	22	C	2023/02/28	Barium, total	mg/L	0.0900
UA	22	C	2023/05/31	Barium, total	mg/L	0.0585
UA	22	C	2023/08/25	Barium, total	mg/L	0.0130
UA	22	C	2023/11/15	Barium, total	mg/L	0.0580
UA	22	C	2013/06/07	Boron, total	mg/L	7.66
UA	22	C	2013/09/03	Boron, total	mg/L	7.51
UA	22	C	2015/12/10	Boron, total	mg/L	6.01
UA	22	C	2016/03/09	Boron, total	mg/L	5.85
UA	22	C	2016/06/07	Boron, total	mg/L	6.28
UA	22	C	2016/09/15	Boron, total	mg/L	5.75
UA	22	C	2016/12/07	Boron, total	mg/L	6.72
UA	22	C	2017/02/21	Boron, total	mg/L	5.47
UA	22	C	2017/04/25	Boron, total	mg/L	5.29
UA	22	C	2017/06/08	Boron, total	mg/L	4.99
UA	22	C	2017/11/16	Boron, total	mg/L	5.35
UA	22	C	2018/06/13	Boron, total	mg/L	5.57

UA	22	C	2018/09/12	Boron, total	mg/L	4.66
UA	22	C	2018/12/12	Boron, total	mg/L	4.92
UA	22	C	2019/03/13	Boron, total	mg/L	5.75
UA	22	C	2019/06/19	Boron, total	mg/L	5.62
UA	22	C	2019/09/17	Boron, total	mg/L	5.37
UA	22	C	2019/12/11	Boron, total	mg/L	5.70
UA	22	C	2020/03/11	Boron, total	mg/L	5.20
UA	22	C	2020/06/03	Boron, total	mg/L	5.07
UA	22	C	2020/09/02	Boron, total	mg/L	4.72
UA	22	C	2020/12/09	Boron, total	mg/L	4.77
UA	22	C	2021/02/24	Boron, total	mg/L	4.92
UA	22	C	2021/03/04	Boron, total	mg/L	5.10
UA	22	C	2021/03/09	Boron, total	mg/L	1.90
UA	22	C	2021/03/17	Boron, total	mg/L	2.00
UA	22	C	2021/03/19	Boron, total	mg/L	4.89
UA	22	C	2021/03/30	Boron, total	mg/L	1.17
UA	22	C	2021/06/23	Boron, total	mg/L	4.91
UA	22	C	2021/09/08	Boron, total	mg/L	4.39
UA	22	C	2021/12/08	Boron, total	mg/L	3.81
UA	22	C	2022/03/22	Boron, total	mg/L	4.84
UA	22	C	2022/06/07	Boron, total	mg/L	3.95
UA	22	C	2022/09/13	Boron, total	mg/L	3.42
UA	22	C	2022/12/27	Boron, total	mg/L	4.44
UA	22	C	2023/02/28	Boron, total	mg/L	4.51
UA	22	C	2023/05/31	Boron, total	mg/L	3.44
UA	22	C	2023/08/25	Boron, total	mg/L	0.130
UA	22	C	2023/11/15	Boron, total	mg/L	3.20
UA	22	C	2013/06/07	Cadmium, total	mg/L	<0.0003
UA	22	C	2013/09/03	Cadmium, total	mg/L	<0.0003
UA	22	C	2015/12/10	Cadmium, total	mg/L	0.00140
UA	22	C	2016/03/09	Cadmium, total	mg/L	0.00170
UA	22	C	2016/06/07	Cadmium, total	mg/L	0.00230
UA	22	C	2016/09/15	Cadmium, total	mg/L	0.00310
UA	22	C	2016/12/07	Cadmium, total	mg/L	0.00440
UA	22	C	2017/02/21	Cadmium, total	mg/L	0.00390
UA	22	C	2017/04/25	Cadmium, total	mg/L	0.00360
UA	22	C	2017/06/08	Cadmium, total	mg/L	0.00320
UA	22	C	2018/06/13	Cadmium, total	mg/L	0.00430
UA	22	C	2018/09/12	Cadmium, total	mg/L	0.00570
UA	22	C	2018/12/12	Cadmium, total	mg/L	0.00760
UA	22	C	2019/03/13	Cadmium, total	mg/L	0.00570
UA	22	C	2019/06/19	Cadmium, total	mg/L	0.00480
UA	22	C	2019/09/17	Cadmium, total	mg/L	0.00480
UA	22	C	2019/12/11	Cadmium, total	mg/L	0.00550
UA	22	C	2020/03/11	Cadmium, total	mg/L	0.00500
UA	22	C	2020/06/03	Cadmium, total	mg/L	0.00530
UA	22	C	2020/09/02	Cadmium, total	mg/L	0.00530
UA	22	C	2020/12/09	Cadmium, total	mg/L	0.00900
UA	22	C	2021/02/24	Cadmium, total	mg/L	0.00600
UA	22	C	2021/03/19	Cadmium, total	mg/L	0.00590
UA	22	C	2021/06/23	Cadmium, total	mg/L	0.00600
UA	22	C	2021/09/08	Cadmium, total	mg/L	0.00540
UA	22	C	2021/12/08	Cadmium, total	mg/L	0.00540
UA	22	C	2022/03/22	Cadmium, total	mg/L	0.00570
UA	22	C	2022/06/07	Cadmium, total	mg/L	0.00570
UA	22	C	2022/09/13	Cadmium, total	mg/L	0.00570
UA	22	C	2022/12/27	Cadmium, total	mg/L	0.00590
UA	22	C	2023/02/28	Cadmium, total	mg/L	0.00960
UA	22	C	2023/05/31	Cadmium, total	mg/L	0.00520
UA	22	C	2023/08/25	Cadmium, total	mg/L	<0.00017
UA	22	C	2023/11/15	Cadmium, total	mg/L	0.00510
UA	22	C	2015/12/10	Calcium, total	mg/L	117

UA	22	C	2016/03/09	Calcium, total	mg/L	124
UA	22	C	2016/06/07	Calcium, total	mg/L	137
UA	22	C	2016/09/15	Calcium, total	mg/L	118
UA	22	C	2016/12/07	Calcium, total	mg/L	123
UA	22	C	2017/02/21	Calcium, total	mg/L	117
UA	22	C	2017/04/25	Calcium, total	mg/L	101
UA	22	C	2017/06/08	Calcium, total	mg/L	121
UA	22	C	2017/11/16	Calcium, total	mg/L	121
UA	22	C	2018/06/13	Calcium, total	mg/L	123
UA	22	C	2018/09/12	Calcium, total	mg/L	137
UA	22	C	2018/12/12	Calcium, total	mg/L	150
UA	22	C	2019/03/13	Calcium, total	mg/L	116
UA	22	C	2019/06/19	Calcium, total	mg/L	126
UA	22	C	2019/09/17	Calcium, total	mg/L	125
UA	22	C	2019/12/11	Calcium, total	mg/L	124
UA	22	C	2020/03/11	Calcium, total	mg/L	124
UA	22	C	2020/06/03	Calcium, total	mg/L	125
UA	22	C	2020/09/02	Calcium, total	mg/L	120
UA	22	C	2020/12/09	Calcium, total	mg/L	159
UA	22	C	2021/02/24	Calcium, total	mg/L	108
UA	22	C	2021/03/04	Calcium, total	mg/L	108
UA	22	C	2021/03/09	Calcium, total	mg/L	120
UA	22	C	2021/03/17	Calcium, total	mg/L	133
UA	22	C	2021/03/19	Calcium, total	mg/L	113
UA	22	C	2021/03/30	Calcium, total	mg/L	72.2
UA	22	C	2021/06/23	Calcium, total	mg/L	112
UA	22	C	2021/09/08	Calcium, total	mg/L	107
UA	22	C	2021/12/08	Calcium, total	mg/L	97.4
UA	22	C	2022/03/22	Calcium, total	mg/L	108
UA	22	C	2022/06/07	Calcium, total	mg/L	104
UA	22	C	2022/09/13	Calcium, total	mg/L	97.0
UA	22	C	2022/12/27	Calcium, total	mg/L	98.7
UA	22	C	2023/02/28	Calcium, total	mg/L	102
UA	22	C	2023/05/31	Calcium, total	mg/L	87.1
UA	22	C	2023/08/25	Calcium, total	mg/L	23.0
UA	22	C	2023/11/15	Calcium, total	mg/L	87.0
UA	22	C	2013/03/08	Chloride, total	mg/L	31.0
UA	22	C	2013/06/07	Chloride, total	mg/L	38.0
UA	22	C	2013/09/03	Chloride, total	mg/L	34.0
UA	22	C	2013/12/10	Chloride, total	mg/L	38.0
UA	22	C	2014/03/25	Chloride, total	mg/L	36.0
UA	22	C	2014/09/30	Chloride, total	mg/L	40.0
UA	22	C	2015/03/18	Chloride, total	mg/L	56.0
UA	22	C	2015/09/16	Chloride, total	mg/L	56.0
UA	22	C	2015/12/10	Chloride, total	mg/L	65.0
UA	22	C	2016/03/09	Chloride, total	mg/L	76.0
UA	22	C	2016/06/07	Chloride, total	mg/L	76.0
UA	22	C	2016/09/15	Chloride, total	mg/L	78.0
UA	22	C	2016/12/07	Chloride, total	mg/L	85.0
UA	22	C	2017/02/21	Chloride, total	mg/L	77.0
UA	22	C	2017/04/25	Chloride, total	mg/L	81.0
UA	22	C	2017/06/08	Chloride, total	mg/L	77.0
UA	22	C	2017/09/06	Chloride, total	mg/L	83.0
UA	22	C	2017/11/16	Chloride, total	mg/L	83.0
UA	22	C	2018/03/26	Chloride, total	mg/L	88.0
UA	22	C	2018/06/13	Chloride, total	mg/L	88.0
UA	22	C	2018/09/12	Chloride, total	mg/L	90.0
UA	22	C	2018/12/12	Chloride, total	mg/L	89.0
UA	22	C	2019/03/13	Chloride, total	mg/L	86.0
UA	22	C	2019/06/19	Chloride, total	mg/L	79.0
UA	22	C	2019/09/17	Chloride, total	mg/L	84.0
UA	22	C	2019/12/11	Chloride, total	mg/L	87.0

UA	22	C	2020/03/11	Chloride, total	mg/L	84.0
UA	22	C	2020/06/03	Chloride, total	mg/L	86.0
UA	22	C	2020/09/02	Chloride, total	mg/L	83.0
UA	22	C	2020/12/09	Chloride, total	mg/L	85.0
UA	22	C	2021/02/24	Chloride, total	mg/L	79.0
UA	22	C	2021/03/04	Chloride, total	mg/L	88.0
UA	22	C	2021/03/09	Chloride, total	mg/L	97.0
UA	22	C	2021/03/17	Chloride, total	mg/L	92.0
UA	22	C	2021/03/19	Chloride, total	mg/L	79.0
UA	22	C	2021/03/30	Chloride, total	mg/L	97.0
UA	22	C	2021/06/23	Chloride, total	mg/L	93.0
UA	22	C	2021/09/08	Chloride, total	mg/L	93.0
UA	22	C	2021/12/08	Chloride, total	mg/L	23.0
UA	22	C	2022/03/22	Chloride, total	mg/L	90.0
UA	22	C	2022/06/07	Chloride, total	mg/L	92.0
UA	22	C	2022/09/13	Chloride, total	mg/L	97.0
UA	22	C	2022/12/27	Chloride, total	mg/L	104
UA	22	C	2023/02/28	Chloride, total	mg/L	100
UA	22	C	2023/05/31	Chloride, total	mg/L	97.0
UA	22	C	2023/08/25	Chloride, total	mg/L	89.0
UA	22	C	2023/11/15	Chloride, total	mg/L	92.0
UA	22	C	2013/12/10	Iron, dissolved	mg/L	<0.007
UA	22	C	2014/03/25	Iron, dissolved	mg/L	<0.007
UA	22	C	2014/08/19	Iron, dissolved	mg/L	<0.007
UA	22	C	2014/09/30	Iron, dissolved	mg/L	<0.007
UA	22	C	2015/03/18	Iron, dissolved	mg/L	<0.007
UA	22	C	2015/09/16	Iron, dissolved	mg/L	<0.007
UA	22	C	2016/03/09	Iron, dissolved	mg/L	<0.007
UA	22	C	2016/09/15	Iron, dissolved	mg/L	<0.007
UA	22	C	2017/02/21	Iron, dissolved	mg/L	<0.007
UA	22	C	2017/09/06	Iron, dissolved	mg/L	<0.007
UA	22	C	2018/03/26	Iron, dissolved	mg/L	<0.007
UA	22	C	2021/02/24	Iron, dissolved	mg/L	<0.0000115
UA	22	C	2021/03/04	Iron, dissolved	mg/L	<0.0115
UA	22	C	2021/03/09	Iron, dissolved	mg/L	2.20
UA	22	C	2021/03/17	Iron, dissolved	mg/L	2.23
UA	22	C	2021/03/30	Iron, dissolved	mg/L	2.10
UA	22	C	2023/05/31	Iron, dissolved	mg/L	<0.02
UA	22	C	2023/08/25	Iron, dissolved	mg/L	<0.047
UA	22	C	2015/12/10	Lithium, total	mg/L	0.0588
UA	22	C	2016/03/09	Lithium, total	mg/L	0.0594
UA	22	C	2016/06/07	Lithium, total	mg/L	0.0641
UA	22	C	2016/09/15	Lithium, total	mg/L	0.0595
UA	22	C	2016/12/07	Lithium, total	mg/L	0.0552
UA	22	C	2017/02/21	Lithium, total	mg/L	0.0554
UA	22	C	2017/04/25	Lithium, total	mg/L	0.0527
UA	22	C	2017/06/08	Lithium, total	mg/L	0.0543
UA	22	C	2018/06/13	Lithium, total	mg/L	0.0616
UA	22	C	2018/09/12	Lithium, total	mg/L	0.0764
UA	22	C	2018/12/12	Lithium, total	mg/L	0.0550
UA	22	C	2019/03/13	Lithium, total	mg/L	0.0650
UA	22	C	2019/06/19	Lithium, total	mg/L	0.0654
UA	22	C	2019/09/17	Lithium, total	mg/L	0.0610
UA	22	C	2019/12/11	Lithium, total	mg/L	0.0632
UA	22	C	2020/03/11	Lithium, total	mg/L	0.0616
UA	22	C	2020/06/03	Lithium, total	mg/L	0.0580
UA	22	C	2020/09/02	Lithium, total	mg/L	0.0545
UA	22	C	2020/12/09	Lithium, total	mg/L	0.0543
UA	22	C	2021/02/24	Lithium, total	mg/L	0.0529
UA	22	C	2021/03/04	Lithium, total	mg/L	0.0621
UA	22	C	2021/03/09	Lithium, total	mg/L	0.0140
UA	22	C	2021/03/17	Lithium, total	mg/L	0.0160

UA	22	C	2021/03/19	Lithium, total	mg/L	0.0562
UA	22	C	2021/03/30	Lithium, total	mg/L	0.00900
UA	22	C	2021/06/23	Lithium, total	mg/L	0.0583
UA	22	C	2021/09/08	Lithium, total	mg/L	0.0542
UA	22	C	2021/12/08	Lithium, total	mg/L	0.0477
UA	22	C	2022/03/22	Lithium, total	mg/L	0.0620
UA	22	C	2022/06/07	Lithium, total	mg/L	0.0507
UA	22	C	2022/09/13	Lithium, total	mg/L	0.0439
UA	22	C	2022/12/27	Lithium, total	mg/L	0.0584
UA	22	C	2023/02/28	Lithium, total	mg/L	0.0419
UA	22	C	2023/05/31	Lithium, total	mg/L	0.0500
UA	22	C	2023/08/25	Lithium, total	mg/L	0.0490
UA	22	C	2023/11/15	Lithium, total	mg/L	0.0510
UA	22	C	2019/09/17	Magnesium, total	mg/L	33.6
UA	22	C	2020/03/11	Magnesium, total	mg/L	35.1
UA	22	C	2020/06/03	Magnesium, total	mg/L	33.8
UA	22	C	2021/02/24	Magnesium, total	mg/L	32.4
UA	22	C	2021/03/04	Magnesium, total	mg/L	30.4
UA	22	C	2021/03/09	Magnesium, total	mg/L	51.0
UA	22	C	2021/03/17	Magnesium, total	mg/L	44.9
UA	22	C	2021/03/19	Magnesium, total	mg/L	34.0
UA	22	C	2021/03/30	Magnesium, total	mg/L	25.4
UA	22	C	2021/09/08	Magnesium, total	mg/L	30.8
UA	22	C	2022/03/22	Magnesium, total	mg/L	33.4
UA	22	C	2022/09/13	Magnesium, total	mg/L	31.0
UA	22	C	2023/02/28	Magnesium, total	mg/L	34.0
UA	22	C	2023/05/31	Magnesium, total	mg/L	32.0
UA	22	C	2023/08/25	Magnesium, total	mg/L	7.10
UA	22	C	2023/11/15	Magnesium, total	mg/L	32.0
UA	22	C	2013/03/08	Manganese, dissolved	mg/L	0.0500
UA	22	C	2013/12/10	Manganese, dissolved	mg/L	0.0779
UA	22	C	2014/03/25	Manganese, dissolved	mg/L	0.0405
UA	22	C	2014/08/19	Manganese, dissolved	mg/L	0.0354
UA	22	C	2014/09/30	Manganese, dissolved	mg/L	0.0663
UA	22	C	2015/03/18	Manganese, dissolved	mg/L	0.0533
UA	22	C	2015/09/16	Manganese, dissolved	mg/L	0.0835
UA	22	C	2016/03/09	Manganese, dissolved	mg/L	0.104
UA	22	C	2016/09/15	Manganese, dissolved	mg/L	0.125
UA	22	C	2017/02/21	Manganese, dissolved	mg/L	0.123
UA	22	C	2017/09/06	Manganese, dissolved	mg/L	0.120
UA	22	C	2018/03/26	Manganese, dissolved	mg/L	0.120
UA	22	C	2021/02/24	Manganese, dissolved	mg/L	0.0874
UA	22	C	2021/03/04	Manganese, dissolved	mg/L	0.101
UA	22	C	2021/03/09	Manganese, dissolved	mg/L	0.0730
UA	22	C	2021/03/17	Manganese, dissolved	mg/L	0.0726
UA	22	C	2021/03/30	Manganese, dissolved	mg/L	0.0698
UA	22	C	2023/05/31	Manganese, dissolved	mg/L	0.0340
UA	22	C	2023/08/25	Manganese, dissolved	mg/L	0.0360
UA	22	C	2023/05/31	Phosphate, dissolved	mg/L	<0.005
UA	22	C	2023/08/25	Phosphate, dissolved	mg/L	0.300
UA	22	C	2019/09/17	Potassium, total	mg/L	12.4
UA	22	C	2020/03/11	Potassium, total	mg/L	14.0
UA	22	C	2020/06/03	Potassium, total	mg/L	12.8
UA	22	C	2021/02/24	Potassium, total	mg/L	12.4
UA	22	C	2021/03/04	Potassium, total	mg/L	12.7
UA	22	C	2021/03/09	Potassium, total	mg/L	3.30
UA	22	C	2021/03/17	Potassium, total	mg/L	3.50
UA	22	C	2021/03/19	Potassium, total	mg/L	13.1
UA	22	C	2021/03/30	Potassium, total	mg/L	1.84
UA	22	C	2021/09/08	Potassium, total	mg/L	12.2
UA	22	C	2022/03/22	Potassium, total	mg/L	12.3
UA	22	C	2022/09/13	Potassium, total	mg/L	11.4

UA	22	C	2023/02/28	Potassium, total	mg/L	11.5
UA	22	C	2023/05/31	Potassium, total	mg/L	11.4
UA	22	C	2023/08/25	Potassium, total	mg/L	2.50
UA	22	C	2023/11/15	Potassium, total	mg/L	10.0
UA	22	C	2023/05/31	Silicon, dissolved	mg/L	17.2
UA	22	C	2023/08/25	Silicon, dissolved	mg/L	21.0
UA	22	C	2019/09/17	Sodium, total	mg/L	55.8
UA	22	C	2020/03/11	Sodium, total	mg/L	56.1
UA	22	C	2020/06/03	Sodium, total	mg/L	57.0
UA	22	C	2021/02/24	Sodium, total	mg/L	55.6
UA	22	C	2021/03/04	Sodium, total	mg/L	61.1
UA	22	C	2021/03/09	Sodium, total	mg/L	41.0
UA	22	C	2021/03/17	Sodium, total	mg/L	43.9
UA	22	C	2021/03/19	Sodium, total	mg/L	57.5
UA	22	C	2021/03/30	Sodium, total	mg/L	24.5
UA	22	C	2021/09/08	Sodium, total	mg/L	56.3
UA	22	C	2022/03/22	Sodium, total	mg/L	59.3
UA	22	C	2022/09/13	Sodium, total	mg/L	52.6
UA	22	C	2023/02/28	Sodium, total	mg/L	57.4
UA	22	C	2023/05/31	Sodium, total	mg/L	55.8
UA	22	C	2023/08/25	Sodium, total	mg/L	12.0
UA	22	C	2023/11/15	Sodium, total	mg/L	55.0
UA	22	C	2013/03/08	Sulfate, total	mg/L	339
UA	22	C	2013/06/07	Sulfate, total	mg/L	346
UA	22	C	2013/09/03	Sulfate, total	mg/L	341
UA	22	C	2013/12/10	Sulfate, total	mg/L	280
UA	22	C	2014/03/25	Sulfate, total	mg/L	264
UA	22	C	2014/09/30	Sulfate, total	mg/L	242
UA	22	C	2015/03/18	Sulfate, total	mg/L	236
UA	22	C	2015/09/16	Sulfate, total	mg/L	224
UA	22	C	2015/12/10	Sulfate, total	mg/L	221
UA	22	C	2016/03/09	Sulfate, total	mg/L	261
UA	22	C	2016/06/07	Sulfate, total	mg/L	255
UA	22	C	2016/09/15	Sulfate, total	mg/L	208
UA	22	C	2016/12/07	Sulfate, total	mg/L	204
UA	22	C	2017/02/21	Sulfate, total	mg/L	197
UA	22	C	2017/04/25	Sulfate, total	mg/L	213
UA	22	C	2017/06/08	Sulfate, total	mg/L	229
UA	22	C	2017/09/06	Sulfate, total	mg/L	228
UA	22	C	2017/11/16	Sulfate, total	mg/L	187
UA	22	C	2018/03/26	Sulfate, total	mg/L	224
UA	22	C	2018/06/13	Sulfate, total	mg/L	219
UA	22	C	2018/09/12	Sulfate, total	mg/L	207
UA	22	C	2018/12/12	Sulfate, total	mg/L	181
UA	22	C	2019/03/13	Sulfate, total	mg/L	179
UA	22	C	2019/06/19	Sulfate, total	mg/L	249
UA	22	C	2019/09/17	Sulfate, total	mg/L	204
UA	22	C	2019/12/11	Sulfate, total	mg/L	187
UA	22	C	2020/03/11	Sulfate, total	mg/L	220
UA	22	C	2020/06/03	Sulfate, total	mg/L	214
UA	22	C	2020/09/02	Sulfate, total	mg/L	206
UA	22	C	2020/12/09	Sulfate, total	mg/L	201
UA	22	C	2021/02/24	Sulfate, total	mg/L	182
UA	22	C	2021/03/04	Sulfate, total	mg/L	205
UA	22	C	2021/03/09	Sulfate, total	mg/L	112
UA	22	C	2021/03/17	Sulfate, total	mg/L	101
UA	22	C	2021/03/19	Sulfate, total	mg/L	179
UA	22	C	2021/03/30	Sulfate, total	mg/L	107
UA	22	C	2021/06/23	Sulfate, total	mg/L	168
UA	22	C	2021/09/08	Sulfate, total	mg/L	160
UA	22	C	2021/12/08	Sulfate, total	mg/L	146
UA	22	C	2022/03/22	Sulfate, total	mg/L	145

UA	22	C	2022/06/07	Sulfate, total	mg/L	134
UA	22	C	2022/09/13	Sulfate, total	mg/L	142
UA	22	C	2022/12/27	Sulfate, total	mg/L	141
UA	22	C	2023/02/28	Sulfate, total	mg/L	145
UA	22	C	2023/05/31	Sulfate, total	mg/L	123
UA	22	C	2023/08/25	Sulfate, total	mg/L	120
UA	22	C	2023/11/15	Sulfate, total	mg/L	120
UA	22	C	2013/03/08	Temperature (Celsius)	degrees C	11.7
UA	22	C	2013/06/07	Temperature (Celsius)	degrees C	13.6
UA	22	C	2013/09/03	Temperature (Celsius)	degrees C	13.6
UA	22	C	2013/12/10	Temperature (Celsius)	degrees C	10.1
UA	22	C	2014/03/25	Temperature (Celsius)	degrees C	10.5
UA	22	C	2014/08/19	Temperature (Celsius)	degrees C	13.8
UA	22	C	2014/09/30	Temperature (Celsius)	degrees C	13.1
UA	22	C	2015/03/18	Temperature (Celsius)	degrees C	12.0
UA	22	C	2015/09/16	Temperature (Celsius)	degrees C	13.4
UA	22	C	2015/12/10	Temperature (Celsius)	degrees C	13.2
UA	22	C	2016/03/09	Temperature (Celsius)	degrees C	12.0
UA	22	C	2016/06/07	Temperature (Celsius)	degrees C	12.5
UA	22	C	2016/09/15	Temperature (Celsius)	degrees C	14.0
UA	22	C	2016/12/07	Temperature (Celsius)	degrees C	10.3
UA	22	C	2017/02/21	Temperature (Celsius)	degrees C	14.0
UA	22	C	2017/04/25	Temperature (Celsius)	degrees C	21.0
UA	22	C	2017/06/08	Temperature (Celsius)	degrees C	14.3
UA	22	C	2017/09/06	Temperature (Celsius)	degrees C	13.6
UA	22	C	2017/11/16	Temperature (Celsius)	degrees C	13.3
UA	22	C	2018/03/26	Temperature (Celsius)	degrees C	14.6
UA	22	C	2018/06/13	Temperature (Celsius)	degrees C	15.4
UA	22	C	2018/09/12	Temperature (Celsius)	degrees C	15.8
UA	22	C	2018/12/12	Temperature (Celsius)	degrees C	13.6
UA	22	C	2019/03/13	Temperature (Celsius)	degrees C	13.8
UA	22	C	2019/06/19	Temperature (Celsius)	degrees C	14.4
UA	22	C	2019/09/17	Temperature (Celsius)	degrees C	14.8
UA	22	C	2019/12/11	Temperature (Celsius)	degrees C	14.2
UA	22	C	2020/03/11	Temperature (Celsius)	degrees C	14.5
UA	22	C	2020/06/03	Temperature (Celsius)	degrees C	15.1
UA	22	C	2020/06/25	Temperature (Celsius)	degrees C	15.1
UA	22	C	2020/09/02	Temperature (Celsius)	degrees C	16.0
UA	22	C	2020/12/09	Temperature (Celsius)	degrees C	14.8
UA	22	C	2021/03/19	Temperature (Celsius)	degrees C	15.0
UA	22	C	2021/06/23	Temperature (Celsius)	degrees C	15.8
UA	22	C	2021/09/08	Temperature (Celsius)	degrees C	16.5
UA	22	C	2021/12/08	Temperature (Celsius)	degrees C	15.1
UA	22	C	2022/03/22	Temperature (Celsius)	degrees C	14.6
UA	22	C	2022/06/07	Temperature (Celsius)	degrees C	15.8
UA	22	C	2022/09/13	Temperature (Celsius)	degrees C	15.8
UA	22	C	2022/12/27	Temperature (Celsius)	degrees C	14.3
UA	22	C	2023/02/28	Temperature (Celsius)	degrees C	14.8
UA	22	C	2023/05/31	Temperature (Celsius)	degrees C	15.7
UA	22	C	2023/08/25	Temperature (Celsius)	degrees C	16.1
UA	22	C	2023/11/15	Temperature (Celsius)	degrees C	15.7
UA	22	C	2013/03/08	Total Dissolved Solids	mg/L	646
UA	22	C	2013/06/07	Total Dissolved Solids	mg/L	702
UA	22	C	2013/09/03	Total Dissolved Solids	mg/L	784
UA	22	C	2013/12/10	Total Dissolved Solids	mg/L	694
UA	22	C	2014/03/25	Total Dissolved Solids	mg/L	596
UA	22	C	2014/08/19	Total Dissolved Solids	mg/L	654
UA	22	C	2014/09/30	Total Dissolved Solids	mg/L	688
UA	22	C	2015/03/18	Total Dissolved Solids	mg/L	650
UA	22	C	2015/09/16	Total Dissolved Solids	mg/L	664
UA	22	C	2015/12/10	Total Dissolved Solids	mg/L	660
UA	22	C	2016/03/09	Total Dissolved Solids	mg/L	684

UA	22	C	2016/06/07	Total Dissolved Solids	mg/L	718
UA	22	C	2016/09/15	Total Dissolved Solids	mg/L	706
UA	22	C	2016/12/07	Total Dissolved Solids	mg/L	670
UA	22	C	2017/02/21	Total Dissolved Solids	mg/L	678
UA	22	C	2017/04/25	Total Dissolved Solids	mg/L	730
UA	22	C	2017/06/08	Total Dissolved Solids	mg/L	760
UA	22	C	2017/09/06	Total Dissolved Solids	mg/L	698
UA	22	C	2017/11/16	Total Dissolved Solids	mg/L	694
UA	22	C	2018/03/26	Total Dissolved Solids	mg/L	684
UA	22	C	2018/06/13	Total Dissolved Solids	mg/L	740
UA	22	C	2018/09/12	Total Dissolved Solids	mg/L	800
UA	22	C	2018/12/12	Total Dissolved Solids	mg/L	734
UA	22	C	2019/03/13	Total Dissolved Solids	mg/L	710
UA	22	C	2019/06/19	Total Dissolved Solids	mg/L	774
UA	22	C	2019/09/17	Total Dissolved Solids	mg/L	732
UA	22	C	2019/12/11	Total Dissolved Solids	mg/L	676
UA	22	C	2020/03/11	Total Dissolved Solids	mg/L	722
UA	22	C	2020/06/03	Total Dissolved Solids	mg/L	688
UA	22	C	2020/09/02	Total Dissolved Solids	mg/L	676
UA	22	C	2020/12/09	Total Dissolved Solids	mg/L	684
UA	22	C	2021/02/24	Total Dissolved Solids	mg/L	674
UA	22	C	2021/03/04	Total Dissolved Solids	mg/L	688
UA	22	C	2021/03/09	Total Dissolved Solids	mg/L	646
UA	22	C	2021/03/17	Total Dissolved Solids	mg/L	712
UA	22	C	2021/03/19	Total Dissolved Solids	mg/L	644
UA	22	C	2021/03/30	Total Dissolved Solids	mg/L	618
UA	22	C	2021/06/23	Total Dissolved Solids	mg/L	640
UA	22	C	2021/09/08	Total Dissolved Solids	mg/L	626
UA	22	C	2021/12/08	Total Dissolved Solids	mg/L	588
UA	22	C	2022/03/22	Total Dissolved Solids	mg/L	608
UA	22	C	2022/06/07	Total Dissolved Solids	mg/L	664
UA	22	C	2022/09/13	Total Dissolved Solids	mg/L	662
UA	22	C	2022/12/27	Total Dissolved Solids	mg/L	594
UA	22	C	2023/02/28	Total Dissolved Solids	mg/L	598
UA	22	C	2023/05/31	Total Dissolved Solids	mg/L	586
UA	22	C	2023/08/25	Total Dissolved Solids	mg/L	640
UA	22	C	2023/11/15	Total Dissolved Solids	mg/L	590
UA	22D	C	2019/09/17	pH (field)	SU	7.2
UA	22D	C	2019/12/11	pH (field)	SU	7.3
UA	22D	C	2020/03/11	pH (field)	SU	7.3
UA	22D	C	2020/06/03	pH (field)	SU	7.4
UA	22D	C	2020/06/25	pH (field)	SU	7.5
UA	22D	C	2020/09/02	pH (field)	SU	7.4
UA	22D	C	2020/12/09	pH (field)	SU	7.4
UA	22D	C	2021/03/19	pH (field)	SU	7.3
UA	22D	C	2021/06/23	pH (field)	SU	7.0
UA	22D	C	2021/09/08	pH (field)	SU	7.2
UA	22D	C	2021/12/08	pH (field)	SU	7.2
UA	22D	C	2022/03/22	pH (field)	SU	7.3
UA	22D	C	2022/06/07	pH (field)	SU	7.3
UA	22D	C	2022/09/13	pH (field)	SU	7.2
UA	22D	C	2022/12/27	pH (field)	SU	7.2
UA	22D	C	2023/02/28	pH (field)	SU	7.2
UA	22D	C	2023/05/31	pH (field)	SU	7.2
UA	22D	C	2023/08/22	pH (field)	SU	7.3
UA	22D	C	2023/11/15	pH (field)	SU	7.4
UA	22D	C	2019/09/17	Oxidation Reduction Potential	mV	-124
UA	22D	C	2019/12/11	Oxidation Reduction Potential	mV	-100
UA	22D	C	2020/03/11	Oxidation Reduction Potential	mV	-106
UA	22D	C	2020/06/03	Oxidation Reduction Potential	mV	-122
UA	22D	C	2020/06/25	Oxidation Reduction Potential	mV	-111
UA	22D	C	2020/09/02	Oxidation Reduction Potential	mV	-135

UA	22D	C	2020/12/09	Oxidation Reduction Potential	mV	-139
UA	22D	C	2021/03/19	Oxidation Reduction Potential	mV	-109
UA	22D	C	2021/06/23	Oxidation Reduction Potential	mV	-145
UA	22D	C	2021/09/08	Oxidation Reduction Potential	mV	68.0
UA	22D	C	2021/12/08	Oxidation Reduction Potential	mV	-122
UA	22D	C	2022/03/22	Oxidation Reduction Potential	mV	-155
UA	22D	C	2022/06/07	Oxidation Reduction Potential	mV	42.0
UA	22D	C	2022/09/13	Oxidation Reduction Potential	mV	21.0
UA	22D	C	2022/12/27	Oxidation Reduction Potential	mV	-133
UA	22D	C	2023/02/28	Oxidation Reduction Potential	mV	-107
UA	22D	C	2023/05/31	Oxidation Reduction Potential	mV	-121
UA	22D	C	2023/08/22	Oxidation Reduction Potential	mV	-82.1
UA	22D	C	2023/11/15	Oxidation Reduction Potential	mV	-112
UA	22D	C	2019/09/17	Eh	V	0.072
UA	22D	C	2019/12/11	Eh	V	0.096
UA	22D	C	2020/03/11	Eh	V	0.091
UA	22D	C	2020/06/03	Eh	V	0.073
UA	22D	C	2020/06/25	Eh	V	0.084
UA	22D	C	2020/09/02	Eh	V	0.060
UA	22D	C	2020/12/09	Eh	V	0.057
UA	22D	C	2021/03/19	Eh	V	0.087
UA	22D	C	2021/06/23	Eh	V	0.050
UA	22D	C	2021/09/08	Eh	V	0.26
UA	22D	C	2021/12/08	Eh	V	0.074
UA	22D	C	2022/03/22	Eh	V	0.041
UA	22D	C	2022/06/07	Eh	V	0.24
UA	22D	C	2022/09/13	Eh	V	0.22
UA	22D	C	2022/12/27	Eh	V	0.063
UA	22D	C	2023/02/28	Eh	V	0.088
UA	22D	C	2023/05/31	Eh	V	0.074
UA	22D	C	2023/08/22	Eh	V	0.11
UA	22D	C	2023/11/15	Eh	V	0.083
UA	22D	C	2019/09/17	Alkalinity, bicarbonate	mg/L CaCO3	324
UA	22D	C	2020/03/11	Alkalinity, bicarbonate	mg/L CaCO3	334
UA	22D	C	2021/03/19	Alkalinity, bicarbonate	mg/L CaCO3	340
UA	22D	C	2021/09/08	Alkalinity, bicarbonate	mg/L CaCO3	316
UA	22D	C	2022/03/22	Alkalinity, bicarbonate	mg/L CaCO3	333
UA	22D	C	2022/09/13	Alkalinity, bicarbonate	mg/L CaCO3	346
UA	22D	C	2023/02/28	Alkalinity, bicarbonate	mg/L CaCO3	341
UA	22D	C	2023/05/31	Alkalinity, bicarbonate	mg/L CaCO3	345
UA	22D	C	2023/08/22	Alkalinity, bicarbonate	mg/L CaCO3	340
UA	22D	C	2023/11/15	Alkalinity, bicarbonate	mg/L CaCO3	350
UA	22D	C	2019/09/17	Arsenic, total	mg/L	0.00140
UA	22D	C	2019/12/11	Arsenic, total	mg/L	0.00130
UA	22D	C	2020/03/11	Arsenic, total	mg/L	0.00120
UA	22D	C	2020/06/03	Arsenic, total	mg/L	0.00150
UA	22D	C	2020/09/02	Arsenic, total	mg/L	0.00120
UA	22D	C	2020/12/09	Arsenic, total	mg/L	0.00180
UA	22D	C	2021/03/19	Arsenic, total	mg/L	0.00120
UA	22D	C	2021/06/23	Arsenic, total	mg/L	0.00140
UA	22D	C	2021/09/08	Arsenic, total	mg/L	0.00120
UA	22D	C	2021/12/08	Arsenic, total	mg/L	0.00170
UA	22D	C	2022/03/22	Arsenic, total	mg/L	0.00130
UA	22D	C	2022/09/13	Arsenic, total	mg/L	0.00110
UA	22D	C	2023/02/28	Arsenic, total	mg/L	0.00160
UA	22D	C	2023/05/31	Arsenic, total	mg/L	<0.0087
UA	22D	C	2023/08/22	Arsenic, total	mg/L	0.00130
UA	22D	C	2023/11/15	Arsenic, total	mg/L	0.00120
UA	22D	C	2019/09/17	Barium, total	mg/L	0.0565
UA	22D	C	2019/12/11	Barium, total	mg/L	0.0587
UA	22D	C	2020/03/11	Barium, total	mg/L	0.0601
UA	22D	C	2020/06/03	Barium, total	mg/L	0.0619

UA	22D	C	2020/09/02	Barium, total	mg/L	0.0629
UA	22D	C	2020/12/09	Barium, total	mg/L	0.0881
UA	22D	C	2021/03/19	Barium, total	mg/L	0.0656
UA	22D	C	2021/06/23	Barium, total	mg/L	0.0662
UA	22D	C	2021/09/08	Barium, total	mg/L	0.0627
UA	22D	C	2021/12/08	Barium, total	mg/L	0.0609
UA	22D	C	2022/03/22	Barium, total	mg/L	0.0676
UA	22D	C	2022/09/13	Barium, total	mg/L	0.0739
UA	22D	C	2023/02/28	Barium, total	mg/L	0.0783
UA	22D	C	2023/05/31	Barium, total	mg/L	0.0669
UA	22D	C	2023/08/22	Barium, total	mg/L	0.0660
UA	22D	C	2023/11/15	Barium, total	mg/L	0.0670
UA	22D	C	2019/09/17	Boron, total	mg/L	2.68
UA	22D	C	2019/12/11	Boron, total	mg/L	2.41
UA	22D	C	2020/03/11	Boron, total	mg/L	2.14
UA	22D	C	2020/06/03	Boron, total	mg/L	2.24
UA	22D	C	2020/09/02	Boron, total	mg/L	1.94
UA	22D	C	2020/12/09	Boron, total	mg/L	1.86
UA	22D	C	2021/03/19	Boron, total	mg/L	1.92
UA	22D	C	2021/06/23	Boron, total	mg/L	1.90
UA	22D	C	2021/09/08	Boron, total	mg/L	2.05
UA	22D	C	2021/12/08	Boron, total	mg/L	2.02
UA	22D	C	2022/03/22	Boron, total	mg/L	2.10
UA	22D	C	2022/09/13	Boron, total	mg/L	1.67
UA	22D	C	2023/02/28	Boron, total	mg/L	2.40
UA	22D	C	2023/05/31	Boron, total	mg/L	1.57
UA	22D	C	2023/08/22	Boron, total	mg/L	1.30
UA	22D	C	2023/11/15	Boron, total	mg/L	1.50
UA	22D	C	2019/09/17	Cadmium, total	mg/L	<0.0002
UA	22D	C	2019/12/11	Cadmium, total	mg/L	<0.0002
UA	22D	C	2020/03/11	Cadmium, total	mg/L	<0.0002
UA	22D	C	2020/06/03	Cadmium, total	mg/L	<0.0002
UA	22D	C	2020/09/02	Cadmium, total	mg/L	<0.0002
UA	22D	C	2020/12/09	Cadmium, total	mg/L	<0.0002
UA	22D	C	2021/03/19	Cadmium, total	mg/L	<0.0002
UA	22D	C	2021/06/23	Cadmium, total	mg/L	<0.0002
UA	22D	C	2021/09/08	Cadmium, total	mg/L	<0.0002
UA	22D	C	2021/12/08	Cadmium, total	mg/L	<0.0002
UA	22D	C	2022/03/22	Cadmium, total	mg/L	<0.0002
UA	22D	C	2022/09/13	Cadmium, total	mg/L	<0.0002
UA	22D	C	2023/02/28	Cadmium, total	mg/L	<0.0002
UA	22D	C	2023/05/31	Cadmium, total	mg/L	<0.0005
UA	22D	C	2023/08/22	Cadmium, total	mg/L	<0.00017
UA	22D	C	2023/11/15	Cadmium, total	mg/L	<0.00017
UA	22D	C	2019/09/17	Calcium, total	mg/L	130
UA	22D	C	2019/12/11	Calcium, total	mg/L	125
UA	22D	C	2020/03/11	Calcium, total	mg/L	127
UA	22D	C	2020/06/03	Calcium, total	mg/L	133
UA	22D	C	2020/09/02	Calcium, total	mg/L	124
UA	22D	C	2020/12/09	Calcium, total	mg/L	185
UA	22D	C	2021/03/19	Calcium, total	mg/L	128
UA	22D	C	2021/06/23	Calcium, total	mg/L	135
UA	22D	C	2021/09/08	Calcium, total	mg/L	129
UA	22D	C	2021/12/08	Calcium, total	mg/L	119
UA	22D	C	2022/03/22	Calcium, total	mg/L	132
UA	22D	C	2022/09/13	Calcium, total	mg/L	124
UA	22D	C	2023/02/28	Calcium, total	mg/L	137
UA	22D	C	2023/05/31	Calcium, total	mg/L	113
UA	22D	C	2023/08/22	Calcium, total	mg/L	120
UA	22D	C	2023/11/15	Calcium, total	mg/L	120
UA	22D	C	2019/09/17	Chloride, total	mg/L	71.0
UA	22D	C	2019/12/11	Chloride, total	mg/L	85.0

UA	22D	C	2020/03/11	Chloride, total	mg/L	84.0
UA	22D	C	2020/06/03	Chloride, total	mg/L	94.0
UA	22D	C	2020/09/02	Chloride, total	mg/L	93.0
UA	22D	C	2020/12/09	Chloride, total	mg/L	98.0
UA	22D	C	2021/03/19	Chloride, total	mg/L	95.0
UA	22D	C	2021/06/23	Chloride, total	mg/L	103
UA	22D	C	2021/09/08	Chloride, total	mg/L	100
UA	22D	C	2021/12/08	Chloride, total	mg/L	112
UA	22D	C	2022/03/22	Chloride, total	mg/L	104
UA	22D	C	2022/09/13	Chloride, total	mg/L	103
UA	22D	C	2023/02/28	Chloride, total	mg/L	113
UA	22D	C	2023/05/31	Chloride, total	mg/L	110
UA	22D	C	2023/08/22	Chloride, total	mg/L	97.0
UA	22D	C	2023/11/15	Chloride, total	mg/L	93.0
UA	22D	C	2023/05/31	Iron, dissolved	mg/L	1.92
UA	22D	C	2023/08/22	Iron, dissolved	mg/L	2.20
UA	22D	C	2019/09/17	Lithium, total	mg/L	0.0158
UA	22D	C	2019/12/11	Lithium, total	mg/L	0.0170
UA	22D	C	2020/03/11	Lithium, total	mg/L	0.0168
UA	22D	C	2020/06/03	Lithium, total	mg/L	0.0176
UA	22D	C	2020/09/02	Lithium, total	mg/L	0.0148
UA	22D	C	2020/12/09	Lithium, total	mg/L	0.0147
UA	22D	C	2021/03/19	Lithium, total	mg/L	0.0148
UA	22D	C	2021/06/23	Lithium, total	mg/L	0.0163
UA	22D	C	2021/09/08	Lithium, total	mg/L	0.0155
UA	22D	C	2021/12/08	Lithium, total	mg/L	0.0156
UA	22D	C	2022/03/22	Lithium, total	mg/L	0.0175
UA	22D	C	2022/09/13	Lithium, total	mg/L	0.0123
UA	22D	C	2023/02/28	Lithium, total	mg/L	0.0129
UA	22D	C	2023/05/31	Lithium, total	mg/L	0.0150
UA	22D	C	2023/08/22	Lithium, total	mg/L	0.0170
UA	22D	C	2023/11/15	Lithium, total	mg/L	0.0190
UA	22D	C	2019/09/17	Magnesium, total	mg/L	42.6
UA	22D	C	2020/03/11	Magnesium, total	mg/L	42.4
UA	22D	C	2020/06/03	Magnesium, total	mg/L	41.7
UA	22D	C	2021/03/19	Magnesium, total	mg/L	44.4
UA	22D	C	2021/09/08	Magnesium, total	mg/L	41.9
UA	22D	C	2022/03/22	Magnesium, total	mg/L	43.3
UA	22D	C	2022/09/13	Magnesium, total	mg/L	41.6
UA	22D	C	2023/02/28	Magnesium, total	mg/L	42.2
UA	22D	C	2023/05/31	Magnesium, total	mg/L	39.4
UA	22D	C	2023/08/22	Magnesium, total	mg/L	41.0
UA	22D	C	2023/11/15	Magnesium, total	mg/L	40.0
UA	22D	C	2023/05/31	Manganese, dissolved	mg/L	0.0648
UA	22D	C	2023/08/22	Manganese, dissolved	mg/L	0.0650
UA	22D	C	2023/05/31	Phosphate, dissolved	mg/L	0.0280
UA	22D	C	2023/08/22	Phosphate, dissolved	mg/L	<0.073
UA	22D	C	2019/09/17	Potassium, total	mg/L	3.22
UA	22D	C	2020/03/11	Potassium, total	mg/L	3.38
UA	22D	C	2020/06/03	Potassium, total	mg/L	3.25
UA	22D	C	2021/03/19	Potassium, total	mg/L	3.46
UA	22D	C	2021/09/08	Potassium, total	mg/L	3.30
UA	22D	C	2022/03/22	Potassium, total	mg/L	3.39
UA	22D	C	2022/09/13	Potassium, total	mg/L	3.16
UA	22D	C	2023/02/28	Potassium, total	mg/L	3.30
UA	22D	C	2023/05/31	Potassium, total	mg/L	3.32
UA	22D	C	2023/08/22	Potassium, total	mg/L	3.10
UA	22D	C	2023/11/15	Potassium, total	mg/L	3.20
UA	22D	C	2023/05/31	Silicon, dissolved	mg/L	7.29
UA	22D	C	2023/08/22	Silicon, dissolved	mg/L	9.00
UA	22D	C	2019/09/17	Sodium, total	mg/L	33.0
UA	22D	C	2020/03/11	Sodium, total	mg/L	37.6

UA	22D	C	2020/06/03	Sodium, total	mg/L	40.2
UA	22D	C	2021/03/19	Sodium, total	mg/L	43.3
UA	22D	C	2021/09/08	Sodium, total	mg/L	41.8
UA	22D	C	2022/03/22	Sodium, total	mg/L	45.4
UA	22D	C	2022/09/13	Sodium, total	mg/L	41.9
UA	22D	C	2023/02/28	Sodium, total	mg/L	48.9
UA	22D	C	2023/05/31	Sodium, total	mg/L	47.2
UA	22D	C	2023/08/22	Sodium, total	mg/L	44.0
UA	22D	C	2023/11/15	Sodium, total	mg/L	49.0
UA	22D	C	2019/09/17	Sulfate, total	mg/L	109
UA	22D	C	2019/12/11	Sulfate, total	mg/L	114
UA	22D	C	2020/03/11	Sulfate, total	mg/L	103
UA	22D	C	2020/06/03	Sulfate, total	mg/L	118
UA	22D	C	2020/09/02	Sulfate, total	mg/L	105
UA	22D	C	2020/12/09	Sulfate, total	mg/L	114
UA	22D	C	2021/03/19	Sulfate, total	mg/L	103
UA	22D	C	2021/06/23	Sulfate, total	mg/L	107
UA	22D	C	2021/09/08	Sulfate, total	mg/L	107
UA	22D	C	2021/12/08	Sulfate, total	mg/L	103
UA	22D	C	2022/03/22	Sulfate, total	mg/L	103
UA	22D	C	2022/09/13	Sulfate, total	mg/L	96.0
UA	22D	C	2023/02/28	Sulfate, total	mg/L	112
UA	22D	C	2023/05/31	Sulfate, total	mg/L	104
UA	22D	C	2023/08/22	Sulfate, total	mg/L	96.0
UA	22D	C	2023/11/15	Sulfate, total	mg/L	89.0
UA	22D	C	2019/09/17	Temperature (Celsius)	degrees C	14.9
UA	22D	C	2019/12/11	Temperature (Celsius)	degrees C	14.0
UA	22D	C	2020/03/11	Temperature (Celsius)	degrees C	12.5
UA	22D	C	2020/06/03	Temperature (Celsius)	degrees C	15.1
UA	22D	C	2020/06/25	Temperature (Celsius)	degrees C	15.5
UA	22D	C	2020/09/02	Temperature (Celsius)	degrees C	15.6
UA	22D	C	2020/12/09	Temperature (Celsius)	degrees C	14.5
UA	22D	C	2021/03/19	Temperature (Celsius)	degrees C	14.5
UA	22D	C	2021/06/23	Temperature (Celsius)	degrees C	15.8
UA	22D	C	2021/09/08	Temperature (Celsius)	degrees C	16.3
UA	22D	C	2021/12/08	Temperature (Celsius)	degrees C	14.6
UA	22D	C	2022/03/22	Temperature (Celsius)	degrees C	14.8
UA	22D	C	2022/06/07	Temperature (Celsius)	degrees C	15.8
UA	22D	C	2022/09/13	Temperature (Celsius)	degrees C	16.4
UA	22D	C	2022/12/27	Temperature (Celsius)	degrees C	14.7
UA	22D	C	2023/02/28	Temperature (Celsius)	degrees C	14.8
UA	22D	C	2023/05/31	Temperature (Celsius)	degrees C	15.9
UA	22D	C	2023/08/22	Temperature (Celsius)	degrees C	18.0
UA	22D	C	2023/11/15	Temperature (Celsius)	degrees C	16.2
UA	22D	C	2019/09/17	Total Dissolved Solids	mg/L	660
UA	22D	C	2019/12/11	Total Dissolved Solids	mg/L	590
UA	22D	C	2020/03/11	Total Dissolved Solids	mg/L	636
UA	22D	C	2020/06/03	Total Dissolved Solids	mg/L	616
UA	22D	C	2020/09/02	Total Dissolved Solids	mg/L	550
UA	22D	C	2020/12/09	Total Dissolved Solids	mg/L	608
UA	22D	C	2021/03/19	Total Dissolved Solids	mg/L	630
UA	22D	C	2021/06/23	Total Dissolved Solids	mg/L	640
UA	22D	C	2021/09/08	Total Dissolved Solids	mg/L	582
UA	22D	C	2021/12/08	Total Dissolved Solids	mg/L	578
UA	22D	C	2022/03/22	Total Dissolved Solids	mg/L	616
UA	22D	C	2022/09/13	Total Dissolved Solids	mg/L	686
UA	22D	C	2023/02/28	Total Dissolved Solids	mg/L	680
UA	22D	C	2023/05/31	Total Dissolved Solids	mg/L	640
UA	22D	C	2023/08/22	Total Dissolved Solids	mg/L	690
UA	22D	C	2023/11/15	Total Dissolved Solids	mg/L	640
UA	23	C	2013/03/08	pH (field)	SU	7.1
UA	23	C	2013/06/07	pH (field)	SU	7.2

UA	23	C	2013/09/03	pH (field)	SU	7.6
UA	23	C	2013/12/10	pH (field)	SU	7.5
UA	23	C	2014/03/25	pH (field)	SU	7.6
UA	23	C	2014/08/19	pH (field)	SU	7.5
UA	23	C	2014/09/30	pH (field)	SU	7.5
UA	23	C	2015/03/18	pH (field)	SU	7.5
UA	23	C	2015/09/16	pH (field)	SU	7.4
UA	23	C	2015/12/10	pH (field)	SU	7.5
UA	23	C	2016/03/09	pH (field)	SU	7.4
UA	23	C	2016/06/07	pH (field)	SU	7.5
UA	23	C	2016/09/15	pH (field)	SU	7.5
UA	23	C	2016/12/07	pH (field)	SU	7.4
UA	23	C	2017/02/21	pH (field)	SU	7.3
UA	23	C	2017/04/25	pH (field)	SU	7.3
UA	23	C	2017/06/08	pH (field)	SU	7.3
UA	23	C	2017/09/06	pH (field)	SU	7.4
UA	23	C	2017/11/15	pH (field)	SU	7.8
UA	23	C	2018/03/26	pH (field)	SU	7.6
UA	23	C	2018/06/13	pH (field)	SU	7.1
UA	23	C	2018/09/12	pH (field)	SU	7.4
UA	23	C	2018/12/12	pH (field)	SU	7.5
UA	23	C	2019/03/13	pH (field)	SU	7.6
UA	23	C	2019/06/19	pH (field)	SU	7.4
UA	23	C	2019/09/18	pH (field)	SU	7.5
UA	23	C	2019/12/11	pH (field)	SU	7.5
UA	23	C	2020/03/11	pH (field)	SU	7.3
UA	23	C	2020/06/24	pH (field)	SU	7.7
UA	23	C	2020/09/02	pH (field)	SU	7.6
UA	23	C	2020/12/10	pH (field)	SU	7.6
UA	23	C	2021/03/19	pH (field)	SU	7.5
UA	23	C	2021/06/24	pH (field)	SU	7.3
UA	23	C	2021/09/09	pH (field)	SU	7.4
UA	23	C	2021/12/08	pH (field)	SU	7.3
UA	23	C	2022/03/22	pH (field)	SU	7.4
UA	23	C	2022/06/07	pH (field)	SU	7.4
UA	23	C	2022/09/13	pH (field)	SU	7.4
UA	23	C	2022/12/27	pH (field)	SU	7.4
UA	23	C	2023/02/28	pH (field)	SU	7.4
UA	23	C	2023/05/31	pH (field)	SU	7.4
UA	23	C	2023/08/22	pH (field)	SU	7.4
UA	23	C	2023/11/15	pH (field)	SU	7.5
UA	23	C	2015/12/10	Oxidation Reduction Potential	mV	-27.0
UA	23	C	2016/03/09	Oxidation Reduction Potential	mV	-36.0
UA	23	C	2016/06/07	Oxidation Reduction Potential	mV	24.0
UA	23	C	2016/09/15	Oxidation Reduction Potential	mV	-4.00
UA	23	C	2016/12/07	Oxidation Reduction Potential	mV	105
UA	23	C	2017/02/21	Oxidation Reduction Potential	mV	117
UA	23	C	2017/04/25	Oxidation Reduction Potential	mV	33.0
UA	23	C	2017/06/08	Oxidation Reduction Potential	mV	-16.0
UA	23	C	2017/11/15	Oxidation Reduction Potential	mV	-56.0
UA	23	C	2018/06/13	Oxidation Reduction Potential	mV	21.0
UA	23	C	2018/09/12	Oxidation Reduction Potential	mV	81.0
UA	23	C	2018/12/12	Oxidation Reduction Potential	mV	101
UA	23	C	2019/03/13	Oxidation Reduction Potential	mV	-38.0
UA	23	C	2019/06/19	Oxidation Reduction Potential	mV	17.0
UA	23	C	2019/09/18	Oxidation Reduction Potential	mV	79.0
UA	23	C	2019/12/11	Oxidation Reduction Potential	mV	30.0
UA	23	C	2020/03/11	Oxidation Reduction Potential	mV	139
UA	23	C	2020/06/24	Oxidation Reduction Potential	mV	75.0
UA	23	C	2020/09/02	Oxidation Reduction Potential	mV	45.0
UA	23	C	2020/12/10	Oxidation Reduction Potential	mV	-71.0
UA	23	C	2021/03/19	Oxidation Reduction Potential	mV	-31.0

UA	23	C	2021/06/24	Oxidation Reduction Potential	mV	13.0
UA	23	C	2021/09/09	Oxidation Reduction Potential	mV	-58.0
UA	23	C	2021/12/08	Oxidation Reduction Potential	mV	5.00
UA	23	C	2022/03/22	Oxidation Reduction Potential	mV	-115
UA	23	C	2022/06/07	Oxidation Reduction Potential	mV	18.0
UA	23	C	2022/09/13	Oxidation Reduction Potential	mV	-7.00
UA	23	C	2022/12/27	Oxidation Reduction Potential	mV	-191
UA	23	C	2023/02/28	Oxidation Reduction Potential	mV	-125
UA	23	C	2023/05/31	Oxidation Reduction Potential	mV	-127
UA	23	C	2023/08/22	Oxidation Reduction Potential	mV	-124
UA	23	C	2023/11/15	Oxidation Reduction Potential	mV	-88.1
UA	23	C	2015/12/10	Eh	V	0.17
UA	23	C	2016/03/09	Eh	V	0.16
UA	23	C	2016/06/07	Eh	V	0.22
UA	23	C	2016/09/15	Eh	V	0.19
UA	23	C	2016/12/07	Eh	V	0.30
UA	23	C	2017/02/21	Eh	V	0.31
UA	23	C	2017/04/25	Eh	V	0.22
UA	23	C	2017/06/08	Eh	V	0.18
UA	23	C	2017/11/15	Eh	V	0.14
UA	23	C	2018/06/13	Eh	V	0.22
UA	23	C	2018/09/12	Eh	V	0.28
UA	23	C	2018/12/12	Eh	V	0.30
UA	23	C	2019/03/13	Eh	V	0.16
UA	23	C	2019/06/19	Eh	V	0.21
UA	23	C	2019/09/18	Eh	V	0.28
UA	23	C	2019/12/11	Eh	V	0.23
UA	23	C	2020/03/11	Eh	V	0.34
UA	23	C	2020/06/24	Eh	V	0.27
UA	23	C	2020/09/02	Eh	V	0.24
UA	23	C	2020/12/10	Eh	V	0.13
UA	23	C	2021/03/19	Eh	V	0.17
UA	23	C	2021/06/24	Eh	V	0.21
UA	23	C	2021/09/09	Eh	V	0.14
UA	23	C	2021/12/08	Eh	V	0.20
UA	23	C	2022/03/22	Eh	V	0.082
UA	23	C	2022/06/07	Eh	V	0.22
UA	23	C	2022/09/13	Eh	V	0.19
UA	23	C	2022/12/27	Eh	V	0.0064
UA	23	C	2023/02/28	Eh	V	0.072
UA	23	C	2023/05/31	Eh	V	0.070
UA	23	C	2023/08/22	Eh	V	0.071
UA	23	C	2023/11/15	Eh	V	0.11
UA	23	C	2019/09/18	Alkalinity, bicarbonate	mg/L CaCO3	159
UA	23	C	2020/03/11	Alkalinity, bicarbonate	mg/L CaCO3	163
UA	23	C	2021/02/24	Alkalinity, bicarbonate	mg/L CaCO3	166
UA	23	C	2021/03/04	Alkalinity, bicarbonate	mg/L CaCO3	164
UA	23	C	2021/03/09	Alkalinity, bicarbonate	mg/L CaCO3	161
UA	23	C	2021/03/18	Alkalinity, bicarbonate	mg/L CaCO3	169
UA	23	C	2021/03/19	Alkalinity, bicarbonate	mg/L CaCO3	164
UA	23	C	2021/03/30	Alkalinity, bicarbonate	mg/L CaCO3	179
UA	23	C	2021/09/09	Alkalinity, bicarbonate	mg/L CaCO3	160
UA	23	C	2022/03/22	Alkalinity, bicarbonate	mg/L CaCO3	158
UA	23	C	2022/09/13	Alkalinity, bicarbonate	mg/L CaCO3	162
UA	23	C	2023/02/28	Alkalinity, bicarbonate	mg/L CaCO3	171
UA	23	C	2023/05/31	Alkalinity, bicarbonate	mg/L CaCO3	169
UA	23	C	2023/08/22	Alkalinity, bicarbonate	mg/L CaCO3	150
UA	23	C	2023/11/15	Alkalinity, bicarbonate	mg/L CaCO3	170
UA	23	C	2013/06/07	Arsenic, total	mg/L	<0.0007
UA	23	C	2013/09/03	Arsenic, total	mg/L	<0.0007
UA	23	C	2015/12/10	Arsenic, total	mg/L	<0.0002
UA	23	C	2016/03/09	Arsenic, total	mg/L	<0.0002

UA	23	C	2016/06/07	Arsenic, total	mg/L	<0.0002
UA	23	C	2016/09/15	Arsenic, total	mg/L	<0.0002
UA	23	C	2016/12/07	Arsenic, total	mg/L	<0.0002
UA	23	C	2017/02/21	Arsenic, total	mg/L	<0.0002
UA	23	C	2017/04/25	Arsenic, total	mg/L	<0.0002
UA	23	C	2017/06/08	Arsenic, total	mg/L	<0.0002
UA	23	C	2018/06/13	Arsenic, total	mg/L	<0.0004
UA	23	C	2018/09/12	Arsenic, total	mg/L	<0.0004
UA	23	C	2018/12/12	Arsenic, total	mg/L	<0.0004
UA	23	C	2019/03/13	Arsenic, total	mg/L	<0.0004
UA	23	C	2019/06/19	Arsenic, total	mg/L	<0.0004
UA	23	C	2019/09/18	Arsenic, total	mg/L	<0.0004
UA	23	C	2019/12/11	Arsenic, total	mg/L	<0.0004
UA	23	C	2020/03/11	Arsenic, total	mg/L	<0.0004
UA	23	C	2020/06/24	Arsenic, total	mg/L	<0.0004
UA	23	C	2020/09/02	Arsenic, total	mg/L	<0.0004
UA	23	C	2020/12/10	Arsenic, total	mg/L	<0.0004
UA	23	C	2021/02/24	Arsenic, total	mg/L	<0.0000004
UA	23	C	2021/03/04	Arsenic, total	mg/L	<0.0004
UA	23	C	2021/03/09	Arsenic, total	mg/L	<0.0004
UA	23	C	2021/03/18	Arsenic, total	mg/L	<0.0004
UA	23	C	2021/03/19	Arsenic, total	mg/L	<0.0004
UA	23	C	2021/03/30	Arsenic, total	mg/L	<0.0004
UA	23	C	2021/06/24	Arsenic, total	mg/L	<0.0004
UA	23	C	2021/09/09	Arsenic, total	mg/L	<0.0004
UA	23	C	2021/12/08	Arsenic, total	mg/L	<0.0004
UA	23	C	2022/03/22	Arsenic, total	mg/L	<0.0004
UA	23	C	2022/06/07	Arsenic, total	mg/L	0.000700
UA	23	C	2022/09/13	Arsenic, total	mg/L	0.000500
UA	23	C	2022/12/27	Arsenic, total	mg/L	0.00110
UA	23	C	2023/02/28	Arsenic, total	mg/L	0.00130
UA	23	C	2023/05/31	Arsenic, total	mg/L	<0.0087
UA	23	C	2023/08/22	Arsenic, total	mg/L	0.000890
UA	23	C	2023/11/15	Arsenic, total	mg/L	0.000830
UA	23	C	2013/06/07	Barium, total	mg/L	0.116
UA	23	C	2013/09/03	Barium, total	mg/L	0.0500
UA	23	C	2015/12/10	Barium, total	mg/L	0.0530
UA	23	C	2016/03/09	Barium, total	mg/L	0.0792
UA	23	C	2016/06/07	Barium, total	mg/L	0.0588
UA	23	C	2016/09/15	Barium, total	mg/L	0.0359
UA	23	C	2016/12/07	Barium, total	mg/L	0.0307
UA	23	C	2017/02/21	Barium, total	mg/L	0.0289
UA	23	C	2017/04/25	Barium, total	mg/L	0.0283
UA	23	C	2017/06/08	Barium, total	mg/L	0.0291
UA	23	C	2018/06/13	Barium, total	mg/L	0.0317
UA	23	C	2018/09/12	Barium, total	mg/L	0.0359
UA	23	C	2018/12/12	Barium, total	mg/L	0.0342
UA	23	C	2019/03/13	Barium, total	mg/L	0.0261
UA	23	C	2019/06/19	Barium, total	mg/L	0.0352
UA	23	C	2019/09/18	Barium, total	mg/L	0.0347
UA	23	C	2019/12/11	Barium, total	mg/L	0.0362
UA	23	C	2020/03/11	Barium, total	mg/L	0.0354
UA	23	C	2020/06/24	Barium, total	mg/L	0.0344
UA	23	C	2020/09/02	Barium, total	mg/L	0.0360
UA	23	C	2020/12/10	Barium, total	mg/L	0.0515
UA	23	C	2021/02/24	Barium, total	mg/L	0.0379
UA	23	C	2021/03/19	Barium, total	mg/L	0.0378
UA	23	C	2021/06/24	Barium, total	mg/L	0.0360
UA	23	C	2021/09/09	Barium, total	mg/L	0.0363
UA	23	C	2021/12/08	Barium, total	mg/L	0.0367
UA	23	C	2022/03/22	Barium, total	mg/L	0.0412
UA	23	C	2022/06/07	Barium, total	mg/L	0.0410

UA	23	C	2022/09/13	Barium, total	mg/L	0.0445
UA	23	C	2022/12/27	Barium, total	mg/L	0.0467
UA	23	C	2023/02/28	Barium, total	mg/L	0.0685
UA	23	C	2023/05/31	Barium, total	mg/L	0.0481
UA	23	C	2023/08/22	Barium, total	mg/L	0.0420
UA	23	C	2023/11/15	Barium, total	mg/L	0.0400
UA	23	C	2013/06/07	Boron, total	mg/L	2.88
UA	23	C	2013/09/03	Boron, total	mg/L	7.43
UA	23	C	2015/12/10	Boron, total	mg/L	5.63
UA	23	C	2016/03/09	Boron, total	mg/L	7.24
UA	23	C	2016/06/07	Boron, total	mg/L	8.50
UA	23	C	2016/09/15	Boron, total	mg/L	8.25
UA	23	C	2016/12/07	Boron, total	mg/L	7.99
UA	23	C	2017/02/21	Boron, total	mg/L	7.78
UA	23	C	2017/04/25	Boron, total	mg/L	7.31
UA	23	C	2017/06/08	Boron, total	mg/L	7.04
UA	23	C	2017/11/15	Boron, total	mg/L	8.09
UA	23	C	2018/06/13	Boron, total	mg/L	8.93
UA	23	C	2018/09/12	Boron, total	mg/L	7.68
UA	23	C	2018/12/12	Boron, total	mg/L	8.47
UA	23	C	2019/03/13	Boron, total	mg/L	7.49
UA	23	C	2019/06/19	Boron, total	mg/L	8.47
UA	23	C	2019/09/18	Boron, total	mg/L	9.35
UA	23	C	2019/12/11	Boron, total	mg/L	8.83
UA	23	C	2020/03/11	Boron, total	mg/L	8.26
UA	23	C	2020/06/24	Boron, total	mg/L	8.38
UA	23	C	2020/09/02	Boron, total	mg/L	8.07
UA	23	C	2020/12/10	Boron, total	mg/L	10.2
UA	23	C	2021/02/24	Boron, total	mg/L	8.52
UA	23	C	2021/03/04	Boron, total	mg/L	8.53
UA	23	C	2021/03/09	Boron, total	mg/L	7.60
UA	23	C	2021/03/18	Boron, total	mg/L	8.30
UA	23	C	2021/03/19	Boron, total	mg/L	8.09
UA	23	C	2021/03/30	Boron, total	mg/L	8.92
UA	23	C	2021/06/24	Boron, total	mg/L	8.22
UA	23	C	2021/09/09	Boron, total	mg/L	9.05
UA	23	C	2021/12/08	Boron, total	mg/L	8.05
UA	23	C	2022/03/22	Boron, total	mg/L	9.61
UA	23	C	2022/06/07	Boron, total	mg/L	9.40
UA	23	C	2022/09/13	Boron, total	mg/L	8.20
UA	23	C	2022/12/27	Boron, total	mg/L	9.90
UA	23	C	2023/02/28	Boron, total	mg/L	12.8
UA	23	C	2023/05/31	Boron, total	mg/L	8.79
UA	23	C	2023/08/22	Boron, total	mg/L	8.10
UA	23	C	2023/11/15	Boron, total	mg/L	8.70
UA	23	C	2013/06/07	Cadmium, total	mg/L	<0.0003
UA	23	C	2013/09/03	Cadmium, total	mg/L	<0.0003
UA	23	C	2015/12/10	Cadmium, total	mg/L	<0.0002
UA	23	C	2016/03/09	Cadmium, total	mg/L	<0.0002
UA	23	C	2016/06/07	Cadmium, total	mg/L	<0.0002
UA	23	C	2016/09/15	Cadmium, total	mg/L	<0.0002
UA	23	C	2016/12/07	Cadmium, total	mg/L	<0.0002
UA	23	C	2017/02/21	Cadmium, total	mg/L	<0.0002
UA	23	C	2017/04/25	Cadmium, total	mg/L	<0.0002
UA	23	C	2017/06/08	Cadmium, total	mg/L	<0.0002
UA	23	C	2018/06/13	Cadmium, total	mg/L	<0.0002
UA	23	C	2018/09/12	Cadmium, total	mg/L	<0.0002
UA	23	C	2018/12/12	Cadmium, total	mg/L	<0.0002
UA	23	C	2019/03/13	Cadmium, total	mg/L	<0.0002
UA	23	C	2019/06/19	Cadmium, total	mg/L	<0.0002
UA	23	C	2019/09/18	Cadmium, total	mg/L	<0.0002
UA	23	C	2019/12/11	Cadmium, total	mg/L	<0.0002

UA	23	C	2020/03/11	Cadmium, total	mg/L	<0.0002
UA	23	C	2020/06/24	Cadmium, total	mg/L	<0.0002
UA	23	C	2020/09/02	Cadmium, total	mg/L	<0.0002
UA	23	C	2020/12/10	Cadmium, total	mg/L	<0.0002
UA	23	C	2021/02/24	Cadmium, total	mg/L	<0.0000002
UA	23	C	2021/03/19	Cadmium, total	mg/L	<0.0002
UA	23	C	2021/06/24	Cadmium, total	mg/L	<0.0002
UA	23	C	2021/09/09	Cadmium, total	mg/L	<0.0002
UA	23	C	2021/12/08	Cadmium, total	mg/L	<0.0002
UA	23	C	2022/03/22	Cadmium, total	mg/L	<0.0002
UA	23	C	2022/06/07	Cadmium, total	mg/L	<0.0002
UA	23	C	2022/09/13	Cadmium, total	mg/L	<0.0002
UA	23	C	2022/12/27	Cadmium, total	mg/L	<0.0002
UA	23	C	2023/02/28	Cadmium, total	mg/L	<0.0002
UA	23	C	2023/05/31	Cadmium, total	mg/L	<0.0005
UA	23	C	2023/08/22	Cadmium, total	mg/L	<0.00017
UA	23	C	2023/11/15	Cadmium, total	mg/L	<0.00017
UA	23	C	2015/12/10	Calcium, total	mg/L	105
UA	23	C	2016/03/09	Calcium, total	mg/L	136
UA	23	C	2016/06/07	Calcium, total	mg/L	148
UA	23	C	2016/09/15	Calcium, total	mg/L	119
UA	23	C	2016/12/07	Calcium, total	mg/L	115
UA	23	C	2017/02/21	Calcium, total	mg/L	114
UA	23	C	2017/04/25	Calcium, total	mg/L	110
UA	23	C	2017/06/08	Calcium, total	mg/L	119
UA	23	C	2017/11/15	Calcium, total	mg/L	119
UA	23	C	2018/06/13	Calcium, total	mg/L	120
UA	23	C	2018/09/12	Calcium, total	mg/L	123
UA	23	C	2018/12/12	Calcium, total	mg/L	117
UA	23	C	2019/03/13	Calcium, total	mg/L	91.9
UA	23	C	2019/06/19	Calcium, total	mg/L	125
UA	23	C	2019/09/18	Calcium, total	mg/L	125
UA	23	C	2019/12/11	Calcium, total	mg/L	121
UA	23	C	2020/03/11	Calcium, total	mg/L	120
UA	23	C	2020/06/24	Calcium, total	mg/L	113
UA	23	C	2020/09/02	Calcium, total	mg/L	117
UA	23	C	2020/12/10	Calcium, total	mg/L	114
UA	23	C	2021/02/24	Calcium, total	mg/L	118
UA	23	C	2021/03/04	Calcium, total	mg/L	109
UA	23	C	2021/03/09	Calcium, total	mg/L	110
UA	23	C	2021/03/18	Calcium, total	mg/L	117
UA	23	C	2021/03/19	Calcium, total	mg/L	115
UA	23	C	2021/03/30	Calcium, total	mg/L	118
UA	23	C	2021/06/24	Calcium, total	mg/L	120
UA	23	C	2021/09/09	Calcium, total	mg/L	121
UA	23	C	2021/12/08	Calcium, total	mg/L	106
UA	23	C	2022/03/22	Calcium, total	mg/L	116
UA	23	C	2022/06/07	Calcium, total	mg/L	115
UA	23	C	2022/09/13	Calcium, total	mg/L	115
UA	23	C	2022/12/27	Calcium, total	mg/L	120
UA	23	C	2023/02/28	Calcium, total	mg/L	122
UA	23	C	2023/05/31	Calcium, total	mg/L	105
UA	23	C	2023/08/22	Calcium, total	mg/L	110
UA	23	C	2023/11/15	Calcium, total	mg/L	110
UA	23	C	2013/03/08	Chloride, total	mg/L	57.0
UA	23	C	2013/06/07	Chloride, total	mg/L	22.0
UA	23	C	2013/09/03	Chloride, total	mg/L	62.0
UA	23	C	2013/12/10	Chloride, total	mg/L	54.0
UA	23	C	2014/03/25	Chloride, total	mg/L	<1
UA	23	C	2014/09/30	Chloride, total	mg/L	63.0
UA	23	C	2015/03/18	Chloride, total	mg/L	62.0
UA	23	C	2015/09/16	Chloride, total	mg/L	58.0

UA	23	C	2015/12/10	Chloride, total	mg/L	44.0
UA	23	C	2016/03/09	Chloride, total	mg/L	68.0
UA	23	C	2016/06/07	Chloride, total	mg/L	70.0
UA	23	C	2016/09/15	Chloride, total	mg/L	68.0
UA	23	C	2016/12/07	Chloride, total	mg/L	64.0
UA	23	C	2017/02/21	Chloride, total	mg/L	58.0
UA	23	C	2017/04/25	Chloride, total	mg/L	62.0
UA	23	C	2017/06/08	Chloride, total	mg/L	66.0
UA	23	C	2017/09/06	Chloride, total	mg/L	63.0
UA	23	C	2017/11/15	Chloride, total	mg/L	60.0
UA	23	C	2018/03/26	Chloride, total	mg/L	60.0
UA	23	C	2018/06/13	Chloride, total	mg/L	63.0
UA	23	C	2018/09/12	Chloride, total	mg/L	61.0
UA	23	C	2018/12/12	Chloride, total	mg/L	57.0
UA	23	C	2019/03/13	Chloride, total	mg/L	58.0
UA	23	C	2019/06/19	Chloride, total	mg/L	58.0
UA	23	C	2019/09/18	Chloride, total	mg/L	56.0
UA	23	C	2019/12/11	Chloride, total	mg/L	60.0
UA	23	C	2020/03/11	Chloride, total	mg/L	59.0
UA	23	C	2020/06/24	Chloride, total	mg/L	65.0
UA	23	C	2020/09/02	Chloride, total	mg/L	61.0
UA	23	C	2020/12/10	Chloride, total	mg/L	62.0
UA	23	C	2021/02/24	Chloride, total	mg/L	64.0
UA	23	C	2021/03/04	Chloride, total	mg/L	63.0
UA	23	C	2021/03/09	Chloride, total	mg/L	61.0
UA	23	C	2021/03/18	Chloride, total	mg/L	55.0
UA	23	C	2021/03/19	Chloride, total	mg/L	60.0
UA	23	C	2021/03/30	Chloride, total	mg/L	58.0
UA	23	C	2021/06/24	Chloride, total	mg/L	58.0
UA	23	C	2021/09/09	Chloride, total	mg/L	57.0
UA	23	C	2021/12/08	Chloride, total	mg/L	58.0
UA	23	C	2022/03/22	Chloride, total	mg/L	58.0
UA	23	C	2022/06/07	Chloride, total	mg/L	53.0
UA	23	C	2022/09/13	Chloride, total	mg/L	50.0
UA	23	C	2022/12/27	Chloride, total	mg/L	64.0
UA	23	C	2023/02/28	Chloride, total	mg/L	66.0
UA	23	C	2023/05/31	Chloride, total	mg/L	55.0
UA	23	C	2023/08/22	Chloride, total	mg/L	53.0
UA	23	C	2023/11/15	Chloride, total	mg/L	56.0
UA	23	C	2013/12/10	Iron, dissolved	mg/L	<0.007
UA	23	C	2014/03/25	Iron, dissolved	mg/L	<0.007
UA	23	C	2014/08/19	Iron, dissolved	mg/L	<0.007
UA	23	C	2014/09/30	Iron, dissolved	mg/L	<0.007
UA	23	C	2015/03/18	Iron, dissolved	mg/L	<0.007
UA	23	C	2015/09/16	Iron, dissolved	mg/L	<0.007
UA	23	C	2016/03/09	Iron, dissolved	mg/L	<0.007
UA	23	C	2016/09/15	Iron, dissolved	mg/L	<0.007
UA	23	C	2017/02/21	Iron, dissolved	mg/L	<0.007
UA	23	C	2017/09/06	Iron, dissolved	mg/L	<0.007
UA	23	C	2018/03/26	Iron, dissolved	mg/L	<0.007
UA	23	C	2021/02/24	Iron, dissolved	mg/L	0.0418
UA	23	C	2021/03/04	Iron, dissolved	mg/L	0.0786
UA	23	C	2021/03/09	Iron, dissolved	mg/L	0.0550
UA	23	C	2021/03/18	Iron, dissolved	mg/L	0.0278
UA	23	C	2021/03/30	Iron, dissolved	mg/L	<0.0115
UA	23	C	2023/05/31	Iron, dissolved	mg/L	0.148
UA	23	C	2023/08/22	Iron, dissolved	mg/L	0.140
UA	23	C	2015/12/10	Lithium, total	mg/L	0.00360
UA	23	C	2016/03/09	Lithium, total	mg/L	0.00390
UA	23	C	2016/06/07	Lithium, total	mg/L	0.00520
UA	23	C	2016/09/15	Lithium, total	mg/L	0.00520
UA	23	C	2016/12/07	Lithium, total	mg/L	0.00550

UA	23	C	2017/02/21	Lithium, total	mg/L	0.00490
UA	23	C	2017/04/25	Lithium, total	mg/L	0.00570
UA	23	C	2017/06/08	Lithium, total	mg/L	0.00480
UA	23	C	2018/06/13	Lithium, total	mg/L	0.00530
UA	23	C	2018/09/12	Lithium, total	mg/L	0.00670
UA	23	C	2018/12/12	Lithium, total	mg/L	0.00570
UA	23	C	2019/03/13	Lithium, total	mg/L	0.00480
UA	23	C	2019/06/19	Lithium, total	mg/L	0.00560
UA	23	C	2019/09/18	Lithium, total	mg/L	0.00600
UA	23	C	2019/12/11	Lithium, total	mg/L	0.00560
UA	23	C	2020/03/11	Lithium, total	mg/L	0.00520
UA	23	C	2020/06/24	Lithium, total	mg/L	0.00540
UA	23	C	2020/09/02	Lithium, total	mg/L	0.00460
UA	23	C	2020/12/10	Lithium, total	mg/L	0.00500
UA	23	C	2021/02/24	Lithium, total	mg/L	<0.005
UA	23	C	2021/03/04	Lithium, total	mg/L	0.00510
UA	23	C	2021/03/09	Lithium, total	mg/L	0.00450
UA	23	C	2021/03/18	Lithium, total	mg/L	0.00500
UA	23	C	2021/03/19	Lithium, total	mg/L	0.00490
UA	23	C	2021/03/30	Lithium, total	mg/L	0.00560
UA	23	C	2021/06/24	Lithium, total	mg/L	0.00490
UA	23	C	2021/09/09	Lithium, total	mg/L	0.00500
UA	23	C	2021/12/08	Lithium, total	mg/L	0.00470
UA	23	C	2022/03/22	Lithium, total	mg/L	0.00560
UA	23	C	2022/06/07	Lithium, total	mg/L	0.00460
UA	23	C	2022/09/13	Lithium, total	mg/L	0.00390
UA	23	C	2022/12/27	Lithium, total	mg/L	0.00520
UA	23	C	2023/02/28	Lithium, total	mg/L	0.00420
UA	23	C	2023/05/31	Lithium, total	mg/L	<0.0019
UA	23	C	2023/08/22	Lithium, total	mg/L	0.00630
UA	23	C	2023/11/15	Lithium, total	mg/L	0.00660
UA	23	C	2019/09/18	Magnesium, total	mg/L	83.4
UA	23	C	2020/03/11	Magnesium, total	mg/L	84.1
UA	23	C	2020/06/24	Magnesium, total	mg/L	84.0
UA	23	C	2021/02/24	Magnesium, total	mg/L	85.5
UA	23	C	2021/03/04	Magnesium, total	mg/L	76.3
UA	23	C	2021/03/09	Magnesium, total	mg/L	79.0
UA	23	C	2021/03/18	Magnesium, total	mg/L	83.7
UA	23	C	2021/03/19	Magnesium, total	mg/L	81.0
UA	23	C	2021/03/30	Magnesium, total	mg/L	85.6
UA	23	C	2021/09/09	Magnesium, total	mg/L	86.5
UA	23	C	2022/03/22	Magnesium, total	mg/L	79.0
UA	23	C	2022/09/13	Magnesium, total	mg/L	78.9
UA	23	C	2023/02/28	Magnesium, total	mg/L	80.5
UA	23	C	2023/05/31	Magnesium, total	mg/L	77.5
UA	23	C	2023/08/22	Magnesium, total	mg/L	78.0
UA	23	C	2023/11/15	Magnesium, total	mg/L	75.0
UA	23	C	2013/03/08	Manganese, dissolved	mg/L	0.600
UA	23	C	2013/12/10	Manganese, dissolved	mg/L	0.148
UA	23	C	2014/03/25	Manganese, dissolved	mg/L	0.0123
UA	23	C	2014/08/19	Manganese, dissolved	mg/L	0.0231
UA	23	C	2014/09/30	Manganese, dissolved	mg/L	0.0681
UA	23	C	2015/03/18	Manganese, dissolved	mg/L	0.147
UA	23	C	2015/09/16	Manganese, dissolved	mg/L	0.0510
UA	23	C	2016/03/09	Manganese, dissolved	mg/L	0.0266
UA	23	C	2016/09/15	Manganese, dissolved	mg/L	0.274
UA	23	C	2017/02/21	Manganese, dissolved	mg/L	0.542
UA	23	C	2017/09/06	Manganese, dissolved	mg/L	0.680
UA	23	C	2018/03/26	Manganese, dissolved	mg/L	0.725
UA	23	C	2021/02/24	Manganese, dissolved	mg/L	1.04
UA	23	C	2021/03/04	Manganese, dissolved	mg/L	1.21
UA	23	C	2021/03/09	Manganese, dissolved	mg/L	0.970

UA	23	C	2021/03/18	Manganese, dissolved	mg/L	0.955
UA	23	C	2021/03/30	Manganese, dissolved	mg/L	1.01
UA	23	C	2023/05/31	Manganese, dissolved	mg/L	1.16
UA	23	C	2023/08/22	Manganese, dissolved	mg/L	1.10
UA	23	C	2023/05/31	Phosphate, dissolved	mg/L	0.0310
UA	23	C	2023/08/22	Phosphate, dissolved	mg/L	<0.073
UA	23	C	2019/09/18	Potassium, total	mg/L	3.08
UA	23	C	2020/03/11	Potassium, total	mg/L	3.23
UA	23	C	2020/06/24	Potassium, total	mg/L	3.02
UA	23	C	2021/02/24	Potassium, total	mg/L	2.80
UA	23	C	2021/03/04	Potassium, total	mg/L	2.92
UA	23	C	2021/03/09	Potassium, total	mg/L	2.60
UA	23	C	2021/03/18	Potassium, total	mg/L	3.25
UA	23	C	2021/03/19	Potassium, total	mg/L	3.18
UA	23	C	2021/03/30	Potassium, total	mg/L	3.07
UA	23	C	2021/09/09	Potassium, total	mg/L	3.35
UA	23	C	2022/03/22	Potassium, total	mg/L	3.08
UA	23	C	2022/09/13	Potassium, total	mg/L	3.08
UA	23	C	2023/02/28	Potassium, total	mg/L	2.99
UA	23	C	2023/05/31	Potassium, total	mg/L	3.16
UA	23	C	2023/08/22	Potassium, total	mg/L	2.90
UA	23	C	2023/11/15	Potassium, total	mg/L	3.00
UA	23	C	2023/05/31	Silicon, dissolved	mg/L	5.38
UA	23	C	2023/08/22	Silicon, dissolved	mg/L	6.60
UA	23	C	2019/09/18	Sodium, total	mg/L	42.6
UA	23	C	2020/03/11	Sodium, total	mg/L	42.1
UA	23	C	2020/06/24	Sodium, total	mg/L	45.3
UA	23	C	2021/02/24	Sodium, total	mg/L	47.9
UA	23	C	2021/03/04	Sodium, total	mg/L	46.2
UA	23	C	2021/03/09	Sodium, total	mg/L	43.0
UA	23	C	2021/03/18	Sodium, total	mg/L	46.6
UA	23	C	2021/03/19	Sodium, total	mg/L	45.2
UA	23	C	2021/03/30	Sodium, total	mg/L	47.3
UA	23	C	2021/09/09	Sodium, total	mg/L	40.5
UA	23	C	2022/03/22	Sodium, total	mg/L	45.0
UA	23	C	2022/09/13	Sodium, total	mg/L	43.4
UA	23	C	2023/02/28	Sodium, total	mg/L	46.3
UA	23	C	2023/05/31	Sodium, total	mg/L	46.0
UA	23	C	2023/08/22	Sodium, total	mg/L	44.0
UA	23	C	2023/11/15	Sodium, total	mg/L	44.0
UA	23	C	2013/03/08	Sulfate, total	mg/L	478
UA	23	C	2013/06/07	Sulfate, total	mg/L	152
UA	23	C	2013/09/03	Sulfate, total	mg/L	456
UA	23	C	2013/12/10	Sulfate, total	mg/L	357
UA	23	C	2014/03/25	Sulfate, total	mg/L	17.0
UA	23	C	2014/09/30	Sulfate, total	mg/L	472
UA	23	C	2015/03/18	Sulfate, total	mg/L	421
UA	23	C	2015/09/16	Sulfate, total	mg/L	458
UA	23	C	2015/12/10	Sulfate, total	mg/L	323
UA	23	C	2016/03/09	Sulfate, total	mg/L	477
UA	23	C	2016/06/07	Sulfate, total	mg/L	483
UA	23	C	2016/09/15	Sulfate, total	mg/L	470
UA	23	C	2016/12/07	Sulfate, total	mg/L	408
UA	23	C	2017/02/21	Sulfate, total	mg/L	390
UA	23	C	2017/04/25	Sulfate, total	mg/L	439
UA	23	C	2017/06/08	Sulfate, total	mg/L	485
UA	23	C	2017/09/06	Sulfate, total	mg/L	456
UA	23	C	2017/11/15	Sulfate, total	mg/L	420
UA	23	C	2018/03/26	Sulfate, total	mg/L	402
UA	23	C	2018/06/13	Sulfate, total	mg/L	489
UA	23	C	2018/09/12	Sulfate, total	mg/L	462
UA	23	C	2018/12/12	Sulfate, total	mg/L	420

UA	23	C	2019/03/13	Sulfate, total	mg/L	382
UA	23	C	2019/06/19	Sulfate, total	mg/L	424
UA	23	C	2019/09/18	Sulfate, total	mg/L	475
UA	23	C	2019/12/11	Sulfate, total	mg/L	433
UA	23	C	2020/03/11	Sulfate, total	mg/L	440
UA	23	C	2020/06/24	Sulfate, total	mg/L	473
UA	23	C	2020/09/02	Sulfate, total	mg/L	451
UA	23	C	2020/12/10	Sulfate, total	mg/L	554
UA	23	C	2021/02/24	Sulfate, total	mg/L	407
UA	23	C	2021/03/04	Sulfate, total	mg/L	404
UA	23	C	2021/03/09	Sulfate, total	mg/L	431
UA	23	C	2021/03/18	Sulfate, total	mg/L	423
UA	23	C	2021/03/19	Sulfate, total	mg/L	397
UA	23	C	2021/03/30	Sulfate, total	mg/L	426
UA	23	C	2021/06/24	Sulfate, total	mg/L	429
UA	23	C	2021/09/09	Sulfate, total	mg/L	455
UA	23	C	2021/12/08	Sulfate, total	mg/L	413
UA	23	C	2022/03/22	Sulfate, total	mg/L	421
UA	23	C	2022/06/07	Sulfate, total	mg/L	442
UA	23	C	2022/09/13	Sulfate, total	mg/L	471
UA	23	C	2022/12/27	Sulfate, total	mg/L	441
UA	23	C	2023/02/28	Sulfate, total	mg/L	433
UA	23	C	2023/05/31	Sulfate, total	mg/L	450
UA	23	C	2023/08/22	Sulfate, total	mg/L	460
UA	23	C	2023/11/15	Sulfate, total	mg/L	430
UA	23	C	2013/03/08	Temperature (Celsius)	degrees C	11.2
UA	23	C	2013/06/07	Temperature (Celsius)	degrees C	12.7
UA	23	C	2013/09/03	Temperature (Celsius)	degrees C	14.3
UA	23	C	2013/12/10	Temperature (Celsius)	degrees C	9.90
UA	23	C	2014/03/25	Temperature (Celsius)	degrees C	10.4
UA	23	C	2014/08/19	Temperature (Celsius)	degrees C	13.3
UA	23	C	2014/09/30	Temperature (Celsius)	degrees C	12.0
UA	23	C	2015/03/18	Temperature (Celsius)	degrees C	12.2
UA	23	C	2015/09/16	Temperature (Celsius)	degrees C	12.6
UA	23	C	2015/12/10	Temperature (Celsius)	degrees C	12.6
UA	23	C	2016/03/09	Temperature (Celsius)	degrees C	11.3
UA	23	C	2016/06/07	Temperature (Celsius)	degrees C	11.5
UA	23	C	2016/09/15	Temperature (Celsius)	degrees C	13.4
UA	23	C	2016/12/07	Temperature (Celsius)	degrees C	10.1
UA	23	C	2017/02/21	Temperature (Celsius)	degrees C	12.9
UA	23	C	2017/04/25	Temperature (Celsius)	degrees C	20.2
UA	23	C	2017/06/08	Temperature (Celsius)	degrees C	20.8
UA	23	C	2017/09/06	Temperature (Celsius)	degrees C	11.9
UA	23	C	2017/11/15	Temperature (Celsius)	degrees C	11.9
UA	23	C	2018/03/26	Temperature (Celsius)	degrees C	12.8
UA	23	C	2018/06/13	Temperature (Celsius)	degrees C	13.3
UA	23	C	2018/09/12	Temperature (Celsius)	degrees C	12.5
UA	23	C	2018/12/12	Temperature (Celsius)	degrees C	11.5
UA	23	C	2019/03/13	Temperature (Celsius)	degrees C	12.4
UA	23	C	2019/06/19	Temperature (Celsius)	degrees C	12.0
UA	23	C	2019/09/18	Temperature (Celsius)	degrees C	12.4
UA	23	C	2019/12/11	Temperature (Celsius)	degrees C	11.7
UA	23	C	2020/03/11	Temperature (Celsius)	degrees C	11.3
UA	23	C	2020/06/24	Temperature (Celsius)	degrees C	12.6
UA	23	C	2020/09/02	Temperature (Celsius)	degrees C	12.4
UA	23	C	2020/12/10	Temperature (Celsius)	degrees C	11.8
UA	23	C	2021/03/19	Temperature (Celsius)	degrees C	11.9
UA	23	C	2021/06/24	Temperature (Celsius)	degrees C	12.4
UA	23	C	2021/09/09	Temperature (Celsius)	degrees C	12.7
UA	23	C	2021/12/08	Temperature (Celsius)	degrees C	12.5
UA	23	C	2022/03/22	Temperature (Celsius)	degrees C	12.5
UA	23	C	2022/06/07	Temperature (Celsius)	degrees C	12.8

UA	23	C	2022/09/13	Temperature (Celsius)	degrees C	12.9
UA	23	C	2022/12/27	Temperature (Celsius)	degrees C	12.3
UA	23	C	2023/02/28	Temperature (Celsius)	degrees C	12.5
UA	23	C	2023/05/31	Temperature (Celsius)	degrees C	13.0
UA	23	C	2023/08/22	Temperature (Celsius)	degrees C	15.0
UA	23	C	2023/11/15	Temperature (Celsius)	degrees C	13.6
UA	23	C	2013/03/08	Total Dissolved Solids	mg/L	840
UA	23	C	2013/06/07	Total Dissolved Solids	mg/L	574
UA	23	C	2013/09/03	Total Dissolved Solids	mg/L	1,030
UA	23	C	2013/12/10	Total Dissolved Solids	mg/L	852
UA	23	C	2014/03/25	Total Dissolved Solids	mg/L	166
UA	23	C	2014/08/19	Total Dissolved Solids	mg/L	952
UA	23	C	2014/09/30	Total Dissolved Solids	mg/L	1,010
UA	23	C	2015/03/18	Total Dissolved Solids	mg/L	894
UA	23	C	2015/09/16	Total Dissolved Solids	mg/L	964
UA	23	C	2015/12/10	Total Dissolved Solids	mg/L	858
UA	23	C	2016/03/09	Total Dissolved Solids	mg/L	908
UA	23	C	2016/06/07	Total Dissolved Solids	mg/L	1,000
UA	23	C	2016/09/15	Total Dissolved Solids	mg/L	992
UA	23	C	2016/12/07	Total Dissolved Solids	mg/L	820
UA	23	C	2017/02/21	Total Dissolved Solids	mg/L	848
UA	23	C	2017/04/25	Total Dissolved Solids	mg/L	908
UA	23	C	2017/06/08	Total Dissolved Solids	mg/L	990
UA	23	C	2017/09/06	Total Dissolved Solids	mg/L	926
UA	23	C	2017/11/15	Total Dissolved Solids	mg/L	944
UA	23	C	2018/03/26	Total Dissolved Solids	mg/L	864
UA	23	C	2018/06/13	Total Dissolved Solids	mg/L	956
UA	23	C	2018/09/12	Total Dissolved Solids	mg/L	996
UA	23	C	2018/12/12	Total Dissolved Solids	mg/L	880
UA	23	C	2019/03/13	Total Dissolved Solids	mg/L	862
UA	23	C	2019/06/19	Total Dissolved Solids	mg/L	884
UA	23	C	2019/09/18	Total Dissolved Solids	mg/L	980
UA	23	C	2019/12/11	Total Dissolved Solids	mg/L	916
UA	23	C	2020/03/11	Total Dissolved Solids	mg/L	930
UA	23	C	2020/06/24	Total Dissolved Solids	mg/L	978
UA	23	C	2020/09/02	Total Dissolved Solids	mg/L	908
UA	23	C	2020/12/10	Total Dissolved Solids	mg/L	892
UA	23	C	2021/02/24	Total Dissolved Solids	mg/L	884
UA	23	C	2021/03/04	Total Dissolved Solids	mg/L	880
UA	23	C	2021/03/09	Total Dissolved Solids	mg/L	874
UA	23	C	2021/03/18	Total Dissolved Solids	mg/L	912
UA	23	C	2021/03/19	Total Dissolved Solids	mg/L	870
UA	23	C	2021/03/30	Total Dissolved Solids	mg/L	860
UA	23	C	2021/06/24	Total Dissolved Solids	mg/L	840
UA	23	C	2021/09/09	Total Dissolved Solids	mg/L	868
UA	23	C	2021/12/08	Total Dissolved Solids	mg/L	828
UA	23	C	2022/03/22	Total Dissolved Solids	mg/L	826
UA	23	C	2022/06/07	Total Dissolved Solids	mg/L	984
UA	23	C	2022/09/13	Total Dissolved Solids	mg/L	1,020
UA	23	C	2022/12/27	Total Dissolved Solids	mg/L	880
UA	23	C	2023/02/28	Total Dissolved Solids	mg/L	856
UA	23	C	2023/05/31	Total Dissolved Solids	mg/L	876
UA	23	C	2023/08/22	Total Dissolved Solids	mg/L	950
UA	23	C	2023/11/15	Total Dissolved Solids	mg/L	890
UA	27	C	2013/03/08	pH (field)	SU	7.2
UA	27	C	2013/06/26	pH (field)	SU	7.3
UA	27	C	2013/09/03	pH (field)	SU	8.0
UA	27	C	2013/12/10	pH (field)	SU	7.8
UA	27	C	2014/03/25	pH (field)	SU	7.2
UA	27	C	2014/08/19	pH (field)	SU	7.4
UA	27	C	2014/09/30	pH (field)	SU	7.4
UA	27	C	2015/03/18	pH (field)	SU	7.4

UA	27	C	2015/09/16	pH (field)	SU	7.4
UA	27	C	2016/03/08	pH (field)	SU	7.2
UA	27	C	2016/09/15	pH (field)	SU	7.4
UA	27	C	2017/02/21	pH (field)	SU	7.3
UA	27	C	2017/09/06	pH (field)	SU	7.1
UA	27	C	2018/03/26	pH (field)	SU	7.3
UA	27	C	2018/09/12	pH (field)	SU	7.1
UA	27	C	2018/12/12	pH (field)	SU	7.2
UA	27	C	2019/03/13	pH (field)	SU	7.2
UA	27	C	2019/12/11	pH (field)	SU	7.2
UA	27	C	2020/03/11	pH (field)	SU	7.2
UA	27	C	2020/09/02	pH (field)	SU	7.3
UA	27	C	2020/12/09	pH (field)	SU	7.2
UA	27	C	2021/03/17	pH (field)	SU	7.1
UA	27	C	2021/06/24	pH (field)	SU	7.0
UA	27	C	2021/09/09	pH (field)	SU	7.0
UA	27	C	2021/12/08	pH (field)	SU	7.1
UA	27	C	2022/03/22	pH (field)	SU	7.1
UA	27	C	2022/06/07	pH (field)	SU	7.1
UA	27	C	2022/09/13	pH (field)	SU	7.1
UA	27	C	2022/12/27	pH (field)	SU	7.2
UA	27	C	2023/02/28	pH (field)	SU	7.0
UA	27	C	2023/05/31	pH (field)	SU	7.0
UA	27	C	2023/08/24	pH (field)	SU	7.3
UA	27	C	2023/11/14	pH (field)	SU	7.3
UA	27	C	2018/09/12	Oxidation Reduction Potential	mV	-41.0
UA	27	C	2018/12/12	Oxidation Reduction Potential	mV	-29.0
UA	27	C	2019/03/13	Oxidation Reduction Potential	mV	-38.0
UA	27	C	2019/12/11	Oxidation Reduction Potential	mV	-30.0
UA	27	C	2020/03/11	Oxidation Reduction Potential	mV	9.00
UA	27	C	2020/09/02	Oxidation Reduction Potential	mV	-11.0
UA	27	C	2020/12/09	Oxidation Reduction Potential	mV	-7.00
UA	27	C	2021/03/17	Oxidation Reduction Potential	mV	-51.0
UA	27	C	2021/06/24	Oxidation Reduction Potential	mV	-63.0
UA	27	C	2021/09/09	Oxidation Reduction Potential	mV	-14.0
UA	27	C	2021/12/08	Oxidation Reduction Potential	mV	-21.0
UA	27	C	2022/03/22	Oxidation Reduction Potential	mV	-60.0
UA	27	C	2022/06/07	Oxidation Reduction Potential	mV	63.0
UA	27	C	2022/09/13	Oxidation Reduction Potential	mV	104
UA	27	C	2022/12/27	Oxidation Reduction Potential	mV	-80.0
UA	27	C	2023/02/28	Oxidation Reduction Potential	mV	-49.1
UA	27	C	2023/05/31	Oxidation Reduction Potential	mV	-16.0
UA	27	C	2023/08/24	Oxidation Reduction Potential	mV	-33.7
UA	27	C	2023/11/14	Oxidation Reduction Potential	mV	-50.4
UA	27	C	2018/09/12	Eh	V	0.15
UA	27	C	2018/12/12	Eh	V	0.17
UA	27	C	2019/03/13	Eh	V	0.16
UA	27	C	2019/12/11	Eh	V	0.17
UA	27	C	2020/03/11	Eh	V	0.21
UA	27	C	2020/09/02	Eh	V	0.19
UA	27	C	2020/12/09	Eh	V	0.19
UA	27	C	2021/03/17	Eh	V	0.15
UA	27	C	2021/06/24	Eh	V	0.13
UA	27	C	2021/09/09	Eh	V	0.18
UA	27	C	2021/12/08	Eh	V	0.18
UA	27	C	2022/03/22	Eh	V	0.14
UA	27	C	2022/06/07	Eh	V	0.26
UA	27	C	2022/09/13	Eh	V	0.30
UA	27	C	2022/12/27	Eh	V	0.12
UA	27	C	2023/02/28	Eh	V	0.15
UA	27	C	2023/05/31	Eh	V	0.18
UA	27	C	2023/08/24	Eh	V	0.16

UA	27	C	2023/11/14	Eh	V	0.15
UA	27	C	2020/03/11	Alkalinity, bicarbonate	mg/L CaCO3	352
UA	27	C	2021/03/17	Alkalinity, bicarbonate	mg/L CaCO3	326
UA	27	C	2021/09/09	Alkalinity, bicarbonate	mg/L CaCO3	342
UA	27	C	2022/03/22	Alkalinity, bicarbonate	mg/L CaCO3	333
UA	27	C	2023/02/28	Alkalinity, bicarbonate	mg/L CaCO3	323
UA	27	C	2023/05/31	Alkalinity, bicarbonate	mg/L CaCO3	334
UA	27	C	2023/08/24	Alkalinity, bicarbonate	mg/L CaCO3	340
UA	27	C	2023/11/14	Alkalinity, bicarbonate	mg/L CaCO3	350
UA	27	C	2013/06/26	Arsenic, total	mg/L	<0.0007
UA	27	C	2013/09/03	Arsenic, total	mg/L	<0.0007
UA	27	C	2018/09/12	Arsenic, total	mg/L	<0.0004
UA	27	C	2018/12/12	Arsenic, total	mg/L	0.00110
UA	27	C	2019/03/13	Arsenic, total	mg/L	0.00150
UA	27	C	2019/12/11	Arsenic, total	mg/L	0.00120
UA	27	C	2020/03/11	Arsenic, total	mg/L	<0.0004
UA	27	C	2020/09/02	Arsenic, total	mg/L	<0.0004
UA	27	C	2020/12/09	Arsenic, total	mg/L	<0.0004
UA	27	C	2021/03/17	Arsenic, total	mg/L	0.00110
UA	27	C	2021/06/24	Arsenic, total	mg/L	<0.0004
UA	27	C	2021/09/09	Arsenic, total	mg/L	<0.0004
UA	27	C	2021/12/08	Arsenic, total	mg/L	<0.0004
UA	27	C	2022/03/22	Arsenic, total	mg/L	<0.0004
UA	27	C	2022/06/07	Arsenic, total	mg/L	0.000500
UA	27	C	2022/09/13	Arsenic, total	mg/L	0.000700
UA	27	C	2022/12/27	Arsenic, total	mg/L	0.00110
UA	27	C	2023/02/28	Arsenic, total	mg/L	0.00130
UA	27	C	2023/05/31	Arsenic, total	mg/L	<0.0087
UA	27	C	2023/08/24	Arsenic, total	mg/L	0.00100
UA	27	C	2023/11/14	Arsenic, total	mg/L	0.00120
UA	27	C	2013/06/26	Barium, total	mg/L	0.130
UA	27	C	2013/09/03	Barium, total	mg/L	0.0905
UA	27	C	2018/09/12	Barium, total	mg/L	0.111
UA	27	C	2018/12/12	Barium, total	mg/L	0.0892
UA	27	C	2019/03/13	Barium, total	mg/L	0.0895
UA	27	C	2019/12/11	Barium, total	mg/L	0.0919
UA	27	C	2020/03/11	Barium, total	mg/L	0.0818
UA	27	C	2020/09/02	Barium, total	mg/L	0.0918
UA	27	C	2020/12/09	Barium, total	mg/L	0.122
UA	27	C	2021/03/17	Barium, total	mg/L	0.0923
UA	27	C	2021/06/24	Barium, total	mg/L	0.0874
UA	27	C	2021/09/09	Barium, total	mg/L	0.0913
UA	27	C	2021/12/08	Barium, total	mg/L	0.0885
UA	27	C	2022/03/22	Barium, total	mg/L	0.0863
UA	27	C	2022/06/07	Barium, total	mg/L	0.0838
UA	27	C	2022/09/13	Barium, total	mg/L	0.0806
UA	27	C	2022/12/27	Barium, total	mg/L	0.0731
UA	27	C	2023/02/28	Barium, total	mg/L	0.0971
UA	27	C	2023/05/31	Barium, total	mg/L	0.0837
UA	27	C	2023/08/24	Barium, total	mg/L	0.0840
UA	27	C	2023/11/14	Barium, total	mg/L	0.0840
UA	27	C	2013/06/26	Boron, total	mg/L	3.98
UA	27	C	2013/09/03	Boron, total	mg/L	4.68
UA	27	C	2018/09/12	Boron, total	mg/L	3.94
UA	27	C	2018/12/12	Boron, total	mg/L	4.02
UA	27	C	2019/03/13	Boron, total	mg/L	4.31
UA	27	C	2019/12/11	Boron, total	mg/L	3.21
UA	27	C	2020/03/11	Boron, total	mg/L	2.82
UA	27	C	2020/09/02	Boron, total	mg/L	2.29
UA	27	C	2020/12/09	Boron, total	mg/L	2.12
UA	27	C	2021/03/17	Boron, total	mg/L	2.73
UA	27	C	2021/06/24	Boron, total	mg/L	2.37

UA	27	C	2021/09/09	Boron, total	mg/L	2.57
UA	27	C	2021/12/08	Boron, total	mg/L	2.22
UA	27	C	2022/03/22	Boron, total	mg/L	2.41
UA	27	C	2022/06/07	Boron, total	mg/L	2.22
UA	27	C	2022/09/13	Boron, total	mg/L	2.07
UA	27	C	2022/12/27	Boron, total	mg/L	2.34
UA	27	C	2023/02/28	Boron, total	mg/L	2.73
UA	27	C	2023/05/31	Boron, total	mg/L	2.27
UA	27	C	2023/08/24	Boron, total	mg/L	2.00
UA	27	C	2023/11/14	Boron, total	mg/L	2.40
UA	27	C	2013/06/26	Cadmium, total	mg/L	<0.0003
UA	27	C	2013/09/03	Cadmium, total	mg/L	<0.0003
UA	27	C	2018/09/12	Cadmium, total	mg/L	<0.0002
UA	27	C	2018/12/12	Cadmium, total	mg/L	<0.0002
UA	27	C	2019/03/13	Cadmium, total	mg/L	<0.0002
UA	27	C	2019/12/11	Cadmium, total	mg/L	<0.0002
UA	27	C	2020/03/11	Cadmium, total	mg/L	<0.0002
UA	27	C	2020/09/02	Cadmium, total	mg/L	<0.0002
UA	27	C	2020/12/09	Cadmium, total	mg/L	<0.0002
UA	27	C	2021/03/17	Cadmium, total	mg/L	<0.0002
UA	27	C	2021/06/24	Cadmium, total	mg/L	<0.0002
UA	27	C	2021/09/09	Cadmium, total	mg/L	<0.0002
UA	27	C	2021/12/08	Cadmium, total	mg/L	<0.0002
UA	27	C	2022/03/22	Cadmium, total	mg/L	<0.0002
UA	27	C	2022/06/07	Cadmium, total	mg/L	0.000500
UA	27	C	2022/09/13	Cadmium, total	mg/L	<0.0002
UA	27	C	2022/12/27	Cadmium, total	mg/L	0.000800
UA	27	C	2023/02/28	Cadmium, total	mg/L	0.000300
UA	27	C	2023/05/31	Cadmium, total	mg/L	<0.0005
UA	27	C	2023/08/24	Cadmium, total	mg/L	0.000250
UA	27	C	2023/11/14	Cadmium, total	mg/L	<0.00017
UA	27	C	2018/09/12	Calcium, total	mg/L	169
UA	27	C	2018/12/12	Calcium, total	mg/L	133
UA	27	C	2019/03/13	Calcium, total	mg/L	141
UA	27	C	2019/12/11	Calcium, total	mg/L	139
UA	27	C	2020/03/11	Calcium, total	mg/L	139
UA	27	C	2020/09/02	Calcium, total	mg/L	132
UA	27	C	2020/12/09	Calcium, total	mg/L	197
UA	27	C	2021/03/17	Calcium, total	mg/L	138
UA	27	C	2021/06/24	Calcium, total	mg/L	138
UA	27	C	2021/09/09	Calcium, total	mg/L	141
UA	27	C	2021/12/08	Calcium, total	mg/L	129
UA	27	C	2022/03/22	Calcium, total	mg/L	140
UA	27	C	2022/06/07	Calcium, total	mg/L	132
UA	27	C	2022/09/13	Calcium, total	mg/L	132
UA	27	C	2022/12/27	Calcium, total	mg/L	136
UA	27	C	2023/02/28	Calcium, total	mg/L	141
UA	27	C	2023/05/31	Calcium, total	mg/L	117
UA	27	C	2023/08/24	Calcium, total	mg/L	120
UA	27	C	2023/11/14	Calcium, total	mg/L	120
UA	27	C	2013/03/08	Chloride, total	mg/L	49.0
UA	27	C	2013/06/26	Chloride, total	mg/L	46.0
UA	27	C	2013/09/03	Chloride, total	mg/L	38.0
UA	27	C	2013/12/10	Chloride, total	mg/L	44.0
UA	27	C	2014/03/25	Chloride, total	mg/L	66.0
UA	27	C	2014/09/30	Chloride, total	mg/L	42.0
UA	27	C	2015/03/18	Chloride, total	mg/L	41.0
UA	27	C	2015/09/16	Chloride, total	mg/L	35.0
UA	27	C	2016/03/08	Chloride, total	mg/L	43.0
UA	27	C	2016/09/15	Chloride, total	mg/L	53.0
UA	27	C	2017/02/21	Chloride, total	mg/L	55.0
UA	27	C	2017/09/06	Chloride, total	mg/L	73.0

UA	27	C	2018/03/26	Chloride, total	mg/L	86.0
UA	27	C	2018/09/12	Chloride, total	mg/L	90.0
UA	27	C	2018/12/12	Chloride, total	mg/L	86.0
UA	27	C	2019/03/13	Chloride, total	mg/L	89.0
UA	27	C	2019/12/11	Chloride, total	mg/L	98.0
UA	27	C	2020/03/11	Chloride, total	mg/L	98.0
UA	27	C	2020/09/02	Chloride, total	mg/L	103
UA	27	C	2020/12/09	Chloride, total	mg/L	108
UA	27	C	2021/03/17	Chloride, total	mg/L	98.0
UA	27	C	2021/06/24	Chloride, total	mg/L	103
UA	27	C	2021/09/09	Chloride, total	mg/L	107
UA	27	C	2021/12/08	Chloride, total	mg/L	109
UA	27	C	2022/03/22	Chloride, total	mg/L	101
UA	27	C	2022/06/07	Chloride, total	mg/L	96.0
UA	27	C	2022/09/13	Chloride, total	mg/L	104
UA	27	C	2022/12/27	Chloride, total	mg/L	107
UA	27	C	2023/02/28	Chloride, total	mg/L	99.0
UA	27	C	2023/05/31	Chloride, total	mg/L	107
UA	27	C	2023/08/24	Chloride, total	mg/L	91.0
UA	27	C	2023/11/14	Chloride, total	mg/L	88.0
UA	27	C	2013/03/08	Iron, dissolved	mg/L	1.13
UA	27	C	2013/12/10	Iron, dissolved	mg/L	0.242
UA	27	C	2014/03/25	Iron, dissolved	mg/L	0.0499
UA	27	C	2014/08/19	Iron, dissolved	mg/L	<0.007
UA	27	C	2014/09/30	Iron, dissolved	mg/L	0.0943
UA	27	C	2015/03/18	Iron, dissolved	mg/L	0.274
UA	27	C	2015/09/16	Iron, dissolved	mg/L	0.0817
UA	27	C	2016/03/08	Iron, dissolved	mg/L	0.161
UA	27	C	2016/09/15	Iron, dissolved	mg/L	0.132
UA	27	C	2017/02/21	Iron, dissolved	mg/L	0.219
UA	27	C	2017/09/06	Iron, dissolved	mg/L	0.230
UA	27	C	2018/03/26	Iron, dissolved	mg/L	0.207
UA	27	C	2023/05/31	Iron, dissolved	mg/L	0.257
UA	27	C	2023/08/24	Iron, dissolved	mg/L	0.210
UA	27	C	2018/09/12	Lithium, total	mg/L	0.0227
UA	27	C	2018/12/12	Lithium, total	mg/L	0.0220
UA	27	C	2019/03/13	Lithium, total	mg/L	0.0225
UA	27	C	2019/12/11	Lithium, total	mg/L	0.0266
UA	27	C	2020/03/11	Lithium, total	mg/L	0.0266
UA	27	C	2020/09/02	Lithium, total	mg/L	0.0248
UA	27	C	2020/12/09	Lithium, total	mg/L	0.0234
UA	27	C	2021/03/17	Lithium, total	mg/L	0.0207
UA	27	C	2021/06/24	Lithium, total	mg/L	0.0253
UA	27	C	2021/09/09	Lithium, total	mg/L	0.0254
UA	27	C	2021/12/08	Lithium, total	mg/L	0.0226
UA	27	C	2022/03/22	Lithium, total	mg/L	0.0231
UA	27	C	2022/06/07	Lithium, total	mg/L	0.0224
UA	27	C	2022/09/13	Lithium, total	mg/L	0.0203
UA	27	C	2022/12/27	Lithium, total	mg/L	0.0187
UA	27	C	2023/02/28	Lithium, total	mg/L	0.0174
UA	27	C	2023/05/31	Lithium, total	mg/L	0.0225
UA	27	C	2023/08/24	Lithium, total	mg/L	0.0240
UA	27	C	2023/11/14	Lithium, total	mg/L	0.0230
UA	27	C	2020/03/11	Magnesium, total	mg/L	39.0
UA	27	C	2021/03/17	Magnesium, total	mg/L	40.0
UA	27	C	2021/09/09	Magnesium, total	mg/L	39.8
UA	27	C	2022/03/22	Magnesium, total	mg/L	38.9
UA	27	C	2023/02/28	Magnesium, total	mg/L	39.6
UA	27	C	2023/05/31	Magnesium, total	mg/L	35.4
UA	27	C	2023/08/24	Magnesium, total	mg/L	37.0
UA	27	C	2023/11/14	Magnesium, total	mg/L	37.0
UA	27	C	2013/03/08	Manganese, dissolved	mg/L	0.660

UA	27	C	2013/12/10	Manganese, dissolved	mg/L	0.702
UA	27	C	2014/03/25	Manganese, dissolved	mg/L	0.607
UA	27	C	2014/08/19	Manganese, dissolved	mg/L	0.650
UA	27	C	2014/09/30	Manganese, dissolved	mg/L	0.772
UA	27	C	2015/03/18	Manganese, dissolved	mg/L	0.758
UA	27	C	2015/09/16	Manganese, dissolved	mg/L	0.722
UA	27	C	2016/03/08	Manganese, dissolved	mg/L	0.703
UA	27	C	2016/09/15	Manganese, dissolved	mg/L	0.715
UA	27	C	2017/02/21	Manganese, dissolved	mg/L	0.711
UA	27	C	2017/09/06	Manganese, dissolved	mg/L	0.720
UA	27	C	2018/03/26	Manganese, dissolved	mg/L	0.687
UA	27	C	2023/05/31	Manganese, dissolved	mg/L	0.657
UA	27	C	2023/08/24	Manganese, dissolved	mg/L	0.660
UA	27	C	2023/05/31	Phosphate, dissolved	mg/L	0.147
UA	27	C	2023/08/24	Phosphate, dissolved	mg/L	0.230
UA	27	C	2020/03/11	Potassium, total	mg/L	3.88
UA	27	C	2021/03/17	Potassium, total	mg/L	3.64
UA	27	C	2021/09/09	Potassium, total	mg/L	4.12
UA	27	C	2022/03/22	Potassium, total	mg/L	3.83
UA	27	C	2023/02/28	Potassium, total	mg/L	3.08
UA	27	C	2023/05/31	Potassium, total	mg/L	3.60
UA	27	C	2023/08/24	Potassium, total	mg/L	3.50
UA	27	C	2023/11/14	Potassium, total	mg/L	3.20
UA	27	C	2023/05/31	Silicon, dissolved	mg/L	7.59
UA	27	C	2023/08/24	Silicon, dissolved	mg/L	9.40
UA	27	C	2020/03/11	Sodium, total	mg/L	52.1
UA	27	C	2021/03/17	Sodium, total	mg/L	53.7
UA	27	C	2021/09/09	Sodium, total	mg/L	50.5
UA	27	C	2022/03/22	Sodium, total	mg/L	58.4
UA	27	C	2023/02/28	Sodium, total	mg/L	51.1
UA	27	C	2023/05/31	Sodium, total	mg/L	54.8
UA	27	C	2023/08/24	Sodium, total	mg/L	52.0
UA	27	C	2023/11/14	Sodium, total	mg/L	51.0
UA	27	C	2013/03/08	Sulfate, total	mg/L	219
UA	27	C	2013/06/26	Sulfate, total	mg/L	152
UA	27	C	2013/09/03	Sulfate, total	mg/L	192
UA	27	C	2013/12/10	Sulfate, total	mg/L	169
UA	27	C	2014/03/25	Sulfate, total	mg/L	165
UA	27	C	2014/09/30	Sulfate, total	mg/L	215
UA	27	C	2015/03/18	Sulfate, total	mg/L	216
UA	27	C	2015/09/16	Sulfate, total	mg/L	228
UA	27	C	2016/03/08	Sulfate, total	mg/L	216
UA	27	C	2016/09/15	Sulfate, total	mg/L	173
UA	27	C	2017/02/21	Sulfate, total	mg/L	186
UA	27	C	2017/09/06	Sulfate, total	mg/L	150
UA	27	C	2018/03/26	Sulfate, total	mg/L	144
UA	27	C	2018/09/12	Sulfate, total	mg/L	144
UA	27	C	2018/12/12	Sulfate, total	mg/L	135
UA	27	C	2019/03/13	Sulfate, total	mg/L	124
UA	27	C	2019/12/11	Sulfate, total	mg/L	104
UA	27	C	2020/03/11	Sulfate, total	mg/L	109
UA	27	C	2020/09/02	Sulfate, total	mg/L	112
UA	27	C	2020/12/09	Sulfate, total	mg/L	120
UA	27	C	2021/03/17	Sulfate, total	mg/L	124
UA	27	C	2021/06/24	Sulfate, total	mg/L	122
UA	27	C	2021/09/09	Sulfate, total	mg/L	129
UA	27	C	2021/12/08	Sulfate, total	mg/L	115
UA	27	C	2022/03/22	Sulfate, total	mg/L	123
UA	27	C	2022/06/07	Sulfate, total	mg/L	121
UA	27	C	2022/09/13	Sulfate, total	mg/L	117
UA	27	C	2022/12/27	Sulfate, total	mg/L	139
UA	27	C	2023/02/28	Sulfate, total	mg/L	159

UA	27	C	2023/05/31	Sulfate, total	mg/L	118
UA	27	C	2023/08/24	Sulfate, total	mg/L	110
UA	27	C	2023/11/14	Sulfate, total	mg/L	120
UA	27	C	2013/03/08	Temperature (Celsius)	degrees C	10.9
UA	27	C	2013/06/26	Temperature (Celsius)	degrees C	12.8
UA	27	C	2013/09/03	Temperature (Celsius)	degrees C	12.9
UA	27	C	2013/12/10	Temperature (Celsius)	degrees C	10.0
UA	27	C	2014/03/25	Temperature (Celsius)	degrees C	9.90
UA	27	C	2014/08/19	Temperature (Celsius)	degrees C	13.1
UA	27	C	2014/09/30	Temperature (Celsius)	degrees C	12.1
UA	27	C	2015/03/18	Temperature (Celsius)	degrees C	11.8
UA	27	C	2015/09/16	Temperature (Celsius)	degrees C	13.1
UA	27	C	2016/03/08	Temperature (Celsius)	degrees C	11.3
UA	27	C	2016/09/15	Temperature (Celsius)	degrees C	14.9
UA	27	C	2017/02/21	Temperature (Celsius)	degrees C	12.7
UA	27	C	2017/09/06	Temperature (Celsius)	degrees C	12.7
UA	27	C	2018/03/26	Temperature (Celsius)	degrees C	11.8
UA	27	C	2018/09/12	Temperature (Celsius)	degrees C	17.1
UA	27	C	2018/12/12	Temperature (Celsius)	degrees C	11.5
UA	27	C	2019/03/13	Temperature (Celsius)	degrees C	11.2
UA	27	C	2019/12/11	Temperature (Celsius)	degrees C	11.6
UA	27	C	2020/03/11	Temperature (Celsius)	degrees C	11.1
UA	27	C	2020/09/02	Temperature (Celsius)	degrees C	13.5
UA	27	C	2020/12/09	Temperature (Celsius)	degrees C	12.2
UA	27	C	2021/03/17	Temperature (Celsius)	degrees C	11.7
UA	27	C	2021/06/24	Temperature (Celsius)	degrees C	12.4
UA	27	C	2021/09/09	Temperature (Celsius)	degrees C	12.6
UA	27	C	2021/12/08	Temperature (Celsius)	degrees C	11.9
UA	27	C	2022/03/22	Temperature (Celsius)	degrees C	11.6
UA	27	C	2022/06/07	Temperature (Celsius)	degrees C	12.5
UA	27	C	2022/09/13	Temperature (Celsius)	degrees C	14.7
UA	27	C	2022/12/27	Temperature (Celsius)	degrees C	11.1
UA	27	C	2023/02/28	Temperature (Celsius)	degrees C	11.6
UA	27	C	2023/05/31	Temperature (Celsius)	degrees C	12.0
UA	27	C	2023/08/24	Temperature (Celsius)	degrees C	12.5
UA	27	C	2023/11/14	Temperature (Celsius)	degrees C	12.7
UA	27	C	2013/03/08	Total Dissolved Solids	mg/L	654
UA	27	C	2013/06/26	Total Dissolved Solids	mg/L	600
UA	27	C	2013/09/03	Total Dissolved Solids	mg/L	618
UA	27	C	2013/12/10	Total Dissolved Solids	mg/L	602
UA	27	C	2014/03/25	Total Dissolved Solids	mg/L	518
UA	27	C	2014/08/19	Total Dissolved Solids	mg/L	636
UA	27	C	2014/09/30	Total Dissolved Solids	mg/L	644
UA	27	C	2015/03/18	Total Dissolved Solids	mg/L	652
UA	27	C	2015/09/16	Total Dissolved Solids	mg/L	660
UA	27	C	2016/03/08	Total Dissolved Solids	mg/L	638
UA	27	C	2016/09/15	Total Dissolved Solids	mg/L	634
UA	27	C	2017/02/21	Total Dissolved Solids	mg/L	442
UA	27	C	2017/09/06	Total Dissolved Solids	mg/L	680
UA	27	C	2018/03/26	Total Dissolved Solids	mg/L	666
UA	27	C	2018/09/12	Total Dissolved Solids	mg/L	808
UA	27	C	2018/12/12	Total Dissolved Solids	mg/L	694
UA	27	C	2019/03/13	Total Dissolved Solids	mg/L	700
UA	27	C	2019/12/11	Total Dissolved Solids	mg/L	654
UA	27	C	2020/03/11	Total Dissolved Solids	mg/L	668
UA	27	C	2020/09/02	Total Dissolved Solids	mg/L	642
UA	27	C	2020/12/09	Total Dissolved Solids	mg/L	674
UA	27	C	2021/03/17	Total Dissolved Solids	mg/L	722
UA	27	C	2021/06/24	Total Dissolved Solids	mg/L	670
UA	27	C	2021/09/09	Total Dissolved Solids	mg/L	712
UA	27	C	2021/12/08	Total Dissolved Solids	mg/L	634
UA	27	C	2022/03/22	Total Dissolved Solids	mg/L	648

UA	27	C	2022/06/07	Total Dissolved Solids	mg/L	752
UA	27	C	2022/09/13	Total Dissolved Solids	mg/L	698
UA	27	C	2022/12/27	Total Dissolved Solids	mg/L	634
UA	27	C	2023/02/28	Total Dissolved Solids	mg/L	636
UA	27	C	2023/05/31	Total Dissolved Solids	mg/L	658
UA	27	C	2023/08/24	Total Dissolved Solids	mg/L	660
UA	27	C	2023/11/14	Total Dissolved Solids	mg/L	660
UA	35	C	2015/12/09	pH (field)	SU	7.2
UA	35	C	2016/03/09	pH (field)	SU	7.1
UA	35	C	2016/06/07	pH (field)	SU	7.4
UA	35	C	2016/09/15	pH (field)	SU	7.4
UA	35	C	2016/12/07	pH (field)	SU	7.2
UA	35	C	2017/02/21	pH (field)	SU	7.2
UA	35	C	2017/04/25	pH (field)	SU	7.5
UA	35	C	2017/06/08	pH (field)	SU	7.1
UA	35	C	2017/11/15	pH (field)	SU	7.4
UA	35	C	2018/06/13	pH (field)	SU	6.8
UA	35	C	2018/09/12	pH (field)	SU	7.1
UA	35	C	2018/12/12	pH (field)	SU	6.9
UA	35	C	2019/03/13	pH (field)	SU	7.2
UA	35	C	2019/06/19	pH (field)	SU	7.0
UA	35	C	2019/09/17	pH (field)	SU	7.0
UA	35	C	2019/12/11	pH (field)	SU	7.1
UA	35	C	2020/03/11	pH (field)	SU	6.9
UA	35	C	2020/06/24	pH (field)	SU	7.3
UA	35	C	2020/09/02	pH (field)	SU	7.2
UA	35	C	2020/12/09	pH (field)	SU	7.0
UA	35	C	2021/03/17	pH (field)	SU	7.1
UA	35	C	2021/06/23	pH (field)	SU	7.0
UA	35	C	2021/09/08	pH (field)	SU	7.0
UA	35	C	2021/12/08	pH (field)	SU	6.9
UA	35	C	2022/03/22	pH (field)	SU	7.0
UA	35	C	2022/06/07	pH (field)	SU	7.0
UA	35	C	2022/09/14	pH (field)	SU	6.8
UA	35	C	2022/12/27	pH (field)	SU	7.0
UA	35	C	2023/02/28	pH (field)	SU	7.0
UA	35	C	2023/05/31	pH (field)	SU	6.9
UA	35	C	2023/08/24	pH (field)	SU	7.0
UA	35	C	2023/11/15	pH (field)	SU	6.9
UA	35	C	2015/12/09	Oxidation Reduction Potential	mV	148
UA	35	C	2016/03/09	Oxidation Reduction Potential	mV	162
UA	35	C	2016/06/07	Oxidation Reduction Potential	mV	51.0
UA	35	C	2016/09/15	Oxidation Reduction Potential	mV	145
UA	35	C	2016/12/07	Oxidation Reduction Potential	mV	126
UA	35	C	2017/02/21	Oxidation Reduction Potential	mV	77.0
UA	35	C	2017/04/25	Oxidation Reduction Potential	mV	80.0
UA	35	C	2017/06/08	Oxidation Reduction Potential	mV	65.0
UA	35	C	2017/11/15	Oxidation Reduction Potential	mV	-31.0
UA	35	C	2018/06/13	Oxidation Reduction Potential	mV	11.0
UA	35	C	2018/09/12	Oxidation Reduction Potential	mV	62.0
UA	35	C	2018/12/12	Oxidation Reduction Potential	mV	125
UA	35	C	2019/03/13	Oxidation Reduction Potential	mV	102
UA	35	C	2019/06/19	Oxidation Reduction Potential	mV	158
UA	35	C	2019/09/17	Oxidation Reduction Potential	mV	112
UA	35	C	2019/12/11	Oxidation Reduction Potential	mV	132
UA	35	C	2020/03/11	Oxidation Reduction Potential	mV	105
UA	35	C	2020/06/24	Oxidation Reduction Potential	mV	184
UA	35	C	2020/09/02	Oxidation Reduction Potential	mV	111
UA	35	C	2020/12/09	Oxidation Reduction Potential	mV	28.0
UA	35	C	2021/03/17	Oxidation Reduction Potential	mV	143
UA	35	C	2021/06/23	Oxidation Reduction Potential	mV	-36.0
UA	35	C	2021/09/08	Oxidation Reduction Potential	mV	63.0

UA	35	C	2021/12/08	Oxidation Reduction Potential	mV	17.0
UA	35	C	2022/03/22	Oxidation Reduction Potential	mV	10.0
UA	35	C	2022/06/07	Oxidation Reduction Potential	mV	66.0
UA	35	C	2022/09/14	Oxidation Reduction Potential	mV	191
UA	35	C	2022/12/27	Oxidation Reduction Potential	mV	7.00
UA	35	C	2023/02/28	Oxidation Reduction Potential	mV	108
UA	35	C	2023/05/31	Oxidation Reduction Potential	mV	105
UA	35	C	2023/08/24	Oxidation Reduction Potential	mV	162
UA	35	C	2023/11/15	Oxidation Reduction Potential	mV	228
UA	35	C	2015/12/09	Eh	V	0.34
UA	35	C	2016/03/09	Eh	V	0.36
UA	35	C	2016/06/07	Eh	V	0.25
UA	35	C	2016/09/15	Eh	V	0.34
UA	35	C	2016/12/07	Eh	V	0.32
UA	35	C	2017/02/21	Eh	V	0.27
UA	35	C	2017/04/25	Eh	V	0.28
UA	35	C	2017/06/08	Eh	V	0.26
UA	35	C	2017/11/15	Eh	V	0.16
UA	35	C	2018/06/13	Eh	V	0.21
UA	35	C	2018/09/12	Eh	V	0.26
UA	35	C	2018/12/12	Eh	V	0.32
UA	35	C	2019/03/13	Eh	V	0.30
UA	35	C	2019/06/19	Eh	V	0.36
UA	35	C	2019/09/17	Eh	V	0.31
UA	35	C	2019/12/11	Eh	V	0.33
UA	35	C	2020/03/11	Eh	V	0.30
UA	35	C	2020/06/24	Eh	V	0.38
UA	35	C	2020/09/02	Eh	V	0.31
UA	35	C	2020/12/09	Eh	V	0.22
UA	35	C	2021/03/17	Eh	V	0.34
UA	35	C	2021/06/23	Eh	V	0.16
UA	35	C	2021/09/08	Eh	V	0.26
UA	35	C	2021/12/08	Eh	V	0.21
UA	35	C	2022/03/22	Eh	V	0.21
UA	35	C	2022/06/07	Eh	V	0.26
UA	35	C	2022/09/14	Eh	V	0.39
UA	35	C	2022/12/27	Eh	V	0.20
UA	35	C	2023/02/28	Eh	V	0.31
UA	35	C	2023/05/31	Eh	V	0.30
UA	35	C	2023/08/24	Eh	V	0.36
UA	35	C	2023/11/15	Eh	V	0.42
UA	35	C	2019/09/17	Alkalinity, bicarbonate	mg/L CaCO3	210
UA	35	C	2020/03/11	Alkalinity, bicarbonate	mg/L CaCO3	220
UA	35	C	2021/03/17	Alkalinity, bicarbonate	mg/L CaCO3	195
UA	35	C	2021/09/08	Alkalinity, bicarbonate	mg/L CaCO3	208
UA	35	C	2022/03/22	Alkalinity, bicarbonate	mg/L CaCO3	209
UA	35	C	2022/09/14	Alkalinity, bicarbonate	mg/L CaCO3	215
UA	35	C	2023/02/28	Alkalinity, bicarbonate	mg/L CaCO3	269
UA	35	C	2023/05/31	Alkalinity, bicarbonate	mg/L CaCO3	249
UA	35	C	2023/08/24	Alkalinity, bicarbonate	mg/L CaCO3	210
UA	35	C	2023/11/15	Alkalinity, bicarbonate	mg/L CaCO3	310
UA	35	C	2015/12/09	Arsenic, total	mg/L	<0.0002
UA	35	C	2016/03/09	Arsenic, total	mg/L	<0.0002
UA	35	C	2016/06/07	Arsenic, total	mg/L	<0.0002
UA	35	C	2016/09/15	Arsenic, total	mg/L	<0.0002
UA	35	C	2016/12/07	Arsenic, total	mg/L	<0.0002
UA	35	C	2017/02/21	Arsenic, total	mg/L	<0.0002
UA	35	C	2017/04/25	Arsenic, total	mg/L	<0.0002
UA	35	C	2017/06/08	Arsenic, total	mg/L	<0.0002
UA	35	C	2018/06/13	Arsenic, total	mg/L	<0.0004
UA	35	C	2018/09/12	Arsenic, total	mg/L	<0.0004
UA	35	C	2018/12/12	Arsenic, total	mg/L	<0.0004

UA	35	C	2019/03/13	Arsenic, total	mg/L	0.00260
UA	35	C	2019/06/19	Arsenic, total	mg/L	0.0109
UA	35	C	2019/09/17	Arsenic, total	mg/L	0.00170
UA	35	C	2019/12/11	Arsenic, total	mg/L	0.00140
UA	35	C	2020/03/11	Arsenic, total	mg/L	<0.0004
UA	35	C	2020/06/24	Arsenic, total	mg/L	<0.0004
UA	35	C	2020/09/02	Arsenic, total	mg/L	0.00320
UA	35	C	2020/12/09	Arsenic, total	mg/L	0.00210
UA	35	C	2021/03/17	Arsenic, total	mg/L	<0.0004
UA	35	C	2021/06/23	Arsenic, total	mg/L	<0.0004
UA	35	C	2021/09/08	Arsenic, total	mg/L	<0.0004
UA	35	C	2021/12/08	Arsenic, total	mg/L	<0.0004
UA	35	C	2022/03/22	Arsenic, total	mg/L	<0.0004
UA	35	C	2022/06/07	Arsenic, total	mg/L	0.000500
UA	35	C	2022/09/14	Arsenic, total	mg/L	0.000800
UA	35	C	2022/12/27	Arsenic, total	mg/L	0.000800
UA	35	C	2023/02/28	Arsenic, total	mg/L	0.000800
UA	35	C	2023/05/31	Arsenic, total	mg/L	<0.0087
UA	35	C	2023/08/24	Arsenic, total	mg/L	<0.00023
UA	35	C	2023/11/15	Arsenic, total	mg/L	0.000900
UA	35	C	2015/12/09	Barium, total	mg/L	0.0739
UA	35	C	2016/03/09	Barium, total	mg/L	0.0568
UA	35	C	2016/06/07	Barium, total	mg/L	0.0371
UA	35	C	2016/09/15	Barium, total	mg/L	0.0371
UA	35	C	2016/12/07	Barium, total	mg/L	0.0499
UA	35	C	2017/02/21	Barium, total	mg/L	0.0478
UA	35	C	2017/04/25	Barium, total	mg/L	0.0335
UA	35	C	2017/06/08	Barium, total	mg/L	0.0376
UA	35	C	2018/06/13	Barium, total	mg/L	0.0344
UA	35	C	2018/09/12	Barium, total	mg/L	0.0343
UA	35	C	2018/12/12	Barium, total	mg/L	0.0339
UA	35	C	2019/03/13	Barium, total	mg/L	0.0310
UA	35	C	2019/06/19	Barium, total	mg/L	0.0593
UA	35	C	2019/09/17	Barium, total	mg/L	0.0422
UA	35	C	2019/12/11	Barium, total	mg/L	0.0505
UA	35	C	2020/03/11	Barium, total	mg/L	0.0510
UA	35	C	2020/06/24	Barium, total	mg/L	0.0317
UA	35	C	2020/09/02	Barium, total	mg/L	0.0644
UA	35	C	2020/12/09	Barium, total	mg/L	0.0752
UA	35	C	2021/03/17	Barium, total	mg/L	0.0333
UA	35	C	2021/06/23	Barium, total	mg/L	0.0363
UA	35	C	2021/09/08	Barium, total	mg/L	0.0338
UA	35	C	2021/12/08	Barium, total	mg/L	0.0556
UA	35	C	2022/03/22	Barium, total	mg/L	0.0318
UA	35	C	2022/06/07	Barium, total	mg/L	0.0557
UA	35	C	2022/09/14	Barium, total	mg/L	0.0666
UA	35	C	2022/12/27	Barium, total	mg/L	0.0631
UA	35	C	2023/02/28	Barium, total	mg/L	0.0591
UA	35	C	2023/05/31	Barium, total	mg/L	0.0381
UA	35	C	2023/08/24	Barium, total	mg/L	0.0470
UA	35	C	2023/11/15	Barium, total	mg/L	0.0470
UA	35	C	2015/12/09	Boron, total	mg/L	6.35
UA	35	C	2016/03/09	Boron, total	mg/L	7.02
UA	35	C	2016/06/07	Boron, total	mg/L	5.56
UA	35	C	2016/09/15	Boron, total	mg/L	6.87
UA	35	C	2016/12/07	Boron, total	mg/L	6.60
UA	35	C	2017/02/21	Boron, total	mg/L	6.13
UA	35	C	2017/04/25	Boron, total	mg/L	6.39
UA	35	C	2017/06/08	Boron, total	mg/L	8.19
UA	35	C	2017/11/15	Boron, total	mg/L	11.1
UA	35	C	2018/06/13	Boron, total	mg/L	5.56
UA	35	C	2018/09/12	Boron, total	mg/L	8.29

UA	35	C	2018/12/12	Boron, total	mg/L	5.85
UA	35	C	2019/03/13	Boron, total	mg/L	4.98
UA	35	C	2019/06/19	Boron, total	mg/L	12.0
UA	35	C	2019/09/17	Boron, total	mg/L	12.5
UA	35	C	2019/12/11	Boron, total	mg/L	16.6
UA	35	C	2020/03/11	Boron, total	mg/L	15.3
UA	35	C	2020/06/24	Boron, total	mg/L	11.7
UA	35	C	2020/09/02	Boron, total	mg/L	10.7
UA	35	C	2020/12/09	Boron, total	mg/L	14.0
UA	35	C	2021/03/17	Boron, total	mg/L	11.9
UA	35	C	2021/06/23	Boron, total	mg/L	11.8
UA	35	C	2021/09/08	Boron, total	mg/L	12.0
UA	35	C	2021/12/08	Boron, total	mg/L	12.2
UA	35	C	2022/03/22	Boron, total	mg/L	11.3
UA	35	C	2022/06/07	Boron, total	mg/L	15.3
UA	35	C	2022/09/14	Boron, total	mg/L	16.2
UA	35	C	2022/12/27	Boron, total	mg/L	18.1
UA	35	C	2023/02/28	Boron, total	mg/L	9.58
UA	35	C	2023/05/31	Boron, total	mg/L	12.6
UA	35	C	2023/08/24	Boron, total	mg/L	12.0
UA	35	C	2023/11/15	Boron, total	mg/L	11.0
UA	35	C	2015/12/09	Cadmium, total	mg/L	<0.0002
UA	35	C	2016/03/09	Cadmium, total	mg/L	<0.0002
UA	35	C	2016/06/07	Cadmium, total	mg/L	<0.0002
UA	35	C	2016/09/15	Cadmium, total	mg/L	<0.0002
UA	35	C	2016/12/07	Cadmium, total	mg/L	<0.0002
UA	35	C	2017/02/21	Cadmium, total	mg/L	<0.0002
UA	35	C	2017/04/25	Cadmium, total	mg/L	<0.0002
UA	35	C	2017/06/08	Cadmium, total	mg/L	<0.0002
UA	35	C	2018/06/13	Cadmium, total	mg/L	<0.0002
UA	35	C	2018/09/12	Cadmium, total	mg/L	<0.0002
UA	35	C	2018/12/12	Cadmium, total	mg/L	<0.0002
UA	35	C	2019/03/13	Cadmium, total	mg/L	<0.0002
UA	35	C	2019/06/19	Cadmium, total	mg/L	<0.0002
UA	35	C	2019/09/17	Cadmium, total	mg/L	<0.0002
UA	35	C	2019/12/11	Cadmium, total	mg/L	<0.0002
UA	35	C	2020/03/11	Cadmium, total	mg/L	<0.0002
UA	35	C	2020/06/24	Cadmium, total	mg/L	<0.0002
UA	35	C	2020/09/02	Cadmium, total	mg/L	<0.0002
UA	35	C	2020/12/09	Cadmium, total	mg/L	<0.0002
UA	35	C	2021/03/17	Cadmium, total	mg/L	<0.0002
UA	35	C	2021/06/23	Cadmium, total	mg/L	<0.0002
UA	35	C	2021/09/08	Cadmium, total	mg/L	<0.0002
UA	35	C	2021/12/08	Cadmium, total	mg/L	<0.0002
UA	35	C	2022/03/22	Cadmium, total	mg/L	<0.0002
UA	35	C	2022/06/07	Cadmium, total	mg/L	0.000400
UA	35	C	2022/09/14	Cadmium, total	mg/L	0.000500
UA	35	C	2022/12/27	Cadmium, total	mg/L	0.000500
UA	35	C	2023/02/28	Cadmium, total	mg/L	0.000500
UA	35	C	2023/05/31	Cadmium, total	mg/L	<0.0005
UA	35	C	2023/08/24	Cadmium, total	mg/L	<0.00017
UA	35	C	2023/11/15	Cadmium, total	mg/L	0.000290
UA	35	C	2015/12/09	Calcium, total	mg/L	177
UA	35	C	2016/03/09	Calcium, total	mg/L	203
UA	35	C	2016/06/07	Calcium, total	mg/L	161
UA	35	C	2016/09/15	Calcium, total	mg/L	162
UA	35	C	2016/12/07	Calcium, total	mg/L	175
UA	35	C	2017/02/21	Calcium, total	mg/L	189
UA	35	C	2017/04/25	Calcium, total	mg/L	159
UA	35	C	2017/06/08	Calcium, total	mg/L	211
UA	35	C	2017/11/15	Calcium, total	mg/L	256
UA	35	C	2018/06/13	Calcium, total	mg/L	186

UA	35	C	2018/09/12	Calcium, total	mg/L	180
UA	35	C	2018/12/12	Calcium, total	mg/L	208
UA	35	C	2019/03/13	Calcium, total	mg/L	157
UA	35	C	2019/06/19	Calcium, total	mg/L	257
UA	35	C	2019/09/17	Calcium, total	mg/L	241
UA	35	C	2019/12/11	Calcium, total	mg/L	281
UA	35	C	2020/03/11	Calcium, total	mg/L	340
UA	35	C	2020/06/24	Calcium, total	mg/L	224
UA	35	C	2020/09/02	Calcium, total	mg/L	221
UA	35	C	2020/12/09	Calcium, total	mg/L	425
UA	35	C	2021/03/17	Calcium, total	mg/L	286
UA	35	C	2021/06/23	Calcium, total	mg/L	254
UA	35	C	2021/09/08	Calcium, total	mg/L	259
UA	35	C	2021/12/08	Calcium, total	mg/L	305
UA	35	C	2022/03/22	Calcium, total	mg/L	264
UA	35	C	2022/06/07	Calcium, total	mg/L	423
UA	35	C	2022/09/14	Calcium, total	mg/L	426
UA	35	C	2022/12/27	Calcium, total	mg/L	347
UA	35	C	2023/02/28	Calcium, total	mg/L	268
UA	35	C	2023/05/31	Calcium, total	mg/L	291
UA	35	C	2023/08/24	Calcium, total	mg/L	320
UA	35	C	2023/11/15	Calcium, total	mg/L	320
UA	35	C	2015/12/09	Chloride, total	mg/L	45.0
UA	35	C	2016/03/09	Chloride, total	mg/L	44.0
UA	35	C	2016/06/07	Chloride, total	mg/L	45.0
UA	35	C	2016/09/15	Chloride, total	mg/L	42.0
UA	35	C	2016/12/07	Chloride, total	mg/L	45.0
UA	35	C	2017/02/21	Chloride, total	mg/L	41.0
UA	35	C	2017/04/25	Chloride, total	mg/L	43.0
UA	35	C	2017/06/08	Chloride, total	mg/L	40.0
UA	35	C	2017/11/15	Chloride, total	mg/L	38.0
UA	35	C	2018/06/13	Chloride, total	mg/L	35.0
UA	35	C	2018/09/12	Chloride, total	mg/L	63.0
UA	35	C	2018/12/12	Chloride, total	mg/L	46.0
UA	35	C	2019/03/13	Chloride, total	mg/L	38.0
UA	35	C	2019/06/19	Chloride, total	mg/L	52.0
UA	35	C	2019/09/17	Chloride, total	mg/L	53.0
UA	35	C	2019/12/11	Chloride, total	mg/L	46.0
UA	35	C	2020/03/11	Chloride, total	mg/L	37.0
UA	35	C	2020/06/24	Chloride, total	mg/L	54.0
UA	35	C	2020/09/02	Chloride, total	mg/L	59.0
UA	35	C	2020/12/09	Chloride, total	mg/L	49.0
UA	35	C	2021/03/17	Chloride, total	mg/L	27.0
UA	35	C	2021/06/23	Chloride, total	mg/L	60.0
UA	35	C	2021/09/08	Chloride, total	mg/L	56.0
UA	35	C	2021/12/08	Chloride, total	mg/L	46.0
UA	35	C	2022/03/22	Chloride, total	mg/L	29.0
UA	35	C	2022/06/07	Chloride, total	mg/L	35.0
UA	35	C	2022/09/14	Chloride, total	mg/L	30.0
UA	35	C	2022/12/27	Chloride, total	mg/L	33.0
UA	35	C	2023/02/28	Chloride, total	mg/L	26.0
UA	35	C	2023/05/31	Chloride, total	mg/L	32.0
UA	35	C	2023/08/24	Chloride, total	mg/L	37.0
UA	35	C	2023/11/15	Chloride, total	mg/L	24.0
UA	35	C	2023/05/31	Iron, dissolved	mg/L	<0.02
UA	35	C	2023/08/24	Iron, dissolved	mg/L	<0.047
UA	35	C	2015/12/09	Lithium, total	mg/L	0.0245
UA	35	C	2016/03/09	Lithium, total	mg/L	0.0226
UA	35	C	2016/06/07	Lithium, total	mg/L	0.0248
UA	35	C	2016/09/15	Lithium, total	mg/L	0.0305
UA	35	C	2016/12/07	Lithium, total	mg/L	0.0293
UA	35	C	2017/02/21	Lithium, total	mg/L	0.0226

UA	35	C	2017/04/25	Lithium, total	mg/L	0.0291
UA	35	C	2017/06/08	Lithium, total	mg/L	0.0280
UA	35	C	2018/06/13	Lithium, total	mg/L	0.0217
UA	35	C	2018/09/12	Lithium, total	mg/L	0.0332
UA	35	C	2018/12/12	Lithium, total	mg/L	0.0259
UA	35	C	2019/03/13	Lithium, total	mg/L	0.0183
UA	35	C	2019/06/19	Lithium, total	mg/L	0.0374
UA	35	C	2019/09/17	Lithium, total	mg/L	0.0371
UA	35	C	2019/12/11	Lithium, total	mg/L	0.0355
UA	35	C	2020/03/11	Lithium, total	mg/L	0.0290
UA	35	C	2020/06/24	Lithium, total	mg/L	0.0360
UA	35	C	2020/09/02	Lithium, total	mg/L	0.0337
UA	35	C	2020/12/09	Lithium, total	mg/L	0.0324
UA	35	C	2021/03/17	Lithium, total	mg/L	0.0162
UA	35	C	2021/06/23	Lithium, total	mg/L	0.0330
UA	35	C	2021/09/08	Lithium, total	mg/L	0.0349
UA	35	C	2021/12/08	Lithium, total	mg/L	0.0260
UA	35	C	2022/03/22	Lithium, total	mg/L	0.0190
UA	35	C	2022/06/07	Lithium, total	mg/L	0.0304
UA	35	C	2022/09/14	Lithium, total	mg/L	0.0240
UA	35	C	2022/12/27	Lithium, total	mg/L	0.0293
UA	35	C	2023/02/28	Lithium, total	mg/L	0.0128
UA	35	C	2023/05/31	Lithium, total	mg/L	0.0210
UA	35	C	2023/08/24	Lithium, total	mg/L	0.0340
UA	35	C	2023/11/15	Lithium, total	mg/L	0.0330
UA	35	C	2019/09/17	Magnesium, total	mg/L	37.9
UA	35	C	2020/03/11	Magnesium, total	mg/L	47.7
UA	35	C	2020/06/24	Magnesium, total	mg/L	33.5
UA	35	C	2021/03/17	Magnesium, total	mg/L	37.4
UA	35	C	2021/09/08	Magnesium, total	mg/L	36.7
UA	35	C	2022/03/22	Magnesium, total	mg/L	29.0
UA	35	C	2022/09/14	Magnesium, total	mg/L	47.1
UA	35	C	2023/02/28	Magnesium, total	mg/L	30.6
UA	35	C	2023/05/31	Magnesium, total	mg/L	31.7
UA	35	C	2023/08/24	Magnesium, total	mg/L	42.0
UA	35	C	2023/11/15	Magnesium, total	mg/L	39.0
UA	35	C	2023/05/31	Manganese, dissolved	mg/L	0.566
UA	35	C	2023/08/24	Manganese, dissolved	mg/L	0.500
UA	35	C	2023/05/31	Phosphate, dissolved	mg/L	0.0400
UA	35	C	2023/08/24	Phosphate, dissolved	mg/L	<0.073
UA	35	C	2019/09/17	Potassium, total	mg/L	14.0
UA	35	C	2020/03/11	Potassium, total	mg/L	14.8
UA	35	C	2020/06/24	Potassium, total	mg/L	14.9
UA	35	C	2021/03/17	Potassium, total	mg/L	10.2
UA	35	C	2021/09/08	Potassium, total	mg/L	15.8
UA	35	C	2022/03/22	Potassium, total	mg/L	11.2
UA	35	C	2022/09/14	Potassium, total	mg/L	17.1
UA	35	C	2023/02/28	Potassium, total	mg/L	10.2
UA	35	C	2023/05/31	Potassium, total	mg/L	14.0
UA	35	C	2023/08/24	Potassium, total	mg/L	14.0
UA	35	C	2023/11/15	Potassium, total	mg/L	13.0
UA	35	C	2023/05/31	Silicon, dissolved	mg/L	4.18
UA	35	C	2023/08/24	Silicon, dissolved	mg/L	5.80
UA	35	C	2019/09/17	Sodium, total	mg/L	39.6
UA	35	C	2020/03/11	Sodium, total	mg/L	48.2
UA	35	C	2020/06/24	Sodium, total	mg/L	44.4
UA	35	C	2021/03/17	Sodium, total	mg/L	30.1
UA	35	C	2021/09/08	Sodium, total	mg/L	42.0
UA	35	C	2022/03/22	Sodium, total	mg/L	27.2
UA	35	C	2022/09/14	Sodium, total	mg/L	30.4
UA	35	C	2023/02/28	Sodium, total	mg/L	25.6
UA	35	C	2023/05/31	Sodium, total	mg/L	30.8

UA	35	C	2023/08/24	Sodium, total	mg/L	30.0
UA	35	C	2023/11/15	Sodium, total	mg/L	28.0
UA	35	C	2015/12/09	Sulfate, total	mg/L	352
UA	35	C	2016/03/09	Sulfate, total	mg/L	465
UA	35	C	2016/06/07	Sulfate, total	mg/L	317
UA	35	C	2016/09/15	Sulfate, total	mg/L	374
UA	35	C	2016/12/07	Sulfate, total	mg/L	370
UA	35	C	2017/02/21	Sulfate, total	mg/L	381
UA	35	C	2017/04/25	Sulfate, total	mg/L	398
UA	35	C	2017/06/08	Sulfate, total	mg/L	500
UA	35	C	2017/11/15	Sulfate, total	mg/L	598
UA	35	C	2018/06/13	Sulfate, total	mg/L	420
UA	35	C	2018/09/12	Sulfate, total	mg/L	416
UA	35	C	2018/12/12	Sulfate, total	mg/L	327
UA	35	C	2019/03/13	Sulfate, total	mg/L	255
UA	35	C	2019/06/19	Sulfate, total	mg/L	512
UA	35	C	2019/09/17	Sulfate, total	mg/L	470
UA	35	C	2019/12/11	Sulfate, total	mg/L	637
UA	35	C	2020/03/11	Sulfate, total	mg/L	802
UA	35	C	2020/06/24	Sulfate, total	mg/L	479
UA	35	C	2020/09/02	Sulfate, total	mg/L	443
UA	35	C	2020/12/09	Sulfate, total	mg/L	846
UA	35	C	2021/03/17	Sulfate, total	mg/L	620
UA	35	C	2021/06/23	Sulfate, total	mg/L	530
UA	35	C	2021/09/08	Sulfate, total	mg/L	568
UA	35	C	2021/12/08	Sulfate, total	mg/L	818
UA	35	C	2022/03/22	Sulfate, total	mg/L	549
UA	35	C	2022/06/07	Sulfate, total	mg/L	939
UA	35	C	2022/09/14	Sulfate, total	mg/L	1,190
UA	35	C	2022/12/27	Sulfate, total	mg/L	819
UA	35	C	2023/02/28	Sulfate, total	mg/L	476
UA	35	C	2023/05/31	Sulfate, total	mg/L	670
UA	35	C	2023/08/24	Sulfate, total	mg/L	890
UA	35	C	2023/11/15	Sulfate, total	mg/L	730
UA	35	C	2015/12/09	Temperature (Celsius)	degrees C	14.5
UA	35	C	2016/03/09	Temperature (Celsius)	degrees C	10.1
UA	35	C	2016/06/07	Temperature (Celsius)	degrees C	12.1
UA	35	C	2016/09/15	Temperature (Celsius)	degrees C	16.6
UA	35	C	2016/12/07	Temperature (Celsius)	degrees C	11.9
UA	35	C	2017/02/21	Temperature (Celsius)	degrees C	12.2
UA	35	C	2017/04/25	Temperature (Celsius)	degrees C	15.1
UA	35	C	2017/06/08	Temperature (Celsius)	degrees C	13.3
UA	35	C	2017/11/15	Temperature (Celsius)	degrees C	14.4
UA	35	C	2018/06/13	Temperature (Celsius)	degrees C	14.1
UA	35	C	2018/09/12	Temperature (Celsius)	degrees C	16.0
UA	35	C	2018/12/12	Temperature (Celsius)	degrees C	17.8
UA	35	C	2019/03/13	Temperature (Celsius)	degrees C	9.90
UA	35	C	2019/06/19	Temperature (Celsius)	degrees C	12.6
UA	35	C	2019/09/17	Temperature (Celsius)	degrees C	15.7
UA	35	C	2019/12/11	Temperature (Celsius)	degrees C	12.8
UA	35	C	2020/03/11	Temperature (Celsius)	degrees C	9.80
UA	35	C	2020/06/24	Temperature (Celsius)	degrees C	13.5
UA	35	C	2020/09/02	Temperature (Celsius)	degrees C	16.0
UA	35	C	2020/12/09	Temperature (Celsius)	degrees C	14.5
UA	35	C	2021/03/17	Temperature (Celsius)	degrees C	10.0
UA	35	C	2021/06/23	Temperature (Celsius)	degrees C	13.1
UA	35	C	2021/09/08	Temperature (Celsius)	degrees C	15.9
UA	35	C	2021/12/08	Temperature (Celsius)	degrees C	14.5
UA	35	C	2022/03/22	Temperature (Celsius)	degrees C	10.5
UA	35	C	2022/06/07	Temperature (Celsius)	degrees C	12.6
UA	35	C	2022/09/14	Temperature (Celsius)	degrees C	15.7
UA	35	C	2022/12/27	Temperature (Celsius)	degrees C	13.2

UA	35	C	2023/02/28	Temperature (Celsius)	degrees C	11.1
UA	35	C	2023/05/31	Temperature (Celsius)	degrees C	12.9
UA	35	C	2023/08/24	Temperature (Celsius)	degrees C	16.2
UA	35	C	2023/11/15	Temperature (Celsius)	degrees C	15.6
UA	35	C	2015/12/09	Total Dissolved Solids	mg/L	860
UA	35	C	2016/03/09	Total Dissolved Solids	mg/L	978
UA	35	C	2016/06/07	Total Dissolved Solids	mg/L	802
UA	35	C	2016/09/15	Total Dissolved Solids	mg/L	864
UA	35	C	2016/12/07	Total Dissolved Solids	mg/L	854
UA	35	C	2017/02/21	Total Dissolved Solids	mg/L	868
UA	35	C	2017/04/25	Total Dissolved Solids	mg/L	866
UA	35	C	2017/06/08	Total Dissolved Solids	mg/L	1,010
UA	35	C	2017/11/15	Total Dissolved Solids	mg/L	1,260
UA	35	C	2018/06/13	Total Dissolved Solids	mg/L	972
UA	35	C	2018/09/12	Total Dissolved Solids	mg/L	1,000
UA	35	C	2018/12/12	Total Dissolved Solids	mg/L	872
UA	35	C	2019/03/13	Total Dissolved Solids	mg/L	708
UA	35	C	2019/06/19	Total Dissolved Solids	mg/L	1,130
UA	35	C	2019/09/17	Total Dissolved Solids	mg/L	1,110
UA	35	C	2019/12/11	Total Dissolved Solids	mg/L	1,240
UA	35	C	2020/03/11	Total Dissolved Solids	mg/L	1,520
UA	35	C	2020/06/24	Total Dissolved Solids	mg/L	1,070
UA	35	C	2020/09/02	Total Dissolved Solids	mg/L	1,010
UA	35	C	2020/12/09	Total Dissolved Solids	mg/L	1,470
UA	35	C	2021/03/17	Total Dissolved Solids	mg/L	1,210
UA	35	C	2021/06/23	Total Dissolved Solids	mg/L	1,150
UA	35	C	2021/09/08	Total Dissolved Solids	mg/L	1,140
UA	35	C	2021/12/08	Total Dissolved Solids	mg/L	1,330
UA	35	C	2022/03/22	Total Dissolved Solids	mg/L	1,020
UA	35	C	2022/06/07	Total Dissolved Solids	mg/L	1,840
UA	35	C	2022/09/14	Total Dissolved Solids	mg/L	1,940
UA	35	C	2022/12/27	Total Dissolved Solids	mg/L	1,520
UA	35	C	2023/02/28	Total Dissolved Solids	mg/L	918
UA	35	C	2023/05/31	Total Dissolved Solids	mg/L	1,300
UA	35	C	2023/08/24	Total Dissolved Solids	mg/L	1,600
UA	35	C	2023/11/15	Total Dissolved Solids	mg/L	1,500
UA	49	C	2015/12/10	pH (field)	SU	7.4
UA	49	C	2016/03/09	pH (field)	SU	7.2
UA	49	C	2016/06/07	pH (field)	SU	7.2
UA	49	C	2016/09/15	pH (field)	SU	7.3
UA	49	C	2016/12/07	pH (field)	SU	7.1
UA	49	C	2017/02/21	pH (field)	SU	7.2
UA	49	C	2017/04/25	pH (field)	SU	7.0
UA	49	C	2017/06/08	pH (field)	SU	7.0
UA	49	C	2017/11/16	pH (field)	SU	7.2
UA	49	C	2018/06/13	pH (field)	SU	6.9
UA	49	C	2018/09/12	pH (field)	SU	7.1
UA	49	C	2018/12/12	pH (field)	SU	7.1
UA	49	C	2019/03/13	pH (field)	SU	7.3
UA	49	C	2019/06/19	pH (field)	SU	7.1
UA	49	C	2019/09/18	pH (field)	SU	7.1
UA	49	C	2019/12/11	pH (field)	SU	7.2
UA	49	C	2020/03/11	pH (field)	SU	7.1
UA	49	C	2020/06/03	pH (field)	SU	7.2
UA	49	C	2020/06/25	pH (field)	SU	7.3
UA	49	C	2020/09/02	pH (field)	SU	7.2
UA	49	C	2020/12/09	pH (field)	SU	7.2
UA	49	C	2021/03/19	pH (field)	SU	7.2
UA	49	C	2021/06/23	pH (field)	SU	6.9
UA	49	C	2021/09/08	pH (field)	SU	7.0
UA	49	C	2021/12/08	pH (field)	SU	6.9
UA	49	C	2022/03/22	pH (field)	SU	7.1

UA	49	C	2022/06/07	pH (field)	SU	7.1
UA	49	C	2022/09/13	pH (field)	SU	7.0
UA	49	C	2022/12/27	pH (field)	SU	7.0
UA	49	C	2023/02/28	pH (field)	SU	7.0
UA	49	C	2023/05/31	pH (field)	SU	7.0
UA	49	C	2023/08/25	pH (field)	SU	7.1
UA	49	C	2023/11/15	pH (field)	SU	7.2
UA	49	C	2015/12/10	Oxidation Reduction Potential	mV	-2.00
UA	49	C	2016/03/09	Oxidation Reduction Potential	mV	8.00
UA	49	C	2016/06/07	Oxidation Reduction Potential	mV	65.0
UA	49	C	2016/09/15	Oxidation Reduction Potential	mV	36.0
UA	49	C	2016/12/07	Oxidation Reduction Potential	mV	119
UA	49	C	2017/02/21	Oxidation Reduction Potential	mV	120
UA	49	C	2017/04/25	Oxidation Reduction Potential	mV	37.0
UA	49	C	2017/06/08	Oxidation Reduction Potential	mV	68.0
UA	49	C	2017/11/16	Oxidation Reduction Potential	mV	190
UA	49	C	2018/06/13	Oxidation Reduction Potential	mV	64.0
UA	49	C	2018/09/12	Oxidation Reduction Potential	mV	158
UA	49	C	2018/12/12	Oxidation Reduction Potential	mV	-23.0
UA	49	C	2019/03/13	Oxidation Reduction Potential	mV	13.0
UA	49	C	2019/06/19	Oxidation Reduction Potential	mV	50.0
UA	49	C	2019/09/18	Oxidation Reduction Potential	mV	118
UA	49	C	2019/12/11	Oxidation Reduction Potential	mV	86.0
UA	49	C	2020/03/11	Oxidation Reduction Potential	mV	128
UA	49	C	2020/06/03	Oxidation Reduction Potential	mV	-12.0
UA	49	C	2020/06/25	Oxidation Reduction Potential	mV	152
UA	49	C	2020/09/02	Oxidation Reduction Potential	mV	35.0
UA	49	C	2020/12/09	Oxidation Reduction Potential	mV	24.0
UA	49	C	2021/03/19	Oxidation Reduction Potential	mV	78.0
UA	49	C	2021/06/23	Oxidation Reduction Potential	mV	8.00
UA	49	C	2021/09/08	Oxidation Reduction Potential	mV	20.0
UA	49	C	2021/12/08	Oxidation Reduction Potential	mV	83.0
UA	49	C	2022/03/22	Oxidation Reduction Potential	mV	-50.0
UA	49	C	2022/06/07	Oxidation Reduction Potential	mV	35.0
UA	49	C	2022/09/13	Oxidation Reduction Potential	mV	43.0
UA	49	C	2022/12/27	Oxidation Reduction Potential	mV	-55.0
UA	49	C	2023/02/28	Oxidation Reduction Potential	mV	33.4
UA	49	C	2023/05/31	Oxidation Reduction Potential	mV	-19.0
UA	49	C	2023/08/25	Oxidation Reduction Potential	mV	58.2
UA	49	C	2023/11/15	Oxidation Reduction Potential	mV	11.1
UA	49	C	2015/12/10	Eh	V	0.20
UA	49	C	2016/03/09	Eh	V	0.21
UA	49	C	2016/06/07	Eh	V	0.26
UA	49	C	2016/09/15	Eh	V	0.23
UA	49	C	2016/12/07	Eh	V	0.32
UA	49	C	2017/02/21	Eh	V	0.32
UA	49	C	2017/04/25	Eh	V	0.23
UA	49	C	2017/06/08	Eh	V	0.26
UA	49	C	2017/11/16	Eh	V	0.39
UA	49	C	2018/06/13	Eh	V	0.26
UA	49	C	2018/09/12	Eh	V	0.35
UA	49	C	2018/12/12	Eh	V	0.17
UA	49	C	2019/03/13	Eh	V	0.21
UA	49	C	2019/06/19	Eh	V	0.25
UA	49	C	2019/09/18	Eh	V	0.31
UA	49	C	2019/12/11	Eh	V	0.28
UA	49	C	2020/03/11	Eh	V	0.33
UA	49	C	2020/06/03	Eh	V	0.18
UA	49	C	2020/06/25	Eh	V	0.35
UA	49	C	2020/09/02	Eh	V	0.23
UA	49	C	2020/12/09	Eh	V	0.22
UA	49	C	2021/03/19	Eh	V	0.27

UA	49	C	2021/06/23	Eh	V	0.20
UA	49	C	2021/09/08	Eh	V	0.22
UA	49	C	2021/12/08	Eh	V	0.28
UA	49	C	2022/03/22	Eh	V	0.15
UA	49	C	2022/06/07	Eh	V	0.23
UA	49	C	2022/09/13	Eh	V	0.24
UA	49	C	2022/12/27	Eh	V	0.14
UA	49	C	2023/02/28	Eh	V	0.23
UA	49	C	2023/05/31	Eh	V	0.18
UA	49	C	2023/08/25	Eh	V	0.25
UA	49	C	2023/11/15	Eh	V	0.21
UA	49	C	2019/09/18	Alkalinity, bicarbonate	mg/L CaCO3	340
UA	49	C	2020/03/11	Alkalinity, bicarbonate	mg/L CaCO3	346
UA	49	C	2021/03/19	Alkalinity, bicarbonate	mg/L CaCO3	326
UA	49	C	2021/09/08	Alkalinity, bicarbonate	mg/L CaCO3	332
UA	49	C	2022/03/22	Alkalinity, bicarbonate	mg/L CaCO3	322
UA	49	C	2022/09/13	Alkalinity, bicarbonate	mg/L CaCO3	342
UA	49	C	2023/02/28	Alkalinity, bicarbonate	mg/L CaCO3	347
UA	49	C	2023/05/31	Alkalinity, bicarbonate	mg/L CaCO3	339
UA	49	C	2023/08/25	Alkalinity, bicarbonate	mg/L CaCO3	330
UA	49	C	2023/11/15	Alkalinity, bicarbonate	mg/L CaCO3	340
UA	49	C	2015/12/10	Arsenic, total	mg/L	<0.0002
UA	49	C	2016/03/09	Arsenic, total	mg/L	<0.0002
UA	49	C	2016/06/07	Arsenic, total	mg/L	<0.0002
UA	49	C	2016/09/15	Arsenic, total	mg/L	<0.0002
UA	49	C	2016/12/07	Arsenic, total	mg/L	<0.0002
UA	49	C	2017/02/21	Arsenic, total	mg/L	<0.0002
UA	49	C	2017/04/25	Arsenic, total	mg/L	<0.0002
UA	49	C	2017/06/08	Arsenic, total	mg/L	<0.0002
UA	49	C	2018/06/13	Arsenic, total	mg/L	<0.0004
UA	49	C	2018/09/12	Arsenic, total	mg/L	<0.0004
UA	49	C	2018/12/12	Arsenic, total	mg/L	<0.0004
UA	49	C	2019/03/13	Arsenic, total	mg/L	0.00110
UA	49	C	2019/06/19	Arsenic, total	mg/L	<0.0004
UA	49	C	2019/09/18	Arsenic, total	mg/L	<0.0004
UA	49	C	2019/12/11	Arsenic, total	mg/L	<0.0004
UA	49	C	2020/03/11	Arsenic, total	mg/L	<0.0004
UA	49	C	2020/06/03	Arsenic, total	mg/L	<0.0004
UA	49	C	2020/09/02	Arsenic, total	mg/L	<0.0004
UA	49	C	2020/12/09	Arsenic, total	mg/L	<0.0004
UA	49	C	2021/03/19	Arsenic, total	mg/L	<0.0004
UA	49	C	2021/06/23	Arsenic, total	mg/L	<0.0004
UA	49	C	2021/09/08	Arsenic, total	mg/L	<0.0004
UA	49	C	2021/12/08	Arsenic, total	mg/L	<0.0004
UA	49	C	2022/03/22	Arsenic, total	mg/L	<0.0004
UA	49	C	2022/06/07	Arsenic, total	mg/L	<0.0004
UA	49	C	2022/09/13	Arsenic, total	mg/L	<0.0004
UA	49	C	2022/12/27	Arsenic, total	mg/L	<0.0004
UA	49	C	2023/02/28	Arsenic, total	mg/L	0.000600
UA	49	C	2023/05/31	Arsenic, total	mg/L	<0.0087
UA	49	C	2023/08/25	Arsenic, total	mg/L	0.000490
UA	49	C	2023/11/15	Arsenic, total	mg/L	0.000280
UA	49	C	2015/12/10	Barium, total	mg/L	0.0537
UA	49	C	2016/03/09	Barium, total	mg/L	0.0546
UA	49	C	2016/06/07	Barium, total	mg/L	0.0500
UA	49	C	2016/09/15	Barium, total	mg/L	0.0509
UA	49	C	2016/12/07	Barium, total	mg/L	0.0534
UA	49	C	2017/02/21	Barium, total	mg/L	0.0512
UA	49	C	2017/04/25	Barium, total	mg/L	0.0479
UA	49	C	2017/06/08	Barium, total	mg/L	0.0497
UA	49	C	2018/06/13	Barium, total	mg/L	0.0510
UA	49	C	2018/09/12	Barium, total	mg/L	0.0623

UA	49	C	2018/12/12	Barium, total	mg/L	0.0660
UA	49	C	2019/03/13	Barium, total	mg/L	0.0558
UA	49	C	2019/06/19	Barium, total	mg/L	0.0564
UA	49	C	2019/09/18	Barium, total	mg/L	0.0538
UA	49	C	2019/12/11	Barium, total	mg/L	0.0677
UA	49	C	2020/03/11	Barium, total	mg/L	0.0575
UA	49	C	2020/06/03	Barium, total	mg/L	0.0584
UA	49	C	2020/09/02	Barium, total	mg/L	0.0595
UA	49	C	2020/12/09	Barium, total	mg/L	0.0713
UA	49	C	2021/03/19	Barium, total	mg/L	0.0588
UA	49	C	2021/06/23	Barium, total	mg/L	0.0600
UA	49	C	2021/09/08	Barium, total	mg/L	0.0596
UA	49	C	2021/12/08	Barium, total	mg/L	0.0639
UA	49	C	2022/03/22	Barium, total	mg/L	0.0638
UA	49	C	2022/06/07	Barium, total	mg/L	0.0576
UA	49	C	2022/09/13	Barium, total	mg/L	0.0576
UA	49	C	2022/12/27	Barium, total	mg/L	0.0617
UA	49	C	2023/02/28	Barium, total	mg/L	0.0827
UA	49	C	2023/05/31	Barium, total	mg/L	0.0711
UA	49	C	2023/08/25	Barium, total	mg/L	0.0620
UA	49	C	2023/11/15	Barium, total	mg/L	0.0600
UA	49	C	2015/12/10	Boron, total	mg/L	1.64
UA	49	C	2016/03/09	Boron, total	mg/L	1.70
UA	49	C	2016/06/07	Boron, total	mg/L	1.50
UA	49	C	2016/09/15	Boron, total	mg/L	1.52
UA	49	C	2016/12/07	Boron, total	mg/L	1.42
UA	49	C	2017/02/21	Boron, total	mg/L	1.25
UA	49	C	2017/04/25	Boron, total	mg/L	1.21
UA	49	C	2017/06/08	Boron, total	mg/L	1.14
UA	49	C	2017/11/16	Boron, total	mg/L	1.12
UA	49	C	2018/06/13	Boron, total	mg/L	1.19
UA	49	C	2018/09/12	Boron, total	mg/L	1.06
UA	49	C	2018/12/12	Boron, total	mg/L	0.960
UA	49	C	2019/03/13	Boron, total	mg/L	1.07
UA	49	C	2019/06/19	Boron, total	mg/L	0.961
UA	49	C	2019/09/18	Boron, total	mg/L	1.00
UA	49	C	2019/12/11	Boron, total	mg/L	0.966
UA	49	C	2020/03/11	Boron, total	mg/L	0.883
UA	49	C	2020/06/03	Boron, total	mg/L	0.829
UA	49	C	2020/09/02	Boron, total	mg/L	0.764
UA	49	C	2020/12/09	Boron, total	mg/L	0.771
UA	49	C	2021/03/19	Boron, total	mg/L	0.702
UA	49	C	2021/06/23	Boron, total	mg/L	0.806
UA	49	C	2021/09/08	Boron, total	mg/L	0.796
UA	49	C	2021/12/08	Boron, total	mg/L	0.844
UA	49	C	2022/03/22	Boron, total	mg/L	0.858
UA	49	C	2022/06/07	Boron, total	mg/L	0.680
UA	49	C	2022/09/13	Boron, total	mg/L	0.701
UA	49	C	2022/12/27	Boron, total	mg/L	0.689
UA	49	C	2023/02/28	Boron, total	mg/L	0.703
UA	49	C	2023/05/31	Boron, total	mg/L	0.758
UA	49	C	2023/08/25	Boron, total	mg/L	0.690
UA	49	C	2023/11/15	Boron, total	mg/L	0.890
UA	49	C	2015/12/10	Cadmium, total	mg/L	<0.0002
UA	49	C	2016/03/09	Cadmium, total	mg/L	<0.0002
UA	49	C	2016/06/07	Cadmium, total	mg/L	<0.0002
UA	49	C	2016/09/15	Cadmium, total	mg/L	<0.0002
UA	49	C	2016/12/07	Cadmium, total	mg/L	<0.0002
UA	49	C	2017/02/21	Cadmium, total	mg/L	<0.0002
UA	49	C	2017/04/25	Cadmium, total	mg/L	<0.0002
UA	49	C	2017/06/08	Cadmium, total	mg/L	<0.0002
UA	49	C	2018/06/13	Cadmium, total	mg/L	0.00110

UA	49	C	2018/09/12	Cadmium, total	mg/L	0.00130
UA	49	C	2018/12/12	Cadmium, total	mg/L	0.00160
UA	49	C	2019/03/13	Cadmium, total	mg/L	0.00140
UA	49	C	2019/06/19	Cadmium, total	mg/L	0.00130
UA	49	C	2019/09/18	Cadmium, total	mg/L	0.00150
UA	49	C	2019/12/11	Cadmium, total	mg/L	0.00180
UA	49	C	2020/03/11	Cadmium, total	mg/L	0.00150
UA	49	C	2020/06/03	Cadmium, total	mg/L	0.00170
UA	49	C	2020/09/02	Cadmium, total	mg/L	0.00170
UA	49	C	2020/12/09	Cadmium, total	mg/L	0.00230
UA	49	C	2021/03/19	Cadmium, total	mg/L	0.00160
UA	49	C	2021/06/23	Cadmium, total	mg/L	0.00170
UA	49	C	2021/09/08	Cadmium, total	mg/L	0.00160
UA	49	C	2021/12/08	Cadmium, total	mg/L	0.00180
UA	49	C	2022/03/22	Cadmium, total	mg/L	0.00160
UA	49	C	2022/06/07	Cadmium, total	mg/L	0.00140
UA	49	C	2022/09/13	Cadmium, total	mg/L	0.00120
UA	49	C	2022/12/27	Cadmium, total	mg/L	0.00140
UA	49	C	2023/02/28	Cadmium, total	mg/L	0.00250
UA	49	C	2023/05/31	Cadmium, total	mg/L	0.00110
UA	49	C	2023/08/25	Cadmium, total	mg/L	0.00130
UA	49	C	2023/11/15	Cadmium, total	mg/L	0.00120
UA	49	C	2015/12/10	Calcium, total	mg/L	133
UA	49	C	2016/03/09	Calcium, total	mg/L	144
UA	49	C	2016/06/07	Calcium, total	mg/L	134
UA	49	C	2016/09/15	Calcium, total	mg/L	130
UA	49	C	2016/12/07	Calcium, total	mg/L	131
UA	49	C	2017/02/21	Calcium, total	mg/L	133
UA	49	C	2017/04/25	Calcium, total	mg/L	113
UA	49	C	2017/06/08	Calcium, total	mg/L	126
UA	49	C	2017/11/16	Calcium, total	mg/L	134
UA	49	C	2018/06/13	Calcium, total	mg/L	125
UA	49	C	2018/09/12	Calcium, total	mg/L	139
UA	49	C	2018/12/12	Calcium, total	mg/L	151
UA	49	C	2019/03/13	Calcium, total	mg/L	123
UA	49	C	2019/06/19	Calcium, total	mg/L	120
UA	49	C	2019/09/18	Calcium, total	mg/L	121
UA	49	C	2019/12/11	Calcium, total	mg/L	118
UA	49	C	2020/03/11	Calcium, total	mg/L	117
UA	49	C	2020/06/03	Calcium, total	mg/L	122
UA	49	C	2020/09/02	Calcium, total	mg/L	113
UA	49	C	2020/12/09	Calcium, total	mg/L	140
UA	49	C	2021/03/19	Calcium, total	mg/L	117
UA	49	C	2021/06/23	Calcium, total	mg/L	118
UA	49	C	2021/09/08	Calcium, total	mg/L	113
UA	49	C	2021/12/08	Calcium, total	mg/L	110
UA	49	C	2022/03/22	Calcium, total	mg/L	114
UA	49	C	2022/06/07	Calcium, total	mg/L	113
UA	49	C	2022/09/13	Calcium, total	mg/L	113
UA	49	C	2022/12/27	Calcium, total	mg/L	116
UA	49	C	2023/02/28	Calcium, total	mg/L	127
UA	49	C	2023/05/31	Calcium, total	mg/L	115
UA	49	C	2023/08/25	Calcium, total	mg/L	99.0
UA	49	C	2023/11/15	Calcium, total	mg/L	100
UA	49	C	2015/12/10	Chloride, total	mg/L	73.0
UA	49	C	2016/03/09	Chloride, total	mg/L	96.0
UA	49	C	2016/06/07	Chloride, total	mg/L	98.0
UA	49	C	2016/09/15	Chloride, total	mg/L	91.0
UA	49	C	2016/12/07	Chloride, total	mg/L	105
UA	49	C	2017/02/21	Chloride, total	mg/L	103
UA	49	C	2017/04/25	Chloride, total	mg/L	111
UA	49	C	2017/06/08	Chloride, total	mg/L	110

UA	49	C	2017/11/16	Chloride, total	mg/L	100
UA	49	C	2018/06/13	Chloride, total	mg/L	106
UA	49	C	2018/09/12	Chloride, total	mg/L	114
UA	49	C	2018/12/12	Chloride, total	mg/L	105
UA	49	C	2019/03/13	Chloride, total	mg/L	104
UA	49	C	2019/06/19	Chloride, total	mg/L	100
UA	49	C	2019/09/18	Chloride, total	mg/L	97.0
UA	49	C	2019/12/11	Chloride, total	mg/L	100
UA	49	C	2020/03/11	Chloride, total	mg/L	97.0
UA	49	C	2020/06/03	Chloride, total	mg/L	108
UA	49	C	2020/09/02	Chloride, total	mg/L	115
UA	49	C	2020/12/09	Chloride, total	mg/L	101
UA	49	C	2021/03/19	Chloride, total	mg/L	94.0
UA	49	C	2021/06/23	Chloride, total	mg/L	102
UA	49	C	2021/09/08	Chloride, total	mg/L	100
UA	49	C	2021/12/08	Chloride, total	mg/L	106
UA	49	C	2022/03/22	Chloride, total	mg/L	103
UA	49	C	2022/06/07	Chloride, total	mg/L	108
UA	49	C	2022/09/13	Chloride, total	mg/L	103
UA	49	C	2022/12/27	Chloride, total	mg/L	110
UA	49	C	2023/02/28	Chloride, total	mg/L	104
UA	49	C	2023/05/31	Chloride, total	mg/L	102
UA	49	C	2023/08/25	Chloride, total	mg/L	95.0
UA	49	C	2023/11/15	Chloride, total	mg/L	95.0
UA	49	C	2023/05/31	Iron, dissolved	mg/L	<0.02
UA	49	C	2023/08/25	Iron, dissolved	mg/L	<0.047
UA	49	C	2015/12/10	Lithium, total	mg/L	0.0243
UA	49	C	2016/03/09	Lithium, total	mg/L	0.0257
UA	49	C	2016/06/07	Lithium, total	mg/L	0.0233
UA	49	C	2016/09/15	Lithium, total	mg/L	0.0270
UA	49	C	2016/12/07	Lithium, total	mg/L	0.0256
UA	49	C	2017/02/21	Lithium, total	mg/L	0.0238
UA	49	C	2017/04/25	Lithium, total	mg/L	0.0279
UA	49	C	2017/06/08	Lithium, total	mg/L	0.0236
UA	49	C	2018/06/13	Lithium, total	mg/L	0.0273
UA	49	C	2018/09/12	Lithium, total	mg/L	0.0260
UA	49	C	2018/12/12	Lithium, total	mg/L	0.0245
UA	49	C	2019/03/13	Lithium, total	mg/L	0.0297
UA	49	C	2019/06/19	Lithium, total	mg/L	0.0263
UA	49	C	2019/09/18	Lithium, total	mg/L	0.0268
UA	49	C	2019/12/11	Lithium, total	mg/L	0.0272
UA	49	C	2020/03/11	Lithium, total	mg/L	0.0262
UA	49	C	2020/06/03	Lithium, total	mg/L	0.0263
UA	49	C	2020/09/02	Lithium, total	mg/L	0.0229
UA	49	C	2020/12/09	Lithium, total	mg/L	0.0231
UA	49	C	2021/03/19	Lithium, total	mg/L	0.0254
UA	49	C	2021/06/23	Lithium, total	mg/L	0.0245
UA	49	C	2021/09/08	Lithium, total	mg/L	0.0229
UA	49	C	2021/12/08	Lithium, total	mg/L	0.0250
UA	49	C	2022/03/22	Lithium, total	mg/L	0.0274
UA	49	C	2022/06/07	Lithium, total	mg/L	0.0218
UA	49	C	2022/09/13	Lithium, total	mg/L	0.0245
UA	49	C	2022/12/27	Lithium, total	mg/L	0.0249
UA	49	C	2023/02/28	Lithium, total	mg/L	0.0207
UA	49	C	2023/05/31	Lithium, total	mg/L	0.0202
UA	49	C	2023/08/25	Lithium, total	mg/L	0.0230
UA	49	C	2023/11/15	Lithium, total	mg/L	0.0240
UA	49	C	2019/09/18	Magnesium, total	mg/L	33.9
UA	49	C	2020/03/11	Magnesium, total	mg/L	36.2
UA	49	C	2020/06/03	Magnesium, total	mg/L	34.7
UA	49	C	2021/03/19	Magnesium, total	mg/L	35.1
UA	49	C	2021/09/08	Magnesium, total	mg/L	33.6

UA	49	C	2022/03/22	Magnesium, total	mg/L	33.5
UA	49	C	2022/09/13	Magnesium, total	mg/L	34.9
UA	49	C	2023/02/28	Magnesium, total	mg/L	36.3
UA	49	C	2023/05/31	Magnesium, total	mg/L	35.9
UA	49	C	2023/08/25	Magnesium, total	mg/L	32.0
UA	49	C	2023/11/15	Magnesium, total	mg/L	34.0
UA	49	C	2023/05/31	Manganese, dissolved	mg/L	0.00450
UA	49	C	2023/08/25	Manganese, dissolved	mg/L	0.00440
UA	49	C	2023/05/31	Phosphate, dissolved	mg/L	0.0340
UA	49	C	2023/08/25	Phosphate, dissolved	mg/L	0.170
UA	49	C	2019/09/18	Potassium, total	mg/L	11.9
UA	49	C	2020/03/11	Potassium, total	mg/L	13.1
UA	49	C	2020/06/03	Potassium, total	mg/L	12.8
UA	49	C	2021/03/19	Potassium, total	mg/L	15.4
UA	49	C	2021/09/08	Potassium, total	mg/L	12.3
UA	49	C	2022/03/22	Potassium, total	mg/L	13.0
UA	49	C	2022/09/13	Potassium, total	mg/L	12.7
UA	49	C	2023/02/28	Potassium, total	mg/L	14.7
UA	49	C	2023/05/31	Potassium, total	mg/L	12.3
UA	49	C	2023/08/25	Potassium, total	mg/L	11.0
UA	49	C	2023/11/15	Potassium, total	mg/L	11.0
UA	49	C	2023/05/31	Silicon, dissolved	mg/L	7.59
UA	49	C	2023/08/25	Silicon, dissolved	mg/L	9.30
UA	49	C	2019/09/18	Sodium, total	mg/L	60.2
UA	49	C	2020/03/11	Sodium, total	mg/L	65.6
UA	49	C	2020/06/03	Sodium, total	mg/L	64.0
UA	49	C	2021/03/19	Sodium, total	mg/L	65.0
UA	49	C	2021/09/08	Sodium, total	mg/L	60.2
UA	49	C	2022/03/22	Sodium, total	mg/L	60.1
UA	49	C	2022/09/13	Sodium, total	mg/L	60.8
UA	49	C	2023/02/28	Sodium, total	mg/L	62.8
UA	49	C	2023/05/31	Sodium, total	mg/L	57.9
UA	49	C	2023/08/25	Sodium, total	mg/L	56.0
UA	49	C	2023/11/15	Sodium, total	mg/L	56.0
UA	49	C	2015/12/10	Sulfate, total	mg/L	114
UA	49	C	2016/03/09	Sulfate, total	mg/L	107
UA	49	C	2016/06/07	Sulfate, total	mg/L	109
UA	49	C	2016/09/15	Sulfate, total	mg/L	105
UA	49	C	2016/12/07	Sulfate, total	mg/L	101
UA	49	C	2017/02/21	Sulfate, total	mg/L	96.0
UA	49	C	2017/04/25	Sulfate, total	mg/L	105
UA	49	C	2017/06/08	Sulfate, total	mg/L	104
UA	49	C	2017/11/16	Sulfate, total	mg/L	89.0
UA	49	C	2018/06/13	Sulfate, total	mg/L	97.0
UA	49	C	2018/09/12	Sulfate, total	mg/L	100
UA	49	C	2018/12/12	Sulfate, total	mg/L	84.0
UA	49	C	2019/03/13	Sulfate, total	mg/L	82.0
UA	49	C	2019/06/19	Sulfate, total	mg/L	88.0
UA	49	C	2019/09/18	Sulfate, total	mg/L	71.0
UA	49	C	2019/12/11	Sulfate, total	mg/L	79.0
UA	49	C	2020/03/11	Sulfate, total	mg/L	75.0
UA	49	C	2020/06/03	Sulfate, total	mg/L	85.0
UA	49	C	2020/09/02	Sulfate, total	mg/L	81.0
UA	49	C	2020/12/09	Sulfate, total	mg/L	96.0
UA	49	C	2021/03/19	Sulfate, total	mg/L	84.0
UA	49	C	2021/06/23	Sulfate, total	mg/L	83.0
UA	49	C	2021/09/08	Sulfate, total	mg/L	79.0
UA	49	C	2021/12/08	Sulfate, total	mg/L	95.0
UA	49	C	2022/03/22	Sulfate, total	mg/L	82.0
UA	49	C	2022/06/07	Sulfate, total	mg/L	83.0
UA	49	C	2022/09/13	Sulfate, total	mg/L	75.0
UA	49	C	2022/12/27	Sulfate, total	mg/L	84.0

UA	49	C	2023/02/28	Sulfate, total	mg/L	108
UA	49	C	2023/05/31	Sulfate, total	mg/L	84.0
UA	49	C	2023/08/25	Sulfate, total	mg/L	78.0
UA	49	C	2023/11/15	Sulfate, total	mg/L	77.0
UA	49	C	2015/12/10	Temperature (Celsius)	degrees C	12.8
UA	49	C	2016/03/09	Temperature (Celsius)	degrees C	11.6
UA	49	C	2016/06/07	Temperature (Celsius)	degrees C	12.0
UA	49	C	2016/09/15	Temperature (Celsius)	degrees C	13.4
UA	49	C	2016/12/07	Temperature (Celsius)	degrees C	9.41
UA	49	C	2017/02/21	Temperature (Celsius)	degrees C	13.2
UA	49	C	2017/04/25	Temperature (Celsius)	degrees C	20.2
UA	49	C	2017/06/08	Temperature (Celsius)	degrees C	20.1
UA	49	C	2017/11/16	Temperature (Celsius)	degrees C	12
UA	49	C	2018/06/13	Temperature (Celsius)	degrees C	14.3
UA	49	C	2018/09/12	Temperature (Celsius)	degrees C	13.4
UA	49	C	2018/12/12	Temperature (Celsius)	degrees C	12.0
UA	49	C	2019/03/13	Temperature (Celsius)	degrees C	12.6
UA	49	C	2019/06/19	Temperature (Celsius)	degrees C	13.0
UA	49	C	2019/09/18	Temperature (Celsius)	degrees C	13.3
UA	49	C	2019/12/11	Temperature (Celsius)	degrees C	12.5
UA	49	C	2020/03/11	Temperature (Celsius)	degrees C	12.5
UA	49	C	2020/06/03	Temperature (Celsius)	degrees C	13.7
UA	49	C	2020/06/25	Temperature (Celsius)	degrees C	13.8
UA	49	C	2020/09/02	Temperature (Celsius)	degrees C	14.1
UA	49	C	2020/12/09	Temperature (Celsius)	degrees C	13.4
UA	49	C	2021/03/19	Temperature (Celsius)	degrees C	13.5
UA	49	C	2021/06/23	Temperature (Celsius)	degrees C	14.0
UA	49	C	2021/09/08	Temperature (Celsius)	degrees C	14.4
UA	49	C	2021/12/08	Temperature (Celsius)	degrees C	13.6
UA	49	C	2022/03/22	Temperature (Celsius)	degrees C	14.1
UA	49	C	2022/06/07	Temperature (Celsius)	degrees C	14.5
UA	49	C	2022/09/13	Temperature (Celsius)	degrees C	14.5
UA	49	C	2022/12/27	Temperature (Celsius)	degrees C	13.7
UA	49	C	2023/02/28	Temperature (Celsius)	degrees C	13.9
UA	49	C	2023/05/31	Temperature (Celsius)	degrees C	14.9
UA	49	C	2023/08/25	Temperature (Celsius)	degrees C	15.3
UA	49	C	2023/11/15	Temperature (Celsius)	degrees C	14.9
UA	49	C	2015/12/10	Total Dissolved Solids	mg/L	662
UA	49	C	2016/03/09	Total Dissolved Solids	mg/L	640
UA	49	C	2016/06/07	Total Dissolved Solids	mg/L	684
UA	49	C	2016/09/15	Total Dissolved Solids	mg/L	706
UA	49	C	2016/12/07	Total Dissolved Solids	mg/L	676
UA	49	C	2017/02/21	Total Dissolved Solids	mg/L	630
UA	49	C	2017/04/25	Total Dissolved Solids	mg/L	678
UA	49	C	2017/06/08	Total Dissolved Solids	mg/L	662
UA	49	C	2017/11/16	Total Dissolved Solids	mg/L	686
UA	49	C	2018/06/13	Total Dissolved Solids	mg/L	692
UA	49	C	2018/09/12	Total Dissolved Solids	mg/L	710
UA	49	C	2018/12/12	Total Dissolved Solids	mg/L	670
UA	49	C	2019/03/13	Total Dissolved Solids	mg/L	656
UA	49	C	2019/06/19	Total Dissolved Solids	mg/L	642
UA	49	C	2019/09/18	Total Dissolved Solids	mg/L	654
UA	49	C	2019/12/11	Total Dissolved Solids	mg/L	612
UA	49	C	2020/03/11	Total Dissolved Solids	mg/L	630
UA	49	C	2020/06/03	Total Dissolved Solids	mg/L	606
UA	49	C	2020/09/02	Total Dissolved Solids	mg/L	604
UA	49	C	2020/12/09	Total Dissolved Solids	mg/L	602
UA	49	C	2021/03/19	Total Dissolved Solids	mg/L	600
UA	49	C	2021/06/23	Total Dissolved Solids	mg/L	628
UA	49	C	2021/09/08	Total Dissolved Solids	mg/L	596
UA	49	C	2021/12/08	Total Dissolved Solids	mg/L	566
UA	49	C	2022/03/22	Total Dissolved Solids	mg/L	594

UA	49	C	2022/06/07	Total Dissolved Solids	mg/L	658
UA	49	C	2022/09/13	Total Dissolved Solids	mg/L	658
UA	49	C	2022/12/27	Total Dissolved Solids	mg/L	620
UA	49	C	2023/02/28	Total Dissolved Solids	mg/L	618
UA	49	C	2023/05/31	Total Dissolved Solids	mg/L	602
UA	49	C	2023/08/25	Total Dissolved Solids	mg/L	620
UA	49	C	2023/11/15	Total Dissolved Solids	mg/L	580
UA	50	C	2019/09/17	pH (field)	SU	6.9
UA	50	C	2019/12/11	pH (field)	SU	7.2
UA	50	C	2020/03/11	pH (field)	SU	7.3
UA	50	C	2020/06/03	pH (field)	SU	7.3
UA	50	C	2020/06/25	pH (field)	SU	7.3
UA	50	C	2020/09/02	pH (field)	SU	7.2
UA	50	C	2020/12/09	pH (field)	SU	7.3
UA	50	C	2021/03/19	pH (field)	SU	7.4
UA	50	C	2021/06/23	pH (field)	SU	7.1
UA	50	C	2021/09/08	pH (field)	SU	7.0
UA	50	C	2021/12/08	pH (field)	SU	7.3
UA	50	C	2022/03/22	pH (field)	SU	7.4
UA	50	C	2022/06/07	pH (field)	SU	7.3
UA	50	C	2022/09/13	pH (field)	SU	7.3
UA	50	C	2022/12/27	pH (field)	SU	7.4
UA	50	C	2023/02/28	pH (field)	SU	7.4
UA	50	C	2023/05/31	pH (field)	SU	7.3
UA	50	C	2023/08/25	pH (field)	SU	7.5
UA	50	C	2023/11/14	pH (field)	SU	7.5
UA	50	C	2019/09/17	Oxidation Reduction Potential	mV	153
UA	50	C	2019/12/11	Oxidation Reduction Potential	mV	43.0
UA	50	C	2020/03/11	Oxidation Reduction Potential	mV	49.0
UA	50	C	2020/06/03	Oxidation Reduction Potential	mV	108
UA	50	C	2020/06/25	Oxidation Reduction Potential	mV	120
UA	50	C	2020/09/02	Oxidation Reduction Potential	mV	117
UA	50	C	2020/12/09	Oxidation Reduction Potential	mV	56.0
UA	50	C	2021/03/19	Oxidation Reduction Potential	mV	200
UA	50	C	2021/06/23	Oxidation Reduction Potential	mV	137
UA	50	C	2021/09/08	Oxidation Reduction Potential	mV	64.0
UA	50	C	2021/12/08	Oxidation Reduction Potential	mV	-65.0
UA	50	C	2022/03/22	Oxidation Reduction Potential	mV	-71.0
UA	50	C	2022/06/07	Oxidation Reduction Potential	mV	47.0
UA	50	C	2022/09/13	Oxidation Reduction Potential	mV	55.0
UA	50	C	2022/12/27	Oxidation Reduction Potential	mV	-67.0
UA	50	C	2023/02/28	Oxidation Reduction Potential	mV	24.1
UA	50	C	2023/05/31	Oxidation Reduction Potential	mV	34.0
UA	50	C	2023/08/25	Oxidation Reduction Potential	mV	88.0
UA	50	C	2023/11/14	Oxidation Reduction Potential	mV	206
UA	50	C	2019/09/17	Eh	V	0.35
UA	50	C	2019/12/11	Eh	V	0.24
UA	50	C	2020/03/11	Eh	V	0.24
UA	50	C	2020/06/03	Eh	V	0.30
UA	50	C	2020/06/25	Eh	V	0.31
UA	50	C	2020/09/02	Eh	V	0.31
UA	50	C	2020/12/09	Eh	V	0.25
UA	50	C	2021/03/19	Eh	V	0.40
UA	50	C	2021/06/23	Eh	V	0.33
UA	50	C	2021/09/08	Eh	V	0.26
UA	50	C	2021/12/08	Eh	V	0.13
UA	50	C	2022/03/22	Eh	V	0.12
UA	50	C	2022/06/07	Eh	V	0.24
UA	50	C	2022/09/13	Eh	V	0.25
UA	50	C	2022/12/27	Eh	V	0.13
UA	50	C	2023/02/28	Eh	V	0.22
UA	50	C	2023/05/31	Eh	V	0.23

UA	50	C	2023/08/25	Eh	V	0.28
UA	50	C	2023/11/14	Eh	V	0.40
UA	50	C	2019/09/17	Alkalinity, bicarbonate	mg/L CaCO3	356
UA	50	C	2020/03/11	Alkalinity, bicarbonate	mg/L CaCO3	370
UA	50	C	2021/03/19	Alkalinity, bicarbonate	mg/L CaCO3	270
UA	50	C	2021/09/08	Alkalinity, bicarbonate	mg/L CaCO3	335
UA	50	C	2022/03/22	Alkalinity, bicarbonate	mg/L CaCO3	281
UA	50	C	2022/09/13	Alkalinity, bicarbonate	mg/L CaCO3	326
UA	50	C	2023/02/28	Alkalinity, bicarbonate	mg/L CaCO3	251
UA	50	C	2023/05/31	Alkalinity, bicarbonate	mg/L CaCO3	324
UA	50	C	2023/08/25	Alkalinity, bicarbonate	mg/L CaCO3	280
UA	50	C	2023/11/14	Alkalinity, bicarbonate	mg/L CaCO3	290
UA	50	C	2019/09/17	Arsenic, total	mg/L	<0.0004
UA	50	C	2019/12/11	Arsenic, total	mg/L	<0.0004
UA	50	C	2020/03/11	Arsenic, total	mg/L	<0.0004
UA	50	C	2020/06/03	Arsenic, total	mg/L	<0.0004
UA	50	C	2020/09/02	Arsenic, total	mg/L	<0.0004
UA	50	C	2020/12/09	Arsenic, total	mg/L	<0.0004
UA	50	C	2021/03/19	Arsenic, total	mg/L	<0.0004
UA	50	C	2021/06/23	Arsenic, total	mg/L	<0.0004
UA	50	C	2021/09/08	Arsenic, total	mg/L	<0.0004
UA	50	C	2021/12/08	Arsenic, total	mg/L	<0.0004
UA	50	C	2022/03/22	Arsenic, total	mg/L	<0.0004
UA	50	C	2022/09/13	Arsenic, total	mg/L	0.000800
UA	50	C	2023/02/28	Arsenic, total	mg/L	0.00100
UA	50	C	2023/05/31	Arsenic, total	mg/L	<0.0087
UA	50	C	2023/08/25	Arsenic, total	mg/L	<0.00023
UA	50	C	2023/11/14	Arsenic, total	mg/L	0.000760
UA	50	C	2019/09/17	Barium, total	mg/L	0.0969
UA	50	C	2019/12/11	Barium, total	mg/L	0.112
UA	50	C	2020/03/11	Barium, total	mg/L	0.0983
UA	50	C	2020/06/03	Barium, total	mg/L	0.0980
UA	50	C	2020/09/02	Barium, total	mg/L	0.0954
UA	50	C	2020/12/09	Barium, total	mg/L	0.0821
UA	50	C	2021/03/19	Barium, total	mg/L	0.0862
UA	50	C	2021/06/23	Barium, total	mg/L	0.0901
UA	50	C	2021/09/08	Barium, total	mg/L	0.0977
UA	50	C	2021/12/08	Barium, total	mg/L	0.0912
UA	50	C	2022/03/22	Barium, total	mg/L	0.0925
UA	50	C	2022/09/13	Barium, total	mg/L	0.105
UA	50	C	2023/02/28	Barium, total	mg/L	0.103
UA	50	C	2023/05/31	Barium, total	mg/L	0.0888
UA	50	C	2023/08/25	Barium, total	mg/L	0.0640
UA	50	C	2023/11/14	Barium, total	mg/L	0.0870
UA	50	C	2019/09/17	Boron, total	mg/L	0.815
UA	50	C	2019/12/11	Boron, total	mg/L	0.820
UA	50	C	2020/03/11	Boron, total	mg/L	0.732
UA	50	C	2020/06/03	Boron, total	mg/L	0.816
UA	50	C	2020/09/02	Boron, total	mg/L	0.681
UA	50	C	2020/12/09	Boron, total	mg/L	0.777
UA	50	C	2021/03/19	Boron, total	mg/L	0.862
UA	50	C	2021/06/23	Boron, total	mg/L	0.790
UA	50	C	2021/09/08	Boron, total	mg/L	0.696
UA	50	C	2021/12/08	Boron, total	mg/L	0.690
UA	50	C	2022/03/22	Boron, total	mg/L	1.24
UA	50	C	2022/09/13	Boron, total	mg/L	0.618
UA	50	C	2023/02/28	Boron, total	mg/L	1.43
UA	50	C	2023/05/31	Boron, total	mg/L	0.784
UA	50	C	2023/08/25	Boron, total	mg/L	0.590
UA	50	C	2023/11/14	Boron, total	mg/L	1.00
UA	50	C	2019/09/17	Cadmium, total	mg/L	0.00120
UA	50	C	2019/12/11	Cadmium, total	mg/L	0.00140

UA	50	C	2020/03/11	Cadmium, total	mg/L	0.00140
UA	50	C	2020/06/03	Cadmium, total	mg/L	0.00140
UA	50	C	2020/09/02	Cadmium, total	mg/L	0.00130
UA	50	C	2020/12/09	Cadmium, total	mg/L	0.00150
UA	50	C	2021/03/19	Cadmium, total	mg/L	0.00140
UA	50	C	2021/06/23	Cadmium, total	mg/L	0.00110
UA	50	C	2021/09/08	Cadmium, total	mg/L	0.00150
UA	50	C	2021/12/08	Cadmium, total	mg/L	0.00130
UA	50	C	2022/03/22	Cadmium, total	mg/L	0.00100
UA	50	C	2022/09/13	Cadmium, total	mg/L	0.00140
UA	50	C	2023/02/28	Cadmium, total	mg/L	0.00370
UA	50	C	2023/05/31	Cadmium, total	mg/L	<0.0005
UA	50	C	2023/08/25	Cadmium, total	mg/L	0.00140
UA	50	C	2023/11/14	Cadmium, total	mg/L	0.00150
UA	50	C	2019/09/17	Calcium, total	mg/L	128
UA	50	C	2019/12/11	Calcium, total	mg/L	128
UA	50	C	2020/03/11	Calcium, total	mg/L	125
UA	50	C	2020/06/03	Calcium, total	mg/L	124
UA	50	C	2020/09/02	Calcium, total	mg/L	111
UA	50	C	2020/12/09	Calcium, total	mg/L	110
UA	50	C	2021/03/19	Calcium, total	mg/L	113
UA	50	C	2021/06/23	Calcium, total	mg/L	123
UA	50	C	2021/09/08	Calcium, total	mg/L	119
UA	50	C	2021/12/08	Calcium, total	mg/L	111
UA	50	C	2022/03/22	Calcium, total	mg/L	114
UA	50	C	2022/09/13	Calcium, total	mg/L	110
UA	50	C	2023/02/28	Calcium, total	mg/L	121
UA	50	C	2023/05/31	Calcium, total	mg/L	122
UA	50	C	2023/08/25	Calcium, total	mg/L	100
UA	50	C	2023/11/14	Calcium, total	mg/L	110
UA	50	C	2019/09/17	Chloride, total	mg/L	91.0
UA	50	C	2019/12/11	Chloride, total	mg/L	95.0
UA	50	C	2020/03/11	Chloride, total	mg/L	86.0
UA	50	C	2020/06/03	Chloride, total	mg/L	94.0
UA	50	C	2020/09/02	Chloride, total	mg/L	93.0
UA	50	C	2020/12/09	Chloride, total	mg/L	88.0
UA	50	C	2021/03/19	Chloride, total	mg/L	87.0
UA	50	C	2021/06/23	Chloride, total	mg/L	94.0
UA	50	C	2021/09/08	Chloride, total	mg/L	95.0
UA	50	C	2021/12/08	Chloride, total	mg/L	97.0
UA	50	C	2022/03/22	Chloride, total	mg/L	102
UA	50	C	2022/09/13	Chloride, total	mg/L	96.0
UA	50	C	2023/02/28	Chloride, total	mg/L	101
UA	50	C	2023/05/31	Chloride, total	mg/L	90.0
UA	50	C	2023/08/25	Chloride, total	mg/L	87.0
UA	50	C	2023/11/14	Chloride, total	mg/L	83.0
UA	50	C	2023/05/31	Iron, dissolved	mg/L	<0.02
UA	50	C	2023/08/25	Iron, dissolved	mg/L	<0.047
UA	50	C	2019/09/17	Lithium, total	mg/L	0.0231
UA	50	C	2019/12/11	Lithium, total	mg/L	0.0239
UA	50	C	2020/03/11	Lithium, total	mg/L	0.0221
UA	50	C	2020/06/03	Lithium, total	mg/L	0.0229
UA	50	C	2020/09/02	Lithium, total	mg/L	0.0180
UA	50	C	2020/12/09	Lithium, total	mg/L	0.0232
UA	50	C	2021/03/19	Lithium, total	mg/L	0.0238
UA	50	C	2021/06/23	Lithium, total	mg/L	0.0245
UA	50	C	2021/09/08	Lithium, total	mg/L	0.0197
UA	50	C	2021/12/08	Lithium, total	mg/L	0.0206
UA	50	C	2022/03/22	Lithium, total	mg/L	0.0225
UA	50	C	2022/09/13	Lithium, total	mg/L	0.0201
UA	50	C	2023/02/28	Lithium, total	mg/L	0.0242
UA	50	C	2023/05/31	Lithium, total	mg/L	0.00710

UA	50	C	2023/08/25	Lithium, total	mg/L	0.0250
UA	50	C	2023/11/14	Lithium, total	mg/L	0.0300
UA	50	C	2019/09/17	Magnesium, total	mg/L	35.7
UA	50	C	2020/03/11	Magnesium, total	mg/L	37.4
UA	50	C	2020/06/03	Magnesium, total	mg/L	36.6
UA	50	C	2021/03/19	Magnesium, total	mg/L	30.2
UA	50	C	2021/09/08	Magnesium, total	mg/L	33.4
UA	50	C	2022/03/22	Magnesium, total	mg/L	29.4
UA	50	C	2022/09/13	Magnesium, total	mg/L	32.9
UA	50	C	2023/02/28	Magnesium, total	mg/L	27.4
UA	50	C	2023/05/31	Magnesium, total	mg/L	30.1
UA	50	C	2023/08/25	Magnesium, total	mg/L	31.0
UA	50	C	2023/11/14	Magnesium, total	mg/L	23.0
UA	50	C	2023/05/31	Manganese, dissolved	mg/L	0.176
UA	50	C	2023/08/25	Manganese, dissolved	mg/L	0.270
UA	50	C	2023/05/31	Phosphate, dissolved	mg/L	0.0310
UA	50	C	2023/08/25	Phosphate, dissolved	mg/L	0.180
UA	50	C	2019/09/17	Potassium, total	mg/L	9.07
UA	50	C	2020/03/11	Potassium, total	mg/L	8.72
UA	50	C	2020/06/03	Potassium, total	mg/L	8.02
UA	50	C	2021/03/19	Potassium, total	mg/L	9.71
UA	50	C	2021/09/08	Potassium, total	mg/L	9.69
UA	50	C	2022/03/22	Potassium, total	mg/L	9.08
UA	50	C	2022/09/13	Potassium, total	mg/L	9.32
UA	50	C	2023/02/28	Potassium, total	mg/L	9.20
UA	50	C	2023/05/31	Potassium, total	mg/L	9.45
UA	50	C	2023/08/25	Potassium, total	mg/L	11.0
UA	50	C	2023/11/14	Potassium, total	mg/L	8.30
UA	50	C	2023/05/31	Silicon, dissolved	mg/L	14.5
UA	50	C	2023/08/25	Silicon, dissolved	mg/L	17.0
UA	50	C	2019/09/17	Sodium, total	mg/L	65.7
UA	50	C	2020/03/11	Sodium, total	mg/L	70.2
UA	50	C	2020/06/03	Sodium, total	mg/L	70.5
UA	50	C	2021/03/19	Sodium, total	mg/L	57.5
UA	50	C	2021/09/08	Sodium, total	mg/L	58.6
UA	50	C	2022/03/22	Sodium, total	mg/L	59.5
UA	50	C	2022/09/13	Sodium, total	mg/L	61.0
UA	50	C	2023/02/28	Sodium, total	mg/L	56.5
UA	50	C	2023/05/31	Sodium, total	mg/L	59.7
UA	50	C	2023/08/25	Sodium, total	mg/L	54.0
UA	50	C	2023/11/14	Sodium, total	mg/L	51.0
UA	50	C	2019/09/17	Sulfate, total	mg/L	83.0
UA	50	C	2019/12/11	Sulfate, total	mg/L	113
UA	50	C	2020/03/11	Sulfate, total	mg/L	98.0
UA	50	C	2020/06/03	Sulfate, total	mg/L	107
UA	50	C	2020/09/02	Sulfate, total	mg/L	81.0
UA	50	C	2020/12/09	Sulfate, total	mg/L	89.0
UA	50	C	2021/03/19	Sulfate, total	mg/L	96.0
UA	50	C	2021/06/23	Sulfate, total	mg/L	90.0
UA	50	C	2021/09/08	Sulfate, total	mg/L	85.0
UA	50	C	2021/12/08	Sulfate, total	mg/L	104
UA	50	C	2022/03/22	Sulfate, total	mg/L	90.0
UA	50	C	2022/09/13	Sulfate, total	mg/L	81.0
UA	50	C	2023/02/28	Sulfate, total	mg/L	136
UA	50	C	2023/05/31	Sulfate, total	mg/L	88.0
UA	50	C	2023/08/25	Sulfate, total	mg/L	93.0
UA	50	C	2023/11/14	Sulfate, total	mg/L	91.0
UA	50	C	2019/09/17	Temperature (Celsius)	degrees C	16.5
UA	50	C	2019/12/11	Temperature (Celsius)	degrees C	16.4
UA	50	C	2020/03/11	Temperature (Celsius)	degrees C	15.5
UA	50	C	2020/06/03	Temperature (Celsius)	degrees C	15.9
UA	50	C	2020/06/25	Temperature (Celsius)	degrees C	16.4

UA	50	C	2020/09/02	Temperature (Celsius)	degrees C	17.8
UA	50	C	2020/12/09	Temperature (Celsius)	degrees C	16.7
UA	50	C	2021/03/19	Temperature (Celsius)	degrees C	15.5
UA	50	C	2021/06/23	Temperature (Celsius)	degrees C	15.5
UA	50	C	2021/09/08	Temperature (Celsius)	degrees C	15.9
UA	50	C	2021/12/08	Temperature (Celsius)	degrees C	16.7
UA	50	C	2022/03/22	Temperature (Celsius)	degrees C	15.2
UA	50	C	2022/06/07	Temperature (Celsius)	degrees C	14.1
UA	50	C	2022/09/13	Temperature (Celsius)	degrees C	15.9
UA	50	C	2022/12/27	Temperature (Celsius)	degrees C	13.1
UA	50	C	2023/02/28	Temperature (Celsius)	degrees C	14.7
UA	50	C	2023/05/31	Temperature (Celsius)	degrees C	15.5
UA	50	C	2023/08/25	Temperature (Celsius)	degrees C	16.7
UA	50	C	2023/11/14	Temperature (Celsius)	degrees C	15.8
UA	50	C	2019/09/17	Total Dissolved Solids	mg/L	700
UA	50	C	2019/12/11	Total Dissolved Solids	mg/L	672
UA	50	C	2020/03/11	Total Dissolved Solids	mg/L	690
UA	50	C	2020/06/03	Total Dissolved Solids	mg/L	662
UA	50	C	2020/09/02	Total Dissolved Solids	mg/L	622
UA	50	C	2020/12/09	Total Dissolved Solids	mg/L	604
UA	50	C	2021/03/19	Total Dissolved Solids	mg/L	606
UA	50	C	2021/06/23	Total Dissolved Solids	mg/L	692
UA	50	C	2021/09/08	Total Dissolved Solids	mg/L	588
UA	50	C	2021/12/08	Total Dissolved Solids	mg/L	598
UA	50	C	2022/03/22	Total Dissolved Solids	mg/L	598
UA	50	C	2022/09/13	Total Dissolved Solids	mg/L	668
UA	50	C	2023/02/28	Total Dissolved Solids	mg/L	580
UA	50	C	2023/05/31	Total Dissolved Solids	mg/L	632
UA	50	C	2023/08/25	Total Dissolved Solids	mg/L	610
UA	50	C	2023/11/14	Total Dissolved Solids	mg/L	610
UA	51	C	2020/03/11	pH (field)	SU	7.5
UA	51	C	2020/06/24	pH (field)	SU	7.5
UA	51	C	2020/09/02	pH (field)	SU	7.5
UA	51	C	2020/12/10	pH (field)	SU	7.6
UA	51	C	2021/03/17	pH (field)	SU	7.3
UA	51	C	2021/06/23	pH (field)	SU	7.3
UA	51	C	2021/09/09	pH (field)	SU	7.4
UA	51	C	2021/12/09	pH (field)	SU	7.3
UA	51	C	2022/03/22	pH (field)	SU	7.4
UA	51	C	2022/06/07	pH (field)	SU	7.3
UA	51	C	2022/09/13	pH (field)	SU	7.2
UA	51	C	2022/12/27	pH (field)	SU	7.2
UA	51	C	2023/02/28	pH (field)	SU	7.2
UA	51	C	2023/05/31	pH (field)	SU	7.2
UA	51	C	2023/08/22	pH (field)	SU	7.4
UA	51	C	2023/11/15	pH (field)	SU	7.4
UA	51	C	2020/03/11	Oxidation Reduction Potential	mV	-132
UA	51	C	2020/06/24	Oxidation Reduction Potential	mV	-139
UA	51	C	2020/09/02	Oxidation Reduction Potential	mV	-150
UA	51	C	2020/12/10	Oxidation Reduction Potential	mV	-152
UA	51	C	2021/03/17	Oxidation Reduction Potential	mV	-125
UA	51	C	2021/06/23	Oxidation Reduction Potential	mV	-194
UA	51	C	2021/09/09	Oxidation Reduction Potential	mV	-152
UA	51	C	2021/12/09	Oxidation Reduction Potential	mV	-142
UA	51	C	2022/03/22	Oxidation Reduction Potential	mV	-163
UA	51	C	2022/06/07	Oxidation Reduction Potential	mV	15.0
UA	51	C	2022/09/13	Oxidation Reduction Potential	mV	68.0
UA	51	C	2022/12/27	Oxidation Reduction Potential	mV	-141
UA	51	C	2023/02/28	Oxidation Reduction Potential	mV	-119
UA	51	C	2023/05/31	Oxidation Reduction Potential	mV	-135
UA	51	C	2023/08/22	Oxidation Reduction Potential	mV	-129
UA	51	C	2023/11/15	Oxidation Reduction Potential	mV	-125

UA	51	C	2020/03/11	Eh	V	0.066
UA	51	C	2020/06/24	Eh	V	0.058
UA	51	C	2020/09/02	Eh	V	0.046
UA	51	C	2020/12/10	Eh	V	0.046
UA	51	C	2021/03/17	Eh	V	0.074
UA	51	C	2021/06/23	Eh	V	0.0034
UA	51	C	2021/09/09	Eh	V	0.045
UA	51	C	2021/12/09	Eh	V	0.056
UA	51	C	2022/03/22	Eh	V	0.035
UA	51	C	2022/06/07	Eh	V	0.21
UA	51	C	2022/09/13	Eh	V	0.26
UA	51	C	2022/12/27	Eh	V	0.057
UA	51	C	2023/02/28	Eh	V	0.079
UA	51	C	2023/05/31	Eh	V	0.062
UA	51	C	2023/08/22	Eh	V	0.065
UA	51	C	2023/11/15	Eh	V	0.072
UA	51	C	2020/03/11	Alkalinity, bicarbonate	mg/L CaCO3	332
UA	51	C	2021/02/25	Alkalinity, bicarbonate	mg/L CaCO3	344
UA	51	C	2021/03/04	Alkalinity, bicarbonate	mg/L CaCO3	347
UA	51	C	2021/03/09	Alkalinity, bicarbonate	mg/L CaCO3	335
UA	51	C	2021/03/17	Alkalinity, bicarbonate	mg/L CaCO3	349
UA	51	C	2021/03/18	Alkalinity, bicarbonate	mg/L CaCO3	339
UA	51	C	2021/03/30	Alkalinity, bicarbonate	mg/L CaCO3	355
UA	51	C	2021/09/09	Alkalinity, bicarbonate	mg/L CaCO3	356
UA	51	C	2022/03/22	Alkalinity, bicarbonate	mg/L CaCO3	346
UA	51	C	2022/09/13	Alkalinity, bicarbonate	mg/L CaCO3	347
UA	51	C	2023/02/28	Alkalinity, bicarbonate	mg/L CaCO3	357
UA	51	C	2023/05/31	Alkalinity, bicarbonate	mg/L CaCO3	356
UA	51	C	2023/08/22	Alkalinity, bicarbonate	mg/L CaCO3	340
UA	51	C	2023/11/15	Alkalinity, bicarbonate	mg/L CaCO3	360
UA	51	C	2020/03/11	Arsenic, total	mg/L	0.0102
UA	51	C	2020/06/24	Arsenic, total	mg/L	0.0105
UA	51	C	2020/09/02	Arsenic, total	mg/L	0.0132
UA	51	C	2020/12/10	Arsenic, total	mg/L	0.0237
UA	51	C	2021/02/25	Arsenic, total	mg/L	0.0171
UA	51	C	2021/03/04	Arsenic, total	mg/L	0.0168
UA	51	C	2021/03/09	Arsenic, total	mg/L	0.0190
UA	51	C	2021/03/17	Arsenic, total	mg/L	0.0176
UA	51	C	2021/03/18	Arsenic, total	mg/L	0.0180
UA	51	C	2021/03/30	Arsenic, total	mg/L	0.0165
UA	51	C	2021/06/23	Arsenic, total	mg/L	0.0192
UA	51	C	2021/09/09	Arsenic, total	mg/L	0.0174
UA	51	C	2021/12/09	Arsenic, total	mg/L	0.0197
UA	51	C	2022/03/22	Arsenic, total	mg/L	0.0195
UA	51	C	2022/06/07	Arsenic, total	mg/L	0.0192
UA	51	C	2022/09/13	Arsenic, total	mg/L	0.0206
UA	51	C	2022/12/27	Arsenic, total	mg/L	0.0264
UA	51	C	2023/02/28	Arsenic, total	mg/L	0.0308
UA	51	C	2023/05/31	Arsenic, total	mg/L	0.0182
UA	51	C	2023/08/22	Arsenic, total	mg/L	0.0190
UA	51	C	2023/11/15	Arsenic, total	mg/L	0.0190
UA	51	C	2020/03/11	Barium, total	mg/L	0.145
UA	51	C	2020/06/24	Barium, total	mg/L	0.106
UA	51	C	2020/09/02	Barium, total	mg/L	0.112
UA	51	C	2020/12/10	Barium, total	mg/L	0.144
UA	51	C	2021/02/25	Barium, total	mg/L	0.118
UA	51	C	2021/03/17	Barium, total	mg/L	0.126
UA	51	C	2021/06/23	Barium, total	mg/L	0.122
UA	51	C	2021/09/09	Barium, total	mg/L	0.115
UA	51	C	2021/12/09	Barium, total	mg/L	0.112
UA	51	C	2022/03/22	Barium, total	mg/L	0.102
UA	51	C	2022/06/07	Barium, total	mg/L	0.0968

UA	51	C	2022/09/13	Barium, total	mg/L	0.0917
UA	51	C	2022/12/27	Barium, total	mg/L	0.120
UA	51	C	2023/02/28	Barium, total	mg/L	0.134
UA	51	C	2023/05/31	Barium, total	mg/L	0.109
UA	51	C	2023/08/22	Barium, total	mg/L	0.100
UA	51	C	2023/11/15	Barium, total	mg/L	0.100
UA	51	C	2020/03/11	Boron, total	mg/L	3.14
UA	51	C	2020/06/24	Boron, total	mg/L	2.83
UA	51	C	2020/09/02	Boron, total	mg/L	2.40
UA	51	C	2020/12/10	Boron, total	mg/L	2.63
UA	51	C	2021/02/25	Boron, total	mg/L	2.41
UA	51	C	2021/03/04	Boron, total	mg/L	2.32
UA	51	C	2021/03/09	Boron, total	mg/L	2.10
UA	51	C	2021/03/17	Boron, total	mg/L	2.24
UA	51	C	2021/03/18	Boron, total	mg/L	2.37
UA	51	C	2021/03/30	Boron, total	mg/L	2.51
UA	51	C	2021/06/23	Boron, total	mg/L	2.11
UA	51	C	2021/09/09	Boron, total	mg/L	1.96
UA	51	C	2021/12/09	Boron, total	mg/L	1.90
UA	51	C	2022/03/22	Boron, total	mg/L	2.55
UA	51	C	2022/06/07	Boron, total	mg/L	1.72
UA	51	C	2022/09/13	Boron, total	mg/L	1.57
UA	51	C	2022/12/27	Boron, total	mg/L	2.01
UA	51	C	2023/02/28	Boron, total	mg/L	1.54
UA	51	C	2023/05/31	Boron, total	mg/L	1.63
UA	51	C	2023/08/22	Boron, total	mg/L	1.30
UA	51	C	2023/11/15	Boron, total	mg/L	1.60
UA	51	C	2020/03/11	Cadmium, total	mg/L	<0.0002
UA	51	C	2020/06/24	Cadmium, total	mg/L	<0.0002
UA	51	C	2020/09/02	Cadmium, total	mg/L	<0.0002
UA	51	C	2020/12/10	Cadmium, total	mg/L	<0.0002
UA	51	C	2021/02/25	Cadmium, total	mg/L	<0.0000002
UA	51	C	2021/03/17	Cadmium, total	mg/L	<0.0002
UA	51	C	2021/06/23	Cadmium, total	mg/L	<0.0002
UA	51	C	2021/09/09	Cadmium, total	mg/L	<0.0002
UA	51	C	2021/12/09	Cadmium, total	mg/L	<0.0002
UA	51	C	2022/03/22	Cadmium, total	mg/L	<0.0002
UA	51	C	2022/06/07	Cadmium, total	mg/L	<0.0002
UA	51	C	2022/09/13	Cadmium, total	mg/L	<0.0002
UA	51	C	2022/12/27	Cadmium, total	mg/L	<0.0002
UA	51	C	2023/02/28	Cadmium, total	mg/L	<0.0002
UA	51	C	2023/05/31	Cadmium, total	mg/L	<0.0005
UA	51	C	2023/08/22	Cadmium, total	mg/L	<0.00017
UA	51	C	2023/11/15	Cadmium, total	mg/L	<0.00017
UA	51	C	2020/03/11	Calcium, total	mg/L	126
UA	51	C	2020/06/24	Calcium, total	mg/L	116
UA	51	C	2020/09/02	Calcium, total	mg/L	120
UA	51	C	2020/12/10	Calcium, total	mg/L	168
UA	51	C	2021/02/25	Calcium, total	mg/L	129
UA	51	C	2021/03/04	Calcium, total	mg/L	119
UA	51	C	2021/03/09	Calcium, total	mg/L	120
UA	51	C	2021/03/17	Calcium, total	mg/L	127
UA	51	C	2021/03/18	Calcium, total	mg/L	128
UA	51	C	2021/03/30	Calcium, total	mg/L	123
UA	51	C	2021/06/23	Calcium, total	mg/L	128
UA	51	C	2021/09/09	Calcium, total	mg/L	132
UA	51	C	2021/12/09	Calcium, total	mg/L	132
UA	51	C	2022/03/22	Calcium, total	mg/L	121
UA	51	C	2022/06/07	Calcium, total	mg/L	120
UA	51	C	2022/09/13	Calcium, total	mg/L	124
UA	51	C	2022/12/27	Calcium, total	mg/L	128
UA	51	C	2023/02/28	Calcium, total	mg/L	132

UA	51	C	2023/05/31	Calcium, total	mg/L	127
UA	51	C	2023/08/22	Calcium, total	mg/L	110
UA	51	C	2023/11/15	Calcium, total	mg/L	110
UA	51	C	2020/03/11	Chloride, total	mg/L	94.0
UA	51	C	2020/06/24	Chloride, total	mg/L	93.0
UA	51	C	2020/09/02	Chloride, total	mg/L	103
UA	51	C	2020/12/10	Chloride, total	mg/L	99.0
UA	51	C	2021/02/25	Chloride, total	mg/L	97.0
UA	51	C	2021/03/04	Chloride, total	mg/L	100
UA	51	C	2021/03/09	Chloride, total	mg/L	105
UA	51	C	2021/03/17	Chloride, total	mg/L	90.0
UA	51	C	2021/03/18	Chloride, total	mg/L	97.0
UA	51	C	2021/03/30	Chloride, total	mg/L	99.0
UA	51	C	2021/06/23	Chloride, total	mg/L	105
UA	51	C	2021/09/09	Chloride, total	mg/L	101
UA	51	C	2021/12/09	Chloride, total	mg/L	107
UA	51	C	2022/03/22	Chloride, total	mg/L	103
UA	51	C	2022/06/07	Chloride, total	mg/L	111
UA	51	C	2022/09/13	Chloride, total	mg/L	112
UA	51	C	2022/12/27	Chloride, total	mg/L	109
UA	51	C	2023/02/28	Chloride, total	mg/L	110
UA	51	C	2023/05/31	Chloride, total	mg/L	109
UA	51	C	2023/08/22	Chloride, total	mg/L	94.0
UA	51	C	2023/11/15	Chloride, total	mg/L	92.0
UA	51	C	2023/08/22	Ferrous Iron, dissolved	mg/L	1.74
UA	51	C	2021/02/25	Iron, dissolved	mg/L	4.60
UA	51	C	2021/03/04	Iron, dissolved	mg/L	4.39
UA	51	C	2021/03/09	Iron, dissolved	mg/L	5.00
UA	51	C	2021/03/18	Iron, dissolved	mg/L	5.17
UA	51	C	2021/03/30	Iron, dissolved	mg/L	4.72
UA	51	C	2023/05/31	Iron, dissolved	mg/L	6.53
UA	51	C	2023/08/22	Iron, dissolved	mg/L	6.10
UA	51	C	2020/03/11	Lithium, total	mg/L	0.0245
UA	51	C	2020/06/24	Lithium, total	mg/L	0.0232
UA	51	C	2020/09/02	Lithium, total	mg/L	0.0214
UA	51	C	2020/12/10	Lithium, total	mg/L	0.0224
UA	51	C	2021/02/25	Lithium, total	mg/L	0.0230
UA	51	C	2021/03/04	Lithium, total	mg/L	0.0244
UA	51	C	2021/03/09	Lithium, total	mg/L	0.0240
UA	51	C	2021/03/17	Lithium, total	mg/L	0.0242
UA	51	C	2021/03/18	Lithium, total	mg/L	0.0214
UA	51	C	2021/03/30	Lithium, total	mg/L	0.0238
UA	51	C	2021/06/23	Lithium, total	mg/L	0.0241
UA	51	C	2021/09/09	Lithium, total	mg/L	0.0248
UA	51	C	2021/12/09	Lithium, total	mg/L	0.0251
UA	51	C	2022/03/22	Lithium, total	mg/L	0.0250
UA	51	C	2022/06/07	Lithium, total	mg/L	0.0258
UA	51	C	2022/09/13	Lithium, total	mg/L	0.0213
UA	51	C	2022/12/27	Lithium, total	mg/L	0.0302
UA	51	C	2023/02/28	Lithium, total	mg/L	0.0210
UA	51	C	2023/05/31	Lithium, total	mg/L	0.0714
UA	51	C	2023/08/22	Lithium, total	mg/L	0.0250
UA	51	C	2023/11/15	Lithium, total	mg/L	0.0260
UA	51	C	2020/03/11	Magnesium, total	mg/L	41.5
UA	51	C	2020/06/24	Magnesium, total	mg/L	40.8
UA	51	C	2021/02/25	Magnesium, total	mg/L	47.5
UA	51	C	2021/03/04	Magnesium, total	mg/L	42.1
UA	51	C	2021/03/09	Magnesium, total	mg/L	44.0
UA	51	C	2021/03/17	Magnesium, total	mg/L	44.5
UA	51	C	2021/03/18	Magnesium, total	mg/L	45.5
UA	51	C	2021/03/30	Magnesium, total	mg/L	45.1
UA	51	C	2021/09/09	Magnesium, total	mg/L	42.9

UA	51	C	2022/03/22	Magnesium, total	mg/L	37.3
UA	51	C	2022/09/13	Magnesium, total	mg/L	36.7
UA	51	C	2023/02/28	Magnesium, total	mg/L	39.8
UA	51	C	2023/05/31	Magnesium, total	mg/L	40.2
UA	51	C	2023/08/22	Magnesium, total	mg/L	37.0
UA	51	C	2023/11/15	Magnesium, total	mg/L	37.0
UA	51	C	2021/02/25	Manganese, dissolved	mg/L	0.0965
UA	51	C	2021/03/04	Manganese, dissolved	mg/L	0.117
UA	51	C	2021/03/09	Manganese, dissolved	mg/L	0.110
UA	51	C	2021/03/18	Manganese, dissolved	mg/L	0.109
UA	51	C	2021/03/30	Manganese, dissolved	mg/L	0.0991
UA	51	C	2023/05/31	Manganese, dissolved	mg/L	0.169
UA	51	C	2023/08/22	Manganese, dissolved	mg/L	0.150
UA	51	C	2023/05/31	Phosphate, dissolved	mg/L	0.0710
UA	51	C	2023/08/22	Phosphate, dissolved	mg/L	<0.073
UA	51	C	2020/03/11	Potassium, total	mg/L	5.16
UA	51	C	2020/06/24	Potassium, total	mg/L	4.56
UA	51	C	2021/02/25	Potassium, total	mg/L	4.05
UA	51	C	2021/03/04	Potassium, total	mg/L	4.55
UA	51	C	2021/03/09	Potassium, total	mg/L	4.20
UA	51	C	2021/03/17	Potassium, total	mg/L	4.89
UA	51	C	2021/03/18	Potassium, total	mg/L	4.78
UA	51	C	2021/03/30	Potassium, total	mg/L	4.32
UA	51	C	2021/09/09	Potassium, total	mg/L	4.98
UA	51	C	2022/03/22	Potassium, total	mg/L	5.36
UA	51	C	2022/09/13	Potassium, total	mg/L	6.49
UA	51	C	2023/02/28	Potassium, total	mg/L	6.55
UA	51	C	2023/05/31	Potassium, total	mg/L	6.65
UA	51	C	2023/08/22	Potassium, total	mg/L	5.60
UA	51	C	2023/11/15	Potassium, total	mg/L	6.10
UA	51	C	2023/05/31	Silicon, dissolved	mg/L	7.53
UA	51	C	2023/08/22	Silicon, dissolved	mg/L	8.70
UA	51	C	2020/03/11	Sodium, total	mg/L	46.5
UA	51	C	2020/06/24	Sodium, total	mg/L	50.7
UA	51	C	2021/02/25	Sodium, total	mg/L	57.2
UA	51	C	2021/03/04	Sodium, total	mg/L	59.2
UA	51	C	2021/03/09	Sodium, total	mg/L	53.0
UA	51	C	2021/03/17	Sodium, total	mg/L	55.9
UA	51	C	2021/03/18	Sodium, total	mg/L	55.6
UA	51	C	2021/03/30	Sodium, total	mg/L	54.5
UA	51	C	2021/09/09	Sodium, total	mg/L	57.2
UA	51	C	2022/03/22	Sodium, total	mg/L	57.6
UA	51	C	2022/09/13	Sodium, total	mg/L	55.5
UA	51	C	2023/02/28	Sodium, total	mg/L	59.3
UA	51	C	2023/05/31	Sodium, total	mg/L	58.9
UA	51	C	2023/08/22	Sodium, total	mg/L	52.0
UA	51	C	2023/11/15	Sodium, total	mg/L	56.0
UA	51	C	2020/03/11	Sulfate, total	mg/L	120
UA	51	C	2020/06/24	Sulfate, total	mg/L	113
UA	51	C	2020/09/02	Sulfate, total	mg/L	106
UA	51	C	2020/12/10	Sulfate, total	mg/L	124
UA	51	C	2021/02/25	Sulfate, total	mg/L	105
UA	51	C	2021/03/04	Sulfate, total	mg/L	106
UA	51	C	2021/03/09	Sulfate, total	mg/L	127
UA	51	C	2021/03/17	Sulfate, total	mg/L	95.0
UA	51	C	2021/03/18	Sulfate, total	mg/L	106
UA	51	C	2021/03/30	Sulfate, total	mg/L	116
UA	51	C	2021/06/23	Sulfate, total	mg/L	103
UA	51	C	2021/09/09	Sulfate, total	mg/L	101
UA	51	C	2021/12/09	Sulfate, total	mg/L	108
UA	51	C	2022/03/22	Sulfate, total	mg/L	94.0
UA	51	C	2022/06/07	Sulfate, total	mg/L	95.0

UA	51	C	2022/09/13	Sulfate, total	mg/L	105
UA	51	C	2022/12/27	Sulfate, total	mg/L	100
UA	51	C	2023/02/28	Sulfate, total	mg/L	105
UA	51	C	2023/05/31	Sulfate, total	mg/L	97.0
UA	51	C	2023/08/22	Sulfate, total	mg/L	90.0
UA	51	C	2023/11/15	Sulfate, total	mg/L	87.0
UA	51	C	2020/03/11	Temperature (Celsius)	degrees C	11.3
UA	51	C	2020/06/24	Temperature (Celsius)	degrees C	13.1
UA	51	C	2020/09/02	Temperature (Celsius)	degrees C	14.3
UA	51	C	2020/12/10	Temperature (Celsius)	degrees C	11.6
UA	51	C	2021/03/17	Temperature (Celsius)	degrees C	10.1
UA	51	C	2021/06/23	Temperature (Celsius)	degrees C	12.3
UA	51	C	2021/09/09	Temperature (Celsius)	degrees C	12.6
UA	51	C	2021/12/09	Temperature (Celsius)	degrees C	11.9
UA	51	C	2022/03/22	Temperature (Celsius)	degrees C	11.8
UA	51	C	2022/06/07	Temperature (Celsius)	degrees C	12.8
UA	51	C	2022/09/13	Temperature (Celsius)	degrees C	13.1
UA	51	C	2022/12/27	Temperature (Celsius)	degrees C	11.6
UA	51	C	2023/02/28	Temperature (Celsius)	degrees C	11.2
UA	51	C	2023/05/31	Temperature (Celsius)	degrees C	12.9
UA	51	C	2023/08/22	Temperature (Celsius)	degrees C	17.3
UA	51	C	2023/11/15	Temperature (Celsius)	degrees C	13.0
UA	51	C	2020/03/11	Total Dissolved Solids	mg/L	644
UA	51	C	2020/06/24	Total Dissolved Solids	mg/L	652
UA	51	C	2020/09/02	Total Dissolved Solids	mg/L	605
UA	51	C	2020/12/10	Total Dissolved Solids	mg/L	634
UA	51	C	2021/02/25	Total Dissolved Solids	mg/L	628
UA	51	C	2021/03/04	Total Dissolved Solids	mg/L	630
UA	51	C	2021/03/09	Total Dissolved Solids	mg/L	632
UA	51	C	2021/03/17	Total Dissolved Solids	mg/L	676
UA	51	C	2021/03/18	Total Dissolved Solids	mg/L	624
UA	51	C	2021/03/30	Total Dissolved Solids	mg/L	644
UA	51	C	2021/06/23	Total Dissolved Solids	mg/L	702
UA	51	C	2021/09/09	Total Dissolved Solids	mg/L	628
UA	51	C	2021/12/09	Total Dissolved Solids	mg/L	584
UA	51	C	2022/03/22	Total Dissolved Solids	mg/L	622
UA	51	C	2022/06/07	Total Dissolved Solids	mg/L	684
UA	51	C	2022/09/13	Total Dissolved Solids	mg/L	615
UA	51	C	2022/12/27	Total Dissolved Solids	mg/L	624
UA	51	C	2023/02/28	Total Dissolved Solids	mg/L	630
UA	51	C	2023/05/31	Total Dissolved Solids	mg/L	630
UA	51	C	2023/08/22	Total Dissolved Solids	mg/L	680
UA	51	C	2023/11/15	Total Dissolved Solids	mg/L	650
UA	21	C	2013/03/08	pH (field)	SU	7.2
UA	21	C	2013/06/07	pH (field)	SU	8.0
UA	21	C	2013/09/03	pH (field)	SU	7.1
UA	21	C	2013/12/10	pH (field)	SU	7.2
UA	21	C	2014/03/25	pH (field)	SU	7.6
UA	21	C	2014/08/19	pH (field)	SU	7.7
UA	21	C	2014/09/30	pH (field)	SU	7.5
UA	21	C	2015/03/18	pH (field)	SU	7.5
UA	21	C	2015/09/16	pH (field)	SU	7.5
UA	21	C	2015/12/10	pH (field)	SU	7.6
UA	21	C	2016/03/09	pH (field)	SU	7.3
UA	21	C	2016/06/07	pH (field)	SU	7.4
UA	21	C	2016/09/15	pH (field)	SU	7.4
UA	21	C	2016/12/07	pH (field)	SU	7.6
UA	21	C	2017/02/21	pH (field)	SU	7.4
UA	21	C	2017/04/25	pH (field)	SU	7.4
UA	21	C	2017/06/08	pH (field)	SU	7.4
UA	21	C	2017/09/06	pH (field)	SU	7.4
UA	21	C	2017/11/15	pH (field)	SU	7.5

UA	21	C	2018/03/26	pH (field)	SU	7.7
UA	21	C	2018/06/13	pH (field)	SU	6.8
UA	21	C	2018/09/12	pH (field)	SU	7.5
UA	21	C	2018/12/12	pH (field)	SU	7.4
UA	21	C	2019/03/13	pH (field)	SU	7.5
UA	21	C	2019/06/19	pH (field)	SU	7.4
UA	21	C	2015/12/10	Oxidation Reduction Potential	mV	-88.0
UA	21	C	2016/03/09	Oxidation Reduction Potential	mV	-110
UA	21	C	2016/06/07	Oxidation Reduction Potential	mV	-129
UA	21	C	2016/09/15	Oxidation Reduction Potential	mV	-124
UA	21	C	2016/12/07	Oxidation Reduction Potential	mV	-113
UA	21	C	2017/02/21	Oxidation Reduction Potential	mV	-88.0
UA	21	C	2017/04/25	Oxidation Reduction Potential	mV	-139
UA	21	C	2017/06/08	Oxidation Reduction Potential	mV	-187
UA	21	C	2017/11/15	Oxidation Reduction Potential	mV	10.0
UA	21	C	2018/06/13	Oxidation Reduction Potential	mV	-120
UA	21	C	2018/09/12	Oxidation Reduction Potential	mV	-183
UA	21	C	2018/12/12	Oxidation Reduction Potential	mV	-166
UA	21	C	2019/03/13	Oxidation Reduction Potential	mV	32.0
UA	21	C	2019/06/19	Oxidation Reduction Potential	mV	-168
UA	21	C	2015/12/10	Eh	V	0.11
UA	21	C	2016/03/09	Eh	V	0.087
UA	21	C	2016/06/07	Eh	V	0.068
UA	21	C	2016/09/15	Eh	V	0.071
UA	21	C	2016/12/07	Eh	V	0.085
UA	21	C	2017/02/21	Eh	V	0.11
UA	21	C	2017/04/25	Eh	V	0.051
UA	21	C	2017/06/08	Eh	V	0.0087
UA	21	C	2017/11/15	Eh	V	0.21
UA	21	C	2018/06/13	Eh	V	0.075
UA	21	C	2018/09/12	Eh	V	0.012
UA	21	C	2018/12/12	Eh	V	0.031
UA	21	C	2019/03/13	Eh	V	0.23
UA	21	C	2019/06/19	Eh	V	0.029
UA	21	C	2013/06/07	Arsenic, total	mg/L	0.00740
UA	21	C	2013/09/03	Arsenic, total	mg/L	0.00890
UA	21	C	2015/12/10	Arsenic, total	mg/L	0.00980
UA	21	C	2016/03/09	Arsenic, total	mg/L	0.00860
UA	21	C	2016/06/07	Arsenic, total	mg/L	0.00910
UA	21	C	2016/09/15	Arsenic, total	mg/L	0.00940
UA	21	C	2016/12/07	Arsenic, total	mg/L	0.00890
UA	21	C	2017/02/21	Arsenic, total	mg/L	0.00910
UA	21	C	2017/04/25	Arsenic, total	mg/L	0.00920
UA	21	C	2017/06/08	Arsenic, total	mg/L	0.00870
UA	21	C	2018/06/13	Arsenic, total	mg/L	0.0105
UA	21	C	2018/09/12	Arsenic, total	mg/L	0.0128
UA	21	C	2018/12/12	Arsenic, total	mg/L	0.00240
UA	21	C	2019/03/13	Arsenic, total	mg/L	0.00460
UA	21	C	2019/06/19	Arsenic, total	mg/L	0.00530
UA	21	C	2013/06/07	Barium, total	mg/L	0.203
UA	21	C	2013/09/03	Barium, total	mg/L	0.182
UA	21	C	2015/12/10	Barium, total	mg/L	0.179
UA	21	C	2016/03/09	Barium, total	mg/L	0.180
UA	21	C	2016/06/07	Barium, total	mg/L	0.179
UA	21	C	2016/09/15	Barium, total	mg/L	0.183
UA	21	C	2016/12/07	Barium, total	mg/L	0.187
UA	21	C	2017/02/21	Barium, total	mg/L	0.177
UA	21	C	2017/04/25	Barium, total	mg/L	0.175
UA	21	C	2017/06/08	Barium, total	mg/L	0.176
UA	21	C	2018/06/13	Barium, total	mg/L	0.173
UA	21	C	2018/09/12	Barium, total	mg/L	0.237
UA	21	C	2018/12/12	Barium, total	mg/L	0.199

UA	21	C	2019/03/13	Barium, total	mg/L	0.129
UA	21	C	2019/06/19	Barium, total	mg/L	0.221
UA	21	C	2013/06/07	Boron, total	mg/L	5.18
UA	21	C	2013/09/03	Boron, total	mg/L	5.09
UA	21	C	2015/12/10	Boron, total	mg/L	4.20
UA	21	C	2016/03/09	Boron, total	mg/L	4.30
UA	21	C	2016/06/07	Boron, total	mg/L	4.31
UA	21	C	2016/09/15	Boron, total	mg/L	4.60
UA	21	C	2016/12/07	Boron, total	mg/L	4.35
UA	21	C	2017/02/21	Boron, total	mg/L	3.95
UA	21	C	2017/04/25	Boron, total	mg/L	4.17
UA	21	C	2017/06/08	Boron, total	mg/L	4.01
UA	21	C	2017/11/15	Boron, total	mg/L	4.12
UA	21	C	2018/06/13	Boron, total	mg/L	3.89
UA	21	C	2018/09/12	Boron, total	mg/L	3.64
UA	21	C	2018/12/12	Boron, total	mg/L	4.12
UA	21	C	2019/03/13	Boron, total	mg/L	1.25
UA	21	C	2019/06/19	Boron, total	mg/L	3.73
UA	21	C	2013/06/07	Cadmium, total	mg/L	<0.0003
UA	21	C	2013/09/03	Cadmium, total	mg/L	<0.0003
UA	21	C	2015/12/10	Cadmium, total	mg/L	<0.0002
UA	21	C	2016/03/09	Cadmium, total	mg/L	<0.0002
UA	21	C	2016/06/07	Cadmium, total	mg/L	<0.0002
UA	21	C	2016/09/15	Cadmium, total	mg/L	<0.0002
UA	21	C	2016/12/07	Cadmium, total	mg/L	<0.0002
UA	21	C	2017/02/21	Cadmium, total	mg/L	<0.0002
UA	21	C	2017/04/25	Cadmium, total	mg/L	<0.0002
UA	21	C	2017/06/08	Cadmium, total	mg/L	<0.0002
UA	21	C	2018/06/13	Cadmium, total	mg/L	<0.0002
UA	21	C	2018/09/12	Cadmium, total	mg/L	<0.0002
UA	21	C	2018/12/12	Cadmium, total	mg/L	<0.0002
UA	21	C	2019/03/13	Cadmium, total	mg/L	<0.0002
UA	21	C	2019/06/19	Cadmium, total	mg/L	<0.0002
UA	21	C	2015/12/10	Calcium, total	mg/L	97.2
UA	21	C	2016/03/09	Calcium, total	mg/L	99.8
UA	21	C	2016/06/07	Calcium, total	mg/L	99.4
UA	21	C	2016/09/15	Calcium, total	mg/L	100
UA	21	C	2016/12/07	Calcium, total	mg/L	106
UA	21	C	2017/02/21	Calcium, total	mg/L	98.6
UA	21	C	2017/04/25	Calcium, total	mg/L	91.5
UA	21	C	2017/06/08	Calcium, total	mg/L	103
UA	21	C	2017/11/15	Calcium, total	mg/L	104
UA	21	C	2018/06/13	Calcium, total	mg/L	99.5
UA	21	C	2018/09/12	Calcium, total	mg/L	131
UA	21	C	2018/12/12	Calcium, total	mg/L	114
UA	21	C	2019/03/13	Calcium, total	mg/L	75.4
UA	21	C	2019/06/19	Calcium, total	mg/L	108
UA	21	C	2013/03/08	Chloride, total	mg/L	41.0
UA	21	C	2013/06/07	Chloride, total	mg/L	43.0
UA	21	C	2013/09/03	Chloride, total	mg/L	40.0
UA	21	C	2013/12/10	Chloride, total	mg/L	43.0
UA	21	C	2014/03/25	Chloride, total	mg/L	38.0
UA	21	C	2014/09/30	Chloride, total	mg/L	46.0
UA	21	C	2015/03/18	Chloride, total	mg/L	41.0
UA	21	C	2015/09/16	Chloride, total	mg/L	38.0
UA	21	C	2015/12/10	Chloride, total	mg/L	49.0
UA	21	C	2016/03/09	Chloride, total	mg/L	48.0
UA	21	C	2016/06/07	Chloride, total	mg/L	48.0
UA	21	C	2016/09/15	Chloride, total	mg/L	43.0
UA	21	C	2016/12/07	Chloride, total	mg/L	44.0
UA	21	C	2017/02/21	Chloride, total	mg/L	38.0
UA	21	C	2017/04/25	Chloride, total	mg/L	40.0

UA	21	C	2017/06/08	Chloride, total	mg/L	41.0
UA	21	C	2017/09/06	Chloride, total	mg/L	44.0
UA	21	C	2017/11/15	Chloride, total	mg/L	41.0
UA	21	C	2018/03/26	Chloride, total	mg/L	45.0
UA	21	C	2018/06/13	Chloride, total	mg/L	50.0
UA	21	C	2018/09/12	Chloride, total	mg/L	59.0
UA	21	C	2018/12/12	Chloride, total	mg/L	56.0
UA	21	C	2019/03/13	Chloride, total	mg/L	33.0
UA	21	C	2019/06/19	Chloride, total	mg/L	54.0
UA	21	C	2013/03/08	Iron, dissolved	mg/L	0.880
UA	21	C	2013/12/10	Iron, dissolved	mg/L	4.13
UA	21	C	2014/03/25	Iron, dissolved	mg/L	3.47
UA	21	C	2014/08/19	Iron, dissolved	mg/L	<0.007
UA	21	C	2014/09/30	Iron, dissolved	mg/L	3.53
UA	21	C	2015/03/18	Iron, dissolved	mg/L	2.49
UA	21	C	2015/09/16	Iron, dissolved	mg/L	2.77
UA	21	C	2016/03/09	Iron, dissolved	mg/L	3.65
UA	21	C	2016/09/15	Iron, dissolved	mg/L	3.64
UA	21	C	2017/02/21	Iron, dissolved	mg/L	3.06
UA	21	C	2017/09/06	Iron, dissolved	mg/L	1.93
UA	21	C	2018/03/26	Iron, dissolved	mg/L	4.20
UA	21	C	2015/12/10	Lithium, total	mg/L	0.0126
UA	21	C	2016/03/09	Lithium, total	mg/L	0.0136
UA	21	C	2016/06/07	Lithium, total	mg/L	0.0137
UA	21	C	2016/09/15	Lithium, total	mg/L	0.0136
UA	21	C	2016/12/07	Lithium, total	mg/L	0.0138
UA	21	C	2017/02/21	Lithium, total	mg/L	0.0124
UA	21	C	2017/04/25	Lithium, total	mg/L	0.0126
UA	21	C	2017/06/08	Lithium, total	mg/L	0.0138
UA	21	C	2018/06/13	Lithium, total	mg/L	0.0160
UA	21	C	2018/09/12	Lithium, total	mg/L	0.0208
UA	21	C	2018/12/12	Lithium, total	mg/L	0.0158
UA	21	C	2019/03/13	Lithium, total	mg/L	0.00640
UA	21	C	2019/06/19	Lithium, total	mg/L	0.0145
UA	21	C	2013/03/08	Manganese, dissolved	mg/L	0.0800
UA	21	C	2013/12/10	Manganese, dissolved	mg/L	0.121
UA	21	C	2014/03/25	Manganese, dissolved	mg/L	0.0977
UA	21	C	2014/08/19	Manganese, dissolved	mg/L	0.0956
UA	21	C	2014/09/30	Manganese, dissolved	mg/L	0.102
UA	21	C	2015/03/18	Manganese, dissolved	mg/L	0.0918
UA	21	C	2015/09/16	Manganese, dissolved	mg/L	0.0971
UA	21	C	2016/03/09	Manganese, dissolved	mg/L	0.103
UA	21	C	2016/09/15	Manganese, dissolved	mg/L	0.112
UA	21	C	2017/02/21	Manganese, dissolved	mg/L	0.114
UA	21	C	2017/09/06	Manganese, dissolved	mg/L	0.110
UA	21	C	2018/03/26	Manganese, dissolved	mg/L	0.109
UA	21	C	2013/03/08	Sulfate, total	mg/L	144
UA	21	C	2013/06/07	Sulfate, total	mg/L	161
UA	21	C	2013/09/03	Sulfate, total	mg/L	149
UA	21	C	2013/12/10	Sulfate, total	mg/L	119
UA	21	C	2014/03/25	Sulfate, total	mg/L	120
UA	21	C	2014/09/30	Sulfate, total	mg/L	159
UA	21	C	2015/03/18	Sulfate, total	mg/L	123
UA	21	C	2015/09/16	Sulfate, total	mg/L	124
UA	21	C	2015/12/10	Sulfate, total	mg/L	146
UA	21	C	2016/03/09	Sulfate, total	mg/L	146
UA	21	C	2016/06/07	Sulfate, total	mg/L	169
UA	21	C	2016/09/15	Sulfate, total	mg/L	167
UA	21	C	2016/12/07	Sulfate, total	mg/L	149
UA	21	C	2017/02/21	Sulfate, total	mg/L	142
UA	21	C	2017/04/25	Sulfate, total	mg/L	142
UA	21	C	2017/06/08	Sulfate, total	mg/L	163

UA	21	C	2017/09/06	Sulfate, total	mg/L	143
UA	21	C	2017/11/15	Sulfate, total	mg/L	110
UA	21	C	2018/03/26	Sulfate, total	mg/L	130
UA	21	C	2018/06/13	Sulfate, total	mg/L	135
UA	21	C	2018/09/12	Sulfate, total	mg/L	140
UA	21	C	2018/12/12	Sulfate, total	mg/L	91.0
UA	21	C	2019/03/13	Sulfate, total	mg/L	51.0
UA	21	C	2019/06/19	Sulfate, total	mg/L	77.0
UA	21	C	2013/03/08	Temperature (Celsius)	degrees C	10.9
UA	21	C	2013/06/07	Temperature (Celsius)	degrees C	15.1
UA	21	C	2013/09/03	Temperature (Celsius)	degrees C	16.8
UA	21	C	2013/12/10	Temperature (Celsius)	degrees C	10.3
UA	21	C	2014/03/25	Temperature (Celsius)	degrees C	10.3
UA	21	C	2014/08/19	Temperature (Celsius)	degrees C	14.3
UA	21	C	2014/09/30	Temperature (Celsius)	degrees C	13.4
UA	21	C	2015/03/18	Temperature (Celsius)	degrees C	13.2
UA	21	C	2015/09/16	Temperature (Celsius)	degrees C	14.2
UA	21	C	2015/12/10	Temperature (Celsius)	degrees C	14.1
UA	21	C	2016/03/09	Temperature (Celsius)	degrees C	12.6
UA	21	C	2016/06/07	Temperature (Celsius)	degrees C	13.3
UA	21	C	2016/09/15	Temperature (Celsius)	degrees C	15.2
UA	21	C	2016/12/07	Temperature (Celsius)	degrees C	11.5
UA	21	C	2017/02/21	Temperature (Celsius)	degrees C	14.2
UA	21	C	2017/04/25	Temperature (Celsius)	degrees C	22.9
UA	21	C	2017/06/08	Temperature (Celsius)	degrees C	14.6
UA	21	C	2017/09/06	Temperature (Celsius)	degrees C	13.3
UA	21	C	2017/11/15	Temperature (Celsius)	degrees C	13.5
UA	21	C	2018/03/26	Temperature (Celsius)	degrees C	13.7
UA	21	C	2018/06/13	Temperature (Celsius)	degrees C	16.3
UA	21	C	2018/09/12	Temperature (Celsius)	degrees C	15.8
UA	21	C	2018/12/12	Temperature (Celsius)	degrees C	12.7
UA	21	C	2019/03/13	Temperature (Celsius)	degrees C	12.2
UA	21	C	2019/06/19	Temperature (Celsius)	degrees C	13.5
UA	21	C	2013/03/08	Total Dissolved Solids	mg/L	518
UA	21	C	2013/06/07	Total Dissolved Solids	mg/L	564
UA	21	C	2013/09/03	Total Dissolved Solids	mg/L	618
UA	21	C	2013/12/10	Total Dissolved Solids	mg/L	540
UA	21	C	2014/03/25	Total Dissolved Solids	mg/L	442
UA	21	C	2014/08/19	Total Dissolved Solids	mg/L	546
UA	21	C	2014/09/30	Total Dissolved Solids	mg/L	546
UA	21	C	2015/03/18	Total Dissolved Solids	mg/L	542
UA	21	C	2015/09/16	Total Dissolved Solids	mg/L	564
UA	21	C	2015/12/10	Total Dissolved Solids	mg/L	532
UA	21	C	2016/03/09	Total Dissolved Solids	mg/L	560
UA	21	C	2016/06/07	Total Dissolved Solids	mg/L	588
UA	21	C	2016/09/15	Total Dissolved Solids	mg/L	582
UA	21	C	2016/12/07	Total Dissolved Solids	mg/L	532
UA	21	C	2017/02/21	Total Dissolved Solids	mg/L	532
UA	21	C	2017/04/25	Total Dissolved Solids	mg/L	564
UA	21	C	2017/06/08	Total Dissolved Solids	mg/L	558
UA	21	C	2017/09/06	Total Dissolved Solids	mg/L	558
UA	21	C	2017/11/15	Total Dissolved Solids	mg/L	572
UA	21	C	2018/03/26	Total Dissolved Solids	mg/L	560
UA	21	C	2018/06/13	Total Dissolved Solids	mg/L	586
UA	21	C	2018/09/12	Total Dissolved Solids	mg/L	644
UA	21	C	2018/12/12	Total Dissolved Solids	mg/L	568
UA	21	C	2019/03/13	Total Dissolved Solids	mg/L	338
UA	21	C	2019/06/19	Total Dissolved Solids	mg/L	508
UA	24	C	2013/03/08	pH (field)	SU	7.3
UA	24	C	2013/06/07	pH (field)	SU	7.8
UA	24	C	2013/09/03	pH (field)	SU	7.8
UA	24	C	2013/12/10	pH (field)	SU	7.6

UA	24	C	2014/03/25	pH (field)	SU	7.5
UA	24	C	2014/08/19	pH (field)	SU	7.8
UA	24	C	2014/09/30	pH (field)	SU	7.6
UA	24	C	2015/03/18	pH (field)	SU	7.6
UA	24	C	2015/09/16	pH (field)	SU	8.0
UA	24	C	2015/12/10	pH (field)	SU	7.6
UA	24	C	2016/03/09	pH (field)	SU	7.8
UA	24	C	2016/06/07	pH (field)	SU	7.6
UA	24	C	2016/09/15	pH (field)	SU	7.6
UA	24	C	2016/12/07	pH (field)	SU	7.4
UA	24	C	2017/02/21	pH (field)	SU	7.5
UA	24	C	2017/04/25	pH (field)	SU	7.3
UA	24	C	2017/06/08	pH (field)	SU	7.4
UA	24	C	2017/09/06	pH (field)	SU	7.4
UA	24	C	2017/11/15	pH (field)	SU	7.7
UA	24	C	2018/03/26	pH (field)	SU	7.6
UA	24	C	2018/06/13	pH (field)	SU	7.0
UA	24	C	2018/09/12	pH (field)	SU	7.4
UA	24	C	2018/12/12	pH (field)	SU	7.4
UA	24	C	2019/03/13	pH (field)	SU	7.5
UA	24	C	2019/06/19	pH (field)	SU	7.5
UA	24	C	2015/12/10	Oxidation Reduction Potential	mV	-78.0
UA	24	C	2016/03/09	Oxidation Reduction Potential	mV	-155
UA	24	C	2016/06/07	Oxidation Reduction Potential	mV	-114
UA	24	C	2016/09/15	Oxidation Reduction Potential	mV	-123
UA	24	C	2016/12/07	Oxidation Reduction Potential	mV	-90.0
UA	24	C	2017/02/21	Oxidation Reduction Potential	mV	-87.0
UA	24	C	2017/04/25	Oxidation Reduction Potential	mV	-142
UA	24	C	2017/06/08	Oxidation Reduction Potential	mV	-160
UA	24	C	2017/11/15	Oxidation Reduction Potential	mV	-102
UA	24	C	2018/06/13	Oxidation Reduction Potential	mV	-138
UA	24	C	2018/09/12	Oxidation Reduction Potential	mV	-153
UA	24	C	2018/12/12	Oxidation Reduction Potential	mV	-135
UA	24	C	2019/03/13	Oxidation Reduction Potential	mV	-119
UA	24	C	2019/06/19	Oxidation Reduction Potential	mV	-112
UA	24	C	2015/12/10	Eh	V	0.12
UA	24	C	2016/03/09	Eh	V	0.043
UA	24	C	2016/06/07	Eh	V	0.083
UA	24	C	2016/09/15	Eh	V	0.074
UA	24	C	2016/12/07	Eh	V	0.11
UA	24	C	2017/02/21	Eh	V	0.11
UA	24	C	2017/04/25	Eh	V	0.050
UA	24	C	2017/06/08	Eh	V	0.034
UA	24	C	2017/11/15	Eh	V	0.095
UA	24	C	2018/06/13	Eh	V	0.058
UA	24	C	2018/09/12	Eh	V	0.044
UA	24	C	2018/12/12	Eh	V	0.063
UA	24	C	2019/03/13	Eh	V	0.078
UA	24	C	2019/06/19	Eh	V	0.085
UA	24	C	2013/06/07	Arsenic, total	mg/L	0.00890
UA	24	C	2013/09/03	Arsenic, total	mg/L	0.00880
UA	24	C	2015/12/10	Arsenic, total	mg/L	0.0279
UA	24	C	2016/03/09	Arsenic, total	mg/L	0.0263
UA	24	C	2016/06/07	Arsenic, total	mg/L	0.0275
UA	24	C	2016/09/15	Arsenic, total	mg/L	0.0328
UA	24	C	2016/12/07	Arsenic, total	mg/L	0.0343
UA	24	C	2017/02/21	Arsenic, total	mg/L	0.0300
UA	24	C	2017/04/25	Arsenic, total	mg/L	0.0319
UA	24	C	2017/06/08	Arsenic, total	mg/L	0.0313
UA	24	C	2018/06/13	Arsenic, total	mg/L	0.0336
UA	24	C	2018/09/12	Arsenic, total	mg/L	0.0332
UA	24	C	2018/12/12	Arsenic, total	mg/L	0.0332

UA	24	C	2019/03/13	Arsenic, total	mg/L	0.0380
UA	24	C	2019/06/19	Arsenic, total	mg/L	0.0254
UA	24	C	2013/06/07	Barium, total	mg/L	0.0424
UA	24	C	2013/09/03	Barium, total	mg/L	0.0397
UA	24	C	2015/12/10	Barium, total	mg/L	0.0499
UA	24	C	2016/03/09	Barium, total	mg/L	0.0451
UA	24	C	2016/06/07	Barium, total	mg/L	0.0538
UA	24	C	2016/09/15	Barium, total	mg/L	0.0536
UA	24	C	2016/12/07	Barium, total	mg/L	0.0588
UA	24	C	2017/02/21	Barium, total	mg/L	0.0550
UA	24	C	2017/04/25	Barium, total	mg/L	0.0535
UA	24	C	2017/06/08	Barium, total	mg/L	0.0575
UA	24	C	2018/06/13	Barium, total	mg/L	0.0634
UA	24	C	2018/09/12	Barium, total	mg/L	0.0653
UA	24	C	2018/12/12	Barium, total	mg/L	0.0705
UA	24	C	2019/03/13	Barium, total	mg/L	0.0699
UA	24	C	2019/06/19	Barium, total	mg/L	0.0555
UA	24	C	2013/06/07	Boron, total	mg/L	3.02
UA	24	C	2013/09/03	Boron, total	mg/L	2.90
UA	24	C	2015/12/10	Boron, total	mg/L	3.39
UA	24	C	2016/03/09	Boron, total	mg/L	3.19
UA	24	C	2016/06/07	Boron, total	mg/L	3.84
UA	24	C	2016/09/15	Boron, total	mg/L	2.80
UA	24	C	2016/12/07	Boron, total	mg/L	2.81
UA	24	C	2017/02/21	Boron, total	mg/L	2.74
UA	24	C	2017/04/25	Boron, total	mg/L	2.54
UA	24	C	2017/06/08	Boron, total	mg/L	2.41
UA	24	C	2017/11/15	Boron, total	mg/L	2.48
UA	24	C	2018/06/13	Boron, total	mg/L	2.36
UA	24	C	2018/09/12	Boron, total	mg/L	2.22
UA	24	C	2018/12/12	Boron, total	mg/L	2.39
UA	24	C	2019/03/13	Boron, total	mg/L	2.44
UA	24	C	2019/06/19	Boron, total	mg/L	2.11
UA	24	C	2013/06/07	Cadmium, total	mg/L	<0.0003
UA	24	C	2013/09/03	Cadmium, total	mg/L	<0.0003
UA	24	C	2015/12/10	Cadmium, total	mg/L	<0.0002
UA	24	C	2016/03/09	Cadmium, total	mg/L	<0.0002
UA	24	C	2016/06/07	Cadmium, total	mg/L	<0.0002
UA	24	C	2016/09/15	Cadmium, total	mg/L	<0.0002
UA	24	C	2016/12/07	Cadmium, total	mg/L	<0.0002
UA	24	C	2017/02/21	Cadmium, total	mg/L	<0.0002
UA	24	C	2017/04/25	Cadmium, total	mg/L	<0.0002
UA	24	C	2017/06/08	Cadmium, total	mg/L	<0.0002
UA	24	C	2018/06/13	Cadmium, total	mg/L	<0.0002
UA	24	C	2018/09/12	Cadmium, total	mg/L	<0.0002
UA	24	C	2018/12/12	Cadmium, total	mg/L	<0.0002
UA	24	C	2019/03/13	Cadmium, total	mg/L	<0.0002
UA	24	C	2019/06/19	Cadmium, total	mg/L	<0.0002
UA	24	C	2015/12/10	Calcium, total	mg/L	125
UA	24	C	2016/03/09	Calcium, total	mg/L	108
UA	24	C	2016/06/07	Calcium, total	mg/L	152
UA	24	C	2016/09/15	Calcium, total	mg/L	139
UA	24	C	2016/12/07	Calcium, total	mg/L	150
UA	24	C	2017/02/21	Calcium, total	mg/L	142
UA	24	C	2017/04/25	Calcium, total	mg/L	127
UA	24	C	2017/06/08	Calcium, total	mg/L	141
UA	24	C	2017/11/15	Calcium, total	mg/L	152
UA	24	C	2018/06/13	Calcium, total	mg/L	145
UA	24	C	2018/09/12	Calcium, total	mg/L	133
UA	24	C	2018/12/12	Calcium, total	mg/L	141
UA	24	C	2019/03/13	Calcium, total	mg/L	143
UA	24	C	2019/06/19	Calcium, total	mg/L	107

UA	24	C	2013/03/08	Chloride, total	mg/L	45.0
UA	24	C	2013/06/07	Chloride, total	mg/L	38.0
UA	24	C	2013/09/03	Chloride, total	mg/L	40.0
UA	24	C	2013/12/10	Chloride, total	mg/L	45.0
UA	24	C	2014/03/25	Chloride, total	mg/L	43.0
UA	24	C	2014/09/30	Chloride, total	mg/L	55.0
UA	24	C	2015/03/18	Chloride, total	mg/L	55.0
UA	24	C	2015/09/16	Chloride, total	mg/L	46.0
UA	24	C	2015/12/10	Chloride, total	mg/L	47.0
UA	24	C	2016/03/09	Chloride, total	mg/L	51.0
UA	24	C	2016/06/07	Chloride, total	mg/L	63.0
UA	24	C	2016/09/15	Chloride, total	mg/L	69.0
UA	24	C	2016/12/07	Chloride, total	mg/L	75.0
UA	24	C	2017/02/21	Chloride, total	mg/L	70.0
UA	24	C	2017/04/25	Chloride, total	mg/L	82.0
UA	24	C	2017/06/08	Chloride, total	mg/L	77.0
UA	24	C	2017/09/06	Chloride, total	mg/L	85.0
UA	24	C	2017/11/15	Chloride, total	mg/L	86.0
UA	24	C	2018/03/26	Chloride, total	mg/L	89.0
UA	24	C	2018/06/13	Chloride, total	mg/L	99.0
UA	24	C	2018/09/12	Chloride, total	mg/L	106
UA	24	C	2018/12/12	Chloride, total	mg/L	96.0
UA	24	C	2019/03/13	Chloride, total	mg/L	95.0
UA	24	C	2019/06/19	Chloride, total	mg/L	88.0
UA	24	C	2013/03/08	Iron, dissolved	mg/L	2.39
UA	24	C	2013/12/10	Iron, dissolved	mg/L	0.679
UA	24	C	2014/03/25	Iron, dissolved	mg/L	3.02
UA	24	C	2014/08/19	Iron, dissolved	mg/L	0.235
UA	24	C	2014/09/30	Iron, dissolved	mg/L	3.75
UA	24	C	2015/03/18	Iron, dissolved	mg/L	3.27
UA	24	C	2015/09/16	Iron, dissolved	mg/L	1.81
UA	24	C	2016/03/09	Iron, dissolved	mg/L	3.68
UA	24	C	2016/09/15	Iron, dissolved	mg/L	4.83
UA	24	C	2017/02/21	Iron, dissolved	mg/L	3.27
UA	24	C	2017/09/06	Iron, dissolved	mg/L	5.57
UA	24	C	2018/03/26	Iron, dissolved	mg/L	4.43
UA	24	C	2015/12/10	Lithium, total	mg/L	0.0202
UA	24	C	2016/03/09	Lithium, total	mg/L	0.0195
UA	24	C	2016/06/07	Lithium, total	mg/L	0.0241
UA	24	C	2016/09/15	Lithium, total	mg/L	0.0220
UA	24	C	2016/12/07	Lithium, total	mg/L	0.0218
UA	24	C	2017/02/21	Lithium, total	mg/L	0.0202
UA	24	C	2017/04/25	Lithium, total	mg/L	0.0220
UA	24	C	2017/06/08	Lithium, total	mg/L	0.0193
UA	24	C	2018/06/13	Lithium, total	mg/L	0.0242
UA	24	C	2018/09/12	Lithium, total	mg/L	0.0257
UA	24	C	2018/12/12	Lithium, total	mg/L	0.0255
UA	24	C	2019/03/13	Lithium, total	mg/L	0.0270
UA	24	C	2019/06/19	Lithium, total	mg/L	0.0236
UA	24	C	2013/03/08	Manganese, dissolved	mg/L	0.0500
UA	24	C	2013/12/10	Manganese, dissolved	mg/L	0.0663
UA	24	C	2014/03/25	Manganese, dissolved	mg/L	0.0735
UA	24	C	2014/08/19	Manganese, dissolved	mg/L	0.0398
UA	24	C	2014/09/30	Manganese, dissolved	mg/L	0.0835
UA	24	C	2015/03/18	Manganese, dissolved	mg/L	0.0733
UA	24	C	2015/09/16	Manganese, dissolved	mg/L	0.0576
UA	24	C	2016/03/09	Manganese, dissolved	mg/L	0.0860
UA	24	C	2016/09/15	Manganese, dissolved	mg/L	0.101
UA	24	C	2017/02/21	Manganese, dissolved	mg/L	0.100
UA	24	C	2017/09/06	Manganese, dissolved	mg/L	0.110
UA	24	C	2018/03/26	Manganese, dissolved	mg/L	0.100
UA	24	C	2013/03/08	Sulfate, total	mg/L	192

UA	24	C	2013/06/07	Sulfate, total	mg/L	108
UA	24	C	2013/09/03	Sulfate, total	mg/L	75.0
UA	24	C	2013/12/10	Sulfate, total	mg/L	139
UA	24	C	2014/03/25	Sulfate, total	mg/L	154
UA	24	C	2014/09/30	Sulfate, total	mg/L	179
UA	24	C	2015/03/18	Sulfate, total	mg/L	162
UA	24	C	2015/09/16	Sulfate, total	mg/L	135
UA	24	C	2015/12/10	Sulfate, total	mg/L	140
UA	24	C	2016/03/09	Sulfate, total	mg/L	133
UA	24	C	2016/06/07	Sulfate, total	mg/L	135
UA	24	C	2016/09/15	Sulfate, total	mg/L	143
UA	24	C	2016/12/07	Sulfate, total	mg/L	149
UA	24	C	2017/02/21	Sulfate, total	mg/L	131
UA	24	C	2017/04/25	Sulfate, total	mg/L	140
UA	24	C	2017/06/08	Sulfate, total	mg/L	148
UA	24	C	2017/09/06	Sulfate, total	mg/L	141
UA	24	C	2017/11/15	Sulfate, total	mg/L	128
UA	24	C	2018/03/26	Sulfate, total	mg/L	139
UA	24	C	2018/06/13	Sulfate, total	mg/L	120
UA	24	C	2018/09/12	Sulfate, total	mg/L	133
UA	24	C	2018/12/12	Sulfate, total	mg/L	119
UA	24	C	2019/03/13	Sulfate, total	mg/L	101
UA	24	C	2019/06/19	Sulfate, total	mg/L	95.0
UA	24	C	2013/03/08	Temperature (Celsius)	degrees C	11.3
UA	24	C	2013/06/07	Temperature (Celsius)	degrees C	13.2
UA	24	C	2013/09/03	Temperature (Celsius)	degrees C	15.3
UA	24	C	2013/12/10	Temperature (Celsius)	degrees C	9.90
UA	24	C	2014/03/25	Temperature (Celsius)	degrees C	10.2
UA	24	C	2014/08/19	Temperature (Celsius)	degrees C	13.3
UA	24	C	2014/09/30	Temperature (Celsius)	degrees C	12.6
UA	24	C	2015/03/18	Temperature (Celsius)	degrees C	12.4
UA	24	C	2015/09/16	Temperature (Celsius)	degrees C	12.8
UA	24	C	2015/12/10	Temperature (Celsius)	degrees C	13.9
UA	24	C	2016/03/09	Temperature (Celsius)	degrees C	11.6
UA	24	C	2016/06/07	Temperature (Celsius)	degrees C	12.2
UA	24	C	2016/09/15	Temperature (Celsius)	degrees C	13.6
UA	24	C	2016/12/07	Temperature (Celsius)	degrees C	10.7
UA	24	C	2017/02/21	Temperature (Celsius)	degrees C	13.1
UA	24	C	2017/04/25	Temperature (Celsius)	degrees C	20.1
UA	24	C	2017/06/08	Temperature (Celsius)	degrees C	17.2
UA	24	C	2017/09/06	Temperature (Celsius)	degrees C	12.4
UA	24	C	2017/11/15	Temperature (Celsius)	degrees C	12.3
UA	24	C	2018/03/26	Temperature (Celsius)	degrees C	12.8
UA	24	C	2018/06/13	Temperature (Celsius)	degrees C	13.7
UA	24	C	2018/09/12	Temperature (Celsius)	degrees C	13.3
UA	24	C	2018/12/12	Temperature (Celsius)	degrees C	11.7
UA	24	C	2019/03/13	Temperature (Celsius)	degrees C	12.4
UA	24	C	2019/06/19	Temperature (Celsius)	degrees C	12.3
UA	24	C	2013/03/08	Total Dissolved Solids	mg/L	578
UA	24	C	2013/06/07	Total Dissolved Solids	mg/L	376
UA	24	C	2013/09/03	Total Dissolved Solids	mg/L	324
UA	24	C	2013/12/10	Total Dissolved Solids	mg/L	522
UA	24	C	2014/03/25	Total Dissolved Solids	mg/L	526
UA	24	C	2014/08/19	Total Dissolved Solids	mg/L	336
UA	24	C	2014/09/30	Total Dissolved Solids	mg/L	622
UA	24	C	2015/03/18	Total Dissolved Solids	mg/L	630
UA	24	C	2015/09/16	Total Dissolved Solids	mg/L	558
UA	24	C	2015/12/10	Total Dissolved Solids	mg/L	568
UA	24	C	2016/03/09	Total Dissolved Solids	mg/L	458
UA	24	C	2016/06/07	Total Dissolved Solids	mg/L	564
UA	24	C	2016/09/15	Total Dissolved Solids	mg/L	648
UA	24	C	2016/12/07	Total Dissolved Solids	mg/L	632

UA	24	C	2017/02/21	Total Dissolved Solids	mg/L	602
UA	24	C	2017/04/25	Total Dissolved Solids	mg/L	676
UA	24	C	2017/06/08	Total Dissolved Solids	mg/L	658
UA	24	C	2017/09/06	Total Dissolved Solids	mg/L	696
UA	24	C	2017/11/15	Total Dissolved Solids	mg/L	702
UA	24	C	2018/03/26	Total Dissolved Solids	mg/L	654
UA	24	C	2018/06/13	Total Dissolved Solids	mg/L	714
UA	24	C	2018/09/12	Total Dissolved Solids	mg/L	822
UA	24	C	2018/12/12	Total Dissolved Solids	mg/L	722
UA	24	C	2019/03/13	Total Dissolved Solids	mg/L	690
UA	24	C	2019/06/19	Total Dissolved Solids	mg/L	540

Notes:

< = results is less than detection limit
B = Background
C = Compliance
HSU = Hydrostratigraphic Unit
CCR = Coal Combustion Residuals
UA = Uppermost Aquifer
mg/L = milligrams per liter
SU = standard units
V = volts

ADDENDUM TO NATURE AND EXTENT REPORT

(IN DEVELOPMENT)

Appendix E

Groundwater Polishing Report

Geosyntec
consultants

engineers | scientists | innovators

Groundwater Polishing Evaluation Report

Hennepin Power Plant – West Ash Pond System

(IEPA ID No. W1550100002-01 and W1550100002-03)

Prepared for

Dynegy Midwest Generation, LLC

1500 Eastport Plaza Drive
Collinsville, Illinois 62234

Prepared by

Geosyntec Consultants, Inc.
134 N. Lasalle Street, Suite 300
Chicago, Illinois 60602

Project Number: GLP8079

March 2025

TABLE OF CONTENTS

LIST OF INTERNAL TABLES

LIST OF FIGURES

LIST OF ATTACHMENTS

ACRONYMS AND ABBREVIATIONS

BCU	bedrock confining unit
CAAA	Corrective Actions Alternative Analysis
CCR	coal combustion residuals
COC	constituent of concern
GCSM	geochemical conceptual site model
GWB	Geochemist’s Workbench®
GWPS	groundwater protection standard
IEPA	Illinois Environmental Protection Agency
mg/kg	milligrams per kilogram
OWAP	Old West Ash Pond
OWPP	Old West Polishing Pond
redox	oxidation-reduction
SEP	sequential extraction procedure
SU	standard units
TDS	total dissolved solids
UAU	uppermost aquifer unit
µg/g	micrograms per gram
µg/L	micrograms per liter
USEPA	United States Environmental Protection Agency
WAPS	West Ash Pond System
XRD	X-ray diffraction

EXECUTIVE SUMMARY

This document has been prepared as an attachment to the Corrective Actions Alternatives Analysis (CAAA) prepared by Gradient for Hennepin Power Plant West Ash Pond System (WAPS). The constituents of concern (COCs) addressed in this document are arsenic, boron, lithium, sulfate, and total dissolved solids (TDS), which have been identified as having exceedances[1] of the site-specific groundwater protection standards (GWPS) at the time of this analysis. Of these COCs, boron, sulfate, and arsenic were addressed in geochemical modeling efforts. Natural geochemical processes may be appropriate as a "polishing step" for residual plume management after effective source control implementation, if there are no risks to receptors and/or the contaminant plume is not expanding (United States Environmental Protection Agency [USEPA] 1999; USEPA 2015). Source control is a major component of every corrective action considered in the CAAA, and there are no risks to human health or the environment at Hennepin WAPS.

Natural groundwater polishing processes, which include both physical and chemical mechanisms, reduce the concentration of COCs in the groundwater. After source control is implemented, a geochemical trailing gradient may form in the subsurface as conditions undergo a return to background water quality which could affect chemical groundwater polishing mechanisms (Savannah River National Laboratory 2011). This report supports groundwater polishing as a component of the proposed corrective action by evaluating the contribution of chemical mechanisms to groundwater polishing under current conditions and after source control implementation. The groundwater flow and transport model estimated the time to reach the GWPS based on hydraulic properties of the aquifer. The results of this groundwater polishing evaluation contextualize these estimates by evaluating the potential for attenuation of COCs and for previously attenuated COCs to be mobilized to groundwater as groundwater quality returns to background conditions.

Groundwater polishing mechanisms were assessed using speciation and reaction geochemical models: speciation models assess the distribution of constituents between solid and aqueous phases, and reaction models evaluate how that distribution may change with changing site conditions (USEPA 2015). Inputs to the model include geochemically reactive solid mineral phases, compliance well groundwater composition, and background groundwater composition based on site-specific data. Additional modeling and analysis was completed to better understand arsenic speciation, solubility, and mechanisms of mobilization at wells with arsenic GWPS exceedances.

The results of the groundwater polishing evaluation indicate that chemical attenuation of modeled COCs (arsenic, boron, and sulfate) is feasible under current conditions through sorption to iron and aluminum oxide minerals. Though some degree of desorption is predicted with background

---

[1] Throughout this document, "exceedance" or "exceedances" is intended to refer only to potential exceedances of proposed applicable background statistics or Groundwater Protection Standards as described in the proposed groundwater monitoring program which was submitted to the IEPA on October 25, 2021 as part of Dynegy Midwest Generation, LLC's operating permit application for the West Ash Pond System. That operating permit application, including the proposed groundwater monitoring program, remains under review by the IEPA and therefore Dynegy Midwest Generation, LLC has not identified any actual exceedances.

water interaction, aqueous boron and sulfate (and therefore TDS) concentrations should decrease below the GWPS at all wells in the compliance monitoring network following source control. Remobilization of boron and sulfate is unlikely to affect the estimated time to reach the GWPS based on modeling results. Aqueous arsenic concentrations are predicted to increase at wells with current exceedances following remobilization of arsenic under future conditions. Remobilization may impact the time to reach the GWPS for arsenic. Lithium was not evaluated in the geochemical modeling because lithium concentrations continue to decline following unit closure. These results will inform corrective action groundwater monitoring and adaptive site management, critical components every corrective action considered in the CAAA.

1. INTRODUCTION

This document has been prepared as an attachment to the Corrective Actions Alternatives Analysis (CAAA) prepared by Gradient for Hennepin Power Plant West Ash Pond System (WAPS). The purpose of the CAAA is to holistically evaluate potentially viable corrective actions to remediate groundwater and achieve compliance with GWPS for all monitored parameters under Title 35 of the Illinois Administrative Code (35 I.A.C.) § 845.600. The constituents of concern (COCs) addressed in this document are arsenic, boron, lithium, sulfate, and total dissolved solids (TDS)[2], which have been identified as having exceedances of the site-specific groundwater protection standards (GWPS) at the time of this analysis. In the CAAA, all corrective actions considered consist of source control and residual plume management. Natural geochemical processes may be appropriate as a "polishing step" for residual plume management after effective source control implementation, if there are no risks to receptors and/or the contaminant plume is not expanding (United States Environmental Protection Agency [USEPA] 1999; USEPA 2015). Source control is a major component of every corrective action considered in the CAAA, and there are no risks to human health or the environment at Hennepin WAPS.[3]

Groundwater polishing processes include both physical and chemical mechanisms within the subsurface which reduce the concentration of COCs in the groundwater. Physical components of groundwater polishing, including advection, dilution, and dispersion, are assessed by groundwater flow and transport modeling (Groundwater Modeling Technical Memorandum[4]). Chemical mechanisms of groundwater polishing include sorption and mineral precipitation. After source control is implemented, a geochemical trailing gradient may form in the subsurface as conditions undergo a return to background water quality which could affect chemical groundwater polishing mechanisms (Savannah River National Laboratory [SRNL], 2011). The chemical mechanisms of groundwater polishing at Hennepin WAPS are evaluated herein using a geochemical modeling-based approach informed by site-specific data. This report uses geochemical modeling to evaluate the influence of chemical mechanisms on groundwater polishing under current conditions and future conditions. Additional modeling and analyses were conducted to further investigate arsenic distribution, solubility, and mobilization within the western portion of the WAPS.

The groundwater flow and transport model (Groundwater Modeling Technical Memorandum[5]) estimated the time for COCs to reach their respective GWPS under different potential corrective actions based on physical components of groundwater polishing and did not incorporate any potential chemical controls on parameter distribution. The geochemical modeling efforts presented herein support the assessment of groundwater polishing as a component of the proposed corrective

---

[2] TDS measurements represent the total mass of dissolved constituents in a sample rather than a single chemical behavior. Because sulfate is the dominant contributor to TDS, results for sulfate in this analysis also apply to TDS.

[3] The Human Health and Ecological Risk Assessment serves as Appendix A of the CAAA to which this report is attached.

[4] The Groundwater Modeling Technical Memorandum serves as Appendix B.1 of the Corrective Action Supporting Information Report; the Corrective Action Supporting Information Report serves as Appendix B of the CAAA to which this report is attached.

[5] Ibid.

action by evaluating the potential for chemical attenuation of COCs under current and predicted future conditions as a means of contextualizing the times estimated in the flow and transport model. This analysis also provides an initial foundation for understanding groundwater chemistry to inform adaptive site management as a key component of the Corrective Action Groundwater Monitoring Plan[6].

---

[6] The Corrective Action Groundwater Monitoring Plan serves as Appendix B.1 to the Construction Permit Application.

2. SITE BACKGROUND

2.1 Site Overview

A thorough overview of general site characteristics is presented in Section 1 of the CAAA to which this document is attached and summarized here. The Hennepin Power Plant is owned by Dynegy Midwest Generation, LLC and was in operation from the early 1950s to 2019. The facility is located four miles northeast of the Village of Hennepin, Illinois, along the Illinois River. The Hennepin WAPS is located west of the Hennepin Power Plant and adjacent to the Illinois River. The Hennepin Power Plant property is bordered by farm fields to the east and south, low lying floodplains to the west, and the Illinois River to the north.

The WAPS is comprised of two inactive sub-units, the Old West Ash Pond (OWAP) and the Old West Polishing Pond (OWPP). The OWAP includes a 9.3-acre Pond No.1 on the eastern end of the WAPS impoundment and a 16.4-acre Pond No. 3 in the central portion of the impoundment. Pond No. 1 accepted bottom ash and slag and Pond No. 3 accepted mixed coal ash. The 4.7-acre OWPP was used as a secondary pond and is located on the western end of the impoundment. The WAPS operated between 1952 and 1996, and closure occurred between 2019 and 2020 (Dynegy 2020a and 2020b).

A groundwater monitoring network was proposed in the Initial Operating Permit Application (Burns & McDonnell 2021) in accordance with 35 I.A.C. § 845.630 to monitor groundwater quality which passes the waste boundary as part of the Operating Permit Application to Illinois Environmental Protection Agency (IEPA) for the WAPS. The proposed groundwater monitoring network is shown in **Attachment A**. The monitoring network consists of nine compliance monitoring wells (21R, 22, 22D, 23, 27, 35, 49, 50, and 51) and two background wells (32 and 34).

The geology underlying the Site in the vicinity of the WAPS consists of three distinct hydrostratigraphic units (Natural Resource Technology, Inc. 2017):

- **Fill Unit:** The Fill Unit underlies the WAPS and was present in all Pond sub-units prior to closure. The Fill Unit consists of coal combustion residuals (CCR), primarily fly ash and smaller amounts of bottom ash and slag. In some locations within the unit, CCR was mixed with sand, silt, and clay to form constructed berms. The Fill Unit no longer underlies the western end of the WAPS, as CCR and one foot of soil beneath the CCR was removed from the OWPP during closure.

- **Uppermost Aquifer Unit (UAU):** The UAU contains clay, silt, and sand, collectively referred to as Cahokia alluvium, and outwash sand and gravel deposits of the Henry Formation. The UAU is the uppermost aquifer and primary groundwater transport pathway in the vicinity of the WAPS.

- **Bedrock Confining Unit (BCU):** The BCU is a low permeability unit comprised of Pennsylvanian age shale with interbedded limestone, sandstone, and clay.

Groundwater within the UAU and near the WAPS migrates north and west towards the Illinois River, consistent with surface topography. When the WAPS was operational, sluicing of ash created radial flow conditions that caused a portion of the groundwater beneath the WAPS to flow towards wetlands located south and west of the OWAP. Under normal post-closure conditions, groundwater beneath the WAPS flows toward the river. Groundwater typically flows laterally within the hydrostratigraphic units, with converging upward flow near and beneath the river. A map showing representative groundwater flow direction at the site is shown in **Attachment A**.

2.2 Identified Exceedances of the GWPS

The following GWPS exceedances at compliance groundwater monitoring wells likely attributable to the Hennepin WAPS were observed from 2023 Q2 through 2024 Q3 (Ramboll 2024):

- Arsenic – Observed at monitoring wells 21R and 51.
- Boron – Observed at monitoring wells 21R, 22, 23, and 35.
- Lithium – Observed at monitoring well 22.
- Sulfate – Observed at monitoring wells 23 and 35.
- TDS – Observed at monitoring well 35.

The data set for geochemical modeling was finalized after the 2024 Q3 sampling event. Groundwater at these compliance wells is representative of groundwater conditions downgradient of the unit, and samples may be referred to as downgradient groundwater.

GWPS exceedances in the WAPS network occur exclusively in the UAU. Arsenic exceedances are limited to two wells near the northwest corner of the WAPS. Arsenic concentrations at these two monitoring locations have been elevated post-closure. Boron is widely distributed throughout the WAPS network, with multiple locations containing boron exceedances. Boron is generally stable or decreasing over time, except at well 35 which may be influenced by localized post-closure flow conditions near the south boundary of the WAPS. Lithium exceedances are limited to one monitoring location which has exhibited a decreasing trend over time. Sulfate exceedances were observed at two monitoring locations (wells 23 and 35). TDS exceedances are observed at one monitoring location (well 35). Sulfate is the dominant contributor to TDS at well 35, so TDS concentrations are expected to follow sulfate trends at this location.

Modeling parameters with observed exceedances is appropriate to the scope of the CAAA. Additionally, the selected remedy will meet the performance standards of 35 I.A.C. § 845.670(d) and the Corrective Action Plan will be submitted to the Agency on or before May 8, 2025. Once implemented and completed, the selected remedy will attain the GWPSs.

2.3 Geochemical Conceptual Site Model

A Geochemical Conceptual Site Model (GCSM)[7] was developed for the Hennepin WAPS to describe the geochemical processes that contribute to mobilization and attenuation of constituents in the environment under current conditions, including evaluating whether chemical interactions of COCs with aquifer solids contribute to attenuation of aqueous concentrations at compliance monitoring wells (Geosyntec 2024). This discussion relies on lab reports and raw data previously presented in the Nature and Extent Report submitted to IEPA on May 8, 2024 (Ramboll 2024) in accordance with 35 I.A.C. § 845.650(d)(1) and provided again in full and with relevant updates presenting ongoing work as Appendix D of the CAAA to which this report is attached.

The primary source of arsenic, boron, lithium, sulfate, and TDS to UAU groundwater is expected to be WAPS CCR porewater. This finding is based on COC concentrations within the source and relationships to hydrogeological patterns at the site. Arsenic, boron, and lithium were identified in UAU solids adjacent to downgradient and background wells, which suggests that aquifer solids may provide an additional geogenic source of these COCs to the groundwater.

The pH is generally circumneutral and consistent across the site, though compliance wells along the north side of the WAPS tend to have slightly higher pH values than background wells. An oxidation-reduction (redox) gradient is observed across the WAPS monitoring network, with groundwater conditions changing from oxidizing to reducing from east to west, likely due to the observed increased presence of organic-rich silty soils in the subsurface of the western portion of the WAPS monitoring network. Reducing conditions at western monitoring wells likely enhance arsenic solubility and thus aqueous arsenic concentrations at wells 21R and 51.

Arsenic, boron, lithium, and sulfate in the groundwater may be attenuated via surface complexation reactions with metal oxides, such as iron and aluminum oxides. These relationships can be evaluated through analyses of aquifer solids samples, which were collected adjacent to various compliance and background monitoring wells. Detailed discussion of aquifer solids sampling and analytical results is provided in the GCSM. Discussion of additional solids sampling and analyses completed in 2024 is provided in an Addendum to the GCSM[8].

Iron oxides were detected in the initial aquifer solids dataset and are generally predicted to be stable across the network. Magnetite, a crystalline iron oxide, was detected during X-ray diffraction (XRD) analyses of aquifer solids samples with values ranging from 0.2 to 0.5%. An abundance of iron was also detected during total metals analysis of UAU solids, with concentrations ranging from 9,400 to 14,000 milligrams of iron per kilogram of solids (mg/kg). Total iron observations do not correlate well with magnetite concentrations (i.e., samples with higher iron concentrations do not necessarily have higher iron oxide minerals identified in XRD results). This suggests the presence of non-crystalline, amorphous iron oxides in the aquifer solids.

---

[7] The GCSM is a component of the Nature and Extent Report previously submitted to IEPA (Ramboll 2024) and is provided with relevant updates as Appendix D of the CAAA to which this report is attached.

[8] The GCSM is a component of the Nature and Extent Report previously submitted to IEPA (Ramboll 2024) and is provided with relevant updates as Appendix D of the CAAA to which this report is attached.

Amorphous (non-crystalline) iron oxides were confirmed in SEP results from samples collected and analyzed in 2024 which included a non-crystalline analysis component.

Clay minerals (kaolinite and chlorite) were also identified in aquifer solids datasets and may provide an additional attenuation mechanism for COCs due to their large surface area and electrostatic charge. At locations where reducing conditions are present, microbial sulfate reduction may contribute to lower sulfate concentrations in groundwater. TDS trends are generally consistent with the major ions in the WAPS groundwater system. Therefore, attenuation of major ions, particularly sulfate, is expected to contribute to a reduction in TDS in the groundwater.

Batch attenuation testing was conducted for arsenic to evaluate sorption and generate site-specific distribution coefficients between solid and aqueous phases. Testing yielded a K_d value in general agreement with academic studies, thus providing additional evidence of arsenic attenuation via sorption to solids in the UAU.

The GCSM findings suggest the potential for chemical attenuation of arsenic, boron, lithium, and sulfate based on detected abundances of iron oxide and clay minerals and groundwater redox conditions which are generally favorable for the stability of potential sorbing surfaces. These findings are supported by analytical results of supplementary sampling and analyses completed in 2024. Attenuation of major ions, such as sulfate, is expected to contribute to a reduction in TDS in the groundwater.

3. GROUNDWATER POLISHING REMEDY EVALUATION

This groundwater polishing evaluation uses geochemical modeling to evaluate chemical attenuation of COCs under current conditions and to predict changes in attenuation at exceedance locations following source control. This evaluation will therefore further assess if chemical mechanisms of groundwater polishing will contribute to the remedy achieving the GWPS in a reasonable amount of time. Speciation and reaction models are geochemical models that can be used to evaluate the potential for chemical attenuation in groundwater. Speciation models assess the distribution of constituents between solid and aqueous phases, and reaction models evaluate how that distribution may change with changing site conditions (USEPA 2015). The results of geochemical modeling provide insight into groundwater polishing mechanisms and additional context for the time estimated to reach the GWPS determined by the groundwater flow and transport model[9], which is based on hydraulic properties of the aquifer and does not take into account chemical interactions occurring within the hydrologic unit. Additional sampling and analyses were completed to strengthen the conceptual understanding of arsenic speciation and solubility at these two locations. Detailed discussion of additional sample collection, analyses, and results are provided in the GCSM Addendum.

3.1 Methods

Geochemical modeling was done in PHREEQC Version 3 (USGS 2021) using a modified MINTEQ v4 thermodynamic database (as described in relevant sections below). The geochemical modeling of groundwater polishing under current conditions and conditions after source control is completed includes speciation and reaction modeling (USEPA 2015):

1. Speciation: To understand groundwater polishing mechanisms under current conditions, a solid phase representative of site conditions is equilibrated with current downgradient groundwater. The results of speciation modeling represent the association of COCs with the solid phase under current conditions through mechanisms such as sorption or precipitation.
2. Reaction: In the reaction modeling, the solid phase generated during the speciation modeling phase is reacted iteratively with background groundwater. These results represent the geochemical conditions expected after the source is controlled during which a trailing geochemical gradient may be created (SRNL 2011). The reactions with background groundwater assess the potential for a trailing geochemical gradient to drive changes in groundwater chemistry. Persistence of elevated groundwater COC concentrations over several reaction iterations suggests a trailing geochemical gradient may affect the time to reach the GWPS.

The equilibrium thermodynamic modeling approach used herein allows that the solid and aqueous phases reach equilibrium during each step. The primary goal of this model is to assess whether groundwater polishing is an appropriate remedy for the site by evaluating dominant geochemical

---

[9] The Groundwater Modeling Technical Memorandum serves as Appendix B.1 of the Corrective Action Supporting Information Report; the Corrective Action Supporting Information Report serves as Appendix B of the CAAA to which this report is attached.

reactions that may occur at time scales relevant to groundwater flow, including adsorption and certain mineral dissolution/precipitation (i.e., iron and aluminum (hydr)oxides, carbonates, and some sulfates) as identified in the GCSM[10]. The model therefore includes those parameters that are expected to contribute to those reactions (as discussed below) and does not include every constituent of the solid phase and groundwater in order to capture "the salient aspects of the system's behavior without introducing unnecessary complexity" (USEPA 2015). This model is therefore a semi-quantitative estimation of chemical behavior in the subsurface rather than a prediction of groundwater quality, consistent with USEPA guidance that geochemical modeling "is often most helpful for identifying relative changes in contaminant speciation and distribution" (USEPA 2015).

3.1.1 Model Set-Up

Inputs to the model include solid phase composition, downgradient groundwater composition for wells 21R, 22, 23, 35, and 51, representative background groundwater composition, and representative Illinois River composition for select model runs. The PHREEQC input files and modified MINTEQ v4 database are provided in **Attachment B**. The data included for model parameterization is summarized in **Table 1** and discussed in greater detail in **Attachment C**. Most data used in the model and discussed below are provided in the Nature and Extent Report[11], including additional solids data collected in 2024 (iron and aluminum SEP results).

3.1.2 Solid Phase Inputs

Iron hydroxide (ferrihydrite, [$Fe(OH)_3$]) and aluminum hydroxide (gibbsite [$Al(OH)_3$]) are widespread in the environment and known to act as sorbing phases for many groundwater constituents, including arsenic, boron, and sulfate (Dzombak and Morel 1990; Karamalidis and Dzombak 2010). SEP analyses for iron and aluminum from October 2024 sampling were used to populate the ferrihydrite and gibbsite component of the geochemical models, as described in greater detail in **Attachment C**.

Metal oxide concentrations representing the 25th percentile, median, and 75th percentile of the observed data were used to test the sensitivity of the model to the amount of sorbing phase present. Both ferrihydrite and gibbsite were allowed to dissolve or precipitate in the reaction phase of the model.

Calcite and dolomite were included as mineral phases in the model because carbonate mineral formation and dissolution are often major controls on groundwater pH (Stumm and Morgan 1996; Stackelberg et al. 2020). Calcite and dolomite are present in site aquifer solids, and model input concentration were based on site-specific XRD results. Both calcite and dolomite were allowed to dissolve or precipitate in the reaction phase of the model.

---

[10] The GCSM is a component of the Nature and Extent Report previously submitted to IEPA (Ramboll 2024) and is provided with relevant updates as Appendix D of the CAAA to which this report is attached.

[11] The Nature and Extent Report was previously submitted to IEPA (Ramboll 2024) and is provided with relevant updates as Appendix D of the CAAA to which this report is attached. The Nature and Extent report contains laboratory reports and tabulated results from solid phase analysis and tabulated results from groundwater analyses. Laboratory reports for groundwater data are provided quarterly to IEPA and posted to the facility's operating record in accordance with 35 I.A.C. § 845.800(d)(15).

Barite ($BaSO_4$) and gypsum ($CaSO_4$) are minerals that contain sulfate and have the potential to form under ambient environmental conditions in a timeframe consistent with the remedial effort. Therefore, these minerals may affect sulfate attenuation. Neither mineral phase was observed in mineralogical results for WAPS samples; therefore, both were made available to precipitate from the aqueous solution but did not have initial concentrations provided.

3.1.3 Aqueous Inputs

In addition to arsenic, boron, and sulfate, the following parameters are included to capture the expected attenuation and mobilization mechanisms (see **Section 2.3**):

- Temperature, pH and pe[12]
- Major ions: Carbonate and bicarbonate alkalinity, chloride, fluoride, calcium, magnesium, potassium, and sodium
- Oxyanions: Silicon and phosphate
- Redox-active metals: Aluminum, iron, and manganese.
- Remaining constituents regulated under 35 IAC § 845.600[13].

This full suite of geochemical parameters for this model was measured in Quarter 2 and Quarter 3, 2023. The medians of these results were used in the model to represent average groundwater interacting with the solid phase (details provided in **Attachment C**). For downgradient wells with GWPS exceedances, the median for each parameter was calculated for each location individually.

The WAPS exhibits variable redox conditions and groundwater flow patterns across the site. Upgradient wells on the east side of the WAPS are not expected to be representative of background conditions for compliance wells on the west side of the WAPS, and vice-versa. The presence of a silty lens on the west side of the site is believed to contribute to more reducing conditions observed towards the west side of the WAPS, as discussed in Section 2.3. Additionally, groundwater monitoring has indicated the occasional reversal of groundwater flow direction at well 22 (i.e., from the river into the groundwater) due to elevated river levels associated with flooding events. As a result, background water sources in modeling must be specified for individual wells rather than applied to all WAPS compliance wells.

Background groundwater was represented in speciation and reaction modeling efforts for compliance wells 21R and 51 using the median composition of background well 34 from 2023 Q2 and Q3 sampling events (referred to as WAPS-West). Background groundwater was represented in modeling efforts for compliance wells 22, 23, and 35 using the median composition of background well 32 from 2023 Q2 and Q3 sampling events (referred to as WAPS-East).

---

[12] See **Appendix C** for details.

[13] Mercury, thallium, total dissolved solids, and radium were not included in the model. Mercury reactions within the environment are highly complex and would require a separate modeling effort, and the high frequency of non-detect concentrations in the groundwater indicate it would not contribute to model outcomes. Thallium forms a non-reactive monovalent cation and is rarely detected in the groundwater and is therefore not expected to contribute to model outcomes. Total dissolved solids are not a chemical parameter, but rather the result of other chemical abundances taken together. Radium is not included in most thermodynamic databases.

Additionally, the median composition of eight surface water samples collected from three sampling locations in the Illinois River immediately north of the WAPS was used in a separate model scenario to evaluate the Illinois River as a background water source for well 22 during flooding events (referred to as WAPS-River). These data are provided and discussed in the GCSM Addendum[14].

3.2 Results and Discussion

Geochemical modeling results are shown on **Figures 1 through 12** below. Current geochemical conditions are represented in model output figures as 'Speciation Model' and subsequent reaction calculation results are represented with 'First Reaction' and 'Second Reaction'. Full modeling outputs are provided in **Attachment D**. Results of geochemical modeling for WAPS-West model runs (wells 21R and 51) are presented in **Figures 1 to 5**. Results of modeling for WAPS-East model runs (wells 22, 23, and 35) are presented in **Figures 6 to 10**. **Figures 11 to 12** illustrate the effect of river water (WAPS-River) on geochemical reactions at well 22.

3.2.1 Model Results: WAPS West

Figure 1: Percentage of Sorbed Arsenic – West

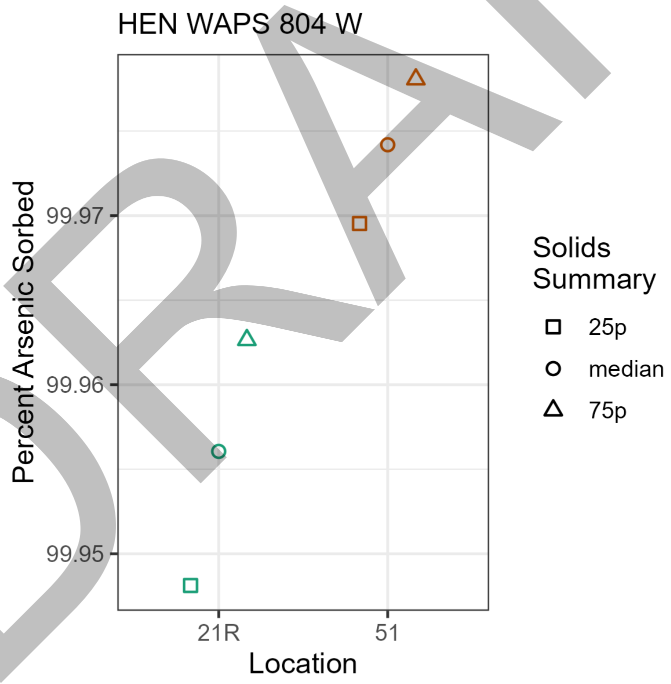

---

[14] The GCSM is a component of the Nature and Extent Report previously submitted to IEPA (Ramboll 2024) and is provided with relevant updates as Appendix D of the CAAA to which this report is attached.

Figure 2: Modeled Arsenic Behavior – West

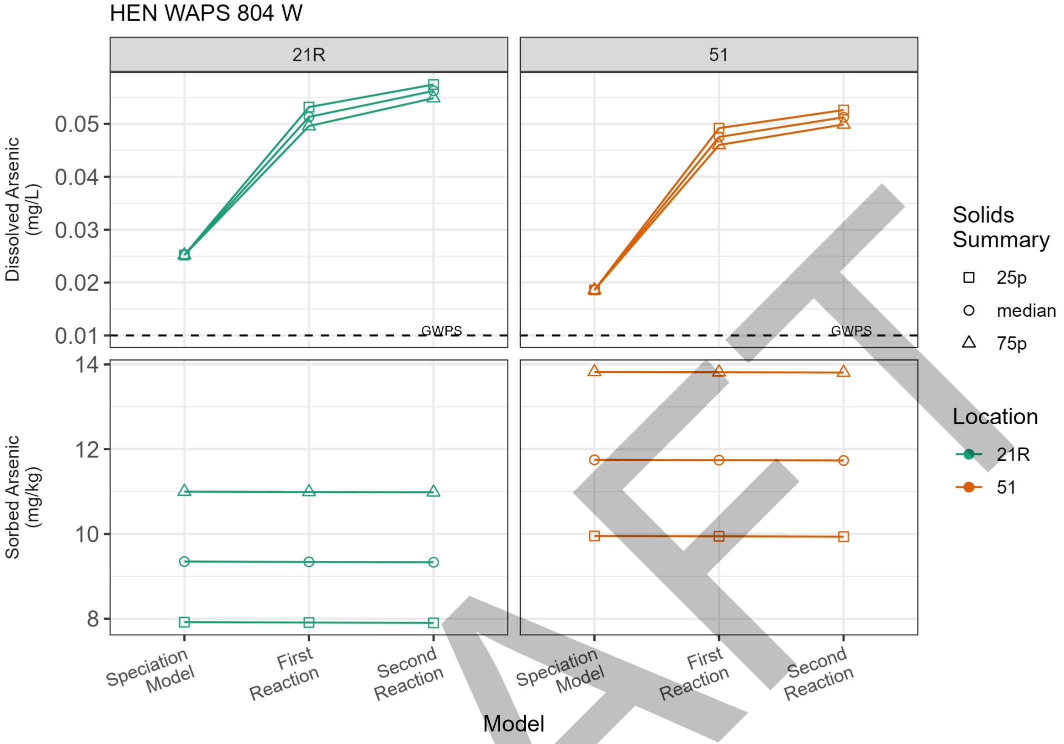

Figure 3: Percentage of Sorbed Boron - West

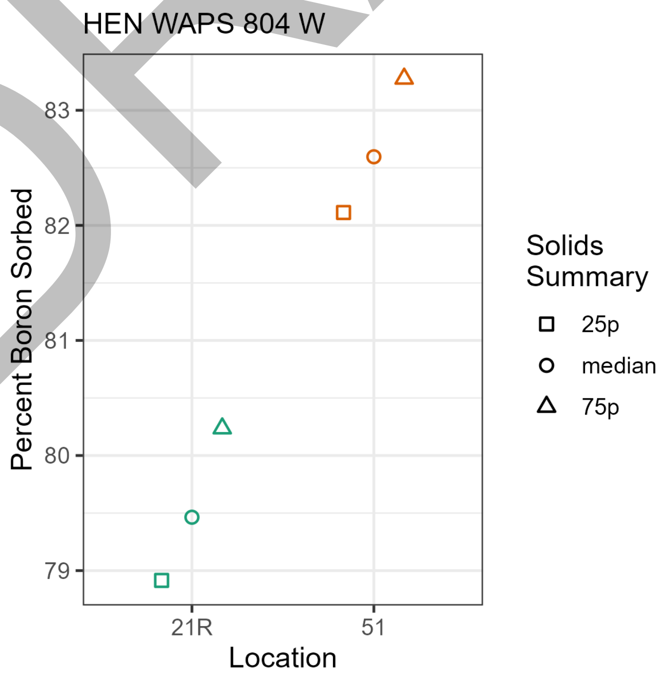

Figure 4: Modeled Boron Behavior – West

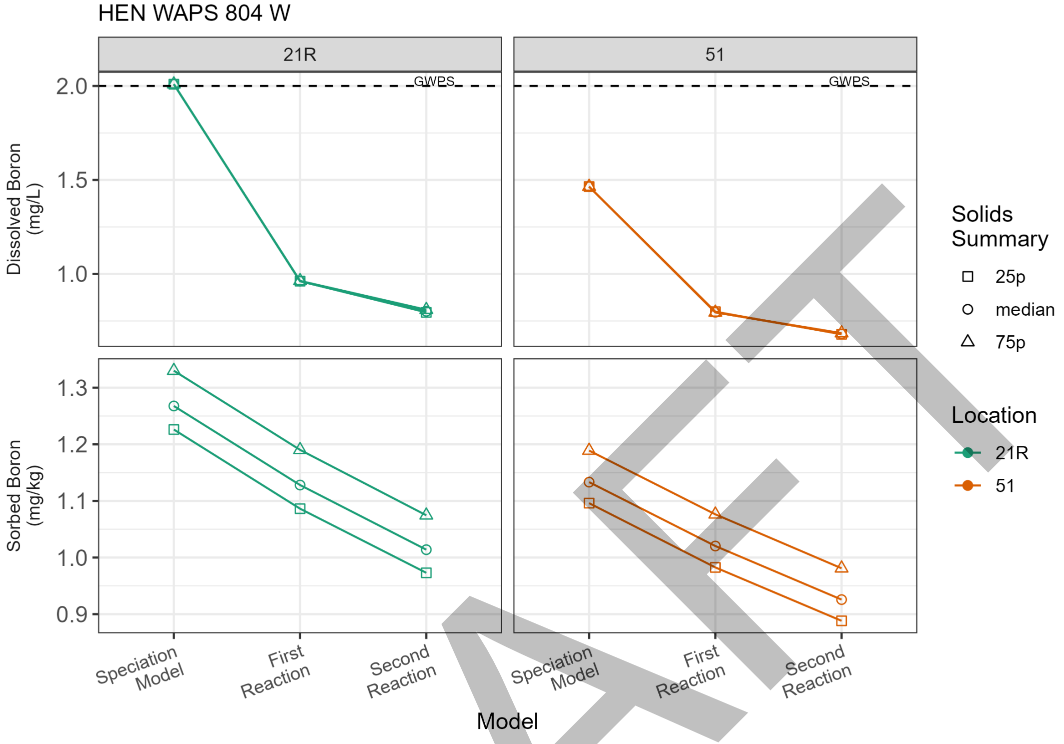

Figure 5: Modeled Sorbing Phase Behavior – West

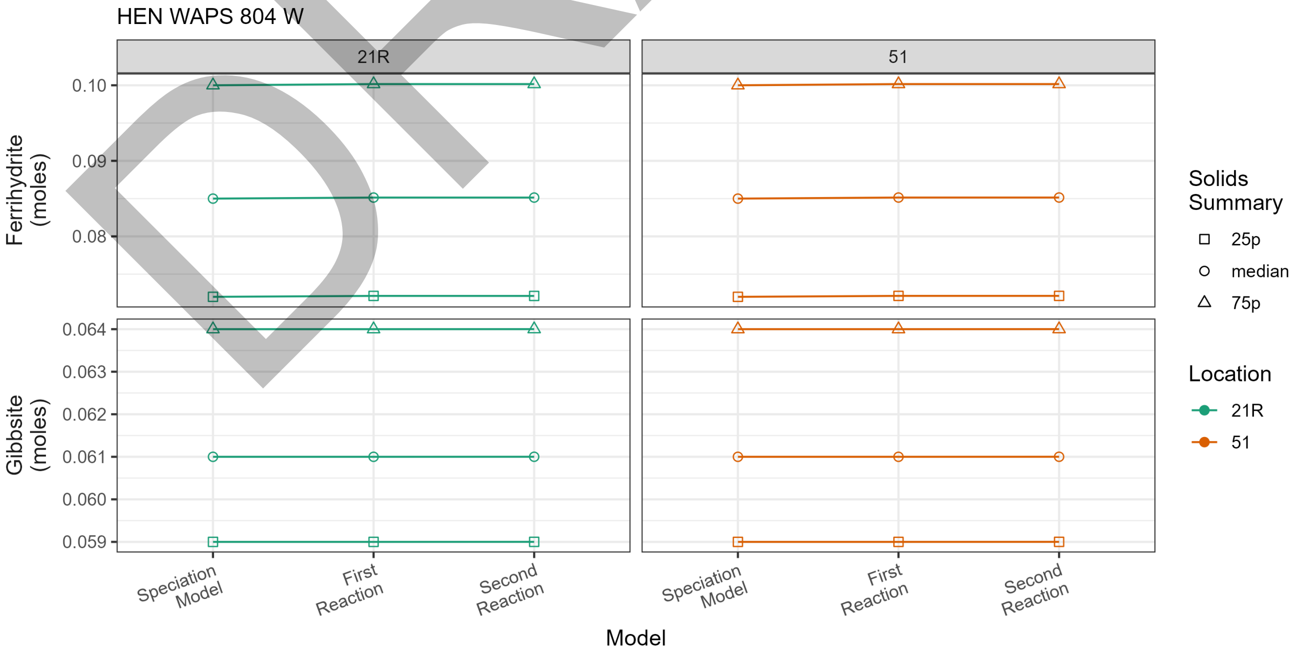

Results of speciation modeling for WAPS-West support the determination of the GCSM that chemical attenuation of arsenic and boron is likely to occur. Speciation calculations indicate that at wells with arsenic exceedances (21R and 51) greater than 99% of the arsenic present at (modeled) compliance wells is sorbed to mineral surfaces (**Figure 1**). Sensitivity assessments demonstrate that the sorbing mineral mass inputs have a minor impact on arsenic sorption, with the 25th and 75th percentile values for mineral mass accounting for differences of less than 1% of aqueous arsenic sorbed under current conditions. These results suggest that arsenic sorption to iron and aluminum hydroxide minerals should occur under current geochemical conditions.

Speciation calculations for boron indicate that at well 21R (the only well with boron exceedances on the western side of the WAPS), between 79 and 80% of boron present in groundwater will sorb to mineral surfaces (**Figure 3**). Sensitivity assessments demonstrate that the mineral mass inputs have a minor impact on boron sorption at well 21R, with the 25th and 75th percentile values for mineral mass accounting for approximately 1% of variability in aqueous boron sorbed under current conditions.

Reaction modeling results of conditions under future conditions for WAPS-West demonstrate that aqueous arsenic and boron concentrations change with interaction with background water. Aqueous arsenic concentrations are predicted to increase at wells with current exceedances (wells 21R and 51) with each iterative reaction (**Figure 2**). The predicted mobilization of arsenic is associated with desorption of arsenic from oxides, particularly ferrihydrite (**Attachment D**). This desorption is predicted to result in aqueous arsenic concentration increases following source control activities, which may impact the observed time to reach GWPS for arsenic. Arsenic speciation, solubility, and mobilization within the western portion of the WAPS is explored in greater detail in Section 3.3 of this document.

Aqueous boron concentrations at well 21R are predicted to decrease with each iterative reaction (**Figure 4**). While some boron desorption (< 0.3 mg/kg over two iterative reactions) is predicted for well 21R, the impact of this desorption on aqueous boron concentrations is offset by the influence of background groundwater containing lower aqueous boron concentrations. Mobilization of boron at well 21R is therefore unlikely to affect the modeled time to reach the GWPS.

3.2.2 Model Results – WAPS East

Results of modeling for WAPS-East model runs (wells 22, 23, and 35 with background well 32) are presented in **Figures 6 to 10**.

Figure 6: Percentage of Sorbed Boron – East

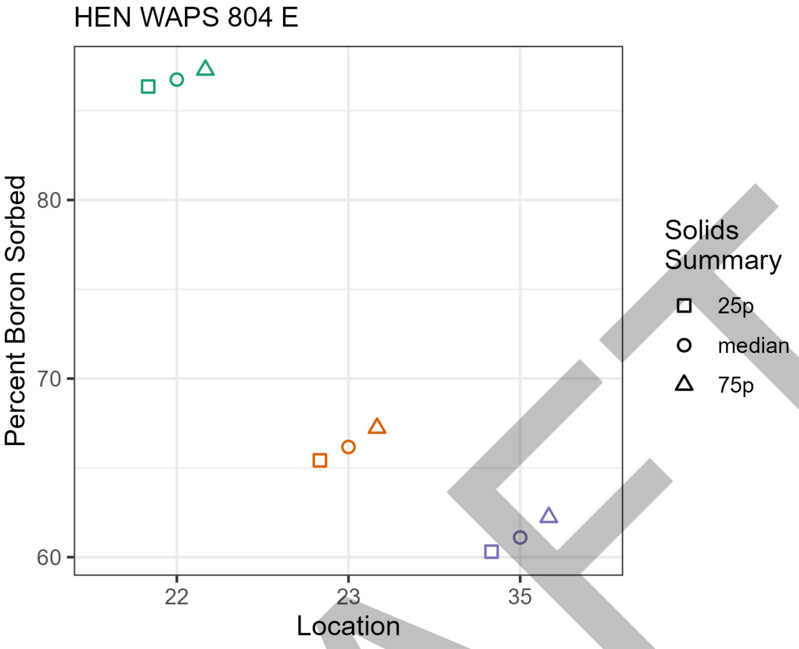

Figure 7: Modeled Boron Behavior – East

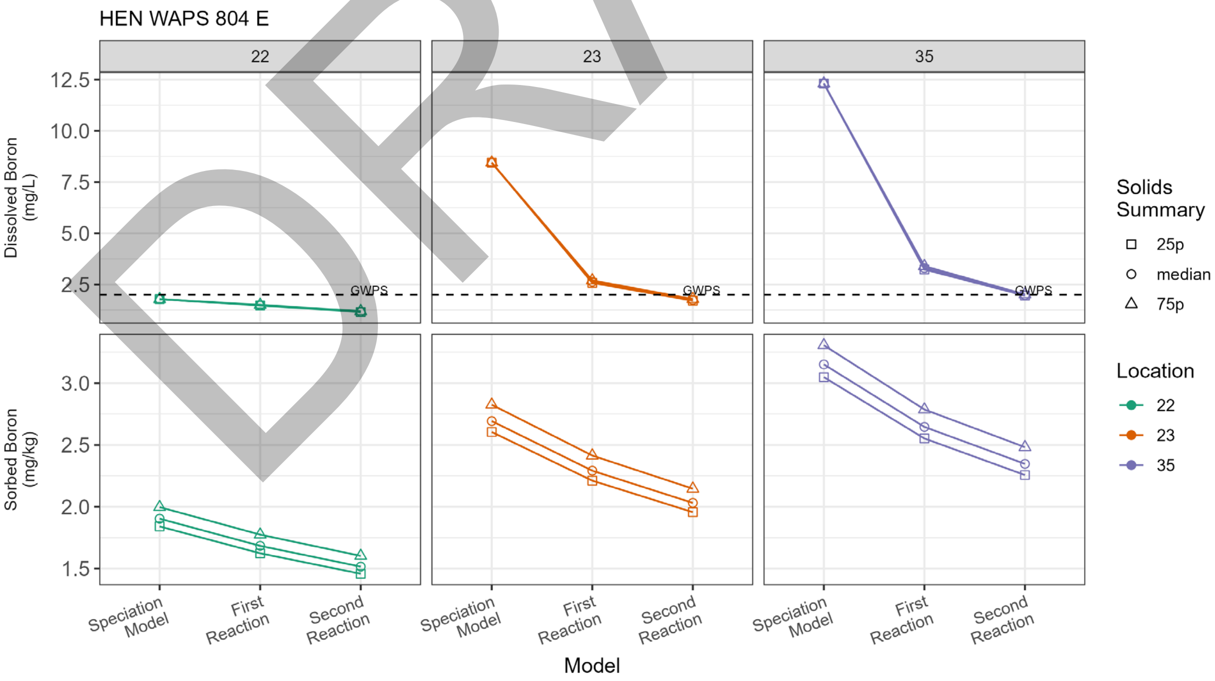

Figure 8: Percentage of Sorbed Sulfate – East

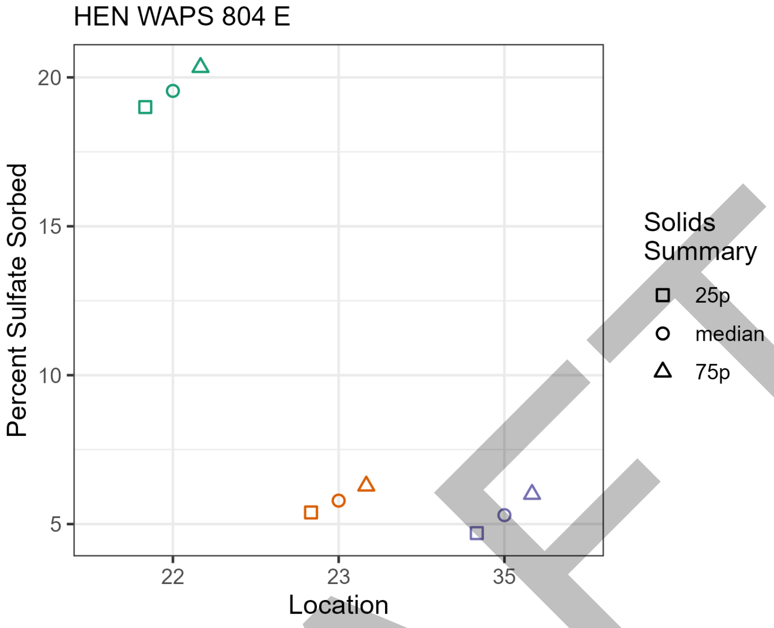

Figure 9: Modeled Sulfate Behavior – East

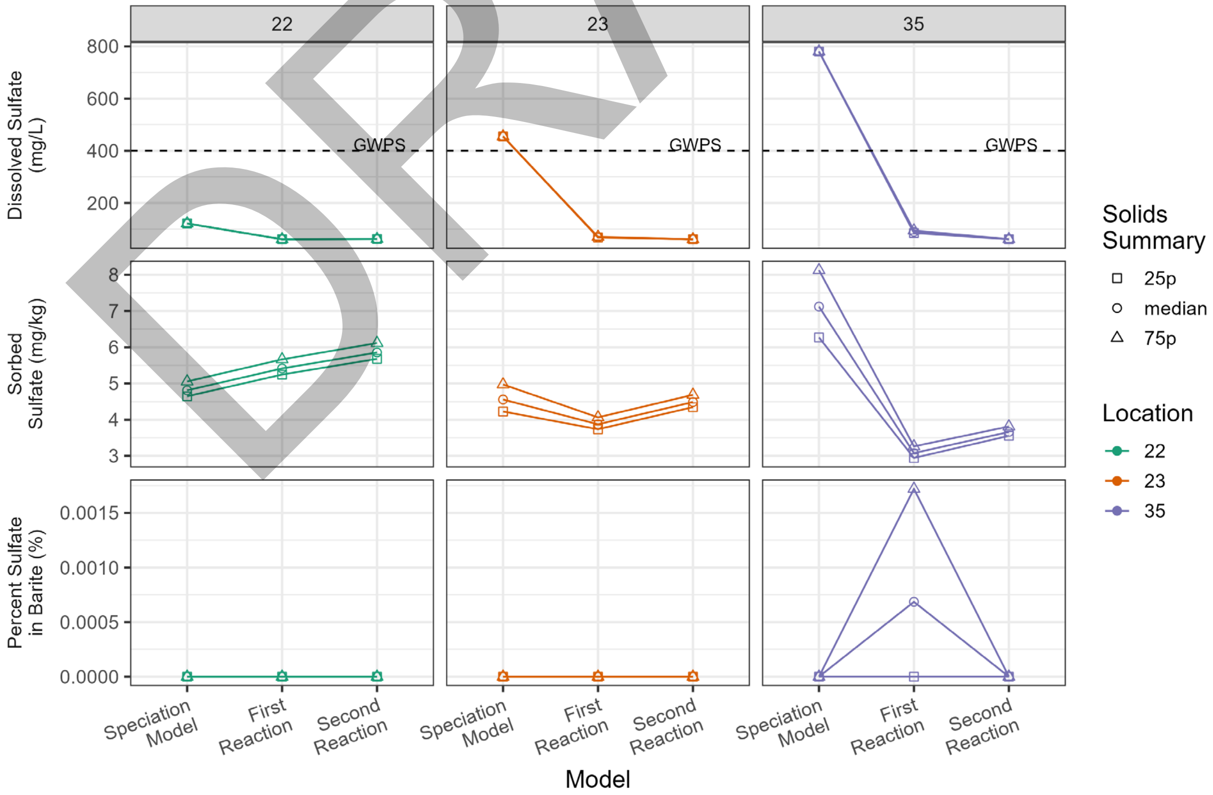

Figure 10: Modeled Sorbing Phase Behavior – East

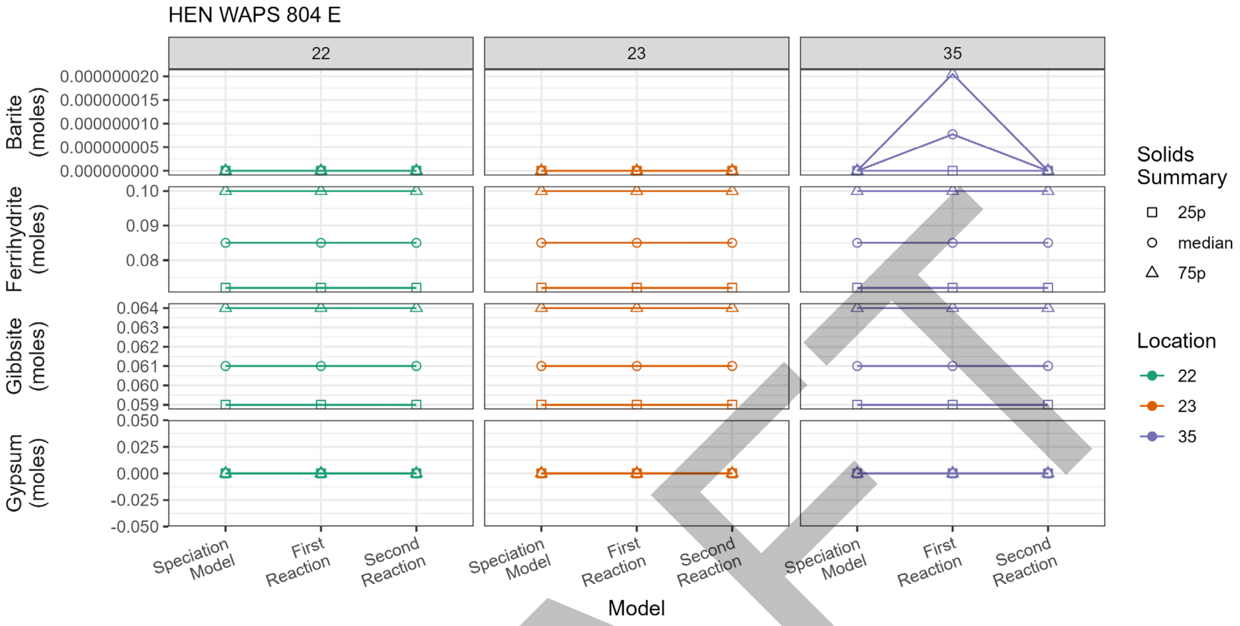

Results of speciation modeling for WAPS-East support the determination of the GCSM that chemical attenuation of boron and (to a lesser extent) sulfate is likely to occur. Wells with boron exceedances on the eastern side of the WAPS (wells 22, 23, and 35) are predicted to have between 60 and 87% of the boron present at (modeled) compliance wells is sorbed to mineral surfaces (**Figure 6**). Well 22 is predicted to experience notably greater boron sorption under current conditions than wells 23 and 35. Sensitivity assessments demonstrate that the mineral mass inputs have a minor impact on boron sorption, with the 25th and 75th percentile values for mineral mass accounting for differences of approximately 3% of aqueous boron sorbed at each well under current conditions. These results suggest that boron sorption is likely to occur under current geochemical conditions across the site, although at different magnitudes depending on well-specific geochemical conditions.

Speciation calculations for sulfate indicate that at wells with sulfate exceedances (wells 23 and 35), between 5 and 8% of sulfate present at (modeled) compliance wells is sorbed to mineral surfaces (**Figure 8**). Sensitivity assessments demonstrate that the mineral mass inputs have a minor impact on sulfate sorption, with the 25th and 75th percentile values for mineral mass accounting for differences of less than 2% of aqueous sulfate sorbed at each well under current conditions (**Figure 8**). These results suggest that some degree of sulfate sorption to iron and aluminum hydroxide minerals is likely to occur under current geochemical conditions, although less sorption is expected for aqueous sulfate relative to other COCs.

Reaction modeling results of conditions under future conditions for WAPS-East demonstrate that aqueous boron and sulfate concentrations change with interaction with background water. Aqueous boron concentrations at wells with exceedances on the eastern side of the WAPS (wells 22, 23, and 35) are predicted to decrease with each iterative reaction (**Figure 7**). Though a small amount of boron desorption (up to 0.8 mg/kg) is predicted at each well, the impact of this desorption on aqueous boron concentrations is offset by the influence of background groundwater containing lower aqueous boron concentrations. Well 22 is predicted to achieve the boron GWPS following the first reaction and wells 23 and 35 are predicted to achieve the boron GWPS following the second reaction. These results indicate that mobilization of currently attenuated boron is unlikely to affect the modeled time to reach the GWPS.

Concentrations of aqueous sulfate at wells with exceedances (wells 23 and 35) are predicted to decrease at both wells with each iterative reaction (**Figure 9**). Some degree (up to 4.5 mg/kg) of sulfate desorption is predicted following the first reaction. However, the impact of this desorption on aqueous sulfate concentrations is offset by interactions with background groundwater containing lower aqueous sulfate concentrations. Barite precipitation is predicted under future conditions, particularly at well 35, which provides an additional attenuation mechanism for aqueous sulfate. These results indicate that mobilization of currently attenuated sulfate is unlikely to affect the modeled time to reach the GWPS.

3.2.3 Model Results – WAPS River

Figures 11 to 12 illustrate the effect of river water (WAPS-River) on geochemical reactions at well 22.

Figure 11: Modeled Boron Behavior – River

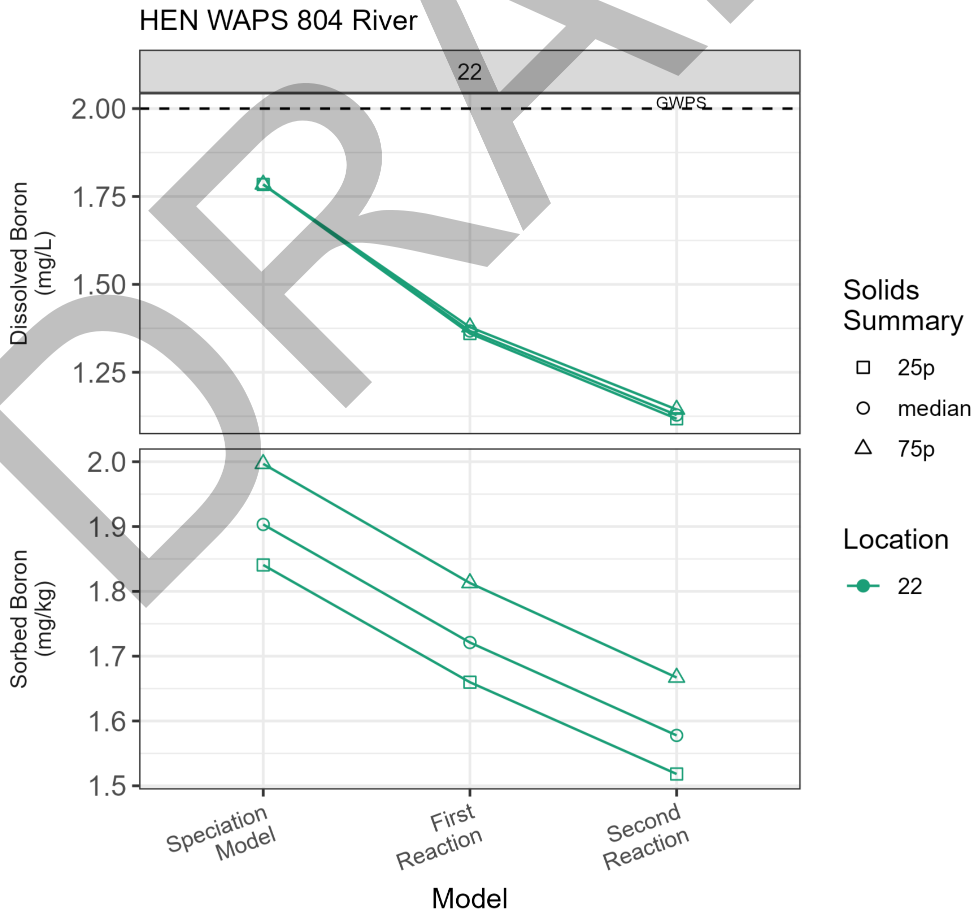

Figure 12: Modeled Sorbing Phase Behavior – River

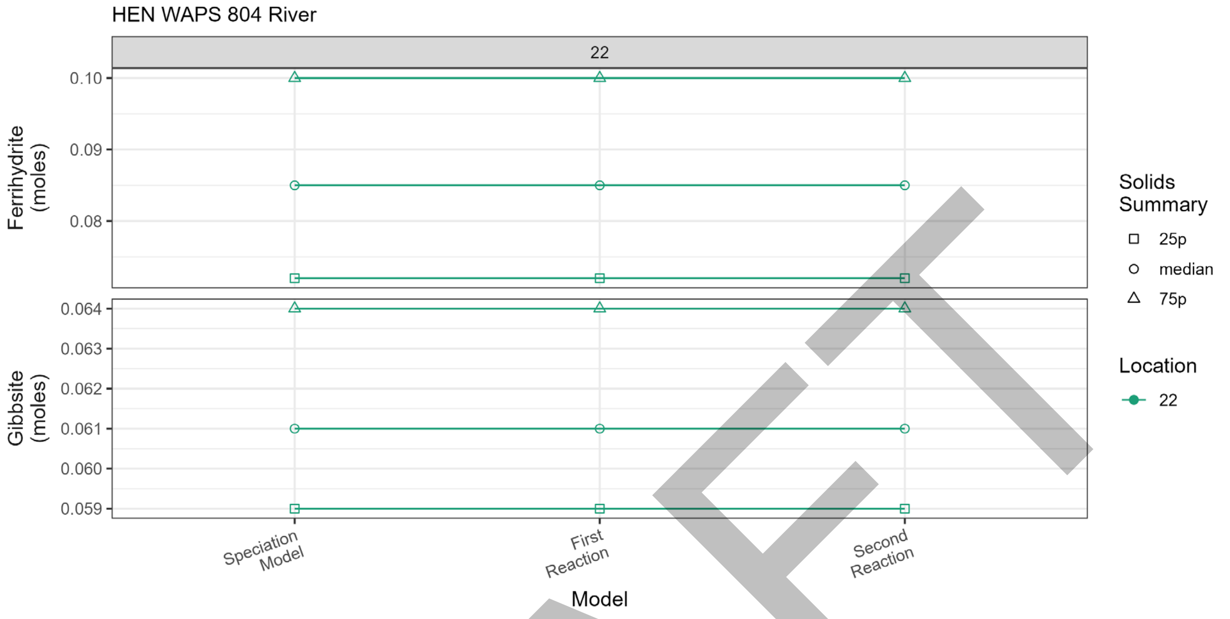

Speciation modeling results for well 22 are identical in the WAPS-River model (**Figure 11**) and the WAPS-East model (**Figure 7**), as both models incorporate the same initial aqueous and solid phase geochemical conditions at well 22.

Reaction modeling results of conditions under future conditions for WAPS-River demonstrate that aqueous boron concentrations change with interaction with background water. Reaction modeling with river water as a background source at well 22 yielded similar results as WAPS-East models with regards to boron behavior (**Figure 11**). Aqueous boron concentrations at well 22 are predicted to decrease with each iterative reaction with river water, and a small amount of boron desorption (approximately 0.3 mg/kg) is predicted.

3.2.4 Reaction Modeling Summary

Arsenic, boron, and sulfate are predicted to sorb to ferrihydrite and gibbsite. Both minerals are predicted to be stable and exhibit minor (less than 1%, **Table 2**) changes due to precipitation or dissolution reactions under future conditions (**Figures 5, 10, and 12**). Minor barite precipitation is predicted under most future conditions. The predicted stability of sorbing mineral phases and precipitation of barite under future conditions demonstrates the continued feasibility of chemical attenuation mechanisms for all COCs in the WAPS.

The primary chemical attenuation mechanism for arsenic and boron is anticipated to be sorption to iron and aluminum oxide mineral phases which are predicted to be stable under future conditions. Chemical attenuation mechanisms for sulfate are expected to include sorption to iron and aluminum oxide minerals and precipitation of barite. Results suggest that the flow and transport model conclusions are approximately correct for boron and sulfate, and that the time to reach the respective GWPS is not anticipated to be affected by desorption of COCs from the solid phase. Chemical attenuation of sulfate is also expected to contribute to a reduction in TDS at well 35. Aqueous arsenic concentrations are predicted to be impacted by remobilization of attenuated arsenic following interaction of representative background groundwater with arsenic-bearing aquifer solids at wells 21R and 51. As such, the time to reach the GWPS for arsenic may be longer than predicted by the groundwater flow and transport model.

3.3 Supplemental Arsenic Geochemical Assessment

Remobilization of arsenic from CCR porewater and natural sources was predicted by reaction modeling and was further explored through additional solid and aqueous phase sampling and geochemical analyses as discussed in an Addendum to the GCSM[15]. The results were used as the basis of supplemental geochemical modeling with the goal of better understanding arsenic speciation, solubility, and mechanisms of mobilization at wells with arsenic GWPS exceedances.

3.3.1 Arsenic Speciation and Association

The reaction modeling results discussed in Section 3.2 predict the presence of a trailing geochemical gradient for arsenic, the result of which is a temporary increase to aqueous arsenic concentrations at wells 21R and 51 after source control is completed.

Solids analyses presented in the GCSM indicate that arsenic is present in the solid phase at background and compliance locations, indicating that a component of arsenic is geogenic. SEP analyses indicate that the majority of arsenic is associated with the oxide component. This finding was supported by XRD results which detected the iron oxide mineral magnetite, as well as other iron-bearing minerals (pyrite and ankerite).

Additional 2024 sampling and SEP analyses also indicated arsenic association with the oxide fraction, as well as notable association with the residual fraction, the sulfide fraction, and the non-crystalline fraction which is commonly associated with amorphous oxide materials; however, XRD results from 2024 sampling did not indicate the presence of iron (hydr)oxide or iron sulfide minerals.

Groundwater at both wells with arsenic GWPS exceedances (21R and 51) and background well 34 was sampled in September 2024 for analysis of aqueous arsenic speciation and aqueous metals (total and dissolved). These results are provided in the GCSM Addendum. Aqueous arsenic concentrations were observed to be approximately two orders of magnitude lower at background well 34 compared to both wells with exceedances, based on total metals and arsenic speciation analyses. While aqueous arsenic at background well 34 was nearly evenly comprised of arsenite (H_3AsO_3; arsenic with a 3^+ oxidation state) and arsenate ($H_2AsO_4^{-}$; arsenic with a 5^+ oxidation state), arsenite was reported as the dominant oxidation state in wells 21R and 51. Arsenic speciation results reflect the elevated arsenic concentrations at the wells with exceedances compared to the nearest background locations and indicate that arsenite, the more mobile oxidation state of the two, dominants aqueous arsenic at these locations.

---

[15] The GCSM is a component of the Nature and Extent Report previously submitted to IEPA (Ramboll 2024) and is provided with relevant updates as Appendix D of the CAAA to which this report is attached.

3.3.2 Thermodynamic Evaluation

Arsenic speciation results were used to calculate electron potential (Eh) values for the arsenite/arsenate redox couple using the Nerst Equation (Panagiotaras et al. 2012). These arsenic redox couple-specific Eh values can be compared to field measured Eh values derived by converting oxidation-reduction potential (ORP) measurements (**Table 3**). Field Eh measurements account for any redox reaction occurring in the groundwater and represent an average, rather than compound-specific, redox state. Therefore, calculated Eh values were compared to Eh values measured in the field during the September sampling event provide an assessment of the discrepancy between methods, with calculated Eh values interpreted to be a more accurate representation of groundwater redox measurements for arsenic. An Eh adjustment factor of -0.08373 (V) was calculated as the difference between the mean value of calculated and measured Eh values for the September 2024 sampling event. This adjustment factor was then applied to historical Eh field measurements from wells 34, 21R, and 51. Pourbaix diagrams were then constructed using the composition of each well from the September 2024 sampling event to construct phase stability boundaries, and samples were plotted using both field-measured and adjusted Eh values (**Figures 13, 14, and 15**). Samples that plot above the red line indicate thermodynamic stability of arsenate aqueous species, whereas samples that plot below the red line indicate thermodynamic stability of arsenite aqueous species.

Figure 13: Well 34 Arsenic Pourbaix Diagram – Calculated Eh Values

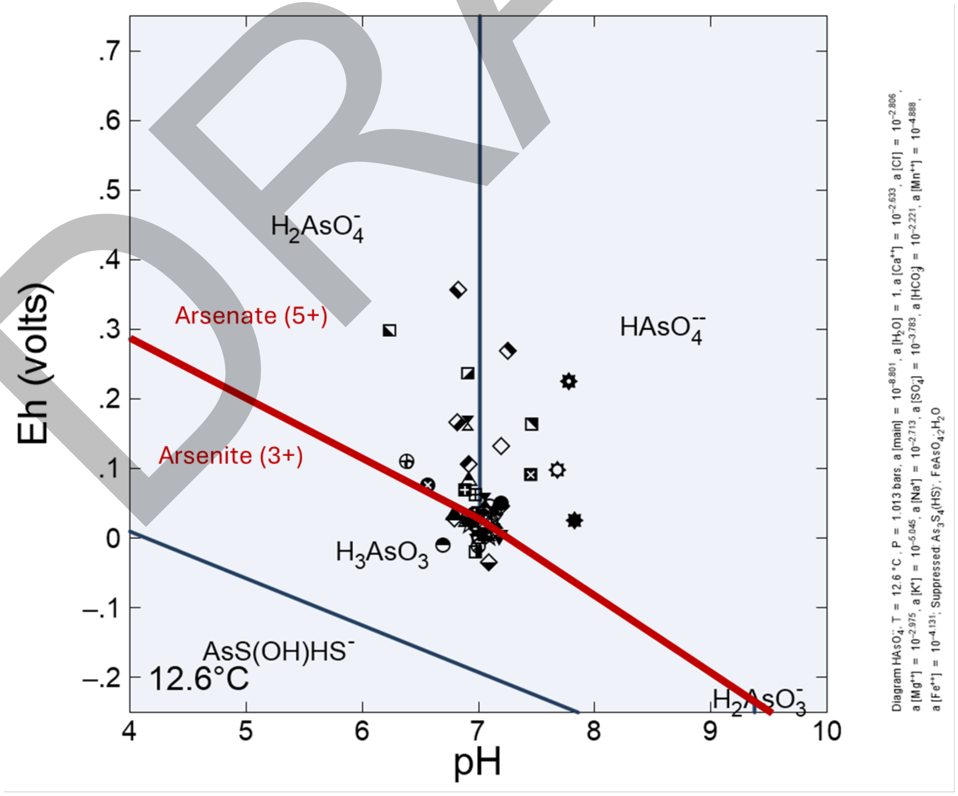

Note: Samples collected between 9/25/1996 and 10/08/2024 are displayed on the diagram

Figure 14: Well 21R Arsenic Pourbaix Diagram – Calculated Eh Values

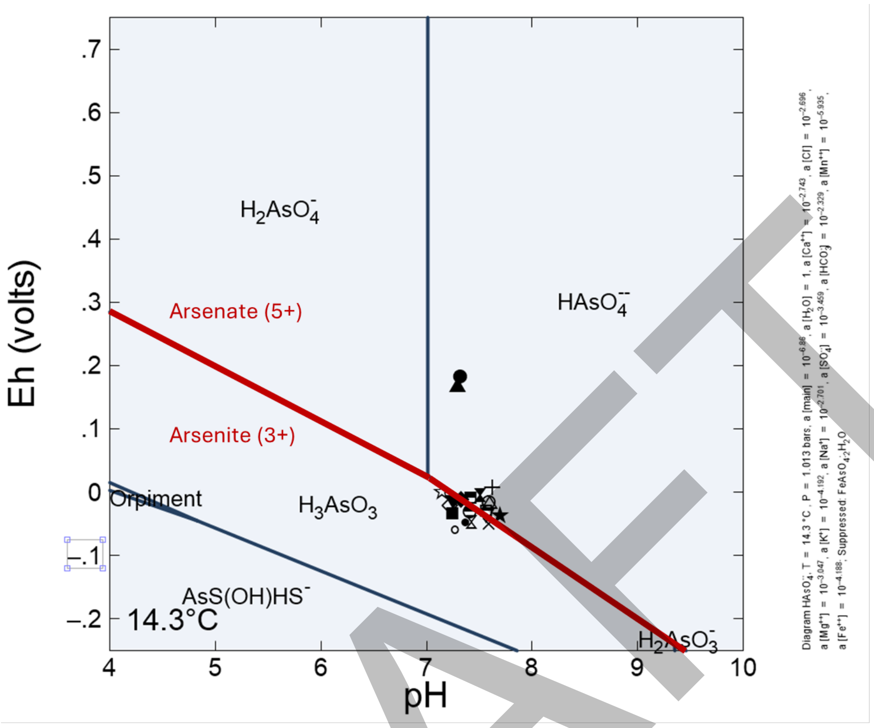

Note: Samples collected from 03/11/2020 through 10/08/2024 are displayed on the diagram

Figure 15: Well 51 Arsenic Pourbaix Diagram – Calculated Eh Values

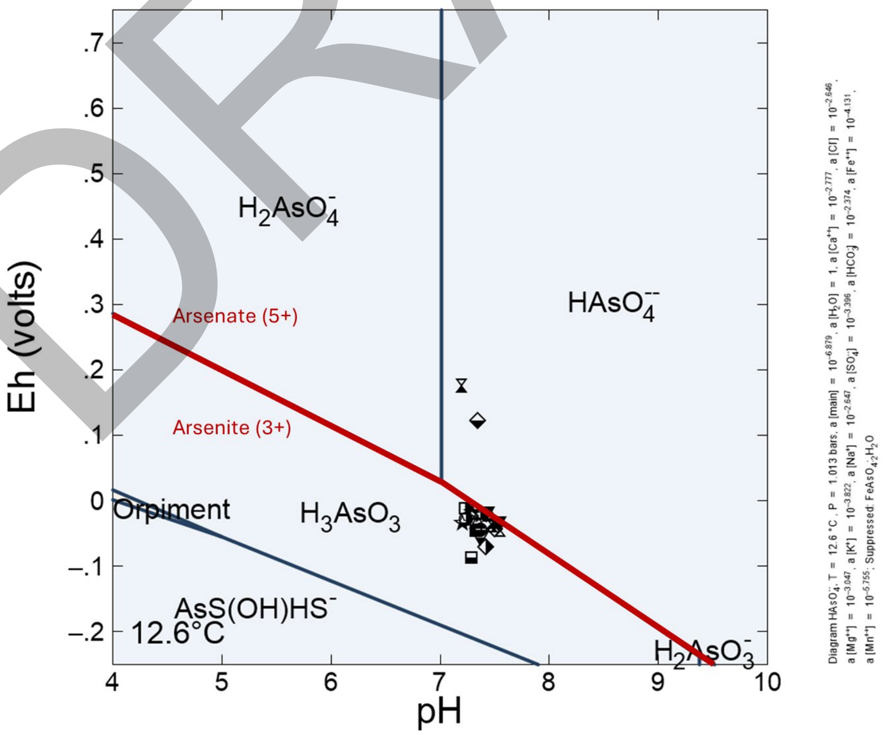

The arsenic speciation results and associated Pourbaix diagram findings contrast with the existing GCSM for arsenic at 21R and 51, which posited that arsenate species may be more prevalent at these locations based on data available at the time the CGSM was prepared. Recently collected data indicate that the consistently reducing conditions at these wells are actually associated with arsenic speciation favoring more mobile species (i.e., arsenite).

Arsenic speciation analyses and thermodynamic evaluations indicate that arsenite species dominate groundwater at locations with arsenic GWPS exceedances, a trait which is likely exclusive to the highly reducing, organic-rich lithology underlying the western portion of the WAPS. The current predominance of arsenite species at these locations is linked to elevated aqueous arsenic concentrations following source control, suggesting that the dominant arsenite will more readily desorb from aquifer solids with migration of background groundwater.

3.3.3 Reaction Pathway Modeling

Supplemental reaction pathway modeling was completed for well 21R to investigate the impact of dynamic geochemical conditions potentially associated with closure activities on arsenic mobility at this location. Similar to the geochemical reaction modeling described in Section 3.2, reaction pathway modeling predicts how aqueous and solid arsenic concentrations will change following source control during interaction with background water. However, reaction pathway modeling adjusts single geochemical parameters (i.e., pH and Eh) to understand their potential impacts on sorption and aqueous concentrations in isolation from the effect of desorption due to re-equilibration with a lower concentration solution. Reaction pathway modeling was only completed for well 21R as it was the only location with contemporaneous arsenic speciation and aquifer solids data collected.

Geochemist's Workbench (GWB) software package was used for reaction pathway modeling. The MINTEQ v4 database[16] was used in model calculations. Sorption to iron oxides was incorporated into the model calculations using the Dzombak and Morel (1990) two-layer surface complexation model, which is provided in GWB for the MINTEQ database as sorption dataset FeOH_minteq.sdat. Sorption sites to iron oxide materials are defined in this sorption dataset for the mineral ferrihydrite. A porosity value of 22% was used for the UAU (Natural Resource Technology, Inc., 2017).

Solids sampling adjacent to well 21R produced an SEP dataset containing results for fractions associated with oxides and non-crystalline components, which are typically representative of amorphous oxide components. These components were incorporated into the reaction pathway model to reflect the impact of arsenic sorption to well-specific aquifer solids within the model.

The initial aqueous component of the geochemical model was populated using the groundwater composition of the sample collected at well 21R in September 2024 (the nearest sampling event to the collection of aquifer solids near 21R). The model was run twice utilizing varying geochemical conditions to evaluate separately the impact of pH and redox variability on arsenic sorption and

---

[16] The standard MINTEQ v4 database contains identical thermodynamic data for arsenic species as the modified MINTEQ v4 database used in speciation and reaction modeling efforts. Usage of the modified database was therefore not required to maintain thermodynamic database consistence between modeling efforts.

mobility; initially fixing the pH value and setting Eh values to vary along a sliding scale towards conditions more similar to background, and secondly fixing Eh and setting pH values to vary along a sliding scale towards conditions more similar to background. Fixed pH and Eh values for the aqueous component within the model were set at values measured from well 21R during the September 2024 sampling event (pH value of 7.4 standard units [SU]; Eh value of 0.0256 mV). pH values were set to slide from 8.0 to 6.0 SU, a value inclusive of both the pH value measured at background well 34 during the September 2024 sampling event (6.8 SU) and typical range of pH values measured at well 21R. Eh values were set to slide from 0.02 to 0.20 V, a value inclusive of the less reducing groundwater conditions at well 34 (the September 2024 sampling event Eh reported value was 0.0672 V; previously observed Eh values varied from 0.0517 V to 0.443 V, with an average of 0.1630 V). Solid-phase iron reactants incorporated for sorption assessment were defined based on SEP results for iron oxides and non-crystalline materials (analytical data provided in the GCSM Addendum). Ferrihydrite was included at a mass of 4,400 micrograms per gram (µg/g), calculated by averaging the sum of iron associated with the iron oxide and iron non-crystalline material fractions for SEP samples from both well 21R solid sample intervals.

The geochemical models were used to calculate the anticipated individual effects of pH and redox variability on aqueous arsenic concentrations. Aqueous arsenic concentrations as a function of pH are shown on **Figure 16**, and concentrations as a function of Eh are shown on **Figure 17**.

Figure 16: 21R Aqueous Arsenic Concentrations as a Function of pH Variability

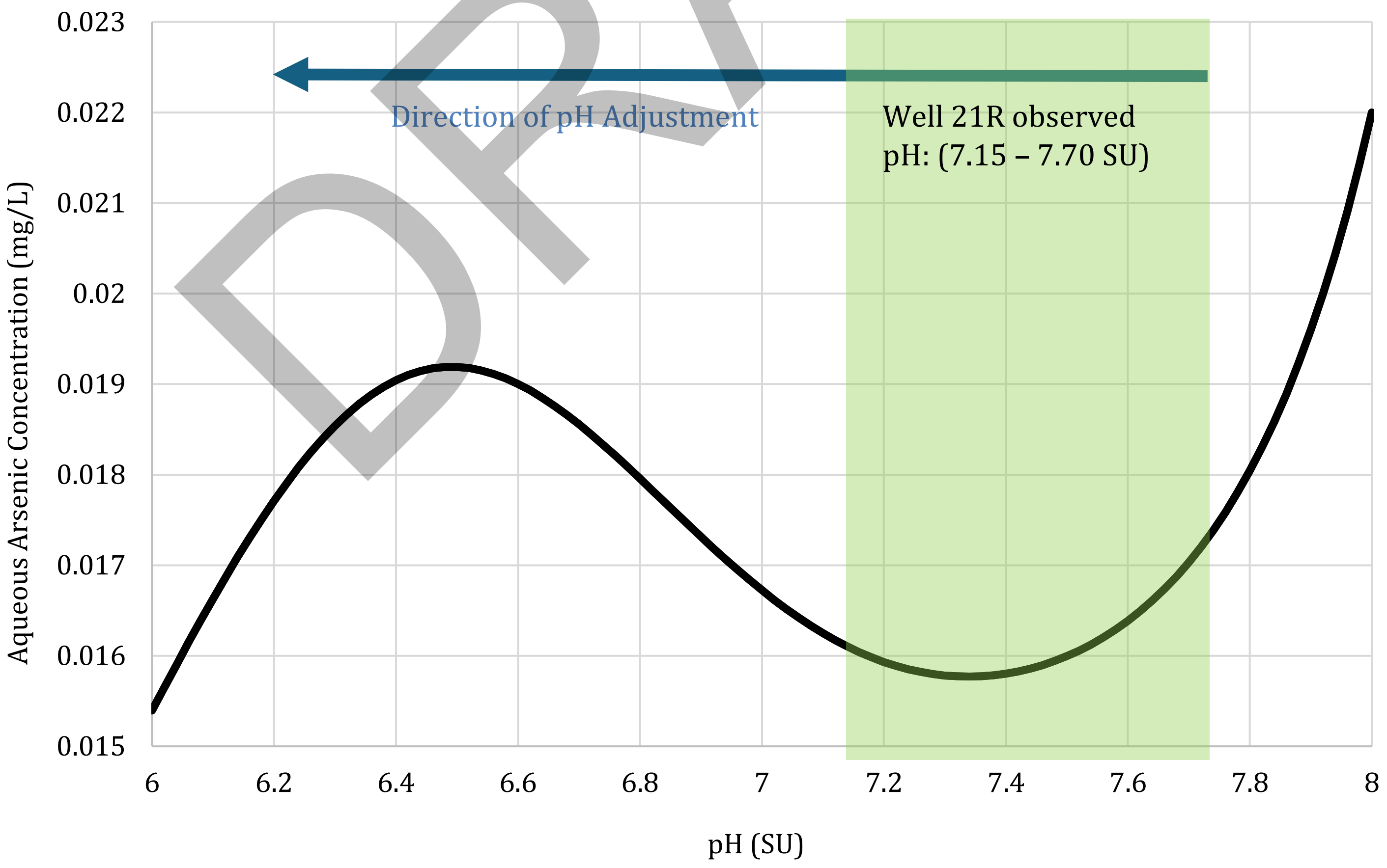

Figure 17: 21R Aqueous Arsenic Concentrations as a Function of Eh Variability

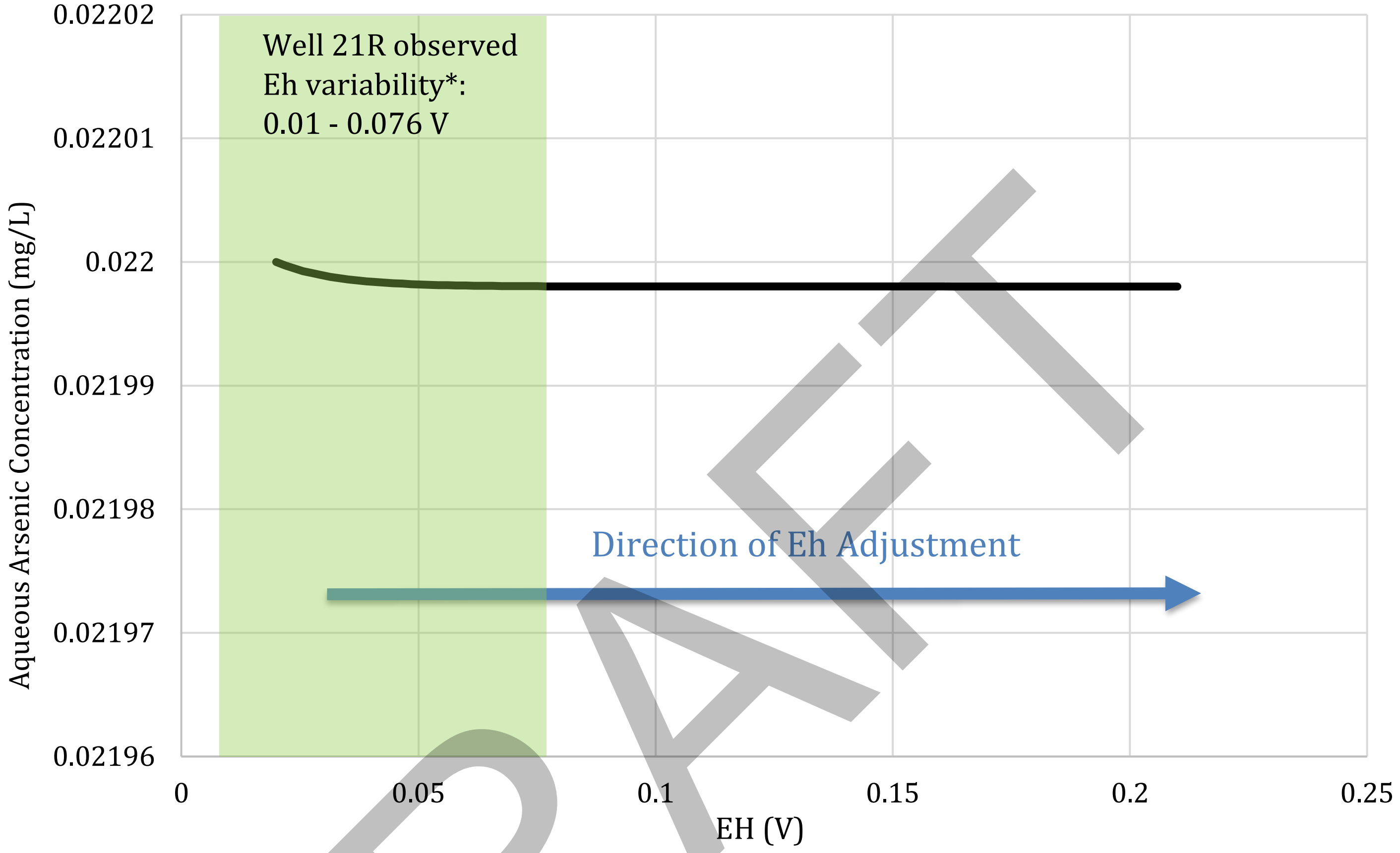

*: 21R Eh measurement variability excludes two outlier measurements of 0.252 and 0.237 V measured on 6/7/2022 and 9/13/2022 respectively

The results of the reaction pathway modeling presented in **Figures 16 and 17** indicate that while fluctuations in pH (and to a notably lesser extent, redox conditions) have a degree of influence on aqueous arsenic concentrations, the predicted aqueous arsenic increases from reaction modeling presented in Section 3.2 are unable to be achieved without interaction with low arsenic-concentration water. Reaction pathway modeling results predict that aqueous arsenic concentrations should vary from a minimum of 0.0158 mg/L (at pH 7.32 SU) to a maximum of 0.0170 mg/L (at pH 7.7 SU) within the pH range observed at well 21R to date; however, further decreases in pH values associated with background conditions are expected to influence arsenic concentrations, potentially increasing aqueous concentrations to a predicted maximum of 0.0192 mg/L at pH 6.5 (**Figure 16**). This maximum predicted value is still well below the predicted aqueous arsenic concentrations from reaction modeling presented in Section 3.2 (maximum aqueous concentrations of approximately 0.0600 mg/L, **Figure 2**).

In comparison, redox conditions (represented by Eh in the modeling effort) have less influence on aqueous arsenic concentrations, with aqueous arsenic concentrations predicted to vary negligibly as a function of Eh changes (**Figure 17**).

Combined, Section 3.2 and Section 3.3 modeling results suggest that previously modeled aqueous arsenic increases are anticipated to be caused primarily by the physical migration of lower arsenic concentration groundwater from background locations (represented by well 34 in the WAPS-West model) triggering re-equilibration leading to the subsequent desorption of arsenic from UAU solids. However, a component of aqueous arsenic mobilization is also predicted to be associated with pH changes at wells with arsenic exceedances. If groundwater flow conditions or remedial activities at the site drive substantial pH changes, additional arsenic mobilization may occur.

4. CONCLUSIONS

This report evaluated the contribution of chemical mechanisms to groundwater polishing using geochemical modeling. The results of the groundwater polishing evaluation also contextualize estimates of the modeled time to reach the GWPS by evaluating potential changes in COC attenuation as groundwater quality returns to background conditions.

Geochemical modeling of current WAPS conditions demonstrates chemical attenuation of arsenic, boron, and (to a lesser extent) sulfate via sorption to aquifer solids, particularly iron and aluminum oxides. Modeling of anticipated future conditions predicts some desorption of arsenic, boron, and sulfate from solids. Aqueous arsenic concentrations are predicted to increase at wells with current exceedances following remobilization of previously attenuated arsenic (whether due to the influence of the WAPS or from geogenic sources) under future conditions. Modeling predicts that iron and aluminum oxide sorbing mineral phases will remain stable in post-source control conditions, and as a result this chemical attenuation mechanism will remain viable for boron and sulfate. Barite precipitation is predicted under future conditions which will provide an additional attenuation mechanism for sulfate. It is expected that attenuation of sulfate will also contribute to a reduction in TDS, as sulfate is the primary contributor to TDS at well 35. Lithium was not addressed in the geochemical modeling, but lithium concentrations have steadily declined following initiation of closure activities.

Results of the geochemical modeling suggest that the time to reach boron and sulfate GWPS is not anticipated to be impacted by desorption from aquifer solids under future conditions. The observed time to reach the GWPS for arsenic may be longer than predicted by the groundwater flow and transport model due to remobilization of previously attenuated arsenic. Arsenic speciation and mobilization were further investigated in a supplemental assessment which included evaluation of recently collected solid and aqueous phase data as well as geochemical modeling. Results indicate that arsenic exists in the solid and aqueous phase at wells with arsenic GWPS exceedances, and the majority of aqueous arsenic is in the arsenic (III) oxidation state at these locations. Supplemental geochemical modeling determined that changes to pH (and to a lesser extent, redox) conditions at wells with exceedances will influence arsenic mobility somewhat. However, modeling results generally suggest that re-equilibration of aquifer solids containing sorbed or geogenic arsenic with background groundwater containing lower aqueous arsenic concentration is the primary driver of aqueous arsenic increases at wells with exceedances. These results will inform corrective action groundwater monitoring and adaptive site management, critical components of every corrective action considered in the CAAA.

5. REFERENCES

Burns and McDonnell. 2021. Initial Operating Permit, Hennepin West Ash Pond System. October.

Dynegy Midwest Generation, LLC. 2020. Hennepin Power Station; Old West Ash Pond, Ash Pond No. 2, Notification of Completion of Closure. December. 2020-Hennepin-Notification of Completion of Closure -OWAP and AP No. 2.pdf

Dynegy Midwest Generation, LLC. 2020. Hennepin Power Station; Old West Polishing Pond, Notification of Completion of Closure. December. 2020-Hennepin-Notification of Completion of Closure -Old West Polishing Pond.pdf

Dzombak D.A. and Morel F.M.M. 1990. Surface Complexation Modeling: Hydrous Ferric Oxide. John Wiley & Sons, New York.

Geosyntec. 2024. Geochemical Conceptual Site Model – Hennepin Power Plant, West Ash Pond System (CCR Unit #804).

Karamalidis A.K. and Dzombak D.A. 2010. Surface Complexation Modeling: Gibbsite. John Wiley & Sons, New York.

Natural Resource Technology, Inc. 2017. Hydrogeologic Site Characterization Report, Hennepin West Ash Pond System, Hennepin, Illinois. December.

Panagiotaras, D., Panagopoulos, G., Papoulis, D., and Avramidis, P. 2012. Arsenic Geochemistry in Groundwater Systems. In *Geochemistry – Earth's System Processes*. p.27-38. InTech.

Ramboll. 2021. Hydrogeologic Site Characterization Report, Hennepin Power Plant East Ash Pond. October.

Ramboll. 2024. Nature and Extent Report. Hennepin Power Plant, West Ash Pond System, IEPA ID No. W1550100002-01 and W1550100002-03. May.

Savannah River National Laboratory. 2011. The Scenarios Approach to Attenuation-Based Remedies for Inorganic and Radionuclide Contaminants. SRNL-STI-2011-00459. August.

Stackelberg P.E., Belitz K., Brown C.J., Erickson M.L., Elliot S.M., Kauffman L.J., Ransom K.M., and Reddy J.E. 2020. Machine Learning Predictions of pH in the Glacial Aquifer System, Northern USA. Groundwater, 59(3):352-368. https://doi.org/10.1111/gwat.13063

Stumm W. and Morgan J.J. 1996. Aquatic Chemistry: Chemical Equilibria and Rates in Natural Waters. Third edition. John Wiley & Sons, New York.

USEPA. 1999. Use of Monitored Natural Attenuation at Superfund, RCRA Corrective Action, and Underground Storage Tank Sites. Office of Solid Waste and Emergency Response. Directive 9200.4-17P. April.

USEPA. 2015. Use of Monitored Natural Attenuation for Inorganic Contaminants in Groundwater at Superfund Sites. Office of Solid Waste and Emergency Response. Directive 9283.1-36. August.

United States Geological Survey (USGS). 2021. PHREEQC Version 3. December. https://www.usgs.gov/software/phreeqc-version-3

TABLES

Table 1. Summary of Geochemical Model Inputs
Groundwater Polishing Evaluation Report
Hennepin Power Plant - West Ash Pond System

Model Component	Parameters	Data source(s)
Solid Phase	Iron (hydr)oxides, aluminum (hydr)oxides	Site-specific sequential extraction results from October 2024 sampling
	Calcite and dolomite	X-ray diffraction results
Downgradient groundwater (COC exceedance locations)	Arsenic, boron, sulfate, iron, manganese, major ions[1], 845 constituents[1]	Median concentrations per well from data collected in Q2 and Q3 2023
Background groundwater		Median concentrations from network background wells using data collected in Q2 and Q3 2023 (West and East model runs). Median concentrations from eight Illinois River water sampling events (River model run)

[1] See Section 3.1.1.2 for details.

Table 2: Geochemical Modeling Response of Sorbing Phases
Groundwater Polishing Evaluation
Hennepin Power Plant - West Ash Pond System

Program ID	Parameter	Hydrostratigraphic Unit	Location	Summary Type	First Reaction Change		Second Reaction Change	
					mg/kg	%	mg/kg	%
HEN 804 W	Barite	UA	21R	25p	0.008	NA	0.007	85.90
HEN 804 W	Barite	UA	21R	median	0.008	NA	0.007	84.86
HEN 804 W	Barite	UA	21R	75p	0.008	NA	0.007	83.77
HEN 804 W	Barite	UA	51	25p	0.008	NA	0.007	88.84
HEN 804 W	Barite	UA	51	median	0.008	NA	0.007	87.94
HEN 804 W	Barite	UA	51	75p	0.008	NA	0.007	86.98
HEN 804 W	Ferrihydrite	UA	21R	25p	2.146	0.17	-0.067	<0.01
HEN 804 W	Ferrihydrite	UA	21R	median	2.418	0.16	-0.037	<0.01
HEN 804 W	Ferrihydrite	UA	21R	75p	2.723	0.16	-0.006	<0.01
HEN 804 W	Ferrihydrite	UA	51	25p	2.194	0.17	-0.002	<0.01
HEN 804 W	Ferrihydrite	UA	51	median	2.455	0.17	0.026	<0.01
HEN 804 W	Ferrihydrite	UA	51	75p	2.748	0.16	0.054	<0.01
HEN 804 W	Gibbsite	UA	21R	25p	0.004	<0.01	0.004	<0.01
HEN 804 W	Gibbsite	UA	21R	median	0.004	<0.01	0.004	<0.01
HEN 804 W	Gibbsite	UA	21R	75p	0.004	<0.01	0.004	<0.01
HEN 804 W	Gibbsite	UA	51	25p	0.004	<0.01	0.004	<0.01
HEN 804 W	Gibbsite	UA	51	median	0.004	<0.01	0.004	<0.01
HEN 804 W	Gibbsite	UA	51	75p	0.004	<0.01	0.004	<0.01
HEN 804 E	Barite	UA	22	25p	0.000	NA	0.000	NA
HEN 804 E	Barite	UA	22	median	0.000	NA	0.000	NA
HEN 804 E	Barite	UA	22	75p	0.000	NA	0.000	NA
HEN 804 E	Barite	UA	23	25p	0.000	NA	0.000	NA
HEN 804 E	Barite	UA	23	median	0.000	NA	0.000	NA
HEN 804 E	Barite	UA	23	75p	0.000	NA	0.000	NA
HEN 804 E	Barite	UA	35	25p	0.000	NA	0.000	NA
HEN 804 E	Barite	UA	35	median	0.000	NA	-0.000	<0.01
HEN 804 E	Barite	UA	35	75p	0.001	NA	-0.001	<0.01
HEN 804 E	Ferrihydrite	UA	22	25p	0.005	<0.01	0.005	<0.01
HEN 804 E	Ferrihydrite	UA	22	median	0.005	<0.01	0.005	<0.01
HEN 804 E	Ferrihydrite	UA	22	75p	0.005	<0.01	0.005	<0.01
HEN 804 E	Ferrihydrite	UA	23	25p	0.005	<0.01	0.005	<0.01
HEN 804 E	Ferrihydrite	UA	23	median	0.005	<0.01	0.005	<0.01
HEN 804 E	Ferrihydrite	UA	23	75p	0.005	<0.01	0.005	<0.01
HEN 804 E	Ferrihydrite	UA	35	25p	0.005	<0.01	0.005	<0.01
HEN 804 E	Ferrihydrite	UA	35	median	0.005	<0.01	0.005	<0.01
HEN 804 E	Ferrihydrite	UA	35	75p	0.005	<0.01	0.005	<0.01
HEN 804 E	Gibbsite	UA	22	25p	0.004	<0.01	0.004	<0.01
HEN 804 E	Gibbsite	UA	22	median	0.004	<0.01	0.004	<0.01
HEN 804 E	Gibbsite	UA	22	75p	0.004	<0.01	0.004	<0.01
HEN 804 E	Gibbsite	UA	23	25p	0.004	<0.01	0.004	<0.01
HEN 804 E	Gibbsite	UA	23	median	0.004	<0.01	0.004	<0.01
HEN 804 E	Gibbsite	UA	23	75p	0.004	<0.01	0.004	<0.01

Table 2: Geochemical Modeling Response of Sorbing Phases
Groundwater Polishing Evaluation
Hennepin Power Plant - West Ash Pond System

Program ID	Parameter	Hydrostratigraphic Unit	Location	Summary Type	First Reaction Change		Second Reaction Change	
					mg/kg	%	mg/kg	%
HEN 804 E	Gibbsite	UA	35	25p	0.004	<0.01	0.004	<0.01
HEN 804 E	Gibbsite	UA	35	median	0.004	<0.01	0.004	<0.01
HEN 804 E	Gibbsite	UA	35	75p	0.004	<0.01	0.004	<0.01
HEN 804 River	Barite	UA	22	25p	0.008	NA	0.008	101.37
HEN 804 River	Barite	UA	22	median	0.008	NA	0.008	101.15
HEN 804 River	Barite	UA	22	75p	0.008	NA	0.008	100.88
HEN 804 River	Ferrihydrite	UA	22	25p	0.039	<0.01	0.039	<0.01
HEN 804 River	Ferrihydrite	UA	22	median	0.039	<0.01	0.039	<0.01
HEN 804 River	Ferrihydrite	UA	22	75p	0.039	<0.01	0.039	<0.01
HEN 804 River	Gibbsite	UA	22	25p	0.002	<0.01	0.002	<0.01
HEN 804 River	Gibbsite	UA	22	median	0.002	<0.01	0.002	<0.01
HEN 804 River	Gibbsite	UA	22	75p	0.002	<0.01	0.002	<0.01

Notes:

% = percent
25p = 25th percentile
75p = 75th percentile
mg/kg = milligram/kilogram
NA = not applicable
UA = Uppermost Aquifer

Table 3 - Groundwater Oxidation-Reduction (Redox) Conditions
Groundwater Polishing Report
Hennepin West Ash Pond System, Illinois

Constituent	Units	Background	Compliance	
		34	21R	51
pH	SU	6.85	7.38	7.23
Arsenic (III)	µg/L	0.141	21.0	18.1
Arsenic (V)	µg/L	0.103	2.36	2.48
Field ORP Measurement	mV	-132.8	-174.4	-146.2
Eh - Calculated from ORP	V	0.0672	0.0256	0.0538
Eh - Calculated from Nernst Equation	V	-0.0204	-0.0444	-0.0398

Notes

Nernst equation used to calculate Eh for the arsenite/arsenate oxidation-reduction couple using methods from Panagiotaras et al. 2012.

An Ag/AgCl electrode was assumed for the calculation of Eh from field ORP measurements.

SU - standard units
µg/L - microgram per liter
mV - millivolt
V - volt

ATTACHMENT A

Potentiometric Surface Map – August 21 and 22, 2023

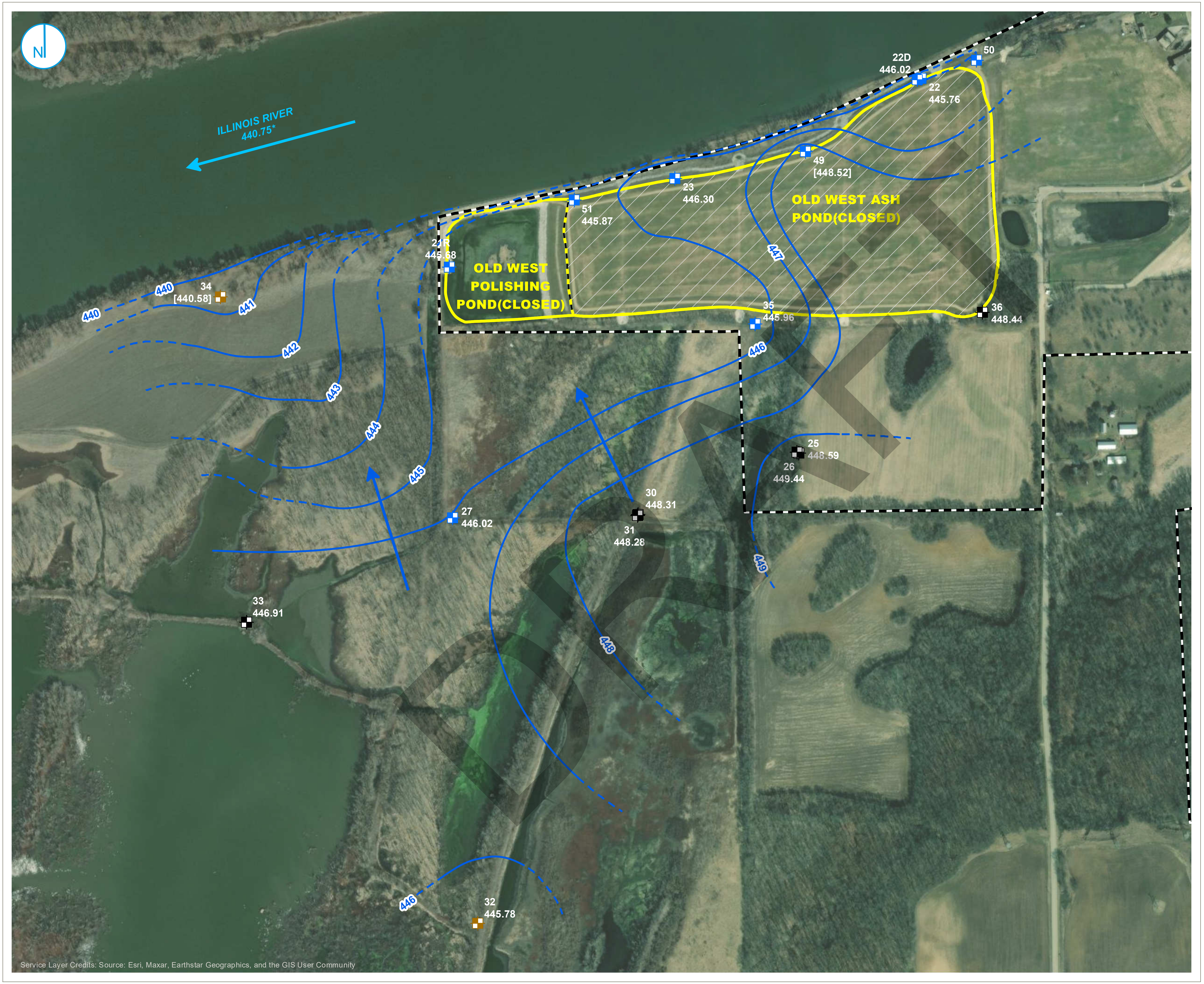

Y:\Mapping\Projects\22\2285\MXD\GW_Contours\Round_2023\Hennepin\OWAP_804\HEN 804 OWAP Pot Surface 20230821.mxd

PROJECT: 169000XXXX | DATED: 12/18/2023 | DESIGNER: GALARNMC

🟦 COMPLIANCE MONITORING WELL

🟧 BACKGROUND MONITORING WELL

⬛ MONITORING WELL

— GROUNDWATER ELEVATION CONTOUR (1 FT CONTOUR INTERVAL, NAVD88)

- - INFERRED GROUNDWATER ELEVATION CONTOUR

→ GROUNDWATER FLOW DIRECTION

🟨 REGULATED UNIT (SUBJECT UNIT)

▨ LIMITS OF FINAL COVER

⬚ PROPERTY BOUNDARY

NOTES:

1.ELEVATIONS IN PARENTHESES WERE NOT USED FOR CONTOURING.

2. ELEVATIONS IN BRACKETS WERE OBTAINED OUTSIDE OF THE 24 HOUR PERIOD FROM INITIATION OF DEPTH TO GROUNDWATER MEASUREMENTS BUT WITHIN THE SAME SAMPLING EVENT.

3. ELEVATION CONTOURS SHOWN IN FEET, NORTH AMERICAN VERTICAL DATUM OF 1988 (NAVD88)

*ILLINOIS RIVER ELEVATION OBTAINED FROM STAFF GAGE SG02, LOCATED AT THE HENNEPIN POWER PLANT

0 200 400
Feet

POTENTIOMETRIC SURFACE MAP
AUGUST 21 AND 22, 2023

2023 ANNUAL GROUNDWATER MONITORING AND CORRECTIVE ACTION REPORT
OLD WEST ASH POND
HENNEPIN POWER PLANT
HENNEPIN, ILLINOIS

RAMBOLL AMERICAS
ENGINEERING SOLUTIONS, INC.

RAMBOLL

ATTACHMENT B

PHREEQC Input Files and Thermodynamic Database

804W - 25th Percentile Metal Oxides/No Charge Balance

```
SELECTED_OUTPUT 1
-file HEN_845_804W_25p_cb-false_out.csv
-charge_balance true
-percent_error true
-totals S(6) B Li As C(4) Cl F Ca Mg Na K Ba Si P Mn Fe Al Sb Be Cd Cr Co Pb Mo Se Hfo_s
Hfo_w Hao_
-molalities Hfo_wOH Hfo_wOH2+ Hfo_wOHSO4-2 Hfo_wSO4- Hfo_wOSi(OH)3
Hfo_wOSiO(OH)2- Hfo_wHCO3 Hfo_wCO3- Hfo_wPO4-2
Hfo_wHPO4- Hfo_wH2PO4 Hfo_sCO3- Hfo_sHCO3
Hfo_sHPO4- Hfo_sH2BO3 Hfo_sH2PO4 Hfo_sOSi(OH)3
Hfo_sOSiO(OH)2- Hfo_sOHSO4-2 Hfo_sSO4-
Hao_SO4- Hao_OHSO4-2 Hao_H2BO3 Hao_H3BO4-
Hfo_sH2AsO3 Hfo_sH2AsO4 Hfo_sHAsO4- Hfo_sOHAsO4-3
Hfo_wOHAsO4-3 Hfo_wHAsO4- Hfo_wH2AsO4 Hfo_wH2AsO3
-equilibrium_phases Ferrihydrite Gibbsite Barite Calcite Dolomite(ordered) Gypsum
-saturation_indices Ferrihydrite Gibbsite Barite Calcite Dolomite(ordered) Gypsum

SOLUTION 1 #21R (C - UA)
redox pe
units mg/l
density 1
pH 7.44
pe 0.98
temp 14.9
S(6) 92.5 as SO4
B 2.01
Li 0.02135
As 0.0252
C(4) 227.5 as CO3
Cl 99
F 0.175
Ca 120.5
Mg 40.35
Na 47.2
K 2.905
Ba 0.298
Si 9.085
P 0.217
Mn 0.1105
Fe 5.52
Al 0.009425
Sb 0.000425
Be 0.0001825
Cd 0.0001675
Cr 0.002
Co 0.00135
Pb 0.0024
Mo 0.00885
Se 0.000395
end

SOLUTION 2 #51 (C - UA)
redox pe
```

```
units mg/l
density 1
pH 7.305
pe 1.42
temp 15.1
S(6) 93.5 as SO4
B 1.465
Li 0.0482
As 0.0186
C(4) 208.5 as CO3
Cl 101.5
F 0.17
Ca 118.5
Mg 38.6
Na 55.45
K 6.125
Ba 0.1045
Si 8.115
P 0.023
Mn 0.1595
Fe 6.315
Al 0.009425
Sb 0.000425
Be 0.0001825
Cd 0.0001675
Cr 0.00125
Co 0.00083
Pb 0.0016
Mo 0.0078
Se 0.000395
end

EQUILIBRIUM_PHASES 1 #21R (C - UA) - 25p
Barite 0 0
Gypsum 0 0
Gibbsite 0 0.059
Ferrihydrite 0 0.072
Calcite 0 6
Dolomite(ordered) 0 2

SURFACE 1
Hfo_wOH Ferrihydrite equilibrium_phase 0.2 53400
Hfo_sOH Ferrihydrite equilibrium_phase 0.005 53400
Hao_OH Gibbsite equilibrium_phase 0.033 2496
-equil 1
save surface 1
end

EQUILIBRIUM_PHASES 2 #51 (C - UA) - 25p
Barite 0 0
Gypsum 0 0
Gibbsite 0 0.059
Ferrihydrite 0 0.072
Calcite 0 6
Dolomite(ordered) 0 2
```

```
SURFACE 2
Hfo_wOH Ferrihydrite equilibrium_phase 0.2 53400
Hfo_sOH Ferrihydrite equilibrium_phase 0.005 53400
Hao_OH Gibbsite equilibrium_phase 0.033 2496
-equil 2
save surface 2
end

SOLUTION 3 #average background
redox pe
units mg/l
density 1
pH 7
pe 2.08
temp 12.55
S(6) 47.5
B 0.1
Li 0.0081
As 0.0022325
C(4) 327
Cl 70 charge
F 0.155
Ca 149.5
Mg 40.9
Na 48.75
K 0.435
Ba 0.10475
Si 12.2
P 0.119
Mn 1.21
Fe 5.825
Al 0.009425
Sb 0.000425
Be 0.0001825
Cd 0.0001675
Cr 0.000975
Co 0.00045
Pb 0.0010475
Mo 0.00155
Se 0.000395

SAVE solution 3

end

#FIRST REACTION

#21R (C - UA) - First Reaction
USE SOLUTION 3
USE EQUILIBRIUM_PHASES 1
USE SURFACE 1
SAVE equilibrium_phases 1
SAVE surface 1
end

#21R (C - UA) - Second Reaction
USE SOLUTION 3
```

```
USE EQUILIBRIUM_PHASES 1
USE SURFACE 1
SAVE equilibrium_phases 1
SAVE surface 1
end

#51 (C - UA) - First Reaction
USE SOLUTION 3
USE EQUILIBRIUM_PHASES 2
USE SURFACE 2
SAVE equilibrium_phases 2
SAVE surface 2
end

#51 (C - UA) - Second Reaction
USE SOLUTION 3
USE EQUILIBRIUM_PHASES 2
USE SURFACE 2
SAVE equilibrium_phases 2
SAVE surface 2
end
```

804W - 25th Percentile Metal Oxides/Charge Balance on Chloride

```
SELECTED_OUTPUT 1
-file HEN_845_804W_25p_cb-true_out.csv
-charge_balance true
-percent_error true
-totals S(6) B Li As C(4) Cl F Ca Mg Na K Ba Si P Mn Fe Al Sb Be Cd Cr Co Pb Mo Se Hfo_s
Hfo_w Hao_
-molalities Hfo_wOH Hfo_wOH2+ Hfo_wOHSO4-2 Hfo_wSO4- Hfo_wOSi(OH)3
Hfo_wOSiO(OH)2- Hfo_wHCO3 Hfo_wCO3- Hfo_wPO4-2
Hfo_wHPO4- Hfo_wH2PO4 Hfo_sCO3- Hfo_sHCO3
Hfo_sHPO4- Hfo_sH2BO3 Hfo_sH2PO4 Hfo_sOSi(OH)3
Hfo_sOSiO(OH)2- Hfo_sOHSO4-2 Hfo_sSO4-
Hao_SO4- Hao_OHSO4-2 Hao_H2BO3 Hao_H3BO4-
Hfo_sH2AsO3 Hfo_sH2AsO4 Hfo_sHAsO4- Hfo_sOHAsO4-3
Hfo_wOHAsO4-3 Hfo_wHAsO4- Hfo_wH2AsO4 Hfo_wH2AsO3
-equilibrium_phases Ferrihydrite Gibbsite Barite Calcite Dolomite(ordered) Gypsum
-saturation_indices Ferrihydrite Gibbsite Barite Calcite Dolomite(ordered) Gypsum

SOLUTION 1 #21R (C - UA)
redox pe
units mg/l
density 1
pH 7.44
pe 0.98
temp 14.9
S(6) 92.5 as SO4
B 2.01
Li 0.02135
As 0.0252
C(4) 227.5 as CO3
Cl 99 charge
F 0.175
Ca 120.5
Mg 40.35
Na 47.2
K 2.905
Ba 0.298
Si 9.085
P 0.217
Mn 0.1105
Fe 5.52
Al 0.009425
Sb 0.000425
Be 0.0001825
Cd 0.0001675
Cr 0.002
Co 0.00135
Pb 0.0024
Mo 0.00885
Se 0.000395
end

SOLUTION 2 #51 (C - UA)
redox pe
```

```
units mg/l
density 1
pH 7.305
pe 1.42
temp 15.1
S(6) 93.5 as SO4
B 1.465
Li 0.0482
As 0.0186
C(4) 208.5 as CO3
Cl 101.5 charge
F 0.17
Ca 118.5
Mg 38.6
Na 55.45
K 6.125
Ba 0.1045
Si 8.115
P 0.023
Mn 0.1595
Fe 6.315
Al 0.009425
Sb 0.000425
Be 0.0001825
Cd 0.0001675
Cr 0.00125
Co 0.00083
Pb 0.0016
Mo 0.0078
Se 0.000395
end

EQUILIBRIUM_PHASES 1 #21R (C - UA) - 25p
Barite 0 0
Gypsum 0 0
Gibbsite 0 0.059
Ferrihydrite 0 0.072
Calcite 0 6
Dolomite(ordered) 0 2

SURFACE 1
Hfo_wOH Ferrihydrite equilibrium_phase 0.2 53400
Hfo_sOH Ferrihydrite equilibrium_phase 0.005 53400
Hao_OH Gibbsite equilibrium_phase 0.033 2496
-equil 1
save surface 1
end

EQUILIBRIUM_PHASES 2 #51 (C - UA) - 25p
Barite 0 0
Gypsum 0 0
Gibbsite 0 0.059
Ferrihydrite 0 0.072
Calcite 0 6
Dolomite(ordered) 0 2
```

```
SURFACE 2
Hfo_wOH Ferrihydrite equilibrium_phase 0.2 53400
Hfo_sOH Ferrihydrite equilibrium_phase 0.005 53400
Hao_OH Gibbsite equilibrium_phase 0.033 2496
-equil 2
save surface 2
end

SOLUTION 3 #average background
redox pe
units mg/l
density 1
pH 7
pe 2.08
temp 12.55
S(6) 47.5
B 0.1
Li 0.0081
As 0.0022325
C(4) 327
Cl 70 charge
F 0.155
Ca 149.5
Mg 40.9
Na 48.75
K 0.435
Ba 0.10475
Si 12.2
P 0.119
Mn 1.21
Fe 5.825
Al 0.009425
Sb 0.000425
Be 0.0001825
Cd 0.0001675
Cr 0.000975
Co 0.00045
Pb 0.0010475
Mo 0.00155
Se 0.000395

SAVE solution 3

end

#FIRST REACTION

#21R (C - UA) - First Reaction
USE SOLUTION 3
USE EQUILIBRIUM_PHASES 1
USE SURFACE 1
SAVE equilibrium_phases 1
SAVE surface 1
end

#21R (C - UA) - Second Reaction
USE SOLUTION 3
```

```
USE EQUILIBRIUM_PHASES 1
USE SURFACE 1
SAVE equilibrium_phases 1
SAVE surface 1
end

#51 (C - UA) - First Reaction
USE SOLUTION 3
USE EQUILIBRIUM_PHASES 2
USE SURFACE 2
SAVE equilibrium_phases 2
SAVE surface 2
end

#51 (C - UA) - Second Reaction
USE SOLUTION 3
USE EQUILIBRIUM_PHASES 2
USE SURFACE 2
SAVE equilibrium_phases 2
SAVE surface 2
end
```

804W - 75th Percentile Metal Oxides/No Charge Balance

```
SELECTED_OUTPUT 1
-file HEN_845_804W_75p_cb-false_out.csv
-charge_balance true
-percent_error true
-totals S(6) B Li As C(4) Cl F Ca Mg Na K Ba Si P Mn Fe Al Sb Be Cd Cr Co Pb Mo Se Hfo_s
Hfo_w Hao_
-molalities Hfo_wOH Hfo_wOH2+ Hfo_wOHSO4-2 Hfo_wSO4- Hfo_wOSi(OH)3
Hfo_wOSiO(OH)2- Hfo_wHCO3 Hfo_wCO3- Hfo_wPO4-2
Hfo_wHPO4- Hfo_wH2PO4 Hfo_sCO3- Hfo_sHCO3
Hfo_sHPO4- Hfo_sH2BO3 Hfo_sH2PO4 Hfo_sOSi(OH)3
Hfo_sOSiO(OH)2- Hfo_sOHSO4-2 Hfo_sSO4-
Hao_SO4- Hao_OHSO4-2 Hao_H2BO3 Hao_H3BO4-
Hfo_sH2AsO3 Hfo_sH2AsO4 Hfo_sHAsO4- Hfo_sOHAsO4-3
Hfo_wOHAsO4-3 Hfo_wHAsO4- Hfo_wH2AsO4 Hfo_wH2AsO3
-equilibrium_phases Ferrihydrite Gibbsite Barite Calcite Dolomite(ordered) Gypsum
-saturation_indices Ferrihydrite Gibbsite Barite Calcite Dolomite(ordered) Gypsum

SOLUTION 1 #21R (C - UA)
redox pe
units mg/l
density 1
pH 7.44
pe 0.98
temp 14.9
S(6) 92.5 as SO4
B 2.01
Li 0.02135
As 0.0252
C(4) 227.5 as CO3
Cl 99
F 0.175
Ca 120.5
Mg 40.35
Na 47.2
K 2.905
Ba 0.298
Si 9.085
P 0.217
Mn 0.1105
Fe 5.52
Al 0.009425
Sb 0.000425
Be 0.0001825
Cd 0.0001675
Cr 0.002
Co 0.00135
Pb 0.0024
Mo 0.00885
Se 0.000395
end

SOLUTION 2 #51 (C - UA)
redox pe
```

```
units mg/l
density 1
pH 7.305
pe 1.42
temp 15.1
S(6) 93.5 as SO4
B 1.465
Li 0.0482
As 0.0186
C(4) 208.5 as CO3
Cl 101.5
F 0.17
Ca 118.5
Mg 38.6
Na 55.45
K 6.125
Ba 0.1045
Si 8.115
P 0.023
Mn 0.1595
Fe 6.315
Al 0.009425
Sb 0.000425
Be 0.0001825
Cd 0.0001675
Cr 0.00125
Co 0.00083
Pb 0.0016
Mo 0.0078
Se 0.000395
end

EQUILIBRIUM_PHASES 1 #21R (C - UA) - 75p
Barite 0 0
Gypsum 0 0
Gibbsite 0 0.064
Ferrihydrite 0 0.1
Calcite 0 6
Dolomite(ordered) 0 2

SURFACE 1
Hfo_wOH Ferrihydrite equilibrium_phase 0.2 53400
Hfo_sOH Ferrihydrite equilibrium_phase 0.005 53400
Hao_OH Gibbsite equilibrium_phase 0.033 2496
-equil 1
save surface 1
end

EQUILIBRIUM_PHASES 2 #51 (C - UA) - 75p
Barite 0 0
Gypsum 0 0
Gibbsite 0 0.064
Ferrihydrite 0 0.1
Calcite 0 6
Dolomite(ordered) 0 2
```

```
SURFACE 2
Hfo_wOH Ferrihydrite equilibrium_phase 0.2 53400
Hfo_sOH Ferrihydrite equilibrium_phase 0.005 53400
Hao_OH Gibbsite equilibrium_phase 0.033 2496
-equil 2
save surface 2
end

SOLUTION 3 #average background
redox pe
units mg/l
density 1
pH 7
pe 2.08
temp 12.55
S(6) 47.5
B 0.1
Li 0.0081
As 0.0022325
C(4) 327
Cl 70 charge
F 0.155
Ca 149.5
Mg 40.9
Na 48.75
K 0.435
Ba 0.10475
Si 12.2
P 0.119
Mn 1.21
Fe 5.825
Al 0.009425
Sb 0.000425
Be 0.0001825
Cd 0.0001675
Cr 0.000975
Co 0.00045
Pb 0.0010475
Mo 0.00155
Se 0.000395

SAVE solution 3

end

#FIRST REACTION

#21R (C - UA) - First Reaction
USE SOLUTION 3
USE EQUILIBRIUM_PHASES 1
USE SURFACE 1
SAVE equilibrium_phases 1
SAVE surface 1
end

#21R (C - UA) - Second Reaction
USE SOLUTION 3
```

```
USE EQUILIBRIUM_PHASES 1
USE SURFACE 1
SAVE equilibrium_phases 1
SAVE surface 1
end

#51 (C - UA) - First Reaction
USE SOLUTION 3
USE EQUILIBRIUM_PHASES 2
USE SURFACE 2
SAVE equilibrium_phases 2
SAVE surface 2
end

#51 (C - UA) - Second Reaction
USE SOLUTION 3
USE EQUILIBRIUM_PHASES 2
USE SURFACE 2
SAVE equilibrium_phases 2
SAVE surface 2
end
```

804W - 75th Percentile Metal Oxides/Charge Balance on Chloride

```
SELECTED_OUTPUT 1
-file HEN_845_804W_75p_cb-true_out.csv
-charge_balance true
-percent_error true
-totals S(6) B Li As C(4) Cl F Ca Mg Na K Ba Si P Mn Fe Al Sb Be Cd Cr Co Pb Mo Se Hfo_s
Hfo_w Hao_
-molalities Hfo_wOH Hfo_wOH2+ Hfo_wOHSO4-2 Hfo_wSO4- Hfo_wOSi(OH)3
Hfo_wOSiO(OH)2- Hfo_wHCO3 Hfo_wCO3- Hfo_wPO4-2
Hfo_wHPO4- Hfo_wH2PO4 Hfo_sCO3- Hfo_sHCO3
Hfo_sHPO4- Hfo_sH2BO3 Hfo_sH2PO4 Hfo_sOSi(OH)3
Hfo_sOSiO(OH)2- Hfo_sOHSO4-2 Hfo_sSO4-
Hao_SO4- Hao_OHSO4-2 Hao_H2BO3 Hao_H3BO4-
Hfo_sH2AsO3 Hfo_sH2AsO4 Hfo_sHAsO4- Hfo_sOHAsO4-3
Hfo_wOHAsO4-3 Hfo_wHAsO4- Hfo_wH2AsO4 Hfo_wH2AsO3
-equilibrium_phases Ferrihydrite Gibbsite Barite Calcite Dolomite(ordered) Gypsum
-saturation_indices Ferrihydrite Gibbsite Barite Calcite Dolomite(ordered) Gypsum

SOLUTION 1 #21R (C - UA)
redox pe
units mg/l
density 1
pH 7.44
pe 0.98
temp 14.9
S(6) 92.5 as SO4
B 2.01
Li 0.02135
As 0.0252
C(4) 227.5 as CO3
Cl 99 charge
F 0.175
Ca 120.5
Mg 40.35
Na 47.2
K 2.905
Ba 0.298
Si 9.085
P 0.217
Mn 0.1105
Fe 5.52
Al 0.009425
Sb 0.000425
Be 0.0001825
Cd 0.0001675
Cr 0.002
Co 0.00135
Pb 0.0024
Mo 0.00885
Se 0.000395
end

SOLUTION 2 #51 (C - UA)
redox pe
```

```
units mg/l
density 1
pH 7.305
pe 1.42
temp 15.1
S(6) 93.5 as SO4
B 1.465
Li 0.0482
As 0.0186
C(4) 208.5 as CO3
Cl 101.5 charge
F 0.17
Ca 118.5
Mg 38.6
Na 55.45
K 6.125
Ba 0.1045
Si 8.115
P 0.023
Mn 0.1595
Fe 6.315
Al 0.009425
Sb 0.000425
Be 0.0001825
Cd 0.0001675
Cr 0.00125
Co 0.00083
Pb 0.0016
Mo 0.0078
Se 0.000395
end

EQUILIBRIUM_PHASES 1 #21R (C - UA) - 75p
Barite 0 0
Gypsum 0 0
Gibbsite 0 0.064
Ferrihydrite 0 0.1
Calcite 0 6
Dolomite(ordered) 0 2

SURFACE 1
Hfo_wOH Ferrihydrite equilibrium_phase 0.2 53400
Hfo_sOH Ferrihydrite equilibrium_phase 0.005 53400
Hao_OH Gibbsite equilibrium_phase 0.033 2496
-equil 1
save surface 1
end

EQUILIBRIUM_PHASES 2 #51 (C - UA) - 75p
Barite 0 0
Gypsum 0 0
Gibbsite 0 0.064
Ferrihydrite 0 0.1
Calcite 0 6
Dolomite(ordered) 0 2
```

```
SURFACE 2
Hfo_wOH Ferrihydrite equilibrium_phase 0.2 53400
Hfo_sOH Ferrihydrite equilibrium_phase 0.005 53400
Hao_OH Gibbsite equilibrium_phase 0.033 2496
-equil 2
save surface 2
end

SOLUTION 3 #average background
redox pe
units mg/l
density 1
pH 7
pe 2.08
temp 12.55
S(6) 47.5
B 0.1
Li 0.0081
As 0.0022325
C(4) 327
Cl 70 charge
F 0.155
Ca 149.5
Mg 40.9
Na 48.75
K 0.435
Ba 0.10475
Si 12.2
P 0.119
Mn 1.21
Fe 5.825
Al 0.009425
Sb 0.000425
Be 0.0001825
Cd 0.0001675
Cr 0.000975
Co 0.00045
Pb 0.0010475
Mo 0.00155
Se 0.000395

SAVE solution 3

end

#FIRST REACTION

#21R (C - UA) - First Reaction
USE SOLUTION 3
USE EQUILIBRIUM_PHASES 1
USE SURFACE 1
SAVE equilibrium_phases 1
SAVE surface 1
end

#21R (C - UA) - Second Reaction
USE SOLUTION 3
```

```
USE EQUILIBRIUM_PHASES 1
USE SURFACE 1
SAVE equilibrium_phases 1
SAVE surface 1
end

#51 (C - UA) - First Reaction
USE SOLUTION 3
USE EQUILIBRIUM_PHASES 2
USE SURFACE 2
SAVE equilibrium_phases 2
SAVE surface 2
end

#51 (C - UA) - Second Reaction
USE SOLUTION 3
USE EQUILIBRIUM_PHASES 2
USE SURFACE 2
SAVE equilibrium_phases 2
SAVE surface 2
end
```

804W - Median Metal Oxides/No Charge Balance

```
SELECTED_OUTPUT 1
-file HEN_845_804W_median_cb-false_out.csv
-charge_balance true
-percent_error true
-totals S(6) B Li As C(4) Cl F Ca Mg Na K Ba Si P Mn Fe Al Sb Be Cd Cr Co Pb Mo Se Hfo_s
Hfo_w Hao_
-molalities Hfo_wOH Hfo_wOH2+ Hfo_wOHSO4-2 Hfo_wSO4- Hfo_wOSi(OH)3
Hfo_wOSiO(OH)2- Hfo_wHCO3 Hfo_wCO3- Hfo_wPO4-2
Hfo_wHPO4- Hfo_wH2PO4 Hfo_sCO3- Hfo_sHCO3
Hfo_sHPO4- Hfo_sH2BO3 Hfo_sH2PO4 Hfo_sOSi(OH)3
Hfo_sOSiO(OH)2- Hfo_sOHSO4-2 Hfo_sSO4-
Hao_SO4- Hao_OHSO4-2 Hao_H2BO3 Hao_H3BO4-
Hfo_sH2AsO3 Hfo_sH2AsO4 Hfo_sHAsO4- Hfo_sOHAsO4-3
Hfo_wOHAsO4-3 Hfo_wHAsO4- Hfo_wH2AsO4 Hfo_wH2AsO3
-equilibrium_phases Ferrihydrite Gibbsite Barite Calcite Dolomite(ordered) Gypsum
-saturation_indices Ferrihydrite Gibbsite Barite Calcite Dolomite(ordered) Gypsum

SOLUTION 1 #21R (C - UA)
redox pe
units mg/l
density 1
pH 7.44
pe 0.98
temp 14.9
S(6) 92.5 as SO4
B 2.01
Li 0.02135
As 0.0252
C(4) 227.5 as CO3
Cl 99
F 0.175
Ca 120.5
Mg 40.35
Na 47.2
K 2.905
Ba 0.298
Si 9.085
P 0.217
Mn 0.1105
Fe 5.52
Al 0.009425
Sb 0.000425
Be 0.0001825
Cd 0.0001675
Cr 0.002
Co 0.00135
Pb 0.0024
Mo 0.00885
Se 0.000395
end

SOLUTION 2 #51 (C - UA)
redox pe
```

```
units mg/l
density 1
pH 7.305
pe 1.42
temp 15.1
S(6) 93.5 as SO4
B 1.465
Li 0.0482
As 0.0186
C(4) 208.5 as CO3
Cl 101.5
F 0.17
Ca 118.5
Mg 38.6
Na 55.45
K 6.125
Ba 0.1045
Si 8.115
P 0.023
Mn 0.1595
Fe 6.315
Al 0.009425
Sb 0.000425
Be 0.0001825
Cd 0.0001675
Cr 0.00125
Co 0.00083
Pb 0.0016
Mo 0.0078
Se 0.000395
end

EQUILIBRIUM_PHASES 1 #21R (C - UA) - median
Barite 0 0
Gypsum 0 0
Gibbsite 0 0.061
Ferrihydrite 0 0.085
Calcite 0 6
Dolomite(ordered) 0 2

SURFACE 1
Hfo_wOH Ferrihydrite equilibrium_phase 0.2 53400
Hfo_sOH Ferrihydrite equilibrium_phase 0.005 53400
Hao_OH Gibbsite equilibrium_phase 0.033 2496
-equil 1
save surface 1
end

EQUILIBRIUM_PHASES 2 #51 (C - UA) - median
Barite 0 0
Gypsum 0 0
Gibbsite 0 0.061
Ferrihydrite 0 0.085
Calcite 0 6
Dolomite(ordered) 0 2
```

```
SURFACE 2
Hfo_wOH Ferrihydrite equilibrium_phase 0.2 53400
Hfo_sOH Ferrihydrite equilibrium_phase 0.005 53400
Hao_OH Gibbsite equilibrium_phase 0.033 2496
-equil 2
save surface 2
end

SOLUTION 3 #average background
redox pe
units mg/l
density 1
pH 7
pe 2.08
temp 12.55
S(6) 47.5
B 0.1
Li 0.0081
As 0.0022325
C(4) 327
Cl 70 charge
F 0.155
Ca 149.5
Mg 40.9
Na 48.75
K 0.435
Ba 0.10475
Si 12.2
P 0.119
Mn 1.21
Fe 5.825
Al 0.009425
Sb 0.000425
Be 0.0001825
Cd 0.0001675
Cr 0.000975
Co 0.00045
Pb 0.0010475
Mo 0.00155
Se 0.000395

SAVE solution 3

end

#FIRST REACTION

#21R (C - UA) - First Reaction
USE SOLUTION 3
USE EQUILIBRIUM_PHASES 1
USE SURFACE 1
SAVE equilibrium_phases 1
SAVE surface 1
end

#21R (C - UA) - Second Reaction
USE SOLUTION 3
```

```
USE EQUILIBRIUM_PHASES 1
USE SURFACE 1
SAVE equilibrium_phases 1
SAVE surface 1
end

#51 (C - UA) - First Reaction
USE SOLUTION 3
USE EQUILIBRIUM_PHASES 2
USE SURFACE 2
SAVE equilibrium_phases 2
SAVE surface 2
end

#51 (C - UA) - Second Reaction
USE SOLUTION 3
USE EQUILIBRIUM_PHASES 2
USE SURFACE 2
SAVE equilibrium_phases 2
SAVE surface 2
end
```

804W - Median Metal Oxides/Charge Balance on Chloride

```
SELECTED_OUTPUT 1
-file HEN_845_804W_median_cb-true_out.csv
-charge_balance true
-percent_error true
-totals S(6) B Li As C(4) Cl F Ca Mg Na K Ba Si P Mn Fe Al Sb Be Cd Cr Co Pb Mo Se Hfo_s
Hfo_w Hao_
-molalities Hfo_wOH Hfo_wOH2+ Hfo_wOHSO4-2 Hfo_wSO4- Hfo_wOSi(OH)3
Hfo_wOSiO(OH)2- Hfo_wHCO3 Hfo_wCO3- Hfo_wPO4-2
Hfo_wHPO4- Hfo_wH2PO4 Hfo_sCO3- Hfo_sHCO3
Hfo_sHPO4- Hfo_sH2BO3 Hfo_sH2PO4 Hfo_sOSi(OH)3
Hfo_sOSiO(OH)2- Hfo_sOHSO4-2 Hfo_sSO4-
Hao_SO4- Hao_OHSO4-2 Hao_H2BO3 Hao_H3BO4-
Hfo_sH2AsO3 Hfo_sH2AsO4 Hfo_sHAsO4- Hfo_sOHAsO4-3
Hfo_wOHAsO4-3 Hfo_wHAsO4- Hfo_wH2AsO4 Hfo_wH2AsO3
-equilibrium_phases Ferrihydrite Gibbsite Barite Calcite Dolomite(ordered) Gypsum
-saturation_indices Ferrihydrite Gibbsite Barite Calcite Dolomite(ordered) Gypsum

SOLUTION 1 #21R (C - UA)
redox pe
units mg/l
density 1
pH 7.44
pe 0.98
temp 14.9
S(6) 92.5 as SO4
B 2.01
Li 0.02135
As 0.0252
C(4) 227.5 as CO3
Cl 99 charge
F 0.175
Ca 120.5
Mg 40.35
Na 47.2
K 2.905
Ba 0.298
Si 9.085
P 0.217
Mn 0.1105
Fe 5.52
Al 0.009425
Sb 0.000425
Be 0.0001825
Cd 0.0001675
Cr 0.002
Co 0.00135
Pb 0.0024
Mo 0.00885
Se 0.000395
end

SOLUTION 2 #51 (C - UA)
redox pe
```

```
units mg/l
density 1
pH 7.305
pe 1.42
temp 15.1
S(6) 93.5 as SO4
B 1.465
Li 0.0482
As 0.0186
C(4) 208.5 as CO3
Cl 101.5 charge
F 0.17
Ca 118.5
Mg 38.6
Na 55.45
K 6.125
Ba 0.1045
Si 8.115
P 0.023
Mn 0.1595
Fe 6.315
Al 0.009425
Sb 0.000425
Be 0.0001825
Cd 0.0001675
Cr 0.00125
Co 0.00083
Pb 0.0016
Mo 0.0078
Se 0.000395
end

EQUILIBRIUM_PHASES 1 #21R (C - UA) - median
Barite 0 0
Gypsum 0 0
Gibbsite 0 0.061
Ferrihydrite 0 0.085
Calcite 0 6
Dolomite(ordered) 0 2

SURFACE 1
Hfo_wOH Ferrihydrite equilibrium_phase 0.2 53400
Hfo_sOH Ferrihydrite equilibrium_phase 0.005 53400
Hao_OH Gibbsite equilibrium_phase 0.033 2496
-equil 1
save surface 1
end

EQUILIBRIUM_PHASES 2 #51 (C - UA) - median
Barite 0 0
Gypsum 0 0
Gibbsite 0 0.061
Ferrihydrite 0 0.085
Calcite 0 6
Dolomite(ordered) 0 2
```

```
SURFACE 2
Hfo_wOH Ferrihydrite equilibrium_phase 0.2 53400
Hfo_sOH Ferrihydrite equilibrium_phase 0.005 53400
Hao_OH Gibbsite equilibrium_phase 0.033 2496
-equil 2
save surface 2
end

SOLUTION 3 #average background
redox pe
units mg/l
density 1
pH 7
pe 2.08
temp 12.55
S(6) 47.5
B 0.1
Li 0.0081
As 0.0022325
C(4) 327
Cl 70 charge
F 0.155
Ca 149.5
Mg 40.9
Na 48.75
K 0.435
Ba 0.10475
Si 12.2
P 0.119
Mn 1.21
Fe 5.825
Al 0.009425
Sb 0.000425
Be 0.0001825
Cd 0.0001675
Cr 0.000975
Co 0.00045
Pb 0.0010475
Mo 0.00155
Se 0.000395

SAVE solution 3

end

#FIRST REACTION

#21R (C - UA) - First Reaction
USE SOLUTION 3
USE EQUILIBRIUM_PHASES 1
USE SURFACE 1
SAVE equilibrium_phases 1
SAVE surface 1
end

#21R (C - UA) - Second Reaction
USE SOLUTION 3
```

```
USE EQUILIBRIUM_PHASES 1
USE SURFACE 1
SAVE equilibrium_phases 1
SAVE surface 1
end

#51 (C - UA) - First Reaction
USE SOLUTION 3
USE EQUILIBRIUM_PHASES 2
USE SURFACE 2
SAVE equilibrium_phases 2
SAVE surface 2
end

#51 (C - UA) - Second Reaction
USE SOLUTION 3
USE EQUILIBRIUM_PHASES 2
USE SURFACE 2
SAVE equilibrium_phases 2
SAVE surface 2
end
```

804E - 25th Percentile Metal Oxides/No Charge Balance

```
SELECTED_OUTPUT 1
-file HEN_845_804E_25p_cb-false_out.csv
-charge_balance true
-percent_error true
-totals S(6) B Li As C(4) Cl F Ca Mg Na K Ba Si P Mn Fe Al Sb Be Cd Cr Co Pb Mo Se Hfo_s
Hfo_w Hao_
-molalities Hfo_wOH Hfo_wOH2+ Hfo_wOHSO4-2 Hfo_wSO4- Hfo_wOSi(OH)3
Hfo_wOSiO(OH)2- Hfo_wHCO3 Hfo_wCO3- Hfo_wPO4-2
Hfo_wHPO4- Hfo_wH2PO4 Hfo_sCO3- Hfo_sHCO3
Hfo_sHPO4- Hfo_sH2BO3 Hfo_sH2PO4 Hfo_sOSi(OH)3
Hfo_sOSiO(OH)2- Hfo_sOHSO4-2 Hfo_sSO4-
Hao_SO4- Hao_OHSO4-2 Hao_H2BO3 Hao_H3BO4-
Hfo_sH2AsO3 Hfo_sH2AsO4 Hfo_sHAsO4- Hfo_sOHAsO4-3
Hfo_wOHAsO4-3 Hfo_wHAsO4- Hfo_wH2AsO4 Hfo_wH2AsO3
-equilibrium_phases Ferrihydrite Gibbsite Barite Calcite Dolomite(ordered) Gypsum
-saturation_indices Ferrihydrite Gibbsite Barite Calcite Dolomite(ordered) Gypsum

SOLUTION 1 #22 (C - UA)
redox pe
units mg/l
density 1
pH 7.625
pe 4.815
temp 15.9
S(6) 121.5 as SO4
B 1.785
Li 0.0495
As 0.0022325
C(4) 145 as CO3
Cl 93
F 0.175
Ca 55.05
Mg 19.55
Na 33.9
K 6.95
Ba 0.03575
Si 19.1
P 0.0025
Mn 0.035
Fe 0.01675
Al 0.009425
Sb 0.000725
Be 0.0001825
Cd 0.0026425
Cr 0.000975
Co 0.00158
Pb 0.0010475
Mo 0.04395
Se 0.01535
end

SOLUTION 2 #23 (C - UA)
redox pe
```

```
units mg/l
density 1
pH 7.405
pe 1.545
temp 14
S(6) 455 as SO4
B 8.445
Li 0.003625
As 0.00262
C(4) 95.45 as CO3
Cl 54
F 0.185
Ca 107.5
Mg 77.75
Na 45
K 3.03
Ba 0.04505
Si 5.99
P 0.01
Mn 1.13
Fe 0.144
Al 0.009425
Sb 0.000425
Be 0.0002825
Cd 0.0001675
Cr 0.000975
Co 0.000435
Pb 0.0010475
Mo 0.0148
Se 0.000395
end

SOLUTION 3 #35 (C - UA)
redox pe
units mg/l
density 1
pH 6.955
pe 6.075
temp 14.55
S(6) 780 as SO4
B 12.3
Li 0.0275
As 0.0022325
C(4) 137.5 as CO3
Cl 34.5
F 0.155
Ca 305.5
Mg 36.85
Na 30.4
K 14
Ba 0.04255
Si 4.99
P 0.013
Mn 0.533
```

```
Fe 0.01675
Al 0.009425
Sb 0.000425
Be 0.0001825
Cd 0.0001675
Cr 0.000975
Co 0.0013
Pb 0.0010475
Mo 0.0779
Se 0.000395
end

EQUILIBRIUM_PHASES 1 #22 (C - UA) - 25p
Barite 0 0
Gypsum 0 0
Gibbsite 0 0.059
Ferrihydrite 0 0.072
Calcite 0 6
Dolomite(ordered) 0 2

SURFACE 1
Hfo_wOH Ferrihydrite equilibrium_phase 0.2 53400
Hfo_sOH Ferrihydrite equilibrium_phase 0.005 53400
Hao_OH Gibbsite equilibrium_phase 0.033 2496
-equil 1
save surface 1
end

EQUILIBRIUM_PHASES 2 #23 (C - UA) - 25p
Barite 0 0
Gypsum 0 0
Gibbsite 0 0.059
Ferrihydrite 0 0.072
Calcite 0 6
Dolomite(ordered) 0 2

SURFACE 2
Hfo_wOH Ferrihydrite equilibrium_phase 0.2 53400
Hfo_sOH Ferrihydrite equilibrium_phase 0.005 53400
Hao_OH Gibbsite equilibrium_phase 0.033 2496
-equil 2
save surface 2
end

EQUILIBRIUM_PHASES 3 #35 (C - UA) - 25p
Barite 0 0
Gypsum 0 0
Gibbsite 0 0.059
Ferrihydrite 0 0.072
Calcite 0 6
Dolomite(ordered) 0 2

SURFACE 3
Hfo_wOH Ferrihydrite equilibrium_phase 0.2 53400
Hfo_sOH Ferrihydrite equilibrium_phase 0.005 53400
Hao_OH Gibbsite equilibrium_phase 0.033 2496
-equil 3
```

```
save surface 3
end

SOLUTION 4 #average background
redox pe
units mg/l
density 1
pH 7.005
pe 5.89
temp 12.4
S(6) 64.5
B 0.1415
Li 0.00385
As 0.00242
C(4) 194.5
Cl 69 charge
F 0.16
Ca 101
Mg 39.25
Na 39.05
K 2.16
Ba 0.04
Si 6.275
P 0.057
Mn 0.07075
Fe 0.01675
Al 0.009425
Sb 0.000425
Be 0.0001825
Cd 0.00023
Cr 0.000975
Co 0.0016
Pb 0.0010475
Mo 0.00155
Se 0.000395

SAVE solution 4

end

#FIRST REACTION

#22 (C - UA) - First Reaction
USE SOLUTION 4
USE EQUILIBRIUM_PHASES 1
USE SURFACE 1
SAVE equilibrium_phases 1
SAVE surface 1
end

#22 (C - UA) - Second Reaction
USE SOLUTION 4
USE EQUILIBRIUM_PHASES 1
USE SURFACE 1
SAVE equilibrium_phases 1
SAVE surface 1
end
```

```
#23 (C - UA) - First Reaction
USE SOLUTION 4
USE EQUILIBRIUM_PHASES 2
USE SURFACE 2
SAVE equilibrium_phases 2
SAVE surface 2
end

#23 (C - UA) - Second Reaction
USE SOLUTION 4
USE EQUILIBRIUM_PHASES 2
USE SURFACE 2
SAVE equilibrium_phases 2
SAVE surface 2
end

#35 (C - UA) - First Reaction
USE SOLUTION 4
USE EQUILIBRIUM_PHASES 3
USE SURFACE 3
SAVE equilibrium_phases 3
SAVE surface 3
end

#35 (C - UA) - Second Reaction
USE SOLUTION 4
USE EQUILIBRIUM_PHASES 3
USE SURFACE 3
SAVE equilibrium_phases 3
SAVE surface 3
end
```

804E - 25th Percentile Metal Oxides/Charge Balance on Chloride

```
SELECTED_OUTPUT 1
-file HEN_845_804E_25p_cb-true_out.csv
-charge_balance true
-percent_error true
-totals S(6) B Li As C(4) Cl F Ca Mg Na K Ba Si P Mn Fe Al Sb Be Cd Cr Co Pb Mo Se Hfo_s
Hfo_w Hao_
-molalities Hfo_wOH Hfo_wOH2+ Hfo_wOHSO4-2 Hfo_wSO4- Hfo_wOSi(OH)3
Hfo_wOSiO(OH)2- Hfo_wHCO3 Hfo_wCO3- Hfo_wPO4-2
Hfo_wHPO4- Hfo_wH2PO4 Hfo_sCO3- Hfo_sHCO3
Hfo_sHPO4- Hfo_sH2BO3 Hfo_sH2PO4 Hfo_sOSi(OH)3
Hfo_sOSiO(OH)2- Hfo_sOHSO4-2 Hfo_sSO4-
Hao_SO4- Hao_OHSO4-2 Hao_H2BO3 Hao_H3BO4-
Hfo_sH2AsO3 Hfo_sH2AsO4 Hfo_sHAsO4- Hfo_sOHAsO4-3
Hfo_wOHAsO4-3 Hfo_wHAsO4- Hfo_wH2AsO4 Hfo_wH2AsO3
-equilibrium_phases Ferrihydrite Gibbsite Barite Calcite Dolomite(ordered) Gypsum
-saturation_indices Ferrihydrite Gibbsite Barite Calcite Dolomite(ordered) Gypsum

SOLUTION 1 #22 (C - UA)
redox pe
units mg/l
density 1
pH 7.625
pe 4.815
temp 15.9
S(6) 121.5 as SO4
B 1.785
Li 0.0495
As 0.0022325
C(4) 145 as CO3
Cl 93 charge
F 0.175
Ca 55.05
Mg 19.55
Na 33.9
K 6.95
Ba 0.03575
Si 19.1
P 0.0025
Mn 0.035
Fe 0.01675
Al 0.009425
Sb 0.000725
Be 0.0001825
Cd 0.0026425
Cr 0.000975
Co 0.00158
Pb 0.0010475
Mo 0.04395
Se 0.01535
end

SOLUTION 2 #23 (C - UA)
redox pe
```

```
units mg/l
density 1
pH 7.405
pe 1.545
temp 14
S(6) 455 as SO4
B 8.445
Li 0.003625
As 0.00262
C(4) 95.45 as CO3
Cl 54 charge
F 0.185
Ca 107.5
Mg 77.75
Na 45
K 3.03
Ba 0.04505
Si 5.99
P 0.01
Mn 1.13
Fe 0.144
Al 0.009425
Sb 0.000425
Be 0.0002825
Cd 0.0001675
Cr 0.000975
Co 0.000435
Pb 0.0010475
Mo 0.0148
Se 0.000395
end

SOLUTION 3 #35 (C - UA)
redox pe
units mg/l
density 1
pH 6.955
pe 6.075
temp 14.55
S(6) 780 as SO4
B 12.3
Li 0.0275
As 0.0022325
C(4) 137.5 as CO3
Cl 34.5 charge
F 0.155
Ca 305.5
Mg 36.85
Na 30.4
K 14
Ba 0.04255
Si 4.99
P 0.013
Mn 0.533
```

```
Fe 0.01675
Al 0.009425
Sb 0.000425
Be 0.0001825
Cd 0.0001675
Cr 0.000975
Co 0.0013
Pb 0.0010475
Mo 0.0779
Se 0.000395
end

EQUILIBRIUM_PHASES 1 #22 (C - UA) - 25p
Barite 0 0
Gypsum 0 0
Gibbsite 0 0.059
Ferrihydrite 0 0.072
Calcite 0 6
Dolomite(ordered) 0 2

SURFACE 1
Hfo_wOH Ferrihydrite equilibrium_phase 0.2 53400
Hfo_sOH Ferrihydrite equilibrium_phase 0.005 53400
Hao_OH Gibbsite equilibrium_phase 0.033 2496
-equil 1
save surface 1
end

EQUILIBRIUM_PHASES 2 #23 (C - UA) - 25p
Barite 0 0
Gypsum 0 0
Gibbsite 0 0.059
Ferrihydrite 0 0.072
Calcite 0 6
Dolomite(ordered) 0 2

SURFACE 2
Hfo_wOH Ferrihydrite equilibrium_phase 0.2 53400
Hfo_sOH Ferrihydrite equilibrium_phase 0.005 53400
Hao_OH Gibbsite equilibrium_phase 0.033 2496
-equil 2
save surface 2
end

EQUILIBRIUM_PHASES 3 #35 (C - UA) - 25p
Barite 0 0
Gypsum 0 0
Gibbsite 0 0.059
Ferrihydrite 0 0.072
Calcite 0 6
Dolomite(ordered) 0 2

SURFACE 3
Hfo_wOH Ferrihydrite equilibrium_phase 0.2 53400
Hfo_sOH Ferrihydrite equilibrium_phase 0.005 53400
Hao_OH Gibbsite equilibrium_phase 0.033 2496
-equil 3
```

```
save surface 3
end

SOLUTION 4 #average background
redox pe
units mg/l
density 1
pH 7.005
pe 5.89
temp 12.4
S(6) 64.5
B 0.1415
Li 0.00385
As 0.00242
C(4) 194.5
Cl 69 charge
F 0.16
Ca 101
Mg 39.25
Na 39.05
K 2.16
Ba 0.04
Si 6.275
P 0.057
Mn 0.07075
Fe 0.01675
Al 0.009425
Sb 0.000425
Be 0.0001825
Cd 0.00023
Cr 0.000975
Co 0.0016
Pb 0.0010475
Mo 0.00155
Se 0.000395

SAVE solution 4

end

#FIRST REACTION

#22 (C - UA) - First Reaction
USE SOLUTION 4
USE EQUILIBRIUM_PHASES 1
USE SURFACE 1
SAVE equilibrium_phases 1
SAVE surface 1
end

#22 (C - UA) - Second Reaction
USE SOLUTION 4
USE EQUILIBRIUM_PHASES 1
USE SURFACE 1
SAVE equilibrium_phases 1
SAVE surface 1
end
```

```
#23 (C - UA) - First Reaction
USE SOLUTION 4
USE EQUILIBRIUM_PHASES 2
USE SURFACE 2
SAVE equilibrium_phases 2
SAVE surface 2
end

#23 (C - UA) - Second Reaction
USE SOLUTION 4
USE EQUILIBRIUM_PHASES 2
USE SURFACE 2
SAVE equilibrium_phases 2
SAVE surface 2
end

#35 (C - UA) - First Reaction
USE SOLUTION 4
USE EQUILIBRIUM_PHASES 3
USE SURFACE 3
SAVE equilibrium_phases 3
SAVE surface 3
end

#35 (C - UA) - Second Reaction
USE SOLUTION 4
USE EQUILIBRIUM_PHASES 3
USE SURFACE 3
SAVE equilibrium_phases 3
SAVE surface 3
end
```

804E - 75th Percentile Metal Oxides/No Charge Balance

```
SELECTED_OUTPUT 1
-file HEN_845_804E_75p_cb-false_out.csv
-charge_balance true
-percent_error true
-totals S(6) B Li As C(4) Cl F Ca Mg Na K Ba Si P Mn Fe Al Sb Be Cd Cr Co Pb Mo Se Hfo_s
Hfo_w Hao_
-molalities Hfo_wOH Hfo_wOH2+ Hfo_wOHSO4-2 Hfo_wSO4- Hfo_wOSi(OH)3
Hfo_wOSiO(OH)2- Hfo_wHCO3 Hfo_wCO3- Hfo_wPO4-2
Hfo_wHPO4- Hfo_wH2PO4 Hfo_sCO3- Hfo_sHCO3
Hfo_sHPO4- Hfo_sH2BO3 Hfo_sH2PO4 Hfo_sOSi(OH)3
Hfo_sOSiO(OH)2- Hfo_sOHSO4-2 Hfo_sSO4-
Hao_SO4- Hao_OHSO4-2 Hao_H2BO3 Hao_H3BO4-
Hfo_sH2AsO3 Hfo_sH2AsO4 Hfo_sHAsO4- Hfo_sOHAsO4-3
Hfo_wOHAsO4-3 Hfo_wHAsO4- Hfo_wH2AsO4 Hfo_wH2AsO3
-equilibrium_phases Ferrihydrite Gibbsite Barite Calcite Dolomite(ordered) Gypsum
-saturation_indices Ferrihydrite Gibbsite Barite Calcite Dolomite(ordered) Gypsum
```

```
SOLUTION 1 #22 (C - UA)
redox pe
units mg/l
density 1
pH 7.625
pe 4.815
temp 15.9
S(6) 121.5 as SO4
B 1.785
Li 0.0495
As 0.0022325
C(4) 145 as CO3
Cl 93
F 0.175
Ca 55.05
Mg 19.55
Na 33.9
K 6.95
Ba 0.03575
Si 19.1
P 0.0025
Mn 0.035
Fe 0.01675
Al 0.009425
Sb 0.000725
Be 0.0001825
Cd 0.0026425
Cr 0.000975
Co 0.00158
Pb 0.0010475
Mo 0.04395
Se 0.01535
end
```

```
SOLUTION 2 #23 (C - UA)
redox pe
```

```
units mg/l
density 1
pH 7.405
pe 1.545
temp 14
S(6) 455 as SO4
B 8.445
Li 0.003625
As 0.00262
C(4) 95.45 as CO3
Cl 54
F 0.185
Ca 107.5
Mg 77.75
Na 45
K 3.03
Ba 0.04505
Si 5.99
P 0.01
Mn 1.13
Fe 0.144
Al 0.009425
Sb 0.000425
Be 0.0002825
Cd 0.0001675
Cr 0.000975
Co 0.000435
Pb 0.0010475
Mo 0.0148
Se 0.000395
end
SOLUTION 3 #35 (C - UA)
redox pe
units mg/l
density 1
pH 6.955
pe 6.075
temp 14.55
S(6) 780 as SO4
B 12.3
Li 0.0275
As 0.0022325
C(4) 137.5 as CO3
Cl 34.5
F 0.155
Ca 305.5
Mg 36.85
Na 30.4
K 14
Ba 0.04255
Si 4.99
P 0.013
Mn 0.533
```

```
Fe 0.01675
Al 0.009425
Sb 0.000425
Be 0.0001825
Cd 0.0001675
Cr 0.000975
Co 0.0013
Pb 0.0010475
Mo 0.0779
Se 0.000395
end

EQUILIBRIUM_PHASES 1 #22 (C - UA) - 75p
Barite 0 0
Gypsum 0 0
Gibbsite 0 0.064
Ferrihydrite 0 0.1
Calcite 0 6
Dolomite(ordered) 0 2

SURFACE 1
Hfo_wOH Ferrihydrite equilibrium_phase 0.2 53400
Hfo_sOH Ferrihydrite equilibrium_phase 0.005 53400
Hao_OH Gibbsite equilibrium_phase 0.033 2496
-equil 1
save surface 1
end

EQUILIBRIUM_PHASES 2 #23 (C - UA) - 75p
Barite 0 0
Gypsum 0 0
Gibbsite 0 0.064
Ferrihydrite 0 0.1
Calcite 0 6
Dolomite(ordered) 0 2

SURFACE 2
Hfo_wOH Ferrihydrite equilibrium_phase 0.2 53400
Hfo_sOH Ferrihydrite equilibrium_phase 0.005 53400
Hao_OH Gibbsite equilibrium_phase 0.033 2496
-equil 2
save surface 2
end

EQUILIBRIUM_PHASES 3 #35 (C - UA) - 75p
Barite 0 0
Gypsum 0 0
Gibbsite 0 0.064
Ferrihydrite 0 0.1
Calcite 0 6
Dolomite(ordered) 0 2

SURFACE 3
Hfo_wOH Ferrihydrite equilibrium_phase 0.2 53400
Hfo_sOH Ferrihydrite equilibrium_phase 0.005 53400
Hao_OH Gibbsite equilibrium_phase 0.033 2496
-equil 3
```

```
save surface 3
end

SOLUTION 4 #average background
redox pe
units mg/l
density 1
pH 7.005
pe 5.89
temp 12.4
S(6) 64.5
B 0.1415
Li 0.00385
As 0.00242
C(4) 194.5
Cl 69 charge
F 0.16
Ca 101
Mg 39.25
Na 39.05
K 2.16
Ba 0.04
Si 6.275
P 0.057
Mn 0.07075
Fe 0.01675
Al 0.009425
Sb 0.000425
Be 0.0001825
Cd 0.00023
Cr 0.000975
Co 0.0016
Pb 0.0010475
Mo 0.00155
Se 0.000395

SAVE solution 4

end

#FIRST REACTION

#22 (C - UA) - First Reaction
USE SOLUTION 4
USE EQUILIBRIUM_PHASES 1
USE SURFACE 1
SAVE equilibrium_phases 1
SAVE surface 1
end

#22 (C - UA) - Second Reaction
USE SOLUTION 4
USE EQUILIBRIUM_PHASES 1
USE SURFACE 1
SAVE equilibrium_phases 1
SAVE surface 1
end
```

```
#23 (C - UA) - First Reaction
USE SOLUTION 4
USE EQUILIBRIUM_PHASES 2
USE SURFACE 2
SAVE equilibrium_phases 2
SAVE surface 2
end

#23 (C - UA) - Second Reaction
USE SOLUTION 4
USE EQUILIBRIUM_PHASES 2
USE SURFACE 2
SAVE equilibrium_phases 2
SAVE surface 2
end

#35 (C - UA) - First Reaction
USE SOLUTION 4
USE EQUILIBRIUM_PHASES 3
USE SURFACE 3
SAVE equilibrium_phases 3
SAVE surface 3
end

#35 (C - UA) - Second Reaction
USE SOLUTION 4
USE EQUILIBRIUM_PHASES 3
USE SURFACE 3
SAVE equilibrium_phases 3
SAVE surface 3
end
```

804E - 75th Percentile Metal Oxides/Charge Balance on Chloride

```
SELECTED_OUTPUT 1
-file HEN_845_804E_75p_cb-true_out.csv
-charge_balance true
-percent_error true
-totals S(6) B Li As C(4) Cl F Ca Mg Na K Ba Si P Mn Fe Al Sb Be Cd Cr Co Pb Mo Se Hfo_s
Hfo_w Hao_
-molalities Hfo_wOH Hfo_wOH2+ Hfo_wOHSO4-2 Hfo_wSO4- Hfo_wOSi(OH)3
Hfo_wOSiO(OH)2- Hfo_wHCO3 Hfo_wCO3- Hfo_wPO4-2
Hfo_wHPO4- Hfo_wH2PO4 Hfo_sCO3- Hfo_sHCO3
Hfo_sHPO4- Hfo_sH2BO3 Hfo_sH2PO4 Hfo_sOSi(OH)3
Hfo_sOSiO(OH)2- Hfo_sOHSO4-2 Hfo_sSO4-
Hao_SO4- Hao_OHSO4-2 Hao_H2BO3 Hao_H3BO4-
Hfo_sH2AsO3 Hfo_sH2AsO4 Hfo_sHAsO4- Hfo_sOHAsO4-3
Hfo_wOHAsO4-3 Hfo_wHAsO4- Hfo_wH2AsO4 Hfo_wH2AsO3
-equilibrium_phases Ferrihydrite Gibbsite Barite Calcite Dolomite(ordered) Gypsum
-saturation_indices Ferrihydrite Gibbsite Barite Calcite Dolomite(ordered) Gypsum

SOLUTION 1 #22 (C - UA)
redox pe
units mg/l
density 1
pH 7.625
pe 4.815
temp 15.9
S(6) 121.5 as SO4
B 1.785
Li 0.0495
As 0.0022325
C(4) 145 as CO3
Cl 93 charge
F 0.175
Ca 55.05
Mg 19.55
Na 33.9
K 6.95
Ba 0.03575
Si 19.1
P 0.0025
Mn 0.035
Fe 0.01675
Al 0.009425
Sb 0.000725
Be 0.0001825
Cd 0.0026425
Cr 0.000975
Co 0.00158
Pb 0.0010475
Mo 0.04395
Se 0.01535
end

SOLUTION 2 #23 (C - UA)
redox pe
```

```
units mg/l
density 1
pH 7.405
pe 1.545
temp 14
S(6) 455 as SO4
B 8.445
Li 0.003625
As 0.00262
C(4) 95.45 as CO3
Cl 54 charge
F 0.185
Ca 107.5
Mg 77.75
Na 45
K 3.03
Ba 0.04505
Si 5.99
P 0.01
Mn 1.13
Fe 0.144
Al 0.009425
Sb 0.000425
Be 0.0002825
Cd 0.0001675
Cr 0.000975
Co 0.000435
Pb 0.0010475
Mo 0.0148
Se 0.000395
end
```

```
SOLUTION 3 #35 (C - UA)
redox pe
units mg/l
density 1
pH 6.955
pe 6.075
temp 14.55
S(6) 780 as SO4
B 12.3
Li 0.0275
As 0.0022325
C(4) 137.5 as CO3
Cl 34.5 charge
F 0.155
Ca 305.5
Mg 36.85
Na 30.4
K 14
Ba 0.04255
Si 4.99
P 0.013
Mn 0.533
```

```
Fe 0.01675
Al 0.009425
Sb 0.000425
Be 0.0001825
Cd 0.0001675
Cr 0.000975
Co 0.0013
Pb 0.0010475
Mo 0.0779
Se 0.000395
end

EQUILIBRIUM_PHASES 1 #22 (C - UA) - 75p
Barite 0 0
Gypsum 0 0
Gibbsite 0 0.064
Ferrihydrite 0 0.1
Calcite 0 6
Dolomite(ordered) 0 2

SURFACE 1
Hfo_wOH Ferrihydrite equilibrium_phase 0.2 53400
Hfo_sOH Ferrihydrite equilibrium_phase 0.005 53400
Hao_OH Gibbsite equilibrium_phase 0.033 2496
-equil 1
save surface 1
end

EQUILIBRIUM_PHASES 2 #23 (C - UA) - 75p
Barite 0 0
Gypsum 0 0
Gibbsite 0 0.064
Ferrihydrite 0 0.1
Calcite 0 6
Dolomite(ordered) 0 2

SURFACE 2
Hfo_wOH Ferrihydrite equilibrium_phase 0.2 53400
Hfo_sOH Ferrihydrite equilibrium_phase 0.005 53400
Hao_OH Gibbsite equilibrium_phase 0.033 2496
-equil 2
save surface 2
end

EQUILIBRIUM_PHASES 3 #35 (C - UA) - 75p
Barite 0 0
Gypsum 0 0
Gibbsite 0 0.064
Ferrihydrite 0 0.1
Calcite 0 6
Dolomite(ordered) 0 2

SURFACE 3
Hfo_wOH Ferrihydrite equilibrium_phase 0.2 53400
Hfo_sOH Ferrihydrite equilibrium_phase 0.005 53400
Hao_OH Gibbsite equilibrium_phase 0.033 2496
-equil 3
```

```
save surface 3
end

SOLUTION 4 #average background
redox pe
units mg/l
density 1
pH 7.005
pe 5.89
temp 12.4
S(6) 64.5
B 0.1415
Li 0.00385
As 0.00242
C(4) 194.5
Cl 69 charge
F 0.16
Ca 101
Mg 39.25
Na 39.05
K 2.16
Ba 0.04
Si 6.275
P 0.057
Mn 0.07075
Fe 0.01675
Al 0.009425
Sb 0.000425
Be 0.0001825
Cd 0.00023
Cr 0.000975
Co 0.0016
Pb 0.0010475
Mo 0.00155
Se 0.000395

SAVE solution 4

end

#FIRST REACTION

#22 (C - UA) - First Reaction
USE SOLUTION 4
USE EQUILIBRIUM_PHASES 1
USE SURFACE 1
SAVE equilibrium_phases 1
SAVE surface 1
end

#22 (C - UA) - Second Reaction
USE SOLUTION 4
USE EQUILIBRIUM_PHASES 1
USE SURFACE 1
SAVE equilibrium_phases 1
SAVE surface 1
end
```

```
#23 (C - UA) - First Reaction
USE SOLUTION 4
USE EQUILIBRIUM_PHASES 2
USE SURFACE 2
SAVE equilibrium_phases 2
SAVE surface 2
end

#23 (C - UA) - Second Reaction
USE SOLUTION 4
USE EQUILIBRIUM_PHASES 2
USE SURFACE 2
SAVE equilibrium_phases 2
SAVE surface 2
end

#35 (C - UA) - First Reaction
USE SOLUTION 4
USE EQUILIBRIUM_PHASES 3
USE SURFACE 3
SAVE equilibrium_phases 3
SAVE surface 3
end

#35 (C - UA) - Second Reaction
USE SOLUTION 4
USE EQUILIBRIUM_PHASES 3
USE SURFACE 3
SAVE equilibrium_phases 3
SAVE surface 3
end
```

804E - Median Metal Oxides/No Charge Balance

```
SELECTED_OUTPUT 1
-file HEN_845_804E_median_cb-false_out.csv
-charge_balance true
-percent_error true
-totals S(6) B Li As C(4) Cl F Ca Mg Na K Ba Si P Mn Fe Al Sb Be Cd Cr Co Pb Mo Se Hfo_s
Hfo_w Hao_
-molalities Hfo_wOH Hfo_wOH2+ Hfo_wOHSO4-2 Hfo_wSO4- Hfo_wOSi(OH)3
Hfo_wOSiO(OH)2- Hfo_wHCO3 Hfo_wCO3- Hfo_wPO4-2
Hfo_wHPO4- Hfo_wH2PO4 Hfo_sCO3- Hfo_sHCO3
Hfo_sHPO4- Hfo_sH2BO3 Hfo_sH2PO4 Hfo_sOSi(OH)3
Hfo_sOSiO(OH)2- Hfo_sOHSO4-2 Hfo_sSO4-
Hao_SO4- Hao_OHSO4-2 Hao_H2BO3 Hao_H3BO4-
Hfo_sH2AsO3 Hfo_sH2AsO4 Hfo_sHAsO4- Hfo_sOHAsO4-3
Hfo_wOHAsO4-3 Hfo_wHAsO4- Hfo_wH2AsO4 Hfo_wH2AsO3
-equilibrium_phases Ferrihydrite Gibbsite Barite Calcite Dolomite(ordered) Gypsum
-saturation_indices Ferrihydrite Gibbsite Barite Calcite Dolomite(ordered) Gypsum

SOLUTION 1 #22 (C - UA)
redox pe
units mg/l
density 1
pH 7.625
pe 4.815
temp 15.9
S(6) 121.5 as SO4
B 1.785
Li 0.0495
As 0.0022325
C(4) 145 as CO3
Cl 93
F 0.175
Ca 55.05
Mg 19.55
Na 33.9
K 6.95
Ba 0.03575
Si 19.1
P 0.0025
Mn 0.035
Fe 0.01675
Al 0.009425
Sb 0.000725
Be 0.0001825
Cd 0.0026425
Cr 0.000975
Co 0.00158
Pb 0.0010475
Mo 0.04395
Se 0.01535
end

SOLUTION 2 #23 (C - UA)
redox pe
```

```
units mg/l
density 1
pH 7.405
pe 1.545
temp 14
S(6) 455 as SO4
B 8.445
Li 0.003625
As 0.00262
C(4) 95.45 as CO3
Cl 54
F 0.185
Ca 107.5
Mg 77.75
Na 45
K 3.03
Ba 0.04505
Si 5.99
P 0.01
Mn 1.13
Fe 0.144
Al 0.009425
Sb 0.000425
Be 0.0002825
Cd 0.0001675
Cr 0.000975
Co 0.000435
Pb 0.0010475
Mo 0.0148
Se 0.000395
end

SOLUTION 3 #35 (C - UA)
redox pe
units mg/l
density 1
pH 6.955
pe 6.075
temp 14.55
S(6) 780 as SO4
B 12.3
Li 0.0275
As 0.0022325
C(4) 137.5 as CO3
Cl 34.5
F 0.155
Ca 305.5
Mg 36.85
Na 30.4
K 14
Ba 0.04255
Si 4.99
P 0.013
Mn 0.533
```

```
Fe 0.01675
Al 0.009425
Sb 0.000425
Be 0.0001825
Cd 0.0001675
Cr 0.000975
Co 0.0013
Pb 0.0010475
Mo 0.0779
Se 0.000395
end

EQUILIBRIUM_PHASES 1 #22 (C - UA) - median
Barite 0 0
Gypsum 0 0
Gibbsite 0 0.061
Ferrihydrite 0 0.085
Calcite 0 6
Dolomite(ordered) 0 2

SURFACE 1
Hfo_wOH Ferrihydrite equilibrium_phase 0.2 53400
Hfo_sOH Ferrihydrite equilibrium_phase 0.005 53400
Hao_OH Gibbsite equilibrium_phase 0.033 2496
-equil 1
save surface 1
end

EQUILIBRIUM_PHASES 2 #23 (C - UA) - median
Barite 0 0
Gypsum 0 0
Gibbsite 0 0.061
Ferrihydrite 0 0.085
Calcite 0 6
Dolomite(ordered) 0 2

SURFACE 2
Hfo_wOH Ferrihydrite equilibrium_phase 0.2 53400
Hfo_sOH Ferrihydrite equilibrium_phase 0.005 53400
Hao_OH Gibbsite equilibrium_phase 0.033 2496
-equil 2
save surface 2
end

EQUILIBRIUM_PHASES 3 #35 (C - UA) - median
Barite 0 0
Gypsum 0 0
Gibbsite 0 0.061
Ferrihydrite 0 0.085
Calcite 0 6
Dolomite(ordered) 0 2

SURFACE 3
Hfo_wOH Ferrihydrite equilibrium_phase 0.2 53400
Hfo_sOH Ferrihydrite equilibrium_phase 0.005 53400
Hao_OH Gibbsite equilibrium_phase 0.033 2496
-equil 3
```

```
save surface 3
end

SOLUTION 4 #average background
redox pe
units mg/l
density 1
pH 7.005
pe 5.89
temp 12.4
S(6) 64.5
B 0.1415
Li 0.00385
As 0.00242
C(4) 194.5
Cl 69 charge
F 0.16
Ca 101
Mg 39.25
Na 39.05
K 2.16
Ba 0.04
Si 6.275
P 0.057
Mn 0.07075
Fe 0.01675
Al 0.009425
Sb 0.000425
Be 0.0001825
Cd 0.00023
Cr 0.000975
Co 0.0016
Pb 0.0010475
Mo 0.00155
Se 0.000395

SAVE solution 4

end

#FIRST REACTION

#22 (C - UA) - First Reaction
USE SOLUTION 4
USE EQUILIBRIUM_PHASES 1
USE SURFACE 1
SAVE equilibrium_phases 1
SAVE surface 1
end

#22 (C - UA) - Second Reaction
USE SOLUTION 4
USE EQUILIBRIUM_PHASES 1
USE SURFACE 1
SAVE equilibrium_phases 1
SAVE surface 1
end
```

```
#23 (C - UA) - First Reaction
USE SOLUTION 4
USE EQUILIBRIUM_PHASES 2
USE SURFACE 2
SAVE equilibrium_phases 2
SAVE surface 2
end

#23 (C - UA) - Second Reaction
USE SOLUTION 4
USE EQUILIBRIUM_PHASES 2
USE SURFACE 2
SAVE equilibrium_phases 2
SAVE surface 2
end

#35 (C - UA) - First Reaction
USE SOLUTION 4
USE EQUILIBRIUM_PHASES 3
USE SURFACE 3
SAVE equilibrium_phases 3
SAVE surface 3
end

#35 (C - UA) - Second Reaction
USE SOLUTION 4
USE EQUILIBRIUM_PHASES 3
USE SURFACE 3
SAVE equilibrium_phases 3
SAVE surface 3
end
```

804E - Median Metal Oxides/Charge Balance on Chloride

```
SELECTED_OUTPUT 1
-file HEN_845_804E_median_cb-true_out.csv
-charge_balance true
-percent_error true
-totals S(6) B Li As C(4) Cl F Ca Mg Na K Ba Si P Mn Fe Al Sb Be Cd Cr Co Pb Mo Se Hfo_s
Hfo_w Hao_
-molalities Hfo_wOH Hfo_wOH2+ Hfo_wOHSO4-2 Hfo_wSO4- Hfo_wOSi(OH)3
Hfo_wOSiO(OH)2- Hfo_wHCO3 Hfo_wCO3- Hfo_wPO4-2
Hfo_wHPO4- Hfo_wH2PO4 Hfo_sCO3- Hfo_sHCO3
Hfo_sHPO4- Hfo_sH2BO3 Hfo_sH2PO4 Hfo_sOSi(OH)3
Hfo_sOSiO(OH)2- Hfo_sOHSO4-2 Hfo_sSO4-
Hao_SO4- Hao_OHSO4-2 Hao_H2BO3 Hao_H3BO4-
Hfo_sH2AsO3 Hfo_sH2AsO4 Hfo_sHAsO4- Hfo_sOHAsO4-3
Hfo_wOHAsO4-3 Hfo_wHAsO4- Hfo_wH2AsO4 Hfo_wH2AsO3
-equilibrium_phases Ferrihydrite Gibbsite Barite Calcite Dolomite(ordered) Gypsum
-saturation_indices Ferrihydrite Gibbsite Barite Calcite Dolomite(ordered) Gypsum

SOLUTION 1 #22 (C - UA)
redox pe
units mg/l
density 1
pH 7.625
pe 4.815
temp 15.9
S(6) 121.5 as SO4
B 1.785
Li 0.0495
As 0.0022325
C(4) 145 as CO3
Cl 93 charge
F 0.175
Ca 55.05
Mg 19.55
Na 33.9
K 6.95
Ba 0.03575
Si 19.1
P 0.0025
Mn 0.035
Fe 0.01675
Al 0.009425
Sb 0.000725
Be 0.0001825
Cd 0.0026425
Cr 0.000975
Co 0.00158
Pb 0.0010475
Mo 0.04395
Se 0.01535
end

SOLUTION 2 #23 (C - UA)
redox pe
```

```
units mg/l
density 1
pH 7.405
pe 1.545
temp 14
S(6) 455 as SO4
B 8.445
Li 0.003625
As 0.00262
C(4) 95.45 as CO3
Cl 54 charge
F 0.185
Ca 107.5
Mg 77.75
Na 45
K 3.03
Ba 0.04505
Si 5.99
P 0.01
Mn 1.13
Fe 0.144
Al 0.009425
Sb 0.000425
Be 0.0002825
Cd 0.0001675
Cr 0.000975
Co 0.000435
Pb 0.0010475
Mo 0.0148
Se 0.000395
end

SOLUTION 3 #35 (C - UA)
redox pe
units mg/l
density 1
pH 6.955
pe 6.075
temp 14.55
S(6) 780 as SO4
B 12.3
Li 0.0275
As 0.0022325
C(4) 137.5 as CO3
Cl 34.5 charge
F 0.155
Ca 305.5
Mg 36.85
Na 30.4
K 14
Ba 0.04255
Si 4.99
P 0.013
Mn 0.533
```

```
Fe 0.01675
Al 0.009425
Sb 0.000425
Be 0.0001825
Cd 0.0001675
Cr 0.000975
Co 0.0013
Pb 0.0010475
Mo 0.0779
Se 0.000395
end

EQUILIBRIUM_PHASES 1 #22 (C - UA) - median
Barite 0 0
Gypsum 0 0
Gibbsite 0 0.061
Ferrihydrite 0 0.085
Calcite 0 6
Dolomite(ordered) 0 2

SURFACE 1
Hfo_wOH Ferrihydrite equilibrium_phase 0.2 53400
Hfo_sOH Ferrihydrite equilibrium_phase 0.005 53400
Hao_OH Gibbsite equilibrium_phase 0.033 2496
-equil 1
save surface 1
end

EQUILIBRIUM_PHASES 2 #23 (C - UA) - median
Barite 0 0
Gypsum 0 0
Gibbsite 0 0.061
Ferrihydrite 0 0.085
Calcite 0 6
Dolomite(ordered) 0 2

SURFACE 2
Hfo_wOH Ferrihydrite equilibrium_phase 0.2 53400
Hfo_sOH Ferrihydrite equilibrium_phase 0.005 53400
Hao_OH Gibbsite equilibrium_phase 0.033 2496
-equil 2
save surface 2
end

EQUILIBRIUM_PHASES 3 #35 (C - UA) - median
Barite 0 0
Gypsum 0 0
Gibbsite 0 0.061
Ferrihydrite 0 0.085
Calcite 0 6
Dolomite(ordered) 0 2

SURFACE 3
Hfo_wOH Ferrihydrite equilibrium_phase 0.2 53400
Hfo_sOH Ferrihydrite equilibrium_phase 0.005 53400
Hao_OH Gibbsite equilibrium_phase 0.033 2496
-equil 3
```

```
save surface 3
end

SOLUTION 4 #average background
redox pe
units mg/l
density 1
pH 7.005
pe 5.89
temp 12.4
S(6) 64.5
B 0.1415
Li 0.00385
As 0.00242
C(4) 194.5
Cl 69 charge
F 0.16
Ca 101
Mg 39.25
Na 39.05
K 2.16
Ba 0.04
Si 6.275
P 0.057
Mn 0.07075
Fe 0.01675
Al 0.009425
Sb 0.000425
Be 0.0001825
Cd 0.00023
Cr 0.000975
Co 0.0016
Pb 0.0010475
Mo 0.00155
Se 0.000395

SAVE solution 4

end

#FIRST REACTION

#22 (C - UA) - First Reaction
USE SOLUTION 4
USE EQUILIBRIUM_PHASES 1
USE SURFACE 1
SAVE equilibrium_phases 1
SAVE surface 1
end

#22 (C - UA) - Second Reaction
USE SOLUTION 4
USE EQUILIBRIUM_PHASES 1
USE SURFACE 1
SAVE equilibrium_phases 1
SAVE surface 1
end
```

```
#23 (C - UA) - First Reaction
USE SOLUTION 4
USE EQUILIBRIUM_PHASES 2
USE SURFACE 2
SAVE equilibrium_phases 2
SAVE surface 2
end

#23 (C - UA) - Second Reaction
USE SOLUTION 4
USE EQUILIBRIUM_PHASES 2
USE SURFACE 2
SAVE equilibrium_phases 2
SAVE surface 2
end

#35 (C - UA) - First Reaction
USE SOLUTION 4
USE EQUILIBRIUM_PHASES 3
USE SURFACE 3
SAVE equilibrium_phases 3
SAVE surface 3
end

#35 (C - UA) - Second Reaction
USE SOLUTION 4
USE EQUILIBRIUM_PHASES 3
USE SURFACE 3
SAVE equilibrium_phases 3
SAVE surface 3
end
```

804R - 25th Percentile Metal Oxides/No Charge Balance

```
SELECTED_OUTPUT 1
-file HEN_845_804R_25p_cb-false_out.csv
-charge_balance true
-percent_error true
-totals S(6) B Li As C(4) Cl F Ca Mg Na K Ba Si P Mn Fe Al Sb Be Cd Cr Co Pb Mo Se Hfo_s
Hfo_w Hao_
-molalities Hfo_wOH Hfo_wOH2+ Hfo_wOHSO4-2 Hfo_wSO4- Hfo_wOSi(OH)3
Hfo_wOSiO(OH)2- Hfo_wHCO3 Hfo_wCO3- Hfo_wPO4-2
Hfo_wHPO4- Hfo_wH2PO4 Hfo_sCO3- Hfo_sHCO3
Hfo_sHPO4- Hfo_sH2BO3 Hfo_sH2PO4 Hfo_sOSi(OH)3
Hfo_sOSiO(OH)2- Hfo_sOHSO4-2 Hfo_sSO4-
Hao_SO4- Hao_OHSO4-2 Hao_H2BO3 Hao_H3BO4-
Hfo_sH2AsO3 Hfo_sH2AsO4 Hfo_sHAsO4- Hfo_sOHAsO4-3
Hfo_wOHAsO4-3 Hfo_wHAsO4- Hfo_wH2AsO4 Hfo_wH2AsO3
-equilibrium_phases Ferrihydrite Gibbsite Barite Calcite Dolomite(ordered) Gypsum
-saturation_indices Ferrihydrite Gibbsite Barite Calcite Dolomite(ordered) Gypsum

SOLUTION 1 #22 (C - UA)
redox pe
units mg/l
density 1
pH 7.625
pe 4.815
temp 15.9
S(6) 121.5 as SO4
B 1.785
Li 0.0495
As 0.0022325
C(4) 145 as CO3
Cl 93
F 0.175
Ca 55.05
Mg 19.55
Na 33.9
K 6.95
Ba 0.03575
Si 19.1
P 0.0025
Mn 0.035
Fe 0.01675
Al 0.009425
Sb 0.000725
Be 0.0001825
Cd 0.0026425
Cr 0.000975
Co 0.00158
Pb 0.0010475
Mo 0.04395
Se 0.01535
end

EQUILIBRIUM_PHASES 1 #22 (C - UA) - 25p
Barite 0 0
```

```
Gypsum 0 0
Gibbsite 0 0.059
Ferrihydrite 0 0.072
Calcite 0 6
Dolomite(ordered) 0 2

SURFACE 1
Hfo_wOH Ferrihydrite equilibrium_phase 0.2 53400
Hfo_sOH Ferrihydrite equilibrium_phase 0.005 53400
Hao_OH Gibbsite equilibrium_phase 0.033 2496
-equil 1
save surface 1
end

SOLUTION 2 #average background
redox pe
units mg/l
density 1
pH 7.665
pe 5.995
temp 10.73
S(6) 48.5
B 0.249
Li 0.01965
As 0.003
C(4) 248
Cl 8 charge
F 0.41
Ca 46.2
Mg 29
Na 102.025
K 3.775
Ba 0.0807
Si 8.49
P 0.009
Mn 0.02275
Fe 0.12425
Al 0.00635
Sb 0.0002
Be 0.0001
Cd 0.00025
Cr 0.0014
Co 0.00005
Pb 0.002
Mo 0.00355
Se 0.0003

SAVE solution 2

end

#FIRST REACTION

#22 (C - UA) - First Reaction
USE SOLUTION 2
USE EQUILIBRIUM_PHASES 1
USE SURFACE 1
```

```
SAVE equilibrium_phases 1
SAVE surface 1
end

#22 (C - UA) - Second Reaction
USE SOLUTION 2
USE EQUILIBRIUM_PHASES 1
USE SURFACE 1
SAVE equilibrium_phases 1
SAVE surface 1
end
```

804R - 25th Percentile Metal Oxides/Charge Balance on Chloride

```
SELECTED_OUTPUT 1
-file HEN_845_804R_25p_cb-true_out.csv
-charge_balance true
-percent_error true
-totals S(6) B Li As C(4) Cl F Ca Mg Na K Ba Si P Mn Fe Al Sb Be Cd Cr Co Pb Mo Se Hfo_s
Hfo_w Hao_
-molalities Hfo_wOH Hfo_wOH2+ Hfo_wOHSO4-2 Hfo_wSO4- Hfo_wOSi(OH)3
Hfo_wOSiO(OH)2- Hfo_wHCO3 Hfo_wCO3- Hfo_wPO4-2
Hfo_wHPO4- Hfo_wH2PO4 Hfo_sCO3- Hfo_sHCO3
Hfo_sHPO4- Hfo_sH2BO3 Hfo_sH2PO4 Hfo_sOSi(OH)3
Hfo_sOSiO(OH)2- Hfo_sOHSO4-2 Hfo_sSO4-
Hao_SO4- Hao_OHSO4-2 Hao_H2BO3 Hao_H3BO4-
Hfo_sH2AsO3 Hfo_sH2AsO4 Hfo_sHAsO4- Hfo_sOHAsO4-3
Hfo_wOHAsO4-3 Hfo_wHAsO4- Hfo_wH2AsO4 Hfo_wH2AsO3
-equilibrium_phases Ferrihydrite Gibbsite Barite Calcite Dolomite(ordered) Gypsum
-saturation_indices Ferrihydrite Gibbsite Barite Calcite Dolomite(ordered) Gypsum

SOLUTION 1 #22 (C - UA)
redox pe
units mg/l
density 1
pH 7.625
pe 4.815
temp 15.9
S(6) 121.5 as SO4
B 1.785
Li 0.0495
As 0.0022325
C(4) 145 as CO3
Cl 93 charge
F 0.175
Ca 55.05
Mg 19.55
Na 33.9
K 6.95
Ba 0.03575
Si 19.1
P 0.0025
Mn 0.035
Fe 0.01675
Al 0.009425
Sb 0.000725
Be 0.0001825
Cd 0.0026425
Cr 0.000975
Co 0.00158
Pb 0.0010475
Mo 0.04395
Se 0.01535
end

EQUILIBRIUM_PHASES 1 #22 (C - UA) - 25p
Barite 0 0
```

```
Gypsum 0 0
Gibbsite 0 0.059
Ferrihydrite 0 0.072
Calcite 0 6
Dolomite(ordered) 0 2

SURFACE 1
Hfo_wOH Ferrihydrite equilibrium_phase 0.2 53400
Hfo_sOH Ferrihydrite equilibrium_phase 0.005 53400
Hao_OH Gibbsite equilibrium_phase 0.033 2496
-equil 1
save surface 1
end

SOLUTION 2 #average background
redox pe
units mg/l
density 1
pH 7.665
pe 5.995
temp 10.73
S(6) 48.5
B 0.249
Li 0.01965
As 0.003
C(4) 248
Cl 8 charge
F 0.41
Ca 46.2
Mg 29
Na 102.025
K 3.775
Ba 0.0807
Si 8.49
P 0.009
Mn 0.02275
Fe 0.12425
Al 0.00635
Sb 0.0002
Be 0.0001
Cd 0.00025
Cr 0.0014
Co 0.00005
Pb 0.002
Mo 0.00355
Se 0.0003

SAVE solution 2

end

#FIRST REACTION

#22 (C - UA) - First Reaction
USE SOLUTION 2
USE EQUILIBRIUM_PHASES 1
USE SURFACE 1
```

```
SAVE equilibrium_phases 1
SAVE surface 1
end

#22 (C - UA) - Second Reaction
USE SOLUTION 2
USE EQUILIBRIUM_PHASES 1
USE SURFACE 1
SAVE equilibrium_phases 1
SAVE surface 1
end
```

804R - 75th Percentile Metal Oxides/No Charge Balance

```
SELECTED_OUTPUT 1
-file HEN_845_804R_75p_cb-false_out.csv
-charge_balance true
-percent_error true
-totals S(6) B Li As C(4) Cl F Ca Mg Na K Ba Si P Mn Fe Al Sb Be Cd Cr Co Pb Mo Se Hfo_s
Hfo_w Hao_
-molalities Hfo_wOH Hfo_wOH2+ Hfo_wOHSO4-2 Hfo_wSO4- Hfo_wOSi(OH)3
Hfo_wOSiO(OH)2- Hfo_wHCO3 Hfo_wCO3- Hfo_wPO4-2
Hfo_wHPO4- Hfo_wH2PO4 Hfo_sCO3- Hfo_sHCO3
Hfo_sHPO4- Hfo_sH2BO3 Hfo_sH2PO4 Hfo_sOSi(OH)3
Hfo_sOSiO(OH)2- Hfo_sOHSO4-2 Hfo_sSO4-
Hao_SO4- Hao_OHSO4-2 Hao_H2BO3 Hao_H3BO4-
Hfo_sH2AsO3 Hfo_sH2AsO4 Hfo_sHAsO4- Hfo_sOHAsO4-3
Hfo_wOHAsO4-3 Hfo_wHAsO4- Hfo_wH2AsO4 Hfo_wH2AsO3
-equilibrium_phases Ferrihydrite Gibbsite Barite Calcite Dolomite(ordered) Gypsum
-saturation_indices Ferrihydrite Gibbsite Barite Calcite Dolomite(ordered) Gypsum

SOLUTION 1 #22 (C - UA)
redox pe
units mg/l
density 1
pH 7.625
pe 4.815
temp 15.9
S(6) 121.5 as SO4
B 1.785
Li 0.0495
As 0.0022325
C(4) 145 as CO3
Cl 93
F 0.175
Ca 55.05
Mg 19.55
Na 33.9
K 6.95
Ba 0.03575
Si 19.1
P 0.0025
Mn 0.035
Fe 0.01675
Al 0.009425
Sb 0.000725
Be 0.0001825
Cd 0.0026425
Cr 0.000975
Co 0.00158
Pb 0.0010475
Mo 0.04395
Se 0.01535
end

EQUILIBRIUM_PHASES 1 #22 (C - UA) - 75p
Barite 0 0
```

```
Gypsum 0 0
Gibbsite 0 0.064
Ferrihydrite 0 0.1
Calcite 0 6
Dolomite(ordered) 0 2

SURFACE 1
Hfo_wOH Ferrihydrite equilibrium_phase 0.2 53400
Hfo_sOH Ferrihydrite equilibrium_phase 0.005 53400
Hao_OH Gibbsite equilibrium_phase 0.033 2496
-equil 1
save surface 1
end

SOLUTION 2 #average background
redox pe
units mg/l
density 1
pH 7.665
pe 5.995
temp 10.73
S(6) 48.5
B 0.249
Li 0.01965
As 0.003
C(4) 248
Cl 8 charge
F 0.41
Ca 46.2
Mg 29
Na 102.025
K 3.775
Ba 0.0807
Si 8.49
P 0.009
Mn 0.02275
Fe 0.12425
Al 0.00635
Sb 0.0002
Be 0.0001
Cd 0.00025
Cr 0.0014
Co 0.00005
Pb 0.002
Mo 0.00355
Se 0.0003

SAVE solution 2

end

#FIRST REACTION

#22 (C - UA) - First Reaction
USE SOLUTION 2
USE EQUILIBRIUM_PHASES 1
USE SURFACE 1
```

```
SAVE equilibrium_phases 1
SAVE surface 1
end

#22 (C - UA) - Second Reaction
USE SOLUTION 2
USE EQUILIBRIUM_PHASES 1
USE SURFACE 1
SAVE equilibrium_phases 1
SAVE surface 1
end
```

804R - 75th Percentile Metal Oxides/Charge Balance on Chloride

```
SELECTED_OUTPUT 1
-file HEN_845_804R_75p_cb-true_out.csv
-charge_balance true
-percent_error true
-totals S(6) B Li As C(4) Cl F Ca Mg Na K Ba Si P Mn Fe Al Sb Be Cd Cr Co Pb Mo Se Hfo_s
Hfo_w Hao_
-molalities Hfo_wOH Hfo_wOH2+ Hfo_wOHSO4-2 Hfo_wSO4- Hfo_wOSi(OH)3
Hfo_wOSiO(OH)2- Hfo_wHCO3 Hfo_wCO3- Hfo_wPO4-2
Hfo_wHPO4- Hfo_wH2PO4 Hfo_sCO3- Hfo_sHCO3
Hfo_sHPO4- Hfo_sH2BO3 Hfo_sH2PO4 Hfo_sOSi(OH)3
Hfo_sOSiO(OH)2- Hfo_sOHSO4-2 Hfo_sSO4-
Hao_SO4- Hao_OHSO4-2 Hao_H2BO3 Hao_H3BO4-
Hfo_sH2AsO3 Hfo_sH2AsO4 Hfo_sHAsO4- Hfo_sOHAsO4-3
Hfo_wOHAsO4-3 Hfo_wHAsO4- Hfo_wH2AsO4 Hfo_wH2AsO3
-equilibrium_phases Ferrihydrite Gibbsite Barite Calcite Dolomite(ordered) Gypsum
-saturation_indices Ferrihydrite Gibbsite Barite Calcite Dolomite(ordered) Gypsum

SOLUTION 1 #22 (C - UA)
redox pe
units mg/l
density 1
pH 7.625
pe 4.815
temp 15.9
S(6) 121.5 as SO4
B 1.785
Li 0.0495
As 0.0022325
C(4) 145 as CO3
Cl 93 charge
F 0.175
Ca 55.05
Mg 19.55
Na 33.9
K 6.95
Ba 0.03575
Si 19.1
P 0.0025
Mn 0.035
Fe 0.01675
Al 0.009425
Sb 0.000725
Be 0.0001825
Cd 0.0026425
Cr 0.000975
Co 0.00158
Pb 0.0010475
Mo 0.04395
Se 0.01535
end

EQUILIBRIUM_PHASES 1 #22 (C - UA) - 75p
Barite 0 0
```

```
Gypsum 0 0
Gibbsite 0 0.064
Ferrihydrite 0 0.1
Calcite 0 6
Dolomite(ordered) 0 2

SURFACE 1
Hfo_wOH Ferrihydrite equilibrium_phase 0.2 53400
Hfo_sOH Ferrihydrite equilibrium_phase 0.005 53400
Hao_OH Gibbsite equilibrium_phase 0.033 2496
-equil 1
save surface 1
end

SOLUTION 2 #average background
redox pe
units mg/l
density 1
pH 7.665
pe 5.995
temp 10.73
S(6) 48.5
B 0.249
Li 0.01965
As 0.003
C(4) 248
Cl 8 charge
F 0.41
Ca 46.2
Mg 29
Na 102.025
K 3.775
Ba 0.0807
Si 8.49
P 0.009
Mn 0.02275
Fe 0.12425
Al 0.00635
Sb 0.0002
Be 0.0001
Cd 0.00025
Cr 0.0014
Co 0.00005
Pb 0.002
Mo 0.00355
Se 0.0003

SAVE solution 2

end

#FIRST REACTION

#22 (C - UA) - First Reaction
USE SOLUTION 2
USE EQUILIBRIUM_PHASES 1
USE SURFACE 1
```

```
SAVE equilibrium_phases 1
SAVE surface 1
end

#22 (C - UA) - Second Reaction
USE SOLUTION 2
USE EQUILIBRIUM_PHASES 1
USE SURFACE 1
SAVE equilibrium_phases 1
SAVE surface 1
end
```

804R - Median Metal Oxides/No Charge Balance

```
SELECTED_OUTPUT 1
-file HEN_845_804R_median_cb-false_out.csv
-charge_balance true
-percent_error true
-totals S(6) B Li As C(4) Cl F Ca Mg Na K Ba Si P Mn Fe Al Sb Be Cd Cr Co Pb Mo Se Hfo_s
Hfo_w Hao_
-molalities Hfo_wOH Hfo_wOH2+ Hfo_wOHSO4-2 Hfo_wSO4- Hfo_wOSi(OH)3
Hfo_wOSiO(OH)2- Hfo_wHCO3 Hfo_wCO3- Hfo_wPO4-2
Hfo_wHPO4- Hfo_wH2PO4 Hfo_sCO3- Hfo_sHCO3
Hfo_sHPO4- Hfo_sH2BO3 Hfo_sH2PO4 Hfo_sOSi(OH)3
Hfo_sOSiO(OH)2- Hfo_sOHSO4-2 Hfo_sSO4-
Hao_SO4- Hao_OHSO4-2 Hao_H2BO3 Hao_H3BO4-
Hfo_sH2AsO3 Hfo_sH2AsO4 Hfo_sHAsO4- Hfo_sOHAsO4-3
Hfo_wOHAsO4-3 Hfo_wHAsO4- Hfo_wH2AsO4 Hfo_wH2AsO3
-equilibrium_phases Ferrihydrite Gibbsite Barite Calcite Dolomite(ordered) Gypsum
-saturation_indices Ferrihydrite Gibbsite Barite Calcite Dolomite(ordered) Gypsum

SOLUTION 1 #22 (C - UA)
redox pe
units mg/l
density 1
pH 7.625
pe 4.815
temp 15.9
S(6) 121.5 as SO4
B 1.785
Li 0.0495
As 0.0022325
C(4) 145 as CO3
Cl 93
F 0.175
Ca 55.05
Mg 19.55
Na 33.9
K 6.95
Ba 0.03575
Si 19.1
P 0.0025
Mn 0.035
Fe 0.01675
Al 0.009425
Sb 0.000725
Be 0.0001825
Cd 0.0026425
Cr 0.000975
Co 0.00158
Pb 0.0010475
Mo 0.04395
Se 0.01535
end

EQUILIBRIUM_PHASES 1 #22 (C - UA) - median
Barite 0 0
```

```
Gypsum 0 0
Gibbsite 0 0.061
Ferrihydrite 0 0.085
Calcite 0 6
Dolomite(ordered) 0 2

SURFACE 1
Hfo_wOH Ferrihydrite equilibrium_phase 0.2 53400
Hfo_sOH Ferrihydrite equilibrium_phase 0.005 53400
Hao_OH Gibbsite equilibrium_phase 0.033 2496
-equil 1
save surface 1
end

SOLUTION 2 #average background
redox pe
units mg/l
density 1
pH 7.665
pe 5.995
temp 10.73
S(6) 48.5
B 0.249
Li 0.01965
As 0.003
C(4) 248
Cl 8 charge
F 0.41
Ca 46.2
Mg 29
Na 102.025
K 3.775
Ba 0.0807
Si 8.49
P 0.009
Mn 0.02275
Fe 0.12425
Al 0.00635
Sb 0.0002
Be 0.0001
Cd 0.00025
Cr 0.0014
Co 0.00005
Pb 0.002
Mo 0.00355
Se 0.0003

SAVE solution 2

end

#FIRST REACTION

#22 (C - UA) - First Reaction
USE SOLUTION 2
USE EQUILIBRIUM_PHASES 1
USE SURFACE 1
```

```
SAVE equilibrium_phases 1
SAVE surface 1
end

#22 (C - UA) - Second Reaction
USE SOLUTION 2
USE EQUILIBRIUM_PHASES 1
USE SURFACE 1
SAVE equilibrium_phases 1
SAVE surface 1
end
```

804R - Median Metal Oxides/Charge Balance on Chloride

```
SELECTED_OUTPUT 1
-file HEN_845_804R_median_cb-true_out.csv
-charge_balance true
-percent_error true
-totals S(6) B Li As C(4) Cl F Ca Mg Na K Ba Si P Mn Fe Al Sb Be Cd Cr Co Pb Mo Se Hfo_s
Hfo_w Hao_
-molalities Hfo_wOH Hfo_wOH2+ Hfo_wOHSO4-2 Hfo_wSO4- Hfo_wOSi(OH)3
Hfo_wOSiO(OH)2- Hfo_wHCO3 Hfo_wCO3- Hfo_wPO4-2
Hfo_wHPO4- Hfo_wH2PO4 Hfo_sCO3- Hfo_sHCO3
Hfo_sHPO4- Hfo_sH2BO3 Hfo_sH2PO4 Hfo_sOSi(OH)3
Hfo_sOSiO(OH)2- Hfo_sOHSO4-2 Hfo_sSO4-
Hao_SO4- Hao_OHSO4-2 Hao_H2BO3 Hao_H3BO4-
Hfo_sH2AsO3 Hfo_sH2AsO4 Hfo_sHAsO4- Hfo_sOHAsO4-3
Hfo_wOHAsO4-3 Hfo_wHAsO4- Hfo_wH2AsO4 Hfo_wH2AsO3
-equilibrium_phases Ferrihydrite Gibbsite Barite Calcite Dolomite(ordered) Gypsum
-saturation_indices Ferrihydrite Gibbsite Barite Calcite Dolomite(ordered) Gypsum

SOLUTION 1 #22 (C - UA)
redox pe
units mg/l
density 1
pH 7.625
pe 4.815
temp 15.9
S(6) 121.5 as SO4
B 1.785
Li 0.0495
As 0.0022325
C(4) 145 as CO3
Cl 93 charge
F 0.175
Ca 55.05
Mg 19.55
Na 33.9
K 6.95
Ba 0.03575
Si 19.1
P 0.0025
Mn 0.035
Fe 0.01675
Al 0.009425
Sb 0.000725
Be 0.0001825
Cd 0.0026425
Cr 0.000975
Co 0.00158
Pb 0.0010475
Mo 0.04395
Se 0.01535
end

EQUILIBRIUM_PHASES 1 #22 (C - UA) - median
Barite 0 0
```

```
Gypsum 0 0
Gibbsite 0 0.061
Ferrihydrite 0 0.085
Calcite 0 6
Dolomite(ordered) 0 2

SURFACE 1
Hfo_wOH Ferrihydrite equilibrium_phase 0.2 53400
Hfo_sOH Ferrihydrite equilibrium_phase 0.005 53400
Hao_OH Gibbsite equilibrium_phase 0.033 2496
-equil 1
save surface 1
end

SOLUTION 2 #average background
redox pe
units mg/l
density 1
pH 7.665
pe 5.995
temp 10.73
S(6) 48.5
B 0.249
Li 0.01965
As 0.003
C(4) 248
Cl 8 charge
F 0.41
Ca 46.2
Mg 29
Na 102.025
K 3.775
Ba 0.0807
Si 8.49
P 0.009
Mn 0.02275
Fe 0.12425
Al 0.00635
Sb 0.0002
Be 0.0001
Cd 0.00025
Cr 0.0014
Co 0.00005
Pb 0.002
Mo 0.00355
Se 0.0003

SAVE solution 2

end

#FIRST REACTION

#22 (C - UA) - First Reaction
USE SOLUTION 2
USE EQUILIBRIUM_PHASES 1
USE SURFACE 1
```

```
SAVE equilibrium_phases 1
SAVE surface 1
end

#22 (C - UA) - Second Reaction
USE SOLUTION 2
USE EQUILIBRIUM_PHASES 1
USE SURFACE 1
SAVE equilibrium_phases 1
SAVE surface 1
end
```

Database

```
#$Id: minteq.v4.dat 12387 2017-02-09 16:41:47Z dlpark $
SOLUTION_MASTER_SPECIES
Alkalinity CO3-2 2.0 HCO3 61.0173
E e- 0 0 0
O H2O 0 O 16.00
O(-2) H2O 0 O
O(0) O2 0 O
Ag Ag+ 0.0 Ag 107.868
Al Al+3 0.0 Al 26.9815
As H3AsO4 -1.0 As 74.9216
As(3) H3AsO3 0.0 As
As(5) H3AsO4 -1.0 As
B H3BO3 0.0 B 10.81
Ba Ba+2 0.0 Ba 137.33
Be Be+2 0.0 Be 9.0122
Br Br- 0.0 Br 79.904
C CO3-2 2.0 CO3 12.0111
C(4) CO3-2 2.0 CO3 12.0111
Cyanide Cyanide- 1.0 Cyanide 26.0177
Dom_a Dom_a 0.0 C 12.0111
Dom_b Dom_b 0.0 C 12.0111
Dom_c Dom_c 0.0 C 12.0111
Ca Ca+2 0.0 Ca 40.078
Cd Cd+2 0.0 Cd 112.41
Cl Cl- 0.0 Cl 35.453
Co Co+3 -1.0 Co 58.9332
Co(2) Co+2 0.0 Co
Co(3) Co+3 -1.0 Co
Cr CrO4-2 1.0 Cr 51.996
Cr(2) Cr+2 0.0 Cr
Cr(3) Cr(OH)2+ 0.0 Cr
Cr(6) CrO4-2 1.0 Cr
Cu Cu+2 0.0 Cu 63.546
Cu(1) Cu+ 0.0 Cu
Cu(2) Cu+2 0.0 Cu
F F- 0.0 F 18.9984
Fe Fe+3 -2.0 Fe 55.847
Fe(2) Fe+2 0.0 Fe
Fe(3) Fe+3 -2.0 Fe
H H+ -1.0 H 1.0079
H(0) H2 0 H
H(1) H+ -1.0 H
Hg Hg(OH)2 0.0 Hg 200.59
Hg(0) Hg 0.0 Hg
Hg(1) Hg2+2 0.0 Hg
Hg(2) Hg(OH)2 0.0 Hg
I I- 0.0 I 126.904
K K+ 0.0 K 39.0983
Li Li+ 0.0 Li 6.941
Mg Mg+2 0.0 Mg 24.305
Mn Mn+3 0.0 Mn 54.938
```

```
Mn(2) Mn+2 0.0 Mn
Mn(3) Mn+3 0.0 Mn
Mn(6) MnO4-2 0.0 Mn
Mn(7) MnO4- 0.0 Mn
Mo MoO4-2 0.0 Mo 95.94
N NO3- 0.0 N 14.0067
N(-3) NH4+ 0.0 N
N(3) NO2- 0.0 N
N(5) NO3- 0.0 N
Na Na+ 0.0 Na 22.9898
Ni Ni+2 0.0 Ni 58.69
P PO4-3 2.0 P 30.9738
Pb Pb+2 0.0 Pb 207.2
S SO4-2 0.0 SO4 32.066
S(-2) HS- 1.0 S
#S(0) S 0.0 S
S(6) SO4-2 0.0 SO4
Sb Sb(OH)6- 0.0 Sb 121.75
Sb(3) Sb(OH)3 0.0 Sb
Sb(5) Sb(OH)6- 0.0 Sb
Se SeO4-2 0.0 Se 78.96
Se(-2) HSe- 0.0 Se
Se(4) HSeO3- 0.0 Se
Se(6) SeO4-2 0.0 Se
Si H4SiO4 0.0 SiO2 28.0843
Sn Sn(OH)6-2 0.0 Sn 118.71
Sn(2) Sn(OH)2 0.0 Sn
Sn(4) Sn(OH)6-2 0.0 Sn
Sr Sr+2 0.0 Sr 87.62
Tl Tl(OH)3 0.0 Tl 204.383
Tl(1) Tl+ 0.0 Tl
Tl(3) Tl(OH)3 0.0 Tl
U UO2+2 0.0 U 238.029
U(3) U+3 0.0 U
U(4) U+4 -4.0 U
U(5) UO2+ 0.0 U
U(6) UO2+2 0.0 U
V VO2+ -2.0 V 50.94
V(2) V+2 0.0 V
V(3) V+3 -3.0 V
V(4) VO+2 0.0 V
V(5) VO2+ -2.0 V
Zn Zn+2 0.0 Zn 65.39
Benzoate Benzoate- 0.0 121.116 121.116
Phenylacetate Phenylacetate- 0.0 135.142 135.142
Isophthalate Isophthalate-2 0.0 164.117 164.117
Diethylamine Diethylamine 1.0 73.138 73.138
Butylamine Butylamine 1.0 73.138 73.138
Methylamine Methylamine 1.0 31.057 31.057
Dimethylamine Dimethylamine 1.0 45.084 45.084
Hexylamine Hexylamine 1.0 101.192 101.192
Ethylenediamine Ethylenediamine 2.0 60.099 60.099
Propylamine Propylamine 1.0 59.111 59.111
Isopropylamine Isopropylamine 1.0 59.111 59.111
```

```
Trimethylamine Trimethylamine 1.0 59.111 59.111
Citrate Citrate-3 2.0 189.102 189.102
Nta Nta-3 1.0 188.117 188.117
Edta Edta-4 2.0 288.214 288.214
Propionate Propionate- 1.0 73.072 73.072
Butyrate Butyrate- 1.0 87.098 87.098
Isobutyrate Isobutyrate- 1.0 87.098 87.098
Two_picoline Two_picoline 1.0 93.128 93.128
Three_picoline Three_picoline 1.0 93.128 93.128
Four_picoline Four_picoline 1.0 93.128 93.128
Formate Formate- 0.0 45.018 45.018
Isovalerate Isovalerate- 1.0 101.125 101.125
Valerate Valerate- 1.0 101.125 101.125
Acetate Acetate- 1.0 59.045 59.045
Tartarate Tartarate-2 0.0 148.072 148.072
Glycine Glycine- 1.0 74.059 74.059
Salicylate Salicylate-2 1.0 136.107 136.107
Glutamate Glutamate-2 1.0 145.115 145.115
Phthalate Phthalate-2 1.0 164.117 164.117
SOLUTION_SPECIES
e- = e-
log_k 0
H2O = H2O
log_k 0
Ag+ = Ag+
log_k 0
Al+3 = Al+3
log_k 0
H3AsO4 = H3AsO4
log_k 0
H3BO3 = H3BO3
log_k 0
Ba+2 = Ba+2
log_k 0
Be+2 = Be+2
log_k 0
Br- = Br-
log_k 0
CO3-2 = CO3-2
log_k 0
Cyanide- = Cyanide-
log_k 0
Dom_a = Dom_a
log_k 0
Dom_b = Dom_b
log_k 0
Dom_c = Dom_c
log_k 0
Ca+2 = Ca+2
log_k 0
Cd+2 = Cd+2
log_k 0
Cl- = Cl-
log_k 0
```

```
Co+3 = Co+3
log_k 0
CrO4-2 = CrO4-2
log_k 0
Cu+2 = Cu+2
log_k 0
F- = F-
log_k 0
Fe+3 = Fe+3
log_k 0
H+ = H+
log_k 0
Hg(OH)2 = Hg(OH)2
log_k 0
I- = I-
log_k 0
K+ = K+
log_k 0
Li+ = Li+
log_k 0
Mg+2 = Mg+2
log_k 0
Mn+3 = Mn+3
log_k 0
MoO4-2 = MoO4-2
log_k 0
NO3- = NO3-
log_k 0
Na+ = Na+
log_k 0
Ni+2 = Ni+2
log_k 0
PO4-3 = PO4-3
log_k 0
Pb+2 = Pb+2
log_k 0
SO4-2 = SO4-2
log_k 0
Sb(OH)6- = Sb(OH)6-
log_k 0
SeO4-2 = SeO4-2
log_k 0
H4SiO4 = H4SiO4
log_k 0
Sn(OH)6-2 = Sn(OH)6-2
log_k 0
Sr+2 = Sr+2
log_k 0
Tl(OH)3 = Tl(OH)3
log_k 0
UO2+2 = UO2+2
log_k 0
VO2+ = VO2+
log_k 0
```

```
Benzoate- = Benzoate-
log_k 0
Phenylacetate- = Phenylacetate-
log_k 0
Isophthalate-2 = Isophthalate-2
log_k 0
Zn+2 = Zn+2
log_k 0
Diethylamine = Diethylamine
log_k 0
Butylamine = Butylamine
log_k 0
Methylamine = Methylamine
log_k 0
Dimethylamine = Dimethylamine
log_k 0
Hexylamine = Hexylamine
log_k 0
Ethylenediamine = Ethylenediamine
log_k 0
Propylamine = Propylamine
log_k 0
Isopropylamine = Isopropylamine
log_k 0
Trimethylamine = Trimethylamine
log_k 0
Citrate-3 = Citrate-3
log_k 0
Nta-3 = Nta-3
log_k 0
Edta-4 = Edta-4
log_k 0
Propionate- = Propionate-
log_k 0
Butyrate- = Butyrate-
log_k 0
Isobutyrate- = Isobutyrate-
log_k 0
Two_picoline = Two_picoline
log_k 0
Three_picoline = Three_picoline
log_k 0
Four_picoline = Four_picoline
log_k 0
Formate- = Formate-
log_k 0
Isovalerate- = Isovalerate-
log_k 0
Valerate- = Valerate-
log_k 0
Acetate- = Acetate-
log_k 0
Tartarate-2 = Tartarate-2
log_k 0
```

```
Glycine- = Glycine-
log_k 0
Salicylate-2 = Salicylate-2
log_k 0
Glutamate-2 = Glutamate-2
log_k 0
Phthalate-2 = Phthalate-2
log_k 0
SOLUTION_SPECIES
Fe+3 + e- = Fe+2
log_k 13.032
delta_h -42.7 kJ
-gamma 0 0
# Id: 2802810
# log K source: Bard85
# Delta H source: Bard85
#T and ionic strength:
H3AsO4 + 2e- + 2H+ = H3AsO3 + H2O
log_k 18.898
delta_h -125.6 kJ
-gamma 0 0
# Id: 600610
# log K source: Bard85
# Delta H source: MTQ3.11
#T and ionic strength:
Sb(OH)6- + 2e- + 3H+ = Sb(OH)3 + 3H2O
log_k 24.31
delta_h 0 kJ
-gamma 0 0
# Id: 7407410
# log K source: Bard85
# Delta H source: MTQ3.11
#T and ionic strength:
UO2+2 + 3e- + 4H+ = U+3 + 2H2O
log_k 0.42
delta_h -42 kJ
-gamma 0 0
# Id: 8908930
# log K source: MTQ3.11
# Delta H source: MTQ3.11
#T and ionic strength:
UO2+2 + 2e- + 4H+ = U+4 + 2H2O
log_k 9.216
delta_h -144.1 kJ
-gamma 0 0
# Id: 8918930
# log K source: MTQ3.11
# Delta H source: MTQ3.11
#T and ionic strength:
UO2+2 + e- = UO2+
log_k 2.785
delta_h -13.8 kJ
-gamma 0 0
# Id: 8928930
```

```
# log K source: MTQ3.11
# Delta H source: MTQ3.11
#T and ionic strength:
e- + Mn+3 = Mn+2
log_k 25.35
delta_h -107.8 kJ
-gamma 0 0
# Id: 4704710
# log K source: Bard85
# Delta H source: MTQ3.11
#T and ionic strength:
Co+3 + e- = Co+2
log_k 32.4
delta_h 0 kJ
-gamma 0 0
# Id: 2002010
# log K source: Bard85
# Delta H source: MTQ3.11
#T and ionic strength:
Cu+2 + e- = Cu+
log_k 2.69
delta_h 6.9 kJ
-gamma 0 0
# Id: 2302310
# log K source: Bard85
# Delta H source: MTQ3.11
#T and ionic strength:
V+3 + e- = V+2
log_k -4.31
delta_h 0 kJ
-gamma 0 0
# Id: 9009010
# log K source: Bard85
# Delta H source: MTQ3.11
#T and ionic strength:
VO+2 + e- + 2H+ = V+3 + H2O
log_k 5.696
delta_h 0 kJ
-gamma 0 0
# Id: 9019020
# log K source: Bard85
# Delta H source: MTQ3.11
#T and ionic strength:
VO2+ + e- + 2H+ = VO+2 + H2O
log_k 16.903
delta_h -122.7 kJ
-gamma 0 0
# Id: 9029030
# log K source: Bard85
# Delta H source: MTQ3.11
#T and ionic strength:
SO4-2 + 9H+ + 8e- = HS- + 4H2O
log_k 33.66
delta_h -60.14 kJ
```

```
-gamma 0 0
# Id: 7307320
# log K source: MTQ3.11
# Delta H source: MTQ3.11
#T and ionic strength:
Sn(OH)6-2 + 2e- + 4H+ = Sn(OH)2 + 4H2O
log_k 19.2
delta_h 0 kJ
-gamma 0 0
# Id: 7907910
# log K source: Bard85
# Delta H source: MTQ3.11
#T and ionic strength:
Tl(OH)3 + 2e- + 3H+ = Tl+ + 3H2O
log_k 45.55
delta_h 0 kJ
-gamma 0 0
# Id: 8708710
# log K source: Bard85
# Delta H source: MTQ3.11
#T and ionic strength:
HSeO3- + 6e- + 6H+ = HSe- + 3H2O
log_k 44.86
delta_h 0 kJ
-gamma 0 0
# Id: 7607610
# log K source: Bard85
# Delta H source: MTQ3.11
#T and ionic strength:
SeO4-2 + 2e- + 3H+ = HSeO3- + H2O
log_k 36.308
delta_h -201.2 kJ
-gamma 0 0
# Id: 7617620
# log K source: Bard85
# Delta H source: MTQ3.11
#T and ionic strength:
0.5Hg2+2 + e- = Hg
log_k 6.5667
delta_h -45.735 kJ
-gamma 0 0
# Id: 3600000
# log K source: NIST2.1.1
# Delta H source: NIST2.1.1
#T and ionic strength:

2Hg(OH)2 + 4H+ + 2e- = Hg2+2 + 4H2O
log_k 43.185
delta_h -63.59 kJ
-gamma 0 0
# Id: 3603610
# log K source: Bard85
# Delta H source: MTQ3.11
#T and ionic strength:
```

```
Cr(OH)2+ + 2H+ + e- = Cr+2 + 2H2O
log_k 2.947
delta_h 6.36 kJ
-gamma 0 0
# Id: 2102110
# log K source: MTQ3.11
# Delta H source: MTQ3.11
#T and ionic strength:
CrO4-2 + 6H+ + 3e- = Cr(OH)2+ + 2H2O
log_k 67.376
delta_h -103 kJ
-gamma 0 0
# Id: 2112120
# log K source: MTQ3.11
# Delta H source: MTQ3.11
#T and ionic strength:

2H2O = O2 + 4H+ + 4e-
# Adjusted for equation to aqueous species
log_k -85.9951
-analytic 38.0229 7.99407E-03 -2.7655e+004 -1.4506e+001 199838.45

2 H+ + 2 e- = H2
log_k -3.15
delta_h -1.759 kcal

NO3- + 2 H+ + 2 e- = NO2- + H2O
log_k 28.570
delta_h -43.760 kcal
-gamma 3.0000 0.0000

NO3- + 10 H+ + 8 e- = NH4+ + 3 H2O
log_k 119.077
delta_h -187.055 kcal
-gamma 2.5000 0.0000

Mn+2 + 4H2O = MnO4- + 8H+ + 5e-
log_k -127.794
delta_h 822.67 kJ
-gamma 3 0
# Id: 4700020
# log K source: NIST2.1.1
# Delta H source: NIST2.1.1
#T and ionic strength:
Mn+2 + 4H2O = MnO4-2 + 8H+ + 4e-
log_k -118.422
delta_h 711.07 kJ
-gamma 5 0
# Id: 4700021
# log K source: NIST2.1.1
# Delta H source: NIST2.1.1
#T and ionic strength:
HS- = S-2 + H+
log_k -17.3
delta_h 49.4 kJ
-gamma 5 0
# Id: 3307301
```

```
# log K source: LMa1987
# Delta H source: NIST2.1.1
#T and ionic strength: 0.00 25.0
HSe- = Se-2 + H+
log_k -15
delta_h 48.116 kJ
-gamma 0 0
# Id: 3307601
# log K source: SCD3.02 (1968 DKa)
# Delta H source: MTQ3.11
#T and ionic strength: 0.00 25.0
Tl(OH)3 + 3H+ = Tl+3 + 3H2O
log_k 3.291
delta_h 0 kJ
-gamma 0 0
# Id: 8713300
# log K source: NIST46.3
# Delta H source: MTQ3.11
#T and ionic strength: 0.00 25.0
0.5Hg2+2 + e- = Hg
log_k 6.5667
delta_h -45.735 kJ
-gamma 0 0
# Id: 3600000
# log K source: NIST2.1.1
# Delta H source: NIST2.1.1
#T and ionic strength:
Hg(OH)2 + 2H+ = Hg+2 + 2H2O
log_k 6.194
delta_h -39.72 kJ
-gamma 0 0
# Id: 3613300
# log K source: NIST46.3
# Delta H source: NIST46.3
#T and ionic strength: 0.00 25.0
Cr(OH)2+ + 2H+ = Cr+3 + 2H2O
log_k 9.5688
delta_h -129.62 kJ
-gamma 0 0
# Id: 2113300
# log K source: NIST46.3
# Delta H source: NIST46.3
#T and ionic strength: 0.10 20.0
H2O = OH- + H+
log_k -13.997
delta_h 55.81 kJ
-gamma 3.5 0
# Id: 3300020
# log K source: NIST46.4
# Delta H source: NIST46.4
#T and ionic strength: 0.00 25.0
Sn(OH)2 + 2H+ = Sn+2 + 2H2O
log_k 7.094
delta_h 0 kJ
```

```
-gamma 0 0
# Id: 7903301
# log K source: NIST46.4
# Delta H source: MTQ3.11
#T and ionic strength: 0.00 25.0
Sn(OH)2 + H+ = SnOH+ + H2O
log_k 3.697
delta_h 0 kJ
-gamma 0 0
# Id: 7903302
# log K source: NIST46.4
# Delta H source: MTQ3.11
#T and ionic strength: 0.00 25.0
Sn(OH)2 + H2O = Sn(OH)3- + H+
log_k -9.497
delta_h 0 kJ
-gamma 0 0
# Id: 7903303
# log K source: NIST46.4
# Delta H source: MTQ3.11
#T and ionic strength: 0.00 25.0
2Sn(OH)2 + 2H+ = Sn2(OH)2+2 + 2H2O
log_k 9.394
delta_h 0 kJ
-gamma 0 0
# Id: 7903304
# log K source: NIST46.4
# Delta H source: MTQ3.11
#T and ionic strength: 0.00 25.0
3Sn(OH)2 + 2H+ = Sn3(OH)4+2 + 2H2O
log_k 14.394
delta_h 0 kJ
-gamma 0 0
# Id: 7903305
# log K source: NIST46.4
# Delta H source: MTQ3.11
#T and ionic strength: 0.00 25.0
Sn(OH)2 = HSnO2- + H+
log_k -8.9347
delta_h 0 kJ
-gamma 0 0
# Id: 7903306
# log K source: Bard85
# Delta H source: MTQ3.11
#T and ionic strength:
Sn(OH)6-2 + 6H+ = Sn+4 + 6H2O
log_k 21.2194
delta_h 0 kJ
-gamma 0 0
# Id: 7913301
# log K source: Bard85
# Delta H source: MTQ3.11
#T and ionic strength:
Sn(OH)6-2 = SnO3-2 + 3H2O
```

```
log_k -2.2099
delta_h 0 kJ
-gamma 0 0
# Id: 7913302
# log K source: Bard85
# Delta H source: MTQ3.11
#T and ionic strength:
Pb+2 + H2O = PbOH+ + H+
log_k -7.597
delta_h 0 kJ
-gamma 0 0
# Id: 6003300
# log K source: NIST46.3
# Delta H source: MTQ3.11
#T and ionic strength: 0.00 25.0
Pb+2 + 2H2O = Pb(OH)2 + 2H+
log_k -17.094
delta_h 0 kJ
-gamma 0 0
# Id: 6003301
# log K source: NIST46.3
# Delta H source: MTQ3.11
#T and ionic strength: 0.00 25.0
Pb+2 + 3H2O = Pb(OH)3- + 3H+
log_k -28.091
delta_h 0 kJ
-gamma 0 0
# Id: 6003302
# log K source: NIST46.3
# Delta H source: MTQ3.11
#T and ionic strength: 0.00 25.0
2Pb+2 + H2O = Pb2OH+3 + H+
log_k -6.397
delta_h 0 kJ
-gamma 0 0
# Id: 6003303
# log K source: NIST46.3
# Delta H source: MTQ3.11
#T and ionic strength: 0.00 25.0
3Pb+2 + 4H2O = Pb3(OH)4+2 + 4H+
log_k -23.888
delta_h 115.24 kJ
-gamma 0 0
# Id: 6003304
# log K source: NIST46.3
# Delta H source: NIST46.3
#T and ionic strength: 0.00 25.0
Pb+2 + 4H2O = Pb(OH)4-2 + 4H+
log_k -39.699
delta_h 0 kJ
-gamma 0 0
# Id: 6003305
# log K source: MTQ3.11
# Delta H source: MTQ3.11
```

```
#T and ionic strength:
4Pb+2 + 4H2O = Pb4(OH)4+4 + 4H+
log_k -19.988
delta_h 88.24 kJ
-gamma 0 0
# Id: 6003306
# log K source: NIST46.4
# Delta H source: NIST46.4
#T and ionic strength: 0.00 25.0
H3BO3 + F- = BF(OH)3-
log_k -0.399
delta_h 7.7404 kJ
-gamma 2.5 0
# Id: 902700
# log K source: MTQ3.11
# Delta H source: MTQ3.11
#T and ionic strength:
H3BO3 + 2F- + H+ = BF2(OH)2- + H2O
log_k 7.63
delta_h 6.8408 kJ
-gamma 2.5 0
# Id: 902701
# log K source: MTQ3.11
# Delta H source: MTQ3.11
#T and ionic strength:
H3BO3 + 3F- + 2H+ = BF3OH- + 2H2O
log_k 13.22
delta_h -20.4897 kJ
-gamma 2.5 0
# Id: 902702
# log K source: NIST2.1.1
# Delta H source: NIST2.1.1
#T and ionic strength:
Al+3 + H2O = AlOH+2 + H+
log_k -4.997
delta_h 47.81 kJ
-gamma 5.4 0
# Id: 303300
# log K source: NIST46.3
# Delta H source: NIST46.3
#T and ionic strength: 0.00 25.0
Al+3 + 2H2O = Al(OH)2+ + 2H+
log_k -10.094
delta_h 0 kJ
-gamma 5.4 0
# Id: 303301
# log K source: NIST46.3
# Delta H source: MTQ3.11
#T and ionic strength: 0.00 25.0
Al+3 + 3H2O = Al(OH)3 + 3H+
log_k -16.791
delta_h 0 kJ
-gamma 0 0
# Id: 303303
```

```
# log K source: NIST46.3
# Delta H source: MTQ3.11
#T and ionic strength: 0.00 25.0
Al+3 + 4H2O = Al(OH)4- + 4H+
log_k -22.688
delta_h 173.24 kJ
-gamma 4.5 0
# Id: 303302
# log K source: NIST46.3
# Delta H source: NIST46.3
#T and ionic strength: 0.00 25.0
Tl+ + H2O = TlOH + H+
log_k -13.207
delta_h 56.81 kJ
-gamma 0 0
# Id: 8703300
# log K source: NIST46.3
# Delta H source: NIST46.3
#T and ionic strength: 0.00 25.0
Tl(OH)3 + 2H+ = TlOH+2 + 2H2O
log_k 2.694
delta_h 0 kJ
-gamma 0 0
# Id: 8713301
# log K source: NIST46.3
# Delta H source: NIST46.3
#T and ionic strength: 0.00 25.0
Tl(OH)3 + H+ = Tl(OH)2+ + H2O
log_k 1.897
delta_h 0 kJ
-gamma 0 0
# Id: 8713302
# log K source: NIST46.3
# Delta H source: MTQ3.11
#T and ionic strength: 0.00 25.0
Tl(OH)3 + H2O = Tl(OH)4- + H+
log_k -11.697
delta_h 0 kJ
-gamma 0 0
# Id: 8713303
# log K source: NIST46.3
# Delta H source: MTQ3.11
#T and ionic strength: 0.00 25.0
Zn+2 + H2O = ZnOH+ + H+
log_k -8.997
delta_h 55.81 kJ
-gamma 0 0
# Id: 9503300
# log K source: NIST46.3
# Delta H source: NIST46.3
#T and ionic strength: 0.00 25.0
Zn+2 + 2H2O = Zn(OH)2 + 2H+
log_k -17.794
delta_h 0 kJ
```

```
-gamma 0 0
# Id: 9503301
# log K source: NIST46.3
# Delta H source: MTQ3.11
#T and ionic strength: 0.00 25.0
Zn+2 + 3H2O = Zn(OH)3- + 3H+
log_k -28.091
delta_h 0 kJ
-gamma 0 0
# Id: 9503302
# log K source: NIST46.3
# Delta H source: MTQ3.11
#T and ionic strength: 0.00 25.0
Zn+2 + 4H2O = Zn(OH)4-2 + 4H+
log_k -40.488
delta_h 0 kJ
-gamma 0 0
# Id: 9503303
# log K source: NIST46.3
# Delta H source: MTQ3.11
#T and ionic strength: 0.00 25.0
Cd+2 + H2O = CdOH+ + H+
log_k -10.097
delta_h 54.81 kJ
-gamma 0 0
# Id: 1603300
# log K source: NIST46.3
# Delta H source: NIST46.3
#T and ionic strength: 0.00 25.0
Cd+2 + 2H2O = Cd(OH)2 + 2H+
log_k -20.294
delta_h 0 kJ
-gamma 0 0
# Id: 1603301
# log K source: NIST46.3
# Delta H source: MTQ3.11
#T and ionic strength: 0.00 25.0
Cd+2 + 3H2O = Cd(OH)3- + 3H+
log_k -32.505
delta_h 0 kJ
-gamma 0 0
# Id: 1603302
# log K source: NIST46.3
# Delta H source: MTQ3.11
#T and ionic strength: 3.00 25.0
Cd+2 + 4H2O = Cd(OH)4-2 + 4H+
log_k -47.288
delta_h 0 kJ
-gamma 0 0
# Id: 1603303
# log K source: NIST46.3
# Delta H source: MTQ3.11
#T and ionic strength: 0.00 25.0
2Cd+2 + H2O = Cd2OH+3 + H+
```

```
log_k -9.397
delta_h 45.81 kJ
-gamma 0 0
# Id: 1603304
# log K source: NIST46.3
# Delta H source: NIST46.3
#T and ionic strength: 0.00 25.0
Hg(OH)2 + H+ = HgOH+ + H2O
log_k 2.797
delta_h -18.91 kJ
-gamma 0 0
# Id: 3613302
# log K source: NIST46.3
# Delta H source: NIST46.3
#T and ionic strength: 0.00 25.0
Hg(OH)2 + H2O = Hg(OH)3- + H+
log_k -14.897
delta_h 0 kJ
-gamma 0 0
# Id: 3613303
# log K source: NIST46.3
# Delta H source: MTQ3.11
#T and ionic strength: 0.00 25.0
Cu+2 + H2O = CuOH+ + H+
log_k -7.497
delta_h 35.81 kJ
-gamma 4 0
# Id: 2313300
# log K source: NIST46.3
# Delta H source: NIST46.3
#T and ionic strength: 0.00 25.0
Cu+2 + 2H2O = Cu(OH)2 + 2H+
log_k -16.194
delta_h 0 kJ
-gamma 0 0
# Id: 2313301
# log K source: NIST46.3
# Delta H source: MTQ3.11
#T and ionic strength: 0.00 25.0
Cu+2 + 3H2O = Cu(OH)3- + 3H+
log_k -26.879
delta_h 0 kJ
-gamma 0 0
# Id: 2313302
# log K source: NIST46.3
# Delta H source: MTQ3.11
#T and ionic strength: 1.00 25.0
Cu+2 + 4H2O = Cu(OH)4-2 + 4H+
log_k -39.98
delta_h 0 kJ
-gamma 0 0
# Id: 2313303
# log K source: NIST46.3
# Delta H source: MTQ3.11
```

```
#T and ionic strength: 1.00 25.0
2Cu+2 + 2H2O = Cu2(OH)2+2 + 2H+
log_k -10.594
delta_h 76.62 kJ
-gamma 0 0
# Id: 2313304
# log K source: NIST46.3
# Delta H source: NIST46.3
#T and ionic strength: 0.00 25.0
Ag+ + H2O = AgOH + H+
log_k -11.997
delta_h 0 kJ
-gamma 0 0
# Id: 203300
# log K source: NIST46.3
# Delta H source: MTQ3.11
#T and ionic strength: 0.00 25.0
Ag+ + 2H2O = Ag(OH)2- + 2H+
log_k -24.004
delta_h 0 kJ
-gamma 0 0
# Id: 203301
# log K source: NIST46.3
# Delta H source: MTQ3.11
#T and ionic strength: 0.00 25.0
Ni+2 + H2O = NiOH+ + H+
log_k -9.897
delta_h 51.81 kJ
-gamma 0 0
# Id: 5403300
# log K source: NIST46.3
# Delta H source: NIST46.3
#T and ionic strength: 0.00 25.0
Ni+2 + 2H2O = Ni(OH)2 + 2H+
log_k -18.994
delta_h 0 kJ
-gamma 0 0
# Id: 5403301
# log K source: NIST46.3
# Delta H source: MTQ3.11
#T and ionic strength: 0.00 25.0
Ni+2 + 3H2O = Ni(OH)3- + 3H+
log_k -29.991
delta_h 0 kJ
-gamma 0 0
# Id: 5403302
# log K source: NIST46.3
# Delta H source: MTQ3.11
#T and ionic strength: 0.00 25.0
Co+2 + H2O = CoOH+ + H+
log_k -9.697
delta_h 0 kJ
-gamma 0 0
# Id: 2003300
```

```
# log K source: NIST46.4
# Delta H source: MTQ3.11
#T and ionic strength: 0.00 25.0
Co+2 + 2H2O = Co(OH)2 + 2H+
log_k -18.794
delta_h 0 kJ
-gamma 0 0
# Id: 2003301
# log K source: NIST46.4
# Delta H source: MTQ3.11
#T and ionic strength: 0.00 25.0
Co+2 + 3H2O = Co(OH)3- + 3H+
log_k -31.491
delta_h 0 kJ
-gamma 0 0
# Id: 2003302
# log K source: NIST46.4
# Delta H source: MTQ3.11
#T and ionic strength: 0.00 25.0
Co+2 + 4H2O = Co(OH)4-2 + 4H+
log_k -46.288
delta_h 0 kJ
-gamma 0 0
# Id: 2003303
# log K source: NIST46.4
# Delta H source: MTQ3.11
#T and ionic strength: 0.00 25.0
2Co+2 + H2O = Co2OH+3 + H+
log_k -10.997
delta_h 0 kJ
-gamma 0 0
# Id: 2003304
# log K source: NIST46.4
# Delta H source: MTQ3.11
#T and ionic strength: 0.00 25.0
4Co+2 + 4H2O = Co4(OH)4+4 + 4H+
log_k -30.488
delta_h 0 kJ
-gamma 0 0
# Id: 2003306
# log K source: NIST46.4
# Delta H source: MTQ3.11
#T and ionic strength: 0.00 25.0
Co+2 + 2H2O = CoOOH- + 3H+
log_k -32.0915
delta_h 260.454 kJ
-gamma 0 0
# Id: 2003305
# log K source: NIST2.1.1
# Delta H source: MTQ3.11
#T and ionic strength:
Co+3 + H2O = CoOH+2 + H+
log_k -1.291
delta_h 0 kJ
```

```
-gamma 0 0
# Id: 2013300
# log K source: NIST46.4
# Delta H source: MTQ3.11
#T and ionic strength: 3.00 25.0
Fe+2 + H2O = FeOH+ + H+
log_k -9.397
delta_h 55.81 kJ
-gamma 5 0
# Id: 2803300
# log K source: NIST46.3
# Delta H source: NIST46.3
#T and ionic strength: 0.00 25.0
Fe+2 + 2H2O = Fe(OH)2 + 2H+
log_k -20.494
delta_h 119.62 kJ
-gamma 0 0
# Id: 2803302
# log K source: NIST46.3
# Delta H source: NIST46.3
#T and ionic strength: 0.00 25.0
Fe+2 + 3H2O = Fe(OH)3- + 3H+
log_k -28.991
delta_h 126.43 kJ
-gamma 5 0
# Id: 2803301
# log K source: NIST46.3
# Delta H source: NIST46.3
#T and ionic strength: 0.00 25.0
Fe+3 + H2O = FeOH+2 + H+
log_k -2.187
delta_h 41.81 kJ
-gamma 5 0
# Id: 2813300
# log K source: NIST46.3
# Delta H source: NIST46.3
#T and ionic strength: 0.00 25.0
Fe+3 + 2H2O = Fe(OH)2+ + 2H+
log_k -4.594
delta_h 0 kJ
-gamma 5.4 0
# Id: 2813301
# log K source: NIST46.3
# Delta H source: MTQ3.11
#T and ionic strength: 0.00 25.0
Fe+3 + 3H2O = Fe(OH)3 + 3H+
log_k -12.56
delta_h 103.8 kJ
-gamma 0 0
# Id: 2813302
# log K source: Nord90
# Delta H source: Nord90
#T and ionic strength: 0.00 25.0
Fe+3 + 4H2O = Fe(OH)4- + 4H+
```

```
log_k -21.588
delta_h 0 kJ
-gamma 5.4 0
# Id: 2813303
# log K source: NIST46.3
# Delta H source: MTQ3.11
#T and ionic strength: 0.00 25.0
2Fe+3 + 2H2O = Fe2(OH)2+4 + 2H+
log_k -2.854
delta_h 57.62 kJ
-gamma 0 0
# Id: 2813304
# log K source: NIST46.3
# Delta H source: NIST46.3
#T and ionic strength: 0.00 25.0
3Fe+3 + 4H2O = Fe3(OH)4+5 + 4H+
log_k -6.288
delta_h 65.24 kJ
-gamma 0 0
# Id: 2813305
# log K source: NIST46.3
# Delta H source: NIST46.3
#T and ionic strength: 0.00 25.0
Mn+2 + H2O = MnOH+ + H+
log_k -10.597
delta_h 55.81 kJ
-gamma 5 0
# Id: 4703300
# log K source: NIST46.3
# Delta H source: NIST46.3
#T and ionic strength: 0.00 25.0
Mn+2 + 3H2O = Mn(OH)3- + 3H+
log_k -34.8
delta_h 0 kJ
-gamma 5 0
# Id: 4703301
# log K source: MTQ3.11
# Delta H source: MTQ3.11
#T and ionic strength:
Mn+2 + 4H2O = Mn(OH)4-2 + 4H+
log_k -48.288
delta_h 0 kJ
-gamma 5 0
# Id: 4703302
# log K source: NIST46.4
# Delta H source: MTQ3.11
#T and ionic strength: 0.00 25.0
Mn+2 + 4H2O = MnO4- + 8H+ + 5e-
log_k -127.794
delta_h 822.67 kJ
-gamma 3 0
# Id: 4700020
# log K source: NIST2.1.1
# Delta H source: NIST2.1.1
```

```
#T and ionic strength:
Mn+2 + 4H2O = MnO4-2 + 8H+ + 4e-
log_k -118.422
delta_h 711.07 kJ
-gamma 5 0
# Id: 4700021
# log K source: NIST2.1.1
# Delta H source: NIST2.1.1
#T and ionic strength:
Cr(OH)2+ + H+ = Cr(OH)+2 + H2O
log_k 5.9118
delta_h -77.91 kJ
-gamma 0 0
# Id: 2113301
# log K source: NIST46.3
# Delta H source: NIST46.3
#T and ionic strength: 0.00 25.0
Cr(OH)2+ + H2O = Cr(OH)3 + H+
log_k -8.4222
delta_h 0 kJ
-gamma 0 0
# Id: 2113302
# log K source: SCD3.02 (1983 RCa)
# Delta H source: MTQ3.11
#T and ionic strength: 0.00 25.0
Cr(OH)2+ + 2H2O = Cr(OH)4- + 2H+
log_k -17.8192
delta_h 0 kJ
-gamma 0 0
# Id: 2113303
# log K source: SCD3.02 (1983 RCa)
# Delta H source: MTQ3.11
#T and ionic strength: 0.00 25.0
Cr(OH)2+ = CrO2- + 2H+
log_k -17.7456
delta_h 0 kJ
-gamma 0 0
# Id: 2113304
# log K source: MTQ3.11
# Delta H source: MTQ3.11
#T and ionic strength:
V+2 + H2O = VOH+ + H+
log_k -6.487
delta_h 59.81 kJ
-gamma 0 0
# Id: 9003300
# log K source: NIST46.3
# Delta H source: NIST46.3
#T and ionic strength: 0.00 25.0
V+3 + H2O = VOH+2 + H+
log_k -2.297
delta_h 43.81 kJ
-gamma 0 0
# Id: 9013300
```

```
# log K source: NIST46.3
# Delta H source: NIST46.3
#T and ionic strength: 0.00 25.0
V+3 + 2H2O = V(OH)2+ + 2H+
log_k -6.274
delta_h 0 kJ
-gamma 0 0
# Id: 9013301
# log K source: NIST46.3
# Delta H source: MTQ3.11
#T and ionic strength: 1.00 20.0
V+3 + 3H2O = V(OH)3 + 3H+
log_k -3.0843
delta_h 0 kJ
-gamma 0 0
# Id: 9013302
# log K source: SCD3.02 (1978 TKa)
# Delta H source: MTQ3.11
#T and ionic strength: 0.10 20.0
2V+3 + 2H2O = V2(OH)2+4 + 2H+
log_k -3.794
delta_h 0 kJ
-gamma 0 0
# Id: 9013304
# log K source: NIST46.3
# Delta H source: MTQ3.11
#T and ionic strength: 0.00 25.0
2V+3 + 3H2O = V2(OH)3+3 + 3H+
log_k -10.1191
delta_h 0 kJ
-gamma 0 0
# Id: 9013303
# log K source: NIST46.3
# Delta H source: MTQ3.11
#T and ionic strength: 3.00 25.0
VO+2 + 2H2O = V(OH)3+ + H+
log_k -5.697
delta_h 0 kJ
-gamma 0 0
# Id: 9023300
# log K source: NIST46.4
# Delta H source: MTQ3.11
#T and ionic strength: 0.00 25.0
2VO+2 + 2H2O = H2V2O4+2 + 2H+
log_k -6.694
delta_h 53.62 kJ
-gamma 0 0
# Id: 9023301
# log K source: NIST46.4
# Delta H source: NIST46.4
#T and ionic strength: 0.00 25.0
U+4 + H2O = UOH+3 + H+
log_k -0.597
delta_h 47.81 kJ
```

```
-gamma 0 0
# Id: 8913300
# log K source: NIST46.3
# Delta H source: NIST46.3
#T and ionic strength: 0.00 25.0
U+4 + 2H2O = U(OH)2+2 + 2H+
log_k -2.27
delta_h 74.1823 kJ
-gamma 0 0
# Id: 8913301
# log K source: MTQ3.11
# Delta H source: MTQ3.11
#T and ionic strength:
U+4 + 3H2O = U(OH)3+ + 3H+
log_k -4.935
delta_h 94.7467 kJ
-gamma 0 0
# Id: 8913302
# log K source: MTQ3.11
# Delta H source: MTQ3.11
#T and ionic strength:
U+4 + 4H2O = U(OH)4 + 4H+
log_k -8.498
delta_h 103.596 kJ
-gamma 0 0
# Id: 8913303
# log K source: MTQ3.11
# Delta H source: MTQ3.11
#T and ionic strength:
U+4 + 5H2O = U(OH)5- + 5H+
log_k -13.12
delta_h 115.374 kJ
-gamma 0 0
# Id: 8913304
# log K source: MTQ3.11
# Delta H source: MTQ3.11
#T and ionic strength:
6U+4 + 15H2O = U6(OH)15+9 + 15H+
log_k -17.155
delta_h 0 kJ
-gamma 0 0
# Id: 8913305
# log K source: NIST46.3
# Delta H source: MTQ3.11
#T and ionic strength: 0.00 25.0
UO2+2 + H2O = UO2OH+ + H+
log_k -5.897
delta_h 47.81 kJ
-gamma 0 0
# Id: 8933300
# log K source: NIST46.3
# Delta H source: NIST46.3
#T and ionic strength: 0.00 25.0
2UO2+2 + 2H2O = (UO2)2(OH)2+2 + 2H+
```

```
log_k -5.574
delta_h 41.82 kJ
-gamma 0 0
# Id: 8933301
# log K source: NIST46.3
# Delta H source: NIST46.3
#T and ionic strength: 0.00 25.0
3UO2+2 + 5H2O = (UO2)3(OH)5+ + 5H+
log_k -15.585
delta_h 108.05 kJ
-gamma 0 0
# Id: 8933302
# log K source: NIST46.3
# Delta H source: NIST46.3
#T and ionic strength: 0.00 25.0
Be+2 + H2O = BeOH+ + H+
log_k -5.397
delta_h 0 kJ
-gamma 6.5 0
# Id: 1103301
# log K source: NIST46.4
# Delta H source: MTQ3.11
#T and ionic strength: 0.00 25.0
Be+2 + 2H2O = Be(OH)2 + 2H+
log_k -13.594
delta_h 0 kJ
-gamma 6.5 0
# Id: 1103302
# log K source: NIST46.4
# Delta H source: MTQ3.11
#T and ionic strength: 0.00 25.0
Be+2 + 3H2O = Be(OH)3- + 3H+
log_k -23.191
delta_h 0 kJ
-gamma 6.5 0
# Id: 1103303
# log K source: NIST46.4
# Delta H source: MTQ3.11
#T and ionic strength: 0.00 25.0
Be+2 + 4H2O = Be(OH)4-2 + 4H+
log_k -37.388
delta_h 0 kJ
-gamma 6.5 0
# Id: 1103304
# log K source: NIST46.4
# Delta H source: MTQ3.11
#T and ionic strength: 0.00 25.0
2Be+2 + H2O = Be2OH+3 + H+
log_k -3.177
delta_h 0 kJ
-gamma 6.5 0
# Id: 1103305
# log K source: NIST46.4
# Delta H source: MTQ3.11
```

```
#T and ionic strength: 0.10 25.0
3Be+2 + 3H2O = Be3(OH)3+3 + 3H+
log_k -8.8076
delta_h 0 kJ
-gamma 6.5 0
# Id: 1103306
# log K source: NIST46.4
# Delta H source: MTQ3.11
#T and ionic strength: 0.10 25.0
Mg+2 + H2O = MgOH+ + H+
log_k -11.397
delta_h 67.81 kJ
-gamma 6.5 0
# Id: 4603300
# log K source: NIST46.3
# Delta H source: NIST46.3
#T and ionic strength: 0.00 25.0
Ca+2 + H2O = CaOH+ + H+
log_k -12.697
delta_h 64.11 kJ
-gamma 6 0
# Id: 1503300
# log K source: NIST46.3
# Delta H source: NIST46.3
#T and ionic strength: 0.00 25.0
Sr+2 + H2O = SrOH+ + H+
log_k -13.177
delta_h 60.81 kJ
-gamma 5 0
# Id: 8003300
# log K source: NIST46.3
# Delta H source: NIST46.3
#T and ionic strength: 0.00 25.0
Ba+2 + H2O = BaOH+ + H+
log_k -13.357
delta_h 60.81 kJ
-gamma 5 0
# Id: 1003300
# log K source: NIST46.3
# Delta H source: NIST46.3
#T and ionic strength: 0.00 25.0
H+ + F- = HF
log_k 3.17
delta_h 13.3 kJ
-gamma 0 0
# Id: 3302700
# log K source: NIST46.3
# Delta H source: NIST46.3
#T and ionic strength: 0.00 25.0
H+ + 2F- = HF2-
log_k 3.75
delta_h 17.4 kJ
-gamma 3.5 0
# Id: 3302701
```

```
# log K source: NIST46.3
# Delta H source: NIST46.3
#T and ionic strength: 0.00 25.0
2F- + 2H+ = H2F2
log_k 6.768
delta_h 0 kJ
-gamma 0 0
# Id: 3302702
# log K source: MTQ3.11
# Delta H source: MTQ3.11
#T and ionic strength:
Sb(OH)3 + F- + H+ = SbOF + 2H2O
log_k 6.1864
delta_h 0 kJ
-gamma 0 0
# Id: 7402700
# log K source: PNL89
# Delta H source: PNL89
#T and ionic strength:
Sb(OH)3 + F- + H+ = Sb(OH)2F + H2O
log_k 6.1937
delta_h 0 kJ
-gamma 0 0
# Id: 7402702
# log K source: PNL89
# Delta H source: PNL89
#T and ionic strength:
H4SiO4 + 4H+ + 6F- = SiF6-2 + 4H2O
log_k 30.18
delta_h -68 kJ
-gamma 5 0
# Id: 7702700
# log K source: Nord90
# Delta H source: Nord90
#T and ionic strength: 0.00 25.0
Sn(OH)2 + 2H+ + F- = SnF+ + 2H2O
log_k 11.582
delta_h 0 kJ
-gamma 0 0
# Id: 7902701
# log K source: NIST46.4
# Delta H source: MTQ3.11
#T and ionic strength: 1.00 25.0
Sn(OH)2 + 2H+ + 2F- = SnF2 + 2H2O
log_k 14.386
delta_h 0 kJ
-gamma 0 0
# Id: 7902702
# log K source: NIST46.4
# Delta H source: MTQ3.11
#T and ionic strength: 1.00 25.0
Sn(OH)2 + 2H+ + 3F- = SnF3- + 2H2O
log_k 17.206
delta_h 0 kJ
```

```
-gamma 0 0
# Id: 7902703
# log K source: NIST46.4
# Delta H source: MTQ3.11
#T and ionic strength: 1.00 25.0
Sn(OH)6-2 + 6H+ + 6F- = SnF6-2 + 6H2O
log_k 33.5844
delta_h 0 kJ
-gamma 0 0
# Id: 7912701
# log K source: Bard85
# Delta H source: MTQ3.11
#T and ionic strength:
Pb+2 + F- = PbF+
log_k 1.848
delta_h 0 kJ
-gamma 0 0
# Id: 6002700
# log K source: NIST46.3
# Delta H source: MTQ3.11
#T and ionic strength: 1.00 25.0
Pb+2 + 2F- = PbF2
log_k 3.142
delta_h 0 kJ
-gamma 0 0
# Id: 6002701
# log K source: NIST46.3
# Delta H source: MTQ3.11
#T and ionic strength: 1.00 25.0
Pb+2 + 3F- = PbF3-
log_k 3.42
delta_h 0 kJ
-gamma 0 0
# Id: 6002702
# log K source: SCD3.02 (1956 TKa)
# Delta H source: MTQ3.11
#T and ionic strength: 0.00 25.0
Pb+2 + 4F- = PbF4-2
log_k 3.1
delta_h 0 kJ
-gamma 0 0
# Id: 6002703
# log K source: SCD3.02 (1956 TKa)
# Delta H source: MTQ3.11
#T and ionic strength: 0.00 25.0
H3BO3 + 3H+ + 4F- = BF4- + 3H2O
log_k 19.912
delta_h -18.67 kJ
-gamma 2.5 0
# Id: 902703
# log K source: NIST46.3
# Delta H source: NIST2.1.1
#T and ionic strength: 1.00 25.0
Al+3 + F- = AlF+2
```

```
log_k 7
delta_h 4.6 kJ
-gamma 5.4 0
# Id: 302700
# log K source: NIST46.3
# Delta H source: NIST46.3
#T and ionic strength: 0.00 25.0
Al+3 + 2F- = AlF2+
log_k 12.6
delta_h 8.3 kJ
-gamma 5.4 0
# Id: 302701
# log K source: NIST46.3
# Delta H source: NIST46.3
#T and ionic strength: 0.00 25.0
Al+3 + 3F- = AlF3
log_k 16.7
delta_h 8.7 kJ
-gamma 0 0
# Id: 302702
# log K source: NIST46.3
# Delta H source: NIST46.3
#T and ionic strength: 0.00 25.0
Al+3 + 4F- = AlF4-
log_k 19.4
delta_h 8.7 kJ
-gamma 4.5 0
# Id: 302703
# log K source: NIST46.3
# Delta H source: NIST46.3
#T and ionic strength: 0.00 25.0
Tl+ + F- = TlF
log_k 0.1
delta_h 0 kJ
-gamma 0 0
# Id: 8702700
# log K source: NIST46.3
# Delta H source: MTQ3.11
#T and ionic strength: 0.00 25.0
Zn+2 + F- = ZnF+
log_k 1.3
delta_h 11 kJ
-gamma 0 0
# Id: 9502700
# log K source: NIST46.3
# Delta H source: NIST46.3
#T and ionic strength: 0.00 25.0
Cd+2 + F- = CdF+
log_k 1.2
delta_h 5 kJ
-gamma 0 0
# Id: 1602700
# log K source: NIST46.3
# Delta H source: NIST46.3
```

```
#T and ionic strength: 0.00 25.0
Cd+2 + 2F- = CdF2
log_k 1.5
delta_h 0 kJ
-gamma 0 0
# Id: 1602701
# log K source: MTQ3.11
# Delta H source: MTQ3.11
#T and ionic strength:
Hg(OH)2 + 2H+ + F- = HgF+ + 2H2O
log_k 7.763
delta_h -35.72 kJ
-gamma 0 0
# Id: 3612701
# log K source: NIST46.3
# Delta H source: NIST46.3
#T and ionic strength: 0.50 25.0
Cu+2 + F- = CuF+
log_k 1.8
delta_h 13 kJ
-gamma 0 0
# Id: 2312700
# log K source: NIST46.3
# Delta H source: NIST46.3
#T and ionic strength: 0.00 25.0
Ag+ + F- = AgF
log_k 0.4
delta_h 12 kJ
-gamma 0 0
# Id: 202700
# log K source: NIST46.3
# Delta H source: NIST46.3
#T and ionic strength: 0.00 25.0
Ni+2 + F- = NiF+
log_k 1.4
delta_h 7.1 kJ
-gamma 0 0
# Id: 5402700
# log K source: NIST46.3
# Delta H source: NIST46.3
#T and ionic strength: 0.00 25.0
Co+2 + F- = CoF+
log_k 1.5
delta_h 9.2 kJ
-gamma 0 0
# Id: 2002700
# log K source: NIST46.4
# Delta H source: NIST46.4
#T and ionic strength: 0.00 25.0
Fe+3 + F- = FeF+2
log_k 6.04
delta_h 10 kJ
-gamma 5 0
# Id: 2812700
```

```
# log K source: NIST46.3
# Delta H source: NIST46.3
#T and ionic strength: 0.00 25.0
Fe+3 + 2F- = FeF2+
log_k 10.4675
delta_h 17 kJ
-gamma 5 0
# Id: 2812701
# log K source: NIST46.3
# Delta H source: NIST46.3
#T and ionic strength: 0.50 25.0
Fe+3 + 3F- = FeF3
log_k 13.617
delta_h 29 kJ
-gamma 0 0
# Id: 2812702
# log K source: NIST46.3
# Delta H source: NIST46.3
#T and ionic strength: 0.50 25.0
Mn+2 + F- = MnF+
log_k 1.6
delta_h 11 kJ
-gamma 5 0
# Id: 4702700
# log K source: NIST46.3
# Delta H source: NIST46.3
#T and ionic strength: 0.00 25.0
Cr(OH)2+ + 2H+ + F- = CrF+2 + 2H2O
log_k 14.7688
delta_h -70.2452 kJ
-gamma 0 0
# Id: 2112700
# log K source: NIST46.3
# Delta H source: MTQ3.11
#T and ionic strength: 0.00 25.0
VO+2 + F- = VOF+
log_k 3.778
delta_h 7.9 kJ
-gamma 0 0
# Id: 9022700
# log K source: NIST46.3
# Delta H source: NIST46.3
#T and ionic strength: 1.00 25.0
VO+2 + 2F- = VOF2
log_k 6.352
delta_h 14 kJ
-gamma 0 0
# Id: 9022701
# log K source: NIST46.3
# Delta H source: NIST46.3
#T and ionic strength: 1.00 25.0
VO+2 + 3F- = VOF3-
log_k 7.902
delta_h 20 kJ
```

```
-gamma 0 0
# Id: 9022702
# log K source: NIST46.3
# Delta H source: NIST46.3
#T and ionic strength: 1.00 25.0
VO+2 + 4F- = VOF4-2
log_k 8.508
delta_h 26 kJ
-gamma 0 0
# Id: 9022703
# log K source: NIST46.3
# Delta H source: NIST46.3
#T and ionic strength: 1.00 25.0
VO2+ + F- = VO2F
log_k 3.244
delta_h 0 kJ
-gamma 0 0
# Id: 9032700
# log K source: NIST46.3
# Delta H source: MTQ3.11
#T and ionic strength: 1.00 25.0
VO2+ + 2F- = VO2F2-
log_k 5.804
delta_h 0 kJ
-gamma 0 0
# Id: 9032701
# log K source: NIST46.3
# Delta H source: MTQ3.11
#T and ionic strength: 1.00 20.0
VO2+ + 3F- = VO2F3-2
log_k 6.9
delta_h 0 kJ
-gamma 0 0
# Id: 9032702
# log K source: NIST46.3
# Delta H source: MTQ3.11
#T and ionic strength: 1.00 20.0
VO2+ + 4F- = VO2F4-3
log_k 6.592
delta_h 0 kJ
-gamma 0 0
# Id: 9032703
# log K source: NIST46.3
# Delta H source: MTQ3.11
#T and ionic strength: 1.00 20.0
U+4 + F- = UF+3
log_k 9.3
delta_h 21.1292 kJ
-gamma 0 0
# Id: 8912700
# log K source: NIST46.3
# Delta H source: MTQ3.11
#T and ionic strength: 0.00 25.0
U+4 + 2F- = UF2+2
```

```
log_k 16.4
delta_h 30.1248 kJ
-gamma 0 0
# Id: 8912701
# log K source: NIST46.3
# Delta H source: MTQ3.11
#T and ionic strength: 0.00 25.0
U+4 + 3F- = UF3+
log_k 21.6
delta_h 29.9156 kJ
-gamma 0 0
# Id: 8912702
# log K source: NIST46.3
# Delta H source: MTQ3.11
#T and ionic strength: 0.00 25.0
U+4 + 4F- = UF4
log_k 23.64
delta_h 19.2464 kJ
-gamma 0 0
# Id: 8912703
# log K source: MTQ3.11
# Delta H source: MTQ3.11
#T and ionic strength:
U+4 + 5F- = UF5-
log_k 25.238
delta_h 20.2924 kJ
-gamma 0 0
# Id: 8912704
# log K source: MTQ3.11
# Delta H source: MTQ3.11
#T and ionic strength:
U+4 + 6F- = UF6-2
log_k 27.718
delta_h 13.8072 kJ
-gamma 0 0
# Id: 8912705
# log K source: MTQ3.11
# Delta H source: MTQ3.11
#T and ionic strength:
UO2+2 + F- = UO2F+
log_k 5.14
delta_h 1 kJ
-gamma 0 0
# Id: 8932700
# log K source: NIST46.3
# Delta H source: NIST46.3
#T and ionic strength: 0.00 25.0
UO2+2 + 2F- = UO2F2
log_k 8.6
delta_h 2 kJ
-gamma 0 0
# Id: 8932701
# log K source: NIST46.3
# Delta H source: NIST46.3
```

```
#T and ionic strength: 0.00 25.0
UO2+2 + 3F- = UO2F3-
log_k 11
delta_h 2 kJ
-gamma 0 0
# Id: 8932702
# log K source: NIST46.3
# Delta H source: NIST46.3
#T and ionic strength: 0.00 25.0
UO2+2 + 4F- = UO2F4-2
log_k 11.9
delta_h 0.4 kJ
-gamma 0 0
# Id: 8932703
# log K source: NIST46.3
# Delta H source: NIST46.3
#T and ionic strength: 0.00 25.0
Be+2 + F- = BeF+
log_k 5.249
delta_h 0 kJ
-gamma 0 0
# Id: 1102701
# log K source: NIST46.4
# Delta H source: NIST46.4
#T and ionic strength: 0.50 25.0
Be+2 + 2F- = BeF2
log_k 9.1285
delta_h -4 kJ
-gamma 0 0
# Id: 1102702
# log K source: NIST46.4
# Delta H source: NIST46.4
#T and ionic strength: 0.50 25.0
Be+2 + 3F- = BeF3-
log_k 11.9085
delta_h -8 kJ
-gamma 0 0
# Id: 1102703
# log K source: NIST46.4
# Delta H source: NIST46.4
#T and ionic strength: 0.50 25.0
Mg+2 + F- = MgF+
log_k 2.05
delta_h 13 kJ
-gamma 4.5 0
# Id: 4602700
# log K source: NIST46.3
# Delta H source: NIST46.3
#T and ionic strength: 0.00 25.0
Ca+2 + F- = CaF+
log_k 1.038
delta_h 14 kJ
-gamma 5 0
# Id: 1502700
```

```
# log K source: NIST46.3
# Delta H source: NIST46.3
#T and ionic strength: 1.00 25.0
Sr+2 + F- = SrF+
log_k 0.548
delta_h 16 kJ
-gamma 0 0
# Id: 8002701
# log K source: NIST46.4
# Delta H source: NIST46.4
#T and ionic strength: 1.00 25.0
Na+ + F- = NaF
log_k -0.2
delta_h 12 kJ
-gamma 0 0
# Id: 5002700
# log K source: NIST46.3
# Delta H source: NIST46.3
#T and ionic strength: 0.00 25.0
Sn(OH)2 + 2H+ + Cl- = SnCl+ + 2H2O
log_k 8.734
delta_h 0 kJ
-gamma 0 0
# Id: 7901801
# log K source: NIST46.4
# Delta H source: NIST46.4
#T and ionic strength: 0.00 25.0
Sn(OH)2 + 2H+ + 2Cl- = SnCl2 + 2H2O
log_k 9.524
delta_h 0 kJ
-gamma 0 0
# Id: 7901802
# log K source: NIST46.4
# Delta H source: NIST46.4
#T and ionic strength: 0.00 25.0
Sn(OH)2 + 2H+ + 3Cl- = SnCl3- + 2H2O
log_k 8.3505
delta_h 0 kJ
-gamma 0 0
# Id: 7901803
# log K source: NIST46.4
# Delta H source: NIST46.4
#T and ionic strength: 2.00 25.0
Pb+2 + Cl- = PbCl+
log_k 1.55
delta_h 8.7 kJ
-gamma 0 0
# Id: 6001800
# log K source: NIST46.3
# Delta H source: NIST46.3
#T and ionic strength: 0.00 25.0
Pb+2 + 2Cl- = PbCl2
log_k 2.2
delta_h 12 kJ
```

```
-gamma 0 0
# Id: 6001801
# log K source: NIST46.3
# Delta H source: NIST46.3
#T and ionic strength: 0.00 25.0
Pb+2 + 3Cl- = PbCl3-
log_k 1.8
delta_h 4 kJ
-gamma 0 0
# Id: 6001802
# log K source: NIST46.3
# Delta H source: NIST46.3
#T and ionic strength: 0.00 25.0
Pb+2 + 4Cl- = PbCl4-2
log_k 1.46
delta_h 14.7695 kJ
-gamma 0 0
# Id: 6001803
# log K source: SCD3.02 (1984 SEa)
# Delta H source: MTQ3.11
#T and ionic strength: 0.00 25.0
Tl+ + Cl- = TlCl
log_k 0.51
delta_h -6.2 kJ
-gamma 0 0
# Id: 8701800
# log K source: NIST46.3
# Delta H source: NIST46.3
#T and ionic strength: 0.00 25.0
Tl+ + 2Cl- = TlCl2-
log_k 0.28
delta_h 0 kJ
-gamma 0 0
# Id: 8701801
# log K source: SCD3.02 (1992 RAb)
# Delta H source: MTQ3.11
#T and ionic strength: 0.00 25.0
Tl(OH)3 + 3H+ + Cl- = TlCl+2 + 3H2O
log_k 11.011
delta_h 0 kJ
-gamma 0 0
# Id: 8711800
# log K source: NIST46.3
# Delta H source: NIST46.3
#T and ionic strength: 0.00 25.0
Tl(OH)3 + 3H+ + 2Cl- = TlCl2+ + 3H2O
log_k 16.771
delta_h 0 kJ
-gamma 0 0
# Id: 8711801
# log K source: NIST46.3
# Delta H source: NIST46.3
#T and ionic strength: 0.00 25.0
Tl(OH)3 + 3H+ + 3Cl- = TlCl3 + 3H2O
```

```
log_k 19.791
delta_h 0 kJ
-gamma 0 0
# Id: 8711802
# log K source: NIST46.3
# Delta H source: NIST46.3
#T and ionic strength: 0.00 25.0
Tl(OH)3 + 3H+ + 4Cl- = TlCl4- + 3H2O
log_k 21.591
delta_h 0 kJ
-gamma 0 0
# Id: 8711803
# log K source: NIST46.3
# Delta H source: NIST46.3
#T and ionic strength: 0.00 25.0
Tl(OH)3 + Cl- + 2H+ = TlOHCl+ + 2H2O
log_k 10.629
delta_h 0 kJ
-gamma 0 0
# Id: 8711804
# log K source: MTQ3.11
# Delta H source: MTQ3.11
#T and ionic strength:
Zn+2 + Cl- = ZnCl+
log_k 0.4
delta_h 5.4 kJ
-gamma 4 0
# Id: 9501800
# log K source: NIST46.3
# Delta H source: NIST46.3
#T and ionic strength: 0.00 25.0
Zn+2 + 2Cl- = ZnCl2
log_k 0.6
delta_h 37 kJ
-gamma 0 0
# Id: 9501801
# log K source: NIST46.3
# Delta H source: NIST46.3
#T and ionic strength: 0.00 25.0
Zn+2 + 3Cl- = ZnCl3-
log_k 0.5
delta_h 39.999 kJ
-gamma 4 0
# Id: 9501802
# log K source: MTQ3.11
# Delta H source: MTQ3.11
#T and ionic strength:
Zn+2 + 4Cl- = ZnCl4-2
log_k 0.199
delta_h 45.8566 kJ
-gamma 5 0
# Id: 9501803
# log K source: MTQ3.11
# Delta H source: MTQ3.11
```

```
#T and ionic strength:
Zn+2 + H2O + Cl- = ZnOHCl + H+
log_k -7.48
delta_h 0 kJ
-gamma 0 0
# Id: 9501804
# log K source: MTQ3.11
# Delta H source: MTQ3.11
#T and ionic strength:
Cd+2 + Cl- = CdCl+
log_k 1.98
delta_h 1 kJ
-gamma 0 0
# Id: 1601800
# log K source: NIST46.3
# Delta H source: NIST46.3
#T and ionic strength: 0.00 25.0
Cd+2 + 2Cl- = CdCl2
log_k 2.6
delta_h 3 kJ
-gamma 0 0
# Id: 1601801
# log K source: NIST46.3
# Delta H source: NIST46.3
#T and ionic strength: 0.00 25.0
Cd+2 + 3Cl- = CdCl3-
log_k 2.4
delta_h 10 kJ
-gamma 0 0
# Id: 1601802
# log K source: NIST46.3
# Delta H source: NIST46.3
#T and ionic strength: 0.00 25.0
Cd+2 + H2O + Cl- = CdOHCl + H+
log_k -7.404
delta_h 18.2213 kJ
-gamma 0 0
# Id: 1601803
# log K source: MTQ3.11
# Delta H source: MTQ3.11
#T and ionic strength:
Hg(OH)2 + 2H+ + Cl- = HgCl+ + 2H2O
log_k 13.494
delta_h -62.72 kJ
-gamma 0 0
# Id: 3611800
# log K source: NIST46.3
# Delta H source: NIST46.3
#T and ionic strength: 0.00 25.0
Hg(OH)2 + 2H+ + 2Cl- = HgCl2 + 2H2O
log_k 20.194
delta_h -92.42 kJ
-gamma 0 0
# Id: 3611801
```

```
# log K source: NIST46.3
# Delta H source: NIST46.3
#T and ionic strength: 0.00 25.0
Hg(OH)2 + 2H+ + 3Cl- = HgCl3- + 2H2O
log_k 21.194
delta_h -94.02 kJ
-gamma 0 0
# Id: 3611802
# log K source: NIST46.3
# Delta H source: NIST46.3
#T and ionic strength: 0.00 25.0
Hg(OH)2 + 2H+ + 4Cl- = HgCl4-2 + 2H2O
log_k 21.794
delta_h -100.72 kJ
-gamma 0 0
# Id: 3611803
# log K source: NIST46.3
# Delta H source: NIST46.3
#T and ionic strength: 0.00 25.0
Hg(OH)2 + Cl- + I- + 2H+ = HgClI + 2H2O
log_k 25.532
delta_h -135.3 kJ
-gamma 0 0
# Id: 3611804
# log K source: NIST2.1.1
# Delta H source: NIST2.1.1
#T and ionic strength:
Hg(OH)2 + H+ + Cl- = HgClOH + H2O
log_k 10.444
delta_h -42.72 kJ
-gamma 0 0
# Id: 3611805
# log K source: NIST46.3
# Delta H source: NIST46.3
#T and ionic strength: 1.00 25.0
Cu+2 + Cl- = CuCl+
log_k 0.2
delta_h 8.3 kJ
-gamma 4 0
# Id: 2311800
# log K source: NIST46.3
# Delta H source: NIST46.3
#T and ionic strength: 0.00 25.0
Cu+2 + 2Cl- = CuCl2
log_k -0.26
delta_h 44.183 kJ
-gamma 0 0
# Id: 2311801
# log K source: SCD3.02 (1989 IPa)
# Delta H source: MTQ3.11
#T and ionic strength: 0.00 25.0
Cu+2 + 3Cl- = CuCl3-
log_k -2.29
delta_h 57.279 kJ
```

```
-gamma 4 0
# Id: 2311802
# log K source: MTQ3.11
# Delta H source: MTQ3.11
#T and ionic strength:
Cu+2 + 4Cl- = CuCl4-2
log_k -4.59
delta_h 32.5515 kJ
-gamma 5 0
# Id: 2311803
# log K source: MTQ3.11
# Delta H source: MTQ3.11
#T and ionic strength:
Cu+ + 2Cl- = CuCl2-
log_k 5.42
delta_h -1.7573 kJ
-gamma 4 0
# Id: 2301800
# log K source: NIST46.3
# Delta H source: MTQ3.11
#T and ionic strength: 0.00 25.0
Cu+ + 3Cl- = CuCl3-2
log_k 4.75
delta_h 1.0878 kJ
-gamma 5 0
# Id: 2301801
# log K source: NIST46.3
# Delta H source: MTQ3.11
#T and ionic strength: 0.00 25.0
Cu+ + Cl- = CuCl
log_k 3.1
delta_h 0 kJ
-gamma 0 0
# Id: 2301802
# log K source: NIST46.4
# Delta H source: MTQ3.11
#T and ionic strength: 0.00 25.0
Ag+ + Cl- = AgCl
log_k 3.31
delta_h -12 kJ
-gamma 0 0
# Id: 201800
# log K source: NIST46.3
# Delta H source: NIST46.3
#T and ionic strength: 0.00 25.0
Ag+ + 2Cl- = AgCl2-
log_k 5.25
delta_h -16 kJ
-gamma 0 0
# Id: 201801
# log K source: NIST46.3
# Delta H source: NIST46.3
#T and ionic strength: 0.00 25.0
Ag+ + 3Cl- = AgCl3-2
```

```
log_k 5.2
delta_h 0 kJ
-gamma 0 0
# Id: 201802
# log K source: NIST46.3
# Delta H source: MTQ3.11
#T and ionic strength: 0.00 25.0
Ag+ + 4Cl- = AgCl4-3
log_k 5.51
delta_h 0 kJ
-gamma 0 0
# Id: 201803
# log K source: MTQ3.11
# Delta H source: MTQ3.11
#T and ionic strength:
Ni+2 + Cl- = NiCl+
log_k 0.408
delta_h 2 kJ
-gamma 0 0
# Id: 5401800
# log K source: NIST46.3
# Delta H source: NIST46.3
#T and ionic strength: 1.00 25.0
Ni+2 + 2Cl- = NiCl2
log_k -1.89
delta_h 0 kJ
-gamma 0 0
# Id: 5401801
# log K source: SCD3.02 (1989 IPa)
# Delta H source: MTQ3.11
#T and ionic strength: 0.00 25.0
Co+2 + Cl- = CoCl+
log_k 0.539
delta_h 2 kJ
-gamma 0 0
# Id: 2001800
# log K source: NIST46.4
# Delta H source: NIST46.4
#T and ionic strength: 0.50 25.0
Co+3 + Cl- = CoCl+2
log_k 2.3085
delta_h 16 kJ
-gamma 0 0
# Id: 2011800
# log K source: NIST46.4
# Delta H source: NIST46.4
#T and ionic strength: 0.50 25.0
Fe+3 + Cl- = FeCl+2
log_k 1.48
delta_h 23 kJ
-gamma 5 0
# Id: 2811800
# log K source: NIST46.3
# Delta H source: NIST46.3
```

```
#T and ionic strength: 0.00 25.0
Fe+3 + 2Cl- = FeCl2+
log_k 2.13
delta_h 0 kJ
-gamma 5 0
# Id: 2811801
# log K source: NIST46.3
# Delta H source: MTQ3.11
#T and ionic strength: 0.00 25.0
Fe+3 + 3Cl- = FeCl3
log_k 1.13
delta_h 0 kJ
-gamma 0 0
# Id: 2811802
# log K source: Nord90
# Delta H source: MTQ3.11
#T and ionic strength: 0.00 25.0
Mn+2 + Cl- = MnCl+
log_k 0.1
delta_h 0 kJ
-gamma 5 0
# Id: 4701800
# log K source: NIST46.3
# Delta H source: MTQ3.11
#T and ionic strength: 0.00 20.0
Mn+2 + 2Cl- = MnCl2
log_k 0.25
delta_h 0 kJ
-gamma 0 0
# Id: 4701801
# log K source: Nord90
# Delta H source: MTQ3.11
#T and ionic strength: 0.00 25.0
Mn+2 + 3Cl- = MnCl3-
log_k -0.31
delta_h 0 kJ
-gamma 5 0
# Id: 4701802
# log K source: Nord90
# Delta H source: MTQ3.11
#T and ionic strength: 0.00 25.0
Cr(OH)2+ + 2H+ + Cl- = CrCl+2 + 2H2O
log_k 9.6808
delta_h -103.62 kJ
-gamma 0 0
# Id: 2111800
# log K source: NIST46.3
# Delta H source: NIST46.3
#T and ionic strength: 1.00 25.0
Cr(OH)2+ + 2Cl- + 2H+ = CrCl2+ + 2H2O
log_k 8.658
delta_h -39.2208 kJ
-gamma 0 0
# Id: 2111801
```

```
# log K source: MTQ3.11
# Delta H source: MTQ3.11
#T and ionic strength:
Cr(OH)2+ + 2Cl- + H+ = CrOHCl2 + H2O
log_k 2.9627
delta_h 0 kJ
-gamma 0 0
# Id: 2111802
# log K source: MTQ3.11
# Delta H source: MTQ3.11
#T and ionic strength:
VO+2 + Cl- = VOCl+
log_k 0.448
delta_h 0 kJ
-gamma 0 0
# Id: 9021800
# log K source: NIST46.3
# Delta H source: MTQ3.11
#T and ionic strength: 1.00 20.0
U+4 + Cl- = UCl+3
log_k 1.7
delta_h -20 kJ
-gamma 0 0
# Id: 8911800
# log K source: NIST46.3
# Delta H source: NIST46.3
#T and ionic strength: 0.00 25.0
UO2+2 + Cl- = UO2Cl+
log_k 0.21
delta_h 16 kJ
-gamma 0 0
# Id: 8931800
# log K source: NIST46.3
# Delta H source: NIST46.3
#T and ionic strength: 0.00 25.0
Be+2 + Cl- = BeCl+
log_k 0.2009
delta_h 0 kJ
-gamma 5 0
# Id: 1101801
# log K source: NIST46.4
# Delta H source: MTQ3.11
#T and ionic strength: 0.70 20.0
Sn(OH)2 + 2H+ + Br- = SnBr+ + 2H2O
log_k 8.254
delta_h 0 kJ
-gamma 0 0
# Id: 7901301
# log K source: NIST46.4
# Delta H source: NIST46.4
#T and ionic strength: 0.00 25.0
Sn(OH)2 + 2H+ + 2Br- = SnBr2 + 2H2O
log_k 8.794
delta_h 0 kJ
```

```
-gamma 0 0
# Id: 7901302
# log K source: NIST46.4
# Delta H source: NIST46.4
#T and ionic strength: 0.00 25.0
Sn(OH)2 + 2H+ + 3Br- = SnBr3- + 2H2O
log_k 7.48
delta_h 0 kJ
-gamma 0 0
# Id: 7901303
# log K source: NIST46.4
# Delta H source: NIST46.4
#T and ionic strength: 3.00 25.0
Pb+2 + Br- = PbBr+
log_k 1.7
delta_h 8 kJ
-gamma 0 0
# Id: 6001300
# log K source: NIST46.3
# Delta H source: NIST46.3
#T and ionic strength: 0.00 25.0
Pb+2 + 2Br- = PbBr2
log_k 2.6
delta_h -4 kJ
-gamma 0 0
# Id: 6001301
# log K source: NIST46.3
# Delta H source: NIST46.3
#T and ionic strength: 0.00 25.0
Tl+ + Br- = TlBr
log_k 0.91
delta_h -12 kJ
-gamma 0 0
# Id: 8701300
# log K source: NIST46.3
# Delta H source: NIST46.3
#T and ionic strength: 0.00 25.0
Tl+ + 2Br- = TlBr2-
log_k -0.384
delta_h 12.36 kJ
-gamma 0 0
# Id: 8701301
# log K source: NIST46.3
# Delta H source: NIST2.1.1
#T and ionic strength: 4.00 25.0
Tl+ + Br- + Cl- = TlBrCl-
log_k 0.8165
delta_h 0 kJ
-gamma 0 0
# Id: 8701302
# log K source: MTQ3.11
# Delta H source: MTQ3.11
#T and ionic strength:
Tl+ + I- + Br- = TlIBr-
```

```
log_k 2.185
delta_h 0 kJ
-gamma 0 0
# Id: 8703802
# log K source: MTQ3.11
# Delta H source: MTQ3.11
#T and ionic strength:
Tl(OH)3 + 3H+ + Br- = TlBr+2 + 3H2O
log_k 12.803
delta_h 0 kJ
-gamma 0 0
# Id: 8711300
# log K source: NIST46.3
# Delta H source: MTQ3.11
#T and ionic strength: 1.00 25.0
Tl(OH)3 + 3H+ + 2Br- = TlBr2+ + 3H2O
log_k 20.711
delta_h 0 kJ
-gamma 0 0
# Id: 8711301
# log K source: NIST46.3
# Delta H source: MTQ3.11
#T and ionic strength: 1.00 25.0
Tl(OH)3 + 3Br- + 3H+ = TlBr3 + 3H2O
log_k 27.0244
delta_h 0 kJ
-gamma 0 0
# Id: 8711302
# log K source: MTQ3.11
# Delta H source: MTQ3.11
#T and ionic strength:
Tl(OH)3 + 4Br- + 3H+ = TlBr4- + 3H2O
log_k 31.1533
delta_h 0 kJ
-gamma 0 0
# Id: 8711303
# log K source: MTQ3.11
# Delta H source: MTQ3.11
#T and ionic strength:
Zn+2 + Br- = ZnBr+
log_k -0.07
delta_h 1 kJ
-gamma 0 0
# Id: 9501300
# log K source: NIST46.3
# Delta H source: NIST46.3
#T and ionic strength: 0.00 25.0
Zn+2 + 2Br- = ZnBr2
log_k -0.98
delta_h 0 kJ
-gamma 0 0
# Id: 9501301
# log K source: MTQ3.11
# Delta H source: MTQ3.11
```

```
#T and ionic strength:
Cd+2 + Br- = CdBr+
log_k 2.15
delta_h -3 kJ
-gamma 0 0
# Id: 1601300
# log K source: NIST46.3
# Delta H source: NIST46.3
#T and ionic strength: 0.00 25.0
Cd+2 + 2Br- = CdBr2
log_k 3
delta_h -3 kJ
-gamma 0 0
# Id: 1601301
# log K source: NIST46.3
# Delta H source: NIST46.3
#T and ionic strength: 0.00 25.0
Hg(OH)2 + 2H+ + Br- = HgBr+ + 2H2O
log_k 15.803
delta_h -81.92 kJ
-gamma 0 0
# Id: 3611301
# log K source: NIST46.3
# Delta H source: NIST46.3
#T and ionic strength: 0.50 25.0
Hg(OH)2 + 2H+ + 2Br- = HgBr2 + 2H2O
log_k 24.2725
delta_h -127.12 kJ
-gamma 0 0
# Id: 3611302
# log K source: NIST46.3
# Delta H source: NIST46.3
#T and ionic strength: 0.50 25.0
Hg(OH)2 + 2H+ + 3Br- = HgBr3- + 2H2O
log_k 26.7025
delta_h -138.82 kJ
-gamma 0 0
# Id: 3611303
# log K source: NIST46.3
# Delta H source: NIST46.3
#T and ionic strength: 0.50 25.0
Hg(OH)2 + 2H+ + 4Br- = HgBr4-2 + 2H2O
log_k 27.933
delta_h -153.72 kJ
-gamma 0 0
# Id: 3611304
# log K source: NIST46.3
# Delta H source: NIST46.3
#T and ionic strength: 0.50 25.0
Hg(OH)2 + Br- + Cl- + 2H+ = HgBrCl + 2H2O
log_k 22.1811
delta_h -113.77 kJ
-gamma 0 0
# Id: 3611305
```

```
# log K source: NIST2.1.1
# Delta H source: NIST2.1.1
#T and ionic strength:
Hg(OH)2 + Br- + I- + 2H+ = HgBrI + 2H2O
log_k 27.3133
delta_h -151.27 kJ
-gamma 0 0
# Id: 3611306
# log K source: NIST2.1.1
# Delta H source: NIST2.1.1
#T and ionic strength:
Hg(OH)2 + Br- + 3I- + 2H+ = HgBrI3-2 + 2H2O
log_k 34.2135
delta_h 0 kJ
-gamma 0 0
# Id: 3611307
# log K source: MTQ3.11
# Delta H source: MTQ3.11
#T and ionic strength:
Hg(OH)2 + 2Br- + 2I- + 2H+ = HgBr2I2-2 + 2H2O
log_k 32.3994
delta_h 0 kJ
-gamma 0 0
# Id: 3611308
# log K source: MTQ3.11
# Delta H source: MTQ3.11
#T and ionic strength:
Hg(OH)2 + 3Br- + I- + 2H+ = HgBr3I-2 + 2H2O
log_k 30.1528
delta_h 0 kJ
-gamma 0 0
# Id: 3611309
# log K source: MTQ3.11
# Delta H source: MTQ3.11
#T and ionic strength:
Hg(OH)2 + H+ + Br- = HgBrOH + H2O
log_k 12.433
delta_h 0 kJ
-gamma 0 0
# Id: 3613301
# log K source: NIST46.3
# Delta H source: MTQ3.11
#T and ionic strength: 0.50 25.0
Ag+ + Br- = AgBr
log_k 4.6
delta_h 0 kJ
-gamma 0 0
# Id: 201300
# log K source: NIST46.3
# Delta H source: MTQ3.11
#T and ionic strength: 0.00 25.0
Ag+ + 2Br- = AgBr2-
log_k 7.5
delta_h 0 kJ
```

```
-gamma 0 0
# Id: 201301
# log K source: NIST46.3
# Delta H source: MTQ3.11
#T and ionic strength: 0.00 25.0
Ag+ + 3Br- = AgBr3-2
log_k 8.1
delta_h 0 kJ
-gamma 0 0
# Id: 201302
# log K source: NIST46.3
# Delta H source: MTQ3.11
#T and ionic strength: 0.00 25.0
Ni+2 + Br- = NiBr+
log_k 0.5
delta_h 0 kJ
-gamma 0 0
# Id: 5401300
# log K source: MTQ3.11
# Delta H source: MTQ3.11
#T and ionic strength:
Cr(OH)2+ + Br- + 2H+ = CrBr+2 + 2H2O
log_k 7.5519
delta_h -46.9068 kJ
-gamma 0 0
# Id: 2111300
# log K source: MTQ3.11
# Delta H source: MTQ3.11
#T and ionic strength:
Be+2 + Br- = BeBr+
log_k 0.1009
delta_h 0 kJ
-gamma 5 0
# Id: 1101301
# log K source: NIST46.4
# Delta H source: MTQ3.11
#T and ionic strength: 0.70 20.0
Pb+2 + I- = PbI+
log_k 2
delta_h 0 kJ
-gamma 0 0
# Id: 6003800
# log K source: NIST46.3
# Delta H source: MTQ3.11
#T and ionic strength: 0.00 25.0
Pb+2 + 2I- = PbI2
log_k 3.2
delta_h 0 kJ
-gamma 0 0
# Id: 6003801
# log K source: NIST46.3
# Delta H source: MTQ3.11
#T and ionic strength: 0.00 25.0
Tl+ + I- = TlI
```

```
log_k 1.4279
delta_h 0 kJ
-gamma 0 0
# Id: 8703800
# log K source: MTQ3.11
# Delta H source: MTQ3.11
#T and ionic strength:
Tl+ + 2I- = TlI2-
log_k 1.8588
delta_h 0 kJ
-gamma 0 0
# Id: 8703801
# log K source: MTQ3.11
# Delta H source: MTQ3.11
#T and ionic strength:
Tl(OH)3 + 4I- + 3H+ = TlI4- + 3H2O
log_k 34.7596
delta_h 0 kJ
-gamma 0 0
# Id: 8713800
# log K source: MTQ3.11
# Delta H source: MTQ3.11
#T and ionic strength:
Zn+2 + I- = ZnI+
log_k -2.0427
delta_h -4 kJ
-gamma 0 0
# Id: 9503800
# log K source: NIST46.3
# Delta H source: NIST46.3
#T and ionic strength: 3.00 25.0
Zn+2 + 2I- = ZnI2
log_k -1.69
delta_h 0 kJ
-gamma 0 0
# Id: 9503801
# log K source: MTQ3.11
# Delta H source: MTQ3.11
#T and ionic strength:
Cd+2 + I- = CdI+
log_k 2.28
delta_h -9.6 kJ
-gamma 0 0
# Id: 1603800
# log K source: NIST46.3
# Delta H source: NIST46.3
#T and ionic strength: 0.00 25.0
Cd+2 + 2I- = CdI2
log_k 3.92
delta_h -12 kJ
-gamma 0 0
# Id: 1603801
# log K source: NIST46.3
# Delta H source: NIST46.3
```

```
#T and ionic strength: 0.00 25.0
Hg(OH)2 + 2H+ + I- = HgI+ + 2H2O
log_k 19.603
delta_h -111.22 kJ
-gamma 0 0
# Id: 3613801
# log K source: NIST46.4
# Delta H source: NIST46.4
#T and ionic strength: 0.50 25.0
Hg(OH)2 + 2H+ + 2I- = HgI2 + 2H2O
log_k 30.8225
delta_h -182.72 kJ
-gamma 0 0
# Id: 3613802
# log K source: NIST46.4
# Delta H source: NIST46.4
#T and ionic strength: 0.50 25.0
Hg(OH)2 + 2H+ + 3I- = HgI3- + 2H2O
log_k 34.6025
delta_h -194.22 kJ
-gamma 0 0
# Id: 3613803
# log K source: NIST46.4
# Delta H source: NIST2.1.1
#T and ionic strength: 0.50 25.0
Hg(OH)2 + 2H+ + 4I- = HgI4-2 + 2H2O
log_k 36.533
delta_h -220.72 kJ
-gamma 0 0
# Id: 3613804
# log K source: NIST46.4
# Delta H source: NIST46.4
#T and ionic strength: 0.50 25.0
Ag+ + I- = AgI
log_k 6.6
delta_h 0 kJ
-gamma 0 0
# Id: 203800
# log K source: NIST46.3
# Delta H source: MTQ3.11
#T and ionic strength: 0.00 18.0
Ag+ + 2I- = AgI2-
log_k 11.7
delta_h 0 kJ
-gamma 0 0
# Id: 203801
# log K source: NIST46.3
# Delta H source: MTQ3.11
#T and ionic strength: 0.00 18.0
Ag+ + 3I- = AgI3-2
log_k 12.6
delta_h -122 kJ
-gamma 0 0
# Id: 203802
```

```
# log K source: NIST46.3
# Delta H source: NIST46.3
#T and ionic strength: 0.00 25.0
Ag+ + 4I- = AgI4-3
log_k 14.229
delta_h 0 kJ
-gamma 0 0
# Id: 203803
# log K source: NIST46.3
# Delta H source: MTQ3.11
#T and ionic strength: 2.00 25.0
Cr(OH)2+ + I- + 2H+ = CrI+2 + 2H2O
log_k 4.8289
delta_h 0 kJ
-gamma 0 0
# Id: 2113800
# log K source: MTQ3.11
# Delta H source: MTQ3.11
#T and ionic strength:
H+ + HS- = H2S
log_k 7.02
delta_h -22 kJ
-gamma 0 0
# Id: 3307300
# log K source: NIST46.3
# Delta H source: NIST46.3
#T and ionic strength: 0.00 25.0
Pb+2 + 2HS- = Pb(HS)2
log_k 15.27
delta_h 0 kJ
-gamma 0 0
# Id: 6007300
# log K source: MTQ3.11
# Delta H source: MTQ3.11
#T and ionic strength:
Pb+2 + 3HS- = Pb(HS)3-
log_k 16.57
delta_h 0 kJ
-gamma 0 0
# Id: 6007301
# log K source: MTQ3.11
# Delta H source: MTQ3.11
#T and ionic strength:
Tl+ + HS- = TlHS
log_k 2.474
delta_h 0 kJ
-gamma 0 0
# Id: 8707300
# log K source: NIST46.3
# Delta H source: MTQ3.11
#T and ionic strength: 1.00 25.0
2Tl+ + HS- = Tl2HS+
log_k 5.974
delta_h 0 kJ
```

```
-gamma 0 0
# Id: 8707301
# log K source: NIST46.3
# Delta H source: MTQ3.11
#T and ionic strength: 1.00 25.0
2Tl+ + 3HS- + H2O = Tl2OH(HS)3-2 + H+
log_k 1.0044
delta_h 0 kJ
-gamma 0 0
# Id: 8707302
# log K source: MTQ3.11
# Delta H source: MTQ3.11
#T and ionic strength:
2Tl+ + 2HS- + 2H2O = Tl2(OH)2(HS)2-2 + 2H+
log_k -11.0681
delta_h 0 kJ
-gamma 0 0
# Id: 8707303
# log K source: MTQ3.11
# Delta H source: MTQ3.11
#T and ionic strength:
Zn+2 + 2HS- = Zn(HS)2
log_k 12.82
delta_h 0 kJ
-gamma 0 0
# Id: 9507300
# log K source: DHa1993
# Delta H source: MTQ3.11
#T and ionic strength: 0.00 25.0
Zn+2 + 3HS- = Zn(HS)3-
log_k 16.1
delta_h 0 kJ
-gamma 0 0
# Id: 9507301
# log K source: MTQ3.11
# Delta H source: MTQ3.11
#T and ionic strength:
Zn+2 + 3HS- = ZnS(HS)2-2 + H+
log_k 6.12
delta_h 0 kJ
-gamma 0 0
# Id: 9507302
# log K source: DHa1993
# Delta H source: MTQ3.11
#T and ionic strength: 0.00 25.0
Zn+2 + 2HS- + 2HS- = Zn(HS)4-2
log_k 14.64
delta_h 0 kJ
-gamma 0 0
# Id: 9507303
# log K source: DHa1993
# Delta H source: MTQ3.11
#T and ionic strength: 0.00 25.0
Zn+2 + 2HS- = ZnS(HS)- + H+
```

```
log_k 6.81
delta_h 0 kJ
-gamma 0 0
# Id: 9507304
# log K source: DHa1993
# Delta H source: MTQ3.11
#T and ionic strength: 0.00 25.0
Cd+2 + HS- = CdHS+
log_k 8.008
delta_h 0 kJ
-gamma 0 0
# Id: 1607300
# log K source: NIST46.3
# Delta H source: MTQ3.11
#T and ionic strength: 1.00 25.0
Cd+2 + 2HS- = Cd(HS)2
log_k 15.212
delta_h 0 kJ
-gamma 0 0
# Id: 1607301
# log K source: NIST46.3
# Delta H source: MTQ3.11
#T and ionic strength: 1.00 25.0
Cd+2 + 3HS- = Cd(HS)3-
log_k 17.112
delta_h 0 kJ
-gamma 0 0
# Id: 1607302
# log K source: NIST46.3
# Delta H source: MTQ3.11
#T and ionic strength: 1.00 25.0
Cd+2 + 4HS- = Cd(HS)4-2
log_k 19.308
delta_h 0 kJ
-gamma 0 0
# Id: 1607303
# log K source: NIST46.3
# Delta H source: MTQ3.11
#T and ionic strength: 1.00 25.0
Hg(OH)2 + 2HS- = HgS2-2 + 2H2O
log_k 29.414
delta_h 0 kJ
-gamma 0 0
# Id: 3617300
# log K source: NIST46.4
# Delta H source: MTQ3.11
#T and ionic strength: 1.00 20.0
Hg(OH)2 + 2H+ + 2HS- = Hg(HS)2 + 2H2O
log_k 44.516
delta_h 0 kJ
-gamma 0 0
# Id: 3617301
# log K source: NIST46.3
# Delta H source: MTQ3.11
```

```
#T and ionic strength: 1.00 20.0
Hg(OH)2 + H+ + 2HS- = HgHS2- + 2H2O
log_k 38.122
delta_h 0 kJ
-gamma 0 0
# Id: 3617302
# log K source: NIST46.4
# Delta H source: MTQ3.11
#T and ionic strength: 1.00 20.0
Cu+2 + 3HS- = Cu(HS)3-
log_k 25.899
delta_h 0 kJ
-gamma 0 0
# Id: 2317300
# log K source: MTQ3.11
# Delta H source: MTQ3.11
#T and ionic strength:
Ag+ + HS- = AgHS
log_k 13.8145
delta_h 0 kJ
-gamma 0 0
# Id: 207300
# log K source: NIST46.3
# Delta H source: MTQ3.11
#T and ionic strength: 0.10 20.0
Ag+ + 2HS- = Ag(HS)2-
log_k 17.9145
delta_h 0 kJ
-gamma 0 0
# Id: 207301
# log K source: NIST46.3
# Delta H source: MTQ3.11
#T and ionic strength: 0.10 20.0
Fe+2 + 2HS- = Fe(HS)2
log_k 8.95
delta_h 0 kJ
-gamma 0 0
# Id: 2807300
# log K source: MTQ3.11
# Delta H source: MTQ3.11
#T and ionic strength:
Fe+2 + 3HS- = Fe(HS)3-
log_k 10.987
delta_h 0 kJ
-gamma 0 0
# Id: 2807301
# log K source: MTQ3.11
# Delta H source: MTQ3.11
#T and ionic strength:
HS- = S2-2 + H+
log_k -11.7828
delta_h 46.4 kJ
-gamma 0 0
-no_check
```

```
# Id: 7317300
# log K source: NIST2.1.1
# Delta H source: NIST2.1.1
#T and ionic strength:
HS- = S3-2 + H+
log_k -10.7667
delta_h 42.2 kJ
-gamma 0 0
-no_check
# Id: 7317301
# log K source: NIST2.1.1
# Delta H source: NIST2.1.1
#T and ionic strength:
HS- = S4-2 + H+
log_k -9.9608
delta_h 39.3 kJ
-gamma 0 0
-no_check
# Id: 7317302
# log K source: NIST2.1.1
# Delta H source: NIST2.1.1
#T and ionic strength:
HS- = S5-2 + H+
log_k -9.3651
delta_h 37.6 kJ
-gamma 0 0
-no_check
# Id: 7317303
# log K source: NIST2.1.1
# Delta H source: NIST2.1.1
#T and ionic strength:
HS- = S6-2 + H+
log_k -9.881
delta_h 0 kJ
-gamma 0 0
-no_check
# Id: 7317304
# log K source: MTQ3.11
# Delta H source: MTQ3.11
#T and ionic strength:
2Sb(OH)3 + 4HS- + 2H+ = Sb2S4-2 + 6H2O
log_k 49.3886
delta_h -321.78 kJ
-gamma 0 0
# Id: 7407300
# log K source: NIST2.1.1
# Delta H source: NIST2.1.1
#T and ionic strength:
Cu+ + 2HS- = Cu(S4)2-3 + 2H+
log_k 3.39
delta_h 0 kJ
-gamma 23 0
-no_check
# Id: 2307300
```

```
# log K source: MTQ3.11
# Delta H source: MTQ3.11
#T and ionic strength:
Cu+ + 2HS- = CuS4S5-3 + 2H+
log_k 2.66
delta_h 0 kJ
-gamma 25 0
-no_check
# Id: 2307301
# log K source: MTQ3.11
# Delta H source: MTQ3.11
#T and ionic strength:
Ag+ + 2HS- = Ag(S4)2-3 + 2H+
log_k 0.991
delta_h 0 kJ
-gamma 22 0
-no_check
# Id: 207302
# log K source: MTQ3.11
# Delta H source: MTQ3.11
#T and ionic strength:
Ag+ + 2HS- = AgS4S5-3 + 2H+
log_k 0.68
delta_h 0 kJ
-gamma 24 0
-no_check
# Id: 207303
# log K source: MTQ3.11
# Delta H source: MTQ3.11
#T and ionic strength:
Ag+ + 2HS- = Ag(HS)S4-2 + H+
log_k 10.431
delta_h 0 kJ
-gamma 15 0
-no_check
# Id: 207304
# log K source: MTQ3.11
# Delta H source: MTQ3.11
#T and ionic strength:
H+ + SO4-2 = HSO4-
log_k 1.99
delta_h 22 kJ
-gamma 4.5 0
# Id: 3307320
# log K source: NIST46.3
# Delta H source: NIST46.3
#T and ionic strength: 0.00 25.0
NH4+ + SO4-2 = NH4SO4-
log_k 1.03
delta_h 0 kJ
-gamma 5 0
# Id: 4907320
# log K source: NIST46.3
# Delta H source: MTQ3.11
```

```
#T and ionic strength: 0.00 25.0
Pb+2 + SO4-2 = PbSO4
log_k 2.69
delta_h 0 kJ
-gamma 0 0
# Id: 6007320
# log K source: NIST46.3
# Delta H source: MTQ3.11
#T and ionic strength: 0.00 25.0
Pb+2 + 2SO4-2 = Pb(SO4)2-2
log_k 3.47
delta_h 0 kJ
-gamma 0 0
# Id: 6007321
# log K source: SCD3.02 (1960 RKa)
# Delta H source: MTQ3.11
#T and ionic strength: 0.00 25.0
Al+3 + SO4-2 = AlSO4+
log_k 3.89
delta_h 28 kJ
-gamma 4.5 0
# Id: 307320
# log K source: NIST46.3
# Delta H source: NIST46.3
#T and ionic strength: 0.00 25.0
Al+3 + 2SO4-2 = Al(SO4)2-
log_k 4.92
delta_h 11.9 kJ
-gamma 4.5 0
# Id: 307321
# log K source: Nord90
# Delta H source: Nord90
#T and ionic strength: 0.00 25.0
Tl+ + SO4-2 = TlSO4-
log_k 1.37
delta_h -0.8 kJ
-gamma 0 0
# Id: 8707320
# log K source: NIST46.3
# Delta H source: NIST46.3
#T and ionic strength: 0.00 25.0
Zn+2 + SO4-2 = ZnSO4
log_k 2.34
delta_h 6.2 kJ
-gamma 0 0
# Id: 9507320
# log K source: NIST46.3
# Delta H source: NIST46.3
#T and ionic strength: 0.00 25.0
Zn+2 + 2SO4-2 = Zn(SO4)2-2
log_k 3.28
delta_h 0 kJ
-gamma 0 0
# Id: 9507321
```

```
# log K source: MTQ3.11
# Delta H source: MTQ3.11
#T and ionic strength:
Cd+2 + SO4-2 = CdSO4
log_k 2.37
delta_h 8.7 kJ
-gamma 0 0
# Id: 1607320
# log K source: NIST46.3
# Delta H source: NIST46.3
#T and ionic strength: 0.00 25.0
Cd+2 + 2SO4-2 = Cd(SO4)2-2
log_k 3.5
delta_h 0 kJ
-gamma 0 0
# Id: 1607321
# log K source: MTQ3.11
# Delta H source: MTQ3.11
#T and ionic strength:
Hg(OH)2 + 2H+ + SO4-2 = HgSO4 + 2H2O
log_k 8.612
delta_h 0 kJ
-gamma 0 0
# Id: 3617320
# log K source: NIST46.3
# Delta H source: MTQ3.11
#T and ionic strength: 0.50 25.0
Cu+2 + SO4-2 = CuSO4
log_k 2.36
delta_h 8.7 kJ
-gamma 0 0
# Id: 2317320
# log K source: NIST46.3
# Delta H source: NIST46.3
#T and ionic strength: 0.00 25.0
Ag+ + SO4-2 = AgSO4-
log_k 1.3
delta_h 6.2 kJ
-gamma 0 0
# Id: 207320
# log K source: NIST46.3
# Delta H source: NIST46.3
#T and ionic strength: 0.00 25.0
Ni+2 + SO4-2 = NiSO4
log_k 2.3
delta_h 5.8 kJ
-gamma 0 0
# Id: 5407320
# log K source: NIST46.3
# Delta H source: NIST46.3
#T and ionic strength: 0.00 25.0
Ni+2 + 2SO4-2 = Ni(SO4)2-2
log_k 0.82
delta_h 0 kJ
```

```
-gamma 0 0
# Id: 5407321
# log K source: SCD3.02 (1978 BLa)
# Delta H source: MTQ3.11
#T and ionic strength: 0.00 25.0
Co+2 + SO4-2 = CoSO4
log_k 2.3
delta_h 6.2 kJ
-gamma 0 0
# Id: 2007320
# log K source: NIST46.4
# Delta H source: NIST46.4
#T and ionic strength: 0.00 25.0
Fe+2 + SO4-2 = FeSO4
log_k 2.39
delta_h 8 kJ
-gamma 0 0
# Id: 2807320
# log K source: NIST46.3
# Delta H source: NIST46.3
#T and ionic strength: 0.00 25.0
Fe+3 + SO4-2 = FeSO4+
log_k 4.05
delta_h 25 kJ
-gamma 5 0
# Id: 2817320
# log K source: NIST46.3
# Delta H source: NIST46.3
#T and ionic strength: 0.00 25.0
Fe+3 + 2SO4-2 = Fe(SO4)2-
log_k 5.38
delta_h 19.2 kJ
-gamma 0 0
# Id: 2817321
# log K source: Nord90
# Delta H source: Nord90
#T and ionic strength: 0.00 25.0
Mn+2 + SO4-2 = MnSO4
log_k 2.25
delta_h 8.7 kJ
-gamma 0 0
# Id: 4707320
# log K source: NIST46.3
# Delta H source: NIST46.3
#T and ionic strength: 0.00 25.0
Cr(OH)2+ + 2H+ + SO4-2 = CrSO4+ + 2H2O
log_k 12.9371
delta_h -98.62 kJ
-gamma 0 0
# Id: 2117320
# log K source: NIST46.3
# Delta H source: NIST46.3
#T and ionic strength: 1.00 50.0
Cr(OH)2+ + H+ + SO4-2 = CrOHSO4 + H2O
```

```
log_k 8.2871
delta_h 0 kJ
-gamma 0 0
# Id: 2117321
# log K source: NIST46.3
# Delta H source: MTQ3.11
#T and ionic strength: 0.10 25.0
2Cr(OH)2+ + SO4-2 + 2H+ = Cr2(OH)2SO4+2 + 2H2O
log_k 16.155
delta_h 0 kJ
-gamma 0 0
# Id: 2117323
# log K source: MTQ3.11
# Delta H source: MTQ3.11
#T and ionic strength:
2Cr(OH)2+ + 2SO4-2 + 2H+ = Cr2(OH)2(SO4)2 + 2H2O
log_k 17.9288
delta_h 0 kJ
-gamma 0 0
# Id: 2117324
# log K source: MTQ3.11
# Delta H source: MTQ3.11
#T and ionic strength:
U+4 + SO4-2 = USO4+2
log_k 6.6
delta_h 8 kJ
-gamma 0 0
# Id: 8917320
# log K source: NIST46.3
# Delta H source: NIST46.3
#T and ionic strength: 0.00 25.0
U+4 + 2SO4-2 = U(SO4)2
log_k 10.5
delta_h 33 kJ
-gamma 0 0
# Id: 8917321
# log K source: NIST46.3
# Delta H source: NIST46.3
#T and ionic strength: 0.00 25.0
UO2+2 + SO4-2 = UO2SO4
log_k 3.18
delta_h 20 kJ
-gamma 0 0
# Id: 8937320
# log K source: NIST46.3
# Delta H source: NIST46.3
#T and ionic strength: 0.00 25.0
UO2+2 + 2SO4-2 = UO2(SO4)2-2
log_k 4.3
delta_h 38 kJ
-gamma 0 0
# Id: 8937321
# log K source: NIST46.3
# Delta H source: NIST46.3
```

```
#T and ionic strength: 0.00 25.0
V+3 + SO4-2 = VSO4+
log_k 2.674
delta_h 0 kJ
-gamma 0 0
# Id: 9017320
# log K source: NIST46.3
# Delta H source: MTQ3.11
#T and ionic strength: 1.00 25.0
VO+2 + SO4-2 = VOSO4
log_k 2.44
delta_h 17 kJ
-gamma 0 0
# Id: 9027320
# log K source: NIST46.3
# Delta H source: NIST46.3
#T and ionic strength: 0.00 25.0
VO2+ + SO4-2 = VO2SO4-
log_k 1.378
delta_h 0 kJ
-gamma 0 0
# Id: 9037320
# log K source: NIST46.3
# Delta H source: MTQ3.11
#T and ionic strength: 1.00 20.0
Be+2 + SO4-2 = BeSO4
log_k 2.19
delta_h 29 kJ
-gamma 0 0
# Id: 1107321
# log K source: NIST46.4
# Delta H source: NIST46.4
#T and ionic strength: 0.00 25.0
Be+2 + 2SO4-2 = Be(SO4)2-2
log_k 2.596
delta_h 0 kJ
-gamma 0 0
# Id: 1107322
# log K source: NIST46.4
# Delta H source: MTQ3.11
#T and ionic strength: 1.00 25.0
Mg+2 + SO4-2 = MgSO4
log_k 2.26
delta_h 5.8 kJ
-gamma 0 0
# Id: 4607320
# log K source: NIST46.3
# Delta H source: NIST46.3
#T and ionic strength: 0.00 25.0
Ca+2 + SO4-2 = CaSO4
log_k 2.36
delta_h 7.1 kJ
-gamma 0 0
# Id: 1507320
```

```
# log K source: NIST46.3
# Delta H source: NIST46.3
#T and ionic strength: 0.00 25.0
Sr+2 + SO4-2 = SrSO4
log_k 2.3
delta_h 8 kJ
-gamma 0 0
# Id: 8007321
# log K source: NIST46.4
# Delta H source: NIST46.4
#T and ionic strength: 0.00 25.0
Li+ + SO4-2 = LiSO4-
log_k 0.64
delta_h 0 kJ
-gamma 5 0
# Id: 4407320
# log K source: NIST46.3
# Delta H source: NIST46.3
#T and ionic strength: 0.00 25.0
Na+ + SO4-2 = NaSO4-
log_k 0.73
delta_h 1 kJ
-gamma 5.4 0
# Id: 5007320
# log K source: NIST46.3
# Delta H source: NIST46.3
#T and ionic strength: 0.00 25.0
K+ + SO4-2 = KSO4-
log_k 0.85
delta_h 4.1 kJ
-gamma 5.4 0
# Id: 4107320
# log K source: NIST46.3
# Delta H source: NIST46.3
#T and ionic strength: 0.00 25.0
HSe- + H+ = H2Se
log_k 3.89
delta_h 3.3 kJ
-gamma 0 0
# Id: 3307600
# log K source: NIST46.3
# Delta H source: NIST2.1.1
#T and ionic strength: 0.00 25.0
2Ag+ + HSe- = Ag2Se + H+
log_k 34.911
delta_h 0 kJ
-gamma 0 0
# Id: 207600
# log K source: NIST46.3
# Delta H source: MTQ3.11
#T and ionic strength: 1.00 25.0
Ag+ + H2O + 2HSe- = AgOH(Se)2-4 + 3H+
log_k -20.509
delta_h 0 kJ
```

```
-gamma 0 0
# Id: 207601
# log K source: NIST46.3
# Delta H source: MTQ3.11
#T and ionic strength: 1.00 25.0
Mn+2 + HSe- = MnSe + H+
log_k -5.385
delta_h 0 kJ
-gamma 0 0
# Id: 4707600
# log K source: NIST46.3
# Delta H source: MTQ3.11
#T and ionic strength: 1.00 25.0
HSeO3- = SeO3-2 + H+
log_k -8.4
delta_h 5.02 kJ
-gamma 0 0
# Id: 3307611
# log K source: NIST46.3
# Delta H source: NIST46.3
#T and ionic strength: 0.00 25.0
HSeO3- + H+ = H2SeO3
log_k 2.63
delta_h 6.2 kJ
-gamma 0 0
# Id: 3307610
# log K source: NIST46.3
# Delta H source: NIST46.3
#T and ionic strength: 0.00 25.0
Cd+2 + 2HSeO3- = Cd(SeO3)2-2 + 2H+
log_k -10.884
delta_h 0 kJ
-gamma 0 0
# Id: 1607610
# log K source: NIST46.4
# Delta H source: MTQ3.11
#T and ionic strength: 1.00 25.0
Ag+ + HSeO3- = AgSeO3- + H+
log_k -5.592
delta_h 0 kJ
-gamma 0 0
# Id: 207610
# log K source: NIST46.3
# Delta H source: MTQ3.11
#T and ionic strength: 1.00 25.0
Ag+ + 2HSeO3- = Ag(SeO3)2-3 + 2H+
log_k -13.04
delta_h 0 kJ
-gamma 0 0
# Id: 207611
# log K source: NIST46.3
# Delta H source: MTQ3.11
#T and ionic strength: 1.00 25.0
Fe+3 + HSeO3- = FeHSeO3+2
```

```
log_k 3.422
delta_h 25 kJ
-gamma 0 0
# Id: 2817610
# log K source: NIST46.3
# Delta H source: NIST46.3
#T and ionic strength: 1.00 25.0
SeO4-2 + H+ = HSeO4-
log_k 1.7
delta_h 23 kJ
-gamma 0 0
# Id: 3307620
# log K source: NIST46.4
# Delta H source: NIST46.4
#T and ionic strength: 0.00 25.0
Zn+2 + SeO4-2 = ZnSeO4
log_k 2.19
delta_h 0 kJ
-gamma 0 0
# Id: 9507620
# log K source: NIST46.4
# Delta H source: MTQ3.11
#T and ionic strength: 0.00 25.0
Zn+2 + 2SeO4-2 = Zn(SeO4)2-2
log_k 2.196
delta_h 0 kJ
-gamma 0 0
# Id: 9507621
# log K source: NIST46.4
# Delta H source: MTQ3.11
#T and ionic strength: 1.00 25.0
Cd+2 + SeO4-2 = CdSeO4
log_k 2.27
delta_h 0 kJ
-gamma 0 0
# Id: 1607620
# log K source: NIST46.4
# Delta H source: MTQ3.11
#T and ionic strength: 0.00 25.0
Ni+2 + SeO4-2 = NiSeO4
log_k 2.67
delta_h 14 kJ
-gamma 0 0
# Id: 5407620
# log K source: NIST46.4
# Delta H source: NIST46.4
#T and ionic strength: 0.00 25.0
Co+2 + SeO4-2 = CoSeO4
log_k 2.7
delta_h 12 kJ
-gamma 0 0
# Id: 2007621
# log K source: NIST46.4
# Delta H source: NIST46.4
```

```
#T and ionic strength: 0.00 25.0
Mn+2 + SeO4-2 = MnSeO4
log_k 2.43
delta_h 14 kJ
-gamma 0 0
# Id: 4707620
# log K source: NIST46.4
# Delta H source: NIST46.4
#T and ionic strength: 0.00 25.0
NH4+ = NH3 + H+
log_k -9.244
delta_h 52 kJ
-gamma 0 0
# Id: 3304900
# log K source: NIST46.3
# Delta H source: NIST46.3
#T and ionic strength: 0.00 25.0
Ag+ + NH4+ = AgNH3+ + H+
log_k -5.934
delta_h -72 kJ
-gamma 0 0
# Id: 204901
# log K source: NIST46.4
# Delta H source: NIST46.4
#T and ionic strength: 0.00 25.0
Ag+ + 2NH4+ = Ag(NH3)2+ + 2H+
log_k -11.268
delta_h -160 kJ
-gamma 0 0
# Id: 204902
# log K source: NIST46.4
# Delta H source: NIST46.4
#T and ionic strength: 0.00 25.0
Hg(OH)2 + H+ + NH4+ = HgNH3+2 + 2H2O
log_k 5.75
delta_h 0 kJ
-gamma 0 0
# Id: 3614900
# log K source: NIST46.3
# Delta H source: MTQ3.11
#T and ionic strength: 2.00 22.0
Hg(OH)2 + 2NH4+ = Hg(NH3)2+2 + 2H2O
log_k 5.506
delta_h -246.72 kJ
-gamma 0 0
# Id: 3614901
# log K source: NIST46.3
# Delta H source: NIST46.3
#T and ionic strength: 1.00 25.0
Hg(OH)2 + 3NH4+ = Hg(NH3)3+2 + 2H2O + H+
log_k -3.138
delta_h -312.72 kJ
-gamma 0 0
# Id: 3614902
```

```
# log K source: NIST46.3
# Delta H source: NIST46.3
#T and ionic strength: 2.00 25.0
Hg(OH)2 + 4NH4+ = Hg(NH3)4+2 + 2H2O + 2H+
log_k -11.482
delta_h -379.72 kJ
-gamma 0 0
# Id: 3614903
# log K source: NIST46.3
# Delta H source: NIST46.3
#T and ionic strength: 0.10 25.0
Cu+2 + NH4+ = CuNH3+2 + H+
log_k -5.234
delta_h -72 kJ
-gamma 0 0
# Id: 2314901
# log K source: NIST46.4
# Delta H source: NIST46.4
#T and ionic strength: 0.00 25.0
Ni+2 + NH4+ = NiNH3+2 + H+
log_k -6.514
delta_h -67 kJ
-gamma 0 0
# Id: 5404901
# log K source: NIST46.4
# Delta H source: NIST46.4
#T and ionic strength: 0.10 25.0
Ni+2 + 2NH4+ = Ni(NH3)2+2 + 2H+
log_k -13.598
delta_h -111.6 kJ
-gamma 0 0
# Id: 5404902
# log K source: NIST46.4
# Delta H source: NIST46.4
#T and ionic strength: 0.10 25.0
Co+2 + NH4+ = Co(NH3)+2 + H+
log_k -7.164
delta_h -65 kJ
-gamma 0 0
# Id: 2004900
# log K source: NIST46.4
# Delta H source: NIST46.4
#T and ionic strength: 0.10 25.0
Co+2 + 2NH4+ = Co(NH3)2+2 + 2H+
log_k -14.778
delta_h 0 kJ
-gamma 0 0
# Id: 2004901
# log K source: NIST46.4
# Delta H source: MTQ3.11
#T and ionic strength: 2.00 25.0
Co+2 + 3NH4+ = Co(NH3)3+2 + 3H+
log_k -22.922
delta_h 0 kJ
```

```
-gamma 0 0
# Id: 2004902
# log K source: NIST46.4
# Delta H source: MTQ3.11
#T and ionic strength: 2.00 25.0
Co+2 + 4NH4+ = Co(NH3)4+2 + 4H+
log_k -31.446
delta_h 0 kJ
-gamma 0 0
# Id: 2004903
# log K source: NIST46.4
# Delta H source: MTQ3.11
#T and ionic strength: 2.00 30.0
Co+2 + 5NH4+ = Co(NH3)5+2 + 5H+
log_k -40.47
delta_h 0 kJ
-gamma 0 0
# Id: 2004904
# log K source: NIST46.4
# Delta H source: MTQ3.11
#T and ionic strength: 2.00 30.0
Co+3 + 6NH4+ + H2O = Co(NH3)6OH+2 + 7H+
log_k -43.7148
delta_h 0 kJ
-gamma 0 0
# Id: 2014901
# log K source: NIST2.1.1
# Delta H source: MTQ3.11
#T and ionic strength:
Co+3 + 5NH4+ + Cl- = Co(NH3)5Cl+2 + 5H+
log_k -17.9584
delta_h 113.38 kJ
-gamma 0 0
# Id: 2014902
# log K source: NIST2.1.1
# Delta H source: NIST2.1.1
#T and ionic strength:
Co+3 + 6NH4+ + Cl- = Co(NH3)6Cl+2 + 6H+
log_k -33.9179
delta_h 104.34 kJ
-gamma 0 0
# Id: 2014903
# log K source: NIST2.1.1
# Delta H source: NIST2.1.1
#T and ionic strength:
Co+3 + 6NH4+ + Br- = Co(NH3)6Br+2 + 6H+
log_k -33.8884
delta_h 110.57 kJ
-gamma 0 0
# Id: 2014904
# log K source: NIST2.1.1
# Delta H source: NIST2.1.1
#T and ionic strength:
Co+3 + 6NH4+ + I- = Co(NH3)6I+2 + 6H+
```

```
log_k -33.4808
delta_h 115.44 kJ
-gamma 0 0
# Id: 2014905
# log K source: NIST2.1.1
# Delta H source: NIST2.1.1
#T and ionic strength:
Co+3 + 6NH4+ + SO4-2 = Co(NH3)6SO4+ + 6H+
log_k -28.9926
delta_h 124.5 kJ
-gamma 0 0
# Id: 2014906
# log K source: NIST2.1.1
# Delta H source: NIST2.1.1
#T and ionic strength:
Cr(OH)2+ + 6NH4+ = Cr(NH3)6+3 + 2H2O + 4H+
log_k -32.8952
delta_h 0 kJ
-gamma 0 0
# Id: 2114900
# log K source: NIST46.3
# Delta H source: MTQ3.11
#T and ionic strength: 4.50 25.0
Cr(OH)2+ + 5NH4+ = Cr(NH3)5OH+2 + 4H+ + H2O
log_k -30.2759
delta_h 0 kJ
-gamma 0 0
# Id: 2114901
# log K source: MTQ3.11
# Delta H source: MTQ3.11
#T and ionic strength:
Cr(OH)2+ + 6NH4+ + Cl- = Cr(NH3)6Cl+2 + 2H2O + 4H+
log_k -31.7932
delta_h 0 kJ
-gamma 0 0
# Id: 2114904
# log K source: MTQ3.11
# Delta H source: MTQ3.11
#T and ionic strength:
Cr(OH)2+ + 6NH4+ + Br- = Cr(NH3)6Br+2 + 4H+ + 2H2O
log_k -31.887
delta_h 0 kJ
-gamma 0 0
# Id: 2114905
# log K source: MTQ3.11
# Delta H source: MTQ3.11
#T and ionic strength:
Cr(OH)2+ + 6NH4+ + I- = Cr(NH3)6I+2 + 4H+ + 2H2O
log_k -32.008
delta_h 0 kJ
-gamma 0 0
# Id: 2114906
# log K source: MTQ3.11
# Delta H source: MTQ3.11
```

```
#T and ionic strength:
#Cr(OH)2+ + 4NH4+ = cis+ + 4H+
# log_k -29.8574
# delta_h 0 kJ
# -gamma 0 0
# # Id: 4902113
# # log K source: MTQ3.11
# # Delta H source: MTQ3.11
# #T and ionic strength:
#Cr(OH)2+ + 4NH4+ = trans+ + 4H+
# log_k -30.5537
# delta_h 0 kJ
# -gamma 0 0
# # Id: 4902114
# # log K source: MTQ3.11
# # Delta H source: MTQ3.11
# #T and ionic strength:
Ca+2 + NH4+ = CaNH3+2 + H+
log_k -9.144
delta_h 0 kJ
-gamma 0 0
# Id: 1504901
# log K source: NIST46.4
# Delta H source: MTQ3.11
#T and ionic strength: 0.50 25.0
Ca+2 + 2NH4+ = Ca(NH3)2+2 + 2H+
log_k -18.788
delta_h 0 kJ
-gamma 0 0
# Id: 1504902
# log K source: NIST46.4
# Delta H source: MTQ3.11
#T and ionic strength: 0.50 25.0
Sr+2 + NH4+ = SrNH3+2 + H+
log_k -9.344
delta_h 0 kJ
-gamma 0 0
# Id: 8004901
# log K source: NIST46.4
# Delta H source: MTQ3.11
#T and ionic strength: 0.50 25.0
Ba+2 + NH4+ = BaNH3+2 + H+
log_k -9.444
delta_h 0 kJ
-gamma 0 0
# Id: 1004901
# log K source: NIST46.4
# Delta H source: MTQ3.11
#T and ionic strength: 0.50 25.0
Tl+ + NO2- = TlNO2
log_k 0.83
delta_h 0 kJ
-gamma 0 0
# Id: 8704910
```

```
# log K source: NIST46.3
# Delta H source: MTQ3.11
#T and ionic strength: 0.00 25.0
Ag+ + NO2- = AgNO2
log_k 2.32
delta_h -29 kJ
-gamma 0 0
# Id: 204911
# log K source: NIST46.4
# Delta H source: NIST46.4
#T and ionic strength: 0.00 25.0
Ag+ + 2NO2- = Ag(NO2)2-
log_k 2.51
delta_h -46 kJ
-gamma 0 0
# Id: 204910
# log K source: NIST46.3
# Delta H source: NIST46.3
#T and ionic strength: 0.00 25.0
Cu+2 + NO2- = CuNO2+
log_k 2.02
delta_h 0 kJ
-gamma 0 0
# Id: 2314911
# log K source: NIST46.4
# Delta H source: MTQ3.11
#T and ionic strength: 0.00 25.0
Cu+2 + 2NO2- = Cu(NO2)2
log_k 3.03
delta_h 0 kJ
-gamma 0 0
# Id: 2314912
# log K source: NIST46.4
# Delta H source: MTQ3.11
#T and ionic strength: 0.00 25.0
Co+2 + NO2- = CoNO2+
log_k 0.848
delta_h 0 kJ
-gamma 0 0
# Id: 2004911
# log K source: NIST46.4
# Delta H source: MTQ3.11
#T and ionic strength: 1.00 25.0
Sn(OH)2 + 2H+ + NO3- = SnNO3+ + 2H2O
log_k 7.942
delta_h 0 kJ
-gamma 0 0
# Id: 7904921
# log K source: NIST46.4
# Delta H source: MTQ3.11
#T and ionic strength: 1.00 25.0
Pb+2 + NO3- = PbNO3+
log_k 1.17
delta_h 2 kJ
```

```
-gamma 0 0
# Id: 6004920
# log K source: NIST46.3
# Delta H source: NIST46.3
#T and ionic strength: 0.00 25.0
Pb+2 + 2NO3- = Pb(NO3)2
log_k 1.4
delta_h -6.6 kJ
-gamma 0 0
# Id: 6004921
# log K source: NIST46.4
# Delta H source: NIST46.4
#T and ionic strength: 0.00 25.0
Tl+ + NO3- = TlNO3
log_k 0.33
delta_h -2 kJ
-gamma 0 0
# Id: 8704920
# log K source: NIST46.3
# Delta H source: NIST46.3
#T and ionic strength: 0.00 25.0
Tl(OH)3 + NO3- + 3H+ = TlNO3+2 + 3H2O
log_k 7.0073
delta_h 0 kJ
-gamma 0 0
# Id: 8714920
# log K source: MTQ3.11
# Delta H source: MTQ3.11
#T and ionic strength:
Cd+2 + NO3- = CdNO3+
log_k 0.5
delta_h -21 kJ
-gamma 0 0
# Id: 1604920
# log K source: NIST46.3
# Delta H source: NIST46.3
#T and ionic strength: 0.00 25.0
Cd+2 + 2NO3- = Cd(NO3)2
log_k 0.2
delta_h 0 kJ
-gamma 0 0
# Id: 1604921
# log K source: NIST46.4
# Delta H source: MTQ3.11
#T and ionic strength: 0.00 25.0
Hg(OH)2 + 2H+ + NO3- = HgNO3+ + 2H2O
log_k 5.7613
delta_h 0 kJ
-gamma 0 0
# Id: 3614920
# log K source: NIST46.3
# Delta H source: MTQ3.11
#T and ionic strength: 3.00 25.0
Hg(OH)2 + 2H+ + 2NO3- = Hg(NO3)2 + 2H2O
```

```
log_k 5.38
delta_h 0 kJ
-gamma 0 0
# Id: 3614921
# log K source: NIST46.3
# Delta H source: MTQ3.11
#T and ionic strength: 3.00 25.0
Cu+2 + NO3- = CuNO3+
log_k 0.5
delta_h -4.1 kJ
-gamma 0 0
# Id: 2314921
# log K source: NIST46.4
# Delta H source: NIST46.4
#T and ionic strength: 0.00 25.0
Cu+2 + 2NO3- = Cu(NO3)2
log_k -0.4
delta_h 0 kJ
-gamma 0 0
# Id: 2314922
# log K source: NIST46.4
# Delta H source: MTQ3.11
#T and ionic strength: 0.00 25.0
Zn+2 + NO3- = ZnNO3+
log_k 0.4
delta_h -4.6 kJ
-gamma 0 0
# Id: 9504921
# log K source: NIST46.4
# Delta H source: NIST46.4
#T and ionic strength: 0.00 25.0
Zn+2 + 2NO3- = Zn(NO3)2
log_k -0.3
delta_h 0 kJ
-gamma 0 0
# Id: 9504922
# log K source: NIST46.4
# Delta H source: MTQ3.11
#T and ionic strength: 0.00 25.0
Ag+ + NO3- = AgNO3
log_k -0.1
delta_h 22.6 kJ
-gamma 0 0
# Id: 204920
# log K source: NIST46.3
# Delta H source: NIST46.3
#T and ionic strength: 0.00 25.0
Ni+2 + NO3- = NiNO3+
log_k 0.4
delta_h 0 kJ
-gamma 0 0
# Id: 5404921
# log K source: NIST46.4
# Delta H source: MTQ3.11
```

```
#T and ionic strength: 0.00 25.0
Co+2 + NO3- = CoNO3+
log_k 0.2
delta_h 0 kJ
-gamma 0 0
# Id: 2004921
# log K source: NIST46.4
# Delta H source: MTQ3.11
#T and ionic strength: 0.00 25.0
Co+2 + 2NO3- = Co(NO3)2
log_k 0.5085
delta_h 0 kJ
-gamma 0 0
# Id: 2004922
# log K source: NIST46.4
# Delta H source: MTQ3.11
#T and ionic strength: 0.50 25.0
Fe+3 + NO3- = FeNO3+2
log_k 1
delta_h -37 kJ
-gamma 0 0
# Id: 2814921
# log K source: NIST46.4
# Delta H source: NIST46.4
#T and ionic strength: 0.00 25.0
Mn+2 + NO3- = MnNO3+
log_k 0.2
delta_h 0 kJ
-gamma 0 0
# Id: 4704921
# log K source: NIST46.4
# Delta H source: MTQ3.11
#T and ionic strength: 0.00 25.0
Mn+2 + 2NO3- = Mn(NO3)2
log_k 0.6
delta_h -1.6569 kJ
-gamma 0 0
# Id: 4704920
# log K source: NIST46.3
# Delta H source: MTQ3.11
#T and ionic strength: 0.00 25.0
Cr(OH)2+ + NO3- + 2H+ = CrNO3+2 + 2H2O
log_k 8.2094
delta_h -65.4378 kJ
-gamma 0 0
# Id: 2114920
# log K source: MTQ3.11
# Delta H source: MTQ3.11
#T and ionic strength:
UO2+2 + NO3- = UO2NO3+
log_k 0.3
delta_h -12 kJ
-gamma 0 0
# Id: 8934921
```

```
# log K source: NIST46.4
# Delta H source: NIST46.4
#T and ionic strength: 0.00 25.0
VO2+ + NO3- = VO2NO3
log_k -0.296
delta_h 0 kJ
-gamma 0 0
# Id: 9034920
# log K source: NIST46.3
# Delta H source: MTQ3.11
#T and ionic strength: 1.00 20.0
Ca+2 + NO3- = CaNO3+
log_k 0.5
delta_h -5.4 kJ
-gamma 0 0
# Id: 1504921
# log K source: NIST46.4
# Delta H source: NIST46.4
#T and ionic strength: 0.00 25.0
Sr+2 + NO3- = SrNO3+
log_k 0.6
delta_h -10 kJ
-gamma 0 0
# Id: 8004921
# log K source: NIST46.4
# Delta H source: NIST46.4
#T and ionic strength: 0.00 25.0
Ba+2 + NO3- = BaNO3+
log_k 0.7
delta_h -13 kJ
-gamma 0 0
# Id: 1004921
# log K source: NIST46.4
# Delta H source: NIST46.4
#T and ionic strength: 0.00 25.0
H+ + Cyanide- = HCyanide
log_k 9.21
delta_h -43.63 kJ
-gamma 0 0
# Id: 3301431
# log K source: NIST46.4
# Delta H source: NIST46.4
#T and ionic strength: 0.00 25.0
Cd+2 + Cyanide- = CdCyanide+
log_k 6.01
delta_h -30 kJ
-gamma 0 0
# Id: 1601431
# log K source: NIST46.4
# Delta H source: NIST46.4
#T and ionic strength: 0.00 25.0
Cd+2 + 2Cyanide- = Cd(Cyanide)2
log_k 11.12
delta_h -54.3 kJ
```

```
-gamma 0 0
# Id: 1601432
# log K source: NIST46.4
# Delta H source: NIST46.4
#T and ionic strength: 0.00 25.0
Cd+2 + 3Cyanide- = Cd(Cyanide)3-
log_k 15.65
delta_h -90.3 kJ
-gamma 0 0
# Id: 1601433
# log K source: NIST46.4
# Delta H source: NIST46.4
#T and ionic strength: 0.00 25.0
Cd+2 + 4Cyanide- = Cd(Cyanide)4-2
log_k 17.92
delta_h -112 kJ
-gamma 0 0
# Id: 1601434
# log K source: NIST46.4
# Delta H source: NIST46.4
#T and ionic strength: 0.00 25.0
Hg(OH)2 + 2H+ + Cyanide- = HgCyanide+ + 2H2O
log_k 23.194
delta_h -136.72 kJ
-gamma 0 0
# Id: 3611431
# log K source: NIST46.4
# Delta H source: NIST46.4
#T and ionic strength: 0.00 25.0
Hg(OH)2 + 2H+ + 2Cyanide- = Hg(Cyanide)2 + 2H2O
log_k 38.944
delta_h 154.28 kJ
-gamma 0 0
# Id: 3611432
# log K source: NIST46.4
# Delta H source: NIST46.4
#T and ionic strength: 0.00 25.0
Hg(OH)2 + 2H+ + 3Cyanide- = Hg(Cyanide)3- + 2H2O
log_k 42.504
delta_h -262.72 kJ
-gamma 0 0
# Id: 3611433
# log K source: NIST46.4
# Delta H source: NIST46.4
#T and ionic strength: 0.00 25.0
Hg(OH)2 + 2H+ + 4Cyanide- = Hg(Cyanide)4-2 + 2H2O
log_k 45.164
delta_h -288.72 kJ
-gamma 0 0
# Id: 3611434
# log K source: NIST46.4
# Delta H source: NIST46.4
#T and ionic strength: 0.00 25.0
Cu+ + 2Cyanide- = Cu(Cyanide)2-
```

```
log_k 21.9145
delta_h -121 kJ
-gamma 0 0
# Id: 2301432
# log K source: NIST46.4
# Delta H source: NIST46.4
#T and ionic strength: 0.10 25.0
Cu+ + 3Cyanide- = Cu(Cyanide)3-2
log_k 27.2145
delta_h -167.4 kJ
-gamma 0 0
# Id: 2301433
# log K source: NIST46.4
# Delta H source: NIST46.4
#T and ionic strength: 0.00 25.0
Cu+ + 4Cyanide- = Cu(Cyanide)4-3
log_k 28.7145
delta_h -214.2 kJ
-gamma 0 0
# Id: 2301431
# log K source: NIST46.4
# Delta H source: NIST46.4
#T and ionic strength: 0.00 25.0
Ag+ + 2Cyanide- = Ag(Cyanide)2-
log_k 20.48
delta_h -137 kJ
-gamma 0 0
# Id: 201432
# log K source: NIST46.4
# Delta H source: NIST46.4
#T and ionic strength: 0.00 25.0
Ag+ + 3Cyanide- = Ag(Cyanide)3-2
log_k 21.7
delta_h -140 kJ
-gamma 0 0
# Id: 201433
# log K source: NIST46.4
# Delta H source: NIST46.4
#T and ionic strength: 0.00 25.0
Ag+ + H2O + Cyanide- = Ag(Cyanide)OH- + H+
log_k -0.777
delta_h 0 kJ
-gamma 0 0
# Id: 201431
# log K source: NIST46.4
# Delta H source: MTQ3.11
#T and ionic strength: 0.00 25.0
Ni+2 + 4Cyanide- = Ni(Cyanide)4-2
log_k 30.2
delta_h -180 kJ
-gamma 0 0
# Id: 5401431
# log K source: NIST46.4
# Delta H source: NIST46.4
```

```
#T and ionic strength: 0.00 25.0
Ni+2 + 4Cyanide- + H+ = NiH(Cyanide)4-
log_k 36.0289
delta_h 0 kJ
-gamma 0 0
# Id: 5401432
# log K source: NIST46.4
# Delta H source: MTQ3.11
#T and ionic strength: 0.10 25.0
Ni+2 + 4Cyanide- + 2H+ = NiH2Cyanide4
log_k 40.7434
delta_h 0 kJ
-gamma 0 0
# Id: 5401433
# log K source: NIST46.4
# Delta H source: MTQ3.11
#T and ionic strength: 0.10 25.0
Ni+2 + 4Cyanide- + 3H+ = NiH3(Cyanide)4+
log_k 43.3434
delta_h 0 kJ
-gamma 0 0
# Id: 5401434
# log K source: NIST46.4
# Delta H source: MTQ3.11
#T and ionic strength: 0.10 25.0
Co+2 + 3Cyanide- = Co(Cyanide)3-
log_k 14.312
delta_h 0 kJ
-gamma 0 0
# Id: 2001431
# log K source: NIST46.4
# Delta H source: MTQ3.11
#T and ionic strength: 1.00 25.0
Co+2 + 5Cyanide- = Co(Cyanide)5-3
log_k 23
delta_h -257 kJ
-gamma 0 0
# Id: 2001432
# log K source: NIST46.4
# Delta H source: NIST46.4
#T and ionic strength: 1.00 25.0
Fe+2 + 6Cyanide- = Fe(Cyanide)6-4
log_k 35.4
delta_h -358 kJ
-gamma 0 0
# Id: 2801431
# log K source: NIST46.4
# Delta H source: NIST46.4
#T and ionic strength: 0.00 25.0
H+ + Fe+2 + 6Cyanide- = HFe(Cyanide)6-3
log_k 39.71
delta_h -356 kJ
-gamma 0 0
# Id: 2801432
```

```
# log K source: NIST46.4
# Delta H source: NIST46.4
#T and ionic strength: 0.00 25.0
2H+ + Fe+2 + 6Cyanide- = H2Fe(Cyanide)6-2
log_k 42.11
delta_h -352 kJ
-gamma 0 0
# Id: 2801433
# log K source: NIST46.4
# Delta H source: NIST46.4
#T and ionic strength: 0.00 25.0
Fe+3 + 6Cyanide- = Fe(Cyanide)6-3
log_k 43.6
delta_h -293 kJ
-gamma 0 0
# Id: 2811431
# log K source: NIST46.4
# Delta H source: NIST46.4
#T and ionic strength: 0.00 25.0
2Fe+3 + 6Cyanide- = Fe2(Cyanide)6
log_k 47.6355
delta_h -218 kJ
-gamma 0 0
# Id: 2811432
# log K source: NIST46.4
# Delta H source: NIST46.4
#T and ionic strength: 0.50 25.0
Sn(OH)2 + Fe+3 + 6Cyanide- + 2H+ = SnFe(Cyanide)6- + 2H2O
log_k 53.54
delta_h 0 kJ
-gamma 0 0
# Id: 7901431
# log K source: Ba1987
# Delta H source:
#T and ionic strength: 0.00 25.0
NH4+ + Fe+2 + 6Cyanide- = NH4Fe(Cyanide)6-3
log_k 37.7
delta_h -354 kJ
-gamma 0 0
# Id: 4901431
# log K source: NIST46.4
# Delta H source: NIST46.4
#T and ionic strength: 0.00 25.0
Tl+ + Fe+2 + 6Cyanide- = TlFe(Cyanide)6-3
log_k 38.4
delta_h -365.5 kJ
-gamma 0 0
# Id: 8701432
# log K source: NIST46.4
# Delta H source: NIST46.4
#T and ionic strength: 0.00 25.0
Mg+2 + Fe+3 + 6Cyanide- = MgFe(Cyanide)6-
log_k 46.39
delta_h -290 kJ
```

```
-gamma 0 0
# Id: 4601431
# log K source: NIST46.4
# Delta H source: NIST46.4
#T and ionic strength: 0.00 25.0
Mg+2 + Fe+2 + 6Cyanide- = MgFe(Cyanide)6-2
log_k 39.21
delta_h -346 kJ
-gamma 0 0
# Id: 4601432
# log K source: NIST46.4
# Delta H source: NIST46.4
#T and ionic strength: 0.00 25.0
Ca+2 + Fe+3 + 6Cyanide- = CaFe(Cyanide)6-
log_k 46.43
delta_h -291 kJ
-gamma 0 0
# Id: 1501431
# log K source: NIST46.4
# Delta H source: NIST46.4
#T and ionic strength: 0.00 25.0
Ca+2 + Fe+2 + 6Cyanide- = CaFe(Cyanide)6-2
log_k 39.1
delta_h -347 kJ
-gamma 0 0
# Id: 1501432
# log K source: NIST46.4
# Delta H source: NIST46.4
#T and ionic strength: 0.00 25.0
2Ca+2 + Fe+2 + 6Cyanide- = Ca2Fe(Cyanide)6
log_k 40.6
delta_h -350.201 kJ
-gamma 0 0
# Id: 1501433
# log K source: NIST46.4
# Delta H source: MTQ3.11
#T and ionic strength: 0.00 25.0
Sr+2 + Fe+3 + 6Cyanide- = SrFe(Cyanide)6-
log_k 46.45
delta_h -292 kJ
-gamma 0 0
# Id: 8001431
# log K source: NIST46.4
# Delta H source: NIST46.4
#T and ionic strength: 0.00 25.0
Sr+2 + Fe+2 + 6Cyanide- = SrFe(Cyanide)6-2
log_k 39.1
delta_h -350 kJ
-gamma 0 0
# Id: 8001432
# log K source: NIST46.4
# Delta H source: NIST46.4
#T and ionic strength: 0.00 25.0
Ba+2 + Fe+2 + 6Cyanide- = BaFe(Cyanide)6-2
```

```
log_k 39.19
delta_h -342 kJ
-gamma 0 0
# Id: 1001430
# log K source: NIST46.4
# Delta H source: NIST46.4
#T and ionic strength: 0.00 25.0
Ba+2 + Fe+3 + 6Cyanide- = BaFe(Cyanide)6-
log_k 46.48
delta_h -292 kJ
-gamma 0 0
# Id: 1001431
# log K source: NIST46.4
# Delta H source: NIST46.4
#T and ionic strength: 0.00 25.0
Na+ + Fe+2 + 6Cyanide- = NaFe(Cyanide)6-3
log_k 37.6
delta_h -354 kJ
-gamma 0 0
# Id: 5001431
# log K source: NIST46.4
# Delta H source: NIST46.4
#T and ionic strength: 0.00 25.0
K+ + Fe+2 + 6Cyanide- = KFe(Cyanide)6-3
log_k 37.75
delta_h -353.9 kJ
-gamma 0 0
# Id: 4101433
# log K source: NIST46.4
# Delta H source: NIST46.4
#T and ionic strength: 0.00 25.0
K+ + Fe+3 + 6Cyanide- = KFe(Cyanide)6-2
log_k 45.04
delta_h -291 kJ
-gamma 0 0
# Id: 4101430
# log K source: NIST46.4
# Delta H source: NIST46.4
#T and ionic strength: 0.00 25.0
H+ + PO4-3 = HPO4-2
log_k 12.375
delta_h -15 kJ
-gamma 5 0
# Id: 3305800
# log K source: NIST46.3
# Delta H source: NIST46.3
#T and ionic strength: 0.00 25.0
2H+ + PO4-3 = H2PO4-
log_k 19.573
delta_h -18 kJ
-gamma 5.4 0
# Id: 3305801
# log K source: NIST46.3
# Delta H source: NIST46.3
```

```
#T and ionic strength: 0.00 25.0
3H+ + PO4-3 = H3PO4
log_k 21.721
delta_h -10.1 kJ
-gamma 0 0
# Id: 3305802
# log K source: NIST46.3
# Delta H source: NIST46.3
#T and ionic strength: 0.00 25.0
Co+2 + H+ + PO4-3 = CoHPO4
log_k 15.4128
delta_h 0 kJ
-gamma 0 0
# Id: 2005800
# log K source: NIST46.4
# Delta H source: MTQ3.11
#T and ionic strength: 0.10 25.0
Fe+2 + 2H+ + PO4-3 = FeH2PO4+
log_k 22.273
delta_h 0 kJ
-gamma 5.4 0
# Id: 2805800
# log K source: NIST46.3
# Delta H source: MTQ3.11
#T and ionic strength: 0.00 25.0
Fe+2 + H+ + PO4-3 = FeHPO4
log_k 15.975
delta_h 0 kJ
-gamma 0 0
# Id: 2805801
# log K source: NIST46.3
# Delta H source: MTQ3.11
#T and ionic strength: 0.00 25.0
Fe+3 + 2H+ + PO4-3 = FeH2PO4+2
log_k 23.8515
delta_h 0 kJ
-gamma 5.4 0
# Id: 2815801
# log K source: NIST46.3
# Delta H source: MTQ3.11
#T and ionic strength: 0.50 25.0
Fe+3 + H+ + PO4-3 = FeHPO4+
log_k 22.292
delta_h -30.5432 kJ
-gamma 5.4 0
# Id: 2815800
# log K source: NIST46.3
# Delta H source: MTQ3.11
#T and ionic strength: 0.50 25.0
Cr(OH)2+ + 4H+ + PO4-3 = CrH2PO4+2 + 2H2O
log_k 31.9068
delta_h 0 kJ
-gamma 0 0
# Id: 2115800
```

```
# log K source: MTQ3.11
# Delta H source: MTQ3.11
#T and ionic strength:
U+4 + PO4-3 + H+ = UHPO4+2
log_k 24.443
delta_h 31.38 kJ
-gamma 0 0
# Id: 8915800
# log K source: MTQ3.11
# Delta H source: MTQ3.11
#T and ionic strength:
U+4 + 2PO4-3 + 2H+ = U(HPO4)2
log_k 46.833
delta_h 7.1128 kJ
-gamma 0 0
# Id: 8915801
# log K source: MTQ3.11
# Delta H source: MTQ3.11
#T and ionic strength:
U+4 + 3PO4-3 + 3H+ = U(HPO4)3-2
log_k 67.564
delta_h -32.6352 kJ
-gamma 0 0
# Id: 8915802
# log K source: MTQ3.11
# Delta H source: MTQ3.11
#T and ionic strength:
U+4 + 4PO4-3 + 4H+ = U(HPO4)4-4
log_k 88.483
delta_h -110.876 kJ
-gamma 0 0
# Id: 8915803
# log K source: MTQ3.11
# Delta H source: MTQ3.11
#T and ionic strength:
UO2+2 + H+ + PO4-3 = UO2HPO4
log_k 19.655
delta_h -8.7864 kJ
-gamma 0 0
# Id: 8935800
# log K source: NIST46.3
# Delta H source: MTQ3.11
#T and ionic strength: 0.00 25.0
UO2+2 + 2PO4-3 + 2H+ = UO2(HPO4)2-2
log_k 42.988
delta_h -47.6934 kJ
-gamma 0 0
# Id: 8935801
# log K source: MTQ3.11
# Delta H source: MTQ3.11
#T and ionic strength:
UO2+2 + 2H+ + PO4-3 = UO2H2PO4+
log_k 22.833
delta_h -15.4808 kJ
```

```
-gamma 0 0
# Id: 8935802
# log K source: NIST46.3
# Delta H source: MTQ3.11
#T and ionic strength: 0.00 25.0
UO2+2 + 2PO4-3 + 4H+ = UO2(H2PO4)2
log_k 44.7
delta_h -69.036 kJ
-gamma 0 0
# Id: 8935803
# log K source: MTQ3.11
# Delta H source: MTQ3.11
#T and ionic strength:
UO2+2 + 3PO4-3 + 6H+ = UO2(H2PO4)3-
log_k 66.245
delta_h -119.662 kJ
-gamma 0 0
# Id: 8935804
# log K source: MTQ3.11
# Delta H source: MTQ3.11
#T and ionic strength:
UO2+2 + PO4-3 = UO2PO4-
log_k 13.25
delta_h 0 kJ
-gamma 0 0
# Id: 8935805
# log K source: NIST46.4
# Delta H source: MTQ3.11
#T and ionic strength: 0.00 25.0
Mg+2 + PO4-3 = MgPO4-
log_k 4.654
delta_h 12.9704 kJ
-gamma 5.4 0
# Id: 4605800
# log K source: SCD3.02 (1993 GMa)
# Delta H source: MTQ3.11
#T and ionic strength: 0.20 25.0
Mg+2 + 2H+ + PO4-3 = MgH2PO4+
log_k 21.2561
delta_h -4.6861 kJ
-gamma 5.4 0
# Id: 4605801
# log K source: NIST46.3
# Delta H source: MTQ3.11
#T and ionic strength: 0.00 37.0
Mg+2 + H+ + PO4-3 = MgHPO4
log_k 15.175
delta_h -3 kJ
-gamma 0 0
# Id: 4605802
# log K source: NIST46.3
# Delta H source: NIST46.3
#T and ionic strength: 0.00 25.0
Ca+2 + H+ + PO4-3 = CaHPO4
```

```
log_k 15.035
delta_h -3 kJ
-gamma 0 0
# Id: 1505800
# log K source: NIST46.3
# Delta H source: NIST46.3
#T and ionic strength: 0.00 25.0
Ca+2 + PO4-3 = CaPO4-
log_k 6.46
delta_h 12.9704 kJ
-gamma 5.4 0
# Id: 1505801
# log K source: SCD3.02 (1993 GMa)
# Delta H source: MTQ3.11
#T and ionic strength: 0.00 25.0
Ca+2 + 2H+ + PO4-3 = CaH2PO4+
log_k 20.923
delta_h -6 kJ
-gamma 5.4 0
# Id: 1505802
# log K source: NIST46.3
# Delta H source: NIST46.3
#T and ionic strength: 0.00 25.0
Sr+2 + H+ + PO4-3 = SrHPO4
log_k 14.8728
delta_h 0 kJ
-gamma 0 0
# Id: 8005800
# log K source: NIST46.4
# Delta H source: MTQ3.11
#T and ionic strength: 0.10 25.0
Sr+2 + 2H+ + PO4-3 = SrH2PO4+
log_k 20.4019
delta_h 0 kJ
-gamma 0 0
# Id: 8005801
# log K source: NIST46.4
# Delta H source: MTQ3.11
#T and ionic strength: 0.10 20.0
Na+ + H+ + PO4-3 = NaHPO4-
log_k 13.445
delta_h 0 kJ
-gamma 5.4 0
# Id: 5005800
# log K source: NIST46.3
# Delta H source: MTQ3.11
#T and ionic strength: 0.00 25.0
K+ + H+ + PO4-3 = KHPO4-
log_k 13.255
delta_h 0 kJ
-gamma 5.4 0
# Id: 4105800
# log K source: NIST46.3
# Delta H source: MTQ3.11
```

```
#T and ionic strength: 0.00 25.0
H3AsO3 = AsO3-3 + 3H+
log_k -34.744
delta_h 84.726 kJ
-gamma 0 0
# Id: 3300602
# log K source: MTQ3.11
# Delta H source: MTQ3.11
#T and ionic strength:
H3AsO3 = HAsO3-2 + 2H+
log_k -21.33
delta_h 59.4086 kJ
-gamma 0 0
# Id: 3300601
# log K source: MTQ3.11
# Delta H source: MTQ3.11
#T and ionic strength:
H3AsO3 = H2AsO3- + H+
log_k -9.29
delta_h 27.41 kJ
-gamma 0 0
# Id: 3300600
# log K source: NIST46.4
# Delta H source: NIST2.1.1
#T and ionic strength: 0.00 25.0
H3AsO3 + H+ = H4AsO3+
log_k -0.305
delta_h 0 kJ
-gamma 0 0
# Id: 3300603
# log K source: MTQ3.11
# Delta H source: MTQ3.11
#T and ionic strength:
H3AsO4 = AsO4-3 + 3H+
log_k -20.7
delta_h 12.9 kJ
-gamma 0 0
# Id: 3300613
# log K source: NIST46.4
# Delta H source: NIST46.4
#T and ionic strength: 0.00 25.0
H3AsO4 = HAsO4-2 + 2H+
log_k -9.2
delta_h -4.1 kJ
-gamma 0 0
# Id: 3300612
# log K source: NIST46.4
# Delta H source: NIST46.4
#T and ionic strength: 0.00 25.0
H3AsO4 = H2AsO4- + H+
log_k -2.24
delta_h -7.1 kJ
-gamma 0 0
# Id: 3300611
```

```
# log K source: NIST46.4
# Delta H source: NIST46.4
#T and ionic strength: 0.00 25.0
Sb(OH)3 + H2O = Sb(OH)4- + H+
log_k -12.0429
delta_h 69.8519 kJ
-gamma 0 0
# Id: 7400020
# log K source: PNL89
# Delta H source: PNL89
#T and ionic strength:
Sb(OH)3 + H+ = Sb(OH)2+ + H2O
log_k 1.3853
delta_h 0 kJ
-gamma 0 0
# Id: 7403302
# log K source: PNL89
# Delta H source: PNL89
#T and ionic strength:
Sb(OH)3 = HSbO2 + H2O
log_k -0.0105
delta_h -0.13 kJ
-gamma 0 0
# Id: 7400021
# log K source: NIST2.1.1
# Delta H source: NIST2.1.1
#T and ionic strength:
Sb(OH)3 = SbO2- + H2O + H+
log_k -11.8011
delta_h 70.1866 kJ
-gamma 0 0
# Id: 7403301
# log K source: PNL89
# Delta H source: PNL89
#T and ionic strength:
Sb(OH)3 + H+ = SbO+ + 2H2O
log_k 0.9228
delta_h 8.2425 kJ
-gamma 0 0
# Id: 7403300
# log K source: PNL89
# Delta H source: PNL89
#T and ionic strength:
Sb(OH)6- = SbO3- + 3H2O
log_k 2.9319
delta_h 0 kJ
-gamma 0 0
# Id: 7410021
# log K source: PNL89
# Delta H source: PNL89
#T and ionic strength:
Sb(OH)6- + 2H+ = SbO2+ + 4H2O
log_k 2.3895
delta_h 0 kJ
```

```
-gamma 0 0
# Id: 7413300
# log K source: PNL89
# Delta H source: PNL89
#T and ionic strength:
H+ + CO3-2 = HCO3-
log_k 10.329
delta_h -14.6 kJ
-gamma 5.4 0
# Id: 3301400
# log K source: NIST46.4
# Delta H source: NIST46.4
#T and ionic strength: 0.00 25.0
2H+ + CO3-2 = H2CO3
log_k 16.681
delta_h -23.76 kJ
-gamma 0 0
# Id: 3301401
# log K source: NIST46.4
# Delta H source: NIST46.4
#T and ionic strength: 0.00 25.0
Pb+2 + 2CO3-2 = Pb(CO3)2-2
log_k 9.938
delta_h 0 kJ
-gamma 0 0
# Id: 6001400
# log K source: NIST46.3
# Delta H source: MTQ3.11
#T and ionic strength: 0.50 25.0
Pb+2 + CO3-2 = PbCO3
log_k 6.478
delta_h 0 kJ
-gamma 0 0
# Id: 6001401
# log K source: NIST46.3
# Delta H source: MTQ3.11
#T and ionic strength: 0.50 25.0
Pb+2 + CO3-2 + H+ = PbHCO3+
log_k 13.2
delta_h 0 kJ
-gamma 0 0
# Id: 6001402
# log K source: MTQ3.11
# Delta H source: MTQ3.11
#T and ionic strength:
Zn+2 + CO3-2 = ZnCO3
log_k 4.76
delta_h 0 kJ
-gamma 0 0
# Id: 9501401
# log K source: NIST46.4
# Delta H source: MTQ3.11
#T and ionic strength: 0.00 25.0
Zn+2 + H+ + CO3-2 = ZnHCO3+
```

```
log_k 11.829
delta_h 0 kJ
-gamma 0 0
# Id: 9501400
# log K source: NIST46.4
# Delta H source: MTQ3.11
#T and ionic strength: 0.00 25.0
Hg(OH)2 + 2H+ + CO3-2 = HgCO3 + 2H2O
log_k 18.272
delta_h 0 kJ
-gamma 0 0
# Id: 3611401
# log K source: NIST46.4
# Delta H source: MTQ3.11
#T and ionic strength: 0.50 25.0
Hg(OH)2 + 2H+ + 2CO3-2 = Hg(CO3)2-2 + 2H2O
log_k 21.772
delta_h 0 kJ
-gamma 0 0
# Id: 3611402
# log K source: NIST46.4
# Delta H source: MTQ3.11
#T and ionic strength: 0.50 25.0
Hg(OH)2 + 3H+ + CO3-2 = HgHCO3+ + 2H2O
log_k 22.542
delta_h 0 kJ
-gamma 0 0
# Id: 3611403
# log K source: NIST46.4
# Delta H source: MTQ3.11
#T and ionic strength: 0.50 25.0
Cd+2 + CO3-2 = CdCO3
log_k 4.3578
delta_h 0 kJ
-gamma 0 0
# Id: 1601401
# log K source: NIST46.4
# Delta H source: MTQ3.11
#T and ionic strength: 0.10 25.0
Cd+2 + H+ + CO3-2 = CdHCO3+
log_k 10.6863
delta_h 0 kJ
-gamma 0 0
# Id: 1601400
# log K source: NIST46.4
# Delta H source: MTQ3.11
#T and ionic strength: 3.00 25.0
Cd+2 + 2CO3-2 = Cd(CO3)2-2
log_k 7.2278
delta_h 0 kJ
-gamma 0 0
# Id: 1601403
# log K source: NIST46.4
# Delta H source: MTQ3.11
```

```
#T and ionic strength: 0.10 20.0
Cu+2 + CO3-2 = CuCO3
log_k 6.77
delta_h 0 kJ
-gamma 0 0
# Id: 2311400
# log K source: NIST46.4
# Delta H source: MTQ3.11
#T and ionic strength: 0.00 25.0
Cu+2 + H+ + CO3-2 = CuHCO3+
log_k 12.129
delta_h 0 kJ
-gamma 0 0
# Id: 2311402
# log K source: NIST46.4
# Delta H source: MTQ3.11
#T and ionic strength: 0.00 25.0
Cu+2 + 2CO3-2 = Cu(CO3)2-2
log_k 10.2
delta_h 0 kJ
-gamma 0 0
# Id: 2311401
# log K source: NIST46.4
# Delta H source: MTQ3.11
#T and ionic strength: 0.00 25.0
Ni+2 + CO3-2 = NiCO3
log_k 4.5718
delta_h 0 kJ
-gamma 0 0
# Id: 5401401
# log K source: NIST46.3
# Delta H source: MTQ3.11
#T and ionic strength: 0.70 25.0
Ni+2 + H+ + CO3-2 = NiHCO3+
log_k 12.4199
delta_h 0 kJ
-gamma 0 0
# Id: 5401400
# log K source: NIST46.3
# Delta H source: MTQ3.11
#T and ionic strength: 0.70 25.0
Co+2 + CO3-2 = CoCO3
log_k 4.228
delta_h 0 kJ
-gamma 0 0
# Id: 2001400
# log K source: NIST46.4
# Delta H source: MTQ3.11
#T and ionic strength: 0.50 25.0
Co+2 + H+ + CO3-2 = CoHCO3+
log_k 12.2199
delta_h 0 kJ
-gamma 0 0
# Id: 2001401
```

```
# log K source: NIST46.4
# Delta H source: MTQ3.11
#T and ionic strength: 0.70 25.0
Fe+2 + H+ + CO3-2 = FeHCO3+
log_k 11.429
delta_h 0 kJ
-gamma 6 0
# Id: 2801400
# log K source: NIST46.4
# Delta H source: MTQ3.11
#T and ionic strength: 0.00 25.0
Mn+2 + H+ + CO3-2 = MnHCO3+
log_k 11.629
delta_h -10.6 kJ
-gamma 5 0
# Id: 4701400
# log K source: NIST46.4
# Delta H source: NIST46.4
#T and ionic strength: 0.00 25.0
UO2+2 + CO3-2 = UO2CO3
log_k 9.6
delta_h 4 kJ
-gamma 0 0
# Id: 8931400
# log K source: NIST46.3
# Delta H source: NIST46.3
#T and ionic strength: 0.00 25.0
UO2+2 + 2CO3-2 = UO2(CO3)2-2
log_k 16.9
delta_h 16 kJ
-gamma 0 0
# Id: 8931401
# log K source: NIST46.3
# Delta H source: NIST46.3
#T and ionic strength: 0.00 25.0
UO2+2 + 3CO3-2 = UO2(CO3)3-4
log_k 21.6
delta_h -40 kJ
-gamma 0 0
# Id: 8931402
# log K source: NIST46.3
# Delta H source: NIST46.3
#T and ionic strength: 0.00 25.0
Be+2 + CO3-2 = BeCO3
log_k 6.2546
delta_h 0 kJ
-gamma 0 0
# Id: 1101401
# log K source: NIST46.4
# Delta H source: MTQ3.11
#T and ionic strength: 3.00 25.0
Mg+2 + CO3-2 = MgCO3
log_k 2.92
delta_h 12 kJ
```

```
-gamma 0 0
# Id: 4601400
# log K source: NIST46.3
# Delta H source: NIST46.3
#T and ionic strength: 0.00 25.0
Mg+2 + H+ + CO3-2 = MgHCO3+
log_k 11.339
delta_h -10.6 kJ
-gamma 4 0
# Id: 4601401
# log K source: NIST46.3
# Delta H source: NIST46.3
#T and ionic strength: 0.00 25.0
Ca+2 + H+ + CO3-2 = CaHCO3+
log_k 11.599
delta_h 5.4 kJ
-gamma 6 0
# Id: 1501400
# log K source: NIST46.3
# Delta H source: NIST46.3
#T and ionic strength: 0.00 25.0
CO3-2 + Ca+2 = CaCO3
log_k 3.2
delta_h 16 kJ
-gamma 0 0
# Id: 1501401
# log K source: NIST46.3
# Delta H source: NIST46.3
#T and ionic strength: 0.00 25.0
Sr+2 + CO3-2 = SrCO3
log_k 2.81
delta_h 20 kJ
-gamma 0 0
# Id: 8001401
# log K source: NIST46.4
# Delta H source: NIST46.4
#T and ionic strength: 0.00 25.0
Sr+2 + H+ + CO3-2 = SrHCO3+
log_k 11.539
delta_h 10.4 kJ
-gamma 6 0
# Id: 8001400
# log K source: NIST46.4
# Delta H source: NIST46.4
#T and ionic strength: 0.00 25.0
Ba+2 + CO3-2 = BaCO3
log_k 2.71
delta_h 16 kJ
-gamma 0 0
# Id: 1001401
# log K source: NIST46.4
# Delta H source: NIST46.4
#T and ionic strength: 0.00 25.0
Ba+2 + H+ + CO3-2 = BaHCO3+
```

```
log_k 11.309
delta_h 10.4 kJ
-gamma 6 0
# Id: 1001400
# log K source: NIST46.4
# Delta H source: NIST46.4
#T and ionic strength: 0.00 25.0
Na+ + CO3-2 = NaCO3-
log_k 1.27
delta_h -20.35 kJ
-gamma 5.4 0
# Id: 5001400
# log K source: NIST46.3
# Delta H source: NIST2.1.1
#T and ionic strength: 0.00 25.0
Na+ + H+ + CO3-2 = NaHCO3
log_k 10.079
delta_h -28.3301 kJ
-gamma 0 0
# Id: 5001401
# log K source: NIST46.3
# Delta H source: NIST2.1.1
#T and ionic strength: 0.00 25.0
H4SiO4 = H2SiO4-2 + 2H+
log_k -23.04
delta_h 61 kJ
-gamma 5.4 0
# Id: 3307701
# log K source: NIST46.4
# Delta H source: NIST46.4
#T and ionic strength: 0.00 25.0
H4SiO4 = H3SiO4- + H+
log_k -9.84
delta_h 20 kJ
-gamma 4 0
# Id: 3307700
# log K source: NIST46.4
# Delta H source: NIST46.4
#T and ionic strength: 0.00 25.0
UO2+2 + H4SiO4 = UO2H3SiO4+ + H+
log_k -1.9111
delta_h 0 kJ
-gamma 0 0
# Id: 8937700
# log K source: NIST46.4
# Delta H source: MTQ3.11
#T and ionic strength: 0.10 25.0
H3BO3 = H2BO3- + H+
log_k -9.236
delta_h 13 kJ
-gamma 2.5 0
# Id: 3300900
# log K source: NIST46.4
# Delta H source: NIST46.4
```

```
#T and ionic strength: 0.00 25.0
2H3BO3 = H5(BO3)2- + H+
log_k -9.306
delta_h 8.4 kJ
-gamma 2.5 0
# Id: 3300901
# log K source: NIST46.4
# Delta H source: NIST46.4
#T and ionic strength: 0.00 25.0
3H3BO3 = H8(BO3)3- + H+
log_k -7.306
delta_h 29.4 kJ
-gamma 2.5 0
# Id: 3300902
# log K source: NIST46.4
# Delta H source: NIST46.4
#T and ionic strength: 0.00 25.0
Ag+ + H3BO3 = AgH2BO3 + H+
log_k -8.036
delta_h 0 kJ
-gamma 2.5 0
# Id: 200901
# log K source: NIST46.4
# Delta H source: MTQ3.11
#T and ionic strength: 0.00 25.0
Mg+2 + H3BO3 = MgH2BO3+ + H+
log_k -7.696
delta_h 13 kJ
-gamma 2.5 0
# Id: 4600901
# log K source: NIST46.4
# Delta H source: NIST46.4
#T and ionic strength: 0.00 25.0
Ca+2 + H3BO3 = CaH2BO3+ + H+
log_k -7.476
delta_h 17 kJ
-gamma 2.5 0
# Id: 1500901
# log K source: NIST46.4
# Delta H source: NIST46.4
#T and ionic strength: 0.00 25.0
Sr+2 + H3BO3 = SrH2BO3+ + H+
log_k -7.686
delta_h 17 kJ
-gamma 2.5 0
# Id: 8000901
# log K source: NIST46.4
# Delta H source: NIST46.4
#T and ionic strength: 0.00 25.0
Ba+2 + H3BO3 = BaH2BO3+ + H+
log_k -7.746
delta_h 17 kJ
-gamma 2.5 0
# Id: 1000901
```

```
# log K source: NIST46.4
# Delta H source: NIST46.4
#T and ionic strength: 0.00 25.0
Na+ + H3BO3 = NaH2BO3 + H+
log_k -9.036
delta_h 0 kJ
-gamma 2.5 0
# Id: 5000901
# log K source: NIST46.4
# Delta H source: MTQ3.11
#T and ionic strength: 0.00 25.0
CrO4-2 + H+ = HCrO4-
log_k 6.51
delta_h 2 kJ
-gamma 0 0
# Id: 2123300
# log K source: NIST46.4
# Delta H source: NIST46.4
#T and ionic strength: 0.00 25.0
CrO4-2 + 2H+ = H2CrO4
log_k 6.4188
delta_h 39 kJ
-gamma 0 0
# Id: 2123301
# log K source: NIST46.4
# Delta H source: NIST46.4
#T and ionic strength: 0.00 20.0
2CrO4-2 + 2H+ = Cr2O7-2 + H2O
log_k 14.56
delta_h -15 kJ
-gamma 0 0
# Id: 2123302
# log K source: NIST46.4
# Delta H source: NIST46.4
#T and ionic strength: 0.00 25.0
CrO4-2 + Cl- + 2H+ = CrO3Cl- + H2O
log_k 7.3086
delta_h 0 kJ
-gamma 0 0
# Id: 2121800
# log K source: MTQ3.11
# Delta H source: MTQ3.11
#T and ionic strength:
CrO4-2 + SO4-2 + 2H+ = CrO3SO4-2 + H2O
log_k 8.9937
delta_h 0 kJ
-gamma 0 0
# Id: 2127320
# log K source: MTQ3.11
# Delta H source: MTQ3.11
#T and ionic strength:
CrO4-2 + 4H+ + PO4-3 = CrO3H2PO4- + H2O
log_k 29.3634
delta_h 0 kJ
```

```
-gamma 0 0
# Id: 2125800
# log K source: MTQ3.11
# Delta H source: MTQ3.11
#T and ionic strength:
CrO4-2 + 3H+ + PO4-3 = CrO3HPO4-2 + H2O
log_k 26.6806
delta_h 0 kJ
-gamma 0 0
# Id: 2125801
# log K source: MTQ3.11
# Delta H source: MTQ3.11
#T and ionic strength:
CrO4-2 + Na+ = NaCrO4-
log_k 0.6963
delta_h 0 kJ
-gamma 0 0
# Id: 5002120
# log K source: MTQ3.11
# Delta H source: MTQ3.11
#T and ionic strength:
K+ + CrO4-2 = KCrO4-
log_k 0.57
delta_h 0 kJ
-gamma 0 0
# Id: 4102120
# log K source: NIST46.4
# Delta H source: MTQ3.11
#T and ionic strength: 0.00 18.0
MoO4-2 + H+ = HMoO4-
log_k 4.2988
delta_h 20 kJ
-gamma 0 0
# Id: 3304801
# log K source: NIST46.4
# Delta H source: NIST46.4
#T and ionic strength: 0.00 20.0
MoO4-2 + 2H+ = H2MoO4
log_k 8.1636
delta_h -26 kJ
-gamma 0 0
# Id: 3304802
# log K source: NIST46.4
# Delta H source: NIST46.4
#T and ionic strength: 0.00 20.0
7MoO4-2 + 8H+ = Mo7O24-6 + 4H2O
log_k 52.99
delta_h -228 kJ
-gamma 0 0
# Id: 3304803
# log K source: NIST46.4
# Delta H source: NIST46.4
#T and ionic strength: 0.10 25.0
7MoO4-2 + 9H+ = HMo7O24-5 + 4H2O
```

```
log_k 59.3768
delta_h -218 kJ
-gamma 0 0
# Id: 3304804
# log K source: NIST46.4
# Delta H source: NIST46.4
#T and ionic strength: 0.10 25.0
7MoO4-2 + 10H+ = H2Mo7O24-4 + 4H2O
log_k 64.159
delta_h -215 kJ
-gamma 0 0
# Id: 3304805
# log K source: NIST46.4
# Delta H source: NIST46.4
#T and ionic strength: 0.10 25.0
7MoO4-2 + 11H+ = H3Mo7O24-3 + 4H2O
log_k 67.405
delta_h -217 kJ
-gamma 0 0
# Id: 3304806
# log K source: NIST46.4
# Delta H source: NIST46.4
#T and ionic strength: 1.00 25.0
6MoO4-2 + Al+3 + 6H+ = AlMo6O21-3 + 3H2O
log_k 54.9925
delta_h 0 kJ
-gamma 0 0
# Id: 304801
# log K source: NIST46.4
# Delta H source: MTQ3.11
#T and ionic strength: 0.50 25.0
MoO4-2 + 2Ag+ = Ag2MoO4
log_k -0.4219
delta_h -1.18 kJ
-gamma 0 0
# Id: 204801
# log K source: Bard85
# Delta H source: Bard85
#T and ionic strength:
VO2+ + 2H2O = VO4-3 + 4H+
log_k -30.2
delta_h -25 kJ
-gamma 0 0
# Id: 9033303
# log K source: NIST46.4
# Delta H source: NIST46.4
#T and ionic strength: 0.00 25.0
VO2+ + 2H2O = HVO4-2 + 3H+
log_k -15.9
delta_h 0 kJ
-gamma 0 0
# Id: 9033302
# log K source: NIST46.3
# Delta H source: NIST46.3
```

```
#T and ionic strength: 0.00 25.0
VO2+ + 2H2O = H2VO4- + 2H+
log_k -7.3
delta_h 0 kJ
-gamma 0 0
# Id: 9033301
# log K source: NIST46.3
# Delta H source: NIST46.3
#T and ionic strength: 0.00 25.0
VO2+ + 2H2O = H3VO4 + H+
log_k -3.3
delta_h 44.4759 kJ
-gamma 0 0
# Id: 9033300
# log K source: MTQ3.11
# Delta H source: MTQ3.11
#T and ionic strength:
2VO2+ + 3H2O = V2O7-4 + 6H+
log_k -31.24
delta_h -28 kJ
-gamma 0 0
# Id: 9030020
# log K source: NIST46.3
# Delta H source: NIST46.3
#T and ionic strength: 0.00 25.0
2VO2+ + 3H2O = HV2O7-3 + 5H+
log_k -20.67
delta_h 0 kJ
-gamma 0 0
# Id: 9030021
# log K source: NIST46.3
# Delta H source: MTQ3.11
#T and ionic strength: 0.00 25.0
2VO2+ + 3H2O = H3V2O7- + 3H+
log_k -3.79
delta_h 0 kJ
-gamma 0 0
# Id: 9030022
# log K source: MTQ3.11
# Delta H source: MTQ3.11
#T and ionic strength:
3VO2+ + 3H2O = V3O9-3 + 6H+
log_k -15.88
delta_h 0 kJ
-gamma 0 0
# Id: 9030023
# log K source: MTQ3.11
# Delta H source: MTQ3.11
#T and ionic strength:
4VO2+ + 4H2O = V4O12-4 + 8H+
log_k -20.56
delta_h -87 kJ
-gamma 0 0
# Id: 9030024
```

```
# log K source: NIST46.3
# Delta H source: NIST46.3
#T and ionic strength: 0.00 25.0
10VO2+ + 8H2O = V10O28-6 + 16H+
log_k -24.0943
delta_h 0 kJ
-gamma 0 0
# Id: 9030025
# log K source: NIST46.4
# Delta H source: MTQ3.11
#T and ionic strength: 0.10 20.0
10VO2+ + 8H2O = HV10O28-5 + 15H+
log_k -15.9076
delta_h 90.0397 kJ
-gamma 0 0
# Id: 9030026
# log K source: NIST46.4
# Delta H source: MTQ3.11
#T and ionic strength: 0.10 20.0
10VO2+ + 8H2O = H2V10O28-4 + 14H+
log_k -10.7
delta_h 0 kJ
-gamma 0 0
# Id: 9030027
# log K source: NIST46.3
# Delta H source: MTQ3.11
#T and ionic strength: 0.00 25.0
Benzoate- + H+ = H(Benzoate)
log_k 4.202
delta_h -0.4602 kJ
-gamma 0 0
# Id: 3309171
# log K source: NIST46.2
# Delta H source: NIST46.2
#T and ionic strength:
Benzoate- + Pb+2 = Pb(Benzoate)+
log_k 2.4
delta_h 0 kJ
-gamma 0 0
# Id: 6009171
# log K source: NIST46.2
# Delta H source: NIST46.2
#T and ionic strength:
Benzoate- + Al+3 = Al(Benzoate)+2
log_k 2.05
delta_h 0 kJ
-gamma 0 0
# Id: 309171
# log K source: NIST46.2
# Delta H source: NIST46.2
#T and ionic strength:
Benzoate- + Al+3 + H2O = AlOH(Benzoate)+ + H+
log_k -0.56
delta_h 0 kJ
```

```
-gamma 0 0
# Id: 309172
# log K source: NIST46.2
# Delta H source: NIST46.2
#T and ionic strength:
Benzoate- + Zn+2 = Zn(Benzoate)+
log_k 1.7
delta_h 0 kJ
-gamma 0 0
# Id: 9509171
# log K source: SCD2.62
# Delta H source: SCD2.62
#T and ionic strength:
Benzoate- + Cd+2 = Cd(Benzoate)+
log_k 1.8
delta_h 0 kJ
-gamma 0 0
# Id: 1609171
# log K source: NIST46.2
# Delta H source: NIST46.2
#T and ionic strength:
2Benzoate- + Cd+2 = Cd(Benzoate)2
log_k 1.82
delta_h 0 kJ
-gamma 0 0
# Id: 1609172
# log K source: SCD2.62
# Delta H source: SCD2.62
#T and ionic strength:
Benzoate- + Cu+2 = Cu(Benzoate)+
log_k 2.19
delta_h 0 kJ
-gamma 0 0
# Id: 2319171
# log K source: NIST46.2
# Delta H source: NIST46.2
#T and ionic strength:
Benzoate- + Ag+ = Ag(Benzoate)
log_k 0.91
delta_h 0 kJ
-gamma 0 0
# Id: 209171
# log K source: NIST46.2
# Delta H source: NIST46.2
#T and ionic strength:
Benzoate- + Ni+2 = Ni(Benzoate)+
log_k 1.86
delta_h 0 kJ
-gamma 0 0
# Id: 5409171
# log K source: SCD2.62
# Delta H source: SCD2.62
#T and ionic strength:
Co+2 + Benzoate- = Co(Benzoate)+
```

```
log_k 1.0537
delta_h 12 kJ
-gamma 0 0
# Id: 2009171
# log K source: NIST46.4
# Delta H source: NIST46.4
#T and ionic strength: 0.50 30.0
Benzoate- + Mn+2 = Mn(Benzoate)+
log_k 2.06
delta_h 0 kJ
-gamma 0 0
# Id: 4709171
# log K source: NIST46.2
# Delta H source: NIST46.2
#T and ionic strength:
Benzoate- + Mg+2 = Mg(Benzoate)+
log_k 1.26
delta_h 0 kJ
-gamma 0 0
# Id: 4609171
# log K source: SCD2.62
# Delta H source: SCD2.62
#T and ionic strength:
Benzoate- + Ca+2 = Ca(Benzoate)+
log_k 1.55
delta_h 0 kJ
-gamma 0 0
# Id: 1509171
# log K source: SCD2.62
# Delta H source: SCD2.62
#T and ionic strength:
Phenylacetate- + H+ = H(Phenylacetate)
log_k 4.31
delta_h 2.1757 kJ
-gamma 0 0
# Id: 3309181
# log K source: NIST46.2
# Delta H source: NIST46.2
#T and ionic strength:
Phenylacetate- + Zn+2 = Zn(Phenylacetate)+
log_k 1.57
delta_h 0 kJ
-gamma 0 0
# Id: 9509181
# log K source: NIST46.2
# Delta H source: NIST46.2
#T and ionic strength:
Phenylacetate- + Cu+2 = Cu(Phenylacetate)+
log_k 1.97
delta_h 0 kJ
-gamma 0 0
# Id: 2319181
# log K source: NIST46.2
# Delta H source: NIST46.2
```

```
#T and ionic strength:
Co+2 + Phenylacetate- = Co(Phenylacetate)+
log_k 0.591
delta_h 0 kJ
-gamma 0 0
# Id: 2009181
# log K source: NIST46.4
# Delta H source: NIST46.2
#T and ionic strength: 2.00 25.0
Co+2 + 2Phenylacetate- = Co(Phenylacetate)2
log_k 0.4765
delta_h 0 kJ
-gamma 0 0
# Id: 2009182
# log K source: NIST46.4
# Delta H source: NIST46.2
#T and ionic strength: 2.00 25.0
Isophthalate-2 + H+ = H(Isophthalate)-
log_k 4.5
delta_h 1.6736 kJ
-gamma 0 0
# Id: 3309201
# log K source: NIST46.2
# Delta H source: NIST46.2
#T and ionic strength:
Isophthalate-2 + 2H+ = H2(Isophthalate)
log_k 8
delta_h 1.6736 kJ
-gamma 0 0
# Id: 3309202
# log K source: NIST46.2
# Delta H source: NIST46.2
#T and ionic strength:
Isophthalate-2 + Pb+2 = Pb(Isophthalate)
log_k 2.99
delta_h 0 kJ
-gamma 0 0
# Id: 6009201
# log K source: NIST46.2
# Delta H source: NIST46.2
#T and ionic strength:
2Isophthalate-2 + Pb+2 = Pb(Isophthalate)2-2
log_k 4.18
delta_h 0 kJ
-gamma 0 0
# Id: 6009202
# log K source: NIST46.2
# Delta H source: NIST46.2
#T and ionic strength:
Isophthalate-2 + Pb+2 + H+ = PbH(Isophthalate)+
log_k 6.69
delta_h 0 kJ
-gamma 0 0
# Id: 6009203
```

```
# log K source: NIST46.2
# Delta H source: NIST46.2
#T and ionic strength:
Isophthalate-2 + Cd+2 = Cd(Isophthalate)
log_k 2.15
delta_h 0 kJ
-gamma 0 0
# Id: 1609201
# log K source: NIST46.2
# Delta H source: NIST46.2
#T and ionic strength:
2Isophthalate-2 + Cd+2 = Cd(Isophthalate)2-2
log_k 2.99
delta_h 0 kJ
-gamma 0 0
# Id: 1609202
# log K source: NIST46.2
# Delta H source: NIST46.2
#T and ionic strength:
Isophthalate-2 + Cd+2 + H+ = CdH(Isophthalate)+
log_k 5.73
delta_h 0 kJ
-gamma 0 0
# Id: 1609203
# log K source: NIST46.2
# Delta H source: NIST46.2
#T and ionic strength:
Isophthalate-2 + Ca+2 = Ca(Isophthalate)
log_k 2
delta_h 0 kJ
-gamma 0 0
# Id: 1509200
# log K source: NIST46.2
# Delta H source: NIST46.2
#T and ionic strength:
Isophthalate-2 + Ba+2 = Ba(Isophthalate)
log_k 1.55
delta_h 0 kJ
-gamma 0 0
# Id: 1009201
# log K source: NIST46.2
# Delta H source: NIST46.2
#T and ionic strength:
H+ + Diethylamine = H(Diethylamine)+
log_k 10.933
delta_h -53.1368 kJ
-gamma 0 0
# Id: 3309551
# log K source: NIST46.2
# Delta H source: NIST46.2
#T and ionic strength:
Zn+2 + Diethylamine = Zn(Diethylamine)+2
log_k 2.74
delta_h 0 kJ
```

```
-gamma 0 0
# Id: 9509551
# log K source: SCD2.62
# Delta H source: SCD2.62
#T and ionic strength:
Zn+2 + 2Diethylamine = Zn(Diethylamine)2+2
log_k 5.27
delta_h 0 kJ
-gamma 0 0
# Id: 9509552
# log K source: SCD2.62
# Delta H source: SCD2.62
#T and ionic strength:
Zn+2 + 3Diethylamine = Zn(Diethylamine)3+2
log_k 7.71
delta_h 0 kJ
-gamma 0 0
# Id: 9509553
# log K source: SCD2.62
# Delta H source: SCD2.62
#T and ionic strength:
Zn+2 + 4Diethylamine = Zn(Diethylamine)4+2
log_k 9.84
delta_h 0 kJ
-gamma 0 0
# Id: 9509554
# log K source: SCD2.62
# Delta H source: SCD2.62
#T and ionic strength:
Cd+2 + Diethylamine = Cd(Diethylamine)+2
log_k 2.73
delta_h 0 kJ
-gamma 0 0
# Id: 1609551
# log K source: SCD2.62
# Delta H source: SCD2.62
#T and ionic strength:
Cd+2 + 2Diethylamine = Cd(Diethylamine)2+2
log_k 4.86
delta_h 0 kJ
-gamma 0 0
# Id: 1609552
# log K source: SCD2.62
# Delta H source: SCD2.62
#T and ionic strength:
Cd+2 + 3Diethylamine = Cd(Diethylamine)3+2
log_k 6.37
delta_h 0 kJ
-gamma 0 0
# Id: 1609553
# log K source: SCD2.62
# Delta H source: SCD2.62
#T and ionic strength:
Cd+2 + 4Diethylamine = Cd(Diethylamine)4+2
```

```
log_k 7.32
delta_h 0 kJ
-gamma 0 0
# Id: 1609554
# log K source: SCD2.62
# Delta H source: SCD2.62
#T and ionic strength:
Ag+ + Diethylamine = Ag(Diethylamine)+
log_k 2.98
delta_h 0 kJ
-gamma 0 0
# Id: 209551
# log K source: NIST46.2
# Delta H source: NIST46.2
#T and ionic strength:
Ag+ + 2Diethylamine = Ag(Diethylamine)2+
log_k 6.38
delta_h -44.7688 kJ
-gamma 0 0
# Id: 209552
# log K source: NIST46.2
# Delta H source: NIST46.2
#T and ionic strength:
Ni+2 + Diethylamine = Ni(Diethylamine)+2
log_k 2.78
delta_h 0 kJ
-gamma 0 0
# Id: 5409551
# log K source: SCD2.62
# Delta H source: SCD2.62
#T and ionic strength:
Ni+2 + 2Diethylamine = Ni(Diethylamine)2+2
log_k 4.97
delta_h 0 kJ
-gamma 0 0
# Id: 5409552
# log K source: SCD2.62
# Delta H source: SCD2.62
#T and ionic strength:
Ni+2 + 3Diethylamine = Ni(Diethylamine)3+2
log_k 6.72
delta_h 0 kJ
-gamma 0 0
# Id: 5409553
# log K source: SCD2.62
# Delta H source: SCD2.62
#T and ionic strength:
Ni+2 + 4Diethylamine = Ni(Diethylamine)4+2
log_k 7.93
delta_h 0 kJ
-gamma 0 0
# Id: 5409554
# log K source: SCD2.62
# Delta H source: SCD2.62
```

```
#T and ionic strength:
Ni+2 + 5Diethylamine = Ni(Diethylamine)5+2
log_k 8.87
delta_h 0 kJ
-gamma 0 0
# Id: 5409555
# log K source: SCD2.62
# Delta H source: SCD2.62
#T and ionic strength:
H+ + Butylamine = H(Butylamine)+
log_k 10.64
delta_h -58.2831 kJ
-gamma 0 0
# Id: 3309561
# log K source: NIST46.2
# Delta H source: NIST46.2
#T and ionic strength:
Hg(OH)2 + Butylamine + 2H+ = Hg(Butylamine)+2 + 2H2O
log_k 14.84
delta_h 0 kJ
-gamma 0 0
# Id: 3619561
# log K source: NIST46.2
# Delta H source: NIST46.2
#T and ionic strength:
Hg(OH)2 + 2Butylamine + 2H+ = Hg(Butylamine)2+2 + 2H2O
log_k 24.24
delta_h 0 kJ
-gamma 0 0
# Id: 3619562
# log K source: NIST46.2
# Delta H source: NIST46.2
#T and ionic strength:
Hg(OH)2 + 3Butylamine + 2H+ = Hg(Butylamine)3+2 + 2H2O
log_k 25.1
delta_h 0 kJ
-gamma 0 0
# Id: 3619563
# log K source: NIST46.2
# Delta H source: NIST46.2
#T and ionic strength:
Hg(OH)2 + 4Butylamine + 2H+ = Hg(Butylamine)4+2 + 2H2O
log_k 26.1
delta_h 0 kJ
-gamma 0 0
# Id: 3619564
# log K source: NIST46.2
# Delta H source: NIST46.2
#T and ionic strength:
Ag+ + Butylamine = Ag(Butylamine)+
log_k 3.42
delta_h -16.736 kJ
-gamma 0 0
# Id: 209561
```

```
# log K source: NIST46.2
# Delta H source: NIST46.2
#T and ionic strength:
Ag+ + 2Butylamine = Ag(Butylamine)2+
log_k 7.47
delta_h -52.7184 kJ
-gamma 0 0
# Id: 209562
# log K source: NIST46.2
# Delta H source: NIST46.2
#T and ionic strength:
H+ + Methylamine = H(Methylamine)+
log_k 10.64
delta_h -55.2288 kJ
-gamma 0 0
# Id: 3309581
# log K source: NIST46.2
# Delta H source: NIST46.2
#T and ionic strength:
Cd+2 + Methylamine = Cd(Methylamine)+2
log_k 2.75
delta_h 0 kJ
-gamma 0 0
# Id: 1609581
# log K source: NIST46.2
# Delta H source: NIST46.2
#T and ionic strength:
Cd+2 + 2Methylamine = Cd(Methylamine)2+2
log_k 4.81
delta_h -29.288 kJ
-gamma 0 0
# Id: 1609582
# log K source: NIST46.2
# Delta H source: NIST46.2
#T and ionic strength:
Cd+2 + 3Methylamine = Cd(Methylamine)3+2
log_k 5.94
delta_h 0 kJ
-gamma 0 0
# Id: 1609583
# log K source: NIST46.2
# Delta H source: NIST46.2
#T and ionic strength:
Cd+2 + 4Methylamine = Cd(Methylamine)4+2
log_k 6.55
delta_h -58.576 kJ
-gamma 0 0
# Id: 1609584
# log K source: NIST46.2
# Delta H source: NIST46.2
#T and ionic strength:
Hg(OH)2 + Methylamine + 2H+ = Hg(Methylamine)+2 + 2H2O
log_k 14.76
delta_h 0 kJ
```

```
-gamma 0 0
# Id: 3619581
# log K source: NIST46.2
# Delta H source: NIST46.2
#T and ionic strength:
Hg(OH)2 + 2Methylamine + 2H+ = Hg(Methylamine)2+2 + 2H2O
log_k 23.96
delta_h 0 kJ
-gamma 0 0
# Id: 3619582
# log K source: NIST46.2
# Delta H source: NIST46.2
#T and ionic strength:
Hg(OH)2 + 3Methylamine + 2H+ = Hg(Methylamine)3+2 + 2H2O
log_k 24.3
delta_h 0 kJ
-gamma 0 0
# Id: 3619583
# log K source: NIST46.2
# Delta H source: NIST46.2
#T and ionic strength:
Hg(OH)2 + 4Methylamine + 2H+ = Hg(Methylamine)4+2 + 2H2O
log_k 24.6
delta_h 0 kJ
-gamma 0 0
# Id: 3619584
# log K source: NIST46.2
# Delta H source: NIST46.2
#T and ionic strength:
Cu+2 + Methylamine = Cu(Methylamine)+2
log_k 4.11
delta_h 0 kJ
-gamma 0 0
# Id: 2319581
# log K source: NIST46.2
# Delta H source: NIST46.2
#T and ionic strength:
Cu+2 + 2Methylamine = Cu(Methylamine)2+2
log_k 7.51
delta_h 0 kJ
-gamma 0 0
# Id: 2319582
# log K source: NIST46.2
# Delta H source: NIST46.2
#T and ionic strength:
Cu+2 + 3Methylamine = Cu(Methylamine)3+2
log_k 10.21
delta_h 0 kJ
-gamma 0 0
# Id: 2319583
# log K source: NIST46.2
# Delta H source: NIST46.2
#T and ionic strength:
Cu+2 + 4Methylamine = Cu(Methylamine)4+2
```

```
log_k 12.08
delta_h 0 kJ
-gamma 0 0
# Id: 2319584
# log K source: NIST46.2
# Delta H source: NIST46.2
#T and ionic strength:
Ag+ + Methylamine = Ag(Methylamine)+
log_k 3.07
delta_h -12.552 kJ
-gamma 0 0
# Id: 209581
# log K source: NIST46.2
# Delta H source: NIST46.2
#T and ionic strength:
Ag+ + 2Methylamine = Ag(Methylamine)2+
log_k 6.89
delta_h -48.9528 kJ
-gamma 0 0
# Id: 209582
# log K source: NIST46.2
# Delta H source: NIST46.2
#T and ionic strength:
Ni+2 + Methylamine = Ni(Methylamine)+2
log_k 2.23
delta_h 0 kJ
-gamma 0 0
# Id: 5409581
# log K source: NIST46.2
# Delta H source: NIST46.2
#T and ionic strength:
H+ + Dimethylamine = H(Dimethylamine)+
log_k 10.774
delta_h -50.208 kJ
-gamma 0 0
# Id: 3309591
# log K source: NIST46.2
# Delta H source: NIST46.2
#T and ionic strength:
Ag+ + 2Dimethylamine = Ag(Dimethylamine)2+
log_k 5.37
delta_h -40.5848 kJ
-gamma 0 0
# Id: 209591
# log K source: NIST46.2
# Delta H source: NIST46.2
#T and ionic strength:
Ni+2 + Dimethylamine = Ni(Dimethylamine)+2
log_k 1.47
delta_h 0 kJ
-gamma 0 0
# Id: 5409591
# log K source: NIST46.2
# Delta H source: NIST46.2
```

```
#T and ionic strength:
H+ + Hexylamine = H(Hexylamine)+
log_k 10.63
delta_h -58.576 kJ
-gamma 0 0
# Id: 3309611
# log K source: NIST46.2
# Delta H source: NIST46.2
#T and ionic strength:
Ag+ + Hexylamine = Ag(Hexylamine)+
log_k 3.54
delta_h -25.104 kJ
-gamma 0 0
# Id: 209611
# log K source: NIST46.2
# Delta H source: NIST46.2
#T and ionic strength:
Ag+ + 2Hexylamine = Ag(Hexylamine)2+
log_k 7.55
delta_h -53.1368 kJ
-gamma 0 0
# Id: 209612
# log K source: NIST46.2
# Delta H source: NIST46.2
#T and ionic strength:
H+ + Ethylenediamine = H(Ethylenediamine)+
log_k 9.928
delta_h -49.7896 kJ
-gamma 0 0
# Id: 3309631
# log K source: NIST46.2
# Delta H source: NIST46.2
#T and ionic strength:
2H+ + Ethylenediamine = H2(Ethylenediamine)+2
log_k 16.776
delta_h -95.3952 kJ
-gamma 0 0
# Id: 3309632
# log K source: NIST46.2
# Delta H source: NIST46.2
#T and ionic strength:
Pb+2 + Ethylenediamine = Pb(Ethylenediamine)+2
log_k 5.04
delta_h 0 kJ
-gamma 0 0
# Id: 6009631
# log K source: NIST46.2
# Delta H source: NIST46.2
#T and ionic strength:
Pb+2 + 2Ethylenediamine = Pb(Ethylenediamine)2+2
log_k 8.5
delta_h 0 kJ
-gamma 0 0
# Id: 6009632
```

```
# log K source: NIST46.2
# Delta H source: NIST46.2
#T and ionic strength:
Zn+2 + Ethylenediamine = Zn(Ethylenediamine)+2
log_k 5.66
delta_h -29.288 kJ
-gamma 0 0
# Id: 9509631
# log K source: NIST46.2
# Delta H source: NIST46.2
#T and ionic strength:
Zn+2 + 2Ethylenediamine = Zn(Ethylenediamine)2+2
log_k 10.6
delta_h -48.116 kJ
-gamma 0 0
# Id: 9509632
# log K source: NIST46.2
# Delta H source: NIST46.2
#T and ionic strength:
Zn+2 + 3Ethylenediamine = Zn(Ethylenediamine)3+2
log_k 13.9
delta_h -71.5464 kJ
-gamma 0 0
# Id: 9509633
# log K source: NIST46.2
# Delta H source: NIST46.2
#T and ionic strength:
Cd+2 + Ethylenediamine = Cd(Ethylenediamine)+2
log_k 5.41
delta_h -28.4512 kJ
-gamma 0 0
# Id: 1609631
# log K source: NIST46.2
# Delta H source: NIST46.2
#T and ionic strength:
Cd+2 + 2Ethylenediamine = Cd(Ethylenediamine)2+2
log_k 9.9
delta_h -55.6472 kJ
-gamma 0 0
# Id: 1609632
# log K source: NIST46.2
# Delta H source: NIST46.2
#T and ionic strength:
Cd+2 + 3Ethylenediamine = Cd(Ethylenediamine)3+2
log_k 11.6
delta_h -82.4248 kJ
-gamma 0 0
# Id: 1609633
# log K source: NIST46.2
# Delta H source: NIST46.2
#T and ionic strength:
Hg(OH)2 + Ethylenediamine + 2H+ = Hg(Ethylenediamine)+2 + 2H2O
log_k 20.4
delta_h 0 kJ
```

```
-gamma 0 0
# Id: 3619631
# log K source: NIST46.2
# Delta H source: NIST46.2
#T and ionic strength:
Hg(OH)2 + 2Ethylenediamine + 2H+ = Hg(Ethylenediamine)2+2 + 2H2O
log_k 29.3
delta_h -173.218 kJ
-gamma 0 0
# Id: 3619632
# log K source: NIST46.2
# Delta H source: NIST46.2
#T and ionic strength:
Hg(OH)2 + 2Ethylenediamine + 3H+ = HgH(Ethylenediamine)2+3 + 2H2O
log_k 34.7
delta_h 0 kJ
-gamma 0 0
# Id: 3619633
# log K source: NIST46.2
# Delta H source: NIST46.2
#T and ionic strength:
Cu+ + 2Ethylenediamine = Cu(Ethylenediamine)2+
log_k 11.2
delta_h 0 kJ
-gamma 0 0
# Id: 2309631
# log K source: NIST46.2
# Delta H source: NIST46.2
#T and ionic strength:
Cu+2 + Ethylenediamine = Cu(Ethylenediamine)+2
log_k 10.5
delta_h -52.7184 kJ
-gamma 0 0
# Id: 2319631
# log K source: NIST46.2
# Delta H source: NIST46.2
#T and ionic strength:
Cu+2 + 2Ethylenediamine = Cu(Ethylenediamine)2+2
log_k 19.6
delta_h -105.437 kJ
-gamma 0 0
# Id: 2319632
# log K source: NIST46.2
# Delta H source: NIST46.2
#T and ionic strength:
Ag+ + Ethylenediamine = Ag(Ethylenediamine)+
log_k 4.6
delta_h -48.9528 kJ
-gamma 0 0
# Id: 209631
# log K source: NIST46.2
# Delta H source: NIST46.2
#T and ionic strength:
Ag+ + 2Ethylenediamine = Ag(Ethylenediamine)2+
```

```
log_k 7.5
delta_h -52.3 kJ
-gamma 0 0
# Id: 209632
# log K source: NIST46.2
# Delta H source: NIST46.2
#T and ionic strength:
Ag+ + Ethylenediamine + H+ = AgH(Ethylenediamine)+2
log_k 11.99
delta_h -75.312 kJ
-gamma 0 0
# Id: 209633
# log K source: NIST46.2
# Delta H source: NIST46.2
#T and ionic strength:
2Ag+ + Ethylenediamine = Ag2(Ethylenediamine)+2
log_k 6.5
delta_h 0 kJ
-gamma 0 0
# Id: 209634
# log K source: NIST46.2
# Delta H source: NIST46.2
#T and ionic strength:
2Ag+ + 2Ethylenediamine = Ag2(Ethylenediamine)2+2
log_k 12.7
delta_h -97.0688 kJ
-gamma 0 0
# Id: 209635
# log K source: NIST46.2
# Delta H source: NIST46.2
#T and ionic strength:
Ag+ + 2Ethylenediamine + 2H+ = Ag(HEthylenediamine)2+3
log_k 24
delta_h -150.206 kJ
-gamma 0 0
# Id: 209636
# log K source: NIST46.2
# Delta H source: NIST46.2
#T and ionic strength:
Ag+ + 2Ethylenediamine + H+ = AgH(Ethylenediamine)2+2
log_k 8.4
delta_h -47.6976 kJ
-gamma 0 0
# Id: 209637
# log K source: NIST46.2
# Delta H source: NIST46.2
#T and ionic strength:
Ni+2 + Ethylenediamine = Ni(Ethylenediamine)+2
log_k 7.32
delta_h -37.656 kJ
-gamma 0 0
# Id: 5409631
# log K source: NIST46.2
# Delta H source: NIST46.2
```

```
#T and ionic strength:
Ni+2 + 2Ethylenediamine = Ni(Ethylenediamine)2+2
log_k 13.5
delta_h -76.5672 kJ
-gamma 0 0
# Id: 5409632
# log K source: NIST46.2
# Delta H source: NIST46.2
#T and ionic strength:
Ni+2 + 3Ethylenediamine = Ni(Ethylenediamine)3+2
log_k 17.6
delta_h -117.152 kJ
-gamma 0 0
# Id: 5409633
# log K source: NIST46.2
# Delta H source: NIST46.2
#T and ionic strength:
Co+2 + Ethylenediamine = Co(Ethylenediamine)+2
log_k 5.5
delta_h -28 kJ
-gamma 0 0
# Id: 2009631
# log K source: NIST46.4
# Delta H source: NIST46.4
#T and ionic strength: 0.10 25.0
Co+2 + 2Ethylenediamine = Co(Ethylenediamine)2+2
log_k 10.1
delta_h -58.5 kJ
-gamma 0 0
# Id: 2009632
# log K source: NIST46.4
# Delta H source: NIST46.4
#T and ionic strength: 0.10 25.0
Co+2 + 3Ethylenediamine = Co(Ethylenediamine)3+2
log_k 13.2
delta_h -92.8 kJ
-gamma 0 0
# Id: 2009633
# log K source: NIST46.4
# Delta H source: NIST46.4
#T and ionic strength: 0.10 25.0
Co+3 + 2Ethylenediamine = Co(Ethylenediamine)2+3
log_k 34.7
delta_h 0 kJ
-gamma 0 0
# Id: 2019631
# log K source: NIST46.4
# Delta H source: NIST46.2
#T and ionic strength: 1.00 25.0
Co+3 + 3Ethylenediamine = Co(Ethylenediamine)3+3
log_k 48.69
delta_h 0 kJ
-gamma 0 0
# Id: 2019632
```

```
# log K source: NIST46.4
# Delta H source: NIST46.2
#T and ionic strength: 1.50 30.0
Fe+2 + Ethylenediamine = Fe(Ethylenediamine)+2
log_k 4.26
delta_h 0 kJ
-gamma 0 0
# Id: 2809631
# log K source: NIST46.2
# Delta H source: NIST46.2
#T and ionic strength:
Fe+2 + 2Ethylenediamine = Fe(Ethylenediamine)2+2
log_k 7.73
delta_h 0 kJ
-gamma 0 0
# Id: 2809632
# log K source: NIST46.2
# Delta H source: NIST46.2
#T and ionic strength:
Fe+2 + 3Ethylenediamine = Fe(Ethylenediamine)3+2
log_k 10.17
delta_h 0 kJ
-gamma 0 0
# Id: 2809633
# log K source: NIST46.2
# Delta H source: NIST46.2
#T and ionic strength:
Mn+2 + Ethylenediamine = Mn(Ethylenediamine)+2
log_k 2.74
delta_h -11.7152 kJ
-gamma 0 0
# Id: 4709631
# log K source: NIST46.2
# Delta H source: NIST46.2
#T and ionic strength:
Mn+2 + 2Ethylenediamine = Mn(Ethylenediamine)2+2
log_k 4.8
delta_h -25.104 kJ
-gamma 0 0
# Id: 4709632
# log K source: NIST46.2
# Delta H source: NIST46.2
#T and ionic strength:
Cr(OH)2+ + 2Ethylenediamine + 2H+ = Cr(Ethylenediamine)2+3 + 2H2O
log_k 22.57
delta_h 0 kJ
-gamma 0 0
# Id: 2119631
# log K source: NIST46.2
# Delta H source: NIST46.2
#T and ionic strength:
Cr(OH)2+ + 3Ethylenediamine + 2H+ = Cr(Ethylenediamine)3+3 + 2H2O
log_k 29
delta_h 0 kJ
```

```
-gamma 0 0
# Id: 2119632
# log K source: NIST46.2
# Delta H source: NIST46.2
#T and ionic strength:
Mg+2 + Ethylenediamine = Mg(Ethylenediamine)+2
log_k 0.37
delta_h 0 kJ
-gamma 0 0
# Id: 4609631
# log K source: NIST46.2
# Delta H source: NIST46.2
#T and ionic strength:
Ca+2 + Ethylenediamine = Ca(Ethylenediamine)+2
log_k 0.11
delta_h 0 kJ
-gamma 0 0
# Id: 1509631
# log K source: NIST46.2
# Delta H source: NIST46.2
#T and ionic strength:
H+ + Propylamine = H(Propylamine)+
log_k 10.566
delta_h -57.53 kJ
-gamma 0 0
# Id: 3309641
# log K source: NIST46.2
# Delta H source: NIST46.2
#T and ionic strength:
Zn+2 + Propylamine = Zn(Propylamine)+2
log_k 2.42
delta_h 0 kJ
-gamma 0 0
# Id: 9509641
# log K source: SCD2.62
# Delta H source: SCD2.62
#T and ionic strength:
Zn+2 + 2Propylamine = Zn(Propylamine)2+2
log_k 4.85
delta_h 0 kJ
-gamma 0 0
# Id: 9509642
# log K source: SCD2.62
# Delta H source: SCD2.62
#T and ionic strength:
Zn+2 + 3Propylamine = Zn(Propylamine)3+2
log_k 7.38
delta_h 0 kJ
-gamma 0 0
# Id: 9509643
# log K source: SCD2.62
# Delta H source: SCD2.62
#T and ionic strength:
Zn+2 + 4Propylamine = Zn(Propylamine)4+2
```

```
log_k 9.49
delta_h 0 kJ
-gamma 0 0
# Id: 9509644
# log K source: SCD2.62
# Delta H source: SCD2.62
#T and ionic strength:
Cd+2 + Propylamine = Cd(Propylamine)+2
log_k 2.62
delta_h 0 kJ
-gamma 0 0
# Id: 1609641
# log K source: SCD2.62
# Delta H source: SCD2.62
#T and ionic strength:
Cd+2 + 2Propylamine = Cd(Propylamine)2+2
log_k 4.64
delta_h 0 kJ
-gamma 0 0
# Id: 1609642
# log K source: SCD2.62
# Delta H source: SCD2.62
#T and ionic strength:
Cd+2 + 3Propylamine = Cd(Propylamine)3+2
log_k 6.03
delta_h 0 kJ
-gamma 0 0
# Id: 1609643
# log K source: SCD2.62
# Delta H source: SCD2.62
#T and ionic strength:
Ag+ + Propylamine = Ag(Propylamine)+
log_k 3.45
delta_h -12.552 kJ
-gamma 0 0
# Id: 209641
# log K source: NIST46.2
# Delta H source: NIST46.2
#T and ionic strength:
Ag+ + 2Propylamine = Ag(Propylamine)2+
log_k 7.44
delta_h -53.1368 kJ
-gamma 0 0
# Id: 209642
# log K source: NIST46.2
# Delta H source: NIST46.2
#T and ionic strength:
Ni+2 + Propylamine = Ni(Propylamine)+2
log_k 2.81
delta_h 0 kJ
-gamma 0 0
# Id: 5409641
# log K source: SCD2.62
# Delta H source: SCD2.62
```

```
#T and ionic strength:
Ni+2 + 2Propylamine = Ni(Propylamine)2+2
log_k 5.02
delta_h 0 kJ
-gamma 0 0
# Id: 5409642
# log K source: SCD2.62
# Delta H source: SCD2.62
#T and ionic strength:
Ni+2 + 3Propylamine = Ni(Propylamine)3+2
log_k 6.79
delta_h 0 kJ
-gamma 0 0
# Id: 5409643
# log K source: SCD2.62
# Delta H source: SCD2.62
#T and ionic strength:
Ni+2 + 4Propylamine = Ni(Propylamine)4+2
log_k 8.31
delta_h 0 kJ
-gamma 0 0
# Id: 5409644
# log K source: SCD2.62
# Delta H source: SCD2.62
#T and ionic strength:
H+ + Isopropylamine = H(Isopropylamine)+
log_k 10.67
delta_h -58.3668 kJ
-gamma 0 0
# Id: 3309651
# log K source: NIST46.2
# Delta H source: NIST46.2
#T and ionic strength:
Zn+2 + Isopropylamine = Zn(Isopropylamine)+2
log_k 2.37
delta_h 0 kJ
-gamma 0 0
# Id: 9509651
# log K source: SCD2.62
# Delta H source: SCD2.62
#T and ionic strength:
Zn+2 + 2Isopropylamine = Zn(Isopropylamine)2+2
log_k 4.67
delta_h 0 kJ
-gamma 0 0
# Id: 9509652
# log K source: SCD2.62
# Delta H source: SCD2.62
#T and ionic strength:
Zn+2 + 3Isopropylamine = Zn(Isopropylamine)3+2
log_k 7.14
delta_h 0 kJ
-gamma 0 0
# Id: 9509653
```

```
# log K source: SCD2.62
# Delta H source: SCD2.62
#T and ionic strength:
Zn+2 + 4Isopropylamine = Zn(Isopropylamine)4+2
log_k 9.44
delta_h 0 kJ
-gamma 0 0
# Id: 9509654
# log K source: SCD2.62
# Delta H source: SCD2.62
#T and ionic strength:
Cd+2 + Isopropylamine = Cd(Isopropylamine)+2
log_k 2.55
delta_h 0 kJ
-gamma 0 0
# Id: 1609651
# log K source: SCD2.62
# Delta H source: SCD2.62
#T and ionic strength:
Cd+2 + 2Isopropylamine = Cd(Isopropylamine)2+2
log_k 4.57
delta_h 0 kJ
-gamma 0 0
# Id: 1609652
# log K source: SCD2.62
# Delta H source: SCD2.62
#T and ionic strength:
Cd+2 + 3Isopropylamine = Cd(Isopropylamine)3+2
log_k 6.07
delta_h 0 kJ
-gamma 0 0
# Id: 1609653
# log K source: SCD2.62
# Delta H source: SCD2.62
#T and ionic strength:
Cd+2 + 4Isopropylamine = Cd(Isopropylamine)4+2
log_k 6.9
delta_h 0 kJ
-gamma 0 0
# Id: 1609654
# log K source: SCD2.62
# Delta H source: SCD2.62
#T and ionic strength:
Hg(OH)2 + Isopropylamine + 2H+ = Hg(Isopropylamine)+2 + 2H2O
log_k 14.85
delta_h 0 kJ
-gamma 0 0
# Id: 3619651
# log K source: NIST46.2
# Delta H source: NIST46.2
#T and ionic strength:
Hg(OH)2 + 2Isopropylamine + 2H+ = Hg(Isopropylamine)2+2 + 2H2O
log_k 24.37
delta_h 0 kJ
```

```
-gamma 0 0
# Id: 3619652
# log K source: NIST46.2
# Delta H source: NIST46.2
#T and ionic strength:
Ag+ + Isopropylamine = Ag(Isopropylamine)+
log_k 3.67
delta_h -23.8488 kJ
-gamma 0 0
# Id: 209651
# log K source: NIST46.2
# Delta H source: NIST46.2
#T and ionic strength:
Ag+ + 2Isopropylamine = Ag(Isopropylamine)2+
log_k 7.77
delta_h -59.8312 kJ
-gamma 0 0
# Id: 209652
# log K source: NIST46.2
# Delta H source: NIST46.2
#T and ionic strength:
Ni+2 + Isopropylamine = Ni(Isopropylamine)+2
log_k 2.71
delta_h 0 kJ
-gamma 0 0
# Id: 5409651
# log K source: SCD2.62
# Delta H source: SCD2.62
#T and ionic strength:
Ni+2 + 2Isopropylamine = Ni(Isopropylamine)2+2
log_k 4.86
delta_h 0 kJ
-gamma 0 0
# Id: 5409652
# log K source: SCD2.62
# Delta H source: SCD2.62
#T and ionic strength:
Ni+2 + 3Isopropylamine = Ni(Isopropylamine)3+2
log_k 6.57
delta_h 0 kJ
-gamma 0 0
# Id: 5409653
# log K source: SCD2.62
# Delta H source: SCD2.62
#T and ionic strength:
Ni+2 + 4Isopropylamine = Ni(Isopropylamine)4+2
log_k 7.83
delta_h 0 kJ
-gamma 0 0
# Id: 5409654
# log K source: SCD2.62
# Delta H source: SCD2.62
#T and ionic strength:
Ni+2 + 5Isopropylamine = Ni(Isopropylamine)5+2
```

```
log_k 8.43
delta_h 0 kJ
-gamma 0 0
# Id: 5409655
# log K source: SCD2.62
# Delta H source: SCD2.62
#T and ionic strength:
H+ + Trimethylamine = H(Trimethylamine)+
log_k 9.8
delta_h -36.8192 kJ
-gamma 0 0
# Id: 3309661
# log K source: NIST46.2
# Delta H source: NIST46.2
#T and ionic strength:
Ag+ + Trimethylamine = Ag(Trimethylamine)+
log_k 1.701
delta_h 0 kJ
-gamma 0 0
# Id: 209661
# log K source: SCD2.62
# Delta H source: SCD2.62
#T and ionic strength:
H+ + Citrate-3 = H(Citrate)-2
log_k 6.396
delta_h 3.3472 kJ
-gamma 0 0
# Id: 3309671
# log K source: NIST46.2
# Delta H source: NIST46.2
#T and ionic strength:
2H+ + Citrate-3 = H2(Citrate)-
log_k 11.157
delta_h 1.297 kJ
-gamma 0 0
# Id: 3309672
# log K source: NIST46.2
# Delta H source: NIST46.2
#T and ionic strength:
3H+ + Citrate-3 = H3(Citrate)
log_k 14.285
delta_h -2.7614 kJ
-gamma 0 0
# Id: 3309673
# log K source: NIST46.2
# Delta H source: NIST46.2
#T and ionic strength:
Pb+2 + Citrate-3 = Pb(Citrate)-
log_k 7.27
delta_h 0 kJ
-gamma 0 0
# Id: 6009671
# log K source: SCD2.62
# Delta H source: SCD2.62
```

```
#T and ionic strength:
Pb+2 + 2Citrate-3 = Pb(Citrate)2-4
log_k 6.53
delta_h 0 kJ
-gamma 0 0
# Id: 6009672
# log K source: NIST46.2
# Delta H source: NIST46.2
#T and ionic strength:
Al+3 + Citrate-3 = Al(Citrate)
log_k 9.97
delta_h 0 kJ
-gamma 0 0
# Id: 309671
# log K source: NIST46.2
# Delta H source: NIST46.2
#T and ionic strength:
Al+3 + 2Citrate-3 = Al(Citrate)2-3
log_k 14.8
delta_h 0 kJ
-gamma 0 0
# Id: 309672
# log K source: NIST46.2
# Delta H source: NIST46.2
#T and ionic strength:
Al+3 + Citrate-3 + H+ = AlH(Citrate)+
log_k 12.85
delta_h 0 kJ
-gamma 0 0
# Id: 309673
# log K source: NIST46.2
# Delta H source: NIST46.2
#T and ionic strength:
Tl+ + Citrate-3 = Tl(Citrate)-2
log_k 1.48
delta_h 0 kJ
-gamma 0 0
# Id: 8709671
# log K source: NIST46.2
# Delta H source: NIST46.2
#T and ionic strength:
Zn+2 + Citrate-3 = Zn(Citrate)-
log_k 6.21
delta_h 8.368 kJ
-gamma 0 0
# Id: 9509671
# log K source: NIST46.2
# Delta H source: NIST46.2
#T and ionic strength:
Zn+2 + 2Citrate-3 = Zn(Citrate)2-4
log_k 7.4
delta_h 25.104 kJ
-gamma 0 0
# Id: 9509672
```

```
# log K source: NIST46.2
# Delta H source: NIST46.2
#T and ionic strength:
Zn+2 + Citrate-3 + H+ = ZnH(Citrate)
log_k 10.2
delta_h 3.3472 kJ
-gamma 0 0
# Id: 9509673
# log K source: NIST46.2
# Delta H source: NIST46.2
#T and ionic strength:
Zn+2 + Citrate-3 + 2H+ = ZnH2(Citrate)+
log_k 12.84
delta_h 0 kJ
-gamma 0 0
# Id: 9509674
# log K source: SCD2.62
# Delta H source: SCD2.62
#T and ionic strength:
Cd+2 + Citrate-3 = Cd(Citrate)-
log_k 4.98
delta_h 8.368 kJ
-gamma 0 0
# Id: 1609671
# log K source: NIST46.2
# Delta H source: NIST46.2
#T and ionic strength:
Cd+2 + Citrate-3 + H+ = CdH(Citrate)
log_k 9.44
delta_h 3.3472 kJ
-gamma 0 0
# Id: 1609672
# log K source: NIST46.2
# Delta H source: NIST46.2
#T and ionic strength:
Cd+2 + Citrate-3 + 2H+ = CdH2(Citrate)+
log_k 12.9
delta_h 0 kJ
-gamma 0 0
# Id: 1609673
# log K source: NIST46.2
# Delta H source: NIST46.2
#T and ionic strength:
Cd+2 + 2Citrate-3 = Cd(Citrate)2-4
log_k 5.9
delta_h 20.92 kJ
-gamma 0 0
# Id: 1609674
# log K source: NIST46.2
# Delta H source: NIST46.2
#T and ionic strength:
Hg(OH)2 + Citrate-3 + 2H+ = Hg(Citrate)- + 2H2O
log_k 18.3
delta_h 0 kJ
```

```
-gamma 0 0
# Id: 3619671
# log K source: NIST46.2
# Delta H source: NIST46.2
#T and ionic strength:
Cu+2 + Citrate-3 = Cu(Citrate)-
log_k 7.57
delta_h 0 kJ
-gamma 0 0
# Id: 2319671
# log K source: SCD2.62
# Delta H source: SCD2.62
#T and ionic strength:
Cu+2 + 2Citrate-3 = Cu(Citrate)2-4
log_k 8.9
delta_h 0 kJ
-gamma 0 0
# Id: 2319672
# log K source: SCD2.62
# Delta H source: SCD2.62
#T and ionic strength:
Cu+2 + Citrate-3 + H+ = CuH(Citrate)
log_k 10.87
delta_h 11.7152 kJ
-gamma 0 0
# Id: 2319673
# log K source: NIST46.2
# Delta H source: NIST46.2
#T and ionic strength:
Cu+2 + Citrate-3 + 2H+ = CuH2(Citrate)+
log_k 13.23
delta_h 0 kJ
-gamma 0 0
# Id: 2319674
# log K source: SCD2.62
# Delta H source: SCD2.62
#T and ionic strength:
2Cu+2 + 2Citrate-3 = Cu2(Citrate)2-2
log_k 16.9
delta_h 41.84 kJ
-gamma 0 0
# Id: 2319675
# log K source: NIST46.2
# Delta H source: NIST46.2
#T and ionic strength:
Ni+2 + Citrate-3 = Ni(Citrate)-
log_k 6.59
delta_h 16.736 kJ
-gamma 0 0
# Id: 5409671
# log K source: NIST46.2
# Delta H source: NIST46.2
#T and ionic strength:
Ni+2 + Citrate-3 + H+ = NiH(Citrate)
```

```
log_k 10.5
delta_h 15.8992 kJ
-gamma 0 0
# Id: 5409672
# log K source: NIST46.2
# Delta H source: NIST46.2
#T and ionic strength:
Ni+2 + Citrate-3 + 2H+ = NiH2(Citrate)+
log_k 13.3
delta_h 0 kJ
-gamma 0 0
# Id: 5409673
# log K source: NIST46.2
# Delta H source: NIST46.2
#T and ionic strength:
Ni+2 + 2Citrate-3 = Ni(Citrate)2-4
log_k 8.77
delta_h 12.552 kJ
-gamma 0 0
# Id: 5409674
# log K source: NIST46.2
# Delta H source: NIST46.2
#T and ionic strength:
Ni+2 + 2Citrate-3 + H+ = NiH(Citrate)2-3
log_k 14.9
delta_h 32.6352 kJ
-gamma 0 0
# Id: 5409675
# log K source: NIST46.2
# Delta H source: NIST46.2
#T and ionic strength:
Co+2 + Citrate-3 = Co(Citrate)-
log_k 6.1867
delta_h 0 kJ
-gamma 0 0
# Id: 2009671
# log K source: NIST46.4
# Delta H source: NIST46.2
#T and ionic strength: 0.10 25.0
Co+2 + H+ + Citrate-3 = CoHCitrate
log_k 10.4438
delta_h 0 kJ
-gamma 0 0
# Id: 2009672
# log K source: NIST46.4
# Delta H source: NIST46.2
#T and ionic strength: 0.10 25.0
Co+2 + 2H+ + Citrate-3 = CoH2Citrate+
log_k 12.7859
delta_h 0 kJ
-gamma 0 0
# Id: 2009673
# log K source: NIST46.4
# Delta H source: NIST46.2
```

```
#T and ionic strength: 0.10 20.0
Fe+2 + Citrate-3 = Fe(Citrate)-
log_k 6.1
delta_h 0 kJ
-gamma 0 0
# Id: 2809671
# log K source: NIST46.2
# Delta H source: NIST46.2
#T and ionic strength:
Fe+2 + Citrate-3 + H+ = FeH(Citrate)
log_k 10.2
delta_h 0 kJ
-gamma 0 0
# Id: 2809672
# log K source: NIST46.2
# Delta H source: NIST46.2
#T and ionic strength:
Fe+3 + Citrate-3 = Fe(Citrate)
log_k 13.1
delta_h 0 kJ
-gamma 0 0
# Id: 2819671
# log K source: NIST46.2
# Delta H source: NIST46.2
#T and ionic strength:
Fe+3 + Citrate-3 + H+ = FeH(Citrate)+
log_k 14.4
delta_h 0 kJ
-gamma 0 0
# Id: 2819672
# log K source: NIST46.2
# Delta H source: NIST46.2
#T and ionic strength:
Mn+2 + Citrate-3 = Mn(Citrate)-
log_k 4.28
delta_h 0 kJ
-gamma 0 0
# Id: 4709671
# log K source: SCD2.62
# Delta H source: SCD2.62
#T and ionic strength:
Mn+2 + Citrate-3 + H+ = MnH(Citrate)
log_k 9.6
delta_h 0 kJ
-gamma 0 0
# Id: 4709672
# log K source: NIST46.2
# Delta H source: NIST46.2
#T and ionic strength:
Be+2 + Citrate-3 = Be(Citrate)-
log_k 5.534
delta_h 0 kJ
-gamma 0 0
# Id: 1109671
```

```
# log K source: NIST46.4
# Delta H source: NIST46.2
#T and ionic strength: 1.00 25.0
Be+2 + H+ + Citrate-3 = BeH(Citrate)
log_k 9.442
delta_h 0 kJ
-gamma 0 0
# Id: 1109672
# log K source: NIST46.4
# Delta H source: NIST46.2
#T and ionic strength: 1.00 25.0
Ca+2 + Citrate-3 = Ca(Citrate)-
log_k 4.87
delta_h -8.368 kJ
-gamma 0 0
# Id: 1509671
# log K source: NIST46.2
# Delta H source: NIST46.2
#T and ionic strength:
Ca+2 + Citrate-3 + H+ = CaH(Citrate)
log_k 9.26
delta_h -0.8368 kJ
-gamma 0 0
# Id: 1509672
# log K source: NIST46.2
# Delta H source: NIST46.2
#T and ionic strength:
Ca+2 + Citrate-3 + 2H+ = CaH2(Citrate)+
log_k 12.257
delta_h 0 kJ
-gamma 0 0
# Id: 1509673
# log K source: SCD2.62
# Delta H source: SCD2.62
#T and ionic strength:
Mg+2 + Citrate-3 = Mg(Citrate)-
log_k 4.89
delta_h 8.368 kJ
-gamma 0 0
# Id: 4609671
# log K source: NIST46.2
# Delta H source: NIST46.2
#T and ionic strength:
Mg+2 + Citrate-3 + H+ = MgH(Citrate)
log_k 8.91
delta_h 3.3472 kJ
-gamma 0 0
# Id: 4609672
# log K source: NIST46.2
# Delta H source: NIST46.2
#T and ionic strength:
Mg+2 + Citrate-3 + 2H+ = MgH2(Citrate)+
log_k 12.2
delta_h 0 kJ
```

```
-gamma 0 0
# Id: 4609673
# log K source: SCD2.62
# Delta H source: SCD2.62
#T and ionic strength:
Sr+2 + Citrate-3 = Sr(Citrate)-
log_k 4.3367
delta_h 0 kJ
-gamma 0 0
# Id: 8009671
# log K source: NIST46.4
# Delta H source: NIST46.2
#T and ionic strength: 0.10 25.0
Sr+2 + H+ + Citrate-3 = SrH(Citrate)
log_k 8.9738
delta_h 0 kJ
-gamma 0 0
# Id: 8009672
# log K source: NIST46.4
# Delta H source: NIST46.2
#T and ionic strength: 0.10 25.0
Sr+2 + 2H+ + Citrate-3 = SrH2(Citrate)+
log_k 12.4859
delta_h 0 kJ
-gamma 0 0
# Id: 8009673
# log K source: NIST46.4
# Delta H source: NIST46.2
#T and ionic strength: 0.10 25.0
Ba+2 + Citrate-3 = Ba(Citrate)-
log_k 4.1
delta_h 0 kJ
-gamma 0 0
# Id: 1009671
# log K source: NIST46.2
# Delta H source: NIST46.2
#T and ionic strength:
Ba+2 + Citrate-3 + H+ = BaH(Citrate)
log_k 8.74
delta_h 0 kJ
-gamma 0 0
# Id: 1009672
# log K source: NIST46.2
# Delta H source: NIST46.2
#T and ionic strength:
Ba+2 + Citrate-3 + 2H+ = BaH2(Citrate)+
log_k 12.3
delta_h 0 kJ
-gamma 0 0
# Id: 1009673
# log K source: NIST46.2
# Delta H source: NIST46.2
#T and ionic strength:
Na+ + Citrate-3 = Na(Citrate)-2
```

```
log_k 1.03
delta_h -2.8033 kJ
-gamma 0 0
# Id: 5009671
# log K source: SCD2.62
# Delta H source: SCD2.62
#T and ionic strength:
2Na+ + Citrate-3 = Na2(Citrate)-
log_k 1.5
delta_h -5.1045 kJ
-gamma 0 0
# Id: 5009672
# log K source: SCD2.62
# Delta H source: SCD2.62
#T and ionic strength:
Na+ + Citrate-3 + H+ = NaH(Citrate)-
log_k 6.45
delta_h -3.5982 kJ
-gamma 0 0
# Id: 5009673
# log K source: SCD2.62
# Delta H source: SCD2.62
#T and ionic strength:
K+ + Citrate-3 = K(Citrate)-2
log_k 1.1
delta_h 5.4392 kJ
-gamma 0 0
# Id: 4109671
# log K source: NIST46.2
# Delta H source: NIST46.2
#T and ionic strength:
H+ + Nta-3 = H(Nta)-2
log_k 10.278
delta_h -18.828 kJ
-gamma 0 0
# Id: 3309681
# log K source: NIST46.2
# Delta H source: NIST46.2
#T and ionic strength:
2H+ + Nta-3 = H2(Nta)-
log_k 13.22
delta_h -17.9912 kJ
-gamma 0 0
# Id: 3309682
# log K source: NIST46.2
# Delta H source: NIST46.2
#T and ionic strength:
3H+ + Nta-3 = H3(Nta)
log_k 15.22
delta_h -16.3176 kJ
-gamma 0 0
# Id: 3309683
# log K source: NIST46.2
# Delta H source: NIST46.2
```

```
#T and ionic strength:
4H+ + Nta-3 = H4(Nta)+
log_k 16.22
delta_h -16.3176 kJ
-gamma 0 0
# Id: 3309684
# log K source: NIST46.2
# Delta H source: NIST46.2
#T and ionic strength:
Pb+2 + Nta-3 = Pb(Nta)-
log_k 12.7
delta_h -15.8992 kJ
-gamma 0 0
# Id: 6009681
# log K source: NIST46.2
# Delta H source: NIST46.2
#T and ionic strength:
Pb+2 + Nta-3 + H+ = PbH(Nta)
log_k 15.3
delta_h 0 kJ
-gamma 0 0
# Id: 6009682
# log K source: NIST46.2
# Delta H source: NIST46.2
#T and ionic strength:
Al+3 + Nta-3 = Al(Nta)
log_k 13.3
delta_h 0 kJ
-gamma 0 0
# Id: 309681
# log K source: NIST46.2
# Delta H source: NIST46.2
#T and ionic strength:
Al+3 + Nta-3 + H+ = AlH(Nta)+
log_k 15.2
delta_h 0 kJ
-gamma 0 0
# Id: 309682
# log K source: NIST46.2
# Delta H source: NIST46.2
#T and ionic strength:
Al+3 + Nta-3 + H2O = AlOH(Nta)- + H+
log_k 8
delta_h 0 kJ
-gamma 0 0
# Id: 309683
# log K source: NIST46.2
# Delta H source: NIST46.2
#T and ionic strength:
Tl+ + Nta-3 = Tl(Nta)-2
log_k 5.39
delta_h 0 kJ
-gamma 0 0
# Id: 8709681
```

```
# log K source: NIST46.2
# Delta H source: NIST46.2
#T and ionic strength:
Zn+2 + Nta-3 = Zn(Nta)-
log_k 11.95
delta_h -3.7656 kJ
-gamma 0 0
# Id: 9509681
# log K source: NIST46.2
# Delta H source: NIST46.2
#T and ionic strength:
Zn+2 + 2Nta-3 = Zn(Nta)2-4
log_k 14.88
delta_h -15.0624 kJ
-gamma 0 0
# Id: 9509682
# log K source: NIST46.2
# Delta H source: NIST46.2
#T and ionic strength:
Zn+2 + Nta-3 + H2O = ZnOH(Nta)-2 + H+
log_k 1.46
delta_h 46.4424 kJ
-gamma 0 0
# Id: 9509683
# log K source: NIST46.2
# Delta H source: NIST46.2
#T and ionic strength:
Cd+2 + Nta-3 = Cd(Nta)-
log_k 11.07
delta_h -16.736 kJ
-gamma 0 0
# Id: 1609681
# log K source: NIST46.2
# Delta H source: NIST46.2
#T and ionic strength:
Cd+2 + 2Nta-3 = Cd(Nta)2-4
log_k 15.03
delta_h -38.0744 kJ
-gamma 0 0
# Id: 1609682
# log K source: NIST46.2
# Delta H source: NIST46.2
#T and ionic strength:
Cd+2 + Nta-3 + H2O = CdOH(Nta)-2 + H+
log_k -0.61
delta_h 29.288 kJ
-gamma 0 0
# Id: 1609683
# log K source: NIST46.2
# Delta H source: NIST46.2
#T and ionic strength:
Hg(OH)2 + Nta-3 + 2H+ = Hg(Nta)- + 2H2O
log_k 21.7
delta_h 0 kJ
```

```
-gamma 0 0
# Id: 3619681
# log K source: NIST46.2
# Delta H source: NIST46.2
#T and ionic strength:
Cu+2 + Nta-3 = Cu(Nta)-
log_k 14.4
delta_h -7.9496 kJ
-gamma 0 0
# Id: 2319681
# log K source: NIST46.2
# Delta H source: NIST46.2
#T and ionic strength:
Cu+2 + 2Nta-3 = Cu(Nta)2-4
log_k 18.1
delta_h -37.2376 kJ
-gamma 0 0
# Id: 2319682
# log K source: NIST46.2
# Delta H source: NIST46.2
#T and ionic strength:
Cu+2 + Nta-3 + H+ = CuH(Nta)
log_k 16.2
delta_h 0 kJ
-gamma 0 0
# Id: 2319683
# log K source: NIST46.2
# Delta H source: NIST46.2
#T and ionic strength:
Cu+2 + Nta-3 + H2O = CuOH(Nta)-2 + H+
log_k 4.8
delta_h 25.5224 kJ
-gamma 0 0
# Id: 2319684
# log K source: NIST46.2
# Delta H source: NIST46.2
#T and ionic strength:
Ag+ + Nta-3 = Ag(Nta)-2
log_k 6
delta_h -26.3592 kJ
-gamma 0 0
# Id: 209681
# log K source: NIST46.2
# Delta H source: NIST46.2
#T and ionic strength:
Ni+2 + Nta-3 = Ni(Nta)-
log_k 12.79
delta_h -10.0416 kJ
-gamma 0 0
# Id: 5409681
# log K source: NIST46.2
# Delta H source: NIST46.2
#T and ionic strength:
Ni+2 + 2Nta-3 = Ni(Nta)2-4
```

```
log_k 16.96
delta_h -32.6352 kJ
-gamma 0 0
# Id: 5409682
# log K source: NIST46.2
# Delta H source: NIST46.2
#T and ionic strength:
Ni+2 + Nta-3 + H2O = NiOH(Nta)-2 + H+
log_k 1.5
delta_h 15.0624 kJ
-gamma 0 0
# Id: 5409683
# log K source: NIST46.2
# Delta H source: NIST46.2
#T and ionic strength:
Co+2 + Nta-3 = Co(Nta)-
log_k 11.6667
delta_h -0.4 kJ
-gamma 0 0
# Id: 2009681
# log K source: NIST46.4
# Delta H source: NIST46.4
#T and ionic strength: 0.10 25.0
Co+2 + 2Nta-3 = Co(Nta)2-4
log_k 14.9734
delta_h -20 kJ
-gamma 0 0
# Id: 2009682
# log K source: NIST46.4
# Delta H source: NIST46.4
#T and ionic strength: 0.10 25.0
Co+2 + Nta-3 + H2O = CoOH(Nta)-2 + H+
log_k 0.4378
delta_h 45.6 kJ
-gamma 0 0
# Id: 2009683
# log K source: NIST46.4
# Delta H source: NIST46.4
#T and ionic strength: 0.10 25.0
Fe+2 + Nta-3 = Fe(Nta)-
log_k 10.19
delta_h 0 kJ
-gamma 0 0
# Id: 2809681
# log K source: NIST46.2
# Delta H source: NIST46.2
#T and ionic strength:
Fe+2 + 2Nta-3 = Fe(Nta)2-4
log_k 12.62
delta_h 0 kJ
-gamma 0 0
# Id: 2809682
# log K source: NIST46.2
# Delta H source: NIST46.2
```

```
#T and ionic strength:
Fe+2 + Nta-3 + H+ = FeH(Nta)
log_k 12.29
delta_h 0 kJ
-gamma 0 0
# Id: 2809683
# log K source: NIST46.2
# Delta H source: NIST46.2
#T and ionic strength:
Fe+2 + Nta-3 + H2O = FeOH(Nta)-2 + H+
log_k -1.06
delta_h 0 kJ
-gamma 0 0
# Id: 2809684
# log K source: NIST46.2
# Delta H source: NIST46.2
#T and ionic strength:
Fe+3 + Nta-3 = Fe(Nta)
log_k 17.8
delta_h 13.3888 kJ
-gamma 0 0
# Id: 2819681
# log K source: NIST46.2
# Delta H source: NIST46.2
#T and ionic strength:
Fe+3 + 2Nta-3 = Fe(Nta)2-3
log_k 25.9
delta_h 0 kJ
-gamma 0 0
# Id: 2819682
# log K source: NIST46.2
# Delta H source: NIST46.2
#T and ionic strength:
Fe+3 + Nta-3 + H2O = FeOH(Nta)- + H+
log_k 13.23
delta_h 0 kJ
-gamma 0 0
# Id: 2819683
# log K source: NIST46.2
# Delta H source: NIST46.2
#T and ionic strength:
Mn+2 + Nta-3 = Mn(Nta)-
log_k 8.573
delta_h 5.8576 kJ
-gamma 0 0
# Id: 4709681
# log K source: NIST46.2
# Delta H source: NIST46.2
#T and ionic strength:
Mn+2 + 2Nta-3 = Mn(Nta)2-4
log_k 11.58
delta_h -17.1544 kJ
-gamma 0 0
# Id: 4709682
```

```
# log K source: NIST46.2
# Delta H source: NIST46.2
#T and ionic strength:
Cr(OH)2+ + Nta-3 + 2H+ = Cr(Nta) + 2H2O
log_k 21.2
delta_h 0 kJ
-gamma 0 0
# Id: 2119681
# log K source: SCD2.62
# Delta H source: SCD2.62
#T and ionic strength:
Cr(OH)2+ + 2Nta-3 + 2H+ = Cr(Nta)2-3 + 2H2O
log_k 29.5
delta_h 0 kJ
-gamma 0 0
# Id: 2119682
# log K source: SCD2.62
# Delta H source: SCD2.62
#T and ionic strength:
MoO4-2 + 2H+ + Nta-3 = MoO3(Nta)-3 + H2O
log_k 19.5434
delta_h -69 kJ
-gamma 0 0
# Id: 4809681
# log K source: NIST46.4
# Delta H source: NIST46.4
#T and ionic strength: 0.10 25.0
MoO4-2 + 3H+ + Nta-3 = MoO3H(Nta)-2 + H2O
log_k 23.3954
delta_h -71 kJ
-gamma 0 0
# Id: 4809682
# log K source: NIST46.4
# Delta H source: NIST46.4
#T and ionic strength: 1.00 25.0
MoO4-2 + 4H+ + Nta-3 = MoO3H2(Nta)- + H2O
log_k 25.3534
delta_h -71 kJ
-gamma 0 0
# Id: 4809683
# log K source: NIST46.4
# Delta H source: NIST46.4
#T and ionic strength: 1.00 25.0
Be+2 + Nta-3 = Be(Nta)-
log_k 9.0767
delta_h 25 kJ
-gamma 0 0
# Id: 1109681
# log K source: NIST46.4
# Delta H source: NIST46.4
#T and ionic strength: 0.10 25.0
Mg+2 + Nta-3 = Mg(Nta)-
log_k 6.5
delta_h 17.9912 kJ
```

```
-gamma 0 0
# Id: 4609681
# log K source: NIST46.2
# Delta H source: NIST46.2
#T and ionic strength:
Ca+2 + Nta-3 = Ca(Nta)-
log_k 7.608
delta_h -5.6902 kJ
-gamma 0 0
# Id: 1509681
# log K source: NIST46.2
# Delta H source: NIST46.2
#T and ionic strength:
Ca+2 + 2Nta-3 = Ca(Nta)2-4
log_k 8.81
delta_h -32.6352 kJ
-gamma 0 0
# Id: 1509682
# log K source: NIST46.2
# Delta H source: NIST46.2
#T and ionic strength:
Sr+2 + Nta-3 = Sr(Nta)-
log_k 6.2767
delta_h -2.2 kJ
-gamma 0 0
# Id: 8009681
# log K source: NIST46.4
# Delta H source: NIST46.4
#T and ionic strength: 0.10 25.0
Ba+2 + Nta-3 = Ba(Nta)-
log_k 5.875
delta_h -6.025 kJ
-gamma 0 0
# Id: 1009681
# log K source: NIST46.2
# Delta H source: NIST46.2
#T and ionic strength:
H+ + Edta-4 = H(Edta)-3
log_k 10.948
delta_h -23.4304 kJ
-gamma 0 0
# Id: 3309691
# log K source: NIST46.2
# Delta H source: NIST46.2
#T and ionic strength:
2H+ + Edta-4 = H2(Edta)-2
log_k 17.221
delta_h -41.0032 kJ
-gamma 0 0
# Id: 3309692
# log K source: NIST46.2
# Delta H source: NIST46.2
#T and ionic strength:
3H+ + Edta-4 = H3(Edta)-
```

```
log_k 20.34
delta_h -35.564 kJ
-gamma 0 0
# Id: 3309693
# log K source: NIST46.2
# Delta H source: NIST46.2
#T and ionic strength:
4H+ + Edta-4 = H4(Edta)
log_k 22.5
delta_h -34.3088 kJ
-gamma 0 0
# Id: 3309694
# log K source: NIST46.2
# Delta H source: NIST46.2
#T and ionic strength:
5H+ + Edta-4 = H5(Edta)+
log_k 24
delta_h -32.2168 kJ
-gamma 0 0
# Id: 3309695
# log K source: NIST46.2
# Delta H source: NIST46.2
#T and ionic strength:
Sn(OH)2 + 2H+ + Edta-4 = Sn(Edta)-2 + 2H2O
log_k 27.026
delta_h 0 kJ
-gamma 0 0
# Id: 7909691
# log K source: NIST46.4
# Delta H source: NIST46.2
#T and ionic strength: 1.00 20.0
Sn(OH)2 + 3H+ + Edta-4 = SnH(Edta)- + 2H2O
log_k 29.934
delta_h 0 kJ
-gamma 0 0
# Id: 7909692
# log K source: NIST46.4
# Delta H source: NIST46.2
#T and ionic strength: 1.00 20.0
Sn(OH)2 + 4H+ + Edta-4 = SnH2(Edta) + 2H2O
log_k 31.638
delta_h 0 kJ
-gamma 0 0
# Id: 7909693
# log K source: NIST46.4
# Delta H source: NIST46.2
#T and ionic strength: 1.00 20.0
Pb+2 + Edta-4 = Pb(Edta)-2
log_k 19.8
delta_h -54.8104 kJ
-gamma 0 0
# Id: 6009691
# log K source: NIST46.2
# Delta H source: NIST46.2
```

```
#T and ionic strength:
Pb+2 + Edta-4 + H+ = PbH(Edta)-
log_k 23
delta_h 0 kJ
-gamma 0 0
# Id: 6009692
# log K source: NIST46.2
# Delta H source: NIST46.2
#T and ionic strength:
Pb+2 + Edta-4 + 2H+ = PbH2(Edta)
log_k 24.9
delta_h 0 kJ
-gamma 0 0
# Id: 6009693
# log K source: NIST46.2
# Delta H source: NIST46.2
#T and ionic strength:
Al+3 + Edta-4 = Al(Edta)-
log_k 19.1
delta_h 52.7184 kJ
-gamma 0 0
# Id: 309690
# log K source: NIST46.2
# Delta H source: NIST46.2
#T and ionic strength:
Al+3 + Edta-4 + H+ = AlH(Edta)
log_k 21.8
delta_h 36.4008 kJ
-gamma 0 0
# Id: 309691
# log K source: NIST46.2
# Delta H source: NIST46.2
#T and ionic strength:
Al+3 + Edta-4 + H2O = AlOH(Edta)-2 + H+
log_k 12.8
delta_h 73.6384 kJ
-gamma 0 0
# Id: 309692
# log K source: NIST46.2
# Delta H source: NIST46.2
#T and ionic strength:
Tl+ + Edta-4 = Tl(Edta)-3
log_k 7.27
delta_h -43.5136 kJ
-gamma 0 0
# Id: 8709691
# log K source: NIST46.2
# Delta H source: NIST46.2
#T and ionic strength:
Tl+ + Edta-4 + H+ = TlH(Edta)-2
log_k 13.68
delta_h 0 kJ
-gamma 0 0
# Id: 8709692
```

```
# log K source: NIST46.2
# Delta H source: NIST46.2
#T and ionic strength:
Zn+2 + Edta-4 = Zn(Edta)-2
log_k 18
delta_h -19.2464 kJ
-gamma 0 0
# Id: 9509691
# log K source: NIST46.2
# Delta H source: NIST46.2
#T and ionic strength:
Zn+2 + Edta-4 + H+ = ZnH(Edta)-
log_k 21.4
delta_h -28.4512 kJ
-gamma 0 0
# Id: 9509692
# log K source: NIST46.2
# Delta H source: NIST46.2
#T and ionic strength:
Zn+2 + Edta-4 + H2O = ZnOH(Edta)-3 + H+
log_k 5.8
delta_h 0 kJ
-gamma 0 0
# Id: 9509693
# log K source: NIST46.2
# Delta H source: NIST46.2
#T and ionic strength:
Cd+2 + Edta-4 = Cd(Edta)-2
log_k 18.2
delta_h -38.0744 kJ
-gamma 0 0
# Id: 1609691
# log K source: NIST46.2
# Delta H source: NIST46.2
#T and ionic strength:
Cd+2 + Edta-4 + H+ = CdH(Edta)-
log_k 21.5
delta_h -39.748 kJ
-gamma 0 0
# Id: 1609692
# log K source: NIST46.2
# Delta H source: NIST46.2
#T and ionic strength:
Hg(OH)2 + Edta-4 + 2H+ = Hg(Edta)-2 + 2H2O
log_k 29.3
delta_h -125.102 kJ
-gamma 0 0
# Id: 3619691
# log K source: NIST46.2
# Delta H source: NIST46.2
#T and ionic strength:
Hg(OH)2 + Edta-4 + 3H+ = HgH(Edta)- + 2H2O
log_k 32.9
delta_h -128.449 kJ
```

```
-gamma 0 0
# Id: 3619692
# log K source: NIST46.2
# Delta H source: NIST46.2
#T and ionic strength:
Cu+2 + Edta-4 = Cu(Edta)-2
log_k 20.5
delta_h -34.7272 kJ
-gamma 0 0
# Id: 2319691
# log K source: NIST46.2
# Delta H source: NIST46.2
#T and ionic strength:
Cu+2 + Edta-4 + H+ = CuH(Edta)-
log_k 24
delta_h -43.0952 kJ
-gamma 0 0
# Id: 2319692
# log K source: NIST46.2
# Delta H source: NIST46.2
#T and ionic strength:
Cu+2 + Edta-4 + 2H+ = CuH2(Edta)
log_k 26.2
delta_h 0 kJ
-gamma 0 0
# Id: 2319693
# log K source: NIST46.2
# Delta H source: NIST46.2
#T and ionic strength:
Cu+2 + Edta-4 + H2O = CuOH(Edta)-3 + H+
log_k 8.5
delta_h 0 kJ
-gamma 0 0
# Id: 2319694
# log K source: NIST46.2
# Delta H source: NIST46.2
#T and ionic strength:
Ag+ + Edta-4 = Ag(Edta)-3
log_k 8.08
delta_h -31.38 kJ
-gamma 0 0
# Id: 209691
# log K source: NIST46.2
# Delta H source: NIST46.2
#T and ionic strength:
Ag+ + Edta-4 + H+ = AgH(Edta)-2
log_k 15.21
delta_h 0 kJ
-gamma 0 0
# Id: 209693
# log K source: SCD2.62
# Delta H source: SCD2.62
#T and ionic strength:
Ni+2 + Edta-4 = Ni(Edta)-2
```

```
log_k 20.1
delta_h -30.9616 kJ
-gamma 0 0
# Id: 5409691
# log K source: NIST46.2
# Delta H source: NIST46.2
#T and ionic strength:
Ni+2 + Edta-4 + H+ = NiH(Edta)-
log_k 23.6
delta_h -38.4928 kJ
-gamma 0 0
# Id: 5409692
# log K source: NIST46.2
# Delta H source: NIST46.2
#T and ionic strength:
Ni+2 + Edta-4 + H2O = NiOH(Edta)-3 + H+
log_k 7.6
delta_h 0 kJ
-gamma 0 0
# Id: 5409693
# log K source: NIST46.2
# Delta H source: NIST46.2
#T and ionic strength:
Co+2 + Edta-4 = Co(Edta)-2
log_k 18.1657
delta_h -15 kJ
-gamma 0 0
# Id: 2009691
# log K source: NIST46.4
# Delta H source: NIST46.4
#T and ionic strength: 0.10 25.0
Co+2 + Edta-4 + H+ = CoH(Edta)-
log_k 21.5946
delta_h -22.9 kJ
-gamma 0 0
# Id: 2009692
# log K source: NIST46.4
# Delta H source: NIST46.4
#T and ionic strength: 0.10 25.0
Co+2 + Edta-4 + 2H+ = CoH2(Edta)
log_k 23.4986
delta_h 0 kJ
-gamma 0 0
# Id: 2009693
# log K source: NIST46.4
# Delta H source: NIST46.2
#T and ionic strength: 1.00 25.0
Co+3 + Edta-4 = Co(Edta)-
log_k 43.9735
delta_h 0 kJ
-gamma 0 0
# Id: 2019691
# log K source: NIST46.4
# Delta H source: NIST46.2
```

```
#T and ionic strength: 0.10 25.0
Co+3 + Edta-4 + H+ = CoH(Edta)
log_k 47.168
delta_h 0 kJ
-gamma 0 0
# Id: 2019692
# log K source: NIST46.4
# Delta H source: NIST46.2
#T and ionic strength: 0.10 20.0
Fe+2 + Edta-4 = Fe(Edta)-2
log_k 16
delta_h -16.736 kJ
-gamma 0 0
# Id: 2809690
# log K source: NIST46.2
# Delta H source: NIST46.2
#T and ionic strength:
Fe+2 + Edta-4 + H+ = FeH(Edta)-
log_k 19.06
delta_h -27.6144 kJ
-gamma 0 0
# Id: 2809691
# log K source: NIST46.2
# Delta H source: NIST46.2
#T and ionic strength:
Fe+2 + Edta-4 + H2O = FeOH(Edta)-3 + H+
log_k 6.5
delta_h 0 kJ
-gamma 0 0
# Id: 2809692
# log K source: SCD2.62
# Delta H source: SCD2.62
#T and ionic strength:
Fe+2 + Edta-4 + 2H2O = Fe(OH)2(Edta)-4 + 2H+
log_k -4
delta_h 0 kJ
-gamma 0 0
# Id: 2809693
# log K source: SCD2.62
# Delta H source: SCD2.62
#T and ionic strength:
Fe+3 + Edta-4 = Fe(Edta)-
log_k 27.7
delta_h -11.2968 kJ
-gamma 0 0
# Id: 2819690
# log K source: NIST46.2
# Delta H source: NIST46.2
#T and ionic strength:
Fe+3 + Edta-4 + H+ = FeH(Edta)
log_k 29.2
delta_h -11.7152 kJ
-gamma 0 0
# Id: 2819691
```

```
# log K source: NIST46.2
# Delta H source: NIST46.2
#T and ionic strength:
Fe+3 + Edta-4 + H2O = FeOH(Edta)-2 + H+
log_k 19.9
delta_h 0 kJ
-gamma 0 0
# Id: 2819692
# log K source: NIST46.2
# Delta H source: NIST46.2
#T and ionic strength:
Fe+3 + Edta-4 + 2H2O = Fe(OH)2(Edta)-3 + 2H+
log_k 9.85
delta_h 0 kJ
-gamma 0 0
# Id: 2819693
# log K source: SCD2.62
# Delta H source: SCD2.62
#T and ionic strength:
Mn+2 + Edta-4 = Mn(Edta)-2
log_k 15.6
delta_h -19.2464 kJ
-gamma 0 0
# Id: 4709691
# log K source: NIST46.2
# Delta H source: NIST46.2
#T and ionic strength:
Mn+2 + Edta-4 + H+ = MnH(Edta)-
log_k 19.1
delta_h -24.2672 kJ
-gamma 0 0
# Id: 4709692
# log K source: NIST46.2
# Delta H source: NIST46.2
#T and ionic strength:
Cr+2 + Edta-4 = Cr(Edta)-2
log_k 15.3
delta_h 0 kJ
-gamma 0 0
# Id: 2109691
# log K source: NIST46.2
# Delta H source: NIST46.2
#T and ionic strength:
Cr+2 + Edta-4 + H+ = CrH(Edta)-
log_k 19.1
delta_h 0 kJ
-gamma 0 0
# Id: 2109692
# log K source: SCD2.62
# Delta H source: SCD2.62
#T and ionic strength:
Cr(OH)2+ + Edta-4 + 2H+ = Cr(Edta)- + 2H2O
log_k 35.5
delta_h 0 kJ
```

```
-gamma 0 0
# Id: 2119691
# log K source: NIST46.2
# Delta H source: NIST46.2
#T and ionic strength:
Cr(OH)2+ + Edta-4 + 3H+ = CrH(Edta) + 2H2O
log_k 37.4
delta_h 0 kJ
-gamma 0 0
# Id: 2119692
# log K source: NIST46.2
# Delta H source: NIST46.2
#T and ionic strength:
Cr(OH)2+ + Edta-4 + H+ = CrOH(Edta)-2 + H2O
log_k 27.7
delta_h 0 kJ
-gamma 0 0
# Id: 2119693
# log K source: NIST46.2
# Delta H source: NIST46.2
#T and ionic strength:
Be+2 + Edta-4 = Be(Edta)-2
log_k 11.4157
delta_h 41 kJ
-gamma 0 0
# Id: 1109691
# log K source: NIST46.4
# Delta H source: NIST46.4
#T and ionic strength: 0.10 25.0
Mg+2 + Edta-4 = Mg(Edta)-2
log_k 10.57
delta_h 13.8072 kJ
-gamma 0 0
# Id: 4609690
# log K source: NIST46.2
# Delta H source: NIST46.2
#T and ionic strength:
Mg+2 + Edta-4 + H+ = MgH(Edta)-
log_k 14.97
delta_h 0 kJ
-gamma 0 0
# Id: 4609691
# log K source: NIST46.2
# Delta H source: NIST46.2
#T and ionic strength:
Ca+2 + Edta-4 = Ca(Edta)-2
log_k 12.42
delta_h -25.5224 kJ
-gamma 0 0
# Id: 1509690
# log K source: NIST46.2
# Delta H source: NIST46.2
#T and ionic strength:
Ca+2 + Edta-4 + H+ = CaH(Edta)-
```

```
log_k 15.9
delta_h 0 kJ
-gamma 0 0
# Id: 1509691
# log K source: NIST46.2
# Delta H source: NIST46.2
#T and ionic strength:
Sr+2 + Edta-4 = Sr(Edta)-2
log_k 10.4357
delta_h -17 kJ
-gamma 0 0
# Id: 8009691
# log K source: NIST46.4
# Delta H source: NIST46.4
#T and ionic strength: 0.10 25.0
Sr+2 + Edta-4 + H+ = SrH(Edta)-
log_k 14.7946
delta_h 0 kJ
-gamma 0 0
# Id: 8009692
# log K source: NIST46.4
# Delta H source: NIST46.2
#T and ionic strength: 0.10 20.0
Ba+2 + Edta-4 = Ba(Edta)-2
log_k 7.72
delta_h -20.5016 kJ
-gamma 0 0
# Id: 1009691
# log K source: SCD2.62
# Delta H source: SCD2.62
#T and ionic strength:
Na+ + Edta-4 = Na(Edta)-3
log_k 2.7
delta_h -5.8576 kJ
-gamma 0 0
# Id: 5009690
# log K source: NIST46.2
# Delta H source: NIST46.2
#T and ionic strength:
K+ + Edta-4 = K(Edta)-3
log_k 1.7
delta_h 0 kJ
-gamma 0 0
# Id: 4109690
# log K source: NIST46.2
# Delta H source: NIST46.2
#T and ionic strength:
H+ + Propionate- = H(Propionate)
log_k 4.874
delta_h 0.66 kJ
-gamma 0 0
# Id: 3309711
# log K source: NIST46.4
# Delta H source: NIST46.4
```

```
#T and ionic strength: 0.00 25.0
Pb+2 + Propionate- = Pb(Propionate)+
log_k 2.64
delta_h 0 kJ
-gamma 0 0
# Id: 6009711
# log K source: NIST46.4
# Delta H source: SCD2.62
#T and ionic strength: 0.00 35.0
Pb+2 + 2Propionate- = Pb(Propionate)2
log_k 3.1765
delta_h 0 kJ
-gamma 0 0
# Id: 6009712
# log K source: NIST46.4
# Delta H source: SCD2.62
#T and ionic strength: 2.00 25.0
Zn+2 + Propionate- = Zn(Propionate)+
log_k 1.4389
delta_h 0 kJ
-gamma 0 0
# Id: 9509711
# log K source: NIST46.4
# Delta H source: NIST46.2
#T and ionic strength: 0.10 25.0
Zn+2 + 2Propionate- = Zn(Propionate)2
log_k 1.842
delta_h 0 kJ
-gamma 0 0
# Id: 9509712
# log K source: NIST46.4
# Delta H source: NIST46.2
#T and ionic strength: 1.00 25.0
Cd+2 + Propionate- = Cd(Propionate)+
log_k 1.598
delta_h 0 kJ
-gamma 0 0
# Id: 1609711
# log K source: NIST46.4
# Delta H source: NIST46.2
#T and ionic strength: 1.00 25.0
Cd+2 + 2Propionate- = Cd(Propionate)2
log_k 2.472
delta_h 0 kJ
-gamma 0 0
# Id: 1609712
# log K source: NIST46.4
# Delta H source: NIST46.2
#T and ionic strength: 1.00 25.0
Hg(OH)2 + 2H+ + Propionate- = Hg(Propionate)+ + 2H2O
log_k 10.594
delta_h 0 kJ
-gamma 0 0
# Id: 3619711
```

```
# log K source: NIST46.4
# Delta H source: NIST46.2
#T and ionic strength: 0.00 25.0
Cu+2 + Propionate- = Cu(Propionate)+
log_k 2.22
delta_h 4.1 kJ
-gamma 0 0
# Id: 2319711
# log K source: NIST46.4
# Delta H source: NIST46.4
#T and ionic strength: 0.00 25.0
Cu+2 + 2Propionate- = Cu(Propionate)2
log_k 3.5
delta_h 0 kJ
-gamma 0 0
# Id: 2319712
# log K source: NIST46.4
# Delta H source: NIST46.2
#T and ionic strength: 0.00 25.0
Ni+2 + Propionate- = Ni(Propionate)+
log_k 0.908
delta_h 0 kJ
-gamma 0 0
# Id: 5409711
# log K source: NIST46.4
# Delta H source: SCD2.62
#T and ionic strength: 1.00 25.0
Co+2 + Propionate- = Co(Propionate)+
log_k 0.671
delta_h 4.6 kJ
-gamma 0 0
# Id: 2009711
# log K source: NIST46.4
# Delta H source: NIST46.4
#T and ionic strength: 2.00 25.0
Co+2 + 2Propionate- = Co(Propionate)2
log_k 0.5565
delta_h 16 kJ
-gamma 0 0
# Id: 2009712
# log K source: NIST46.4
# Delta H source: NIST46.4
#T and ionic strength: 2.00 25.0
Fe+3 + Propionate- = Fe(Propionate)+2
log_k 4.012
delta_h 0 kJ
-gamma 0 0
# Id: 2819711
# log K source: NIST46.4
# Delta H source: NIST46.2
#T and ionic strength: 1.00 20.0
Cr(OH)2+ + 2H+ + Propionate- = Cr(Propionate)+2 + 2H2O
log_k 15.0773
delta_h 0 kJ
```

```
-gamma 0 0
# Id: 2119711
# log K source: NIST46.4
# Delta H source: SCD2.62
#T and ionic strength: 0.50 25.0
Cr(OH)2+ + 2H+ + 2Propionate- = Cr(Propionate)2+ + 2H2O
log_k 17.9563
delta_h 0 kJ
-gamma 0 0
# Id: 2119712
# log K source: NIST46.4
# Delta H source: SCD2.62
#T and ionic strength: 0.50 25.0
Cr(OH)2+ + 2H+ + 3Propionate- = Cr(Propionate)3 + 2H2O
log_k 20.8858
delta_h 0 kJ
-gamma 0 0
# Id: 2119713
# log K source: NIST46.4
# Delta H source: SCD2.62
#T and ionic strength: 0.50 25.0
Mg+2 + Propionate- = Mg(Propionate)+
log_k 0.9689
delta_h 4.2677 kJ
-gamma 0 0
# Id: 4609710
# log K source: NIST46.4
# Delta H source: SCD2.62
#T and ionic strength: 0.10 25.0
Ca+2 + Propionate- = Ca(Propionate)+
log_k 0.9289
delta_h 3.3472 kJ
-gamma 0 0
# Id: 1509710
# log K source: NIST46.4
# Delta H source: SCD2.62
#T and ionic strength: 0.10 25.0
Sr+2 + Propionate- = Sr(Propionate)+
log_k 0.8589
delta_h 0 kJ
-gamma 0 0
# Id: 8009711
# log K source: NIST46.4
# Delta H source: NIST46.2
#T and ionic strength: 0.10 25.0
Ba+2 + Propionate- = Ba(Propionate)+
log_k 0.7689
delta_h 0 kJ
-gamma 0 0
# Id: 1009711
# log K source: NIST46.4
# Delta H source: SCD2.62
#T and ionic strength: 0.10 25.0
Ba+2 + 2Propionate- = Ba(Propionate)2
```

```
log_k 0.9834
delta_h 0 kJ
-gamma 0 0
# Id: 1009712
# log K source: NIST46.4
# Delta H source: SCD2.62
#T and ionic strength: 0.10 25.0
H+ + Butyrate- = H(Butyrate)
log_k 4.819
delta_h 2.8 kJ
-gamma 0 0
# Id: 3309721
# log K source: NIST46.4
# Delta H source: NIST46.4
#T and ionic strength: 0.00 25.0
Pb+2 + Butyrate- = Pb(Butyrate)+
log_k 2.101
delta_h 0 kJ
-gamma 0 0
# Id: 6009721
# log K source: NIST46.4
# Delta H source: SCD2.62
#T and ionic strength: 2.00 25.0
Zn+2 + Butyrate- = Zn(Butyrate)+
log_k 1.4289
delta_h 0 kJ
-gamma 0 0
# Id: 9509721
# log K source: NIST46.4
# Delta H source: NIST46.2
#T and ionic strength: 0.10 25.0
Hg(OH)2 + 2H+ + Butyrate- = Hg(Butyrate)+ + 2H2O
log_k 10.3529
delta_h 0 kJ
-gamma 0 0
# Id: 3619721
# log K source: NIST46.4
# Delta H source: NIST46.2
#T and ionic strength: 0.10 25.0
Cu+2 + Butyrate- = Cu(Butyrate)+
log_k 2.14
delta_h 0 kJ
-gamma 0 0
# Id: 2319721
# log K source: NIST46.4
# Delta H source: NIST46.2
#T and ionic strength: 0.00 25.0
Ni+2 + Butyrate- = Ni(Butyrate)+
log_k 0.691
delta_h 0 kJ
-gamma 0 0
# Id: 5409721
# log K source: NIST46.4
# Delta H source: SCD2.62
```

```
#T and ionic strength: 2.00 25.0
Co+2 + Butyrate- = Co(Butyrate)+
log_k 0.591
delta_h 0 kJ
-gamma 0 0
# Id: 2009721
# log K source: NIST46.4
# Delta H source: NIST46.2
#T and ionic strength: 2.00 25.0
Co+2 + 2Butyrate- = Co(Butyrate)2
log_k 0.7765
delta_h 0 kJ
-gamma 0 0
# Id: 2009722
# log K source: NIST46.4
# Delta H source: NIST46.2
#T and ionic strength: 2.00 25.0
Mg+2 + Butyrate- = Mg(Butyrate)+
log_k 0.9589
delta_h 0 kJ
-gamma 0 0
# Id: 4609720
# log K source: NIST46.4
# Delta H source: SCD2.62
#T and ionic strength: 0.10 25.0
Ca+2 + Butyrate- = Ca(Butyrate)+
log_k 0.9389
delta_h 3.3472 kJ
-gamma 0 0
# Id: 1509720
# log K source: NIST46.4
# Delta H source: SCD2.62
#T and ionic strength: 0.10 25.0
Sr+2 + Butyrate- = Sr(Butyrate)+
log_k 0.7889
delta_h 0 kJ
-gamma 0 0
# Id: 8009721
# log K source: NIST46.4
# Delta H source: NIST46.2
#T and ionic strength: 0.10 25.0
Ba+2 + Butyrate- = Ba(Butyrate)+
log_k 0.7389
delta_h 0 kJ
-gamma 0 0
# Id: 1009721
# log K source: NIST46.4
# Delta H source: SCD2.62
#T and ionic strength: 0.10 25.0
Ba+2 + 2Butyrate- = Ba(Butyrate)2
log_k 0.88
delta_h 0 kJ
-gamma 0 0
# Id: 1009722
```

```
# log K source: SCD2.62
# Delta H source: SCD2.62
#T and ionic strength:
H+ + Isobutyrate- = H(Isobutyrate)
log_k 4.849
delta_h 3.2217 kJ
-gamma 0 0
# Id: 3309731
# log K source: NIST46.2
# Delta H source: NIST46.2
#T and ionic strength:
Zn+2 + Isobutyrate- = Zn(Isobutyrate)+
log_k 1.44
delta_h 0 kJ
-gamma 0 0
# Id: 9509731
# log K source: NIST46.2
# Delta H source: NIST46.2
#T and ionic strength:
Cu+2 + Isobutyrate- = Cu(Isobutyrate)+
log_k 2.17
delta_h 0 kJ
-gamma 0 0
# Id: 2319731
# log K source: NIST46.2
# Delta H source: NIST46.2
#T and ionic strength:
Cu+2 + 2Isobutyrate- = Cu(Isobutyrate)2
log_k 3.3
delta_h 0 kJ
-gamma 0 0
# Id: 2319732
# log K source: NIST46.2
# Delta H source: NIST46.2
#T and ionic strength:
Fe+3 + Isobutyrate- = Fe(Isobutyrate)+2
log_k 4.2
delta_h 0 kJ
-gamma 0 0
# Id: 2819731
# log K source: NIST46.2
# Delta H source: NIST46.2
#T and ionic strength:
Ca+2 + Isobutyrate- = Ca(Isobutyrate)+
log_k 0.51
delta_h 0 kJ
-gamma 0 0
# Id: 1509731
# log K source: SCD2.62
# Delta H source: SCD2.62
#T and ionic strength:
H+ + Two_picoline = H(Two_picoline)+
log_k 5.95
delta_h -25.5224 kJ
```

```
-gamma 0 0
# Id: 3309801
# log K source: NIST46.2
# Delta H source: NIST46.2
#T and ionic strength:
Cu+2 + Two_picoline = Cu(Two_picoline)+2
log_k 1.3
delta_h 0 kJ
-gamma 0 0
# Id: 2319801
# log K source: NIST46.2
# Delta H source: NIST46.2
#T and ionic strength:
Cu+2 + 2Two_picoline = Cu(Two_picoline)2+2
log_k 2.8
delta_h 0 kJ
-gamma 0 0
# Id: 2319802
# log K source: NIST46.2
# Delta H source: NIST46.2
#T and ionic strength:
Cu+ + Two_picoline = Cu(Two_picoline)+
log_k 5.4
delta_h 0 kJ
-gamma 0 0
# Id: 2309801
# log K source: NIST46.2
# Delta H source: NIST46.2
#T and ionic strength:
Cu+ + 2Two_picoline = Cu(Two_picoline)2+
log_k 7.65
delta_h 0 kJ
-gamma 0 0
# Id: 2309802
# log K source: NIST46.2
# Delta H source: NIST46.2
#T and ionic strength:
Cu+ + 3Two_picoline = Cu(Two_picoline)3+
log_k 8.5
delta_h 0 kJ
-gamma 0 0
# Id: 2309803
# log K source: NIST46.2
# Delta H source: NIST46.2
#T and ionic strength:
Ag+ + Two_picoline = Ag(Two_picoline)+
log_k 2.32
delta_h -24.2672 kJ
-gamma 0 0
# Id: 209801
# log K source: NIST46.2
# Delta H source: NIST46.2
#T and ionic strength:
Ag+ + 2Two_picoline = Ag(Two_picoline)2+
```

```
log_k 4.68
delta_h -42.6768 kJ
-gamma 0 0
# Id: 209802
# log K source: NIST46.2
# Delta H source: NIST46.2
#T and ionic strength:
Ni+2 + Two_picoline = Ni(Two_picoline)+2
log_k 0.4
delta_h 0 kJ
-gamma 0 0
# Id: 5409801
# log K source: NIST46.2
# Delta H source: NIST46.2
#T and ionic strength:
H+ + Three_picoline = H(Three_picoline)+
log_k 5.7
delta_h -23.8488 kJ
-gamma 0 0
# Id: 3309811
# log K source: NIST46.2
# Delta H source: NIST46.2
#T and ionic strength:
Zn+2 + Three_picoline = Zn(Three_picoline)+2
log_k 1
delta_h 0 kJ
-gamma 0 0
# Id: 9509811
# log K source: NIST46.2
# Delta H source: NIST46.2
#T and ionic strength:
Zn+2 + 2Three_picoline = Zn(Three_picoline)2+2
log_k 2.1
delta_h 0 kJ
-gamma 0 0
# Id: 9509812
# log K source: NIST46.2
# Delta H source: NIST46.2
#T and ionic strength:
Zn+2 + 3Three_picoline = Zn(Three_picoline)3+2
log_k 2.6
delta_h 0 kJ
-gamma 0 0
# Id: 9509813
# log K source: NIST46.2
# Delta H source: NIST46.2
#T and ionic strength:
Zn+2 + 4Three_picoline = Zn(Three_picoline)4+2
log_k 3.7
delta_h 0 kJ
-gamma 0 0
# Id: 9509814
# log K source: NIST46.2
# Delta H source: NIST46.2
```

```
#T and ionic strength:
Cd+2 + Three_picoline = Cd(Three_picoline)+2
log_k 1.42
delta_h 0 kJ
-gamma 0 0
# Id: 1609811
# log K source: SCD2.62
# Delta H source: SCD2.62
#T and ionic strength:
Cd+2 + 2Three_picoline = Cd(Three_picoline)2+2
log_k 2.27
delta_h 0 kJ
-gamma 0 0
# Id: 1609812
# log K source: SCD2.62
# Delta H source: SCD2.62
#T and ionic strength:
Cd+2 + 3Three_picoline = Cd(Three_picoline)3+2
log_k 3.6
delta_h 0 kJ
-gamma 0 0
# Id: 1609813
# log K source: NIST46.2
# Delta H source: NIST46.2
#T and ionic strength:
Cd+2 + 4Three_picoline = Cd(Three_picoline)4+2
log_k 4
delta_h 0 kJ
-gamma 0 0
# Id: 1609814
# log K source: NIST46.2
# Delta H source: NIST46.2
#T and ionic strength:
Cu+ + Three_picoline = Cu(Three_picoline)+
log_k 5.6
delta_h 0 kJ
-gamma 0 0
# Id: 2309811
# log K source: NIST46.2
# Delta H source: NIST46.2
#T and ionic strength:
Cu+ + 2Three_picoline = Cu(Three_picoline)2+
log_k 7.78
delta_h 0 kJ
-gamma 0 0
# Id: 2309812
# log K source: NIST46.2
# Delta H source: NIST46.2
#T and ionic strength:
Cu+ + 3Three_picoline = Cu(Three_picoline)3+
log_k 8.6
delta_h 0 kJ
-gamma 0 0
# Id: 2309813
```

```
# log K source: NIST46.2
# Delta H source: NIST46.2
#T and ionic strength:
Cu+ + 4Three_picoline = Cu(Three_picoline)4+
log_k 9
delta_h 0 kJ
-gamma 0 0
# Id: 2309814
# log K source: NIST46.2
# Delta H source: NIST46.2
#T and ionic strength:
Cu+2 + Three_picoline = Cu(Three_picoline)+2
log_k 2.77
delta_h 0 kJ
-gamma 0 0
# Id: 2319811
# log K source: NIST46.2
# Delta H source: NIST46.2
#T and ionic strength:
Cu+2 + 2Three_picoline = Cu(Three_picoline)2+2
log_k 4.8
delta_h 0 kJ
-gamma 0 0
# Id: 2319812
# log K source: NIST46.2
# Delta H source: NIST46.2
#T and ionic strength:
Cu+2 + 3Three_picoline = Cu(Three_picoline)3+2
log_k 6.3
delta_h 0 kJ
-gamma 0 0
# Id: 2319813
# log K source: NIST46.2
# Delta H source: NIST46.2
#T and ionic strength:
Cu+2 + 4Three_picoline = Cu(Three_picoline)4+2
log_k 7.2
delta_h 0 kJ
-gamma 0 0
# Id: 2319814
# log K source: NIST46.2
# Delta H source: NIST46.2
#T and ionic strength:
Ag+ + Three_picoline = Ag(Three_picoline)+
log_k 2.2
delta_h -21.7568 kJ
-gamma 0 0
# Id: 209811
# log K source: NIST46.2
# Delta H source: NIST46.2
#T and ionic strength:
Ag+ + 2Three_picoline = Ag(Three_picoline)2+
log_k 4.46
delta_h -49.7896 kJ
```

```
-gamma 0 0
# Id: 209812
# log K source: NIST46.2
# Delta H source: NIST46.2
#T and ionic strength:
Ni+2 + Three_picoline = Ni(Three_picoline)+2
log_k 1.87
delta_h 0 kJ
-gamma 0 0
# Id: 5409811
# log K source: NIST46.2
# Delta H source: NIST46.2
#T and ionic strength:
Ni+2 + 2Three_picoline = Ni(Three_picoline)2+2
log_k 3.3
delta_h 0 kJ
-gamma 0 0
# Id: 5409812
# log K source: NIST46.2
# Delta H source: NIST46.2
#T and ionic strength:
Ni+2 + 3Three_picoline = Ni(Three_picoline)3+2
log_k 4.1
delta_h 0 kJ
-gamma 0 0
# Id: 5409813
# log K source: NIST46.2
# Delta H source: NIST46.2
#T and ionic strength:
Ni+2 + 4Three_picoline = Ni(Three_picoline)4+2
log_k 4.6
delta_h 0 kJ
-gamma 0 0
# Id: 5409814
# log K source: NIST46.2
# Delta H source: NIST46.2
#T and ionic strength:
Co+2 + Three_picoline = Co(Three_picoline)+2
log_k 1.4
delta_h 0 kJ
-gamma 0 0
# Id: 2009811
# log K source: NIST46.4
# Delta H source: NIST46.2
#T and ionic strength: 0.50 25.0
Co+2 + 2Three_picoline = Co(Three_picoline)2+2
log_k 2.2
delta_h 0 kJ
-gamma 0 0
# Id: 2009812
# log K source: NIST46.4
# Delta H source: NIST46.2
#T and ionic strength: 0.50 25.0
Co+2 + 3Three_picoline = Co(Three_picoline)3+2
```

```
log_k 2.5
delta_h 0 kJ
-gamma 0 0
# Id: 2009813
# log K source: NIST46.4
# Delta H source: NIST46.2
#T and ionic strength: 0.50 25.0
H+ + Four_picoline = H(Four_picoline)+
log_k 6.03
delta_h -25.3132 kJ
-gamma 0 0
# Id: 3309821
# log K source: NIST46.2
# Delta H source: NIST46.2
#T and ionic strength:
Zn+2 + Four_picoline = Zn(Four_picoline)+2
log_k 1.4
delta_h 0 kJ
-gamma 0 0
# Id: 9509821
# log K source: NIST46.2
# Delta H source: NIST46.2
#T and ionic strength:
Zn+2 + 2Four_picoline = Zn(Four_picoline)2+2
log_k 2.11
delta_h 0 kJ
-gamma 0 0
# Id: 9509822
# log K source: NIST46.2
# Delta H source: NIST46.2
#T and ionic strength:
Zn+2 + 3Four_picoline = Zn(Four_picoline)3+2
log_k 2.85
delta_h 0 kJ
-gamma 0 0
# Id: 9509823
# log K source: NIST46.2
# Delta H source: NIST46.2
#T and ionic strength:
Cd+2 + Four_picoline = Cd(Four_picoline)+2
log_k 1.59
delta_h 0 kJ
-gamma 0 0
# Id: 1609821
# log K source: SCD2.62
# Delta H source: SCD2.62
#T and ionic strength:
Cd+2 + 2Four_picoline = Cd(Four_picoline)2+2
log_k 2.4
delta_h 0 kJ
-gamma 0 0
# Id: 1609822
# log K source: SCD2.62
# Delta H source: SCD2.62
```

```
#T and ionic strength:
Cd+2 + 3Four_picoline = Cd(Four_picoline)3+2
log_k 3.18
delta_h 0 kJ
-gamma 0 0
# Id: 1609823
# log K source: SCD2.62
# Delta H source: SCD2.62
#T and ionic strength:
Cd+2 + 4Four_picoline = Cd(Four_picoline)4+2
log_k 4
delta_h 0 kJ
-gamma 0 0
# Id: 1609824
# log K source: NIST46.2
# Delta H source: NIST46.2
#T and ionic strength:
Cu+ + Four_picoline = Cu(Four_picoline)+
log_k 5.65
delta_h 0 kJ
-gamma 0 0
# Id: 2309821
# log K source: NIST46.2
# Delta H source: NIST46.2
#T and ionic strength:
Cu+ + 2Four_picoline = Cu(Four_picoline)2+
log_k 8.2
delta_h 0 kJ
-gamma 0 0
# Id: 2309822
# log K source: NIST46.2
# Delta H source: NIST46.2
#T and ionic strength:
Cu+ + 3Four_picoline = Cu(Four_picoline)3+
log_k 8.8
delta_h 0 kJ
-gamma 0 0
# Id: 2309823
# log K source: NIST46.2
# Delta H source: NIST46.2
#T and ionic strength:
Cu+ + 4Four_picoline = Cu(Four_picoline)4+
log_k 9.2
delta_h 0 kJ
-gamma 0 0
# Id: 2309824
# log K source: NIST46.2
# Delta H source: NIST46.2
#T and ionic strength:
Cu+2 + Four_picoline = Cu(Four_picoline)+2
log_k 2.88
delta_h 0 kJ
-gamma 0 0
# Id: 2319821
```

```
# log K source: NIST46.2
# Delta H source: NIST46.2
#T and ionic strength:
Cu+2 + 2Four_picoline = Cu(Four_picoline)2+2
log_k 5.16
delta_h 0 kJ
-gamma 0 0
# Id: 2319822
# log K source: NIST46.2
# Delta H source: NIST46.2
#T and ionic strength:
Cu+2 + 3Four_picoline = Cu(Four_picoline)3+2
log_k 6.77
delta_h 0 kJ
-gamma 0 0
# Id: 2319823
# log K source: NIST46.2
# Delta H source: NIST46.2
#T and ionic strength:
Cu+2 + 4Four_picoline = Cu(Four_picoline)4+2
log_k 8.08
delta_h 0 kJ
-gamma 0 0
# Id: 2319824
# log K source: NIST46.2
# Delta H source: NIST46.2
#T and ionic strength:
Cu+2 + 5Four_picoline = Cu(Four_picoline)5+2
log_k 8.3
delta_h 0 kJ
-gamma 0 0
# Id: 2319825
# log K source: NIST46.2
# Delta H source: NIST46.2
#T and ionic strength:
Ag+ + Four_picoline = Ag(Four_picoline)+
log_k 2.03
delta_h -25.5224 kJ
-gamma 0 0
# Id: 209821
# log K source: NIST46.2
# Delta H source: NIST46.2
#T and ionic strength:
Ag+ + 2Four_picoline = Ag(Four_picoline)2+
log_k 4.39
delta_h -53.5552 kJ
-gamma 0 0
# Id: 209822
# log K source: NIST46.2
# Delta H source: NIST46.2
#T and ionic strength:
Ni+2 + Four_picoline = Ni(Four_picoline)+2
log_k 2.11
delta_h 0 kJ
```

```
-gamma 0 0
# Id: 5409821
# log K source: NIST46.2
# Delta H source: NIST46.2
#T and ionic strength:
Ni+2 + 2Four_picoline = Ni(Four_picoline)2+2
log_k 3.59
delta_h 0 kJ
-gamma 0 0
# Id: 5409822
# log K source: NIST46.2
# Delta H source: NIST46.2
#T and ionic strength:
Ni+2 + 3Four_picoline = Ni(Four_picoline)3+2
log_k 4.34
delta_h 0 kJ
-gamma 0 0
# Id: 5409823
# log K source: NIST46.2
# Delta H source: NIST46.2
#T and ionic strength:
Ni+2 + 4Four_picoline = Ni(Four_picoline)4+2
log_k 4.7
delta_h 0 kJ
-gamma 0 0
# Id: 5409824
# log K source: NIST46.2
# Delta H source: NIST46.2
#T and ionic strength:
Co+2 + Four_picoline = Co(Four_picoline)+2
log_k 1.56
delta_h 0 kJ
-gamma 0 0
# Id: 2009821
# log K source: NIST46.4
# Delta H source: NIST46.2
#T and ionic strength: 0.50 25.0
Co+2 + 2Four_picoline = Co(Four_picoline)2+2
log_k 2.51
delta_h 0 kJ
-gamma 0 0
# Id: 2009822
# log K source: NIST46.4
# Delta H source: NIST46.2
#T and ionic strength: 0.50 25.0
Co+2 + 3Four_picoline = Co(Four_picoline)3+2
log_k 2.94
delta_h 0 kJ
-gamma 0 0
# Id: 2009823
# log K source: NIST46.4
# Delta H source: NIST46.2
#T and ionic strength: 0.50 25.0
Co+2 + 4Four_picoline = Co(Four_picoline)4+2
```

```
log_k 3.17
delta_h 0 kJ
-gamma 0 0
# Id: 2009824
# log K source: NIST46.4
# Delta H source: NIST46.2
#T and ionic strength: 0.50 25.0
H+ + Formate- = H(Formate)
log_k 3.745
delta_h 0.1674 kJ
-gamma 0 0
# Id: 3309831
# log K source: NIST46.2
# Delta H source: NIST46.2
#T and ionic strength:
Pb+2 + Formate- = Pb(Formate)+
log_k 2.2
delta_h 0 kJ
-gamma 0 0
# Id: 6009831
# log K source: SCD2.62
# Delta H source: SCD2.62
#T and ionic strength:
Zn+2 + Formate- = Zn(Formate)+
log_k 1.44
delta_h 0 kJ
-gamma 0 0
# Id: 9509831
# log K source: NIST46.2
# Delta H source: NIST46.2
#T and ionic strength:
Cd+2 + Formate- = Cd(Formate)+
log_k 1.7
delta_h 0 kJ
-gamma 0 0
# Id: 1609831
# log K source: SCD2.62
# Delta H source: SCD2.62
#T and ionic strength:
Hg(OH)2 + Formate- + 2H+ = Hg(Formate)+ + 2H2O
log_k 9.6
delta_h 0 kJ
-gamma 0 0
# Id: 3619831
# log K source: NIST46.2
# Delta H source: NIST46.2
#T and ionic strength:
Cu+2 + Formate- = Cu(Formate)+
log_k 2
delta_h 0 kJ
-gamma 0 0
# Id: 2319831
# log K source: NIST46.2
# Delta H source: NIST46.2
```

```
#T and ionic strength:
Ni+2 + Formate- = Ni(Formate)+
log_k 1.22
delta_h 0 kJ
-gamma 0 0
# Id: 5409831
# log K source: SCD2.62
# Delta H source: SCD2.62
#T and ionic strength:
Co+2 + Formate- = Co(Formate)+
log_k 1.209
delta_h 0 kJ
-gamma 0 0
# Id: 2009831
# log K source: NIST46.4
# Delta H source: NIST46.2
#T and ionic strength: 0.50 30.0
Co+2 + 2Formate- = Co(Formate)2
log_k 1.1365
delta_h 0 kJ
-gamma 0 0
# Id: 2009832
# log K source: NIST46.4
# Delta H source: NIST46.2
#T and ionic strength: 2.00 25.0
Cr+2 + Formate- = Cr(Formate)+
log_k 1.07
delta_h 0 kJ
-gamma 0 0
# Id: 2109831
# log K source: NIST46.2
# Delta H source: NIST46.2
#T and ionic strength:
Mg+2 + Formate- = Mg(Formate)+
log_k 1.43
delta_h 0 kJ
-gamma 0 0
# Id: 4609831
# log K source: NIST46.2
# Delta H source: NIST46.2
#T and ionic strength:
Ca+2 + Formate- = Ca(Formate)+
log_k 1.43
delta_h 4.184 kJ
-gamma 0 0
# Id: 1509831
# log K source: NIST46.2
# Delta H source: NIST46.2
#T and ionic strength:
Sr+2 + Formate- = Sr(Formate)+
log_k 1.39
delta_h 4 kJ
-gamma 0 0
# Id: 8009831
```

```
# log K source: NIST46.4
# Delta H source: NIST46.4
#T and ionic strength: 0.00 25.0
Ba+2 + Formate- = Ba(Formate)+
log_k 1.38
delta_h 0 kJ
-gamma 0 0
# Id: 1009831
# log K source: NIST46.2
# Delta H source: NIST46.2
#T and ionic strength:
H+ + Isovalerate- = H(Isovalerate)
log_k 4.781
delta_h 4.5606 kJ
-gamma 0 0
# Id: 3309841
# log K source: NIST46.2
# Delta H source: NIST46.2
#T and ionic strength:
Zn+2 + Isovalerate- = Zn(Isovalerate)+
log_k 1.39
delta_h 0 kJ
-gamma 0 0
# Id: 9509841
# log K source: NIST46.2
# Delta H source: NIST46.2
#T and ionic strength:
Cu+2 + Isovalerate- = Cu(Isovalerate)+
log_k 2.08
delta_h 0 kJ
-gamma 0 0
# Id: 2319841
# log K source: NIST46.2
# Delta H source: NIST46.2
#T and ionic strength:
Ca+2 + Isovalerate- = Ca(Isovalerate)+
log_k 0.2
delta_h 0 kJ
-gamma 0 0
# Id: 1509841
# log K source: SCD2.62
# Delta H source: SCD2.62
#T and ionic strength:
H+ + Valerate- = H(Valerate)
log_k 4.843
delta_h 2.887 kJ
-gamma 0 0
# Id: 3309851
# log K source: NIST46.2
# Delta H source: NIST46.2
#T and ionic strength:
Cu+2 + Valerate- = Cu(Valerate)+
log_k 2.12
delta_h 0 kJ
```

```
-gamma 0 0
# Id: 2319851
# log K source: NIST46.2
# Delta H source: NIST46.2
#T and ionic strength:
Ca+2 + Valerate- = Ca(Valerate)+
log_k 0.3
delta_h 0 kJ
-gamma 0 0
# Id: 1509851
# log K source: SCD2.62
# Delta H source: SCD2.62
#T and ionic strength:
Ba+2 + Valerate- = Ba(Valerate)+
log_k -0.2
delta_h 0 kJ
-gamma 0 0
# Id: 1009851
# log K source: SCD2.62
# Delta H source: SCD2.62
#T and ionic strength:
H+ + Acetate- = H(Acetate)
log_k 4.757
delta_h 0.41 kJ
-gamma 0 0
# Id: 3309921
# log K source: NIST46.4
# Delta H source: NIST46.4
#T and ionic strength: 0.00 25.0
Sn(OH)2 + 2H+ + Acetate- = Sn(Acetate)+ + 2H2O
log_k 10.0213
delta_h 0 kJ
-gamma 0 0
# Id: 7909921
# log K source: NIST46.4
# Delta H source: NIST46.2
#T and ionic strength: 3.00 25.0
Sn(OH)2 + 2H+ + 2Acetate- = Sn(Acetate)2 + 2H2O
log_k 12.32
delta_h 0 kJ
-gamma 0 0
# Id: 7909922
# log K source: NIST46.4
# Delta H source: NIST46.2
#T and ionic strength: 3.00 25.0
Sn(OH)2 + 2H+ + 3Acetate- = Sn(Acetate)3- + 2H2O
log_k 13.55
delta_h 0 kJ
-gamma 0 0
# Id: 7909923
# log K source: NIST46.4
# Delta H source: NIST46.2
#T and ionic strength: 3.00 25.0
Pb+2 + Acetate- = Pb(Acetate)+
```

```
log_k 2.68
delta_h -0.4 kJ
-gamma 0 0
# Id: 6009921
# log K source: NIST46.4
# Delta H source: NIST46.4
#T and ionic strength: 0.00 25.0
Pb+2 + 2Acetate- = Pb(Acetate)2
log_k 4.08
delta_h -0.8 kJ
-gamma 0 0
# Id: 6009922
# log K source: NIST46.4
# Delta H source: NIST46.4
#T and ionic strength: 0.00 25.0
Tl+ + Acetate- = Tl(Acetate)
log_k -0.11
delta_h 0 kJ
-gamma 0 0
# Id: 8709921
# log K source: NIST46.4
# Delta H source: NIST46.2
#T and ionic strength: 0.00 25.0
Zn+2 + Acetate- = Zn(Acetate)+
log_k 1.58
delta_h 8.3 kJ
-gamma 0 0
# Id: 9509921
# log K source: NIST46.4
# Delta H source: NIST46.4
#T and ionic strength: 0.00 25.0
Zn+2 + 2Acetate- = Zn(Acetate)2
log_k 2.6434
delta_h 22 kJ
-gamma 0 0
# Id: 9509922
# log K source: NIST46.4
# Delta H source: NIST46.4
#T and ionic strength: 0.10 25.0
Cd+2 + Acetate- = Cd(Acetate)+
log_k 1.93
delta_h 9.6 kJ
-gamma 0 0
# Id: 1609921
# log K source: NIST46.4
# Delta H source: NIST46.4
#T and ionic strength: 0.00 25.0
Cd+2 + 2Acetate- = Cd(Acetate)2
log_k 2.86
delta_h 15 kJ
-gamma 0 0
# Id: 1609922
# log K source: NIST46.4
# Delta H source: NIST46.4
```

```
#T and ionic strength: 0.00 25.0
Hg(OH)2 + 2H+ + Acetate- = Hg(Acetate)+ + 2H2O
log_k 10.494
delta_h 0 kJ
-gamma 0 0
# Id: 3619920
# log K source: NIST46.4
# Delta H source: NIST46.2
#T and ionic strength: 0.00 25.0
Hg(OH)2 + 2H+ + 2Acetate- = Hg(Acetate)2 + 2H2O
log_k 13.83
delta_h 0 kJ
-gamma 0 0
# Id: 3619921
# log K source: NIST46.4
# Delta H source: SCD2.62
#T and ionic strength: 3.00 25.0
Cu+2 + Acetate- = Cu(Acetate)+
log_k 2.21
delta_h 7.1 kJ
-gamma 0 0
# Id: 2319921
# log K source: NIST46.4
# Delta H source: NIST46.4
#T and ionic strength: 0.00 25.0
Cu+2 + 2Acetate- = Cu(Acetate)2
log_k 3.4
delta_h 12 kJ
-gamma 0 0
# Id: 2319922
# log K source: NIST46.4
# Delta H source: NIST46.4
#T and ionic strength: 0.00 25.0
Cu+2 + 3Acetate- = Cu(Acetate)3-
log_k 3.9434
delta_h 6.2 kJ
-gamma 0 0
# Id: 2319923
# log K source: NIST46.4
# Delta H source: NIST46.4
#T and ionic strength: 0.10 25.0
Ag+ + Acetate- = Ag(Acetate)
log_k 0.73
delta_h 3 kJ
-gamma 0 0
# Id: 209921
# log K source: NIST46.4
# Delta H source: NIST46.4
#T and ionic strength: 0.00 25.0
Ag+ + 2Acetate- = Ag(Acetate)2-
log_k 0.64
delta_h 3 kJ
-gamma 0 0
# Id: 209922
```

```
# log K source: NIST46.4
# Delta H source: NIST46.4
#T and ionic strength: 0.00 25.0
Ni+2 + Acetate- = Ni(Acetate)+
log_k 1.37
delta_h 8.7 kJ
-gamma 0 0
# Id: 5409921
# log K source: NIST46.4
# Delta H source: NIST46.4
#T and ionic strength: 0.00 25.0
Ni+2 + 2Acetate- = Ni(Acetate)2
log_k 2.1
delta_h 10 kJ
-gamma 0 0
# Id: 5409922
# log K source: NIST46.4
# Delta H source: NIST46.4
#T and ionic strength: 0.00 25.0
Co+2 + Acetate- = Co(Acetate)+
log_k 1.38
delta_h 0 kJ
-gamma 0 0
# Id: 2009921
# log K source: NIST46.4
# Delta H source: NIST46.2
#T and ionic strength: 0.00 25.0
Co+2 + 2Acetate- = Co(Acetate)2
log_k 0.7565
delta_h 0 kJ
-gamma 0 0
# Id: 2009922
# log K source: NIST46.4
# Delta H source: NIST46.2
#T and ionic strength: 2.00 25.0
Fe+2 + Acetate- = Fe(Acetate)+
log_k 1.4
delta_h 0 kJ
-gamma 0 0
# Id: 2809920
# log K source: NIST46.4
# Delta H source: NIST46.2
#T and ionic strength: 0.00 25.0
Fe+3 + Acetate- = Fe(Acetate)+2
log_k 4.0234
delta_h 0 kJ
-gamma 0 0
# Id: 2819920
# log K source: NIST46.4
# Delta H source: NIST46.2
#T and ionic strength: 0.10 20.0
Fe+3 + 2Acetate- = Fe(Acetate)2+
log_k 7.5723
delta_h 0 kJ
```

```
-gamma 0 0
# Id: 2819921
# log K source: NIST46.4
# Delta H source: NIST46.2
#T and ionic strength: 0.10 20.0
Fe+3 + 3Acetate- = Fe(Acetate)3
log_k 9.5867
delta_h 0 kJ
-gamma 0 0
# Id: 2819922
# log K source: NIST46.4
# Delta H source: NIST46.2
#T and ionic strength: 0.10 20.0
Mn+2 + Acetate- = Mn(Acetate)+
log_k 1.4
delta_h 0 kJ
-gamma 0 0
# Id: 4709920
# log K source: NIST46.4
# Delta H source: NIST46.2
#T and ionic strength: 0.00 25.0
Cr+2 + Acetate- = Cr(Acetate)+
log_k 1.8
delta_h 0 kJ
-gamma 0 0
# Id: 2109921
# log K source: NIST46.4
# Delta H source: NIST46.2
#T and ionic strength: 0.00 25.0
Cr+2 + 2Acetate- = Cr(Acetate)2
log_k 2.92
delta_h 0 kJ
-gamma 0 0
# Id: 2109922
# log K source: NIST46.4
# Delta H source: NIST46.2
#T and ionic strength: 0.00 25.0
Cr(OH)2+ + 2H+ + Acetate- = Cr(Acetate)+2 + 2H2O
log_k 15.0073
delta_h -125.62 kJ
-gamma 0 0
# Id: 2119921
# log K source: NIST46.4
# Delta H source: NIST46.4
#T and ionic strength: 0.50 25.0
Cr(OH)2+ + 2H+ + 2Acetate- = Cr(Acetate)2+ + 2H2O
log_k 17.9963
delta_h -117.62 kJ
-gamma 0 0
# Id: 2119922
# log K source: NIST46.4
# Delta H source: NIST46.4
#T and ionic strength: 0.50 25.0
Cr(OH)2+ + 2H+ + 3Acetate- = Cr(Acetate)3 + 2H2O
```

```
log_k 20.7858
delta_h -96.62 kJ
-gamma 0 0
# Id: 2119923
# log K source: NIST46.4
# Delta H source: NIST46.4
#T and ionic strength: 0.50 25.0
Be+2 + Acetate- = Be(Acetate)+
log_k 2.0489
delta_h 0 kJ
-gamma 0 0
# Id: 1109921
# log K source: NIST46.4
# Delta H source: NIST46.2
#T and ionic strength: 0.10 25.0
Be+2 + 2Acetate- = Be(Acetate)2
log_k 3.0034
delta_h 0 kJ
-gamma 0 0
# Id: 1109922
# log K source: NIST46.4
# Delta H source: NIST46.2
#T and ionic strength: 0.10 25.0
Mg+2 + Acetate- = Mg(Acetate)+
log_k 1.27
delta_h 0 kJ
-gamma 0 0
# Id: 4609920
# log K source: NIST46.4
# Delta H source: NIST46.2
#T and ionic strength: 0.00 25.0
Ca+2 + Acetate- = Ca(Acetate)+
log_k 1.18
delta_h 4 kJ
-gamma 0 0
# Id: 1509920
# log K source: NIST46.4
# Delta H source: NIST46.4
#T and ionic strength: 0.00 25.0
Sr+2 + Acetate- = Sr(Acetate)+
log_k 1.14
delta_h 0 kJ
-gamma 0 0
# Id: 8009921
# log K source: NIST46.4
# Delta H source: NIST46.2
#T and ionic strength: 0.00 25.0
Ba+2 + Acetate- = Ba(Acetate)+
log_k 1.07
delta_h 0 kJ
-gamma 0 0
# Id: 1009921
# log K source: NIST46.4
# Delta H source: NIST46.2
```

```
#T and ionic strength: 0.00 25.0
Na+ + Acetate- = Na(Acetate)
log_k -0.18
delta_h 12 kJ
-gamma 0 0
# Id: 5009920
# log K source: NIST46.4
# Delta H source: NIST46.4
#T and ionic strength: 0.00 25.0
K+ + Acetate- = K(Acetate)
log_k -0.1955
delta_h 4.184 kJ
-gamma 0 0
# Id: 4109921
# log K source: NIST46.4
# Delta H source: NIST46.2
#T and ionic strength: 0.10 25.0
H+ + Tartarate-2 = H(Tartarate)-
log_k 4.366
delta_h -0.7531 kJ
-gamma 0 0
# Id: 3309931
# log K source: NIST46.2
# Delta H source: NIST46.2
#T and ionic strength:
2H+ + Tartarate-2 = H2(Tartarate)
log_k 7.402
delta_h -3.6819 kJ
-gamma 0 0
# Id: 3309932
# log K source: NIST46.2
# Delta H source: NIST46.2
#T and ionic strength:
Sn(OH)2 + 2H+ + Tartarate-2 = Sn(Tartarate) + 2H2O
log_k 13.1518
delta_h 0 kJ
-gamma 0 0
# Id: 7909931
# log K source: NIST46.4
# Delta H source: NIST46.2
#T and ionic strength: 0.10 20.0
Pb+2 + Tartarate-2 = Pb(Tartarate)
log_k 3.98
delta_h 0 kJ
-gamma 0 0
# Id: 6009931
# log K source: NIST46.2
# Delta H source: NIST46.2
#T and ionic strength:
Al+3 + 2Tartarate-2 = Al(Tartarate)2-
log_k 9.37
delta_h 0 kJ
-gamma 0 0
# Id: 309931
```

```
# log K source: NIST46.2
# Delta H source: NIST46.2
#T and ionic strength:
Tl+ + Tartarate-2 = Tl(Tartarate)-
log_k 1.4
delta_h 0 kJ
-gamma 0 0
# Id: 8709931
# log K source: NIST46.2
# Delta H source: NIST46.2
#T and ionic strength:
Tl+ + Tartarate-2 + H+ = TlH(Tartarate)
log_k 4.8
delta_h 0 kJ
-gamma 0 0
# Id: 8709932
# log K source: NIST46.2
# Delta H source: NIST46.2
#T and ionic strength:
Zn+2 + Tartarate-2 = Zn(Tartarate)
log_k 3.43
delta_h 0 kJ
-gamma 0 0
# Id: 9509931
# log K source: NIST46.2
# Delta H source: NIST46.2
#T and ionic strength:
Zn+2 + 2Tartarate-2 = Zn(Tartarate)2-2
log_k 5.5
delta_h 0 kJ
-gamma 0 0
# Id: 9509932
# log K source: NIST46.2
# Delta H source: NIST46.2
#T and ionic strength:
Zn+2 + Tartarate-2 + H+ = ZnH(Tartarate)+
log_k 5.9
delta_h 0 kJ
-gamma 0 0
# Id: 9509933
# log K source: NIST46.2
# Delta H source: NIST46.2
#T and ionic strength:
Cd+2 + Tartarate-2 = Cd(Tartarate)
log_k 2.7
delta_h 0 kJ
-gamma 0 0
# Id: 1609931
# log K source: NIST46.2
# Delta H source: NIST46.2
#T and ionic strength:
Cd+2 + 2Tartarate-2 = Cd(Tartarate)2-2
log_k 4.1
delta_h 0 kJ
```

```
-gamma 0 0
# Id: 1609932
# log K source: NIST46.2
# Delta H source: NIST46.2
#T and ionic strength:
Hg(OH)2 + Tartarate-2 + 2H+ = Hg(Tartarate) + 2H2O
log_k 14
delta_h 0 kJ
-gamma 0 0
# Id: 3619931
# log K source: NIST46.2
# Delta H source: NIST46.2
#T and ionic strength:
Cu+2 + Tartarate-2 = Cu(Tartarate)
log_k 3.97
delta_h 0 kJ
-gamma 0 0
# Id: 2319931
# log K source: NIST46.2
# Delta H source: NIST46.2
#T and ionic strength:
Cu+2 + Tartarate-2 + H+ = CuH(Tartarate)+
log_k 6.7
delta_h 0 kJ
-gamma 0 0
# Id: 2319932
# log K source: NIST46.2
# Delta H source: NIST46.2
#T and ionic strength:
Ni+2 + Tartarate-2 = Ni(Tartarate)
log_k 3.46
delta_h 0 kJ
-gamma 0 0
# Id: 5409931
# log K source: NIST46.2
# Delta H source: NIST46.2
#T and ionic strength:
Ni+2 + Tartarate-2 + H+ = NiH(Tartarate)+
log_k 5.89
delta_h 0 kJ
-gamma 0 0
# Id: 5409932
# log K source: NIST46.2
# Delta H source: NIST46.2
#T and ionic strength:
Co+2 + Tartarate-2 = Co(Tartarate)
log_k 3.05
delta_h 0 kJ
-gamma 0 0
# Id: 2009931
# log K source: NIST46.4
# Delta H source: NIST46.2
#T and ionic strength: 0.00 25.0
Co+2 + 2Tartarate-2 = Co(Tartarate)2-2
```

```
log_k 4
delta_h 0 kJ
-gamma 0 0
# Id: 2009932
# log K source: NIST46.4
# Delta H source: NIST46.2
#T and ionic strength: 0.00 25.0
Co+2 + H+ + Tartarate-2 = CoH(Tartarate)+
log_k 5.754
delta_h 0 kJ
-gamma 0 0
# Id: 2009933
# log K source: NIST46.4
# Delta H source: NIST46.2
#T and ionic strength: 1.00 20.0
Fe+2 + Tartarate-2 = Fe(Tartarate)
log_k 3.1
delta_h 0 kJ
-gamma 0 0
# Id: 2809931
# log K source: NIST46.2
# Delta H source: NIST46.2
#T and ionic strength:
Fe+3 + Tartarate-2 = Fe(Tartarate)+
log_k 7.78
delta_h 0 kJ
-gamma 0 0
# Id: 2819931
# log K source: NIST46.2
# Delta H source: NIST46.2
#T and ionic strength:
Mn+2 + Tartarate-2 = Mn(Tartarate)
log_k 3.38
delta_h 0 kJ
-gamma 0 0
# Id: 4709931
# log K source: NIST46.2
# Delta H source: NIST46.2
#T and ionic strength:
Mn+2 + Tartarate-2 + H+ = MnH(Tartarate)+
log_k 6
delta_h 0 kJ
-gamma 0 0
# Id: 4709932
# log K source: NIST46.2
# Delta H source: NIST46.2
#T and ionic strength:
Mg+2 + Tartarate-2 = Mg(Tartarate)
log_k 2.3
delta_h 0 kJ
-gamma 0 0
# Id: 4609931
# log K source: NIST46.2
# Delta H source: NIST46.2
```

```
#T and ionic strength:
Mg+2 + Tartarate-2 + H+ = MgH(Tartarate)+
log_k 5.75
delta_h 0 kJ
-gamma 0 0
# Id: 4609932
# log K source: NIST46.2
# Delta H source: NIST46.2
#T and ionic strength:
Be+2 + Tartarate-2 = Be(Tartarate)
log_k 2.768
delta_h 0 kJ
-gamma 0 0
# Id: 1109931
# log K source: NIST46.4
# Delta H source: NIST46.2
#T and ionic strength: 0.50 25.0
Be+2 + 2Tartarate-2 = Be(Tartarate)2-2
log_k 4.008
delta_h 0 kJ
-gamma 0 0
# Id: 1109932
# log K source: NIST46.4
# Delta H source: NIST46.2
#T and ionic strength: 0.50 25.0
Ca+2 + Tartarate-2 = Ca(Tartarate)
log_k 2.8
delta_h -8.368 kJ
-gamma 0 0
# Id: 1509931
# log K source: NIST46.2
# Delta H source: NIST46.2
#T and ionic strength:
Ca+2 + Tartarate-2 + H+ = CaH(Tartarate)+
log_k 5.86
delta_h -9.1211 kJ
-gamma 0 0
# Id: 1509932
# log K source: NIST46.2
# Delta H source: NIST46.2
#T and ionic strength:
Sr+2 + Tartarate-2 = Sr(Tartarate)
log_k 2.55
delta_h 0 kJ
-gamma 0 0
# Id: 8009931
# log K source: NIST46.4
# Delta H source: NIST46.2
#T and ionic strength: 0.00 20.0
Sr+2 + H+ + Tartarate-2 = SrH(Tartarate)+
log_k 5.8949
delta_h 0 kJ
-gamma 0 0
# Id: 8009932
```

```
# log K source: NIST46.4
# Delta H source: NIST46.2
#T and ionic strength: 0.10 25.0
Ba+2 + Tartarate-2 = Ba(Tartarate)
log_k 2.54
delta_h 0 kJ
-gamma 0 0
# Id: 1009931
# log K source: NIST46.2
# Delta H source: NIST46.2
#T and ionic strength:
Ba+2 + Tartarate-2 + H+ = BaH(Tartarate)+
log_k 5.77
delta_h 0 kJ
-gamma 0 0
# Id: 1009932
# log K source: NIST46.2
# Delta H source: NIST46.2
#T and ionic strength:
Na+ + Tartarate-2 = Na(Tartarate)-
log_k 0.9
delta_h -0.8368 kJ
-gamma 0 0
# Id: 5009931
# log K source: NIST46.2
# Delta H source: NIST46.2
#T and ionic strength:
Na+ + Tartarate-2 + H+ = NaH(Tartarate)
log_k 4.58
delta_h -2.8451 kJ
-gamma 0 0
# Id: 5009932
# log K source: NIST46.2
# Delta H source: NIST46.2
#T and ionic strength:
K+ + Tartarate-2 = K(Tartarate)-
log_k 0.8
delta_h 0 kJ
-gamma 0 0
# Id: 4109931
# log K source: NIST46.2
# Delta H source: NIST46.2
#T and ionic strength:
H+ + Glycine- = H(Glycine)
log_k 9.778
delta_h -44.3504 kJ
-gamma 0 0
# Id: 3309941
# log K source: NIST46.2
# Delta H source: NIST46.2
#T and ionic strength:
2H+ + Glycine- = H2(Glycine)+
log_k 12.128
delta_h -48.4507 kJ
```

```
-gamma 0 0
# Id: 3309942
# log K source: NIST46.2
# Delta H source: NIST46.2
#T and ionic strength:
Pb+2 + Glycine- = Pb(Glycine)+
log_k 5.47
delta_h 0 kJ
-gamma 0 0
# Id: 6009941
# log K source: NIST46.2
# Delta H source: NIST46.2
#T and ionic strength:
Pb+2 + 2Glycine- = Pb(Glycine)2
log_k 8.86
delta_h 0 kJ
-gamma 0 0
# Id: 6009942
# log K source: SCD2.62
# Delta H source: SCD2.62
#T and ionic strength:
Tl+ + Glycine- = Tl(Glycine)
log_k 1.72
delta_h 0 kJ
-gamma 0 0
# Id: 8709941
# log K source: NIST46.2
# Delta H source: NIST46.2
#T and ionic strength:
Zn+2 + Glycine- = Zn(Glycine)+
log_k 5.38
delta_h -11.7152 kJ
-gamma 0 0
# Id: 9509941
# log K source: NIST46.2
# Delta H source: NIST46.2
#T and ionic strength:
Zn+2 + 2Glycine- = Zn(Glycine)2
log_k 9.81
delta_h -24.2672 kJ
-gamma 0 0
# Id: 9509942
# log K source: NIST46.2
# Delta H source: NIST46.2
#T and ionic strength:
Zn+2 + 3Glycine- = Zn(Glycine)3-
log_k 12.3
delta_h -39.748 kJ
-gamma 0 0
# Id: 9509943
# log K source: NIST46.2
# Delta H source: NIST46.2
#T and ionic strength:
Cd+2 + Glycine- = Cd(Glycine)+
```

```
log_k 4.69
delta_h -8.7864 kJ
-gamma 0 0
# Id: 1609941
# log K source: NIST46.2
# Delta H source: NIST46.2
#T and ionic strength:
Cd+2 + 2Glycine- = Cd(Glycine)2
log_k 8.4
delta_h -22.5936 kJ
-gamma 0 0
# Id: 1609942
# log K source: NIST46.2
# Delta H source: NIST46.2
#T and ionic strength:
Cd+2 + 3Glycine- = Cd(Glycine)3-
log_k 10.7
delta_h -35.9824 kJ
-gamma 0 0
# Id: 1609943
# log K source: NIST46.2
# Delta H source: NIST46.2
#T and ionic strength:
Hg(OH)2 + Glycine- + 2H+ = Hg(Glycine)+ + 2H2O
log_k 17
delta_h 0 kJ
-gamma 0 0
# Id: 3619941
# log K source: SCD2.62
# Delta H source: SCD2.62
#T and ionic strength:
Hg(OH)2 + 2Glycine- + 2H+ = Hg(Glycine)2 + 2H2O
log_k 25.8
delta_h 0 kJ
-gamma 0 0
# Id: 3619942
# log K source: SCD2.62
# Delta H source: SCD2.62
#T and ionic strength:
Cu+ + 2Glycine- = Cu(Glycine)2-
log_k 10.3
delta_h 0 kJ
-gamma 0 0
# Id: 2309941
# log K source: NIST46.2
# Delta H source: NIST46.2
#T and ionic strength:
Cu+2 + Glycine- = Cu(Glycine)+
log_k 8.57
delta_h -25.104 kJ
-gamma 0 0
# Id: 2319941
# log K source: NIST46.2
# Delta H source: NIST46.2
```

```
#T and ionic strength:
Cu+2 + 2Glycine- = Cu(Glycine)2
log_k 15.7
delta_h -54.8104 kJ
-gamma 0 0
# Id: 2319942
# log K source: NIST46.2
# Delta H source: NIST46.2
#T and ionic strength:
Ag+ + Glycine- = Ag(Glycine)
log_k 3.51
delta_h -19.2464 kJ
-gamma 0 0
# Id: 209941
# log K source: NIST46.2
# Delta H source: NIST46.2
#T and ionic strength:
Ag+ + 2Glycine- = Ag(Glycine)2-
log_k 6.89
delta_h -48.116 kJ
-gamma 0 0
# Id: 209942
# log K source: NIST46.2
# Delta H source: NIST46.2
#T and ionic strength:
Ni+2 + Glycine- = Ni(Glycine)+
log_k 6.15
delta_h -18.828 kJ
-gamma 0 0
# Id: 5409941
# log K source: NIST46.2
# Delta H source: NIST46.2
#T and ionic strength:
Ni+2 + 2Glycine- = Ni(Glycine)2
log_k 11.12
delta_h -38.0744 kJ
-gamma 0 0
# Id: 5409942
# log K source: NIST46.2
# Delta H source: NIST46.2
#T and ionic strength:
Ni+2 + 3Glycine- = Ni(Glycine)3-
log_k 14.63
delta_h -62.3416 kJ
-gamma 0 0
# Id: 5409943
# log K source: SCD2.62
# Delta H source: SCD2.62
#T and ionic strength:
Co+2 + Glycine- = Co(Glycine)+
log_k 5.07
delta_h -12 kJ
-gamma 0 0
# Id: 2009941
```

```
# log K source: NIST46.4
# Delta H source: NIST46.4
#T and ionic strength: 0.00 25.0
Co+2 + 2Glycine- = Co(Glycine)2
log_k 9.07
delta_h -26 kJ
-gamma 0 0
# Id: 2009942
# log K source: NIST46.4
# Delta H source: NIST46.4
#T and ionic strength: 0.00 25.0
Co+2 + 3Glycine- = Co(Glycine)3-
log_k 11.6
delta_h -41 kJ
-gamma 0 0
# Id: 2009943
# log K source: NIST46.4
# Delta H source: NIST46.4
#T and ionic strength: 0.00 25.0
Co+2 + Glycine- + H2O = CoOH(Glycine) + H+
log_k -5.02
delta_h 0 kJ
-gamma 0 0
# Id: 2009944
# log K source: NIST46.4
# Delta H source: NIST46.2
#T and ionic strength: 0.10 25.0
Fe+2 + Glycine- = Fe(Glycine)+
log_k 4.31
delta_h -15.0624 kJ
-gamma 0 0
# Id: 2809941
# log K source: NIST46.2
# Delta H source: NIST46.2
#T and ionic strength:
Fe+2 + 2Glycine- = Fe(Glycine)2
log_k 8.29
delta_h 0 kJ
-gamma 0 0
# Id: 2809942
# log K source: NIST46.2
# Delta H source: NIST46.2
#T and ionic strength:
Fe+3 + Glycine- = Fe(Glycine)+2
log_k 9.38
delta_h 0 kJ
-gamma 0 0
# Id: 2819941
# log K source: NIST46.2
# Delta H source: NIST46.2
#T and ionic strength:
Fe+3 + Glycine- + H+ = FeH(Glycine)+3
log_k 11.55
delta_h 0 kJ
```

```
-gamma 0 0
# Id: 2819942
# log K source: NIST46.2
# Delta H source: NIST46.2
#T and ionic strength:
Mn+2 + Glycine- = Mn(Glycine)+
log_k 3.19
delta_h -1.2552 kJ
-gamma 0 0
# Id: 4709941
# log K source: NIST46.2
# Delta H source: NIST46.2
#T and ionic strength:
Mn+2 + 2Glycine- = Mn(Glycine)2
log_k 5.4
delta_h 0 kJ
-gamma 0 0
# Id: 4709942
# log K source: NIST46.2
# Delta H source: NIST46.2
#T and ionic strength:
Cr(OH)2+ + Glycine- + 2H+ = Cr(Glycine)+2 + 2H2O
log_k 18.7
delta_h 0 kJ
-gamma 0 0
# Id: 2119941
# log K source: SCD2.62
# Delta H source: SCD2.62
#T and ionic strength:
Cr(OH)2+ + 2Glycine- + 2H+ = Cr(Glycine)2+ + 2H2O
log_k 25.6
delta_h 0 kJ
-gamma 0 0
# Id: 2119942
# log K source: SCD2.62
# Delta H source: SCD2.62
#T and ionic strength:
Cr(OH)2+ + 3Glycine- + 2H+ = Cr(Glycine)3 + 2H2O
log_k 31.6
delta_h 0 kJ
-gamma 0 0
# Id: 2119943
# log K source: SCD2.62
# Delta H source: SCD2.62
#T and ionic strength:
Mg+2 + Glycine- = Mg(Glycine)+
log_k 2.08
delta_h 4.184 kJ
-gamma 0 0
# Id: 4609941
# log K source: NIST46.2
# Delta H source: NIST46.2
#T and ionic strength:
Ca+2 + Glycine- = Ca(Glycine)+
```

```
log_k 1.39
delta_h -4.184 kJ
-gamma 0 0
# Id: 1509941
# log K source: NIST46.2
# Delta H source: NIST46.2
#T and ionic strength:
Ca+2 + Glycine- + H+ = CaH(Glycine)+2
log_k 10.1
delta_h -35.9824 kJ
-gamma 0 0
# Id: 1509942
# log K source: NIST46.2
# Delta H source: NIST46.2
#T and ionic strength:
Sr+2 + Glycine- = Sr(Glycine)+
log_k 0.91
delta_h 0 kJ
-gamma 0 0
# Id: 8009941
# log K source: NIST46.4
# Delta H source: NIST46.2
#T and ionic strength: 0.00 25.0
Ba+2 + Glycine- = Ba(Glycine)+
log_k 0.77
delta_h 0 kJ
-gamma 0 0
# Id: 1009941
# log K source: NIST46.2
# Delta H source: NIST46.2
#T and ionic strength:
H+ + Salicylate-2 = H(Salicylate)-
log_k 13.7
delta_h -35.7732 kJ
-gamma 0 0
# Id: 3309951
# log K source: NIST46.2
# Delta H source: NIST46.2
#T and ionic strength:
2H+ + Salicylate-2 = H2(Salicylate)
log_k 16.8
delta_h -38.7857 kJ
-gamma 0 0
# Id: 3309952
# log K source: NIST46.2
# Delta H source: NIST46.2
#T and ionic strength:
Zn+2 + Salicylate-2 = Zn(Salicylate)
log_k 7.71
delta_h 0 kJ
-gamma 0 0
# Id: 9509951
# log K source: SCD2.62
# Delta H source: SCD2.62
```

```
#T and ionic strength:
Zn+2 + Salicylate-2 + H+ = ZnH(Salicylate)+
log_k 15.5
delta_h 0 kJ
-gamma 0 0
# Id: 9509952
# log K source: NIST46.2
# Delta H source: NIST46.2
#T and ionic strength:
Cd+2 + Salicylate-2 = Cd(Salicylate)
log_k 6.2
delta_h 0 kJ
-gamma 0 0
# Id: 1609951
# log K source: NIST46.2
# Delta H source: NIST46.2
#T and ionic strength:
Cd+2 + Salicylate-2 + H+ = CdH(Salicylate)+
log_k 16
delta_h 0 kJ
-gamma 0 0
# Id: 1609952
# log K source: NIST46.2
# Delta H source: NIST46.2
#T and ionic strength:
Cu+2 + Salicylate-2 = Cu(Salicylate)
log_k 11.3
delta_h -17.9912 kJ
-gamma 0 0
# Id: 2319951
# log K source: NIST46.2
# Delta H source: NIST46.2
#T and ionic strength:
Cu+2 + 2Salicylate-2 = Cu(Salicylate)2-2
log_k 19.3
delta_h 0 kJ
-gamma 0 0
# Id: 2319952
# log K source: NIST46.2
# Delta H source: NIST46.2
#T and ionic strength:
Cu+2 + Salicylate-2 + H+ = CuH(Salicylate)+
log_k 14.8
delta_h 0 kJ
-gamma 0 0
# Id: 2319953
# log K source: NIST46.2
# Delta H source: NIST46.2
#T and ionic strength:
Ni+2 + Salicylate-2 = Ni(Salicylate)
log_k 8.2
delta_h 0 kJ
-gamma 0 0
# Id: 5409951
```

```
# log K source: NIST46.2
# Delta H source: NIST46.2
#T and ionic strength:
Ni+2 + 2Salicylate-2 = Ni(Salicylate)2-2
log_k 12.64
delta_h 0 kJ
-gamma 0 0
# Id: 5409952
# log K source: SCD2.62
# Delta H source: SCD2.62
#T and ionic strength:
Co+2 + Salicylate-2 = Co(Salicylate)
log_k 7.4289
delta_h 0 kJ
-gamma 0 0
# Id: 2009951
# log K source: NIST46.4
# Delta H source: NIST46.2
#T and ionic strength: 0.10 20.0
Co+2 + 2Salicylate-2 = Co(Salicylate)2-2
log_k 11.8
delta_h 0 kJ
-gamma 0 0
# Id: 2009952
# log K source: NIST46.4
# Delta H source: NIST46.2
#T and ionic strength: 0.10 20.0
Fe+2 + Salicylate-2 = Fe(Salicylate)
log_k 7.2
delta_h 0 kJ
-gamma 0 0
# Id: 2809951
# log K source: NIST46.2
# Delta H source: NIST46.2
#T and ionic strength:
Fe+2 + 2Salicylate-2 = Fe(Salicylate)2-2
log_k 11.6
delta_h 0 kJ
-gamma 0 0
# Id: 2809952
# log K source: NIST46.2
# Delta H source: NIST46.2
#T and ionic strength:
Fe+3 + Salicylate-2 = Fe(Salicylate)+
log_k 17.6
delta_h 0 kJ
-gamma 0 0
# Id: 2819951
# log K source: NIST46.2
# Delta H source: NIST46.2
#T and ionic strength:
Fe+3 + 2Salicylate-2 = Fe(Salicylate)2-
log_k 29.3
delta_h 0 kJ
```

```
-gamma 0 0
# Id: 2819952
# log K source: NIST46.2
# Delta H source: NIST46.2
#T and ionic strength:
Mn+2 + Salicylate-2 = Mn(Salicylate)
log_k 6.5
delta_h 0 kJ
-gamma 0 0
# Id: 4709951
# log K source: NIST46.2
# Delta H source: NIST46.2
#T and ionic strength:
Mn+2 + 2Salicylate-2 = Mn(Salicylate)2-2
log_k 10.1
delta_h 0 kJ
-gamma 0 0
# Id: 4709952
# log K source: NIST46.2
# Delta H source: NIST46.2
#T and ionic strength:
Be+2 + Salicylate-2 = Be(Salicylate)
log_k 13.3889
delta_h -31.7732 kJ
-gamma 0 0
# Id: 1109951
# log K source: NIST46.4
# Delta H source: NIST46.4
#T and ionic strength: 0.10 25.0
Be+2 + 2Salicylate-2 = Be(Salicylate)2-2
log_k 23.25
delta_h 0 kJ
-gamma 0 0
# Id: 1109952
# log K source: NIST46.4
# Delta H source: NIST46.2
#T and ionic strength: 0.10 25.0
Mg+2 + Salicylate-2 = Mg(Salicylate)
log_k 5.76
delta_h 0 kJ
-gamma 0 0
# Id: 4609951
# log K source: NIST46.2
# Delta H source: NIST46.2
#T and ionic strength:
Mg+2 + Salicylate-2 + H+ = MgH(Salicylate)+
log_k 15.3
delta_h 0 kJ
-gamma 0 0
# Id: 4609952
# log K source: SCD2.62
# Delta H source: SCD2.62
#T and ionic strength:
Ca+2 + Salicylate-2 = Ca(Salicylate)
```

```
log_k 4.05
delta_h 0 kJ
-gamma 0 0
# Id: 1509951
# log K source: NIST46.2
# Delta H source: NIST46.2
#T and ionic strength:
Ca+2 + Salicylate-2 + H+ = CaH(Salicylate)+
log_k 14.3
delta_h 0 kJ
-gamma 0 0
# Id: 1509952
# log K source: NIST46.2
# Delta H source: NIST46.2
#T and ionic strength:
Ba+2 + Salicylate-2 + H+ = BaH(Salicylate)+
log_k 13.9
delta_h 0 kJ
-gamma 0 0
# Id: 1009951
# log K source: SCD2.62
# Delta H source: SCD2.62
#T and ionic strength:
H+ + Glutamate-2 = H(Glutamate)-
log_k 9.96
delta_h -41.0032 kJ
-gamma 0 0
# Id: 3309961
# log K source: NIST46.2
# Delta H source: NIST46.2
#T and ionic strength:
2H+ + Glutamate-2 = H2(Glutamate)
log_k 14.26
delta_h -43.5136 kJ
-gamma 0 0
# Id: 3309962
# log K source: NIST46.2
# Delta H source: NIST46.2
#T and ionic strength:
3H+ + Glutamate-2 = H3(Glutamate)+
log_k 16.42
delta_h -46.8608 kJ
-gamma 0 0
# Id: 3309963
# log K source: NIST46.2
# Delta H source: NIST46.2
#T and ionic strength:
Pb+2 + Glutamate-2 = Pb(Glutamate)
log_k 6.43
delta_h 0 kJ
-gamma 0 0
# Id: 6009961
# log K source: SCD2.62
# Delta H source: SCD2.62
```

```
#T and ionic strength:
Pb+2 + 2Glutamate-2 = Pb(Glutamate)2-2
log_k 8.61
delta_h 0 kJ
-gamma 0 0
# Id: 6009962
# log K source: SCD2.62
# Delta H source: SCD2.62
#T and ionic strength:
Pb+2 + Glutamate-2 + H+ = PbH(Glutamate)+
log_k 14.08
delta_h 0 kJ
-gamma 0 0
# Id: 6009963
# log K source: SCD2.62
# Delta H source: SCD2.62
#T and ionic strength:
Al+3 + Glutamate-2 + H+ = AlH(Glutamate)+2
log_k 13.07
delta_h 0 kJ
-gamma 0 0
# Id: 309961
# log K source: NIST46.2
# Delta H source: NIST46.2
#T and ionic strength:
Zn+2 + Glutamate-2 = Zn(Glutamate)
log_k 6.2
delta_h 0 kJ
-gamma 0 0
# Id: 9509961
# log K source: SCD2.62
# Delta H source: SCD2.62
#T and ionic strength:
Zn+2 + 2Glutamate-2 = Zn(Glutamate)2-2
log_k 9.13
delta_h 0 kJ
-gamma 0 0
# Id: 9509962
# log K source: SCD2.62
# Delta H source: SCD2.62
#T and ionic strength:
Zn+2 + 3Glutamate-2 = Zn(Glutamate)3-4
log_k 9.8
delta_h 0 kJ
-gamma 0 0
# Id: 9509963
# log K source: SCD2.62
# Delta H source: SCD2.62
#T and ionic strength:
Cd+2 + Glutamate-2 = Cd(Glutamate)
log_k 4.7
delta_h 0 kJ
-gamma 0 0
# Id: 1609961
```

```
# log K source: NIST46.2
# Delta H source: NIST46.2
#T and ionic strength:
Cd+2 + 2Glutamate-2 = Cd(Glutamate)2-2
log_k 7.59
delta_h 0 kJ
-gamma 0 0
# Id: 1609962
# log K source: NIST46.2
# Delta H source: NIST46.2
#T and ionic strength:
Hg(OH)2 + Glutamate-2 + 2H+ = Hg(Glutamate) + 2H2O
log_k 19.8
delta_h 0 kJ
-gamma 0 0
# Id: 3619961
# log K source: SCD2.62
# Delta H source: SCD2.62
#T and ionic strength:
Hg(OH)2 + 2Glutamate-2 + 2H+ = Hg(Glutamate)2-2 + 2H2O
log_k 26.2
delta_h 0 kJ
-gamma 0 0
# Id: 3619962
# log K source: SCD2.62
# Delta H source: SCD2.62
#T and ionic strength:
Cu+2 + Glutamate-2 = Cu(Glutamate)
log_k 9.17
delta_h -20.92 kJ
-gamma 0 0
# Id: 2319961
# log K source: NIST46.2
# Delta H source: NIST46.2
#T and ionic strength:
Cu+2 + 2Glutamate-2 = Cu(Glutamate)2-2
log_k 15.78
delta_h -48.116 kJ
-gamma 0 0
# Id: 2319962
# log K source: NIST46.2
# Delta H source: NIST46.2
#T and ionic strength:
Cu+2 + Glutamate-2 + H+ = CuH(Glutamate)+
log_k 13.3
delta_h -28.0328 kJ
-gamma 0 0
# Id: 2319963
# log K source: NIST46.2
# Delta H source: NIST46.2
#T and ionic strength:
Ag+ + Glutamate-2 = Ag(Glutamate)-
log_k 4.22
delta_h 0 kJ
```

```
-gamma 0 0
# Id: 209961
# log K source: NIST46.2
# Delta H source: NIST46.2
#T and ionic strength:
Ag+ + 2Glutamate-2 = Ag(Glutamate)2-3
log_k 7.36
delta_h 0 kJ
-gamma 0 0
# Id: 209962
# log K source: SCD2.62
# Delta H source: SCD2.62
#T and ionic strength:
2Ag+ + Glutamate-2 = Ag2(Glutamate)
log_k 3.4
delta_h 0 kJ
-gamma 0 0
# Id: 209963
# log K source: NIST46.2
# Delta H source: NIST46.2
#T and ionic strength:
Ni+2 + Glutamate-2 = Ni(Glutamate)
log_k 6.47
delta_h 0 kJ
-gamma 0 0
# Id: 5409961
# log K source: NIST46.2
# Delta H source: NIST46.2
#T and ionic strength:
Ni+2 + 2Glutamate-2 = Ni(Glutamate)2-2
log_k 10.7
delta_h -30.9616 kJ
-gamma 0 0
# Id: 5409962
# log K source: NIST46.2
# Delta H source: NIST46.2
#T and ionic strength:
Co+2 + Glutamate-2 = Co(Glutamate)
log_k 5.4178
delta_h 0 kJ
-gamma 0 0
# Id: 2009961
# log K source: NIST46.4
# Delta H source: NIST46.2
#T and ionic strength: 0.10 25.0
Co+2 + 2Glutamate-2 = Co(Glutamate)2-2
log_k 8.7178
delta_h 0 kJ
-gamma 0 0
# Id: 2009962
# log K source: NIST46.4
# Delta H source: NIST46.2
#T and ionic strength: 0.10 25.0
Mn+2 + Glutamate-2 = Mn(Glutamate)
```

```
log_k 4.95
delta_h 0 kJ
-gamma 0 0
# Id: 4709961
# log K source: SCD2.62
# Delta H source: SCD2.62
#T and ionic strength:
Mn+2 + 2Glutamate-2 = Mn(Glutamate)2-2
log_k 8.48
delta_h 0 kJ
-gamma 0 0
# Id: 4709962
# log K source: SCD2.62
# Delta H source: SCD2.62
#T and ionic strength:
Cr(OH)2+ + Glutamate-2 + 2H+ = Cr(Glutamate)+ + 2H2O
log_k 22.6
delta_h 0 kJ
-gamma 0 0
# Id: 2119961
# log K source: SCD2.62
# Delta H source: SCD2.62
#T and ionic strength:
Cr(OH)2+ + 2Glutamate-2 + 2H+ = Cr(Glutamate)2- + 2H2O
log_k 30.7
delta_h 0 kJ
-gamma 0 0
# Id: 2119962
# log K source: SCD2.62
# Delta H source: SCD2.62
#T and ionic strength:
Cr(OH)2+ + Glutamate-2 + 3H+ = CrH(Glutamate)+2 + 2H2O
log_k 25.2
delta_h 0 kJ
-gamma 0 0
# Id: 2119963
# log K source: SCD2.62
# Delta H source: SCD2.62
#T and ionic strength:
Mg+2 + Glutamate-2 = Mg(Glutamate)
log_k 2.8
delta_h 0 kJ
-gamma 0 0
# Id: 4609961
# log K source: NIST46.2
# Delta H source: NIST46.2
#T and ionic strength:
Ca+2 + Glutamate-2 = Ca(Glutamate)
log_k 2.06
delta_h 0 kJ
-gamma 0 0
# Id: 1509961
# log K source: NIST46.2
# Delta H source: NIST46.2
```

```
#T and ionic strength:
Ca+2 + Glutamate-2 + H+ = CaH(Glutamate)+
log_k 11.13
delta_h 0 kJ
-gamma 0 0
# Id: 1509962
# log K source: NIST46.2
# Delta H source: NIST46.2
#T and ionic strength:
Sr+2 + Glutamate-2 = Sr(Glutamate)
log_k 2.2278
delta_h 0 kJ
-gamma 0 0
# Id: 8009961
# log K source: NIST46.4
# Delta H source: NIST46.2
#T and ionic strength: 0.10 25.0
Ba+2 + Glutamate-2 = Ba(Glutamate)
log_k 2.14
delta_h 0 kJ
-gamma 0 0
# Id: 1009961
# log K source: NIST46.2
# Delta H source: NIST46.2
#T and ionic strength:
H+ + Phthalate-2 = H(Phthalate)-
log_k 5.408
delta_h 2.1757 kJ
-gamma 0 0
# Id: 3309971
# log K source: NIST46.2
# Delta H source: NIST46.2
#T and ionic strength:
2H+ + Phthalate-2 = H2(Phthalate)
log_k 8.358
delta_h 4.8534 kJ
-gamma 0 0
# Id: 3309972
# log K source: NIST46.2
# Delta H source: NIST46.2
#T and ionic strength:
Pb+2 + Phthalate-2 = Pb(Phthalate)
log_k 4.26
delta_h 0 kJ
-gamma 0 0
# Id: 6009971
# log K source: SCD2.62
# Delta H source: SCD2.62
#T and ionic strength:
Pb+2 + 2Phthalate-2 = Pb(Phthalate)2-2
log_k 4.83
delta_h 0 kJ
-gamma 0 0
# Id: 6009972
```

```
# log K source: NIST46.2
# Delta H source: NIST46.2
#T and ionic strength:
Pb+2 + Phthalate-2 + H+ = PbH(Phthalate)+
log_k 6.98
delta_h 0 kJ
-gamma 0 0
# Id: 6009973
# log K source: NIST46.2
# Delta H source: NIST46.2
#T and ionic strength:
Al+3 + Phthalate-2 = Al(Phthalate)+
log_k 4.56
delta_h 0 kJ
-gamma 0 0
# Id: 309971
# log K source: NIST46.2
# Delta H source: NIST46.2
#T and ionic strength:
Al+3 + 2Phthalate-2 = Al(Phthalate)2-
log_k 7.2
delta_h 0 kJ
-gamma 0 0
# Id: 309972
# log K source: NIST46.2
# Delta H source: NIST46.2
#T and ionic strength:
Zn+2 + Phthalate-2 = Zn(Phthalate)
log_k 2.91
delta_h 13.3888 kJ
-gamma 0 0
# Id: 9509971
# log K source: NIST46.2
# Delta H source: NIST46.2
#T and ionic strength:
Zn+2 + 2Phthalate-2 = Zn(Phthalate)2-2
log_k 4.2
delta_h 0 kJ
-gamma 0 0
# Id: 9509972
# log K source: NIST46.2
# Delta H source: NIST46.2
#T and ionic strength:
Cd+2 + Phthalate-2 = Cd(Phthalate)
log_k 3.43
delta_h 0 kJ
-gamma 0 0
# Id: 1609971
# log K source: NIST46.2
# Delta H source: NIST46.2
#T and ionic strength:
Cd+2 + Phthalate-2 + H+ = CdH(Phthalate)+
log_k 6.3
delta_h 0 kJ
```

```
-gamma 0 0
# Id: 1609973
# log K source: NIST46.2
# Delta H source: NIST46.2
#T and ionic strength:
Cd+2 + 2Phthalate-2 = Cd(Phthalate)2-2
log_k 3.7
delta_h 0 kJ
-gamma 0 0
# Id: 1609972
# log K source: NIST46.2
# Delta H source: NIST46.2
#T and ionic strength:
Cu+2 + Phthalate-2 = Cu(Phthalate)
log_k 4.02
delta_h 8.368 kJ
-gamma 0 0
# Id: 2319971
# log K source: NIST46.2
# Delta H source: NIST46.2
#T and ionic strength:
Cu+2 + Phthalate-2 + H+ = CuH(Phthalate)+
log_k 7.1
delta_h 3.8493 kJ
-gamma 0 0
# Id: 2319970
# log K source: NIST46.2
# Delta H source: NIST46.2
#T and ionic strength:
Cu+2 + 2Phthalate-2 = Cu(Phthalate)2-2
log_k 5.3
delta_h 15.8992 kJ
-gamma 0 0
# Id: 2319972
# log K source: NIST46.2
# Delta H source: NIST46.2
#T and ionic strength:
Ni+2 + Phthalate-2 = Ni(Phthalate)
log_k 2.95
delta_h 7.5312 kJ
-gamma 0 0
# Id: 5409971
# log K source: NIST46.2
# Delta H source: NIST46.2
#T and ionic strength:
Ni+2 + Phthalate-2 + H+ = NiH(Phthalate)+
log_k 6.6
delta_h 0 kJ
-gamma 0 0
# Id: 5409972
# log K source: NIST46.2
# Delta H source: NIST46.2
#T and ionic strength:
Co+2 + Phthalate-2 = Co(Phthalate)
```

```
log_k 2.83
delta_h 7.9 kJ
-gamma 0 0
# Id: 2009971
# log K source: NIST46.4
# Delta H source: NIST46.4
#T and ionic strength: 0.00 25.0
Co+2 + H+ + Phthalate-2 = CoH(Phthalate)+
log_k 7.227
delta_h 0 kJ
-gamma 0 0
# Id: 2009972
# log K source: NIST46.4
# Delta H source: NIST46.2
#T and ionic strength: 0.50 25.0
Mn+2 + Phthalate-2 = Mn(Phthalate)
log_k 2.74
delta_h 10.0416 kJ
-gamma 0 0
# Id: 4709971
# log K source: NIST46.2
# Delta H source: NIST46.2
#T and ionic strength:
Cr(OH)2+ + Phthalate-2 + 2H+ = Cr(Phthalate)+ + 2H2O
log_k 16.3
delta_h 0 kJ
-gamma 0 0
# Id: 2119971
# log K source: SCD2.62
# Delta H source: SCD2.62
#T and ionic strength:
Cr(OH)2+ + 2Phthalate-2 + 2H+ = Cr(Phthalate)2- + 2H2O
log_k 21.2
delta_h 0 kJ
-gamma 0 0
# Id: 2119972
# log K source: SCD2.62
# Delta H source: SCD2.62
#T and ionic strength:
Cr(OH)2+ + 3Phthalate-2 + 2H+ = Cr(Phthalate)3-3 + 2H2O
log_k 23.3
delta_h 0 kJ
-gamma 0 0
# Id: 2119973
# log K source: SCD2.62
# Delta H source: SCD2.62
#T and ionic strength:
Be+2 + Phthalate-2 = Be(Phthalate)
log_k 4.8278
delta_h 0 kJ
-gamma 0 0
# Id: 1109971
# log K source: NIST46.4
# Delta H source: NIST46.2
```

```
#T and ionic strength: 0.10 25.0
Be+2 + 2Phthalate-2 = Be(Phthalate)2-2
log_k 6.5478
delta_h 0 kJ
-gamma 0 0
# Id: 1109972
# log K source: NIST46.4
# Delta H source: NIST46.2
#T and ionic strength: 0.10 25.0
Mg+2 + Phthalate-2 = Mg(Phthalate)
log_k 2.49
delta_h 0 kJ
-gamma 0 0
# Id: 4609971
# log K source: SCD2.62
# Delta H source: SCD2.62
#T and ionic strength:
Ca+2 + Phthalate-2 = Ca(Phthalate)
log_k 2.45
delta_h 0 kJ
-gamma 0 0
# Id: 1509970
# log K source: NIST46.2
# Delta H source: NIST46.2
#T and ionic strength:
Ca+2 + Phthalate-2 + H+ = CaH(Phthalate)+
log_k 6.43
delta_h 0 kJ
-gamma 0 0
# Id: 1509971
# log K source: NIST46.2
# Delta H source: NIST46.2
#T and ionic strength:
Ba+2 + Phthalate-2 = Ba(Phthalate)
log_k 2.33
delta_h 0 kJ
-gamma 0 0
# Id: 1009971
# log K source: NIST46.2
# Delta H source: NIST46.2
#T and ionic strength:
Na+ + Phthalate-2 = Na(Phthalate)-
log_k 0.8
delta_h 4.184 kJ
-gamma 0 0
# Id: 5009970
# log K source: NIST46.2
# Delta H source: NIST46.2
#T and ionic strength:
K+ + Phthalate-2 = K(Phthalate)-
log_k 0.7
delta_h 3.7656 kJ
-gamma 0 0
# Id: 4109971
```

```
# log K source: NIST46.2
# Delta H source: NIST46.2
#T and ionic strength:
PHASES
Sulfur
S + H+ + 2e- = HS-
log_k -2.1449
delta_h -16.3 kJ
Semetal(hex
Se + H+ + 2e- = HSe-
log_k -7.7084
delta_h 15.9 kJ
Semetal(am)
Se + H+ + 2e- = HSe-
log_k -7.1099
delta_h 10.8784 kJ
Sbmetal
Sb + 3H2O = Sb(OH)3 + 3H+ + 3e-
log_k -11.6889
delta_h 83.89 kJ
Snmetal(wht)
Sn + 2H2O = Sn(OH)2 + 2H+ + 2e-
log_k -2.3266
delta_h -0 kJ
Pbmetal
Pb = Pb+2 + 2e-
log_k 4.2462
delta_h 0.92 kJ
Tlmetal
Tl = Tl+ + e-
log_k 5.6762
delta_h 5.36 kJ
Znmetal
Zn = Zn+2 + 2e-
log_k 25.7886
delta_h -153.39 kJ
Cdmetal(alpha)
Cd = Cd+2 + 2e-
log_k 13.5147
delta_h -75.33 kJ
Cdmetal(gamma)
Cd = Cd+2 + 2e-
log_k 13.618
delta_h -75.92 kJ
Hgmetal(l)
Hg = 0.5Hg2+2 + e-
log_k -13.4517
delta_h 83.435 kJ
Cumetal
Cu = Cu+ + e-
log_k -8.756
delta_h 71.67 kJ
Agmetal
Ag = Ag+ + e-
```

```
log_k -13.5065
delta_h 105.79 kJ
Crmetal
Cr = Cr+2 + 2e-
log_k 30.4831
delta_h -172 kJ
Vmetal
V = V+3 + 3e-
log_k 44.0253
delta_h -259 kJ
Stibnite
Sb2S3 + 6H2O = 2Sb(OH)3 + 3H+ + 3HS-
log_k -50.46
delta_h 293.78 kJ
Orpiment
As2S3 + 6H2O = 2H3AsO3 + 3HS- + 3H+
log_k -61.0663
delta_h 350.68 kJ
Realgar
AsS + 3H2O = H3AsO3 + HS- + 2H+ + e-
log_k -19.747
delta_h 127.8 kJ
SnS
SnS + 2H2O = Sn(OH)2 + H+ + HS-
log_k -19.114
delta_h -0 kJ
SnS2
SnS2 + 6H2O = Sn(OH)6-2 + 4H+ + 2HS-
log_k -57.4538
delta_h -0 kJ
Galena
PbS + H+ = Pb+2 + HS-
log_k -13.97
delta_h 80 kJ
Tl2S
Tl2S + H+ = 2Tl+ + HS-
log_k -7.19
delta_h 91.52 kJ
ZnS(am)
ZnS + H+ = Zn+2 + HS-
log_k -9.052
delta_h 15.3553 kJ
Sphalerite
ZnS + H+ = Zn+2 + HS-
log_k -11.45
delta_h 30 kJ
Wurtzite
ZnS + H+ = Zn+2 + HS-
log_k -8.95
delta_h 21.171 kJ
Greenockite
CdS + H+ = Cd+2 + HS-
log_k -14.36
delta_h 55 kJ
```

```
Hg2S
Hg2S + H+ = Hg2+2 + HS-
log_k -11.6765
delta_h 69.7473 kJ
Cinnabar
HgS + 2H2O = Hg(OH)2 + H+ + HS-
log_k -45.694
delta_h 253.76 kJ
Metacinnabar
HgS + 2H2O = Hg(OH)2 + H+ + HS-
log_k -45.094
delta_h 253.72 kJ
Chalcocite
Cu2S + H+ = 2Cu+ + HS-
log_k -34.92
delta_h 168 kJ
Djurleite
Cu0.066Cu1.868S + H+ = 0.066Cu+2 + 1.868Cu+ + HS-
log_k -33.92
delta_h 200.334 kJ
Anilite
Cu0.25Cu1.5S + H+ = 0.25Cu+2 + 1.5Cu+ + HS-
log_k -31.878
delta_h 182.15 kJ
BlaubleiII
Cu0.6Cu0.8S + H+ = 0.6Cu+2 + 0.8Cu+ + HS-
log_k -27.279
delta_h -0 kJ
BlaubleiI
Cu0.9Cu0.2S + H+ = 0.9Cu+2 + 0.2Cu+ + HS-
log_k -24.162
delta_h -0 kJ
Covellite
CuS + H+ = Cu+2 + HS-
log_k -22.3
delta_h 97 kJ
Chalcopyrite
CuFeS2 + 2H+ = Cu+2 + Fe+2 + 2HS-
log_k -35.27
delta_h 148.448 kJ
Acanthite
Ag2S + H+ = 2Ag+ + HS-
log_k -36.22
delta_h 227 kJ
NiS(alpha)
NiS + H+ = Ni+2 + HS-
log_k -5.6
delta_h -0 kJ
NiS(beta)
NiS + H+ = Ni+2 + HS-
log_k -11.1
delta_h -0 kJ
NiS(gamma)
NiS + H+ = Ni+2 + HS-
```

```
log_k -12.8
delta_h -0 kJ
CoS(alpha)
CoS + H+ = Co+2 + HS-
log_k -7.44
delta_h -0 kJ
CoS(beta)
CoS + H+ = Co+2 + HS-
log_k -11.07
delta_h -0 kJ
FeS(ppt)
FeS + H+ = Fe+2 + HS-
log_k -2.95
delta_h -11 kJ
Greigite
Fe3S4 + 4H+ = 2Fe+3 + Fe+2 + 4HS-
log_k -45.035
delta_h -0 kJ
Mackinawite
FeS + H+ = Fe+2 + HS-
log_k -3.6
delta_h -0 kJ
Pyrite
FeS2 + 2H+ + 2e- = Fe+2 + 2HS-
log_k -18.5082
delta_h 49.844 kJ
MnS(grn)
MnS + H+ = Mn+2 + HS-
log_k 0.17
delta_h -32 kJ
MnS(pnk)
MnS + H+ = Mn+2 + HS-
log_k 3.34
delta_h -0 kJ
MoS2
MoS2 + 4H2O = MoO4-2 + 6H+ + 2HS- + 2e-
log_k -70.2596
delta_h 389.02 kJ
BeS
BeS + H+ = Be+2 + HS-
log_k 19.38
delta_h -0 kJ
BaS
BaS + H+ = Ba+2 + HS-
log_k 16.18
delta_h -0 kJ
Hg2(Cyanide)2
Hg2(Cyanide)2 = Hg2+2 + 2Cyanide-
log_k -39.3
delta_h -0 kJ
CuCyanide
CuCyanide = Cu+ + Cyanide-
log_k -19.5
delta_h -19 kJ
```

```
AgCyanide
AgCyanide = Ag+ + Cyanide-
log_k -15.74
delta_h 110.395 kJ
Ag2(Cyanide)2
Ag2(Cyanide)2 = 2Ag+ + 2Cyanide-
log_k -11.3289
delta_h -0 kJ
NaCyanide(cubic)
NaCyanide = Cyanide- + Na+
log_k 1.6012
delta_h 0.969 kJ
KCyanide(cubic)
KCyanide = Cyanide- + K+
log_k 1.4188
delta_h 11.93 kJ
Pb2Fe(Cyanide)6
Pb2Fe(Cyanide)6 = 2Pb+2 + Fe+2 + 6Cyanide-
log_k -53.42
delta_h -0 kJ
Zn2Fe(Cyanide)6
Zn2Fe(Cyanide)6 = 2Zn+2 + Fe+2 + 6Cyanide-
log_k -51.08
delta_h -0 kJ
Cd2Fe(Cyanide)6
Cd2Fe(Cyanide)6 = 2Cd+2 + Fe+2 + 6Cyanide-
log_k -52.78
delta_h -0 kJ
Ag4Fe(Cyanide)6
Ag4Fe(Cyanide)6 = 4Ag+ + Fe+2 + 6Cyanide-
log_k -79.47
delta_h -0 kJ
Ag3Fe(Cyanide)6
Ag3Fe(Cyanide)6 = 3Ag+ + Fe+3 + 6Cyanide-
log_k -72.7867
delta_h -0 kJ
Mn3(Fe(Cyanide)6)2
Mn3(Fe(Cyanide)6)2 = 3Mn+2 + 2Fe+3 + 12Cyanide-
log_k -105.4
delta_h -0 kJ
Sb2Se3
Sb2Se3 + 6H2O = 2Sb(OH)3 + 3HSe- + 3H+
log_k -67.7571
delta_h 343.046 kJ
SnSe
SnSe + 2H2O = Sn(OH)2 + H+ + HSe-
log_k -30.494
delta_h -0 kJ
SnSe2
SnSe2 + 6H2O = Sn(OH)6-2 + 4H+ + 2HSe-
log_k -65.1189
delta_h -0 kJ
Clausthalite
PbSe + H+ = Pb+2 + HSe-
```

```
log_k -27.1
delta_h 119.72 kJ
Tl2Se
Tl2Se + H+ = 2Tl+ + HSe-
log_k -18.1
delta_h 85.62 kJ
ZnSe
ZnSe + H+ = Zn+2 + HSe-
log_k -14.4
delta_h 25.51 kJ
CdSe
CdSe + H+ = Cd+2 + HSe-
log_k -20.2
delta_h 75.9814 kJ
HgSe
HgSe + 2H2O = Hg(OH)2 + H+ + HSe-
log_k -55.694
delta_h -0 kJ
Cu2Se(alpha)
Cu2Se + H+ = 2Cu+ + HSe-
log_k -45.8
delta_h 214.263 kJ
Cu3Se2
Cu3Se2 + 2H+ = 2HSe- + 2Cu+ + Cu+2
log_k -63.4911
delta_h 340.327 kJ
CuSe
CuSe + H+ = Cu+2 + HSe-
log_k -33.1
delta_h 121.127 kJ
CuSe2
CuSe2 + 2H+ + 2e- = 2HSe- + Cu+2
log_k -33.3655
delta_h 140.582 kJ
Ag2Se
Ag2Se + H+ = 2Ag+ + HSe-
log_k -48.7
delta_h 265.48 kJ
NiSe
NiSe + H+ = Ni+2 + HSe-
log_k -17.7
delta_h -0 kJ
CoSe
CoSe + H+ = Co+2 + HSe-
log_k -16.2
delta_h -0 kJ
FeSe
FeSe + H+ = Fe+2 + HSe-
log_k -11
delta_h 2.092 kJ
Ferroselite
FeSe2 + 2H+ + 2e- = 2HSe- + Fe+2
log_k -18.5959
delta_h 47.2792 kJ
```

```
MnSe
MnSe + H+ = Mn+2 + HSe-
log_k 3.5
delta_h -98.15 kJ
AlSb
AlSb + 3H2O = Sb(OH)3 + 6e- + Al+3 + 3H+
log_k 65.6241
delta_h -0 kJ
ZnSb
ZnSb + 3H2O = Sb(OH)3 + 5e- + Zn+2 + 3H+
log_k 11.0138
delta_h -54.8773 kJ
CdSb
CdSb + 3H2O = Sb(OH)3 + 5e- + 3H+ + Cd+2
log_k -0.3501
delta_h 22.36 kJ
Cu2Sb:3H2O
Cu2Sb:3H2O = Sb(OH)3 + 6e- + 3H+ + Cu+ + Cu+2
log_k -34.8827
delta_h 233.237 kJ
Cu3Sb
Cu3Sb + 3H2O = Sb(OH)3 + 6e- + 3H+ + 3Cu+
log_k -42.5937
delta_h 308.131 kJ
#Ag4Sb
# Ag4Sb + 3H2O = Sb(OH)3 + 6e- + 3Ag+ + 3H+
# log_k -56.1818
# delta_h -0 kJ
Breithauptite
NiSb + 3H2O = Sb(OH)3 + 5e- + 3H+ + Ni+2
log_k -18.5225
delta_h 96.0019 kJ
MnSb
MnSb + 3H2O = Mn+3 + Sb(OH)3 + 6e- + 3H+
log_k -2.9099
delta_h 21.1083 kJ
Mn2Sb
Mn2Sb + 3H2O = 2Mn+2 + Sb(OH)3 + 7e- + 3H+
log_k 61.0796
delta_h -0 kJ
USb2
USb2 + 8H2O = UO2+2 + 2Sb(OH)3 + 12e- + 10H+
log_k 29.5771
delta_h -103.56 kJ
U3Sb4
U3Sb4 + 12H2O = 3U+4 + 4Sb(OH)3 + 24e- + 12H+
log_k 152.383
delta_h -986.04 kJ
Mg2Sb3
Mg2Sb3 + 9H2O = 2Mg+2 + 3Sb(OH)3 + 9H+ + 13e-
log_k 74.6838
delta_h -0 kJ
Ca3Sb2
Ca3Sb2 + 6H2O = 3Ca+2 + 2Sb(OH)3 + 6H+ + 12e-
```

```
log_k 142.974
delta_h -732.744 kJ
NaSb
NaSb + 3H2O = Na+ + Sb(OH)3 + 3H+ + 4e-
log_k 23.1658
delta_h -93.45 kJ
Na3Sb
Na3Sb + 3H2O = 3Na+ + Sb(OH)3 + 3H+ + 6e-
log_k 94.4517
delta_h -432.13 kJ
SeO2
SeO2 + H2O = HSeO3- + H+
log_k 0.1246
delta_h 1.4016 kJ
SeO3
SeO3 + H2O = SeO4-2 + 2H+
log_k 21.044
delta_h -146.377 kJ
Sb2O5
Sb2O5 + 7H2O = 2Sb(OH)6- + 2H+
log_k -9.6674
delta_h -0 kJ
SbO2
SbO2 + 4H2O = Sb(OH)6- + e- + 2H+
log_k -27.8241
delta_h -0 kJ
Sb2O4
Sb2O4 + 2H2O + 2H+ + 2e- = 2Sb(OH)3
log_k 3.4021
delta_h -68.04 kJ
Sb4O6(cubic)
Sb4O6 + 6H2O = 4Sb(OH)3
log_k -18.2612
delta_h 61.1801 kJ
Sb4O6(orth)
Sb4O6 + 6H2O = 4Sb(OH)3
log_k -17.9012
delta_h 37.6801 kJ
Sb(OH)3
Sb(OH)3 = Sb(OH)3
log_k -7.1099
delta_h 30.1248 kJ
Senarmontite
Sb2O3 + 3H2O = 2Sb(OH)3
log_k -12.3654
delta_h 30.6478 kJ
Valentinite
Sb2O3 + 3H2O = 2Sb(OH)3
log_k -8.4806
delta_h 19.0163 kJ
Chalcedony
SiO2 + 2H2O = H4SiO4
log_k -3.55
delta_h 19.7 kJ
```

```
Cristobalite
SiO2 + 2H2O = H4SiO4
log_k -3.35
delta_h 20.006 kJ
Quartz
SiO2 + 2H2O = H4SiO4
log_k -4
delta_h 22.36 kJ
SiO2(am-gel)
SiO2 + 2H2O = H4SiO4
log_k -2.71
delta_h 14 kJ
SiO2(am-ppt)
SiO2 + 2H2O = H4SiO4
log_k -2.74
delta_h 15.15 kJ
SnO
SnO + H2O = Sn(OH)2
log_k -4.9141
delta_h -0 kJ
SnO2
SnO2 + 4H2O = Sn(OH)6-2 + 2H+
log_k -28.9749
delta_h -0 kJ
Sn(OH)2
Sn(OH)2 = Sn(OH)2
log_k -5.4309
delta_h -0 kJ
Sn(OH)4
Sn(OH)4 + 2H2O = Sn(OH)6-2 + 2H+
log_k -22.2808
delta_h -0 kJ
H2Sn(OH)6
H2Sn(OH)6 = Sn(OH)6-2 + 2H+
log_k -23.5281
delta_h -0 kJ
Massicot
PbO + 2H+ = Pb+2 + H2O
log_k 12.894
delta_h -66.848 kJ
Litharge
PbO + 2H+ = Pb+2 + H2O
log_k 12.694
delta_h -65.501 kJ
PbO:0.3H2O
PbO:0.33H2O + 2H+ = Pb+2 + 1.33H2O
log_k 12.98
delta_h -0 kJ
Plattnerite
PbO2 + 4H+ + 2e- = Pb+2 + 2H2O
log_k 49.6001
delta_h -296.27 kJ
Pb(OH)2
Pb(OH)2 + 2H+ = Pb+2 + 2H2O
```

```
log_k 8.15
delta_h -58.5342 kJ
Pb2O(OH)2
Pb2O(OH)2 + 4H+ = 2Pb+2 + 3H2O
log_k 26.188
delta_h -0 kJ
Al(OH)3(am)
Al(OH)3 + 3H+ = Al+3 + 3H2O
log_k 10.8
delta_h -111 kJ
Boehmite
AlOOH + 3H+ = Al+3 + 2H2O
log_k 8.578
delta_h -117.696 kJ
Diaspore
AlOOH + 3H+ = Al+3 + 2H2O
log_k 6.873
delta_h -103.052 kJ
Gibbsite
Al(OH)3 + 3H+ = Al+3 + 3H2O
log_k 8.291
delta_h -95.3952 kJ
Tl2O
Tl2O + 2H+ = 2Tl+ + H2O
log_k 27.0915
delta_h -96.41 kJ
TlOH
TlOH + H+ = Tl+ + H2O
log_k 12.9186
delta_h -41.57 kJ
Avicennite
Tl2O3 + 3H2O = 2Tl(OH)3
log_k -13
delta_h -0 kJ
Tl(OH)3
Tl(OH)3 = Tl(OH)3
log_k -5.441
delta_h -0 kJ
Zn(OH)2(am)
Zn(OH)2 + 2H+ = Zn+2 + 2H2O
log_k 12.474
delta_h -80.62 kJ
Zn(OH)2
Zn(OH)2 + 2H+ = Zn+2 + 2H2O
log_k 12.2
delta_h -0 kJ
Zn(OH)2(beta)
Zn(OH)2 + 2H+ = Zn+2 + 2H2O
log_k 11.754
delta_h -83.14 kJ
Zn(OH)2(gamma)
Zn(OH)2 + 2H+ = Zn+2 + 2H2O
log_k 11.734
delta_h -0 kJ
```

```
Zn(OH)2(epsilon)
Zn(OH)2 + 2H+ = Zn+2 + 2H2O
log_k 11.534
delta_h -81.8 kJ
ZnO(active)
ZnO + 2H+ = Zn+2 + H2O
log_k 11.1884
delta_h -88.76 kJ
Zincite
ZnO + 2H+ = Zn+2 + H2O
log_k 11.334
delta_h -89.62 kJ
Cd(OH)2(am)
Cd(OH)2 + 2H+ = Cd+2 + 2H2O
log_k 13.73
delta_h -86.9017 kJ
Cd(OH)2
Cd(OH)2 + 2H+ = Cd+2 + 2H2O
log_k 13.644
delta_h -94.62 kJ
Monteponite
CdO + 2H+ = Cd+2 + H2O
log_k 15.1034
delta_h -103.4 kJ
Hg2(OH)2
Hg2(OH)2 + 2H+ = Hg2+2 + 2H2O
log_k 5.2603
delta_h -0 kJ
Montroydite
HgO + H2O = Hg(OH)2
log_k -3.64
delta_h -38.9 kJ
Hg(OH)2
Hg(OH)2 = Hg(OH)2
log_k -3.4963
delta_h -0 kJ
Cuprite
Cu2O + 2H+ = 2Cu+ + H2O
log_k -1.406
delta_h -124.02 kJ
Cu(OH)2
Cu(OH)2 + 2H+ = Cu+2 + 2H2O
log_k 8.674
delta_h -56.42 kJ
Tenorite
CuO + 2H+ = Cu+2 + H2O
log_k 7.644
delta_h -64.867 kJ
Ag2O
Ag2O + 2H+ = 2Ag+ + H2O
log_k 12.574
delta_h -45.62 kJ
Ni(OH)2
Ni(OH)2 + 2H+ = Ni+2 + 2H2O
```

```
log_k 12.794
delta_h -95.96 kJ
Bunsenite
NiO + 2H+ = Ni+2 + H2O
log_k 12.4456
delta_h -100.13 kJ
CoO
CoO + 2H+ = Co+2 + H2O
log_k 13.5864
delta_h -106.295 kJ
Co(OH)2
Co(OH)2 + 2H+ = Co+2 + 2H2O
log_k 13.094
delta_h -0 kJ
Co(OH)3
Co(OH)3 + 3H+ = Co+3 + 3H2O
log_k -2.309
delta_h -92.43 kJ
#Wustite-0.11
# WUSTITE-0.11 + 2H+ = 0.947Fe+2 + H2O
# log_k 11.6879
# delta_h -103.938 kJ
Fe(OH)2
Fe(OH)2 + 2H+ = Fe+2 + 2H2O
log_k 13.564
delta_h -0 kJ
Ferrihydrite
Fe(OH)3 + 3H+ = Fe+3 + 3H2O
log_k 3.191
delta_h -73.374 kJ
Fe3(OH)8
Fe3(OH)8 + 8H+ = 2Fe+3 + Fe+2 + 8H2O
log_k 20.222
delta_h -0 kJ
Goethite
FeOOH + 3H+ = Fe+3 + 2H2O
log_k 0.491
delta_h -60.5843 kJ
Pyrolusite
MnO2 + 4H+ + 2e- = Mn+2 + 2H2O
log_k 41.38
delta_h -272 kJ
Birnessite
MnO2 + 4H+ + e- = Mn+3 + 2H2O
log_k 18.091
delta_h -0 kJ
Nsutite
MnO2 + 4H+ + e- = Mn+3 + 2H2O
log_k 17.504
delta_h -0 kJ
Pyrochroite
Mn(OH)2 + 2H+ = Mn+2 + 2H2O
log_k 15.194
delta_h -97.0099 kJ
```

```
Manganite
MnOOH + 3H+ + e- = Mn+2 + 2H2O
log_k 25.34
delta_h -0 kJ
Cr(OH)2
Cr(OH)2 + 2H+ = Cr+2 + 2H2O
log_k 10.8189
delta_h -35.6058 kJ
Cr(OH)3(am)
Cr(OH)3 + H+ = Cr(OH)2+ + H2O
log_k -0.75
delta_h -0 kJ
Cr(OH)3
Cr(OH)3 + H+ = Cr(OH)2+ + H2O
log_k 1.3355
delta_h -29.7692 kJ
CrO3
CrO3 + H2O = CrO4-2 + 2H+
log_k -3.2105
delta_h -5.2091 kJ
MoO3
MoO3 + H2O = MoO4-2 + 2H+
log_k -8
delta_h -0 kJ
VO
VO + 2H+ = V+3 + H2O + e-
log_k 14.7563
delta_h -113.041 kJ
V(OH)3
V(OH)3 + 3H+ = V+3 + 3H2O
log_k 7.591
delta_h -0 kJ
VO(OH)2
VO(OH)2 + 2H+ = VO+2 + 2H2O
log_k 5.1506
delta_h -0 kJ
Uraninite
UO2 + 4H+ = U+4 + 2H2O
log_k -4.6693
delta_h -77.86 kJ
UO2(am)
UO2 + 4H+ = U+4 + 2H2O
log_k 0.934
delta_h -109.746 kJ
UO3
UO3 + 2H+ = UO2+2 + H2O
log_k 7.7
delta_h -81.0299 kJ
Gummite
UO3 + 2H+ = UO2+2 + H2O
log_k 7.6718
delta_h -81.0299 kJ
UO2(OH)2(beta)
UO2(OH)2 + 2H+ = UO2+2 + 2H2O
```

```
log_k 5.6116
delta_h -56.7599 kJ
Schoepite
UO2(OH)2:H2O + 2H+ = UO2+2 + 3H2O
log_k 5.994
delta_h -49.79 kJ
Be(OH)2(am)
Be(OH)2 + 2H+ = Be+2 + 2H2O
log_k 7.194
delta_h -0 kJ
Be(OH)2(alpha)
Be(OH)2 + 2H+ = Be+2 + 2H2O
log_k 6.894
delta_h -0 kJ
Be(OH)2(beta)
Be(OH)2 + 2H+ = Be+2 + 2H2O
log_k 6.494
delta_h -0 kJ
Brucite
Mg(OH)2 + 2H+ = Mg+2 + 2H2O
log_k 16.844
delta_h -113.996 kJ
Periclase
MgO + 2H+ = Mg+2 + H2O
log_k 21.5841
delta_h -151.23 kJ
Mg(OH)2(active)
Mg(OH)2 + 2H+ = Mg+2 + 2H2O
log_k 18.794
delta_h -0 kJ
Lime
CaO + 2H+ = Ca+2 + H2O
log_k 32.6993
delta_h -193.91 kJ
Portlandite
Ca(OH)2 + 2H+ = Ca+2 + 2H2O
log_k 22.804
delta_h -128.62 kJ
Ba(OH)2:8H2O
Ba(OH)2:8H2O + 2H+ = Ba+2 + 10H2O
log_k 24.394
delta_h -54.32 kJ
Cu(SbO3)2
Cu(SbO3)2 + 6H+ + 4e- = 2Sb(OH)3 + Cu+2
log_k 45.2105
delta_h -0 kJ
Arsenolite
As4O6 + 6H2O = 4H3AsO3
log_k -2.76
delta_h 59.9567 kJ
Claudetite
As4O6 + 6H2O = 4H3AsO3
log_k -3.065
delta_h 55.6054 kJ
```

```
As2O5
As2O5 + 3H2O = 2H3AsO4
log_k 6.7061
delta_h -22.64 kJ
Pb2O3
Pb2O3 + 6H+ + 2e- = 2Pb+2 + 3H2O
log_k 61.04
delta_h -0 kJ
Minium
Pb3O4 + 8H+ + 2e- = 3Pb+2 + 4H2O
log_k 73.5219
delta_h -421.874 kJ
Al2O3
Al2O3 + 6H+ = 2Al+3 + 3H2O
log_k 19.6524
delta_h -258.59 kJ
Co3O4
Co3O4 + 8H+ = Co+2 + 2Co+3 + 4H2O
log_k -10.4956
delta_h -107.5 kJ
CoFe2O4
CoFe2O4 + 8H+ = Co+2 + 2Fe+3 + 4H2O
log_k -3.5281
delta_h -158.82 kJ
Magnetite
Fe3O4 + 8H+ = 2Fe+3 + Fe+2 + 4H2O
log_k 3.4028
delta_h -208.526 kJ
Hercynite
FeAl2O4 + 8H+ = Fe+2 + 2Al+3 + 4H2O
log_k 22.893
delta_h -313.92 kJ
Hematite
Fe2O3 + 6H+ = 2Fe+3 + 3H2O
log_k -1.418
delta_h -128.987 kJ
Maghemite
Fe2O3 + 6H+ = 2Fe+3 + 3H2O
log_k 6.386
delta_h -0 kJ
Lepidocrocite
FeOOH + 3H+ = Fe+3 + 2H2O
log_k 1.371
delta_h -0 kJ
Hausmannite
Mn3O4 + 8H+ + 2e- = 3Mn+2 + 4H2O
log_k 61.03
delta_h -421 kJ
Bixbyite
Mn2O3 + 6H+ = 2Mn+3 + 3H2O
log_k -0.6445
delta_h -124.49 kJ
Cr2O3
Cr2O3 + H2O + 2H+ = 2Cr(OH)2+
```

```
log_k -2.3576
delta_h -50.731 kJ
#V2O3
# V2O3 + 3H+ = V+3 + 1.5H2O
# log_k 4.9
# delta_h -82.5085 kJ
V3O5
V3O5 + 4H+ = 3VO+2 + 2H2O + 2e-
log_k 1.8361
delta_h -98.46 kJ
#V2O4
# V2O4 + 2H+ = VO+2 + H2O
# log_k 4.27
# delta_h -58.8689 kJ
V4O7
V4O7 + 6H+ = 4VO+2 + 3H2O + 2e-
log_k 7.1865
delta_h -163.89 kJ
V6O13
V6O13 + 2H+ = 6VO2+ + H2O + 4e-
log_k -60.86
delta_h 271.5 kJ
V2O5
V2O5 + 2H+ = 2VO2+ + H2O
log_k -1.36
delta_h 34 kJ
U4O9
U4O9 + 18H+ + 2e- = 4U+4 + 9H2O
log_k -3.0198
delta_h -426.87 kJ
U3O8
U3O8 + 16H+ + 4e- = 3U+4 + 8H2O
log_k 21.0834
delta_h -485.44 kJ
Spinel
MgAl2O4 + 8H+ = Mg+2 + 2Al+3 + 4H2O
log_k 36.8476
delta_h -388.012 kJ
Magnesioferrite
Fe2MgO4 + 8H+ = Mg+2 + 2Fe+3 + 4H2O
log_k 16.8597
delta_h -278.92 kJ
Natron
Na2CO3:10H2O = 2Na+ + CO3-2 + 10H2O
log_k -1.311
delta_h 65.8771 kJ
Cuprousferrite
CuFeO2 + 4H+ = Cu+ + Fe+3 + 2H2O
log_k -8.9171
delta_h -15.89 kJ
Cupricferrite
CuFe2O4 + 8H+ = Cu+2 + 2Fe+3 + 4H2O
log_k 5.9882
delta_h -210.21 kJ
```

```
FeCr2O4
FeCr2O4 + 4H+ = 2Cr(OH)2+ + Fe+2
log_k 7.2003
delta_h -140.4 kJ
MgCr2O4
MgCr2O4 + 4H+ = 2Cr(OH)2+ + Mg+2
log_k 16.2007
delta_h -179.4 kJ
SbF3
SbF3 + 3H2O = Sb(OH)3 + 3H+ + 3F-
log_k -10.2251
delta_h -6.7279 kJ
PbF2
PbF2 = Pb+2 + 2F-
log_k -7.44
delta_h 20 kJ
ZnF2
ZnF2 = Zn+2 + 2F-
log_k -0.5343
delta_h -59.69 kJ
CdF2
CdF2 = Cd+2 + 2F-
log_k -1.2124
delta_h -46.22 kJ
Hg2F2
Hg2F2 = Hg2+2 + 2F-
log_k -10.3623
delta_h -18.486 kJ
CuF
CuF = Cu+ + F-
log_k -4.9056
delta_h 16.648 kJ
CuF2
CuF2 = Cu+2 + 2F-
log_k 1.115
delta_h -66.901 kJ
CuF2:2H2O
CuF2:2H2O = Cu+2 + 2F- + 2H2O
log_k -4.55
delta_h -15.2716 kJ
AgF:4H2O
AgF:4H2O = Ag+ + F- + 4H2O
log_k 1.0491
delta_h 15.4202 kJ
CoF2
CoF2 = Co+2 + 2F-
log_k -1.5969
delta_h -57.368 kJ
CoF3
CoF3 = Co+3 + 3F-
log_k -1.4581
delta_h -123.692 kJ
CrF3
CrF3 + 2H2O = Cr(OH)2+ + 3F- + 2H+
```

```
log_k -11.3367
delta_h -23.3901 kJ
VF4
VF4 + H2O = VO+2 + 4F- + 2H+
log_k 14.93
delta_h -199.117 kJ
UF4
UF4 = U+4 + 4F-
log_k -29.5371
delta_h -79.0776 kJ
UF4:2.5H2O
UF4:2.5H2O = U+4 + 4F- + 2.5H2O
log_k -32.7179
delta_h 24.325 kJ
MgF2
MgF2 = Mg+2 + 2F-
log_k -8.13
delta_h -8 kJ
Fluorite
CaF2 = Ca+2 + 2F-
log_k -10.5
delta_h 8 kJ
SrF2
SrF2 = Sr+2 + 2F-
log_k -8.58
delta_h 4 kJ
BaF2
BaF2 = Ba+2 + 2F-
log_k -5.82
delta_h 4 kJ
Cryolite
Na3AlF6 = 3Na+ + Al+3 + 6F-
log_k -33.84
delta_h 38 kJ
SbCl3
SbCl3 + 3H2O = Sb(OH)3 + 3Cl- + 3H+
log_k 0.5719
delta_h -35.18 kJ
SnCl2
SnCl2 + 2H2O = Sn(OH)2 + 2H+ + 2Cl-
log_k -9.2752
delta_h -0 kJ
Cotunnite
PbCl2 = Pb+2 + 2Cl-
log_k -4.78
delta_h 26.166 kJ
Matlockite
PbClF = Pb+2 + Cl- + F-
log_k -8.9733
delta_h 33.19 kJ
Phosgenite
PbCl2:PbCO3 = 2Pb+2 + 2Cl- + CO3-2
log_k -19.81
delta_h -0 kJ
```

```
Laurionite
PbOHCl + H+ = Pb+2 + Cl- + H2O
log_k 0.623
delta_h -0 kJ
Pb2(OH)3Cl
Pb2(OH)3Cl + 3H+ = 2Pb+2 + 3H2O + Cl-
log_k 8.793
delta_h -0 kJ
TlCl
TlCl = Tl+ + Cl-
log_k -3.74
delta_h 41 kJ
ZnCl2
ZnCl2 = Zn+2 + 2Cl-
log_k 7.05
delta_h -72.5 kJ
Zn2(OH)3Cl
Zn2(OH)3Cl + 3H+ = 2Zn+2 + 3H2O + Cl-
log_k 15.191
delta_h -0 kJ
Zn5(OH)8Cl2
Zn5(OH)8Cl2 + 8H+ = 5Zn+2 + 8H2O + 2Cl-
log_k 38.5
delta_h -0 kJ
CdCl2
CdCl2 = Cd+2 + 2Cl-
log_k -0.6588
delta_h -18.58 kJ
CdCl2:1H2O
CdCl2:1H2O = Cd+2 + 2Cl- + H2O
log_k -1.6932
delta_h -7.47 kJ
CdCl2:2.5H2O
CdCl2:2.5H2O = Cd+2 + 2Cl- + 2.5H2O
log_k -1.913
delta_h 7.2849 kJ
CdOHCl
CdOHCl + H+ = Cd+2 + H2O + Cl-
log_k 3.5373
delta_h -30.93 kJ
Calomel
Hg2Cl2 = Hg2+2 + 2Cl-
log_k -17.91
delta_h 92 kJ
HgCl2
HgCl2 + 2H2O = Hg(OH)2 + 2Cl- + 2H+
log_k -21.2621
delta_h 107.82 kJ
Nantokite
CuCl = Cu+ + Cl-
log_k -6.73
delta_h 42.662 kJ
Melanothallite
CuCl2 = Cu+2 + 2Cl-
```

```
log_k 6.2572
delta_h -63.407 kJ
Atacamite
Cu2(OH)3Cl + 3H+ = 2Cu+2 + 3H2O + Cl-
log_k 7.391
delta_h -93.43 kJ
Cerargyrite
AgCl = Ag+ + Cl-
log_k -9.75
delta_h 65.2 kJ
CoCl2
CoCl2 = Co+2 + 2Cl-
log_k 8.2672
delta_h -79.815 kJ
CoCl2:6H2O
CoCl2:6H2O = Co+2 + 2Cl- + 6H2O
log_k 2.5365
delta_h 8.0598 kJ
(Co(NH3)6)Cl3
(Co(NH3)6)Cl3 + 6H+ = Co+3 + 6NH4+ + 3Cl-
log_k 20.0317
delta_h -33.1 kJ
(Co(NH3)5OH2)Cl3
(Co(NH3)5OH2)Cl3 + 5H+ = Co+3 + 5NH4+ + 3Cl- + H2O
log_k 11.7351
delta_h -25.37 kJ
(Co(NH3)5Cl)Cl2
(Co(NH3)5Cl)Cl2 + 5H+ = Co+3 + 5NH4+ + 3Cl-
log_k 4.5102
delta_h -10.74 kJ
Fe(OH)2.7Cl.3
Fe(OH)2.7Cl.3 + 2.7H+ = Fe+3 + 2.7H2O + 0.3Cl-
log_k -3.04
delta_h -0 kJ
MnCl2:4H2O
MnCl2:4H2O = Mn+2 + 2Cl- + 4H2O
log_k 2.7151
delta_h -10.83 kJ
CrCl2
CrCl2 = Cr+2 + 2Cl-
log_k 14.0917
delta_h -110.76 kJ
CrCl3
CrCl3 + 2H2O = Cr(OH)2+ + 3Cl- + 2H+
log_k 15.1145
delta_h -121.08 kJ
VCl2
VCl2 = V+3 + 2Cl- + e-
log_k 18.8744
delta_h -141.16 kJ
VCl3
VCl3 = V+3 + 3Cl-
log_k 23.4326
delta_h -179.54 kJ
```

```
VOCl
VOCl + 2H+ = V+3 + Cl- + H2O
log_k 11.1524
delta_h -104.91 kJ
VOCl2
VOCl2 = VO+2 + 2Cl-
log_k 12.7603
delta_h -117.76 kJ
VO2Cl
VO2Cl = VO2+ + Cl-
log_k 2.8413
delta_h -40.28 kJ
Halite
NaCl = Na+ + Cl-
log_k 1.6025
delta_h 3.7 kJ
SbBr3
SbBr3 + 3H2O = Sb(OH)3 + 3Br- + 3H+
log_k 0.9689
delta_h -20.94 kJ
SnBr2
SnBr2 + 2H2O = Sn(OH)2 + 2H+ + 2Br-
log_k -9.5443
delta_h -0 kJ
SnBr4
SnBr4 + 6H2O = Sn(OH)6-2 + 6H+ + 4Br-
log_k -28.8468
delta_h -0 kJ
PbBr2
PbBr2 = Pb+2 + 2Br-
log_k -5.3
delta_h 35.499 kJ
PbBrF
PbBrF = Pb+2 + Br- + F-
log_k -8.49
delta_h -0 kJ
TlBr
TlBr = Tl+ + Br-
log_k -5.44
delta_h 54 kJ
ZnBr2:2H2O
ZnBr2:2H2O = Zn+2 + 2Br- + 2H2O
log_k 5.2005
delta_h -30.67 kJ
CdBr2:4H2O
CdBr2:4H2O = Cd+2 + 2Br- + 4H2O
log_k -2.425
delta_h 30.5001 kJ
Hg2Br2
Hg2Br2 = Hg2+2 + 2Br-
log_k -22.25
delta_h 133 kJ
HgBr2
HgBr2 + 2H2O = Hg(OH)2 + 2Br- + 2H+
```

```
log_k -25.2734
delta_h 138.492 kJ
CuBr
CuBr = Cu+ + Br-
log_k -8.3
delta_h 54.86 kJ
Cu2(OH)3Br
Cu2(OH)3Br + 3H+ = 2Cu+2 + 3H2O + Br-
log_k 7.9085
delta_h -93.43 kJ
Bromyrite
AgBr = Ag+ + Br-
log_k -12.3
delta_h 84.5 kJ
(Co(NH3)6)Br3
(Co(NH3)6)Br3 + 6H+ = Co+3 + 6NH4+ + 3Br-
log_k 18.3142
delta_h -21.1899 kJ
(Co(NH3)5Cl)Br2
(Co(NH3)5Cl)Br2 + 5H+ = Co+3 + 5NH4+ + Cl- + 2Br-
log_k 5.0295
delta_h -6.4 kJ
CrBr3
CrBr3 + 2H2O = Cr(OH)2+ + 3Br- + 2H+
log_k 19.9086
delta_h -141.323 kJ
AsI3
AsI3 + 3H2O = H3AsO3 + 3I- + 3H+
log_k 4.2307
delta_h 3.15 kJ
SbI3
SbI3 + 3H2O = Sb(OH)3 + 3H+ + 3I-
log_k -0.538
delta_h 13.5896 kJ
PbI2
PbI2 = Pb+2 + 2I-
log_k -8.1
delta_h 62 kJ
TlI
TlI = Tl+ + I-
log_k -7.23
delta_h 75 kJ
ZnI2
ZnI2 = Zn+2 + 2I-
log_k 7.3055
delta_h -58.92 kJ
CdI2
CdI2 = Cd+2 + 2I-
log_k -3.5389
delta_h 13.82 kJ
Hg2I2
Hg2I2 = Hg2+2 + 2I-
log_k -28.34
delta_h 163 kJ
```

```
Coccinite
HgI2 + 2H2O = Hg(OH)2 + 2H+ + 2I-
log_k -34.9525
delta_h 210.72 kJ
HgI2:2NH3
HgI2:2NH3 + 2H2O = Hg(OH)2 + 2I- + 2NH4+
log_k -16.2293
delta_h 132.18 kJ
HgI2:6NH3
HgI2:6NH3 + 2H2O + 4H+ = Hg(OH)2 + 2I- + 6NH4+
log_k 33.7335
delta_h -90.3599 kJ
CuI
CuI = Cu+ + I-
log_k -12
delta_h 82.69 kJ
Iodyrite
AgI = Ag+ + I-
log_k -16.08
delta_h 110 kJ
(Co(NH3)6)I3
(Co(NH3)6)I3 + 6H+ = Co+3 + 6NH4+ + 3I-
log_k 16.5831
delta_h -9.6999 kJ
(Co(NH3)5Cl)I2
(Co(NH3)5Cl)I2 + 5H+ = Co+3 + 5NH4+ + Cl- + 2I-
log_k 5.5981
delta_h 0.66 kJ
CrI3
CrI3 + 2H2O = Cr(OH)2+ + 3I- + 2H+
log_k 20.4767
delta_h -134.419 kJ
Cerussite
PbCO3 = Pb+2 + CO3-2
log_k -13.13
delta_h 24.79 kJ
Pb2OCO3
Pb2OCO3 + 2H+ = 2Pb+2 + H2O + CO3-2
log_k -0.5578
delta_h -40.8199 kJ
Pb3O2CO3
Pb3O2CO3 + 4H+ = 3Pb+2 + CO3-2 + 2H2O
log_k 11.02
delta_h -110.583 kJ
Hydrocerussite
Pb3(OH)2(CO3)2 + 2H+ = 3Pb+2 + 2H2O + 2CO3-2
log_k -18.7705
delta_h -0 kJ
Pb10(OH)6O(CO3)6
Pb10(OH)6O(CO3)6 + 8H+ = 10Pb+2 + 6CO3-2 + 7H2O
log_k -8.76
delta_h -0 kJ
Tl2CO3
Tl2CO3 = 2Tl+ + CO3-2
```

```
log_k -3.8367
delta_h 35.49 kJ
Smithsonite
ZnCO3 = Zn+2 + CO3-2
log_k -10
delta_h -15.84 kJ
ZnCO3:1H2O
ZnCO3:1H2O = Zn+2 + CO3-2 + H2O
log_k -10.26
delta_h -0 kJ
Otavite
CdCO3 = Cd+2 + CO3-2
log_k -12
delta_h -0.55 kJ
Hg2CO3
Hg2CO3 = Hg2+2 + CO3-2
log_k -16.05
delta_h 45.14 kJ
Hg3O2CO3
Hg3O2CO3 + 4H2O = 3Hg(OH)2 + 2H+ + CO3-2
log_k -29.682
delta_h -0 kJ
CuCO3
CuCO3 = Cu+2 + CO3-2
log_k -11.5
delta_h -0 kJ
Malachite
Cu2(OH)2CO3 + 2H+ = 2Cu+2 + 2H2O + CO3-2
log_k -5.306
delta_h 76.38 kJ
Azurite
Cu3(OH)2(CO3)2 + 2H+ = 3Cu+2 + 2H2O + 2CO3-2
log_k -16.906
delta_h -95.22 kJ
Ag2CO3
Ag2CO3 = 2Ag+ + CO3-2
log_k -11.09
delta_h 42.15 kJ
NiCO3
NiCO3 = Ni+2 + CO3-2
log_k -6.87
delta_h -41.589 kJ
CoCO3
CoCO3 = Co+2 + CO3-2
log_k -9.98
delta_h -12.7612 kJ
Siderite
FeCO3 = Fe+2 + CO3-2
log_k -10.24
delta_h -16 kJ
Rhodochrosite
MnCO3 = Mn+2 + CO3-2
log_k -10.58
delta_h -1.88 kJ
```

```
Rutherfordine
UO2CO3 = UO2+2 + CO3-2
log_k -14.5
delta_h -3.03 kJ
Artinite
MgCO3:Mg(OH)2:3H2O + 2H+ = 2Mg+2 + CO3-2 + 5H2O
log_k 9.6
delta_h -120.257 kJ
Hydromagnesite
Mg5(CO3)4(OH)2:4H2O + 2H+ = 5Mg+2 + 4CO3-2 + 6H2O
log_k -8.766
delta_h -218.447 kJ
Magnesite
MgCO3 = Mg+2 + CO3-2
log_k -7.46
delta_h 20 kJ
Nesquehonite
MgCO3:3H2O = Mg+2 + CO3-2 + 3H2O
log_k -4.67
delta_h -24.2212 kJ
Aragonite
CaCO3 = Ca+2 + CO3-2
log_k -8.3
delta_h -12 kJ
Calcite
CaCO3 = Ca+2 + CO3-2
log_k -8.48
delta_h -8 kJ
Dolomite(ordered)
CaMg(CO3)2 = Ca+2 + Mg+2 + 2CO3-2
log_k -17.09
delta_h -39.5 kJ
Dolomite(disordered)
CaMg(CO3)2 = Ca+2 + Mg+2 + 2CO3-2
log_k -16.54
delta_h -46.4 kJ
Huntite
CaMg3(CO3)4 = 3Mg+2 + Ca+2 + 4CO3-2
log_k -29.968
delta_h -107.78 kJ
Strontianite
SrCO3 = Sr+2 + CO3-2
log_k -9.27
delta_h -0 kJ
Witherite
BaCO3 = Ba+2 + CO3-2
log_k -8.57
delta_h 4 kJ
Thermonatrite
Na2CO3:H2O = 2Na+ + CO3-2 + H2O
log_k 0.637
delta_h -10.4799 kJ
TlNO3
TlNO3 = Tl+ + NO3-
```

```
log_k -1.6127
delta_h 42.44 kJ
Zn(NO3)2:6H2O
Zn(NO3)2:6H2O = Zn+2 + 2NO3- + 6H2O
log_k 3.3153
delta_h 24.5698 kJ
Cu2(OH)3NO3
Cu2(OH)3NO3 + 3H+ = 2Cu+2 + 3H2O + NO3-
log_k 9.251
delta_h -72.5924 kJ
(Co(NH3)6)(NO3)3
(Co(NH3)6)(NO3)3 + 6H+ = Co+3 + 6NH4+ + 3NO3-
log_k 17.9343
delta_h 1.59 kJ
(Co(NH3)5Cl)(NO3)2
(Co(NH3)5Cl)(NO3)2 + 5H+ = Co+3 + 5NH4+ + Cl- + 2NO3-
log_k 6.2887
delta_h 6.4199 kJ
UO2(NO3)2
UO2(NO3)2 = UO2+2 + 2NO3-
log_k 12.1476
delta_h -83.3999 kJ
UO2(NO3)2:2H2O
UO2(NO3)2:2H2O = UO2+2 + 2NO3- + 2H2O
log_k 4.851
delta_h -25.355 kJ
UO2(NO3)2:3H2O
UO2(NO3)2:3H2O = UO2+2 + 2NO3- + 3H2O
log_k 3.39
delta_h -9.1599 kJ
UO2(NO3)2:6H2O
UO2(NO3)2:6H2O = UO2+2 + 2NO3- + 6H2O
log_k 2.0464
delta_h 20.8201 kJ
Pb(BO2)2
Pb(BO2)2 + 2H2O + 2H+ = Pb+2 + 2H3BO3
log_k 6.5192
delta_h -15.6119 kJ
Zn(BO2)2
Zn(BO2)2 + 2H2O + 2H+ = Zn+2 + 2H3BO3
log_k 8.29
delta_h -0 kJ
Cd(BO2)2
Cd(BO2)2 + 2H2O + 2H+ = Cd+2 + 2H3BO3
log_k 9.84
delta_h -0 kJ
Co(BO2)2
Co(BO2)2 + 2H2O + 2H+ = Co+2 + 2H3BO3
log_k 27.0703
delta_h -0 kJ
SnSO4
SnSO4 + 2H2O = Sn(OH)2 + 2H+ + SO4-2
log_k -56.9747
delta_h -0 kJ
```

```
Sn(SO4)2
Sn(SO4)2 + 6H2O = Sn(OH)6-2 + 6H+ + 2SO4-2
log_k -15.2123
delta_h -0 kJ
Larnakite
PbO:PbSO4 + 2H+ = 2Pb+2 + SO4-2 + H2O
log_k -0.4344
delta_h -21.83 kJ
Pb3O2SO4
Pb3O2SO4 + 4H+ = 3Pb+2 + SO4-2 + 2H2O
log_k 10.6864
delta_h -79.14 kJ
Pb4O3SO4
Pb4O3SO4 + 6H+ = 4Pb+2 + SO4-2 + 3H2O
log_k 21.8772
delta_h -136.45 kJ
Anglesite
PbSO4 = Pb+2 + SO4-2
log_k -7.79
delta_h 12 kJ
Pb4(OH)6SO4
Pb4(OH)6SO4 + 6H+ = 4Pb+2 + SO4-2 + 6H2O
log_k 21.1
delta_h -0 kJ
AlOHSO4
AlOHSO4 + H+ = Al+3 + SO4-2 + H2O
log_k -3.23
delta_h -0 kJ
Al4(OH)10SO4
Al4(OH)10SO4 + 10H+ = 4Al+3 + SO4-2 + 10H2O
log_k 22.7
delta_h -0 kJ
Tl2SO4
Tl2SO4 = 2Tl+ + SO4-2
log_k -3.7868
delta_h 33.1799 kJ
Zn2(OH)2SO4
Zn2(OH)2SO4 + 2H+ = 2Zn+2 + 2H2O + SO4-2
log_k 7.5
delta_h -0 kJ
Zn4(OH)6SO4
Zn4(OH)6SO4 + 6H+ = 4Zn+2 + 6H2O + SO4-2
log_k 28.4
delta_h -0 kJ
Zn3O(SO4)2
Zn3O(SO4)2 + 2H+ = 3Zn+2 + 2SO4-2 + H2O
log_k 18.9135
delta_h -258.08 kJ
Zincosite
ZnSO4 = Zn+2 + SO4-2
log_k 3.9297
delta_h -82.586 kJ
ZnSO4:1H2O
ZnSO4:1H2O = Zn+2 + SO4-2 + H2O
```

```
log_k -0.638
delta_h -44.0699 kJ
Bianchite
ZnSO4:6H2O = Zn+2 + SO4-2 + 6H2O
log_k -1.765
delta_h -0.6694 kJ
Goslarite
ZnSO4:7H2O = Zn+2 + SO4-2 + 7H2O
log_k -2.0112
delta_h 14.21 kJ
Cd3(OH)4SO4
Cd3(OH)4SO4 + 4H+ = 3Cd+2 + 4H2O + SO4-2
log_k 22.56
delta_h -0 kJ
Cd3(OH)2(SO4)2
Cd3(OH)2(SO4)2 + 2H+ = 3Cd+2 + 2H2O + 2SO4-2
log_k 6.71
delta_h -0 kJ
Cd4(OH)6SO4
Cd4(OH)6SO4 + 6H+ = 4Cd+2 + 6H2O + SO4-2
log_k 28.4
delta_h -0 kJ
CdSO4
CdSO4 = Cd+2 + SO4-2
log_k -0.1722
delta_h -51.98 kJ
CdSO4:1H2O
CdSO4:1H2O = Cd+2 + SO4-2 + H2O
log_k -1.7261
delta_h -31.5399 kJ
CdSO4:2.67H2O
CdSO4:2.67H2O = Cd+2 + SO4-2 + 2.67H2O
log_k -1.873
delta_h -17.9912 kJ
Hg2SO4
Hg2SO4 = Hg2+2 + SO4-2
log_k -6.13
delta_h 5.4 kJ
HgSO4
HgSO4 + 2H2O = Hg(OH)2 + SO4-2 + 2H+
log_k -9.4189
delta_h 14.6858 kJ
Cu2SO4
Cu2SO4 = 2Cu+ + SO4-2
log_k -1.95
delta_h -19.079 kJ
Antlerite
Cu3(OH)4SO4 + 4H+ = 3Cu+2 + 4H2O + SO4-2
log_k 8.788
delta_h -0 kJ
Brochantite
Cu4(OH)6SO4 + 6H+ = 4Cu+2 + 6H2O + SO4-2
log_k 15.222
delta_h -202.86 kJ
```

```
Langite
Cu4(OH)6SO4:H2O + 6H+ = 4Cu+2 + 7H2O + SO4-2
log_k 17.4886
delta_h -165.55 kJ
CuOCuSO4
CuOCuSO4 + 2H+ = 2Cu+2 + H2O + SO4-2
log_k 10.3032
delta_h -137.777 kJ
CuSO4
CuSO4 = Cu+2 + SO4-2
log_k 2.9395
delta_h -73.04 kJ
Chalcanthite
CuSO4:5H2O = Cu+2 + SO4-2 + 5H2O
log_k -2.64
delta_h 6.025 kJ
Ag2SO4
Ag2SO4 = 2Ag+ + SO4-2
log_k -4.82
delta_h 17 kJ
Ni4(OH)6SO4
Ni4(OH)6SO4 + 6H+ = 4Ni+2 + SO4-2 + 6H2O
log_k 32
delta_h -0 kJ
Retgersite
NiSO4:6H2O = Ni+2 + SO4-2 + 6H2O
log_k -2.04
delta_h 4.6024 kJ
Morenosite
NiSO4:7H2O = Ni+2 + SO4-2 + 7H2O
log_k -2.1449
delta_h 12.1802 kJ
CoSO4
CoSO4 = Co+2 + SO4-2
log_k 2.8024
delta_h -79.277 kJ
CoSO4:6H2O
CoSO4:6H2O = Co+2 + SO4-2 + 6H2O
log_k -2.4726
delta_h 1.0801 kJ
Melanterite
FeSO4:7H2O = Fe+2 + SO4-2 + 7H2O
log_k -2.209
delta_h 20.5 kJ
Fe2(SO4)3
Fe2(SO4)3 = 2Fe+3 + 3SO4-2
log_k -3.7343
delta_h -242.028 kJ
H-Jarosite
(H3O)Fe3(SO4)2(OH)6 + 5H+ = 3Fe+3 + 2SO4-2 + 7H2O
log_k -12.1
delta_h -230.748 kJ
Na-Jarosite
NaFe3(SO4)2(OH)6 + 6H+ = Na+ + 3Fe+3 + 2SO4-2 + 6H2O
```

```
log_k -11.2
delta_h -151.377 kJ
K-Jarosite
KFe3(SO4)2(OH)6 + 6H+ = K+ + 3Fe+3 + 2SO4-2 + 6H2O
log_k -14.8
delta_h -130.875 kJ
MnSO4
MnSO4 = Mn+2 + SO4-2
log_k 2.5831
delta_h -64.8401 kJ
Mn2(SO4)3
Mn2(SO4)3 = 2Mn+3 + 3SO4-2
log_k -5.711
delta_h -163.427 kJ
VOSO4
VOSO4 = VO+2 + SO4-2
log_k 3.6097
delta_h -86.7401 kJ
Epsomite
MgSO4:7H2O = Mg+2 + SO4-2 + 7H2O
log_k -2.1265
delta_h 11.5601 kJ
Anhydrite
CaSO4 = Ca+2 + SO4-2
log_k -4.36
delta_h -7.2 kJ
Gypsum
CaSO4:2H2O = Ca+2 + SO4-2 + 2H2O
log_k -4.61
delta_h 1 kJ
Celestite
SrSO4 = Sr+2 + SO4-2
log_k -6.62
delta_h 2 kJ
Barite
BaSO4 = Ba+2 + SO4-2
log_k -9.98
delta_h 23 kJ
Mirabilite
Na2SO4:10H2O = 2Na+ + SO4-2 + 10H2O
log_k -1.114
delta_h 79.4416 kJ
Thenardite
Na2SO4 = 2Na+ + SO4-2
log_k 0.3217
delta_h -9.121 kJ
K-Alum
KAl(SO4)2:12H2O = K+ + Al+3 + 2SO4-2 + 12H2O
log_k -5.17
delta_h 30.2085 kJ
Alunite
KAl3(SO4)2(OH)6 + 6H+ = K+ + 3Al+3 + 2SO4-2 + 6H2O
log_k -1.4
delta_h -210 kJ
```

```
(NH4)2CrO4
(NH4)2CrO4 = CrO4-2 + 2NH4+
log_k 0.4046
delta_h 9.163 kJ
PbCrO4
PbCrO4 = Pb+2 + CrO4-2
log_k -12.6
delta_h 44.18 kJ
Tl2CrO4
Tl2CrO4 = 2Tl+ + CrO4-2
log_k -12.01
delta_h 74.27 kJ
Hg2CrO4
Hg2CrO4 = Hg2+2 + CrO4-2
log_k -8.7
delta_h -0 kJ
CuCrO4
CuCrO4 = Cu+2 + CrO4-2
log_k -5.44
delta_h -0 kJ
Ag2CrO4
Ag2CrO4 = 2Ag+ + CrO4-2
log_k -11.59
delta_h 62 kJ
MgCrO4
MgCrO4 = CrO4-2 + Mg+2
log_k 5.3801
delta_h -88.9518 kJ
CaCrO4
CaCrO4 = Ca+2 + CrO4-2
log_k -2.2657
delta_h -26.945 kJ
SrCrO4
SrCrO4 = Sr+2 + CrO4-2
log_k -4.65
delta_h -10.1253 kJ
BaCrO4
BaCrO4 = Ba+2 + CrO4-2
log_k -9.67
delta_h 33 kJ
Li2CrO4
Li2CrO4 = CrO4-2 + 2Li+
log_k 4.8568
delta_h -45.2792 kJ
Na2CrO4
Na2CrO4 = CrO4-2 + 2Na+
log_k 2.9302
delta_h -19.6301 kJ
Na2Cr2O7
Na2Cr2O7 + H2O = 2CrO4-2 + 2Na+ + 2H+
log_k -9.8953
delta_h 22.1961 kJ
K2CrO4
K2CrO4 = CrO4-2 + 2K+
```

```
log_k -0.5134
delta_h 18.2699 kJ
K2Cr2O7
K2Cr2O7 + H2O = 2CrO4-2 + 2K+ + 2H+
log_k -17.2424
delta_h 80.7499 kJ
Hg2SeO3
Hg2SeO3 + H+ = Hg2+2 + HSeO3-
log_k -4.657
delta_h -0 kJ
HgSeO3
HgSeO3 + 2H2O = Hg(OH)2 + H+ + HSeO3-
log_k -12.43
delta_h -0 kJ
Ag2SeO3
Ag2SeO3 + H+ = 2Ag+ + HSeO3-
log_k -7.15
delta_h 39.68 kJ
CuSeO3:2H2O
CuSeO3:2H2O + H+ = Cu+2 + HSeO3- + 2H2O
log_k 0.5116
delta_h -36.861 kJ
NiSeO3:2H2O
NiSeO3:2H2O + H+ = HSeO3- + Ni+2 + 2H2O
log_k 2.8147
delta_h -31.0034 kJ
CoSeO3
CoSeO3 + H+ = Co+2 + HSeO3-
log_k 1.32
delta_h -0 kJ
Fe2(SeO3)3:2H2O
Fe2(SeO3)3:2H2O + 3H+ = 3HSeO3- + 2Fe+3 + 2H2O
log_k -20.6262
delta_h -0 kJ
Fe2(OH)4SeO3
Fe2(OH)4SeO3 + 5H+ = HSeO3- + 2Fe+3 + 4H2O
log_k 1.5539
delta_h -0 kJ
MnSeO3
MnSeO3 + H+ = Mn+2 + HSeO3-
log_k 1.13
delta_h -0 kJ
MnSeO3:2H2O
MnSeO3:2H2O + H+ = HSeO3- + Mn+2 + 2H2O
log_k 0.9822
delta_h 8.4935 kJ
MgSeO3:6H2O
MgSeO3:6H2O + H+ = Mg+2 + HSeO3- + 6H2O
log_k 3.0554
delta_h 5.23 kJ
CaSeO3:2H2O
CaSeO3:2H2O + H+ = HSeO3- + Ca+2 + 2H2O
log_k 2.8139
delta_h -19.4556 kJ
```

```
SrSeO3
SrSeO3 + H+ = Sr+2 + HSeO3-
log_k 2.3
delta_h -0 kJ
BaSeO3
BaSeO3 + H+ = Ba+2 + HSeO3-
log_k 1.83
delta_h 11.98 kJ
Na2SeO3:5H2O
Na2SeO3:5H2O + H+ = 2Na+ + HSeO3- + 5H2O
log_k 10.3
delta_h -0 kJ
PbSeO4
PbSeO4 = Pb+2 + SeO4-2
log_k -6.84
delta_h 15 kJ
Tl2SeO4
Tl2SeO4 = 2Tl+ + SeO4-2
log_k -4.1
delta_h 43 kJ
ZnSeO4:6H2O
ZnSeO4:6H2O = Zn+2 + SeO4-2 + 6H2O
log_k -1.52
delta_h -0 kJ
CdSeO4:2H2O
CdSeO4:2H2O = Cd+2 + SeO4-2 + 2H2O
log_k -1.85
delta_h -0 kJ
Ag2SeO4
Ag2SeO4 = 2Ag+ + SeO4-2
log_k -8.91
delta_h -43.5 kJ
CuSeO4:5H2O
CuSeO4:5H2O = Cu+2 + SeO4-2 + 5H2O
log_k -2.44
delta_h -0 kJ
NiSeO4:6H2O
NiSeO4:6H2O = Ni+2 + SeO4-2 + 6H2O
log_k -1.52
delta_h -0 kJ
CoSeO4:6H2O
CoSeO4:6H2O = Co+2 + SeO4-2 + 6H2O
log_k -1.53
delta_h -0 kJ
MnSeO4:5H2O
MnSeO4:5H2O = Mn+2 + SeO4-2 + 5H2O
log_k -2.05
delta_h -0 kJ
UO2SeO4:4H2O
UO2SeO4:4H2O = UO2+2 + SeO4-2 + 4H2O
log_k -2.25
delta_h -0 kJ
MgSeO4:6H2O
MgSeO4:6H2O = Mg+2 + SeO4-2 + 6H2O
```

```
log_k -1.2
delta_h -0 kJ
CaSeO4:2H2O
CaSeO4:2H2O = Ca+2 + SeO4-2 + 2H2O
log_k -3.02
delta_h -8.3 kJ
SrSeO4
SrSeO4 = Sr+2 + SeO4-2
log_k -4.4
delta_h 0.4 kJ
BaSeO4
BaSeO4 = Ba+2 + SeO4-2
log_k -7.46
delta_h 22 kJ
BeSeO4:4H2O
BeSeO4:4H2O = Be+2 + SeO4-2 + 4H2O
log_k -2.94
delta_h -0 kJ
Na2SeO4
Na2SeO4 = 2Na+ + SeO4-2
log_k 1.28
delta_h -0 kJ
K2SeO4
K2SeO4 = 2K+ + SeO4-2
log_k -0.73
delta_h -0 kJ
(NH4)2SeO4
(NH4)2SeO4 = 2NH4+ + SeO4-2
log_k 0.45
delta_h -0 kJ
H2MoO4
H2MoO4 = MoO4-2 + 2H+
log_k -12.8765
delta_h 49 kJ
PbMoO4
PbMoO4 = Pb+2 + MoO4-2
log_k -15.62
delta_h 53.93 kJ
Al2(MoO4)3
Al2(MoO4)3 = 3MoO4-2 + 2Al+3
log_k 2.3675
delta_h -260.8 kJ
Tl2MoO4
Tl2MoO4 = MoO4-2 + 2Tl+
log_k -7.9887
delta_h -0 kJ
ZnMoO4
ZnMoO4 = MoO4-2 + Zn+2
log_k -10.1254
delta_h -10.6901 kJ
CdMoO4
CdMoO4 = MoO4-2 + Cd+2
log_k -14.1497
delta_h 19.48 kJ
```

```
CuMoO4
CuMoO4 = MoO4-2 + Cu+2
log_k -13.0762
delta_h 12.2 kJ
Ag2MoO4
Ag2MoO4 = 2Ag+ + MoO4-2
log_k -11.55
delta_h 52.7 kJ
NiMoO4
NiMoO4 = MoO4-2 + Ni+2
log_k -11.1421
delta_h 1.3 kJ
CoMoO4
CoMoO4 = MoO4-2 + Co+2
log_k -7.7609
delta_h -23.3999 kJ
FeMoO4
FeMoO4 = MoO4-2 + Fe+2
log_k -10.091
delta_h -11.1 kJ
BeMoO4
BeMoO4 = MoO4-2 + Be+2
log_k -1.7817
delta_h -56.4 kJ
MgMoO4
MgMoO4 = Mg+2 + MoO4-2
log_k -1.85
delta_h -0 kJ
CaMoO4
CaMoO4 = Ca+2 + MoO4-2
log_k -7.95
delta_h -2 kJ
BaMoO4
BaMoO4 = MoO4-2 + Ba+2
log_k -6.9603
delta_h 10.96 kJ
Li2MoO4
Li2MoO4 = MoO4-2 + 2Li+
log_k 2.4416
delta_h -33.9399 kJ
Na2MoO4
Na2MoO4 = MoO4-2 + 2Na+
log_k 1.4901
delta_h -9.98 kJ
Na2MoO4:2H2O
Na2MoO4:2H2O = MoO4-2 + 2Na+ + 2H2O
log_k 1.224
delta_h -0 kJ
Na2Mo2O7
Na2Mo2O7 + H2O = 2MoO4-2 + 2Na+ + 2H+
log_k -16.5966
delta_h 56.2502 kJ
K2MoO4
K2MoO4 = MoO4-2 + 2K+
```

```
log_k 3.2619
delta_h -3.38 kJ
PbHPO4
PbHPO4 = Pb+2 + H+ + PO4-3
log_k -23.805
delta_h -0 kJ
Pb3(PO4)2
Pb3(PO4)2 = 3Pb+2 + 2PO4-3
log_k -43.53
delta_h -0 kJ
Pyromorphite
Pb5(PO4)3Cl = 5Pb+2 + 3PO4-3 + Cl-
log_k -84.43
delta_h -0 kJ
Hydroxylpyromorphite
Pb5(PO4)3OH + H+ = 5Pb+2 + 3PO4-3 + H2O
log_k -62.79
delta_h -0 kJ
Plumbgummite
PbAl3(PO4)2(OH)5:H2O + 5H+ = Pb+2 + 3Al+3 + 2PO4-3 + 6H2O
log_k -32.79
delta_h -0 kJ
Hinsdalite
PbAl3PO4SO4(OH)6 + 6H+ = Pb+2 + 3Al+3 + PO4-3 + SO4-2 + 6H2O
log_k -2.5
delta_h -0 kJ
Tsumebite
Pb2CuPO4(OH)3:3H2O + 3H+ = 2Pb+2 + Cu+2 + PO4-3 + 6H2O
log_k -9.79
delta_h -0 kJ
Zn3(PO4)2:4H2O
Zn3(PO4)2:4H2O = 3Zn+2 + 2PO4-3 + 4H2O
log_k -35.42
delta_h -0 kJ
Cd3(PO4)2
Cd3(PO4)2 = 3Cd+2 + 2PO4-3
log_k -32.6
delta_h -0 kJ
Hg2HPO4
Hg2HPO4 = Hg2+2 + H+ + PO4-3
log_k -24.775
delta_h -0 kJ
Cu3(PO4)2
Cu3(PO4)2 = 3Cu+2 + 2PO4-3
log_k -36.85
delta_h -0 kJ
Cu3(PO4)2:3H2O
Cu3(PO4)2:3H2O = 3Cu+2 + 2PO4-3 + 3H2O
log_k -35.12
delta_h -0 kJ
Ag3PO4
Ag3PO4 = 3Ag+ + PO4-3
log_k -17.59
delta_h -0 kJ
```

```
Ni3(PO4)2
Ni3(PO4)2 = 3Ni+2 + 2PO4-3
log_k -31.3
delta_h -0 kJ
CoHPO4
CoHPO4 = Co+2 + PO4-3 + H+
log_k -19.0607
delta_h -0 kJ
Co3(PO4)2
Co3(PO4)2 = 3Co+2 + 2PO4-3
log_k -34.6877
delta_h -0 kJ
Vivianite
Fe3(PO4)2:8H2O = 3Fe+2 + 2PO4-3 + 8H2O
log_k -36
delta_h -0 kJ
Strengite
FePO4:2H2O = Fe+3 + PO4-3 + 2H2O
log_k -26.4
delta_h -9.3601 kJ
Mn3(PO4)2
Mn3(PO4)2 = 3Mn+2 + 2PO4-3
log_k -23.827
delta_h 8.8701 kJ
MnHPO4
MnHPO4 = Mn+2 + PO4-3 + H+
log_k -25.4
delta_h -0 kJ
(VO)3(PO4)2
(VO)3(PO4)2 = 3VO+2 + 2PO4-3
log_k -25.1
delta_h -0 kJ
Mg3(PO4)2
Mg3(PO4)2 = 3Mg+2 + 2PO4-3
log_k -23.28
delta_h -0 kJ
MgHPO4:3H2O
MgHPO4:3H2O = Mg+2 + H+ + PO4-3 + 3H2O
log_k -18.175
delta_h -0 kJ
FCO3Apatite
Ca9.316Na0.36Mg0.144(PO4)4.8(CO3)1.2F2.48 = 9.316Ca+2 + 0.36Na+ + 0.144Mg+2 + 4.8PO4-3 + 1.2CO3-2 + 2.48F-
log_k -114.4
delta_h 164.808 kJ
Hydroxylapatite
Ca5(PO4)3OH + H+ = 5Ca+2 + 3PO4-3 + H2O
log_k -44.333
delta_h -0 kJ
CaHPO4:2H2O
CaHPO4:2H2O = Ca+2 + H+ + PO4-3 + 2H2O
log_k -18.995
delta_h 23 kJ
CaHPO4
```

```
CaHPO4 = Ca+2 + H+ + PO4-3
log_k -19.275
delta_h 31 kJ
Ca3(PO4)2(beta)
Ca3(PO4)2 = 3Ca+2 + 2PO4-3
log_k -28.92
delta_h 54 kJ
Ca4H(PO4)3:3H2O
Ca4H(PO4)3:3H2O = 4Ca+2 + H+ + 3PO4-3 + 3H2O
log_k -47.08
delta_h -0 kJ
SrHPO4
SrHPO4 = Sr+2 + H+ + PO4-3
log_k -19.295
delta_h -0 kJ
BaHPO4
BaHPO4 = Ba+2 + H+ + PO4-3
log_k -19.775
delta_h -0 kJ
U(HPO4)2:4H2O
U(HPO4)2:4H2O = U+4 + 2PO4-3 + 2H+ + 4H2O
log_k -51.584
delta_h 16.0666 kJ
(UO2)3(PO4)2
(UO2)3(PO4)2 = 3UO2+2 + 2PO4-3
log_k -49.4
delta_h 397.062 kJ
UO2HPO4
UO2HPO4 = UO2+2 + H+ + PO4-3
log_k -24.225
delta_h -0 kJ
Uramphite
(NH4)2(UO2)2(PO4)2 = 2UO2+2 + 2NH4+ + 2PO4-3
log_k -51.749
delta_h 40.5848 kJ
Przhevalskite
Pb(UO2)2(PO4)2 = 2UO2+2 + Pb+2 + 2PO4-3
log_k -44.365
delta_h -46.024 kJ
Torbernite
Cu(UO2)2(PO4)2 = 2UO2+2 + Cu+2 + 2PO4-3
log_k -45.279
delta_h -66.5256 kJ
Bassetite
Fe(UO2)2(PO4)2 = 2UO2+2 + Fe+2 + 2PO4-3
log_k -44.485
delta_h -83.2616 kJ
Saleeite
Mg(UO2)2(PO4)2 = 2UO2+2 + Mg+2 + 2PO4-3
log_k -43.646
delta_h -84.4331 kJ
Ningyoite
CaU(PO4)2:2H2O = U+4 + Ca+2 + 2PO4-3 + 2H2O
log_k -53.906
```

```
delta_h -9.4977 kJ
H-Autunite
H2(UO2)2(PO4)2 = 2UO2+2 + 2H+ + 2PO4-3
log_k -47.931
delta_h -15.0624 kJ
Autunite
Ca(UO2)2(PO4)2 = 2UO2+2 + Ca+2 + 2PO4-3
log_k -43.927
delta_h -59.9986 kJ
Sr-Autunite
Sr(UO2)2(PO4)2 = 2UO2+2 + Sr+2 + 2PO4-3
log_k -44.457
delta_h -54.6012 kJ
Na-Autunite
Na2(UO2)2(PO4)2 = 2UO2+2 + 2Na+ + 2PO4-3
log_k -47.409
delta_h -1.9246 kJ
K-Autunite
K2(UO2)2(PO4)2 = 2UO2+2 + 2K+ + 2PO4-3
log_k -48.244
delta_h 24.5182 kJ
Uranocircite
Ba(UO2)2(PO4)2 = 2UO2+2 + Ba+2 + 2PO4-3
log_k -44.631
delta_h -42.2584 kJ
Pb3(AsO4)2
Pb3(AsO4)2 + 6H+ = 3Pb+2 + 2H3AsO4
log_k 5.8
delta_h -0 kJ
AlAsO4:2H2O
AlAsO4:2H2O + 3H+ = Al+3 + H3AsO4 + 2H2O
log_k 4.8
delta_h -0 kJ
Zn3(AsO4)2:2.5H2O
Zn3(AsO4)2:2.5H2O + 6H+ = 3Zn+2 + 2H3AsO4 + 2.5H2O
log_k 13.65
delta_h -0 kJ
Cu3(AsO4)2:2H2O
Cu3(AsO4)2:2H2O + 6H+ = 3Cu+2 + 2H3AsO4 + 2H2O
log_k 6.1
delta_h -0 kJ
Ag3AsO3
Ag3AsO3 + 3H+ = 3Ag+ + H3AsO3
log_k 2.1573
delta_h -0 kJ
Ag3AsO4
Ag3AsO4 + 3H+ = 3Ag+ + H3AsO4
log_k -2.7867
delta_h -0 kJ
Ni3(AsO4)2:8H2O
Ni3(AsO4)2:8H2O + 6H+ = 3Ni+2 + 2H3AsO4 + 8H2O
log_k 15.7
delta_h -0 kJ
Co3(AsO4)2
```

```
Co3(AsO4)2 + 6H+ = 3Co+2 + 2H3AsO4
log_k 13.0341
delta_h -0 kJ
FeAsO4:2H2O
FeAsO4:2H2O + 3H+ = Fe+3 + H3AsO4 + 2H2O
log_k 0.4
delta_h -0 kJ
Mn3(AsO4)2:8H2O
Mn3(AsO4)2:8H2O + 6H+ = 3Mn+2 + 2H3AsO4 + 8H2O
log_k 12.5
delta_h -0 kJ
Ca3(AsO4)2:4H2O
Ca3(AsO4)2:4H2O + 6H+ = 3Ca+2 + 2H3AsO4 + 4H2O
log_k 22.3
delta_h -0 kJ
Ba3(AsO4)2
Ba3(AsO4)2 + 6H+ = 3Ba+2 + 2H3AsO4
log_k -8.91
delta_h 11.0458 kJ
#NH4VO3
# NH4VO3 + 2H+ = 2VO2+ + H2O
# log_k 3.8
# delta_h 30 kJ
Pb3(VO4)2
Pb3(VO4)2 + 8H+ = 3Pb+2 + 2VO2+ + 4H2O
log_k 6.14
delta_h -72.6342 kJ
Pb2V2O7
Pb2V2O7 + 6H+ = 2Pb+2 + 2VO2+ + 3H2O
log_k -1.9
delta_h -26.945 kJ
AgVO3
AgVO3 + 2H+ = Ag+ + VO2+ + H2O
log_k 0.77
delta_h -0 kJ
Ag2HVO4
Ag2HVO4 + 3H+ = 2Ag+ + VO2+ + 2H2O
log_k 1.48
delta_h -0 kJ
Ag3H2VO5
Ag3H2VO5 + 4H+ = 3Ag+ + VO2+ + 3H2O
log_k 5.18
delta_h -0 kJ
Fe(VO3)2
Fe(VO3)2 + 4H+ = Fe+2 + 2VO2+ + 2H2O
log_k -3.72
delta_h -61.6722 kJ
Mn(VO3)2
Mn(VO3)2 + 4H+ = Mn+2 + 2VO2+ + 2H2O
log_k 4.9
delta_h -92.4664 kJ
Mg(VO3)2
Mg(VO3)2 + 4H+ = Mg+2 + 2VO2+ + 2H2O
log_k 11.28
```

```
delta_h -136.649 kJ
Mg2V2O7
Mg2V2O7 + 6H+ = 2Mg+2 + 2VO2+ + 3H2O
log_k 26.36
delta_h -255.224 kJ
Carnotite
KUO2VO4 + 4H+ = K+ + UO2+2 + VO2+ + 2H2O
log_k 0.23
delta_h -36.4008 kJ
Tyuyamunite
Ca(UO2)2(VO4)2 + 8H+ = Ca+2 + 2UO2+2 + 2VO2+ + 4H2O
log_k 4.08
delta_h -153.134 kJ
Ca(VO3)2
Ca(VO3)2 + 4H+ = Ca+2 + 2VO2+ + 2H2O
log_k 5.66
delta_h -84.7678 kJ
Ca3(VO4)2
Ca3(VO4)2 + 8H+ = 3Ca+2 + 2VO2+ + 4H2O
log_k 38.96
delta_h -293.466 kJ
Ca2V2O7
Ca2V2O7 + 6H+ = 2Ca+2 + 2VO2+ + 3H2O
log_k 17.5
delta_h -159.494 kJ
Ca3(VO4)2:4H2O
Ca3(VO4)2:4H2O + 8H+ = 3Ca+2 + 2VO2+ + 8H2O
log_k 39.86
delta_h -0 kJ
Ca2V2O7:2H2O
Ca2V2O7:2H2O + 6H+ = 2Ca+2 + 2VO2+ + 5H2O
log_k 21.552
delta_h -0 kJ
Ba3(VO4)2:4H2O
Ba3(VO4)2:4H2O + 8H+ = 3Ba+2 + 2VO2+ + 8H2O
log_k 32.94
delta_h -0 kJ
Ba2V2O7:2H2O
Ba2V2O7:2H2O + 6H+ = 2Ba+2 + 2VO2+ + 5H2O
log_k 15.872
delta_h -0 kJ
NaVO3
NaVO3 + 2H+ = Na+ + VO2+ + H2O
log_k 3.8582
delta_h -30.1799 kJ
Na3VO4
Na3VO4 + 4H+ = 3Na+ + VO2+ + 2H2O
log_k 36.6812
delta_h -184.61 kJ
Na4V2O7
Na4V2O7 + 6H+ = 4Na+ + 2VO2+ + 3H2O
log_k 37.4
delta_h -201.083 kJ
Halloysite
```

```
Al2Si2O5(OH)4 + 6H+ = 2Al+3 + 2H4SiO4 + H2O
log_k 9.5749
delta_h -181.43 kJ
Kaolinite
Al2Si2O5(OH)4 + 6H+ = 2Al+3 + 2H4SiO4 + H2O
log_k 7.435
delta_h -148 kJ
Greenalite
Fe3Si2O5(OH)4 + 6H+ = 3Fe+2 + 2H4SiO4 + H2O
log_k 20.81
delta_h -0 kJ
Chrysotile
Mg3Si2O5(OH)4 + 6H+ = 3Mg+2 + 2H4SiO4 + H2O
log_k 32.2
delta_h -196 kJ
Sepiolite
Mg2Si3O7.5OH:3H2O + 4H+ + 0.5H2O = 2Mg+2 + 3H4SiO4
log_k 15.76
delta_h -114.089 kJ
Sepiolite(A)
Mg2Si3O7.5OH:3H2O + 0.5H2O + 4H+ = 2Mg+2 + 3H4SiO4
log_k 18.78
delta_h -0 kJ
PHASES
O2(g)
O2 + 4H+ + 4e- = 2H2O
log_k 83.0894
delta_h -571.66 kJ
CH4(g)
CH4 + 3H2O = CO3-2 + 8e- + 10H+
log_k -41.0452
delta_h 257.133 kJ
CO2(g)
CO2 + H2O = 2H+ + CO3-2
log_k -18.147
delta_h 4.06 kJ
H2S(g)
H2S = H+ + HS-
log_k -8.01
delta_h -0 kJ
H2Se(g)
H2Se = HSe- + H+
log_k -4.96
delta_h -15.3 kJ
Hg(g)
Hg = 0.5Hg2+2 + e-
log_k -7.8733
delta_h 22.055 kJ
Hg2(g)
Hg2 = Hg2+2 + 2e-
log_k -14.9554
delta_h 58.07 kJ
Hg(CH3)2(g)
Hg(CH3)2 + 8H2O = Hg(OH)2 + 2CO3-2 + 16e- + 20H+
```

```
log_k -73.7066
delta_h 481.99 kJ
HgF(g)
HgF = 0.5Hg2+2 + F-
log_k 32.6756
delta_h -254.844 kJ
HgF2(g)
HgF2 + 2H2O = Hg(OH)2 + 2F- + 2H+
log_k 12.5652
delta_h -165.186 kJ
HgCl(g)
HgCl = 0.5Hg2+2 + Cl-
log_k 19.4966
delta_h -162.095 kJ
HgBr(g)
HgBr = 0.5Hg2+2 + Br-
log_k 16.7566
delta_h -142.157 kJ
HgBr2(g)
HgBr2 + 2H2O = Hg(OH)2 + 2Br- + 2H+
log_k -18.3881
delta_h 54.494 kJ
HgI(g)
HgI = 0.5Hg2+2 + I-
log_k 11.3322
delta_h -106.815 kJ
HgI2(g)
HgI2 + 2H2O = Hg(OH)2 + 2I- + 2H+
log_k -27.2259
delta_h 114.429 kJ
SURFACE_MASTER_SPECIES
Hfo_s Hfo_sOH
Hfo_w Hfo_wOH
Hao_ Hao_OH #hydrous aluminum oxides - gibbsite
SURFACE_SPECIES
Hfo_wOH = Hfo_wOH
log_k 0.0
Hfo_sOH = Hfo_sOH
log_k 0.0
Hao_OH = Hao_OH
log_k 0.0

Hfo_sOH + H+ = Hfo_sOH2+
log_k 7.29
delta_h 0 kJ
# Id: 8113302
# log K source:
# Delta H source:
#T and ionic strength:
Hfo_sOH = Hfo_sO- + H+
log_k -8.93
delta_h 0 kJ
# Id: 8113301
# log K source:
```

```
# Delta H source:
#T and ionic strength:
Hfo_wOH + H+ = Hfo_wOH2+
log_k 7.29
delta_h 0 kJ
# Id: 8123302
# log K source:
# Delta H source:
#T and ionic strength:
Hfo_wOH = Hfo_wO- + H+
log_k -8.93
delta_h 0 kJ
# Id: 8123301
# log K source:
# Delta H source:
#T and ionic strength:
Hfo_sOH + Ba+2 = Hfo_sOHBa+2
log_k 5.46
delta_h 0 kJ
# Id: 8111000
# log K source:
# Delta H source:
#T and ionic strength:
Hfo_wOH + Ba+2 = Hfo_wOBa+ + H+
log_k -7.2
delta_h 0 kJ
# Id: 8121000
# log K source:
# Delta H source:
#T and ionic strength:
Hfo_sOH + Ca+2 = Hfo_sOHCa+2
log_k 4.97
delta_h 0 kJ
# Id: 8111500
# log K source:
# Delta H source:
#T and ionic strength:
Hfo_wOH + Ca+2 = Hfo_wOCa+ + H+
log_k -5.85
delta_h 0 kJ
# Id: 8121500
# log K source:
# Delta H source:
#T and ionic strength:
Hfo_wOH + Mg+2 = Hfo_wOMg+ + H+
log_k -4.6
delta_h 0 kJ
# Id: 8124600
# log K source:
# Delta H source:
#T and ionic strength:
Hfo_sOH + Ag+ = Hfo_sOAg + H+
log_k -1.72
delta_h 0 kJ
```

```
# Id: 8110200
# log K source:
# Delta H source:
#T and ionic strength:
Hfo_wOH + Ag+ = Hfo_wOAg + H+
log_k -5.3
delta_h 0 kJ
# Id: 8120200
# log K source:
# Delta H source:
#T and ionic strength:
Hfo_sOH + Ni+2 = Hfo_sONi+ + H+
log_k 0.37
delta_h 0 kJ
# Id: 8115400
# log K source:
# Delta H source:
#T and ionic strength:
Hfo_wOH + Ni+2 = Hfo_wONi+ + H+
log_k -2.5
delta_h 0 kJ
# Id: 8125400
# log K source:
# Delta H source:
#T and ionic strength:
Hfo_sOH + Cd+2 = Hfo_sOCd+ + H+
log_k 0.47
delta_h 0 kJ
# Id: 8111600
# log K source:
# Delta H source:
#T and ionic strength:
Hfo_wOH + Cd+2 = Hfo_wOCd+ + H+
log_k -2.9
delta_h 0 kJ
# Id: 8121600
# log K source:
# Delta H source:
#T and ionic strength:
Hfo_sOH + Co+2 = Hfo_sOCo+ + H+
log_k -0.46
delta_h 0 kJ
# Id: 8112000
# log K source:
# Delta H source:
#T and ionic strength:
Hfo_wOH + Co+2 = Hfo_wOCo+ + H+
log_k -3.01
delta_h 0 kJ
# Id: 8122000
# log K source:
# Delta H source:
#T and ionic strength:
Hfo_sOH + Zn+2 = Hfo_sOZn+ + H+
```

```
log_k 0.99
delta_h 0 kJ
# Id: 8119500
# log K source:
# Delta H source:
#T and ionic strength:
Hfo_wOH + Zn+2 = Hfo_wOZn+ + H+
log_k -1.99
delta_h 0 kJ
# Id: 8129500
# log K source:
# Delta H source:
#T and ionic strength:
Hfo_sOH + Cu+2 = Hfo_sOCu+ + H+
log_k 2.89
delta_h 0 kJ
# Id: 8112310
# log K source:
# Delta H source:
#T and ionic strength:
Hfo_wOH + Cu+2 = Hfo_wOCu+ + H+
log_k 0.6
delta_h 0 kJ
# Id: 8123100
# log K source:
# Delta H source:
#T and ionic strength:
Hfo_sOH + Pb+2 = Hfo_sOPb+ + H+
log_k 4.65
delta_h 0 kJ
# Id: 8116000
# log K source:
# Delta H source:
#T and ionic strength:
Hfo_wOH + Pb+2 = Hfo_wOPb+ + H+
log_k 0.3
delta_h 0 kJ
# Id: 8126000
# log K source:
# Delta H source:
#T and ionic strength:
Hfo_sOH + Be+2 = Hfo_sOBe+ + H+
log_k 5.7
delta_h 0 kJ
# Id: 8111100
# log K source:
# Delta H source:
#T and ionic strength:
Hfo_wOH + Be+2 = Hfo_wOBe+ + H+
log_k 3.3
delta_h 0 kJ
# Id: 8121100
# log K source:
# Delta H source:
```

```
#T and ionic strength:
Hfo_sOH + Hg(OH)2 + H+ = Hfo_sOHg+ + 2H2O
log_k 13.95
delta_h 0 kJ
# Id: 8113610
# log K source:
# Delta H source:
#T and ionic strength:
Hfo_wOH + Hg(OH)2 + H+ = Hfo_wOHg+ + 2H2O
log_k 12.64
delta_h 0 kJ
# Id: 8123610
# log K source:
# Delta H source:
#T and ionic strength:
Hfo_sOH + Sn(OH)2 + H+ = Hfo_sOSn+ + 2H2O
log_k 15.1
delta_h 0 kJ
# Id: 8117900
# log K source:
# Delta H source:
#T and ionic strength:
Hfo_wOH + Sn(OH)2 + H+ = Hfo_wOSn+ + 2H2O
log_k 13
delta_h 0 kJ
# Id: 8127900
# log K source:
# Delta H source:
#T and ionic strength:
Hfo_sOH + Cr(OH)2+ = Hfo_sOCrOH+ + H2O
log_k 11.63
delta_h 0 kJ
# Id: 8112110
# log K source:
# Delta H source:
#T and ionic strength:
Hfo_sOH + H3AsO3 = Hfo_sH2AsO3 + H2O
log_k 5.41
delta_h 0 kJ
# Id: 8110600
# log K source:
# Delta H source:
#T and ionic strength:
Hfo_wOH + H3AsO3 = Hfo_wH2AsO3 + H2O
log_k 5.41
delta_h 0 kJ
# Id: 8120600
# log K source:
# Delta H source:
#T and ionic strength:
Hfo_sOH + H3BO3 = Hfo_sH2BO3 + H2O
log_k 0.62
delta_h 0 kJ
# Id: 8110900
```

```
# log K source:
# Delta H source:
#T and ionic strength:
Hfo_wOH + H3BO3 = Hfo_wH2BO3 + H2O
log_k 0.62
delta_h 0 kJ
# Id: 8120900
# log K source:
# Delta H source:
#T and ionic strength:
Hfo_sOH + PO4-3 + 3H+ = Hfo_sH2PO4 + H2O
log_k 31.29
delta_h 0 kJ
# Id: 8115800
# log K source:
# Delta H source:
#T and ionic strength:
Hfo_wOH + PO4-3 + 3H+ = Hfo_wH2PO4 + H2O
log_k 31.29
delta_h 0 kJ
# Id: 8125800
# log K source:
# Delta H source:
#T and ionic strength:
Hfo_sOH + PO4-3 + 2H+ = Hfo_sHPO4- + H2O
log_k 25.39
delta_h 0 kJ
# Id: 8115801
# log K source:
# Delta H source:
#T and ionic strength:
Hfo_wOH + PO4-3 + 2H+ = Hfo_wHPO4- + H2O
log_k 25.39
delta_h 0 kJ
# Id: 8125801
# log K source:
# Delta H source:
#T and ionic strength:
Hfo_sOH + PO4-3 + H+ = Hfo_sPO4-2 + H2O
log_k 17.72
delta_h 0 kJ
# Id: 8115802
# log K source:
# Delta H source:
#T and ionic strength:
Hfo_wOH + PO4-3 + H+ = Hfo_wPO4-2 + H2O
log_k 17.72
delta_h 0 kJ
# Id: 8125802
# log K source:
# Delta H source:
#T and ionic strength:
Hfo_sOH + H3AsO4 = Hfo_sH2AsO4 + H2O
log_k 8.61
```

```
delta_h 0 kJ
# Id: 8110610
# log K source:
# Delta H source:
#T and ionic strength:
Hfo_wOH + H3AsO4 = Hfo_wH2AsO4 + H2O
log_k 8.61
delta_h 0 kJ
# Id: 8120610
# log K source:
# Delta H source:
#T and ionic strength:
Hfo_sOH + H3AsO4 = Hfo_sHAsO4- + H2O + H+
log_k 2.81
delta_h 0 kJ
# Id: 8110611
# log K source:
# Delta H source:
#T and ionic strength:
Hfo_wOH + H3AsO4 = Hfo_wHAsO4- + H2O + H+
log_k 2.81
delta_h 0 kJ
# Id: 8120611
# log K source:
# Delta H source:
#T and ionic strength:
Hfo_sOH + H3AsO4 = Hfo_sOHAsO4-3 + 3H+
log_k -10.12
delta_h 0 kJ
# Id: 8110613
# log K source:
# Delta H source:
#T and ionic strength:
Hfo_wOH + H3AsO4 = Hfo_wOHAsO4-3 + 3H+
log_k -10.12
delta_h 0 kJ
# Id: 8120613
# log K source:
# Delta H source:
#T and ionic strength:
Hfo_sOH + VO2+ + 2H2O = Hfo_sOHVO4-3 + 4H+
log_k -16.63
delta_h 0 kJ
# Id: 8119031
# log K source:
# Delta H source:
#T and ionic strength:
Hfo_wOH + VO2+ + 2H2O = Hfo_wOHVO4-3 + 4H+
log_k -16.63
delta_h 0 kJ
# Id: 8129031
# log K source:
# Delta H source:
#T and ionic strength:
```

```
Hfo_sOH + SO4-2 + H+ = Hfo_sSO4- + H2O
log_k 7.78
delta_h 0 kJ
# Id: 8117320
# log K source:
# Delta H source:
#T and ionic strength:
Hfo_wOH + SO4-2 + H+ = Hfo_wSO4- + H2O
log_k 7.78
delta_h 0 kJ
# Id: 8127320
# log K source:
# Delta H source:
#T and ionic strength:
Hfo_sOH + SO4-2 = Hfo_sOHSO4-2
log_k 0.79
delta_h 0 kJ
# Id: 8117321
# log K source:
# Delta H source:
#T and ionic strength:
Hfo_wOH + SO4-2 = Hfo_wOHSO4-2
log_k 0.79
delta_h 0 kJ
# Id: 8127321
# log K source:
# Delta H source:
#T and ionic strength:
Hfo_sOH + HSeO3- = Hfo_sSeO3- + H2O
log_k 4.29
delta_h 0 kJ
# Id: 8117610
# log K source:
# Delta H source:
#T and ionic strength:
Hfo_wOH + HSeO3- = Hfo_wSeO3- + H2O
log_k 4.29
delta_h 0 kJ
# Id: 8127610
# log K source:
# Delta H source:
#T and ionic strength:
Hfo_sOH + HSeO3- = Hfo_sOHSeO3-2 + H+
log_k -3.23
delta_h 0 kJ
# Id: 8117611
# log K source:
# Delta H source:
#T and ionic strength:
Hfo_wOH + HSeO3- = Hfo_wOHSeO3-2 + H+
log_k -3.23
delta_h 0 kJ
# Id: 8127611
# log K source:
```

```
# Delta H source:
#T and ionic strength:
Hfo_sOH + SeO4-2 + H+ = Hfo_sSeO4- + H2O
log_k 7.73
delta_h 0 kJ
# Id: 8117620
# log K source:
# Delta H source:
#T and ionic strength:
Hfo_wOH + SeO4-2 + H+ = Hfo_wSeO4- + H2O
log_k 7.73
delta_h 0 kJ
# Id: 8127620
# log K source:
# Delta H source:
#T and ionic strength:
Hfo_sOH + SeO4-2 = Hfo_sOHSeO4-2
log_k 0.8
delta_h 0 kJ
# Id: 8117621
# log K source:
# Delta H source:
#T and ionic strength:
Hfo_wOH + SeO4-2 = Hfo_wOHSeO4-2
log_k 0.8
delta_h 0 kJ
# Id: 8127621
# log K source:
# Delta H source:
#T and ionic strength:
Hfo_sOH + CrO4-2 + H+ = Hfo_sCrO4- + H2O
log_k 10.85
delta_h 0 kJ
# Id: 8112120
# log K source:
# Delta H source:
#T and ionic strength:
Hfo_wOH + CrO4-2 + H+ = Hfo_wCrO4- + H2O
log_k 10.85
delta_h 0 kJ
# Id: 8122120
# log K source:
# Delta H source:
#T and ionic strength:
Hfo_sOH + CrO4-2 = Hfo_sOHCrO4-2
log_k 3.9
delta_h 0 kJ
# Id: 8112121
# log K source:
# Delta H source:
#T and ionic strength:
Hfo_wOH + CrO4-2 = Hfo_wOHCrO4-2
log_k 3.9
delta_h 0 kJ
```

```
# Id: 8122121
# log K source:
# Delta H source:
#T and ionic strength:
Hfo_sOH + MoO4-2 + H+ = Hfo_sMoO4- + H2O
log_k 9.5
delta_h 0 kJ
# Id: 8114800
# log K source:
# Delta H source:
#T and ionic strength:
Hfo_wOH + MoO4-2 + H+ = Hfo_wMoO4- + H2O
log_k 9.5
delta_h 0 kJ
# Id: 8124800
# log K source:
# Delta H source:
#T and ionic strength:
Hfo_sOH + MoO4-2 = Hfo_sOHMoO4-2
log_k 2.4
delta_h 0 kJ
# Id: 8114801
# log K source:
# Delta H source:
#T and ionic strength:
Hfo_wOH + MoO4-2 = Hfo_wOHMoO4-2
log_k 2.4
delta_h 0 kJ
# Id: 8124801
# log K source:
# Delta H source:
#T and ionic strength:
Hfo_sOH + Sb(OH)6- + H+ = Hfo_sSbO(OH)4 + 2H2O
log_k 8.4
delta_h 0 kJ
# Id: 8117410
# log K source:
# Delta H source:
#T and ionic strength:
Hfo_wOH + Sb(OH)6- + H+ = Hfo_wSbO(OH)4 + 2H2O
log_k 8.4
delta_h 0 kJ
# Id: 8127410
# log K source:
# Delta H source:
#T and ionic strength:
Hfo_sOH + Sb(OH)6- = Hfo_sOHSbO(OH)4- + H2O
log_k 1.3
delta_h 0 kJ
# Id: 8117411
# log K source:
# Delta H source:
#T and ionic strength:
Hfo_wOH + Sb(OH)6- = Hfo_wOHSbO(OH)4- + H2O
```

```
log_k 1.3
delta_h 0 kJ
# Id: 8127411
# log K source:
# Delta H source:
#T and ionic strength:
Hfo_sOH + Cyanide- + H+ = Hfo_sCyanide + H2O
log_k 13
delta_h 0 kJ
# Id: 8111430
# log K source:
# Delta H source:
#T and ionic strength:
Hfo_wOH + Cyanide- + H+ = Hfo_wCyanide + H2O
log_k 13
delta_h 0 kJ
# Id: 8121430
# log K source:
# Delta H source:
#T and ionic strength:
Hfo_sOH + Cyanide- = Hfo_sOHCyanide-
log_k 5.7
delta_h 0 kJ
# Id: 8111431
# log K source:
# Delta H source:
#T and ionic strength:
Hfo_wOH + Cyanide- = Hfo_wOHCyanide-
log_k 5.7
delta_h 0 kJ
# Id: 8121431
# log K source:
# Delta H source:
#T and ionic strength:
#Additions from GWB Minteq
Hfo_wOH + H4SiO4 = Hfo_wOSi(OH)3 + H2O
log_k 4.28
delta_h 0 kJ
Hfo_wOH + H4SiO4 = Hfo_wOSiO(OH)2- + H+ + H2O
log_k -3.22
delta_h 0 kJ
Hfo_sOH + H4SiO4 = Hfo_sOSi(OH)3 + H2O
log_k 4.28
delta_h 0
Hfo_sOH + H4SiO4 = Hfo_sOSiO(OH)2- + H+ + H2O
log_k -3.22
delta_h 0
Hfo_wOH + CO3-2 + H+ = Hfo_wCO3- + H2O
log_k 12.56
delta_h 0
Hfo_wOH + CO3-2 + 2H+= Hfo_wHCO3 + H2O
log_k 20.62
delta_h 0
Hfo_sOH + CO3-2 + H+ = Hfo_sCO3- + H2O
```

```
log_k 12.56
delta_h 0
Hfo_sOH + CO3-2 + 2H+= Hfo_sHCO3 + H2O
log_k 20.62
delta_h 0

#Karamalidis and Dzombak sorption to gibbsite (hao) as compiled in Cravotta 2021 (https://doi.org/10.1016/j.apgeochem.2020.104845) Table S4 unless otherwise noted
Hao_OH + Cu+2 = Hao_OCu+ + H+
log_k 0.25
Hao_OH + Pb+2 = Hao_OPb+ + H+
log_k 0.37
Hao_OH + Co+2 = Hao_OCo+ + H+
log_k -2.52
Hao_OH + Cd+2 = Hao_OCd+ + H+
log_k -2.73
Hao_OH + Mn+2 = Hao_OMn+ + H+
log_k -5.49
Hao_OH + Fe+2 = Hao_OFe+ + H+
log_k -3.77
Hao_OH + Ca+2 = Hao_OCa+ + H+
log_k -10.49
Hao_OH + Mg+2 = Hao_OMg+ + H+
log_k -5.93
Hao_OH + Ba+2 = Hao_OBa+ + H+
log_k -8.5
Hao_OH + Sr+2 = Hao_OSr+ + H+
log_k -8.26
Hao_OH + Zn+2 = Hao_OZn+ + H+
log_k -0.96
Hao_OH + PO4-3 + 3 H+ = Hao_H2PO4 + H2O
log_k 26.89
Hao_OH + PO4-3 + 2H+ = Hao_HPO4- + H2O
log_k 19.37
Hao_OH + PO4-3 + H+ = Hao_PO4-2 + H2O
log_k 13.57
#Hao_OH + SO4-2 + H+ = Hao_SO4- + H2O
# log_k -0.45
#Hao_OH + SO4-2 = Hao_OHSO4-2
# log_k 1.19
Hao_OH + F- + H+ = Hao_F + H2O
log_k 8.78
Hao_OH + F- = Hao_OHF-
log_k 2.88
Hao_OH + 2 F- + H+ = Hao_F2- + H2O
log_k 11.94
Hao_OH + H4SiO4 = Hao_OH4SiO4- + H+
log_k -4.16

#Modified value from Goldberg and Glaubig (1985)
Hao_OH + H3BO3 = Hao_H2BO3 + H2O
Log_k 4.83
Hao_OH + H3BO3 = Hao_H3BO4- + H+
Log_k -7.40

#Modified value from Kitadai et al. (2018)
```

```
Hao_OH + SO4-2 + H+ = Hao_SO4- + H2O
log_k 2.4
#Modified value from Kitadai et al. (2018)
Hao_OH + SO4-2 = Hao_OHSO4-2
log_k 7.5

END
```

ATTACHMENT C

Details of Geochemical Model Parameterization

Attachment C. Details of Geochemical Model Parameterization

Introduction

This appendix to the Groundwater Polishing Report for the Hennepin Power Plant West Ash Pond System (WAPS) provides detailed information regarding geochemical model parameterization. The information provided includes sources of thermodynamic data, sources of data used in model parameterization, summarized values, and calculation methods. All solid-phase data is fully documented in the Nature and Extent Report.[1] All aqueous data have been posted to the facility's operating record in accordance with 35 I.A.C. § 845.800(d)(15).

Solid Phase Inputs

The solid phase inputs to the model included iron (hydr)oxides and aluminum (hydr)oxides. These phases tend to have relatively rapid precipitation kinetics and form an outer layer on the surfaces of aquifer solids, creating surface area for sorption and attenuation of boron. Sequential extraction procedure (SEP) methods are described in the Geochemical Conceptual Site Model (GCSM)[2] and employ chemical extractants to dissolve metals from specific solid-associated phases. SEP methods use progressively stronger reagents to solubilize metals from increasingly recalcitrant phases. Although these procedures do not identify the discrete solid phases in a soil/aquifer matrix, they provide a means to evaluate the characterize the metal binding mechanisms and relative stability of metals in each phase, and to estimate the available mass of the respective attenuating phase(s) (i.e., aluminum and iron [hydr]oxide). While SEP analyses were completed on WAPS aquifer solids samples in March 2021 and were presented in the GCSM, the SEP methodology used to analyze these samples did not include extraction stages associated with non-crystalline or sulfide materials, both of which are important to solid-phase iron distribution. Therefore, this SEP data was not included in model set up.

SEP data from the October 2024 sampling event included two samples collected adjacent to monitoring location 21R from within the uppermost aquifer unit (UAU) at depths associated with the screened interval of 21R. The SEP analyses used for WAPS samples included a more reactive non-crystalline metal oxide fraction and a less reactive metal hydroxide fraction, as well as a sulfide fraction. Input concentrations for iron and aluminum (hydr)oxides were derived using SEP data from

---

[1] The Nature and Extent Report was previously submitted to IEPA in May 2024 and provided with relevant updates as Appendix D of the CAAA to which this report is attached.

[2] Ibid.; the GCSM is an appendix of the Nature and Extent Report.

aquifer solids samples collected in October 2024 and discussed in the Groundwater Polishing Evaluation Report primary document.

Sorption of inorganic constituents to iron (hydr)oxides in the MINTEQ v4 database[3] is represented by the hydrous ferric oxide (HFO) thermodynamic data set presented in Dzombak and Morel (1990). Sorption of inorganic constituents to aluminum (hydr)oxides is represented by the hydrous aluminum oxide (HAO) thermodynamic data presented in Karamalidis and Dzombak (2010), Goldberg and Glaubig (1985) (boron), and Kitadai et al. (2018) (sulfate). These sorption data are based on gibbsite, a nearly ubiquitous crystalline aluminum hydroxide mineral (Karamalidis and Dzombak 2010).

In thermodynamic modeling, the amount of sorbing phase present is typically the dominant control on the concentration of constituents sorbed. Therefore, different amounts of metal oxides were used to test the sensitivity of the model to the amount of sorbing phase present. The amount of metal oxides used were derived from the 25th percentile, mean, and 75th percentile of the SEP results for the relevant iron and aluminum phases.

The quantities of HFO and HAO in the model are represented by ferrihydrite ($Fe(OH)_3$) and gibbsite ($Al(OH)_3$), respectively. Ferrihydrite is the most similar naturally occurring iron oxide to HFO (Dzombak and Morel, 1990), and sorption data for HAO was determined using gibbsite (Karamalidis and Dzombak 2010). Metal concentrations are presented in milligrams per kilogram of dry weight (mg/kg dw), whereas ferrihydrite and gibbsite inputs to the model represent moles of solid phase associated with one liter (L) of aqueous phase. The concentrations of iron and aluminum were converted to moles of ferrihydrite and gibbsite (respectively) according to the following:

The mass in kilograms (kg) of solid in the model (i.e., per 1 L of water) was calculated by:

$$Solid\ Mass\ In\ Model\ (kg) = \frac{(1-\phi)}{\phi} \times \frac{1000\ cm^3\ water}{L\ water} \times 1\ L\ water\ \times \rho\ \times \frac{1\ kg\ solid}{1000\ g\ solid}$$

Where:

ϕ = porosity (water volume in cubic centimeters [cm^3] / total volume in cm^3)

ρ = density of the solid (grams [g]/cm^3)

Porosity and density represent the median of measurements each hydrostratigraphic unit as reported in the Hydrogeologic Characterization Report[4].

Moles of ferrihydrite and gibbsite were determined using metals concentrations as described above, the molar mass of iron or aluminum, and the mass of solid phase in the model:

---

[3] The default MINTEQ v4 database for PHREEQC does not include sorption data for carbonate and silicate to HFO. Thermodynamic constants for sorption of carbonate and silicate to HFO were added from the MINTEQ database associated with the Geochemist's Workbench software program.

[4] The Hydrogeologic Characterization Report was previously submitted to IEPA as part of the Closure Permit Application and is provided as Appendix B.3 to the Construction Permit Application.

$$Moles\ of\ Metal\ Oxide = \frac{mg\ Fe\ or\ Al}{kg\ solid} \times \frac{g}{1000\ mg} \times \frac{moles\ Fe\ or\ Al}{g\ Fe\ or\ Al} \times kg\ Solid\ Mass\ in\ Model$$

The moles of ferrihydrite and gibbsite are represented by moles of Fe or Al (respectively) in a 1:1 ratio mased on the mineral formula. Ferrihydrite and gibbsite were allowed to precipitate or dissolve in the reaction phase of the model to evaluate the impact of source control on sorbing phase availability.

Calcite and dolomite were included as mineral phases in the model because carbonate mineral formation and dissolution are often major controls on groundwater pH. Calcite and dolomite are common carbonate minerals and were detected at levels of greater than 1% by weight in X-ray diffraction (XRD) analysis and are therefore considered to be present in excess within the aquifer. Therefore, the mass fractions reported in the XRD results presented in the GCSM are used as model inputs. Both calcite and dolomite were allowed to precipitate in the reaction phase of the model.

Barite and gypsum are common sulfate minerals that have the potential to form under ambient environmental conditions. Neither mineral was detected in XRD results at well locations containing exceedances of groundwater protection standards (GWPS). Therefore, barite and gypsum did not have initial concentrations in the model but were allowed to precipitate or dissolve in the reaction phase of the model.

Aqueous Inputs

In addition to the constituent of concern boron, the following parameters are included in the model and are anticipated to capture the expected attenuation and mobilization mechanisms for reasons detailed below:

- Temperature, pH and pe: pH and pe (a measure of redox potential) are major controls on chemical attenuation and mobility.
- Chloride, potassium, and sodium: Major ions in groundwater typically required for the model to reach charge balance.
- Carbonate ion, calcium, and magnesium: Major ions in groundwater that may also form common minerals, including carbonates. Carbonate mineral formation and dissolution is often a major control on groundwater pH. Bicarbonate and carbonate ions, a major component of groundwater alkalinity, may also compete with sulfate/boron for sorbing sites.
- Silicon and phosphate: Silicate and phosphate are oxyanions that compete with sulfate/boron for sorbing sites.
- Aluminum, iron, and manganese: As discussed above, iron and aluminum form reactive metal (hydr)oxide minerals which have high capacities for sorbing other ions on their surfaces. Although sorption to manganese oxides was not considered in this model, manganese behaves similarly to iron and is included for completeness.

- Remaining constituents regulated under 35 IAC § 845.600[5]: Although these parameters are not subject to corrective action at NEW PAP, they are included in the model for completeness.

Values for pe and carbonate ion concentrations were derived from values previously reported in the analytical data according to the following methods.

pe is a non-dimension scale of redox potential and is calculated from oxidation reduction potential (ORP). First, the field-measured ORP was converted to Eh (i.e., the redox potential normalized to the standard hydrogen electrode). The following equation provided in the Horiba water quality meter instruction manual[6] was used:

$$Eh = ORP + 206 - 0.7*(T - 25)$$

Where both Eh and ORP are in volts (V) and T is temperature in degrees Celsius. Eh is then converted to pe:

$$pe = (Eh * F) / (2.303 * R * T)$$

Where:

F = Faraday constant (96,500 Joules (J) / V-equivalent)

R = Molar gas constant (8.31 J / Kelvin (K)-mole)

T = temperature in Kelvin

Data reported for groundwater at the site include carbonate and bicarbonate alkalinity in units of mg of calcium carbonate per liter (mg $CaCO_3$/L). For use in modeling, it is convenient to convert these values to a single carbonate (CO_3^{2-}) ion concentration. Because carbonate and bicarbonate alkalinity are reported in the same units (i.e., standardized to mg $CaCO_3$) and represent different protonation states of the same inorganic carbon oxyanion, they were summed to represent total alkalinity due to carbonate. This summed alkalinity was converted to concentration of carbonate ion according to the following equation:

$$\frac{mg\ CO_3^{2-}}{L} = \frac{mg\ CaCO_3}{L} \times \frac{mole\ CaCO_3}{100.1\ mg\ CaCO_3} \times \frac{1\ mole\ CO_3^{2-}}{1\ mole\ CaCO_3} \times \frac{60\ mg\ CO_3^{2-}}{mole\ CO_3^{2-}}$$

The full suite of geochemical parameters for the modeling effort were measured in Quarter 2 and Quarter 3, 2023, for all compliance monitoring wells with exceedances of GWPS. The medians of these results were used in the model to represent average groundwater interacting with the solid phase.

As discussed in detail in the Groundwater Polishing Evaluation Report primary document, groundwater flow conditions at and near the WAPS are variable and warrant consideration of

---

[5] Mercury, thallium, total dissolved solids, and radium were not included in the model. Mercury reactions within the environment are highly complex and would require a separate modeling effort. Thallium forms a non-reactive monovalent cation and is rarely detected in the groundwater and is therefore not expected to contribute to model outcomes. Total dissolved solids are not a chemical parameter, but rather the result of other chemical abundances taken together. Radium is not included in most thermodynamic databases.

[6] https://static.horiba.com/fileadmin/Horiba/Products/Process_and_Environmental/Water_Pollution/Instruction_Manuals/U-50/U-50_Manual.pdf

appropriate background groundwater sources for individual compliance wells. Background groundwater was represented in modeling efforts for compliance wells 21R and 51 using the average composition of background well 34 from 2024 Q1 and Q2 sampling events (referred to as HEN – West). Background groundwater was represented in modeling efforts for compliance wells 22, 23, and 35 using the average composition of background well 32 from 2024 Q1 and Q2 sampling events (referred to as HEN – East). Additionally, the average composition of eight surface water samples collected from three sampling locations in the Illinois River immediately north of the WAPS was used in a separate model scenario to evaluate the Illinois River as a background water source for well 22 during flooding events (referred to as HEN – River).

The model was run without charge balancing and with charge balancing on chloride. The results during the reaction modeling did not substantially differ with and without charge balancing on chloride. The results presented in the Groundwater Polishing Evaluation Report therefore represent the model results using charge balancing on chloride.

References

Appelo C.A.J. and Postma D. 2005. Geochemistry, Groundwater, and Pollution. 2nd Edition. A.A. Balkema Publishers, member of Taylor & Francis Group. The Netherlands.

Dzombak D.A. and Morel F.M.M. 1990. Surface Complexation Modeling: Hydrous Ferric Oxide. John Wiley & Sons, New York.

Goldberg S. and Glaubig R.A. 1985. Boron Adsorption on Aluminum and Iron Oxide Minerals. *Soil Science Society of America Journal* **49**(6):1374-1379.

Karamalidis A.K. and Dzombak D.A. 2010. Surface Complexation Modeling: Gibbsite. John Wiley & Sons, New York.

Kitadai N., Nishiuchi K, and Tanaka M. 2018. A comprehensive predictive model for sulfate adsorption on oxide minerals. *Geochimica et Cosmochimica Acta* **238**:150-168.

ATTACHMENT D

Complete Geochemical Modeling Output

Attachment D. PHREEQC modeling output

Groundwater Polishing Report
West Ash Pond System
Hennepin Power Plant
Hennepin, IL

program_id	Location	Location Description	Model	Charge Balance
HEN_845_804W	21R	C - UA	Initial Soln	TRUE
HEN_845_804W	51	C - UA	Initial Soln	TRUE
HEN_845_804W	21R	C - UA	Speciation Model	TRUE
HEN_845_804W	51	C - UA	Speciation Model	TRUE
HEN_845_804W	21R	C - UA	First Reaction	TRUE
HEN_845_804W	21R	C - UA	Second Reaction	TRUE
HEN_845_804W	51	C - UA	First Reaction	TRUE
HEN_845_804W	51	C - UA	Second Reaction	TRUE
HEN_845_804W	21R	C - UA	Initial Soln	TRUE
HEN_845_804W	51	C - UA	Initial Soln	TRUE
HEN_845_804W	21R	C - UA	Speciation Model	TRUE
HEN_845_804W	51	C - UA	Speciation Model	TRUE
HEN_845_804W	21R	C - UA	First Reaction	TRUE
HEN_845_804W	21R	C - UA	Second Reaction	TRUE
HEN_845_804W	51	C - UA	First Reaction	TRUE
HEN_845_804W	51	C - UA	Second Reaction	TRUE
HEN_845_804W	21R	C - UA	Initial Soln	TRUE
HEN_845_804W	51	C - UA	Initial Soln	TRUE
HEN_845_804W	21R	C - UA	Speciation Model	TRUE
HEN_845_804W	51	C - UA	Speciation Model	TRUE
HEN_845_804W	21R	C - UA	First Reaction	TRUE
HEN_845_804W	21R	C - UA	Second Reaction	TRUE
HEN_845_804W	51	C - UA	First Reaction	TRUE
HEN_845_804W	51	C - UA	Second Reaction	TRUE
HEN_845_804W	21R	C - UA	Initial Soln	FALSE
HEN_845_804W	51	C - UA	Initial Soln	FALSE
HEN_845_804W	21R	C - UA	Speciation Model	FALSE
HEN_845_804W	51	C - UA	Speciation Model	FALSE
HEN_845_804W	21R	C - UA	First Reaction	FALSE
HEN_845_804W	21R	C - UA	Second Reaction	FALSE
HEN_845_804W	51	C - UA	First Reaction	FALSE
HEN_845_804W	51	C - UA	Second Reaction	FALSE
HEN_845_804W	21R	C - UA	Initial Soln	FALSE
HEN_845_804W	51	C - UA	Initial Soln	FALSE
HEN_845_804W	21R	C - UA	Speciation Model	FALSE
HEN_845_804W	51	C - UA	Speciation Model	FALSE
HEN_845_804W	21R	C - UA	First Reaction	FALSE
HEN_845_804W	21R	C - UA	Second Reaction	FALSE
HEN_845_804W	51	C - UA	First Reaction	FALSE
HEN_845_804W	51	C - UA	Second Reaction	FALSE
HEN_845_804W	21R	C - UA	Initial Soln	FALSE
HEN_845_804W	51	C - UA	Initial Soln	FALSE
HEN_845_804W	21R	C - UA	Speciation Model	FALSE

HEN_845_804W	51	C - UA	Speciation Model	FALSE
HEN_845_804W	21R	C - UA	First Reaction	FALSE
HEN_845_804W	21R	C - UA	Second Reaction	FALSE
HEN_845_804W	51	C - UA	First Reaction	FALSE
HEN_845_804W	51	C - UA	Second Reaction	FALSE
HEN_845_804E	22	C - UA	Initial Soln	TRUE
HEN_845_804E	23	C - UA	Initial Soln	TRUE
HEN_845_804E	35	C - UA	Initial Soln	TRUE
HEN_845_804E	22	C - UA	Speciation Model	TRUE
HEN_845_804E	23	C - UA	Speciation Model	TRUE
HEN_845_804E	35	C - UA	Speciation Model	TRUE
HEN_845_804E	22	C - UA	First Reaction	TRUE
HEN_845_804E	22	C - UA	Second Reaction	TRUE
HEN_845_804E	23	C - UA	First Reaction	TRUE
HEN_845_804E	23	C - UA	Second Reaction	TRUE
HEN_845_804E	35	C - UA	First Reaction	TRUE
HEN_845_804E	35	C - UA	Second Reaction	TRUE
HEN_845_804E	22	C - UA	Initial Soln	TRUE
HEN_845_804E	23	C - UA	Initial Soln	TRUE
HEN_845_804E	35	C - UA	Initial Soln	TRUE
HEN_845_804E	22	C - UA	Speciation Model	TRUE
HEN_845_804E	23	C - UA	Speciation Model	TRUE
HEN_845_804E	35	C - UA	Speciation Model	TRUE
HEN_845_804E	22	C - UA	First Reaction	TRUE
HEN_845_804E	22	C - UA	Second Reaction	TRUE
HEN_845_804E	23	C - UA	First Reaction	TRUE
HEN_845_804E	23	C - UA	Second Reaction	TRUE
HEN_845_804E	35	C - UA	First Reaction	TRUE
HEN_845_804E	35	C - UA	Second Reaction	TRUE
HEN_845_804E	22	C - UA	Initial Soln	TRUE
HEN_845_804E	23	C - UA	Initial Soln	TRUE
HEN_845_804E	35	C - UA	Initial Soln	TRUE
HEN_845_804E	22	C - UA	Speciation Model	TRUE
HEN_845_804E	23	C - UA	Speciation Model	TRUE
HEN_845_804E	35	C - UA	Speciation Model	TRUE
HEN_845_804E	22	C - UA	First Reaction	TRUE
HEN_845_804E	22	C - UA	Second Reaction	TRUE
HEN_845_804E	23	C - UA	First Reaction	TRUE
HEN_845_804E	23	C - UA	Second Reaction	TRUE
HEN_845_804E	35	C - UA	First Reaction	TRUE
HEN_845_804E	35	C - UA	Second Reaction	TRUE
HEN_845_804E	22	C - UA	Initial Soln	FALSE
HEN_845_804E	23	C - UA	Initial Soln	FALSE
HEN_845_804E	35	C - UA	Initial Soln	FALSE
HEN_845_804E	22	C - UA	Speciation Model	FALSE
HEN_845_804E	23	C - UA	Speciation Model	FALSE
HEN_845_804E	35	C - UA	Speciation Model	FALSE
HEN_845_804E	22	C - UA	First Reaction	FALSE
HEN_845_804E	22	C - UA	Second Reaction	FALSE
HEN_845_804E	23	C - UA	First Reaction	FALSE

HEN_845_804E	23	C - UA	Second Reaction	FALSE
HEN_845_804E	35	C - UA	First Reaction	FALSE
HEN_845_804E	35	C - UA	Second Reaction	FALSE
HEN_845_804E	22	C - UA	Initial Soln	FALSE
HEN_845_804E	23	C - UA	Initial Soln	FALSE
HEN_845_804E	35	C - UA	Initial Soln	FALSE
HEN_845_804E	22	C - UA	Speciation Model	FALSE
HEN_845_804E	23	C - UA	Speciation Model	FALSE
HEN_845_804E	35	C - UA	Speciation Model	FALSE
HEN_845_804E	22	C - UA	First Reaction	FALSE
HEN_845_804E	22	C - UA	Second Reaction	FALSE
HEN_845_804E	23	C - UA	First Reaction	FALSE
HEN_845_804E	23	C - UA	Second Reaction	FALSE
HEN_845_804E	35	C - UA	First Reaction	FALSE
HEN_845_804E	35	C - UA	Second Reaction	FALSE
HEN_845_804E	22	C - UA	Initial Soln	FALSE
HEN_845_804E	23	C - UA	Initial Soln	FALSE
HEN_845_804E	35	C - UA	Initial Soln	FALSE
HEN_845_804E	22	C - UA	Speciation Model	FALSE
HEN_845_804E	23	C - UA	Speciation Model	FALSE
HEN_845_804E	35	C - UA	Speciation Model	FALSE
HEN_845_804E	22	C - UA	First Reaction	FALSE
HEN_845_804E	22	C - UA	Second Reaction	FALSE
HEN_845_804E	23	C - UA	First Reaction	FALSE
HEN_845_804E	23	C - UA	Second Reaction	FALSE
HEN_845_804E	35	C - UA	First Reaction	FALSE
HEN_845_804E	35	C - UA	Second Reaction	FALSE
HEN_845_804R	22	C - UA	Initial Soln	TRUE
HEN_845_804R	22	C - UA	Speciation Model	TRUE
HEN_845_804R	22	C - UA	First Reaction	TRUE
HEN_845_804R	22	C - UA	Second Reaction	TRUE
HEN_845_804R	22	C - UA	Initial Soln	TRUE
HEN_845_804R	22	C - UA	Speciation Model	TRUE
HEN_845_804R	22	C - UA	First Reaction	TRUE
HEN_845_804R	22	C - UA	Second Reaction	TRUE
HEN_845_804R	22	C - UA	Initial Soln	TRUE
HEN_845_804R	22	C - UA	Speciation Model	TRUE
HEN_845_804R	22	C - UA	First Reaction	TRUE
HEN_845_804R	22	C - UA	Second Reaction	TRUE
HEN_845_804R	22	C - UA	Initial Soln	FALSE
HEN_845_804R	22	C - UA	Speciation Model	FALSE
HEN_845_804R	22	C - UA	First Reaction	FALSE
HEN_845_804R	22	C - UA	Second Reaction	FALSE
HEN_845_804R	22	C - UA	Initial Soln	FALSE
HEN_845_804R	22	C - UA	Speciation Model	FALSE
HEN_845_804R	22	C - UA	First Reaction	FALSE
HEN_845_804R	22	C - UA	Second Reaction	FALSE
HEN_845_804R	22	C - UA	Initial Soln	FALSE
HEN_845_804R	22	C - UA	Speciation Model	FALSE
HEN_845_804R	22	C - UA	First Reaction	FALSE

HEN_845_804R	22	C - UA	Second Reaction	FALSE

NOTES:

All model results are in units of moles with the exceptions of:
- pH and pe (standard units)
- charge (equivalents)
- Results beginning with 'd_' (change from prior model step)
- Results beginning with 'si_' (saturation index)

Solids Summary	pH	pe	charge	pct_err
25p	7.44	0.980	1.00e-16	4.53e-13
25p	7.30	1.42	1.69e-12	7.46e-09
25p	7.44	0.980	1.02e-16	4.61e-13
25p	7.30	1.42	1.69e-12	7.46e-09
25p	7.29	-3.11e-01	-7.49e-05	-2.94e-01
25p	7.25	-2.12e-01	-1.43e-05	-5.46e-02
25p	7.25	-2.34e-01	-3.55e-05	-1.36e-01
25p	7.23	-1.78e-01	-5.91e-06	-2.23e-02
75p	7.44	0.980	1.00e-16	4.53e-13
75p	7.30	1.42	1.69e-12	7.46e-09
75p	7.44	0.980	1.01e-16	4.57e-13
75p	7.30	1.42	1.69e-12	7.46e-09
75p	7.31	-3.17e-01	-9.53e-05	-3.78e-01
75p	7.26	-2.23e-01	-1.98e-05	-7.65e-02
75p	7.26	-2.24e-01	-4.34e-05	-1.67e-01
75p	7.24	-1.73e-01	-9.03e-06	-3.43e-02
median	7.44	0.980	1.00e-16	4.53e-13
median	7.30	1.42	1.69e-12	7.46e-09
median	7.44	0.980	1.02e-16	4.61e-13
median	7.30	1.42	1.69e-12	7.46e-09
median	7.30	-3.14e-01	-8.46e-05	-3.34e-01
median	7.25	-2.17e-01	-1.70e-05	-6.54e-02
median	7.26	-2.28e-01	-3.93e-05	-1.51e-01
median	7.23	-1.75e-01	-7.45e-06	-2.82e-02
25p	7.44	0.980	0.00340	18.2
25p	7.30	1.42	0.00393	21.1
25p	7.44	0.980	0.00340	18.2
25p	7.30	1.42	0.00393	21.1
25p	7.29	-3.13e-01	-7.30e-05	-2.87e-01
25p	7.25	-2.14e-01	-1.42e-05	-5.44e-02
25p	7.25	-2.36e-01	-3.80e-05	-1.46e-01
25p	7.23	-1.80e-01	-5.91e-06	-2.24e-02
75p	7.44	0.980	0.00340	18.2
75p	7.30	1.42	0.00393	21.1
75p	7.44	0.980	0.00340	18.2
75p	7.30	1.42	0.00393	21.1
75p	7.31	-3.19e-01	-9.39e-05	-3.73e-01
75p	7.26	-2.24e-01	-1.97e-05	-7.62e-02
75p	7.26	-2.26e-01	-4.81e-05	-1.85e-01
75p	7.24	-1.75e-01	-9.09e-06	-3.45e-02
median	7.44	0.980	0.00340	18.2
median	7.30	1.42	0.00393	21.1
median	7.44	0.980	0.00340	18.2

median	7.30	1.42	0.00393	21.1
median	7.30	-3.16e-01	-8.29e-05	-3.28e-01
median	7.25	-2.18e-01	-1.70e-05	-6.51e-02
median	7.26	-2.31e-01	-4.28e-05	-1.65e-01
median	7.23	-1.77e-01	-7.48e-06	-2.84e-02
25p	7.62	4.82	3.46e-18	3.10e-14
25p	7.41	1.54	-1.47e-18	-6.33e-15
25p	6.96	6.08	-7.91e-18	-2.58e-14
25p	7.62	4.82	3.46e-18	3.10e-14
25p	7.41	1.54	-3.27e-17	-1.41e-13
25p	6.96	6.08	-1.14e-17	-3.71e-14
25p	7.52	3.11	-7.88e-05	-3.93e-01
25p	7.50	3.20	-1.56e-05	-7.72e-02
25p	7.51	0.924	5.58e-05	0.274
25p	7.49	1.11	-1.29e-06	-6.34e-03
25p	7.31	4.32	0.000160	0.686
25p	7.37	4.21	1.08e-05	0.0495
75p	7.62	4.82	3.46e-18	3.10e-14
75p	7.41	1.54	-1.47e-18	-6.33e-15
75p	6.96	6.08	-7.91e-18	-2.58e-14
75p	7.62	4.82	3.46e-18	3.10e-14
75p	7.41	1.54	-3.27e-17	-1.41e-13
75p	6.96	6.08	-1.14e-17	-3.71e-14
75p	7.52	3.09	-1.03e-04	-5.13e-01
75p	7.51	3.18	-1.88e-05	-9.30e-02
75p	7.52	0.897	9.09e-05	0.446
75p	7.50	1.07	1.30e-07	0.000643
75p	7.29	4.36	0.000238	0.999
75p	7.35	4.27	1.91e-05	0.0865
median	7.62	4.82	3.46e-18	3.10e-14
median	7.41	1.54	-1.47e-18	-6.33e-15
median	6.96	6.08	-7.91e-18	-2.58e-14
median	7.62	4.82	3.46e-18	3.10e-14
median	7.41	1.54	-3.27e-17	-1.41e-13
median	6.96	6.08	-1.14e-17	-3.71e-14
median	7.52	3.10	-9.00e-05	-4.49e-01
median	7.51	3.19	-1.72e-05	-8.50e-02
median	7.51	0.911	7.24e-05	0.356
median	7.50	1.09	-7.78e-07	-3.84e-03
median	7.30	4.34	0.000197	0.836
median	7.36	4.24	1.45e-05	0.0658
25p	7.62	4.82	-1.46e-03	-1.15e+01
25p	7.41	1.54	0.00136	6.21
25p	6.96	6.08	0.000895	3.01
25p	7.62	4.82	-1.46e-03	-1.15e+01
25p	7.41	1.54	0.00136	6.21
25p	6.96	6.08	0.000895	3.01
25p	7.52	3.11	-8.22e-05	-4.09e-01
25p	7.50	3.20	-1.56e-05	-7.73e-02
25p	7.51	0.919	5.35e-05	0.263

25p	7.50	1.10	-1.32e-06	-6.51e-03
25p	7.31	4.32	0.000158	0.676
25p	7.37	4.21	1.08e-05	0.0493
75p	7.62	4.82	-1.46e-03	-1.15e+01
75p	7.41	1.54	0.00136	6.21
75p	6.96	6.08	0.000895	3.01
75p	7.62	4.82	-1.46e-03	-1.15e+01
75p	7.41	1.54	0.00136	6.21
75p	6.96	6.08	0.000895	3.01
75p	7.52	3.09	-1.06e-04	-5.31e-01
75p	7.51	3.18	-1.88e-05	-9.31e-02
75p	7.52	0.892	8.70e-05	0.427
75p	7.50	1.07	4.39e-08	0.000217
75p	7.29	4.36	0.000235	0.984
75p	7.35	4.26	1.91e-05	0.0861
median	7.62	4.82	-1.46e-03	-1.15e+01
median	7.41	1.54	0.00136	6.21
median	6.96	6.08	0.000895	3.01
median	7.62	4.82	-1.46e-03	-1.15e+01
median	7.41	1.54	0.00136	6.21
median	6.96	6.08	0.000895	3.01
median	7.52	3.10	-9.35e-05	-4.66e-01
median	7.51	3.19	-1.72e-05	-8.51e-02
median	7.51	0.906	6.94e-05	0.341
median	7.50	1.09	-8.35e-07	-4.12e-03
median	7.30	4.34	0.000194	0.824
median	7.36	4.24	1.44e-05	0.0656
25p	7.62	4.82	3.46e-18	3.10e-14
25p	7.62	4.82	3.46e-18	3.10e-14
25p	7.67	2.97	-1.64e-06	-9.02e-03
25p	7.69	3.01	-5.76e-06	-3.19e-02
75p	7.62	4.82	3.46e-18	3.10e-14
75p	7.62	4.82	3.46e-18	3.10e-14
75p	7.67	2.98	2.19e-06	0.0120
75p	7.68	3.01	-5.32e-06	-2.95e-02
median	7.62	4.82	3.46e-18	3.10e-14
median	7.62	4.82	3.46e-18	3.10e-14
median	7.67	2.98	2.05e-07	0.00113
median	7.69	3.01	-5.60e-06	-3.10e-02
25p	7.62	4.82	-1.46e-03	-1.15e+01
25p	7.62	4.82	-1.46e-03	-1.15e+01
25p	7.67	2.97	-4.96e-06	-2.73e-02
25p	7.69	3.01	-5.78e-06	-3.21e-02
75p	7.62	4.82	-1.46e-03	-1.15e+01
75p	7.62	4.82	-1.46e-03	-1.15e+01
75p	7.67	2.98	-1.49e-06	-8.17e-03
75p	7.68	3.01	-5.35e-06	-2.96e-02
median	7.62	4.82	-1.46e-03	-1.15e+01
median	7.62	4.82	-1.46e-03	-1.15e+01
median	7.67	2.98	-3.27e-06	-1.80e-02

median	7.69	3.01	-5.63e-06	-3.12e-02

S(6)	B	Li	As	C(4)
0.000964	0.000186	3.08e-06	3.37e-07	0.00379
0.000974	0.000136	6.95e-06	2.48e-07	0.00348
0.000964	0.000186	3.08e-06	3.37e-07	0.00379
0.000974	0.000136	6.95e-06	2.48e-07	0.00348
0.000485	8.90e-05	1.17e-06	7.10e-07	0.00492
0.000476	7.37e-05	1.17e-06	7.67e-07	0.00539
0.000492	7.40e-05	1.17e-06	6.57e-07	0.00530
0.000479	6.29e-05	1.17e-06	7.03e-07	0.00558
0.000964	0.000186	3.08e-06	3.37e-07	0.00379
0.000974	0.000136	6.95e-06	2.48e-07	0.00348
0.000964	0.000186	3.08e-06	3.37e-07	0.00379
0.000974	0.000136	6.95e-06	2.48e-07	0.00348
0.000487	8.92e-05	1.17e-06	6.62e-07	0.00477
0.000475	7.50e-05	1.17e-06	7.33e-07	0.00524
0.000496	7.36e-05	1.17e-06	6.14e-07	0.00521
0.000479	6.34e-05	1.17e-06	6.66e-07	0.00549
0.000964	0.000186	3.08e-06	3.37e-07	0.00379
0.000974	0.000136	6.95e-06	2.48e-07	0.00348
0.000964	0.000186	3.08e-06	3.37e-07	0.00379
0.000974	0.000136	6.95e-06	2.48e-07	0.00348
0.000486	8.90e-05	1.17e-06	6.85e-07	0.00485
0.000476	7.42e-05	1.17e-06	7.51e-07	0.00532
0.000494	7.37e-05	1.17e-06	6.35e-07	0.00526
0.000479	6.30e-05	1.17e-06	6.84e-07	0.00553
0.000964	0.000186	3.08e-06	3.37e-07	0.00379
0.000974	0.000136	6.95e-06	2.48e-07	0.00348
0.000964	0.000186	3.08e-06	3.37e-07	0.00379
0.000974	0.000136	6.95e-06	2.48e-07	0.00348
0.000485	8.75e-05	1.17e-06	7.30e-07	0.00492
0.000476	7.25e-05	1.17e-06	7.91e-07	0.00539
0.000492	7.25e-05	1.17e-06	6.79e-07	0.00530
0.000480	6.17e-05	1.17e-06	7.28e-07	0.00558
0.000964	0.000186	3.08e-06	3.37e-07	0.00379
0.000974	0.000136	6.95e-06	2.48e-07	0.00348
0.000964	0.000186	3.08e-06	3.37e-07	0.00379
0.000974	0.000136	6.95e-06	2.48e-07	0.00348
0.000487	8.76e-05	1.17e-06	6.80e-07	0.00476
0.000476	7.38e-05	1.17e-06	7.54e-07	0.00523
0.000496	7.20e-05	1.17e-06	6.35e-07	0.00521
0.000479	6.22e-05	1.17e-06	6.89e-07	0.00549
0.000964	0.000186	3.08e-06	3.37e-07	0.00379
0.000974	0.000136	6.95e-06	2.48e-07	0.00348
0.000964	0.000186	3.08e-06	3.37e-07	0.00379

0.000974	0.000136	6.95e-06	2.48e-07	0.00348
0.000486	8.74e-05	1.17e-06	7.04e-07	0.00484
0.000476	7.30e-05	1.17e-06	7.73e-07	0.00531
0.000494	7.21e-05	1.17e-06	6.56e-07	0.00525
0.000480	6.18e-05	1.17e-06	7.08e-07	0.00553
0.00127	0.000165	7.14e-06	2.98e-08	0.00242
0.00474	0.000782	5.23e-07	3.50e-08	0.00159
0.00813	0.00114	3.97e-06	2.98e-08	0.00229
0.00127	0.000165	7.14e-06	2.98e-08	0.00242
0.00474	0.000782	5.23e-07	3.50e-08	0.00159
0.00813	0.00114	3.97e-06	2.98e-08	0.00229
0.000633	0.000137	5.55e-07	2.25e-08	0.00335
0.000644	0.000107	5.55e-07	1.78e-08	0.00341
0.000703	0.000239	5.55e-07	5.55e-08	0.00333
0.000633	0.000158	5.55e-07	5.75e-08	0.00347
0.000884	0.000299	5.55e-07	3.42e-08	0.00482
0.000633	0.000181	5.55e-07	2.83e-08	0.00442
0.00127	0.000165	7.14e-06	2.98e-08	0.00242
0.00474	0.000782	5.23e-07	3.50e-08	0.00159
0.00813	0.00114	3.97e-06	2.98e-08	0.00229
0.00127	0.000165	7.14e-06	2.98e-08	0.00242
0.00474	0.000782	5.23e-07	3.50e-08	0.00159
0.00813	0.00114	3.97e-06	2.98e-08	0.00229
0.000633	0.000140	5.55e-07	2.41e-08	0.00333
0.000643	0.000111	5.55e-07	1.99e-08	0.00338
0.000730	0.000250	5.55e-07	5.47e-08	0.00328
0.000632	0.000166	5.55e-07	5.70e-08	0.00342
0.000983	0.000314	5.55e-07	3.61e-08	0.00494
0.000637	0.000187	5.55e-07	3.03e-08	0.00459
0.00127	0.000165	7.14e-06	2.98e-08	0.00242
0.00474	0.000782	5.23e-07	3.50e-08	0.00159
0.00813	0.00114	3.97e-06	2.98e-08	0.00229
0.00127	0.000165	7.14e-06	2.98e-08	0.00242
0.00474	0.000782	5.23e-07	3.50e-08	0.00159
0.00813	0.00114	3.97e-06	2.98e-08	0.00229
0.000633	0.000138	5.55e-07	2.33e-08	0.00334
0.000644	0.000109	5.55e-07	1.89e-08	0.00339
0.000716	0.000244	5.55e-07	5.51e-08	0.00331
0.000632	0.000162	5.55e-07	5.73e-08	0.00345
0.000930	0.000306	5.55e-07	3.52e-08	0.00488
0.000634	0.000183	5.55e-07	2.93e-08	0.00451
0.00127	0.000165	7.14e-06	2.98e-08	0.00242
0.00474	0.000782	5.23e-07	3.50e-08	0.00159
0.00813	0.00114	3.97e-06	2.98e-08	0.00229
0.00127	0.000165	7.14e-06	2.98e-08	0.00242
0.00474	0.000782	5.23e-07	3.50e-08	0.00159
0.00813	0.00114	3.97e-06	2.98e-08	0.00229
0.000634	0.000137	5.55e-07	2.21e-08	0.00336
0.000644	0.000108	5.55e-07	1.75e-08	0.00341
0.000703	0.000239	5.55e-07	5.63e-08	0.00333

0.000633	0.000158	5.55e-07	5.84e-08	0.00347
0.000884	0.000299	5.55e-07	3.44e-08	0.00482
0.000633	0.000181	5.55e-07	2.85e-08	0.00442
0.00127	0.000165	7.14e-06	2.98e-08	0.00242
0.00474	0.000782	5.23e-07	3.50e-08	0.00159
0.00813	0.00114	3.97e-06	2.98e-08	0.00229
0.00127	0.000165	7.14e-06	2.98e-08	0.00242
0.00474	0.000782	5.23e-07	3.50e-08	0.00159
0.00813	0.00114	3.97e-06	2.98e-08	0.00229
0.000634	0.000140	5.55e-07	2.37e-08	0.00334
0.000643	0.000111	5.55e-07	1.96e-08	0.00338
0.000730	0.000250	5.55e-07	5.55e-08	0.00328
0.000632	0.000166	5.55e-07	5.78e-08	0.00342
0.000983	0.000315	5.55e-07	3.64e-08	0.00494
0.000637	0.000187	5.55e-07	3.05e-08	0.00459
0.00127	0.000165	7.14e-06	2.98e-08	0.00242
0.00474	0.000782	5.23e-07	3.50e-08	0.00159
0.00813	0.00114	3.97e-06	2.98e-08	0.00229
0.00127	0.000165	7.14e-06	2.98e-08	0.00242
0.00474	0.000782	5.23e-07	3.50e-08	0.00159
0.00813	0.00114	3.97e-06	2.98e-08	0.00229
0.000634	0.000139	5.55e-07	2.30e-08	0.00335
0.000643	0.000109	5.55e-07	1.86e-08	0.00339
0.000715	0.000243	5.55e-07	5.59e-08	0.00331
0.000633	0.000161	5.55e-07	5.81e-08	0.00345
0.000930	0.000306	5.55e-07	3.54e-08	0.00488
0.000634	0.000183	5.55e-07	2.94e-08	0.00451
0.00127	0.000165	7.14e-06	2.98e-08	0.00242
0.00127	0.000165	7.14e-06	2.98e-08	0.00242
0.000482	0.000126	2.83e-06	3.51e-08	0.00425
0.000482	0.000104	2.83e-06	2.87e-08	0.00417
0.00127	0.000165	7.14e-06	2.98e-08	0.00242
0.00127	0.000165	7.14e-06	2.98e-08	0.00242
0.000483	0.000128	2.83e-06	3.72e-08	0.00427
0.000481	0.000106	2.83e-06	3.16e-08	0.00420
0.00127	0.000165	7.14e-06	2.98e-08	0.00242
0.00127	0.000165	7.14e-06	2.98e-08	0.00242
0.000482	0.000127	2.83e-06	3.62e-08	0.00426
0.000482	0.000104	2.83e-06	3.02e-08	0.00418
0.00127	0.000165	7.14e-06	2.98e-08	0.00242
0.00127	0.000165	7.14e-06	2.98e-08	0.00242
0.000482	0.000127	2.83e-06	3.45e-08	0.00426
0.000482	0.000104	2.83e-06	2.82e-08	0.00417
0.00127	0.000165	7.14e-06	2.98e-08	0.00242
0.00127	0.000165	7.14e-06	2.98e-08	0.00242
0.000483	0.000128	2.83e-06	3.66e-08	0.00428
0.000481	0.000106	2.83e-06	3.11e-08	0.00420
0.00127	0.000165	7.14e-06	2.98e-08	0.00242
0.00127	0.000165	7.14e-06	2.98e-08	0.00242
0.000483	0.000127	2.83e-06	3.56e-08	0.00427

0.000482	0.000105	2.83e-06	2.97e-08	0.00419

Cl	F	Ca	Mg	Na
0.00619	9.22e-06	0.00301	0.00166	0.00205
0.00680	8.95e-06	0.00296	0.00159	0.00241
0.00619	9.22e-06	0.00301	0.00166	0.00205
0.00680	8.95e-06	0.00296	0.00159	0.00241
0.00776	8.15e-06	0.00256	0.00283	0.00212
0.00776	8.16e-06	0.00266	0.00293	0.00212
0.00776	8.15e-06	0.00264	0.00292	0.00212
0.00776	8.16e-06	0.00269	0.00297	0.00212
0.00619	9.22e-06	0.00301	0.00166	0.00205
0.00680	8.95e-06	0.00296	0.00159	0.00241
0.00619	9.22e-06	0.00301	0.00166	0.00205
0.00680	8.95e-06	0.00296	0.00159	0.00241
0.00776	8.15e-06	0.00253	0.00280	0.00212
0.00776	8.16e-06	0.00263	0.00290	0.00212
0.00776	8.15e-06	0.00263	0.00290	0.00212
0.00776	8.16e-06	0.00267	0.00296	0.00212
0.00619	9.22e-06	0.00301	0.00166	0.00205
0.00680	8.95e-06	0.00296	0.00159	0.00241
0.00619	9.22e-06	0.00301	0.00166	0.00205
0.00680	8.95e-06	0.00296	0.00159	0.00241
0.00776	8.15e-06	0.00255	0.00282	0.00212
0.00776	8.16e-06	0.00264	0.00292	0.00212
0.00776	8.15e-06	0.00263	0.00291	0.00212
0.00776	8.16e-06	0.00268	0.00296	0.00212
0.00279	9.22e-06	0.00301	0.00166	0.00205
0.00286	8.95e-06	0.00296	0.00159	0.00241
0.00279	9.22e-06	0.00301	0.00166	0.00205
0.00286	8.95e-06	0.00296	0.00159	0.00241
0.00776	8.15e-06	0.00256	0.00283	0.00212
0.00776	8.16e-06	0.00265	0.00293	0.00212
0.00776	8.15e-06	0.00264	0.00292	0.00212
0.00776	8.16e-06	0.00269	0.00297	0.00212
0.00279	9.22e-06	0.00301	0.00166	0.00205
0.00286	8.95e-06	0.00296	0.00159	0.00241
0.00279	9.22e-06	0.00301	0.00166	0.00205
0.00286	8.95e-06	0.00296	0.00159	0.00241
0.00776	8.15e-06	0.00253	0.00280	0.00212
0.00776	8.16e-06	0.00263	0.00290	0.00212
0.00776	8.15e-06	0.00262	0.00290	0.00212
0.00776	8.16e-06	0.00267	0.00296	0.00212
0.00279	9.22e-06	0.00301	0.00166	0.00205
0.00286	8.95e-06	0.00296	0.00159	0.00241
0.00279	9.22e-06	0.00301	0.00166	0.00205

0.00286	8.95e-06	0.00296	0.00159	0.00241
0.00776	8.15e-06	0.00255	0.00282	0.00212
0.00776	8.16e-06	0.00264	0.00292	0.00212
0.00776	8.15e-06	0.00263	0.00291	0.00212
0.00776	8.16e-06	0.00268	0.00296	0.00212
0.00117	9.22e-06	0.00137	0.000805	0.00148
0.00288	9.75e-06	0.00268	0.00320	0.00196
0.00187	8.17e-06	0.00763	0.00152	0.00132
0.00117	9.22e-06	0.00137	0.000805	0.00148
0.00288	9.75e-06	0.00268	0.00320	0.00196
0.00187	8.17e-06	0.00763	0.00152	0.00132
0.00603	8.42e-06	0.00204	0.00227	0.00170
0.00603	8.42e-06	0.00207	0.00230	0.00170
0.00603	8.42e-06	0.00210	0.00233	0.00170
0.00603	8.42e-06	0.00208	0.00232	0.00170
0.00603	8.42e-06	0.00251	0.00278	0.00170
0.00603	8.42e-06	0.00228	0.00253	0.00170
0.00117	9.22e-06	0.00137	0.000805	0.00148
0.00288	9.75e-06	0.00268	0.00320	0.00196
0.00187	8.17e-06	0.00763	0.00152	0.00132
0.00117	9.22e-06	0.00137	0.000805	0.00148
0.00288	9.75e-06	0.00268	0.00320	0.00196
0.00187	8.17e-06	0.00763	0.00152	0.00132
0.00603	8.42e-06	0.00203	0.00226	0.00170
0.00603	8.42e-06	0.00207	0.00229	0.00170
0.00603	8.42e-06	0.00211	0.00235	0.00170
0.00603	8.42e-06	0.00207	0.00230	0.00170
0.00603	8.42e-06	0.00260	0.00287	0.00170
0.00603	8.42e-06	0.00231	0.00257	0.00170
0.00117	9.22e-06	0.00137	0.000805	0.00148
0.00288	9.75e-06	0.00268	0.00320	0.00196
0.00187	8.17e-06	0.00763	0.00152	0.00132
0.00117	9.22e-06	0.00137	0.000805	0.00148
0.00288	9.75e-06	0.00268	0.00320	0.00196
0.00187	8.17e-06	0.00763	0.00152	0.00132
0.00603	8.42e-06	0.00204	0.00226	0.00170
0.00603	8.42e-06	0.00207	0.00230	0.00170
0.00603	8.42e-06	0.00211	0.00234	0.00170
0.00603	8.42e-06	0.00208	0.00231	0.00170
0.00603	8.42e-06	0.00255	0.00282	0.00170
0.00603	8.42e-06	0.00229	0.00255	0.00170
0.00262	9.22e-06	0.00137	0.000805	0.00148
0.00152	9.75e-06	0.00268	0.00320	0.00196
0.000974	8.17e-06	0.00763	0.00152	0.00132
0.00262	9.22e-06	0.00137	0.000805	0.00148
0.00152	9.75e-06	0.00268	0.00320	0.00196
0.000974	8.17e-06	0.00763	0.00152	0.00132
0.00603	8.42e-06	0.00204	0.00227	0.00170
0.00603	8.42e-06	0.00207	0.00230	0.00170
0.00603	8.42e-06	0.00210	0.00233	0.00170

0.00603	8.42e-06	0.00208	0.00232	0.00170
0.00603	8.42e-06	0.00251	0.00278	0.00170
0.00603	8.42e-06	0.00228	0.00253	0.00170
0.00262	9.22e-06	0.00137	0.000805	0.00148
0.00152	9.75e-06	0.00268	0.00320	0.00196
0.000974	8.17e-06	0.00763	0.00152	0.00132
0.00262	9.22e-06	0.00137	0.000805	0.00148
0.00152	9.75e-06	0.00268	0.00320	0.00196
0.000974	8.17e-06	0.00763	0.00152	0.00132
0.00603	8.42e-06	0.00203	0.00226	0.00170
0.00603	8.42e-06	0.00207	0.00230	0.00170
0.00603	8.42e-06	0.00211	0.00234	0.00170
0.00603	8.42e-06	0.00207	0.00230	0.00170
0.00603	8.42e-06	0.00260	0.00287	0.00170
0.00603	8.42e-06	0.00231	0.00257	0.00170
0.00262	9.22e-06	0.00137	0.000805	0.00148
0.00152	9.75e-06	0.00268	0.00320	0.00196
0.000974	8.17e-06	0.00763	0.00152	0.00132
0.00262	9.22e-06	0.00137	0.000805	0.00148
0.00152	9.75e-06	0.00268	0.00320	0.00196
0.000974	8.17e-06	0.00763	0.00152	0.00132
0.00603	8.42e-06	0.00204	0.00226	0.00170
0.00603	8.42e-06	0.00207	0.00230	0.00170
0.00603	8.42e-06	0.00210	0.00234	0.00170
0.00603	8.42e-06	0.00208	0.00231	0.00170
0.00603	8.42e-06	0.00255	0.00282	0.00170
0.00603	8.42e-06	0.00229	0.00255	0.00170
0.00117	9.22e-06	0.00137	0.000805	0.00148
0.00117	9.22e-06	0.00137	0.000805	0.00148
0.00426	2.16e-05	0.00109	0.00129	0.00444
0.00426	2.16e-05	0.00108	0.00127	0.00444
0.00117	9.22e-06	0.00137	0.000805	0.00148
0.00117	9.22e-06	0.00137	0.000805	0.00148
0.00426	2.16e-05	0.00110	0.00130	0.00444
0.00426	2.16e-05	0.00108	0.00127	0.00444
0.00117	9.22e-06	0.00137	0.000805	0.00148
0.00117	9.22e-06	0.00137	0.000805	0.00148
0.00426	2.16e-05	0.00110	0.00129	0.00444
0.00426	2.16e-05	0.00108	0.00127	0.00444
0.00262	9.22e-06	0.00137	0.000805	0.00148
0.00262	9.22e-06	0.00137	0.000805	0.00148
0.00426	2.16e-05	0.00109	0.00129	0.00444
0.00426	2.16e-05	0.00108	0.00127	0.00444
0.00262	9.22e-06	0.00137	0.000805	0.00148
0.00262	9.22e-06	0.00137	0.000805	0.00148
0.00426	2.16e-05	0.00110	0.00130	0.00444
0.00426	2.16e-05	0.00108	0.00128	0.00444
0.00262	9.22e-06	0.00137	0.000805	0.00148
0.00262	9.22e-06	0.00137	0.000805	0.00148
0.00426	2.16e-05	0.00110	0.00129	0.00444

0.00426	2.16e-05	0.00108	0.00127	0.00444

K	Ba	Si	P	Mn
7.43e-05	2.17e-06	0.000151	7.01e-06	2.01e-06
0.000157	7.61e-07	0.000135	7.43e-07	2.91e-06
7.43e-05	2.17e-06	0.000151	7.01e-06	2.01e-06
0.000157	7.61e-07	0.000135	7.43e-07	2.91e-06
1.11e-05	5.58e-07	0.000207	6.39e-06	1.97e-05
1.11e-05	5.81e-07	0.000233	6.45e-06	2.19e-05
1.11e-05	5.59e-07	0.000187	9.86e-07	1.97e-05
1.11e-05	5.80e-07	0.000203	1.03e-06	2.18e-05
7.43e-05	2.17e-06	0.000151	7.01e-06	2.01e-06
0.000157	7.61e-07	0.000135	7.43e-07	2.91e-06
7.43e-05	2.17e-06	0.000151	7.01e-06	2.01e-06
0.000157	7.61e-07	0.000135	7.43e-07	2.91e-06
1.11e-05	5.52e-07	0.000200	6.40e-06	1.93e-05
1.11e-05	5.78e-07	0.000227	6.50e-06	2.18e-05
1.11e-05	5.53e-07	0.000182	9.80e-07	1.94e-05
1.11e-05	5.79e-07	0.000199	1.02e-06	2.17e-05
7.43e-05	2.17e-06	0.000151	7.01e-06	2.01e-06
0.000157	7.61e-07	0.000135	7.43e-07	2.91e-06
7.43e-05	2.17e-06	0.000151	7.01e-06	2.01e-06
0.000157	7.61e-07	0.000135	7.43e-07	2.91e-06
1.11e-05	5.55e-07	0.000203	6.40e-06	1.95e-05
1.11e-05	5.79e-07	0.000230	6.48e-06	2.19e-05
1.11e-05	5.56e-07	0.000185	9.83e-07	1.96e-05
1.11e-05	5.80e-07	0.000201	1.02e-06	2.18e-05
7.43e-05	2.17e-06	0.000151	7.01e-06	2.01e-06
0.000157	7.61e-07	0.000135	7.43e-07	2.91e-06
7.43e-05	2.17e-06	0.000151	7.01e-06	2.01e-06
0.000157	7.61e-07	0.000135	7.43e-07	2.91e-06
1.11e-05	5.59e-07	0.000206	6.38e-06	1.96e-05
1.11e-05	5.80e-07	0.000232	6.45e-06	2.19e-05
1.11e-05	5.60e-07	0.000186	9.87e-07	1.97e-05
1.11e-05	5.80e-07	0.000202	1.03e-06	2.18e-05
7.43e-05	2.17e-06	0.000151	7.01e-06	2.01e-06
0.000157	7.61e-07	0.000135	7.43e-07	2.91e-06
7.43e-05	2.17e-06	0.000151	7.01e-06	2.01e-06
0.000157	7.61e-07	0.000135	7.43e-07	2.91e-06
1.11e-05	5.53e-07	0.000198	6.40e-06	1.93e-05
1.11e-05	5.77e-07	0.000226	6.50e-06	2.18e-05
1.11e-05	5.53e-07	0.000181	9.80e-07	1.94e-05
1.11e-05	5.78e-07	0.000198	1.02e-06	2.17e-05
7.43e-05	2.17e-06	0.000151	7.01e-06	2.01e-06
0.000157	7.61e-07	0.000135	7.43e-07	2.91e-06
7.43e-05	2.17e-06	0.000151	7.01e-06	2.01e-06

0.000157	7.61e-07	0.000135	7.43e-07	2.91e-06
1.11e-05	5.56e-07	0.000202	6.39e-06	1.95e-05
1.11e-05	5.79e-07	0.000229	6.48e-06	2.19e-05
1.11e-05	5.57e-07	0.000184	9.84e-07	1.96e-05
1.11e-05	5.79e-07	0.000200	1.02e-06	2.18e-05
0.000178	2.60e-07	0.000318	8.08e-08	6.37e-07
7.76e-05	3.28e-07	9.98e-05	3.23e-07	2.06e-05
0.000359	3.10e-07	8.32e-05	4.20e-07	9.71e-06
0.000178	2.60e-07	0.000318	8.08e-08	6.37e-07
7.76e-05	3.28e-07	9.98e-05	3.23e-07	2.06e-05
0.000359	3.10e-07	8.32e-05	4.20e-07	9.71e-06
5.53e-05	2.93e-07	0.000346	9.49e-08	1.30e-06
5.53e-05	2.91e-07	0.000303	9.45e-08	1.25e-06
5.53e-05	2.91e-07	0.000122	5.73e-07	2.68e-06
5.53e-05	2.91e-07	0.000126	5.76e-07	1.48e-06
5.53e-05	2.90e-07	7.29e-05	9.77e-07	1.37e-06
5.53e-05	2.91e-07	6.27e-05	9.36e-07	1.19e-06
0.000178	2.60e-07	0.000318	8.08e-08	6.37e-07
7.76e-05	3.28e-07	9.98e-05	3.23e-07	2.06e-05
0.000359	3.10e-07	8.32e-05	4.20e-07	9.71e-06
0.000178	2.60e-07	0.000318	8.08e-08	6.37e-07
7.76e-05	3.28e-07	9.98e-05	3.23e-07	2.06e-05
0.000359	3.10e-07	8.32e-05	4.20e-07	9.71e-06
5.53e-05	2.93e-07	0.000360	9.49e-08	1.31e-06
5.53e-05	2.91e-07	0.000323	9.37e-08	1.25e-06
5.53e-05	2.91e-07	0.000121	5.72e-07	2.79e-06
5.53e-05	2.91e-07	0.000125	5.76e-07	1.51e-06
5.53e-05	2.70e-07	7.64e-05	9.89e-07	1.39e-06
5.53e-05	3.11e-07	6.60e-05	9.49e-07	1.19e-06
0.000178	2.60e-07	0.000318	8.08e-08	6.37e-07
7.76e-05	3.28e-07	9.98e-05	3.23e-07	2.06e-05
0.000359	3.10e-07	8.32e-05	4.20e-07	9.71e-06
0.000178	2.60e-07	0.000318	8.08e-08	6.37e-07
7.76e-05	3.28e-07	9.98e-05	3.23e-07	2.06e-05
0.000359	3.10e-07	8.32e-05	4.20e-07	9.71e-06
5.53e-05	2.93e-07	0.000353	9.48e-08	1.31e-06
5.53e-05	2.91e-07	0.000313	9.40e-08	1.25e-06
5.53e-05	2.91e-07	0.000121	5.73e-07	2.72e-06
5.53e-05	2.91e-07	0.000125	5.76e-07	1.50e-06
5.53e-05	2.82e-07	7.47e-05	9.83e-07	1.38e-06
5.53e-05	2.98e-07	6.43e-05	9.42e-07	1.19e-06
0.000178	2.60e-07	0.000318	8.08e-08	6.37e-07
7.76e-05	3.28e-07	9.98e-05	3.23e-07	2.06e-05
0.000359	3.10e-07	8.32e-05	4.20e-07	9.71e-06
0.000178	2.60e-07	0.000318	8.08e-08	6.37e-07
7.76e-05	3.28e-07	9.98e-05	3.23e-07	2.06e-05
0.000359	3.10e-07	8.32e-05	4.20e-07	9.71e-06
5.53e-05	2.93e-07	0.000347	9.45e-08	1.30e-06
5.53e-05	2.91e-07	0.000303	9.42e-08	1.25e-06
5.53e-05	2.91e-07	0.000122	5.75e-07	2.70e-06

5.53e-05	2.91e-07	0.000126	5.78e-07	1.49e-06
5.53e-05	2.90e-07	7.29e-05	9.78e-07	1.37e-06
5.53e-05	2.91e-07	6.27e-05	9.37e-07	1.19e-06
0.000178	2.60e-07	0.000318	8.08e-08	6.37e-07
7.76e-05	3.28e-07	9.98e-05	3.23e-07	2.06e-05
0.000359	3.10e-07	8.32e-05	4.20e-07	9.71e-06
0.000178	2.60e-07	0.000318	8.08e-08	6.37e-07
7.76e-05	3.28e-07	9.98e-05	3.23e-07	2.06e-05
0.000359	3.10e-07	8.32e-05	4.20e-07	9.71e-06
5.53e-05	2.93e-07	0.000361	9.46e-08	1.30e-06
5.53e-05	2.91e-07	0.000324	9.34e-08	1.25e-06
5.53e-05	2.91e-07	0.000120	5.74e-07	2.81e-06
5.53e-05	2.91e-07	0.000125	5.78e-07	1.52e-06
5.53e-05	2.69e-07	7.64e-05	9.91e-07	1.39e-06
5.53e-05	3.11e-07	6.60e-05	9.51e-07	1.19e-06
0.000178	2.60e-07	0.000318	8.08e-08	6.37e-07
7.76e-05	3.28e-07	9.98e-05	3.23e-07	2.06e-05
0.000359	3.10e-07	8.32e-05	4.20e-07	9.71e-06
0.000178	2.60e-07	0.000318	8.08e-08	6.37e-07
7.76e-05	3.28e-07	9.98e-05	3.23e-07	2.06e-05
0.000359	3.10e-07	8.32e-05	4.20e-07	9.71e-06
5.53e-05	2.93e-07	0.000354	9.45e-08	1.30e-06
5.53e-05	2.91e-07	0.000314	9.37e-08	1.25e-06
5.53e-05	2.91e-07	0.000121	5.75e-07	2.74e-06
5.53e-05	2.91e-07	0.000125	5.78e-07	1.50e-06
5.53e-05	2.82e-07	7.46e-05	9.84e-07	1.38e-06
5.53e-05	2.98e-07	6.43e-05	9.43e-07	1.19e-06
0.000178	2.60e-07	0.000318	8.08e-08	6.37e-07
0.000178	2.60e-07	0.000318	8.08e-08	6.37e-07
9.66e-05	3.90e-07	0.000337	1.20e-07	5.48e-07
9.66e-05	3.87e-07	0.000292	1.09e-07	4.34e-07
0.000178	2.60e-07	0.000318	8.08e-08	6.37e-07
0.000178	2.60e-07	0.000318	8.08e-08	6.37e-07
9.66e-05	3.90e-07	0.000352	1.24e-07	5.58e-07
9.66e-05	3.88e-07	0.000312	1.14e-07	4.39e-07
0.000178	2.60e-07	0.000318	8.08e-08	6.37e-07
0.000178	2.60e-07	0.000318	8.08e-08	6.37e-07
9.66e-05	3.90e-07	0.000345	1.22e-07	5.52e-07
9.66e-05	3.88e-07	0.000302	1.12e-07	4.36e-07
0.000178	2.60e-07	0.000318	8.08e-08	6.37e-07
0.000178	2.60e-07	0.000318	8.08e-08	6.37e-07
9.66e-05	3.89e-07	0.000338	1.20e-07	5.44e-07
9.66e-05	3.88e-07	0.000293	1.08e-07	4.33e-07
0.000178	2.60e-07	0.000318	8.08e-08	6.37e-07
0.000178	2.60e-07	0.000318	8.08e-08	6.37e-07
9.66e-05	3.89e-07	0.000353	1.23e-07	5.54e-07
9.66e-05	3.89e-07	0.000312	1.14e-07	4.38e-07
0.000178	2.60e-07	0.000318	8.08e-08	6.37e-07
0.000178	2.60e-07	0.000318	8.08e-08	6.37e-07
9.66e-05	3.89e-07	0.000346	1.21e-07	5.48e-07

9.66e-05	3.88e-07	0.000303	1.11e-07	4.35e-07

Fe	Al	Sb	Be	Cd
9.89e-05	3.50e-07	3.49e-09	2.03e-08	1.49e-09
0.000113	3.50e-07	3.49e-09	2.03e-08	1.49e-09
9.89e-05	3.50e-07	3.49e-09	2.03e-08	1.49e-09
0.000113	3.50e-07	3.49e-09	2.03e-08	1.49e-09
6.88e-05	4.46e-08	3.49e-09	3.22e-08	1.44e-09
7.60e-05	4.29e-08	3.49e-09	3.69e-08	1.50e-09
7.52e-05	4.32e-08	3.49e-09	2.99e-08	1.30e-09
7.90e-05	4.24e-08	3.49e-09	3.23e-08	1.31e-09
9.89e-05	3.50e-07	3.49e-09	2.03e-08	1.49e-09
0.000113	3.50e-07	3.49e-09	2.03e-08	1.49e-09
9.89e-05	3.50e-07	3.49e-09	2.03e-08	1.49e-09
0.000113	3.50e-07	3.49e-09	2.03e-08	1.49e-09
6.24e-05	4.52e-08	3.49e-09	3.07e-08	1.39e-09
7.02e-05	4.34e-08	3.49e-09	3.52e-08	1.48e-09
6.93e-05	4.35e-08	3.49e-09	2.90e-08	1.25e-09
7.38e-05	4.26e-08	3.49e-09	3.14e-08	1.29e-09
9.89e-05	3.50e-07	3.49e-09	2.03e-08	1.49e-09
0.000113	3.50e-07	3.49e-09	2.03e-08	1.49e-09
9.89e-05	3.50e-07	3.49e-09	2.03e-08	1.49e-09
0.000113	3.50e-07	3.49e-09	2.03e-08	1.49e-09
6.54e-05	4.49e-08	3.49e-09	3.15e-08	1.42e-09
7.31e-05	4.31e-08	3.49e-09	3.61e-08	1.49e-09
7.21e-05	4.33e-08	3.49e-09	2.95e-08	1.27e-09
7.64e-05	4.25e-08	3.49e-09	3.19e-08	1.30e-09
9.89e-05	3.50e-07	3.49e-09	2.03e-08	1.49e-09
0.000113	3.50e-07	3.49e-09	2.03e-08	1.49e-09
9.89e-05	3.50e-07	3.49e-09	2.03e-08	1.49e-09
0.000113	3.50e-07	3.49e-09	2.03e-08	1.49e-09
6.89e-05	4.46e-08	3.49e-09	3.21e-08	1.67e-09
7.62e-05	4.29e-08	3.49e-09	3.68e-08	1.74e-09
7.53e-05	4.32e-08	3.49e-09	2.98e-08	1.53e-09
7.92e-05	4.24e-08	3.49e-09	3.22e-08	1.55e-09
9.89e-05	3.50e-07	3.49e-09	2.03e-08	1.49e-09
0.000113	3.50e-07	3.49e-09	2.03e-08	1.49e-09
9.89e-05	3.50e-07	3.49e-09	2.03e-08	1.49e-09
0.000113	3.50e-07	3.49e-09	2.03e-08	1.49e-09
6.24e-05	4.53e-08	3.49e-09	3.06e-08	1.61e-09
7.03e-05	4.34e-08	3.49e-09	3.51e-08	1.72e-09
6.93e-05	4.35e-08	3.49e-09	2.89e-08	1.48e-09
7.40e-05	4.26e-08	3.49e-09	3.13e-08	1.52e-09
9.89e-05	3.50e-07	3.49e-09	2.03e-08	1.49e-09
0.000113	3.50e-07	3.49e-09	2.03e-08	1.49e-09
9.89e-05	3.50e-07	3.49e-09	2.03e-08	1.49e-09

0.000113	3.50e-07	3.49e-09	2.03e-08	1.49e-09
6.55e-05	4.49e-08	3.49e-09	3.13e-08	1.64e-09
7.32e-05	4.31e-08	3.49e-09	3.59e-08	1.73e-09
7.21e-05	4.34e-08	3.49e-09	2.94e-08	1.50e-09
7.65e-05	4.25e-08	3.49e-09	3.18e-08	1.53e-09
3.00e-07	3.49e-07	5.96e-09	2.03e-08	2.35e-08
2.58e-06	3.50e-07	3.49e-09	3.14e-08	1.49e-09
3.00e-07	3.50e-07	3.50e-09	2.03e-08	1.49e-09
3.00e-07	3.49e-07	5.96e-09	2.03e-08	2.35e-08
2.58e-06	3.50e-07	3.49e-09	3.14e-08	1.49e-09
3.00e-07	3.50e-07	3.50e-09	2.03e-08	1.49e-09
1.07e-08	5.72e-08	3.49e-09	3.01e-08	5.87e-08
1.02e-08	5.64e-08	3.49e-09	2.91e-08	5.10e-08
8.68e-07	5.68e-08	3.49e-09	3.37e-08	7.03e-10
6.31e-07	5.57e-08	3.49e-09	3.44e-08	5.56e-10
9.77e-09	4.54e-08	3.49e-09	1.44e-08	3.55e-10
8.46e-09	4.81e-08	3.49e-09	1.26e-08	2.40e-10
3.00e-07	3.49e-07	5.96e-09	2.03e-08	2.35e-08
2.58e-06	3.50e-07	3.49e-09	3.14e-08	1.49e-09
3.00e-07	3.50e-07	3.50e-09	2.03e-08	1.49e-09
3.00e-07	3.49e-07	5.96e-09	2.03e-08	2.35e-08
2.58e-06	3.50e-07	3.49e-09	3.14e-08	1.49e-09
3.00e-07	3.50e-07	3.50e-09	2.03e-08	1.49e-09
1.07e-08	5.75e-08	3.49e-09	3.04e-08	5.91e-08
1.02e-08	5.67e-08	3.49e-09	2.96e-08	5.19e-08
8.94e-07	5.72e-08	3.49e-09	3.34e-08	7.26e-10
6.51e-07	5.62e-08	3.49e-09	3.40e-08	5.77e-10
1.02e-08	4.47e-08	3.49e-09	1.50e-08	3.79e-10
8.81e-09	4.71e-08	3.49e-09	1.31e-08	2.54e-10
3.00e-07	3.49e-07	5.96e-09	2.03e-08	2.35e-08
2.58e-06	3.50e-07	3.49e-09	3.14e-08	1.49e-09
3.00e-07	3.50e-07	3.50e-09	2.03e-08	1.49e-09
3.00e-07	3.49e-07	5.96e-09	2.03e-08	2.35e-08
2.58e-06	3.50e-07	3.49e-09	3.14e-08	1.49e-09
3.00e-07	3.50e-07	3.50e-09	2.03e-08	1.49e-09
1.07e-08	5.74e-08	3.49e-09	3.02e-08	5.89e-08
1.02e-08	5.66e-08	3.49e-09	2.94e-08	5.14e-08
8.79e-07	5.70e-08	3.49e-09	3.35e-08	7.13e-10
6.39e-07	5.59e-08	3.49e-09	3.42e-08	5.66e-10
9.98e-09	4.50e-08	3.49e-09	1.47e-08	3.66e-10
8.63e-09	4.76e-08	3.49e-09	1.28e-08	2.46e-10
3.00e-07	3.49e-07	5.96e-09	2.03e-08	2.35e-08
2.58e-06	3.50e-07	3.49e-09	3.14e-08	1.49e-09
3.00e-07	3.50e-07	3.50e-09	2.03e-08	1.49e-09
3.00e-07	3.49e-07	5.96e-09	2.03e-08	2.35e-08
2.58e-06	3.50e-07	3.49e-09	3.14e-08	1.49e-09
3.00e-07	3.50e-07	3.50e-09	2.03e-08	1.49e-09
1.07e-08	5.72e-08	3.49e-09	3.01e-08	5.41e-08
1.01e-08	5.64e-08	3.49e-09	2.91e-08	4.69e-08
8.76e-07	5.69e-08	3.49e-09	3.36e-08	7.45e-10

6.37e-07	5.57e-08	3.49e-09	3.43e-08	5.90e-10
9.77e-09	4.54e-08	3.49e-09	1.44e-08	3.68e-10
8.46e-09	4.81e-08	3.49e-09	1.26e-08	2.48e-10
3.00e-07	3.49e-07	5.96e-09	2.03e-08	2.35e-08
2.58e-06	3.50e-07	3.49e-09	3.14e-08	1.49e-09
3.00e-07	3.50e-07	3.50e-09	2.03e-08	1.49e-09
3.00e-07	3.49e-07	5.96e-09	2.03e-08	2.35e-08
2.58e-06	3.50e-07	3.49e-09	3.14e-08	1.49e-09
3.00e-07	3.50e-07	3.50e-09	2.03e-08	1.49e-09
1.07e-08	5.75e-08	3.49e-09	3.04e-08	5.45e-08
1.02e-08	5.67e-08	3.49e-09	2.96e-08	4.78e-08
9.02e-07	5.73e-08	3.49e-09	3.33e-08	7.70e-10
6.57e-07	5.62e-08	3.49e-09	3.39e-08	6.11e-10
1.02e-08	4.47e-08	3.49e-09	1.50e-08	3.93e-10
8.81e-09	4.71e-08	3.49e-09	1.31e-08	2.63e-10
3.00e-07	3.49e-07	5.96e-09	2.03e-08	2.35e-08
2.58e-06	3.50e-07	3.49e-09	3.14e-08	1.49e-09
3.00e-07	3.50e-07	3.50e-09	2.03e-08	1.49e-09
3.00e-07	3.49e-07	5.96e-09	2.03e-08	2.35e-08
2.58e-06	3.50e-07	3.49e-09	3.14e-08	1.49e-09
3.00e-07	3.50e-07	3.50e-09	2.03e-08	1.49e-09
1.07e-08	5.73e-08	3.49e-09	3.03e-08	5.42e-08
1.01e-08	5.65e-08	3.49e-09	2.94e-08	4.73e-08
8.87e-07	5.71e-08	3.49e-09	3.34e-08	7.56e-10
6.45e-07	5.59e-08	3.49e-09	3.41e-08	6.00e-10
9.98e-09	4.51e-08	3.49e-09	1.47e-08	3.79e-10
8.63e-09	4.76e-08	3.49e-09	1.28e-08	2.55e-10
3.00e-07	3.49e-07	5.96e-09	2.03e-08	2.35e-08
3.00e-07	3.49e-07	5.96e-09	2.03e-08	2.35e-08
7.54e-09	6.79e-08	1.64e-09	2.41e-08	3.31e-08
6.92e-09	6.92e-08	1.64e-09	2.26e-08	2.82e-08
3.00e-07	3.49e-07	5.96e-09	2.03e-08	2.35e-08
3.00e-07	3.49e-07	5.96e-09	2.03e-08	2.35e-08
7.64e-09	6.75e-08	1.64e-09	2.45e-08	3.36e-08
7.02e-09	6.88e-08	1.64e-09	2.32e-08	2.89e-08
3.00e-07	3.49e-07	5.96e-09	2.03e-08	2.35e-08
3.00e-07	3.49e-07	5.96e-09	2.03e-08	2.35e-08
7.59e-09	6.77e-08	1.64e-09	2.43e-08	3.33e-08
6.97e-09	6.90e-08	1.64e-09	2.29e-08	2.85e-08
3.00e-07	3.49e-07	5.96e-09	2.03e-08	2.35e-08
3.00e-07	3.49e-07	5.96e-09	2.03e-08	2.35e-08
7.55e-09	6.79e-08	1.64e-09	2.41e-08	3.05e-08
6.92e-09	6.91e-08	1.64e-09	2.27e-08	2.60e-08
3.00e-07	3.49e-07	5.96e-09	2.03e-08	2.35e-08
3.00e-07	3.49e-07	5.96e-09	2.03e-08	2.35e-08
7.64e-09	6.75e-08	1.64e-09	2.46e-08	3.10e-08
7.02e-09	6.88e-08	1.64e-09	2.32e-08	2.66e-08
3.00e-07	3.49e-07	5.96e-09	2.03e-08	2.35e-08
3.00e-07	3.49e-07	5.96e-09	2.03e-08	2.35e-08
7.59e-09	6.77e-08	1.64e-09	2.43e-08	3.07e-08

6.97e-09	6.90e-08	1.64e-09	2.29e-08	2.62e-08

Cr	Co	Pb	Mo	Se
3.85e-08	2.29e-08	1.16e-08	9.23e-08	5.01e-09
2.41e-08	1.41e-08	7.73e-09	8.14e-08	5.01e-09
3.85e-08	2.29e-08	1.16e-08	9.23e-08	5.01e-09
2.41e-08	1.41e-08	7.73e-09	8.14e-08	5.01e-09
5.30e-08	2.02e-08	1.05e-08	2.94e-08	1.37e-07
5.98e-08	2.11e-08	1.10e-08	1.91e-08	8.63e-09
3.31e-08	1.19e-08	8.42e-09	3.86e-08	1.98e-07
3.55e-08	1.20e-08	8.56e-09	2.26e-08	1.63e-08
3.85e-08	2.29e-08	1.16e-08	9.23e-08	5.01e-09
2.41e-08	1.41e-08	7.73e-09	8.14e-08	5.01e-09
3.85e-08	2.29e-08	1.16e-08	9.23e-08	5.01e-09
2.41e-08	1.41e-08	7.73e-09	8.14e-08	5.01e-09
5.09e-08	1.93e-08	1.03e-08	3.32e-08	1.85e-07
5.76e-08	2.05e-08	1.10e-08	2.10e-08	1.29e-08
3.22e-08	1.14e-08	8.26e-09	4.43e-08	2.60e-07
3.46e-08	1.17e-08	8.53e-09	2.63e-08	3.06e-08
3.85e-08	2.29e-08	1.16e-08	9.23e-08	5.01e-09
2.41e-08	1.41e-08	7.73e-09	8.14e-08	5.01e-09
3.85e-08	2.29e-08	1.16e-08	9.23e-08	5.01e-09
2.41e-08	1.41e-08	7.73e-09	8.14e-08	5.01e-09
5.19e-08	1.97e-08	1.04e-08	3.13e-08	1.59e-07
5.87e-08	2.08e-08	1.10e-08	2.00e-08	1.04e-08
3.26e-08	1.16e-08	8.34e-09	4.14e-08	2.27e-07
3.51e-08	1.18e-08	8.55e-09	2.43e-08	2.23e-08
3.85e-08	2.29e-08	1.16e-08	9.23e-08	5.01e-09
2.41e-08	1.41e-08	7.73e-09	8.14e-08	5.01e-09
3.85e-08	2.29e-08	1.16e-08	9.23e-08	5.01e-09
2.41e-08	1.41e-08	7.73e-09	8.14e-08	5.01e-09
5.29e-08	2.05e-08	1.04e-08	2.98e-08	1.38e-07
5.97e-08	2.14e-08	1.09e-08	1.92e-08	8.56e-09
3.31e-08	1.21e-08	8.36e-09	3.92e-08	1.99e-07
3.55e-08	1.22e-08	8.51e-09	2.28e-08	1.61e-08
3.85e-08	2.29e-08	1.16e-08	9.23e-08	5.01e-09
2.41e-08	1.41e-08	7.73e-09	8.14e-08	5.01e-09
3.85e-08	2.29e-08	1.16e-08	9.23e-08	5.01e-09
2.41e-08	1.41e-08	7.73e-09	8.14e-08	5.01e-09
5.08e-08	1.95e-08	1.02e-08	3.36e-08	1.86e-07
5.75e-08	2.07e-08	1.09e-08	2.12e-08	1.28e-08
3.22e-08	1.15e-08	8.20e-09	4.50e-08	2.62e-07
3.47e-08	1.18e-08	8.48e-09	2.65e-08	3.03e-08
3.85e-08	2.29e-08	1.16e-08	9.23e-08	5.01e-09
2.41e-08	1.41e-08	7.73e-09	8.14e-08	5.01e-09
3.85e-08	2.29e-08	1.16e-08	9.23e-08	5.01e-09

2.41e-08	1.41e-08	7.73e-09	8.14e-08	5.01e-09
5.18e-08	1.99e-08	1.03e-08	3.16e-08	1.60e-07
5.87e-08	2.11e-08	1.09e-08	2.01e-08	1.03e-08
3.26e-08	1.18e-08	8.27e-09	4.20e-08	2.29e-07
3.51e-08	1.20e-08	8.50e-09	2.45e-08	2.20e-08
1.88e-08	2.68e-08	5.06e-09	4.58e-07	1.94e-07
1.88e-08	7.39e-09	5.06e-09	1.54e-07	5.01e-09
1.88e-08	2.21e-08	5.06e-09	8.13e-07	5.01e-09
1.88e-08	2.68e-08	5.06e-09	4.58e-07	1.94e-07
1.88e-08	7.39e-09	5.06e-09	1.54e-07	5.01e-09
1.88e-08	2.21e-08	5.06e-09	8.13e-07	5.01e-09
3.00e-08	5.71e-08	9.68e-09	6.49e-08	1.59e-07
2.82e-08	4.97e-08	8.45e-09	2.30e-08	1.29e-07
1.77e-08	3.13e-09	4.73e-09	1.06e-07	7.40e-09
1.76e-08	2.50e-09	3.84e-09	4.75e-08	7.53e-09
1.03e-08	4.56e-09	2.84e-09	9.27e-07	6.66e-09
8.64e-09	2.95e-09	1.96e-09	4.30e-07	5.90e-09
1.88e-08	2.68e-08	5.06e-09	4.58e-07	1.94e-07
1.88e-08	7.39e-09	5.06e-09	1.54e-07	5.01e-09
1.88e-08	2.21e-08	5.06e-09	8.13e-07	5.01e-09
1.88e-08	2.68e-08	5.06e-09	4.58e-07	1.94e-07
1.88e-08	7.39e-09	5.06e-09	1.54e-07	5.01e-09
1.88e-08	2.21e-08	5.06e-09	8.13e-07	5.01e-09
3.03e-08	5.74e-08	9.76e-09	8.10e-08	1.69e-07
2.87e-08	5.04e-08	8.61e-09	2.77e-08	1.43e-07
1.78e-08	3.21e-09	4.91e-09	1.25e-07	7.34e-09
1.75e-08	2.56e-09	4.06e-09	6.32e-08	7.52e-09
1.08e-08	4.89e-09	3.03e-09	1.09e-06	6.91e-09
9.07e-09	3.14e-09	2.12e-09	5.91e-07	6.17e-09
1.88e-08	2.68e-08	5.06e-09	4.58e-07	1.94e-07
1.88e-08	7.39e-09	5.06e-09	1.54e-07	5.01e-09
1.88e-08	2.21e-08	5.06e-09	8.13e-07	5.01e-09
1.88e-08	2.68e-08	5.06e-09	4.58e-07	1.94e-07
1.88e-08	7.39e-09	5.06e-09	1.54e-07	5.01e-09
1.88e-08	2.21e-08	5.06e-09	8.13e-07	5.01e-09
3.01e-08	5.72e-08	9.71e-09	7.26e-08	1.64e-07
2.85e-08	5.00e-08	8.52e-09	2.51e-08	1.36e-07
1.77e-08	3.17e-09	4.82e-09	1.16e-07	7.37e-09
1.76e-08	2.53e-09	3.95e-09	5.49e-08	7.53e-09
1.05e-08	4.71e-09	2.93e-09	1.01e-06	6.79e-09
8.85e-09	3.04e-09	2.04e-09	5.08e-07	6.03e-09
1.88e-08	2.68e-08	5.06e-09	4.58e-07	1.94e-07
1.88e-08	7.39e-09	5.06e-09	1.54e-07	5.01e-09
1.88e-08	2.21e-08	5.06e-09	8.13e-07	5.01e-09
1.88e-08	2.68e-08	5.06e-09	4.58e-07	1.94e-07
1.88e-08	7.39e-09	5.06e-09	1.54e-07	5.01e-09
1.88e-08	2.21e-08	5.06e-09	8.13e-07	5.01e-09
3.00e-08	5.63e-08	9.68e-09	6.42e-08	1.58e-07
2.82e-08	4.89e-08	8.44e-09	2.28e-08	1.28e-07
1.77e-08	3.16e-09	4.76e-09	1.06e-07	7.44e-09

1.76e-08	2.53e-09	3.87e-09	4.77e-08	7.58e-09
1.03e-08	4.60e-09	2.86e-09	9.31e-07	6.68e-09
8.66e-09	2.98e-09	1.98e-09	4.32e-07	5.91e-09
1.88e-08	2.68e-08	5.06e-09	4.58e-07	1.94e-07
1.88e-08	7.39e-09	5.06e-09	1.54e-07	5.01e-09
1.88e-08	2.21e-08	5.06e-09	8.13e-07	5.01e-09
1.88e-08	2.68e-08	5.06e-09	4.58e-07	1.94e-07
1.88e-08	7.39e-09	5.06e-09	1.54e-07	5.01e-09
1.88e-08	2.21e-08	5.06e-09	8.13e-07	5.01e-09
3.02e-08	5.66e-08	9.76e-09	8.00e-08	1.68e-07
2.87e-08	4.97e-08	8.61e-09	2.75e-08	1.42e-07
1.78e-08	3.25e-09	4.94e-09	1.26e-07	7.38e-09
1.75e-08	2.59e-09	4.08e-09	6.35e-08	7.56e-09
1.08e-08	4.93e-09	3.05e-09	1.10e-06	6.93e-09
9.09e-09	3.17e-09	2.14e-09	5.94e-07	6.18e-09
1.88e-08	2.68e-08	5.06e-09	4.58e-07	1.94e-07
1.88e-08	7.39e-09	5.06e-09	1.54e-07	5.01e-09
1.88e-08	2.21e-08	5.06e-09	8.13e-07	5.01e-09
1.88e-08	2.68e-08	5.06e-09	4.58e-07	1.94e-07
1.88e-08	7.39e-09	5.06e-09	1.54e-07	5.01e-09
1.88e-08	2.21e-08	5.06e-09	8.13e-07	5.01e-09
3.01e-08	5.64e-08	9.71e-09	7.17e-08	1.63e-07
2.85e-08	4.92e-08	8.51e-09	2.49e-08	1.35e-07
1.77e-08	3.20e-09	4.85e-09	1.16e-07	7.41e-09
1.76e-08	2.56e-09	3.97e-09	5.51e-08	7.57e-09
1.06e-08	4.75e-09	2.95e-09	1.02e-06	6.81e-09
8.87e-09	3.06e-09	2.05e-09	5.10e-07	6.04e-09
1.88e-08	2.68e-08	5.06e-09	4.58e-07	1.94e-07
1.88e-08	2.68e-08	5.06e-09	4.58e-07	1.94e-07
2.34e-08	3.48e-08	9.51e-09	8.86e-08	2.12e-07
2.16e-08	2.96e-08	8.26e-09	4.13e-08	1.75e-07
1.88e-08	2.68e-08	5.06e-09	4.58e-07	1.94e-07
1.88e-08	2.68e-08	5.06e-09	4.58e-07	1.94e-07
2.38e-08	3.54e-08	9.60e-09	1.07e-07	2.24e-07
2.21e-08	3.03e-08	8.41e-09	4.49e-08	1.92e-07
1.88e-08	2.68e-08	5.06e-09	4.58e-07	1.94e-07
1.88e-08	2.68e-08	5.06e-09	4.58e-07	1.94e-07
2.36e-08	3.51e-08	9.55e-09	9.71e-08	2.18e-07
2.18e-08	2.99e-08	8.32e-09	4.29e-08	1.84e-07
1.88e-08	2.68e-08	5.06e-09	4.58e-07	1.94e-07
1.88e-08	2.68e-08	5.06e-09	4.58e-07	1.94e-07
2.34e-08	3.43e-08	9.51e-09	8.77e-08	2.11e-07
2.16e-08	2.92e-08	8.26e-09	4.12e-08	1.74e-07
1.88e-08	2.68e-08	5.06e-09	4.58e-07	1.94e-07
1.88e-08	2.68e-08	5.06e-09	4.58e-07	1.94e-07
2.38e-08	3.49e-08	9.60e-09	1.05e-07	2.23e-07
2.20e-08	2.98e-08	8.40e-09	4.47e-08	1.91e-07
1.88e-08	2.68e-08	5.06e-09	4.58e-07	1.94e-07
1.88e-08	2.68e-08	5.06e-09	4.58e-07	1.94e-07
2.36e-08	3.46e-08	9.55e-09	9.61e-08	2.17e-07

2.18e-08	2.94e-08	8.32e-09	4.28e-08	1.83e-07

Hfo_s	Hfo_w	Hao_	m_Hfo_wOH	m_Hfo_wOH2+
0	0	0	0	0
0	0	0	0	0
0.000360	0.0144	0.00195	0.000778	0.000459
0.000360	0.0144	0.00195	0.000910	0.000570
0.000361	0.0144	0.00195	0.000600	0.000397
0.000361	0.0144	0.00195	0.000545	0.000385
0.000361	0.0144	0.00195	0.000672	0.000437
0.000361	0.0144	0.00195	0.000632	0.000429
0	0	0	0	0
0	0	0	0	0
0.000500	0.0200	0.00211	0.00108	0.000637
0.000500	0.0200	0.00211	0.00126	0.000792
0.000501	0.0200	0.00211	0.000859	0.000558
0.000501	0.0200	0.00211	0.000778	0.000541
0.000501	0.0200	0.00211	0.000952	0.000614
0.000501	0.0200	0.00211	0.000894	0.000602
0	0	0	0	0
0	0	0	0	0
0.000425	0.0170	0.00201	0.000918	0.000541
0.000425	0.0170	0.00201	0.00107	0.000673
0.000426	0.0170	0.00201	0.000719	0.000471
0.000426	0.0170	0.00201	0.000652	0.000457
0.000426	0.0170	0.00201	0.000801	0.000519
0.000426	0.0170	0.00201	0.000752	0.000509
0	0	0	0	0
0	0	0	0	0
0.000360	0.0144	0.00195	0.000775	0.000457
0.000360	0.0144	0.00195	0.000906	0.000569
0.000361	0.0144	0.00195	0.000601	0.000398
0.000361	0.0144	0.00195	0.000546	0.000386
0.000361	0.0144	0.00195	0.000673	0.000439
0.000361	0.0144	0.00195	0.000632	0.000431
0	0	0	0	0
0	0	0	0	0
0.000500	0.0200	0.00211	0.00108	0.000635
0.000500	0.0200	0.00211	0.00126	0.000790
0.000501	0.0200	0.00211	0.000861	0.000561
0.000501	0.0200	0.00211	0.000780	0.000544
0.000501	0.0200	0.00211	0.000954	0.000618
0.000501	0.0200	0.00211	0.000894	0.000605
0	0	0	0	0
0	0	0	0	0
0.000425	0.0170	0.00201	0.000915	0.000540

0.000425	0.0170	0.00201	0.00107	0.000672
0.000426	0.0170	0.00201	0.000721	0.000474
0.000426	0.0170	0.00201	0.000653	0.000459
0.000426	0.0170	0.00201	0.000802	0.000522
0.000426	0.0170	0.00201	0.000753	0.000511
0	0	0	0	0
0	0	0	0	0
0	0	0	0	0
0.000360	0.0144	0.00195	0.000587	0.000270
0.000360	0.0144	0.00195	0.00101	0.000338
0.000360	0.0144	0.00195	0.00126	0.000948
0.000360	0.0144	0.00195	0.000514	0.000230
0.000360	0.0144	0.00195	0.000562	0.000243
0.000360	0.0144	0.00195	0.000802	0.000255
0.000360	0.0144	0.00195	0.000787	0.000257
0.000360	0.0144	0.00195	0.00119	0.000595
0.000360	0.0144	0.00195	0.00132	0.000596
0	0	0	0	0
0	0	0	0	0
0	0	0	0	0
0.000500	0.0200	0.00211	0.000816	0.000375
0.000500	0.0200	0.00211	0.00141	0.000470
0.000500	0.0200	0.00211	0.00175	0.00132
0.000500	0.0200	0.00211	0.000695	0.000313
0.000500	0.0200	0.00211	0.000748	0.000329
0.000500	0.0200	0.00211	0.00112	0.000353
0.000500	0.0200	0.00211	0.00110	0.000356
0.000500	0.0200	0.00211	0.00160	0.000824
0.000500	0.0200	0.00211	0.00177	0.000828
0	0	0	0	0
0	0	0	0	0
0	0	0	0	0
0.000425	0.0170	0.00201	0.000694	0.000319
0.000425	0.0170	0.00201	0.00120	0.000400
0.000425	0.0170	0.00201	0.00149	0.00112
0.000425	0.0170	0.00201	0.000599	0.000269
0.000425	0.0170	0.00201	0.000649	0.000283
0.000425	0.0170	0.00201	0.000950	0.000300
0.000425	0.0170	0.00201	0.000932	0.000303
0.000425	0.0170	0.00201	0.00138	0.000701
0.000425	0.0170	0.00201	0.00153	0.000704
0	0	0	0	0
0	0	0	0	0
0	0	0	0	0
0.000360	0.0144	0.00195	0.000588	0.000270
0.000360	0.0144	0.00195	0.00101	0.000338
0.000360	0.0144	0.00195	0.00126	0.000947
0.000360	0.0144	0.00195	0.000513	0.000229
0.000360	0.0144	0.00195	0.000561	0.000242
0.000360	0.0144	0.00195	0.000802	0.000255

0.000360	0.0144	0.00195	0.000787	0.000258
0.000360	0.0144	0.00195	0.00119	0.000595
0.000360	0.0144	0.00195	0.00132	0.000596
0	0	0	0	0
0	0	0	0	0
0	0	0	0	0
0.000500	0.0200	0.00211	0.000817	0.000376
0.000500	0.0200	0.00211	0.00141	0.000470
0.000500	0.0200	0.00211	0.00175	0.00132
0.000500	0.0200	0.00211	0.000694	0.000313
0.000500	0.0200	0.00211	0.000747	0.000328
0.000500	0.0200	0.00211	0.00112	0.000353
0.000500	0.0200	0.00211	0.00110	0.000357
0.000500	0.0200	0.00211	0.00160	0.000824
0.000500	0.0200	0.00211	0.00177	0.000828
0	0	0	0	0
0	0	0	0	0
0	0	0	0	0
0.000425	0.0170	0.00201	0.000694	0.000319
0.000425	0.0170	0.00201	0.00120	0.000399
0.000425	0.0170	0.00201	0.00149	0.00112
0.000425	0.0170	0.00201	0.000598	0.000268
0.000425	0.0170	0.00201	0.000648	0.000282
0.000425	0.0170	0.00201	0.000950	0.000301
0.000425	0.0170	0.00201	0.000933	0.000304
0.000425	0.0170	0.00201	0.00138	0.000702
0.000425	0.0170	0.00201	0.00153	0.000704
0	0	0	0	0
0.000360	0.0144	0.00195	0.000587	0.000270
0.000360	0.0144	0.00195	0.000512	0.000214
0.000360	0.0144	0.00195	0.000560	0.000222
0	0	0	0	0
0.000500	0.0200	0.00211	0.000816	0.000375
0.000500	0.0200	0.00211	0.000691	0.000294
0.000500	0.0200	0.00211	0.000747	0.000303
0	0	0	0	0
0.000425	0.0170	0.00201	0.000694	0.000319
0.000425	0.0170	0.00201	0.000595	0.000251
0.000425	0.0170	0.00201	0.000648	0.000259
0	0	0	0	0
0.000360	0.0144	0.00195	0.000588	0.000270
0.000360	0.0144	0.00195	0.000511	0.000214
0.000360	0.0144	0.00195	0.000560	0.000221
0	0	0	0	0
0.000500	0.0200	0.00211	0.000817	0.000376
0.000500	0.0200	0.00211	0.000690	0.000294
0.000500	0.0200	0.00211	0.000746	0.000303
0	0	0	0	0
0.000425	0.0170	0.00201	0.000694	0.000319
0.000425	0.0170	0.00201	0.000594	0.000251

0.000425	0.0170	0.00201	0.000647	0.000259

m_Hfo_wOHSO4-2	m_Hfo_wSO4-	m_Hfo_wOSi(OH)3	m_Hfo_wOSiO(OH)2-	m_Hfo_wHCO3
0	0	0	0	0
0	0	0	0	0
3.06e-06	9.05e-07	0.00224	0.00235	0.00135
5.98e-06	1.88e-06	0.00235	0.00231	0.00193
1.80e-06	5.97e-07	0.00237	0.00221	0.00174
1.72e-06	6.09e-07	0.00243	0.00213	0.00190
2.49e-06	8.12e-07	0.00240	0.00227	0.00226
2.33e-06	7.94e-07	0.00245	0.00222	0.00235
0	0	0	0	0
0	0	0	0	0
4.25e-06	1.26e-06	0.00312	0.00326	0.00187
8.31e-06	2.61e-06	0.00326	0.00321	0.00268
2.51e-06	8.17e-07	0.00327	0.00311	0.00234
2.37e-06	8.27e-07	0.00337	0.00299	0.00256
3.48e-06	1.13e-06	0.00332	0.00317	0.00310
3.24e-06	1.09e-06	0.00339	0.00310	0.00322
0	0	0	0	0
0	0	0	0	0
3.62e-06	1.07e-06	0.00265	0.00277	0.00159
7.06e-06	2.22e-06	0.00277	0.00273	0.00228
2.13e-06	6.99e-07	0.00279	0.00263	0.00202
2.02e-06	7.11e-07	0.00287	0.00252	0.00221
2.95e-06	9.58e-07	0.00283	0.00269	0.00265
2.75e-06	9.34e-07	0.00289	0.00263	0.00276
0	0	0	0	0
0	0	0	0	0
3.08e-06	9.12e-07	0.00223	0.00233	0.00135
6.01e-06	1.89e-06	0.00234	0.00229	0.00193
1.79e-06	5.95e-07	0.00236	0.00220	0.00174
1.71e-06	6.08e-07	0.00242	0.00211	0.00190
2.47e-06	8.07e-07	0.00239	0.00226	0.00226
2.31e-06	7.90e-07	0.00244	0.00221	0.00235
0	0	0	0	0
0	0	0	0	0
4.28e-06	1.27e-06	0.00310	0.00324	0.00187
8.35e-06	2.63e-06	0.00324	0.00319	0.00268
2.49e-06	8.14e-07	0.00326	0.00309	0.00234
2.36e-06	8.26e-07	0.00336	0.00297	0.00256
3.45e-06	1.12e-06	0.00331	0.00315	0.00309
3.21e-06	1.09e-06	0.00338	0.00308	0.00322
0	0	0	0	0
0	0	0	0	0
3.64e-06	1.08e-06	0.00264	0.00276	0.00159

7.10e-06	2.23e-06	0.00276	0.00271	0.00228
2.12e-06	6.97e-07	0.00278	0.00261	0.00202
2.01e-06	7.09e-07	0.00286	0.00251	0.00221
2.92e-06	9.52e-07	0.00282	0.00267	0.00265
2.73e-06	9.30e-07	0.00288	0.00261	0.00276
0	0	0	0	0
0	0	0	0	0
0	0	0	0	0
2.68e-06	6.18e-07	0.00355	0.00476	0.000463
6.98e-05	1.17e-05	0.00193	0.00357	0.000772
0.000202	7.61e-05	0.00201	0.00165	0.00337
1.72e-06	3.84e-07	0.00339	0.00468	0.000640
2.13e-06	4.62e-07	0.00324	0.00463	0.000727
5.96e-06	9.49e-07	0.00186	0.00362	0.00100
5.35e-06	8.77e-07	0.00189	0.00357	0.00106
1.06e-05	2.65e-06	0.00166	0.00204	0.00324
8.09e-06	1.83e-06	0.00158	0.00216	0.00293
0	0	0	0	0
0	0	0	0	0
0	0	0	0	0
3.73e-06	8.58e-07	0.00493	0.00662	0.000643
9.69e-05	1.62e-05	0.00268	0.00495	0.00107
0.000281	0.000106	0.00280	0.00230	0.00468
2.24e-06	5.05e-07	0.00477	0.00652	0.000853
2.69e-06	5.92e-07	0.00461	0.00647	0.000950
8.61e-06	1.36e-06	0.00257	0.00505	0.00136
7.39e-06	1.20e-06	0.00261	0.00499	0.00144
1.60e-05	4.14e-06	0.00233	0.00279	0.00462
1.10e-05	2.59e-06	0.00223	0.00293	0.00424
0	0	0	0	0
0	0	0	0	0
0	0	0	0	0
3.17e-06	7.29e-07	0.00419	0.00562	0.000547
8.24e-05	1.38e-05	0.00228	0.00421	0.000912
0.000239	8.98e-05	0.00238	0.00195	0.00398
1.96e-06	4.40e-07	0.00403	0.00554	0.000739
2.39e-06	5.23e-07	0.00387	0.00548	0.000831
7.17e-06	1.14e-06	0.00219	0.00428	0.00117
6.30e-06	1.03e-06	0.00223	0.00423	0.00124
1.30e-05	3.31e-06	0.00197	0.00239	0.00388
9.47e-06	2.18e-06	0.00188	0.00252	0.00353
0	0	0	0	0
0	0	0	0	0
0	0	0	0	0
2.65e-06	6.11e-07	0.00355	0.00476	0.000462
7.01e-05	1.17e-05	0.00193	0.00356	0.000773
0.000203	7.62e-05	0.00201	0.00165	0.00337
1.71e-06	3.84e-07	0.00339	0.00468	0.000640
2.13e-06	4.62e-07	0.00324	0.00463	0.000726
5.93e-06	9.46e-07	0.00186	0.00361	0.00100

5.33e-06	8.75e-07	0.00189	0.00356	0.00106
1.06e-05	2.65e-06	0.00166	0.00204	0.00324
8.09e-06	1.83e-06	0.00158	0.00216	0.00293
0	0	0	0	0
0	0	0	0	0
0	0	0	0	0
3.68e-06	8.49e-07	0.00494	0.00662	0.000642
9.73e-05	1.63e-05	0.00268	0.00495	0.00107
0.000281	0.000106	0.00279	0.00230	0.00468
2.23e-06	5.05e-07	0.00477	0.00653	0.000853
2.68e-06	5.91e-07	0.00461	0.00647	0.000950
8.57e-06	1.35e-06	0.00257	0.00504	0.00136
7.36e-06	1.20e-06	0.00261	0.00498	0.00144
1.60e-05	4.14e-06	0.00233	0.00279	0.00462
1.10e-05	2.59e-06	0.00223	0.00293	0.00424
0	0	0	0	0
0	0	0	0	0
0	0	0	0	0
3.13e-06	7.22e-07	0.00420	0.00563	0.000546
8.27e-05	1.38e-05	0.00228	0.00421	0.000912
0.000239	9.00e-05	0.00237	0.00195	0.00398
1.96e-06	4.41e-07	0.00403	0.00554	0.000739
2.39e-06	5.22e-07	0.00388	0.00548	0.000831
7.13e-06	1.13e-06	0.00219	0.00427	0.00117
6.27e-06	1.02e-06	0.00223	0.00422	0.00124
1.30e-05	3.31e-06	0.00197	0.00239	0.00388
9.46e-06	2.18e-06	0.00188	0.00252	0.00353
0	0	0	0	0
2.68e-06	6.18e-07	0.00355	0.00476	0.000463
8.13e-07	1.70e-07	0.00328	0.00484	0.000562
9.39e-07	1.86e-07	0.00311	0.00485	0.000587
0	0	0	0	0
3.73e-06	8.58e-07	0.00493	0.00662	0.000643
1.08e-06	2.31e-07	0.00462	0.00671	0.000770
1.21e-06	2.46e-07	0.00443	0.00674	0.000793
0	0	0	0	0
3.17e-06	7.29e-07	0.00419	0.00562	0.000547
9.39e-07	1.99e-07	0.00390	0.00571	0.000658
1.07e-06	2.14e-07	0.00372	0.00573	0.000683
0	0	0	0	0
2.65e-06	6.11e-07	0.00355	0.00476	0.000462
8.13e-07	1.70e-07	0.00328	0.00484	0.000562
9.38e-07	1.86e-07	0.00312	0.00485	0.000586
0	0	0	0	0
3.68e-06	8.49e-07	0.00494	0.00662	0.000642
1.08e-06	2.31e-07	0.00463	0.00671	0.000770
1.21e-06	2.46e-07	0.00443	0.00674	0.000793
0	0	0	0	0
3.13e-06	7.22e-07	0.00420	0.00563	0.000546
9.39e-07	1.99e-07	0.00391	0.00571	0.000658

1.07e-06	2.14e-07	0.00372	0.00573	0.000682

m_Hfo_wCO3-	m_Hfo_wPO4-2	m_Hfo_wHPO4-	m_Hfo_wH2PO4	m_Hfo_sCO3-
0	0	0	0	0
0	0	0	0	0
0.000388	0.000377	0.000533	1.28e-05	1.49e-08
0.000524	7.24e-05	0.000109	2.78e-06	3.29e-08
0.000447	0.000350	0.000555	1.50e-05	2.20e-08
0.000457	0.000335	0.000566	1.63e-05	2.34e-08
0.000590	7.17e-05	0.000112	2.97e-06	4.29e-08
0.000588	7.09e-05	0.000115	3.19e-06	4.35e-08
0	0	0	0	0
0	0	0	0	0
0.000539	0.000523	0.000740	1.78e-05	2.08e-08
0.000727	0.000101	0.000151	3.85e-06	4.57e-08
0.000611	0.000492	0.000767	2.03e-05	2.97e-08
0.000624	0.000470	0.000784	2.22e-05	3.14e-08
0.000815	9.98e-05	0.000154	4.06e-06	5.88e-08
0.000813	9.82e-05	0.000159	4.35e-06	5.97e-08
0	0	0	0	0
0	0	0	0	0
0.000458	0.000445	0.000629	1.51e-05	1.76e-08
0.000618	8.54e-05	0.000128	3.28e-06	3.89e-08
0.000523	0.000416	0.000654	1.75e-05	2.56e-08
0.000535	0.000397	0.000668	1.91e-05	2.72e-08
0.000695	8.47e-05	0.000132	3.48e-06	5.03e-08
0.000692	8.35e-05	0.000136	3.74e-06	5.11e-08
0	0	0	0	0
0	0	0	0	0
0.000388	0.000375	0.000531	1.28e-05	1.48e-08
0.000523	7.19e-05	0.000108	2.77e-06	3.26e-08
0.000446	0.000348	0.000554	1.49e-05	2.19e-08
0.000456	0.000333	0.000565	1.63e-05	2.32e-08
0.000588	7.12e-05	0.000112	2.97e-06	4.24e-08
0.000585	7.04e-05	0.000115	3.20e-06	4.31e-08
0	0	0	0	0
0	0	0	0	0
0.000539	0.000521	0.000738	1.77e-05	2.06e-08
0.000726	9.99e-05	0.000150	3.85e-06	4.52e-08
0.000610	0.000490	0.000764	2.03e-05	2.95e-08
0.000622	0.000467	0.000782	2.22e-05	3.12e-08
0.000811	9.90e-05	0.000154	4.06e-06	5.82e-08
0.000809	9.74e-05	0.000158	4.36e-06	5.91e-08
0	0	0	0	0
0	0	0	0	0
0.000458	0.000443	0.000627	1.51e-05	1.75e-08

0.000617	8.49e-05	0.000128	3.27e-06	3.84e-08
0.000522	0.000414	0.000652	1.74e-05	2.55e-08
0.000533	0.000395	0.000666	1.91e-05	2.70e-08
0.000692	8.41e-05	0.000131	3.48e-06	4.98e-08
0.000689	8.29e-05	0.000135	3.74e-06	5.05e-08
0	0	0	0	0
0	0	0	0	0
0	0	0	0	0
0.000171	3.46e-06	3.82e-06	7.14e-08	1.26e-08
0.000393	7.95e-05	6.37e-05	8.66e-07	3.55e-08
0.000763	0.000138	0.000249	7.62e-06	9.67e-08
0.000243	4.35e-06	4.66e-06	8.48e-08	1.80e-08
0.000286	5.28e-06	5.47e-06	9.62e-08	2.19e-08
0.000535	8.20e-05	6.25e-05	8.09e-07	5.19e-08
0.000551	8.17e-05	6.40e-05	8.52e-07	5.52e-08
0.00110	0.000178	0.000214	4.35e-06	1.42e-07
0.00110	0.000189	0.000205	3.76e-06	1.44e-07
0	0	0	0	0
0	0	0	0	0
0	0	0	0	0
0.000238	4.81e-06	5.30e-06	9.92e-08	1.75e-08
0.000546	0.000110	8.84e-05	1.20e-06	4.93e-08
0.00106	0.000192	0.000346	1.06e-05	1.34e-07
0.000321	5.69e-06	6.15e-06	1.13e-07	2.38e-08
0.000367	6.61e-06	6.97e-06	1.25e-07	2.80e-08
0.000736	0.000114	8.61e-05	1.10e-06	7.08e-08
0.000755	0.000113	8.80e-05	1.16e-06	7.50e-08
0.00152	0.000243	0.000301	6.31e-06	1.97e-07
0.00154	0.000257	0.000289	5.50e-06	2.01e-07
0	0	0	0	0
0	0	0	0	0
0	0	0	0	0
0.000202	4.09e-06	4.51e-06	8.43e-08	1.48e-08
0.000464	9.39e-05	7.52e-05	1.02e-06	4.19e-08
0.000901	0.000164	0.000294	9.00e-06	1.14e-07
0.000280	4.98e-06	5.35e-06	9.79e-08	2.07e-08
0.000324	5.90e-06	6.17e-06	1.09e-07	2.47e-08
0.000629	9.69e-05	7.35e-05	9.46e-07	6.07e-08
0.000646	9.64e-05	7.52e-05	9.95e-07	6.45e-08
0.00130	0.000208	0.000254	5.25e-06	1.68e-07
0.00131	0.000221	0.000243	4.56e-06	1.70e-07
0	0	0	0	0
0	0	0	0	0
0	0	0	0	0
0.000171	3.44e-06	3.80e-06	7.11e-08	1.26e-08
0.000393	7.95e-05	6.37e-05	8.66e-07	3.55e-08
0.000763	0.000139	0.000249	7.62e-06	9.66e-08
0.000243	4.33e-06	4.64e-06	8.44e-08	1.81e-08
0.000286	5.26e-06	5.45e-06	9.58e-08	2.19e-08
0.000534	8.20e-05	6.26e-05	8.11e-07	5.16e-08

0.000549	8.17e-05	6.41e-05	8.55e-07	5.50e-08
0.00110	0.000178	0.000214	4.36e-06	1.41e-07
0.00110	0.000189	0.000205	3.77e-06	1.43e-07
0	0	0	0	0
0	0	0	0	0
0	0	0	0	0
0.000237	4.78e-06	5.27e-06	9.88e-08	1.74e-08
0.000546	0.000110	8.85e-05	1.20e-06	4.92e-08
0.00106	0.000192	0.000346	1.06e-05	1.34e-07
0.000321	5.66e-06	6.12e-06	1.12e-07	2.38e-08
0.000367	6.58e-06	6.94e-06	1.24e-07	2.80e-08
0.000734	0.000114	8.62e-05	1.11e-06	7.04e-08
0.000753	0.000113	8.81e-05	1.16e-06	7.47e-08
0.00152	0.000243	0.000301	6.32e-06	1.96e-07
0.00154	0.000257	0.000289	5.51e-06	2.00e-07
0	0	0	0	0
0	0	0	0	0
0	0	0	0	0
0.000202	4.06e-06	4.48e-06	8.40e-08	1.48e-08
0.000464	9.39e-05	7.52e-05	1.02e-06	4.19e-08
0.000901	0.000164	0.000294	9.00e-06	1.14e-07
0.000280	4.95e-06	5.33e-06	9.75e-08	2.07e-08
0.000324	5.87e-06	6.14e-06	1.09e-07	2.48e-08
0.000627	9.69e-05	7.36e-05	9.49e-07	6.04e-08
0.000644	9.64e-05	7.53e-05	9.99e-07	6.42e-08
0.00130	0.000209	0.000254	5.26e-06	1.67e-07
0.00130	0.000221	0.000244	4.56e-06	1.70e-07
0	0	0	0	0
0.000171	3.46e-06	3.82e-06	7.14e-08	1.26e-08
0.000228	3.73e-06	3.74e-06	6.36e-08	1.62e-08
0.000252	3.92e-06	3.72e-06	6.00e-08	1.81e-08
0	0	0	0	0
0.000238	4.81e-06	5.30e-06	9.92e-08	1.75e-08
0.000308	5.10e-06	5.19e-06	8.99e-08	2.19e-08
0.000332	5.31e-06	5.16e-06	8.52e-08	2.40e-08
0	0	0	0	0
0.000202	4.09e-06	4.51e-06	8.43e-08	1.48e-08
0.000265	4.36e-06	4.41e-06	7.58e-08	1.89e-08
0.000289	4.57e-06	4.39e-06	7.16e-08	2.09e-08
0	0	0	0	0
0.000171	3.44e-06	3.80e-06	7.11e-08	1.26e-08
0.000228	3.70e-06	3.71e-06	6.33e-08	1.62e-08
0.000252	3.90e-06	3.70e-06	5.97e-08	1.82e-08
0	0	0	0	0
0.000237	4.78e-06	5.27e-06	9.88e-08	1.74e-08
0.000308	5.06e-06	5.17e-06	8.95e-08	2.20e-08
0.000332	5.28e-06	5.13e-06	8.48e-08	2.41e-08
0	0	0	0	0
0.000202	4.06e-06	4.48e-06	8.40e-08	1.48e-08
0.000265	4.34e-06	4.39e-06	7.54e-08	1.89e-08

0.000289	4.54e-06	4.37e-06	7.13e-08	2.09e-08

m_Hfo_sHCO3	m_Hfo_sHPO4-	m_Hfo_sH2BO3	m_Hfo_sH2PO4	m_Hfo_sOSi(OH)3
0	0	0	0	0
0	0	0	0	0
5.19e-08	2.05e-08	2.29e-11	4.92e-10	8.63e-08
1.21e-07	6.84e-09	3.21e-11	1.75e-10	1.48e-07
8.58e-08	2.74e-08	1.09e-11	7.38e-10	1.17e-07
9.71e-08	2.90e-08	8.52e-12	8.33e-10	1.24e-07
1.64e-07	8.14e-09	1.50e-11	2.16e-10	1.74e-07
1.74e-07	8.55e-09	1.22e-11	2.36e-10	1.81e-07
0	0	0	0	0
0	0	0	0	0
7.20e-08	2.85e-08	3.18e-11	6.84e-10	1.20e-07
1.69e-07	9.50e-09	4.46e-11	2.42e-10	2.05e-07
1.14e-07	3.73e-08	1.54e-11	9.87e-10	1.59e-07
1.29e-07	3.95e-08	1.22e-11	1.12e-09	1.70e-07
2.24e-07	1.11e-08	2.10e-11	2.93e-10	2.40e-07
2.37e-07	1.17e-08	1.73e-11	3.20e-10	2.49e-07
0	0	0	0	0
0	0	0	0	0
6.12e-08	2.42e-08	2.71e-11	5.81e-10	1.02e-07
1.43e-07	8.08e-09	3.79e-11	2.06e-10	1.74e-07
9.89e-08	3.20e-08	1.30e-11	8.55e-10	1.37e-07
1.12e-07	3.39e-08	1.02e-11	9.69e-10	1.46e-07
1.92e-07	9.54e-09	1.77e-11	2.52e-10	2.05e-07
2.03e-07	1.00e-08	1.45e-11	2.76e-10	2.13e-07
0	0	0	0	0
0	0	0	0	0
5.15e-08	2.03e-08	2.27e-11	4.88e-10	8.54e-08
1.20e-07	6.75e-09	3.16e-11	1.73e-10	1.46e-07
8.55e-08	2.72e-08	1.07e-11	7.35e-10	1.16e-07
9.68e-08	2.88e-08	8.37e-12	8.30e-10	1.24e-07
1.63e-07	8.06e-09	1.46e-11	2.15e-10	1.73e-07
1.73e-07	8.47e-09	1.19e-11	2.35e-10	1.80e-07
0	0	0	0	0
0	0	0	0	0
7.16e-08	2.82e-08	3.15e-11	6.78e-10	1.19e-07
1.67e-07	9.37e-09	4.39e-11	2.40e-10	2.02e-07
1.13e-07	3.70e-08	1.51e-11	9.82e-10	1.58e-07
1.28e-07	3.93e-08	1.20e-11	1.12e-09	1.69e-07
2.22e-07	1.10e-08	2.04e-11	2.91e-10	2.37e-07
2.35e-07	1.15e-08	1.68e-11	3.18e-10	2.47e-07
0	0	0	0	0
0	0	0	0	0
6.08e-08	2.40e-08	2.68e-11	5.76e-10	1.01e-07

1.42e-07	7.97e-09	3.74e-11	2.04e-10	1.72e-07
9.85e-08	3.18e-08	1.27e-11	8.51e-10	1.36e-07
1.12e-07	3.37e-08	1.00e-11	9.65e-10	1.45e-07
1.91e-07	9.45e-09	1.73e-11	2.51e-10	2.03e-07
2.02e-07	9.91e-09	1.42e-11	2.74e-10	2.11e-07
0	0	0	0	0
0	0	0	0	0
0	0	0	0	0
3.40e-08	2.80e-10	2.91e-11	5.25e-12	2.61e-07
6.98e-08	5.76e-09	2.96e-10	7.83e-11	1.75e-07
4.27e-07	3.16e-08	7.61e-10	9.66e-10	2.55e-07
4.74e-08	3.45e-10	2.14e-11	6.28e-12	2.51e-07
5.56e-08	4.18e-10	1.89e-11	7.35e-12	2.48e-07
9.71e-08	6.06e-09	7.63e-11	7.84e-11	1.81e-07
1.06e-07	6.42e-09	5.14e-11	8.55e-11	1.90e-07
4.18e-07	2.76e-08	1.90e-10	5.62e-10	2.14e-07
3.82e-07	2.67e-08	1.29e-10	4.90e-10	2.06e-07
0	0	0	0	0
0	0	0	0	0
0	0	0	0	0
4.72e-08	3.89e-10	4.04e-11	7.29e-12	3.62e-07
9.70e-08	7.99e-09	4.11e-10	1.09e-10	2.42e-07
5.94e-07	4.39e-08	1.06e-09	1.34e-09	3.54e-07
6.30e-08	4.55e-10	2.94e-11	8.35e-12	3.52e-07
7.24e-08	5.31e-10	2.59e-11	9.50e-12	3.51e-07
1.31e-07	8.28e-09	1.11e-10	1.06e-10	2.47e-07
1.43e-07	8.74e-09	7.44e-11	1.15e-10	2.60e-07
5.98e-07	3.89e-08	2.69e-10	8.17e-10	3.02e-07
5.54e-07	3.77e-08	1.78e-10	7.19e-10	2.91e-07
0	0	0	0	0
0	0	0	0	0
0	0	0	0	0
4.01e-08	3.31e-10	3.43e-11	6.19e-12	3.08e-07
8.24e-08	6.79e-09	3.49e-10	9.24e-11	2.06e-07
5.05e-07	3.73e-08	8.98e-10	1.14e-09	3.01e-07
5.47e-08	3.96e-10	2.51e-11	7.25e-12	2.98e-07
6.35e-08	4.71e-10	2.21e-11	8.35e-12	2.96e-07
1.13e-07	7.09e-09	9.18e-11	9.13e-11	2.12e-07
1.23e-07	7.50e-09	6.18e-11	9.94e-11	2.22e-07
5.01e-07	3.28e-08	2.26e-10	6.79e-10	2.54e-07
4.61e-07	3.18e-08	1.51e-10	5.95e-10	2.45e-07
0	0	0	0	0
0	0	0	0	0
0	0	0	0	0
3.40e-08	2.79e-10	2.91e-11	5.23e-12	2.61e-07
6.97e-08	5.75e-09	2.95e-10	7.81e-11	1.74e-07
4.27e-07	3.16e-08	7.59e-10	9.64e-10	2.54e-07
4.75e-08	3.45e-10	2.15e-11	6.27e-12	2.52e-07
5.57e-08	4.17e-10	1.90e-11	7.34e-12	2.49e-07
9.68e-08	6.05e-09	7.60e-11	7.85e-11	1.80e-07

1.06e-07	6.42e-09	5.13e-11	8.56e-11	1.89e-07
4.17e-07	2.75e-08	1.90e-10	5.61e-10	2.13e-07
3.81e-07	2.66e-08	1.29e-10	4.90e-10	2.06e-07
0	0	0	0	0
0	0	0	0	0
0	0	0	0	0
4.72e-08	3.88e-10	4.05e-11	7.27e-12	3.63e-07
9.68e-08	7.98e-09	4.09e-10	1.09e-10	2.42e-07
5.93e-07	4.38e-08	1.05e-09	1.34e-09	3.53e-07
6.32e-08	4.54e-10	2.96e-11	8.34e-12	3.54e-07
7.25e-08	5.30e-10	2.61e-11	9.48e-12	3.52e-07
1.31e-07	8.27e-09	1.10e-10	1.06e-10	2.47e-07
1.42e-07	8.73e-09	7.42e-11	1.15e-10	2.59e-07
5.97e-07	3.88e-08	2.69e-10	8.16e-10	3.01e-07
5.53e-07	3.77e-08	1.78e-10	7.18e-10	2.90e-07
0	0	0	0	0
0	0	0	0	0
0	0	0	0	0
4.01e-08	3.30e-10	3.44e-11	6.18e-12	3.09e-07
8.23e-08	6.78e-09	3.48e-10	9.22e-11	2.05e-07
5.04e-07	3.72e-08	8.96e-10	1.14e-09	3.00e-07
5.48e-08	3.95e-10	2.52e-11	7.23e-12	2.99e-07
6.36e-08	4.70e-10	2.22e-11	8.34e-12	2.97e-07
1.13e-07	7.08e-09	9.14e-11	9.14e-11	2.11e-07
1.23e-07	7.50e-09	6.16e-11	9.95e-11	2.22e-07
5.00e-07	3.28e-08	2.25e-10	6.79e-10	2.54e-07
4.60e-07	3.17e-08	1.51e-10	5.94e-10	2.45e-07
0	0	0	0	0
3.40e-08	2.80e-10	2.91e-11	5.25e-12	2.61e-07
3.98e-08	2.65e-10	1.86e-11	4.51e-12	2.33e-07
4.23e-08	2.68e-10	1.70e-11	4.32e-12	2.24e-07
0	0	0	0	0
4.72e-08	3.89e-10	4.04e-11	7.29e-12	3.62e-07
5.49e-08	3.70e-10	2.57e-11	6.41e-12	3.30e-07
5.74e-08	3.73e-10	2.33e-11	6.16e-12	3.20e-07
0	0	0	0	0
4.01e-08	3.31e-10	3.43e-11	6.19e-12	3.08e-07
4.68e-08	3.14e-10	2.19e-11	5.39e-12	2.78e-07
4.93e-08	3.17e-10	1.99e-11	5.17e-12	2.69e-07
0	0	0	0	0
3.40e-08	2.79e-10	2.91e-11	5.23e-12	2.61e-07
3.99e-08	2.64e-10	1.88e-11	4.50e-12	2.33e-07
4.23e-08	2.67e-10	1.71e-11	4.31e-12	2.25e-07
0	0	0	0	0
4.72e-08	3.88e-10	4.05e-11	7.27e-12	3.63e-07
5.50e-08	3.69e-10	2.58e-11	6.39e-12	3.31e-07
5.75e-08	3.72e-10	2.34e-11	6.14e-12	3.21e-07
0	0	0	0	0
4.01e-08	3.30e-10	3.44e-11	6.18e-12	3.09e-07
4.69e-08	3.13e-10	2.20e-11	5.38e-12	2.79e-07

4.94e-08	3.16e-10	2.00e-11	5.16e-12	2.69e-07

m_Hfo_sOSiO(OH)2-	m_Hfo_sOHSO4-2	m_Hfo_sSO4-	m_Hao_SO4-	m_Hao_OHSO4-2
0	0	0	0	0
0	0	0	0	0
9.03e-08	1.18e-10	3.48e-11	5.25e-15	0.000422
1.45e-07	3.76e-10	1.18e-10	8.17e-15	0.000444
1.09e-07	8.89e-11	2.95e-11	7.07e-15	0.000434
1.09e-07	8.81e-11	3.12e-11	8.22e-15	0.000453
1.65e-07	1.81e-10	5.90e-11	8.22e-15	0.000451
1.65e-07	1.73e-10	5.88e-11	8.98e-15	0.000467
0	0	0	0	0
0	0	0	0	0
1.25e-07	1.64e-10	4.84e-11	5.70e-15	0.000458
2.02e-07	5.23e-10	1.64e-10	8.87e-15	0.000482
1.51e-07	1.22e-10	3.97e-11	7.45e-15	0.000468
1.51e-07	1.20e-10	4.17e-11	8.61e-15	0.000487
2.29e-07	2.51e-10	8.13e-11	8.83e-15	0.000487
2.28e-07	2.38e-10	8.04e-11	9.59e-15	0.000502
0	0	0	0	0
0	0	0	0	0
1.07e-07	1.39e-10	4.11e-11	5.43e-15	0.000437
1.72e-07	4.44e-10	1.40e-10	8.45e-15	0.000459
1.29e-07	1.04e-10	3.43e-11	7.21e-15	0.000447
1.28e-07	1.03e-10	3.61e-11	8.36e-15	0.000466
1.95e-07	2.13e-10	6.93e-11	8.46e-15	0.000465
1.94e-07	2.03e-10	6.89e-11	9.22e-15	0.000481
0	0	0	0	0
0	0	0	0	0
8.92e-08	1.18e-10	3.48e-11	5.26e-15	0.000424
1.43e-07	3.75e-10	1.18e-10	8.19e-15	0.000446
1.08e-07	8.81e-11	2.93e-11	7.10e-15	0.000436
1.08e-07	8.74e-11	3.10e-11	8.25e-15	0.000455
1.63e-07	1.78e-10	5.83e-11	8.26e-15	0.000454
1.62e-07	1.70e-10	5.82e-11	9.02e-15	0.000469
0	0	0	0	0
0	0	0	0	0
1.24e-07	1.63e-10	4.84e-11	5.71e-15	0.000460
1.99e-07	5.21e-10	1.64e-10	8.88e-15	0.000484
1.50e-07	1.21e-10	3.95e-11	7.47e-15	0.000470
1.49e-07	1.18e-10	4.14e-11	8.65e-15	0.000489
2.26e-07	2.48e-10	8.04e-11	8.87e-15	0.000490
2.25e-07	2.35e-10	7.97e-11	9.64e-15	0.000505
0	0	0	0	0
0	0	0	0	0
1.05e-07	1.39e-10	4.11e-11	5.44e-15	0.000439

1.69e-07	4.42e-10	1.39e-10	8.46e-15	0.000461
1.28e-07	1.03e-10	3.40e-11	7.23e-15	0.000450
1.27e-07	1.02e-10	3.59e-11	8.40e-15	0.000468
1.92e-07	2.10e-10	6.86e-11	8.50e-15	0.000468
1.92e-07	2.00e-10	6.82e-11	9.26e-15	0.000483
0	0	0	0	0
0	0	0	0	0
0	0	0	0	0
3.50e-07	1.97e-10	4.54e-11	4.80e-15	0.000294
3.22e-07	6.31e-09	1.06e-09	5.90e-15	0.000189
2.10e-07	2.56e-08	9.64e-09	1.45e-14	0.000122
3.47e-07	1.27e-10	2.84e-11	4.37e-15	0.000333
3.54e-07	1.63e-10	3.53e-11	5.02e-15	0.000360
3.51e-07	5.78e-10	9.20e-11	3.42e-15	0.000232
3.58e-07	5.37e-10	8.79e-11	4.20e-15	0.000271
2.64e-07	1.37e-09	3.42e-10	4.89e-15	0.000175
2.81e-07	1.05e-09	2.39e-10	4.94e-15	0.000217
0	0	0	0	0
0	0	0	0	0
0	0	0	0	0
4.86e-07	2.74e-10	6.30e-11	5.21e-15	0.000318
4.48e-07	8.76e-09	1.47e-09	6.40e-15	0.000205
2.91e-07	3.56e-08	1.34e-08	1.58e-14	0.000133
4.82e-07	1.65e-10	3.73e-11	4.65e-15	0.000359
4.93e-07	2.05e-10	4.51e-11	5.31e-15	0.000387
4.85e-07	8.28e-10	1.30e-10	3.65e-15	0.000250
4.95e-07	7.35e-10	1.19e-10	4.38e-15	0.000291
3.61e-07	2.07e-09	5.36e-10	5.66e-15	0.000188
3.83e-07	1.44e-09	3.38e-10	5.49e-15	0.000230
0	0	0	0	0
0	0	0	0	0
0	0	0	0	0
4.13e-07	2.33e-10	5.36e-11	4.96e-15	0.000304
3.81e-07	7.45e-09	1.25e-09	6.10e-15	0.000195
2.47e-07	3.03e-08	1.14e-08	1.50e-14	0.000126
4.10e-07	1.45e-10	3.26e-11	4.48e-15	0.000344
4.19e-07	1.83e-10	3.99e-11	5.13e-15	0.000371
4.13e-07	6.92e-10	1.10e-10	3.51e-15	0.000239
4.22e-07	6.29e-10	1.02e-10	4.27e-15	0.000279
3.09e-07	1.68e-09	4.28e-10	5.23e-15	0.000180
3.29e-07	1.24e-09	2.85e-10	5.18e-15	0.000222
0	0	0	0	0
0	0	0	0	0
0	0	0	0	0
3.51e-07	1.95e-10	4.50e-11	4.78e-15	0.000293
3.21e-07	6.32e-09	1.06e-09	5.91e-15	0.000188
2.09e-07	2.56e-08	9.64e-09	1.45e-14	0.000122
3.48e-07	1.27e-10	2.85e-11	4.37e-15	0.000332
3.55e-07	1.63e-10	3.54e-11	5.01e-15	0.000359
3.49e-07	5.74e-10	9.15e-11	3.42e-15	0.000232

3.56e-07	5.33e-10	8.76e-11	4.20e-15	0.000272
2.63e-07	1.36e-09	3.41e-10	4.89e-15	0.000175
2.81e-07	1.05e-09	2.38e-10	4.94e-15	0.000217
0	0	0	0	0
0	0	0	0	0
0	0	0	0	0
4.87e-07	2.71e-10	6.25e-11	5.19e-15	0.000318
4.46e-07	8.78e-09	1.47e-09	6.41e-15	0.000204
2.90e-07	3.56e-08	1.34e-08	1.57e-14	0.000132
4.84e-07	1.66e-10	3.74e-11	4.65e-15	0.000358
4.94e-07	2.05e-10	4.51e-11	5.30e-15	0.000387
4.83e-07	8.22e-10	1.30e-10	3.65e-15	0.000250
4.93e-07	7.30e-10	1.18e-10	4.38e-15	0.000291
3.60e-07	2.07e-09	5.34e-10	5.66e-15	0.000188
3.82e-07	1.44e-09	3.38e-10	5.49e-15	0.000230
0	0	0	0	0
0	0	0	0	0
0	0	0	0	0
4.14e-07	2.30e-10	5.31e-11	4.94e-15	0.000303
3.79e-07	7.46e-09	1.25e-09	6.11e-15	0.000195
2.47e-07	3.03e-08	1.14e-08	1.50e-14	0.000126
4.11e-07	1.45e-10	3.27e-11	4.48e-15	0.000343
4.20e-07	1.83e-10	4.00e-11	5.12e-15	0.000370
4.11e-07	6.87e-10	1.09e-10	3.51e-15	0.000240
4.20e-07	6.25e-10	1.02e-10	4.27e-15	0.000280
3.08e-07	1.68e-09	4.27e-10	5.23e-15	0.000180
3.28e-07	1.23e-09	2.84e-10	5.18e-15	0.000222
0	0	0	0	0
3.50e-07	1.97e-10	4.54e-11	4.80e-15	0.000294
3.43e-07	5.77e-11	1.21e-11	2.92e-15	0.000319
3.50e-07	6.76e-11	1.34e-11	3.10e-15	0.000342
0	0	0	0	0
4.86e-07	2.74e-10	6.30e-11	5.21e-15	0.000318
4.78e-07	7.73e-11	1.65e-11	3.18e-15	0.000344
4.87e-07	8.76e-11	1.78e-11	3.36e-15	0.000367
0	0	0	0	0
4.13e-07	2.33e-10	5.36e-11	4.96e-15	0.000304
4.06e-07	6.68e-11	1.41e-11	3.03e-15	0.000329
4.14e-07	7.70e-11	1.55e-11	3.21e-15	0.000352
0	0	0	0	0
3.51e-07	1.95e-10	4.50e-11	4.78e-15	0.000293
3.44e-07	5.78e-11	1.21e-11	2.92e-15	0.000318
3.50e-07	6.77e-11	1.34e-11	3.10e-15	0.000341
0	0	0	0	0
4.87e-07	2.71e-10	6.25e-11	5.19e-15	0.000318
4.80e-07	7.75e-11	1.65e-11	3.18e-15	0.000343
4.88e-07	8.77e-11	1.78e-11	3.35e-15	0.000366
0	0	0	0	0
4.14e-07	2.30e-10	5.31e-11	4.94e-15	0.000303
4.07e-07	6.69e-11	1.42e-11	3.02e-15	0.000328

4.15e-07	7.71e-11	1.55e-11	3.20e-15	0.000351

m_Hao_H2BO3	m_Hao_H3BO4-	m_Hfo_sH2AsO3	m_Hfo_sH2AsO4	m_Hfo_sHAsO4-
0	0	0	0	0
0	0	0	0	0
0.000696	2.62e-10	1.57e-12	3.67e-12	1.93e-10
0.000622	1.58e-10	9.13e-13	9.05e-12	4.46e-10
0.000617	1.77e-10	2.98e-09	6.01e-12	2.81e-10
0.000553	1.42e-10	2.95e-09	7.58e-12	3.32e-10
0.000558	1.43e-10	4.48e-09	1.08e-11	5.14e-10
0.000504	1.23e-10	4.50e-09	1.25e-11	5.70e-10
0	0	0	0	0
0	0	0	0	0
0.000755	2.84e-10	2.17e-12	5.10e-12	2.67e-10
0.000675	1.72e-10	1.27e-12	1.26e-11	6.20e-10
0.000676	1.99e-10	3.74e-09	7.88e-12	3.75e-10
0.000610	1.62e-10	3.82e-09	1.00e-11	4.45e-10
0.000611	1.58e-10	5.58e-09	1.47e-11	7.03e-10
0.000557	1.37e-10	5.74e-09	1.70e-11	7.78e-10
0	0	0	0	0
0	0	0	0	0
0.000720	2.71e-10	1.85e-12	4.34e-12	2.27e-10
0.000644	1.64e-10	1.08e-12	1.07e-11	5.27e-10
0.000641	1.86e-10	3.34e-09	6.90e-12	3.25e-10
0.000576	1.50e-10	3.37e-09	8.75e-12	3.86e-10
0.000579	1.49e-10	5.00e-09	1.26e-11	6.02e-10
0.000526	1.28e-10	5.09e-09	1.46e-11	6.67e-10
0	0	0	0	0
0	0	0	0	0
0.000687	2.59e-10	1.59e-12	3.74e-12	1.96e-10
0.000612	1.56e-10	9.29e-13	9.20e-12	4.53e-10
0.000609	1.75e-10	3.07e-09	6.14e-12	2.86e-10
0.000546	1.41e-10	3.04e-09	7.76e-12	3.39e-10
0.000549	1.41e-10	4.62e-09	1.11e-11	5.24e-10
0.000497	1.21e-10	4.65e-09	1.28e-11	5.81e-10
0	0	0	0	0
0	0	0	0	0
0.000746	2.81e-10	2.21e-12	5.19e-12	2.72e-10
0.000664	1.69e-10	1.29e-12	1.28e-11	6.29e-10
0.000668	1.97e-10	3.84e-09	8.04e-12	3.82e-10
0.000603	1.60e-10	3.93e-09	1.02e-11	4.54e-10
0.000602	1.55e-10	5.75e-09	1.50e-11	7.17e-10
0.000549	1.35e-10	5.91e-09	1.74e-11	7.94e-10
0	0	0	0	0
0	0	0	0	0
0.000711	2.68e-10	1.88e-12	4.41e-12	2.31e-10

0.000633	1.61e-10	1.10e-12	1.09e-11	5.35e-10
0.000633	1.84e-10	3.44e-09	7.05e-12	3.32e-10
0.000569	1.49e-10	3.47e-09	8.96e-12	3.94e-10
0.000571	1.47e-10	5.15e-09	1.29e-11	6.14e-10
0.000518	1.26e-10	5.25e-09	1.50e-11	6.81e-10
0	0	0	0	0
0	0	0	0	0
0	0	0	0	0
0.00105	2.99e-10	8.04e-22	2.48e-13	1.67e-11
0.00148	2.21e-10	5.57e-14	1.27e-12	1.18e-10
0.00173	6.82e-11	2.84e-21	1.04e-11	4.27e-10
0.000922	3.29e-10	6.09e-18	2.30e-13	1.59e-11
0.000828	2.78e-10	3.91e-18	2.15e-13	1.54e-11
0.00126	3.98e-10	7.44e-13	1.18e-12	1.15e-10
0.00111	3.36e-10	3.86e-13	1.32e-12	1.25e-10
0.00145	2.42e-10	8.08e-19	3.15e-12	1.94e-10
0.00128	2.64e-10	7.37e-19	2.34e-12	1.60e-10
0	0	0	0	0
0	0	0	0	0
0	0	0	0	0
0.00113	3.24e-10	1.12e-21	3.45e-13	2.32e-11
0.00160	2.40e-10	7.74e-14	1.77e-12	1.64e-10
0.00188	7.40e-11	3.94e-21	1.44e-11	5.93e-10
0.00101	3.64e-10	9.14e-18	3.28e-13	2.25e-11
0.000910	3.11e-10	6.12e-18	3.13e-13	2.20e-11
0.00137	4.39e-10	1.10e-12	1.57e-12	1.55e-10
0.00122	3.78e-10	5.87e-13	1.77e-12	1.69e-10
0.00158	2.46e-10	1.10e-18	4.80e-12	2.88e-10
0.00141	2.76e-10	9.87e-19	3.63e-12	2.40e-10
0	0	0	0	0
0	0	0	0	0
0	0	0	0	0
0.00108	3.09e-10	9.50e-22	2.93e-13	1.97e-11
0.00153	2.29e-10	6.58e-14	1.50e-12	1.39e-10
0.00179	7.05e-11	3.35e-21	1.22e-11	5.04e-10
0.000956	3.43e-10	7.47e-18	2.75e-13	1.90e-11
0.000861	2.91e-10	4.90e-18	2.60e-13	1.84e-11
0.00130	4.15e-10	9.04e-13	1.36e-12	1.33e-10
0.00115	3.53e-10	4.75e-13	1.53e-12	1.46e-10
0.00150	2.42e-10	9.45e-19	3.90e-12	2.37e-10
0.00133	2.67e-10	8.54e-19	2.92e-12	1.96e-10
0	0	0	0	0
0	0	0	0	0
0	0	0	0	0
0.00105	3.01e-10	7.94e-22	2.45e-13	1.65e-11
0.00148	2.20e-10	5.61e-14	1.28e-12	1.19e-10
0.00173	6.80e-11	2.85e-21	1.04e-11	4.28e-10
0.000925	3.29e-10	5.98e-18	2.27e-13	1.57e-11
0.000831	2.79e-10	3.83e-18	2.11e-13	1.51e-11
0.00125	3.98e-10	7.69e-13	1.19e-12	1.16e-10

0.00111	3.36e-10	3.99e-13	1.34e-12	1.27e-10
0.00145	2.42e-10	8.17e-19	3.16e-12	1.95e-10
0.00128	2.64e-10	7.43e-19	2.35e-12	1.61e-10
0	0	0	0	0
0	0	0	0	0
0	0	0	0	0
0.00114	3.26e-10	1.10e-21	3.40e-13	2.29e-11
0.00160	2.39e-10	7.79e-14	1.78e-12	1.65e-10
0.00188	7.38e-11	3.95e-21	1.44e-11	5.95e-10
0.00101	3.64e-10	8.98e-18	3.23e-13	2.21e-11
0.000913	3.11e-10	6.00e-18	3.08e-13	2.17e-11
0.00137	4.39e-10	1.14e-12	1.59e-12	1.56e-10
0.00122	3.79e-10	6.07e-13	1.79e-12	1.70e-10
0.00158	2.46e-10	1.11e-18	4.82e-12	2.89e-10
0.00141	2.76e-10	9.95e-19	3.65e-12	2.41e-10
0	0	0	0	0
0	0	0	0	0
0	0	0	0	0
0.00108	3.11e-10	9.37e-22	2.89e-13	1.94e-11
0.00153	2.28e-10	6.62e-14	1.51e-12	1.40e-10
0.00179	7.03e-11	3.36e-21	1.23e-11	5.05e-10
0.000959	3.44e-10	7.34e-18	2.71e-13	1.87e-11
0.000863	2.92e-10	4.80e-18	2.56e-13	1.82e-11
0.00130	4.15e-10	9.34e-13	1.38e-12	1.35e-10
0.00115	3.53e-10	4.91e-13	1.55e-12	1.47e-10
0.00150	2.42e-10	9.55e-19	3.91e-12	2.38e-10
0.00133	2.68e-10	8.62e-19	2.93e-12	1.97e-10
0	0	0	0	0
0.00105	2.99e-10	8.04e-22	2.48e-13	1.67e-11
0.000943	4.81e-10	5.85e-18	1.81e-13	1.34e-11
0.000862	4.44e-10	4.03e-18	1.56e-13	1.22e-11
0	0	0	0	0
0.00113	3.24e-10	1.12e-21	3.45e-13	2.32e-11
0.00103	5.21e-10	8.54e-18	2.65e-13	1.93e-11
0.000947	4.85e-10	6.11e-18	2.33e-13	1.78e-11
0	0	0	0	0
0.00108	3.09e-10	9.50e-22	2.93e-13	1.97e-11
0.000977	4.97e-10	7.07e-18	2.20e-13	1.61e-11
0.000896	4.60e-10	4.97e-18	1.91e-13	1.48e-11
0	0	0	0	0
0.00105	3.01e-10	7.94e-22	2.45e-13	1.65e-11
0.000946	4.82e-10	5.74e-18	1.78e-13	1.32e-11
0.000865	4.45e-10	3.96e-18	1.53e-13	1.20e-11
0	0	0	0	0
0.00114	3.26e-10	1.10e-21	3.40e-13	2.29e-11
0.00103	5.22e-10	8.39e-18	2.61e-13	1.90e-11
0.000950	4.86e-10	6.00e-18	2.30e-13	1.75e-11
0	0	0	0	0
0.00108	3.11e-10	9.37e-22	2.89e-13	1.94e-11
0.000981	4.98e-10	6.95e-18	2.16e-13	1.59e-11

0.000899	4.61e-10	4.87e-18	1.88e-13	1.45e-11

m_Hfo_sOHAsO4-3	m_Hfo_wOHAsO4-3	m_Hfo_wHAsO4-	m_Hfo_wH2AsO4	m_Hfo_wH2AsO3
0	0	0	0	0
0	0	0	0	0
2.47e-08	0.000643	5.01e-06	9.55e-08	4.07e-08
5.08e-08	0.000808	7.10e-06	1.44e-07	1.45e-08
2.87e-08	0.000582	5.69e-06	1.22e-07	6.04e-05
2.98e-08	0.000583	6.49e-06	1.48e-07	5.76e-05
5.42e-08	0.000745	7.07e-06	1.49e-07	6.16e-05
5.52e-08	0.000745	7.69e-06	1.69e-07	6.07e-05
0	0	0	0	0
0	0	0	0	0
3.44e-08	0.000894	6.95e-06	1.33e-07	5.65e-08
7.06e-08	0.00112	9.86e-06	2.00e-07	2.02e-08
3.97e-08	0.000815	7.70e-06	1.62e-07	7.69e-05
4.10e-08	0.000814	8.83e-06	1.99e-07	7.59e-05
7.54e-08	0.00104	9.74e-06	2.03e-07	7.74e-05
7.66e-08	0.00104	1.06e-05	2.31e-07	7.81e-05
0	0	0	0	0
0	0	0	0	0
2.92e-08	0.000759	5.91e-06	1.13e-07	4.80e-08
6.00e-08	0.000954	8.38e-06	1.70e-07	1.71e-08
3.38e-08	0.000690	6.64e-06	1.41e-07	6.82e-05
3.51e-08	0.000690	7.59e-06	1.72e-07	6.63e-05
6.40e-08	0.000884	8.32e-06	1.75e-07	6.90e-05
6.51e-08	0.000883	9.05e-06	1.98e-07	6.89e-05
0	0	0	0	0
0	0	0	0	0
2.51e-08	0.000656	5.12e-06	9.78e-08	4.17e-08
5.13e-08	0.000823	7.27e-06	1.48e-07	1.49e-08
2.91e-08	0.000592	5.82e-06	1.25e-07	6.24e-05
3.03e-08	0.000593	6.65e-06	1.52e-07	5.97e-05
5.48e-08	0.000759	7.25e-06	1.53e-07	6.39e-05
5.58e-08	0.000758	7.90e-06	1.74e-07	6.31e-05
0	0	0	0	0
0	0	0	0	0
3.48e-08	0.000911	7.11e-06	1.36e-07	5.79e-08
7.13e-08	0.00114	1.01e-05	2.05e-07	2.07e-08
4.03e-08	0.000831	7.88e-06	1.66e-07	7.93e-05
4.16e-08	0.000830	9.04e-06	2.04e-07	7.84e-05
7.63e-08	0.00106	9.99e-06	2.09e-07	8.01e-05
7.75e-08	0.00106	1.09e-05	2.38e-07	8.10e-05
0	0	0	0	0
0	0	0	0	0
2.96e-08	0.000775	6.04e-06	1.15e-07	4.92e-08

6.06e-08	0.000972	8.58e-06	1.74e-07	1.76e-08
3.43e-08	0.000703	6.79e-06	1.44e-07	7.04e-05
3.56e-08	0.000703	7.78e-06	1.77e-07	6.85e-05
6.48e-08	0.000900	8.53e-06	1.80e-07	7.16e-05
6.59e-08	0.000899	9.29e-06	2.04e-07	7.16e-05
0	0	0	0	0
0	0	0	0	0
0	0	0	0	0
3.53e-09	4.81e-05	2.27e-07	3.38e-09	1.10e-17
4.73e-08	0.000523	1.30e-06	1.41e-08	6.16e-10
3.39e-08	0.000267	3.37e-06	8.18e-08	2.24e-17
3.57e-09	4.81e-05	2.15e-07	3.10e-09	8.22e-14
3.68e-09	4.82e-05	2.01e-07	2.81e-09	5.11e-14
5.07e-08	0.000523	1.18e-06	1.21e-08	7.68e-09
5.24e-08	0.000523	1.25e-06	1.32e-08	3.85e-09
3.47e-08	0.000269	1.51e-06	2.44e-08	6.26e-15
3.51e-08	0.000269	1.23e-06	1.80e-08	5.65e-15
0	0	0	0	0
0	0	0	0	0
0	0	0	0	0
4.91e-09	6.68e-05	3.16e-07	4.69e-09	1.52e-17
6.56e-08	0.000726	1.81e-06	1.96e-08	8.56e-10
4.70e-08	0.000371	4.68e-06	1.14e-07	3.11e-17
4.94e-09	6.69e-05	3.04e-07	4.43e-09	1.24e-13
5.10e-09	6.69e-05	2.89e-07	4.10e-09	8.03e-14
6.98e-08	0.000726	1.61e-06	1.64e-08	1.15e-08
7.21e-08	0.000726	1.70e-06	1.78e-08	5.91e-09
4.83e-08	0.000374	2.22e-06	3.71e-08	8.52e-15
4.89e-08	0.000374	1.84e-06	2.78e-08	7.55e-15
0	0	0	0	0
0	0	0	0	0
0	0	0	0	0
4.17e-09	5.68e-05	2.68e-07	3.99e-09	1.29e-17
5.58e-08	0.000617	1.54e-06	1.66e-08	7.28e-10
4.00e-08	0.000315	3.98e-06	9.66e-08	2.64e-17
4.21e-09	5.68e-05	2.56e-07	3.72e-09	1.01e-13
4.34e-09	5.69e-05	2.42e-07	3.41e-09	6.41e-14
5.96e-08	0.000617	1.38e-06	1.41e-08	9.36e-09
6.16e-08	0.000617	1.46e-06	1.54e-08	4.75e-09
4.11e-08	0.000318	1.83e-06	3.02e-08	7.31e-15
4.15e-08	0.000318	1.50e-06	2.24e-08	6.55e-15
0	0	0	0	0
0	0	0	0	0
0	0	0	0	0
3.47e-09	4.72e-05	2.24e-07	3.33e-09	1.08e-17
4.76e-08	0.000527	1.32e-06	1.42e-08	6.22e-10
3.40e-08	0.000268	3.38e-06	8.22e-08	2.25e-17
3.51e-09	4.72e-05	2.11e-07	3.05e-09	8.05e-14
3.62e-09	4.73e-05	1.97e-07	2.76e-09	5.00e-14
5.10e-08	0.000527	1.20e-06	1.23e-08	7.95e-09

5.28e-08	0.000527	1.27e-06	1.34e-08	3.99e-09
3.48e-08	0.000270	1.52e-06	2.45e-08	6.34e-15
3.52e-08	0.000271	1.24e-06	1.81e-08	5.71e-15
0	0	0	0	0
0	0	0	0	0
0	0	0	0	0
4.83e-09	6.56e-05	3.11e-07	4.62e-09	1.50e-17
6.61e-08	0.000732	1.83e-06	1.97e-08	8.64e-10
4.72e-08	0.000373	4.70e-06	1.14e-07	3.12e-17
4.86e-09	6.56e-05	2.99e-07	4.36e-09	1.21e-13
5.01e-09	6.56e-05	2.84e-07	4.03e-09	7.85e-14
7.02e-08	0.000733	1.63e-06	1.66e-08	1.19e-08
7.26e-08	0.000732	1.72e-06	1.80e-08	6.13e-09
4.85e-08	0.000375	2.24e-06	3.73e-08	8.63e-15
4.90e-08	0.000376	1.85e-06	2.80e-08	7.63e-15
0	0	0	0	0
0	0	0	0	0
0	0	0	0	0
4.10e-09	5.58e-05	2.64e-07	3.93e-09	1.27e-17
5.62e-08	0.000622	1.55e-06	1.68e-08	7.34e-10
4.01e-08	0.000317	4.00e-06	9.70e-08	2.66e-17
4.14e-09	5.58e-05	2.52e-07	3.66e-09	9.89e-14
4.27e-09	5.58e-05	2.37e-07	3.35e-09	6.27e-14
6.00e-08	0.000623	1.40e-06	1.43e-08	9.70e-09
6.20e-08	0.000623	1.48e-06	1.56e-08	4.93e-09
4.12e-08	0.000319	1.85e-06	3.03e-08	7.40e-15
4.16e-08	0.000319	1.51e-06	2.25e-08	6.62e-15
0	0	0	0	0
3.53e-09	4.81e-05	2.27e-07	3.38e-09	1.10e-17
3.42e-09	4.82e-05	1.88e-07	2.55e-09	8.25e-14
3.47e-09	4.82e-05	1.69e-07	2.16e-09	5.60e-14
0	0	0	0	0
4.91e-09	6.68e-05	3.16e-07	4.69e-09	1.52e-17
4.77e-09	6.69e-05	2.70e-07	3.72e-09	1.20e-13
4.84e-09	6.69e-05	2.46e-07	3.23e-09	8.45e-14
0	0	0	0	0
4.17e-09	5.68e-05	2.68e-07	3.99e-09	1.29e-17
4.04e-09	5.69e-05	2.26e-07	3.09e-09	9.94e-14
4.11e-09	5.69e-05	2.04e-07	2.65e-09	6.88e-14
0	0	0	0	0
3.47e-09	4.72e-05	2.24e-07	3.33e-09	1.08e-17
3.36e-09	4.73e-05	1.85e-07	2.51e-09	8.08e-14
3.41e-09	4.73e-05	1.66e-07	2.12e-09	5.48e-14
0	0	0	0	0
4.83e-09	6.56e-05	3.11e-07	4.62e-09	1.50e-17
4.69e-09	6.56e-05	2.66e-07	3.66e-09	1.17e-13
4.76e-09	6.57e-05	2.42e-07	3.17e-09	8.27e-14
0	0	0	0	0
4.10e-09	5.58e-05	2.64e-07	3.93e-09	1.27e-17
3.98e-09	5.58e-05	2.22e-07	3.04e-09	9.74e-14

4.04e-09	5.58e-05	2.01e-07	2.60e-09	6.74e-14

Ferrihydrite	d_Ferrihydrite	Gibbsite	d_Gibbsite	Barite
0	0	0	0	0
0	0	0	0	0
0.0720	0	0.0590	0	0
0.0720	0	0.0590	0	0
0.0721	0.000123	0.0590	3.05e-07	2.13e-07
0.0721	-3.82e-06	0.0590	3.07e-07	3.96e-07
0.0721	0.000126	0.0590	3.06e-07	2.06e-07
0.0721	-8.62e-08	0.0590	3.07e-07	3.89e-07
0	0	0	0	0
0	0	0	0	0
0.100	0	0.0640	0	0
0.100	0	0.0640	0	0
0.100	0.000156	0.0640	3.04e-07	2.22e-07
0.100	-3.70e-07	0.0640	3.06e-07	4.08e-07
0.100	0.000158	0.0640	3.06e-07	2.12e-07
0.100	3.10e-06	0.0640	3.07e-07	3.97e-07
0	0	0	0	0
0	0	0	0	0
0.0850	0	0.0610	0	0
0.0850	0	0.0610	0	0
0.0851	0.000139	0.0610	3.05e-07	2.17e-07
0.0851	-2.15e-06	0.0610	3.06e-07	4.02e-07
0.0851	0.000141	0.0610	3.06e-07	2.09e-07
0.0851	1.50e-06	0.0610	3.07e-07	3.93e-07
0	0	0	0	0
0	0	0	0	0
0.0720	0	0.0590	0	0
0.0720	0	0.0590	0	0
0.0721	0.000127	0.0590	3.05e-07	2.13e-07
0.0721	-3.74e-06	0.0590	3.07e-07	3.96e-07
0.0721	0.000131	0.0590	3.06e-07	2.06e-07
0.0721	4.32e-08	0.0590	3.07e-07	3.89e-07
0	0	0	0	0
0	0	0	0	0
0.100	0	0.0640	0	0
0.100	0	0.0640	0	0
0.100	0.000161	0.0640	3.04e-07	2.22e-07
0.100	-1.45e-07	0.0640	3.06e-07	4.08e-07
0.100	0.000163	0.0640	3.06e-07	2.12e-07
0.100	3.36e-06	0.0640	3.07e-07	3.98e-07
0	0	0	0	0
0	0	0	0	0
0.0850	0	0.0610	0	0

0.0850	0	0.0610	0	0
0.0851	0.000143	0.0610	3.05e-07	2.17e-07
0.0851	-1.99e-06	0.0610	3.06e-07	4.02e-07
0.0851	0.000146	0.0610	3.06e-07	2.09e-07
0.0851	1.69e-06	0.0610	3.07e-07	3.93e-07
0	0	0	0	0
0	0	0	0	0
0	0	0	0	0
0.0720	0	0.0590	0	0
0.0720	0	0.0590	0	0
0.0720	0	0.0590	0	0
0.0720	2.89e-07	0.0590	2.92e-07	0
0.0720	2.89e-07	0.0590	2.93e-07	0
0.0720	3.04e-07	0.0590	2.93e-07	0
0.0720	2.82e-07	0.0590	2.94e-07	0
0.0720	2.86e-07	0.0590	3.04e-07	0
0.0720	2.87e-07	0.0590	3.01e-07	0
0	0	0	0	0
0	0	0	0	0
0	0	0	0	0
0.100	0	0.0640	0	0
0.100	0	0.0640	0	0
0.100	0	0.0640	0	0
0.100	2.89e-07	0.0640	2.92e-07	0
0.100	2.89e-07	0.0640	2.93e-07	0
0.100	3.11e-07	0.0640	2.92e-07	0
0.100	2.78e-07	0.0640	2.93e-07	0
0.100	2.86e-07	0.0640	3.05e-07	2.05e-08
0.100	2.87e-07	0.0640	3.02e-07	0
0	0	0	0	0
0	0	0	0	0
0	0	0	0	0
0.0850	0	0.0610	0	0
0.0850	0	0.0610	0	0
0.0850	0	0.0610	0	0
0.0850	2.89e-07	0.0610	2.92e-07	0
0.0850	2.89e-07	0.0610	2.93e-07	0
0.0850	3.07e-07	0.0610	2.92e-07	0
0.0850	2.80e-07	0.0610	2.94e-07	0
0.0850	2.86e-07	0.0610	3.04e-07	7.72e-09
0.0850	2.87e-07	0.0610	3.02e-07	0
0	0	0	0	0
0	0	0	0	0
0	0	0	0	0
0.0720	0	0.0590	0	0
0.0720	0	0.0590	0	0
0.0720	0	0.0590	0	0
0.0720	2.89e-07	0.0590	2.92e-07	0
0.0720	2.89e-07	0.0590	2.93e-07	0
0.0720	3.04e-07	0.0590	2.93e-07	0

0.0720	2.81e-07	0.0590	2.94e-07	0
0.0720	2.86e-07	0.0590	3.04e-07	0
0.0720	2.87e-07	0.0590	3.01e-07	0
0	0	0	0	0
0	0	0	0	0
0	0	0	0	0
0.100	0	0.0640	0	0
0.100	0	0.0640	0	0
0.100	0	0.0640	0	0
0.100	2.89e-07	0.0640	2.92e-07	0
0.100	2.89e-07	0.0640	2.93e-07	0
0.100	3.12e-07	0.0640	2.92e-07	0
0.100	2.78e-07	0.0640	2.93e-07	0
0.100	2.86e-07	0.0640	3.05e-07	2.06e-08
0.100	2.87e-07	0.0640	3.02e-07	0
0	0	0	0	0
0	0	0	0	0
0	0	0	0	0
0.0850	0	0.0610	0	0
0.0850	0	0.0610	0	0
0.0850	0	0.0610	0	0
0.0850	2.89e-07	0.0610	2.92e-07	0
0.0850	2.89e-07	0.0610	2.93e-07	0
0.0850	3.07e-07	0.0610	2.92e-07	0
0.0850	2.80e-07	0.0610	2.94e-07	0
0.0850	2.86e-07	0.0610	3.04e-07	7.81e-09
0.0850	2.87e-07	0.0610	3.02e-07	0
0	0	0	0	0
0.0720	0	0.0590	0	0
0.0720	2.22e-06	0.0590	1.68e-07	1.98e-07
0.0720	2.22e-06	0.0590	1.66e-07	3.98e-07
0	0	0	0	0
0.100	0	0.0640	0	0
0.100	2.22e-06	0.0640	1.68e-07	1.97e-07
0.100	2.22e-06	0.0640	1.67e-07	3.97e-07
0	0	0	0	0
0.0850	0	0.0610	0	0
0.0850	2.22e-06	0.0610	1.68e-07	1.97e-07
0.0850	2.22e-06	0.0610	1.66e-07	3.97e-07
0	0	0	0	0
0.0720	0	0.0590	0	0
0.0720	2.22e-06	0.0590	1.68e-07	1.98e-07
0.0720	2.22e-06	0.0590	1.66e-07	3.98e-07
0	0	0	0	0
0.100	0	0.0640	0	0
0.100	2.22e-06	0.0640	1.68e-07	1.98e-07
0.100	2.22e-06	0.0640	1.67e-07	3.97e-07
0	0	0	0	0
0.0850	0	0.0610	0	0
0.0850	2.22e-06	0.0610	1.68e-07	1.98e-07

0.0850	2.22e-06	0.0610	1.66e-07	3.98e-07

d_Barite	Calcite	d_Calcite	Dolomite(ordered)	d_Dolomite(ordered)
0	0	0	0	0
0	0	0	0	0
0	6.00	0	2.00	0
0	6.00	0	2.00	0
2.13e-07	6.00	0.00232	2.00	-1.12e-03
1.83e-07	6.00	0.00227	2.00	-1.19e-03
2.06e-07	6.00	0.00246	2.00	-1.35e-03
1.83e-07	6.00	0.00230	2.00	-1.26e-03
0	0	0	0	0
0	0	0	0	0
0	6.00	0	2.00	0
0	6.00	0	2.00	0
2.22e-07	6.00	0.00233	2.00	-1.09e-03
1.86e-07	6.00	0.00224	2.00	-1.13e-03
2.12e-07	6.00	0.00251	2.00	-1.38e-03
1.85e-07	6.00	0.00228	2.00	-1.22e-03
0	0	0	0	0
0	0	0	0	0
0	6.00	0	2.00	0
0	6.00	0	2.00	0
2.17e-07	6.00	0.00232	2.00	-1.10e-03
1.84e-07	6.00	0.00225	2.00	-1.16e-03
2.09e-07	6.00	0.00248	2.00	-1.37e-03
1.84e-07	6.00	0.00229	2.00	-1.24e-03
0	0	0	0	0
0	0	0	0	0
0	6.00	0	2.00	0
0	6.00	0	2.00	0
2.13e-07	6.00	0.00231	2.00	-1.11e-03
1.83e-07	6.00	0.00227	2.00	-1.19e-03
2.06e-07	6.00	0.00246	2.00	-1.35e-03
1.83e-07	6.00	0.00230	2.00	-1.26e-03
0	0	0	0	0
0	0	0	0	0
0	6.00	0	2.00	0
0	6.00	0	2.00	0
2.22e-07	6.00	0.00233	2.00	-1.09e-03
1.86e-07	6.00	0.00223	2.00	-1.12e-03
2.12e-07	6.00	0.00251	2.00	-1.38e-03
1.85e-07	6.00	0.00228	2.00	-1.22e-03
0	0	0	0	0
0	0	0	0	0
0	6.00	0	2.00	0

0	6.00	0	2.00	0
2.17e-07	6.00	0.00232	2.00	-1.10e-03
1.85e-07	6.00	0.00225	2.00	-1.16e-03
2.09e-07	6.00	0.00248	2.00	-1.36e-03
1.84e-07	6.00	0.00229	2.00	-1.24e-03
0	0	0	0	0
0	0	0	0	0
0	0	0	0	0
0	6.00	0	2.00	0
0	6.00	0	2.00	0
0	6.00	0	2.00	0
0	6.00	0.00134	2.00	-8.49e-04
0	6.00	0.00119	2.00	-7.42e-04
0	6.00	0.00129	2.00	-8.76e-04
0	6.00	0.00118	2.00	-7.43e-04
0	6.00	0.00179	2.00	-1.78e-03
0	6.00	0.00135	2.00	-1.12e-03
0	0	0	0	0
0	0	0	0	0
0	0	0	0	0
0	6.00	0	2.00	0
0	6.00	0	2.00	0
0	6.00	0	2.00	0
0	6.00	0.00139	2.00	-8.85e-04
0	6.00	0.00119	2.00	-7.35e-04
0	6.00	0.00132	2.00	-9.22e-04
0	6.00	0.00117	2.00	-7.23e-04
2.05e-08	6.00	0.00193	2.00	-2.01e-03
-2.05e-08	6.00	0.00138	2.00	-1.18e-03
0	0	0	0	0
0	0	0	0	0
0	0	0	0	0
0	6.00	0	2.00	0
0	6.00	0	2.00	0
0	6.00	0	2.00	0
0	6.00	0.00136	2.00	-8.65e-04
0	6.00	0.00119	2.00	-7.38e-04
0	6.00	0.00131	2.00	-8.96e-04
0	6.00	0.00118	2.00	-7.33e-04
7.72e-09	6.00	0.00185	2.00	-1.89e-03
-7.72e-09	6.00	0.00137	2.00	-1.15e-03
0	0	0	0	0
0	0	0	0	0
0	0	0	0	0
0	6.00	0	2.00	0
0	6.00	0	2.00	0
0	6.00	0	2.00	0
0	6.00	0.00134	2.00	-8.53e-04
0	6.00	0.00119	2.00	-7.43e-04
0	6.00	0.00129	2.00	-8.74e-04

0	6.00	0.00118	2.00	-7.43e-04
0	6.00	0.00179	2.00	-1.78e-03
0	6.00	0.00135	2.00	-1.12e-03
0	0	0	0	0
0	0	0	0	0
0	0	0	0	0
0	6.00	0	2.00	0
0	6.00	0	2.00	0
0	6.00	0	2.00	0
0	6.00	0.00139	2.00	-8.90e-04
0	6.00	0.00119	2.00	-7.36e-04
0	6.00	0.00132	2.00	-9.19e-04
0	6.00	0.00117	2.00	-7.22e-04
2.06e-08	6.00	0.00193	2.00	-2.01e-03
-2.06e-08	6.00	0.00138	2.00	-1.18e-03
0	0	0	0	0
0	0	0	0	0
0	0	0	0	0
0	6.00	0	2.00	0
0	6.00	0	2.00	0
0	6.00	0	2.00	0
0	6.00	0.00136	2.00	-8.70e-04
0	6.00	0.00119	2.00	-7.39e-04
0	6.00	0.00130	2.00	-8.94e-04
0	6.00	0.00118	2.00	-7.32e-04
7.81e-09	6.00	0.00185	2.00	-1.89e-03
-7.81e-09	6.00	0.00137	2.00	-1.15e-03
0	0	0	0	0
0	6.00	0	2.00	0
1.98e-07	6.00	0.000404	2.00	-3.39e-04
2.00e-07	6.00	0.000234	2.00	-1.60e-04
0	0	0	0	0
0	6.00	0	2.00	0
1.97e-07	6.00	0.000463	2.00	-4.00e-04
1.99e-07	6.00	0.000246	2.00	-1.78e-04
0	0	0	0	0
0	6.00	0	2.00	0
1.97e-07	6.00	0.000432	2.00	-3.68e-04
2.00e-07	6.00	0.000240	2.00	-1.69e-04
0	0	0	0	0
0	6.00	0	2.00	0
1.98e-07	6.00	0.000408	2.00	-3.42e-04
2.00e-07	6.00	0.000234	2.00	-1.61e-04
0	0	0	0	0
0	6.00	0	2.00	0
1.98e-07	6.00	0.000467	2.00	-4.05e-04
1.99e-07	6.00	0.000247	2.00	-1.79e-04
0	0	0	0	0
0	6.00	0	2.00	0
1.98e-07	6.00	0.000436	2.00	-3.72e-04

2.00e-07	6.00	0.000240	2.00	-1.70e-04

Gypsum	d_Gypsum	si_Ferrihydrite	si_Gibbsite	si_Barite
0	0	2.07	0.793	0.881
0	0	2.17	0.877	0.428
0	0	2.07	0.793	0.881
0	0	2.17	0.877	0.428
0	0	0	0	0
0	0	0	0	0
0	0	0	0	0
0	0	0	0	0
0	0	2.07	0.793	0.881
0	0	2.17	0.877	0.428
0	0	2.07	0.793	0.881
0	0	2.17	0.877	0.428
0	0	0	0	0
0	0	0	0	0
0	0	0	0	0
0	0	0	0	0
0	0	2.07	0.793	0.881
0	0	2.17	0.877	0.428
0	0	2.07	0.793	0.881
0	0	2.17	0.877	0.428
0	0	0	0	0
0	0	0	0	0
0	0	0	0	0
0	0	0	0	0
0	0	2.08	0.795	0.896
0	0	2.19	0.879	0.446
0	0	2.08	0.795	0.896
0	0	2.19	0.879	0.446
0	0	0	0	0
0	0	0	0	0
0	0	0	0	0
0	0	0	0	0
0	0	2.08	0.795	0.896
0	0	2.19	0.879	0.446
0	0	2.08	0.795	0.896
0	0	2.19	0.879	0.446
0	0	0	0	0
0	0	0	0	0
0	0	0	0	0
0	0	0	0	0
0	0	2.08	0.795	0.896
0	0	2.19	0.879	0.446
0	0	2.08	0.795	0.896

0	0	2.19	0.879	0.446
0	0	0	0	0
0	0	0	0	0
0	0	0	0	0
0	0	0	0	0
0	0	2.00	0.634	0.216
0	0	0.783	0.828	0.737
0	0	1.29	1.00	0.840
0	0	2.00	0.634	0.216
0	0	0.783	0.828	0.737
0	0	1.29	1.00	0.840
0	0	0	0	-1.04e-01
0	0	0	0	-1.02e-01
0	0	0	0	-6.63e-02
0	0	0	0	-1.10e-01
0	0	0	0	-6.60e-03
0	0	0	0	-1.31e-01
0	0	2.00	0.634	0.216
0	0	0.783	0.828	0.737
0	0	1.29	1.00	0.840
0	0	2.00	0.634	0.216
0	0	0.783	0.828	0.737
0	0	1.29	1.00	0.840
0	0	0	0	-1.03e-01
0	0	0	0	-1.02e-01
0	0	0	0	-5.10e-02
0	0	0	0	-1.10e-01
0	0	0	0	0
0	0	0	0	-1.03e-01
0	0	2.00	0.634	0.216
0	0	0.783	0.828	0.737
0	0	1.29	1.00	0.840
0	0	2.00	0.634	0.216
0	0	0.783	0.828	0.737
0	0	1.29	1.00	0.840
0	0	0	0	-1.03e-01
0	0	0	0	-1.02e-01
0	0	0	0	-5.91e-02
0	0	0	0	-1.10e-01
0	0	0	0	0
0	0	0	0	-1.20e-01
0	0	2.00	0.633	0.205
0	0	0.787	0.829	0.742
0	0	1.29	1.00	0.843
0	0	2.00	0.633	0.205
0	0	0.787	0.829	0.742
0	0	1.29	1.00	0.843
0	0	0	0	-1.04e-01
0	0	0	0	-1.02e-01
0	0	0	0	-6.64e-02

0	0	0	0	-1.10e-01
0	0	0	0	-6.50e-03
0	0	0	0	-1.31e-01
0	0	2.00	0.633	0.205
0	0	0.787	0.829	0.742
0	0	1.29	1.00	0.843
0	0	2.00	0.633	0.205
0	0	0.787	0.829	0.742
0	0	1.29	1.00	0.843
0	0	0	0	-1.03e-01
0	0	0	0	-1.02e-01
0	0	0	0	-5.10e-02
0	0	0	0	-1.10e-01
0	0	0	0	0
0	0	0	0	-1.03e-01
0	0	2.00	0.633	0.205
0	0	0.787	0.829	0.742
0	0	1.29	1.00	0.843
0	0	2.00	0.633	0.205
0	0	0.787	0.829	0.742
0	0	1.29	1.00	0.843
0	0	0	0	-1.03e-01
0	0	0	0	-1.02e-01
0	0	0	0	-5.91e-02
0	0	0	0	-1.10e-01
0	0	0	0	0
0	0	0	0	-1.20e-01
0	0	2.00	0.634	0.216
0	0	2.00	0.634	0.216
0	0	0	0	0
0	0	0	0	0
0	0	2.00	0.634	0.216
0	0	2.00	0.634	0.216
0	0	0	0	0
0	0	0	0	0
0	0	2.00	0.634	0.216
0	0	2.00	0.634	0.216
0	0	0	0	0
0	0	0	0	0
0	0	2.00	0.633	0.205
0	0	2.00	0.633	0.205
0	0	0	0	0
0	0	0	0	0
0	0	2.00	0.633	0.205
0	0	2.00	0.633	0.205
0	0	0	0	0
0	0	0	0	0
0	0	2.00	0.633	0.205
0	0	2.00	0.633	0.205
0	0	0	0	0

0	0	0	0	0

si_Calcite	si_Dolomite(ordered)	si_Gypsum
0.154	0.0446	-1.51e+00
-3.35e-02	-3.41e-01	-1.51e+00
0.154	0.0446	-1.51e+00
-3.35e-02	-3.41e-01	-1.51e+00
0	0	-1.90e+00
0	0	-1.90e+00
0	0	-1.88e+00
0	0	-1.89e+00
0.154	0.0446	-1.51e+00
-3.35e-02	-3.41e-01	-1.51e+00
0.154	0.0446	-1.51e+00
-3.35e-02	-3.41e-01	-1.51e+00
0	0	-1.90e+00
0	0	-1.90e+00
0	0	-1.88e+00
0	0	-1.89e+00
0.154	0.0446	-1.51e+00
-3.35e-02	-3.41e-01	-1.51e+00
0.154	0.0446	-1.51e+00
-3.35e-02	-3.41e-01	-1.51e+00
0	0	-1.90e+00
0	0	-1.90e+00
0	0	-1.88e+00
0	0	-1.89e+00
0.165	0.0667	-1.50e+00
-2.09e-02	-3.15e-01	-1.50e+00
0.165	0.0667	-1.50e+00
-2.09e-02	-3.15e-01	-1.50e+00
0	0	-1.90e+00
0	0	-1.90e+00
0	0	-1.88e+00
0	0	-1.89e+00
0.165	0.0667	-1.50e+00
-2.09e-02	-3.15e-01	-1.50e+00
0.165	0.0667	-1.50e+00
-2.09e-02	-3.15e-01	-1.50e+00
0	0	-1.90e+00
0	0	-1.90e+00
0	0	-1.88e+00
0	0	-1.89e+00
0.165	0.0667	-1.50e+00
-2.09e-02	-3.15e-01	-1.50e+00
0.165	0.0667	-1.50e+00

-2.09e-02	-3.15e-01	-1.50e+00
0	0	-1.90e+00
0	0	-1.90e+00
0	0	-1.88e+00
0	0	-1.89e+00
-1.18e-01	-4.57e-01	-1.60e+00
-4.11e-01	-7.56e-01	-9.68e-01
-3.76e-01	-1.45e+00	-4.10e-01
-1.18e-01	-4.57e-01	-1.60e+00
-4.11e-01	-7.56e-01	-9.68e-01
-3.76e-01	-1.45e+00	-4.10e-01
0	0	-1.82e+00
0	0	-1.81e+00
0	0	-1.77e+00
0	0	-1.82e+00
0	0	-1.64e+00
0	0	-1.80e+00
-1.18e-01	-4.57e-01	-1.60e+00
-4.11e-01	-7.56e-01	-9.68e-01
-3.76e-01	-1.45e+00	-4.10e-01
-1.18e-01	-4.57e-01	-1.60e+00
-4.11e-01	-7.56e-01	-9.68e-01
-3.76e-01	-1.45e+00	-4.10e-01
0	0	-1.82e+00
0	0	-1.81e+00
0	0	-1.75e+00
0	0	-1.82e+00
0	0	-1.59e+00
0	0	-1.79e+00
-1.18e-01	-4.57e-01	-1.60e+00
-4.11e-01	-7.56e-01	-9.68e-01
-3.76e-01	-1.45e+00	-4.10e-01
-1.18e-01	-4.57e-01	-1.60e+00
-4.11e-01	-7.56e-01	-9.68e-01
-3.76e-01	-1.45e+00	-4.10e-01
0	0	-1.82e+00
0	0	-1.81e+00
0	0	-1.76e+00
0	0	-1.82e+00
0	0	-1.61e+00
0	0	-1.80e+00
-1.24e-01	-4.70e-01	-1.61e+00
-4.08e-01	-7.50e-01	-9.64e-01
-3.74e-01	-1.45e+00	-4.08e-01
-1.24e-01	-4.70e-01	-1.61e+00
-4.08e-01	-7.50e-01	-9.64e-01
-3.74e-01	-1.45e+00	-4.08e-01
0	0	-1.82e+00
0	0	-1.81e+00
0	0	-1.77e+00

0	0	-1.82e+00
0	0	-1.64e+00
0	0	-1.80e+00
-1.24e-01	-4.70e-01	-1.61e+00
-4.08e-01	-7.50e-01	-9.64e-01
-3.74e-01	-1.45e+00	-4.08e-01
-1.24e-01	-4.70e-01	-1.61e+00
-4.08e-01	-7.50e-01	-9.64e-01
-3.74e-01	-1.45e+00	-4.08e-01
0	0	-1.82e+00
0	0	-1.81e+00
0	0	-1.76e+00
0	0	-1.82e+00
0	0	-1.59e+00
0	0	-1.79e+00
-1.24e-01	-4.70e-01	-1.61e+00
-4.08e-01	-7.50e-01	-9.64e-01
-3.74e-01	-1.45e+00	-4.08e-01
-1.24e-01	-4.70e-01	-1.61e+00
-4.08e-01	-7.50e-01	-9.64e-01
-3.74e-01	-1.45e+00	-4.08e-01
0	0	-1.82e+00
0	0	-1.81e+00
0	0	-1.76e+00
0	0	-1.82e+00
0	0	-1.61e+00
0	0	-1.80e+00
-1.18e-01	-4.57e-01	-1.60e+00
-1.18e-01	-4.57e-01	-1.60e+00
0	0	-2.14e+00
0	0	-2.14e+00
-1.18e-01	-4.57e-01	-1.60e+00
-1.18e-01	-4.57e-01	-1.60e+00
0	0	-2.14e+00
0	0	-2.14e+00
-1.18e-01	-4.57e-01	-1.60e+00
-1.18e-01	-4.57e-01	-1.60e+00
0	0	-2.14e+00
0	0	-2.14e+00
-1.24e-01	-4.70e-01	-1.61e+00
-1.24e-01	-4.70e-01	-1.61e+00
0	0	-2.14e+00
0	0	-2.14e+00
-1.24e-01	-4.70e-01	-1.61e+00
-1.24e-01	-4.70e-01	-1.61e+00
0	0	-2.14e+00
0	0	-2.14e+00
-1.24e-01	-4.70e-01	-1.61e+00
-1.24e-01	-4.70e-01	-1.61e+00
0	0	-2.14e+00

0	0	-2.14e+00

APPENDIX B
DRAWINGS AND MATERIALS SPECIFICATIONS FOR SELECTED REMEDY

SAVED: 3/5/25 11:42 AM

C:\DC\ACCDOCS\RAMBOLL GRUPPEN AS\RUS-1940106781-008 VISTRA - HENNEPIN WAPS\PROJECT FILES\4 DELIVERY\40 WIP\401 CIVIL\DRAWINGS\G-000_HEN-WAPS.DWG

CORRECTIVE ACTION PERMIT-LEVEL DESIGN

West Ash Pond System

Hennepin Power Plant

HENNEPIN, ILLINOIS

AERIAL IMAGERY: ESRI WORLD IMAGERY

LOCATION MAP

500' 0 500'
SCALE: 1"=500'

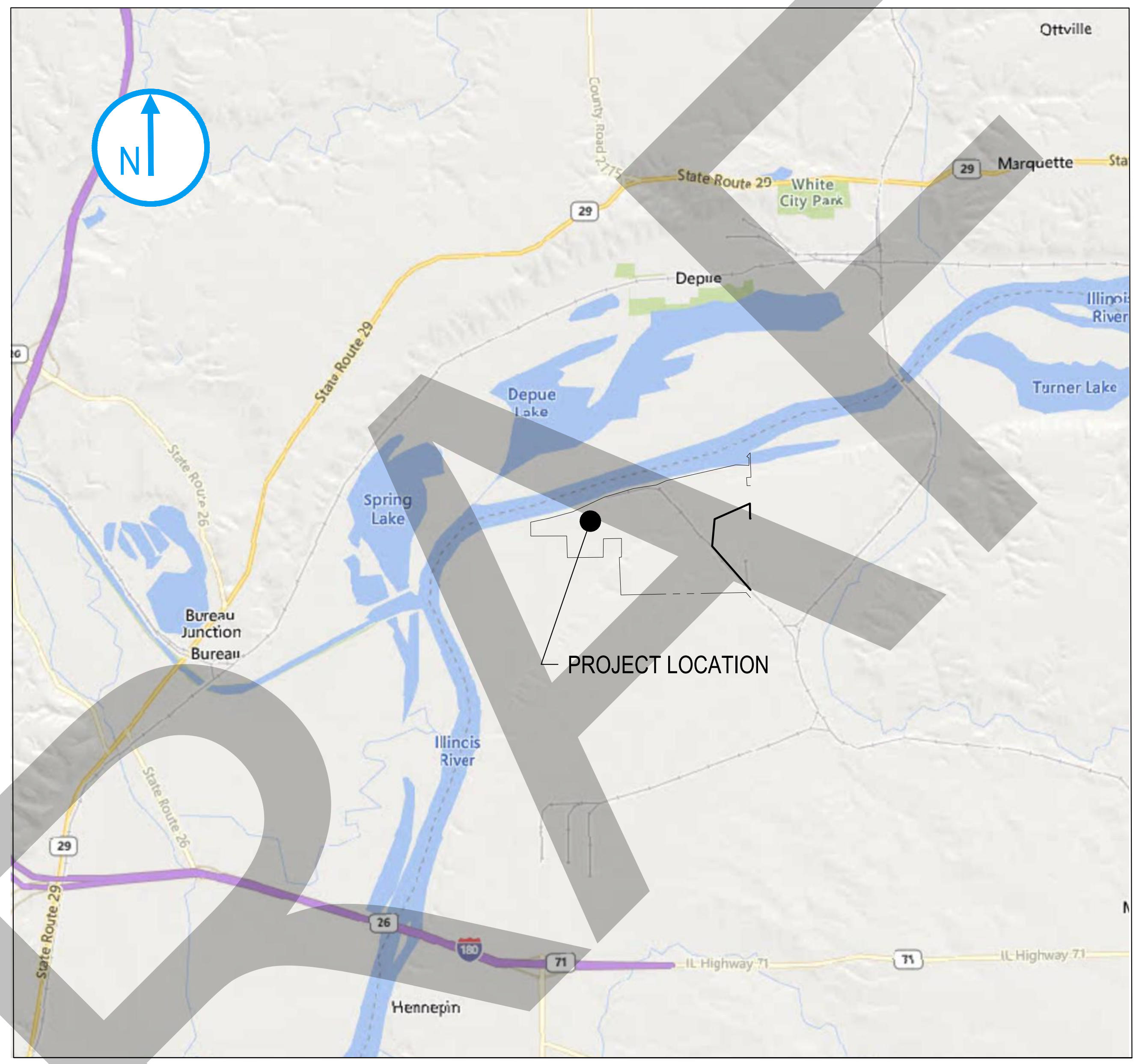

SOURCE: ESRI WORLD STREET MAP

VICINITY MAP

5000' 0 5000'
SCALE: 1"=5000'

SHEET INDEX

	General
G-000	Cover
	Civil
C-101	Overall Site Plan
C-301	Cross Sections A-A' & B-B'
C-302	Cross Sections C-C' & F-F'
C-303	Cross Section Details

DYNEGY MIDWEST GENERATION, LLC

Hennepin Power Plant
13498 E 800th St
Hennepin, IL 61327
April 2025

RAMBOLL

RAMBOLL AMERICAS ENGINEERING SOLUTIONS, INC.

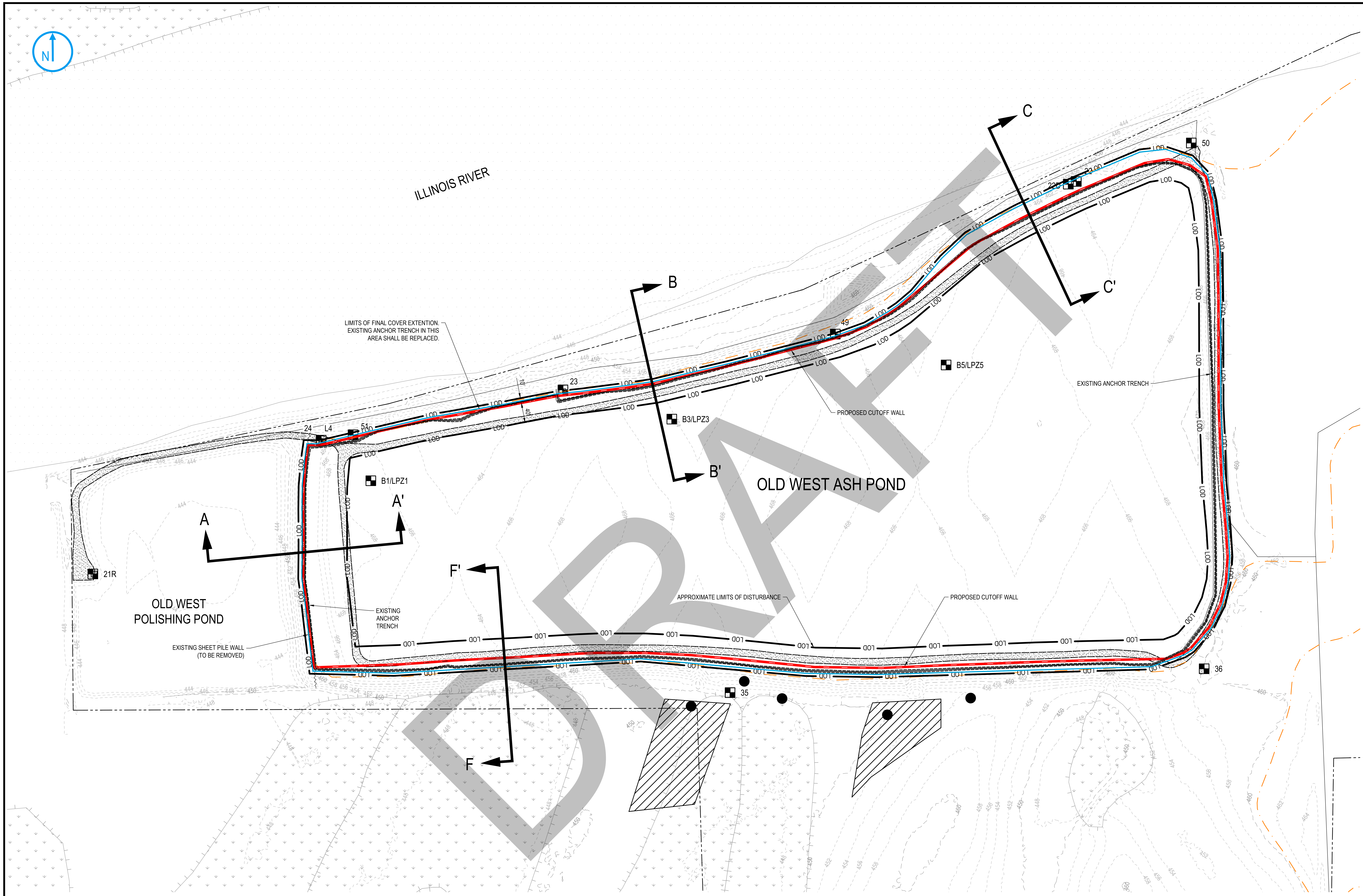

LEGEND

EXISTING

— — 360 — —	MAJOR CONTOUR
- - 358 - -	MINOR CONTOUR
— - - — - - —	APPROXIMATE SITE BOUNDARY
— — — —	100-YR FLOODPLAIN (APPROXIMATE LIMITS)
	WETLANDS (APPROXIMATE LIMITS)
	BODY OF WATER (LAKE, POND, RAVINE, ETC.) (APPROXIMATE LIMITS)
	MONITORING WELLS
●	BOLTONIA POINTS (APPROXIMATE LOCATION)
▨	BOLTONIA AREAS (APPROXIMATE LIMITS)
	SHEETPILE WALL
	EXISTING ANCHOR TRENCH
	GRAVEL ACCESS ROAD

PROPOSED

	CUTOFF WALL
	LIMITS OF FINAL COVER
—— LOD ——	APPROXIMATE LIMITS OF DISTURBANCE

NOTE:

1. EXISTING CONTOURS ARE BASED ON FINAL CLOSURE DRAWINGS OF OLD WEST ASH POND AND OLD WEST POLISHING POND, COMPLETED BY CEC, OCTOBER 2020.
2. WETLANDS REPRESENTED AS PER ILLINOIS NATIONAL WETLANDS INVENTORY AND ADAPTED TO REPRESENT ACTUAL SITE CONDITIONS.
3. BOLTONIA PLANTS AND AREAS BASED ON SCI'S DECURRENT FALSE ASTER SURVEY, SEPTEMBER 27, 2019.
4. 100-YEAR FLOODPLAIN REPRESENTED AS PER FEDERAL EMERGENCY MANAGEMENT AGENCY,"FLOOD INSURANCE RATE MAP, PUTNAM COUNTY, ILLINOIS AND UNINCORPORATED AREAS," NATIONAL FLOOD INSURANCE PROGRAM, JUNE 23, 2022 AND ADAPTED TO REPRESENT BASE FLOOD LEVEL EL. 461.9 FT.
5. THE CONTINUOUS CONTAINMENT SYSTEM DESIGN WILL BE FURTHER REFINED AS PART OF FINAL DESIGN ACTIVITIES THAT WILL BE INITIATED AFTER A CORRECTIVE ACTION CONSTRUCTION PERMIT HAS BEEN ISSUED FOR THE WEST ASH POND SYSTEM THESE ACTIVITIES MAY INCLUDE, BUT ARE NOT LIMITED TO, THE COLLECTION OF ADDITIONAL SITE SURVEY AND/OR SUBSURFACE INVESTIGATION DATA, MORE REFINED DESIGN EVALUATIONS, ADDITIONAL ENGINEERING ANALYSES, AND/OR PERMIT-RELATED CONSIDERATIONS. ELEMENTS OF THE CONTINUOUS CONTAINMENT SYSTEM DESIGN THAT WILL BE REFINED INCLUDE, BUT ARE NOT LIMITED TO, THE LIMITS OF DISTURBANCE, THE DIMENSIONS AND GEOMETRY OF THE WORK PAD, LIMITS OF THE FINAL COVER SYSTEM, TIE-IN DETAILS BETWEEN THE FINAL COVER SYSTEM, TIE-IN DETAILS BETWEEN THE DEEP CUTOFF WALL AND STORMWATER MANAGEMENT FEATURES, AND THE LOCATION OF THE DEEP CUTOFF WALL WITHIN THE WEST ASH POND SYSTEM PERIMETER DIKES.

OVERALL SITE PLAN

100' 0 100'
SCALE: 1"=100'

ISSUED FOR
PERMIT REVIEW
NOT FOR
CONSTRUCTION
DATE: 3/7/2025

NO.	REV DATE	REVISION	INT.

Project Details
DYNEGY MIDWEST GENERATION, LLC
West Ash Pond System
Hennepin Power Plant
13498 E 800th St Hennepin, IL 61327

Drawing Title
OVERALL SITE PLAN

RAMBOLL
RAMBOLL AMERICAS ENGINEERING SOLUTIONS, INC.

Location:

Designer / Professional Engineer Responsible:
B. RICHTER

Project Number **1940110241-006**	Designed by S. LEE	Drawn by B. LEMMON	Checked by L. CARR	Approved by	Date April 2025
Project Status Corrective Action Permit-Level Design	Drawing Number **C-101**			Scale AS NOTED	Sc x

Rev.
x

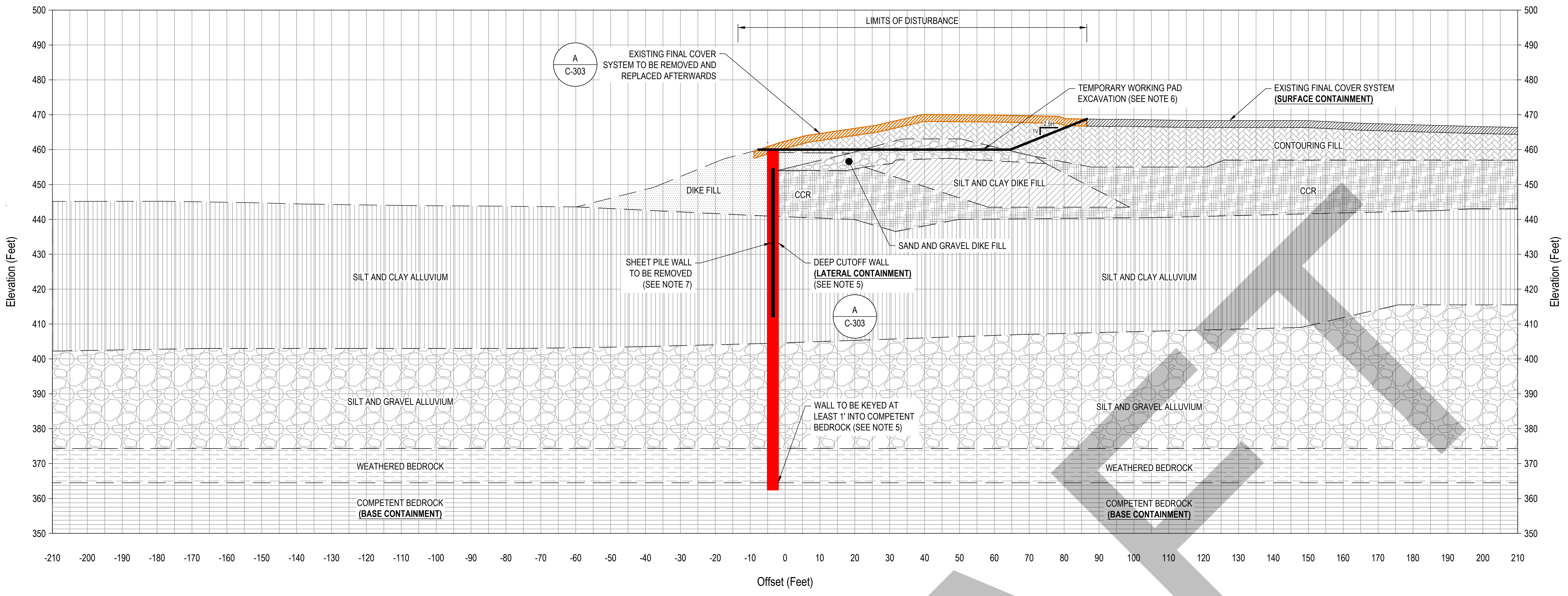

CROSS SECTION A-A'

20' 0 20'
SCALE HORZ. 1" = 20'

20' 0 20'
SCALE: VERT. 1"=20'

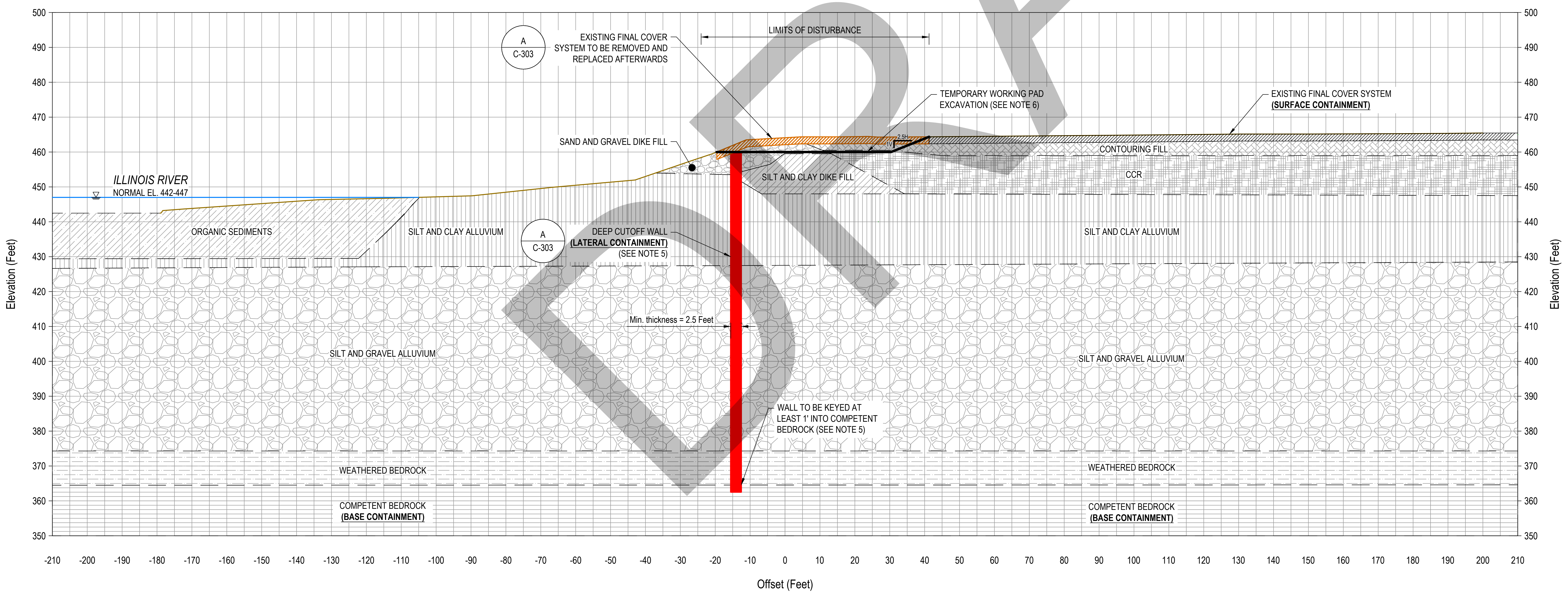

CROSS SECTION B-B'

20' 0 20'
SCALE HORZ. 1" = 20'

20' 0 20'
SCALE: VERT. 1"=20'

NOTES:

1. THE DEEP CUTOFF WALL IS TO:
    a. BE CONSTRUCTED USING SOIL-BENTONITE OR CEMENT-BENTONITE MATERIALS
    b. HAVE A DESIGN HYDRAULIC CONDUCTIVITY OF $1X10^{-7}$CENTIMETERS PER SECOND
    c. HAVE A THICKNESS OF AT LEAST 2.5 FEET
    d. HAVE A DESIGN COMPRESSIVE STRENGTH OF 50 PSI AFTER 28 DAYS OF CURING, UNLESS A LOWER STRENGTH IS JUSTIFIED BASED ON A STABILITY ANALYSIS
    e. BE KEYED AT LEAST 1 FT INTO COMPETENT SHALE BEDROCK, AS DETERMINED BY THE OBSERVATIONS OF CUTTINGS AND MACHINE INSTRUMENTATION OBTAINED DURING WALL INSTALLATION
2. THE TEMPORARY WORKING PLATFORM IS TO BE CONSTRUCTED AFTER THE FINAL COVER SYSTEM IS REMOVED AND BEFORE WALL CONSTRUCTION IS COMPLETED.
3. THE EXISTING NZ-26 STEEL SHEET PILE WALL IS TO BE REMOVED BEFORE OR AFTER WORKING PAD CONSTRUCTION BUT PRIOR TO INSTALLATION OF THE CUTOFF WALL.
4. ALL SUBSURFACE MATERIAL INTERFACES ARE APPROXIMATE AND ARE BASED ON THE INTERPOLATION OF AVAILABLE INVESTIGATION DATA. ADDITIONAL SUBSURFACE INVESTIGATIONS WILL BE ADVANCED ALONG THE CUTOFF WALL PROFILE AS PART OF FUTURE PRE-DESIGN INVESTIGATION ACTIVITIES TO VERIFY MATERIAL INTERFACES AND REFINE THE DESIGN PROFILE OF THE CUTOFF WALL.
5. SUBSURFACE LAYERING WAS TAKEN FROM THE 2020 GEOSYTNEC FINAL CLOSURE DESIGN GEOTECHNICAL CALCULATIONS.
6. THE TOP OF WEATHERED BEDROCK AND COMPETENT BEDROCK (BASE CONTAINMENT) WERE ARE GENERALIZED AND WERE SELECTED BASED ON BORINGS AND PACKER TESTING COMPLETED BY RAMBOLL IN 2024.
7. THE CONTINUOUS CONTAINMENT SYSTEM DESIGN WILL BE FURTHER REFINED AS PART OF FINAL DESIGN ACTIVITIES THAT WILL BE INITIATED AFTER A CORRECTIVE ACTION CONSTRUCTION PERMIT HAS BEEN ISSUED FOR THE WEST ASH POND SYSTEM THESE ACTIVITIES MAY INCLUDE, BUT ARE NOT LIMITED TO, THE COLLECTION OF ADDITIONAL SITE SURVEY AND/OR SUBSURFACE INVESTIGATION DATA, MORE REFINED DESIGN EVALUATIONS, ADDITIONAL ENGINEERING ANALYSES, AND/OR PERMIT-RELATED CONSIDERATIONS. ELEMENTS OF THE CONTINUOUS CONTAINMENT SYSTEM DESIGN THAT WILL BE REFINED INCLUDE, BUT ARE NOT LIMITED TO, THE LIMITS OF DISTURBANCE, THE DIMENSIONS AND GEOMETRY OF THE WORK PAD, LIMITS OF THE FINAL COVER SYSTEM, TIE-IN DETAILS BETWEEN THE FINAL COVER SYSTEM, TIE-IN DETAILS BETWEEN THE DEEP CUTOFF WALL AND STORMWATER MANAGEMENT FEATURES, AND THE LOCATION OF THE DEEP CUTOFF WALL WITHIN THE WEST ASH POND SYSTEM PERIMETER DIKES.

NO.	REV DATE	REVISION	INT.

ISSUED FOR
PERMIT REVIEW
NOT FOR
CONSTRUCTION

DATE: 3/7/2025

Project Details
DYNEGY MIDWEST GENERATION, LLC
West Ash Pond System
Hennepin Power Plant
13498 E 800th St Hennepin, IL 61327

Drawing Title
CROSS SECTIONS A-A' & B-B'

RAMBOLL
RAMBOLL AMERICAS ENGINEERING SOLUTIONS, INC.

Location:

Designer / Professional Engineer Responsible:
B. RICHTER

Project Number **1940110241-006**

Designed by	Drawn by	Checked by	Approved by	Date
S. LEE	B. LEMMON	L. CARR		April 2025

Project Status Corrective Action Permit-Level Design

Drawing Number **C-301**

Scale	Sc	Rev.
AS NOTED	x	x

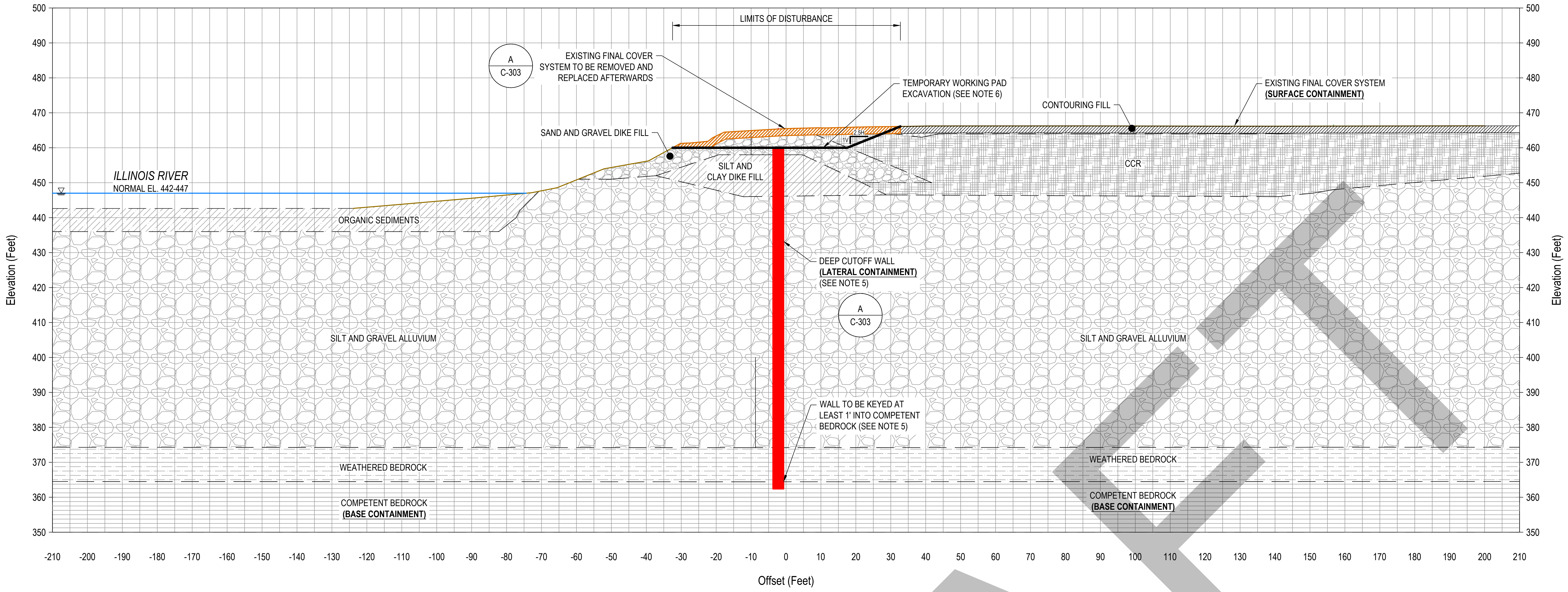

CROSS SECTION C-C'

20' 0 20'
SCALE HORZ. 1" = 20'

20' 0 20'
SCALE: VERT. 1"=20'

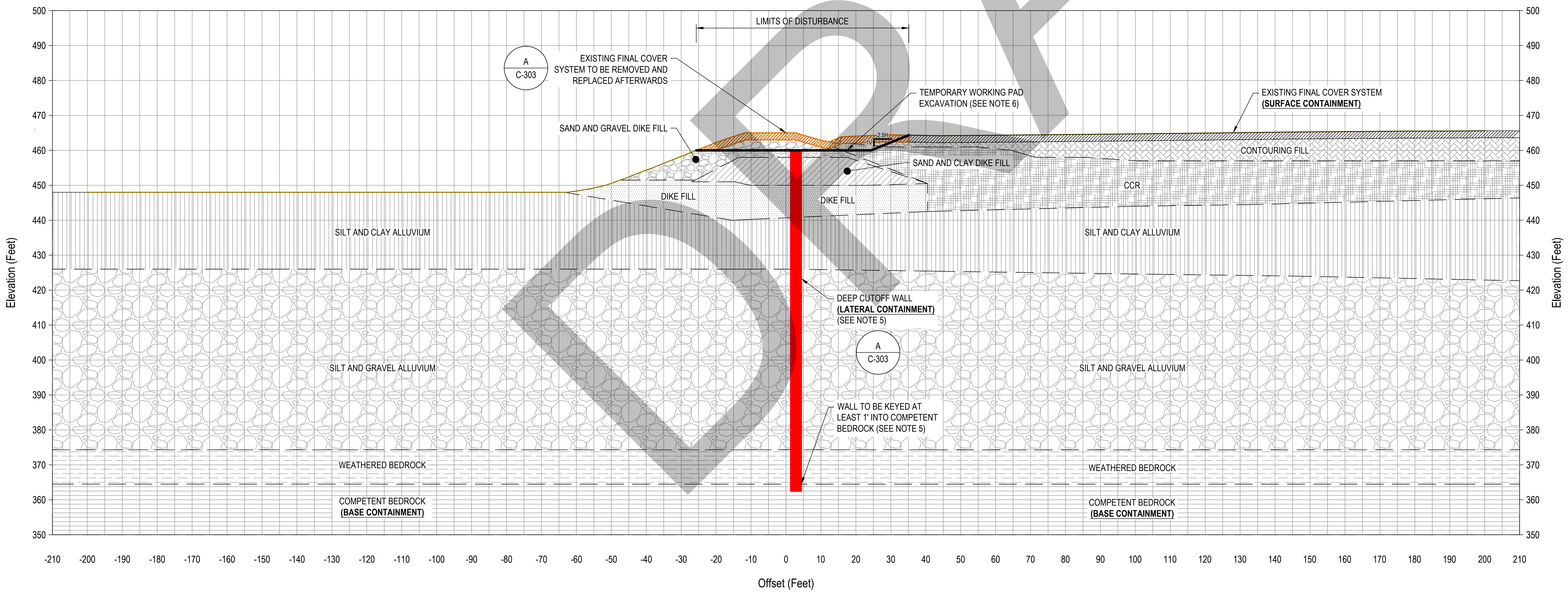

CROSS SECTION F-F'

20' 0 20'
SCALE HORZ. 1" = 20'

20' 0 20'
SCALE: VERT. 1"=20'

NOTES:

1. THE DEEP CUTOFF WALL IS TO:
    a. BE CONSTRUCTED USING SOIL-BENTONITE OR CEMENT-BENTONITE MATERIALS
    b. HAVE A DESIGN HYDRAULIC CONDUCTIVITY OF $1X10^{-7}$CENTIMETERS PER SECOND
    c. HAVE A THICKNESS OF AT LEAST 2.5 FEET
    d. HAVE A DESIGN COMPRESSIVE STRENGTH OF 50 PSI AFTER 28 DAYS OF CURING, UNLESS A LOWER STRENGTH IS JUSTIFIED BASED ON A STABILITY ANALYSIS
    e. BE KEYED AT LEAST 1 FT INTO COMPETENT SHALE BEDROCK, AS DETERMINED BY THE OBSERVATIONS OF CUTTINGS AND MACHINE INSTRUMENTATION OBTAINED DURING WALL INSTALLATION
2. THE TEMPORARY WORKING PLATFORM IS TO BE CONSTRUCTED AFTER THE FINAL COVER SYSTEM IS REMOVED AND BEFORE WALL CONSTRUCTION IS COMPLETED.
3. THE EXISTING NZ-26 STEEL SHEET PILE WALL IS TO BE REMOVED BEFORE OR AFTER WORKING PAD CONSTRUCTION BUT PRIOR TO INSTALLATION OF THE CUTOFF WALL.
4. ALL SUBSURFACE MATERIAL INTERFACES ARE APPROXIMATE AND ARE BASED ON THE INTERPOLATION OF AVAILABLE INVESTIGATION DATA. ADDITIONAL SUBSURFACE INVESTIGATIONS WILL BE ADVANCED ALONG THE CUTOFF WALL PROFILE AS PART OF FUTURE PRE-DESIGN INVESTIGATION ACTIVITIES TO VERIFY MATERIAL INTERFACES AND REFINE THE DESIGN PROFILE OF THE CUTOFF WALL.
5. SUBSURFACE LAYERING WAS TAKEN FROM THE 2020 GEOSYTNEC FINAL CLOSURE DESIGN GEOTECHNICAL CALCULATIONS.
6. THE TOP OF WEATHERED BEDROCK AND COMPETENT BEDROCK (BASE CONTAINMENT) WERE ARE GENERALIZED AND WERE SELECTED BASED ON BORINGS AND PACKER TESTING COMPLETED BY RAMBOLL IN 2024.
7. THE CONTINUOUS CONTAINMENT SYSTEM DESIGN WILL BE FURTHER REFINED AS PART OF FINAL DESIGN ACTIVITIES THAT WILL BE INITIATED AFTER A CORRECTIVE ACTION CONSTRUCTION PERMIT HAS BEEN ISSUED FOR THE WEST ASH POND SYSTEM THESE ACTIVITIES MAY INCLUDE, BUT ARE NOT LIMITED TO, THE COLLECTION OF ADDITIONAL SITE SURVEY AND/OR SUBSURFACE INVESTIGATION DATA, MORE REFINED DESIGN EVALUATIONS, ADDITIONAL ENGINEERING ANALYSES, AND/OR PERMIT-RELATED CONSIDERATIONS. ELEMENTS OF THE CONTINUOUS CONTAINMENT SYSTEM DESIGN THAT WILL BE REFINED INCLUDE, BUT ARE NOT LIMITED TO, THE LIMITS OF DISTURBANCE, THE DIMENSIONS AND GEOMETRY OF THE WORK PAD, LIMITS OF THE FINAL COVER SYSTEM, TIE-IN DETAILS BETWEEN THE FINAL COVER SYSTEM, TIE-IN DETAILS BETWEEN THE DEEP CUTOFF WALL AND STORMWATER MANAGEMENT FEATURES, AND THE LOCATION OF THE DEEP CUTOFF WALL WITHIN THE WEST ASH POND SYSTEM PERIMETER DIKES.

NO.	REV DATE	REVISION	INT.

ISSUED FOR
PERMIT REVIEW
NOT FOR
CONSTRUCTION

DATE: 3/7/2025

Project Details
DYNEGY MIDWEST GENERATION, LLC
West Ash Pond System
Hennepin Power Plant
13498 E 800th St Hennepin, IL 61327

Drawing Title
CROSS SECTIONS C-C' & F-F'

RAMBOLL
RAMBOLL AMERICAS ENGINEERING SOLUTIONS, INC.

Location:

Designer / Professional Engineer Responsible:
B. RICHTER

Project Number **1940110241-006**

Designed by
S. LEE

Drawn by
B. LEMMON

Checked by
L. CARR

Approved by

Date
April 2025

Project Status Corrective Action Permit-Level Design

Drawing Number **C-302**

Scale
AS NOTED

Sc
x

Rev.
x

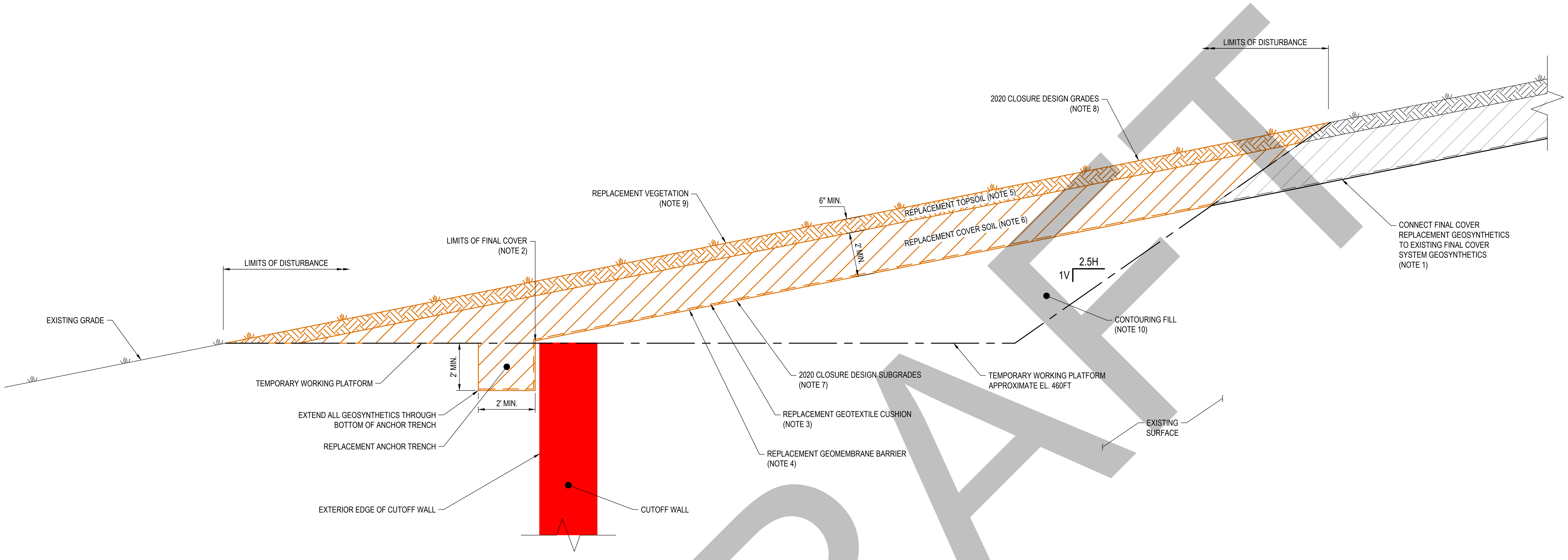

A FINAL COVER REPLACEMENT DETAIL

NOT TO SCALE

NOTES:

1. THE FINAL COVER REPLACEMENT GEOSYNTHETICS IS TO BE CONNECTED TO THE EXISTING FINAL COVER GEOSYNTHETICS AT THE LIMITS OF DISTURBANCE. THIS SHOULD INCLUDE THE FOLLOWING:
   a. FUSION OR EXTRUSION OF THE REPLACEMENT GEOMEMBRANE TO THE EXISTING GEOMEMBRANE
   b. ATTACHING THE REPLACEMENT GEOTEXTILE CUSHION TO THE EXISTING GEOTEXTILE CUSHION BY OVERLAPPING IT BY AT LEAST ONE FOOT AND EITHER MACHINE-SEWING OR THERMALLY BONDING THEM TO ONE ANOTHER.

2. WHERE THE EXISTING FINAL COVER SYSTEM EXTENDS BEYOND THE DEEP CUTOFF WALL, THE LIMITS OF THE FINAL COVER IS TO BE EQUAL TO THE LIMITS OF THE 2020 FINAL CLOSURE (E.G. EXISTING ANCHOR TRENCH LOCATION). WHERE THE CUTOFF WALL IS LOCATED BEYOND THE LIMITS OF THE EXISTING FINAL COVER SYSTEM (E.G., BEYOND THE LIMITS OF THE EXISTING ANCHOR TRENCH), THE REPLACEMENT FINAL COVER SYSTEM IS TO BE EXTENDED BEYOND THE LIMITS OF THE CUTOFF WALL, WITH THE REPLACEMENT ANCHOR TRENCH INSTALLED IMMEDIATELY ADJACENT TO THE EXTERIOR EDGE OF THE CUTOFF WALL.

3. THE REPLACEMENT GEOTEXTILE IS TO CONSIST OF A NONWOVEN POLYPROPYLENE MATERIAL THAT MANUFACTURED IN ACCORDANCE WITH THE LATEST VERSION OF GEOSYNTHETIC INSTITUTE GRI-GT12(A) STANDARD SPECIFICATION, AND WITH THE FOLLOWING REQUIREMENTS:
   a. MINIMUM MASS PER UNIT AREA OF 16 OZ/YD2 (PER ASTM D5261)
   b. MINIMUM GRAB STRENGTH OF 270 LB (PER ASTM D4632)
   c. MINIMUM TEAR STRENGTH OF 105 LB (PER ASTM D4533), AND
   d. MINIMUM PUNCTURE STRENGTH OF 725 LB (PER ASTM D6241).

   GEOTEXTILE SEAMS ARE TO BE OVERLAPPED BY 1 FT DURING PLACEMENT AND EITHER MACHINE SEWN OR THERMALLY BONDED TO ONE ANOTHER.

4. THE REPLACEMENT GEOMEMBRANE IS TO CONSIST OF A LINEAR, LOW-DENSITY POLYETHYLENE (LLDPE) MATERIAL, TEXTURED ON BOTH SIDES, MANUFACTURED IN ACCORDANCE WITH THE LATEST VERSION OF GEOSYNTHETIC INSTITUTE GM17 STANDARD SPECIFICATION, AND WITH THE FOLLOWING REQUIREMENTS:
   a. MINIMUM NOMINAL HEIGHT OF 40 MIL (PER ASTM D5994)
   b. MINIMUM ASPERITY HEIGHT OF 16 MIL (PER ASTM D7466)
   c. MAXIMUM DENSITY OF 0.939 G/ML (PER ASTM D792, OR ASTM D1505)
   d. MINIMUM TENSILE STRENGTH AT BREAK OF 60 LB/IN (PER ASTM D6693)
   e. MINIMUM ELONGATION AT BREAK OF 250% (PER ASTM D6693)
   f. MINIMUM TEAR RESISTANCE OF 22 LB (PER ASTM D1004), AND
   g. MINIMUM PUNCTURE RESISTANCE OF 44 LB (PER ASTM D3895)

   GEOMEMBRANE SEAMS ARE TO BE FUSION WELDED; REPAIRS AND PENETRATION FOR PIPE BOOTS ARE TO BE EXTRUSION WELDED.

5. THE REPLACEMENT TOPSOIL IS TO CONSIST OF A NATURAL SOIL MATERIAL THAT IS RELATIVELY HOMOGENOUS, FREE OF DEBRIS, FOREIGN OBJECTS, AND LARGE ROCK FRAGMENTS. THE TOPSOIL IS TO:
   a. BE CLASSIFIED AS A SC, CL, ML, OR OL (PER ASTM D2487), AND
   b. BE FERTILIZED, AS NECESSARY, BASED ON AGRONOMIC TESTING TO SUPPORT VEGETATION GROWTH AT THE SITE.

   TOPSOIL REMOVED FROM THE EXISTING FINAL COVER SYSTEM, WITHIN THE LIMITS OF DISTURBANCE, MAY BE STOCKPILED AND RE-USED AS REPLACEMENT TOPSOIL, IF APPROPRIATELY SEGREGATED.

6. THE REPLACEMENT COVER SOIL IS TO CONSIST OF A NATURAL SOIL MATERIAL THAT IS RELATIVELY HOMOGENEOUS, FREE OF DEBRIS, FOREIGN OBJECTS, AND LARGE ROCK FRAGMENTS. THE COVER SOIL IS TO:
   a. BE CLASSIFIED AS A CL, CH, SL-CH, CL-ML, SC, SM, SP, SW, OR SW-SP (PER ASTM D2487), AND
   b. HAVE A MAXIMUM PARTICLE SIZE OF 1.5 INCHES (PER ASTM D422 OR D6943), OR LARGER IF SUPPORTED BY A GEOMEMBRANE PUNCTURE ANALYSIS.

   COVER SOIL REMOVED FROM THE EXISTING FINAL COVER SYSTEM, WITHIN THE LIMITS OF DISTURBANCE, MAY BE STOCKPILED AND RE-USED WITH REPLACEMENT TOPSOIL, IF APPROPRIATELY SEGREGATED.

7. THE FINAL COVER SYSTEM WITHIN THE LIMITS OF DISTURBANCE IS TO BE RECONSTRUCTED TO THE SAME DESIGN SUBGRADES AS THE COMPLETED 2020 FINAL CLOSURE.

8. THE FINAL COVER SYSTEM WITHIN THE LIMITS OF DISTURBANCE IS TO BE RECONSTRUCTED TO THE SAME SURFACE GRADES AS THE COMPLETED 2020 FINAL CLOSURE.

9. VEGETATION IS TO BE RESTORED AFTER THE RECONSTRUCTION OF THE FINAL COVER SYSTEM.

10. CONTOURING FILL OR COMPACTED CCR IS TO CONSIST OF MATERIAL REMOVED DURING CONSTRUCTION TO CREATE THE WORKING PLATFORM. THE MATERIALS ARE TO BE REPLACED AFTER WALL CONSTRUCTION TO CREATE THE FINAL COVER SYSTEM SUBGRADES.

11. ANY STORMWATER CHUTES DISTURBED DURING CONSTRUCTION SHOULD BE RECONSTRUCTED TO THE SAME CONFIGURATION AS THE COMPLETED 2020 FINAL CLOSURE.

12. THE CONTINUOUS CONTAINMENT SYSTEM DESIGN WILL BE FURTHER REFINED AS PART OF FINAL DESIGN ACTIVITIES THAT WILL BE INITIATED AFTER A CORRECTIVE ACTION CONSTRUCTION PERMIT HAS BEEN ISSUED FOR THE WEST ASH POND SYSTEM THESE ACTIVITIES MAY INCLUDE, BUT ARE NOT LIMITED TO, THE COLLECTION OF ADDITIONAL SITE SURVEY AND/OR SUBSURFACE INVESTIGATION DATA, MORE REFINED DESIGN EVALUATIONS, ADDITIONAL ENGINEERING ANALYSES, AND/OR PERMIT-RELATED CONSIDERATIONS. ELEMENTS OF THE CONTINUOUS CONTAINMENT SYSTEM DESIGN THAT WILL BE REFINED INCLUDE, BUT ARE NOT LIMITED TO, THE LIMITS OF DISTURBANCE, THE DIMENSIONS AND GEOMETRY OF THE WORK PAD, LIMITS OF THE FINAL COVER SYSTEM, TIE-IN DETAILS BETWEEN THE FINAL COVER SYSTEM, TIE-IN DETAILS BETWEEN THE DEEP CUTOFF WALL AND STORMWATER MANAGEMENT FEATURES, AND THE LOCATION OF THE DEEP CUTOFF WALL WITHIN THE WEST ASH POND SYSTEM PERIMETER DIKES.

ISSUED FOR
PERMIT REVIEW
NOT FOR
CONSTRUCTION
DATE: 3/7/2025

NO.	REV DATE	REVISION	INT.

IT IS A VIOLATION OF LAW FOR ANY PERSON, UNLESS ACTING UNDER THE DIRECTION OF A LICENSED ENGINEER, TO ALTER THIS DOCUMENT. THIS DRAWING WAS PREPARED AT THE SCALE INDICATED. INACCURACIES IN THE STATED SCALE MAY BE INTRODUCED WHEN DRAWINGS ARE REPRODUCED BY ANY MEANS. USE THE GRAPHIC SCALE BAR TO DETERMINE THE ACTUAL SIZE. DRAWING IS NOT SCALABLE IF NO SCALE BAR IS PRESENT.

Project Details **DYNEGY MIDWEST GENERATION, LLC** West Ash Pond System Hennepin Power Plant 13498 E 800th St Hennepin, IL 61327	Drawing Title **CROSS SECTION DETAILS**		RAMBOLL **RAMBOLL AMERICAS ENGINEERING SOLUTIONS, INC.**		
Location:	Designer / Professional Engineer Responsible: B. RICHTER				
Project Number **1940110241-006**	Designed by S. LEE	Drawn by B. LEMMON	Checked by L. CARR	Approved by	Date April 2025
Project Status Corrective Action Permit-Level Design	Drawing Number **C-303**		Scale AS NOTED	Sc x	Rev. x